Sixth Australia-New Zealand Conference on Geomechanics

GEOTECHNICAL RISK — IDENTIFICATION, EVALUATION, AND SOLUTIONS.

CHRISTCHURCH, NEW ZEALAND 3-7 FEBRUARY 1992

CONFERENCE PROCEEDINGS

Organised by the New Zealand Geomechanics Society, a technical group of the Institute of Professional Engineers, New Zealand (IPENZ).

Sponsored by New Zealand Earthquake and War Damage Commission (EQC).

Endorsed by International Society of Soil Mechanics and Foundation Engineering (ISSMFE), International Association of Engineering Geologists (IAEG), and International Society of Rock Mechanics (ISRM).

ORGANISING COMMITTEE

Nick Traylen (Chairman)

Mark Yetton

Marton Sinclair

Don Elder

Tony Lingley

Steve Mathuson

Rob Davis

Dave Bell

John Berrill

Dave Jennings

Bruce Riddolls

Tim Sinclair

Trevor Matuschka

ISBN 0-473-01506-4

Published by The New Zealand Geomechanics Society

PREFACE

The 6th Australia-New Zealand Conference on Geomechanics is the Regional Conference of the International Society for Soil Mechanics and Foundation Engineering, the International Association of Engineering Geology and the International Society for Rock Mechanics. The conference is held at four year intervals with very third conference held in New Zealand.

The conference is organized by the New Zealand Geomechanics Society, a technical group of the New Zealand Institute of Professional Engineers, in co-operation with the Australian Geomechanics Society.

Accepted papers cover the three geomechanics fields of Soil Mechanics, Rock Mechanics and Engineering Geology with an overall theme "Geotechnical Risk — Identification and Solutions". The Conference programme includes a Keynote Address, seven technical sessions, the John Jaeger Memorial Address and the Geomechanics Lecture of the New Zealand Geomechanics Society. Poster sessions are available to allow authors to present their papers. The proceedings are published in a single volume which contains the Keynote Address, all session reports, all technical papers and the John Jaeger address. The Geomechanics Lecture will be published after the conference in Geomechanics News.

The support of our major sponsor, the New Zealand Earthquake and War Damages Commission (EQC) is gratefully acknowledged.

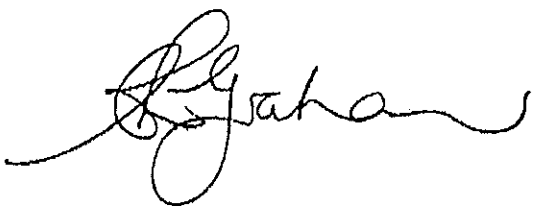

C.J. Graham
Chairman
New Zealand Geomechanics Society

LIST OF PAPERS

SESSION THREE
MINING, TUNNELS AND EXCAVATIONS

SESSION FOUR
SOIL PROPERTIES AND TESTING

SESSION FIVE
ANALYTICAL AND PROBABILISTIC METHODS

SESSION SIX
SLOPE STABILITY AND SEISMIC HAZARD

SESSION SEVEN
PROFESSIONAL AND LEGAL ISSUES

Mitigation of Ground Failure Risk – Some Lessons From the Loma Prieta Earthquake

JAMES K. MITCHELL
B.C.E., S.M., Sc.D.
Edward G. Cahill and John R. Cahill Professor of Civil Engineering, University of California, Berkeley

SUMMARY The identification, evaluation, and mitigation of risk increasingly defines the nature of modern geotechnical engineering practice. The aftermath of the October 17, 1989 Loma Prieta earthquake in California is used to illustrate how geotechnical risk has been identified and evaluated in the Marina District of San Francisco as a basis for recommendations for mitigative actions by both private citizens and the government in order to prevent loss of life and massive damage in a large earthquake which is predicted with a high degree of probability to occur within the next 30 years.

Special studies were done in the Marina District which showed that the heavy damage was the result of deep soft soil layers, uncompacted liquefiable fills, and structurally deficient buildings. The methodologies used in these studies are summarized. Actions that can be taken to prevent loss of life and even more devastation in future earthquakes include ground improvement to prevent liquefaction and lateral spreading, seismic retrofitting of structures, upgrading of utility systems, and the development of emergency response plans.

Geotechnical risks are ubiquitous in the world we live in, and as geotechnical engineers we have a special obligation to apply our special scientific and technical skills for their identification, evaluation, and mitigation. These include zonation studies for mapping of high risk areas, keeping the public and governments informed, early participation in site selection, helping in the development of consensus on assumption of responsibilities, participation in the development of emergency response plans, and helping to insure that the public and policy makers have correct perceptions and understanding of those geotechnical issues that directly affect their safety and well-being and that of the environment around them.

1. INTRODUCTION

"Geotechnical Risk - Identification, Evaluation and Solutions", the theme for this Sixth Australia-New Zealand Conference on Geomechanics, increasingly defines the nature of present geotechnical engineering practice. The 25 year period from the end of World War II in 1945 until 1970 saw major growth in both the scope and technical depth of our discipline. Projects ranging from small to large megaprojects were largely of the new facility type; e.g., foundations for structures of all types, dams, power plants, roads, and airfields. Our work was driven by migrating populations and expanding economies at home and the need for infrastructure development in the developing regions of the world. Few of these projects included formal analysis of risk and its mitigation, and in most cases risk and reliability issues were considered only implicitly, such as by selection of "conservative" values of soil properties and safety factors.

Starting in the 1970's, however, the nature of our geotechnical challenges began to change. There came realizations that resources are finite, that the environment is fragile and must be protected, that safe storage must be found for hazardous and radioactive wastes, and that the public needed better protection from natural hazards. The public, working through the political system and by means of new special interest groups, became much more vocal and influential. Economic and social priorities have undergone change, government involvement and regulation has increased.

The impacts of these changes on the development and practice of geotechnics have been profound. No longer are disciplines clearly defined or separated from each other. No longer are projects conceived, sited, and constructed by planners, designers, and builders without careful prior review and evaluation by representatives of all potentially affected interests. There are few new megaprojects, as environmental concerns dominate at home and economic difficulties plague the developing parts of the world.

As a consequence of these transformations, and because the earth and its immediate environment are central to so many natural and man-made hazards, many, if not most, of today's geotechnical engineering studies are undertaken because of concerns that relate to risk and its identification, evaluation, and mitigation. In short, our field has become very heavily risk-driven, and we do our work in cooperation with many others; e.g., government and business decision makers, the public, earth scientists, engineers of a variety of types, architects, and even media specialists.

The aftermath of the Loma Prieta earthquake of October 17, 1989, which caused significant loss of life and enormous economic losses in northern California, provides an excellent example of the importance of geotechnical issues in the identification of seismic risk, the evaluation of its potential consequences in future earthquakes, and the development of strategies for mitigating these consequences. The Marina District of San Francisco was particularly hard hit by the Loma Prieta earthquake, and it remains at great risk in an anticipated future large earthquake. I use it in this keynote paper to illustrate how

geotechnical risk has been identified and evaluated as a basis for recommendations for mitigative actions by both private citizens and the government. The following reports provide detailed information and data upon which most of this paper is based: BAREPP (1990), Mitchell et al. (1990), Seed et al. (1990), Harding Lawson Associates et al. (1991), U. S. Geological Survey (USGS) (1990), and Mitchell and Wentz (1991).

2. THE 1989 LOMA PRIETA EARTHQUAKE

At 5:04 pm on October 17, 1989, a 40-km long segment of the San Andreas fault ruptured, with the epicenter located about 15-km east of Santa Cruz, California, as shown on Fig. 1. The fault break resulted in a 3-m offset to the northwest at depth of the Pacific Plate on the west side of the fault. This side of the fault also moved upward a distance of more than 1.3-m. Such a fault rupture was not unexpected, as it occurred along one of the six fault segments in California that was judged most likely to generate a magnitude 6.5 or greater earthquake during the period 1988 to 2018, according to The Working Group on Earthquake Probabilities convened in 1988 by the U.S. Geological Survey.

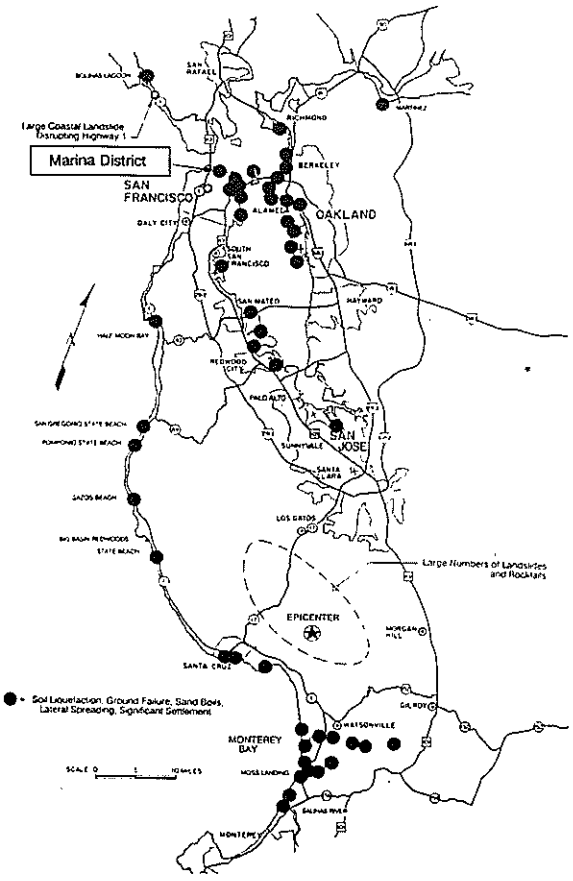

Figure 1 Map showing the region of Northern California affected by the Loma Prieta earthquake of October 17, 1989. Dots indicate zones of soil liquefaction, ground failure, sand boils, lateral spreading, and significant settlement.

The duration of strong ground shaking was about 15 seconds. This is very short for a magnitude 7.1 earthquake. The reason for this short duration was that the fault ruptured simultaneously from the center towards each end. Had the slip initiated at one end of the rupture zone and proceeded in one direction only along the full 40-km of fault rupture, the shaking would have lasted about twice as long, and the resulting damage would undoubtedly have been much greater.

Nonetheless, with estimated damages of more than $6 billion, the Loma Prieta earthquake was the costliest natural disaster in United States history. There were 62 deaths, more than 3,500 injuries, over 18,000 homes damaged, and about 12,000 displaced persons. The collapse of a section of the San Francisco-Oakland Bay Bridge and the failure and near failure of several sections of elevated freeway structures had major impacts on Bay Area transportation, several of which remain. Locations that experienced soil liquefaction, ground failure, lateral spreading, and significant settlement are shown on Fig. 1. Locally, structures and facilities founded on bayshore sites underlain by deep, soft soils sustained unusually high levels of damage due to strong shaking compared to developments founded on rock or shallow, stiff soil.

The results of studies following the earthquake have provided explanations for almost all of the observed behavior and damage. From a geotechnical standpoint there were very few surprises. Seismic zonation studies done prior to the earthquake had generally identified those areas at greatest risk of liquefaction. In general those sites identified as having the greatest liquefaction potential did liquefy and suffered the greatest damage.

Recorded horizontal ground motions were from 1½ to 4 times greater on soft (cohesive) soil sites than on rock in the San Francisco-Oakland area. Damage concentrations in San Francisco and Oakland, some 100 km from the epicenter were much greater than in the San Jose area to the south which is much closer to the epicenter. Both the presence of soft soil profiles and the influence of the underlying geological conditions were responsible for this apparent anomaly of increased damage at 100 km than at 25-40 km from the energy source (Borcherdt, 1991).

2.1 Effects in the Marina District

In San Francisco, the Marina District was one of the most severely damaged of the soft soil areas. The Marina District, located at the northern end of the San Francisco peninsula, as indicated in Fig. 1, sustained extensive damage to structures, utilities, and streets. The Marina District is primarily residential. An air photo taken the day after the earthquake is shown in Fig.2, and a street map is given in Fig. 3.

The heavy damage in the Marina District could be attributed to several factors: (1) ground shaking and its effects on older homes that were constructed or modified prior to the development of modern building codes, which suffered structural deficiencies resulting from deterioration, or which had "soft" ground floors with little resistance to seismic lateral forces due to large, open ground floor garages, (2) soil liquefaction, (3) ruptured water and gas lines, (4) fire, and (5) lateral spreading of the ground.

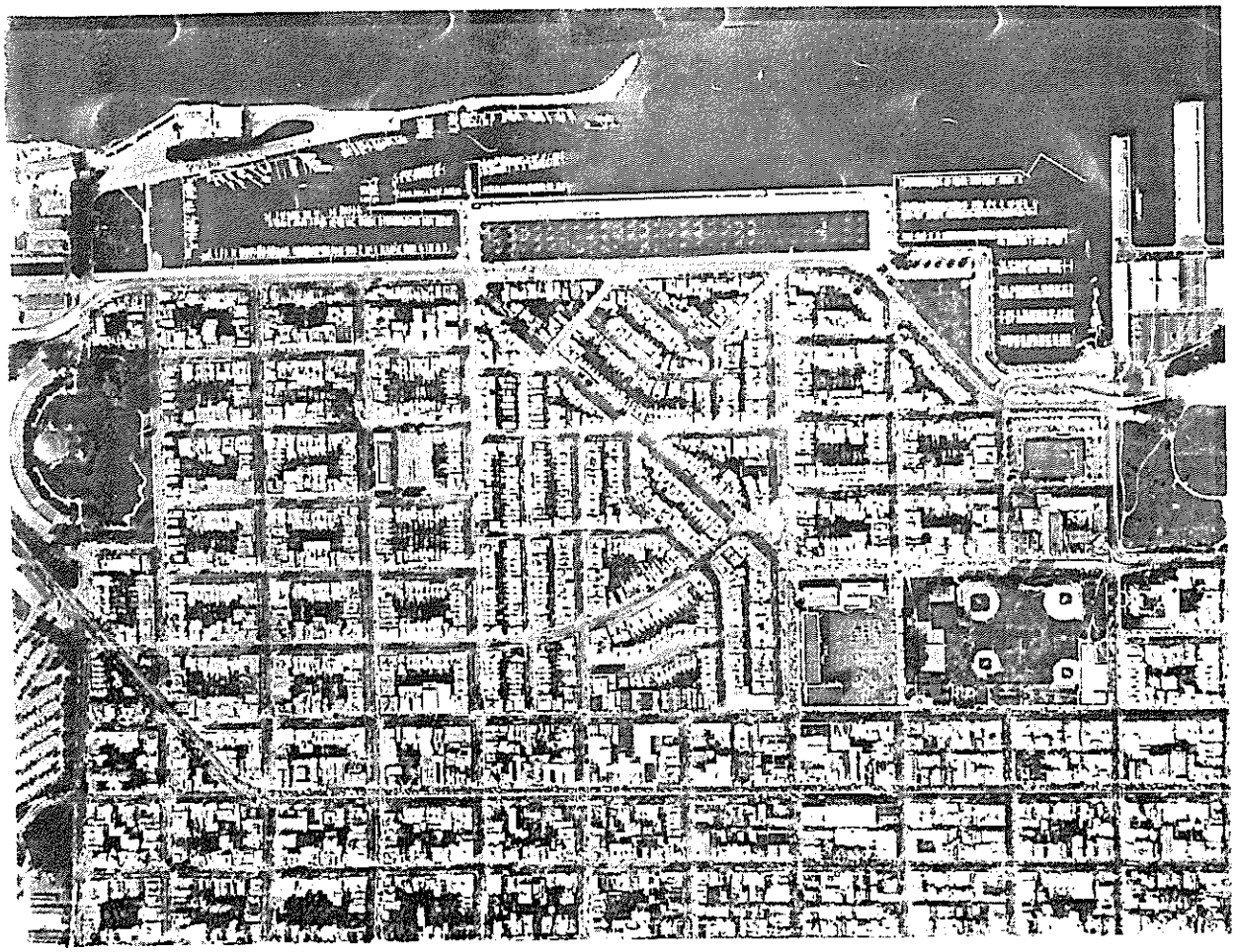

Figure 2 An aerial view of the Marina District of San Francisco

Ground shaking and related ground failure were responsible for extensive building damage as well as the collapse of several structures, as shown in Fig. 4. Liquefaction was widespread and manifested itself by sand boils (Fig. 5) and the ejection of sand through cracks and fissures. In addition, liquefaction resulted in cracked and ruptured pavements, sidewalks, and water and gas lines, and settled and tilted buildings (Fig. 6).

Fissures developed parallel to sea walls as a result of lateral spreading. Damage to the sea wall and settlement at the Marina yacht harbor are shown in Fig. 7. There was almost 0.6-m of lateral spreading towards the Bay at the St. Francis Yacht Club which displaced the deck away from the main clubhouse. Although there may have been local lateral spreading south of Marina Boulevard, the pattern of cracking and surface ruptures in the streets did not indicate any overall movements of large magnitude (O'Rourke et al., 1990).

Several fires started immediately after the earthquake, and the loss of water supplies because of the rupture of water lines prevented their rapid extinction. In fact, the largest fire, located at the corner of Beach and Divisadero Streets, could only be extinguished after the City's fireboat was brought to the edge of the Marina harbor and used to pump water through hoses that were run from the fireboat to the fire. Fortunately, at the time of the earthquake and fires there was no wind. Otherwise the loss by fire could well have exceeded that due to the earthquake itself or that of the devastating Oakland hills brushfire of October 20, 1991, which caused losses estimated at $1.5 to $2 billion.

Inspections in the days following the earthquake resulted in building classifications based on recently developed procedures for post-earthquake safety evaluation that were used for the first time. Each building was inspected and tagged by a color that indicated its condition:

Red Tag	-	unsafe, do not enter or occupy
Yellow Tag	-	limited entry, off limits to unauthorized persons
Green Tag	-	inspected, no restriction on use or occupancy

A map showing the locations of the demolished buildings and the red and yellow tagged buildings is shown in Fig. 8. A line showing the location of the shoreline as it existed in 1869 is also shown. The location of the damaged structures relative to this shoreline is significant, as will be noted further later. The locations of major water line and sewer line breaks, which were caused by both liquefaction of the soil in which they were embedded and from differential movements, are shown in Fig. 9. The majority of these breaks are located in the same area as is the building damage.

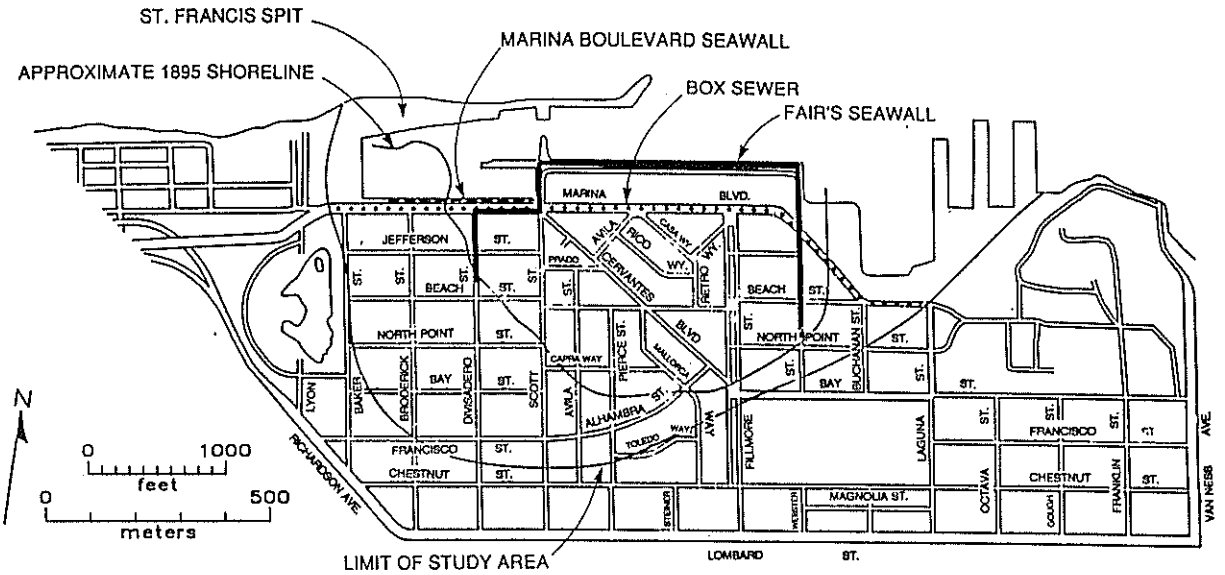

Figure 3 Street map of the Marina District of San Francisco. (modified from USGS, 1990).

Figure 4 Structure collapse as a result of ground shaking.

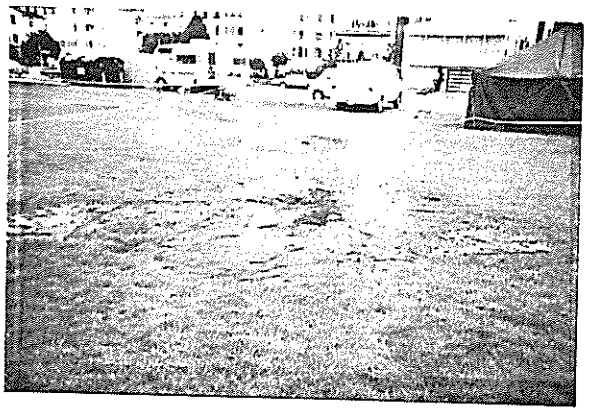

Figure 5 Sand boils caused by liquefaction in the Marina District.

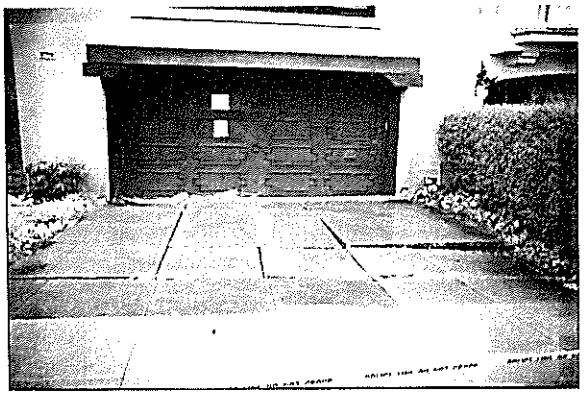

Figure 6 Building settlement as a result of sand liquefaction.

Figure 7 Lateral spreading, settlement, and damage to the seawall at the Marina yacht harbor.

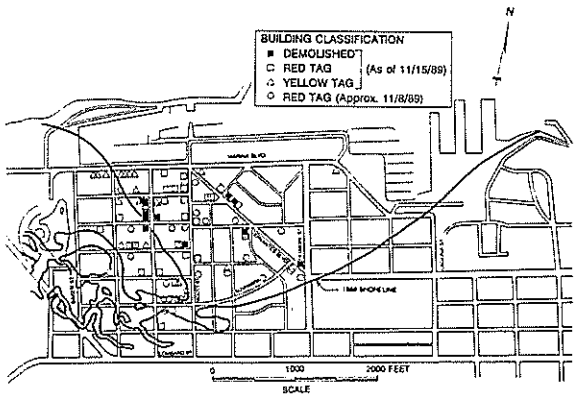

Figure 8 Locations of demolished and red- and yellow-tagged structures in the Marina District.

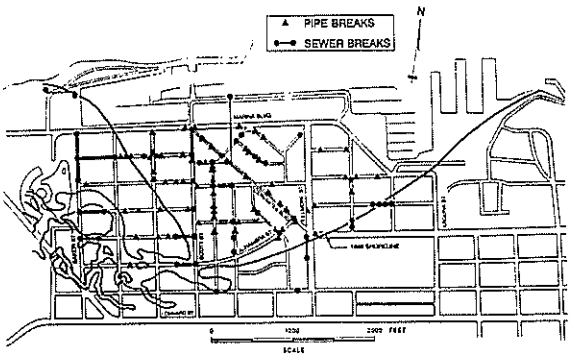

Figure 9 Locations of major water pipe and sewer line breaks.

3. PUBLIC RESPONSE IN THE MARINA DISTRICT

The Marina District was not the only area of San Francisco that sustained heavy damage in the Loma Prieta earthquake. Other areas (as shown on Fig. 18) included Sullivan Marsh (also called South of Market), Mission Creek, South Beach, the Embarcadero Waterfront, and the Telegraph Hill/ North Beach area. These areas sustained even greater damage in the 1906 San Francisco earthquake, because of the stronger and longer duration shaking in that event. The Marina District had not yet been developed at that time.

In the days immediately following the Loma Prieta earthquake the residents of the Marina District organized themselves to provide mutual assistance and to begin the rebuilding process. They also were well aware that their District would be at great risk in any future large earthquake and that there is a two to one probability that a magnitude 7 or larger earthquake will occur prior to 2018 on one of the segments of the Hayward or San Andreas faults that is much closer to the Marina District than the Loma Prieta epicenter (U.S. Geological Survey, 1989). Accordingly, they appealed to the Mayor of San Francisco for a study of the special geologic and soil conditions in the Marina District and their relation to the damage that occurred, and, more important, the likely impact of these conditions on ground response, soil and structure stability, and public safety and welfare in future earthquakes. In essence, the citizens were appealing for an assessment of geotechnical risk and for advice on measures to be undertaken both by the City and by themselves for its mitigation.

A request was then made that the study by done by the University of California, Berkeley, and the author was put in charge of the work, which culminated in a report to Mayor of San Francisco (Mitchell et al., 1990), which was widely circulated among the residents of the Marina District. Because the U. S. Geological Survey (1990) had chosen the Marina District as one of its main post-earthquake study areas, a comprehensive survey had been made of pipeline damage (O'Rourke et al., 1990), and other detailed evaluations had been made of building and utility damage. Thus there was considerable data available for evaluation as a basis for the conclusions and recommendations in the report. The main findings of the study are summarized in the following sections.

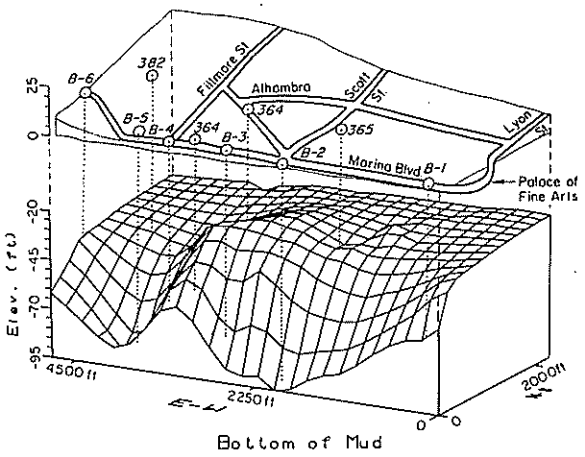

Figure 10 Three-dimensional view of the bottom surface of the Bay mud underlying the Marina District of San Francisco. (prepared by T. D. O'Rourke and B. L. Roth, Cornell University, 1990).

4. WHY WAS THE MARINA DISTRICT SO HARD HIT?

One of the most important conclusions, and one that was difficult to pass on to the residents, since no one likes to be the bearer of bad news, is that much of the structural damage in the Marina District caused by the Loma Prieta earthquake was a direct result of ground shaking and the inability of the structures to withstand it. Liquefaction and the associated ground displacements were responsible primarily for building settlements, utility line and pavement breaks and some structural damage. However, liquefaction was neither the cause of the amplified ground shaking, nor can ground treatment to prevent liquefaction in the future be expected to reduce ground surface shaking significantly. Similarly, the fact that the relatively moderate levels and short duration of shaking in the Loma Prieta earthquake caused liquefaction over large areas suggests that considerable risk for soil liquefaction still exists in the area, and this poses a major risk in future, larger and more near-field seismic events.

4.1 Soil Deposits

The depth to bedrock beneath the Marina District is not known in detail; however, drill holes reached rock at depths of 45 m below mean sea level at Lombard Street west of Fillmore (Fig. 3), 42 m on the west side of Fillmore Street north of Lombard, 78 m on Buchanan Street south of Bay, 80 m at the corner of Beach and Divisadero Streets, and at about 23 m at Lyon Street north of Bay, thus defining a half bowl that deepens to the north.

The bedrock is overlain by a complex series of sediments. The uppermost layer, San Francisco Bay mud, is very soft and compressible and consists primarily of silt and clay. It formed the bottom of a shallow bay which underlay most of the present Marina District prior to filling. A three-dimensional view of the bottom surface of the Bay mud is shown in Fig. 10. The Bay mud varies in thickness from 0 in the vicinity of Chestnut Street in the south to a maximum of 29 m beneath the Marina Green to the north. Tidal marsh deposits of clay and silt with some vegetation extend in a narrow band across the southwest part of the Marina District and west into the Presidio of San Francisco. The northwest part of the District is underlain by clean, uniform beach sand. This part is referred to as Strawberry Island. This sand also forms a narrow strip in the southeast part of the Marina District. Wind-deposited dune sand underlies the eastern and southeastern part of the District.

The significance of these natural soil conditions is that (1) the deep clayey soil column amplifies moderate levels of rock motions of the type produced in this area by the Loma Prieta earthquake, (2) the soft Bay mud provides poor support for foundations extending through the overlying fills and is the source of significant long-term settlements when loaded by fills and structures placed upon it, and (3) some of the naturally deposited sands may be susceptible to liquefaction.

4.2 Marina District Fills

Most of the present Marina District is founded on fills of various types that were constructed to provide greater land area above water. These fills were placed prior to the development of modern engineering understanding of ground response to earthquakes and of soil liquefaction. A composite map showing major fill units is shown in Fig. 11. The dredged hydraulic fill that was placed in Marina Cove in 1912 to provide land for the Panama Pacific International Exhibition has the lowest resistance to liquefaction. In general the fills in the Marina District are primarily sand. However, both the performance of these materials during the Loma Prieta earthquake and subsequent field testing (Bennett, 1990) have shown that they are not equal in terms of liquefaction resistance. This is further illustrated by Fig. 12, which shows the locations of sand boils formed as a result of the earthquake. The post-earthquake field data, primarily in the form of Standard Penetration Test N-values and Cone Penetration Test tip resistance values, are consistent with the sand boil distributions and provided accurate measures of the liquefaction potential of the fills in different areas.

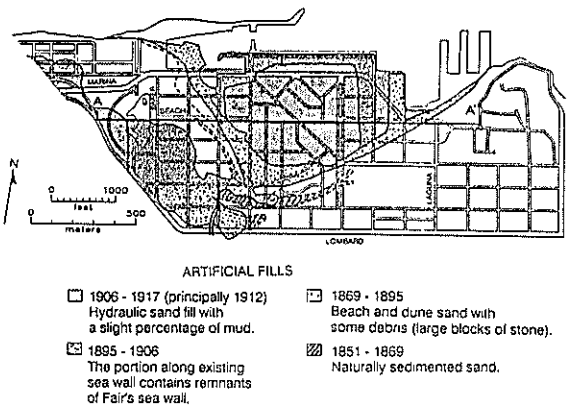

Figure 11 Marina District fills. (from Bonilla, 1990).

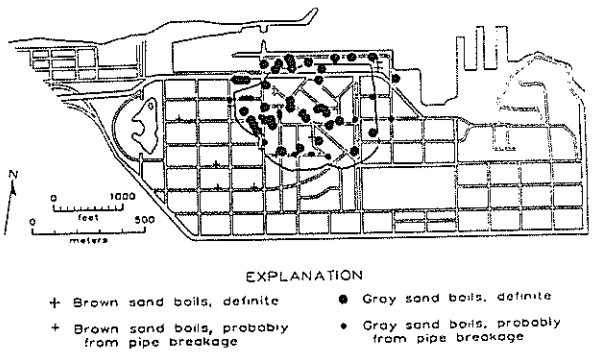

Figure 12 Locations of sand boils formed by liquefaction during the Loma Prieta earthquake. (from Bennett, 1990).

4.3 Soil Profiles

Although insufficient data are available to define all the soil types and their thicknesses at all locations, approximate soil profiles have been developed for the conditions along Marina Boulevard in an east-west direction and for a north-south section parallel to and about 90 m west of Fillmore Street, as shown in Figs. 13 and 14, respectively. These cross sections show that the soil conditions are not uniform across the Marina District. The thickness of the recent Bay mud, which varies from 0 to 23 m, and the thicknesses and types of fill and natural beach and dune sands above the mud influence both the susceptibility of the ground to liquefaction and the choice of any remedial measures that might be used to prevent liquefaction in future earthquakes. Fills susceptible to liquefaction are up to 9 m thick.

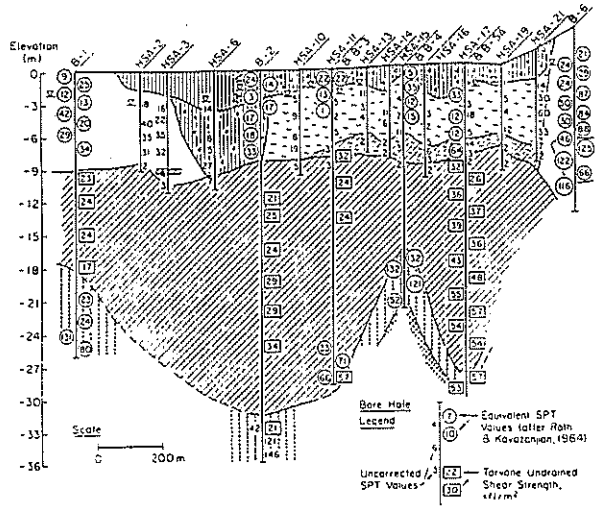

Note: Various soil units are explained in Fig. 14

Figure 13 Soil profile along Marina Boulevard. (from O'Rourke et al., 1990).

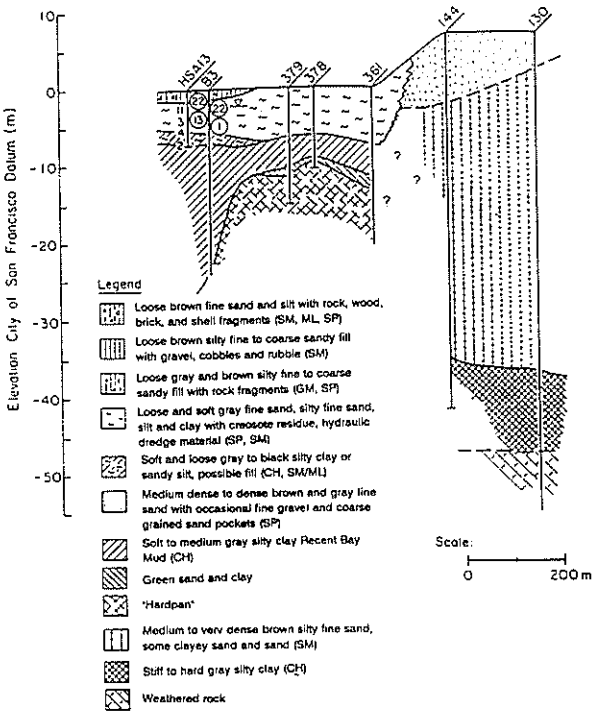

Figure 14 North-south profile about 90 m west of Fillmore Street. (from O'Rourke et al., 1990).

4.4 Reasons for the Extensive Damage

From the evaluations of the soil conditions and structures, it was evident that there are three primary reasons why the Marina District sustained so much damage in the Loma Prieta earthquake.

1. **The deep soil column amplified ground motions.** Rock motions can be amplified as they travel upwards through soft soils to the ground surface. The result is stronger surface shaking and a longer period that is more damaging than the high frequency motions that are more typical of those on rock or rock overlain by shallow, stiff soil layers. Estimates in several ways indicate amplifications of peak accelerations by factors from 2 to 6, with values of 2 to 3 being typical for the levels of shaking produced by the Loma Prieta earthquake, as may be seen in Fig. 15 developed by Idriss (1990). For two to four story stucco-clad wood-frame buildings, which are the predominant type in the Marina District, the motions of the structures are further amplified by as much as a factor of two as a result of resonant interaction with the long period ground surface motions produced by the soft soil conditions.

2. **There was liquefaction of some of the fills.** Some of the sandy fill materials were (and still are) loose. In addition, the water table is shallow, thus producing conditions that were (and still are) particularly susceptible to liquefaction. As a result there were differential settlements, pipeline breakage, and some local lateral spreading that were sources of damage to structures, pavements and utilities.

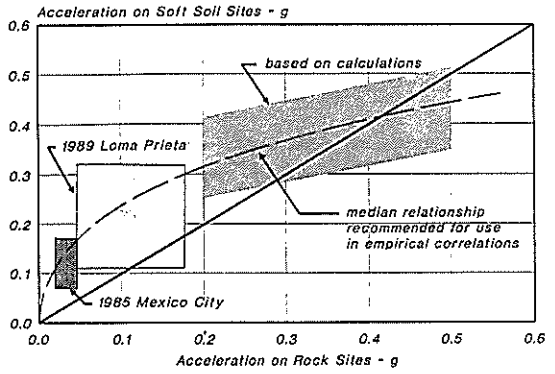

Figure 15 Amplification of rock accelerations by soft soil sites. (from Idriss, 1990).

3. **Many structures had inadequate seismic resistance.** Many buildings were designed prior to the development of modern building codes which provide for suitable earthquake resistant design. Unreinforced masonry buildings, which are common in San Francisco, were particularly hard hit. In a study by Holmes et al. (1990) it was found that there was a correlation between the amount of damage, the softness of the soil site, and the story height, as shown in Fig. 16. In Fig. 16 the average damage ratio is the estimated percent of replacement value, and the range of shear wave velocities is from poor or soft soil (150 m/s) to rock (700 m/s). The damage ratio for story heights greater than 12 ft was much greater at soft soil sites.

An additional major factor in the Marina District was the "soft first story" situation which resulted from the lack of internal bracing on the first floor of may structures because of large open areas to accommodate garage parking. In addition many houses sustained damage as a result of structural deficiencies caused by dry rot or other processes of deterioration. Some well-designed and constructed structures that were in good condition fared quite well; however, others were damaged as a result of substantial total and differential settlements. Any actions to improve

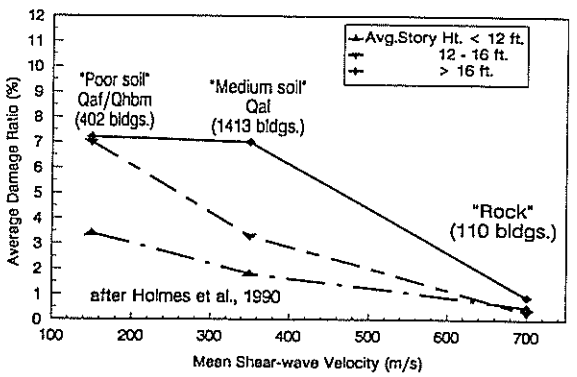

Figure 16 The influence of soil conditions, as measured by shear wave velocity, on the damage ratio for unreinforced masonry structures in San Francisco during the Loma Prieta earthquake (from Holmes et al., 1990).

the soils so that they will maintain their supporting capacity in future earthquakes will be of little value if the intrinsic seismic stability of the structures that they are called upon to support is inadequate.

4.5 Implications

Given that the Loma Prieta earthquake was of unusually short duration (about 15 seconds, as opposed to 30 seconds or more for most magnitude 7.1 events) and that an earthquake of equal or greater magnitude with a closer epicenter is probable within the next 25 to 30 years, the inescapable conclusion is that there is a high probability of even greater damage in the future if seismic retrofitting of structures and ground improvement in some areas are not undertaken. Just what to do, how, and by whom became issues of considerable importance, however, because different technical options were being proposed to the homeowners, most remediation methods are very expensive, both public and private land is involved, privately owned utilities serve the residents, and jurisdictions are not always clear.

5. THE ROLE OF GROUND IMPROVEMENT

Demolition of and removal of structures that could not be saved was carried out rapidly in the days immediately following the earthquake. Equally rapidly a number of salvageable structures were underpinned and structural repairs were initiated. Some individual homeowners chose to have mini-piles installed or compaction grouting done in the potentially unstable fill beneath their homes. There were proposals that a special assessment district be established and the whole Marina District fill be densified by compaction grouting. Most property owners were unable or unwilling to undertake expensive remediation until the extent of government assistance was known, the responsibilities to be assumed by the City were defined, and they had received the results of the University of California report. All were vitally interested in the results of the soil study and its implications for their future safety.

Consequently, it was considered essential that the citizens be fully aware of the usefulness and limitations of ground improvement for seismic hazard mitigation. The conclusions on this point related to the causes of damage and were:

1. Damage directly due to ground shaking. A majority of the structural damage and the collapse of a number of structures appeared to have been caused directly by strong ground shaking. The deep, unconsolidated deposits amplified bedrock motions, and ground improvement cannot significantly reduce this amplification. Consequently, the solution to the ground shaking problem must include structural improvement.

2. Damage due to ground failure and ground displacement. Liquefaction of the saturated, sandy surface fills can result in building foundation bearing failures, differential settlement and distortion of structures, lateral spreading which can pull apart both structures and buried utilities, and in some cases complete stability failure and lateral sliding. Ground strengthening by various means can be used to prevent liquefaction and lateral spreading. Alternative structural support systems providing

improved levels of both vertical support and resistance to differential lateral displacements can be used in lieu of ground treatment for support of buildings; however, this will not mitigate against pavement and utility damage.

It was also pointed out that all areas in the Marina District are not equally at risk of liquefaction. Both observed behavior in the Loma Prieta earthquake and analyses show that the hydraulic fill in the Marina Cove (the 1906-1917 fill area in Fig. 11) has the lowest liquefaction resistance. The beach and dune sand deposits do not appear to have liquefied, and it is probable that they can withstand more intense shaking without liquefaction, although some accounts of the 1906 earthquake suggest that some of these materials may have liquefied then. Detailed study of the response of other artificial fills has not yet been completed. It was recommended that site specific soil investigations to evaluate liquefaction potential be made prior to any new construction or rehabilitation of existing structures.

Furthermore, it was emphasized that actions for mitigation of seismic risk should recognize that (1) building code requirements are intended to prevent loss of life and to protect against building collapse under the maximum ground shaking, even though some damage may occur, and (2) public safety requires that the infrastructure and utilities; i.e., the lifelines, be protected. A general strategy for achieving building safety includes (1) seismic evaluation of the structure and retrofitting if necessary, (2) tying the building foundation together to resist lateral distortions, and (3) treatment of the underlying soil or provision of alternative support. Prevention of large ground displacements and lateral spreading is necessary for protection of the integrity of gas, water and electrical lines, as well as for the safety of structures.

It was considered important also to convey to the public that even though much of the liquefaction at many locations around the Bay area had occurred in fills, in almost every case it was in fills that had not been adequately densified during or after placement. This was to counter the general impression that had developed among the public that "fill" is synonymous with "bad" as far as performance in an earthquake is concerned. An attempt has been made, therefore, in published reports and discussion with the media to make the point that the same sandy hydraulic fill material that was pumped into areas such as the Marina Cove in 1912 and which liquefied during the 1989 Loma Prieta earthquake, could, if properly densified after placement, be used for earthquake resistant support of structures or for construction of barrier walls against the lateral spreading of adjacent liquefied soil.

6. GROUND STABILIZATION AND STRUCTURE SUPPORT OPTIONS

Methods for ground improvement and their applicability and limitations were described in general terms in the University of California report to enable the property owners and policy makers to better assess what could and what could not be done. Remedial actions for improving the soil and foundation support conditions can be considered in three categories:

1. Prevention of lateral spreading of liquefied ground.
2. Prevention of liquefaction.
3. Provision of improved or alternative support for structures presently founded on liquefied ground.

It was pointed out also that because the Marina District, except for the area of the Marina Green (Fig. 3), is already built up with structures, streets and utilities, this greatly limits the ability to use some types of ground improvement.

6.1 Prevention of Lateral Spreading

Large masses of soil that have liquefied during earthquakes have been known to flow laterally for long distances on slopes as flat as 0.5 degree. Given the topography in the area as well as the locations of sea walls and other potential barriers to lateral movement, a separate study was recommended to assess whether additional containment was needed to prevent lateral spreading. In the event that it is, then densified soil walls, concrete slurry walls, stone column buttresses, and mix-in-place soil and cement columns might be possible types of new barrier systems to provide edge containment for the Marina District fills.

6.2 Prevention of Liquefaction

Improving sandy soils to prevent liquefaction is best done by densification. In some cases it may be feasible to prevent liquefaction by drainage or by filling the voids in a loose sand by penetration grouting. However, when structures and utilities already exist, the number of available options is greatly reduced, because of restricted space, vibrations and noise, and the need to minimize ground settlement. Thus, whereas deep dynamic compaction, vibro-compaction, vibro-replacement stone columns, compaction piles, drains, and grouting of various types might be suitable options for open areas, only grouting, small vibrating probes, compaction grouting, or small displacement piles that are jacked into place might be reasonable options for use under existing foundations and around buried utilities. Before any of the methods is undertaken on a large scale, however, it would by useful to know if it is likely to be effective in protecting against liquefaction or other forms of ground failure.

7. THE PERFORMANCE OF IMPROVED GROUND IN THE LOMA PRIETA EARTHQUAKE

The Loma Prieta earthquake, while so destructive in so many ways, also provided one of the few full scale tests available so far of whether ground that has been improved to increase its seismic stability can really carry the earthquake stresses and deformations without distress or failure. In a separate study the post-earthquake condition of twelve sites, located as shown in Fig. 17, where ground improvement had been used were evaluated (Mitchell and Wentz, 1991). The sites and the methods used for ground improvement are listed in Table 1. The distances of the sites from the epicenter, the design accelerations, and the actual peak accelerations and duration of shaking between the first and last peaks of 0.1g acceleration or greater are listed in Table 2.

Although in most cases both the intensity of shaking and duration were less than the design values, the performance of the treated ground at all sites was excellent. No damage of consequence was reported in any case; however, at several of the locations the adjacent untreated ground

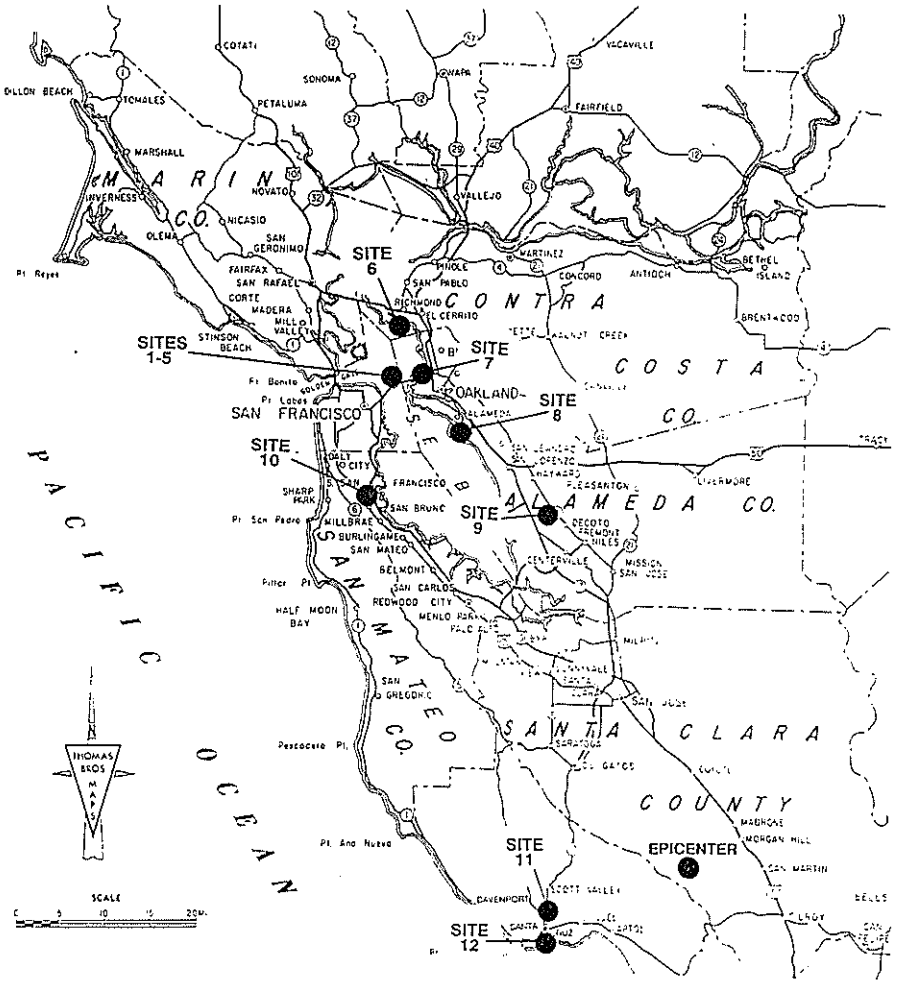

Figure 17 Location of sites where ground improvement had been used prior to the Loma Prieta earthquake. (from Mitchell and Wentz, 1991).

liquefied. Thus, there are now field performance results to attest to the merit of ground improvement for mitigation of seismic risk.

8. RECOMMENDATIONS FROM THE MARINA DISTRICT STUDY

Several conclusions and recommendations were offered in the report to the Mayor and the citizens of the Marina District concerning the identification, evaluation, and mitigation of future seismic risk. These included:

1. Just because an existing building sustained little or no damage from the Loma Prieta earthquake does not guarantee adequate performance in future earthquakes.

2. As new structures must be designed and constructed in conformance with the latest building code (1988), they should withstand future earthquakes provided the supporting soils do not liquefy or displace laterally.

3. An area-wide study was needed to confirm the existing barriers to lateral ground spreading, with special attention given to reducing hazards posed by gas and water line rupture, especially with regard to the fire hazard, wherever these lifelines pass through potentially liquefiable ground.

4. The selection of specific ground improvement methods in any area should only be made after more detailed site-specific soil exploration and engineering studies are made that take into account the costs and benefits.

5. Both the City of San Francisco and individual property owners should address future seismic safety. In particular, the City should evaluate area-wide concerns such as lateral spreading and the integrity of the streets and utilities, but the individual property owners should accept responsibility for their own safety and the adequacy of their homes (and their foundation systems) to withstand the next major earthquake.

TABLE I

GROUND IMPROVEMENT PROJECTS

NAME	LOCATION	SOIL CONDITIONS	METHOD	YEAR OF TREATMENT
1. Medical/Dental Clinic	Treasure Island	Hydraulic Sand Fill	Stone Columns	1989
2. Office Building No. 450	Treasure Island	Hydraulic Sand Fill	Sand Compaction Piles	1967
3. Facilities 487 - 489	Treasure Island	Hydraulic Sand Fill	Vibrocompaction	1972
4. Approach Area, Pier 1	Treasure Island	Hydraulic Sand Fill	Stone Columns	1984
5. Building 453	Treasure Island	Hydraulic Sand Fill	Non-Structural Timber Piles	1969
6. Esplanade Extension East Shore, Marina Bay	Richmond	Silty, Sandy, and Gravelly Fill	Stone Columns	1986
7. East Bay Park Condominiums	Emeryville	Silty Sand Fill	Vibrocompaction	1981
8. Harbor Bay Business Park	Alameda	Hydraulic Sand Fill	Deep Dynamic Compaction	1985
9. Hanover Properties	Union City	Silty Sand Fill	Deep Dynamic Compaction	1988
10. Kaiser Hospital	South San Francisco	Hydraulic Sand Fill	Compaction Grout	1978
11. Riverside Avenue Bridge	Santa Cruz	Sands and Gravels	Chemical Grout	1986
12. Adult Detention Facility	Santa Cruz	Silty, Sandy Fill	Deep Dynamic Compaction	1978

TABLE II

PEAK GROUND ACCELERATIONS - DESIGN EARTHQUAKE AND LOMA PRIETA EARTHQUAKE

NAME	LOCATION	DISTANCE FROM EPICENTER (MILES)	ACCELERATION (g's) ACTUAL	DESIGN	BRACKETED DURATION** (A ≥ 0.10 g) (SEC)
Medical/Dental Clinic	Treasure Island	60	0.16	0.35	2.5
Office Building No. 450	Treasure Island	60	0.16	0.43*	2.5
Facilities 487 - 489	Treasure Island	60	0.16	0.43*	2.5
Approach Area Pier 1	Treasure Island	60	0.16	0.35	2.5
Building 453	Treasure Island	60	0.16	0.45*	2.5
Esplanade Extension East Shore, Marina Bay	Richmond	68	0.11	0.35	1.0
East Bay Park Condominiums	Emeryville	60	0.26	0.35	2.0
Harbor Bay Business Park	Bay Farm Island	49	0.25	0.35	4.0
Hanover Properties	Union City	39	0.16	N/A	3.0
Kaiser Hospital	South San Francisco	51	0.11	N/A	2.0
Riverside Avenue Bridge	Santa Cruz	10	0.45	N/A	15.0
Adult Detention Facility	Santa Cruz	10	0.45	0.40	15.0

* These projects were completed in the late 1960's and the design earthquake used was the 1940 El Centro earthquake (scaled to a peak horizontal ground acceleration of 0.43 to 0.45 g).
** The bracketed duration is the elapsed time period between the first and last waves with accelerations greater than some specified value.

6. The Marina District is not the only area of San Francisco or California that is at risk in future earthquakes. Although the hazards are likely to be similar in the other high risk areas, the acceptable risks and the mitigation strategies may differ. Nonetheless, studies similar to that for the Marina District can be useful for the identification of potentially suitable ground stabilization options and the development of strategies for their implementation.

9. RESPONSE OF THE CITY

In response to the recommendations in the University of California report the City of San Francisco commissioned a project to "provide evaluations and recommendations as to what actions the City can take to minimize damage to public underground facilities in a future 8.3 Richter Scale earthquake." The study was conducted by a team of four firms: Harding Lawson Associates, Dames & Moore, EQE Engineering, Inc., and Kennedy/Jenks/Chilton. Independent review of the study was made by a separate committee chaired by the author.

Six areas within San Francisco were to be included in the study. In addition to the Marina District they included Sullivan Marsh (South of Market), Mission Creek Area, South Beach Area, Embarcadero Waterfront, and the Telegraph Hill/North Beach Area, as shown on Fig. 18. The Marina District is located off the northwest corner of the map just beyond Fort Mason. The study includes an evaluation of the stability of existing seawalls along the San Francisco waterfront at several critical locations. The following tasks were included in the study:

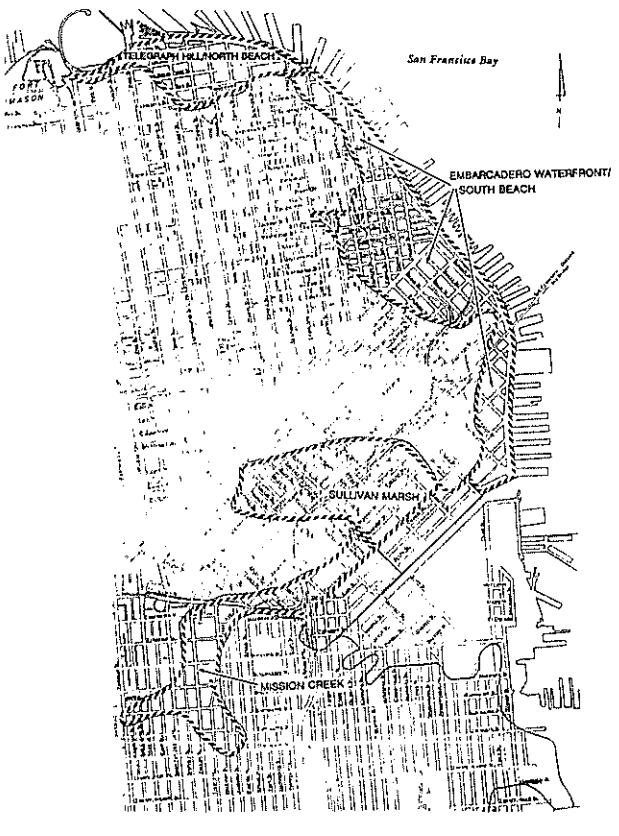

Figure 18 Locations of study areas, San Francisco Liquefaction Study.

1. Collection and evaluation of available geotechnical data.

2. Inventory of type, location, construction material, type of support, type of connection, deterioration, and other relevant information about City-owned underground utilities. These utilities included the Auxiliary and Municipal Water Supply Systems (AWSS and MWSS) and the City sewer system. It is significant to note that the gas, electric, and phone systems were not included in the study, as these systems are not City-owned.

3. Earthquake engineering analyses to evaluate the expected ground response, liquefaction potential of fill and suspect natural soils, and associated ground movements during a 1906 type earthquake, and the performance of underground utilities.

4. Estimation of damage to underground utilities, including all AWSS and MWSS mains, but not service lines, and sewers 200 mm diameter or larger.

5. Evaluation of mitigation options. These options were to include increasing the liquefaction resistance of soils by ground improvement, provision of alternative methods to fulfill facility function, improvements in system operations, increasing the structural capacity of key system components to withstand earthquake loadings and ground movements, and rerouting portions of utility systems to minimize impact to the rest of the City of failures in the study areas.

6. Recommendations for mitigation measures. These recommendations were to be based on the results of the evaluations and cost comparisons.

At the time of writing of this paper the studies for the Marina District and Sullivan Marsh Area have been completed and are reported in Harding Lawson Associates et al. (1991). Studies of the remaining areas are in progress, with the final report due by late 1991. A brief summary of the methodology, conclusions, and recommendations for the Marina District portion of the study abstracted from the Harding Lawson et al. (1991) report is given in the remainder of this section.

9.1 Geotechnical Analyses

Ground motions. Input ground motions were chosen based on experience in the San Francisco area with probabilistic seismic hazard (PSHA) studies for major building projects and were derived from the synthetic record used by Seed and Sun (1989) for analysis of soft soil response in the San Francisco Bay area. Ground response analyses were done using program SHAKE to evaluate the effects of different soil conditions. SHAKE is a one-dimensional site response analysis program for shear wave propagation in horizontally layered strata based on equivalent linear soil modeling.

Three representative profiles within the Marina District were analyzed. Using shear wave velocities for the different soil layers determined by prior experience and by seismic cone and geophysical methods following the Loma Prieta earthquake, the initially computed ground surface

accelerations varied from 0.46g to 0.57g. These values were considered to be too high, however, because the computed shear stresses in the Bay mud exceeded the shear strength. Consequently, accounting for the effects of soil nonlinearity, more reasonable surface accelerations for the postulated 8.3 magnitude event were taken to be on the order of $a_{max} \approx 0.4$ to 0.45g.

Liquefaction-induced settlements. To estimate probable settlements due to post-liquefaction consolidation, zones were defined within the Marina District, each of which enveloped a cluster of borings. The borings indicating the poorest and the best soil conditions based on SPT blow counts were identified in each zone. Depths of potentially liquefiable soil were determined using the method of Seed et al. (1985). Potential settlements were then determined using the method of Tokimatsu and Seed (1987).

The settlements of the hydraulic fill area of the Marina District computed by this procedure were reduced based on experience in the Loma Prieta earthquake that indicated smaller settlements in this material than predicted. The reason given for this overprediction is the presence of fines in the hydraulic fill, although other factors may be important as well, including the short duration of the Loma Prieta earthquake and actual accelerations that were less than assumed.

The results of the analysis were then used to prepare Fig. 19, which indicates zones within which the estimated settlements will be between 6 and 12 inches (150 and 300 mm), 3 and 6 inches (75 and 150 mm) or less than 3 inches (75 mm). The numbers on the map indicate computed minimum and maximum values of settlement in that specific area. Although these settlements are approximate, and deviations of up to 100 percent may occur, the values are about 1.5 to 2 times greater for the assumed magnitude 8.3 earthquake than were experienced in the magnitude 7.1 Loma Prieta earthquake.

Lateral displacements. Lateral movements in the Marina District could result from loss of ground by sand boils, lateral spreading caused by liquefaction, and lateral movement of liquefied sand toward depressions formed by vertical settlement. It was concluded that the largest lateral movements are likely both within the hydraulic fill area and near its margins. The gentle slope of the Marina District (about 0.4 percent) is not likely to spawn large area lateral spreading due to liquefaction. Analyses made using Towhata's method (Towhata et al., 1990) supported this conclusion.

Stability analyses of seawalls and large box sewer. The stabilities of Fair's Seawall, the Marina Boulevard Seawall and the large box sewer beneath Marina Boulevard, located as shown in Fig.3, were evaluated in order to assess the ability of these structures to prevent lateral spreading to the north into San Francisco Bay in the event of liquefaction of Marina District soils. Detailed information about the geometry of Fair's Seawall is not available; therefore, it was necessary to make assumptions about the rockfill structure. These resulted in the geometry in relation to the soil profile as shown in Fig. 20. Assumptions were made for both properties and loading conditions, and limit analyses indicated that the wall would translate laterally in the event of major earthquake (Harding Lawson Associates, 1991). Displacement analyses were made using the Newmark sliding block method (Newmark, 1965; Makdisi and Seed, 1978).

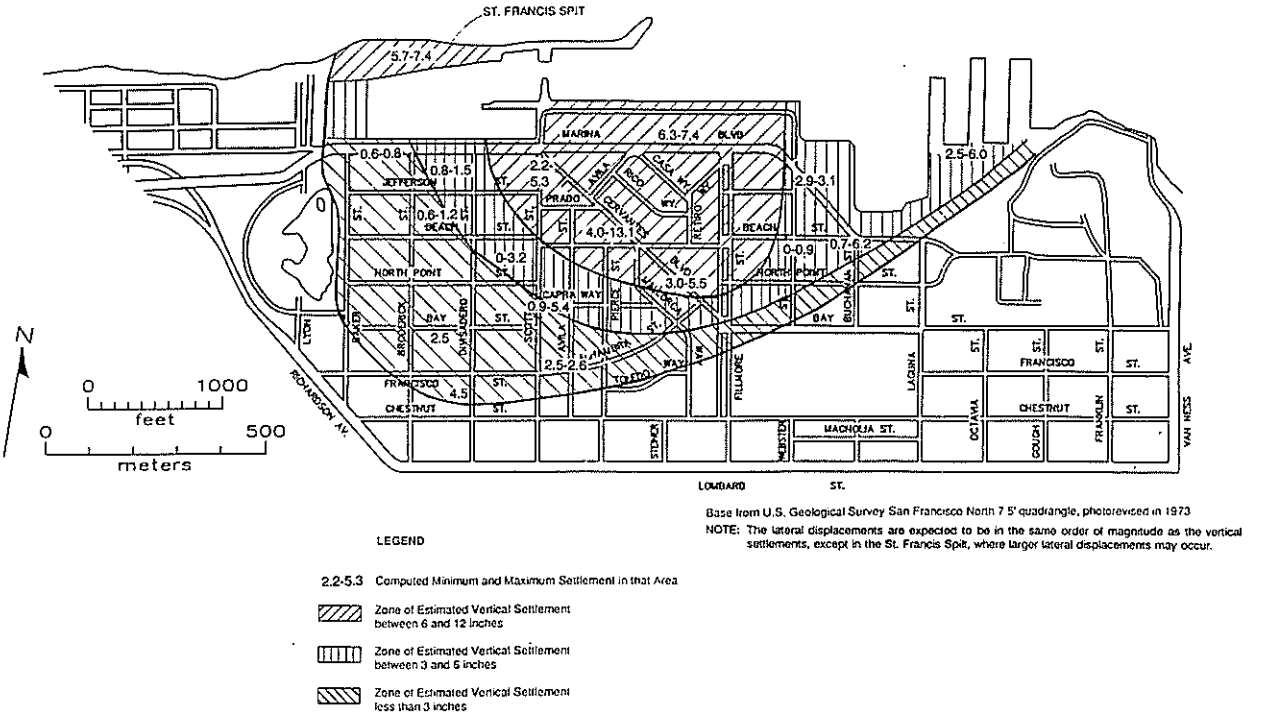

Figure 19 Estimated ground settlements due to liquefaction in the Marina District. (from Harding Lawson Associates et al., 1991).

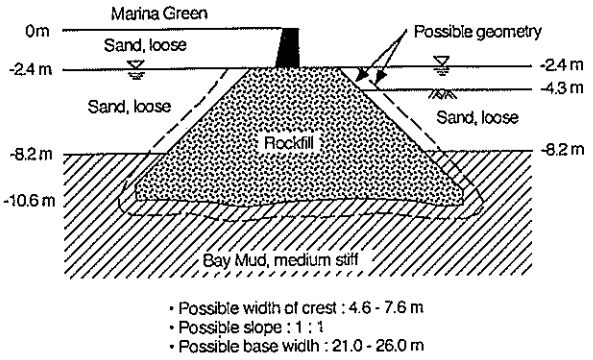

Figure 20 Assumed geometry of Fair's Seawall. (after Harding Lawson Associates et al., 1991).

From the results of the analyses, as well as considerations of the facts that (1) there were no reported movements in the 1906 earthquake when the wall height was not as great and the area behind the wall had not yet been filled completely, and (2) there were no apparent movements in the 1989 earthquake, it was concluded by Harding Lawson et al. (1991) that the wall may move between 1.2 and 2.4 m laterally in a future magnitude 8.3 event. It was also concluded that the wall could withstand these displacements because of its large base width and rockfill construction which can deform without rupture. If the large box sewer along Marina Boulevard prevents lateral ground movements from extending south of Marina Boulevard, then an average ground settlement up to 300 mm might occur in the Marina Green.

The top of the concrete box stormwater sewer beneath Marina Boulevard is about 0.6 m below the ground surface. The cross section increases from 3.35 m wide by 3.66 m high at Baker Street in the west to about 6.40 m wide by 7.00 m high at Buchanan Street in the east. The box is surrounded by a 0.3 m thick layer of drain rock which is intended to reduce the uplift pressure in the event underlying fills liquefy. Analysis of the lateral resistance of the box sewer under earthquake loading was made assuming that the sand above the water table had a friction angle of 35 degrees, the loose sand below the water table on each side of the box sewer has an undrained strength of 0 to 10 kPa (Seed and Harder, 1990), and there is no friction along the base. The resulting factors of safety against lateral translation of the sewer were 1.4 and 2.1 for the assumed residual strengths of the liquefied sand of 0 and 10 kPa, respectively. It was concluded that the box sewer would prevent major ground displacements south of Marina Boulevard. There might be some cracking of the concrete, however.

The Marina Boulevard seawall, located as shown in Fig. 3, was built during 1933-34 and is a cantilever concrete wall supported by composite concrete/wood piles, as shown in Fig. 21. The piles on the land side are vertical and spaced at 4 m center to center, and those on the yacht harbor side are alternates of three batter piles (3V:1H) and one vertical pile spaced at 2 m center to center. The connections between the wood and concrete sections of the piles cannot resist tensile forces, and this was concluded to be the weakest link in the structure. Accordingly, the uplift acting on the land side piles was calculated and compared with

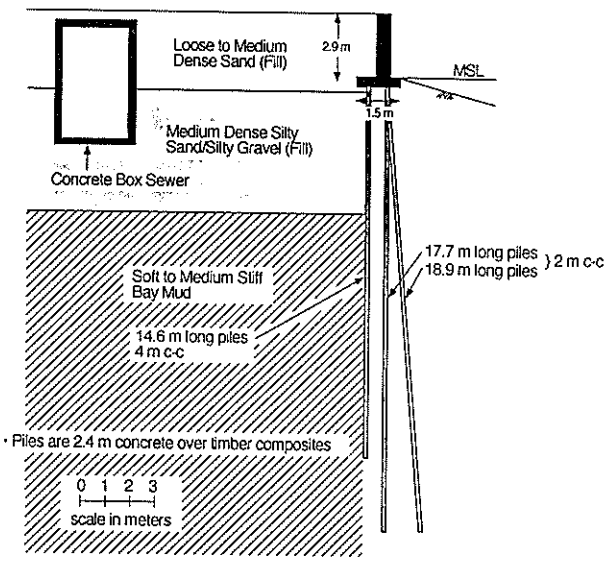

Figure 21 Typical cross section of Marina Boulevard Seawall. (after Harding Lawson Associates et al., 1991).

the skin friction that could be mobilized along the 2.4 m-long concrete pile section which connects the piles to the base of the wall. It was found that the average uplift force was about equal to the available skin resistance, but that the peak uplift force was much greater than the available resistance. Thus, the Harding Lawson Associates et al. (1991) analysis indicates that the wall may displace towards the Bay in a major earthquake. There is some risk that the concrete box sewer could be displaced in this area as well.

9.2 Utility Damage Evaluation

Systems. San Francisco owns three water supply systems: two for firefighting only, and one for both firefighting and municipal water supply (MWSS). The firefighting systems are the below ground Auxiliary Water Supply System (AWSS) and the truck-borne Portable Water Supply System (PWSS). The high pressure AWSS was built following the 1906 earthquake to protect against massive fires such as occurred then. The PWSS was not of concern for the present study. The City operates a combined sewage collection system for sewage and stormwater runoff.
Complete inventories of the water and sewer systems are being made, to include pipe types, lengths, and locations, valve and hydrant types and locations, condition of the components, etc., as a part of the liquefaction studies.

Damage in the 1989 Loma Prieta earthquake. The AWSS was not damaged structurally in the Marina District by the Loma Prieta earthquake. Unfortunately, however, damage to other parts of the system resulted in complete loss of water pressure, so the AWSS was not available for fighting the fires in the Marina District, which was the only area that experienced major fires following the EQ. On the other hand, there were about 120 main and service line breaks in the Marina District MWSS, of which about 80 were breaks in the mains. The differences in behavior between the AWSS and MWSS resulted from differences in length of lines, flexibility of pipes and joints, strength, and specific locations.

Extensive damage was suffered by the sewer lines in the Marina District. Most was incurred by old vitrified clay pipe, with some also to brick sewers. Damage was extensive at connections between buried sewers and those on pile supports. The locations of major water pipe and sewer line breaks are shown in Fig. 9.

Estimated damage in future earthquakes. Pipeline damage mechanisms and failure modes were analyzed and state-of-the-art loss estimation techniques were utilized by the study team to assess probable behavior in future earthquakes (Harding Lawson Associates et al., 1991). It was estimated that for an 8.3 earthquake on the San Andreas fault there will be 11 AWSS main breaks and 82 MWSS main breaks within the Marina District. These breaks would put the systems out of service temporarily, and require expenditures of about $1 million for the AWSS and $7 million for the MWSS, exclusive of the costs to restore service lines. Neither the AWSS nor the MWSS would have pressure for firefighting immediately after the earthquake, and drinking water would have to be imported until the MWSS system was restored.

It was estimated that almost 40 percent of the sewer pipes would be broken, with about 70 percent of this amount occurring in old style vitrified clay pipes with rigid joints. The large box sewer beneath Marina Boulevard would probably experience some cracking. The estimated repair cost for the sewer system in the Marina District is $5.3 million.

9.3 Mitigation Options

Options of four types for mitigation of future earthquake damage and the improvement of water and sewer system reliability were proposed by the liquefaction study team (Harding Lawson Associates et al., 1991):

1. **Geotechnical**, in which the soils are improved.
2. **Structural**, in which pipes and joints are strengthened, special connections are used, etc.
3. **Systemic**, in which system layout is changed to enhance redundancy, avoid poor soil areas, etc.
4. **Operational**, consisting of emergency procedures for operation of water systems and rapid and efficient system repair.

Each of these was analyzed in terms of costs and benefits, and specific series of actions and improvements were recommended to the City. Life safety (fire protection) is given the highest priority, followed by public health (potable water and sewage disposal).

Ground improvement. To improve all potentially liquefiable soils in the Marina District would be economically infeasible because of the high cost of ground improvement, and impractical because of the extensive existing urban development. However, the selective use of ground improvement within strategic areas and the stabilization of "utility corridors" could reduce substantially the risks of utility system failures.

Compaction grouting, stone columns, deep soil mixing, and jet grouting were identified as potentially the most useful methods; however, the effects on the utilities of their implementation would require careful evaluation. Preliminary cost estimates to treat an area 12 m wide, 300 m long, and 9 m deep, exclusive of pavement and utility replacement or relocation, engineering, etc., are $500,000 to $800,000 for stone columns, $1.2 to $2.8 million for compaction grouting, $2.5 million for deep soil mixing, and over $4.5 million for jet grouting.

Stabilization of the ground adjacent to Fair's Seawall, the existing concrete wall along the western section of Marina Boulevard and in the St. Francis Yacht Club spit (Fig. 3) could be done using stone columns, deep soil mixing, and deep dynamic compaction (away from structures). Dynamic compaction of the Marina Green adjacent to Fair's Seawall is estimated to cost $300,000, compared to $1.8 million for stone columns. Installation of additional piles to resist uplift and prevent overturning of the Marina Boulevard seawall is estimated to cost $50,000, exclusive of necessary excavation.

Water supply systems and sewers. Three phases of risk management are noted: pre-emergency measures, emergency operational plans, and post-earthquake recovery plans. Specific changes and improvements in the AWSS are proposed, as well as increasing the size of the Portable Water Supply System, and designation of a San Francisco Fire Department water supply officer for earthquake response. The cost estimate for these improvements is $5.5 million. Additionally, it was recommended that the City consider hardening corridors for the AWSS mains at fireboat manifolds using new pipes on piles (estimated cost $5 million). Given the absolutely critical importance of the water supply systems for fire prevention and the fact that the AWSS water was lost in the Loma Prieta earthquake due to lateral failure of a pile supported pipe south of Market Street, it will be essential that new hardened corridors and pile supported pipes be designed to withstand lateral movements. Proposed improvements to the MWSS include new feeder main routings, installation of flexible joints where mains cross pile-supported sewers, establishment of mutual aid agreements with other fire districts, and other actions, at a total estimated cost of about $8 million.

Finally, the study team recommends that mitigation measures for sewers should include training repair crews in emergency earthquake response, maintaining access to high capacity sewage pumps, maintenance of an inventory of equipment and construction materials, use of seismic resistant materials and construction for all new installations, and replacement of structurally weak sewers in areas subject to liquefaction.

10. DISCUSSION

The foregoing review of the impacts of the Loma Prieta earthquake on the Marina District of San Francisco has illustrated how geotechnical issues can be central to the identification, evaluation, and mitigation of seismic risk. It also illustrates our abilities to identify and solve technical problems, but at the same time it points out broader issues wherein our special expertise can and should be used for the public good.

The current states of knowledge in soil mechanics, geotechnical earthquake engineering, ground improvement,

seismology, and geology, while in many ways still incomplete and imperfect, are sufficient to identify and evaluate ground related seismic risks and to design and evaluate means for their minimization. For example, the amplification of rock motions by soft ground, methods for analysis of ground response and assessment of liquefaction potential, and techniques for ground improvement were available prior to the Loma Prieta earthquake. Among the major lessons from the event from a geotechnical standpoint are that in general the analysis and predictive methods give reasonable results and that ground improvement procedures do mitigate ground failure risk.

However, this apparent "success" is no cause for complacency, because there is continued need to do things better and more efficiently, especially when geological and soil conditions are incompletely known. Improvement in our ability to estimate more accurately the settlements and lateral spreading that will accompany liquefaction is needed, as well as to decide what type and how much ground improvement will be sufficient to mitigate the risks.

Nonetheless, solving technical problems such as these is likely to be the easier of the challenges that we face. As noted in the introduction to this paper, geotechnical engineering has changed greatly over the past 20 years in response to a changing set of world priorities and economies, and there is a much greater public involvement in the acceptance and approval of projects of all types. The greater challenge is to utilize our special technical abilities and insights in such a way that they help in reaching the right political decisions and in establishing the best priorities in the face of many conflicting interests and demands.

Geotechnical experts are uniquely qualified to evaluate and advise on issues such as the following:

1. Seismic zonation and the suitability of different sites for different purposes.

2. Siting of specific projects so as to minimize the risks of ground failure and adverse environmental impacts.

3. Keeping government agencies and the public informed about geotechnical risks that affect them and providing guidance in actions that can be taken to mitigate them and the establishment of priorities for their implementation.

4. Helping both the government and the public reach consensus on who should assume responsibility for risk identification, identification, and mitigation. This has been a particularly difficult issue in the wake of the Loma Prieta earthquake because of the many interests that are involved, including a large number of different municipalities, different state and local government agencies that are responsible for different parts of the area-wide transportation systems, separately and privately owned utilities, and land and structures that are both publicly and privately owned. In almost all cases each of these groups has responded independently in the two years since the earthquake, looking almost exclusively towards its own responsibilities and interests. This approach works against cooperative actions that could achieve greater protection at less cost.

5. Providing assistance in the development of emergency response plans.

6. Helping to insure that the public and policy makers have correct perceptions and understanding of geotechnical issues. As a simple example, the fact that liquefaction and lateral spreading were extensive in filled areas has resulted in the public perception that fills are inherently poor foundation materials. We all know, of course that with proper soil selection, placement and densification fills can be among the best foundation materials, and this type of knowledge must be made available to the public.

11. CONCLUSION

The Marina District of San Francisco, which was heavily damaged in the October 17, 1989 Loma Prieta earthquake in northern California, has been used as a case study for the identification, evaluation, and mitigation of geotechnical risk. What happened there is readily explained in terms of the deep soft soil profiles and the types and conditions of structures. Even greater damage is likely in a large future earthquake which is predicted with a high degree of probability to occur within the next 30 years. The studies that have been made to evaluate the risk and to define strategies and methods for its mitigation have been described. Carefully designed and coordinated site specific programs of ground improvement to prevent liquefaction and lateral spreading in critical areas, seismic retrofitting of deficient structures, upgrading of utility systems, and the development of emergency response plans are required to insure life safety, the prevention of catastrophic fires, and large property damage losses.

Geotechnical risks are ubiquitous. Their identification, evaluation, and mitigation are among the most important and challenging activities in modern geotechnical engineering. Not only are the technical problems difficult, but also dealing effectively with geotechnical risk requires extensive interaction with the public and with the government and participation in the political process, activities that have been foreign to many of us in the past. Nonetheless, public safety requires that we extend ourselves into these new areas and that we become as effective in helping to solve socio-economic-political problems that can benefit from our special technical knowledge as we are in solving purely technical problems.

12. ACKNOWLEDGEMENTS

I thank Professor Raymond B. Seed for review of the paper and his helpful comments and Liz Turner for her careful preparation of the manuscript.

13. REFERENCES

1. BAREPP (1990). "Putting the Pieces Together," Proceedings, Bay Area Regional Earthquake Preparedness Project, October 15-17, 1990, San Francisco.

2. Bennett, M. (1990). "Reconnaissance Report, Geotechnical Characteristics, Ground Effects, Leveling Survey, and Liquefaction Analysis," in U.S. Geological Survey Open File Report on the Effects of the Loma Prieta Earthquake in the Marina District of San Francisco.

3. Bonilla, M. G. (1990). "Natural and Artificial Deposits in the Marina District," in U. S. Geological Survey Open File Report on the Effects of the Loma Prieta Earthquake in the Marina District of San Francisco.

4. Borcherdt, R. D. (1991). "On the Observation, Characterization, and Predictive GIS Mapping of Strong Ground Shaking for Seismic Zonation," Keynote Lecture for Pacific Conference on Earthquake Engineering, Auckland, New Zealand, Nov. 20-23, 1991.

5. Harding Lawson Associates, Dames & Moore, Kennedy/Jenks/Chilton, and EQE Engineering (1991). "Final Report: Liquefaction Study - Marina District and Sullivan Marsh Area, San Francisco, California," Report prepared for the City and County of San Francisco, Department of Public Works, August 21, 1991.

6. Holmes, W. T., Lizundia, B., Brinkman, S., Conrad, J., Reitherman, I., Dong, W., Burton, J. and Bailey, A. (1990). "Preliminary Report on Damaged Unreinforced Buildings," The Loma Preita Earthquake Report, Rutherford and Chekene, San Francisco, California.

7. Idriss, I. M. (1990). "Response of Soft Soil Sites During Earthquakes," Proc. H. Bolton Seed Memorial Symposium, Vol. 2, BiTech Publishers Ltd., Vancouver, B. C., pp. 273-289.

8. Makdisi, F. I. and Seed, H.B. (1978). "Simplified Procedure for Estimating Dam and Embankment Earthquake-Induced Deformations," Journal of the Geotechnical Engineering Division, A.S.C.E., Vol. 104, No. GT7, pp. 849-867.

9. Mitchell, J. K., Masood, T., Kayen, R. E., and Seed, R. B. (1990). "Soil Conditions and Earthquake Hazard Mitigation in the Marina District of San Francisco," University of California, Berkeley, Earthquake Engineering Research Center, Report No. UCB/EERC-90/08, 59 pp.

10. Mitchell, J. K. and Wentz, F. J., Jr. (1991). "Performance of Improved Ground During the Loma Prieta Earthquake," University of California, Berkeley, Earthquake Engineering Research Center, Report No. UCB/EERC-91/12.

11. Newmark, N. M. (1965). "Effects of Earthquakes on Dams and Embankments," Geotechnique, Vol. 15, No. 2, pp.139-160.

12. O'Rourke, T. D., Stewart, H. E., Blackburn, F.T., and Dickerman, T. S. (1990). "Geotechnical and Lifeline Aspects of the October 17, 1989 Loma Prieta Earthquake in San Francisco," Technical Report NCEER-90-001, National Center for Earthquake Engineering Research, State University of New York at Buffalo.

13. Seed, R. B., Dickenson, S. E., Reimer, M. F., Bray, J. D., Sitar, N., Mitchell, J. K., Idriss, I. M., Kayen, R. E., Kropp, A., Harder, L. F., Jr., and Power, M. S. (1990). "Preliminary Report on the Principal Geotechnical Aspects of the October 17, 1989 Loma Prieta Earthquake," University of California, Berkeley, Earthquake Engineering Research Center, Report No. UCB/EERC-90/05.

14. Seed, H. B. and Sun, J.I. (1989). "Implications of Effects in the Mexico City Earthquake of September 19, 1985 for Earthquake Resistant Design Criteria in the San Francisco Bay Area of California," EERC Report No. 89/03, University of California, Berkeley.

15. Seed, H. B., Tokimatsu, K., Harder, L. F., and Chung, R. M. (1985). "Influence of SPT Procedures in Soil Liquefaction Resistance Evaluations," Journal of Geotechnical Engineering, A.S.C.E., Vol. 111, No. 12, pp. 1425-1445.

16. Seed, R. B. and Harder, L. F. (1990). "SPT-Based Analysis of Cyclic Pore Pressure Generation and Undrained Residual Strength," Proc. H. Bolton Seed Memorial Symposium, Vol. 2, pp. 351-376.

17. Tokimatsu, K. and Seed, H. B. (1987). "Evaluation of Settlements in Sands due to Earthquake Shaking," Journal of Geotechnical Engineering, A.S.C.E., Vol. 113, No. 8, pp. 861-878.

18. Towhata, I., Tokida, K., Tamari, Y., Matsumoto, H., and Yamada, K. (1990). "Prediction of Permanent Lateral Displacement of Liquefied Ground by Means of Variational Principle, "Proc. Third Japan-U.S. Workshop on Earthquake Resistant Design of Lifeline Facilities and Countermeasures for Soil Liquefaction, San Francisco, December.

19. U. S. Geological Survey (1989). "The Loma Prieta Earthquake of October 17, 1989," Pamphlet by P. L. Ward and R. A. Page, U. S. Government Printing Office.

20. U. S. Geological Survey (1990). "Effects of the Loma Prieta Earthquake on the Marina District of San Francisco, California," Open-File Report 90-253.

John Jaeger Memorial Address

Modelling Interactive Load-Deformation and Flow Processes in Soils, including Unsaturated and Swelling Soils

B.G. RICHARDS
B.E. (Hons), M.Sc,D.Eng., F.I.E.Aust.
CSIRO Division of soils

SUMMARY This paper presents a general conceptual model for the practical simulation of a number of interactive physical processes in a wide range of soils. This model has been developed over more than 25 years as a finite element computer program incorporating the theoretical and practical experience gained by the author during this period. The processes simulated are load - deformation - failure and the simultaneous flow of water, solutes and heat. While a wide range of soils and soil conditions have been analysed successfully, the modelling procedures were originally developed to handle the particular problems of unsaturated and swelling soils, which are of great significance in Australia and which because of their nature need to be analysed as non-linear and hysteretic materials. The procedures presented are designed so that they can be related to currently available experimental measurements, rather than to idealized theories developed for materials other than soils. As such, this model has been applied successfully to a wide range of practical problems, involving a variety of soil types. A brief description of the procedures used in the model, comparisons with previous theoretical and experimental data, and some practical applications are given in this paper.

1. INTRODUCTION

The problems of unsaturated and swelling soils have attracted much attention over the years since the 1940's. Much of the published work in these fields has been highly empirical with the most common moisture variables being gravimetric water content and degree of saturation, and with soil mechanics properties being related to these variables. This empirical approach can work for a given soil in a given area, but generally the results and even trends cannot be extrapolated to other soils or even to the same soils in other areas.

The early work at the Road Research Laboratories in England in the 1940's and 50's, Imperial College in England, the Road and Building Research Laboratories and the University of Witwatersrand in South Africa and the Soil Mechanics Section, CSIRO in Australia during the 1950's and 60's clearly showed that the only useful moisture variable for describing the state and the properties of unsaturated soils was negative pore water pressure or soil water suction. The soil water potential, which is composed of the soil water suction and gravitational components also defines the water flow processes in unsaturated soils (Richards, 1931). A summary of the state of knowledge as understood by the author in 1966 was given in Richards (1967). A more recent discussion of the definition, measurement and application of soil water suction and its various components was presented by the author in Richards and Peter (1987).

The early attempts at developing theoretical models for unsaturated soils were based on the effective stress theory originally introduced for saturated soils (Terzaghi, 1923). This work on unsaturated soils carried out in England, South Africa and Australia was summarized in the conference on "Pore Pressure and Suction in Soils", London, 1961, eg. Skempton (1961), Croney and Coleman (1961), Jennings (1961) and Aitchison (1961). While applicable to saturated and near saturated soils, the idealized concept of a unique and single valued effective stress parameter, χ, was too restrictive for convenient practical use with unsaturated soils. For example, it is non-linear and hysteretic and both stress path and moisture path dependent.

One practical development from this early effective stress approach was to separate stress and soil water suction from the effective stress equation and treat them as independent variables, eg. Richards (1967), Aitchison and Richards (1969), Fredlund (1979), Fredlund and Morgenstern (1977). This approach appears to be the only useful approach at this time.

Another approach has been the extension of the critical state theory developed for saturated soils (Rosco & Wroth 1958; Wroth 1973) to unsaturated soils (Escario and Saez 1986; Toll 1990 and Wheeler 1991). Again it has been necessary for practical usage to treat stress and soil water suction as independent variables (Wheeler 1991). At this time, the same problems that were associated with the effective stress theory have arisen, namely the complexity of the functions adequately defining the critical state variables. It will be interesting to see future developments in this area.

The approach used in this paper could be called an experimentally based stress and moisture path method, which is designed to incorporate experimental data more directly. It is the result of nearly 40 years of development by several workers in CSIRO, Australia, beginning with Aitchison and Donald (1956) and continuing to the present paper. It has been kept as simple and as flexible as experimental procedures and our current knowledge permit, but at the same time it can incorporate the latest theories, such as the critical state theory for saturated soils, where conditions warrant their use. While it has been been successfully used in design procedures, its main use has been as a research tool to test ideas and to back-analyse complex laboratory and field experiments. It has been particularly useful where other current analytical methods have proven inadequate, such as with unsaturated and swelling soils.

2. CONCEPTUAL MODEL

The conceptual model is shown schematically in figure 1. The physical processes have been considered as two initially independent processes. These two basic processes are the undrained load - deformation - failure process and the fluid and heat flow processes. The latter can be water, solute or

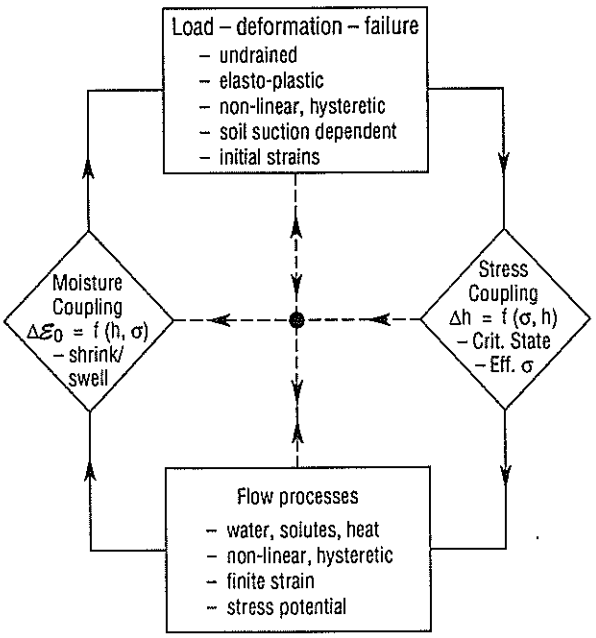

Figure 1. The conceptual model for analysing soil.

heat flow or the simultaneous interactive combination of two or all of them as shown in figure 2.

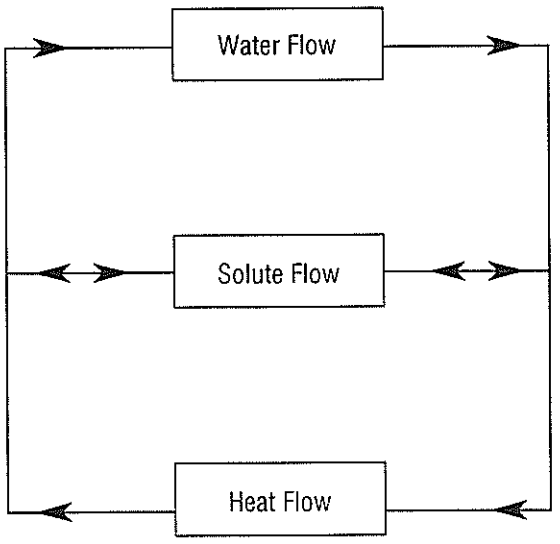

Figure 2. The interactive flow processes.

The interaction between the two basic processes is achieved by the coupling processes or mechanisms as shown in figure 1. These coupling processes are most important in modelling the interaction between water flow and deformation/failure as, for example, in swelling soils, landslides on slopes during rainstorms and in consolidation of high water content soils and mine slurries. One coupling process models the pore water pressure or soil water suction change as a result of the stress or strain change and the other, the change of strain (often called volume change) or stress as a result of a change of pore water pressure or soil water suction.

With this conceptual framework it is possible to model almost any practical problem in soils and soft rocks, using established theories or, where they are not applicable, experimentally based material responses. Each process can be experimentally simulated in laboratory or field tests. This can be done quickly and cheaply by simple tests carried out at the predicted field conditions of stress, moisture, density, etc. Alternately, complex non-linear and hysteretic relationships between model parameters and the relevant soil variables can be developed.

Furthermore it is not necessary to use the whole model framework. Simple quick settlement predictions of a surface load on sand for example requires only the use of the load - deformation - failure process with or without the failure component included and then perhaps implemented as a linear elastic problem. The prediction of seepage from an earth dam or a mine retention pond may only require a simple linear water flow process. On the other hand, an analysis of a concrete slab on or a retaining wall holding back swelling soils would necessitate the use of all processes in the model.

The model can follow time, stress, strain or displacement paths using an iterative - incremental procedure. For each incremental step in non-linear and hysteretic analyses, each process can be repeated iteratively until a selected convergence is achieved before proceeding to the next process. Each path through the model can then also be repeated iteratively until convergence is reached before proceeding to the next increment. This might be thought to require long times on large computers, but the author is currently running large two - dimensional and small three - dimensional problems with up to 10,000 elements on a portable 80386 laptop computer, with 8Mb RAM, a 40Mb hard disk drive and a UNIX operating system.

The art in the use of this model is in the geotechnical engineer being able to assess what processes and material response theories are most applicable to a particular problem and then to plan paths through the model framework to achieve the desired result.

3. A BRIEF DESCRIPTION OF THE PROCESSES

3.1 Load - Deformation - Failure

This process describes the load - deformation - failure response of the soil as a result of a change of stress, load, strain and/or displacement, with all other factors held constant. It includes;

(1) non-linear elastic behaviour of the material as a function of stress, soil water suction and stress history (Richards 1978);

(2) changes of initial stress or strain as a result of swelling or shrinking caused by changes of soil water suction, solute content or temperature (Richards 1984);

(3) stress - strain path dependency or hysteretic behaviour in the load - deformation response of the soil (Richards 1979); and

(4) shear and tensile failure with dilantancy or compression, and with strain softening.

The load - deformation response uses standard incremental elasticity equations, for which the finite element formulations are now well established, eg. Zienkiewicz (1977),

$$(\Delta F)_e = [K](\Delta\delta)_e - [D](\Delta\varepsilon_0)_e \qquad (1)$$

where Δ = the incremental value

F = the nodal forces

δ = the nodal displacements

ε_0 = the initial strains due to moisture or thermal induced strains

[K] = elastic stiffness matrix

[D] = elastic stress matrix

The left hand term for the nodal forces also includes those contributions due to gravitational and other body forces, and boundary conditions. Equation (1) for each element is then used to assemble the global equations for the field problem, which can be solved for $(\Delta\delta)_e$ for each incremental step, either in time, load or displacement from the specified initial values.

The material parameters used in the stiffness matrix [K] and the stress matrix [D] are the normal elastic parameters of bulk modulus, K, and shear modulus, G. These parameters are often highly non-linear for soils and this non-linearity, including irreversible hysteretic behaviour, has been successfully modelled (eg. Richards 1975, 1977,1978, 1980a, 1980b, 1982, 1884 & 1986) using modified 'hyperbolic' formulae (Nelson 1970). The basic relationships for simple stress dependent modulii are

$$K = k_1 \sigma_m^n + k_2 h^m + k_o \qquad (2)$$

$$G = (g_1 \sigma_m^p + g_2 h^r).(1 - [\tau/\tau_f]^q) + g_o \qquad (3)$$

where K = bulk modulus

G = shear modulus

σ_m = previous maximum of the mean stress $(\sigma_1 + \sigma_2 + \sigma_3)/3.0$

h = soil water suction

τ = shear stress

τ_f = yield stress according to the yield criteria adopted eg. Mohr Coulomb given by

$$(\sigma_1-\sigma_3) = 2C \cos\phi + (\sigma_1+\sigma_3) \sin\phi + h \sin\phi_h \qquad (4)$$

σ_1 = maximum principal stress

σ_3 = minimum principal stress

C = cohesion

ϕ = angle of friction for stress

ϕ_h = angle of friction for soil water suction

$k_1,k_2,k_o,g_1,g_2,g_o,n,m,p,r,q$ are empirical material constants.

The above equations are suggested as a guide, but can be altered should experimental data require it. These three equations are programmed into the computer program via the [K] and [D] matrices of equation (1).

Equations (2) - (4), when used in incremental elasticity equations, eg. equation (1), can only model load - deformation behaviour up to yield accurately, although they can model post yield behaviour approximately for soils exhibiting strain hardening. Conventional plasticity theories can be used for post yield behaviour, but with unsaturated soils, often undergoing compression during shearing, they sometimes prove to be unstable or inaccurate in the author's experience. In these cases better results have been obtained (Richards 1980a) by a method which converts the elastic continuum elements to joint or shear elements when yield occurs. These shear elements are based on the joint or interfacial elements proposed by Ghaboussi *et al* (1973).

When yield occurs, the shear stress, t in the element exceeds the yield stress, τ_f, and will continur to exceed it in the case of strain softening. This excess shear stress cannot be resisted by the element and must be redistributed to neighboring elements (Lo and Lee 1973) and this has been achieved by the 'initial stress' method (Zienkiewicz 1977). The direction of the stress redistribution varies from that calculated from the Mohr-Coulomb equations for the associated flow rule ($\phi = \psi$) to the direction of maximum shear strain for the non-associated flow rule with ($\psi = 0$), where y is the angle of dilatancy. The excess stresses to be redistributed in the x-y co-ordinate system are given by

$$\{\Delta\sigma_0\} = \begin{vmatrix} \Delta\sigma_x \\ \Delta\sigma_y \\ \Delta\sigma_z \\ \Delta\tau_{xy} \end{vmatrix} = \begin{vmatrix} -\Delta\tau_\alpha \text{ SIN } 2\alpha \\ \Delta\tau_\alpha \text{ SIN } 2\alpha \\ -\Delta\tau_\alpha \text{ SIN } 2\alpha \\ \Delta\tau_\alpha \text{ COS } 2\alpha \end{vmatrix} \qquad (5)$$

where $\{\Delta\sigma_0\}$ = initial stresses

$\Delta\tau_\alpha$ = excess shear stress $= \tau_\alpha - \tau_{\alpha r}$

τ_α = actual shear stress

$\tau_{\alpha r}$ = residual yield stress

α = angle of yield direction to the horizontal axis.

The finite element formulation for yielded elements can then be written as

$$(F)_e = [K] (\delta)_e + [B] (\delta_o)_e \qquad (6)$$

where [K] = stiffness matrix for shear elements

[B] = strain matrix.

Tensile failure is also included by the redistribution of any tensile stresses exceeding the tensile strength of the material using the 'initial stress' method in the same manner as above (equation 5 & 6).

3.2 Coupling Process for a Change of Stress or Strain.

The soil water potential equation is given by

$$(\Phi)_e = [A].(\sigma)_e/(\gamma_w g) - h + z \qquad (7)$$

where Φ = soil water potential

[A] = pore water coefficient matrix, eg. composedof the coefficients A & B (Skempton (1954)

$\{\sigma\}_e$ = stresses in the element of soil

h = soil water suction = -u

u = pore water pressure

z = height above datum

γ_w = density of water

g = gravitational constant.

While the matrix suction, h_m is generally used for h in equation (7) above and in water flow equations discussed later, it has been found (Richards 1980c) that the total soil suction, h_t, which includes the solute suction, h_s, should be used when modelling swelling soils.

It can also be seen that changes in the soil stresses, $\{\sigma\}_e$ as well as changes in the soil water suction, h, and the height, z, resulting from swelling or shrinkage will all cause changes in soil water potential. This effect of stress on soil water potential is sometimes refered to as the stress potential (Croney and Coleman 1961) or the stress component of field measurements of soil water suction (Richards 1986). The soil water suction, h given in equation (7) was first mentioned in Croney and Coleman (1961) and was defined as the 'unloaded soil suction' (Richards 1986), as it is the soil water suction measured on a sample sitting unloaded on the workbench and is the suction resulting solely from the water in the soil. It is the soil water suction which must be used in all equations defining the material properties of the soil. In a salt free soil, it is also what has been defined as the matrix suction.

The load - deformation analysis gives data for the two factors $\{\sigma\}_e$ and z in equation (7) and so enables the changes in soil water potential to be calculated for inclusion in subsequent water flow analyses. The displacements can also be used to calculate the new geometry and material velocities required for the analysis of water flow in soils undergoing finite strain as described later.

3.3 Flow Processes

3.3.1 Water Flow

The original water flow equation (Richards 1973a) was based on the water flow equation for non-swelling soils (Terzaghi 1923; Richards 1931). Subsequently Richards (1974a & 1984) modified the one-dimensional equations of Philip & Smiles (1969) to incorporate the water 'convected' with the solid phase due to three-dimensional strain in swelling soils. This 'finite strain' theory is important for the modelling of water flow in swelling soils and mine slurries with high water contents, but it can be ignored for simpler analyses of non-swelling soils or consolidated soils.

The theory of Philip & Smiles (1969) describing one-dimensional flow of water in a swelling system can be used to develope the basic flow equation,

$$[\frac{\partial \nu}{\partial t_m}] = \frac{\partial}{\partial_m} [K_m(\nu) \frac{\partial \Phi}{\partial_m}]_t \qquad (8)$$

where ν = moisture ratio of the soil θ

$= \theta_w/\theta_s$

θ_w = volumetric water content

θ_s = volumetric solid content

t = time

$K_m(\nu)$ = hydraulic conductivity or permeability of the soil in m-space

m = material co-ordinate

$= X_o \theta_s \, dx$

Φ = soil water potential (total or matrix potential depending on application - see Richards (1986).

This equation is obtained by combining the continuity equations for the liquid and solid components of the system (assuming total stresses remain constant). It recognises (Gersevanor 1937) that Darcy's Law describes the flow of water relative to the solid particles, so that the 'total' flux of water relative to an external observer is the sum of Darcy's flow plus a component 'convected' with the solid framework. As such it describes one-dimensional water flow in a swelling medium with one-dimensional strain assumed equal to the change in volumetric water content. While it applies to the vertical infiltration into and/or drying of a saturated swelling porous medium, it cannot be applied readily to unsaturated soils or where three-dimensional behaviour in both strain and water flow is significant. However, it does have the advantage of being theoretically correct and being capable of solution by analytical procedures. These solutions are valuable in providing accurate checks on numerical solutions, such as those described in this paper.

In order to extend the equation (8) above to three-dimensional flow problems, a knowledge of the three-dimensional displacements arising while the flow process is occurring is required. These displacements will result from water flow under the potential gradients, modified by stress and strain changes resulting from external boundary conditions. Because it is most convenient to express the displacement in terms of physical space, it is also convenient to express the general three-dimensional form of equation (8) in terms of physical space, ie. x, y & z, viz.

$$[\frac{\partial \theta_w}{\partial_t}]_{x,y,z} = [\nabla(K(h).\nabla\Phi)]_t - [\nabla(\frac{\theta_w}{\theta_s} Fs)]_t \qquad (9)$$

where K(h) = permeabilty of the soil according to Darcy's Law

h = soil water suction

F_s = 3-D flux of the solid phase

∇ = mathematical operator $(\partial/\partial x, \partial/\partial y, \partial/\partial z)$

The second term on the right side of equation (9) represents the movement of water 'convected' with the solid phase. The term on the left hand side is the rate of change of θ_w with time in physical space. The complete water flow equation in terms of soil water potential and suction can be written assuming that stress plays no role at this stage. The role of stress is considered in the other processes within the total model. This equation can be written as

$$\left[\frac{\partial \Phi}{\partial t}\right]_{x,y,z} = \frac{dh}{d\theta}\left[\nabla(K(h).\nabla\Phi) - \nabla\left(\frac{\theta_w}{\theta_s} Fs\right)\right]_t \qquad (10)$$

The form of equation (10) has the advantage that the solid flux vector, F_s, which depends on the three-dimensional deformation behaviour of the soil, can be calculated in flow analyses coupled with the load - deformation analyses from the rate of displacement of the soil with time. In analyses not coupled with the load - deformation behaviour, F_s can be calculated from $d\theta_w/dh$ and equation (10) reverts to the equation of Philip & Smiles (1969) for one-dimensional flow.

Using finite elements in space with the finite element formulation (Zienkiewicz 1977) for variation with time, the Crank-Nicholson formula and the Galerkin weighting scheme, equation (10) can be written as

$$\{\Phi_t - \Phi_{to}\}_e = \Delta t\,[P]\,\{[H]\,(0.33\{\Phi_{to}\}_e + 0.67\{\Phi_{t1}\}_e - [B]\,\{\theta_w.F_s/\theta_s\}_e)\} \qquad (11)$$

where the subscript e refers to the nodal values of each element, the subscripts to and t1 refer to the initial and final times for each increment,

Δt = time step for increment

$[P]$ = distribution matrix for $dh/d\theta w$ over the element

$[H]$ = the permeability matrix for the element

$[B]$ = the gradient matrix for the element (ie. a function of $\delta/\delta x$, $\delta/\delta y$, $\delta/\delta z$)

$\{\Phi\}_e$ = vector of nodal values of Φ for the element.

When the various boundary condition terms for known boundary flows or soil water potentials are included in the right hand side of equation (11) and each finite element equation is assembled for the global field problem, equation (4) can be solved for Φ_t for each time step, starting from the known initial values of Φ_{to}. The time steps are usually chosen by experience and a knowledge of the flow parameters, but must always be checked for stability by carrying out a number of runs at different time steps.

3.3.2 Solute Diffusion

In many analyses of the distribution and movement of soil water, the solutes contained in the soil water also need to be considered, as in the seepage from waste deposits. Also, the properties of dispersive and swelling clay soils are significantly affected by the solute concentration in the soil water (Richards 1980b). Two diffusion processes have been used in this program. The first was described by Mitchell, Greenberg and Witherspoon (1973). They developed a theory which describes both chemico-osmotic flow and the soil water diffusion processes, and considered three types of coupling between the flow of salt and water.

(1) chemico-osmotic coupling i.e. the flow of soil water induced by salt concentration gradients;

(2) drag-coupling i.e. the flow of salt induced by soil water potential gradients; and

(3) porosity coupling i.e. the flow of salt induced by soil porosity changes.

This theory results in one equation for the diffusion of water and another for the diffusion of solute e.g. Na^+ as sodium chloride. If more than one solute or ion species is required, then more equations and the relevant flow and coupling parameters can be added.

$$\frac{\partial h}{\partial t} = \frac{dh}{d\theta_w}\nabla(\kappa_{ww}\nabla\Phi) + \frac{1+e}{a_v} k_{ws}\nabla^2 C_s \qquad (12)$$

$$-e\frac{\partial C_s}{\partial t} = \frac{1+e}{\rho_w} K_{sw}\nabla\left(\frac{C_s}{C_{sm}}\nabla h\right) - (1+e) D'_s \nabla^2 C_s - a_v C_s \frac{\partial h}{\partial t} \qquad (13)$$

where k_{ww} = soil water permeability of the soil under soil water potential gradients k_{ws} and k_{sw} chemico-osmotic coupling coefficients

$K_{sw} = k_{sw} + C_s k_{ww}$

$D'_s = D_{ss} + C_s k_{ws}$

D_{ss} = diffusion constant of solute.

e = void ratio of soil

a_v = coefficient of permeability

C_s = solute concentration of soil solution

ρ_w = density of soil solution

C_{sm} = maximum change in solute concentration

This theory has proved to be the most suitable for swelling soils. However for seepage studies with the simultaneous transport of solute and water, an alternate theory (eg. Bear and Verruijt 1987) is used. In this case the water dragged along by solute flow is ignored, but solute flow by advection (or convection), dispersion, diffusion, adsorption or ion exchange, chemical reactions and injection or removal is considered. In this case, the equation (13) above is replaced by

$$\frac{\partial qc}{\partial t} = -\nabla.(cq - \theta D.\nabla c - \theta D^*_d \nabla c) - f + \theta\,\rho T - Pc + Rc_R \qquad (14)$$

where q = volumetric water content

c = solute concentration of the soil water

q = water flux

D = coefficient of dispersion

D^*d = coefficient of molecular diffusion

f = flow of solute leaving water by adsorption

ρ = density of water

T = rate of mass of solute added by chemical reactions within the water per unit mass of water

P = rate of water removed per unit volume of soil

R = rate of water added per unit volume of soil

c_R = concentration of water added.

3.3.3 Thermal Diffusion

Thermal diffusion can also be included by using equations (12) & (13) with the solute diffusion parameters replaced by the corresponding thermal parameters. For simple thermal diffusion problems, the most convenient method is to replace the water flow parameters in the water flow equation with thermal parameters, eg. Carslaw & Jaeger (1959).

3.4 Soil Strains arising from Flow Processes

The flow processes produce new values of soil water potential and suction and water content, as well as solute concentration or temperature if required. These changes will result in potential volume change, i.e. 'initial strains' $\{\varepsilon_o\}$, at the existing stress state, which can be used in consequent load - deformation analyses (equation (1)) to obtain the actual strains. However, in this case it is a drained analysis and drained material parameters must be used in equation (1), not the undrained parameters used in the analyses for changes of load or displacement. One method of calculating $\{\varepsilon_o\}$ for swelling soils from the results of suction controlled consolidation tests is given by

$$\{\nabla\varepsilon_o\} = [Q]\{\log_{10}h\}_e \qquad (15)$$

where $[Q]$ = the volume change matrix which is a function of the soil stresses, h and the drained elastic parameters.

4. VALIDATION AND USES OF THE MODELLING TECHNIQUES

Because of the complexity of the processes and the programming involved in the computer programs used for this model, it cannot be assumed that numerical simulations will prove to be accurate in all situations. The more complex the modelling packages, the more likely they will have general applicability, but at the price of convenience and a higher probability of making serious mistakes. For these reasons, the computer programs have been thoroughly tested against a wide range of available analytical solutions and published experimental results to validate their correctness and assess their applicability. The following section describes some of these test procedures in order to give an indication of the wide range of applications for which these packages can be used.

4.1 Load - Deformation - Failure

4.1.1 Linear Elasticity

The simple linear elastic theory is still being widely used in practice for settlement analyses, because of the availability of accurate dimensionless solutions. Comparisons of typical published results have already been made (Richards 1974b). One such example is shown in Fig. 3a and 3b, giving the results of analyses of stress and surface displacements under a circular vertical load on an elastic half-space (Duncan *et al* 1968). The small differences can be accounted by the fact that the analytical solution considers a true half space, whereas the numerical procedure can only analyse a finite depth, in this case 30 times the loaded area.

4.1.2 Plasticity

For similar reasons, ideal rigid plasticity with Mohr-Coulomb yield criteria is widely used for failure or stability analyses in soils (Wroth 1973). Comparison using the yield model discussed previously with convential plasticity solutions were also made (Richards 1980a). An example with a flexible frictionless strip footing on a linear elasto-plastic soil is shown in Fig. 4. The analytical result (Zienkiewicz *et al* 1975) as

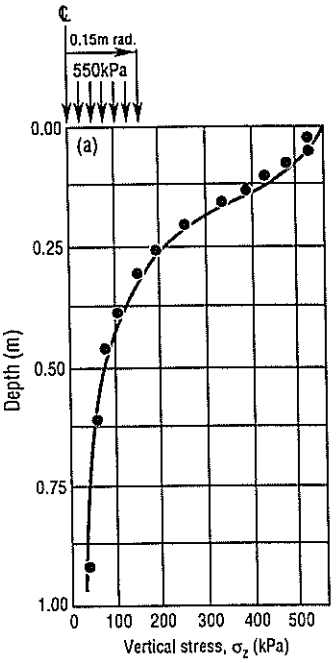

Figure 3a. Analysis of vertical stress under a circular vertical load.

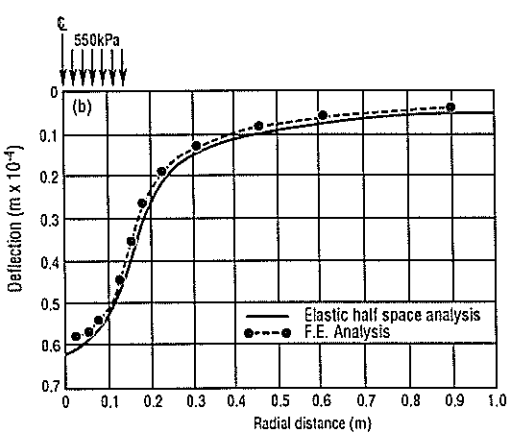

Figure 3b. Results of analysis of surface displacement under a circular vertical load.

reported could only give a collapse load of 1008 kPa, as shown in Fig. 4, whereas the modelling procedures in this paper can give the whole stress - displacement curve.

4.1.3 Non-linear Elasto-plasticity

Perhaps one of the most extensive tests possible was the analyses of laboratory tests carried out during the investigation of stability of spoil piles at the Goonyella coal in the Bowen Basin, Queensland. In this example, all materials were tested as 'intact' cores in undrained triaxial and direct shear tests at their field water content. As shown in Figs. 5 & 6, the basic test apparatus, including membranes, top and bottom caps, etc. was modelled as well as the soil. Also all contact surfaces between the soil and the apparatus were modelled using interfacial elements. The experimental results together with the final results of the modelling are shown in Fig. 7.

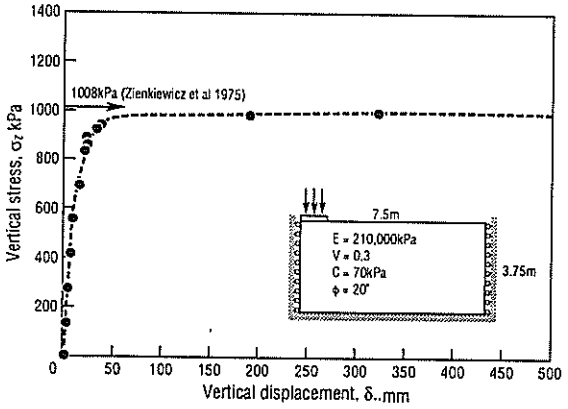

Figure 4. Load - settlement curve for flexible frictionless strip footing (E - elastic modulus, ν = Poisson's ratio, C = cohesion and Φ = friction angle).

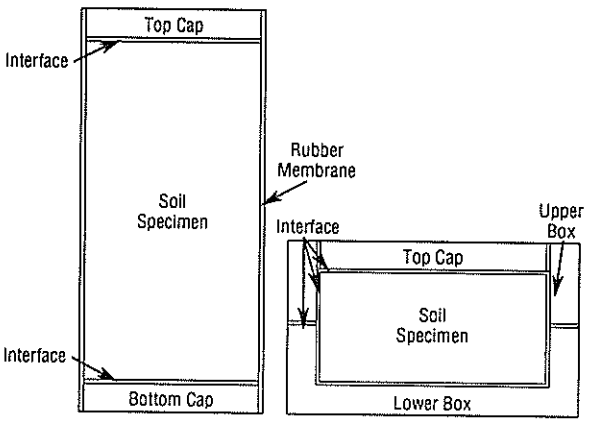

Figure 5. (left) Representation of triaxial test for finite element analysis.
Figure 6. (right) Representation of direct shear test for finite element apparatus.

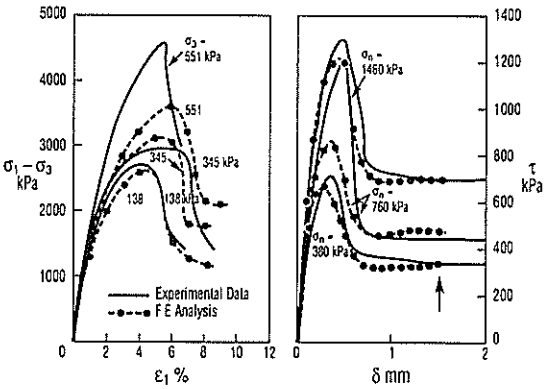

Figure 7. Results of finite element analysis of shear tests on the floor material, Goonyella mine, Qld.

The conventional analyses of these two tests gave two different sets of values for C, ϕ and ϕ_R for the same material as suggested by Davis (1968). Using the values of C, ϕ and ϕ_R calculated from the direct shear test and the non-linear elastic parameters from the triaxial test, and using trial and error fitting, the results in Fig. 7 were obtained. Using this technique, it is possible to model the friction at the soil boundaries, such as end and side friction on the test specimens, as well as the effects of membrane resistance and uneven loading. While these effects are considered sources of errors in conventional analyses of test results, using the method above, they can actually provide more test information for matching the modelling results. For example, the shape of the horizontal displacement of the sample in a triaxial test is one such piece of information.

4.2 Water Flow.

4.2.1 1-D Linear Consolidation

The most common example of water flow in geotechnical engineering is the simple linear one-dimensional consolidation of non-swelling soils (Terzaghi 1923) or the simple diffusion theory for saturated soils (Richards 1931). Fig. 8 shows the dimensionless results for the diffusion of water out of a cylindrical sample, initially at a soil suction of 0 kPa, with the lower bondary held at 100 kPa for times greater than 0 seconds. These results compare very well with the results obtained with conventional analyses.

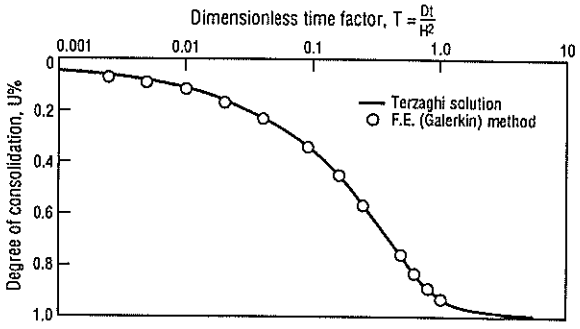

Figure 8. Comparison of results of finite element analysis with conventional linear one-dimensional flow or consolidation in non-swelling soils (D = diffusivity, t = time and H = drainage length).

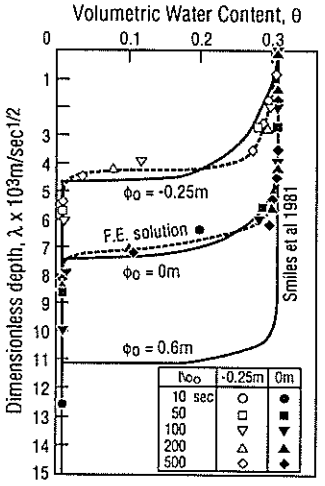

Figure 9. Comparison of the results of finite element analysis with non-linear infiltration of water into a column of Bungendore fine sand under constant surface potential (λ = dimensionless depth, Φ_0 = imposed surface potential, θ = water content, t = time).

4.2.2 Non-linear Infiltration

A more stringent test of water flow analyses is the vertical flow into a column of dry soil with highly non-linear flow properties with various boundary conditions. Smiles *et al* (1980) and Perroux *et al* (1981) have carried out experimental observations and theoretical analyses on various materials under both constant potential and constant flux boundary conditions. Their theoretical analyses were carried out using mathematical relations that approximated the flow properties, while permitting linearization of the mathematical equations, thereby allowing analytical solutions to be obtained. Fig. 9 shows the results of the analysis using the model described in this paper for Bungendore fine sand and a constant soil water potential boundary compared with the previously published data. The non-linear material data used in this analysis are shown in Figs. 10 & 11.

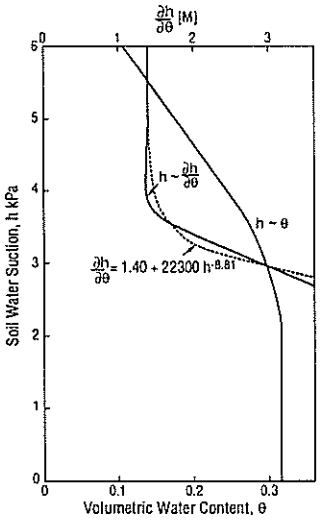

Figure 10. Volumetric water content – soil water suction relationship, θ(h) for Bungendore fine sand.

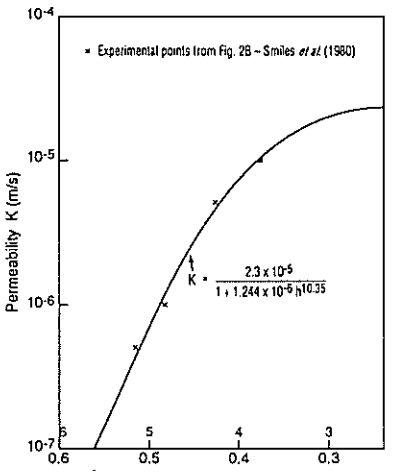

Figure 11. Permeability – soil water suction relationship, K(h) for Bungendore fine sand.

4.2.3 Hysteresis

Apart from non-linearity, irreversible and hysteretic effects in water flow are very important in unsaturated and swelling soils. As no suitable model was found to be available (Richards & Smettem 1991), a simple method was developed, based on the earlier work of Mualem (1974). This method

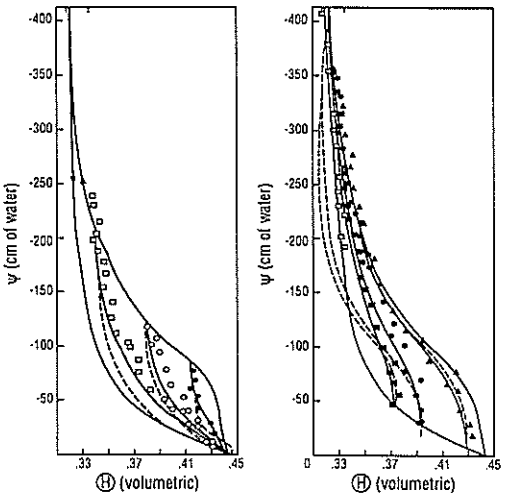

Figure 12. Scanning curves for Caribou silt loam (after Maulem, 1974).

uses the observed similitude of the shape of the family of internal scanning θ(h) curves with the primary wetting and drying curves. It assumes that all internal scanning curves lie within the primary θ(h) curves and that all internal curves have similar shape. An example of this is shown in Fig. 12 for Caribou silt loam (Mualem, 1974) for samples equilibrated on suction plate apparatus.

The application of this method requires only the mathematical definition of the measured primary wetting and drying curves. Possible internal scanning curves can then be predicted knowing the initial water content, θ and soil water suction, h and future variations in h. In general terms, the primary wetting and drying curves are expressed mathematically as

$$\theta_d(h) = f_d(h) \qquad (16a)$$

and

$$\theta_w(h) = w(h) \qquad (16b)$$

where $f_d(h)$ and $f_w(h)$ give the primary wetting and drying curves as functions of h.

Any internal scanning curve can then be expressed as

for drying

$$\theta_d(h) = \theta^*_d + \theta'_d \cdot [f_d(h^*_d - (h^*_d - h)/h'_d) - \theta^*_d] \qquad (17a)$$

for wetting

$$\theta_w(h) = \theta^*_c + \theta'_w \cdot [f_w(h^*_w + (h - h^*_w)/h'_w) - \theta^*_d] \qquad (17b)$$

where $f_d(h'_d)$ and $f_w(h'_w)$ have the same form as equation (16a) & (16b)

θ'_d = reduced volumetric water content for drying

$$= (\theta^*_c - \theta^*_d)/(\theta^*_w - \theta^*_d) \qquad (18a)$$

h'_d = reduced soil water suction for drying

$$= (h^*_d - h^*_c)/(h^*_d - h^*_w) \qquad (18b)$$

q'_w = reduced volumetric water content for wetting

$$= (\theta^*_w - \theta^*_c)/(\theta^*_w - \theta^*_d) \qquad (18c)$$

h'_w = reduced soil water suction for wetting

$$= (h^*_c - h^*_w)(h^*_d - h^*_w) \qquad (18d)$$

and the subscripts *c, *d, and *w refer to the value at c, when the direction was last reversed, and the convergence points d and w in Fig. 13 respectively.

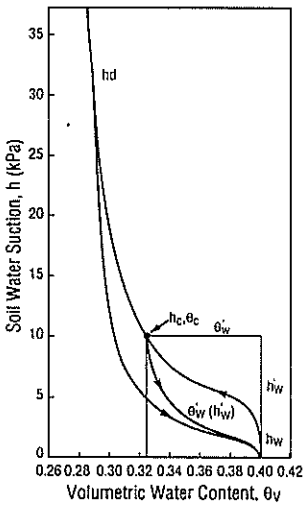

Figure 13. Graphical representation of hysteretic model.

While working along internal scanning curves, the reduced variables in equations (17) & (18) are used, but these equations also give the actual values of θ and h at all times.

This hysteretic model has been used on data for several different soils, giving in each case excellent agreement between theory and experimental data. Figure 14 shows the results for Caribou fine sand.

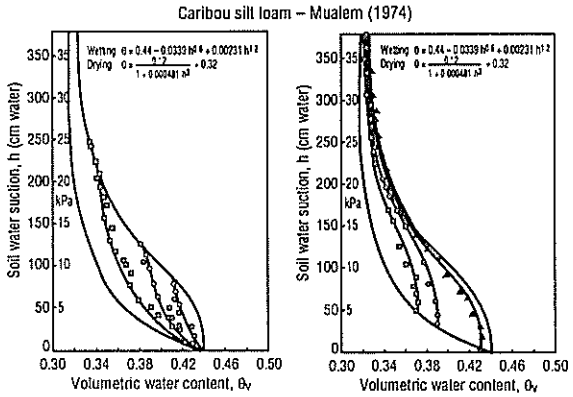

Figure 14. Results of modelling hysteretic behaviour of Caribou silt loam.

4.3 Coupled Solute and Water Flow

4.3.1 Coupled Solute Flow in Swelling Soils

Mitchell *et al* (1973) carried out an experimental program in which they prepared cylindrical disks of various clay minerals consolidated to various water contents, which were subsequently immersed in solute solutions. They showed that chemico-osmosis was very significant for the fine grained swelling clays. In the early stages, water flow is controlled by total suction gradients and only at later stages can the solutes redistribute by solute diffusion in the liquid phase. The result for a bentonite sample is shown in Fig. 15.

The theoretical results of Mitchell *et al* (1973) using equations (12) & (13) are shown in Fig. 16, together with the results from the modelling techniques used in this paper. The Y-axes of Figs. 15 & 16 are different because the experimental measurements were made in terms of total weight change and the theory was expressed in terms of pore pressure change.

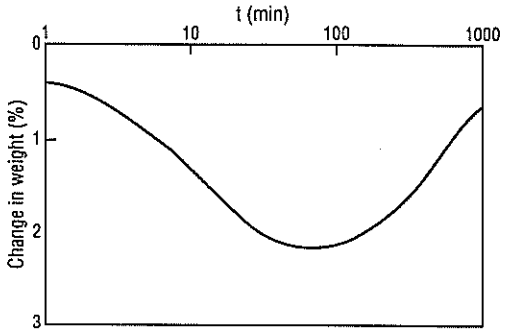

Figure 15. Weight change of bentonite sample due to chemico-osmotic consolidation (after Mitchell et al., 1973).

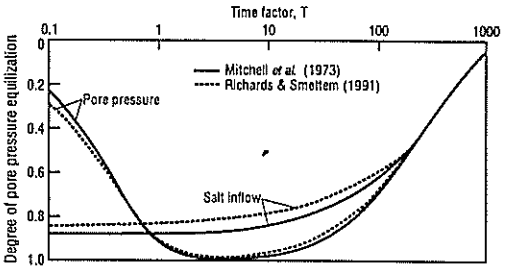

Figure 16. Theoretical prediction of salt inflow and pore pressure equalization during chemico-osmotic consolidation.

4.4 Coupled Water Flow and Load-Deformation Analyses

4.4.1. Biot Consolidation

Biot (1941) developed a theory of consolidation, coupling stress and pore water pressure in saturated porous media, using the effective stress theory. Mandel (1953) produced an exact solution of Biot's equations for two-dimensional plane strain consolidation with constant displacement of the top boundary under constant load. Mandel's solutions together with the results of analyses using the numerical models described in this paper are presented in Figs. 17a & 17b. These figures show the Mandel-Cryer effect (Mandel 1953; Cryer 1963) observed in theoretical solutions of the Biot's equations, where local changes in the total stress may actually cause pore pressure increases during the consolidation or drainage of a clay sample. This effect is clearly seen in Fig. 17b. where u/p increases above the initial value near the centre for low values of dimensionless distance, x/H and for low dimensionless times, T (=Dt/H^2).

The finite element program has also been validated against the two-dimensional loading and drainage tests of Rixner (1968) with a constant stress boundary.

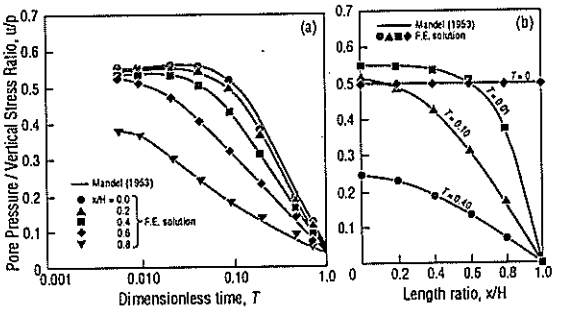

Figure 17. Comparison of consolidation and pore pressure distribution for uniform vertical displacement obtained from Mandel's solution and the finite element solution.

4.5 Water Flow through Swelling Soils

4.5.1. Pressure Filtration of a Swelling Soil

Smiles *et al* (1982) have used the theory of Philip and Smiles (1969) i.e. equation (8) to analyse the constant pressure filtration of a bentonite slurry through a membrane filter. This problem is one where both non-linearity and finite strain are factors, with the initial void ratio equal to about 50. The experimental results and the linearized theoretical analyses of Smiles *et al* (1982) are shown in Fig. 18. together with the results of the modelling techniques described in this paper.

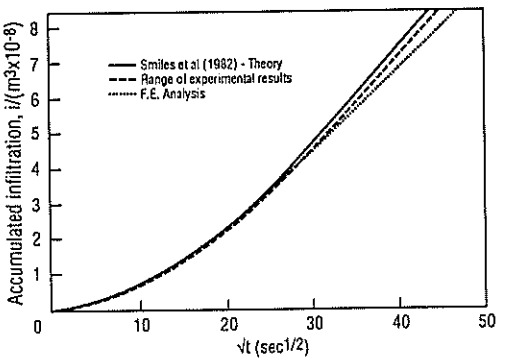

Figure 18. Comparison of experimental, analytical and finite element analysis for constant pressure filtration of a bentonite slurry through a membrane filter.

4.5.2 Consolidation of a Swelling Soil

Carter *et al* (1979) have also used the Biot theory to analyse finite strain consolidation or flow in swelling soil. Their model is similar to that of Philip and Smiles (1969), but is expressed in terms of the consolidation of a saturated elastic soil. This uses a different definition of diffusivity, given by the coefficient of consolidation, Cv = K dσ'/dv, where σ' is the effective stress and v is the volumetric strain. Fig.19 shows one result of Carter *et al* (1979) for one-dimensional consolidation compared with the results using the techniques described in this paper.

4.5.3 Centrifugal Sedimentation of a Swelling Soil

Another interesting and useful test of the model is that of the centrifugal sedimentation of a column of bentonite slurry (e_o>50) (Smiles unpublished data). The results of this experiment at two different times is shown in Figs. 20a & 20b. The material was the same as the bentonite slurry considered in the test shown in Fig. 18 above and therefore must be treated as a finite strain problem. However a further problem

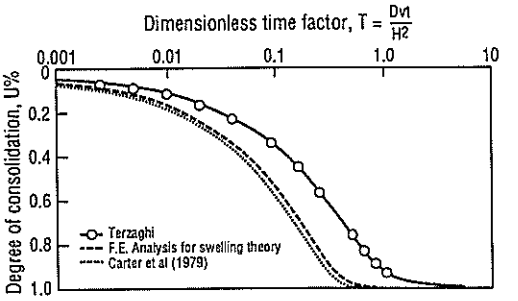

Figure 19. Comparison of finite strain one-dimensional analysis for swelling and non-swelling cases.

arose in analysing this test, namely that the material parameters were determined as a function of soil water suction or negative pore pressure at normal gravitational forces in the laboratory. Because in the case of the filtration test of Fig. 18 above, the stress component of suction (equation (7)) was small, it did not matter whether soil water suction, h or the 'un-loaded soil suction, h' was used. In the centrifuge test with high values of g equal to 360, the stress component of suction becomes very significant and therefore the stress distribution through the slurry must be known accurately. The dashed lines in Figs. 20 are those obtained with the stress component of suction ignored. The solid lines are those obtained with the material parameters and in particular the soil water content as a function of the 'un-loaded' soil suction. The effect of side friction is also very significant in determining the stress distribution in the slurry and therefore the stress component of soil suction is also important, as shown in Figs. 20 for different values of the ratio of side friction to soil friction.

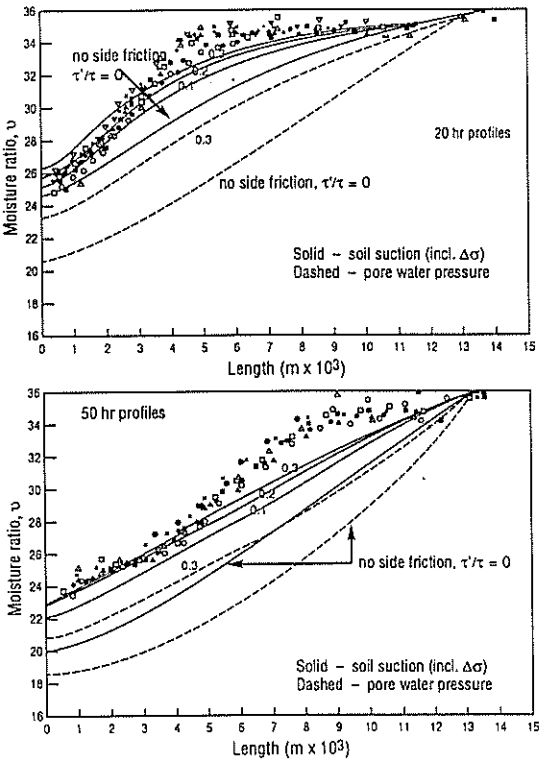

Figure 20. Comparison of experimental and finite element analysis of centrifugal consolidation of a bentonite slurry with and without side friction and various ratio of side friction to soil friction.

4.6 Deformations in a Swelling Soil

4.6.1 Suction Controlled Consolidation Test

One of the least understood mechanisms in geotechnical engineering is that of swelling and shrinking of clay soils. This situation has resulted in a wide range of ad-hoc empirical tests and analytical procedures being used in practice. It is this problem for which the techniques described in this paper were originally developed.

The suction controlled consolidometer (Aitchison *et al* (1973) is probably still the most advanced testing method for swelling soils. It permits soil deformation to be measured as a function of soil stress, soil water suction and, if necessary, solute concentration. An example of tests on a red Riverina clay from near Griffith, NSW is shown in Fig. 21.

Livneh *et al* (1973) and Richards (1979) have shown that data from consolidation tests such as that in Fig. 21 are insufficient to uniquely determine all the drained elastic parameters required. e.g. equation (15). Another test procedure such as a simple unconfined three-dimensional shrink/swell test is necessary. For example, using the data in Fig. 21, and considering Poisson's ratio as the unknown, the theoretical results were obtained for such a test using the model described in this paper as shown in Fig. 22. The experimental results of an unconfined test on the same material are shown superimposed on Fig. 22, from which a value of Poisson's ratio of 0.42 was interpolated.

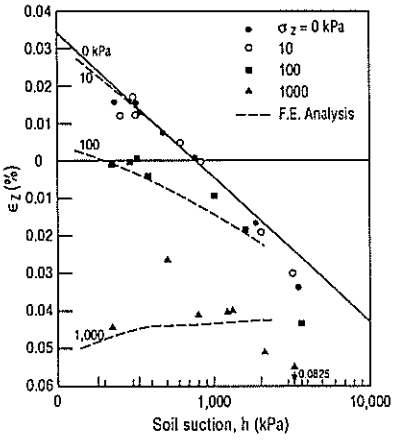

Figure 21. Results of consolidation tests on Riverina clay, Griffith, NSW.

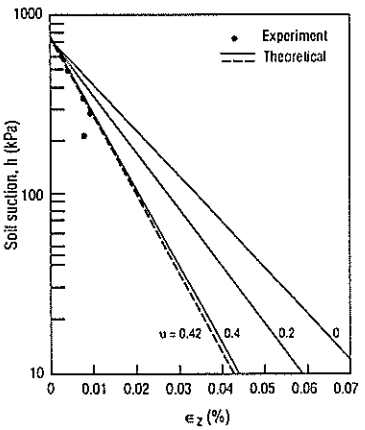

Figure 22. Determination of Poisson's ratio by comparison of experimental data with predicted results.

5. CASE HISTORIES

The model described in this paper has been used on many projects over the past 25 years for the geotechnical, civil, mining, agricultural and environmental industries in the areas of slope stability, landslides, retaining walls, footings, embankments and excavations, compaction and restriction of root growth in agriculture, contaminant transfer in waste management and ground water hydrology. Three such examples have been included here to demonstrate the practical usefulness of the model in differing applications.

5.1 CASE 1: HILL - SLOPE SEEPAGE IN A SOIL WITH CONTRASTING TEXTURE.

5.1.1 Description of Field Experiment

The experimental field site (Smettem *et al*, 1990) is located near the Mt. Bold reservoir within the Onkaringa watershed, 25km SE of Adelaide, South Australia. The experimental plots support a 40 yr. old native pasture and occupy a midslope position with a linear profile and slopes averaging 10 degrees. The mean monthly rainfalls range from 35 mm in February to 150 mm in July with about 40% falling in the winter months and a further 25% in both spring and autumn respectively. Evaporation exceeds precipitation from September to April.

The soil is acidic with a contrasting textural class. The A horizon of fine sandy loam is permeated by cylindrical macropores up to 12 mm diameter with a frequency of 215 m^{-2} at 0.15m depth. Dye tracing has revealed that about 50% of these macropores act as transmission voids. The B-horizon is predominately kaolinitic and consists of weak angular blocky peds permeated by many fine fissures and infrequent cylindrical macropores.

Details of the experimental plots and monitoring equipment have already been described elsewhere (Chittleborough *et al*, in press). Only those features relevant to the modelling work are mentioned here. Rainfall intensities were measured for ten minute intervals. Dip wells were installed to 2 m depth along a transect parallel to the dip of the slope and were monitored on a daily basis.

5.1.2 Material Properties

The soil hydraulic properties were measured by a number of different techniques (Smettem *et al*, 1990). The properties relevant to the modelling work are $\theta(h)$ and $K(h)$, with $dh/d\theta(h)$ being calculated within the computer program. In structured soils with a distinct macropore-matrix dichotomy, characterization of $\theta(h)$ as a continuous function requires parameters to describe the 'size-mean' and the 'size-spread' of both the macropore and matrix pore systems (Smettem *et al*,1991).

The generalized empirical approach to describing $\theta(h)$ of bi-modal soils was described in a previous paper (Richards and Smettem, 1991b).

The $K(h)$ or $K(\theta)$ relations for structured soils are also frequently characterized by a distinct macropore-matrix dichotomy (Clothier and Smettem, 1990). In order to take account of this within the model, the $K(h)$ relation was described by modifying the well known exponential model to account for a macropore domain. Richards and Smettem (1991b) presented typical $K(h)$ curves for this site.

5.1.3 Analyses

In this study, the main concern is the position of the water

table during drainage from known initial soil water contents and suctions. In order to provide realistic boundary conditions, the monitored slope segment is modelled as part of a toposequence that extends 15 m above the top piezometer and 20 m below the bottom piezometer. The upslope limit coincides with the position of the diversion ditch and we assume no throughflow contribution from further upslope. The downslope limit is close to a commonly observed point of seepage. This permits the matrix potential at this point to be fixed close to zero throughout the analyses. The geometry of the region analysed is shown in Figure 23.

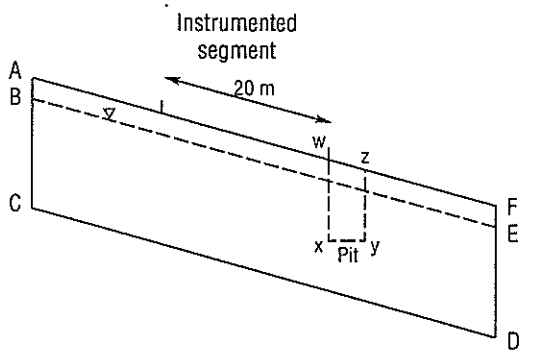

Figure 23. The geometric representation of the region modelled at the Mt Bold hillslope experiment.

Initially two finite element analyses of a drainage event were performed. For the first analysis the instrumented portion of the slope was modelled as the central segment of the toposequence. Measured data at the cessation of a rainfall event were used to define the initial conditions. These comprised a water table at a depth of 0.1 m along the entire slope segment and zero flux into the soil surface. The second simulation was performed to evaluate the effect of the throughflow pit on the subsurface drainage response. This throughflow pit was installed at the lower end of some of the experimental plots to monitor sub-surface water flow and sediment yield.

5.1.4 Results

The measured position of the phreatic line during drainage over a five day period is shown in Figure 24, together with predicted results from the finite element model. The model curves have the correct shape, but show a slightly slower rate of drainage than the measured data. This result shows that it is possible to obtain a reasonable rendition of the drainage response using measured hydraulic properties if the macropore-matrix dichotomy is appropriately parameterized.

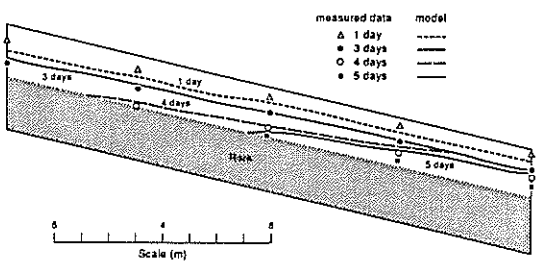

Figure 24. A comparison between the measured and predicted drainage response to winter rainfall.

A particularly close match to the measured data may be obtained simply by altering the slope of the moisture characteristic in the macropore region. Although the model is sensitive in this region, the slope of the moisture characteristic near saturation cannot be measured with a high degree of precision in field soils because macropores are spatially variable and comprise only a small fraction of the total porosity.

The finite element model results from analyses without and with the pit were virtually indistinguishable, indicating that drawdown is negligible over the 5 day period. The throughflow collection system is therefore reasonable for sampling saturated drainage from clay fissure systems.

At present we are unable to extend the model to predict the drainage response during summer storms as this appears to be influenced by processes not explicitly considered in the parameterization of the Richards flow equation.

5.2.2 Material Properties

5.2.2.1 Load - Deformation Properties

The geometry and other details of the londitudinal section through the failed slope are given in Figure 25. The densities of the fill, as determined by sand replacement tests carried out in pits adjacent to the failure, are shown in Figure 26. A density of 1,400 kg/m^3 was considered to be an average value over a depth of 6 m.

Consolidated drained triaxial tests of the fill material gave shear parameters of the order of 15 kPa for cohesion, C', and 34° for the angle of friction, ϕ'. However, the use of these parameters in stability analyses, assuming pore pressure equivalent to down slope flow parallel to the surface, gave a factor of safety of about 1.12. Although low, it was suggested at the time that it was not low enough to cause failure. Back analysis of the failed slope using the Janbu routine method Kong formed an Independent Review Panel on Filled Slopes (1976) to provide an independent authoritative opinion on the cause of the slope failure at Sau Mau Ping in 1976, and on the safety of other similarly constructed slopes. The author of this paper was one of the panelists.

Six major conclusions and recommendations resulted from the Panel's deliberations. The first of these was that "the Sau Mau Ping slope failures of 1976 were the result of infiltration during intense rainfall, in end-tipped, loose fill, followed by loss of strength and consequent conversion of the upper few metres of the fill into a destructive mud avalanche". The other conclusions went on to state that these conditions at Sau Mau Ping were not unique in Hong Kong and recommendations were made in regard to remedial measures and avoiding similar problems in the future.

One of the problems faced by the Panel was the lack of a suitable model for the prediction of the infiltration and slope stability mechanisms and how they interact with each other. The model used in this paper includes the non-linear solution of water flow in unsaturated and saturated soil and the elasto-plastic solution of the load-deformation behaviour of a soil with stress and moisture dependent properties. It also considers the increase in weight of the soil during wetting, the reduction in shear strength of the soil due to water and strain softening, the change in pore pressure with changing stress and the seepage forces due to infiltration and hill-slope flow. In order to test this model for the conditions which existed at Sau Mau Ping on August 25th 1976, analyses of the failed slope were carried out using the limited experimental data available at the time.

5.2. CASE 2: LANDSLIDES IN FILLED SLOPES DURING RAIN STORMS

5.2.1 Description

On August 25, 1976, soon after 10 am., following heavy rain in Hong Kong, which began at 3 am. on August 24th, the fill slope immediately behind Block 9 of the Sau Mau Ping Estate failed. The resulting mud avalanche buried the ground floor of the block killing eighteen people. Considering that an earlier failure had occurred at Sau Mau Ping in 1972, also in filled slopes and the conclusions of a subsequent enquiry at that time, such slopes were considered in more detail. It was quickly recognised that fill slopes, constructed as the result of a need, often urgent, to create land for housing development, are widespread throughout Kowloon and the urban areas of Hong Kong Island. The engineering criteria used in the construction of such fill slopes were thus called into question. It was in these circumstances that the Government of Hong Kong formed an Independent Review Panel on Filled Slopes (1976) to provide an independent authoritative opinion on the cause of the slope failure at Sau Mau Ping in 1976, and on the safety of other similarly constructed slopes. The author of this paper was one of the panelists.

Six major conclusions and recommendations resulted from the Panel's deliberations. The first of these was that "the Sau Mau Ping slope failures of 1976 were the result of infiltration during intense rainfall, in end-tipped, loose fill, followed by loss of strength and consequent conversion of the upper few metres of the fill into a destructive mud avalanche". The other conclusions went on to state that these conditions at Sau Mau Ping were not unique in Hong Kong and recommendations were made in regard to remedial measures and avoiding similar problems in the future.

One of the problems faced by the Panel was the lack of a suitable model for the prediction of the infiltration and slope stability mechanisms and how they interact with each other. The model used in this paper includes the non-linear solution of water flow in unsaturated and saturated soil and the elasto-plastic solution of the load-deformation behaviour of a soil with stress and moisture dependent properties. It also considers the increase in weight of the soil during wetting, the reduction in shear strength of the soil due to water and strain softening, the change in pore pressure with changing stress and the seepage forces due to infiltration and hill-slope flow. In order to test this model for the conditions which existed at Sau Mau Ping on August 25th 1976, analyses of the failed slope were carried out using the limited experimental data available at the time.

5.2.2 Material Properties

5.2.2.1 Load - Deformation Properties

The geometry and other details of the londitudinal section through the failed slope are given in Figure 25. The densities of the fill, as determined by sand replacement tests carried out in pits adjacent to the failure, are shown in Figure 26. A density of 1,400 kg/m^3 was considered to be an average value over a depth of 6 m.

Consolidated drained triaxial tests of the fill material gave shear parameters of the order of 15 kPa for cohesion, C', and 34° for the angle of friction, ϕ'. However, the use of these parameters in stability analyses, assuming pore pressure equivalent to down slope flow parallel to the surface, gave a factor of safety of about 1.12. Although low, it was suggested at the time that it was not low enough to cause failure. Back analysis of the failed slope using the Janbu routine method suggested values of C' = 13 kPa and ϕ' = 30 were more appropiate.

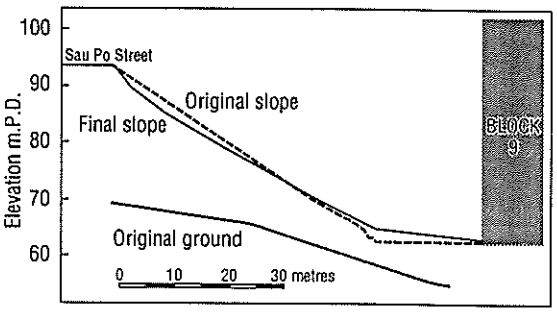

Figure 25. The section through the failed slope at Sau Mau Ping, Hong Kong, 1976.

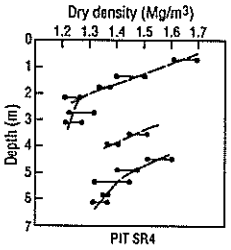

Figure 26. Field densities measured in the failed slope at Sau Mau Ping.

Using the same finite element method as used later for the analysis of the slope, the triaxial tests were themselves back analysed. The following best fit parameters to the experimental data were obtained.

K = 700000 kPa

$G = 3500 \cdot \sigma'^{0.5} + 50$ kPa

C' = 16 kPa

σ' = 34.5°

where K = bulk modulus

G = shear modulus

σ' = effective stress.

It is important to realize that the best fit parameters given above are those which when used in the computer model give the measured experimental response in the triaxial test. They do not necessarily correspond with the traditional theoretical values. Because the soil exhibited compression during the triaxial tests, the non-associated flow rule was used, with the angle of dilatancy, $\psi = 0$.

The change in volume during shear deformation was measured by direct shear box tests. Samples were prepared at various dry densities ranging from very loose to dense, loaded to a vertical pressure of 35 kPa (corresponding to an average soil depth over the failed section of about two metres), and then deformed by shearing the sample at a rate slow enough to allow drained volume change. As the shear dispacement increased, the shear force resistance and the volume changes were measured up to failure of the soil, as shown in Figure 27.

The results in Figure 27 show that dry density affects the volume change characteristics very significantly, although the

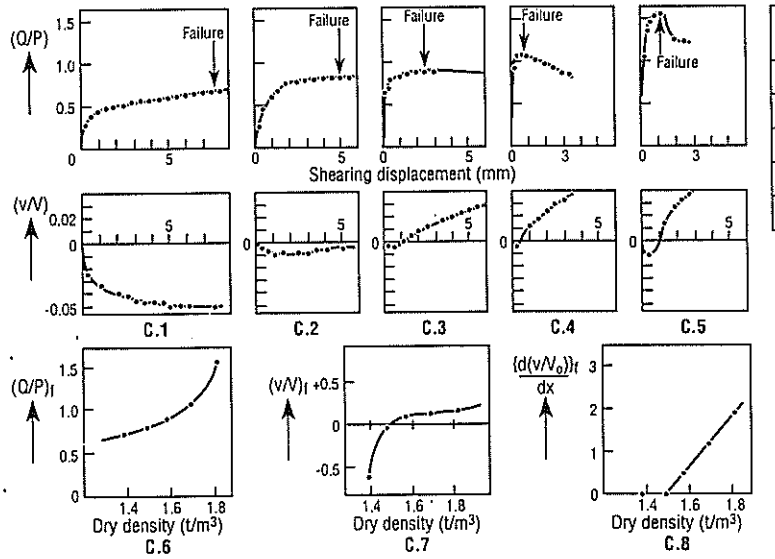

Fig.	Dry density (t/m³)
C.1	1.39
C.2	1.49
C.3	1.57
C.4	1.69
C.5	1.82

Figure 27. Results of the direct shear tests on the fill, sampled from the failed slope at Sau Mau Ping.

strength itself is not affected greatly unless the soil is denser than a dry density of about 1,600 kg/m^3. For loose soil, with dry densities lower than about 1,500 kg/m^3, the soil compresses during shear until it reaches the failure point and then fails at constant volume. With saturated soil undergoing rapid deformation, this compression or more correctly the tendency to compress will cause the pore pressures to rise. If the effective stresses reduce to zero or less, then liquifaction and a mudflow or landslide will occur.

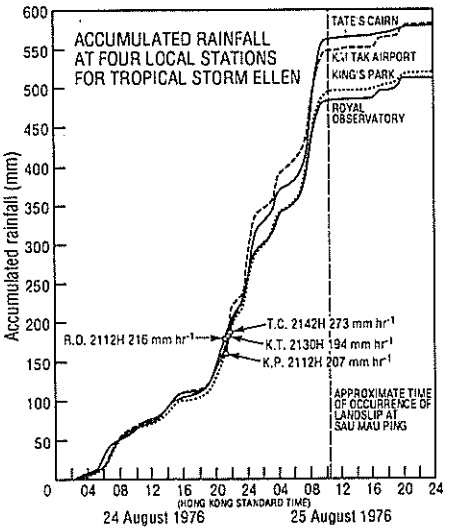

Figure 28. Rainfall at four local stations for tropical storm Ellen.

5.2.2.2. Soil water Flow Parameters

Data on the rainfall that occurred during the 24th and 25th August, 1976, was provided by the Royal Observatory. The data consisted of hourly rainfall in millimetres at local meteorological stations, referred to Hong Kong Standard time. The nearest stations to Sau Mau Ping are those at Hong Kong Airport and Tate's Cairn, which are approximately equidistant from Sau Mau Ping. Figure 28 shows the accumulated rainfall versus time over this period. Up until the failure, 525 mm of rain fell on the slope in 31 hours (ie. an average rate of 17 mm/hr or 0.472x10^{-5}m/s). Permeability measurements of the fill gave saturated permeabilities of about 0.46x10-5m/s, which suggests that the average rainfall intensity equalled the long term infiltration rate of approximately 17 mm/hr (Philip, 1969). Using the data in these figures for rainfall intensity and permeability, and estimated degree of saturation for the soil in its initial and saturated states, a depth of wetting of 2.5 m was calculated. This compared well with the observed thickness of the failed mass.

Wong Hong-Yau (1966) also carried out infiltration studies in similar soils in Hong Kong. Estimates using this data indicate that the depth of wetting would be of the order of 2.9 m.

Considering the soil type and back analyses of the infiltration tests and their assumed wetting profiles, the final K(h) relationship adopted for the fill was

$$K(h) = 0.7\times10^{-5}/(1.0 + 0.05\,h^{2.0}) + 0.1\times10^{-9}\ \text{m/s}. \quad (19)$$

This relationship gives a saturated permeability of 0.7x10^{-5} m/s, which is higher than the mean rainfall intensity, so little ponding or runoff was assumed.

The wetting moisture characteristic θ(h) relationship was estimated from typical saturated water contents, the air dried water contents and the measured particle size distribution. The relationship adopted after fitting the results to the assumed wetting profiles as described below is

$$\theta(h) = 0.42 - 0.119\times10^{-2.0}\,h + 0.130\times10^{-5.0}\,h^{2.0} \quad (20)$$

5.2.3 Analysis

The finite element mesh defining the slope at Sau Mau Ping is shown in Figure 29. As the area represented by this mesh is greater than the actual failure zone, the two vertical boundaries were fixed in the horizontal direction and free in the vertical direction. The lower boundary was fixed in the direction normal to the boundary and free in the direction parallel to the boundary. The upper surface was a completely free boundary.

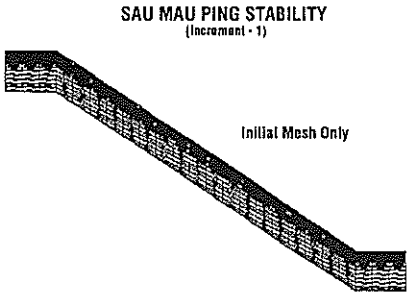

Figure 29. The geometric representation of the region analysed in the failed slope at Sau Mau Ping.

As mentioned above, the infiltration rate at the upper surface boundary of the slope was assumed to equal the rainfall rate and remain constant at 0.472×10^{-5} m/s over the whole analysis. As this rate was lower than the long term infiltration rate, no surface ponding and runoff was expected. However, the program does allow for the decrease in infiltration should pore pressures become positive. The lower boundary was assumed to be impervious, but was deep enough to always be below the wetting front for the elapsed times considered.

The left hand vertical boundary was also assumed to be impervious, as it was located at the top of the slope. The right hand boundary was assumed to be impervious while the pore pressures were negative. However, the pore pressures were controlled to give a mirror image condition whenever they became positive.

5.2.4 Results

The first analyses of the slope were made using only the water flow modules to simulate the infiltration during the infiltration tests and the actual rainfall event. The results using the soil properties above are shown in Figure 30. As these give a depth of wetting of about 2.5 m after 34 hours, the water flow parameters were considered to be a reasonable approximation of properties of the soil in the actual slope.

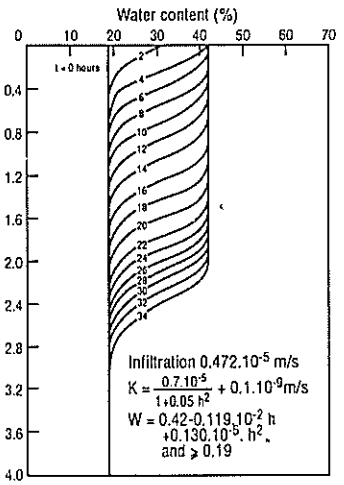

Figure 30. The results of the finite element analysis of infiltration of the rainfall into the failed slope at Sau Mau Ping.

The coupled load - deformation and water flow analyses were carried out using the soil properties and boundary conditions previously discussed. The results showed that displacement of the toe increased with time until mathematical instability, which corresponds to the physical instability or failure of the slope at 36 hours.

The summary of the slope response at 34 hours is shown in Figures 31a,b & c. These results indicate that the failure occurs only in the wetted zone, with the lower boundary of the failure at the depth of wetting. The zone of failure extends from the top of the slope to just above the toe of the slope. In order to check whether the right hand vertical boundary influences the behaviour of the failure at the toe of the slope, an analysis was carried out with this boundary located further from the toe, but the result was not affected. The development of failure is clearly seen by the movements just above the toe of the slope, plotted against time in Figure 32. This figure predicts that failure would occur after 34 hours of rain at the observed rainfall rate, which corresponds with the observed time to failure.

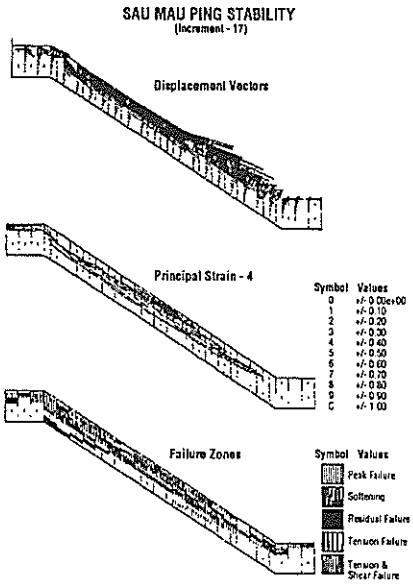

Figure 31. The results of the finite element analysis of the slope stability during infiltration of rainfall into the failed slope at Sau Mau Ping, a Shear strain, b Failure Zones and c Displacements.

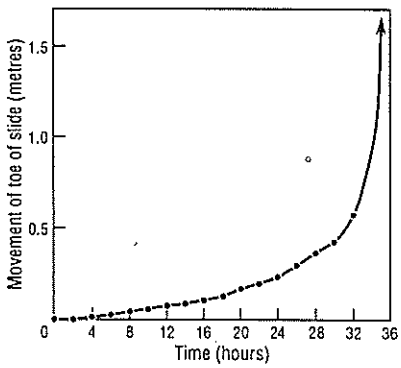

Figure 32. The predicted toe displacements of the failed slope at Sau Mau Ping versus time after commencement of rain.

While the experimental investigation on the fill at Sau Mau Ping was carried out using traditional test methods, with no consideration of the use of the modelling procedures discussed in this paper, it is of interest that the limited data

could be used in the finite element models with reasonable success. It shows that the analytical procedures are capable of modelling the very complex interaction between the mechanisms of water infiltration and slope stability. It also demonstrates that even with limited data, these complex modelling techniques can be made to work in practical situations with good results.

5.3 CASE 3: PRESSURES DUE TO SWELLING SOIL ON A RETAINING WALL.

5.3.1 Description

The basement of the Gouger Street Mail Exchange, Adelaide, South Australia involved the construction of a reinforced concrete retaining wall, 7.5 m deep, which supports stiff Hindmarsh clay over most of its depth (Richards and Kurzeme 1973). The generalized soil profile used in the analyses is shown on the finite element mesh in Figure 33. This clay had been well documented previously and shown to be a highly expansive clay, associated with many structural problems in the Adelaide area (Stapledon 1970). As free water was observed flowing from the top of the clay during the excavation stage, there was concern that subsequent wetting and heaving of the clay might cause large pressures on the wall.

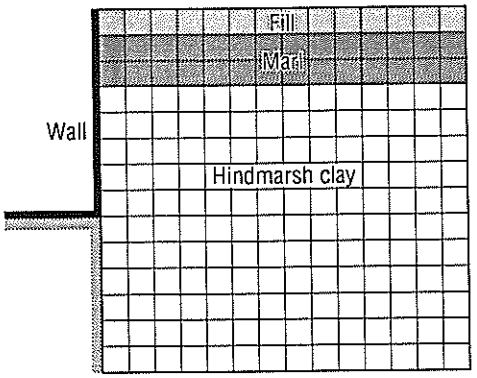

Figure 33. Finite element mesh representing the retaining wall.

In order to investigate the behaviour of the wall, earth pressures on the wall and soil suctions in the clay behind the wall were monitored. The soil water suctions were measured as total suction by 'in-situ' psychrometers. The earth pressures were measured at 6 vertical sections at depths of 2, 4, 6 and 7 metres. The results of measurements made over several years at two sections are shown in Figure 34. While the initial pressures were negible, the earth pressures have increased at the bottom of the wall to values of at least five times the overburden pressure. This pressure increase has moved progressively up the wall with time. At the same time, the soil suction measurements, the nearest being 2m from the wall, showed no significant change. The most likely cause of this pressure increase was thought to be the accumulation of seepage water in the initial gap between the wall and the clay, followed by the local swelling of the clay. When the clay made contact with the wall, this water would no longer be readily available to the clay at that depth. The earth pressures would then only increase until there was an internal redistribution on soil water suction within the clay.

5.3.2 Material Parameters

5.3.2.1 Volume Change Parameters

The volume change parameters, CC1 & CC2 are defined as the slopes of the curves of the vertical and horizontal strain

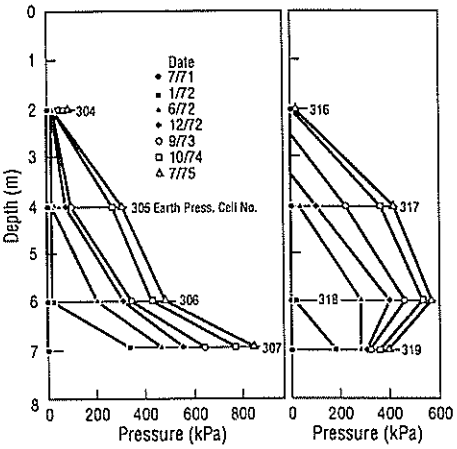

Figure 34. Vertical pressure distribution for the earth pressure cells 304 - 307 and 316 - 319.

respectively due to moisture change at zero vertical stress versus the logarithm of soil water suction, from volume change tests. Over practical changes of soil water suction, these curves approximate straight lines (see Fig. 35). Hence CC1 & CC2 can be considered in many cases to be constants, although the swelling mechanism used in the model is stress dependent, as shown by the back-analysis of a typical test in Figure 36. Results for the three main soil types found behind the retaining wall can be summarized as

Fill	CC1 = 0.012	CC2 = 0.010
Marl	CC1 = 0.030	CC2 = 0.026
Hindmarsh Clay	CC1 = 0.072	CC2 = 0.045

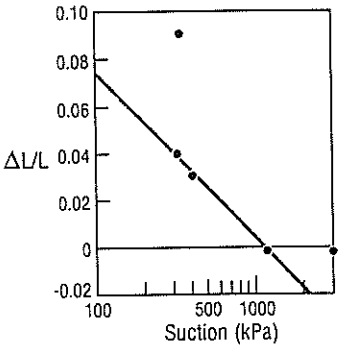

Figure 35. Typical suction – vertical strain relationship for Hindmarsh clay.

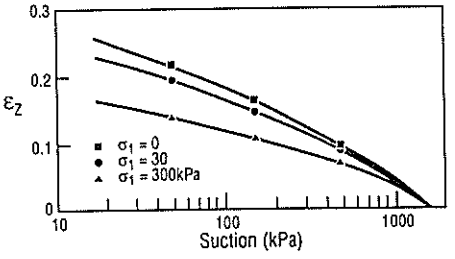

Figure 36. Predicted response of Hindmarsh clay in suction controlled consolidometer.

5.3.2.2 Mohr-Coulomb Yield Criteria

The results of undrained triaxial tests on the Hindmarsh clay under controlled lateral stress and soil water suction are plotted in Figure 37 (Kurzeme and Richards 1973). Due to the high degree of material variability, it was not possible to infer any significant relationship for the undrained parameters C and ϕ for total stress. However when the yield stress was plotted against total suction, a good correlation was obtained (Figure 37) giving C = 0 and ϕ_h for soil suction = 8.3°. The yield criterion used in the analyses is

$$(\sigma_1 - \sigma_3) = 2.h.\tan \phi_h \qquad (21)$$

where σ_1 = vertical stress

σ_3 = horizontal stress

h_t = total suction

ϕ_h = 8.3°

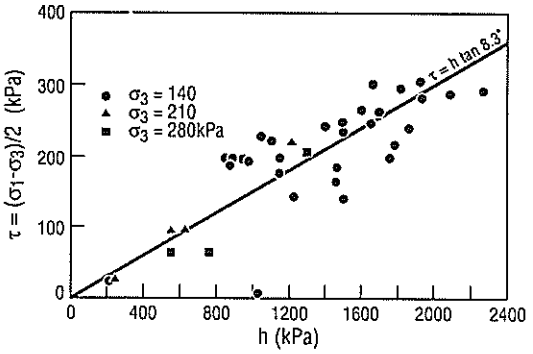

Figure 37. Ultimate shear stress – soil suction relationship for Hindmarsh clay.

5.3.2.3 Stress-Strain Relationships

The triaxial test data was back-analysed using a finite element model of the test procedure to determine the hyperbolic non-linear elastic parameters for the Hindmarsh clay, giving

$$K = 10^6 \text{ kPa}$$

$$G = 107\, h_t^{0.61} (1 - (\tau/\tau_y)^{1.0}) \qquad (20)$$

where τ = shear stress $(\sigma_1 - s_3)/2.0$

τ_y = yield stress (equation) (19)

This relationship gave the predicted stress-strain curve in Figure 38, compared with the typical experimental data with which the parameters were matched.

5.3.3 Analyses

The finite element mesh representing the problem is shown in Figure 33. As no contact was assumed between the wall and the soil, interfacial elements were used to model this interface.

The main unknown was how soil water suction varied with time. According to the psychrometer results, any significant changes were restricted to within a zone 2 metres from the wall. The total suction of the water from the marl - clay interface was 200 kPa due to its electrolyte concentration, and this was therefore assumed to be the limiting soil suction on wetting.

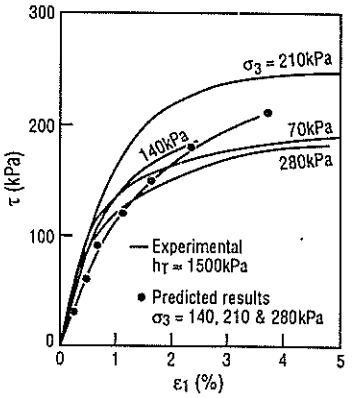

Figure 38. Predicted and experimental stress – strain curves for constant cell pressure triaxial tests on Hindmarsh clay.

The extent to which wetting took place from the wall would be dependent on the volume of water available to the clay. However, as wetting was confined to within 2 m from the wall, this meant that wetting would only take place to the second column of nodes in Figure 33 (the spacing of the nodes was 1 m). Within these constraints several cases were considered (Richards 1977). The two which were most relevant were

(1) Progressive wetting up of the single node at the bottom of the wall from an initial value of 1500 kPa to 200 kPa soil suction before the next node up the wall began to wet up and so on (Figure 39).

(2) Progressive wetting up of two nodes at the bottom of the wall from 1500 - 1000 - 700 - 450 - 300 - 200 kPa while wetting commenced progressively up the wall as the pressure reached 200 kPa (Figure 40).

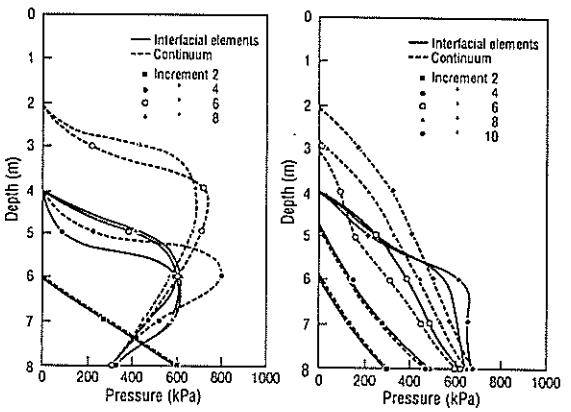

Figure 39. (Left) Results of analysis for Case 1.
Figure 40. (Right) Results of analysis for Case 2.

5.3.4 Results

The results of the above two relevant cases are shown in Figures 39 & 40, together with the results for the case of a continuum between the wall and the soil. They show similar trends to the measured results at the two sections in Figure 34 and help confirm that the mechanisms proposed above can explain the observed behaviour.

6. FINAL DISCUSSION

The modelling techniques described in this paper have been successfully used on a wide range of problems in a wide range of soil and environmental conditions. While developed originally for unsaturated and swelling soils, they seem to

apply equally well to saturated and non-swelling soils, the latter being a particular case of the former.

The techniques have in part resulted because of the author's interests and immediate problems, many of which at the time could not be handled by alternate techniques. They have also provided a theoretical framework within which the author has been able to incorporate his experience in a mathematical form, as a sort of data base. The end product is one that suits the author, handles most of the problems conveniently and successfully and is compatible with his understanding of soils and the experimental techniques which have been available to him. Whether this model is of use for others is for them to judge. Other groups are now using or expressing interest in the model, all currently overseas. However its effective use requires not only the ability to operate the computer programs, but also to understand the basic concepts of the geomechanics used in the techniques.

The main uses of the model have been

(1) to provide a technical framework for planning projects.

(2) to sort out the relevant mechanisms and processes including running preliminary parametric studies.

(3) to develop the relevant test procedures, and by preliminary analyses to determine the appropriate test conditions e.g. stresses and soil water suctions for laboratory tests.

(4) to back analyse laboratory test so as to extract the maximum amount of data from the test results.

(5) to back-analyse failed or problem structures. When good agreement is obtained between the theoretical results and the field observations, conclusions can be drawn on possible failure mechanisms.

(6) to carry out tentative design analyses of new projects. However these analyses should only be used as a guide. The more one becomes experienced with such models, the more one becomes aware of the dangers of relying completely on their results. To use such models in design without a good background of field experience can be most foolhardy indeed.

7. REFERENCES

1. Aitchison, G.D.. The circumstances of unsaturation in soils with particular reference to the Australian environment. Proc. 2nd. Aust. - NZ Conf. Soil Mech. & Fndn. Eng.: (1956) 173-191.

2. Aitchison, G.D. Relationships of moisture stress and effective stress functions in unsaturated soils. In 'Pore Pressure and Suction in Soils', London :(1961).47-52.

3. Aitchison, G.D. and Richards, B.G. (Fundamental mechanisms involved in soil moisture movement and the engineering properties of soils which are important in such movements. Proc. 2nd. Intl. Conf. on Expansive Clay Soils, Texas A & M Univ., Texas, : 66-84.

4. Aitchison, G.D. and Martin, R. A membrane oedometer for complex stress path studies in expansive clay. Proc., 3rd. Intl. Conf. on Expansive Clay Soils. Haifa, Israel, 1 : (1973) 161-176.

5. Bear, J. and Verruijt, A. Modeling groundwater flow and pollution. D. Reidel Publishing Co. (1987).

6. Biot, M.A. General theory of three-dimensional consolidation. J. Applied Physics, **12** : (1941) 155-164.

7. Carslaw, H.S. and Jaeger, J.C. Conduction of heat in solids. Oxford Press (2nd. Edition). (1959)

8. Carter J., Brooker, J.R. and Small, J.C. The analysis of finite elasto-plastic consolidation. Intl. J. for Numerical and Analytical Methods in Geomechanics, **3** : (1980) 107-129.

9. Chittleborough, D.J., Smettem, K.R.J. and Leaney, F.W. Hillslope hydropedology of a soil with a contrasting textural class II. Hydrological Processes, (in press). (1989)

10. Clothier B.E. and Smettem, K.R.J. Combining laboratory and field measurements to define the hydraulic properties of soil. Soil Sci. Soc. Am. J., **54**: 1989) 299-304.

11. Christian, J.T. and Boehmer, J.W. Plane strain consolidation by finite elements. J. Soil Mech. & Fndn. Div., ASCE, **96** (SM4) : 91970) 1435-1457.

12. Croney, D. and Coleman D. Pore pressure and suction in soil. In 'Pore Pressure and Suction in Soil', Butterworths, London : (1961) 31-37.

13. Cryer, C.W. A comparison of the three-dimensional theories of Biot and Terzaghi. Q. J. Mech. Appl. Math., **16** : (1963) 401-412.

14. Davis E.H. Theories of plasticity and the failure of soil masses. In 'Soil Mechanics - Selected Topics' ed. I.K.Lee, Butterworths : (1968) 341-380.

15. Duncan, J.M., Monismith, C.L. and Wilson E.L. Developments in the application of practice of a fundamental procedure fot the design of flexible pavements. Proc. 2nd. Intl. Conf. on Structural Design of Asphalt Pavements. Univ. of Michigan : (1968) 99-108.

16. Escario, V. and Saez, J. The shear strength of partly saturated soils. Geotechnique, 36 (3) : (1986) 453-456.

17. Fredlund, D.G. Stress state variables for unsaturated soils. Proc. ASCE, **103** (GT5) : (1977) 447-466.

18. Fredlund, D.G. Appropriate concepts and technology for unsaturated soils. Canadian Geotech. J., 16: (1979) 121-139.

19. Gersevanor N.M. The foundations of dynamics of soils. 3rd. Edition, Strougdat, Moscow-Leningrad. (1937)

20. Ghaboussi, J., Wilson, E.L. and Isenberg J. Finite element for rock joints and interfaces. Proc., J. Soil Mech. & Fndn. Div., **99** (SM2) : (1973) 833-848.

21. Independent Review Panel on Filled Slopes. Report on the Slope Failures at Sau Mau Ping, August 1976. Government of Hong Kong, 104p. & 8 Drgs. (1976)

22. Jennings, J. A revised effective stress law for use in the prediction of the behaviour of unsaturated soils. In 'Pore Pressure and Suction in Soils', London : (1961) 26-30.

23. Kurzeme M. and Richards, B.G. Earth pressure observations on a retaining wall in expansive clay, Gouger Street Mail Exchange. CSIRO Div. of Applied Geomechanics, Tech. Rept. No. 17. (1973)

24. Llvneh, M., Shklarsky, E. and Uzan J. Cracking of flexible pavements based on swelling clay. Proc., 3rd. Intl. Conf. on Expansive Clay Soils, Haifa, Israel : (1973) 257-266.

25. Lo K.Y. and Lee, C.F. Stress analysis and slope stability in strain softening materials. Geotechnique, **23** (1) : (1973) 1-11.

26. Mandell J. Consolidation of soils. Geotechnique, **111**: (1953) 287-299.

27. Mlitchell,J.K., Greenberg, J.A. and Witherspoon, P.A. Chemico-osmotic effects in fine grained soils. J. Soil Mech. & Fndn. Div., ASCE, 99 (SM4) : (1973) 307-322.

28. Mualem Y. A new model for predicting the hydraulic conductivity of unsaturated porous media. Water Resources Research, **12** (3) : (1976) 513-522.

29. Nelson, I. Investigation of ground shock effects in non-linear hysteretic media. Report 1, Modelling the behaviour of a real soil. Report S-68-1, Contract DCA 39-67-C-0048, Paul Weidlinger Consulting Engineers, US Army Waterways Experiment Station. (1970)

30. Nieber J.L. and Walter M.F. Two-dimensional soil moisture flow in a sloping rectangular region: Experimental and numerical studies. Water Resources Research, **17**: (1981) 1722-1730.

31. Perroux K.M., Smiles, D.E. and White I. Water movement in uniform soils during constant flux infiltration. Soil Sci. Soc. Amer. J., **45** (2) : (1981) 237-240.

32. Philip, J.R. Theory of infiltration. Advances in Hydroscience, **5**: (1969) 215-296.

33. Philip, J.R. and Smiles, D.E. Kinetics of sorption and volume change in 3-component systems. Aust. J. Soil Res., **7** : (1969) 1-19.

34. Richards, B.G. Moisture flow and equilibria in unsaturated soils for shallow foundations. ASTM Symp. on 'Permeability and Capillarity in Soils', ASTM Special Technical Publication 417: (1967) 4-34.

35. Richards, B.G. Mathematical model for moisture flow in Horsham clay. Civil Engng. Trans., Inst. Engrs. Aust., 10 (2) : (1968) 220-224.

36. Richards, B.G. Theoretical transient behaviour of saturated and unsaturated soils under load and changing moisture conditions. CSIRO Australia, Div. of Applied Geomechanics, Tech. Paper 16. (1973)

37. Richards,B.G. Model for slab foundations on expansive clays. Proc. 8th. Intl. Conf. Soil Mech. & Fndn. Engng., Moscow, 2 (2) : (1973) 185-191.

38. Richards B.G. and Kurzeme. M. Observations of earth pressure on a retaining wall at the Gouger Street Mail Exchange, Adelaide. Aust. Geomech. J., **G3** (1) : (1973) 21-26.

39. Richards, B.G. The use of finite element method in the solution of the flow equation in soils. Proc., Intl. Conf. on Finite Element Methods in Engineering. Univ. of NSW, Sydney : (1974) 533-547.

40. Richards, B.G. Analysis of flexible road pavements in the Australian environment - Stresses, strains and displacements under traffic loadings. CSIRO Australia, Div. of Applied Geomechanics, Tech. Paper No. 20. (1974)

41. Richards, B.G. Determination of experimentally based load - deformation properties of a mine fill. Proc., 2nd. Aust-Nz. Conf. on Geomechanics, Brisbane : (1975) 56-62.

42. Richards, B.G. Pressures on a retaining wall by an expansive clay. Proc., 9th. Intl. Conf. on Soil Mech and Fndn. Engng., Tokyo, : (1977) 705-710.

43. Richards, B.G. Application of an experimentally based non-linear constituative model to soils in the laboratory and field tests. Aust. Geomech. J., **G8** : (1978) 20-30.

44. Richards, B.G. The method of analysis of the effects of volume change in unsaturated expansive clays on engineering structures. *Aust. Geomech. J.*, **G9**): (1979) 27-41.

45. Richards, B.G. Use of an automatically generated joint element for the analysis of collapse load in strain softening materials. 3rd. Aust.-NZ Geomech. Conf., Wellington, NZ, 2 : (1980) 233-239.

46. Richards B.G. The measurement of soil suction in expansive clay. Civil Engng. Trans., Inst. Engrs. Aust., CE22 (3) : (1980) 252-261.

47. Richards, B.G. The analysis of the total load-deformation response of an expansive clay subgrade at Macalister, QLD., Proc., 10th. Aust. Road Res. Board Conf., Sydney. (1980).

48. Richards, B.G. The finite element analysis of mine spoil slopes using slip elements to simulate strain softening yield behaviour. Civil Engineering Trans., Inst. Engrs. Aust., CE24 (1) : (1982) 69-76.

49. Richards, B.G. Finite element analysis of volume change in expansive soils. Proc. 5th. Int. Conf. on Expansive Soils, Adelaide, : (1984) 141-148.

50. Richards, B.G. The role of lateral stresses on soil water relations in swelling soils. Aust. J. Soil Res., **24** : (1986) 457-467.

51. Richards, B.G. and Greacen, E.L. Mechanical stresses on an expanding cylindrical root analogue in granular media. Aust. J. Soil Res., 24 : (1986) 393-404.

52. Richards, B.G. and Peter P. Measurement of negative pore pressures or soil water suction. In 'Geotechnical Field Instrumentation', Inst. Engrs. Aust., Melbourne. (1987).

53. Richards B.G. and Smettem K.R.J. Modelling water flow in two and three dimensional application - I: General theory for non-swelling and swelling soils. (Submitted for publication). (1991a).

54. RICHARDS, B.G. and SMETTEM, K.R.J. (1991b) Modelling water flow in two and three dimensional application - II: Characterization of material flow parameters. (Submitted for publication).

55. Richards L.A. Capillary conduction of liquids through pore systems. *Physics.* 1.: (1931) 318-333.

56. Rixner J. Pore pressure dissipation under plane strain conditions. Unpubl. Term Paper, MIT. (1968).

57. Rosco, K.H. & Wroth C.P. On the yielding of Soils, Geotechnique, **8** : (1958) 22.

58. Skempton, A.W. Pore pressure coefficients A and B. Geotechnique, 4 : (1954) 143-147.

59. Skempton, A.W. Address on effective stress in soils, concrete and rocks. In 'Pore Pressure and Suction in Soils', London : (1961) 4-16.

60. Sloan, P.G. and Moore, I.D. Modeling subsurface storm flow on steeply sloping forested watersheds. Water Resources Research, **20:** (1984) 1815-1822.

61. Smettem, K.R.J., Chittleborough, D.J. and Kirkby C. The hydraulic profile of an Ultic Haploxeralf from large undisturbed soil cores. (Submitted for publication). (1990).

62. Smettem K.R.J., Chittleborough, D.J., Richards, B.G. and Leaney, F.W. The influence of macropores on runoff generation from a hillslope soil with a contrasting textural class. J. Hydrol. 122: (1991) 235-252.

63. Smiles, D.E., Perroux, K.M. and Zeglin, S.J. Absorption of water by soil: Some effects of a saturated zone. Soil Sci. Soc. Amer. J., 44 : (1980) 1153-1158.

64. Smiles,D.E., Raats, P.A.C. and Knight J.H. Constant pressure filtration: The effect of a filter membrane. Chem. Engng. Sci., **37** : (1982) 707-714.

65. Stagnitti F., Parlange, M.B., Steenhuis, T.S. and Parlange, J.-Y. Drainage from a uniform soil layer on a hillslope. Water Resources Research, 22:(1986) 631-634.

66. Stapeldon, D.H. Changes and structural defects developed in some South Australian clays and their engineering consequences. Proc., Symp. of Soils and Earth Structures in Arid Climates, Adelaide : (1970) 62-71.

67. Terzaghi K. Reprinted in 'From theory to practice in soil mechanics', John Wiley, New York : (1923) 133-146.

68. Toll, D.G. A framework for unsaturated soil behaviour. Geotechnique, 40 (1) : (1990) 31-44.

69. Wheeler, S.J. An alternative framework for unsaturated soil behaviour. Geotechnique, 41 (2) : (1991) 257-261.

70. Wong H.Y. Infiltration of water into unsaturated soils. MSc(Eng) Thesis, University of Hong Kong, 100p. (1966).

71. Wroth, P. A brief review of the application of plasticity to soil mechanics. Proc. Symp. on the Role of Plasticity in Soil Mechanics. Cambridge : (1973) 1-11.

72. Zienkiewicz, O.C. The finite element method in structural and continuum mechanics. McGraw-Hill, London. (1977).

Earth Structures, Dams, Soil Improvements and Geofabrics – General Report

R. FELL
B.E., M.Eng.Sc., F.I.E.Aust.
School of Civil Engineering, University of New South Wales, Australia

1. INTRODUCTION

A total of twelve papers were submitted for this session, and the brief from the Organising Committee was to "summarise the submissions and present a review paper".

Granted the diversity of the papers presented, and the wide range of topics covered within the title of this session, it was clearly impracticable to present a review paper. I have opted, therefore, to summarise briefly the content of the papers and to comment where this appeared warranted. In several papers, additional information would have made the papers more useful to readers, and I have encouraged the authors to present this in the second volume of the conference proceedings.

In some cases, there are issues which warrant questioning or critical comment, and others where I feel that readers would do well to read alternative or additional information.

If there is a common theme to the review comments, it is that authors fail to include sufficient detailed information in the papers, to allow readers to properly relate the experiences described in the papers to their own projects. This is not always due to the lack of space required by the six page limit for the conference.

2. EMBANKMENTS AND EXCAVATIONS IN SOFT CLAY AND SILT

PALMER, S.J. — Seaview Marina, Geotechnical Design of Breakwaters.

This paper is an interesting case history which describes the investigation and design of a rubble mound breakwater which is up to 8.5m high. The breakwater is founded on 14m of "very soft to soft normally consolidated silt with some clay". The paper describes the soil properties, results of stability analysis, and pore pressures and settlements measured after construction.

There are some unusual features of the soils at the site:

- the effective friction angle of the silt is $\phi'=37°$ in triaxial compression. This is explained by the author as being due to the presence of 20% sand in the sample tested
- the undrained shear strengths determined by vane shear are very high. The lower bound envelope of values is equivalent to $S_u/\sigma'_{vo} = 1.1$.
- there is an artesian aquifer at the base of the silt, with a pressure 20kPa higher than mean sea level.

The monitoring after construction shows settlements in line with predictions, being about 0.7m one year after construction. Pore pressures monitored at mid depth of the silt layer show no dissipation over that period.

COMMENTS:

(a) The presence of 20% sand is unlikely to be the only reason for the high effective friction angle. By analogy with plots of residual strengths versus clay fraction percentage produced by Mesri and Cepeda-Diaz (1986), it would require around 40% to 50% sand before it would dominate properties. One would suspect that the silt must be very angular to give $\phi'=37°$.

(b) The undrained shear strengths obtained by the vane shear appear to be too high for a normally consolidated soil:

- Jamiolkowski et al (1983) give $S_u/\sigma'_{vo} = 0.23 \pm 0.04$.
- using the relationship between S_u and ϕ' in Wroth and Houlsby (1985) $S_u/\sigma'_{vo} = 0.43$, and using Davis in Thorne (1984), $S_u/\sigma'_{vo} = 0.23$ to 0.36 depending on Skempton's A_f.

There are several explanations:

- the soil is overconsolidated. This seems unlikely given the recent accumulation of silt at the site
- the vane is not testing in an undrained manner, ie. the soils are relatively high permeability
- the silt is cemented
- shells are affecting the vane testing.

The author's comment on this would be useful.

(c) The lack of dissipation of pore pressure shown in Figure 5 of the paper is inconsistent with the conclusion that "The accurate prediction of the rate of consolidation settlement (and hence pore pressure dissipation) has provided confidence as to the stability of the embankment".

The author is not alone in having contradictory data on pore pressure dissipation and settlement in silty soils, eg. McDonald (1988) describes similar phenomena.

It raises the question as to whether the strength gain required to raise the embankment has occurred. It would also seem possible that either the artesian pressures are having an influence on the pore pressures, and/or that the settlement is due to secondary consolidation. It would be useful to know what the pore pressures were prior to construction (including the effect of the artesian aquifer). The fluctuations in monitored pore pressure is possibly due to response to total stress loading changes under tidal water level changes. Such effects were noted in the paper by Thorne in this conference, and the general reporter knows of other instances where this has occurred.

It would also be useful to know what the imposed embankment load was for Figure 5, so that the pore pressure response due to the embankment could be assessed.

(d) The vane shear profile used for design is stepped, with relatively high values used at 3m. There does not appear to have been any reduction factor applied as recommended by Bjerrum (1973). Both would seem to be unconservative assumptions.

Overall this is an interesting case history, and it is hoped that some discussion will arise from these comments.

THORNE, C.P. — Trial Loading of Failed Section of River Bank, Fishermans Island.

This paper gives an unfortunately too brief description of a most interesting trial loading of a failed section of river bank. Details have been omitted which would have made the paper more valuable. Even so, the paper does provide some interesting data:

- The response of piezometers to tidal change. The piezometers showed no time lag, and responses varying from 0.7 to 0.3 of the total stress change due to the tidal fluctuation in water level
- pore pressure responses on loading which could be related to changes in principal stresses calculated using finite element analysis, yielding Skempton's pore pressure parameters within the range B=1, A=0.3 and B=1, A=1.0 (in some cases A > 1.0 was required)
- details of how allowance was made to correct for the relatively short length of the trial fill section, allowing adoption of higher strength values for design than those calculated by backanalysing of the trial fill.

COMMENTS:

(a) The range of Skempton's A values calculated, including values up to 1, is described as "representing an extreme response". Given that, these appear to have occurred in the piezometers near the fill/foundation interface and, hence, in material possibly disturbed by sliding, and near normally consolidation conditions, the high values would seem reasonable and consistent with those given by Skempton (1954) for normally consolidated soft clays. The lower values are consistent with slightly overconsolidated behaviour.

(b) The case history is an excellent example of where spending the necessary money on detailed geotechnical investigation and testing, and trial loading has resulted in considerable savings in remedial works. It would have been a brave engineer to ignore the low strengths obtained in residual shear testing without the proof of the trial loading.

(c) As indicated above, the paper would have been more valuable if more details were provided. Possibly the following information could be provided in the second volume of the conference proceedings:
  - the circumstances and backanalysis of the original failure, and details of the remedial works
  - comparison of the Skempton A values obtained in the paper, with those in the triaxial tests
  - discussion of the triaxial extension test(s), and if there was any reduction in undrained shear strength in extension, as compared to triaxial compression tests, as would be expected based on information published by Jamiolkowski et al (1985) and others
  - the time between the failure and the trial
  - a larger version of Figure 2, and Figure 3, with piezometer numbers.

BRABHAHARAN, P. — Ground Improvement to Reduce Geotechnical Risk: Waingate Final Water Treatment Plant.

This paper gives a general description of the use of stone columns to reduce settlements, and to increase bearing capacity under retaining walls and buildings founded on 5m to 12m of soft to firm colluvial clayey silt. The columns were constructed by compacting granular fill through 910mm dia steel casing, withdrawing the casing progressively. The columns were successful in reducing settlements.

The water treatment plant site was identified as being subject to previous overall instability, and subhorizontal drains were installed. Water was observed to flow from most of the drains, with significant flows from some.

COMMENTS:

The paper suffers from lack of detail, particularly in respect to:

- the location and depth of the subhorizontal drains
- piezometric response to the subhorizontal drains (did they reduce the pore pressures, and by how much?)
- effective stress properties and the analysis of overall stability
- the magnitude of settlements including "creep effects" which are likely to occur with the stone columns.

3. DESIGN OF EMBANKMENTS FOR SEISMIC LOADING

ELIAS, D.C., NOVELLO, E.A. and GLENISTER, D. — Design Procedure for the Seismic Analysis of Earth Structures.

This paper presents a simplified design procedure for seismic analysis of earth structures such as dams, tailings dams and embankments. It requires as input the probability, magnitude and maximum ground acceleration of the design earthquake; either in-situ SPT or CPT data, or laboratory cyclic triaxial or simple shear tests, from which liquefaction potential can be assessed; and the geometry of the embankment.

COMMENTS:

(a) While the method is "simplified" compared to full scale dynamic finite element analyses, it encourages the use of cyclic triaxial tests for the design of embankments. In most cases in Australia, this would be an unnecessarily complicated and costly approach for design of embankments, dams and tailings dams constructed of compacted earth and rockfill.

ICOLD (1986), who tend to take a fairly conservative but realistic approach, quote Seed (1979):

> "virtually any well-built dam on a firm foundation can withstand moderate earthquake shaking, say with peak accelerations of about 0.2g, with no detrimental effects"

and

> "since there is ample field evidence that well-built dams can withstand moderate shaking with peak accelerations up to at least 0.2g, with no harmful effects, we should not waste our time and money analysing this type of problem — rather we should concentrate our efforts on those dams likely to present problems either because of strong shaking involving accelerations well in excess of 0.2g or because they incorporate large bodies of cohesionless materials (usually sands) which, if saturated, may lose most of their strength during earthquake shaking and thereby lead to undesirable movements".

(b) Tailings dams constructed of sand or silty sand, using the upstream or centreline methods, need to be considered more carefully. In this case, the author's approach may be justified but readers should also refer to the other "simplified" methods suggested by Lo and Klohn (1990), McLeod, Chambers and Davies (1991), Lo, Klohn and Finn (1991). For more important structures, a method such as that outlined by Finn et al (1990) might be employed.

(c) In many cases, it will be the potential for liquefaction of saturated granular soils in the dam or embankment foundation which will be critical. An initial assessment of this can be done using the method described by Seed and de Alba (1986), with allowance for static driving shear stresses and in-situ effective stresses greater than 100kPa described by Seed and Harder (1990). The general reporter's experience is that this will rule out most sites in Australia as having a problem (but not all).

(d) The general reporter does not agree with the recommendation in section 2 of the paper that "we recommend that an annual probability of exceedance of 1:500 is used for structures with short operating or saturated lives, such as tailings dams, and an annual probability of exceedance of 1:1000 for structures with long design lives such as railway embankments and water supply dams". The design earthquake should be assessed on the basis of the hazard rating of the structures, ie. the consequences of failure of the dam (in ANCOLD terms). ANCOLD (1983). and ICOLD (1986) give guidelines.

4. SEEPAGE CONTROL FROM STORAGE DAMS

O'FLAHERTY, P.J., BARKLEY, D. and TRUSCOTT, E.G. — Seepage and Salinity Control for the Wurdee Boluc Reservoir Enlargement Project.

This paper describes the investigation and design of seepage control measures to allow control of salinity surrounding the Wurdee Boluc Reservoir, when its full supply level is raised. The reservoir is underlain by tertiary clays, silts, silty sand and sand, and tertiary basalt along one boundary of what was a natural lake. Details are provided of seepage analyses, a trial drainage trench and the design of the drainage trench and relief wells, which are needed to control piezometric pressures in saline aquifers. The paper describes how a staged "observational" approach has been adopted to reduce the costs.

COMMENTS:

(a) The permeability of the "organic clay", "surface clay", and "cover clay" are shown as in the range approx 10^{-8} m/sec to 10^{-9} m/sec. The permeability of the basalt is shown as 10^{-7} m/sec to 10^{-8} m/sec approx. These values appear very low for naturally occurring clays, which usually have fissures, relic joints, root holes and/or other lamination and deposits which result in mass permeabilities orders of magnitude higher than those quoted. The value for basalt, in particular, seems low. The permeabilities are said to be based on laboratory and field permeability tests, but no details are given. If the values are based on "pump in" type tests in boreholes, the general reporter would doubt their correctness. Again, it would be the basalt clays where subvertical defects are likely to be present where the greatest error would occur. That this layer may be more permeable is indicated by the recording of saturation and waterlogging along the edge of the basalt flows. It would be useful if the authors commented on the methods used to assess the permeabilities.

(b) The authors adopt a permeability of 10^{-6} m/sec for a slurry trench cutoff wall which was assessed as an alternative. This figure is consistent with the data published by Powell and Morgenstern (1985), and the general reporter would agree it is a realistic figure.

(c) Two and three dimensional seepage analyses were carried out, which included modelling of pressure relief wells. It would be useful to know how the pressure relief wells (which are to be spaced 20m apart) were modelled in the two dimensional model. It would also be useful to know what percentage of seepage is intercepted by the wells.

(d) It is indicated that the seepage collector trenches were sited near the property boundary, rather than at the toe of the dam. While this might be desirable from the viewpoint of intercepting seepage passing outside the property, it is not generally the best location when considering control of seepage pore pressures, under and downstream of the dam. With the presence of confirmed aquifers , such as those at this site, one would normally place the wells at the toe of the dam, or even under a berm to ensure that pore pressures are controlled against the possibility of "blow out" failure.

It is noted that there are few piezometers downstream of the collector trenches, which means that monitoring of the effectiveness of the trenches and wells will apparently be limited.

5. EARTH AND ROCK REINFORCEMENT

HAUSMANN, M.R., SADLIER, M.A.. and BECKINDALE, C. — Geomembranes, Geotextiles and Slope Stability.

This is a useful paper which describes some of the practical problems which may be encountered in designing heap leach facilities for gold or other treatment, where a geomembrane is used as a liner to the base of the heap. It is shown that supporting the geomembrane on geotextile can result in instability, because the friction angle between the two may be low. The information presented would have use in other applications, such as design of landfills.

HOWARTH, D.F. and RENWICK, M.T. — The Development, Testing and Application of a Non-Steel Tendon for Artificial Ground Support.

This paper describes the properties and some application of a highly oriented polyethylene "bar" or "rock bolt". It is claimed to have several advantages over steel and other non-steel bars in some applications, although creep and low melting point and poor bonding resistance between the bolt and grout would seem to be restricting factors in some applications.

BOYD, M.S. — The Application of Reinforcement Materials for Earth Structures — Risk and Acceptability.

This is a useful paper describing the concepts which may be applied to assist in deciding on which system of soil reinforcing might be applicable to a particular project, depending on the assessed risk. In this context, risk is defined in broad terms as a function of "hazard" (the consequences of failure of the structure), the "criticality of the reinforcement" to the structure in terms of stability and deformation, and "uncertainty", ie. the degree of confidence one has of long term behaviour in the particular project environment.

COMMENTS:

(a) The paper emphasises applications where vertical or near vertical faces are required for the structure, where the creep characteristics of polymer reinforcements is potentially more of a problem than it will be in other applications, where some minor long term deformation will not be so important.

(b) The difference between "durability experience", ie. the length of time a particular type of reinforcement has been used in practice, and durability, ie. the ability of the reinforcement to maintain its desired function in the environment of the particular project, is not made clear enough in Table 1. Strictly, it is the latter which is more important.

(c) When discussing the consequences of failure the mode of failure will be important, eg. failure of "inextensible" (the author's term) strips due to strip fracture will occur with little warning, but structures reinforced with the more "extensible" materials should exhibit large strains before collapse, allowing remedial action, and/or reduction of the hazard.

FULLER, S.R.. and WALLACE, K.B. — Strain Compatibility and Design Criteria for Reinforced Earth.

This is an interesting paper which describes the results of analysis of reinforced soil slopes using an analysis method which modifies the Bishop limit equilibrium method, to make some allowance for compatability of strain in the reinforcement and the soil. The results are compared to an elasto-plastic analysis using the finite difference program FLAC.

The "modified displacement method" (MDISMET) has been developed into a computer program by the first author, and can be used as a design aid.

COMMENTS:

(a) Unfortunately the paper does not describe how the displacements along the trial rigid body surfaces within the limit equilibrium analysis are calculated, so one cannot get any feel for the validity of the approach. The method apparently modifies the normal stresses estimated by Bishop analysis, but again details are not provided.

(b) The paper shows that the normal stresses calculated using Bishop, are higher than those using the Fellenius assumption when the angle of the base of the slice exceeds 40°, and uses the FLAC results to indicate the Bishop results are more reasonable. As a word of caution, my colleague Garry Mostyn has noted some inconsistencies with the Bishop method for steep slopes and failure surfaces, such as those being analysed by the authors. In particular, the factor of safety is calculated to increase, as ϕ' decreases. The reason for this is being explored.

(c) There seems to be an inconsistency between Figures 3 and 5, in that from Figure 3 one would expect the normal stresses calculated from the Fellenius method to be lower than those calculated using Bishop, not higher as shown in Figure 5. The authors might clarify this.

(d) Given that FLAC allows the estimation of stress strain behaviour of the soil and the reinforcement, rather than using some empirical approximation to estimate displacements, and the program's ready availability, there would seem some argument that it would be better to concentrate on using FLAC rather than MDISMET. It is not clear what benefits MDISMET would have over FLAC.

6. EXPANSIVE SOILS AND ROADS

HOLDEN, J C. — Reduction of Pavement Damage for Expansive Soils Using Moisture Barriers.

This paper presents the results of trials where vertical moisture barriers, consisting of polythene sheeting placed in trenches backfilled with clay, were used to control seasonal heave of the pavement. For the site of the trials, barriers up to 1.8m deep were not deep enough to prevent significant seasonal movements caused by roadside trees. A barrier 2.5m deep greatly reduced seasonal movements.

The information would be useful not only for road engineers, but would be relevant to building construction.

COMMENTS:

(a) The data would be more useful if shrink-swell test results, suction properties and water content profiles had been presented. Atterberg limits are presented, but they are not a good guide to shrink-swell behaviour

(b) It is indicated that "to substantially stop the lateral moisture migration in the subgrade, the moisture barrier must extend below the depth of any crack which would provide an easy moisture path through the relatively impermeable clay". This could be misunderstood. It is true that vertical cracks will allow easy ingress of rainwater, and hence facilitate swell; and that the depth of cracking is a guide to the depth of seasonal moisture variation (although moisture variation will often extend below the depth of cracking); but the crack will prevent moisture transfer horizontally. Apart from roots, the transfer of moisture horizontally from under the pavement is by soil suction, which will be broken by a crack.

LOOK-HONG, B., WIJEYAKULASURIYA, V.. and REEVES, I. — A Method of Risk Assessment for Roadway Embankments Utilizing Expansive Materials.

This paper sets out to evaluate the risk of distress of road pavements to shrink-swell effects in the subgrade, when roads are constructed on embankments. The paper presents a useful literature review on many of the issues which have to be considered, as well as some data from two field sites.

COMMENTS:

(a) A reader is likely to be left somewhat confused as to what is meant by "risk", because the terminology used in the paper is not consistent. At the beginning of the paper risk is defined as

[Risk] = [Hazard] x [Vulnerability] x [Value]

where	Hazard appears to be defined as the probability of occurrence
	Vulnerability as the degree of damage or loss of functions
and	Value as the value of the road and/or the value to users

but no clear definition is given.

In the next section "hazards" which may produce distress are detailed, including landslips, consolidation of compressible clays and volume changes in expansive clays.

This definition of "hazard" is maintained in section 3.1, but neither definition or assessment seems to be fed back into the risk equation.

Vulnerability is assessed in terms of the swell potential of a pavement under likely changes in soil moisture content, and this is related to acceptable differential movement criteria. However, this is done on acceptable limits (Table VIII) rather than in any way which could allow use of the risk equation. There is no further discussion of "value". Later in the paper (4.1) risk seems to be equated to maximum swell potential, and related to Table VIII. To further confuse the issue in 6.0, Figure 7 is described as showing the vulnerability of embankments to expansive behaviour, but is titled construction risks.

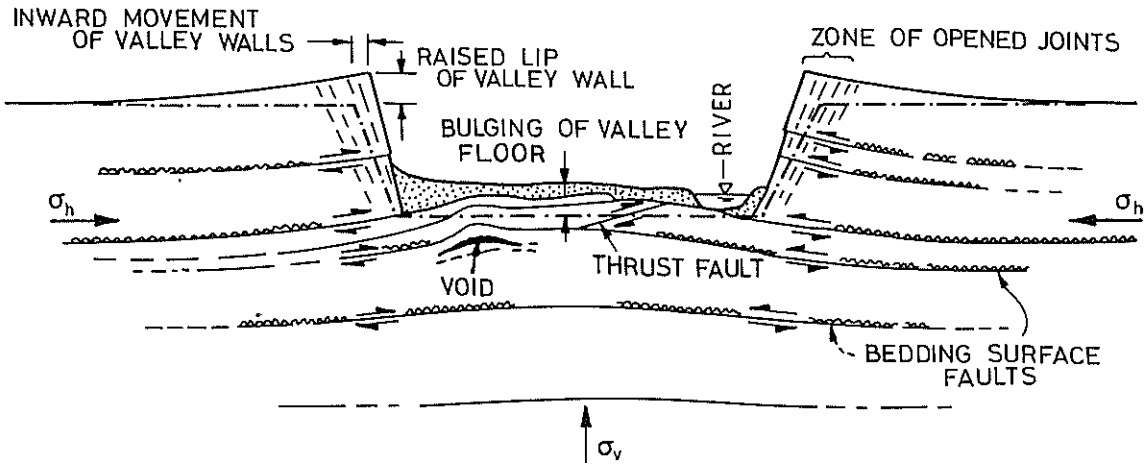

Figure 1 Complex valley structures related to stress release in weak, flat lying rocks (from Fell, MacGregor and Stapledon, 1992, based on Patton and Hendren, 1972).

(b) These problems are unfortunate, because there are some useful concepts in the paper. In reality, the paper seems to set out to develop a method for assessing the magnitude of potential swell, and comparing this to acceptable criteria, and doesn't assess "risk" as originally defined. Methods of construction which will reduce the potential swell are described, including control of construction water content to be near the in service equilibrium water content.

(c) The in service equilibrium water content was found to be near the plastic limit of the embankment soil, and for the soils at the test site, this was 1.3 times the optimum moisture content. Unfortunately, whether this is "standard" or modified optimum water content is not stated. The paper also uses the term relative dry density for what is more commonly called density ratio.

(d) Observed changes in water content at varying depths are shown in Figures 4 and 5, but it is not clear whether these are under the pavement or adjacent. The large changes recorded in Figure 5 would appear to indicate they were not beneath a pavement. It would be helpful if the authors would clarify these points of detail.

7. BEDDING SURFACE SHEARS

JAMES, P.M. — Flexual Slip, An Often Neglected Hazard.

This paper presents a case for engineers and geologists to be aware of the likelihood of the presence of flexual slip seams, particularly in interbedded argillaceous and stronger sedimentary rocks, and metamorphic rocks. Like the general reporter, the author's experience has been that these features, also known as bedding shears, bedding surface faults, or intraformational shears are often missed during site investigations, sometimes with severe consequences, as the effective shear strength on the planes is often near residual.

COMMENTS:

(a) The paper fails to refer to the paper by Hutchinson (1988), which discusses in more detail the formation of such features, and readers are encouraged to refer to that paper. The paper also fails to acknowledge the other potential mechanisms of formation. These include differential consolidation during the formation of the rock, differential slip along bedding and joints, faulting, and stress relief.

One of the most common causes of bedding surface shears is the differential movements which occur on stress relief as valleys are formed. Figure 1 shows examples of such features.

(b) The concentration of differential movement on the contact between "weak" and "strong" layers of rock, when in-situ ground stresses are relieved, has recently been observed in several excavations in the City of Sydney and also occurred in the 40m deep excavation for the Sydney-Newcastle Freeway near Wyong. Given this evidence, there would be a case for expecting the formation of such shear zones in deep excavations in interbedded sedimentary rock, eg. in coal mines, even if they are not present before excavation. This may be considered a form of progressive failure but the result is the same, ie. low strength bedding plane shears.

8. REFERENCES

1. ANCOLD (1983). Guidelines for dam instrumentation and monitoring systems. Australian National Committee on Large Dams.

2. Bjerrum, L. (1973). Problems of soil mechanics and construction on soft clays. State-of-the-art report. Proc. 8th ICSMFE, Vol 3, pp. 111-159.

3. Fell, R., MacGregor, J.P. and Stapledon, D.H. (1992). Geotechnical Engineering of Embankment Dams. Balkema.

4. Finn, W.D., Yogendrokumar, N., Lo, R.C. and Ledbetter, R.H. (1990). Seismic response analysis of tailings dams. ICOLD/ANCOLD Int. Symp. on Safety and Rehabilitation of Tailings Dams, Sydney.

5. ICOLD (1986). Earthquake analysis procedures for dams. International Commission on Large Dams. Bulletin 52.

6. ICOLD (1989). Selecting seismic parameters. Bulletin 72.

7. Jamiolkowski, M., Ladd, C., Germaine, J., Lancellotta, R. (1985). New developments in field and laboratory testing of soils. 11th ICSMFE.

8. Lo, R.L. and Klohn, E.J. (1990). Seismic stability of tailings dams. ICOLD/ANCOLD Int. Symp. on Safety and Rehabilitation of Tailings Dams, Sydney.

9. Lo, R.C., Klohn, E.J. and Finn, W.D.L. (1991). Shear strength of cohesionless materials under seismic loadings. IX Panamerican Conference on Soil Mechanics and Foundation Engineering, pp. 1047-1062.

10. McLeod, H., Chambers, R.W. and Davies, M.P. (1991). Seismic design of hydraulic fill tailings structures. IX Panamerican Conference on Soil Mechanics and Foundation Engineering, pp. 1063-1082.

11.. Mesri, G. and Cepeda-Diaz, A.F. (1986). Residual shear strength of clays and shales. Geotechnique 36, No 2.

12. Patton, F.D. and Hendron, A.J. (1972). General report on mass movements. Proc. 2nd Intl. Congress of International Association of Engineering Geology, V-GR1-V-GR57.

13. Seed, H.B. (1979). Consideration in the earthquake resistant design of earth and rockfill dams. Geotechnique 29, pp. 215-263.

14. Seed, H.B. and De Alba, P. (1986). Use of the SPT and CPT tests for evaluating the liquefaction resistance of sands. In-Situ 86, Conference on Use of In-Situ Tests in Geotechnical Engineering, ASCE Geotechnical Special Publication No 6, Ed. S.P. Clemence.

15. Seed, H.B. and Harder, L:.F. (1990). SPT-based analysis of cyclic pore pressure generation and undrained residual strength, in H. Bolton Seed Memorial Symposium Proceedings. Bi Tech Publishers.

16. Skempton, A.W. (1954). The pore pressure coefficients A and B. Geotechnique Vol 4, pp. 143-147.

17.. Thorne, C.P. (1984). Strength assessment and stability analyses for fissured clays. Geotechnique 34 No 3.

The Application of Reinforcement Materials for Earth Structures – Risk and Acceptability

M.S. BOYD
B.E., M.Eng.Sc., M.I.E.Aust.
Managing Director, Reinforced Earth Pty Limited, Australia

SUMMARY: Reinforcement materials for the reinforcement or stabilisation of earth structures come in many forms. The key characteristics of earth reinforcement are strength, extensibility, soil interaction and durability. In applying reinforcement materials to earth structures an assessment needs to be made of risk. Risk is defined as function of hazard, vulnerability and uncertainty. Hazard relates to the potential for loss of life or function. Vulnerability relates to the criticality of the reinforcement to the performance and stability of the structure. Uncertainty relates primarily to the ability to predict behaviour over the service life required. Application categories for earth reinforcing materials are derived which are based on an overall risk assessment of both the materials and the application. Such categories can be used for the application of material types or for the definition of appropriate safety factors.

1 INTRODUCTION

Since REINFORCED EARTH was invented by Henri Vidal (1966), the technology has been applied to many thousands of structures and its behaviour and application limits are well understood. In the last decade, a number of alternative soil stabilisation and reinforcement systems have been developed. Reinforcement materials are metallic or polymeric, and in strip, bar, grid, mesh or textile form. In particular, a number of reinforced soil wall systems have been promoted with varying degrees of similarity to the REINFORCED EARTH system. Reinforced soil wall systems can be applied efficiently to many structural applications where a high degree of security is required (eg bridge abutments, railway embankments, dams etc). The problem for designers and users is to understand both the similarities and the differences between these systems and to develop appropriate acceptance criteria (Arup,1990). The aim of this paper is to describe a rational basis upon which such criteria can be derived, taking into account the risk associated with both the materials and their application.

2 REINFORCEMENT

Reinforcement may be of different materials and form. The characteristics of primary importance in their application as earth reinforcement are:

- strength
- extensibility
- soil interaction
- durability

These characteristics differ for each of the reinforcement types presently available for earth reinforcement (Table 1). Each of these materials and forms work, but they work in different ways. It is important to understand how they work so that the appropriate design parameters and factors of safety can be applied to different applications, particularly in vertical, or near vertical, faced reinforced soil wall structures where the behaviour of the reinforcement has a direct and usually critical influence on the behaviour of the structure (Boyd,1990).

TABLE 1

Reinforcement Characteristics

Material & Form	Strength	Extensibility	Soil Interaction	Durability Experience
Steel, Ribbed strip	High	Inext.	Friction + Passive	Long
Steel, Grid, Bar mat	High	Inext.	Passive	Long
PET, Strip, Mesh	High	Ext.	Friction	Medium
hdPE, Grid	Medium	Ext.	Passive	Medium
Steel, Woven Mesh	Medium	Ext.	Passive	Medium

2.1 Strength

The allowable design strength per layer may be as high as 100 kN/m or more for both metallic and polymer systems whereas some polymer geotextile systems may provide less than 10 kN/m. The strength of the reinforcement must be predictable over the design life of the structure, taking into account metal corrosion or polymer ageing.

Metal corrosion and polymer ageing are different processes. Design factors must recognise this. Metal corrosion is a physical deterioration resulting in loss of material over time. Sacrificial material is usually provided to "protect" the base section required. The life of this material can be equated to known corrosion rates from the experience of such metals in similar environments for long periods. Polymer ageing is the entirety of all the irreversible chemical and physical processes over time. These processes include - weathering, construction damage, creep, structural change and chemical attack. They are influenced by temperature and may be compounded by the synergistic effects from several processes. Design factors must be applied to cover all possible processes and changes which may occur over the life of the structure based on generally short term data.

2.2 Extensibility

The extensibility or stiffness of the reinforcement has a fundamental influence on the behaviour and performance of reinforced soil structures. The very low working strains (<0.1%) exhibited by inextensible reinforcement promote coherent gravity block behaviour in reinforced soil wall structures, whereas the much larger working strains (>3%) exhibited by extensible reinforcements promote a tied-back wedge action. This can have a significant impact on structural behaviour.

The load/extension characteristics of metals and polymers can be quite different. For comparable strength levels, deformations can be between one and two orders of magnitude different (10 to 100 times). Even for high strength materials, there can still be a large divergence (Fig.1).

The variability of the stiffness characteristics of reinforcement types is highlighted in Fig.2, taken from data presented by Mitchell and Christopher (1990). Stiffness is shown to be function of both material and form, as steel woven mesh exhibits an extensibility closer to that of polymer materials. Default stiffness ratios for inextensible and extensible reinforcement are 75,000 kN/m/m and 2,500 kN/m/m respectively. (Christopher et al, 1990).

Strain compatibility considerations significantly effect both soil and reinforcement stresses and accordingly effect reinforcement design. The time dependency of load/deformation behaviour (creep) has the potential to alter both the state of stress (stability) and the strain behaviour over the life of the structure. For wall structures this can be critical from a serviceability viewpoint. This is recognised in the draft BS8006 (1991) which provides for strains in the reinforcement to not exceed 0.5% for abutments and 1.0% for walls. For long term structures, where the life of the structure is directly related to the life of the reinforcement, caution is required for polymer materials as there simply is no long term creep data available, comparable to such design lives.

2.3 Soil Interaction

The transfer of stress between the soil and the reinforcement is fundamental to an effective soil reinforcement system. Such transfer may be by way of friction or passive (anchorage) resistance depending on the form of the reinforcement and the physical characteristics of the soil.

The shear strength and dimensional stability of fine grained (cohesive) soils, are effected by moisture content. Coarse grained (granular)

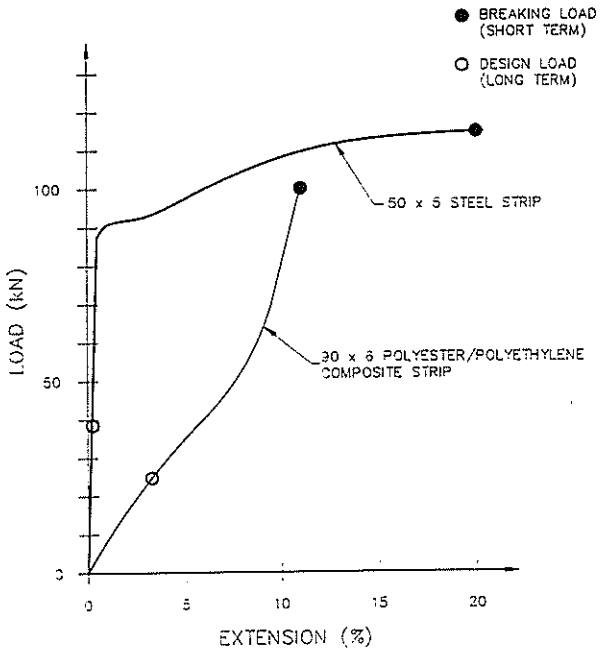

Fig. 1. Load Extension Relationship for Metal and Polymer Reinforcement

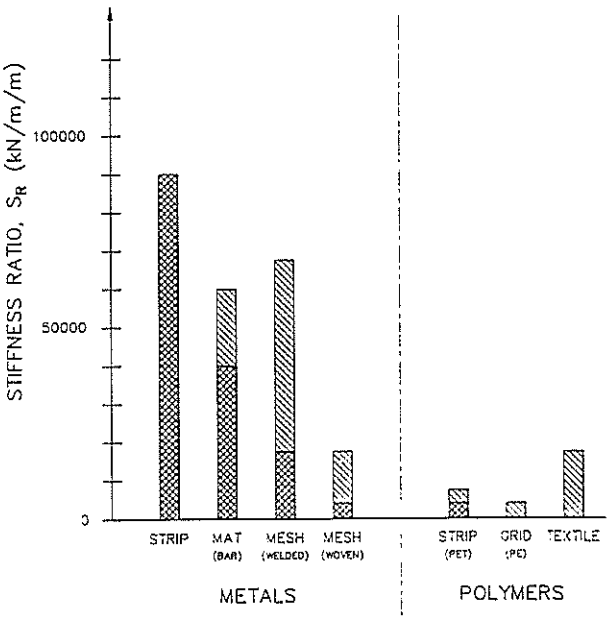

Fig.2 Stiffness Characteristics of Reinforcement (after Mitchell and Christopher, 1990)

soils promote mechanical interlock and are dilatent when sheared promoting good soil interaction with high dimensional stability. Smooth strips rely on frictional transfer. Grids and meshes rely on mechanical interlock. Inextensible reinforcement will mobilise more resistance over the length of the reinforcement, and consequently will promote more composite behaviour within the structure due to its strain compatibility with dense granular earth.

Soil reinforcement interaction factors are compared for several reinforcement types in Fig.3. The predictability and repeatability of such data is important in determining appropriate design factors.

2.4 Durability

All materials will lose strength and change their strain characteristics with time. The only complete method of prediction is from data taken from such materials subject to the same stress and environmental conditions as they would be in the reinforced soil structure, for the time equivalent to the service life.

The present state of knowledge of long term behaviour of materials used as soil reinforcement has been summarised by Jailloux and Segrestin (1988).

For design, the concept of partial factors applied to long-term characteristic strengths is considered appropriate to determine basic design strengths. The draft BS8006 (1991) recommends factors for:

- material variability
- test data extrapolation
- construction damage susceptibility
- environmental attack

Furthermore, it is important that not only should the reinforcement not fail in tension during the life of the structure, but also the strains in the reinforcement should not exceed a prescribed value. This approach is described in Fig.4.

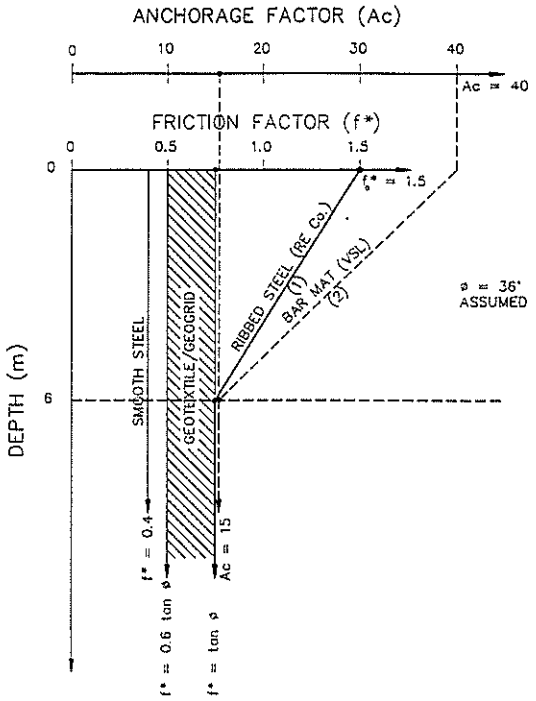

Fig.3 Soil Reinforcement Interaction Factors

Ingold (1991) emphasises the need to apply a consistent approach to both metallic and polymer materials and provides guidelines for partial factors for polymeric materials.

3 RISK

In order to apply reinforcement materials to structures an assessment needs to be made of risk.

Risk is a function of both the potential for failure (vulnerability and uncertainty) and the consequences of failure (hazard). The

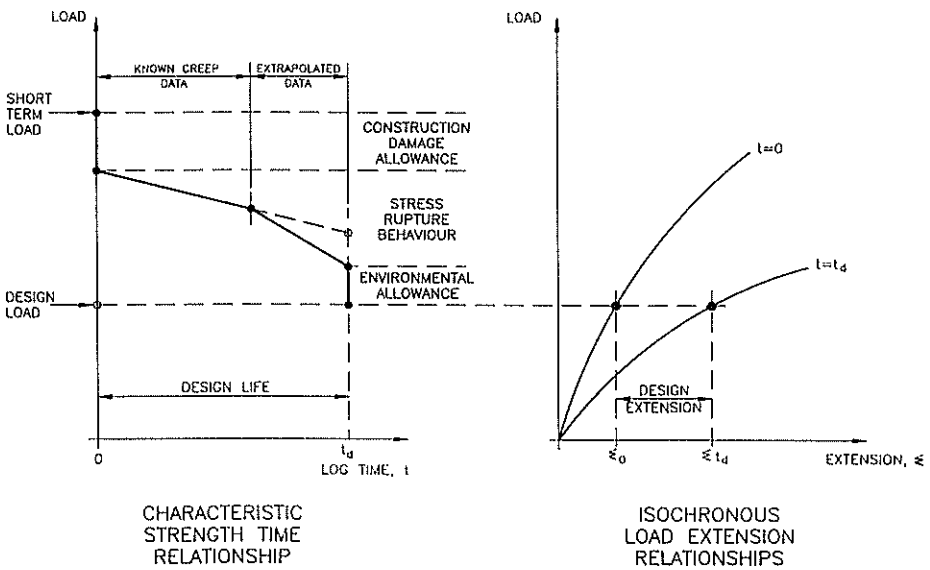

Fig.4 Reinforcement Design for Load and Extension with respect to Design Life.

potential for failure may be increased by reinforcement vulnerability (due to reinforcement criticality) and uncertainty (due to reinforcement experience). The consequences of failure may be increased hazard from loss of life, loss of function and/or economic loss.

Variable design factors should be applied to both the potential for, and the consequences of, failure.

3.1 Hazard

High hazard potential exists where the consequences of failure include the potential for loss of life, excessive economic loss and loss of access on principal roads, railways etc. Low hazard potential could mean no expected loss of life, minimum structural damage and loss of access on minor routes only as defined in the Geotechnical Manual for Slopes used in Hong Kong (GCO,1984).

This differentiation of hazard is reflected in the minimum factors of safety provided for different ultimate limit states in the Model Specification for Reinforced Fill Structures, Geospec 2 (GCO,1989). These are summarised in Table 2.

TABLE 2

Minimum Factors of Safety

Ultimate Limit States		Risk Category	
		High	Low
External	Slope	1.4	1.2
	Sliding	1.5	1.2
	Bearing	2.0	1.6
Internal	Pull-out	1.8	1.5
	Tension	1.7	1.4

Extract from Table A1, Geospec 2 (GCO,1989)

The recommendations issued by the French Ministry of Transport (LCPC/SETRA,1979) distinguish two categories of structure based on their hazard potential:

- "Ordinary" structures
- "High security level" structures

Factors of safety for the limit state of the resistance of the reinforcing material with respect to tension and adherence resistance are summarised for the two categories in Table 3.

TABLE 3

Limit State Coefficients

Limit State	Ordinary	High Security
Internal Tension	1.50	1.65
Adherence	1.35	1.50

Extract from French MoT recommendations (LCPC/SETRA,1979)

The draft BS8006 defines categories of structure depending on the ramifications of failure. This is akin to the hazard potential described above. Furthermore, these categories take some account of the vulnerability of the structure by describing examples of structures for each category which in some cases infer reinforcement criticality. Partial factors are defined with respect to the type of structure and the consequences of failure. These are outlined in Table 4.

TABLE 4

Categories of Structure depending on ramification of failure

Category	Partial Factor	Example of structure
1 (Low)	Not Applicable	Retaining walls and slopes less than 2m in retained height where failure would result in minimal damage and loss of access
2 (Medium)	1.0	Embankments and structures where failure would result in moderate damage and loss of service
3 (High)	1.1	Abutments, structures directly supporting motorway and trunk roads or railways or inhabited buildings, dams, sea walls and slopes, river training walls and slopes

Extract from Table 6.2 draft BS8006 (1991)

A quantitative estimate of the consequences of failure can be made with respect to the structure geometry and the failure mechanism (TAI,1990). This provides a definition of hazard potential. Limiting clearances for loads and associated structures can be defined for different levels of security with respect to material properties and slope geometry as shown in Fig 5.

3.2 Reinforcement Influence

The vulnerability of the structure can be related to the reinforcement where such reinforcement influence is critical to the behaviour of the structure.

The criticality of the reinforcement depends on the relationship between the loads applied, the reinforcement forces and the earth resistance mobilised. Where the behaviour of the structure is directly related to the behaviour of the reinforcement, the reinforcement is critical. This is the case for vertical faced, load bearing structures particularly where direct permanent loads are applied to the active zone. For structures with concrete facing elements directly supported by the reinforcement, the reinforcement behaviour is also critical as the consequences of connection failure may be serious although not necessarily compromising the overall stability of the structure.

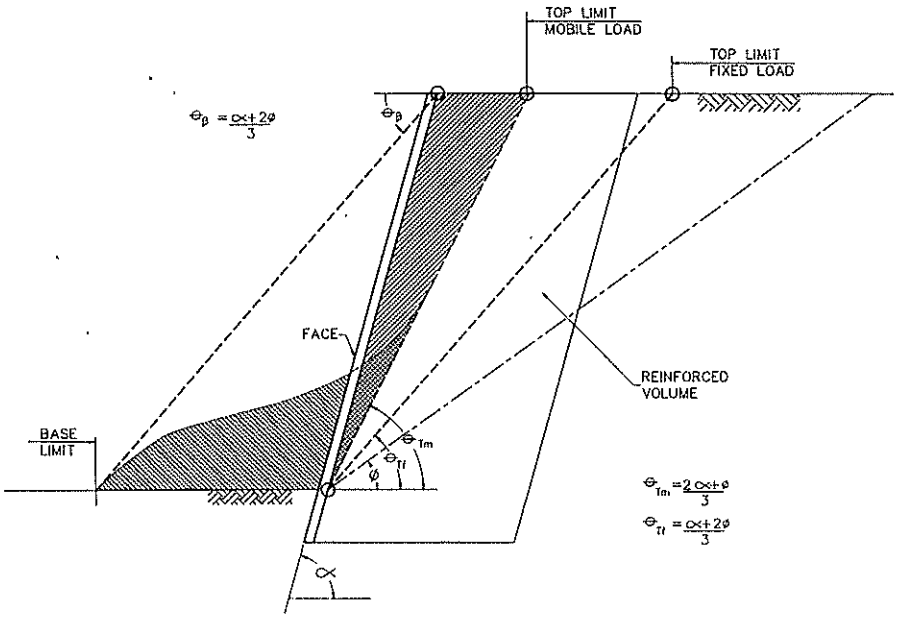

Fig.5 Proposed Clearance Limits for Low Hazard Potential

A distinction may be made between stabilisation and reinforcement in the context of criticality. Stabilisation implies improvement through an indirect influence on material properties and behaviour characteristics. Reinforcement implies direct support through primary structural action.

Rowe (1987) states that only products with sufficient strength, modulus or pullout resistance can be expected to provide significant reinforcing, however, this is not to suggest that a geosynthetic with properties less than that required to provide reinforcement will not improve performance. This could occur by, for example, their functions as separators, filters or drainage mediums.

The criticality or otherwise of reinforcement can be demonstrated by the analysis of a simple wedge in a reinforced soil wall structure as illustrated in Fig 6.

The resultant wedge force Ta, must be resisted by the sum of the reinforcement resistances mobilised across the wedge boundary. This resistance is the lesser of the frictional adherence resistance or tensile (strength) resistance of the reinforcement.

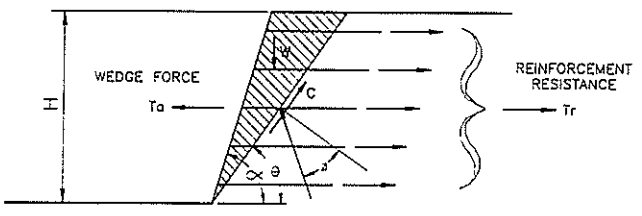

Fig.6 Simple Wedge Analysis of Reinforced Soil

The resultant wedge force can be significantly reduced by reducing the face angle (α), increasing internal friction (ϕ) or mobilising a cohesion (c). This is demonstrated in Table 5. The acquisition of a nominal cohesion to a densely compacted granular earth in time may be sufficient to counteract the wedge force and therefore not mobilise the reinforcement resistance. A cohesion value of 10 kPa could support a vertical face to 3 metres or a sloped face (α = 60 deg) to more than 6 metres. (TAI, 1990). Reinforcement in such cases may not therefore be critical in the longer term.

TABLE 5

Simple Wedge Analysis

Wall Slope α (deg)	Internal Friction ϕ (deg)	Cohesion c (kPa)	Resultant Wedge Force Ta(max) (kN/m)	Reinf. Resist. Tr (kN/m)	Stability Factor Tr/Ta
90	30	0	120	120	1.0
		10	51		2.4
	36	0	93		1.3
		10	32		3.8
	42	0	71		1.7
		10	18		6.7
60	30	0	41	41	1.0
		10	0		-
	36	0	25		1.6
		10	0		-
	42	0	13		3.2
		10	0		-

Assumed wedge height (H) = 6 metres and soil density (γ) = 20 kN/m3
Reinforcement resistance based on ϕ = 30 deg and c = 0 case for Tr/Ta = 1.0

3.3 Service Life

The uncertainty of behaviour is related to time and experience. Some materials and systems have only a limited experience as earth reinforcement and recourse will need to be made to predictions based on time extrapolation or experience in other applications.

Service life requirements are generally defined in the following terms:

- long term or permanent (100 +/- 50 years)
- medium term or semi-permanent (30 +/- 20 years)
- short term or temporary (<10 years)

4 APPLICATION CATEGORIES

On the basis of these considerations it is possible to define application categories which recognise all the elements of risk - the consequences of failure of the structure (hazard), the potential for failure of the reinforcement due to vulnerability (reinforcement criticality) and uncertainty (reinforcement experience). These are described in Table 6.

Where the risk is described as high, medium or low, the appropriate materials and systems can be defined. Furthermore, where additional security levels are required, appropriate partial (safety) factors can be defined.

TABLE 6

Application Categories

Category	Service Life	Reinf. Influence	Potential Hazard	Risk
1	Long	Critical	High	High
2	Long	Critical	Low	Medium
3	Long	Non Crit	High	Medium
4	Long	Non Crit	Low	Low
5	Medium	Critical	High	High
6	Medium	Critical	Low	Medium
7	Medium	Non Crit	High	Medium
8	Medium	Non Crit	Low	Low
9	Short	Critical	High	High
10	Short	Critical	Low	Medium
11	Short	Non Crit	High	Medium
12	Short	Non Crit	Low	Low

5. CONCLUSIONS

Earth reinforcement systems can vary considerably in material and form. The key characteristics required of earth reinforcement are outlined in order to understand the impact of their differences in structural applications, particularly for reinforced soil wall systems. A rational approach to the development of selection and application criteria is presented based on the risk assessment of both the systems and the applications.

6. REFERENCES

ARUP GEOTECHNICS PTY Ltd. (1990). Reinforced Soil Wall System - Technical Direction. Report prepared for the Roads and Traffic Authority of New South Wales. Sydney.

BOYD, M.S. (1991). Elements of Reinforced Soil Wall Systems with particular reference to the design and application of Inextensible (Metallic) Reinforcement Systems. Ground Modification Seminar No.1 The University of Technology, Sydney.

BS 8006 (1991). Code of practice for Strengthened/Reinforced Soils and Other Fills. (Draft). British Standards Institution. London, pp 232.

CHRISTOPHER, B.R. et al (1990). Design and Construction Guidelines for Reinforced Soil Structures. Report No. FHWA - RD - 89.043. Federal Highway Administration, US Department of Transportation.

GCO (1984). Geotechnical Manual for Slopes. Civil Engineering Services Department, Hong Kong, pp 295.

GCO (1989). Model Specification for Reinforced Fill Structures (Geospec 2). Civil Engineering Services Department. Hong Kong, pp 140.

INGOLD, T.S. (1991). Partial Factor Design of Polymer Reinforced Soil Walls. Ground Engineering, Vol. 24, No. 5., London pp 34 - 38.

JAILLOUX, J-M and SEGRESTIN, P. (1988). Present State of Knowledge of Long term Behaviour of Materials used as Soil Reinforcement. International Symposium on Theory and Practice of Earth Reinforcement. Fukuoka, Japan.

LCPC/SETRA (1979). Les Ouvrages en Terre Armee - Recommendations et Regles de l'Art. Minister des Transports. Direction Generale des Transports Interieurs. Paris, pp 195.

MITCHELL, J.K. and CHRISTOPHER, B.R. (1990). North American Practice in Reinforced Soil Systems. Design and Performance of Earth Retaining Structures. ASCE Geotechnical Special Publication No. 25, New York, pp 322 - 346.

ROWE, R.K. (1987), Geosynthetics in Soil Improvement: Functions, Properties and Tests Soil Reinforcement: Mechanics and Design. The University of Sydney. Sydney, pp 1.1 - 1.54

TAI (1990). The Field of Application of Earth Retaining Structures with Synthetic Reinforcements. Terre Armee Internationale. Information Report No.36. Paris

VIDAL, H. (1966). La Terre Armee (Un Materiau Nouveau pour Travaux Publics). Annales de l'Institute Technique du Batiment et des Travaux Publics. Paris.

Ground Improvement to Reduce Geotechnical Risk: Waingake Final Water Treatment Plant

P. BRABHAHARAN
B.Sc.Eng. (Hons), M.Sc.Eng., M.I.C.E., C.Eng., M.I.E.Aust., C.P.Eng., M.I.M.M., R.Eng.
Senior Geotechnical Engineer, Works Consultancy Services Limited

SUMMARY Site Investigations for the Waingake Final Water Treatment Plant near Gisborne in New Zealand identified poor ground conditions under the proposed retaining walls which also carry the treatment plant buildings. Due to the poor ground conditions, there was a potential for damaging settlements and foundation failure. The risk was exacerbated by the potential for strong earthquakes in the region. Ground improvement using stone columns provided a cost effective solution to mitigate the risk of damaging settlements and foundation failure. This solution also allows the retaining wall to undergo small translational movements during large seismic events with minimal disruption to the treatment facility. The stone columns were constructed using a dry compaction technique. Settlement monitoring confirmed the effectiveness of the stone columns in reducing settlements.

1. INTRODUCTION

After the 1988 Cyclone Bola, an interim treatment plant was built at Waingake to reinstate the water supply to Gisborne City in New Zealand. A final water treatment plant was subsequently designed and constructed at the Waingake site, about 50 km southwest of Gisborne City.

The final treatment plant involves the construction of additional filter tanks, a bulk lime silo, chemical dosing buildings, stores, generator and an operations building, see Figure 1. Retaining walls support the operations building, and the excavation behind the filter tanks.

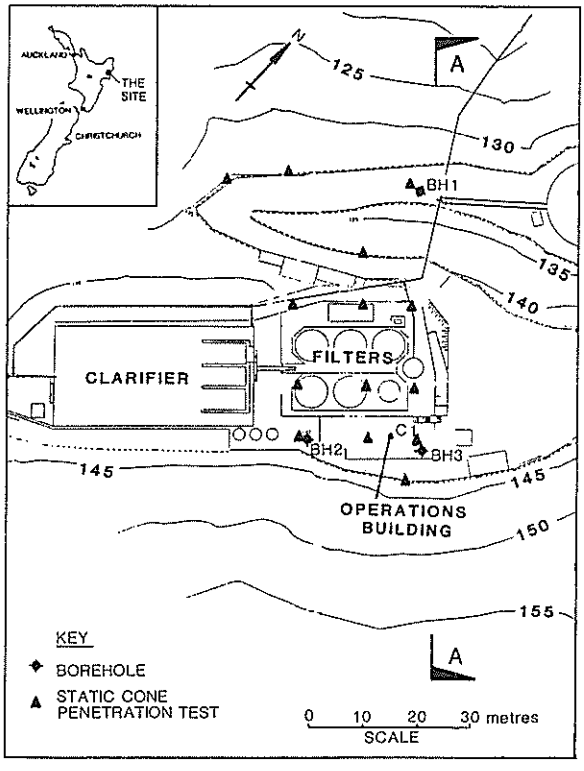

Figure 1 Location Plan

The treatment plant is located on a hillside with an average slope of 20 degrees. At the treatment plant site, colluvium overlies Miocene age massive, sandy to muddy, light blue grey siltstones, occasionally with sandstone beds. The geomorphology of the site together with information from site investigations suggests that past instability of the hillside has resulted in a thick layer of colluvium in a bedrock depression at the site, which is located between bedrock spurs.

The interim treatment plant was located partly on the bedrock spurs, and partly on the intervening colluvium, while the new construction for the final treatment plant is entirely on colluvium.

2. GROUND CONDITIONS

Site investigations comprising boreholes and Static Cone Penetration Tests (CPT) were carried out at the treatment plant site. The site investigations showed the colluvium underlying the site to be up to 25 m thick, and generally comprising soft to firm clayey silt with siltstone / sandstone clasts and some pockets of silty sand. The colluvium was found to be underlain by siltstone and sandstone bedrock. The static cone penetration tests showed the thickness and shear strength of the colluvium to vary across the site. A typical sketch geological section across the site is shown on Figure 2. The cone resistances (q_c) from the cone penetration tests were variable, but were generally less than 1 MPa up to a depth of 6 m to 10 m. Typical results from a static cone penetration test are shown on Figure 3, which illustrates the poor ground conditions under the retaining wall supporting the operations building.

A design undrained shear strength (S_u) of 30 kPa, and a coefficient of volume compressibility (m_v) of 0.34 m^2/MN to 0.13 m^2/MN is assessed from the CPT results, for the colluvium underlying the site. The groundwater level was within 2 m of the ground surface.

3. DESIGN PHILOSOPHY

The stability of the retaining wall supporting the operations building is critical to the final treatment plant. There was assessed to be an unacceptably high risk of failure or significant damage to retaining walls constructed with shallow foundations on existing ground, due to :

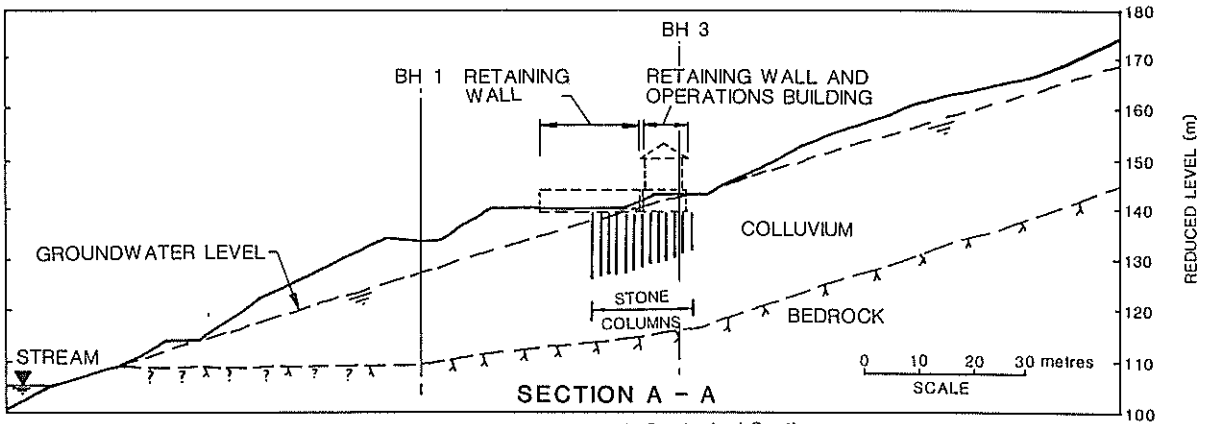

Figure 2 Typical Sketch Geological Section

- an inadequate margin of safety against bearing capacity failure under design seismic events ;
- an inadequate margin of safety against sliding failure of the retaining wall under design seismic events. The poor ground conditions and the large seismic inertia force due to the building supported by the retaining wall contribute to this instability ;
- total consolidation settlements up to 125 mm. Due to the variation of the thickness and compressibility of the colluvium across the site, the estimated differential settlements are of the order of 100 mm, and can cause significant damage.

Deep pile foundations for the retaining walls were discounted for the following reasons :

- The piles would have had to extend to bedrock at a depth of 20 m to 25 m giving an expensive solution ;
- In view of the large lateral seismic forces on the retaining wall, the wall may be designed economically, by allowing the retaining wall to undergo small lateral displacements during large seismic events. However, if pile foundations are chosen, displacement of the wall cannot be allowed for in design, as such displacements would cause shearing at the pile-wall connection. Therefore, ground anchors would have been required to resist the lateral loads. Given the poor ground conditions and the large distance to bedrock, the ground anchors would need to be uneconomically long to achieve the required capacity;
- The slope was assessed to have marginal stability, and any small movements of the slope may impose large lateral loads on the piles, and possibly lead to failure.

Ground improvement using "stone columns" gave an acceptable foundation solution at a reasonable cost. "Stone Columns" are constructed using granular material, through poor ground to a suitable firm stratum. The stone columns were suitable for the Waingake site as they would :

- increase the bearing capacity of the ground ;
- improve the frictional resistance to sliding of the retaining wall along the wall base-ground interface ;
- improve the stability against shallow local slope failures ;
- reduce total and differential settlements. Since the stone columns have a high permeability, they would also accelerate the consolidation settlement by providing drainage in a similar manner to sand drains ;
- accommodate small movements of the slope during extreme events, and
- allow translational displacement of the retaining wall during large seismic events, thus eliminating the need for a costly design to resist the full lateral seismic forces.

Therefore, ground improvement using a stone column foundation solution was adopted for the retaining walls at Waingake.

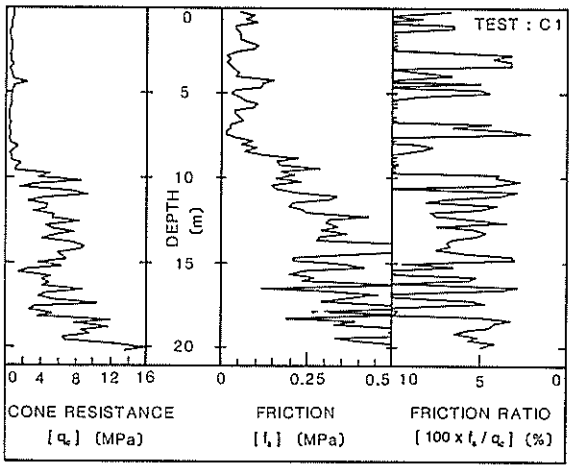

Figure 3 Typical Cone Penetration Test Results

4. RETAINING WALL DESIGN

Various forms of retaining walls were considered for the retaining wall supporting the operations building. To limit the bearing pressures under the retaining wall and provide sufficient resistance against sliding, a rigid reinforced concrete box type retaining structure with a large base slab and counterfort walls was adopted. The retaining wall box structure was designed to be partially filled with soil. Allowance was made in the design to permit small controlled translational movements of the retaining wall during large earthquake events without causing significant disruption to the treatment plant. Calculations indicated that displacements of the order of 60 mm would occur during a design seismic event with a peak ground acceleration of 0.32 g.

5. STONE COLUMN DESIGN

The ultimate load capacity of stone columns was calculated in accordance with the method proposed by Hughes et al (1975). The stress distribution between the granular columns and the soil, and hence the settlement reduction due to construction of the stone columns was derived based on elastic theory (Mitchell, 1981).

Based on these calculations, a design configuration of 1.0 m nominal diameter stone columns at a triangular centre to centre spacing of 1.8 m was chosen. The stone columns were designed to extend between 5 m and 12 m through the soft deposits to a stiffer stratum within the colluvium. The chosen stone column configuration gave a settlement reduction ratio (β) of 0.47, where β is the ratio between the calculated settlements with and without the stone columns. However, since the stone columns do not extend through the full thickness of compressible soils, the overall settlement reduction ratio is smaller than estimated above. The calculations indicated that the consolidation settlements with ground improvement using stone columns would be up to 70 mm. For a flexible foundation, differential settlements would be of the order of 60 mm. However, the retaining wall foundations are rigid, and therefore the actual differential settlements would be much smaller than the 60 mm calculated for flexible foundations.

The stone column layout chosen for the Waingake site is shown on Figure 4. One row of stone columns extends beyond the foundation base for the retaining walls. These columns were sealed at the surface with bentonite-cement grout to prevent ingress of surface water, to avoid any possibility of an increase in the groundwater pressures which could reduce the stability of the overall slope.

6. SLOPE STABILISATION MEASURES

Slope stability analyses indicated that the slope on which the treatment plant is located is marginally stable. There is a potential for slope instability with a failure surface within the colluvium or along the colluvium-bedrock interface, especially following periods of high rainfall.

In view of the assessed marginal slope stability of the Waingake site, and the risk of slope movements following periods of high rainfall, it was considered prudent to undertake remedial measures to improve the stability of the site.

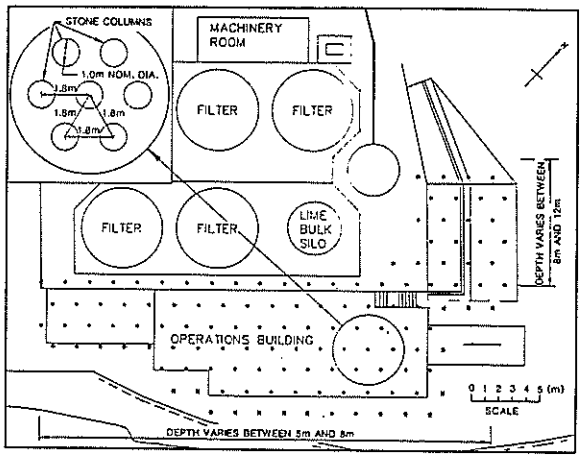

Figure 4 Layout of Stone Columns

Slope stability analyses indicated that lowering the high groundwater levels at the site would provide reasonable improvements in the stability of the slope at a moderate cost. Therefore, surface drains and sub-horizontal drainage holes were incorporated into the scheme to reduce or control the groundwater levels.

7. CONSTRUCTION TECHNIQUES

7.1 Stone Columns

In view of the potential instability of the site, the wet vibroflot process commonly used in Europe to construct stone columns was considered unsuitable for the Waingake site. The wet vibroflot technique would inject large quantities of water into the ground, and may reduce the factor of safety of the marginally stable slope. This consideration coupled with the general unavailability of vibroflot equipment in New Zealand led to the specification of a dry compaction method of stone column construction. To the author's knowledge, this is the first time such a technique has been used in New Zealand. Similar techniques have been used in countries such as India (Datye, 1982) and Australia (Waterton and Foulsham, 1984).

The method of construction adopted is shown in Figure 5. A 920 mm diameter hole to the required depth was drilled using an auger, and cased with a 910 mm outer diameter steel casing.

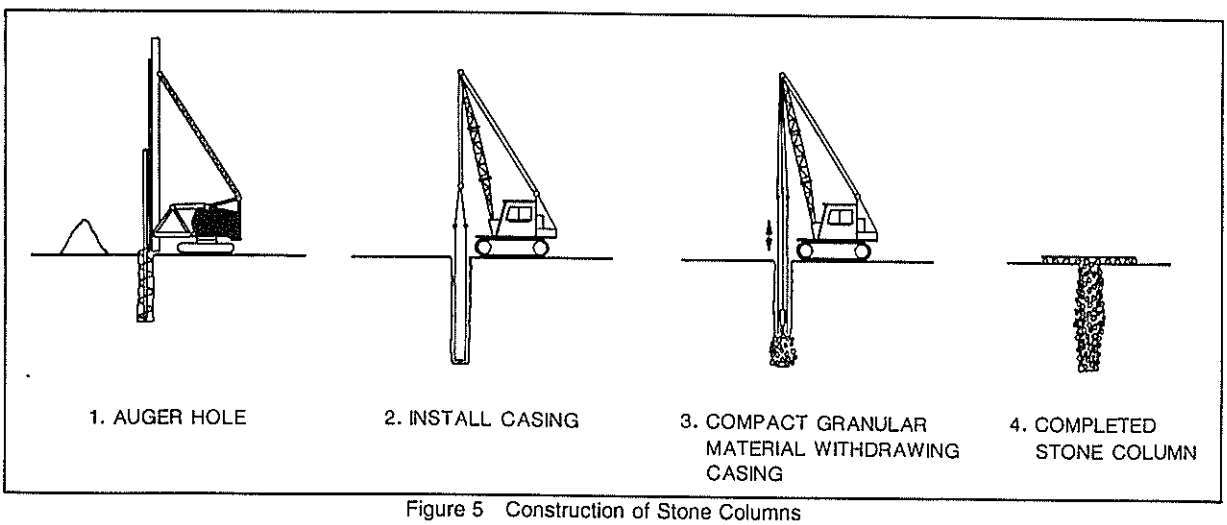

Figure 5 Construction of Stone Columns

Granular material was placed in the cased hole in small lifts, and the casing was withdrawn maintaining the bottom of the casing below the surface of the granular material. The granular material was compacted using a 2000 kg hammer falling through a height of 1.5 m, until a total set of 15 mm for 10 drops of the hammer was achieved. The procedure was repeated till a compacted column is formed to the ground surface. The stone columns were constructed using conventional piling equipment.

7.2 Drainage Measures

Sub-horizontal drainage holes of 86 mm diameter were drilled and lined with 40 mm internal diameter, partially slotted PVC lining tubes. Water flow was observed from most of the drains, and significant flow from some drains, indicating that the sub-horizontal drains were effective in reducing the groundwater pressures in the slope.

Surface drains were installed at the head of the marginally stable slope, and immediately above the treatment plant area, to minimise the surface water run-off entering the slope.

8. MONITORING

A programme of settlement and movement monitoring was implemented to monitor the settlement of the treatment plant structures, and to detect any movement of the slope. Settlement pins were also installed on the existing interim treatment plant structures, to detect any settlement due to lowering of the groundwater levels as a result of the slope drainage measures. Standpipe piezometers were installed to monitor the groundwater levels.

The initial settlement monitoring results indicate very small settlements of the retaining walls founded on stone columns, indicating that the ground improvement has been very effective in reducing settlements.

9. CONCLUSIONS

Site investigations comprising boreholes and static cone penetration tests showed poor ground conditions at the Waingake Treatment Plant site. A geotechnical appraisal identified potential foundation problems and the marginal slope stability of the site.

Shallow foundations for the retaining wall presented a high risk of significant damage due to large differential settlements, and bearing capacity or sliding failure of the walls during design seismic events. Conventional pile foundations together with ground anchors would have given an expensive solution with a risk of pile failure due to small slope movements.

Ground improvement of the soils under the retaining walls was carried out using stone columns to minimise the risk of foundation failure at an acceptable cost. The stone column solution would allow controlled movement of the retaining walls during large seismic events, and would accommodate small slope movements. The stone columns were constructed using a dry compaction technique with conventional piling machinery available in New Zealand.

Surface drains and sub-horizontal drainage holes were incorporated in the scheme to control the groundwater levels in the slope and mitigate the risk of slope failure.

The monitoring programme has shown that the stone columns were effective in reducing the settlement of the retaining walls.

This case study demonstrates the usefulness of site investigations and geotechnical engineering to identify the geotechnical and seismic risks, and to develop appropriate and cost effective solutions to mitigate the risks.

10. ACKNOWLEDGEMENTS

The permission of the Client for the project, Gisborne District Council, to publish this paper is gratefully acknowledged. The author also wishes to acknowledge the contribution of Mr P R Swain, and other colleagues in Works Consultancy Services Limited who have been involved in this project.

11. REFERENCES

Datye, K.R. (1982). Settlement and bearing capacity of foundation system with stone columns. Symposium on Recent Developments in Ground Improvement Techniques, Bangkok. 29 Nov - 3 Dec 1982. pp. 85-103.

Hughes, J.M.O., Withers, N.J. and Greenwood, D.A. (1975). A field trial of the reinforcing effect of a stone column in soil. Symposium on Ground Treatment by Deep Compaction. Geotechnique Vol.25, No.1. March 1975.

Mitchell, J.K. (1981). Soil improvement - state-of-the-art report. Proc. 10th Int. Conf. Soil Mech. and Found. Engrg. Stockholm. Vol.4, pp. 509-565.

Waterton, C.A. and Foulsham, D.A. (1984). The design, construction and performance of a road embankment founded on stone columns. Fourth Australia New Zealand Conf. on Geomechanics. Perth. 14-18 May 1984. Vol.1 Geomechanics Interaction. pp. 351-356.

Design Procedure for the Seismic Analysis of Earth Structures

D.C. ELIAS
B.Eng., C.Eng., M.I.C.E., M.I.E.Aust.
Senior Engineer, Dames & Moore, Perth
E.A. NOVELLO
B.E., Ph.D., Grad. I.E.Aust.
Project Engineer, Dames & Moore, Perth
D. GLENISTER
B.E., M.Eng., M.I.E.Aust.
Civil Engineering and Residue Development Manager, Alcoa of Australia Limited, Perth

SUMMARY A simple procedure is presented for the seismic analysis of earth structures such as dams, tailings dams and embankments. The procedure represents an improvement on the pseudostatic analyses commonly used.

1. INTRODUCTION

A procedure is presented for the seismic analysis of earth structures such as dams, tailings dams and embankments. The procedure is based upon the state of practice used in California, and although by no means a rigorous analysis, represents an improvement over the psuedostatic analysis commonly used in Australia.

An outline of the procedure is presented below.

1. Select the design seismic event.
2. Check whether any of the materials in the structure are subject to loss of strength under cyclic loading.
3. Check whether any of the materials in the structure are subject to liquefaction.
4. If materials are neither prone to significant strength loss (say greater than 20%) nor liquefaction then their probable performance may be assessed by estimating embankment deformations during the design event.
5. If materials are prone to liquefaction under the design earthquake loading then they are not suitable if there is any possibility of the materials becoming saturated.
6. For materials which exhibit significant strength loss under cyclic loading conditions it probably follows that deformations will be excessively high.

The notation used in this paper is summarised in Table I.

2. DESIGN SEISMIC EVENT

The proposed design method requires two parameters relating to the design seismic event. These parameters are:

- the maximum Richter Magnitude (ML_{max}); and
- the maximum ground acceleration at the site.

Australian design values for these parameters may be obtained from References (1) and (2). The first reference gives the estimated maximum Richter Magnitude (ML_{max}) for various zones of Australia, together with estimated data on maximum ground accelerations for an event with a 10% chance of exceedance in 50 years (equivalent to an annual probability of exceedance of one in five hundred). The second reference presents the estimated maximum ground accelerations for an event with a 10% chance of exceedance in 100 years (equivalent to an annual probability of exceedance of one in one thousand). We recommend that an annual probability of exceedance of 1:500 is used for structures with short operating or saturated lives, such as tailings dams, and an annual probability of exceedance of 1:1000 for structures with long design lives such as railway embankments and water supply dams.

The above maximum ground accelerations relate to the bedrock accelerations (a_{max}) experienced during the design seismic event. Soil deposits overlying the bedrock, in general, would tend to amplify the bedrock motion to some degree. In order to be suitably conservative in design, it is recommended that the bedrock accelerations are adjusted in accordance with the design curves shown on Figure 1 (Ref 3) to estimate the peak ground acceleration (a_{max}^*).

To assess the potential of a material to liquefy under seismic loading the average cyclic shear stress (τ_{av}) due to the seismic loading must be estimated. In addition, if laboratory test methods are used to assess liquefaction potential, an appropriate number of τ_{av} stress cycles must be estimated. These parameters may be estimated by the methods described below.

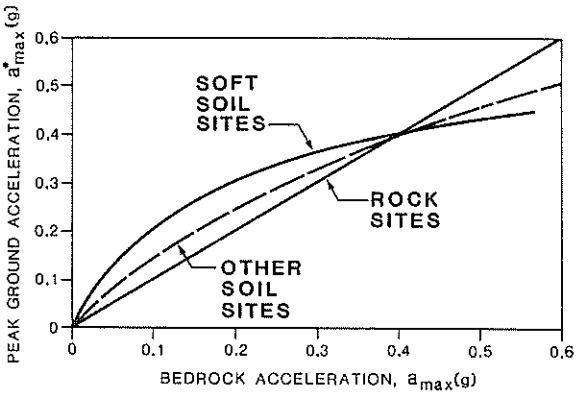

NOTE: SOFT SOILS ARE TYPICALLY NORMALLY CONSOLIDATED MATERIALS WITH UNDRAINED SHEAR STRENGTHS LESS THAN 50kPa

Figure 1 Relationship between peak ground acceleration and bedrock acceleration

The average cyclic shear stress, τ_{av} in a soil deposit during the design seismic event can be determined from the following formula by Seed (4).

$$\frac{\tau_{av}}{\sigma'} = 0.65 \frac{\sigma}{\sigma'} r_d \frac{a_{max}^*}{g} \quad (1)$$

where σ and σ' are the total and effective overburden stresses respectively, g is the acceleration due to gravity, a_{max}^* is the peak particle acceleration at the ground surface and r_d is a stress reduction factor which reduces from unity at the ground surface to about 0.9 at a depth of 10m and 0.5 at a depth of 30m.

The number of τ_{av} stress cycles needed to represent the design seismic event depends on the earthquake magnitude. Appropriate numbers of stress cycles according to Seed (4) are presented as follows:

Richter Earthquake Magnitude	Number of Significant Stress Cycles
5.5	5
6.5	10
7.0	15
7.5	25
8.0	35

3. STRENGTH LOSS, LIQUEFACTION AND CYCLIC MOBILITY UNDER CYCLIC LOADING

3.1 General

The material to be utilised in constructing the earth structure should be checked for strength loss, liquefaction and cyclic mobility when subjected to the level of cyclic loading likely to be experienced in the event of the design earthquake occurring. Generally, cohesive materials and dense granular materials do not suffer significant strength loss in such situations; on the other hand loose, saturated sands and sensitive cohesive soils can experience considerable strength loss due to cyclic loading.

Assessing materials for their susceptibility to liquefaction and cyclic mobility may be achieved using a number of simplified procedures based on field test correlations, e.g. using the standard penetration test, SPT (Ref 5), and the cone penetration test, CPT (Ref 6). Alternatively, a programme of laboratory testing may be undertaken to examine the liquefaction potential of the material.

3.2 Field Test Correlations

On the basis of correlations between field observations of soil liquefaction and N-values measured with the SPT, Seed et al. (5) developed liquefaction resistance curves for sands with different N-values and fines contents. Similar correlations were used by Robertson and Campanella (6) to develop a method for the liquefaction assessment of sand and silts based on the CPT. Both of these methods relate the SPT N-value or the CPT cone resistance value, q_c, to the likely soil liquefaction resistance. The soil liquefaction resistance is expressed as the cyclic shear stress ratio which causes liquefaction or cyclic mobility during an earthquake of a given magnitude. The soil is considered not to be susceptible to liquefaction or cyclic mobility if its liquefaction resistance exceeds the field cyclic shear stress ratio due to the design seismic event (expression (1), Section 2). If liquefaction or cyclic mobility is possible, then the maximum value of shear strain likely to be mobilised in the soil may be estimated from Figure 2.

3.3 Laboratory Test Assessment

Because insitu data will not normally be available at the design stage, a laboratory assessment of field liquefaction potential is necessary. The field liquefaction potential of the embankment material can be assessed from the results of laboratory cyclic shear testing of samples performed at voids ratio, moisture content, pore pressure and loading representative of field conditions. Appropriate testing of materials can be carried out in triaxial or simple shear apparatus with a facility to apply cyclic loading. The level of cyclic loading representative of the design seismic event can be determined using the expression for cyclic stress ratio (τ_{av} / σ') given in Section 2.

The above cyclic shear stress ratio relates to horizontal ground shaking which is the dominant form of earthquake loading. Such conditions can reasonably be simulated in a simple shear apparatus. In a triaxial shear apparatus, however, the applied cyclic shear stress ratio needs to be adjusted to account for the change from horizontal shear conditions during earthquake loading to the isotropic confining conditions of the triaxial test set-up. The adjustment in cyclic shear stress ratio for the testing of normally consolidated materials is given by the following expression:

Triaxial Cyclic Shear Stress Ratio		Earthquake or Simple Shear Cyclic Shear Stress Ratio
$\frac{q'_{cyc}}{2\sigma_c'}$	=	$1.6 \frac{\tau_{av}}{\sigma'}$

(2)

where q'_{cyc} is the applied cyclic deviator stress

and σ_c' is the initial mean effective confining pressure.

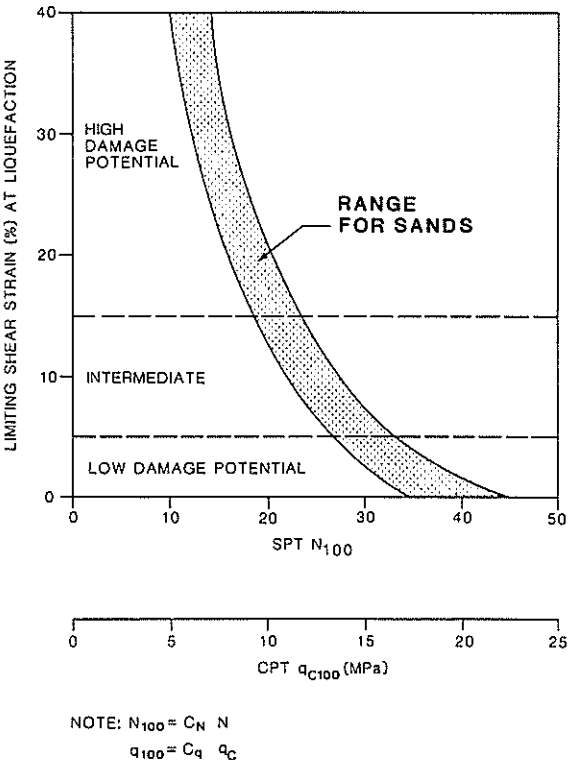

NOTE: $N_{100} = C_N N$

$q_{100} = C_q q_c$

Figure 2 Limiting shear strain at liquefaction

4. ESTIMATING EARTHQUAKE-INDUCED DEFORMATIONS IN EARTH STRUCTURES

If the materials in an earth structure are neither prone to significant strength loss (say greater than 20%) nor liquefaction then their probable performance during the design seismic event may be checked by estimating earthquake-induced deformations in the structure. Makdisi and Seed (7, 8) proposed a simplified procedure for estimating such deformations in dams and embankments constructed of cohesive materials. This procedure is summarised on Figures 3, 4 and 5.

For dams and embankments constructed of granular materials, earthquake induced deformations may be estimated using a relationship proposed by Bureau et al (10) between the earthquake severity index (ESI), the embankment material friction angle and the crest settlement. This relationship is presented on Figure 6.

5. ACCEPTANCE CRITERIA

The methods described above result in an estimate of the measure of performance of a structure under a particular earthquake loading. When assessing the acceptance of the estimated deformation of a structure a number of factors must be taken into consideration, these factors include:

- the type of structure, e.g. railway embankment, water retaining dam, tailings dam;
- the consequence of failure, e.g. downstream effects of spills, potential for loss of life, cost of repair; and
- the probability of the design event occurring during the life of the structure.

Because of these factors there is no simple set of design criteria that may be followed; rather a judgment must be made which will take the above factors into account.

Two of the most important factors to be judged in determining acceptable displacements are:

- the amount of displacement necessary for a breach to occur in the dam (or in the case of a railway embankment sufficient track displacement for a derailment to occur); and
- the amount of displacement available for the embankment material to remain in its elastic range of stress-strain behaviour.

The former of these factors must be dealt with on a case by case basis. The second factor may be assessed by the examination of the stress-strain relationships of the embankment materials. Typically these data would be available from triaxial testing conducted at stress levels appropriate to the embankment configuration. Because of the non-linear stress-strain relationship of many materials the adopted acceptable strain should, in order to preserve a degree of conservatism, preferably be less than the strain to 50% of the peak strength.

As a guide to the probable displacements which may take place without disastrous effects, we have reviewed published data concerning the effects of earthquakes on earth dams primarily in Chile, Mexico and California. The data considered apply to earthquakes of magnitude 5.9 or greater on the Richter scale and would therefore be considered large by Australian conditions. The data concerned a total of 14 dams affected by 24 earthquake events (7) (10) (11) (12) (13) (14) (15). Five of the dams

1. CALCULATE FIRST NATURAL PERIOD OF EMBANKMENT, T_o

   T_o = Function of Embankment Height and Material Type (see Figure 4 for typical values of T_o)

2. DETERMINE PEAK GROUND ACCELERATION, a^*_{max} FOR EARTHQUAKE OF MAGNITUDE, M

   Refer to Section 2 for design values of a^*_{max}.

3. FOR A GIVEN CIRCULAR SLIP SURFACE WITHIN THE EMBANKMENT, CALCULATE YIELD ACCELERATION, k_y

   k_y = Lateral g force to give a factor of safety of unity in a pseudostatic slope stability analysis of the embankment assuming soil undrained shear strength reduced by 20%.

4. CALCULATE MAXIMUM AVERAGE ACCELERATION, k AT BASE OF CIRCULAR SLIP SURFACE (see Figure 5a)

5. CALCULATE EARTHQUAKE-INDUCED LATERAL MOVEMENT, U (see Figure 5b)

   U = Function of T_o, k_y, k and earthquake magnitude M

6. REPEAT STEPS 3 TO 5 FOR DIFFERENT CIRCULAR SLIP SURFACES WITHIN THE EMBANKMENT.
   QUOTE MAXIMUM U VALUE.

Figure 3 Procedure for estimating earthquake induced deformations in cohesive embankments

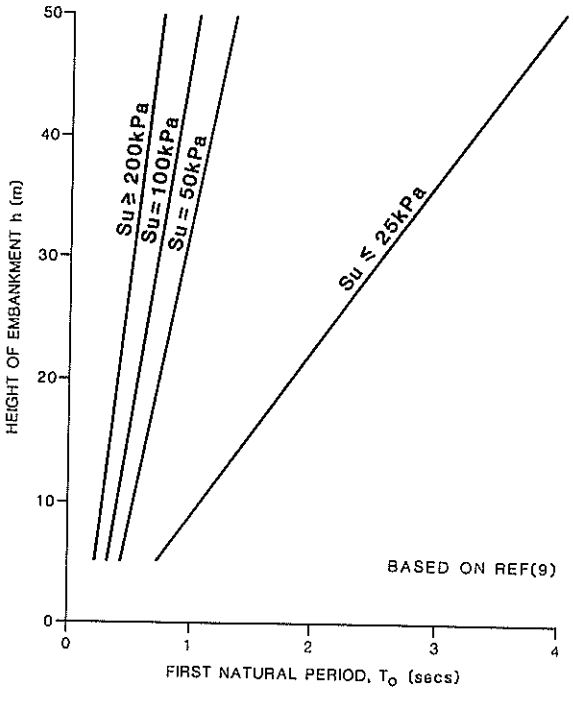

Figure 4 Values of first natural period of embankment

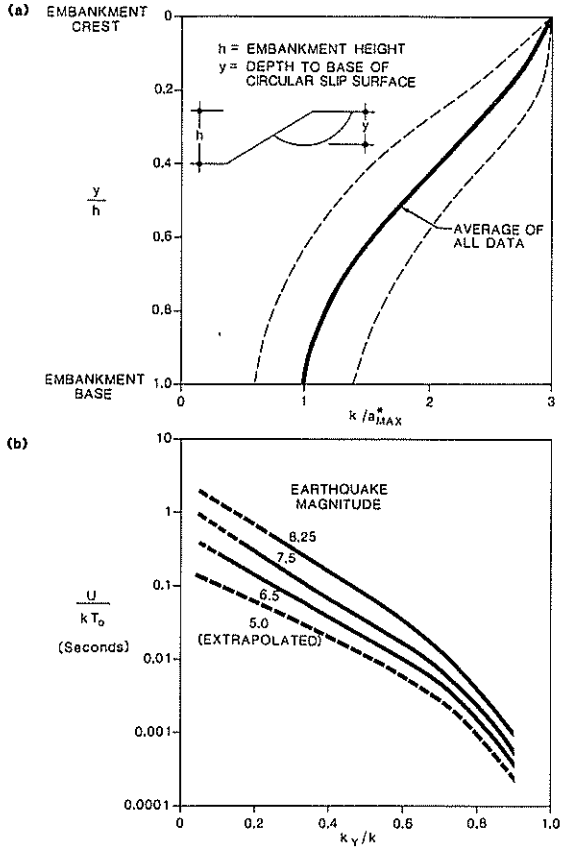

Figure 5 Earthquake induced deformations in cohesive embankments

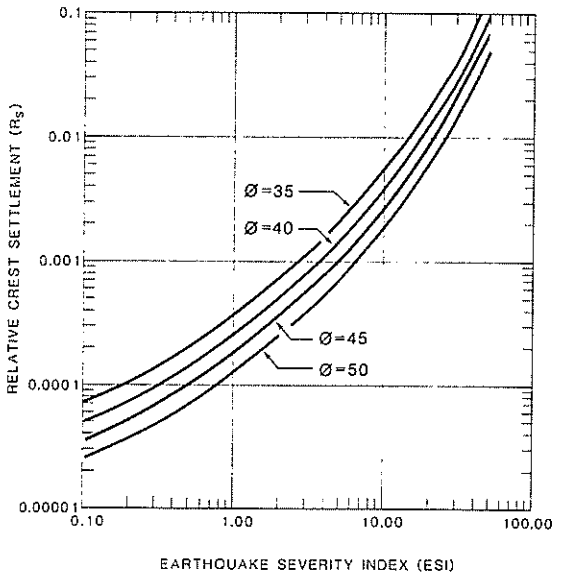

where $ESI = \frac{a^{*}_{max}}{g} (ML_{max} - 4.5)^{3}$

and Crest settlement, $s = R_s \, h$

Figure 6 Procedure for estimating earthquake induced deformations in granular embankments

failed as a result of the seismic loading and experienced large vertical settlements of greater than 8% of their embankment height. The other 9 dams did not fail and experienced serviceable settlements of between 0.01% and 1.5% of the embankment height, with a median value of 0.24%. Perusal of the data and a review of the data source references suggest that embankments can suffer strains in the order of 1.5% without undue distress to their overall integrity. For dams with clay liners and seals we suggest that the tolerable estimated displacement should be limited to 10% of the thickness of the liner/seal, and for dams with plastic membrane liners we suggest that the tolerable estimated displacement should be limited to about 50mm.

This may be summarised:

Type of Structure	Suggested Tolerable Estimated Displacement *
Homogeneous Embankment	1.5% of overall height
Dam with Clay Liner	1.5% of overall height or 10% of liner thickness
Dam with Plastic Membrane	50mm

* Tolerable displacements may be limited by other factors such as consequential damage (e.g. breaches, derailments), or the strain level to limit deformation in the elastic range.

Based on our review of the data cited above and other work described by Seed et al. (16), it is considered that acceptance of the above criteria represents a low probability of seismic failure for the structure. A low failure probability, however, may not equate to an acceptable failure risk, and hence it is important to assess the failure probability in relation to the consequence of failure of the structure.

This may be carried out by the method proposed by Vick et al. (17) summarised on Figure 7 and the relative risk shown on Figure 8. The probability calculations on Figure 7 permit the lifetime probability of seismic failure to be evaluated. Figure 8 gives an indication of the observed risk of failure for various earth structures, and therefore provides some guideline as to what constitutes an acceptable failure risk. By way of example, the probability that an earth structure will fail under the design ground motion for an estimated displacement of 1.5% of the structure height may be less than 5% say, i.e. $p(f/a)=0.05$. Let there be a 10% chance of occurrence or exceedance of this ground motion over the operational life of the dam, i.e. $p(a_i)=0.10$ (refer to Section 2). On this basis, the lifetime probability of failure, $p(f)$ is 0.005, which is within the range of acceptable values for dams presented on Figure 8.

6. CONCLUSIONS

A procedure is presented for the seismic analysis of earth structures such as dams, tailings dams and embankments. The procedure is an improvement over a simple pseudostatic analysis and gives due consideration to the design seismic event, the design ground acceleration, the potential for liquefaction or cyclic mobility of the soil, and a performance assessment of the structure on the basis of acceptable earthquake-induced deformations.

1. CALCULATE PROBABILITY OF GROUND MOTION OCCURRENCE OR EXCEEDANCE DURING DESIGN LIFE

$p(a_i) = 1 - (1-p(a_o))^i$

where:

$p(a_i)$= probability of occurrence or exceedance of design ground motion in i years

$p(a_o)$ = annual probability of occurrence or exceedance of design ground motion

i = life of impoundment (operational or saturated life)

2. CALCULATE LIFETIME PROBABILITY OF SEISMIC FAILURE

$p(f) = p(a_i)\ p(f/a)$

where:

p(f) = lifetime probability of seismic failure

p(f/a)= probability that structure will fail under design motion

Figure 7 Estimation of probability of seismic failure

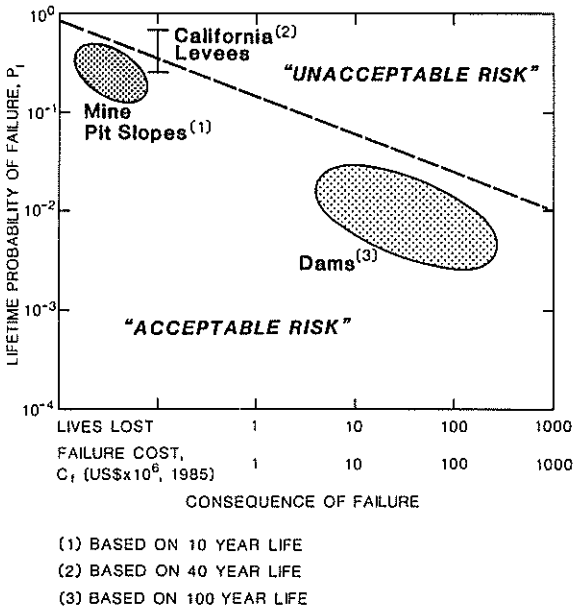

(1) BASED ON 10 YEAR LIFE
(2) BASED ON 40 YEAR LIFE
(3) BASED ON 100 YEAR LIFE

Figure 8 "Accepted" risk - dams and mining-related projects

TABLE I

NOTATION

Symbol	Units	Definition
a		Bedrock acceleration at epicentre
a_{max}		Bedrock acceleration at site
a_{max}^*		Acceleration at natural ground surface
C_N		Depth correction factor for N value
C_q		Depth correction factor for cone resistance
ESI		Earthquake severity index
g	(m/s^2)	Acceleration due to gravity
h	(m)	Embankment height
i	(yrs)	Life of impoundment (operational or saturated life)
k		Acceleration within embankment at a given level
k_y		Yield acceleration of embankment at base of failure surface
M		Earthquake magnitude - Richter scale
ML_{max}		Maximum Richter Magnitude
N		SPT 'N' value
N_{100}		Factored N value
$p(a_i)$		Probability of occurrence or exceedance of design ground motion in i years
$p(a_o)$		Annual probability of occurrence or exceedance of design ground motion
p(f)		Probability of seismic failure
p(f/a)		Probability that structure will fail under design ground motion
q_c	(MPa)	Cone resistance
q_{c100}		Factored cone resistance
q'_{cyc}	(kPa)	Applied cyclic deviator stress
r_d		Stress reduction factor
R_s		Relative crest settlement
s	(m)	Crest settlement
T_o	(sec)	First natural period of embankment
U	(m)	Earthquake induced lateral movement
y	(m)	Depth to base of circular slip surface
τ_{av}liq	(kPa)	Cyclic shear stress to cause liquefaction
τ_{av}	(kPa)	Average cyclic shear stress
σ	(kPa)	Total overburden stress
σ'_c	(kPa)	Initial mean effective confirming pressure
σ'	(kPa)	Effective overburden stress
σ'_{vo}	(kPa)	Effective overburden stress
ϕ	(degrees)	Friction angle of embankment material

Note: Accelerations expressed as a fraction of g.

7. ACKNOWLEDGEMENTS

The authors wish to thank Alcoa of Australia Limited for permission to publish the paper.

8. REFERENCES

1. Gaull, B.A., Michael-Leiba, M.O. and Rynn, J.M.W. "Probabilistic Earthquake Risk Maps of Australia". Australian Journal of Earth Sciences, Vol. 37, No. 2, June 1990, pp.169-187.

2. DR91094:S-1991. "Minimum Design Loads on Structures, Part 4:Earthquake Loads", to be AS1170.4, Standards Association of Australia, 1991.

3. Idriss, I.M. "Response of Soft Soil Sites During Earthquakes". Proceedings H.B. Seed Memorial Symposium, UC Berkeley Calif., Vol. 2, 1991, pp.273-289.

4. Seed, H.B. "Soil Liquefaction and Cyclic Mobility Evaluation for Level Ground During Earthquakes", Journal of Geotech. Engng Div., ASCE, Vol.105, No.GT2, 1979, pp.201-255.

5. Seed, H.B., Tokimatsu, K., Harder, L.F. and Chung, R.M. "Influence of SPT Procedures in Soil Liquefaction Resistance Evaluations", Journal of Geotech. Engng Div., ASCE, Vol.111, No.GT12, 1985, pp.1425-1445.

6. Robertson, P.K. and Campanella R.G. "Liquefaction Potential of Sands Using the CPT", Journal of Geotech. Engng Div., ASCE, Vol.111, No.GT3, 1985, pp.384-403.

7. Makdisi, F.I. and Seed, H.B. "A Simplified Procedure for Estimating Earthquake-Induced Deformations in Dams and Embankments", Earthquake Engineering Research Centre, College of Engineering, UC Berkeley Calif., USA, Report No.UCB/EERC-77/19, August 1977.

8. Makdisi, F.I. and Seed, H.B. "Simplified Procedure for Estimating Dam and Embankment Earthquake-Induced Deformations", Journal of Geotech. Engng Div., ASCE, Vol.104, No.GT7, 1978, pp.849-867.

9. AS2121-1979. "The Design of Earthquake-Resistant Buildings, SAA Earthquake Code", Standards Association of Australia, 1979.

10. Bureau, G., Volpe, R.L., Roth, W.A. and Udaka, T. "Seismic Analysis of Concrete Face Rockfill Dams", closure, Journal of Geotech. Engng Div., ASCE, Vol. 113, No. 10, October 1987, pp.1255-1264.

11. Bureau, G., Bubbitt, D.H., Biachoff, J.A., Volpe, R.L. and Tepel, R.E. "Effects on Dams of the Loma Prieta Earthquake of 17 October 1989", USCOLD Newsletter Issue No. 90, November 1989.

12. Seed, Dickenson, Riemer, Bray, Sito, Mitchell, Idriss, Kayen, Knopp, Harden and Power. "Preliminary Report on the Principal Geotechnical Aspects of the October 17, 1989 Loma Prieta Earthquake". Earthquake Engineering Research Centre, UC Berkeley Calif., USA. Report No. UCB/EERC-90/05, April 1990.

13. De Alba, P.A., Seed, H.B., Retamal, E. and Seed, R.B. "Analysis of Dam Failures in 1985 Chilean Earthquake", Journal of Geotech. Engng Div., ASCE, Vol.114, No.GT12, December 1988.

14. Castro, G., Poulos, S.J. and Leathers, F.D. "Re-examination of Slide of Lower San Fernando Dam". Journal of Geotech. Engng Div., ASCE, Vol.111, No.9, September 1985.

15. Renner, P., Salazar, A. and Wellmann, P. "Tailings Disposal in Seismic Zones". Tailings Disposal Today, Volume 2, Proceedings of the Second International Tailings Symposium, Denver, USA, May 1978.

16. Seed, H.B., Makdisi, F.I. and de Alba, P. "Performance of Earth Dams during Earthquakes". Journal of Geotech. Engng Div., ASCE, Vol. 104, No. GT7, July 1978, pp.967-994.

17. Vick, S.G., Atkinson, G.M. and Wilmot, C.I. "Risk Analysis for Seismic Design of Tailings Dams". Journal of Geotech. Engng Div., ASCE, Vol. 111, No. 7, July 1985, pp.916-933.

Geotechnical Investigations for the Assessment of the Risk of Water Leakage from Pressure Tunnels

J.R. ENEVER
M.Eng.Sc., B.E. (Mining), A.R.M.I.T., member A.G.S.
Senior Principal Research Scientist, CSIRO, Division of Geomechanics
M.B. WOLD
B.Appl.Sc., F.R.M.I.T., member A.G.S.
Senior Research Scientist, CSIRO, Division of Geomechanics
R.J. WALTON
B.Appl. Sc., A.R.M.I.T., member of A.G.S.
Principal Experimental Scientist, CSIRO, Division of Geomechanics

SUMMARY The role of rock stress measurements and borehole pumping tests in the assessment of potential for hydraulic jacking of rock joints and fractures is discussed in relation to three pressure tunnel projects in Australia. Investigations for the siting of steel pressure linings, carried out in varied geological and topographical conditions, have shown that rock stresses and hydraulic jacking potential may vary strongly over short distances within rock masses, with structural effects appearing to have a particularly strong influence on variability. The results of these studies suggest that conventional methods of design for placement of steel linings should be supplemented by direct field measurements to assist in reducing the risk of water leakage from pressure tunnels, and the economical placement of full pressure linings.

1. INTRODUCTION

In the planning and construction of hydro-electric power stations, the design of the headrace pressure tunnel brings together geotechnical risk and economic considerations in a very direct way. The specification of lining requirements can have very significant impact on the placement and design of the machine hall and other excavations, and greatly affect the cost of the pressure tunnel itself. This is particularly true in situations of extreme topographic relief which are common to hydro-electric schemes. Bearing in mind the overall project aspects of efficiency in construction, long term operation, serviceability and safety, a general aim is to minimize the length of the full pressure lining requirements, while achieving an adequately low level of risk of water leakage.

Pressure tunnels which are unlined or have concrete linings, over the major portion of their length, have been widely used in hydro-electric schemes for many years. For instance, three Norwegian unlined pressure shafts were described by Vogt (1922). Provided that suitable conditions are encountered, with no significantly permeable rock structures or erosional paths intersecting the tunnel, and sufficiently high rock stress conditions to overcome hydraulic pressures, low leakage rates and satisfactory long term service have been achieved. However, failures do occur. An early example of hydraulic fracture of the tunnel wall and related leakage, associated with insufficient overburden stress, was at Herlandsfoss, Norway, in 1919 (Selmer-Olsen, 1970). A landslide initiated by increased pore pressure resulting from power tunnel leakage at the Fisher hydro-electric scheme, Tasmania, was described by Paterson et al (1975). More recently, failure of a reinforced concrete pressure tunnel lining and leakage to the surface was described by Sharma et al (1991).

The potential for development of leakage paths by hydraulic jacking of joints and fractures is a prime consideration for pressure-tunnel designers. Essentially, hydraulic jacking can occur when the hydraulic pressure exceeds the normal stress acting across a fissure. The rock stress conditions at any depth will be a function of overburden and tectonic forces, as modified by rock structural features, topography and groundwater. Empirical design criteria for depth of cover, incorporating topography, developed in Norway (Bergh-Christensen and Dannevig, 1971) and Australia (Dann et al, 1964) have been used successfully for many projects. Modern numerical stress analysis methods have confirmed these criteria; however, modelling methods require quantitative stress data as input, and direct measurement of stress conditions can be considered essential for their implementation. However, for the assessment of risk of water leakage, rock stress measurements and hydraulic jacking tests by borehole pumping are directly applicable in their own right.

This paper presents examples of recent stress- and hydraulic jacking measurements, carried out by CSIRO in Australia for design of pressure tunnels. Results are discussed in terms of stress variability associated with structural and topographic features, and their impact on tunnel lining requirements for the prevention of leakage.

2. STRESS MEASUREMENT AND VARIABILITY OF STRESS ESTIMATE

The empirical design rules such as the Norwegian Criterion have been shown to successfully predict adequate cover ratios for many projects, including slopes up to about 55 degrees from horizontal, and are thus very useful for preliminary layout design. By comparison, the use of design methods incorporating numerical stress analysis is much more explicit in the demands it places on rock stress and structural input data. A basic assumption for assessment of hydraulic jacking potential is that the hydraulic pressure within the discontinuity is less than the normal stress acting across it. This ignores any tensile strength component, as might exist for a healed joint, and although pumping tests sometimes reveal initial tensile strength, it is probably well to treat the joints as having no inherent strength. Furthermore, the orientation of the discontinuity with respect to the local stress tensor is obviously important, and for favourable orientations it is possible for the hydraulic pressure to exceed the minimum principal stress without causing hydraulic jacking. However, the question is raised as to the variability in joint spacing and orientation, and of the variability of the stress tensor as measured from point to point in the rock mass. There is ample evidence that stresses vary significantly in magnitude and direction over relatively small distances (e.g. Enever et al, 1990), particularly in metamorphic rock masses of the type in which hydro-electric schemes may often be found. Thus assessment of jacking potential based on measurement and model analysis of stress, must include consideration of the variation in measured stresses. Experience shows that this can be a difficult task, and aspects of the problem are discussed below.

The two most commonly used methods of stress measurement are stress relief by overcoring, and hydraulic fracturing. The individual results are, in essence, point measurements. In overcoring, the commonly used CSIRO HI cell, for instance, measures stresses acting in an essentially intact cylindrical volume of rock of about 150 mm diameter and 250 mm long. It

can be argued that in a jointed rock mass, this method may tend to overestimate the stress level because the intact rock, having a higher effective stiffness than surrounding jointed regions, will be more highly stressed. There will be a critical joint spacing, below which measurements cannot be made, based on the length of the HI cell. Typically, in a stress measurement program, measurements will be made at a number of points within each of several boreholes, the overall spacing of which should match the scale of the excavation and the scales of significant structural features.

The hydraulic fracturing stress measurement method commonly involves a length of borehole of 500 to 1500 mm, and cracks extending several metres into the surrounding rock, and thus samples a considerably larger volume of rock than that by overcoring. Nevertheless, for measurement of rock stress, defect free lengths of borehole are required, and the danger of overestimating stress is again present. Furthermore, on the scales of the excavation and of the major structural features, these dimensions may be small, and the hydraulic fracturing may still be seen as a point measurement. Conceptually, a mean stress tensor could be derived from the point values, using for example, the method described by Walker et al (1990). However, for the problem of hydraulic jacking potential, the minimum principal stress is of critical importance. As a suggested approach, the distribution of normal stress magnitudes and orientations, from the point measurements, should be assessed conjointly with the distributions of discontinuity orientations and the expected hydraulic pressure to obtain a probability function for jacking occurrence. The problem remains to calibrate this probability against real performance.

On the other hand, the long term shut-in pressure from the fracturing test may be taken as a reasonable measure of the stress normal to the fracture created. This principle can be applied for the direct measurement of hydraulic jacking potential using the pumping test, which is the most direct form of risk assessment for the design assumptions. In this method, joints or joint families of known orientation are isolated by packers, and the flow rates at a range of constant pressures are measured over several cycles. The discontinuous transition from low to high leakage rates marks the onset of hydraulic jacking, with differences between initial and subsequent cycles, if evident, providing a measure of tensile strength of the joint. Jacking pressures should be broadly consistent with stress measurements, after adjusting for orientation of the discontinuities, although in view of the suggested concentrations of stress in intact sections of rock between structural features, it could be expected that jacking pressures in the discontinuities could tend to be lower on average than the intact rock stresses.

3 RECENT FIELD INVESTIGATIONS

3.1 General

Stress and hydraulic jacking measurements, from the surface and from underground, have been recently carried out by the CSIRO for three pressure tunnel projects in Australia, to provide the project designers with quantitative data for lining specification. The projects are (locations, Figure 1):

1. the King River hydro-electric development on Tasmania's west coast,
2. the Boomerang Creek water tunnel on the central coast of New South Wales,
3. the Tully Millstream hydro-electric project in northern Queensland, the proposal for which is currently under review by the Queensland and Australian Governments.

These cases provide quite different examples of geological and topographical environment, and of anticipated hydraulic pressures in operation. They indicate the value of in situ measurements in refining knowledge of stress conditions and jacking potential for the purpose of pressure tunnel design.

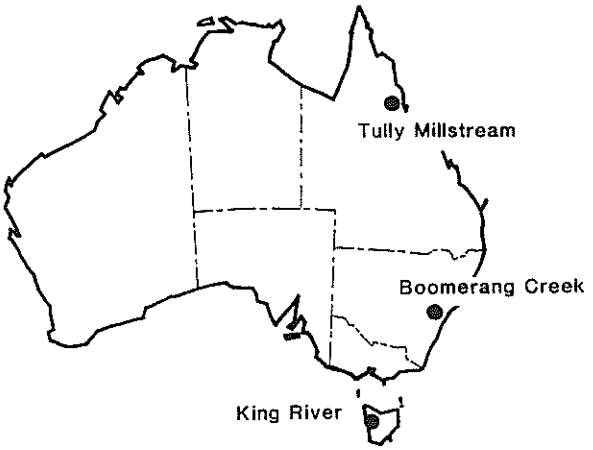

Figure 1 Locations of pressure tunnels subject to investigation

3.2 King River

Construction of the King River project involved a 7 km long pressure tunnel, linking water storages with a surface power station. The pressure tunnel was constructed by drill and blast to a horseshoe profile of 7.2 m crown diameter, with a total change in elevation from source to power station of 200 m. The lower portion of the tunnel is located in a sequence of highly structured volcanics.

From the outset of investigation for the project there was concern that near the lower, power station, end of the tunnel, relatively high water pressure and well developed discontinuity sets could lead to hydraulic jacking of the discontinuities, and unacceptable leakage. The initial design strategy called for a steel pressure lining to be installed upstream from the power station, for a distance that would ensure that hydraulic jacking would not occur. This was based on the notion that any potential jacking surfaces upstream from the upper end of the steel lining would be held closed by the in situ stress, against the maximum water pressure attainable.

During the initial investigation from the surface, hydraulic fracture stress measurements were undertaken in two boreholes, located on the proposed tunnel alignment (Enever et al, 1987a). One of these holes was located near to the critical point at which the rock stress magnitude, based on depth of overburden, would be expected to just balance the hydraulic jacking pressure. Hydraulic fracturing tests undertaken at about 20 m above the projected tunnel level indicated some very low shut-in pressures, in relation to the anticipated overburden pressure and in-service water pressure. Shut-in pressure in this context can be taken as a measure of the minimum stress magnitude in the rock mass. Based on this observation, it was decided to conduct more detailed investigations from within the tunnel when it had been advanced from the power station site to near the anticipated maximum extent of the steel pressure lining. The underground investigation involved overcoring stress measurements using the CSIRO HI cell (Walton and Crawford, 1987), and pumping tests on selected joints with different orientations (Enever et al, 1987b). The sites for these measurements are shown on Figure 2.

The overcoring results indicated the existence of a stress field which varied dramatically from point to point over distances as small as 2 m. Very low magnitudes of minimum stress component, even small tensions, were measured at some points. The variability was attributed to the influence of geological structures prevalent in the rock mass. The measured stresses were compared with the orientations of the joints surveyed in the tunnel in the vicinity of the measurements, and with the design water pressure (1.8-2.3 MPa), to assess hydraulic jacking

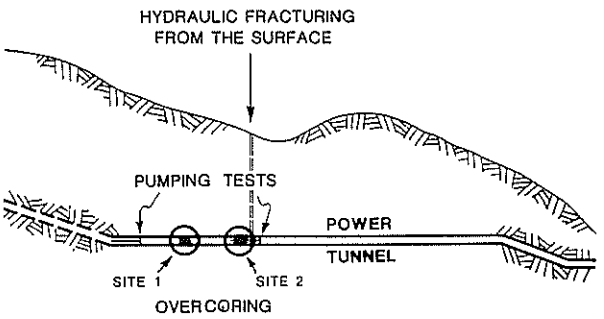

Figure 2 King River pressure tunnel. Vertical section, showing sites for overcoring and pumping tests.

potential (Bowling - personal communication). The results are summarized in Figure 3.

Direct measurement of the hydraulic jacking pressures were made by pumping tests conducted in two boreholes drilled sub-parallel to the tunnel, one of which extended from the end of the tunnel. Using packers to isolate variously orientated joints, these tests demonstrated joint opening and flow at pressures both above and below the design water pressure. Although the majority of both the stress measurements and the pumping test results indicated that the in situ stresses would be adequate to prevent hydraulic jacking, the inherent variability in the data suggested some risk of leakage. Subsequently, a decision was made to place a steel lining from the power station to the vicinity of the investigation site.

3.3 Boomerang Creek Tunnel

The Boomerang Creek Tunnel has been constructed to join the Mangrove Creek Reservoir to the Upper Wyong River as part of a water supply strategy for the Central Coast area of NSW. The circular machine-bored tunnel is 11 km long and approximately 3 m in diameter, and is located predominantly in massive, gently dipping sandstones and interbedded sandstone and siltstone. The lower 2 km of the tunnel, nearer to the Wyong river, is located in a well defined mountain ridge. The tunnel has been designed to perform as a pressure tunnel during downstream flow from the reservoir to river under gravity, and upstream flow under pumping pressure when water is being pumped from river to reservoir.

The initial design concept involved the installation of a full steel pressure lining for a short distance upstream from the lower portal, to guard against the chance of water leakage in the region of very low cover, followed by a "leak proof" concrete lining further upstream, where the tunnel is located within the ridge. In this region, the concern was for the potential existence of a very low horizontal stress within the ridge at the level of the tunnel; much less than the corresponding overburden pressure based on depth of cover. If existent, this low magnitude of stress could result in hydraulic jacking of joints intersecting the tunnel, and/or the formation of hydraulically induced fractures, by the static and dynamic water pressures in the tunnel in service.

During the initial site investigation from the surface, hydraulic fracture stress measurements were carried out in one drillhole located approximately midway along the length of the tunnel sector located within the ridge (Lun et al, 1987). Tests in this hole at the projected tunnel level indicated that the horizontal stress field was not as low as feared, and that the need for a tunnel lining, other than for support purposes, could probably be avoided. This was based on the notion that the stress magnitudes would be high enough to prevent either hydraulic jacking or fracture formation.

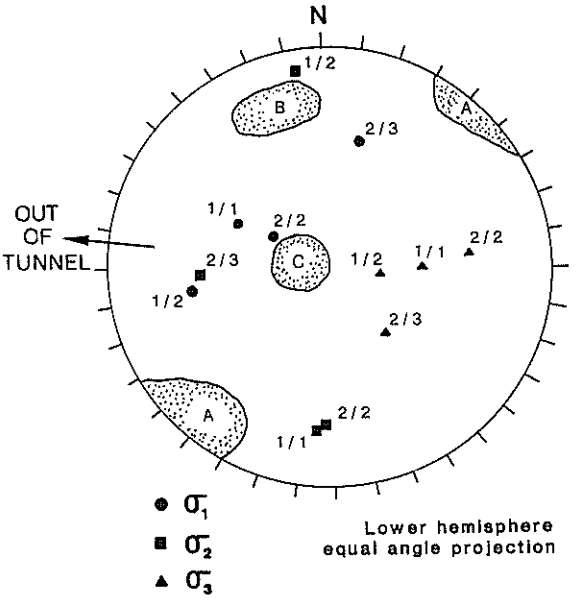

STRESS MAGNITUDES

TEST No.	SITE	σ_1 (MPa)	σ_2 (MPa)	σ_3 (MPa)
1/1	1	8.6	3.6	-0.2*
1/2	1	14.2	9.9	2.3
2/2	2	9.9	4.9	0.1
2/3	2	2.9	0.7	-0.4*

JOINT SETS (POLES TO PLANES) IN THE VICINITY OF THE STRESS MEASUREMENT SITES

* TENSILE STRESS

Figure 3 King River. Stereographic projection showing orientation of principal stresses from overcoring measurements, and poles to planes of joint sets

To confirm this indication, overcoring stress measurements using the CSIRO HI cell were carried out at four locations along the tunnel as it neared completion (Walton and Enever, 1989). The measurement sites were:

(a) near the mid-point of the tunnel under maximum depth of cover, relatively remote from the influence of surface topography,

(b) close to the location of the from-surface measurements, and

(c) at two sites near the region envisaged for the steel lining, near the lower portal.

The main results for sites 2, 3 and 4 are summarized in Figure 4 and Table 1. The results from the site closest to the surface hydraulic fracturing tests (site 2) confirmed the conclusion that the horizontal stresses within the ridge were not generally low in terms of the likelihood of hydraulic jacking or fracturing. The results from further downstream, near the lower portal (sites 3 and 4), indicated a consistently uniform stress field with a minimum principal stress magnitude large enough to prevent leakage upstream of the point already designated as the limit for full pressure lining. The influence of topography on stresses was apparent, with a low measured vertical stress component

TABLE I

BOOMERANG CREEK.
PLANNED WATER PRESSURES AND MEASURED STRESSES AT THREE TEST SITES

Site No.	Storage head pressure (MPa)	Max. steady state pumping head (MPa)	σ_3 (MPa)	Measured vertical stress (MPa)	Calculated vertical stress (MPa)	Ratio: measured / calculated vertical stress
2	0.6	0.88	2.87	3.28	4.35	0.75
3	0.6	0.88	1.15	1.75	2.40	0.73
4	0.6	0.88	1.11	1.32	2.35	0.56

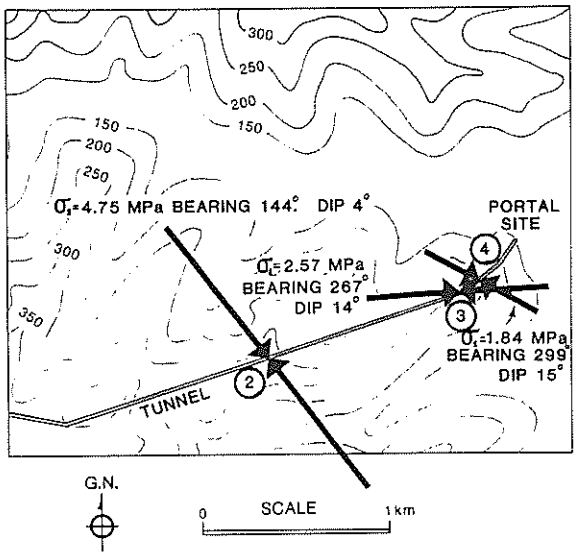

Figure 4a Boomerang Creek. Plan showing topographic contours. Sub-horizontal stresses at three overcoring test sites are indicated.

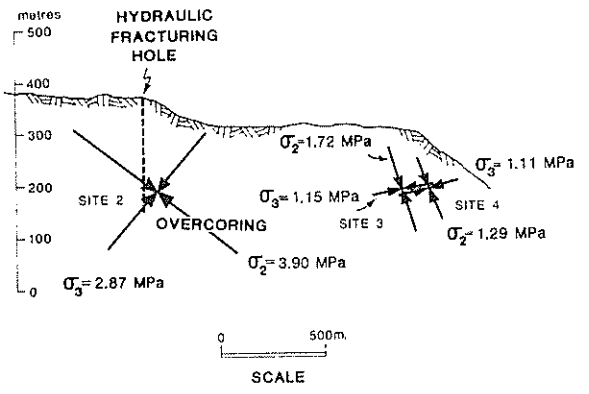

Figure 4b Boomerang Creek. Vertical projection along tunnel alignment, showing intermediate and minor principal stress at three overcoring test sites.

compared to that estimated from depth of cover. This supports the conventional wisdom for pressure tunnel design under ridges or "noses" between valleys, which calls for a notional smoothing of the peaks and an effective reduction of overburden height.

The results of the testing program in this instance confirmed the design strategy calling for a limited extent of steel pressure lining, in conjunction with an essentially unlined tunnel beyond a critical point, based on the measured in situ stress state. Concrete lining could be based on ground support requirements alone, resulting in a substantial cost saving.

3.4 Tully Millstream Project

The Tully Millstream hydro-electric scheme, currently under review by the Federal Government, State Government and Wet Tropics Management Authority, is located on the Tully River in North Queensland. All engineering work on the scheme has been halted pending the outcome of the scheme review. If it goes ahead, the project will involve construction of a large underground power station chamber and a number of service tunnels, including a high pressure headrace tunnel. The headrace tunnel as currently envisaged would have a total change in elevation of 656 m, with a maximum water head on entry to the power station of approximately 690 m. The entire complex will be sited in a volcanic sequence, with a number of well developed joint sets and some prominent shear zones. A generalized longitudinal section is shown in Figure 5, demonstrating the topography of the region.

In light of the high water pressures involved, the concept from the outset of the project has been for the pressure tunnel to be constructed with a section of steel lined penstock at the lower, power station end.

During an initial site investigation from the surface, hydraulic fracture stress measurements and pumping tests on specific joints were undertaken in two drillholes, one of which was located close to the originally proposed power station site (Strata-Tek Pty. Ltd., 1988). The results from these tests indicated a very variable stress field, particularly with regard to orientation, apparently reflecting the influence of topography. The measurements suggested that at the level of the proposed power station, the minimum horizontal stress would approximate the theoretical overburden pressure, based on depth of cover. Subsequently, a comprehensive program of testing was conducted from an exploratory tunnel constructed to within close proximity to the likely location of the power station (Enever and Edgoose, 1991; Walton and Litterbach, 1991; Wold, 1991). The investigations involved overcoring stress measurements using the CSIRO HI cell, hydraulic fracturing using the CSIRO Minifrac System, and pumping tests on selected joints in a 250 m long sub-horizontal hole drilled ahead of the tunnel end. The hydraulic fracturing, which was carried out in three mutually orthoganal drillholes, represented the first civil engineering application of the Minifrac System, which has recently been developed by CSIRO for use in 38 mm diameter holes (Wold et al,1989; Enever et al,1990).

The overcoring and hydraulic fracturing measurements indicated that the stress field varied in both magnitude and direction from

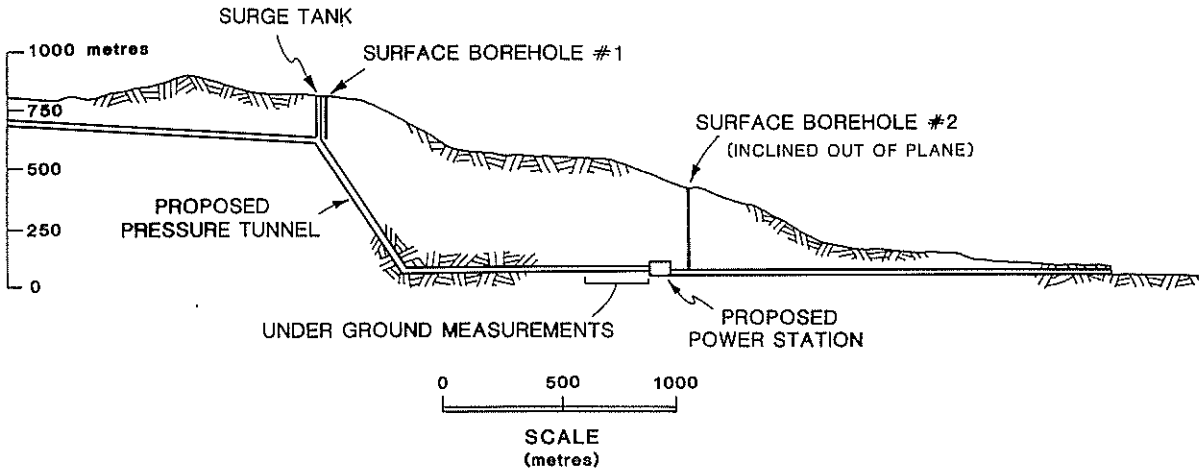

Figure 5 Tully Millstream. Vertical projection of Exploratory Tunnel, showing topography and location of measurement site.

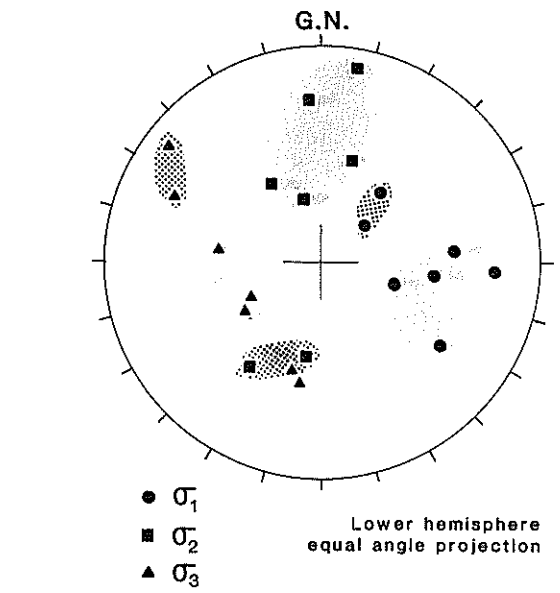

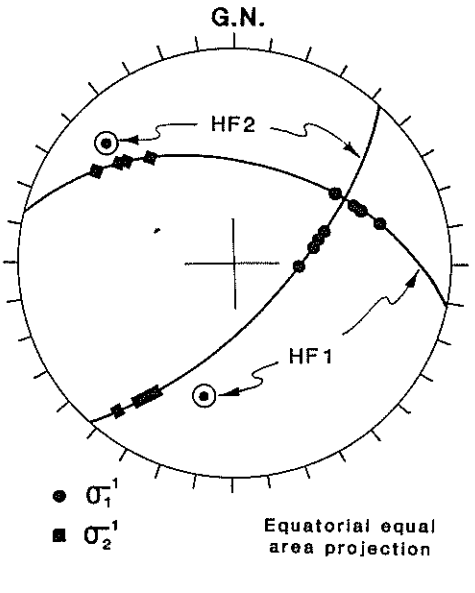

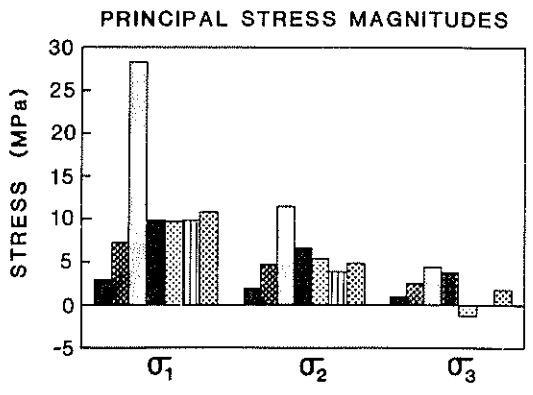

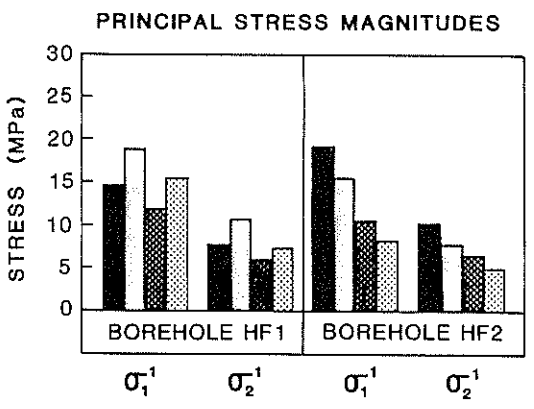

Figure 6a Tully Millstream. Principal stress orientations (lower hemisphere equal angle projection) and magnitudes from overcoring measurements.

Figure 6b Tully Millstream. Secondary principal stress orientations (equatorial equal area projection) and magnitudes from hydraulic fracture tests.

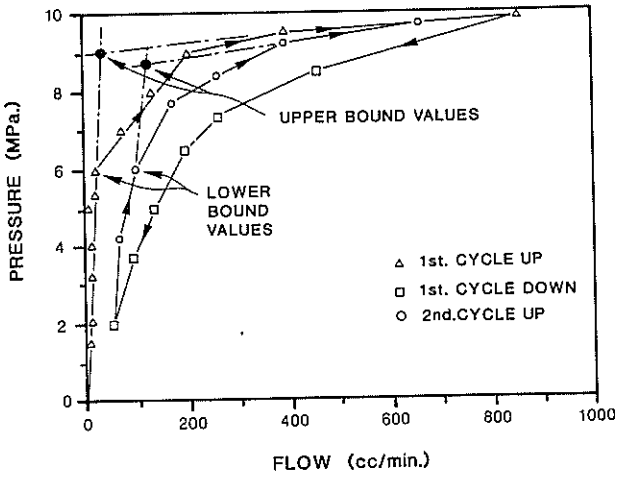

Figure 7 Tully Millstream. Flow vs pressure for initial and second pumping cycle, showing hydraulic jacking pressure, upper and lower bound estimates.

point to point (Figure 6). Both techniques showed the presence of low minimum principal stresses at some points in the rock mass, and high maximum principal stresses at other points. As at King River, this was thought to be related to the influence of structural discontinuities, and to the topography. In terms of the potential for water leakage, some of the measured stress components were low enough, with respect to the maximum anticipated water pressure, to suggest hydraulic jacking of unfavourably oriented discontinuities. This was confirmed by the results of the direct pumping tests, which showed that some joints could be opened at relatively low pressures (Figure 7). However, there was no clear relationship between the orientations of these critical joints, and the measured orientations of the stress field. Likewise, there was no clear spatial relationship between the measured hydraulic jacking pressures and distance into the borehole. Vertical depth of cover was not a dominant variable, at least over the depth range investigated.

4. DISCUSSION AND CONCLUSIONS

The King River project exemplifies the very low rock stresses that can exist at the lower end of pressure tunnels for surface power stations in steep terrain. In this situation, a steel pressure lining is generally recognized as inevitable from the outset, and the geotechnical problem is to determine how far upstream to proceed with the lining. While the majority of stress and pumping measurements in the region selected for investigation suggested adequate resistance to leakage, the occurrence of very low stress components within some units of the rock mass indicated the need for steel lining to this vicinity, at a point above that otherwise considered necessary. This was confirmed by the low pumping pressures required to initiate hydraulic jacking in certain cases.

Like King River, the Boomerang Creek project involves a pressure tunnel under low cover in the region of the down-stream portal, with a steel pressure lining considered necessary in this region. However, in this case the more systematic stress field measured over the region of investigation, and the consistent magnitudes of the minimum stress component near the planned extent of the steel lining confirmed the adequacy of the original lining strategy with regard to steel lining placement.

Compared to the two examples where the pressure tunnel intersected the surface, the planned siting of the Tully Millstream power station under more than 300 m vertical cover might be expected to provide significant confinement of the pressure tunnel by overburden stress, reducing the potential for leakage by hydraulic jacking and lessening lining requirements. However, measured stresses were highly variable, with low minimum stress levels compared to those expected from overburden. The pumping tests indicated correspondingly low jacking pressures. These results can be expected to significantly influence the strategy adopted by the designers of the pressure tunnel lining.

The high variability of stress magnitude and direction in the hard jointed rock at King River and at Tully Millstream, was in marked contrast to the more uniform and systematic stresses at Boomerang Creek, where the sediments were relatively homogeneous. Since at all sites topography is a major feature, this suggests that geological structure has an overriding influence on stress variability, compared to topographical effects.

With respect to site investigation techniques, hydraulic fracture and pumping tests undertaken from the surface were very valuable in that they gave an early indication (with respect to the design procedure) of the general stress regime at critical locations. This knowledge was significantly expanded by the stress and pumping test programs from underground, from where more comprehensive investigations could be undertaken.

It is concluded that programs of stress measurement and direct pumping tests are very important for the assessment of leakage potential for pressure tunnel projects. Because of the generally close proximity of the tunnels to the surface topography, and of the effects of geologic structures in the rock mass, stress fields vary significantly across the regions of interest, and may not be adequately predicted from a priori considerations. Self evidently, mapping of structural discontinuities is essential, and the orientations of joint and fracture planes should be considered in conjunction with the stress field orientations, since the stress components normal to the planes are the critical factor in assessing the risk of hydraulic jacking. Hydraulic pumping of individually isolated, orientated joints is the most direct test of jacking potential.

5. ACKNOWLEDGMENTS

The authors acknowledge, with thanks, the support of the Hydroelectric Commission, Tasmania, the Public Works Department, NSW, and Golder Associates in conjunction with the Queensland Electricity Commission, in the conduct of these field studies. They are grateful to Mr. N. Litterbach of Mining Measurement Services, and Mr. J. Edgoose of Strata-Tek Pty. Ltd., and to their CSIRO colleagues, for their contributions to the field measurements.

6. REFERENCES

Berg - Christensen, J. and Dannevig, N.T. (1971). Engineering geological considerations concerning the unlined pressure shaft at the Mauranger Power Project. A/S GEOTEAM Report No. 2398.03. Oslo, 1971.

Dann, H.E., Hartwig, W.P. and Hunter, J.R. (1964). Unlined tunnels of the Snowy Mountains Hydro-electric Authority, Australia. Jnl. of Power Division, Proc. ASCE. October 1964. pp. 47 - 79.

Enever, J. R., Wooltorton, B. and Johnson, M. (1987a). The application of hydraulic fracturing to the assessment of lining requirements for a pressure tunnel. Proc. VI Australian Tunnelling Conf. Melbourne, March, 1987. pp 109 - 118.

Enever, J. R., Litterbach, N. and Dean, A. (1987b). Pumping tests in the King River power tunnel. Site Investigation Report No. 44, CSIRO Division of Geoemchanics, Aust. November, 1987. 24 p.

Enever, J.R., Wold, M.B. and Walton, R.J. (1990). Scale effects influencing hydraulic fracturing and overcoring stress measurements. Scale Effects in Rock Masses, Pinto da Cunha (ed.) Balkema, Rotterdam, 1990. pp 317 - 326.

Enever, J. R. and Edgoose, J. (1991). Rock stress measurement and hydraulic jacking measurements at the Tully Power Station Site, Tully-Millstream Hydroelectric Project, North Queensland. Vol.1, Part C: Hydraulic jacking tests. CSIRO Division of Geomechanics Internal Report - New Series No. 66. 17 p.

Lun, P.T.W., Enever, J.R., Helm, D.C., Tan, C.P. and Coulthard, M.A. (1987). Stress measurements/stress analysis for the Mangrove Creek Dam - Upper Wyong River pressure tunnel. CSIRO Division of Geoemchanics, Aust., Site Investigation Report No. 38.

Paterson, S.J., Hale, G.E.A. and Ikin, D.B. (1975). Stabilizing a landslide above Fisher penstock, Tasmania. Proc. 2nd Aust. - New Zealand Conf. on Geomechanics. Brisbane, 1975. pp 314 - 318.

Selmer - Olsen, R. (1970). Experience with unlined pressure shafts in Norway. Proc. Int. Symp. on Large Permanent Underground Openings. Oslo. Ed. Brekke and Jorstad. pp. 327 - 332.

Sharma, V.M., Singh, R.B., Kuberan, R., Moza, K.K. and Sharma, T. (1991). In situ stress measurement for design of tunnels. Proc. 7th ISRM Congress, Aachen, Sept., pp 1355-1358.

Strata-Tek Pty. Ltd. (1988). Tully-Millstream Hydro-electric Scheme. A report on hydraulic fracture testing to define in situ stress conditions. Report to Snowy Mountains Engineering Corporation, September 1988. 47 p plus appendices.

Vogt, J.H.L. (1922). Tryktunneler og geologi. Norges Geol. Undersokelse nr. 93, Oslo.

Walker, J.R., Martin, C.D., and Dzik, E.J. (1990). Technical note. Confidence intervals for in situ stress measurements. Int. J. Rock Mech. Min. Sci. & Geomech. Abstr. Vol. 27, No. 2, pp. 139 - 141.

Walton, R.J. and Crawford, G.R. (1987). Rock stress measurements at the King River power tunnel, Tasmania - Part 1: overcoring measurements. CSIRO Division of Geomechanics, Aust. Site Investigation Report No. 43. October, 1987. 37 p.

Walton, R.J. and Enever, J.R. (1989). Rock stress measurements by overcoring at the Boomerang Creek tunnel, NSW. CSIRO Division of Geomechanics Internal Report No.4, 45 p.

Walton, R.J. and Litterbach, N. (1991). Rock stress measurement and hydraulic jacking measurements at the Tully Power Station Site, Tully-Millstream Hydroelectric Project, North Queensland. Vol.1, Part A: Stress measurement by overcoring. CSIRO Division of Geomechanics Internal Report - New Series No. 66, 60 p.

Wold, M.B., Enever, J.R. and Crawford, G.R. (1989) Stress measurements in a burst-prone heterogeneous rock mass using a novel miniature hydraulic fracturing tool. Rock Mechanics as a Guide for Efficient Utilization of Natural Resources, Khair (ed.). 1989 Balkema, Rotterdam. pp. 435 - 442.

Wold, M.B. (1991). Rock stress measurement and hydraulic jacking measurements at the Tully Power Station Stie, Tully-Millstream Hydroelectrie Project, North Queensland. Vol.1, Part B: Stress measurements by hydraulic fracturing. CSIRO Division of Geomechanics Internal Report - New Series No. 66, 21 p.

Strain Compatability and Design Criteria for Reinforced Earth

S.R.FIDLER
B.E., Grad.I.E. Aust.
Geotechnical Engineer, Golder Associates Pty Ltd
K.B. WALLACE
Ph.D., M.I.E.Aust.
Head of School, Civil Engineering, Queensland University of Technology

SUMMARY Semi-empirical design methods are applied successfully to design conventional reinforced earth, geotextile reinforced earth and nailed soil. However, as new types of reinforcing elements are tried in a variety of types of soils and rocks, there is considerable scope for further study of the most appropriate design assumptions and techniques for analysis and design of soil and rock reinforcement.

A method of analysis is described, which is a modification of a working load, displacement based analysis known as the displacement method. The progressive development of displacement as construction proceeds is modelled, as is the stress-strain behaviour of the soil.

Results of analyses using the modified displacement method and analyses using an elasto-plastic finite difference program are studied to provide insight into the effect of the method of determining the normal stress distribition on the failure surface and the significance of choice of Factors of Safety.

1. INTRODUCTION

Semi-empirical design methods are applied successfully to design conventional reinforced earth (Juran et al, 1978), geotextile reinforced earth (Jewell, 1990) and nailed soil (Guillox et al, 1983) and there has been extensive research and field studies of these types of problems. However, as new types of reinforcing elements are tried in a variety of types of soils and rocks, there is considerable scope for further study of the most appropriate design assumptions and techniques for analysis and design of soil and rock reinforcement.

The present work uses a modified "displacement method" of analysis to study the significance of various design assumptions and to provide some insight into choice of appropriate Factors of Safety. It is thought that displacement methods, while relatively simple and expedient, offer significant advantages because they can show the inter-relationship between the relative stiffness of the various components of the system and the safety with respect to failure of these individual components.

The displacement method, as used by Gourc (1986) and others, has been modified to account for the progressive development of displacement as construction proceeds and to model the stress-strain behaviour of the soil in a simple way. A series of potential log spiral "failure" surfaces are considered and for each the rotational displacement required for equilibrium is calculated. The critical surface is chosen as that which undergoes the maximum decrease in potential energy to come to equilibrium.

2. DESIGN METHODS FOR REINFORCED SOIL SYSTEMS

In general, design methods for reinforced soil systems are currently based on analysis of the at-failure condition, and employ limit equilibrium methods of analysis or the limit analysis concept (Juran and Schlosser 1978). In these methods it is most common that the reinforcement force required for equilibrium is calculated, based on the assumption that the soil resistance is fully mobilized.

Most commonly, the Factor of Safety is defined as the maximum available reinforcement tension (limited by either reinforcement strength or soil-reinforcement interface strength), divided by the calculated reinforcement tension required for equilibrium.

The methods currently used for design do not allow the calculation of tensions developed under working loads, and therefore do not allow the assessment of the local Factor of Safety at the level of each reinforcement, with respect to reinforcement rupture or pullout.

The fundamental limitation of the current design methods in this respect is that the requirement of strain compatibility between the soil and the reinforcement is not considered. Strain compatibility must be considered if the load sharing between the soil and the reinforcements and between the reinforcements themselves is to be determined, and hence local Factors of Safety calculated. (The significance of local Factors of Safety will be discussed in some detail in a subsequent section.)

3. THE DISPLACEMENT METHOD

A displacement compatibility design method was proposed by Gourc et al. (1986) and Delmas et al. (1986), and developed further by Ratel (1987). The proposed method, known as the "displacement method", was based on the following assumptions:

- during construction, the active zone (see Figure 1) undergoes a rigid body translation or rotation. No allowance was made for the progressive development of the movement as construction proceeds. The boundary between the active zone and the resistant zone (termed the "failure surface" on Figure 1), is the line along which shear strains are concentrated, and also the locus of maximum tension.
- the relationship between the local deformation of the reinforcement at the potential failure surface, and the

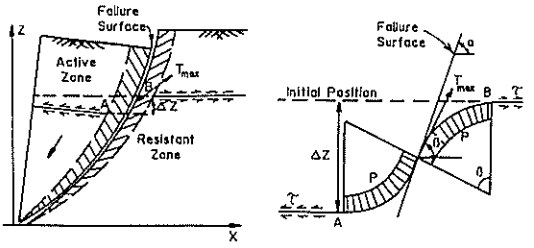

FIG. 1. Anchored Membrane Concept for Geotextile Reinforcement (Gourc et al. 1986)

normal stress acting on the reinforcement through the zone of local deformation is based on the concept of the reaction modulus of an elastic soil.

- the normal stress on the failure plane is determined using a conventional slope stability method of slices (based on the Fellenius assumptions).

The displacement of the active zone that is required to develop sufficient reinforcement tension to ensure global equilibrium of the active zone is calculated for a range of potential failure surfaces. In the determination of global equilibrium, the contribution of shear stresses in the soil to the forces resisting failure is limited to the ultimate resistance reduced by a desired Factor of Safety. The required level of reinforcement is determined such that the developed displacements do not exceed acceptable limits. The application of such a criteria for a reinforced embankment in a practical sense is not clear, since the displacements develop progressively as construction proceeds.

The method as proposed by Gourc et al. (1986) does not therefore fully consider the strain compatibility between the two components of the system since it is based on an assumed Factor of Safety on soil strength.

3.1 Modifications to the Displacement Method

An analysis technique (the "modified displacement method") has been developed by the principal author and is discussed in the following sections. This method is based on the displacement method as outlined above, but which differs from the method as proposed by Gourc et al. (1986), Delmas et al. (1986) and Ratel (1987) in two important aspects:

- the progressive development of displacement as construction proceeds is modelled.
- an attempt is made to model the shear stress - shear strain behaviour of the soil.

A computer program, MDISMET (Modified Displacement Method) has been developed to carry out the large number of calculations required.

3.1.1 Modelling of Construction Process

In the originally proposed formulation of the displacement method, equal translational or rotational displacements (depending on the shape adopted for the failure surface) are experienced at all locations along the failure surface. Consequently, the only difference between the compatible reinforcement strains for the different reinforcing layers is due to changes in the inclination of the failure plane.

It is readily apparent that the displacement of the active zone develops progressively as the construction of a reinforced embankment proceeds. The compatible reinforcement strains are therefore not only a function of the failure surface geometry, but also of the location of the reinforcement. The reinforcements towards the base of the wall develop strain progressively as the material above is placed, and hence the reinforcement strains and tensions are greatest in the lower reinforcements.

In the proposed extension of the displacement method, the displacement required to develop equilibrium is determined *for each stage of construction*, considering the contribution of the layers of reinforcing *that have been installed at that stage of construction*. The final reinforcement strains are equal to the sum of the strains that have been imposed during each of the construction stages.

3.1.2 Modelling of Stress-Strain Behaviour of the Soil

In the proposed extension of the displacement method, the soil is modelled as an elastic, perfectly plastic material with a yield strength defined by the Mohr-Coulomb criteria (see Figure 2). The method adopted is similar to that adopted by Cooper (1988) in the analysis of progressive failure of slopes, except that the soil is assumed not to strain soften, and that a variation of δ_{peak} with normal stress is not considered.

The active zone is assumed to displace as a rigid body. The shear stresses developed along the failure plane are calculated as a function of displacement through the displacement modulus S (see Figure 2), but are limited to the shear strength of the material. The determination of the displacement modulus is currently based on the assumption of a value for δ_{peak} (values in the range of 10-15mm have been used). Definition of the displacement modulus in terms of the shear modulus of the soil is difficult and has not been attempted, since it is necessary to determine the width of the shear zone, which would be a function of the relative reinforcement stiffness.

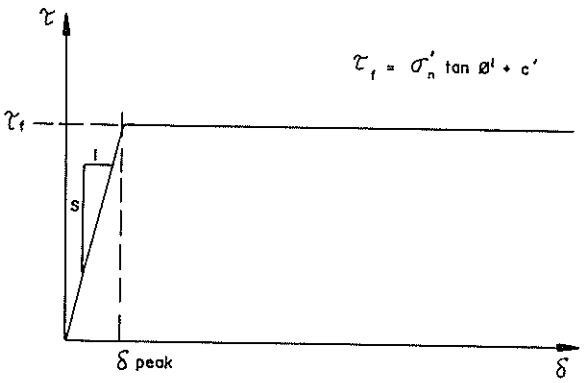

FIG. 2. Stress - Strain Relationship for Soil

3.1.3 Calculation Methodology

In the proposed extension of the displacement method, the active zone is incrementally displaced until the resisting contributions of the soil and the reinforcement are together equal to the disturbing forces. This calculation is carried out for a range of potential failure surfaces. The choice of the critical failure surface is based on the determination of the active zone which undergoes the maximum decrease in potential energy to come to equilibrium.

The reinforcement is considered to provide support to the active zone in two ways:direct support of the active zone through the action of the normal stresses between the reinforcement and the soil in the vicinity of the failure plane (Figure 1), and indirectly through increasing the normal stress on the failure surface (increased lateral confinement).

Separate Factors of Safety can be defined for the soil and for the reinforcement, either locally or globally. Further discussions on the choice and significance of Factors of Safety will be presented in a subsequent section.

4. CHOICE OF THE NORMAL STRESS ASSUMPTION TO BE USED IN THE DISPLACEMENT METHOD

The shape of the failure plane will have a significant effect on the choice of the most appropriate normal stress assumption. In the proposed development of the displacement method, analysis of vertical reinforced walls is based on the assumption that the failure surface will take the form of a log-spiral, which is vertical at its intersection with the ground surface behind the wall. A typical failure surface geometry is illustrated in Figure 4, which is consistent with experimental results published (Bolton et al., 1982).

The difference in normal stress on failure surfaces of such geometry, as determined using a method of slices based on the Fellenius assumptions and the Bishop assumptions has been investigated. Figure 3 illustrates the variation in normal stress with failure plane inclination and mobilized friction angle, as calculated by the two methods. It can be seen that for failure plane inclinations up to about 40 degrees, there is very little difference between the two methods, but that for steeper failure planes the difference is significant. It is therefore significant that the inclination of the failure plane shown in Figure 4 varies from about 55 degrees at the base of the wall up to 90 degrees at its intersection with the ground surface.

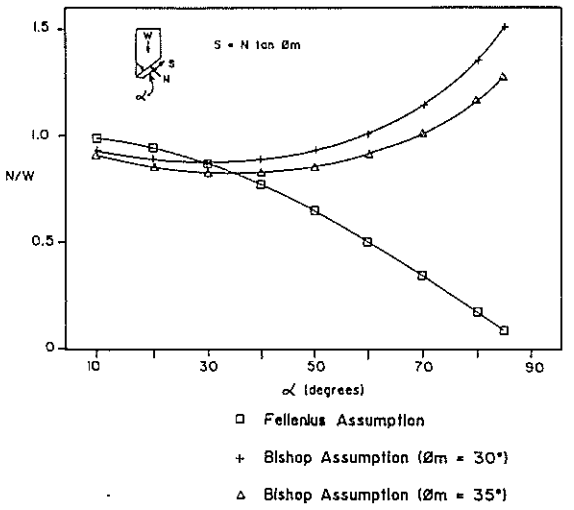

FIG. 3. Variation of Normal Stress on Slice Base with Base Angle for Fellenius and Bishop Assumptions

4.1 Effect of Normal Stress Assumption on the Results of the Displacement Method

Analyses were carried out for a vertical reinforced earth wall using the modified displacement method, to determine the significance of the normal stress assumption on the results of the calculation. Two cases were considered, with reinforcement of different tensile stiffnesses. The conditions analysed are depicted in Figure 4.

The formulation used for calculating normal stresses based on the Bishop assumptions was modified from the conventional formulation to make allowance for the dependance of the shear stress along the failure plane on the displacement of the active zone. The formulation used for the calculation of normal stresses based on the Fellenius method was not modified from the commonly used formulation.

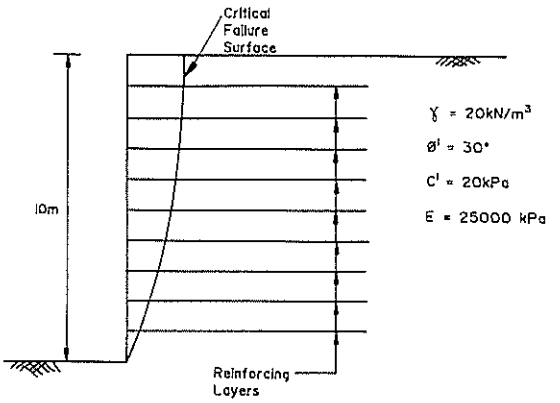

CASE	REINFORCEMENT MODULUS (kN/m)
1 (Relatively Inflexible Reinforcement)	62800
2 (Flexible Reinforcement)	4000

FIG. 4. Conditions Analysed with Modified Displacement Method and with FLAC

The normal stress distributions calculated for the two cases are illustrated in Figure 5, and the effect of the normal stress distribution on the calculated reinforcement tensions is illustrated in Figure 6. The reported results are for the critical failure surface (based on a maximum decrease in potential energy), which is illustrated in Figure 4. It can be seen that the calculated reinforcement tensions are significantly greater if the calculation is based on normal stresses derived from the Fellenius assumptions.

4.2 Finite Difference Analyses to Determine the Most Appropriate Normal Stress Distribution

Since the results of the modified displacement method were significantly dependant on the assumed normal stresses on the failure surface, finite difference analyses were carried out in an attempt to determine which of the two normal stress assumptions that had been considered was more appropriate for use in the modified displacement method, or indeed if neither were appropriate.

The two cases analysed with the modified displacement method were analysed with the finite difference program FLAC. The finite difference grid used for the analysis is illustrated in Figure 7. The construction process involving the sequential placement of layers of fill and reinforcing was modelled. The soil was modelled as an elastic, perfectly plastic material with a yield strength defined by the Mohr-Coulomb criteria, and the reinforcements were modelled with the cable elements provided by FLAC (which have zero bending stress).

The FLAC analysis calculated normal stress distributions (on the critical failure surface that is illustrated in Figure 4) are included on Figure 5. It can be seen that while there is reasonable agreement between the distribution calculated by FLAC and that calculated by using the Bishop assumptions, the correlation between the FLAC calculated normal stresses and those calculated using the Fellenius assumptions is poor. It would therefore seem reasonable that calculation of normal stresses using a method of slices based on the Bishop assumptions would be more appropriate than using a method based on the Fellenius assumptions.

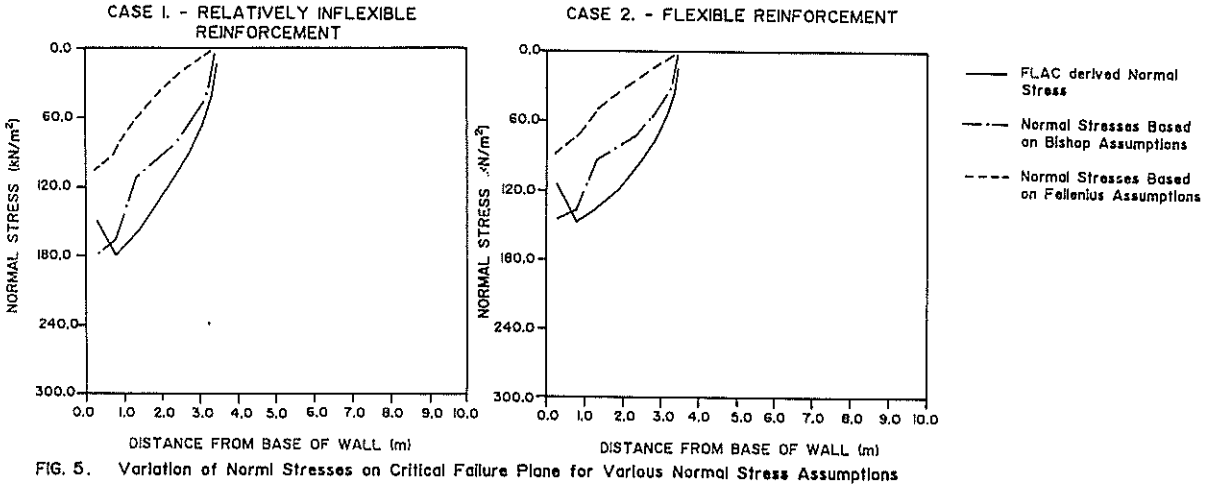

FIG. 5. Variation of Normal Stresses on Critical Failure Plane for Various Normal Stress Assumptions

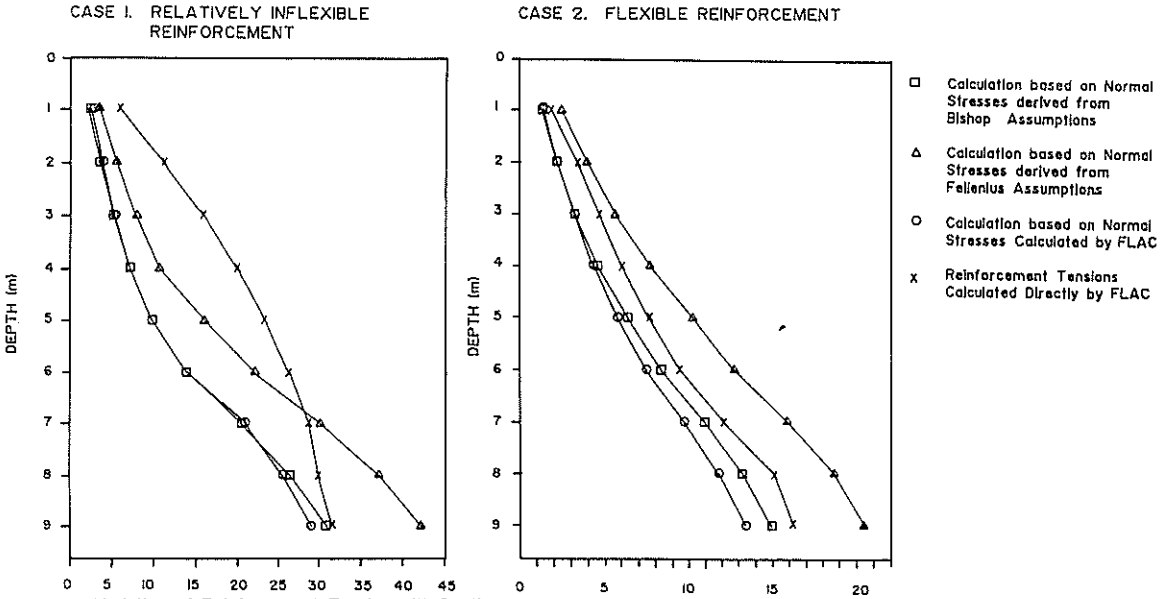

FIG. 6. Variation of Reinforcement Tension with Depth for Various Normal Stress Assumptions

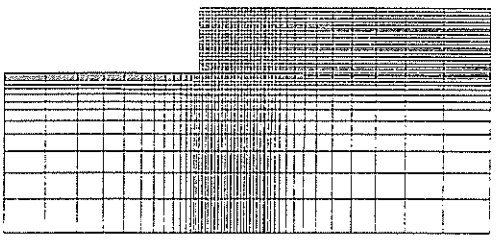

FIG. 7. Finite Difference Grid

This is supported by the comparison of reinforcement tensions that are calculated by the modified displacement method, using the normal stress distribution calculated by FLAC, with the reinforcement tensions calculated using the other normal stress distributions (Figure 6). Again there is a better correlation between the results from the FLAC derived normal stresses and the Bishop derived normal stresses than between the results from the FLAC derived normal stresses and the Fellenius derived normal stresses.

The reinforcement tensions that were calculated directly by FLAC are also illustrated in Figure 6. It can be seen in the case of the stiffer reinforcement that although the maximum reinforcement tension calculated by the modified displacement method using the Bishop assumptions is in good agreement with the maximum value calculated by FLAC, the distribution of reinforcement tensions is significantly different, with the total required reinforcement tension being much less when calculated by the modified displacement method.

In the case of the more flexible reinforcement, there is reasonable correlation between the tensions calculated by the modified displacement method using the Bishop assumptions, and the tensions calculated by FLAC.

The results suggest that the displacement method is more applicable to reinforcements which are flexible in tension than those which are relatively inflexible in tension.

5. SIGNIFICANCE AND CHOICE OF FACTORS OF SAFETY

5.1 General Comments

In general, reinforced soil systems can fail either by rupture of the reinforcements or by pullout of the reinforcements. The consequences of the two types of failure are different, and hence different Factors of Safety are appropriate for the different modes of failure.

Design methods for reinforced soil systems which are based on limit equilibrium concepts commonly calculate a global Factor of Safety on reinforcement rupture or on reinforcement pullout, with no Factor of Safety being applied to soil strength.

The assumption that all reinforcing elements have reached their ultimate strength at failure presumes a ductility and continuity of construction that may be difficult to achieve in practice (Bolton and Pang, 1982). Bolton and Pang (1982) and Juran and Schlosser (1978) identified the progressive nature of failure (in the case of failure by reinforcement rupture), in which the most highly stressed element ruptures first, followed in rapid succession by the remaining elements. This indicates that redistribution of the forces in the most highly stressed element to other elements should not be relied upon. However, limit equilibrium methods automatically redistribute stress away from the most highly stressed element so that all reinforcements have the same calculated Factor of Safety. Evidently, for the case of reinforcement rupture, the safety of a particular design is more directly related to the Factor of Safety against failure of the most highly stressed element than to a global Factor of Safety.

If the ultimate reinforcement pullout load was known with a high degree of confidence, it would seem reasonable to accept lower Factors of Safety on reinforcement pullout if a high Factor of Safety is calculated for the soil shear stresses. Intuitively it would seem that redistribution of stresses to the soil would be possible if a reinforcement failed by pulling out since it maintains the load that it carried at the point of failure, unlike a reinforcement which fails by rupturing and must shed all the load that it was carrying. A similar argument applies to the redistribution of stresses from the soil to the reinforcements once it has reached its ultimate strength. It is noted that the adoption of lower Factors of Safety would require the magnitudes of the loads carried by the soil and the reinforcement to be similar.

It is apparent that a method of calculation is required in which the tension in each individual reinforcement is determined and in which the proportions of the disturbing force carried by the soil and the reinforcements are determined, in order to rationally assess the risks associated with a proposed design.

5.2 Significance of Relative Stiffness

It is apparent that the sharing of load between the reinforcements and the soil is important when considering the appropriate Factors of Safety to be applied.

The effects of relative stiffness on load sharing and on Factors of Safety are illustrated in Figure 8. In this figure it is assumed that the influence of the reinforcement can be taken as an increase in shear resistance along the potential failure plane.

The benefit provided by the reinforcement as shown in Figure 8 is due to direct support to the active zone through the interaction of the reinforcement and the active zone in the vicinity of the failure surface, and due to indirect support provided by increased lateral confinement. The relative magnitudes of these components is not readily apparent but has significance in terms of the ability of the system to redistribute load between the two components.

It can be seen that for the same global Factor of Safety, the local Factors of Safety for the two components are significantly different. It is therefore apparent that if redistribution of stresses between the soil and the reinforcement is not possible, a design method is required in which strain compatibility is considered so that the load sharing between the components of the system can be determined. It would also seem that the acceptable Factors of Safety for the two components should include some provision for uncertainty in the modulus values.

5.3 FLAC Analyses of Load Redistribution

Non-linear finite difference analyses using the computer program FLAC were carried out to determine whether load can effectively be transferred from one component of the system to the other if it has insufficient strength. Analyses were not carried out for the case of reinforcement rupture, since the cable elements provided in FLAC will yield, but do not have a limiting strain at which rupture occurs.

The global Factors of Safety on soil strength and reinforcement pullout (calculated from the FLAC results), for the two cases considered previously, are tabulated below.

Table I - Global Factors of Safety for Cases 1 and 2

Case	Global FOS_{soil}	Global FOS_{rft}
Case 1 Relatively Inflexible Reinforcement	1.75	1.88
Case 2 Flexible Reinforcement	1.4	2.1

Further analyses were carried out using FLAC, in which the strengths of the soil and the reinforcement were separately reduced by the amounts shown above (strength reductions were considered for only one of the two components in any one of the analyses conducted). For example, in the first analysis based on Case 1, the strength of the soil was reduced by a factor of 1.75, and the reinforcement strength was not altered. The calculated global Factors of Safety, after strength reduction, are tabulated below.

Table II - Global Factors of Safety after Strength Reduction

Case	Global FOS_{soil}	Global FOS_{rft}
Case 1 with soil strength reduced by 1.75	1.0	1.25
Case 1 with reinforcement strength reduced by 1.88	1.64	1.46
Case 2 with soil strength reduced by 1.4	1.0	1.42
Case 2 with reinforcement strength reduced by 2.1	1.35	2.33

Failure of the wall did not occur for any of the strength reduction scenarios considered. However, for the case of relatively inflexible reinforcement and reduced soil strength, the results indicated that the system was marginally stable, and that the addition of any extra load would have caused failure. Although the calculated global Factor of Safety for the reinforcement was 1.25, the lowest four reinforcements were at the point of pullout failure.

It can be concluded that there is significantly more capacity, within the systems considered, for load to be transferred from the reinforcements to the soil (under conditions of reinforcement pullout), than for load to be transferred from the soil to the reinforcement. It is apparent that the major contribution of strength improvement provided by the reinforcement is in the form

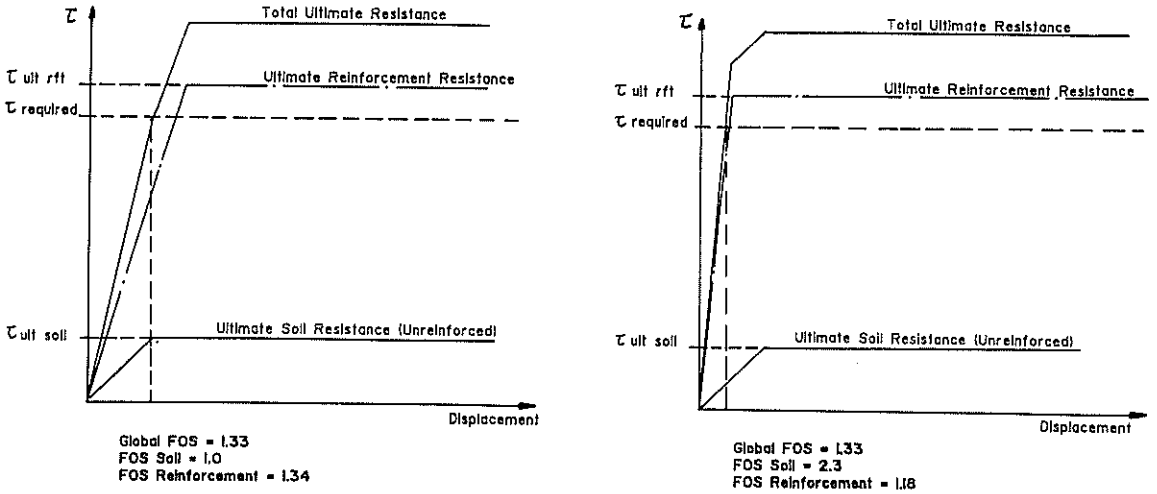

FIG. 8. Effect of Relative Stiffness on Load Sharing and Factors of Safety

of increased lateral confinement. Under conditions of reduced soil strength, this contribution is decreased also, hence the inability of the system to redistribute load from the soil to the reinforcement.

The results indicate that some reductions in the acceptable Factor of Safety may be considered on reinforcement pullout, if high Factors of Safety are calculated for the soil and if the ultimate pullout resistance of the reinforcements is known with confidence. However, similar reductions would not be available for the acceptable Factor of Safety on soil shearing.

6. CONCLUSIONS

The modified displacement method which has been developed offers the advantages of being able to model the influence of relative stiffness on the sharing of load between the soil and the reinforcement, and the progressive development of displacement as construction proceeds.

For the relatively steep potential failure surfaces encountered in reinforced earth systems, it appears that it is more appropriate to calculate normal stresses for use in the modified displacement method based on the Bishop assumptions rather than the Fellenius assumptions.

From the limited comparisons between results for the modified displacement method and more rigorous elasto-plastic finite difference solutions, it is suggested that the displacement method may be more appropriate where reinforcement is relatively flexible in tension.

Design methods for reinforced soil systems which are based on limit equilibrium concepts commonly assume that the ultimate strength of all elements is equally developed, and a global Factor of Safety is calculated. Intuitively, it would seem that redistribution of load would be possible in the cases of reinforcement pullout and full development of soil shear resistance, but that redistribution would not be possible in the case of reinforcement rupture. The ability of the system to redistribute load has significance for the choice of appropriate Factors of Safety for the various components.

Experimental evidence indicates that redistribution of load is not possible in the case of reinforcement rupture. Limited results from finite difference analyses indicate that redistribution is possible in the case of reinforcement pullout, but not in the case of full development of soil shear resistance.

The work has illustrated the potential benefits of the proposed modified displacement method in developing an insight into the significance of load sharing between the two components of reinforced earth systems, and the Factors of Safety for the individual components. Further work is to be directed towards correlation with the results of field and laboratory studies.

REFERENCES

Bolton, M.D. and Pang, P.L.R. (1982). Collapse limit states of reinforced earth retaining walls. Geotechnique, Vol. 32, No. 4, pp. 349-367.

Cooper, M.R. (1988). A displacement based analysis of progressive failure by the reserve capacity method. Proceedings of the Fifth International Symposium on Landlsides, Lausanne, Vol. 1, July, pp.583-589.

Delmas, P., Berche, J.-C. and Gourc, J.-P. (1986). Le dimensionnement des ouvrages reinforces par geotextiles. Bulletin de liaison de LPC, No. 142, Mar.

Gourc, J.P., Ratel, A. and Delmas, P. (1986). Design of fabric retaining walls: the displacement method. Proceedings of the Third International Conference on Geotextiles, Vienna, Vol. 4, Apr, pp. 1067-1072.

Guillox, A., Notte, G. and Gorrin, H. (1983). Experiences on a retaining structure by nailing in moriane soils. Proceedings of the Eighth European Conference on Soil Mechanics and Foundation Engineering, Helsinki, Vol. 1, pp. 499-502.

Jewell, R. (1990). Theory of reinforced walls: Revised design charts for steep reinforced slopes. Reinforced Embankments Theory and Practice, 1st ed., Thomas Telford, London.

Juran, I. and Schosser, F. (1978). Theoretical analysis of failure in reinforced earth structures. Proceedings of the Symposium on Earth Reinforcement, ASCE Annual Convention, Pittsburgh.

Ratel, A. (1987). Modelisation d'un sol renforce par geosynthetique: application de la method en deplacements. Ph.D. Dissertation, University of Grenoble, pp. 141-208.

Flexural Slip, An Often Neglected Hazard

P.M. JAMES
B.Sc., M.Sc.(Eng.), Ph.D., D.I.C., M.I.E.Aust.
Geotechnical Consultant, Brisbane

SUMMARY Flexural slip seams, resulting from tectonic folding, are typically manifest as bedding plane shears in sedimentary rocks and foliation shears in metamorphic rocks. Residual or near residual strengths apply along the seams, depending on the intensity of folding and rock type. Although of great lateral extent and frequent occurrence, these seams are often missed during site investigations; when encountered, they are sometimes incorrectly diagnosed. Major redesign of dams and occasional dam failures have resulted from a non-recognition of the hazard, while landslides initiated by these features have been wrongly attributed to progressive failure. Illustrative examples are described from the literature and the writer's experience.

1 INTRODUCTION

The phenomenon of residual strength was formalised some twenty five years ago (1). The specific case largely responsible for this understanding was a slip on the M6 Motorway at Waltons Wood, U.K., a failure which was essentially a reactivated Pleistocene slide. The failure zone, located in excavation was found to be very thin; along it, the clay platlets had been rotated to an alignment sub parallel to the shearing, thereby producing minimum strength conditions.

The alignment of clay platlets, together with some migration of clay and even mineralogical breakdown on the shear zone, are well documented characteristics of the development of residual strength, both in the laboratory and field situations, (2), (3), and (4). However, a similar development in solid rock formations, by the action of tectonic folding, appears to be less widely recognised in field, although the mechanisms at work are much the same.

During folding, or flexure, there is of necessity some displacement between the various units of a geological formation, Figure 1. In a sedimentary series, this is usually taken up along the bedding planes of the more argillaceous members. In metamorphic rocks, where rapid changes in lithology might not be present, the flexural slip planes tend to be more widely spaced, but again they typically occur on discrete horizons, parallel to the foliations.

The actual amount of strength reduction involved in any flexure will be determined by the intensity of folding and on how this is accomodated by the rock mass concerned. Since the path to the residual is shortest in the direction parallel to the bedding or foliation, (5), most flexural slip seams with the same orientations will tend to have strengths at or near residual. In such cases, highly polished surfaces occur, usually with sufficient striations to indicate the direction of movement during flexure. These striations can serve to distinguish flexural slip seams from shears caused by other phenomena such as translational faults or gravity slides.

The phenomenon of residual strength is well documented in the literature, both for landlsides and for

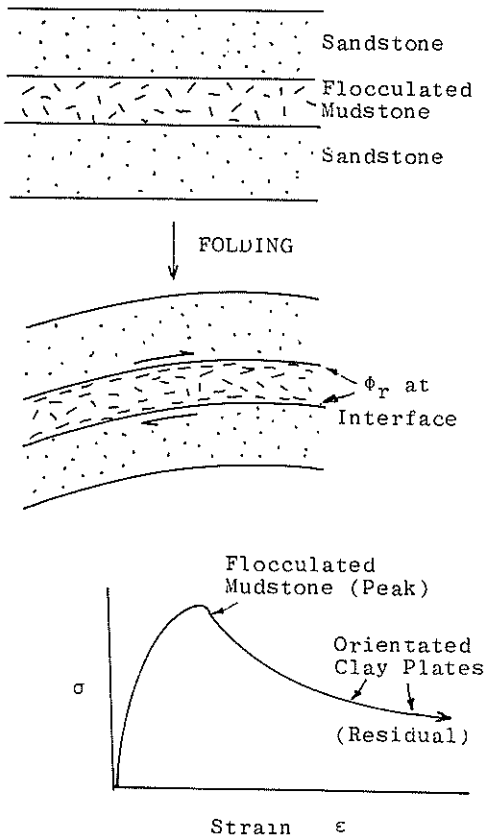

Fig. 1 Folding of a sedimentary sequence to produce residual strength at the argillaceous interfaces.

and for flexure. It might therefore appear redundant to labour the point. However, it has been the writer's experience that, on nearly every site where flexural slip seams have been encountered, they have either been missed during the investigations, or their origin has not been recognised - occasionally even actively disbelieved by engineering geologists.

Case histories are given below to illustrate this point. These have been chosen to include both sites where the problem was identified at an early stage and also sites where the problem was not recognised.

2 CASE HISTORIES - DAMS

2.1 The Hazard Recognised

The first detailed description of the significance of flexural slip seams in sedimentary rocks arose through investigations at Mangla Dam, (6). Here, alternations of clay shales and conglomerates had been moderately folded to produce complex shear patterns which showed a preferential association with the more clayey horizons. Within the shear arrays, flat polished and continuous surfaces were mapped; these were at residual strength.

Soon after Mangla, construction began on a 30 m high concrete dam forming part of the Muda Project, Malaysia; consultants were Sir William Halcrow and Partners. Initial drilling revealed mainly quartzites with mudstone partings, the series forming a dip slope on the right bank of the dam site. No unusual features were reported from the drill cores.

Prior to visiting the site in 1965, the writer identified on air photos what appeared to be a large dip slope slide on the same right bank. It seemed reasonable to assume that sliding had occurred on a mudstone bed and, further, that the mudstone might well have been weakened by flexural slip. Initial excavations for the dam confirmed this view. The mudstone was found to be sheared along its contacts with the quartzite although, elsewhere, it could have been described as a reasonably sound rock. It was, of course, the sound rock which had been retained in the drill cores.

As the strike of the beds approximated to the direction of the dam thrust, the sheared horizons in the mudstone posed a potential hazard to dam stability. A program of testing, with multistage in situ shear tests and complimentary laboratory tests was set up. Residual strengths with $\phi = 18^{\circ}$ were obtained, (7). As a result of these findings, the dam was anchored by high tensile steel cables which are still functioning satisfactorily today, Figure 2. Detailed descriptions of the geology and anchor design are given in (8).

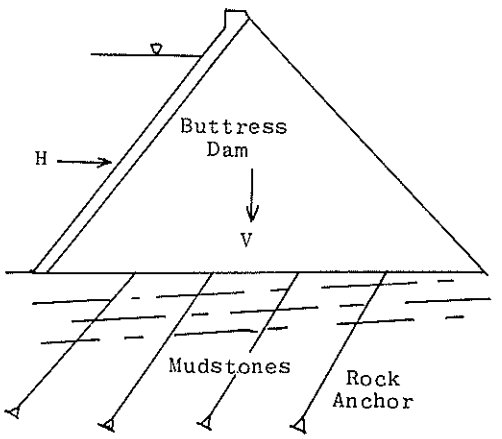

Fig. 2 Muda Dam, a 30 m high concrete buttress dam was founded on a quartzite-mudstone series. As a result of folding, the mudstone interfaces exhibited residual strengths, necessitating foundation improvement in the form of cable anchorages.

A similar situation to Muda has been described for Meadowbank Dam, Tasmania, (9). Here, in situ tests gave ϕ values around twenty degrees along the argillaceous bedding.

Flexural slip seams in almost swarm-like proportions occurred at Sugarloaf Dam, Victoria, (10), although their orientations were not critical to dam stability.

The above discussion was confined to sedimentary rocks. Flexural slip, or foliation, shears are also common in metamorphic rocks and a good account of them can be found in references (11) and (12). One case history is described below.

Kotmale Dam is a 90 m high concrete faced rockfill dam, constructed as part of the Mahaweli Development in Sri Lanka, in the early eighties. As at Muda, the consultants were Sir William Halcrow & Partners.

The rocks of the Kotmale area are hard Pre Cambrian gneisses with interbedded marbles known locally as limestones. The series is strongly foliated and has been moderately folded in Mesozoic times to produce a downstream dip of sixteen to twenty degrees at the dam site, with a component into the left bank. A typical dam section on the foundation is shown in Figure 3.

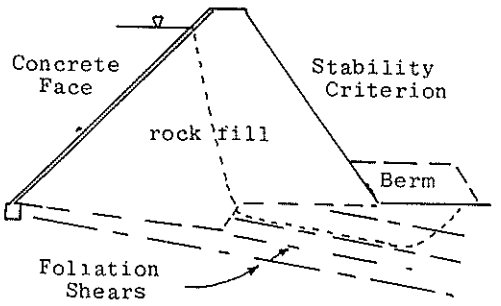

Fig. 3 Kotmale Dam, showing the foliation dip at the dam site. Six or seven major foliation shears were encountered in each abutment, traceable over tens to hundreds of metres.

Nothing unusual had been revealed by several drilling programs prior to construction. However, early excavation for a diversion tunnel revealed a band of highly weathered material in the sound rock, which contained a continuous, polished, surface parallel to the foliation. About this stage, doubts were expressed by client representatives as to the true origin of this and other similar features. Opinions were proferred that the polished surfaces were superficial features. Their continued existence at depth, in the diversion and other tunnels, generally dispelled this view. In any event, striations on the mirror-like surfaces showed movement had been in a direction at right angles to the dip, which ruled out gravity mechanisms. Displaced vertical dykes in the rocks gave direct evidence of the amounts of movement, measurable in tens of centimetres.

Multistage in situ shear tests were undertaken on the seams, together with a comprehensive laboratory program. Minimum strengths of $\phi = 12^{\circ}$ were obtained on first shearing of laboratory specimens. In situ tests gave a corresponding first shear value of $\phi = 15^{\circ}$, in the direction of dam thrust. There was little or no drop in strength on repeated shearing.

During later excavations on site, blocks of fresh rock, ten metres or more in plan dimension, slid down dip on inclinations as low as sixteen degrees. The majority of these were initiated by blasting, but the continued movement of the blocks confirmed that the value of the angle of shearing resistance, for very large areas, do not exceed that obtained for in situ tests by any significant amount.

It is to be remembered that these very low strength values occurred in otherwise hard rock. To neglect such dramatic planes of weakness would be to court disaster.

2.2 The Hazard as a Late Manifestation

At Maroon Dam, in Queensland, the whole right abutment of the dam site moved out abruptly a distance of some tens of centimetres during the excavation of a bottom outlet channel. The base of the movement was located on a subhorizontal plane which was highly polished. Tests on this showed a shear strength at residual, with $\phi = 13^0$, (5). The geological series was quite gently folded in the area. No evidence of any weak or sheared seams had been recorded during the drilling program and the original dam design had to be modified.

The writer was briefly involved in 1988 in the site for a very large concrete dam in south west China. The rock type was similar to Kotmale, above: gneiss with a strong foliation which gradually steepened from downstream to upstream. The formation had been mapped as being crossed by a number of translational faults, each identified by a wide zone of weathering. In each, distinct and slickensided seams were present. It was pointed out by the writer that the striations on these seams ran vertically down dip, rather than horizontally, as might be expected if shearing was through the tear faults. More, the faults in all cases neatly paralleled the changing foliation dip. The "faults" were, in fact, flexural slip seams, highlighted by broad weathering zones, at as Kotmale.

Malpasset Dam, a concrete arch dam founded on phyllites, failed in 1959. A full description of the disaster is given in (13), but some of the essential facst can be ennumerated as follows:-

i) An enormous wedge of rock underlying the left abutment disappeared in the failure. The wedge was bounded on the downstream side by a fault, on the upstream side by a foliation plane, Figure 4.

ii) A stability analysis of the section in Figure 4 a, during design, gave an adequate Factor of Safety.

iii) Measurements showed that initial deformations occurred parallel to the left abutment of the arch.

iv) Sections of the dam were later found with foundation rock adhering to the concrete, indicating that failure along the concrete-rock interface was unlikely.

If we take a three dimensional view of the left abutment, Figure 4 b, we can see that both the line of the fault and the foliation strike lie subparallel to the abutment thrust. This situation produces a wedge of rock bounded on both sides by planes of weakness; this was the wedge which disappeared. The resistance to the dam's thrust along this wedge is provided only by the strength of the two discontinuities: a fault zone and a foliation shear. The strengths along both would be unlikely to exceed and angle of shearing resistance of about twenty degrees.

A simple analysis of the stability of this wedge, (14), makes such a failure mechanism logical, without the need to call on any excessive uplift pressures.

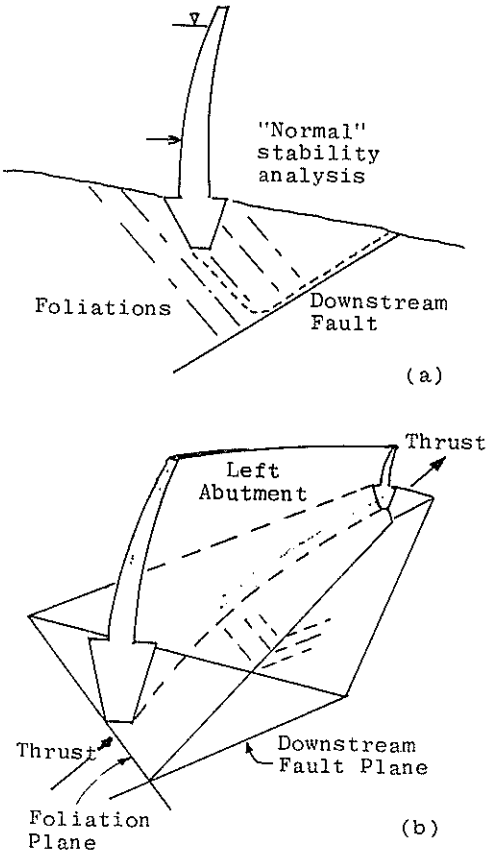

Fig. 4 Malpasset Dam, showing sections a) normal to the axis, which gave an adequate Fof S, and b) along the left abutment alignment, where weak discontinuities bounded the wedge of rock which was removed during the failure.

The St Francis Dam, in California, slid downstream in 1926. The foundation rocks were a series of conglomerates and shales, similar to those at Mangla and failure occurred in the weaker members. At the time, failure was put down to high pore pressures but, with the benefit of hindsight and present day knowledge, we might reasonably assume that flexural slip seams were present and had a large bearing on the failure.

3 CASE HISTORIES - INSTABILITY

Perhaps the most spectacular slope failure in recent times has been that at Mt Toc, above the Vaiont Reservoir. Here, a series of folded Alpine sediments dipped towards the valley, Figure 5. Failure took place in the Malm: thinly bedded limestones and marls. An analysis by Skempton (15) indicated a ϕ value of the order of 16^0 was required, for the relevant ground water and reservoir levels.

This slide thus has all the attributes of an example of failure along bedding plane shears which are the result of flexural slip. It is apparent from the

literature, however, that many engineering geologists are unwilling to accept this explanation and tend to seek corroboration, by analysis, of laboratory strength values obtained from intact rock samples.

Certain open cut coal mines in Central Queensland have suffered slips with basal failures on variously dipping bands of "clay" within the overburden siltstones. The clay is of similar mineralogy to the ambient rock and does not appear to represent a sedimentary hiatus. The clay also contains a sheared horizon which, to the author's knowledge, has received the attention of very little testing; one direct shear test indicated an angle of shearing resistance of twelve degrees.

This clay band, in otherwise sound siltstone, is an obvious flexural slip candidate, yet there again appears to be an unwillingness among mining geotechnical personnel to use this fact.

In Brisbane city, a moderately hard Mesozoic tuff overlies Palaeozoic phyllite unconformably. The phyllite surface exhibits paleoweathering, while folding of the combined formations has produced continuous slickensided shears along this weathered interface zone. In this case, flexural slip occurs on an interface separating formations with an age difference of millions of years. The effect of this interface on stability has been discussed elsewhere, (16).

Limestone poses a special case in flexure. The residual angle of friction for limestone appears to be not much less than the friction value along joints: perhaps thirty five compared to thirty seven or eight degrees. When a massive limestone is folded, adjustment by flexural slip causes a grinding and pulverisation of the rock along the slip plane(s). This makes the horizon more susceptible to solution, so that the flexural slip planes become highlighted by a microkarsticity.

The writer was involved in the excavation of an 80 m. high spillway cutting in massive limestones, in S.W. China. The dip was downstream, with a component out of the valley side. Four or five bedding planes had been mapped as daylighting in the cut; these were characterised by solution planes partly filled with red clay gouge. Rock to rock contact was of the order of 50 - 60 %. The designers had received advice that these clay-filled planes would die out at depth, which advice is believed to indicate a misunderstanding of the origin of the features. In any event, the gouge filled planes were exposed in a diversion tunnel, well below the base of the spillway. The wedges formed by these planes had to be supported by a series of anchors.

4 DISCUSSION

In the foregoing case histories, some emphasis has been placed on the need to differentiate between flexural slip planes and planes of weakness resulting from other causes. This differentiation is not merely of academic interest, and two examples should suffice to illustrate this.

Consider a situation of potential seismic risk at a dam site. This was a concern at one site mentioned above, where an active fault was known in the region, and the mapped "translational faults" at the site ran subparallel to this. Hence the "translational faults" could have been sympathetic features, themselves capable of activity - either natural or reservoir induced.

Recognising the origin of these features, not as translational faults, but as flexural slip planes, the result of Mesozoic folding, was a major factor in allaying concern about their future seismic behaviour.

The case of the slide into the Vaiont Reservoir is one where resistance to the concept of flexural slip is still evident in recently published papers on the topic.

If one does not understand the origin of features which have initiated past slides, one is liable to make errors of judgement when encountering similar phenomena in the future.

5 REFERENCES

1 Skempton, A.W.,"Long Term Stability of Clay Slopes", Geotechnique, 14. 2. 77-101, 1964

2 Morgenstern,N. & Tchalenko, J., "Microscopic Structures in Kaolin Subjected to Direct Shear", Geotechnique, 17.4.308-328, 1967

3 Skempton, A.W., "Some Observations on Tectonic Shear Zones", Proc. 1st Cong. ISRM, Lisbon, pp 329-335, 1966

4 Bishop, A.W., Green,G.E., Garga, V.K. et al, "A New Ring Shear Apparatus and the Measurement of Residual Strength", Geotechnique 21:4:273-328

5 James, P.M., "The Influence of Structure on the Behaviour of Argillaceous Sediments", 1st Aus./N.Z. Geomech. Conf.

6 Binnie, G.M., Clarke, I.F.F. & Skempton, A.W., "The Effect of Discontinuities in the Clay Bedrock on the Design of Dams in the Mangla Project", Trans. 9th ICOLD, 1.165-184, 1967

7 James, P.M., "In Situ Shear Tests at Muda Dam", Conf. In Situ Testing Soils & Rocks, ICE, 2. 45-51, London, 1969

8 Clarke, C.L., Morgenstern,N. & James,P., "Foundation Conditions at Muda Dam", 3rd Internat. Sympos. R.M.

9 Maddox, J.M., Kinster, F.L. & Mather, R.P., "Foundation Studies for Meadowbank Buttress Dam" 9th ICOLD, 1.123-142, 1967

10 Casinader, R.J. & Stapledon,R.H.,"The Effect of Geology on the Treatment of Dam Foundation Interface at Sugarloaf Dam", 13th ICOLD, Q48, R32 New Delhi, 1979

11 Deere, D.U., "The Foliation Shear Zone", Jnl Boston Soc. Civ. Eng., 60.4.163-176, 1973

12 Casinader, R.J., "Systematic Weak Seams in Dam Foundations", Proceed. Sympos. Geotech. Probs & Prac. of Dam Engineering, AIT, pp 253-264, 1980

13 Bellier, J. "The Malpasset Dam, Evaluation of Dam Safety", ASCE Publ. Pacific Grove, Calif., pp 77-136, 1977

14 James, P.M. & Wood, C. "Malpasset Dam - from an Armchair", Aus. Geomechanics 7.23-31, 1984

15 Skempton, A.W., "Bedding Plane Slip, Residual Strength and the Vaiont Landslide", Geotechnique Correspondence, 16:1:82-84, 1966

16 James, P.M., "Cryptic Landslides", 3rd Aus/N.Z. Geomech. Conf., 2.65-68, Wellington, 1980

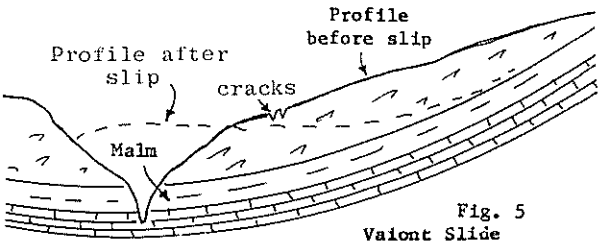

Fig. 5
Vaiont Slide

Geomembranes, Geotextiles and Slope Stability

M.R. HAUSMANN
Associate Professor, University of Technology, Sydney
M.A. SADLIER
Regional Manager, Polyfelt Geosynthetics Pty Ltd, Melbourne
C.BECKINGSALE
Principal Civil Engineer, Minproc Engineers Pty Ltd, Brisbane

SUMMARY Stability and interfacial friction considerations of geomembranes and geotextiles are discussed with particular reference to a sliding failure of a gold mining heap leach pad.

1.0 INTRODUCTION

A significant development in gold ore processing technology over the past 10 years has been the adoption of the heap leaching route for oxidised ores. In concept this involves the stacking of crushed ore on prepared pads for irrigation with a specially prepared cyanide solution. This solution percolates through the heap and can be collected as 'pregnant' liquor in edge drains for further processing to extract the gold. After gold extraction the solution is adjusted prior to recycling to the ore heap. For amenable ores the system offers significant advantages over the conventional grinding/leaching route with respect to energy demand and water demand.

Such heap leach stacks can be 30 metres high with pad areas of several hundred thousand square metres. Ore placement is often by back dumping from dump trucks with conveyor systems sometimes being employed.

A typical system is shown in Figure 1.

A critical component of the heap leaching system is the base liner which must provide a secure means of containment and direction for the leachate. This requirement derives both from the economic aspect in preventing loss of gold bearing liquor, and from the environmental viewpoint in preventing soil contamination by cyanide. Typically the liner is constructed as a heavy duty plastic membrane laid on a suitably prepared base, and installation of the membrane must ensure complete integrity of the lining system.

Typically a heap leach mineral extraction project is seeking to exploit a relatively low grade resource and its viability is often at the lower limit and dependent on the minimisation of construction and operating costs. Since the supply and installation of the pad liner is a major capital item its design must be carefully considered in order to maximise economy while maintaining appropriate factors of safety, which are normally somewhat less than those applied to typical 'permanent' civil engineering works.

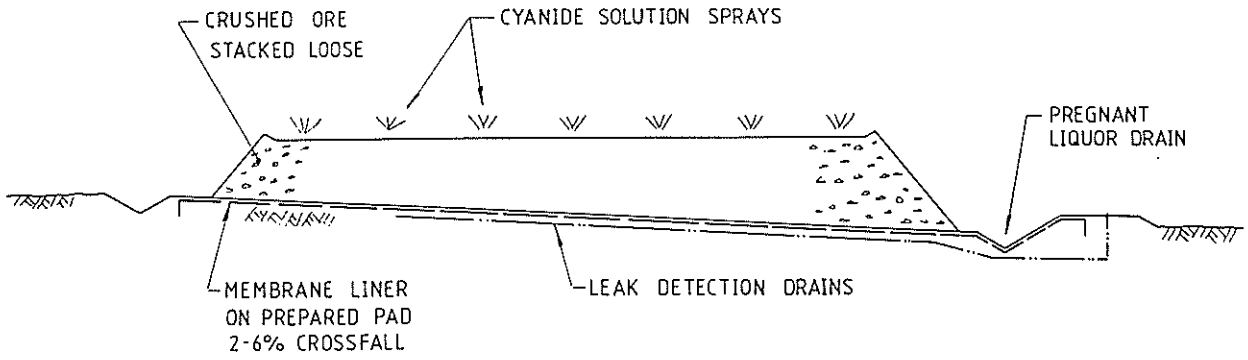

Figure 1. Section Through Typical Heap Leach

2.0 STABILITY AND OPERATIONAL CONSIDERATIONS

The design, construction and operation of a heap leach facility involves a number of compromises which require consideration and appropriate supervision to ensure that satisfactory results are obtained. The actual behaviour of different ores can also vary and lead to a reduction in stability safety factors.

2.1 Ore Stability

The desire to maximise gold recovery dictates that the ore heap is stacked with faces as steep as possible and thus the frictional resistance to sliding at the base is partially mobilised and the degree to which it is not mobilised is the effective safety factor in the structure.

The method by which the ore is placed also affects the stability of the ore heap. Again considerations of gold recovery make it desirable to build the heap close to full height at the starting point and to gradually work the batters out by dumping and pushing. A more stable initial heap body can be obtained by methods such as:

(i) initial part height construction over the major part of the pad with subsequent topping up to full height, or

(ii) provision of horizontal benching particularly in the downhill faces of the heap.

These variations in technique will affect the gold recovery particularly during start-up, an important consideration for capital intensive projects looking for an early cash flow.

Another complicating factor can be the tendency for the crushed ore to acquire a degree of cementitious binding as the solution is percolated through it. This can influence the ore to act less like a granular material and more like a unified cohesive mass. From the point of view of heap stability cementation can be a considerable advantage but it also has the effect of reducing the solution percolation rate and from a gold recovery viewpoint is usually undesirable.

2.2 Pad and Interface Behaviour

Heap leach pads are normally constructed with a fall of 2-6% depending upon such factors as existing topography, length of flow paths, percolation rates and overall layout. Pondage for ore bearing (pregnant) solution and take-off channels are normally at the downhill side so it is normally easier to commence heap construction from the uphill side in spite of the improved stability possible by working from the low side and pushing the ore heap up the slope. Horizontal benching to improve stability has been used in solid waste dumps with synthetic liners but such aids have not been used in heap leaching.

The geomembranes used for heap leach pads are typically thin HDPE extruded sheets with very smooth surfaces, limited tensile capacity and puncture resistance. It is therefore normal to require the prepared base for the liner to offer a smooth surface without protrusions. Improved resistance to puncture can be obtained by using a thick non-woven geotextile underlay or overlay but as the case study which follows illustrates this can severely reduce the friction along the critical interfaces.

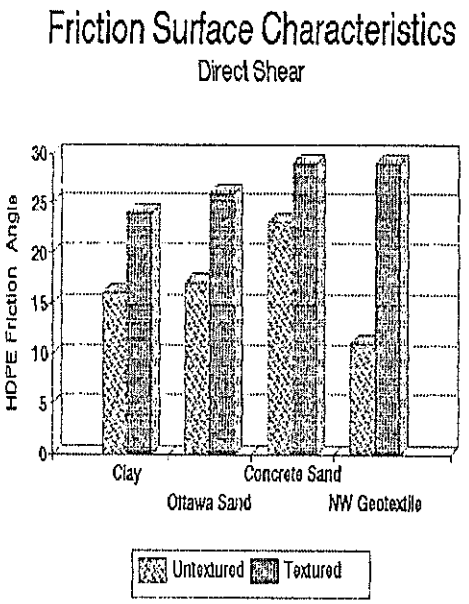

Figure 2. Geomembrane Friction Angles

Friction angles for smooth sheet extruded HDPE liners have been established by shear box testing (e.g. Cadwallader)(1) to be around 15° for clays, 25° or more for sands but reducing to 11° or less for geotextiles depending on their characteristics. This data is summarised in Figure 2 which also shows the capability of co-extruded HDPE sheet with textured surfaces to improve the friction angles for soils and particularly for geotextiles.

There is also a complicating factor for smooth liners, in that once sliding has occurred there is a significant reduction in the friction angle due to a 'polishing effect'. This is discussed by Mitchell et al (2).

2.3 Design and Supervision

As with many other projects contractual arrangements may mean that the designer of the heap is not involved through the construction and operational phases and is not able to observe the behaviour of the heap during loading and operation. If a sliding failure is to occur it will normally be signposted by cracking at the top of the heap and wrinkling of the geosynthetic materials at the toe. It is essential that there is responsible and aware supervision during the loading and initial operation phases that is on the lookout for these telltale signs.

3.0 CASE STUDY LEACH PAD FAILURE

A recent example of a heap leach pad was constructed in Queensland, where a relatively small scale installation was required to provide for economic processing of a gold bearing 'gossan cap' overlying a deeper base-metal ore body.
A leach pad was designed and constructed 100 metres by 210 metres long, consisting of graded and compacted in-situ material, to 3.6% maximum crossfall to receive a fully welded HDPE membrane liner 1.0mm thick.

The pad surface was specified to be finished smooth and unyielding, and free of rocks, stones, sticks or other debris in the top 100mm. However the pad as completed by the earthworks contractor failed to meet these requirements. Importation of suitable clayey sand or loam as a bedding material was considered but associated construction delays and cost penalties led to the decision to adopt instead a geotextile layer as a protective cushion to the underside of the membrane, and Polyfelt TS600 nonwoven polypropylene geotextile was installed.

Following completion of the liner installation construction of the heap was commenced from the uphill end using conventional end dumping and dozing techniques. As the heap progressed down the slope an extensive series of wrinkles formed in the liner in front of the advancing ore, (Figures 3,4) indicating the likelihood of distress in the liner beneath the heap. However due to the inexperience of the operators this potential was not recognised, and cyanide spraying commenced. Large quantities of pregnant solution were subsequently intercepted in the leak detection drains, and spraying was stopped. When ore was removed, extensive tears in the liner were revealed, indicating clearly the leakage path. To avoid further contamination the stacked ore was immediately removed under the direction of the regulatory authority to an adjacent tailings containment, and the base was ripped and limed to neutralise the cyanide.

Inspection of the underside of the failed liner revealed directional polishing marks consistent with relative sliding movement of the liner over the geotextile, down the slope of the pad.

Investigations were carried out by the various parties to the construction, and the consensus was that the primary cause of the failure was low relative friction between the membrane and the geotextile with consequent overstressing of the membrane in tension. This mechanism is analyzed below.

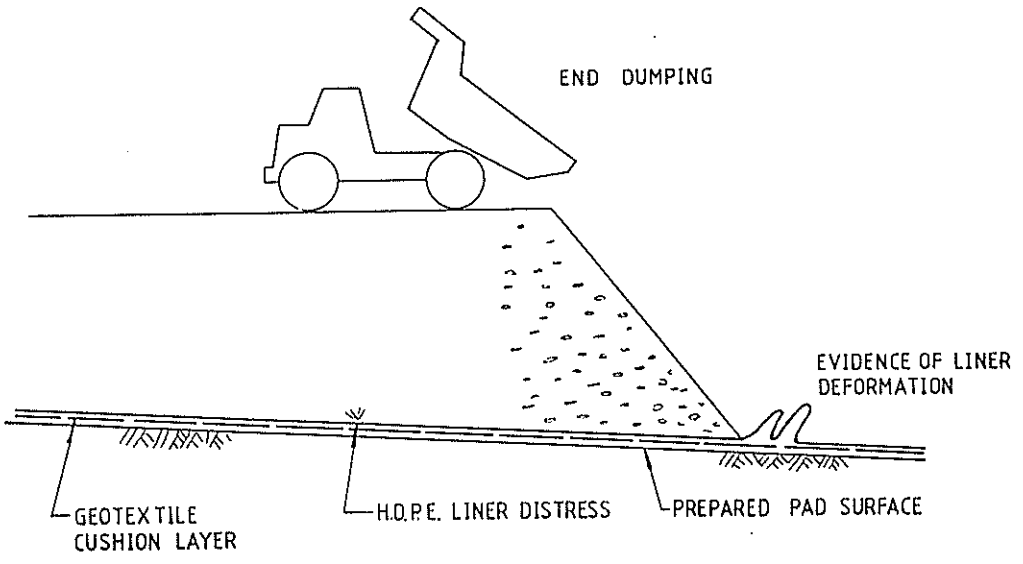

Figure 3. Case Study Heap Construction

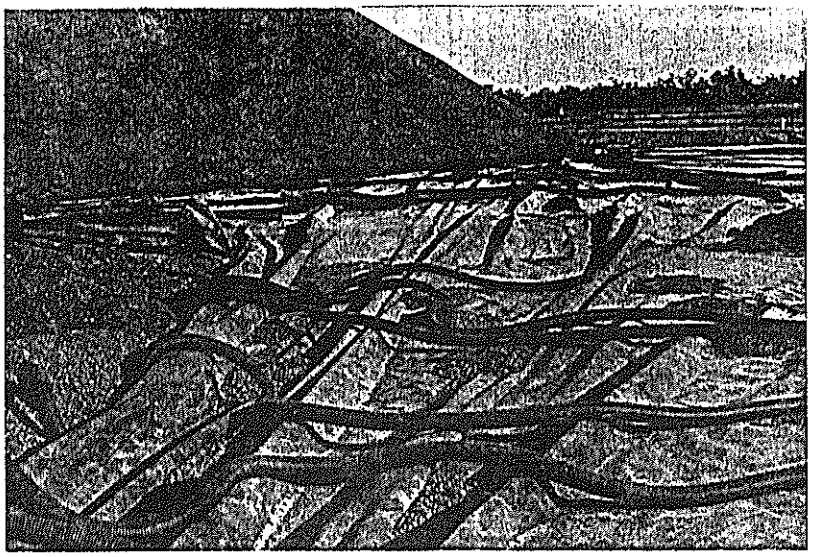

Figure 4. Case Study Liner Deformation

At least one similar experience in the mining sector has been reported from the USA by Thorndycraft (3) where a pad constructed in similar fashion (i.e. HDPE membrane over geotextile) at a gold mine in Nevada failed at 7% base slopes, after similar pads built at 6% and less had survived.

Failure on a 7% base slope suggests that installations on 6% would have rather marginal factors of safety.

The question of geomembranes and slope stability has been a major interest in relation to landfills with incidents such as the Kettleman Hills failure prominent. Kettleman Hills involved a 6 hectare hazardous waste landfill up to 30 metres high with three layers of HDPE liner and various other geosynthetic layers. There was a substantial sliding failure in 1988 as reported by Mitchell et al (2). A recent overview of liner stability on slopes with particular reference to landfills is given by Matichard et al (4).

4.0 CASE STUDY FAILURE ANALYSIS

Consider the forces acting on the toe of a heap being constructed to height H on a base of slope α,

with Γ = material bulk density
ϕ_r = angle of repose
ϕ_i = angle of internal friction
ϕ_b = angle of friction at base
as shown in Fig 4.

Assuming active pressure conditions prevail, and neglecting any surcharge effect or cohesion, which is typically small for an uncompacted crushed ore., the horizontal force per unit width acting on the wedge is

$$P_h = \Gamma.H^2/2N_\phi$$

where $N_\phi = \tan^2 (45° + \phi_i/2)$

The vertical force acting on the wedge is the weight

$$P_v = \Gamma.H^2/2 \tan\phi_r$$

The total force to be resisted along the slope at the base is then

$$P_r = P_h.\cos\alpha + P_v.\sin\alpha$$

The limiting force that can be mobilised by friction at the base is

$$P_f = P_v.\cos\alpha.\tan\phi_b.$$

The resulting tension in the membrane is

$$T_m = T_y$$

Thus the factor of safety against sliding is

$FOS = (P_f + T_y)/P_r$

A minimum value of 1.5 is recommended for design. A calculated value less than 1.0 indicates incipient failure.

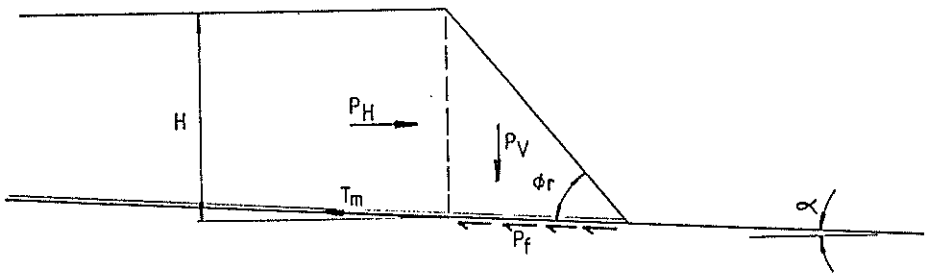

Figure 5. Forces Acting on Toe of Heap

For a heap constructed in thin layers above the liner the maximum tensions would occur near the batter points as illustrated. However for heaps built by end dumping (which is favoured to minimise heap compaction and to maximise permeability), the maximum loads are locked in across the width of the heap.

Using typical parameters for the case study heap :-

$H = 5.0m$
$\Gamma = 18\ kN/m^3$
$\alpha = 2.05°$ ($=\tan^{-1} 0.036$)
$\phi_r = 37°$
and $\phi_i = 33°$

we derive

$P_h = 66.3\ kN/m$
$P_v = 298.6\ kN/m$
and $P_r = 77.0\ kN/m.$

Now for $\phi_b = 11°$(geotextile to HDPE).

$P_f = 58.0\ kN/m.$

and Ty =16.7 kN/m for 1.0 mm HDPE

The calculated factor of safety against sliding is (58.0+16.7)/77.0 = 0.97 indicating incipient failure.

Surcharge effects and applied horizontal loads from dump truck and dozer operations on top of the heap will tend to increase these effects locally.

By comparison for $\phi_b = 19°$ for HDPE to a granular bedding material,

$P'_f = 102.8\ kN/m$

and the calculated factor of safety is (102.8+16.7)/77.0 = 1.55 which is satisfactory.

5.0 SOME REMEDIES AND PRECAUTIONS

It will be evident that the tight cost considerations which are inherent in heap leach mining will ensure that ore heaps are usually built close to the appropriate safety factors. Where circumstances arise that reduce the safety factor below acceptable levels a number of avenues are available to preclude this. The costs associated with the various alternatives will need to be evaluated for each application

5.1 Work from Low Side.

If it is possible to work from the low side stacking the ore up the hill the risk of instability is reduced. Starting from the low side may lead to a short delay in gold production.

5.2 Bench Low Side Slopes

Providing horizontal berms or benching, particularly to the downhill slopes will effectively reduce the mass of ore trying to slip and so improve stability. Benching will effectively reduce the volume of ore exposed to leaching

solution but the edges of the heap are often difficult to treat and are often used for poorer quality ore anyway.

5.3 Build to Part Height First

By building the heap to only part of its full height initially stability can be maintained in the initial phase and the ore will have settled and may be partly cemented when the second stacking phase is carried out. The gold production rate will be reduced because less ore will be exposed to solution in the early phase and because of a reduced percolation rate in the latter phase.

5.4 Use Textured Liner

Using a textured liner will increase the critical base interfacial friction and improve stability. Textured liners are more expensive to manufacture but the extra material cost may be offset by other factors such as reduced pad preparation if a geotextile is to be used.

5.5 Thicker Liner for Tensile Capacity

Having a thicker liner with increased tensile capacity will enable the liner to provide greater resistance to sliding and will also provide improved puncture performance which may be reflected in reduced base preparation costs. Liner cost is directly related to thickness.

5.6 Reinforce Heap

Stronger liner is a fairly inefficient way to make the heap more stable - there are many other geosynthetics such as geogrids and geotextiles able to do this more effectively. Some may also help to improve percolation rates and reduce the impact of fines migration and cementation. The extra cost of these materials may be partially offset by steeper faces and improved percolation.

5.7 Geotextile as Overlay

If a geotextile is needed to guard against liner puncture due to doubtful base preparation then it may be prudent to place it over the liner. If sliding occurs then the heap and geotextile can move without dragging the liner and early observation of this will enable suitable remedial action to be taken.

5.8 Build Pads with Opposing Slopes to a Common Valley

If a series of pads are built to slope towards a common valley with a suitable valley crossfall then the two pads can be built back-to-back and provide support to each other during all phases of construction and operation. On pads which involve substantial base preparation this variation should be possible with very little additional cost.

6.0 CONCLUDING REMARKS

Heap leach pads are by their nature close to the limiting factors for heap stability and care needs to be taken in assessing the interaction of different materials particularly at the critical base interfaces. This is especially so for changes due to circumstances that arise during construction and operation.

If sliding is going to occur it is normally slow to start and should be apparent from astute observation which will allow appropriate remedial action to be taken with minimal impact on cost or production.

7.0 REFERENCES

1. Cadwallader, M. 'Special Concerns of Landfill Closures: VLDPE and Textured Geomembranes' GRI Special Conference on Landfill Closures, Philadelphia, 1990.

2. Mitchell, J., Seed, R., and Seed, H. 'Kettleman Hills Waste Landfill Slope Failure. I: Liner-System Properties' ASCE Journal of Geotechnical Engineering, Vol 116, No. 4, April, 1990

3. Thorndycraft, R.B. 'Heap Leaching in Mountainous Terrain', Proceedings Perth International Gold Conference, Randol International Ltd., 1988.

4. Matichard Y., Delmas, P., Soyez, B., Girard, H, and Mathieu, M. "Stability of Lining Systems on Slopes' Sardinia '91-Third International Symposium on Landfills. University of Cagliari, Sardinia 1991.

Reduction of Pavement Damage from Expansive Soils using Moisture Barriers

J.C. HOLDEN
B.E., M.Eng.Sc., Ph.D., M.I.E.Aust.
Research Engineer, VIC ROADS

SUMMARY: Two field trials were carried out at an experimental site on the Sunraysia Highway, north-western Victoria, where the road had to be reconstructed because of the pavement damage caused by the effects of a Victorian semi-arid climate and trees on the expansive clay subgrade. Using a plastic geomembrane, a vertical moisture barrier was installed in each verge in order to stop the lateral migration of moisture to and from the subgrade. A barrier depth of 1.8 m below verge level was not deep enough to prevent the significant seasonal pavement movements being caused by roadside trees. However, a deeper barrier that was at least 2.5 m below verge level greatly reduced or virtually eliminated seasonal movements.

1. INTRODUCTION

In many countries, including Australia, the damage to structures and roads caused by expansive soils is greater than the damage caused by other natural hazards, such as earthquakes and floods. Road pavements on expansive clay subgrades are affected by seasonal wetting and drying, resulting in two main types of damage: (i) roughness or loss of shape and (ii) longitudinal cracking. The useable life of the pavement can be reduced to a small fraction of its design expectancy.

Loss of shape of the pavement is probably the most serious form of deterioration resulting from shrinking and swelling of expansive soils since this worsens the riding quality of the road and thereby diminishes public safety. It is not readily repairable and hence any remedial works are time consuming and costly. Other consequences of loss of shape are poor surface drainage and damage to existing drainage systems, both leading to ponding of water on, and adjacent to, the road and possible pavement damage.

The problems of loss of pavement shape and pavement cracking resulting from seasonal changes are exacerbated by the presence of roots from roadside trees and shrubs.

Various techniques have been tried with the aim of isolating the foundation soils from the surrounding soils thereby preventing seasonal migration of moisture to and from the pavement subgrade. Methods that have been employed include:

(a) deep, sand-backfilled, sub-surface drains (eg Steinberg, 1979);
(b) encapsulated pavement subgrades;
(c) pressure-injected curtains of lime grout; and
(d) various geomembrane applications, using horizontal, sloping or vertical plastic barriers (eg Steinberg, 1984).

In 1985, the Road Construction Authority (now called Roads Corporation of Victoria, VIC ROADS) commenced a research project at Morton Plains during the reconstruction of a length of the Sunraysia Highway. The aim of the project was to investigate the effect of vertical moisture barriers on the distortion of pavements on expansive soils.

2. ROLE OF VERTICAL MOISTURE BARRIER

Vertical moisture barriers were chosen as the best method for the field trials at Morton Plains because of their proven success in Texas (Picornell et al., 1984) and their prevention of invasion by roots of neighbouring trees (Nazer and Clark, 1982; 1983).

The role of a vertical moisture barrier has been described in detail by Picornell and Lytton (1986). Briefly, its role is to stop the seasonal lateral migration of moisture to and from the subgrade beneath the pavement in order to prevent the subgrade from expanding during wet periods and shrinking, and thereby cracking, during dry periods. To substantially stop the lateral moisture migration in the subgrade, the moisture barrier must extend below the depth of any crack which would provide an easy moisture path through the relatively impermeable clay. Obviously, a vertical barrier cannot stop any vertical moisture movement which may have a significant long-term effect on the expansive soil subgrade.

This long-term effect on the pavement depends upon the subgrade moisture conditions at the time of the barrier installation. To avoid any long-term movements in a new or reconstructed pavement, the soil moisture suction in the subgrade should be equal to the equilibrium suction, ie the value existing in the deeper foundation soils (Aitchison and Richards, 1965).

3. EXPERIMENTAL SECTION

The experimental section, shown in Figure 1, was located on the Sunraysia Highway at Morton Plains, 12 km south of Birchip, which is in the semi-arid Wimmera region of north-western Victoria. Between April and June 1985, the Sunraysia Highway at Morton Plains was reconstructed because the pavement had undergone serious loss of shape, with longitudinal cracking and longitudinal rutting up to 40 mm deep (Martin and Newbegin, 1989). This was only about ten years after the pavement was resheeted and the bituminous spray seal widened from 6.0 m to 7.4 m. The pavement (base/sub-base) comprised 170 to 300 mm depth of weathered sandstone.

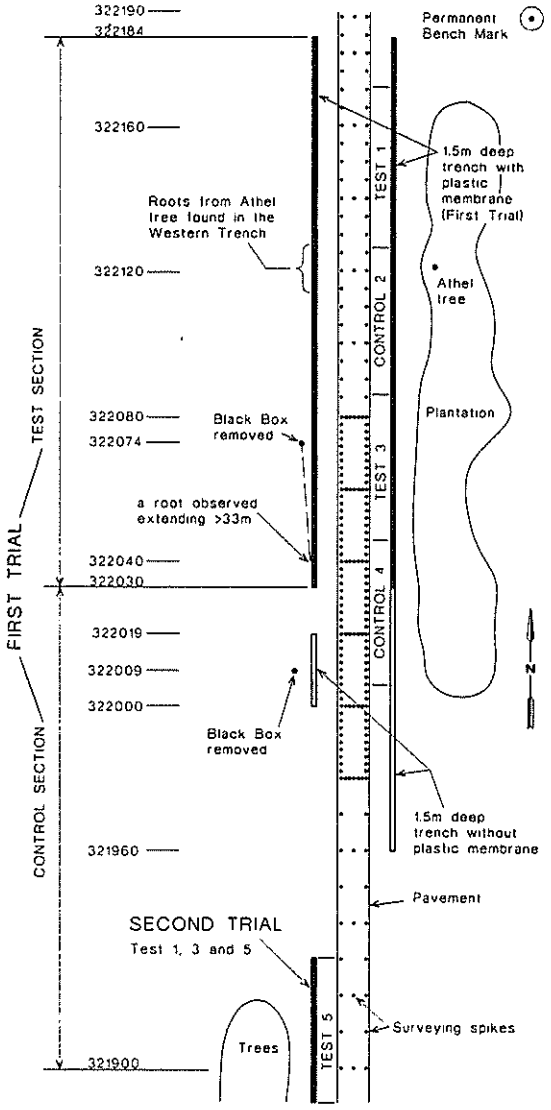

Fig. 1. Plan of Experimental Site

3.1 Geology and Site Conditions

Generally, the geology is similar to that in the Horsham area, where the soil profile consists of grey or black heavy clays to a depth of 0.6 to 2.2 m overlying light brown calcium heavy clays to a depth of up to 3.4 m, above a deep layer of white heavy clay (Kassiff and Holland, 1966). As the area is part of the Murray Basin, the more recent formation is most probably of alluvial origin and is known as "buried gilgai". The development and properties of gilgai are described by Kassiff and Holland (1966). The two characteristic properties of gilgai country are that as the depth increases the swelling potential increases and the permeability decreases. This area is characterised by the creation in winter of depressions known locally as crab holes or sink holes.

The area at the site is low-lying and poorly drained and in winter is flooded for long periods. In summer, through the combined actions of evaporation and tree roots, the soil dries and cracks extensively. An appreciation of the size and extent of the cracking can be gained from the report by Martin and Newbegin (1989).

3.2 Soil Properties

Tests were performed on samples of the subgrade taken from trenches on each side of the highway (Section 4.1). The results indicated that the soil was a highly expansive sandy clay with the following properties: LL = 82-86%, PL = 19-25%, PI = 57-67%, and LS = 21-22%. The moisture content ranged from 27 to 29%.

The base/sub-base material used in this area is weathered sandstone from a local pit. Sandstone in the Wimmera region typically performs well as pavement material but tends to degrade rapidly if it gets wet. Properties of the sandstone, sampled at the bottom of the sub-base, ie at a depth of 0.3 m, are LL = 29%, PL = 23%, PI = 6%, and LS = 4%.

3.3 Vegetation

The experimental section extends over a total distance of 284 m with trees occurring along most of its length. The eastern side of the road is host to a plantation of approximately 70 trees, while the western side has only a few trees, mainly near the southern extremity, and thick patches of lignum bushes and high grasses. There are five different dry-climate species of eucalyptus in the plantation, the trees ranging in height from around 3 m up to about 8 m. Standing some 10 m high, one other tree in the plantation is from the exotic species known as the Athel tree. The understorey is sparse with grasses making up the ground cover.

Two large Black Box trees (Eucalyptus Largiflorens) were removed from the western side of the highway during the reconstruction works in 1985. They were located at Chainages 322009 and 322074 m, as indicated in Figure 1.

4. FIRST FIELD TRIAL

The reconstruction of the Sunraysia Highway at Morton Plains was carried out at the start of the wet season between April and June, 1985, and the experimental section was established between Chainages 321900 and 322184 m (see Figure 1). This distance of 284 m consisted of a 130 m control section and a 154 m test section. In the test section of the first field trial, a thin plastic membrane was placed vertically in a trench on both the east and west sides of the highway.

4.1 Trench Excavation

As shown on the plan in Figure 1, trenches were excavated on both sides of the road about 8 m from the centre-line. On the east side of the road, the trench extended along the test section and well beyond the end of the plantation in the control section, whereas the west side trench was only along the test section and in front of the former site of the removed Black Box at Chainage 322009 m. The reason for the trenches (backfilled without a plastic membrane) in the control section was to sever any roots and thus remove the effect of this variable from the experiment. After the old road formation had been removed down to design subgrade level, the 0.4 m wide trenches were excavated by backhoe to a depth of 1.5 m below sub-base, ie a depth of about 1.5 m below natural surface (N.S.) level (see Figure 2).

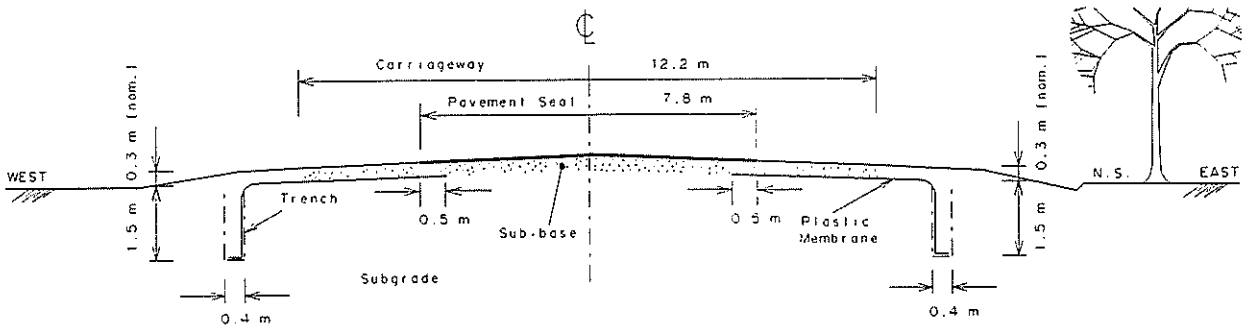

Fig. 2. Typical Cross-Section of Test Section (First Field Trial)

4.2 Placement of Membrane

The barrier chosen to minimise moisture variation beneath the pavement was a 0.2 mm thick black polythene membrane. When unrolled, each sheet was 50 m long by 4 m wide. Two sheets were joined longitudinally with adhesive tape to give a 7 m wide plastic sheet. This was then laid out along the shoulder of the road, so that it would extend 0.5 m under the edge of the future seal (Figure 2). The outer edge of the sheet lay across the bottom of the trench.

Due to the plastic membrane being so thin, several precautions were taken during its placement to avoid puncturing it. For example, sharp objects such as severed tree roots and large stones were removed from the inner face of the trench. Similarly, before placing the membrane horizontally across the shoulder/verge area, a relatively smooth level surface was produced with a grader. However, problems were experienced with the membrane, as discussed later.

Pavement base/sub-base material (weathered sandstone) was placed over the carriageway width on the plastic sheet and compacted in 100 mm layers to form a 300 mm thick pavement, which was surfaced with a 7.8 m wide primerseal.

4.3 Compaction of Backfill

The backfill, the excavated clay material, was shovelled into the trench to form layers of 100 mm (specified) up to about 150 mm thickness. Compaction was difficult due to the narrow width of the trench and the need to protect the plastic sheet. Limited densification of the lower layers of backfill was achieved by applying water from a water tanker. These nominal 100 mm layers were placed up to the top of the trench (ie to a depth of about 300 mm below the finished surface level). The final 300 mm of verge material was placed over the plastic sheet in one layer and compacted by a heavy roller.

4.4 Root Retardant Treatment

In order to eliminate the invasion of tree roots, the trenches were treated with a root retardant. The type chosen was Casoron, whose active ingredient (Dichlorobenil) has been shown to be effective for periods of at least 8 years (Nazer and Clark, 1983). The application of Casoron to each 100 mm layer of backfill followed the guidelines set out by Nazer and Clark (1982).

Root retardant was not placed in the trenches on the western side of the highway, but was placed in both the test and control sections on the eastern side. Also, no retardant was placed in the top 300 mm (ie above the plastic sheet) of the trench as this was compacted in one layer.

5. RESULTS FROM FIRST FIELD TRIAL

The movements of the road pavement were monitored by means of precise levelling (ie to 0.1 mm). To achieve this, the surveyors used a certain QS type bench mark, which was developed to provide a stable datum in expansive soils (Holden, 1987). After the construction works were completed, a number of 100 mm long deck spikes with a domed head were driven into the road pavement. They were placed at 2, 5 or 10 m spacing along the east and west edges of the road as well as at 20 m spacing along the centreline in accordance with the plan shown in Figure 1. A transverse line of 38 spikes at 200 mm spacing was placed at each of Chainages 321980, 322000, 322020, 322040, 322060 and 322080 m. Precise levelling of the spikes was first performed four weeks after completion of the construction works and after that at the end of each dry (summer) and wet (winter) period.

In their report on this project, Martin and Newbegin (1989) have presented all the plots of seasonal heave, seasonal shrinkage, and progressive movement for the east and west sides of the road and the centreline. They have also presented plots of seasonal movement for each of the six transverse lines or cross-sections.

A significant difference between the movements in the test section compared to those in the control section was expected. The movements within the control section should tend to fluctuate greatly due to the seasonal effects on the expansive soil subgrade, whereas in the test section the pavement should undergo a slow steady monotonic movement as the subgrade approaches its equilibrium soil suction. However, from the plots of seasonal heave in **Figure 3** and the plots of seasonal shrinkage, it can be seen that there is no appreciable difference in the magnitude of the seasonal movements between the test and control sections, alongside the plantation. This shows that there is still substantial wetting up and drying out occurring within the subgrade of the test section alongside the plantation.

The effect of the roadside trees can be seen in the typical cross-sections in **Figure 4**, where only the limits of seasonal movements are shown. The seasonal movement of the pavement at Chainages 321980 and 32200 m, where there were few trees set well back, was very small and relatively uniform across the road, over at least the first five years. On the other hand, the four cross-sections from Chainages 322020 to 322080 m show that the pavement was heaving (and shrinking) in a linearly decreasing manner across the road. The greatest

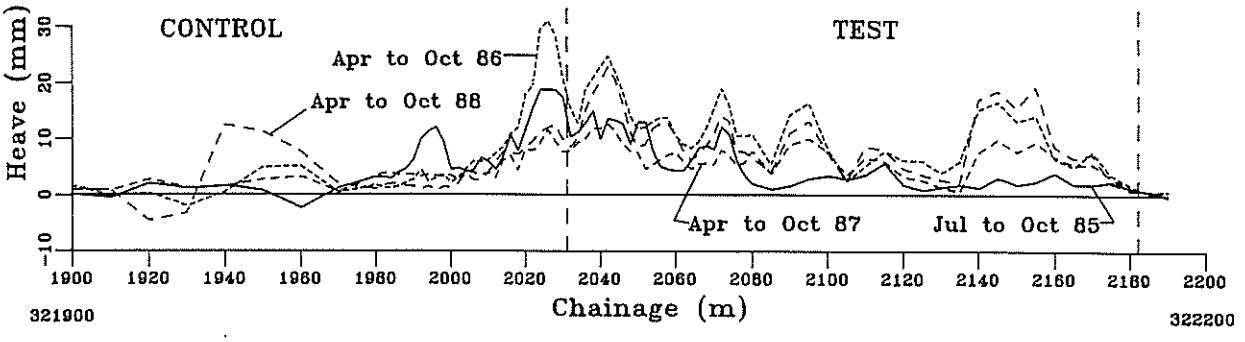

Fig. 3. Seasonal Heave - East Side of Road (First Field Trial)

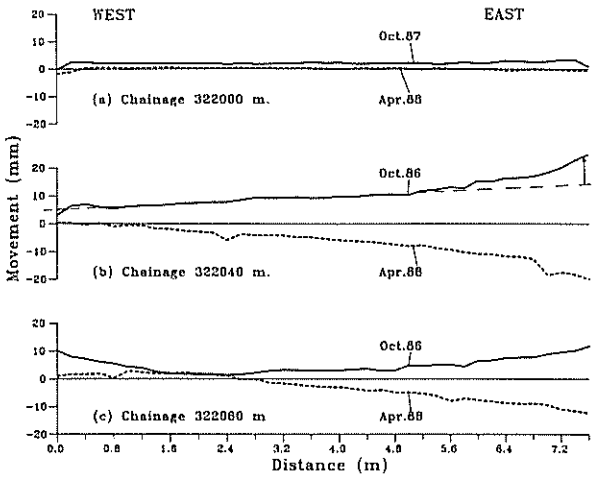

Fig. 4. Seasonal Pavement Movements for Three Cross-Sections (First Field Trial)

movement was always on the eastern side of the highway, where the plantation exists.

Superimposed on this linearly varying heave (and shrinkage) is a phenomenon known as "edge flapping", where the pavement edge moves vertically up or down according to the season. This effect, which can be clearly seen in Figure 4(b) and (c), extends up to 2 m from the pavement edge.

The cyclic movement of the pavement is shown in a typical plot of movement with time in Figure 5. From an examination of the rainfall figures for the area, the expected general influence of rainfall on the magnitude of seasonal movement was observed. The general trend in Figure 5 indicates that, in

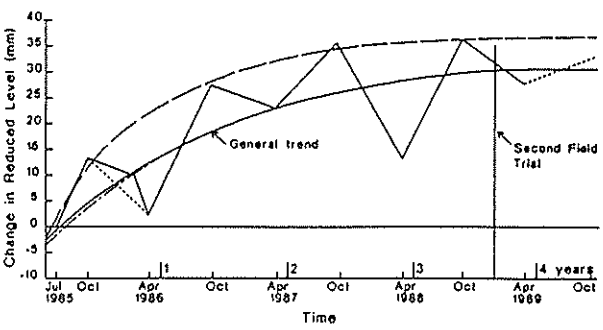

Fig. 5. Cyclic Movement of East Pavement Edge at Chainage 322042 m

the Test Section, it took 3 to 4 years for the subgrade to seemingly recover after cutting the tree roots. This fact should be taken into account when planning a pavement rehabilitation which incorporates moisture/root barriers.

6. SECOND FIELD TRIAL

In the First Field Trial, started in 1985, the junction between the test and control sections was selected to be at Chainage 322030 m, which was approximately half way along the worst section of the original deformed pavement. If the barriers worked, the effect should be shown clearly by contrasting results between the test and control sections. However, as demonstrated over the following 3.5 years, there appeared to be no significant difference between the two sections. Since seasonal movement continued alongside the plantation, it was surmised, after discussions with Prof. R. Lytton, Texas Transportation Institute, that the barrier had not been installed to a sufficient depth. Instead of merely replacing the barrier with a deeper one, it was decided to also relocate the test and control sections.

The Control Section in the First Trial was a poor choice because it had been mainly located in the region sparsely populated with trees on the east side of the highway. For statistical reasons, it was decided to create two separate control sections alternating with two separate test sections alongside the densely populated plantation (see Figure 1). This involved the removal of the vertical component of the plastic membrane from two areas on the east side of the highway, to produce two control sections, each 40 m in length.

The two test sections, on the eastern side only, involved the deepening of two vertical moisture barriers: Test Section 1 was 45 m long (between Chainages 322126 and 322171 m), and Test Section 3 was 40 m long (between Chainages 322046 and 322086 m). These barriers were installed to a depth approximately one metre lower than that previously used on the east side of the highway in 1985.

At the experimental site, a third test section (called Test Section 5), 40 m in length, was established on the western side of the highway between Chainages 321890 and 321930 m (see Figure 1). The pavement in this part of the original control section had undergone very large seasonal movements (Martin and Newbegin, 1989), because it was adjacent to some relatively large trees, and it was decided to determine the effect of a moisture barrier on these movements.

The three new test sections were completed in the order of numbers 5, 3, and 1 during December 1988 and January 1989.

6.1 The Three New Test Sections

During the installation or deepening of the 0.2 mm polythene moisture barriers along the three new test sections, a different approach was adopted for each section, each being an improvement on the previous one; these approaches are described in detail by Martin and Newbegin (1989).

In Test Section 5, a vertical barrier was installed in a trench 40 m long and 2.5 m deep below the road verge surface. There was no horizontal component of the barrier under the shoulder. Compaction of the top metre of backfill against the suspended vertical membrane was carried out with a vibratory rammer.

In Test Section 3, the 40 m long trench was carefully excavated in stages. The tree roots were recorded and an inspection of the original plastic was carried out. The excavation was continued to the new barrier depth of 2.5 m below the verge surface. The new membrane was attached to the old membrane using adhesive plastic tape. Backfilling and compaction to the verge surface level were then completed.

In Test Section 1, a new membrane was installed in a 45 m long trench excavated to 2.5 m below the existing horizontal membrane (ie to a slightly greater depth of approximately 2.8 m below verge level). At each end of the test section, the new plastic membrane was sealed to the wall of the trench, with a bituminous adhesive mixture, since it was thought that a significant horizontal flow of water had occurred in winter behind the old membrane via its ends. Backfilling and compaction were then carried out.

As with the first field trial, a fine granulated root retardant, Casoron, was placed during backfilling in each of the Test Sections 1, 3 and 5. In the top metre, it was sprinkled on successive soil layers which were about 200 mm except in the upper 400 mm where they were only 100 mm thick.

6.2 Observations During Trench Excavation

During the trench excavations for the Test Sections and for removing the vertical membrane from the Control Sections, the diameter, depth and frequency (number of roots per lineal metre) of severed tree roots were recorded and later reported by Martin and Newbegin (1989).

The majority of roots occurred within 400 mm of the surface, growing above the old membrane, with a frequency of up to 160 roots/m. The near-surface roots were generally small in diameter, viz. 1 to 5 mm, although they sometimes reached 10 mm.

Because an intact plastic membrane is impermeable to water, one may expect that roots normally would not have cause to penetrate the membrane. However, studies referred to by Landreth (1991) have shown that certain grass roots do penetrate the membrane used in our field trials. Nevertheless, we observed only that the tree roots, on reaching the membrane, had been diverted horizontally along it in their search for moisture. Some roots up to 18 mm diameter had grown through the membrane, but only at places where sharp stones had punctured holes in the plastic presumably at the time of laying. Those which had made their way through holes in the membrane formed, in some cases, an extensive network of roots behind the membrane. These networks extended horizontally and in some instances down toward the bottom of the trench. Great care was taken to ensure that there were no protruding stones or roots to pierce the new membrane and allow these problems to occur again.

The problems experienced with damage to the 0.2 mm polythene membrane forced us to use thicker membranes in later projects (Nunn et al., 1992).

It was thought that roots diverted by the plastic membrane may grow towards the bottom of the trench in their search for moisture. However, the diverted roots tended to travel horizontally, remaining within 400 mm of the surface. This can be attributed to one of two reasons: either surface roots rarely extend below a depth of 400 mm or the root retardant placed throughout the trench, except for about the top 300 mm, had achieved the desired effect.

7. RESULTS FROM SECOND FIELD TRIAL

As before, the various plots of pavement movement in the Second Field Trial have been presented in the report by Martin and Newbegin (1989).

By comparing these results with those of the first trial, an insight into the improvement in performance can be gained. When analysing the results of the second trial, it must be kept in mind that Control Sections 2 and 4 were not true controls because tree roots had been cut and the trenches backfilled with compacted clay, which is less pervious than the fissured natural clay. The seasonal shrinkage that occurred over three consecutive summers (the last two in the second trial) has been presented for the east side of the road in Figure 6. These plots

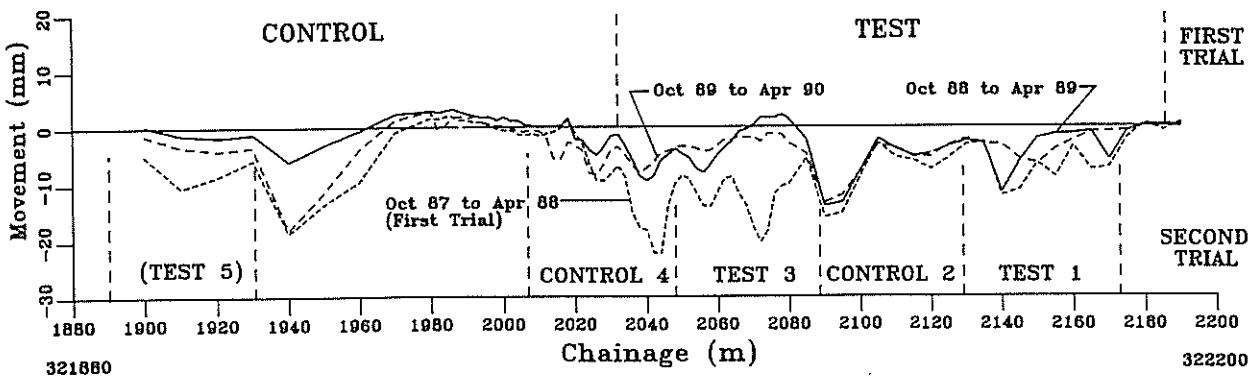

Fig. 6. Seasonal Shrinkage - East Side of Road

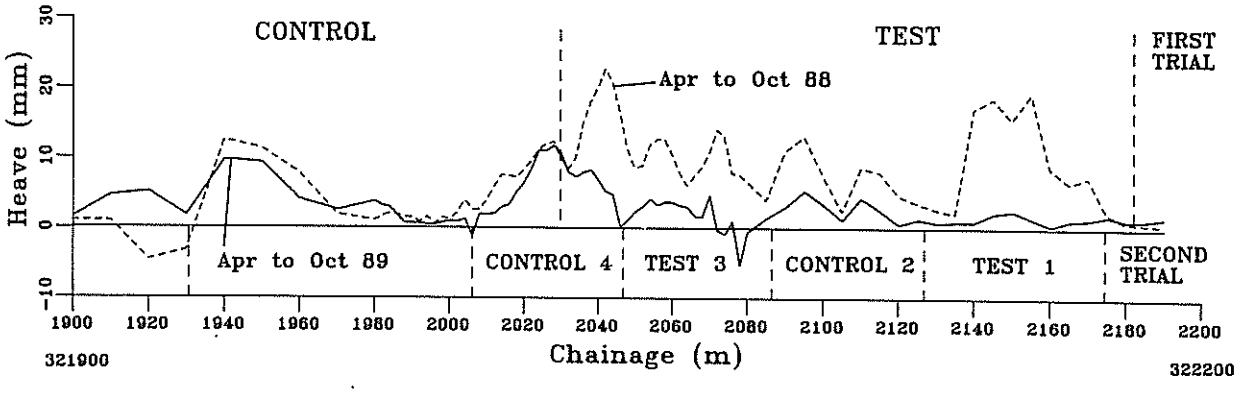

Fig. 7. Seasonal Heave - East Side of Road (First and Second Field Trials)

indicate that shrinkage over the summer has been reduced significantly by the deeper barriers, especially in Test Section 3 where it was only 0 to 2 mm at the centre. In comparison, the seasonal shrinkage for Control Section 2 has remained approximately the same.

The seasonal heave that occurred over two consecutive winters has been presented for the east side of the road in Figure 7. The heave over the winter has been reduced significantly by the deeper barriers, especially in Test Section 1, where the heave was almost eliminated. The partial reduction of heave observed in Control Section 2 and in the disturbed part of Control Section 4 is probably due to the fact that the plastic sheeting, which had some water flowing behind it during winter (see Martin and Newbegin, 1989, for the evidence), was replaced by a relatively impervious compacted clay.

The great value of these barriers can also be seen from the results of Test Section 5 on the western side of the highway (Martin and Newbegin, 1989). For example, the seasonal shrinkage was greatly reduced from a maximum of 43 mm during the summer of 1987/88 (ie without a barrier) to only 10 mm for 1988/89. Moreover in this section, the barrier did not have a horizontal component under the shoulder/verge and it reached to only about 1.7 m below the original natural surface.

8. CONCLUSIONS

Two field trials were carried out at a site on the Sunraysia Highway where the road had to be reconstructed because of the pavement damage caused by the effects of a Victorian semi-arid climate and trees on the expansive clay subgrade.

At this site, a vertical moisture barrier installed in the verge to a depth of 1.8 m below verge level (ie about 1.5 m below design subgrade or N.S. level) was not deep enough to prevent the significant seasonal pavement movements being caused by roadside trees. However, a deeper barrier that was at least 2.5 m below verge level (ie 2.2 m below N.S.) greatly reduced or virtually eliminated seasonal movements.

In a period of 3½ years, many tree roots up to 18 mm diameter had grown across the old trench through the verge material and some had entered the pavement subgrade through small existing puncture holes in the plastic membrane. Because of the risk of puncturing 0.2 mm polythene sheeting during installation, thicker plastic membranes have been used in later projects.

9. ACKNOWLEDGEMENTS

The author wishes to give thanks to God The Father through the Lord Jesus Christ, who is the source and giver of all knowledge, and without whom nothing of value would have been achieved. The considerable assistance of students Graeme Martin, Craig Newbegin (Swinburne Institute of Technology) and many members of the staff of VIC ROADS, especially Michael Ma, is gratefully acknowledged. This paper is presented with the permission of Mr Reg Patterson, Chief Executive, VIC ROADS. The views expressed are those of the author and do not necessarily represent those of the organisation.

10. REFERENCES

AITCHISON, G.D. and RICHARDS, B.G. (1965). A Broad-scale Study of Moisture Conditions in Pavement Subgrades throughout Australia. In G.D. AITCHINSON (Ed.) "Moisture Equilibria and Moisture Changes in Soils beneath Covered Areas", p. 184. Butterworths, Sydney.

GAY, D.A. and LYTTON, R.L. (1987). Pavement Roughness on Expansive Clays Altered by Vertical Moisture Barriers. Texas Transportation Institute, Texas A&M University, College Station, December 1987, 23 pages.

HOLDEN, J.C. (1987). Performance of Stable Survey Marks in Expansive Soils. Proc., 13th National Surveying Conference, Melbourne, September, paper 7.

KASSIFF, G. and HOLLAND, J.E. (1966). Expansive Properties of Dooen Clays. Civil Engineering Transactions, Vol. CE8, No. 2, p. 133.

LANDRETH, R.E. (1991). The Resistance of Membranes in Cover Systems to Root Penetration by Grass and Trees. Proc., Geosynthetics '91 Conference, Atlanta, p. 303.

MARTIN, G. and NEWBEGIN, C. (1989). Effect of Moisture Barriers on Pavement Distortion. VIC ROADS Internal Report No. IR/89-6, October.

NAZER, C.J. and CLARK, J.D. (1982). Prevention of Tree Root Invasion. Parks and Recreation, Australia, Feb., p. 58.

NAZER, C.J. and CLARK, J.D. (1983). Prevention of Tree Root Invasion. Proc., Royal Australia Institute for Parks and Recreation Conference, Melbourne.

NUNN, A.P., HOLDEN, J.C., MA. M. and DIMOS, A. (1992). Restoration of Tree-Affected Building Foundations. Proc., 7th International Conference on Expansive Soils, Dallas, August (in preparation).

PICORNELL, M. and LYTTON, R.L. (1986). Behaviour and Design of Vertical Moisture Barriers. Transportation Research Record 1137, p. 71.

PICORNELL, M. and LYTTON, R.L. and STEINBERG, M.L. (1984). Assessment of the Effectiveness of a Vertical Moisture Barrier. Proc., 5th International Conference on Expansive Soils, Adelaide, May, p. 354.

STEINBERG, M.L. (1979). Subdrainage with a Sand Backfill as a Positive Influence on Pavement Performance. Transportation Research Record 705, p. 71.

STEINBERG, M.L. (1984). Geomembranes Used to Control Expansive Soil. Proc., International Conference on Geomembranes, Denver, U.S.A., June, p. 507.

The Development, Testing and Application of a Non-Steel Tendon for Artificial Ground Support

D.F. HOWARTH
B.Sc., M.E., Ph.D., M.Aus., I.M.M.
Principal Engineer Mining Technology, BHP Engineering
M.T. RENWICK
B.E., M.E., M.Aus., I.M.M.
Senior Engineering Mining Technology, BHP Engineering

1. INTRODUCTION

1.1 Preamble

Ground support problems faced by mine operators are a function of the extraction technique used and geotechnical conditions associated with the mining method (surrounding rock type, stress fields etc) (Gale, 1991). It is probably true to say that the development of rock reinforcement hardware and associated equipment always lags behind the development and implementation of mining methods - this is to be expected.

The lag in the development of suitable rock reinforcement hardware can create adverse situations which may effect the profitability of the mining operations and can lead to hazardous working conditions. For example, highly capitalised underground coal mine operations cannot tolerate unscheduled stoppages of equipment caused directly by ground support problems. Similarly, a large surface mine with a lifespan of many years, is heavily reliant on the ground reinforcement system to continue to operate at its full design capacity for the duration of the mining activity.

Current mining techniques will continue to be used for many years and rock reinforcement hardware is being continually developed and improved to allow the extraction techniques to be exploited to their maximum potential.

The BHP highly oriented polyethylene (HOPE) bar was developed for two specific mining applications - as a cuttable rib bolt for underground coal mining and as a corrosion proof tendon for open pit mining applications. Existing rock reinforcement products for these two applications have proved to be unsatisfactory and there is a market need to reduce risks and uncertainties associated with the use of current products. It is appropriate to briefly review these two applications.

1.2 Underground Coal Operations

Retreat longwall coal mining usually requires the placement of reinforcing elements in the coal seam to control rib deformation and minimise spalling. Timber rib bolts have been used in the past with little success. In recent years, fibreglass rib bolts have been used with limited success. Fibreglass bolts have problems in the areas of load transfer, exceptionally high stiffness and installation.

Steel rib bolts provide adequate support and have been used on a limited basis in some coal mines, however, because rib bolts are mined with the coal, operators are cognizant of the following potential problems.

- Conveyor belt damage.
- Cutter head (shearer) damage.
- Materials handling system blockages (at the mine and the coal washery).
- Ignition of methane due to pick-bolt impact.

1.3 Open Pit Mining Operations

In many large metalliferous mines, corrosion of steel cable bolts is a problem. Mine water is often acidic because of the presence of sulphides within the orebody. Steel tendons in these aggressive conditions corrode rapidly and lose their ability to function. An ensuing ground failure could cause temporary or permanent sterilization of the ore in the affected area.

1.4 Risk Reduction

The HOPE bolt was specifically developed to reduce uncertainties associated with current rock reinforcement hardware in niche applications - ie risks of damage to equipment and personnel and the risk of ground failure due to failure of the support elements.

2. LABORATORY AND FIELD TESTING

2.1 General

Research and preliminary testing was conducted at BHP's Research Laboratory in Melbourne. This was done in close collaboration with operating, consulting and other research bodies within the mining industry. Further product development, engineering implementation and commercialisation has been

undertaken by BHP Engineering, with the co-operation of several mining operations.

The bar has been thoroughly tested in the laboratory and at numerous mine sites using the services of independent consultants including the CSIRO Geomechanics Division in Perth and Strata Control Technology Pty Ltd in Wollongong. Further testing on some particular aspects of the bar's characteristics is planned for the near future.

2.2 Composition and Geometry

The bar is made from die drawn high density polyethylene. The die drawing process aligns the internal moleculuar structure imparting greatly improved mechanical properties to the material.

The bar can be made in a range of sizes, however, current dimensions are: root diameter - 19 mm, outside diameter - 23 mm (these are the dimensions of the bar used in the tests reported in Sections 2.3, 2.4 and 3). Typical maximum production lengths are currently around 25 m.

The bar is threaded over its entire length - this feature ensures good load transfer between the bar and the surrounding grout.

The general properties of polyethylene are as follows.

1. Chemical Resistance: Excellent for all acids and alkalis.

2. Weathering Resistance: Ultraviolet light in the presence of oxygen does degrade the mechanical properties. This can be overcome with appropriate packaging materials (for storage purposes) and the addition of carbon black for surface mining (out-door) applications.

3. Resistance to Attack by Animals and Micro-organisms: Polyethylene is not a nutrient medium and is not attacked by any plant or animal life form.

4. Water Absorption: Polyethylene is water repellent, does not swell when immersed in water and changes in humidity have no effect.

5. Melting Point and Service Temperature: Melting Point is 140°C and it is recommended that the bar is only used in temperatures below 50°C.

6. Flammability: Untreated bars, after ignition, burn with a faintly luminous flame. It continues to burn when the ignition source is removed with burning drips. Spontaneous ignition temperature is approx. 350°C and the temperature at which ignition is induced from an external source is 340°C. Combustion of polyethylene bar produces no environmentally relevant pollutants.

7. Electrical Properties: Surface resistance is greater than 10^{13} ohms. The bar is inclined to become electrostatically charged. This problem can be overcome by the addition of an antistatic agent at manufacture or applying a coating following fabrication.

8. Density: Slightly less than water (1.0) - around 1/8 that of steel.

9. Handling Aspects: Polyethylene emits no vapours and is safe to touch. These properties are reflected in the use of this material for food containers, water pipes, storage crates, etc. The bar does not splinter or fracture. Its light weight makes it extremely easy to man-handle and install.

2.3 Laboratory Testing Methods

A useful laboratory simulation of grouted rock reinforcement performance is the double embedment length test. The specimen can be loaded axially or in shear. The axial test arrangement is shown schematically in Fig 1. The rock is simulated by thick wall steel tubes which are used to contain the grout and reinforcing element. The interface between the two steel tubes represents a rock mass discontinuity. A zero gap (closed joint) was used in the experimental tests detailed below. This is considered to be the most severe test possible since the displacement is concentrated at one point on the bar.

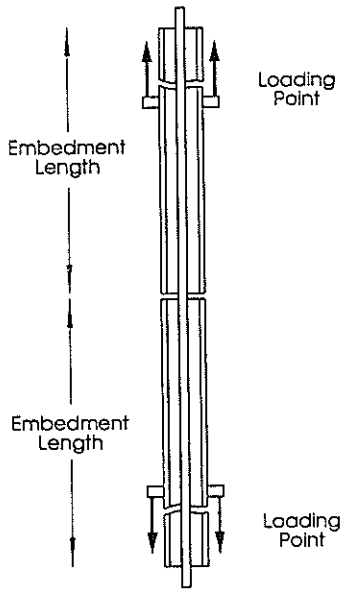

Figure 1 Schematic diagram of the double embedment length laboratory tension test.

Celtite Resifix 2 resin was used to anchor the HOPE bolts in the steel tubes. It is necessary with small diameter tubes to increase the load transfer between the grout and the steel tube by roughening the internal surface. This was achieved in this testing program by machining or tapping a coarse thread inside the steel tube.

A number of different types of loading are possible to provide data relevant to different applications. In this test program, short duration axial tension tests, shear, cyclic axial tension loading and long term axial tension constant loading tests were performed.

2.3.1 Short Duration Tests

The short duration axial tension and shear tests were designed to define the peak capacity of the HOPE bolt, the stiffness of response and the critical embedment length of the bolt in the grout. These parameters are required for comparison with other reinforcing devices and for design purposes.

It is not generally possible to directly extrapolate the results from short embedment length tests to longer lengths to define the minimum embedment length required to transfer the peak capacity of the reinforcing element. Extrapolation can be used only when the load transfer between the reinforcing element and the grout is uniform along the embedment length. Extrapolation is unreliable with a soft material (such as the HOPE bolt) which results in non-uniform load transfer between the reinforcing element and the grout and progressive shearing of the threads.

2.3.2 Cyclic Loading Tests

Mining operations produce changes in the stress regime where reinforcement has been installed. Operations over a period of time may cause cyclic loading of reinforcement. This may have a deleterious effect on the ultimate reinforcement capacity. The cyclic loading tests were designed to determine the ability of the HOPE bolt to recover strain. Elastic materials will show very little or any hysteresis to loading cycles below the elastic limit.

HOPE material is inherently both non-elastic and non-linear. Other materials with these characteristics sometimes exhibit a stabilised response as the number of cycles increases. That is, further damage to the material only occurs when the load is increased beyond the maximum level to which the materials has been subjected previously. The tests were also designed to determine whether progressive damage occurs during the extra cycles of load compared with a test loaded directly to failure. Any damage caused by cycles of load will be reflected by a reduction in the peak capacity.

2.3.3 Creep Tests

Polymeric materials are known to have high creep rates when compared with traditional engineering materials such as steel, aluminium and concrete. The creep characteristics were identified as potentially the most important property which would govern the potential of HOPE material to replace existing reinforcing devices. It was originally intended to perform load relaxation monitoring as a means of evaluating the rate of creep of the HOPE material. Load relaxation tests require the establishment of a load in the reinforcement which is maintained by setting an anchor. Load variations with time are monitored using a load cell whilst maintaining the constant displaced position.

Due to the difficulties associated with anchoring HOPE material, creep tests were performed instead of the planned load relaxation tests. Creep tests involved monitoring the displacement of the specimen whilst maintaining a constant load.

2.4 RESULTS OF LABORATORY TESTS

2.4.1 Critical Embedment

The full load capacity of the bar was developed when the embedment length was greater than 210 mm.

2.4.2 Shear Test

The shear capacity of the 19 mm bolt is 57 kN (further test work is underway to verify and expand on this information).

2.4.3 Short Duration Axial Tension Tests

The summary of the results for the short duration tests with three different embedment lengths is given in Table 1. A typical load-displacement curve is shown in Figure 2.

Typical system stiffness is around 4 kN/mm as indicated in Figure 2.

2.4.4 Cyclic Loading Tests

A typical graph from the cyclic load tests on the HOPE bolt is presented in Figure 3. Specimens were loaded to failure following the cycles of loading. The peak load for the HOPE bolt was marginally lower than the peak loads recorded in the short duration tests.

2.4.5 Creep Tests

A summary of the creep tests is given in Table 2. The four parameters of importance are the load level, rate of creep, displacement and the time to rupture where this form of failure occurred. Rupture occurred in all tests except the one with a nominal constant load of 25 kN.

The bar can tolerate high displacement (when compared to fibreglass bolts) prior to failure as indicated in Table 2. Further test work is being undertaken to provide further details on the long term behaviour of this material.

The results of creep tests are of concern, however, it should be noted that the test adopted was the most severe possible and the relevance of this type of test to

Table 1 Summary of Short Duration Tension Tests

Embedment Length (mm)	Failure Mode	Maximum Load (kN)	Nominal Stress (MPa)
200	S	96	338
	S	96	338
500	R	98	346
	R	98	349
800	R	93	328
	R	93	328

Notes

S = threads stripped from core

R = rupture of core

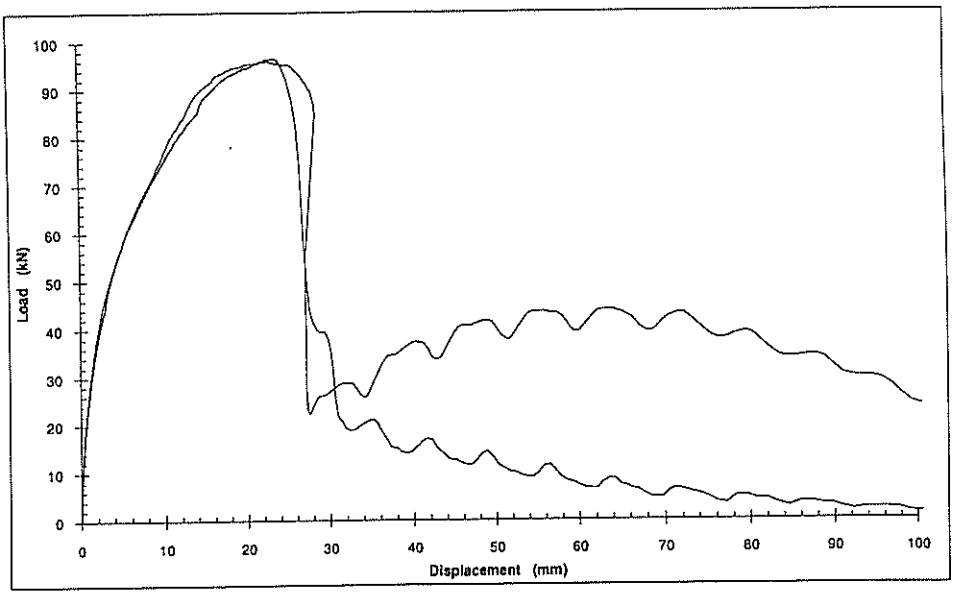

Figure 2 Short duration load-displacement response for 200 mm resin embedment.

Table 2 Summary of Creep Properties for HOPE Bolts

Nominal Load (kN)	Creep Rate (mm/hour)	Displacement (mm)	Failure Mode (hours)
65	0.83	75	R (18)
45	0.40	38	R (50)
25	0.03	16	N/A

Notes

R = rupture of HOPE bolt core

N/A = test discontinued before stability or rupture determined

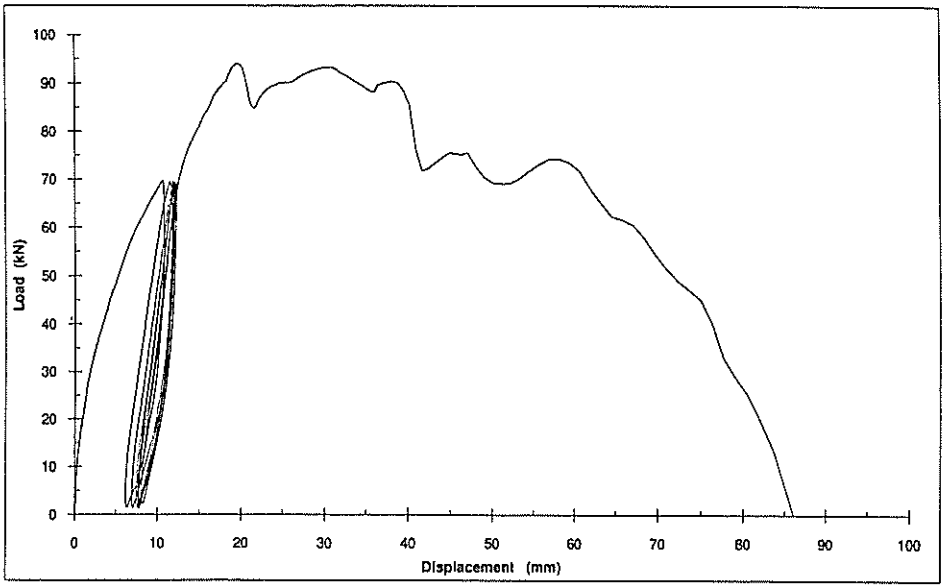

Figure 3 Cyclic load-displacement response curve.

all forms of fully grouted rock and soil reinforcement needs further critical examination.

The creep test described above represents a 'worst case' load situation as could be expected in highly stressed, strong, blocky rock. The most important finding from this test is the amount of deformation required to cause rupture of the HOPE bar. For the two cases where rupture occurred the total displacement was 75 mm and 38 mm for a constant load of 65 kN and 45 kN respectively. These are extremely high dilations for a single discontinuity and would not normally be expected to occur in the access openings of most underground mines.

The creep test also highlighted the inability of HOPE to accept moderate load for a sustained period. HOPE is therefore inappropriate for applications where dead weight loads are experienced.

3. FIELD TESTING

3.1 Rib Bolting in Underground Longwall Coal Mines

The bolt has been field trialled at Tower, Appin, Angus Place and Cordeaux Collieries in NSW. In-situ monitoring, at Tower and Angus Place Collieries was undertaken by Strata Control Technology Pty Ltd. The objective of the Angus Place trial was to compare the in-situ performance of all currently available non-steel rib bolts. The results of this trial are indicative of the results of trials at Tower and Appin Collieries. They can be summarised thus:

1. Generally speaking, there is no significant difference in loads generated by various dowel types. It should be noted however, that it is very difficult to measure loads in HOPE bolts because of the difficulties in cementing strain gauges to the bar's surface.

2. The visual appearance of the ribs reinforced with HOPE bolts, as well as the conditions of the bolts, was noticeably better than the other dowel types.

3. The improved end fixing system and the continuous thread of the HOPE bolt has assisted in maintaining the integrity of the skin of the ribs.

4. Despite the fact that potential creep effects in the HOPE material may tend to lower the long-term effectiveness of the bolt, the improved skin protection of the rib provided by the HOPE bolt provides benefits in all rib conditions.

5. The reduction in total rib deformation measured at the HOPE test site is a reflection of the improved skin provided by this bolt.

In summary, HOPE's in-situ performance is generally better than other non-steel rib bolts Other benefits that may increase the marketability of the bolt are simplicity of installation, easy and safe handling and the fact that the long term projected price is much less than fibreglass bolts (and probably on a par with steel rib bolts). The high stress intensity, short duration nature of this application matches HOPE's current performance characteristics quite well.

3.2 Bolting in Corrosive Environments in Open Pit Mines

The bolt has been trialled at BHP Iron Ore's Mt Newman mine. The mine has an acute groundwater problem where the pH can be as low as 1.5. Steel cable bolts have been known to corrode completely within 3 months of installation.

The HOPE bolt is being trialled in a very low load environment as a mesh pinning bolt. The purpose of this bolt is to assist in maintaining the integrity of slopes by preventing the skin from spalling and ravelling. It is not intended to prevent any deep seated failure.

3.3 Embankment Support

The bolt is being trialled by the Roads and Traffic Authority of NSW as a soil nail. Preliminary results are favourable and further data will be made available in the near future.

4. CONCLUSIONS

4.1 BHP has developed an innovative low cost, non-steel tendon for niche artificial ground support applications.

4.2 The market for the bar is envisaged to be in the area of either

A. Low stress environments (eg mesh pinning), or

B. high intensity, short duration stress environments (eg rib bolting).

coupled with corrosion and/or cuttable requirements.

4.3 The bolt reduces uncertainties in rib bolting and mesh pinning support applications due to its superior performance when compared to existing rock reinforcement products.

4.4 Because the construction material has performance characteristics that are extremely different to steel each application must be carefully reviewed to ensure fitness for purpose.

4.5 The HOPE bolt provides a partial solution to problems in two specific applications and reduces the risks involved - it is not the panacea for ground stabilisation in difficult ground conditions. It is almost certain that continuing development will produce far superior products in the not too distant future.

5. REFERENCES

Gale, W J (1991) Strata Control Utilising rock reinforcement Techniques and Stress Control methods, in Australian Coal Mines.

Mining Engineer, Vol. 150 (352). Jan. pp247-253.

A Method of Risk Assessment for Roadway Embankments utilising expansive materials

BURT LOOK-HONG
B.Sc., D.I.C., M.Sc., M.I.E.Aust.
Post Graduate Student, University of Queensland & Geotechnical Engineer, Queensland Department of Transport
VASANTHA WIJEYAKULASURIYA
B.Sc.(Eng.), M.Eng.
Geotechnical Engineer, Queensland Department of Transport
IAN REEVES
B.E., M.Eng.Sc., M.I.E.Aust., R.P.E.Q.
Principal Advisor (Materials Development), Queensland Department of Transport

SUMMARY : In roadway construction, risk is defined in terms of pavement distress. A risk criterion in terms of the tolerable movements in roadways is proposed for expansive clay road embankments. A design approach is outlined. Valuable information for future designs using expansive clays are found in already constructed road embankments. Their performance in terms of surface distress and associated maintenance requirements can be the yardstick for similar construction.

1.0 INTRODUCTION

In roadway construction, risk is defined in terms of pavement distress. Expansive materials are one of the identified Hazards, and its usage in roadway embankments is often accompanied by heave and roughening of the pavement surface, or longitudinal cracking. This results in a reduction of the design life of the pavement and adds to the maintenance costs. Maintenance costs comprise the costs of road repair as well as the road user costs due to loss of service.

Valuable information for future designs using expansive clays can be obtained from existing road embankments. Their performance in terms of surface distress and associated maintenance requirements can be the yardstick for similar construction. In particular, it has been found that the in-service condition is often not the as-constructed or design condition. Therefore, in theory, if we were to construct at the in-service condition from the start, then the risk of usage can be minimised. This paper presents a review of the risk criteria in roadways and a methodology for the determination of the in-service condition of an expansive clay embankment, prediction of the expected movement accompanying moisture changes, and outlines the risks involved with its usage. A case study is used to illustrate the method.

2.0 RISK ASSESSMENT

2.1 The Definition Of Risk

Statistical and probabilistic methods are tools used to quantify risk. However, in most Geotechnical Engineering applications, risk (of an event) is analysed as "risk of failure" for limiting equilibrium conditions. Factors of safety are used to signify ranging levels of risk. In many cases the factor of safety is really "an experience factor" or equally "a factor of ignorance", against uncertainty in the soil parameters, analytical model, etc.

Where factors of safety are not (or cannot) be applied, risk assessment can be expressed in terms of displacement criteria i.e tolerable movement vs movement to be expected. The tolerable movement is usually based on the structural/ architectural components.

We therefore have two types of risk : (1) Risk of failure, and (2) In - service risk. A definition of risk should describe both types of risks as well as the methods of assessment in terms of probabilities of occurrence, return periods, factors of safety or tolerable movements. Equation (1) - from Ambraseys (1983)[1], seems to provide this broad definition.

$$[\ Risk\ ] = [\ Hazard\ ] \times [\ Vulnerability\ ] \times [\ Value\ ] \qquad (1)$$

Natures's laws determine the Hazards while the human use of an area detefmines the Vulnerability and its Value. In general, Scientists/Geologists/Seismologists identify the Hazard, while Engineers have the responsibility to classify the Hazard and quantify the vulnerability and the Politicians/Economists/Media or Society at large places a value on the works. Typically the design system uses factors of safety to quantify the "acceptable" risk, and the unquantifiable debate of political compromise, etc., is avoided. While ideally the level of risk which society deems acceptable should be the determining criteria, it is often decided by what those "footing the bill" say they can afford.

In roadways the risk is spread over a wider spectrum of society on a recurrent basis. With the advent of more intelligent cars, sophisticated suspension systems, faster, and more sensitive controls, etc. then previously minor movements have now become more noticeable. Surface irregularities on high speed roads have their effects amplified to the driver in proportion to the car speed. This translates into potential loss of control, and risk to the road user. The actual effects of unevenness on user safety and costs are difficult to realistically quantify, given the wide range of variables affecting any accident situation - driver(s), vehicle(s), roadway, time of day, etc. A roadway therefore experiences both types of risks.

2.2 Pavement Distress In Roadways

Climate, material properties and traffic contribute to pavement distress. Cracking, distortion and disintegration are the main types of distress modes (Finn and

Monismith, 1984[2]). One must distinguish among the types of distress modes in terms of :-

- Time to failure[3]. Short Range failures are associated with distress due to gross design and/or construction errors and will be manifested within 5 years after construction. Middle range failures develop due to the magnitude and cyclic action of climate (frost, thermal, precipitation). Thus the design life of the pavement is significantly reduced.

- Surface (only the top pavement) or Structural Distress. In flexible pavements surface distress would be evident by ravelling, aging of binder, wear of surfacing, etc. Structural distress results in cracking and permanent deformation.

- Traffic-load associated or Environmental effects.

Some common types of identifiable hazards which may produce distress to the road are :
1. Poor performance of paving material
2. Landslips (Large or minor movements - including creep)
3. Consolidation of compressible clays
4. Volume changes in expansive clays.

Associated with each hazard is a potential for distress which results in higher maintenance cost, as well as increased road user costs. Expansive behaviour is just one of the many factors affecting the pavement. However, the maintenance costs for roadways on expansive subgrades are roughly 10 times greater than for the same type of pavement constructed on a suitable, non-expansive subgrade (Snethen, 1979)[4]. Expansive clays affect the roadway system with effects on structures (bridges, culverts), the pavement system, stability of slopes, etc.

Pavements on expansive clays may experience two main types of distress :
- Pavement Undulations (distortion)
- Longitudinal edge cracks.

Pavement undulations consist of periodic movements with precipitation and results in pavement roughness and loss in riding quality. Longitudinal edge cracks are typically caused by edge movements due to shrinking and swelling, which are out of phase with the interior of the pavement. This results in cracking and loss of lateral support and acts as a source for further water intrusion leading to other forms of instability.

2.3 Value

The low cost of locally available material from cut and fill operations and the high cost of importing material usually dictates the use of the available expansive material. The true costs for the use of expansive clays in embankments is however the construction costs in addition to the maintenance costs over the design life.

In addition to road maintenance costs, changes in road geometry, cracking and increased roughness all contribute towards increased fuel consumption and vehicle operating costs for the road user. The assigned value is therefore directly proportional to the number of road users for that particular route. As explained previously there is a risk to life as well as the economic risk.

Any cost-benefit analysis would therefore require estimates of :
1. Additional construction costs due to designs incorporating the effects of volume changes.
2. Direct and indirect costs for future maintenance costs.
3. Non-monetary costs for future damage (Human-life factor)

3.0 ASSESSMENT OF EXPANSIVE CLAY EMBANKMENTS

3.1 Identification Of Hazard

As expansive soils, shrink as well as swell, the term therefore refers to a reversible process for volume change behaviour. The first step in any risk assessment is the identification of the expansive materials. Some classification schemes are shown below.

Table I: Classification of potential swell - Snethen, 1979[4]

Liquid Limit %	Plasticity Index %	Natural Soil Suction (kPa)	Potential Swell Classification
> 60	> 35	> 380	High
50 - 60	25 - 35	140 - 380	Marginal
< 50	< 25	140	Low

Table II: Classification of embankment material -DOT, 1991[5]

Class	Plasticity Index %	Potential For Expansion
A	< 12	Low
B	12 - 22	Medium
C	22 - 32	High
D	> 32	Very High

Material classification provides a descriptive assessment of the risks involved, and aids in the identification of the hazard and the extent of measures to be considered.

3.2 Vulnerability

3.2.1 In - Service conditions

In service performance of a pavement is controlled not merely by its traffic loading and as constructed properties but also by its longer term moisture-density equilibrium conditions with its environment. The in-service condition usually take years to attain, and can be significantly different from the initial construction condition. Figure 1 illustrates schematically the equilibration process leading to the in-service condition. The Density and moisture changes which occur after construction are often accompanied by volume changes, and loss of strength. The in-service seasonal movement can be

reduced by a steeper batters, wider seals, moisture barriers, etc. The initial movement should be minimised during design and construction as this can be more easily controlled.

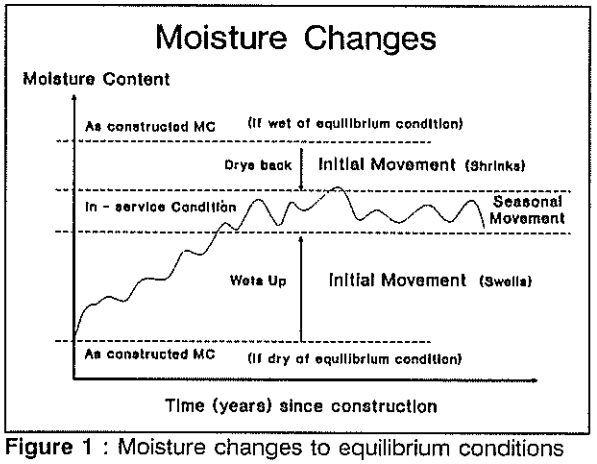

Figure 1 : Moisture changes to equilibrium conditions

The initial movement would generally result in movement of the whole embankment while the in-service seasonal movements would result in differential movement as illustrated in Figure 2. Equilibrium conditions tend to develop in areas of a soil mass that are remote from climatic influences - such as beneath large covered areas and at depth. A roadway embankment experiences climatic influences from 3 sides : part of the top and two side slopes. The effect of groundwater is also felt if it is in close proximity to the base of the embankment. The in-service condition may be wet of optimum or dry of optimum (Richards and Gordon, 1972[6])(Gordon and Waters, 1984[7]), depending on the soil type and climate.

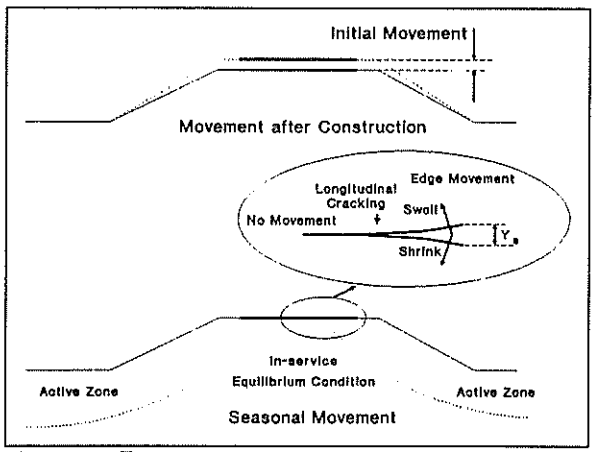

Figure 2 : Types of embankment movement associated with expansive clays.

Haupt (1981)[8] provides various prediction models for equilibrium moisture contents, based on OMC, MDD, Liquid Limit and particle size. Equation (2) is for OMC > 13 %. This provides an in-service moisture condition but does not account for the seasonal variation at the surface and pavement edge. Others such as Livneh and Ishai (1976)[9], provide correlations for the equilibrium moisture condition as well as for CBR (strength).

$$PEMC = 0.38 \times L.L.^{0.7} \times (\%\text{-}0.425)^{0.3} - 1.5$$

where

PEMC = Predicted equilibrium moisture content %
L.L. = Liquid Limit %
%-425 = % pasing the 425 μm sieve (2)

Where areas of inundation are expected, or below the ground water table then in-service moisture conditions can be determined from soaked CBR tests at the in-situ density. However a site specific approach, involving an evaluation of existing roadway performance under conditions of similar road construction with similar materials in the area would usually yield the most reliable assessment at a given site. For most areas the road network is sufficiently developed so as to provide a large databank of information on in-service conditions for construction in a given area. This would be applicable especially for By-Pass roads and addition of lanes at existing roadways.

3.2.2 Evaluation Of Swell potential

Having identified the Hazard of swell potential, then steps must be taken to quantify and reduce the vulnerability. A compromise is often required between the increased maintenance costs associated with shrink/swell behaviour and the control requirements of other hazards i.e. an increase in moisture content to reduce swell could result in a reduction in design strength, increased consolidation potential and an increased shrinkage potential. In order to reduce the swell potential, density, moisture and depth stabilisation are the main elements of construction control.

During design an assessment of vulnerability would include analytical models to quantify the above conditions. Index properties have been used to predict the potential movements in expansive soils, but this approach does not provide for the overburden or lateral restraint, and is based on the assumption that the soil has access to all the water it can absorb. This is often not the case.

Suction has been found to be a more definitive measure of the swell potential. Soil suction is a measure of the intensity with which a soil sample will attract moisture. A change towards a smaller suction (higher MC) or to a larger suction (lower MC) may produce swelling or shrinkage cracking respectively. Soil Suction is dependent on the factors outlined in (3)

$$\textit{Soil Suction} = f\,[\,\textit{Depth, offset, climate, groundwater, Soil type, moisture content, density}\,] \quad (3)$$

Snethen (1979) provides a comprehensive review of soil suction and prediction procedures, using soil suction and other indices. One relationship is that of the (matrix) soil suction with (gravimetric) moisture content (4).

$$\textit{Log}\ \tau_m = A - B \times w$$

where τ_m = *soil suction (kPa)*
A, B = *Constants*
w = *water content (%)* (4)

3.2.3 Concept of the active zone

Maximum change due to climatic effects occur at the surface and decrease with depth. This depth of climatic influence is referred to as the active zone. The active zone in this paper, is associated with movement. Therefore where seasonal moisture changes occur, with no accompanying movement (due to depth of overburden), then that area is not considered an active zone.

The position of the active zone is also dependent on the soil type and depth to the groundwater level. Evaluation of the active zone in roadways provides a good indicator of the depth of stabilisation of material required.

An active zone will show two distinct areas :- a cracked zone (unrestrained), and a uncracked zone (lateral restraint occurs). The cracked zone is a result of desiccation, while the uncracked zone does not experience significant effects of desiccation because of its depth below the surface. The cracked zone may therefore be more likely to experience 3-dimensional volume changes, while the uncracked zone, because of its lateral confinement would undergo 1-dimensional volume change.

3.2.4 Prediction of surface movement

The prediction of surface movement have been applied mainly to buildings. The following discussions therefore draws on some of this "building" experience. Based on the expansion classification, stiffening beams and/or deepened footings would be required. Current roadway technology does not yet have the equivalent of the stiffening beams, but pavement designs would usually involve deepened (thickened) sections as required.

For buildings, A.S. 2870[10, 11] defines the predicted surface movement as a criterion for assessment of the site reactivity and for subsequent foundation design. Methods of calculating the movement is based on the instability Index and a generalised suction profile (5). The instability index, is defined as the vertical strain per unit change in suction and is based on the applied stress, degree of lateral restraint, and suction change.

$$y_s = \Sigma\, I_{ss} \times \Delta z \times \alpha \times \Delta u$$

where

y_s = *predicted surface movement*
I_{ss} = *shrink-swell index*
Δz = *thickness of layer*
α = *restraint factor (Cracked or uncracked zone)*
Δu = *Change in soil suction*

(5)

In the determination of the Shrink-Swell index, the suction range is assumed rather than measured. The reliability of this was checked by Cameron (1988)[12] who provides a review of the tests of reactivity as defined in A.S. 2870, and its relation to other Index properties.

O'Neil and Poormoayed (1980)[13] provide another approach to compute the surface heave for a given foundation (surcharge) (6). The method relies on the swelling pressure of the sample and the measure of the swell (Strain) on inundation. The swelling strain corresponding to the overburden pressure is determined. The

$$y = \Sigma\, s \times h_i \times .01$$

where

y = *heave for the given surcharge pressure*
s (%) = *swell in Layer i for the surcharge*
h_i = *thickness of soil layer i*

(6)

free swell strain is the strain measured without any load. The zero swell pressure is the load required to completely restrain any sample movement when saturated. This is defined in figure 3.

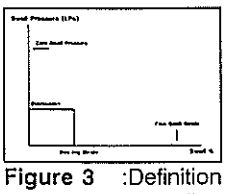

Figure 3 :Definition of terms for swelling pressures

The time for the determination of the full swell for various samples may however be prohibitive, but the method does not involve assumptions of soil suction. The soil suction approach covers both the expansion and shrinkage behaviour of the soil, rather than the wetting up only as implied in (6). However (6) uses complete inundation (a climatic extreme) and considers 1-dimensional swell throughout the active zone. This results in larger deformations than the soil suction model where 1 dimensional movement occurs in the uncracked zone, but 3-D movement occurs in the cracked zone.

Richards (1967)[14] uses soil suction curves to predict moisture content changes in soils. The equilibrium suction is determined from correlations with climatic rating. (7) assumes (i) volume change in the soil is equal to the moisture change and (ii) equal volume changes occur in the vertical and horizontal directions.

$$\frac{\Delta H}{H} = \frac{1}{3} \times \frac{\Delta V}{V} = \frac{1}{3} \times \frac{(w_f - w_i)\, G_s}{100 + w_i\, G_s}$$

where

$\frac{\Delta H}{H}$ = *vertical heave*
$\frac{\Delta V}{V}$ = *volume change*
w_i = *initial water content*
w_f = *final water content*
G_s = *Specific Gravity*

(7)

The terms soil expansion, swell, heave and swelling strain are considered synonymous.

3.3 Assessment Of Serviceability Criteria

In roadways, the criteria for acceptable levels of differential or total movement is not as clearly defined as for structures. For performance assessment of roads with expansive materials or on compressible sub-soils, there is no general guidance on tolerable levels of differential movement. Deformations seen on the surface are the cumulative effect of vertical deformation in each layer of the pavement and subgrade. The different types of distress outlined in Section 2.2 must be kept in perspective.

To evaluate acceptable usage, there is the need to establish criteria for tolerable movements. A review of movement/ deformation criteria for roadways is briefly summarised.

* Surface unevenness increases the hydroplaning potential of the pavement. Rutting can also contribute to hydroplaning. Rutting is probably the best known parameter for characterising deformation of the pavement. Table III (Kaplade, 1990)[15] provides typical requirements for both rutting and water depth threshold limits.

Table III: Threshold values for transverse unevenness - Kaplade, 1990

Speed V_{85} km/h	Rut Depth S_T (mm)	Hypothetical Water Depth S_H (mm)
> 100	20	5
70 < V_{85} < 100	25	8
< 70	30	12

According to Croney (1972)[16] a rut depth of 10mm is considered critical and rut of 20 mm constitutes failure when accompanied by cracking. DOT (1991)[17] evaluates terminal rut on the basis of length of road affected and the number of users (Table IV).

Table IV: Suggested Terminal rut criteria - DOT, 1991

Road Usage	Terminal Rut Depth (mm)	Length of Road exceeding Terminal Rut Depth
Heavily Trafficked Roads >> 2000VPD	20	20 %
Lightly Trafficked Roads << 2000 VPD	30	20 %

* Other approaches are that of Lytton (1973)[18] who characterises the expansive clay roughness in terms of the largest amplitude and wave lengths of the soil type while Jordan (1984)[19] proposes evenness standards.

Table V: Proposed evenness standard for random unevenness on newly surfaced major roads (300 metre test length) - Jordan, 1984

Minimum Peak-to-peak amplitude h (mm)	Allowable number of Bumps relative to a moving average datum of length	
	3 metres	15 metres
5	15	
8	3	
10	0	5
15		0

Table VI: Road subsidence criteria - Jordan, 1984

Riding Quality	Depth of Subsidence
Comfortable / Acceptable	< .04 L^2 / V^2
Uncomfortable / Very Uncomfortable	> 0.1 L^2 / V^2
L = Length of Subsidence (< 30 m) V = max traffic speed (m/s)	

* A.S.2870 (1986) recommends the design of foundations for light foundations on expansive soils be based on the characteristic surface ground movement (y_s) classified in Table VII.

Table VII: Buildings on reactive clays - criteria for assessment and design

y_s (mm)	Reactivity	Design values of differential movements y_m are:
< 20	Slightly to Non - Reactive	0.7 y_s for centre heave 0.5 y_s for edge heave (initially dry site) 0.3 y_s for edge heave (initially wet site)
20 - 40	Moderately Reactive	
40 - 70	Highly Reactive	
> 70	Extremely Reactive	

The literature therefore has general guidance on the quantification of distress in roadways in terms of road surface unevenness, and any surface movement should be within these tolerable limits for suitable performance of the roadway. It should be emphasised that rutting and hydroplaning may be associated with hazards other than expansive material and using these movements as criteria for assessment does not signify the cause. The classification of various Hazards (swelling, collapsing, consolidation potential, etc.) would assist to determine the cause of distress.

Using the criteria presented in Tables III to VII, the movements associated with roadways on expansive soils can be classified as follows :

Table VIII: Summary of differential movement criteria

Criteria	Unacceptable	Concern
Rutting	20 mm	10 mm
Hydroplaning	10 mm	5 mm
Ride Vibration	---	10 - 15 mm
Subsidence - 3m (v=100 km/h) - 10m	--- ---	1 mm 11 mm
Expansive Clays (Residential buildings)	---	10 mm (initially dry site) 6 mm (initially wet site)

4.0 PROPOSED METHOD TO CHARACTERISE EXPANSIVE CLAY EMBANKMENT BEHAVIOUR

4.1 Proposed Method.

The proposed design approach involves the integration of concepts and techniques outlined previously. The stages in the evaluation of expansive clay embankments are :

(i) Identification of the hazard, from Index tests
(ii) Quantification of the associated distress. This involves evaluation of :
1. In - service moisture conditions, and density conditions.
2. Depth of Active zone (cracked and uncracked zones, if possible)
3. Soil suction changes between wet and dry states.
4. Prediction of movement (total since construction and differential due to seasonal variation), by adaptation of existing predictive models to suit roadway embankment conditions (Table IX).

Table IX: Modifications applied to existing methods of movement prediction

Description of method	Adaptation	Reference
Shrink/Swell Index	- Active Zone - Cracked / Uncracked Zone - Suction Profile	Eq 5 - A.S. 2870 (1986)
Swell Pressure	- Use of 1/3 heave in cracked zone & full heave in uncracked zone	Eq 6 - O'Neil & Poormoayed (1980)
Moisture Change	---	Eq 7 - Richards (1967)

(iii) Evaluate the risk associated with the movements as defined in Table VIII, and design alternatives to minimise the risk.

4.2 Field Study

The opportunity to undertake field studies arose when a major deviation of the Bruce Highway at Cooroy was to be designed. Geotechnical investigations along the proposed route indicated that for balanced earthworks only highly expansive clays were available for construction of the embankments. Disposing of excavated materials and substitution with better quality materials (importing over considerable distances) was considered an unacceptable high cost option. The proposed material for the embankments has plasticity Index of 27 to 50% and liquid limit 50 to 80%, with clay content greater than 80%. This material is classified as a high swell potential.

Evaluation of the design conditions for the proposed embankments, involved :
1. Trenches located in embankments, where the proposed Bypass joins the existing Highway
2. Install probes for monitoring of moisture changes.
3. Laboratory CBR tests performed on the proposed material and the effect of lime treatment on the proposed material.

At the time of trenching in-situ CBR, density and moisture values were determined as well as the OMC, and MDD of the material with depth.

Time Domain Reflectivity (T.D.R.) was used to monitor moisture changes. The device operates by sending a voltage pulse, and measuring the rebounded signal. This provides a measure of the dielectric constant, which can be related to the volumetric moisture content. Volumetric moisture content can be converted to gravimetric moisture content (usual Civil Engineering moisture Content reference) by dividing by the dry density. Comparison of the initial TDR readings and the gravimetric moisture content from oven drying were close enough to indicate the instrument was producing reliable results at this site. The full results[20] of the investigation and use of TDR is presented elsewhere (Look-Hong and Reeves, 1991)[21,22].

4.3 In-Service Moisture Conditions

Historically Queensland Roads have been constructed with the moisture content at about 80 to 90% of OMC and the Relative Dry Density (RDD) at or greater than 95%. In-service conditions are typically arrived at in about 3 to 5 years the Bruce Highway is several years old, and therefore assumed to be at its in-service state.

The results of trenching at the existing embankment indicate that the roadway has subsequently wetted up and dedensified, after construction. Therefore for this site, the construction target would be for the dry season "in service" moisture condition in order to minimise the initial movements (refer fig. 1). The in-service movements between the dry and wet season moisture variation should be within tolerable limits as later defined. Figures 4 & 5 provide the TDR readings of volumetric moisture content. This is compared with the rainfall

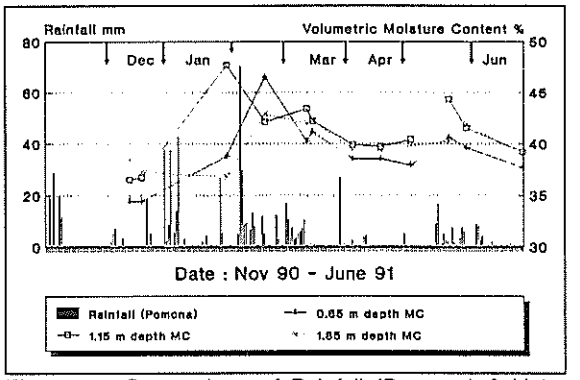

Figure 4 : Comparison of Rainfall (Pomona) & Volumetric moisture Content at varying depths

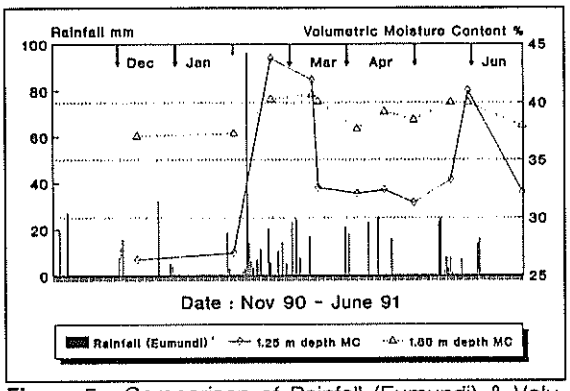

Figure 5 : Comparison of Rainfall (Eumundi) & Volumetric moisture Content at varying depths

records at the nearest rainfall station. The probes were installed at an end of Dry Season Condition, and long term monitoring would involve recording values over at least a full year cycle. Rainfall records indicate the wettest months are typically February and March, for this area. Therefore TDR probe readings during these Wet month periods are assumed to provide the worst condition which occurs at this site. **Note:** There may be a time lag between wetting up and the rainfall event.

Following a rainfall event the probes at 1.15 and 1.25 metres depth seem to wet up first, followed by the higher level (0.6 m), with the lower level (1.8m) being relatively stable. This may indicate the extent of the cracked zone area, where water wets up the base of the cracked area first, then migrates upwards or down. The higher level would however be the first area to dry out. The readings indicate the bottom of the active zone lies at about 1.8 metres or deeper from the pavement surface. The deeper results provide an indication of the stable in-service condition.

Based on these field results, "the seasonal" in-service conditions occur at or above the plastic limit which is wet of optimum at about 1.3 times O.M.C. Field density in the range of 92 to 94 % relative Standard dry density were measured for the in-service condition. In service gravimetric moisture conditions for the driest and wettest condition to date are summarised in Table X. This data represents the 90/91 season condition, which was a relatively dry year - only 2/3 of the expected annual rainfall. Monitoring another dry and wet season will continue in order to assess any variations.

Soil Classification results show the existing embankment material to be an expansive (CH) material with a plasticity index of 30 to 31% and Liquid limit of 52 to 54%, and 90% passing the 425 micron sieve. Using (2) from Haupt (1981) for prediction of the equilibrium moisture content produced a value of 22.7%, which would reflect the "dry in-service condition".

TABLE X: In - service Moisture Content Variation from wet to dry conditions

Trench/ (Depth)	In-Service M.C. (w)		Relative M.C.			
			w/PL		w/OMC	
	Dry	Wet	Dry	Wet	Dry	Wet
T1(0.65)	20.6	27.8	1.1	1.5	1.4	1.8
T1(1.15)	23.7	30.2	1.0	1.3	1.4	1.8
T1(1.85)	23.3	27.1	1.0	1.2	1.3	1.5
T2(1.25)	15.1	25.0	0.7	1.2	0.9	1.5
T2(1.80)	23.0	25.3	1.1	1.2	1.3	1.5

4.4 Use Of Swell Testing To Determine Depth Of Active Zone

One dimensional oedometer swelling tests were conducted on samples from the trenches as part of the determination of the Shrink/Swell index and to evaluate the relationship between overburden pressure and swelling strain. These results are also used to predict the expected movements. Only the results of the latter tests are shown in Table XI.

TABLE XI: Swelling Results

Trench/ (Depth)	Overburden Pressure (kPa)	Swelling Strain (%)	Free Swell Strain (%)	Zero Swell Pressure (kPa)
T1(0.65)	13	2.1	2.5	89
T1(1.15)	22	1.5	2.3	73
T1(1.85)	36	0.0	1.1	36
T2(1.25)	24	1.1	2.8	46
T2(1.80)	35	< 0.0	2.4	11

The zero swelling strain obtained for samples taken at 1.85/1.80 metres depth indicates that at this depth the soil is in an approximate equilibrium condition i.e. Active zone is determined when the existing overburden ≥ zero swell pressure . The results of moisture content monitoring indicates some equilibrium condition at about 1.8 metres and swell testing results support the use of that depth as the active zone. As defined previously, the active zone is considered as the depth at which moisture changes can be associated with movement.

4.5 Prediction Of Soil Suction

By evaluating a nearby site of similar material, then soil type and climate is accounted for. It is assumed that the effect of solute suction is negligible for embankment construction.

At the Cooroy site soil suction (matrix) was measured by the filter paper method. This was limited samples (5) from only two trenches, but nevertheless provides a general guide to the expected suction Snethen's(1979) moisture suction relation (4) was modified as follows :

Using water content as volumetric (θ_v) rather than gravimetric (w) produced a better correlation (8).

$$Log\ \tau_m = 2.737 - .034\ w \qquad r^2 = 0.35$$
$$Log\ \tau_m = 3.026 - .029\ \theta_v \qquad r^2 = 0.41 \qquad (8)$$

In addition, an improved correlation was obtained if the depth (z) at which the sample was taken was included in the regression analysis (9) - refer (3).

$$Log\ \tau_m = 2.770 - .264\ z - .019\ w \qquad r^2 = 0.65$$
$$Log\ \tau_m = 3.021 - .258\ z - .019\ \theta_v \qquad r^2 = 0.71 \qquad (9)$$

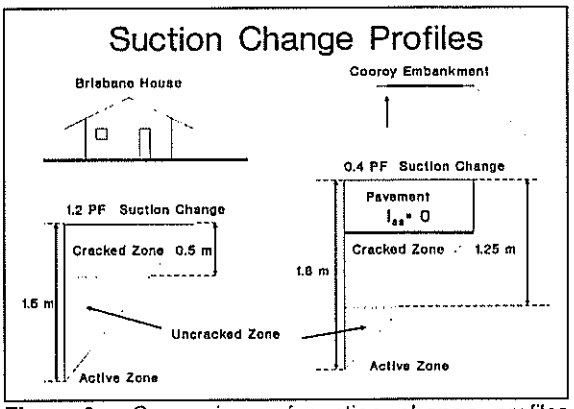

Figure 6 : Comparison of suction **change** profiles beneath flat and embankment areas.

The extreme dry and wet moisture values measured was used to predict suction changes with depth. Ideally the depth of the active zone should have a predicted soil suction change of 0.0 PF. In practice the suction at the surface of the embankment would not be applicable as the pavement thickness would reduce the depth of the active zone. This may be compared with the 1.2 PF suction range in the Brisbane area, as described in A.S. 2870. for "flat" surfaces with 1.5 m depth of active zone (H) for the Brisbane area. The commentary further states, that 0.75 H is a reasonable average for Australia, for an estimate of the cracked zone. However in temperate climate a lower value may be appropriate with H/3 suggested for Sydney, and sometimss applied to Brisbane.

A comparison of the suction profiles is given in figure 6. This is only a guide, but nevertheless indicates the variation for embankments exposed to the elements from 3 sides, even with the top sealed. In this case the effects of only one side, would have been felt as the moisture content directly under the pavement edge was monitored.

In addition, another step in the prediction process was attempted. Embankments are typically constructed at about 90 % OMC, and if this value is used, then an initial Suction of 3.1 PF is backcalculated at the time of construction, compared with 2.8 PF at the present in-service condition.

4.6 Prediction Of Surface Movements

The predicted movements were calculated using the methods described in Table IX are shown in table XII.

Table XII: Predicted seasonal movements

Method	Modification	Predicted Differential Movement
- Shrink/ swell Index tests	Suction Profile Active Zone Cracked/ Uncracked Zone	9 mm
- Swell Pressure tests	Unmodified	14 mm
	1/3 of measured Swelling strain in cracked zone. Full swelling strain in uncracked zone.	8 mm
- Moisture change	---	38 mm
Monitored Movement (March to August 91) - 4 mm max. No Distortion or cracking of pavement observed to date.		

In order to assess the total movements (unmonitored), which would have occurred since construction, the predicted suction at 90% OMC was used. A total movement of 8 to 16 mm is calculated depending on the shrink/swell index value or model profile.

Monitoring will continue through to the next wet season when maximum movement is expected. Whatever magnitude movement occurs is a good guide to the tolerable movements if distortion of the pavement is still not evident, as this is considered a good performing pavement. This will also provide an indication of the suitability of the prediction approach adopted.

As a preliminary consideration from this and other observations, and the criteria outlined in section 3.3, then 10 mm seasonal **differential** movement in the pavement seems to be tolerable, while 20 mm movement would be unacceptable. A **total** heave of approximately 15 mm shows no pavement distress.

5.0 CONSTRUCTION RISKS USING WET CLAYS

Design guidelines for the proposed embankment has been outlined, however this cannot be isolated from effects on construction. Common construction controls are density, and moisture content, with a lower characteristic density being part of the specification requirements for acceptance while, moisture content is used only as a guide to obtain MDD. However there is a need to use moisture content controls in expansive clays, with upper and lower control limits. Overcompaction of the material should be avoided and an RDD below 100 % targeted. This was at a specific site in the South East corner of Queensland. This may vary for the other climatic regions.

While the in-service conditions at this site indicates a 1.3 OMC condition, achievement of this compaction condition may provide difficulties. If the soil is too wet the pore water pressure is increased during compaction, and tends to keep the particles apart. Weaving results

with the compaction plant producing a soil wave as it moves across the fill. Thus weaving is usually a sign of excess moisture for the type of plant in operation and improper compaction would result. A lighter compactor or a reduction in moisture content will reduce or eliminate the weaving.

Farrar (1971)[23] examines the behaviour of wet fill in the laboratory and shows that for heavy clays (PI of 50%) that swelling occurs for compaction under 1.1 PL. Above 1.1 PL (and for low plasticity clays) settlement would generally occur. The magnitude of the settlement or swell being dependent on the height of the embankment. Farrar et. al (1975)[24] further examined the ability of plants operating on wet fill and indicates the most suitable plant for a given type of clay. Depending on the type of plant and % of fines, scrapers would have a "feasible" operation at 1.3 PL max.

6.0 CONCLUSIONS

Risk assessment for roadways can be quantified in terms of distress and tolerable movement. A procedure for the evaluation of the movements in expansive clay embankments is outlined. This was applied and based on the roadway performance, indicate the magnitude for differential movement is approximately :

10 mm - tolerable movement
20 mm - intolerable.

The vulnerability of embankments to expansive material behaviour is summarised in Figure 7. A case study of an expansive clay embankment was checked and, some of the findings at that site are :

1. The suction change profile for a flat surface varies for a roadway embankment. The active zone extends a bit further, possibly because of the side effects.

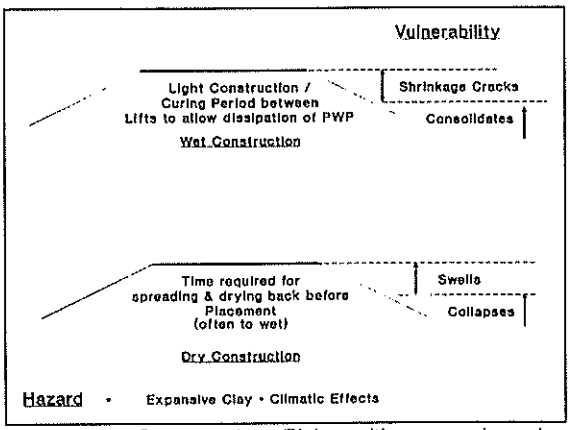

Figure 7 : Construction Risks with expansive clay embankments

2. The in-service moisture condition is approximately 1.3 times the OMC. This is at or above the Plastic Limit of this material.

3. The active zone represents the depth which should ideally be replaced by a higher quality material or deep stabilisation is required. However economic construction may limit this option. Construction using wet of optimum procedures and a reduced compaction density may be an alternative, with some soil stabilisation (surface lime treatment or geofabric) for a working platform.

4. Construction to 1.3 times OMC may provide practical construction difficulties. Curing periods and the use of light compaction plant would be advisable.

7.0 ACKNOWLEDGMENTS : The work described herein forms part of a research program on expansive clay embankments being carried out at the Materials and Geotechnical Services Branch, Queensland Department of Transport. The views expressed do not necessarily reflect those of the Department.

8.0 REFERENCES :

1. Ambraseys, N. (1984), Engineering Seismology Lecture Notes, Imperial College MSc course

2. Finn, F.N. & Monismith, C.L. (1984), "Asphalt Overlay Design Procedures", National Cooperative Highway Research Record No 116, Transportation Research Board, Dec.

3. OECD Report (1988), "Heavy trucks, climate and pavement damage", Road Transport Research

4. Snethen, D.(1979), "An evaluation of methodology for prediction and minimisation of detrimental volume change of expansive soils in highway subgrades : Vol 1" , Federal Highway Administration, Report No FHWA-RD-79-49

5. Queensland Department of Transport (1990), "Draft Specification of embankment material"

6. Richards, B.G. and Gordon, R.(1972), " Prediction and observation of a flexible pavement on an expansive clay subgrade", Proceedings, 3rd International Conf. on structural design of Asphalt pavements, London

7. Gordon, R. and Waters, T. (1984), "A case study of performance of pavements on an expansive soil subgrade", Fifth International Conference on Expansive Soils, Adelaide, South Australia.

8. Haupt, F.J. (1981), "Prediction of subgrade moisture conditions", Tenth International Conference of Soil Mechanics and Foundation Engineering, Vol 1, Stockholm

9. Livneh, M. and Ishai, I. (1975), "Prediction of CBR values under covered areas", 2nd ANZ conference on Geomechanics, Brisbane

10. Standards Australia (1986), "Residential Slabs and Footings", A.S. 2870

11. Standards Australia (1988), "Commentary - Residential Slabs and Footings", A.S. 2870 Supplement

12. Cameron, D.A. (1989), "Tests for Reactivity and prediction of ground movement", Civil Engineering Transactions, I.E. Aust, Vol CE31, No 3

13. O'Neil, M.W. and Poormoayed,N. (1980), "Meth-

odology for foundations on expansive clays", Journal of the Geotechnical Engineering, Proceedings of the American Society of Civil Engineers, Vol 106, No GT12, Dec.

14. Richards, B.G.(1967), "Moisture Flow and equilibria in unsaturated soils for shallow foundations", ASTM, Symposium on Permeability and capillarity ASTM, Spec. Publication 417

15. Kamplade, J. (1990) "Analysis of transverse unevenness with respect to traffic safety", Surface Characteristics of Roadways : International Research and Technologies, ASTM, STP 1031, W.E. Meyer and J. Reichert. Eds, American Society for Testing and Materials, Philadelphia

16. Croney, D.(1972), Proceedings of the 3rd International Conference on the Structural Design of asphalt Pavements

17. Queensland Department of Transport (1991), "Pavement Rehabilitation Manual", Pavements and assets Strategy Branch, Interim Edition

18. Lytton, R.(1973), "Expansive clay roughness in the highway design system", Vol 2 Proceedings of the Workshop on Expansive Clays

19. Jordan, P.G.(1984), " Measurement and assessment of unevenness on major roads", Transport and Road Research Laboratory Report 1125

20. Queensland Department of Transport (1991), "Design Conditions for the proposed Cooroy Bypass Embankment material", Report R1759, Materials and Geotechnical Services Branch

21. Look-Hong, B. and Reeves, I.,(1991), "Application of Time Domain Reflectivity in Geotechnical Instrumentation, Unpublished to date.

22. Look-Hong, B. and Reeves, I. (1991), "Development of Design details for expansive clay embankments based on in-service moisture conditions monitored with Time Domain Reflectometry Instrumentation", Unpublished to date.

23. Farrar, D.M.(1971), " A laboratory study of the use of wet fill in embankments", Road Research Laboratory LR 406

24. Farrar, D.M. and Darley, P. (1975), "The operation of earth moving plant on wet fill", Transportation and Road Research Laboratory Report 688

Seepage & Salinity Control for the Wurdee Boluc Reservoir Enlargement Project

P.J. O'FLAHERTY
M.Sc.(Eng.), M.I.E.Aust, C.P.Eng.
Gutteridge Haskins & Davey Pty Ltd
D. BARKLEY
B.E.(Eng.), M.I.E.Aust., A.W.W.I., C.P.Eng.
Geelong and District Water Board
E.G. TRUSCOTT
Ph.D., B.E.(Eng.), F.I.E.Aust, C.P.Eng.
Gutteridge Haskins and Davey Pty Ltd.

SUMMARY The Geelong and District Water Board operates the Wurdee Boluc Reservoir for purposes of domestic and industrial water supply. The Board is currently raising the reservoir by 4m to increase the capacity from 19 200 ML to 40 000 ML. Groundwater studies have shown that raised groundwater levels and associated salination could result from the enlargement. Computer models have been used to assess the problem and have identified a deep drainage trench supplemented by simple relief wells as the most effective method of seepage control. A sensitivity study indicated that large variations in the required length and depth of the drainage trench occurred depending on the foundation conditions assumed in design. Because the embankment is 8 km long it would have been very expensive to adopt a drainage system that provided an acceptable level of risk against downstream salination. However, as there would be a significant time between increase in reservoir level and spread of salination it was decided to adopt an observational approach to achieve an economic design for the system with minimal risk. An extensive groundwater monitoring system has been installed and field trials carried out. Seepage control measures based on a reasonable but not conservative assessment of ground conditions are now being installed. The changes in groundwater levels are being monitored as the reservoir level is raised and supplementary seepage control measures will be installed if required. This paper discusses the design, monitoring and implementation of the seepage control system.

1. INTRODUCTION

The City of Geelong is located about 70 kilometres south west of Melbourne and is Victoria's second largest city. The Geelong and District Water Board (GDWB) is responsible for collecting, storing and delivering water in the Geelong region supplying water to over 184,000 consumers.

Wurdee Boluc Reservoir is located 32 kilometres south west of Geelong and is owned and operated by GDWB. It is an off stream storage reservoir that provides seventy-five percent of Geelong's industrial and domestic water.

The GDWB has raised and extended the reservoir to increase the capacity from 19,200 ML to 40,000 ML. A general layout of the reservoir is shown on Figure 1. Groundwater studies have shown that raised groundwater levels and associated salination could result from the increased reservoir level.

Computer models have been used to assess the problem and have identified a deep drainage trench supplemented by simple relief wells as the most effective method of seepage control. However, design of an economic foolproof seepage control system prior to the reservoir raising is not possible because of the complex hydrogeology of the site.

An observational approach has therefore been adopted to achieve the most economical solution to the problem and limit the risk of salination. Seepage control measures have been based on a reasonable assessment of ground conditions and an extensive groundwater monitoring system has been installed. The changes in groundwater levels will be monitored during reservoir raising and supplementary seepage control measures installed if required. The relatively long period of filling will provide sufficient time for appropriate supplementary measures to be designed and installed should problems arise.

2. PROJECT DESCRIPTION

The reservoir was first developed as a water storage in 1927 by constructing earthen embankments around a natural depression. In 1955 the embankments were extended and raised to increase the capacity to 19,200 ML.

The GDWB recognised the need to provide additional water resources to meet the growing demand within the Geelong region and determined that the most economic alternative to augment the Board's supply was to increase the capacity of Wurdee Boluc reservoir by raising the existing embankments by 4 metres to a maximum height of 11 metres and extending the embankments to the north and south.

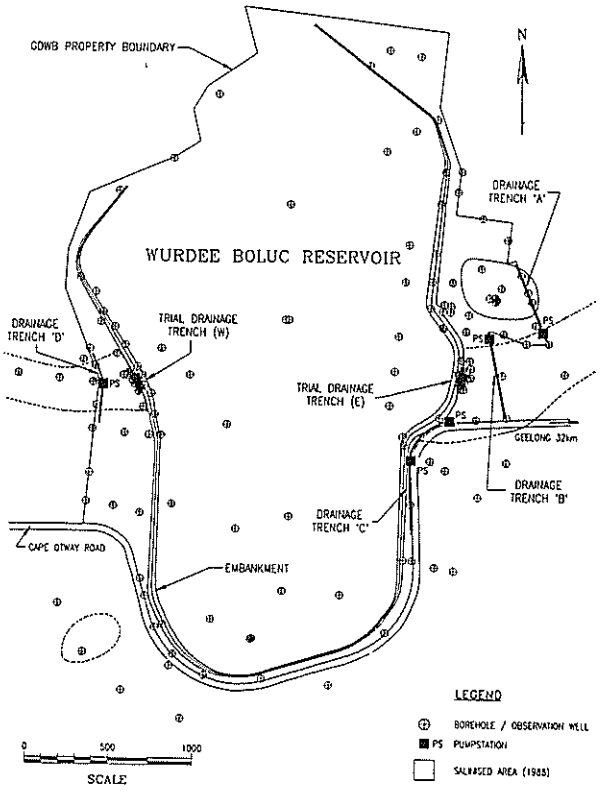

GENERAL LAYOUT
FIGURE 1

Over 800,000 cubic metres of fill for the 8.7 kilometre length embankment was obtained from five on site borrow pits. Where the embankment is over 4 metres in height a downstream toe filter and drain has been included. The upstream face has been

protected with geotextile, coarse filter and rip rap. Construction of the embankment was completed in May 1991 and filling of the reservoir commenced immediately.

3. GEOLOGY

The Wurdee Boluc Reservoir is located in a wide depression between the Barabool Hills to the north, the Otway ranges to the south and gently sloping valleys to the east and west. Prior to the reservoir construction the area formed a natural swamp or lake.

The regional geology of the site is described on the geological sheets for Anglesea and Geelong (Geological Survey of Victoria) and is summarised on Figure 2. The Demon's Bluff Formation which was deposited in a marine environment forms the basement at the site. Pliocene sediments overlie the Demon's Bluff Formation which in turn are overlain by a basalt flow north of the reservoir. The Bambra Fault separates the Pliocene sediments of the lake area from the Tertiary Eastern View Formation to the south. The basalt flow disrupted the drainage and led to the formation of Lake Wurdee Boluc. Subsequent phases of sedimentation have resulted in a complex sequence of sediments including lunette type, aeolian deposits on the eastern and western sides of the reservoir.

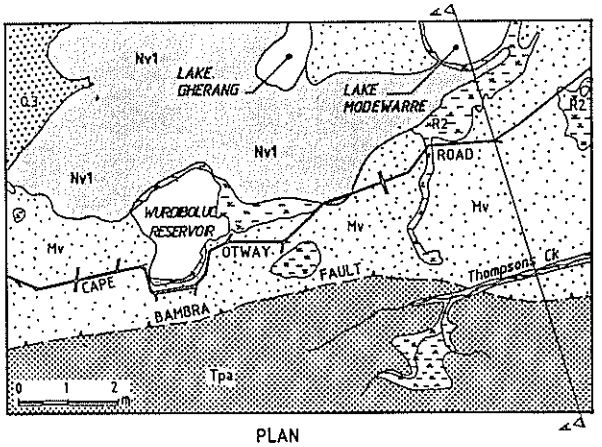

PLAN

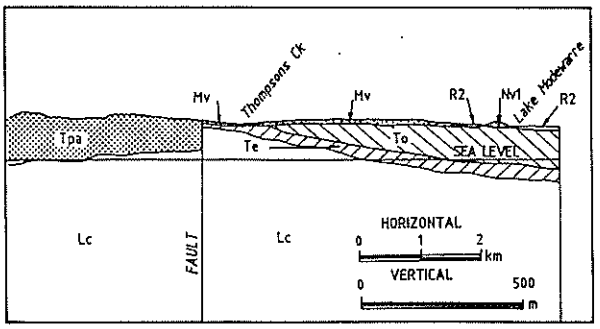

SECTION A-A

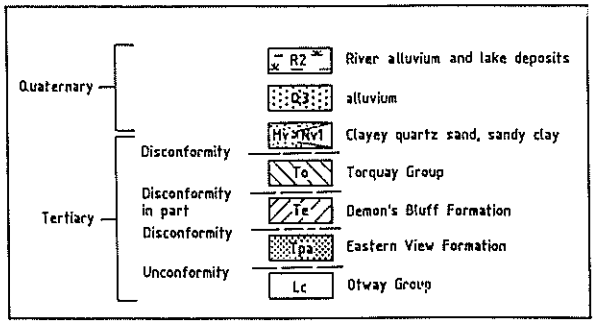

LEGEND

REGIONAL GEOLOGY
FIGURE 2

The Rural Water Commission of Victoria carried out geotechnical investigations in 1988 (RWC) and proposed a time based stratigraphic sequence for the sediments which is summarised in Table I. There is a general fall in the basement (Demon's Bluff Formation) towards the north-east indicating the direction of ancestral drainage. The Basal Sands are relatively thick and continuous throughout the site and form the main aquifer causing salinity. The Basal Clays and Basal Silts are confined to the south/east and west respectively. The Cover Clay unit is relatively thick and has continuity throughout the site.

The Upper Sands and Gravels occur largely as lunette type deposits on the eastern and western sides of the reservoir and form the topographic highs on which the embankments in these areas are constructed. These are overlain by a relatively continuous layer of Surface Clays. The geological model set up by the RWC was retained and used for predicting the hydrogeological behaviour of the complex physical system.

TABLE I
STRATIGRAPHIC SEQUENCE

NAME	USC	CLASSIFICATION	THICKNESS (m)
SURFACE SANDS	SP - SM	SAND-SILTY SAND	0.51 [0 - 3.5]
ORGANIC CLAYS	OI - CI	CLAY	0.68 [0 - 2]
SURFACE CLAYS	CI	SILTY CLAY	1.54 [0 - 4.3]
UPPER SANDS & GRAVELS	SW - SC	SAND-CLAYEY SAND	1.55 [0 - 4.3]
BASALT		BASALT	5.01 [0 - 9.1]
COVER CLAYS	CI - CH	SANDY CLAY	1.92 [0 - 4.5]
BASAL SANDS	SP - SC	SAND - CLAYEY SAND	3.53 [0 - 7.3]
BASAL SILTS	ML (SM - SC)	SANDY CLAYEY SILT	3.27 [0-7.0]
BASAL CLAYS	CL - CI	SILTY CLAY	1.45 [0 - 2.9]
Demon's Bluff Formation	ML	CLAYEY SILT	170+

4. HYDROGEOLOGY

The site has historically been subject to high water tables, and prior to construction of the reservoir, surface runoff and groundwater discharge led to the formation of Lake Wurdee Boluc. The depth to the groundwater table increases to the north and south of the reservoir as the topography rises, but to the east and west remains relatively close to the surface. The natural hydraulic gradient dips slightly to the north east. The hydraulic head from the reservoir is superimposed upon this regional trend.

The geological units identified as having relatively high seepage capacity are the Surface Sands, Upper Sands and Gravels, Basal Sands and Silts. Although these units are described as sands they generally have significant fines content (silt and clay) and in practice have low to medium permeability. The range of permeability from field and laboratory permeability tests is summarised in Figure 3.

In terms of seepage control the Surface Sands are generally shallow and seepage is easily controlled. The Upper Sands and Gravels occur as lunette type deposits which extend a relatively short distance beyond the eastern and western sides of the reservoir and are confined to the GDWB property.

P.J. O'FLAHERTY, D. BARKLEY, and E.G. TRUSCOTT

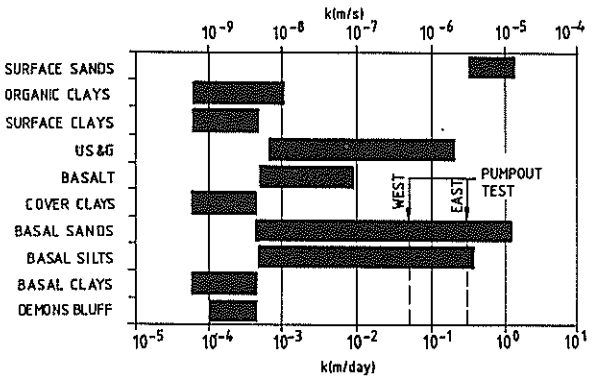

HYDRAULIC CONDUCTIVITIES OF THE GEOLOGICAL UNITS RANGE FROM LABORATORY AND FIELD TESTS

FIGURE 3

The Basal Sands and Silts form a continuous unit throughout the valley and therefore play a significant role in the regional groundwater environment. Seepage in the Basal Sands and Basal Silts is generally much more saline than in the Upper Sands and Gravels. These aquifers are generally overlain by clays which are relatively impervious and restrict seepage into and out of the more permeable units. The Demon's Bluff Formation has relatively low permeability and has been treated as an aquitard.

Salinity problems within this region are generally attributed to a rise in the naturally saline groundwater table as a result of tree clearing and planting of low water usage pastures. Within the study area, salination and waterlogging is apparent in low lying depressions, drainage lines and along the edge of basalt flows where surface seeps and capillary rise and evapotranspiration have resulted in an accumulation of salt near the surface. The salinised areas in close proximity to the reservoir are shown in Figure 1.

5. ALTERNATIVE SEEPAGE CONTROL MEASURES CONSIDERED

The raising of the reservoir level would result in an increase in piezometric level in both the Upper Sands and Gravels and Basal Sands downstream of the dam. As the Upper Sands and Gravels did not generally extend out of the Board's site the only concern with this strata was possible excessive exit gradients at the toe of the dam. However, increased groundwater levels in the Basal Sands stratum could result in an increase in salinised areas beyond the project limits.

A number of alternative measures were studied in order to ensure that this did not happen. The basic design criterion adopted was that the piezometric level in the Basal Sands should not exceed the higher of the piezometric level at the previous full supply level or 2.5 m below the ground surface (estimated as the depth below which the groundwater level did not affect salinity).

The three alternatives investigated were:

- do nothing
- provide a positive cut off through the aquifers
- provide drainage control through the Basal Sands by means of drainage trenches and wells.

These alternatives were investigated by carrying out 2 dimensional seepage studies using the computer programme PC-SEEP on typical transverse sections through the reservoir, extending well outside of the project area. A typical section from these studies is shown on Figure 4.

These studies showed, as expected, that there would be a relatively small increase in groundwater level in the Basal Sands (up to 1.2m) if no control works were undertaken. Hence this approach was only acceptable where the existing maximum groundwater level is well below the ground surface.

A slurry trench cut-off was selected as the most practical positive cut-off for modelling purposes. Assessment of such cut- offs both in the literature and from GHD experience on other jobs indicated that although a material permeability of 10^{-8}m/s could be achieved, the lowest permeability that could be expected for the slurry trench as a whole was 10^{-6} m/s. As shown on Figure 3 this is of higher permeability than the clays and of the same order of permeability as the Basal Silts and Sands. Hence, it was unlikely that the permeability difference between the slurry trench and Basal Silts and Sands would exceed an order of magnitude. As a result the effectiveness of the slurry trench on groundwater pressures is limited as shown on Figure 5.

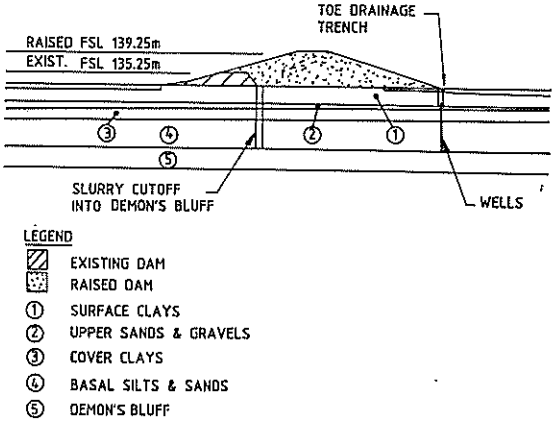

TYPICAL CONTROL MEASURES

FIGURE 4

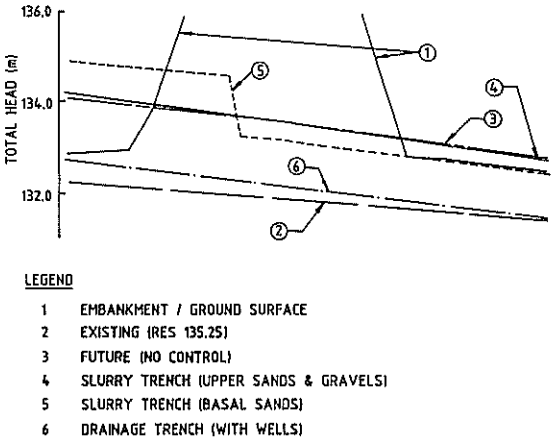

PREDICTED TOTAL HEAD IN BASAL SANDS

FIGURE 5

The effectiveness of the drainage measures depends on the depth of the trench/wells and drawdown. The results shown on Figure 5 assume full penetration of the Basal Silts and Sands and a drawdown to 4 m below the ground surface (ie. easily achieved in a drainage trench).

As can be seen the drainage alternative provides a much more effective control of groundwater levels in the Basal Silts and Sands outside of the project area than the slurry trench cut-off. It has the additional advantages that its effectiveness can be increased at any time by increasing the drawdown level and it is by far the cheaper alternative. Hence this method of groundwater level control was adopted.

6. OBSERVATIONAL METHOD

Having determined that downstream drainage was the most effective method of controlling groundwater levels it was necessary to determine the nature of the drainage system, the lateral extent of the drains and drawdown requirements.

It was decided that the practical depth limit for drainage trenches was 6 m, hence drainage beyond that depth would be achieved by relief wells. Analyses indicated well spacings of 20 m would be effective in controlling water levels.

Three dimensional seepage analyses were used to assess the effect of trenches of different lengths for a range of drawdown levels. The sensitivity of the analyses to aquifer geometry and permeability of the various strata was also checked. It was found difficult to accurately model the piezometric levels measured due, it is believed, to the large variability in the geometry and nature of the Basal Silts and Sands.

The large variation in analysis results meant that a large variety of designs were possible, with a correspondingly large range in costs. In order to avoid excessive costs it was decided to adopt the observational method approach to the design.

In this approach a reasonable design is adopted, the performance of the project is extensively and carefully monitored during reservoir impounding and suitable remedial works can be instituted should measurements indicate the need. This approach was well suited to Wurdee Boluc because an extensive foundation monitoring system was required in any event to demonstrate that groundwater levels were satisfactory.

Hence the design has been based on 6 m deep trenches excavated over the most likely length required. Where the trench does not intersect the Basal Silts and Sands wells are provided at 20 m centres with well starter pipes in between. Where the trench intersects but does not penetrate completely through the Basal Sands well starter pipes are installed at 10 m centres in the trench. The well pump controls in each trench can be adjusted to enable drawdown level to be varied. Piezometers have been installed throughout the site and beyond the site boundary. These piezometers are mainly located in the Basal Silts and Sands but also in higher strata to check exit gradients.

Thus during reservoir impounding the piezometer levels will be carefully monitored. Drawdown levels in the drainage trenches will be varied in order to achieve adequate control of external groundwater levels with minimum pumping of saline water from the trenches. Where it is not practical to control water levels in this way then additional relief wells will be installed. Finally, if piezometric levels in an area not controlled by the drainage trenches become higher than acceptable then either existing trenches can be extended or new trenches installed to control these levels.

7. FIELD TESTING

Preliminary analyses concluded that, because of the complex hydrogeological conditions on site, field trials would be of significant benefit.

Well pump out and recovery tests were carried out on both the eastern and western sides of the reservoir. The tests provided hydraulic properties for the Basal Sands and other relevant information.

Two trial trenches up to 6 metres deep, one of the eastern side and one on the western side of the reservoir were constructed as shown in Figures 6 and 7. Observation wells were installed in both trenches. Relief wells were constructed on the eastern trench for the second stage testing. Drainage pipes which drained to temporary pump stations were placed in the base of the trench and the trench was backfilled with a graded washed silica sand/gravel.

Four tests were carried out on the trenches and the results obtained, along with observations, provided information used to:

- calibrate the seepage model
- determine practical construction methods
- examine the effect on piezometric levels for various drawdown levels in the trench
- examine the effect on piezometric levels of the construction of relief wells
- determine
  - optimum trench depth
  - backfill material properties
  - drawdown levels
  - relief well spacings
  - pump rates
  - probable salinity levels.

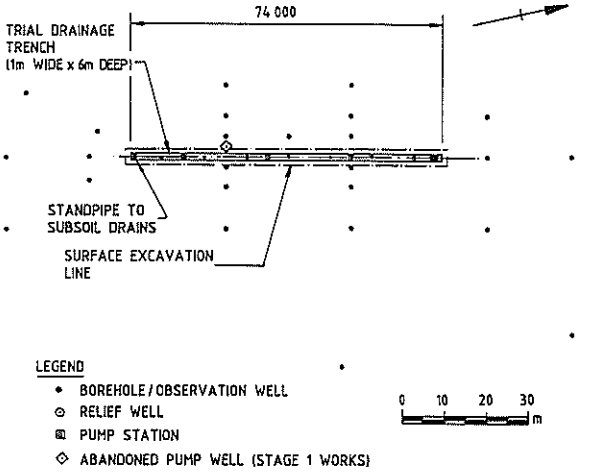

EASTERN TRIAL DRAINAGE TRENCH GENERAL LAYOUT.

FIGURE 6

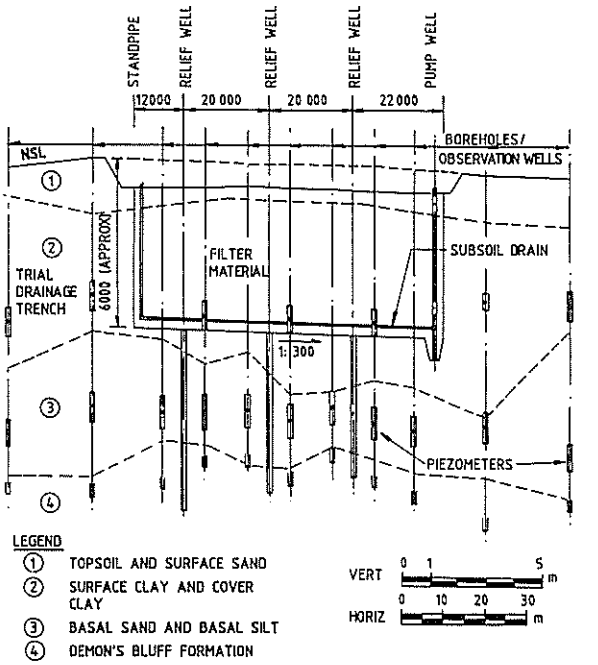

EASTERN TRIAL DRAINAGE TRENCH LONG SECTION

FIGURE 7

8. TRENCH DESIGN

The basic requirement for the seepage control system is to ensure that there is no increase in land salination outside of the Board's property as a direct result of the reservoir enlargement. Therefore the seepage control system has been designed to restrict increases in piezometric level which would otherwise occur as a result of the reservoir raising.

An evapotranspiration extinction depth of 2.5 m was selected for the site and the following criteria adopted for design of the seepage control system:

Piezometric level in Basal Sand for existing reservoir at full supply level*	Allowable increase in piezometric level in Basal Sand*
• Greater than 2.5 m below natural surface level	to within 2.5 m from natural surface level
• equal to or less than 2.5 m below natural surface level	Zero

*Applies to areas outside of the GDWB Property.

As discussed in Section 5.0 preliminary work had shown that increases in the groundwater table could be expected as a result of the reservoir raising and that a drainage trench was the most effective method of control. The design of the seepage control system has been based on analysis of piezometric level data, computer modelling applied with engineering judgement and assisted with field testing.

Two commercially available software packages were used for seepage analysis ie:

- PC SEEP a two dimensional finite element model which can handle both transient and steady state flow. The 'aerial plan' mode was used to model the reservoir effect/trench performance. This is limited in that flow between layers cannot be modelled. Recharge and evaporation can be approximated however for the actual model set up this was not possible because of the limitation on the available number of boundary conditions.

- MODFLOW a pseudo three dimensional difference groundwater flow model capable of simulating both transient and steady state flow. This programme has a modular structure with modules arranged grouped into packages to simulate specific features of the hydrologic system including flow between layers, areal recharge and evapo-transpiration.

The transient flow modelling showed that for the low permeability sediments and high groundwater table conditions at the site that vertical fluxes significantly affected pressure build-up away from the reservoir. This work confirmed that the reservoir enlargement would result in an increase in the potentiometric level beyond the property boundaries and that drainage trenches or relief wells constructed into the Basal Sand would be an effective way of controlling such increases.

Initially the trenches were located at the toe of the dam. However the seepage analyses showed that the trenches were more effective at the site boundary i.e. increased drawdown and reduced pumping rates.

The general layout adopted for the seepage control system is shown on Figure 1. As shown in Figure 8 this comprises a drainage trench approximately 6 m deep, with slotted drain pipes and backfilled with a medium to coarse sand. Simple relief wells at 20 m spacing are used to intercept the Basal Sand where this is below the base of the trench. Manholes are provided at 150 m spacing or less for maintenance. Seepage collected by the trench discharges into pumpstations which is then pumped to the reservoir. Even though the seepage rates are relatively small there is an effect on the reservoir water quality which needs to be carefully monitored.

9. TRENCH CONSTRUCTION

Construction of the seepage control trenches commenced in February 1991, and has been undertaken by the GDWB's own workforce.

Trench D was the first to be constructed. The 420 m long trench including pump station manholes and backfilling was completed within two months. The average trench depth was 6 metres with the Basal Sands being intersected along the entire trench length. Some instability and seepage occurred during construction, however, no major problems were experienced.

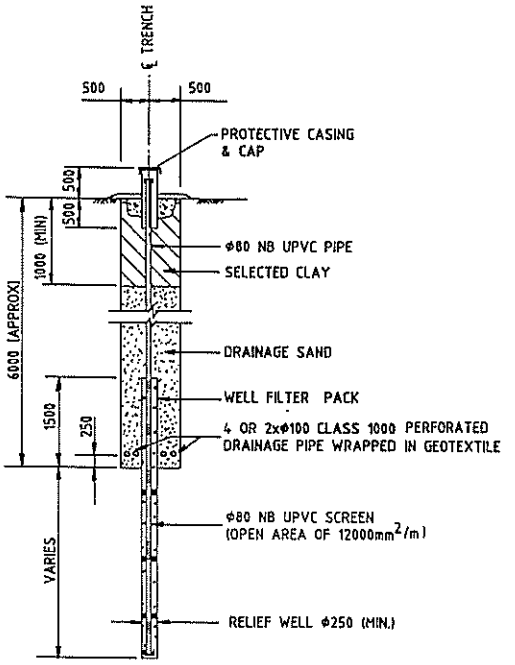

TYPICAL DRAINAGE TRENCH SECTION & RELIEF WELL

FIGURE 8

By August 1991, Trench B, 524 m long, and 400 m of Trench C had been constructed, all of which have intersected the Basal Sands. Again seepage rates were small and no major construction problems have been experienced. Based on seepage inflow measured during construction of trench B it is estimated that up to about 60m^3/day will be intercepted by the trench for the raised reservoir condition compared to 110m^3/day predicted in the design.

The trenches have been excavated with a Hitachi EX300 hydraulic excavator. Temporary trench support has been achieved with 3.5 m long steel trench shields. Temporary relief well casings have been installed at 10 metre intervals along Trenches B and C to aid the construction of relief wells through the trench if the wells are required.

Backfill sand has been supplied from a nearby quarry. The imported sand has been supplemented with Surface Sand obtained on site. As the Surface Sand is not as permeable as the imported sand it has been used sparingly. Compaction of the sand is achieved by flooding the trench. Because of difficulties experienced with compaction of the clay plug above the sand a variety of methods have been trialled with a compaction plate mounted on an excavator proving to be the most successful.

Flexible drain coil pipes wrapped in filter sock have been placed in the base of the trench to collect seepage water. Piezometers located near each trench are monitored daily during construction and significant drawdown has been noted in the piezometric level. Construction of all trenches is expected to be completed by the end of 1991.

10. ASSESSMENT DURING FIRST FILLING

Assessment during first filling will consist of two stages. The first stage includes filling of the reservoir to the pre-enlargement full supply level and holding the reservoir constant at this level until conditions stabilise. This stage will be used to establish relationships between the reservoir level and piezometric level and to establish a base set of data to be used to evaluate the long term performance of the seepage control system. During this stage the seepage control system will be kept out of operation. Monitoring will include routine measurement of piezometric levels, and pH and

salinity measurement of inflows and outflows from the reservoir and in selected piezometers.

Once the base set of data has been established the reservoir will be slowly raised to the new full supply level. During this stage the drainage trenches will be put into operation and testing will be carried out to assess performance and develop operational procedures for the seepage control system. The need for additional seepage control measures will also be determined.

11. LONG TERM MONITORING

It is possible that long term changes may occur to the groundwater regime which could result in increased groundwater levels outside of the project area. Hence piezometric levels will continue to be read in the long term.

These data will be assessed on an annual basis to check for any groundwater level changes and the consequences of such changes. If necessary the operation of the drainage system will be modified to maintain external groundwater levels to acceptable values.

12. CONCLUSIONS

The increased head developed due to raising of the Wurdee Boluc Reservoir will tend to increase the head in the Basal Sands aquifer that passes underneath the reservoir and beyond the limits of the project site. This increase in head would tend to increase the size of salinized areas outside of the project site which is not acceptable.

A comparative study of possible cut offs (slurry trench) and drainage control indicated that the most efficient and effective method of controlling groundwater pressures downstream of the reservoir was to install downstream drainage trenches supplemented by deeper relief wells where the aquifer is below the base of the trench.

A sensitivity study indicated that large variations in the required length and depth of the drainage trench occurred depending on the foundation conditions assumed in design. Because the embankment is 8 km long it would have been very expensive to adopt a drainage system that provided an acceptable level of risk against downstream salination. However, as there would be a significant time between increase in reservoir level and spread of salination it was decided to adopt an observational approach to achieve an economic design for the system with minimal risk. Hence a reasonable design has been selected and extensive monitoring piezometers installed. Detailed monitoring during initial and subsequent impounding will provide a check on the design and enable any supplementary drainage measures to be identified and designed.

REFERENCES

Geological Survey of Victoria, (1980) Australia 1:63 360 Series, Anglesea Sheet.

Rural Water Commission of Victoria (1988), Wurdee Boluc Reservoir Enlargement Project, (Vol II) Geological Investigations, Report for Geelong and District Water Board.

Seaview Marina, Geotechnical Design of Breakwaters

S.J. PALMER
M.I.P.E.N.Z.
Beca Carter Hollings & Ferner Ltd

1 INTRODUCTION

This paper describes the geotechnical investigation, design and construction monitoring of the breakwaters for the Seaview Marina, Wellington.

The breakwaters are of rubble mound type, 630 m in length and rise up to 8.5 m above seabed. They are founded on 14 m thickness of very soft and soft alluvial silts.

2 BACKGROUND

The Seaview Marina is located in the north east corner of Wellington Harbour (refer to Figure 1). The marina will provide 480 berths and 80 fore/aft moorings for pleasure craft. The site is exposed to waves from the south within the harbour and also from Cook Strait. Design wave heights of 2.5 m were predicted and thus breakwaters were required to protect craft moored in the marina.

Construction of the breakwaters commenced late in 1989 and they were substantially complete by April 1991.

3 GEOLOGY

Basement rock in the Wellington region comprises highly disected greywacke and argillite which has been eroded from a former peneplain and disrupted by faulting. The Seaview Marina is located at the foot of the Hutt Valley which is an alluvial filled valley extending north from Wellington Harbour and bounded on both sides by steep hills of the basement rock. (Refer to Figure 1).

In the lower Hutt Valley the alluvial deposits include a layer of relatively permeable sands and gravels overlain by silts and clays. The sands and gravels outcrop in the bed of the Hutt River part way up the valley and the overlying silts and clays provide confinement downstream resulting in the development of artesian pressures within the sands and gravels (Hutt Valley artesian aquifer).

At the marina site the Hutt Valley artesian aquifer is located approximately 14 m below sea bed level and has a piezometric head of approximately 2 m above mean sea level. The overlying aquiclude comprises soft and very soft silt which extends to the seabed level.

Wellington Harbour Board seabed sounding information dating from 1904 to 1985 indicates continuing deposition of silt. Some 2 m to 3 m of deposition occurred across the site from 1904 to the mid-1960's. This period related to the time of early land development projects within the Hutt River's catchment and the formation of the Seaview reclamations adjacent to the marina site during the 1950's. During the past 20 years further deposition has been minimal (less than 10 mm per year average).

The very soft nature of these recent alluvial deposits was a critical factor in the design of the breakwaters.

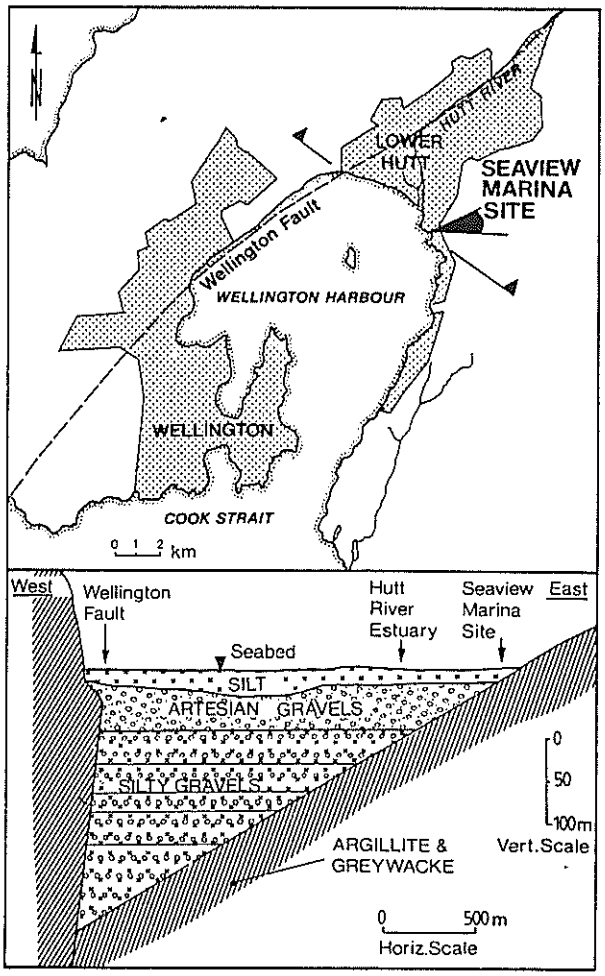

Figure 1: LOCALITY & GEOLOGICAL CROSS SECTION
(After Stevens 1974)

4 SITE INVESTIGATION

4.1 Previous Investigations

Information was available from a number of previous land based investigations and water bores undertaken to the north of the site in the Seaview industrial area, and from a marine based investigation undertaken in 1969 to the south and south west of the site for a wharf development.

Information from these previous investigations was reviewed and allowed the upper surface level of Hutt Valley aquifer to be approximately defined across the site.

4.2 Specific Invesitgations

A site investigation was formulated to investigate specifically the overlying soft alluvial silts. The investigation comprised four land based boreholes, nine marine based boreholes, marine based probing and seabed surface sampling.

Drilling was confined to the alluvial silt and stopped well short of the predicted aquifer level. Had it been anticipated to drill near or into the aquifer the controlling authority would have required special techniques including double casing to protect this valuable water resource.

A truck mounted rotary drilling rig was used for both marine and land based drilling. The marine based drilling platform comprised a 17 m by 6 m self propelled barge which was held over the drilling locations with four comer anchors.

With the help of unusually calm November weather the marine based work was successfully and efficiently completed.

Problems were encountered as a result of the casing sinking up to 1.5 m into the seabed under its own weight. This was resolved by welding an 800 mm square flange plate, 500 mm up from the bottom of the casing, to act as a foot.

Insitu testing and sampling included 75 mm insitu shear vane tests, Standard Penetration Tests and 100 mm diameter push tubes. Good recovery was achieved in the silts, however, some sample loss was experienced in interbedded silts and sands encountered closer to shore and at shallower depths. A piston sampler was employed in these materials and recoveries of 90% to 100% were achieved. The boreholes were advanced by washboring between the testing and sampling locations.

Laboratory testing of selected samples included classification tests, consolidation tests and triaxial compression tests.

4.3 Results of the Investigations

The soil profile along the majority of the breakwater length was found to comprise alluvial silt extending from seabed level to 20 m below mean sea level. Seabed level typically varied between 3 m and 6 m below mean sea level. Previous investigations had indicated that the silt was underlain by dense sandy gravels of the Hutt Valley aquifer.

The properties of the alluvial silt, as determined by the insitu and laboratory testing, are summarised by Table 1 and Figure 2. The silt may be described as soft and very soft, with some clay, and with a trace of shell fragments in parts. It is normally consolidated and of moderate to high plasticity. The upper portion of the layer was noted to include a minor fine sand

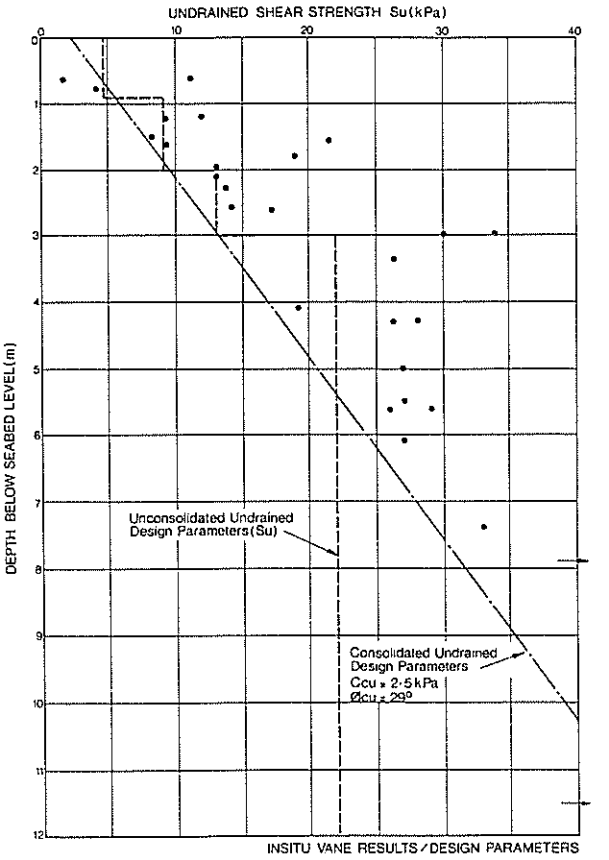

Figure 2 :UNDRAINED SHEAR STRENGTH

TABLE 1: ALLUVIAL SILT TEST RESULTS

Insitu Test Results	Average Laboratory Test Results					
Undrained Shear Strength "S_u" (kPa)	Atterberg Limits (%)	Natural Water Content (%)	Bulk Density (T/m^3)	Dry Density (T/m^3)	Triaxial Compression c' (kPa) Ø' (Deg)	Consolidation $\frac{Cc}{1+eo}$ C_v (m^2/yr)
S_u = 8-30 Refer Figure 2	LL = 67 PL = 38 PI = 29	55	1.60	1.05	C' = 0 Ø' = 37°	Normally Consolidated $\frac{Cc}{1+eo} = 0.18$ $C_v = 10$

content which reduced with depth. The fabric of extruded samples of the silt was studied. There was no evidence of sand beds or partings or other preferential paths for drainage.

Samples tested by triaxial compression were recovered from the upper part of the layer and had sand contents of approximately 20 %. The relatively high internal angles of friction ($\emptyset' = 37°$) recorded by these tests are attributed to this sand content. In general the silt was found to have only a trace of sand content and thus lower $\emptyset'$ values than those recorded above are expected.

5 DESIGN

5.1 Form of the Breakwater

The selected rubble mound form of breakwater (refer to Figure 3) comprises an embankment of low cost weathered greywacke rock fill obtained from local quarries. This core is protected from wave attack by two capping layers of sound rock boulders (armour rock). An intermediate filter layer (filter rock) is provided to avoid piping of the core.

Alternative forms of breakwaters (including floating units, pile screens and vertical seawalls) were discounted in the feasibility stages on technical and economic grounds.

5.2 Design Criteria

For any geotechnical design the aim of the design process is to establish a system that will reduce the risk of failure to an acceptably low value. This is normally done by ensuring that the design has factors of safety against various potential failure modes of greater than appropriate predetermined values.

In the case of the breakwater these risks are due to the possibility of encountering ground conditions weaker than those assumed in design , the risk of extreme environmental conditions (eg severe earthquakes) and due to the limitations of theoretical analysis.

A factor safety of 1.5 (Meyerhof, 1970) is the normal value adopted for long-term earth slopes where failure is not expected to pose a real hazard to human life. A conservative estimate of soil strength parameters is normally taken on the basis of investigation data.

In the short term (i.e. the temporary conditions of high pore pressures and consequently low strengths of the underlying soils that will arise during construction of the breakwater and for a period of months afterwards) a lower factor of safety of 1.3 is generally accepted.

These generally accepted minimum factors of safety of 1.5 for the long term case and 1.3 in the short term have been adopted as the criteria for the geotechnical design of the breakwater. Soil strength parameters based on the insitu shear vane results have been assumed as shown by Figure 2.

5.3 Soil Strength Parameters

5.3.1 Alluvial silts

The rates of displacement within the alluvial silt during a failure are expected to be such that significant pore pressure dissipation during any stability failure would be considered unlikely (Ladd,1991). Undrained conditions would be expected to prevail during a failure and thus undrained soil strength parameters should be applied in the stability analyses.

Three design cases were considered in the design. These design cases and the assumed soil strength parameters are discussed below.

(a) Short Term Unconsolidated Undrained Case

This design case relates to the conditions at the instant the load of the breakwater is imposed on the weak underlying soils, i.e. without dissipation of excess pore water pressures. Undrained soil strength parameters (S_u), as determined directly from the insitu shear vane tests, were assumed. Figure 2 shows the test results and the assumed design parameters.

A minimum factor of safety of 1.3 was the design criteria.

(b) Short Term Partially Consolidated Undrained Case

This design case relates to the conditions during construction and for a short period after. Ten percent of the excess pore water pressures induced by the weight of the breakwater were assumed to have dissipated immediately. This is considered to be a conservative estimate of the dissipation which will occur during construction. Partially consolidated undrained soil strength parameters (C_u) as determined by the relationship $C_u = C_{cu} + \sigma'_v \text{ Tan } \emptyset_{cu}$ were assumed. σ'_v is the effective overburden at the level of the potential failure surface following the partial consolidation. The consolidated undrained parameters C_{cu} and $\emptyset_{cu}$ were determined on the basis of the insitu shear vane results and the calculated effective

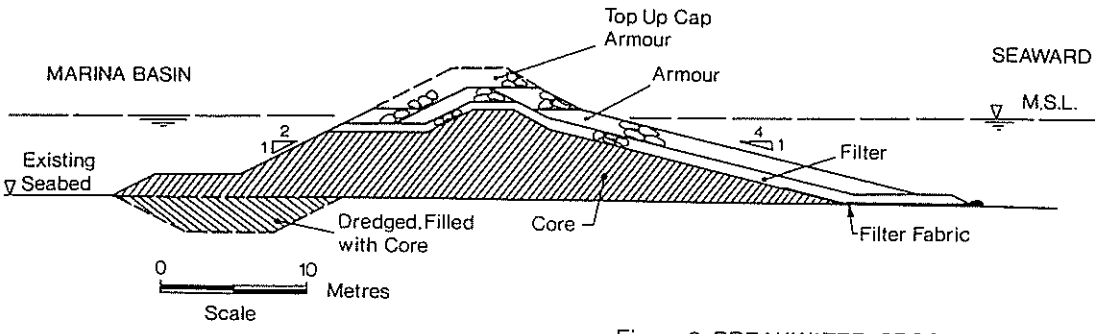

Figure 3: BREAKWATER CROSS SECTION

overburden at the level of each test. These design parameters are shown on Figure 2.

A minimum factor of safety of 1.3 was adopted.

(c) Long Term Consolidated Undrained Case

This design case relates to the conditions once dissipation of excess pore water pressures is virtually complete. These conditions were estimated to occur some two years after the completion of construction. The consolidated undrained design parameters were applied and a factor of safety of 1.5 or greater was considered acceptable.

The factor of safety requirement of 1.3 for the short term unconsolidated and partially consolidated undrained cases are somewhat conservative when compared to the actual situation resulting from construction. For the design, the breakwater is assumed to be constructed virtually instantaneously, whereas in reality construction work will take several weeks to complete any individual breakwater section.

5.3.2 Breakwater construction materials

The construction materials of filter and armour rock and to a lesser extent the core are free draining materials. Drained soil strength parameters of C' = O and $\emptyset' = 35°$ and effective stress analyses were assumed for these materials.

5.4 Stability Analysis

Analyses were carried out using the computer programme SLIPSYST which is based on the theory of Bishop's simplified method of slices. This programme has the facility to search for the critical circular failure surface. Figure 4 shows these critical failure surfaces with associated computed factors of safety for the selected breakwater profile and the design cases discussed above. These critical failure surfaces are discussed further in Section 5.7.

During analysis each profile was modified with the aim of producing an economic design while meeting the selected factor of safety requirements.

5.5 Options Considered

A variety of Breakwater profiles and construction technique options were investigated to determine the most satisfactory and cost effective solution.

Initially a profile comprising a simple continuous batter was considered. A batter slope of 1 vertical to 4 horizontal was found to meet the design criteria. Profiles with a single bench and locally steeper batter slopes were considered. The benched profiles offered reduced core volumes but the locally steep batter slopes required larger armour units to provide protection from wave attack. Due to the high cost of the armour, particularly for larger size units, and the relatively low cost of core, the overall cost of the benched profiles were estimated to be greater than that for the continuous batter.

The continuous 1 vertical to 4 horizontal batter slope offered an economic solution for the seaward batter. However, this profile was undesirable on the internal batter because it encroached on useable water space. Alternatives were considered with the aim of steepening the batter slope. Ground improvements in the form of vertical wick drains coupled with staged construction offered a feasible solution, as did geogrid reinforcement of the base of the breakwater. However the cost of these techniques proved to be prohibitive. A profile including a trench backfilled with core fill at the toe of a 1 vertical to 2 horizontal batter was then examined (refer to Figure 3). This profile offered a cost effective solution and was selected for the internal batter.

5.6 Consolidation Settlement

Settlement due to consolidation of the 14 m thick alluvial silt layer was calculated on the basis of the parameters determined by the site investigation and reported in Table 1.

These calculated consolidation settlements were 1.5 metres where the proposed breakwater is at its maximum height of 8.5 metres above seabed (mean water depth 6.5 metres) and 800 mm where the breakwater stands 5.0 metres above seabed (mean water depth 3.0 metres). Seventy percent of this consolidation was predicted to be complete within approximately 2 years.

To compensate for the consolidation settlements, it is proposed to provide a cap of further armour material on top of the breakwater 18 months to 2 years after its initial construction. This armour cap detail is shown on Figure 3.

5.7 Detailed Stability Analysis of the Selected Profile

Figure 4 shows the critical circular failure surfaces, as determined by application of the SLIPSYST computer programme for the selected breakwater profile.

For the initial construction case factors of safety of greater than 1.3 were calculated assuming the unconsolidated and partially consolidated undrained conditions.

At the time the top up cap of armour material is placed the excess pore water pressures generated in the silt by the loads imposed during initial construction have been assumed to have dissipated to a degree of 75 % (at the level of the critical failure surfaces). The placing of the cap can be expected to generate additional excess pore water pressures. Figure 4 (top up stage) indicates calculated factors of safety under this assumed excess pore water pressure, immediately following the placing of the top up cap. Undrained strengths expected with these partially consolidated conditions were assumed. It can be seen that factors of safety of 1.9 have been calculated.

In the long term the excess pore water pressures will dissipate increasing the factor of safety.

6 CONSTRUCTION

6.1 Construction Materials

Quarry strippings from the local quarries provided suitable low cost core rock comprising moderately to highly weathered, highly fractured Greywacke. These quarries were also able to supply filter rock to meet the quality and grading requirements. However a suitable local supply of armour rock was not found. The tectonic history of the Wellington region has left the local rock highly fractured making it difficult to supply the required 500 kg and 950 kg sound rock units. Consequently marble armour was obtained from Collingwood (north western corner of the South Island) and barged a distance of 200 km across Cook Strait.

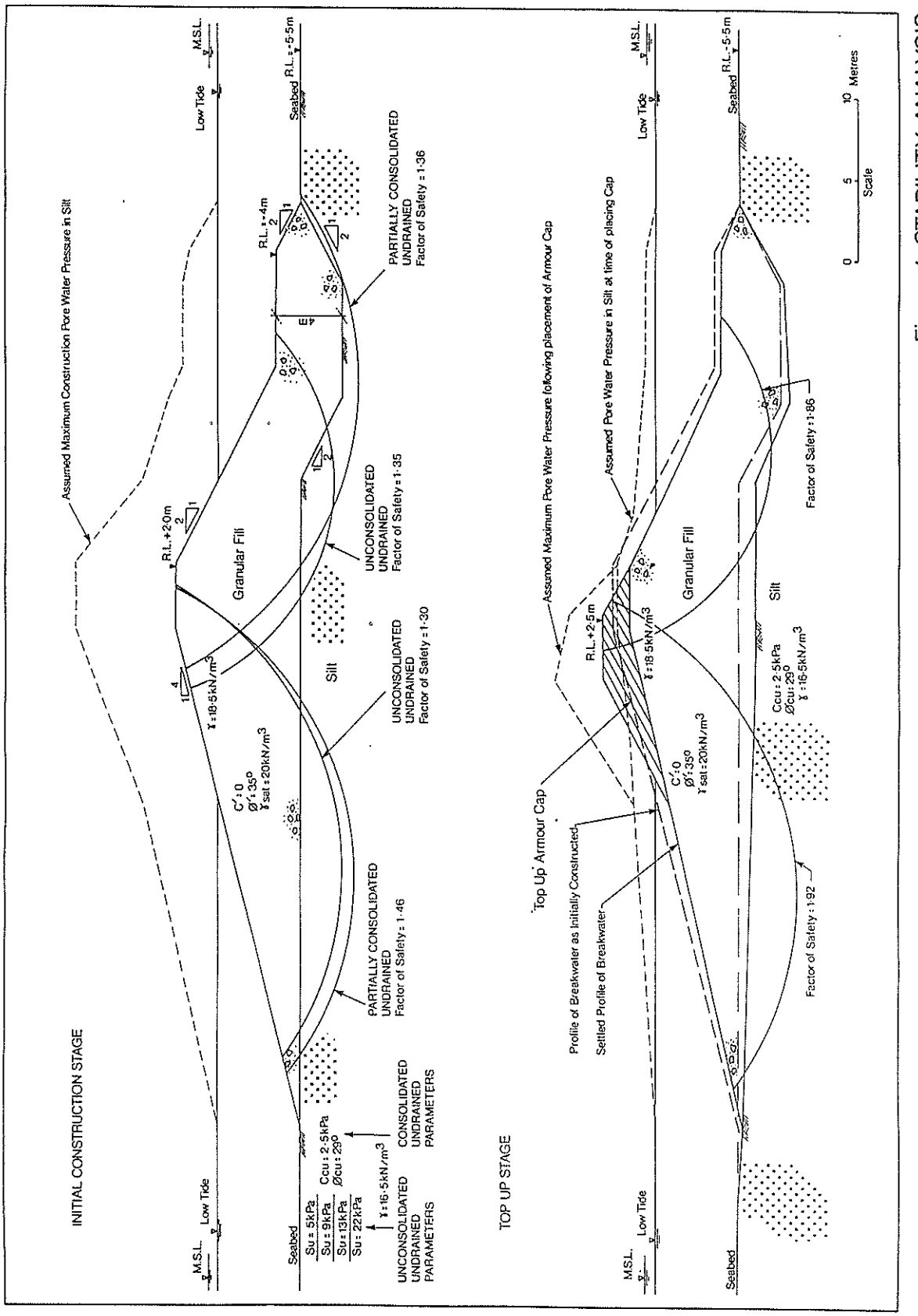

Figure 4 : STABILITY ANALYSIS

6.2 Construction Stability

The initial lift of core rock placement was limited to 1.5 m in height and subsequent lifts to 2 m in height to assure stable profiles during construction. This required marine based construction including bottom dumping barges.

6.3 Settlement and Pore Pressure Monitoring

Six settlement plates and pneumatic piezometers were installed along the length of the breakwaters. A settlement plate comprised a length of 100 mm diameter thick walled steel pipe with a 1.5 m x 1.5 m steel plate welded to the pipe 3 m from one end. The 3 m end of the pipe was pushed into the seabed until the steel plate was level with the surface. The other end of the pipe extended above water level and was monitored for changes in level during and after construction. The pneumatic piezometers were installed through the steel pipe down to a mid height level in the layer of alluvial silt.

The prime purpose of the monitoring was to provide information on the rate and amount of consolidation settlements. This information was required to confirm the appropriate time for placing the top up cap. Sufficient consolidation of the alluvial silt is required before the cap can be placed to ensure the stability of the breakwater during the top up construction work and to ensure that remaining settlements can be adequately predicted and the thickness of the cap can be set to provide a breakwater crest at the required level of 2 m above mean sea level after consolidation has occurred.

Consolidation settlement is following that predicted very closely both with respect to magnitude and rate (refer to Figure 5). Immediate settlements which occured in addition to the consolidation settlement have been deducted in the presentation of this data. The monitored pore pressures have been erratic.

The accurate prediction of the rate of consolidation settlement (and hence pore pressure dissipation) has provided confidence as to the stability of the embankments.

7 CONCLUSIONS

The recently constructed Seaview Marina breakwaters comprise rock fill embankments rising up to 8.5 m above seabed level founded on a 14 m thick layer of very soft and soft normally consolidated alluvial silt. The design of the breakwaters was based on traditional slip circle analyses and undrained soil strength parameters determined by insitu shear vane tests. Consolidation settlement of the breakwaters is closely following that predicted from one dimensional consolidation theory. Monitored staged construction was successfully applied.

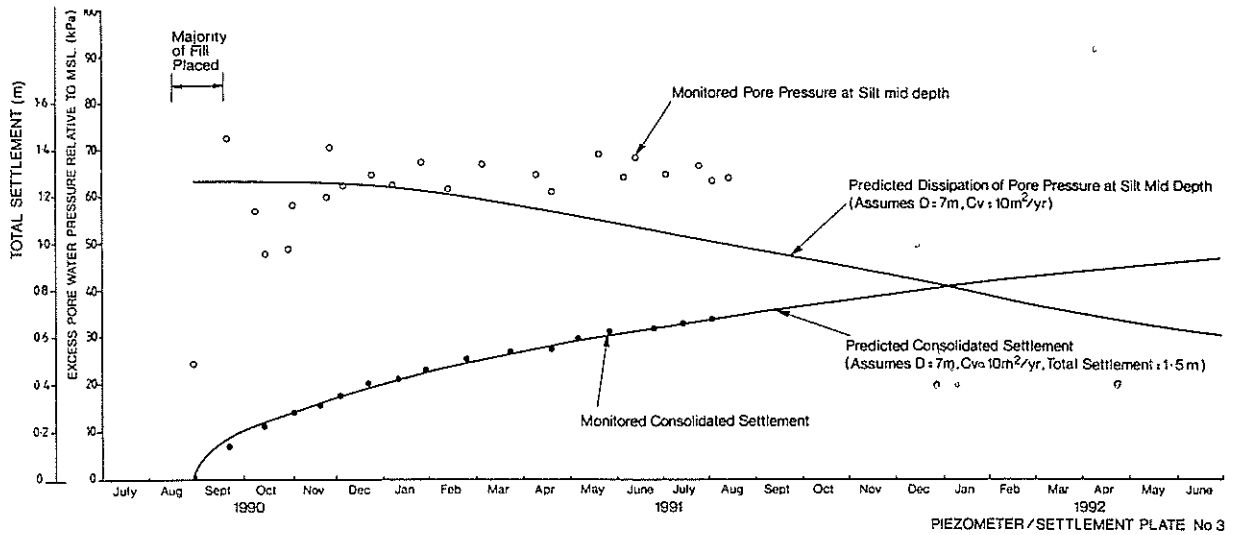

Figure 5: CONSOLIDATION SETTLEMENT & PORE PRESSURE MONITORING

ACKNOWLEDGEMENTS

The Seaview Marina project was initially undertaken by the Wellington Harbour Board. The Lower Hutt City Council took over the project after the Harbour Board was dissolved in 1989. The author acknowledges and thanks Lower Hutt City Council for approval to publish this paper.

Beca Carter Hollings & Ferner Ltd have been the principal consultants through all stages of planning, investigation, design and construction of the marina. Works Construction Ltd have been the main contractor for construction of the breakwaters and reclamation areas.

REFERENCES

BCHF Ltd 1989 "Site Investigation Report, Seaview Marina" Unpublished report.

BCHF Ltd 1989 "A Design Report, Stage 1 Breakwaters Seaview Marina" Unpublished report.

Ladd C 1991 "Stability Evaluation during Staged Construction" J of Geotech Eng. Vol 117, No.4 540-615.

Meyerhof G 1989 "Safety factors in Soil Mechanics" Canadian Geotech J Vol 7 No.4 349-355.

Stevens G 1974 "Rugged Landscape. The Geology of Central New Zealand". AU and AW Reed Ltd, Wellington.

Wroth C 1984 "The Interpretation of Insitu Soil Tests" Geotechnique 34 No.4 449-489.

Trial Loading of Failed Section of River Bank, Fisherman Island

C.P. THORNE
B.E., M.Eng.Sc., F.I.E.Aust.
Director, Coffey Partners International Pty Ltd

SUMMARY A trial loading of a failed section of river bank showed unexpected pore pressure responses. Back-calculation including allowance for end effects is described.

1. INTRODUCTION

The Fisherman Islands berths in Brisbane, Queensland are being developed with initial dredging to RL -12m, with provision for later dredging to RL -16m. The berths are located in an area of recent marine deposits, the surface of which has been raised by the placement of dredged sand. The sequence of soils at the site of Berth No. 3 is shown in Figure 1. The most critical soil unit for the design of the berths is the Unit 6 clay which is a soft to firm, slightly organic clay, with water contents in the order of 55 to 60%.

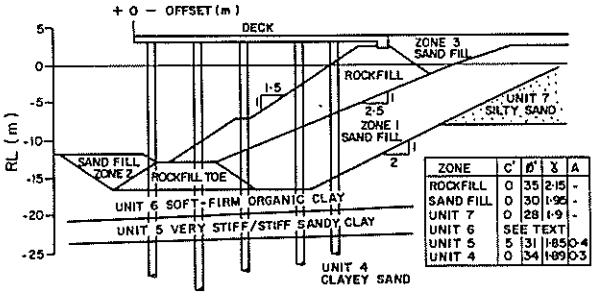

ZONE	c'	φ'	γ	A
ROCKFILL	0	35	2·15	-
SAND FILL	0	30	1·95	-
UNIT 7	0	28	1·9	-
UNIT 6	SEE TEXT			
UNIT 5	5	31	1·85	0·4
UNIT 4	0	34	1·89	0·3

Figure 1 Construction Zones and Soil Conditions

Construction of the wharf involved dredging the rear slope and toe trench (Figure 1), placing the rockfill toe, placing the zone 1 and 2 sandfill, trimming and dredging excess sand to expose the toe rockfill, placing the remaining rockfill and finally placing zone 3 sand. During this final stage a length of 170 metres of the bank failed overnight. The total width of the slide was 70m, the depth 15m and the total volume was 100,000 to 150,000 cubic metres.

Investigations showed that the rockfill toe had moved out about 4m, and that the sand and rockfill zones had slumped. A section through the centre of the slide area is shown in Figure 3.

2. INITIAL STUDIES

Central to any redesign was the remaining strength of the disturbed Unit 6 clays, which had been extensively sheared during the failure. Vane shear tests suggested an average sensitivity of 2.5, with undisturbed undrained shear strengths in the order of 44 kPa near the toe and 33 kPa near the backslope.

The results of effective strength testing are shown in Figure 2. The clay near the toe had, because of unloading by dredging, overconsolidation ratios in the order of 2.5 to 3 and hence reversing shearbox tests were undertaken to investigate whether residual strength behaviour might occur.

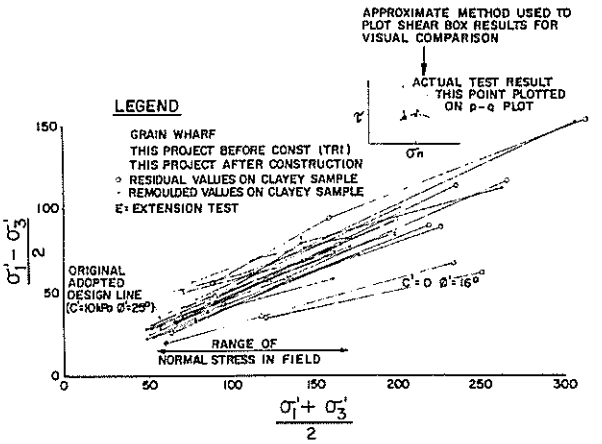

Figure 2 Summary of Effective Strength Results

Two samples did show a reduction in effective strength angle to around 16 degrees from 25 degrees in the undisturbed state. Other samples gave results more like the critical state strength estimated as c'=0, ϕ'=25 degrees.

The laboratory results therefore raised the possibility of a thin failure zone of clay with residual strengths. Initial analyses showed that if this was the case then remedial measures would be extensive, for example extending the deck 10 metres further offshore, 15 metres inshore and adding a row of 1200 diameter dowel piles. On the other hand if parameters closer to the critical state were proven, $A3m to $A4m could be saved.

A proposal was therefore put to the Port of Brisbane Authority for trial loading of the failed section to allow a more reliable assessment of the strength available and to provide information on pore pressure response. Such a trial clearly meant a risk of producing further failures but also held the promise of a substantial saving in the cost of remedial measures.

3. TRIAL LOADING LAYOUT AND INSTRUMENTATION

Figure 3 shows a cross section of the trial loading. An initial causeway was built out to the original crest line and a section of the original crest was rebuilt to allow placement of instrumentation and further sampling.

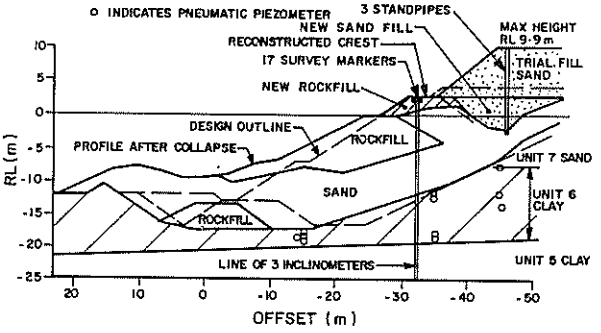

Figure 3 Cross Section of Trial Loading in Failed Area

Seventeen piezometers (there were also piezometers at offset -60m), three standpipes, seventeen survey points and three inclinometers were installed. Pneumatic piezometers with high air entry ceramic tips were used, each one being individually calibrated during installation. Prior to any additional loading, zero readings were taken at all instruments and these were tracked over several tidal cycles.

The fill was placed to roadway level over a 12 day period and subsequent filling was at 0.5m per day, with two or three day rests at RL 3, 5 and 7m. The maximum height of RL 9.9m was maintained for 19 days and sand fill was then removed to RL 3m in stages.

4. TIDAL EFFECTS AND ZERO READINGS

Initial piezometer readings showed that tidal effects were very significant. With only the causeway in place the response of the piezometers in Unit 6 clay had no time lag and varied from 0.7 times the tide range at offset -15m to 0.3 at offset -60m. It was inferred that the response was due to the increase in total stress induced by the weight of the water. Once the fill was extended to the full width the tidal response at offsets -35m and -45m became negligible but those at -15m and -30m were unaltered.

At offset -15m the overlying slope was always submerged and it would have been expected that there would have been a pore pressure response equal to the tide change, whereas it was only 0.7 of this. It was inferred that the most probable reasons for the muted response was that the total stress induced would tend to dissipate with depth because of the proximity of the shoreline and because as the tide fell there was an increase in shear stress in the clay because of reduced water support against slope failure. The increased shear stress resulted in an increase in pore pressure, partially offsetting the drop due to the reduction in direct water load.

All subsequent readings were corrected for tidal influence to a standard tide level of RL0.3m.

Figure 4 shows the initial pore pressures in Unit 6. A finite element analysis was made to estimate the increase in total stress due to the construction of the fill to the reconstructed crest level (RL2.8m). The pore pressure was then calculated assuming both Skempton's A and B were equal to 1.0. These predicted values were then subtracted from the observed values to give an estimate of the post failure pore pressures before the trial.

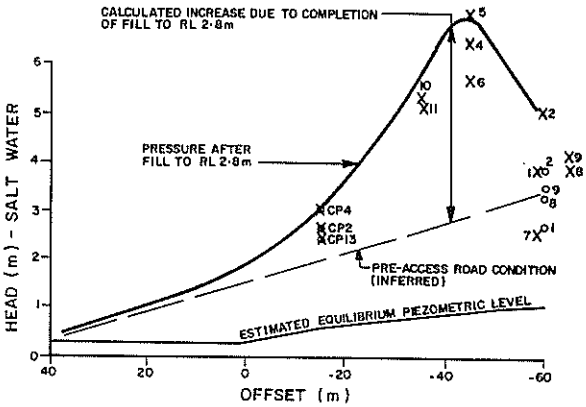

Figure 4 Initial Pore Pressures

5. PORE PRESSURES DURING LOADING AND UNLOADING

Figure 5 shows the increase in pore pressures in the Unit 6 clay as measured during trial fill placement, together with calculated pore pressure increases based on the results of a linear finite element analysis. The upper line represents the case where Skempton's A and B both equal one, in which instance the increase equals the increase in the major principal stress. The lower line represents undrained elastic conditions where B=1 and A=1/3, in which case the pore pressure increase equals the average increase in total stress, ie the bulk stress increase.

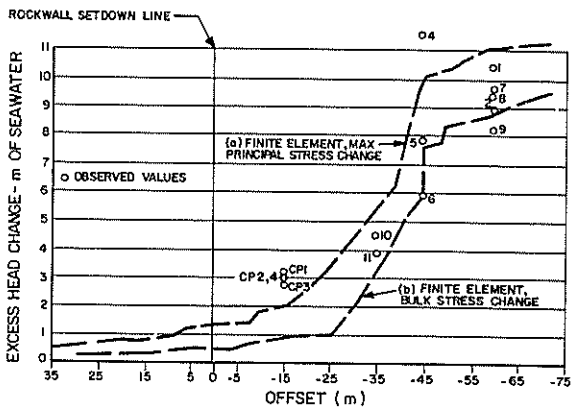

Figure 5 Pore Pressure Changes During Loading

The first represents an extreme response, yet it gives the best approximation to measured pressures, though it still underestimates the actual response at offset -45m. The probable reason for this is thought to be the result of stress concentrations at the interface. Due to numerical accuracy restrictions, the finite element analysis was not able to check magnitudes, though it did suggest that such concentrations would occur near the sand/clay interface.

At offset -15m, the rate of change of pore pressure with increasing fill height rose as the filling progressed. It is thought that yielding further back up the slope was throwing progressively more load onto the toe as the height was increased.

For the purposes of back calculation, "mode" values of pore pressure were used at each offset, joined by straight lines. For the immediate interface on the backslope higher values were adopted similar to that for piezometer 4 which was the only one definitely in that area. For offsets less than -15m the pore pressure was taken as the increase estimated from the finite element maximum principal stress increase plus the inferred initial condition prior to construction, plus an allowance for tide where this varied from RL 0.3m based on a response of 0.7 at -15m changing to 1.0 at offset 0m and beyond.

When the fill was removed, reductions in pore pressure were observed. Once again these were compared with the reductions in total stress predicted from finite element calculations. At offset -15m the reductions were approximately equal to the bulk stress change. However, further back in the slope they varied from about half to one times the bulk stress change. This was important because the remedial work involved redredging the slope and the extent of pore pressure reduction was an important determinant of slope stability.

6. MEASURED MOVEMENTS

Surface movements were measured both horizontally and vertically as loading progressed. In addition three inclinometers monitored horizontal movements in the fill and the underlying ground. The inclinometers confirmed that the main movements occurred in the soft Unit 6 clays just beneath the interface with the fill.

The horizontal surface movements and the horizontal deflection in the worst 0.5m of the inclinometer are shown in Figure 6. The vertical axis is the applied load in kPa above the initial roadway level of RL 2.8m. Horizontal creep was less than 0.3mm per day up to RL 5m (38.9 kPa) but increased to 2.2mm/day at RL 9.9m (115 kPa).

It was important to increase the loading as much as possible without actually producing a catastrophic failure. In judging the maximum height of RL 9.9m, consideration was given to the creep rate, the shape of the movement versus loading curves and the pore pressure response.

7. BACKANALYSIS

The trial was necessarily of limited length and hence some correction for end effects was clearly necessary. Figure 7 shows a long section through the trial fill: at the final height the crest length was about 50 metres (about a third of the original slide length) as compared with a thickness of 15 metres and a transverse width from offshore to inshore of almost 100 metres.

From the slide dimensions the increase in factor of safety due to end effects estimated from the curve in Baligh (1) was 9 to 11%. This is for a uniform material whereas at the trial the end effects involved shearing through rockfill and sand considerably stronger than the Unit 6 clay which formed the bulk of the slide plane.

Further estimates of the restraint were made by assuming shearing on a vertical plane normal to the crest and calculating the resistance on the side of a cylindrical slip as the tangent of the friction angle times the normal stress acting on the ends. Two estimates of the normal stress were made, one being the active pressure and the other from the zero lateral strain finite element analysis. These were applied as restoring moments over a cylindrical segment the same length as the crest for that loading stage. This procedure gave factor of safety increases due to end effects of 13.5% and 15% respectively. The latter method was adopted for backanalysis.

Using this method the mobilised Unit 6 clay strength was c'=0, ϕ' = 21.5 degrees using effective stress. The trial did not actually produce failure and hence the clay is stronger than this. Estimates were made by extrapolation of the load deflection curves and by comparing stress/strain curves to failure from shearbox tests with the observations in the inclinometers. From these it was estimated that the peak strength was about c'=0kPa and ϕ'= 25 degrees.

The load deflection curves all show a marked yield at about 60kPa(RL 6.5m). This is thought to be the onset of local yield, which from the literature would correspond to a true factor of safety of about 1.7 which is also the value obtained for RL 6.5m using the peak parameters given above.

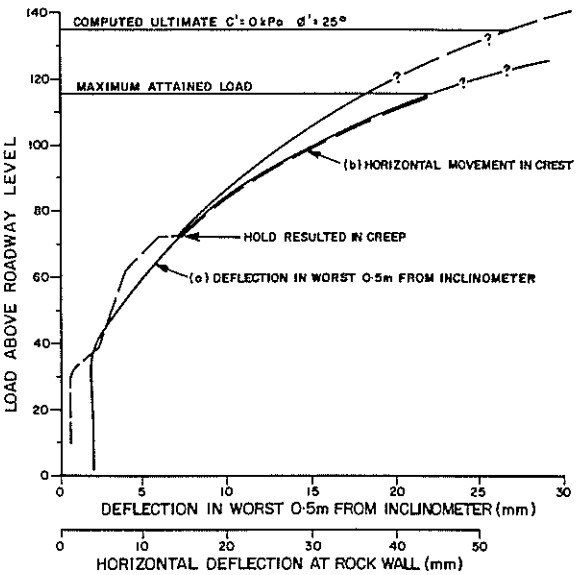

Figure 6 Deflections During Trial Construction

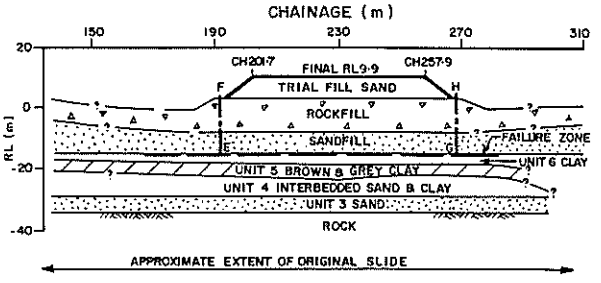

Figure 7 Long Section Through the Trial

8. CONCLUSIONS

The selection of a design factor of safety for stability analyses depends on an assessment of the reliability of the shear strength parameters; uncertainty regarding loading conditions; uncertainty regarding pore pressures; approximations in stability analysis methods; three dimensional effects; and constraints on settlements and lateral movements.

Two alternatives were used in stability analyses associated with further design work.

The first was to adopt peak shear strength parameters in conjunction with conventional factors of safety. The second was to use maximum mobilised shear strength calculated from the trial loading in conjunction with a reduced safety factor which could be justified on the basis that the mobilised strengths were definitely available. Both approaches gave similar results.

Pore pressure data from the trial was used to predict future pore pressure response during loading and unloading associated with reconstruction of the facility. The trial showed that pore pressure reduction associated with unloading was much less than calculated using standard soil mechanics methods. These standard methods proved to be non-conservative.

By accepting the risk of loading an already failed slope and taking the trial close to failure, it was possible to calculate accurate values of mobilised effective stress parameters at a low safety factor. The confidence associated with these parameters allowed the design of economical remedial measures.

9. ACKNOWLEDGMENTS

The project was undertaken as a joint study between Coffey & Partners Pty. Ltd. and the Port of Brisbane Authority. Reading and operation of the instrumentation and construction of the fill was undertaken by the Port of Brisbane Authority.

Permission of the Port of Brisbane Authority to publish this paper is acknowledged.

10. REFERENCES

1. Baligh and Azzouz (1975) "End effects on stability of cohesive slopes" Jnl Geotech Divn ASCE Nov, Vol 101 GT11, pp 1105-1118

General Report: Technical Session 2 – Foundations & Retaining Walls

T.J.E. SINCLAIR
M.A., M.Sc., D.I.C., C.Eng., M.I.C.E., M.I.P.E.N.Z.
Principal, Tonkin & Taylor Ltd, Auckland

1. INTRODUCTION

The intention of this session is to cover the engineering risk associated with foundations and retaining walls. The papers submitted, however, represent a very narrow view of the overall subject and it is perhaps questionable whether they relate to the issues of greatest risk. Is it not self evident that piled structures carry less risk than those founded on shallow footings or that the commonest "failure" of engineering structures is that of retaining walls? Yet this session has 70 percent of the content devoted to piles and nothing to retaining walls.

These questions and statements are spurious and are merely intended to provoke discussion. As suggested in the guidelines to authors, all aspects of geomechanics relate to "risk" of some sort and hence the theme of the conference must be interpreted broadly. The purpose of this report is to highlight the principal points of interest of each paper in the hope that this will stimulate interested parties to read on for more information.

2. GENERAL

The papers assigned to this session fall into the following broad categories:

- Piles:
  - Axial capacity : 4 papers
  - Lateral capacity : 4 papers
  - Practical aspects : 1 paper
- Raft Foundations : 3 papers
- Small footings : 1 paper

Almost all of these are concerned with research projects; only one paper being authored by a designer outside of the research establishments. However, most of the papers are relevant to either design or construction practice despite the content varying widely from mathematical analyses to practical techniques and case histories.

In the following sections, the reporter comments on each paper of this session, always from the perspective of a design engineer.

3. REVIEW OF SESSION PAPERS ON DEEP FOUNDATIONS

3.1 Class A Predictions of Pile Behaviour

Poulos presents here an interesting comparison of predicted pile performance against actual measured performance. He elected to use "... one of the simplest and least sophisticated approaches ..." for the capacity prediction; that of correlating skin friction and end bearing resistance to CPT cone resistance. For the prediction of load-settlement behaviour a boundary element analysis was employed but the input parameters were still based on correlations with CPT data and "... the author's limited experience ...".

The methods themselves are worthy of note, particularly the rationale for the selection of the empirical factors. However, the main points of general interest are well summarised in the papers conclusions, namely:

- Despite relatively favourable circumstances, Class A predictions were "fair only".
- The methods used for prediction are of less significance than the assessment of the parameters.

More specific points of interest may be highlighted as follows:

(a) The pile load distributions (Figures 4 & 5 of the paper) give some clue as to where the predictions may be most in error. However, the reporter believes that this may be one of those occasions where a dimensional plot would be of more value than the normalised plots given, particularly where the measured load differs markedly from the predicted. For example the load distribution for the cased pier would be as shown in Figure 1. If it weren't for the complication of diameter change, the unit skin friction would be proportional to the slopes of these lines. It can be seen that prediction of unit skin friction is reasonable except in the near surface sand above the water table. This also applies to the "slurry pier" to some lesser extent but, for the driven piles, the average unit skin friction has been predicted very closely in soil mechanics terms.

We learn from this, that we should predict higher long term unit skin frictions for the bored piles in non-saturated sand.

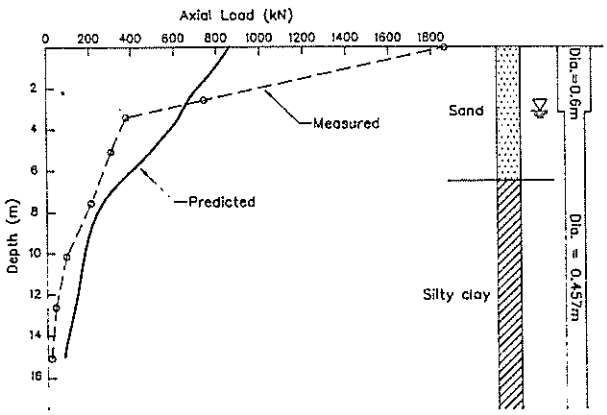

Figure 1: Predicted and measured load distributions for cased pier

(b) The influence of time effects was quite different to that expected by the author. He had expected more benefit from the driven piles and none at all for the bored piles. Table 1 presents the data in terms of proportion of long term load. It will be seen that the time effects are very similar for all piles. This would imply that it is not pore pressure controlling the time effects.

TABLE 1
SUMMARY OF TIME EFFECTS

Pile	Proportion of long tern capacity		
	2 weeks	4 weeks	43 weeks
H-Pile	0.78	0.84	1.0
Pipe	0.61	0.70	1.0
Slurry Pier	0.63	0.82	1.0
Cased Pier	0.61	0.85	1.0
Average	0.66	0.80	1.0

In the light of point (a) above, it would be interesting to know if it were the unsaturated sand which provided the primary influence on the time effects.

(c) Despite the wide range of predicted capacities from the other participants, it would appear that the standard design factor of safety of 3 would rarely result in actual factors of safety being less than 1.8 and would more likely be unnecessarily conservative (and expensive) with actual factors of safety in the 5 to 10 range. Table 2 summarises the actual factors of safety which would result in a real world design situation based on the predictions of the other participants.

TABLE 2
SUMMARY OF ACTUAL FACTORS OF SAFETY

Pile	Most conservative design		Least conservative	
	Predicted allowable load with F=3	Actual factor of safety	Predicted allowable load with F=3	Actual factor of safety
H-Pile	203	5.0	557	1.8
Pipe	187	5.5	550	1.9
Slurry pier	192	9.6	753	2.4
Cased pier	193	9.6	443	4.2

It would appear that the designers of pile foundations could afford to be more adventurous in general.

3.2 The analysis of ancillary loaded piles in layers or non-homogeneous soils

Small and Lee have introduced the "finite layer" method as a means of computing vertical displacements of piles. Despite some confusion with notation, it appears to be a useful addition to the growing list of available numerical methods. This is particularly so because it is intended for use in layered soils or soils with increasing stiffness with depth; circumstances which tend to represent the real would better than the homogeneous elastic half-space.

It is interesting to test some of the results in relation to a typical practical design situation. Take, for example, conditions similar to those described in the previous paper (Poulos, 1992) and assume:

- Axial load = 500 kN
- Sand stiffness = 2 x clay stiffness = 60 MPa
- Pile is concrete with stiffness = 1000 x clay stiffness = 30 GPa
- Depth of sand = 6 m
- length of pile = 15 m

Using Figure 4 of the paper, a settlement of less than 2 mm is predicted and this is compatible with the observed load-displacement curves (see Figures 2 and 3 of Poulos, 1992). However, bearing in mind that it would normally be considered a little adventurous to terminate a pile in clay of shear strength of (say) 60 kPa, the questions must be asked:

- Is settlement an issue with pile foundations?
- Are numerical methods of any real value?

In the reporter's experience, any structure which may be that sensitive to settlement is likely to have piles founded in much stiffer materials than assumed for the example and, though working loads may be considerably greater, measured settlements have rarely been more than about 5 mm at working loads.

3.3 Identification of failure mechanisms in soft rock using stereo-photogrammetry

The title of this paper by Choi & Johnston succinctly describes the content. The problem of bearing capacity in weak rock has taxed both researchers and designers for some time. Current design methods either derive from soil mechanics theory or are based on empirical relationships between capacity and uniaxial compressive strength. The work described in the paper appears to offer a means of starting again from first principles, namely the identification of failure mechanisms in a brittle, crushable material.

The paper concentrates on methodology. We should look forward to seeing the results of a developed research programme.

3.4 Analytical predictions for side resistance of piles in rock

The work for this paper by Kodikara, Johnston and Haberfield clearly complements that of the previous paper (Choi & Johnston, 1992). The paper presents a rational "model" for adhesion in weak rock which, rather than relating simply to uniaxial compressive strength, uses other normalised parameters such as the ratio of modulus to strength (E/q_u) and the ratio of strength to confining stress (q_u/σ_{no}). The simplified design charts for Melbourne mudstone based on this model appear to give good results compared with previous work (Williams et al., 1980) except with low strength materials (q_u < 1 MPa). At these low strengths, the model predicts "adhesion factors" (α) less than 0.5 and yet Williams et al. (1980). present data with α in the range 0.5 to 1.0 for both Melbourne mudstone and "other rocks".

At this point it is worth noting that this rock mechanics "adhesion factor", which relates side shear resistance to uniaxial compression strength, is not the same adhesion factor of soil mechanics which relates side shear resistance to shear strength (e.g. Tomlinson, 1977). There is a factor of two here, despite use of the same symbol (α). This is the cue, perhaps, for a point for discussion. When dealing with transition materials such as strong soils/weak rocks, the separate theories, constitutive models, notation and terminology must all be compatible.

In this respect, the Melbourne mudstone model appears more realistic than the data of Williams et al. (1980) because it predicts lower adhesion factors, more compatible with values

of stiff clay. Figure 2 reproduces Figure 6 of Kodikara et al.(1992) with some values proposed by Tomlinson (1977) for bored piles in stiff clays superimposed. Discussion on why there should be discontinuity in the trends would be of interest.

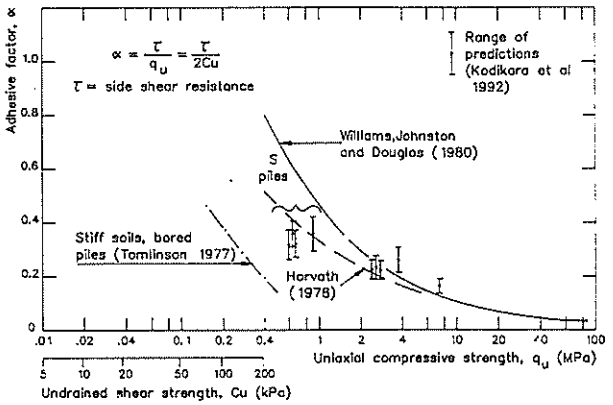

Figure 2: Examples of adhesion factors at soil/rock transition

It is not clear from the paper what makes the model specific to the Melbourne Mudstone. Can the simple design charts be used for other weak rocks?

3.5 Piled bridge abutments on soft clay - experimental data and simple design methods

Stewart, Jewell and Randolf present a clear and useful review of current methods of assessing lateral loads on bridge abutment piles due to embankment loadings. They point out that these tend to be inconsistent and go on to describe a new approach based on centrifuge tests. Results of the new method are promising but the authors readily concede that development must continue.

It is hoped that further research will consider the effects on raked piles, the positions of the piles in relation to the embankment and the effects of downdrag. The latter may contribute far more to bending moments in raked piles than the lateral movement of soil.

3.6 Behaviour of fixed and free head piles in a laterally sliding soil

Hull, Lee and Poulos look at essentially the same problem as the previous paper (Stewart et al., 1992) using a numerical soil-structure interaction method. Their findings are well summarised in the paper's conclusions. The method provides useful in-sight into the behaviour of piles of various stiffness and degree of head fixity in response to laterally sliding soil of various slide depths. The examples use realistic pile sizes so that results could be useful for real problems. However, as the authors point out, the very large predicted displacements (in terms of tens of metres) cast doubt on the validity of using a small displacement formulation.

It appears that the main point of the research work is to determine design procedures for piles used as landslide stabilising measures. The reporter has had this problem on many occasions and welcomes this contribution. However, having come up with a cost effective design with reasonable pile sizes spaced at realistic intervals, the problem invariably degenerates to something more fundamental. The question is asked : What happens downslope of the piles? If this portion of the slip mass continues to slide away, the line of piles then becomes a retaining wall and must now be designed for the internal active forces from the upslope soil mass. These may well be greater than forces calculated for the intact slide because the fixity conditions have changed.

3.7 Lateral soil movement loading on bridge foundation piles

The third paper on the same subject by Hull and McDonald describes a case history of an actual failure and its back analysis. The analysis involved making an assessment of soil movements and then using a computer program (PALLAS) with a long established soil model (Poulos 1973) to analyse the response of the pile. The main point of interest was that the 350 mm square section piles driven through a 10 m layer of soft clay tend to move with the soil; significant relative displacement only occurring in the very soft soil near ground surface.

.

3.8 Sensitivity analysis of laterally loaded piles

Budkowska and Szymczak present a theoretical paper concerned with determining the effects on computed values (e.g. displacements and bending movements) in a lateral pile analysis due to small changes in the design variables. The authors conclude that "... approximation of the changes of the displacements of the pile by means of their first variations is good even for 20 percent change of the design variable".

A reader not familiar with the method adopted ("adjoint method") and some of the notation, may find this paper difficult to follow.

3.9 Risk associated with construction of large diameter bored piles in cavernous marble

In contrast to the preceding paper, this paper by Li is a practical discourse on construction techniques. The risks discussed are those associated with construction rather than permanent risk relating to the finished product. The paper is essential reading for all parties involved in a project of a similar nature.

4. REVIEW OF SESSION PAPERS ON SHALLOW FOUNDATIONS

4.1 An analysis of rectangular rafts of finite flexibility subjected to concentrated loads

Zhang and Small introduce again the finite layer method (see Small and Lee, 1992 - section 3.2 above), this time for analysis of rafts. The method still requires a computer but the formulation is supposed to be comparatively simple in relation to other numerical models such as finite element or finite difference soil-structure interaction codes. This is particularly desirable for analysis of rafts as 3-dimensional effects are significant.

The author's point out that spring models are still widely used for the analysis of rafts. This is certainly true in New Zealand. Yet it has been shown quite convincingly (Hemsley, 1987) that there are serious differences between results of analyses for spring or continuum models. Figures 3 and 4 are reproduced from Hemsley (1987); the former showing that predicted bending moments for the spring model can be as much as 5 times that for the continuum model and the latter showing that the sense of the bending moments can be exactly opposite for the two models. In other words, not only would a design based on a spring model be unnecessarily expensive, but the main reinforcement may be in the wrong place.

But even the elastic continuum model can be significantly in error. It predicts in some circumstances, infinite contact pressures. Clearly, real soil would yield with consequent redistribution of stresses, bending movements and displacements. It is certainly time more attention is given to rigorous analysis of rafts. The paper by Zhang and Small goes some way in the right direction but the method still relies on "elastic" soil. What are needed, of course, are more case histories and instrumentation/monitoring data.

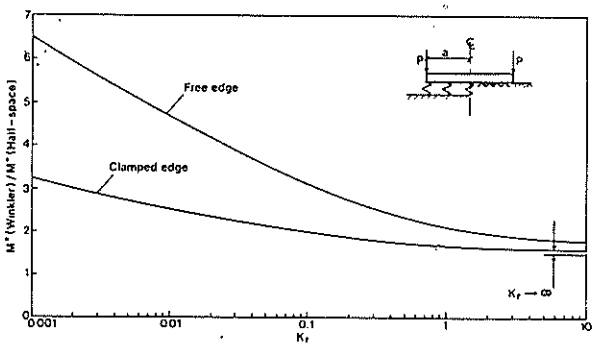

Figure 3: Ratio of maximum bending moments for edge loaded circular raft on spring or half-space foundation (After Hemsley, 1987)

4.2 Prediction and measurement of settlement of a heavily loaded raft

Olds obliges by presenting here a well documented and concise case history of raft design and performance monitoring. The main points of interest are:

(a) The soil modulus profile for design was determined using the unload/reload cycles of pressuremeter tests.

(b) The design was based on the more conservative modulus (i.e. "secant" modulus) of the reload curve but the monitoring data indicated that the stiffer value of the "average" modulus of the unload/reload loop would be more appropriate.

(c) Settlement predictions were reasonable and consistent on the conservative side, as would be expected in a design situation with a critical structure. Settlements may continue to increase with time.

(d) Settlement analyses used a finite element multi-layered, elastic model (program FOCALS). The detailed analysis of the raft was "decoupled" from the analysis of settlement, and is not reported here.

4.3 The cellular raft and horizontal ground strains

This paper by Pellissier and Williams is about mitigation of risk. The paper is devoted to explaining the advantages of using a cellular raft for accommodating horizontal ground strain, particularly in relation to subsidence in longwall mining areas. The arguments are convincing for small structures (i.e. low rise dwellings) and may even be applicable for mitigation of earthquake risk.

The main point of technical interest relates to the tests on the soil/raft slip interface. It would seem that a simple sandwich of cut-back bitumen between sheets of plastic sheeting under the flat bottomed raft may well provide cheap and effective base isolation as well as an effective damp proof course.

The concept of designing flat slabs to accommodate horizontal strain is not new. Bell (1977) describes how systems have been used in Britain since the "fifties". There, however, they favour thin flexible rafts to accommodate curvature also. The authors claim that the stiffer cellular rafts are advantageous in areas of expansive soils. Certainly they would be advantageous in areas prone to differential settlement or, possibly, liquefaction.

This particular cellular raft, termed the Boucell raft, has been patented by the CSIR (South Africa). It is not clear what feature of the raft is patented. It is hoped that it is only a matter of detail and that there would be no restrictions on engineers designing from first principles!

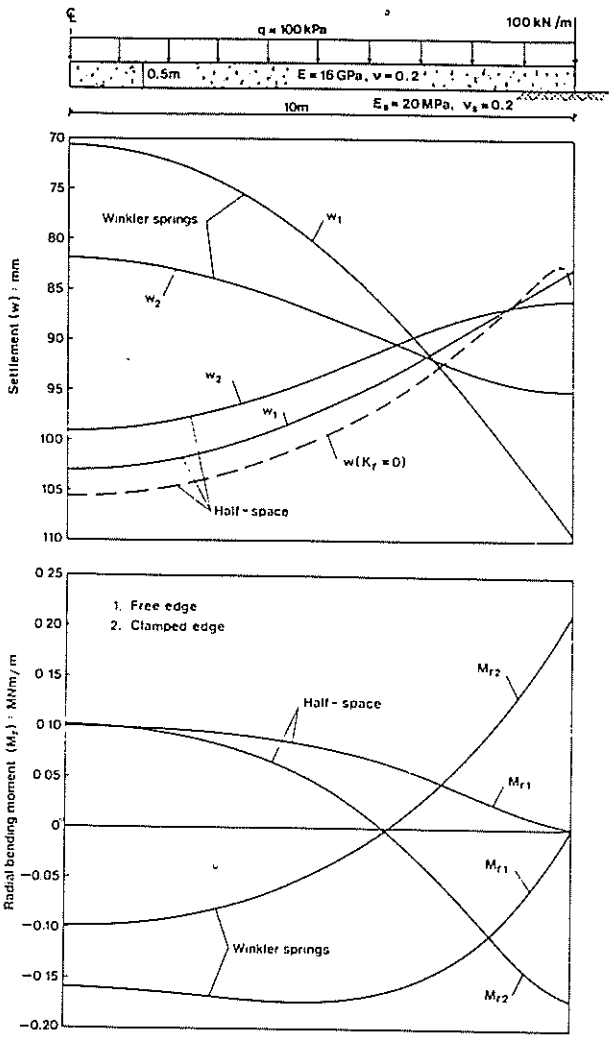

Figure 4: Example results for circular raft with combined edge and uniform distributed loading on spring or half-space foundations (After Hemsley, 1987).

4.4 Study of a case of unsuitable structural system on heterogeneous soil

This paper by Reyad presents a fairly straight forward case history of settlement of dwellings and remedial measures. As the author points out, the selection of simple strip footings to found buildings in an area of very variable ground conditions would appear inappropriate. Certainly the combination of fill, collapsible sand and expansive clay in a situation prone to extreme changes in wetting and drying (watering and arid zone evaporation) should have sounded some alarms. Perhaps the cellular raft of the previous paper (Pellissier & Williams, 1992) would have been the answer here.

It would be interesting to hear if the remedial measures described have been successful.

5.0 CONCLUSIONS

There can only be one conclusion to a session report : If there appears to be anything of interest, read the papers! However, in recognition of the conference theme, the report concludes with some statements which the reporter considers may hold some truth but should be challenged in open discussion:

- There is little risk of catastrophic failure of foundations. Designs are very conservative and unnecessarily expensive.
- The greatest risk in foundation engineering is that due to differential settlement of shallow foundations. Settlements of deep foundations are generally not significant.
- The greatest risk associated with deep basements arises at time of construction. Generally designs of permanent walls are over conservative, despite (or because of) a pre-occupation with the "K_o" fallacy.
- The commonest failures of engineering structures are associated with retaining walls and ground retention systems, yet research is only modest in this field.

6. REFERENCES

6.1 General

Bell, S.E. (1977) Successful design for mining subsidence. Proc.Conf. on Large Ground Movements and Structures, Cardiff, Pentech Press.

Hemsley, J.A. (1987) Elastic solutions for axisymmetrically loaded circular raft with free or damped edges founded on Winkler springs or a half-space. Proc.Instn.Civ.Eng. Part 2, 83, Mar., 61-90.

Tomlinson, M.J. (1977) Pile design and Construction Practice, Viewpoint Publications, London.

6.2 Session papers

The following papers, reviewed in this report, are included in the Proceedings of the 6th ANZ Geomechanics Conference, 1992.

Budkowska, B.B. and Szymczak, C. (1992). Sensitivity analysis of laterally loaded piles.

Choi, S.K. and Johnston, I.W. (1992). Identification of failure mechanisms in soft rock by stereo-photogrammetry.

Hull, T.S., Lee, C.Y. and Poulos, H.G. (1992). Behaviour of fixed and free head piles in a laterally sliding soil.

Hull, T.S. and McDonald, P. (1992). Lateral soil movement loading on bridge foundation piles.

Kodikara, J.K., Johnston, I.W. and Haberfield, C.M. (1992). Analytical predictions for side resistance of piles in rock.

Li, K.S. (1992). Risk associated with construction of large diameter bored piles in cavernous marble.

Olds, R.J. (1992). Prediction and measurement of settlement of a heavily loaded raft.

Pellissier, J.P. and Williams, A.A.B. (1992). The cellular raft and horizontal ground strains.

Poulos, H.G. (1992). Class A predictions of pile behaviour.

Reyad, M.M. (1992). Study of a case of unsuitable structural system on heterogeneous soil.

Small, J.C. and Lee, C.Y. (1992). The analysis of axially loaded piles in layered or non-homogeneous soils.

Stewart, D.P., Jewell, R.J. and Randolph, M.F. (1992). Piled bridge abutments on soft clay - Experimental data and simple design methods.

Zhang, B.Q. and Small, J.C. (1992). The analysis of rectangular rafts of finite flexibility subjected to concentrated loads.

Design of Grouted Offshore Piles in Calcareous Soils

A.F. ABBS
B.Sc. (Eng.), M.I.C.E., M.I.E.Aust.
Principal, Dames & Moore, Perth, Australia

SUMMARY A method is presented for analysing and designing grouted piles in weakly cemented calcareous sediments. The method is based upon correlation with observed field tests and utilises a brittle load transfer curve to calculate pile capacity.

1. INTRODUCTION

It is well known that conventional driven steel pipe piles in calcareous soils may show very low unit skin friction values and as a result drilled and grouted insert piles have generally been used for support of offshore platforms in such soils.

This paper reviews the current state of practice in design of grouted piles in calcareous soils, and proposes a new alternative to the existing methods using cone penetration test cone resistance values to determine peak skin friction for design. The method proposed also uses load transfer analysis and brittle load transfer curves to calculate axial pile capacity.

2. HISTORICAL BACKGROUND

The design for drilled and grouted insert piles in calcareous soils for many years was based upon the work by Angemeer *et al* (1), (2), where field tests were conducted in Bass Strait and on the North West Shelf of Western Australia. These tests showed that grouted piles offered superior load carrying capacity to driven piles in calcareous soils, and the results of the field tests allowed for subsequent installation of grouted piles in many locations.

In his state of the art review Murff(3) concluded that analysis of drilled and grouted piles in calcareous soils was rather "simplistic". A uniform value of unit skin friction of 100kPa was often adopted, loosely based upon the rather crude original test work by Angemeer. This simplistic approach existed until the publication and adoption of the two methods as discussed below.

3. CURRENT PRACTICE

Both methods in current use load transfer analysis to calculate pile capacity in recognition of the brittle load deflection curves typical of grouted piles in these soils. Therefore it is necessary to review not only the method of assessment of pile skin friction but also the form of the load transfer relationship.

3.1 Peak Skin Friction

In the mid to late 1980's, a significant amount of research was performed on this subject, most notably by Esso Australia and Woodside Offshore Petroleum. These programmes of research was driven by the need to resolve real engineering issues in connection with existing offshore structures, and included field tests on drilled and grouted pile sections, (4), (5), followed by analytical work (6), (7), (8). These latter two papers concentrated on back analysis of the grouted pile section tests at the North Rankin A platform and developed innovative techniques for analysis of cyclic loading. However they offer little guidance as how to develop a pile design away from the site specific data of the North Rankin A platform on the North West Shelf of Western Australia.

It is worth noting, however that peak skin friction values of about 300kPa to 680kPa were back analysed from the tests at North Rankin A, significantly higher than the previously used value of 100kPa.

The work reported by Hyden *et al.* (7) did however propose a new design technique. The approach used was to model the soil as frictional in nature, with the peak skin friction given by:

$$\tau_p = F\ \sigma_{rg} \tan \phi_p$$

where:

- σ_{rg} = effective grout pressure
- ϕ_p = peak friction angle from triaxial tests
- F = design correlation factors

The method uses this basic approach, including various empirical factors to account for correlation with the field data and design and construction uncertainties.

Inspection of the method shows that it is conservative with respect to the observed field tests. Typically the method yields design peak skin friction values of up to about 400kPa compared to the field data which gave values in the range 350 to 950kPa, again significantly higher than the previously often adopted 100kPa.

The Hyden *et al.* method is attractively simple and empirical, but it does not recognise the cementation inevitably present in calcareous soils. However it provides a robust rational method to design such piles and has been used in Bass Strait. To the authors knowledge it has also been used on at least one project on the NW Shelf where it was employed as a design check.

In well cemented soils, such as may be found in shallower waters in the NW Shelf of Western Australia, a different approach is often used based upon Abbs & Needham (9).

This method was developed in the early 1980's by the authors during a series of projects in the Arabian Gulf. This approach treats the cemented carbonate soil as a weak rock and adopts a "rock socket" approach to the development of peak skin friction. For this method to be used, the soil must be sufficiently cemented to be successfully cored, normally using wireline triple tube techniques, and as such is really applicable to cemented soils or weak rocks showing an unconfined compressive strength of greater than about 500kPa - 750kPa.

3.2 Load Transfer Curves

Both the methods currently in use employ load transfer analysis to calculate the ultimate axial pile capacity. This has been adopted because of the observation of brittle, strain softening behaviour in pile tests as shown in Figure 1. Different load transfers curves (t-z) have been developed by the two design methods outlined above, but they are broadly similar in shape to each other and the typical field test curve on Figure 1.

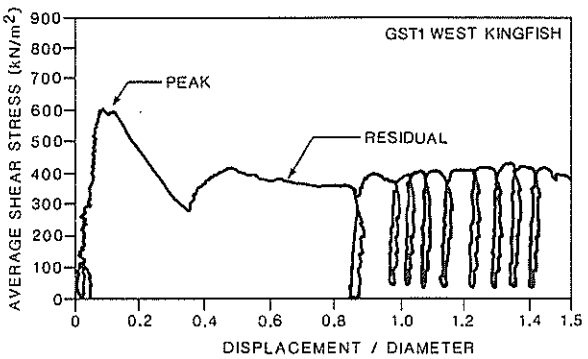

Figure 1 Typical load transfer curve from grouted section test (ref 6)

4. PROPOSED METHOD

4.1 Need for Alternative Method

As discussed above, the two methods in use are different and suffer from some limitations, Abbs & Needham is applicable for well cemented, weak rock materials, whereas Hyden *et al.* assumes no cementation, relying instead upon good quality triaxial tests to measure effective friction angles. Accordingly, there is a need for a method that may be used in the case of weakly cemented soils that are too weak to core successfully, but still with significant cementation. It is also desirable for the method to employ conventional field or laboratory techniques as input. The method selected developed during the foundation design of major offshore structure, opted for cone penetration test data as the basic input for correlation with peak skin friction values.

In cohesive soils it has been common practice to estimate the undrained shear strength of clays and pile capacities using cone resistance data. Therefore it seemed logical that cone resistance values, which provide a repeatable index of a soil's in-situ strength and compressibility, should provide a basis for a method in cemented calcareous soils.

4.2 Correlation of Cone Resistance with Peak Skin Friction

To develop a correlation between cone resistance and unit pile skin friction, it was necessary to assemble a data base of grouted pile tests and cone resistance data in calcareous soils. Figure 2 shows the data assembled during this exercise. The data contains results for piles of a variety of sizes, some of which have failed, some not failed and some failed by cycling.

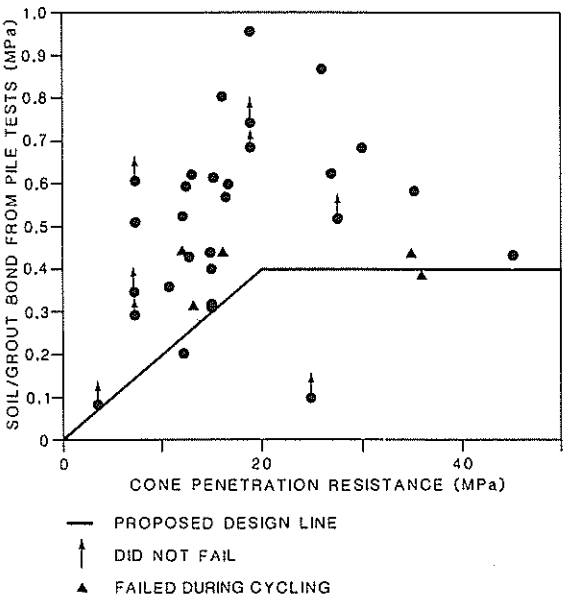

Figure 2 Calcareous Soil Grouted Pile test result data base

A design line was picked as a conservative lower bound to the available test data. This selection of the lower bound accounts for many unknown factors including the effects of pile diameter. It has been found that unit skin friction decreases with increasing pile size Khorshid (10), and reasoning for this has been proposed by Randolph (11).

The proposed correlation is given by:

$$\tau_p = 0.02 q_c$$

where: q_c = cone resistance in MPa

τ_p = peak skin friction in MPa

This ratio may be compared to values quoted in the State of the Art Address to the Carbonate Sediments Conference (11) where it was noted that grouted pile peak skin friction ranged from 0.02 to 0.15 q_c and 0.03 to 0.05 q_c for Bass Strait data.

It was considered that the results reported by Khorshid (10) should be giving the greatest weighting in the selection of a design correlation as these represent a consistent set of high quality test data from one site. Figure 3 presents this sub set of data from one test site, together with the cone resistance profile converted to peak skin friction by the proposed correlation.

The agreement between the proposed correlation and the test data for the full size pile sections is considered encouraging. The figure also illustrates the scatter of laboratory test data from the same site.

The data set indicates that the linear relationship should not continue, and a cut off at τ = 400kPa has been selected. This also has the prudent affect of preventing the pile design relying on a few thin particularly strong layers. In addition, for τ values of greater than about 400kPa the pile design may become governed by allowable stresses between the steel insert pile and the grout.

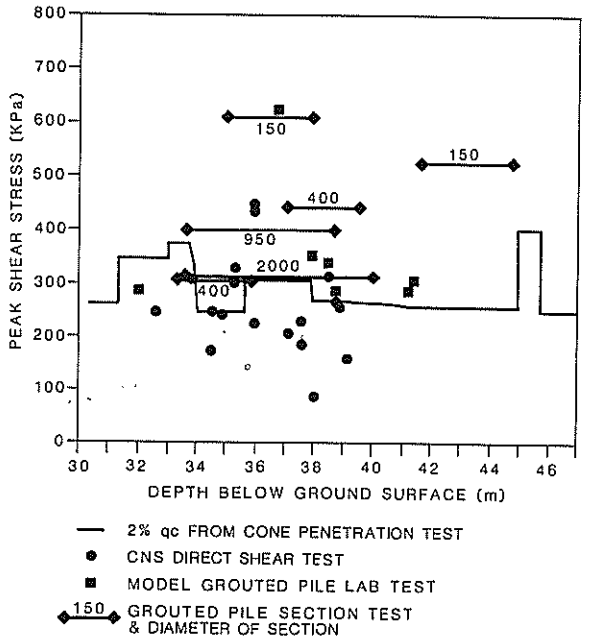

Figure 3 Field and laboratory test data from a calcareous soil test site

For continuous profiles of stronger materials, above say $q_c = 40MPa$, which corresponds to an unconfined compressive strength of 1 to 2MPa, it would be more appropriate to use the Abbs & Needham method for weak rocks, as the cone penetration becomes difficult in these stronger materials.

4.3 Comparison of Design Line with Laboratory Direct Shear Data

As a check, the design line has been compared to laboratory test data. In view of the questions concerning the effects of pile diameter on unit skin friction, it was decided not to use laboratory scale model grouted piles, although these tests do provide valuable insight into the mechanisms (12). Instead, the test selected was the large scale constant normal stiffness direct shear test (CNS tests) (13). This test, which allows the use of large samples tested longitudinally, is considered to be more realistic representation of rough pile/soil interface behaviour during monotonic loading in that it permits dilation or contraction during the shearing process depending upon the radial stresses and stiffness at the soil/grout interface.

Figure 4 shows the data from CNS shear tests which have been performed on samples where CPT data were available from adjacent boreholes. This scatter is due in part to this spatial difference in the data source, but also is due to a variety of initial normal stresses and normal stiffness in the test. These boundary conditions may result in differing peak skin friction values being recorded (13). In spite of the scatter it is reassuring to see that the design line lies conservatively with respect to the data points.

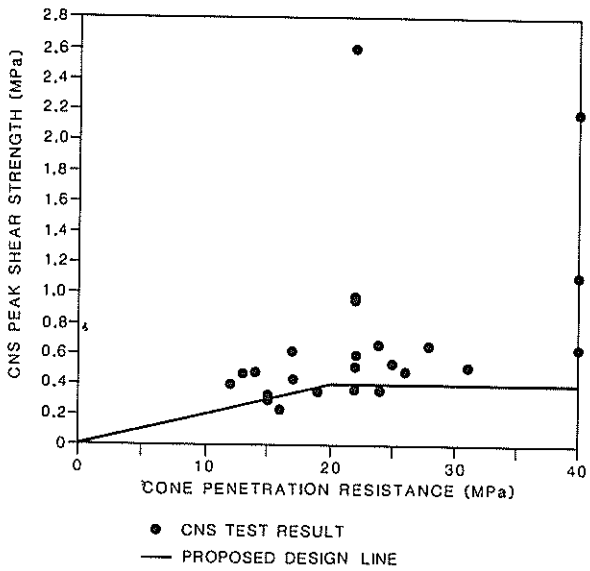

Figure 4 Constant normal stiffness direct shear test data

4.4 Shape of Load Transfer Curve

In conjunction with the peak skin friction relationship, a load transfer curve (t-z curve) is needed to permit calculation of the pile axial capacity and response. The type of curve proposed is that developed by Randolph (7) and Randolph and Jewell (14). The form of the t-z curve is shown on Figure 5. Various parameters need to be selected to define the curve, including:

τ_p	-	peak skin friction
G	-	Soil shear modulus
ξ	-	yield parameter (proportion of linear portion of initial slope of t-z curve)
Δw_{res}	-	displacement to residual skin friction
τ_{res}	-	monotonic residual skin friction
τ_{rc}	-	cyclic residual

Selection of τ_r and Δw_{res} is difficult without site specific tests, but from a review of the data available, τ_{res} appears to range from 10% to 60% of τ_p and Δw_{res} from 5mm (small model piles) to 1000mm (large diameter pile sections).

Generally speaking conservative values for τ_{res} and ΔW_{res} should be selected (say 20% and 50mm-100mm would be typical).

A full discussion of the curve and the source of the somewhat novel cyclic residual is given in reference 14.

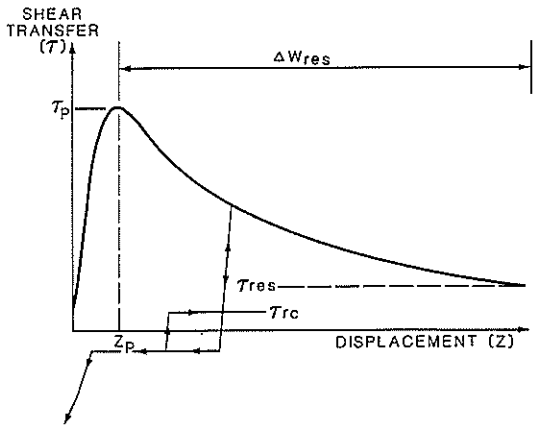

1. $T_p = 0.02q_c + 400kPa$
2. $T_{res} = 0.2T_p$ (TYPICALLY)
3. $T_{rc} = 0.01T_p$ (TYPICALLY)
4. $Z_p \propto \frac{T_p D}{G}$, D= PILE DIAMETER, G= SHEAR MODULUS
5. YIELD PARAMETER ≈ 0

Figure 5 Proposed load transfer curve

4.5 Cyclic Loading

The discussion thus far has been centred around static axial capacity. In calcareous soils, cyclic loading is important, as failure of a pile element may result from repeated cyclic loading at shear stresses below the local peak skin friction. With a strain softening t-z curve this may lead to the pile "unzipping". Cyclic loading may be readily analysed using the Randolph type t-z curve described above and the program RATZ (15). The results of many studies have shown that for properly designed piles with normal safety factors (16), the effects of cyclic loading may often be accommodated within the static safety factor. This would not necessarily be true in every case, however. (In the two methods described above in Section 3 'Current Practice', cyclic loading is implicitly included in this way).

4.6 Example

Figure 6 shows the results of an actual load transfer analysis for a typical offshore pile. Both monotonic and cyclic analyses are shown on this figure. The cyclic analysis shows the reduction in capacity after a period of cyclic loading.

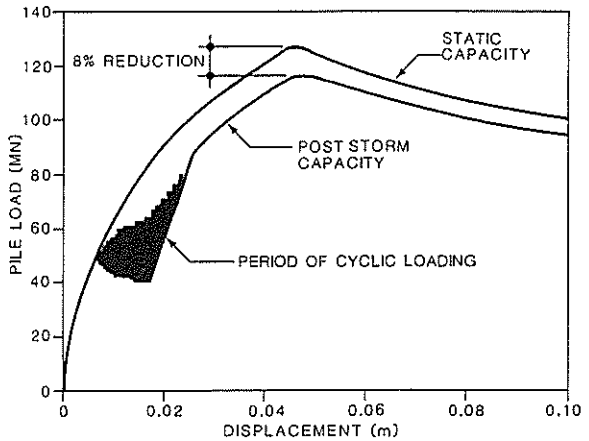

1. 62m LONG x 2mO.D. x 0.05m w.t. TUBULAR IN 2.3m DIA. HOLE

Figure 6 Result of typical load transfer analysis

Figure 7 shows the results of a series of analyses of a 2m diameter insert pile plotted as peak pile capacity versus insert length. The effects of cyclic loading are clearly shown albeit fairly modest in this case. The analyses were run for the static case as well as factored and unfactored cyclic cases.

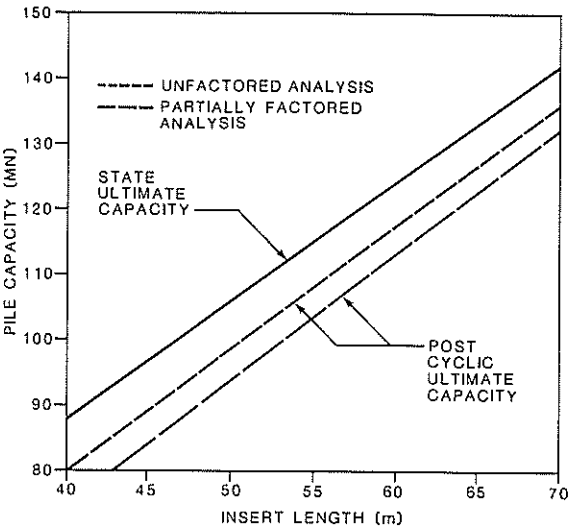

1. 2m O.D. x 0.05m w.t. TUBULAR IN 2.3m DIA. HOLE

Figure 7 Typical pile capacity length relationship

5. CONCLUSION

This paper has presented a new method for analysing and designing grouted insert piles in calcareous soils. The method uses an empirical approach to calculate peak skin friction based upon cone resistance data from cone penetration tests and then uses a load transfer analysis with strain softening t-z wires to calculate pile capacity. While the method is based upon empirical correlation with field data, it should be used with caution in soil types which differ from those on the NW Shelf of Australia. The method compliments the existing approaches described by Abbs & Needham (9) and Hyden *et al* (6), and therefore allows for the use of more than one method if the field and laboratory data are sufficient.

6. REFERENCES

1. Angemeer, J., Carlson, E. and Klick, J.H. "Techniques and Results of Offshore Pile Testing in Calcareous Soil". Proceedings of the Fifth Offshore Technology Conference, Houston 1973.

2. Angemeer, J., Carlson, E., Stroud, S. and Kurzeme, M. "Pile load tests in Calcareous Soils Conducted in 400 feet of Water from a Semi Submersible Exploratory Rig". Proceedings of the Seventh Offshore Technology Conference, Houston 1975.

3. Murff, J.D. "Pile Capacity in Calcareous Sands: State of the Art". Proceedings of the Journal of Geotechnical Engineering, American Society of Civil Engineers, Vol. 113, No. 5, May 1987.

4. Withers, N.J., Kolk, H.T., Lewis, W.M. and Hyden, A.M. "Grouted Section Tests in Calcareous Soils". Proceedings of the Eighteenth Offshore Technology Conference, Houston 1986.

5. Williams, A.F. and van der Zwaag, G.L. "Analysis and Evaluation of Grouted Section Tests". Proceedings of the International Conference on Calcareous Sediments, Perth, 1988.

6. Hyden, A.M., Hylett, J.M., Murff, J.D. and Abbs, A.F. "Design Practice for Grouted Piles in Bass Strait Calcareous Soils". Proceedings of the International Conference on Calcareous Sediments, Perth, 1988.

7. Randolph, M.F. "Evaluation of Grouted Insert Pile Performance". Proceedings of the International Conference on Calcareous Sediments, Perth, 1988.

8. Poulos, H.S. "Evaluation of Grouted Pile Friction from Grouted Section Tests". Proceedings of the International Conference on Calcareous Sediments, Perth, 1988.

9. Abbs, A.F. and Needham, A.D. "Grouted Piles in Weak Carbonate Rocks". Proceedings of the Seventeenth Offshore Technology Conference, Houston, 1985.

10. Khorshid, M.S. "Development of Geotechnical Experience on the North West Shelf". Australian Geomechanics No. 19, December 1990.

11. Randolph, MF. "The Axial Capacity of Deep Foundations in Calcareous Soil". State of the Art Report to the International Conference on Calcareous Sediments, Perth, 1988b.

12. Fahey, M. and Jewell, R.J. "Model Pile Tests in Calcarenite". Proceedings of the International Conference of Calcareous Sediments, Perth, 1988.

13. Johnston, I.W., Carter, J.P., Novello, E.A. and Ooi, L.H. "Constant Normal Stiffness Direct Shear Testing of Calcarenite". Proceedings of the International Conference on Calcareous Sediments, Perth, 1988.

14. Randolph, M.F. and Jewell, R.J. "Load Transfer Model for Piles in Calcareous Soil". 12th International Conference on Soil Mechanics and Foundation Engineering, Rio de Janeiro, 1990.

15. Randolph, M.F. "RATZ. Load Transfer Analysis of Axially Loaded Piles". Department of Civil Engineering, University of Western Australia, 1986.

16. American Petroleum Institute. "Recommended Practice for Planning, designing and Constructing Fixed Offshore Platforms". 1991.

Sensitivity Analysis of Laterally Loaded Piles

B.B. BUDKOWSKA
M.S.C.E., Ph.D.
Assoc. Professor, University of Windsor
C. SZYMCZAK
M.S.C.E., Ph.D.
Professor, University of Windsor (Visiting) and Technical University of Gdansk

SUMMARY The first order variations of an arbitrary displacement and an internal force at a specified cross–section due to some variations of the design variables are derived by means of the adjoint method. The pile cross–section dimensions, the pile material constants and the soil constants are considered to be the design variables. The sensitivity analysis presented is valid for both linear and nonlinear behaviour of the soil and pile material. In some numerical examples dealing with the linear structures the distributions of the underintegral coefficients of the design variable variations determining the increments of the lateral displacement, the angle of cross–section rotation at the pile top due to the changes of the design variables are given. The accuracy of the approximation of the increments of the quantities under consideration due to the design variable variations is also investigated.

1. NOTATION

A – area of the pile cross–section;
D_t – tangent flexural stiffness of the pile;
E – Young's modulus of elasticity of the pile material;
E_t – tangent modulus of elasticity of the pile material;
EJ – flexural stiffness of the pile;
F_v, F_ψ, K_v, K_ψ – underintegral coefficients;
k – stiffness of linear Winkler–type foundation;
k_t – tangent stiffness of the foundation;
L – pile length;
M – moment;
M_x – bending moment;
r – foundation reaction per unit length;
$\bar{s}$ – design variables vector;
v – lateral displacement of the pile;
y, z – coordinate axes;
δ – variational operator;
ϵ – longitudinal strain;
ψ – cross–section rotation;
σ – normal stress;
∂ – first partial derivative.

Subscripts:

a – imposed on adjoint beam;
o – at cross–section $z = z_o$;
, – first partial derivative.

Superscripts:

M – corresponding to moment M;
P – corresponding to concentrated load P;
′ – differentiation with respect to z.

2. INTRODUCTION

Internal forces and displacements in laterally loaded piles can be calculated using a simple one–dimensional idealization in conjunction with the beam–on–elastic–foundation approach (Das, 1990; and Desai and Kuppusamy, 1980). The three displacements of the pile are usually assumed to be uncoupled, thereby superimposition of their effects is possible. However, the internal forces and the displacements may vary due to arbitrary variations of the design variables such as the pile cross–section dimensions, the pile material constants and the soil constants, as well. To facilitate calculations of these changes, without the additional redesign, the first order variations of any displacement or any internal force at the specified cross–section of the pile due to arbitrary variation of the design variables are derived. The considerations are valid for both linear and nonlinear behaviour of the soil and pile material. The adjoint method developed by Mroz et al. (3) is adopted to this case.

The accuracy of the approximations of the pile displacements changes due to the variations of the flexural stiffness of the pile and the foundation stiffness constant by means of their first variations are also discussed. The linear beam resting on the Winkler–type elastic foundation is assumed in this case.

3. FIRST ORDER VARIATION OF DISPLACEMENTS AND INTERNAL FORCES

Consider a pile made of nonlinear elastic material and subjected to lateral loads as shown in Fig. 1. To derive the first order variation of any displacement or any internal force at the specified cross–section of the pile, a simple idealization of one–dimensional beam made of nonlinear elastic material and resting on a nonlinear elastic foundation is used. Using the Bernoulli hypothesis, the increments of the strain $\delta\epsilon$ of the beam may be written as

$$\partial\epsilon = -y\ \delta v'' \tag{1}$$

Hence, the bending moment–curvature incremental relationship can be obtained

$$\delta M_x = -D_t\ \delta v'' \tag{2}$$

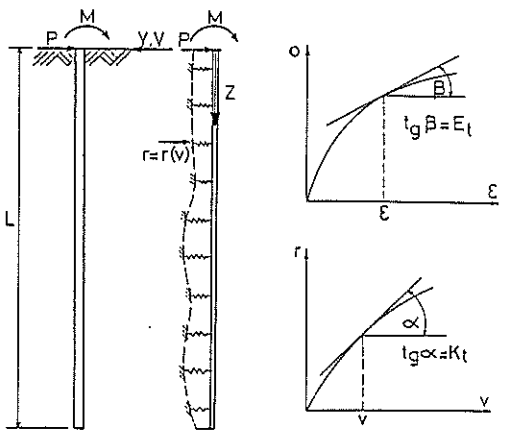

Figure 1. The laterally loaded pile and its model assumed; stress–strain relation (σ–ϵ) of the pile material; reaction–displacement relation (r–v) of the foundation

where

$$D_t = \int_A E_t\, y^2\, dA$$

$$E_t = \frac{d\sigma}{d\epsilon} \tag{3}$$

Regarding the foundation, similarly the foundation reaction–displacement relationship can be written

$$\delta r = k_t\, \delta v \tag{4}$$

According to the adjoint structure concept (Mroz et al., 1985; Szefer et al., 1987) an adjoint beam made of linear elastic material with the tangent modulus of E_t and resting upon the linear Winkler–type foundation described by the tangent foundation stiffness k_t corresponding to the actual stress and displacement fields of the pile and the foundation is introduced. The adjoint beam is subjected to a concentrated load P_a and a concentrated moment M_a at the cross–section $z = z_o$ in which the displacements variations are sought. Consider some statically admissible variations of the displacement field of the primary beam.
Application of the virtual work theorem (Washizu, 1974) yields

$$P_a\, \delta v_o + M_a\, \delta\, \psi_o = -\int_o^L M_{xa}\, \delta v''\, dz + \int_o^L r_a\, \delta v\, dz \tag{5}$$

Taking into account that the statical fields depend on the actual displacements and the vector of the design variables variation $\overline{\delta s}$, the following linear relations are derived

$$\delta M_x = \frac{\partial M_x}{\partial v''}\, \delta v'' + \frac{\partial M_x}{\partial \overline{s}}\, \overline{\delta s} = D_t\, \delta v'' + M_{x,\overline{s}}\, \overline{\delta s} \tag{6}$$

$$\delta r = \frac{\partial r}{\partial v}\, \delta v + \frac{\partial r}{\partial \overline{s}}\, \overline{\delta s} = k_t\, \delta v + r_{,\overline{s}}\, \overline{\delta s}$$

Using relations (6) and (5) and taking into consideration that the statical fields is constant ($\delta M_x = 0$, $\delta r = 0$), after some algebra one can obtain the desired first order variations

$$P_a\, \delta v_o + M_a\, \delta\, \psi_o = \int_o^L (M_{x,\overline{s}}\, v_a'' - r_{,\overline{s}}\, v_a)\overline{\delta s}\, dz \tag{7}$$

If $P_a = 0$, $M_a = 1$ is assumed, then the first variation $\delta v_o'$ is determined, and if $P_a = 1$, $M_a = 0$, then the first variation δv_o is established.
In the case of the linear beam resting on the linear Winkler–type foundation, we arrive at

$$P_a\, \delta v_o + M_a\, \delta\psi_o = -\int_o^L [(EI)_{,\overline{s}}\, v''v_a'' + k_{,\overline{s}}\, vv_a]\overline{\delta s}\, dz \tag{8}$$

The derivation of the first variation of the internal forces proceeds in a similar manner.
The distortions

$$\Delta\psi_{oa} = \psi_{oa}\,(z = z_o^+) - \psi_{oa}\,(z = z_o^-) \text{ and}$$
$$\Delta v_{oa} = v_{oa}\,(z = z_o^+) - v_{oa}\,(z = z_o^-) \tag{9}$$

are imposed on the same adjoint beam. Consider some kinematically admissible variations of static field of the primary beam.
According to the virtual work theorem one can write

$$\delta M_o\, \Delta\psi_{oa} + \delta T_o\, \Delta v_{oa} = -\int_o^L (v_a''\, \delta M_x - v_a\, \delta r)dz \tag{10}$$

Inserting relation (6) in (10) and taking into account that there are no external loads acting at the adjoint beam, one can express the first variation of the internal forces in terms of the design variable variations

$$\delta M_o\, \Delta\psi_{oa} + \delta T_o\, \Delta v_{oa} = -\int_o^L (M_{x,\overline{s}}\, v_a'' - r_{,\overline{s}}\, v_a)\, \overline{\delta s}\, dz \tag{11}$$

Obviously in the case of a linear structure one can obtain

$$\delta M_o\, \Delta\psi_{oa} + \delta T_o\, \Delta v_{oa} = \int_o^L [(EI)_{,\overline{s}}\, v''v_a'' + k_{,\overline{s}}\, vv_a]\, \overline{\delta s}\, dz \tag{12}$$

4. NUMERICAL EXAMPLES

Consider for example a pile made of a linear material with Young's modulus E resting on a linear, uniform Winkler–type foundation and subjected to a unit load P = 1 and a unit moment M = 1 at the pile top, as shown in Fig. 1. Utilizing relation (7), the first variations of the horizontal displacement δv_o and the angle of cross–section rotation $\delta\psi_o$ at the pile top can be expressed in terms of the flexural stiffness variation $\delta(EI)$ and the foundation stiffness variation δk

$$\delta v_o = \int_o^L (F_v^P + F_v^M)\delta k \, dz + \int_o^L (K_v^P + K_v^M)\delta(EI)dz \quad (13)$$

$$\delta\psi_o = \int_o^L (F_\psi^P + F_\psi^M)\,\delta k \, dz + \int_o^L (K_\psi^P + K_\psi^M)\delta(EI)dz$$

The reciprocity theorem (Washizu, 1974) allows us to show that $F_v^M = F_\psi^P$ and $K_v^M = K_\psi^P$. The static analysis of the beam resting on the Winkler–type elastic foundation necessary to find the distribution of the underintegral coefficients is carried out by the finite element method. It is worthwhile noticing that the pile is considered to be a long one (1) because of the ratio of the length L to the characteristic length of the soil–pile system T(L/T = 5). The distributions calculated are shown in Fig. 2 ÷ 3.

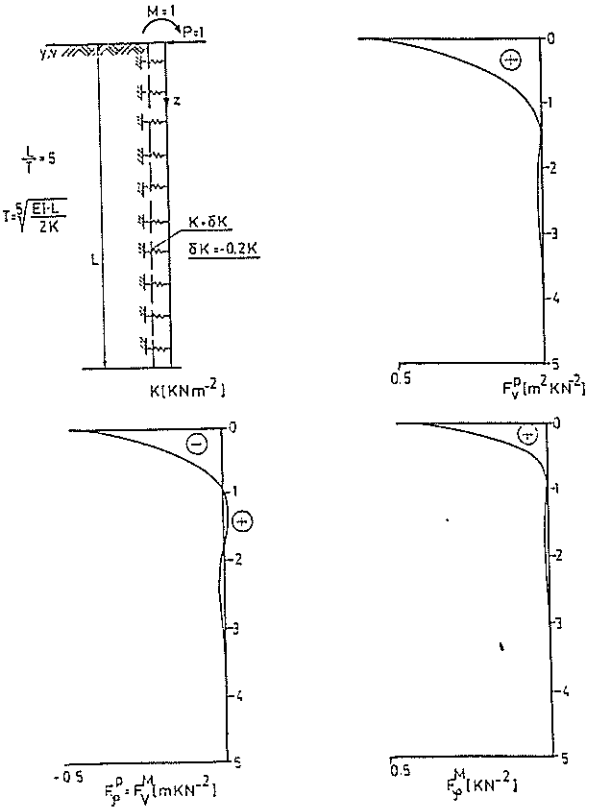

Figure 2. Distributions of underintegral coefficients of foundation stiffness variation δk for uniform foundation stiffness

To estimate the approximation of the change of the displacements due to 20% reduction of the design variable variations by virtue of their first variations, the horizontal displacement and the angle of cross–section rotation at the pile top are determined for the pile with the changed design variation and compare to their approximated values. The results obtained and the errors of approximations are presented in Table I.

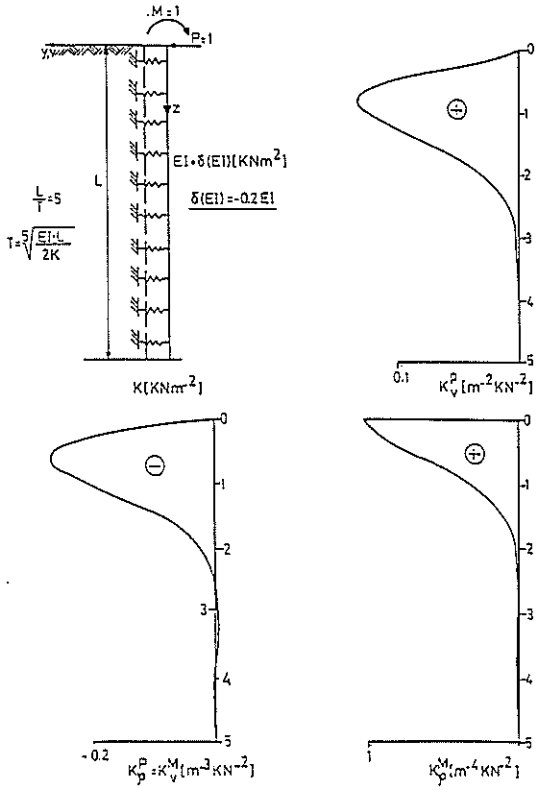

Figure 3. Distributions of underintegral coefficients of flexural stiffness variation of the pile for uniform foundation stiffness

5. CONCLUSIONS

In the paper the first order variations of arbitrary displacements and internal forces of laterally loaded pile due to the design variable increments are derived. The sensitivity analysis discussed is valid for both linear and nonlinear behaviour of the pile material and the soil. The first variations derived enable us to calculate the change of the displacements and the internal forces due to the increments of the pile cross–section dimensions, the pile material constants and the soil constants without full reanalysis of the pile. The latter may be especially interesting for the structures situated in cold regions, where the soil constants may vary due to freezing and thawing effects.

The results presented allow us to draw conclusion that approximation of the changes of the displacements of the pile by means of their first variations is good even for 20 per cent change of the design variable.

6. ACKNOWLEDGEMENT

The financial support of the Natural Science and Engineering Research Council of Canada under grant number OGP 110262 is gratefully acknowledged.

TABLE I

COMPARISON OF EXACT AND APPROXIMATE VALUES OF THE LATERAL DISPLACEMENT AND THE ANGLE OF CROSS-SECTION ROTATION AT THE PILE TOP FOR 20% REDUCTION OF THE DESIGN VARIABLES

	DESIGN VARIABLE (S)			
	FLEXURAL STIFFNESS		FOUNDATION STIFFNESS	
	LOADINGS			
	P = 1	M = 1	P = 1	M = 1
$v_0(s)$	0.71177	–0.63310	0.71177	–0.63310
$v_0(0.8\ s)$	0.84153	–0.70807	0.75249	–0.70759
approx. v_0 (0.8 s)	0.81861	–0.69664	0.74732	–0.69628
Error [%]	2.72	1.61	0.69	1.60
ψ_0 (s)	–0.63310	1.12573	–0.63310	1.12573
ψ_0 (0.8 s)	–0.70807	1.19100	–0.70757	1.33024
approx. ψ_0 (0.8 s)	–0.69664	1.18260	–0.69628	1.29682
Error [%]	1.61	0.71	1.60	2.51

7. REFERENCES

Das, B.M. (1990). Principles of Foundation Engineering. PWS-Kent Publ. Comp., Boston.

Desai, C.S. and Kuppusamy, T. (1980). Application of a Numerical Procedure for Laterally Loaded Substructures. In Numerical Methods of Offshore Piling, Proceedings of a Conference, Institution of Civil Engineers, London, pp. 93–100.

Mroz, Z., Kamat, M.R. and Plant, R.H. (1985). Sensitivity Analysis and Optimal Design of Nonlinear Beams and Plates. J. Struct. Mech., Vol. 13, pp. 245–266.

Szefer, G., Mroz, Z. and Demkowicz, L. (1987). Variational Approach to Sensitivity Analysis in Nonlinear Elasticity. Arch. Mech. Vol. 39, pp. 247–259.

Washizu, K. (1974). Variational Methods in Plasticity and Elasticity. Pergamon Press, Oxford.

Identification of Failure Mechanisms in Soft Rock Using Stereo-Photogrammetry

S.K. CHOI
B.E., Ph.D., M.I.E.Aust.
Senior Research Scientist, CSIRO Division of Geomechanics, Melbourne
I.W. JOHNSTON
B.Sc. (Eng.), Ph.D., F.I.E.Aust.
Associate Professor, Dept of Civil Engineering, Monash University of Melbourne

SUMMARY In order to determine the failure mechanisms which occur when a soft rock is deformed by a loaded foundation, a series of laboratory tests were conducted on a model footing. The footing and foundation rock were modelled by a semi-cylindrical section which was held against the smooth rigid surface of a transparent window. By taking successive photographs from a fixed camera position as the footing was loaded, it was possible to produce a series of stereo-photographic pairs. When these were viewed under a stereoscope, the three dimensional images could be used to produce qualitative and quantitative data on the evolution of the displacement field in the plane of the section examined.

1. INTRODUCTION

In the design of foundations on soils, it is comparatively easy to estimate a maximum allowable bearing pressure by applying a relevant factor of safety to the ultimate bearing capacity and considering the acceptability of the resultant settlement against appropriate serviceability criteria. The ultimate bearing capacity of a soil can be determined with adequate accuracy using plasticity methods such as the slip line method, the method of limit equilibrium and the method of limit analysis, although some of the solutions may not satisfy the conditions for either the lower of upper bound solutions.

However, when a foundation is placed on a rock, the brittleness of rock may render the plasticity methods inappropriate without some modifications. The lack of suitable simple analytical methods make it impossible to employ a reasonable and economic factor of safety against bearing failure for rock. Such a situation leads to the adoption of over-conservative designs to ensure that there is no significant risk of bearing failure.

In an attempt to redress this major shortcoming in foundation design, the authors commenced the development of a numerical model which was capable of predicting the load-settlement response of vertically loaded foundations in soft rock. Particular attention was directed to the prediction of the load capacity of the end bearing component of piles drilled and cast into soft rock.

The model, which was based on the finite element method, required a number of assumptions regarding the constitutive behaviour of the foundation rock to be made in order to obtain a reasonable solution, and it was evident that the solution was highly dependent on the assumptions made. Clearly a wide range of predictions was possible. However, a realistic prediction of the load-settlement response could only be obtained if the numerical model could predict the major actual deformation and failure mechanisms of the prototype foundation. This then raised the additional problem of how to ascertain a clear picture of the failure mechanisms involved so that a suitable constitutive model could be developed and the adequacy of the numerical model assessed.

2. DETERMINATION OF FAILURE MECHANISMS

The use of mechanical and electrical devices for measuring displacements and strains experienced by geotechnical materials is very common. However these techniques are usually limited to the boundaries of the material and can only provide overall average values of deformation or the deformation of a few specific points. In order to obtain the detailed information of displacements within a body of the material to define a failure mechanism, a large number of internal displacements would be required. However, the introduction of meaningful internal measurement points is extremely difficult because of the disturbance caused and the changes in performance brought about by the mere presence of a measuring point or instrument itself. This is particularly true when considering the number of points required to be monitored in order to clearly define a failure mechanism. The only techniques which seem to have moderate success have involved the embedment of lead shot markers in soils, but these have required sophisticated radiographic plotting techniques (e.g. Roscoe et al., 1963).

In the absence of any practical alternative, it appeared that an observational method for investigating failure mechanisms was the only approach available. There seemed to be two principal methods by which this could be carried out. One of these would involve conducting loading tests, and after the application of a significant increment of loading, the test location could be carefully excavated and sectioned to reveal patterns of movement. This technique had in fact been applied to a number of field pile tests in soft rock (Williams, 1980; Williams et al, 1980), but because of the variability of the rock, the mechanisms were not always particularly clear. A much simpler alternative would be to conduct the tests in the laboratory using model foundations bearing on blocks of natural or synthetic rock. However, when considering the number of tests required to cover a reasonable range of foundation geometries and rock characteristics, the method would be very time consuming and labour intensive. This commitment would be even more considerable because, in order to see a mechanism develop, a sectioning process would be required for each of a number of points on a loading curve for just one set of test conditions.

There was also some concern that the identification of mechanisms would be far from easy or as clear cut as would be hoped for.

The other approach would involve the use of a sectioned model such as has often been carried out with sand retained behind a rigid transparent wall which, when loaded with a model footing, will permit the direct observation of overall failure mechanisms. Such an example of this is shown in Figure 1. Unfortunately, while this technique may permit an approximate qualitative picture of deformation patterns, it is sometimes very difficult to translate these observations into a complete failure mechanism without some means of recording and quantification. This would appear to be even more critical for a material such as soft rock which, because it is much less compressible than a sand, would only experience very small deformations. However, as had been demonstrated by Butterfield et al. (1970), stereo-photogrammetric techniques are ideal for the determination of displacement fields in sands. Therefore, these techniques may also be of some considerable use for quantifying the displacement fields, and therefore the failure mechanisms, in soft rock.

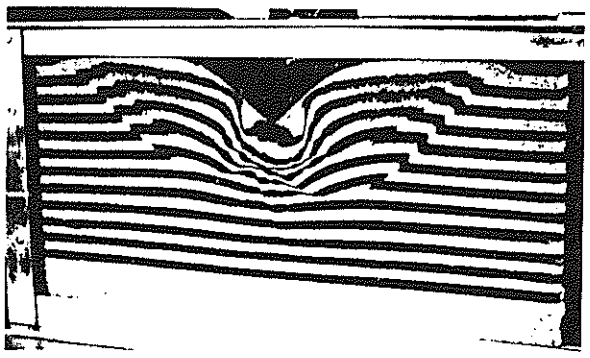

Figure 1 Failure mechanism for a footing on sand

However, as in the early stages of the overall project it was not clear which of the two techniques would be most suitable for soft rock, both were attempted. It was hoped that if both yielded the same failure mechanisms, a great deal more confidence could be placed in the results obtained. This paper describes the principles, techniques and some results obtained with the stereo-photogrammetric method.

3. PRINCIPLE OF THE STEREO-PHOTOGRAMMETRIC TECHNIQUE

Most geotechnical engineers would be familiar with the technique of stereo-photogrammetry as applied to aerial photography and the production of contour maps. Basically, the technique involves a moving vertically oriented camera which takes a series of high quality photographs from an aircraft as it flies over the area to be mapped. By arranging two successive photographs with a significant proportion of subject overlap side by side under a stereo viewer, so that the right eye looks at the right hand photograph and the left eye at the left hand photograph, it is possible to produce a stereo image for the area of overlap. This image is exactly the same as the image of relief that would have been seen by the viewer from an aircraft.

By measuring the difference in parallax between two points in successive photographs, it is possible to establish the difference in the elevations of these points. By continuing this process for a great many points, it is possible to develop contour lines for the whole area. Further details of these well developed techniques may be found in most major textbooks on surveying.

When stereo-photogrammetry is applied to measuring displacement fields, it is no longer the object that stays stationary while the camera moves, but it is the camera which stays stationary while the object (or part of it) moves. The effect is the same with a pair of successive photographs viewed as a stereo pair under a stereoscope. Points which have not moved will appear to be fixed in a constant horizontal plane whereas points that have moved in a specified direction (as will be defined below) will appear on a plane above or below the zero movement or datum plane depending on the direction of relative movement of the corresponding pair of points. The more the displacement experienced by a point, the higher will be the apparent difference in elevation of that point from the datum plane. It follows that a three dimensional image will be produced which can be contoured in exactly the same way as a pair of normal stereo aerial photographs, except that the contours are in terms of displacements rather than elevation.

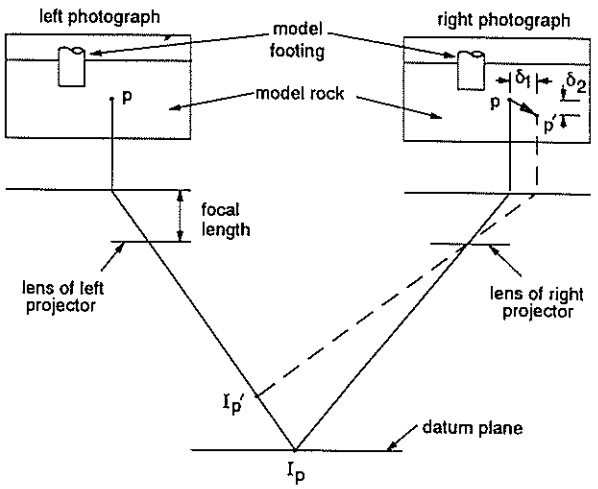

Figure 2: Principle of a stereo image from a displacement field

Figure 2 demonstrates how the stereo image is produced. Consider two successive photographs of a model footing which is embedded in a rock. The photographs have been taken at different points on the loading curve of the footing. The left photograph shows the location of a specific point at p while the right photograph shows that the same point has moved from p to p'. (Note that the amount of movement has been exaggerated for the purposes of clarity). Had there been no movement, then as shown in Figure 2, the image of p would have been at I_p. However, with movement from p to p', the image has moved to $I_{p'}$. Clearly, when viewed as a stereo pair, $I_{p'}$ would appear to be above I_p (or any other zero movement point), and this height difference would be directly proportional to the left-right component of movement, δ_1.

With a knowledge of the focal lengths of the projectors and the geometry of the stereo viewing system, it is possible to derive a contour diagram which would give the horizontal movements of all points in the displacement field. It should be noted that with the pair of photographs oriented as shown in Figure 2, it is only possible to determine horizontal displacements parallel to δ_1. In order to determine the vertical displacements parallel to δ_2, the pair of photographs should be rotated 90° and the contouring process repeated. It may be of interest to note that by comparing displacement measurements of the model footing itself (made directly with displacement transducers) with points that are known not to move, it is possible to check the calibration of the displacement contouring process for any pair of photographs. If the total displacement fields in any component direction were required to be measured, then one of the photographs used should be one taken before loading commenced.

It is important that the image created by the object in the photographs has sufficient texture to permit a clear stereo image. This would normally be possible with materials such as rocks which do contain some form of texture or particle definition such as occurs with sands. However, if the rock appeared to be completely homogeneous as perhaps a remolded clay, then it would not be possible to create a stereo image without some artificially added texture such as ink markings. Further details of the technique may be found in Butterfield et al. (1970). According to Butterfield et al., the method is capable of measuring displacements to an accuracy of at least 0.01 mm.

4. EQUIPMENT AND PROCEDURES

A reasonably robust test rig had to be specifically constructed to house the model pile embedded in rock. Figure 3 shows a diagrammatic plan of the rig, while Figure 4 shows a general view and Figure 5 shows the view from the camera position. It should be noted, however, that the actual photograph taken from the camera for production of the stereo images would have been taken much closer to the test rig so that it was only the test window that was included.

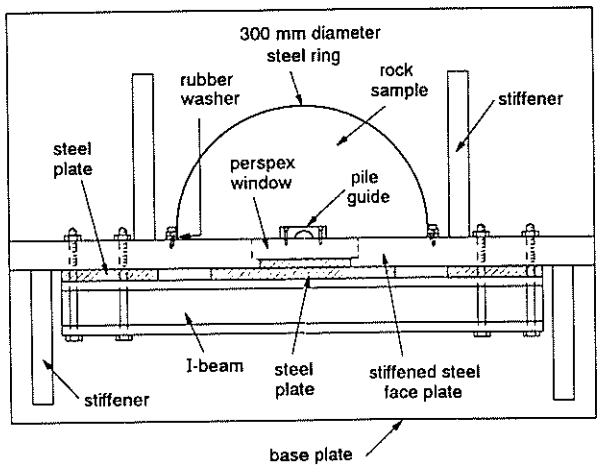

Figure 3: Diagrammatic plan view of test rig

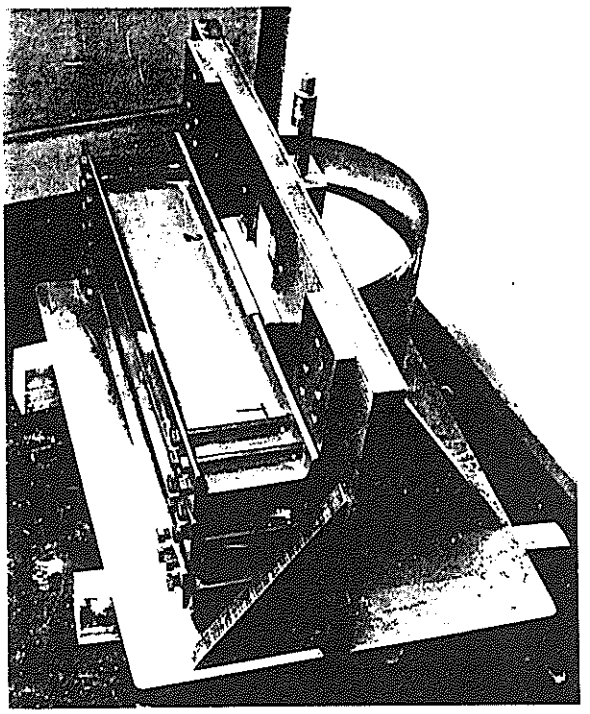

Figure 4: General view of test rig

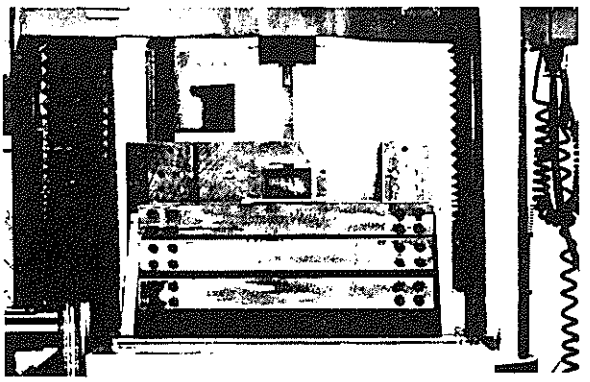

Figure 5: View of front of test rig in loading frame

The actual rock sample consisted of a 300 mm diameter x 300 mm high semi-cylindrical block of synthetic mudstone (Johnston and Choi, 1986) which was contained in a steel ring, the thickness of which was selected to simulate the equivalent stiffness of a semi-infinite rock mass. It should be noted that the smaller diameter plaster sample shown inside the steel ring in Figure 4 was never used for testing. The cut diameter of the block of mudstone was confined by this steel ring to be flush against a 33 mm stiffened steel face plate which contained a 100 mm wide perspex window. Additional steel plates and three I-beams were also used to stiffen the steel face plate. The reason for the large amount of stiffening was to prevent any movement of the perspex away from the test sample when the model pile was loaded. The model pile itself consisted of a 25 mm diameter semi-circular steel rod which passed through a loading guide and was held hard against the perspex window.

When a test was being prepared, the three I-beams were bolted to the face plate in such a way that the area around the base of the model pile could be clearly observed through the window. For example, as shown in Figure 5, where a near surface test is being conducted, the upper I-beam position is left empty while the lowest three positions are occupied. Had the test location been deeper, then one of the lower I-beams would have been omitted.

Each test was conducted with the test rig positioned on the loading platform of a Baldwin universal testing machine. The model pile was connected to the crosshead of this machine (see Figure 5) and it was loaded by lowering the crosshead. The photographs were taken by a good quality 35 mm camera mounted with its focal axis at right angles to the plane of the perspex window. It is important that a cable release be used to activate the shutter mechanism as any movement of the camera would have a major influence on results. The camera was sufficiently close to the test rig so that the field of vision included the whole of the visible test area. It was found that good quality commercial film was adequate when the test location was illuminated by studio lighting. Photographs were taken at suitable intervals so as to observe a reasonable progression of mechanisms as they developed. It was found that about 10 photographs taken from zero load to failure was adequate to clearly define these mechanisms. Further details may be found in Choi (1984).

5. RESULTS

Figure 6 shows one of the photographs taken during the application of load to the surface footing. This was used as one of a pair to establish displacement fields. Unfortunately, while a stereo pair of photographs could be presented here, it would not be possible to view these to produce a three dimensional image without at least a simple stereo viewer. Clearly this is somewhat difficult in the context of a published paper.

When a pair of photographs representing the initial zero movement state of the footing and a relatively advanced state of loading were viewed, the variations of apparent heights representing the different amounts of displacement experienced were very clear.

Indeed, the apparent cliffs which represented the opening of cracks or the development of shear planes were very marked. On the basis of these observations, it was comparatively easy to identify the mechanisms which led to failure.

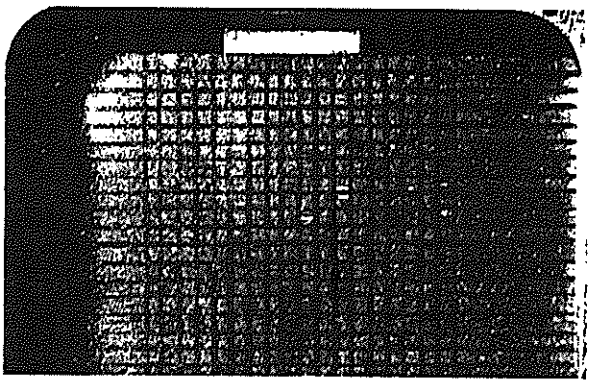

Figure 6: One of a stereo pair of photographs

The mechanisms identified by use of the stereo-photogrammetric method were in reasonable agreement with the limited observations made as a result of sectioning rock samples after conducting model pile tests as described earlier. These in turn were similar to the field mechanisms reported by Williams et al. (1980). Typical mechanisms associated with the development of failure for a model pile (length to diameter ratio greater than 2) in a soft rock are shown in Figure 7.

6. CONCLUSIONS

As part of an investigation into the development of a numerical model to predict the response of a loaded foundation on soft rock, it was considered important that the model should predict the mechanisms of failure that would actually occur. In order to determine these mechanisms, two groups of laboratory model tests were undertaken. One group involved observations made by sectioning test samples after various stages of loading had been applied and the other group involved observations made of a sectioned model test while loading occurred.

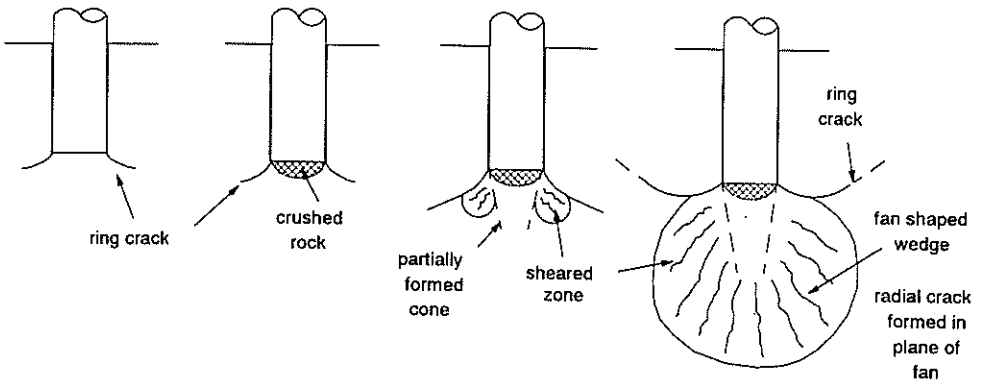

Figure 7: Typical failure mechanisms for a model end-bearing pile in rock (L/D > 2)

The deformations and mechanisms in the latter case were monitored by means of stereo-photogrammetric techniques carried out in accordance with the principles presented by Butterfield et al (1970).

It would appear that the stereo-photogrammetric technique can be applied to quantify displacement fields in soft rock for plane and axisymmetrical problems and represents a considerable saving in time and effort as compared to more conventional methods.

7. REFERENCES

Butterfield, R., Harkness, R.M. and Andrawes, K.Z. (1970). A stereo-photogrammetric method for measuring displacement fields. Geotechnique, Vol. 20, No. 3, pp 308-314.

Choi, S.K. (1984). The bearing capacity of foundations in weak rock. Ph.D. Thesis, Monash University, Melbourne.

Choi, S.K. and Johnston, I.W. (1985). Failure mechanisms of foundations in soft rock. Proc 11th Int. Conf. on Soil Mech. and Foundn Engng, San Francisco, Vol. 2, pp 515-518, A.A. Balkema, Rotterdam.

Johnston, I.W. and Choi, S.K. (1986). A synthetic soft rock for laboratory model studies. Geotechnique, Vol. 36, No. 2, pp 251- 263.

Roscoe, K.H., Arthur, J.R.F. and James, R.G. (1963). The determination of strains in soils by an X-ray method. Civ. Eng. and Publ. Works Rev., Vol. 58, pp 873-876 and 1009-1012.

Williams, A.F. (1980). The design and performance of piles socketed into weak rock. Ph.D. Thesis, Monash University, Melbourne.

Williams, A.F., Johnston, I.W. and Donald, I.B. (1980). The design of socketed piles in weak rock. Proc Int. Conf. on Struct. Foundns on Rock, Sydney, Vol. 1, pp 327-347, A.A. Balkema, Rotterdam.

Determination of Retaining Wall Stability using the Finite Element Method

I.B. DONALD
B.C.E., M.Eng.Sc., D.I.C., Ph.D., M.I.E.Aust.
Associate Professor, Monash University, Melbourne
A.T.C.GOH
B.E., Ph.D. (Monash), M.I.E.Aust.
Lecturer, Swinburne Institute of Technology, Melbourne

SUMMARY Conventional methods of stability analysis for retaining walls are compared with two approaches based on finite element analyses, namely the modified conventional analysis and the recently developed Nodal Displacement Method (NDM). The NDM has considerable potential as it is able to model construction sequences and gives due attention to soil and wall displacements as well as stresses. The physical meaning of safety factor is discussed and the NDM shown to be capable of giving a range of values, depending upon which problem variables are considered to be significant.

1. INTRODUCTION

The safety of gravity and semi-gravity retaining walls is conventionally assessed by limit equilibrium methods in which a failure mechanism is postulated and the restoring and disturbing forces or moments are compared. Many of these analytical methods are unable to take into consideration some of the significant variables likely to affect the stability of the retaining wall. These include the deformation properties of the backfill and foundation subsoil, the stiffness of the retaining wall, the soil-structure interaction and the associated construction sequence.

Application of numerical analyses such as the finite element method permits the calculation of stresses and deformations in walls and retained soil, with reasonably appropriate modelling of most major variables. However, the conversion of stresses and displacements into a meaningful measure of safety against wall instability is not straightforward and the use of stresses from an F.E. analysis in conventional calculations of safety factors against overturning and sliding is highly questionable, as these stresses will not necessarily be valid for a wall on the point of failure.

An alternative method, the Nodal Displacement Method, is currently under development and has shown considerable potential for calculation of the stability of slopes, foundations and retaining structures, in addition to giving valuable information on the deformations of these structures under working conditions. The method is described briefly in this paper and some applications to gravity and cantilever retaining walls discussed.

2. COMPUTER PROGRAM

The program used in this research was written by Goh (1984) and uses an elastic-ideally plastic formulation with either fully associated or non-associated flow rule. The mesh consists of either four or eight noded isoparametric quadrilaterals, with four or six noded slip elements at all soil/concrete interfaces. Incremental excavation and filling may be modelled so that realistic construction sequences may be simulated, e.g. excavation to foundation level, placement of concrete, backfill placing in compacted layers and subsequent rise in ground water level.

3. CONVENTIONAL ANALYSES

In conventional stability analyses it is assumed that fully active conditions have been mobilised behind a wall at the point of failure. Safety factors against sliding and overturning may then be calculated as indicated in Fig. 1 for simplified gravity and cantilever walls.

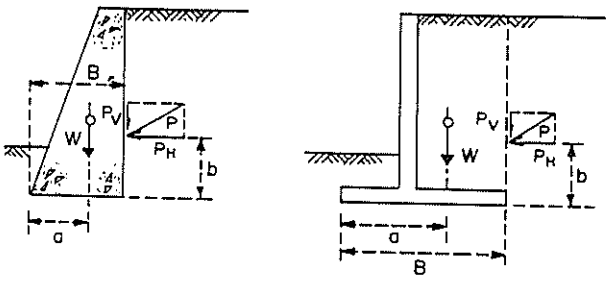

Figure 1 Forces acting on a retaining wall

$$F_{overturning} = \frac{W.a + P_v.b}{P_H.b} \quad (1)$$

$$F_{sliding} = \frac{c_B.B + (W + P_v) \tan \delta_B}{P_H} \quad (2)$$

where P_H and P_v, the components of active force, P_A, may be calculated by approaches such as given in CECP 2 (1951). The method pays no attention to soil stiffness and deformations are not calculated but assumed to be constrained to acceptable values by the choice of appropriate design values of safety factor.

4. MODIFIED CONVENTIONAL ANALYSES

If an F.E. analysis of a wall has been carried out, the stresses acting on the real or virtual back of a wall may be used to derive values of P_v and P_H for insertion in (1) and (2). These stresses are estimates of the actual values on the wall for its in-service condition and, for the active case, may be significantly higher than for fully mobilised active conditions. Their use in such a modified conventional analysis would therefore lead to lower values of safety factor than the simple conventional method. The F.E. stresses would of course be applicable to wall structural design and estimates of wall and soil displacements but, for stability analyses, at best the calculated safety factors could be looked upon only as indications of the likelihood of the

initiation of large scale movements. Such safety factors could be used in design, but adopted values would need to be calibrated against experience.

5. NODAL DISPLACEMENT METHOD

Many of the problems and assumptions of the conventional and modified conventional methods may be avoided by using the Nodal Displacement Method (NDM). In the definition of safety factor used in the majority of limit equilibrium analyses

$$\tau_f = \frac{s}{F} = \frac{1}{F}(c + \sigma \tan\phi) \qquad (3)$$

i.e. the safety factor is a factor on soil strength and implies that, if the field strength should reduce to $\frac{1}{F}$ of its current value, failure would be imminent and large displacements would occur.

In the NDM analysis a series of F.E. calculations of mesh nodal displacements is carried out, while incrementally reducing - or increasing - strength parameters c and ϕ through application of a multiplication factor, N ($\gtrsim 1$). The safety factor is then given by $\frac{1}{N}$ for the situation where displacements at critical nodes in the F.E. mesh show large increases for small changes in N, i.e. a failure mechanism is about to develop. This principle is illustrated in Fig. 2.

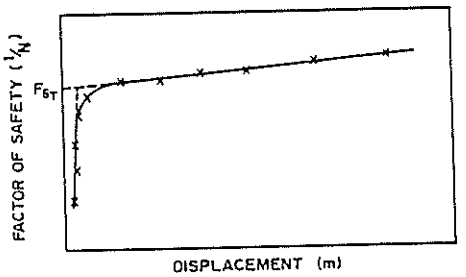

Figure 2 Principle of Nodal Displacement Method

The method possesses a number of obvious advantages - the failure mechanism need not be specified (and is indeed determined by the analysis), soil stress-strain properties are correctly allowed for, critical parameters may be pinpointed by varying them independently and in combination and no assumptions are required concerning changes in soil stresses from the equilibrium to the failure state.

On the debit side considerable computer time may be needed, though with experience this can be minimised, the analysis is carried on to large strains which could limit the accuracy at large displacements and the final result depends on correct choice of critical node. These are not severe criticisms as the critical or turn-over point in the plot normally occurs at relatively small strains and can be clearly defined by simple geometrical constructions and it is usually obvious where excessive deformations will first become apparent, to guide in the selection of critical nodes. It is advisable to prepare nodal displacement plots for a number of presumed significant nodes and it will usually be found that the derived factors of safety fall within a narrow range.

Applications of the NDM to a range of problems have been given by Tan and Donald (1985), Donald et al (1985), Donald and Giam (1988) and Goh (1990).

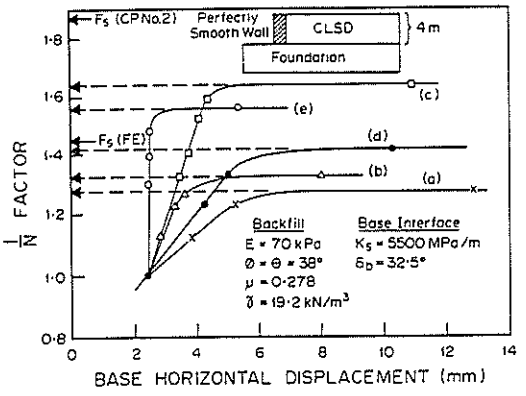

(a) smooth wall

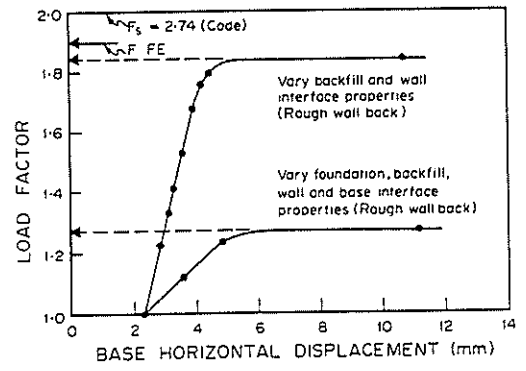

(b) rough wall

Figure 3 NDM plots - gravity retaining wall

6. EXAMPLES

6.1 Gravity Wall

Results for a 4 m high, 1.4 m wide concrete gravity wall with a slightly clayey sand (CLSD) backfill and foundation are shown in Fig. 3.

Both smooth and rough wall/soil interfaces were considered and the design parameters are given in the Figure. The effective stress cohesion for the clayey sand, based on triaxial tests, was small enough to be ignored. The results for a smooth wall back are given in Fig. 3 (a) and for a rough wall back in Fig. 3 (b) and a summary is included in Table I. This Table also contains values of safety factor from conventional and modified conventional sliding and overturning analyses.

For the smooth wall the safety factors cover a wide range from 1.27 to 1.87, the latter being for a conventional sliding analysis. As expected, use of equilibrium F.E. stresses in a sliding analysis gives a lower value of F = 1.45. The NDM values range from 1.27 to 1.64, depending on which parameters are varied - the choice being from ϕ(backfill), ϕ(foundation) and δ(base). The unlikely separation of base interface from foundation soil behaviour has limited the combinations of interest to the five listed in Fig. 3.

TABLE I

COMPARISON OF RESULTS
(INCREMENTAL CONSTRUCTION ONLY)

SAFETY/LOAD FACTOR				
Conventional		Modified Conventional		Nodal Displacement
Sliding	Overturning	Sliding	Overturning	
CLSD BACKFILL AND FOUNDATION				
Smooth Gravity Wall (4 m ht.)				
1.87	1.54	1.45	1.54	(a) 1.27 (b) 1.33 (c) 1.64 (d) 1.41 (e) 1.56
Rough Gravity Wall (4 m ht.)				
2.74	2.55	1.90	2.29	(e) 1.59 (f) 1.27 (g) 1.84
Smooth Cantilever Wall (8 m ht.)				
2.07 (Rankine)	3.90	1.68	3.42	(a) 1.55 (c) 1.60 (e) 2.08
SDCL BACKFILL, CLSD FOUNDATION				
Smooth Cantilever Wall (8 m ht.)				
2.86 (Rankine)	7.83	1.39	3.04	(a) 1.07 (c) 1.25 (e) 1.20

Note: (a) = vary backfill, foundation and base interface prop. (b) = vary backfill and base interface prop.
(c) = vary backfill prop. only (d) = vary foundation and base interface prop.
(e) = vary base interface prop. only (f) = vary backfill, foundation, wall interface and base interface prop.
(g) = vary backfill and wall interface prop.

The conventional sliding factor equation may be rewritten as either

$$P_H \leq \frac{c_B}{F} . B + (W + P_v) \frac{\tan \delta_B}{F} \qquad (4)$$

or $$F.P_H = c_B B + (W + P_v) \tan \delta_B \qquad (5)$$

(4) may be interpreted as applying the safety factor only to the base interface properties, ϕ (backfill) and ϕ (foundation) being presumed reliably known, while (5) implies that only ϕ (backfill) is not known with confidence - i.e. a decrease in backfill tan ϕ to $\frac{1}{F}$. tan ϕ leads, approximately, to an increase of lateral thrust to $F.P_H$.

Neither of these interpretations necessarily represents real situations adequately, but it should be noted that cases (e) and (c) in Fig. 3 are closest to the above interpretations, and the value from (c) of F = 1.64 is not greatly different from the conventional F = 1.87. The value from (e) of F = 1.56 is very close to the conventional overturning value of F = 1.54 but it is worth emphasising that the NDM analysis does not assume a specific failure mechanism but calculates the wall displacements, which include both translational and rotational components. The lowest value of F = 1.27 arises from allowing ϕ (backfill), ϕ (foundation) and δ(base) all to vary by equal proportions, implying that the design values for all three could be equally, unconservatively in error simultaneously. This seems an unlikely occurrence and judgement would have to be exercised when deciding which of the many safety factors is most relevant.

For a rough wall back with δ = 29° the safety factors are generally increased (Table I), though the lowest NDM value remains at 1.27, for simultaneous variation of all four significant parameters. Varying only the backfill ϕ and wall back δ gives F = 1.84, which is still well below the conventional (Code) values for sliding and overturning, though close to the modified conventional value of 1.90. The difference between 1.27 (f) and 1.84 (g) highlights the importance of base interface properties for stability, a conclusion which is reinforced by the results for the smooth wall also. However, other analyses for an increased foundation stiffness (modular ratio 5 : 1) showed that the base interface influence decreases with increasing modular ratio.

6.2 Cantilever wall

Results for an eight meter high cantilever wall are shown in Fig. 4 and Table I for a clayey sand (CLSD) foundation and either a clayey sand or a sandy clay (SDCL) backfill. The SDCL has properties c = 16 kPa, ϕ= 28° while the CLSD has the same properties as in the previous example. Varying all properties together gives the lowest NDM value of F = 1.55, while varying only the base interface properties gives F = 2.08, very close to the conventional sliding factor of F = 2.07. With the SDCL backfill and the critical $\frac{1}{N}$ value of 1.25, for variation of backfill properties only, lateral pressures on the virtual wall back were still significantly higher than fully mobilised active values and $\frac{1}{N}$ = 1.46 , with accompanying lateral movements of 33 mm, was required for full active state

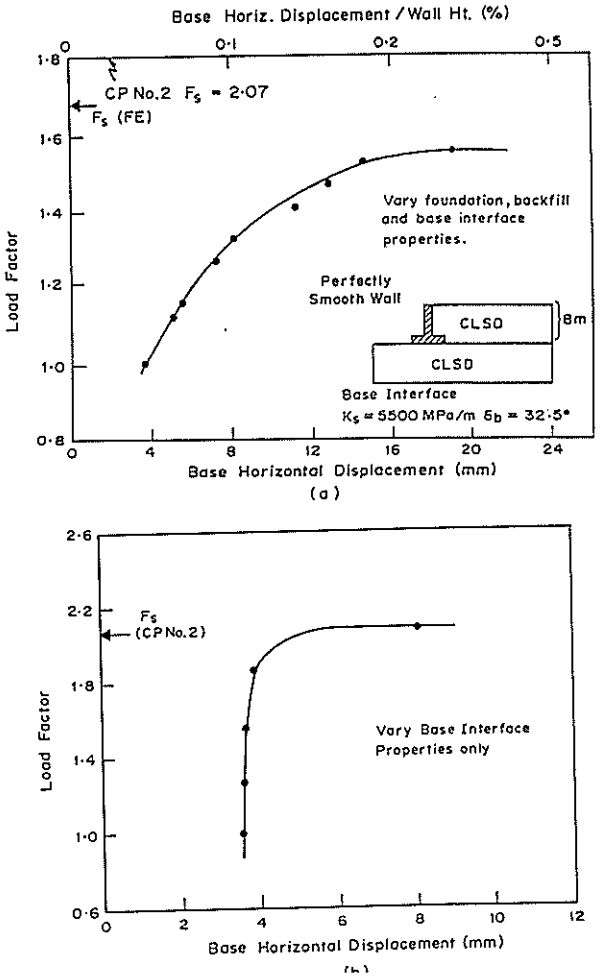

Figure 4 NDM plots - cantilever wall

mobilisation. This indicates that the conventional assumption that lateral pressures will reduce to active values just prior to failure at small displacements may not always be valid. It is also noteworthy that all three NDM values for the SDCL backfill fall in a narrow range, while the conventional analyses give much higher safety factors.

7 DISCUSSION

From the preceding results it may be seen that the concept of safety factor in retaining wall design is a rather imprecise one, unless the conditions and restrictions under which the safety factor has been derived are clearly defined. In some cases a physical meaning may be attached to a particular definition or method of analysis, as was done with (4) and (5), yet it is not immediately obvious what is the correct definition for a particular situation. The Nodal Displacement Method seems to have several advantages over conventional methods, in particular its avoidance of the need to postulate a failure mechanism and its ability to separate the influences of major variables, either individually or in various groupings. The designer may then use knowledge of which parameters are likely to be the least reliable when making a choice of safety factor definition. Application of the NDM obviously needs additional research, particularly in allowing different degrees of variation for various parameters - something akin to a limit state partial load factors approach. Guidelines will also have to be drawn up for acceptable safety factors for the various definitions, as some of the differences in Table I are alarmingly large. Problems involving water behind the wall have not yet been investigated and cohesive backfills obviously require additional investigation.

Based on experience to date it is recommended that the lowest NDM safety factor be calculated, varying all parameters simultaneously, and a value of between 1.25 and 1.50 be accepted for cohesionless soils. For walls where stability is not a problem but deformations are critical, the NDM provides all data required for displacement-controlled design.

8 CONCLUSIONS

An alternative method of retaining wall analysis has been presented, using the Nodal Displacement Method applied to finite element analyses. As the method includes calculations of displacements as well as pressures it provides a more realistic modelling than conventional or modified-conventional limit equilibrium solutions. The method is promising, but further work is required before it may be used in routine practice with confidence.

9 REFERENCES

Civil Engineering Code of Practice, No. 2, (1951). Earth Retaining Structures. Inst. Struct. Eng., London

Donald, I.B. and Giam, P.S.K. (1988) Application of the Nodal Displacement Method to slope stability analysis. Proc. 5th A.N.Z. Conf. Geomech, Sydney, pp 456-460.

Donald, I.B., Tan, C.P. and Goh, A.T.C., (1985) Stability of geomechanical structures assessed by finite element methods. Proc. 2nd Int. Conf. Computing in Civil Engineering, Hangzhou, China, pp 845-856.

Goh, A.T.C, (1984), Finite element analysis of retaining walls, Ph.D. Thesis, Monash University, Melbourne, Australia.

Goh, A.T.C. (1990), Assessment of basal stability for braced excavation systems using the finite element method, Technical Note, Computers and Geotechnics, 10, pp 325-338.

Tan, C.P. and Donald, I.B., (1985), Finite element calculations of dam stability, XIth Int. Conf. Soil Mech. and Fndn. Engg., San Francisco, pp 2041-2044.

Lateral Soil Movement Loading on Bridge Foundation Piles

T.S. HULL
B.E., Ph.D.
Centre for Geotechnical Research, University of Sydney
P. McDONALD
Dip.C.E., B.E., M.Eng.Sc., M.I.E.Aust.
Manager – Geotechnical Group, Roads Corporation of Victoria

SUMMARY The effects of a soft layer of soil moving laterally, due to vertical loading from temporary construction fill, are assessed from the aspect of possible damage to piles supporting bridge pier foundations. An analysis using boundary element methods is used to predict possible damage to the bridge piles as an aid in assessing the risk of the piles having failed owing to lateral soil-pile pressures being generated in the soft soil. The analysis results supported the generally held opinion that the piles without a pile cap were very likely to have failed, while indications were such that the piles already capped were not over-stressed.

1. INTRODUCTION

This paper presents the history of piles at the site of a bridge over Moonee Ponds Creek, Melbourne, Australia. The usual procedure for the construction of piled bridge foundations is to place approach embankment fills prior to piling, so that the soft ground settlements and associated lateral soil movements have substantially completed prior to piling works at bridge piers. Even small lateral soil displacements occurring after pile placement may over-load the piles already driven for the piers. The permanent bridge approaches consisted of piled roadways extending back to the existing ground surface to eliminate long term subsoil settlements and lateral movements, which would have undoubtedly affected the bridge foundations, even if low bridge approach embankments had been used. In this case, contractors placed temporary access filling out into the stream course, allowing pile driving equipment to gain access to pier positions. This procedure is less costly than providing a temporary staging structure. An analytical assessment of the potential damage to pier piles as a result of lateral soil displacements caused by the temporary access fills during construction, is also presented.

2. PROBLEM DEFINITION

The plan of the bridge site is shown in Figure 1. Piers 1, 2, 3 and 4 were affected by the lateral soil movements resulting from access fill placement. When the problem was noticed, the pile caps and piers had been built at two of the pier locations and only the piles had been driven at the other two locations. The un-capped piles at piers 1 and 2 were deemed to be beyond repair owing to the excessive measured deflections from the design position. The integrity of the capped piles at piers 3 and 4, which had moved less, remained to be assessed. The elements of the problem are described below.

2.1 Embankment Loading History

The access fill on the Melbourne side of the creek was placed about two months before driving of piles at pier 4 and three months before driving of pier 3 piles. The filling material was a crushed scoria placed over layers of woven and non-woven geotextiles. The maximum depth of scoria (discovered during drilling through the access fills after pile movement problems had become evident) was of the order

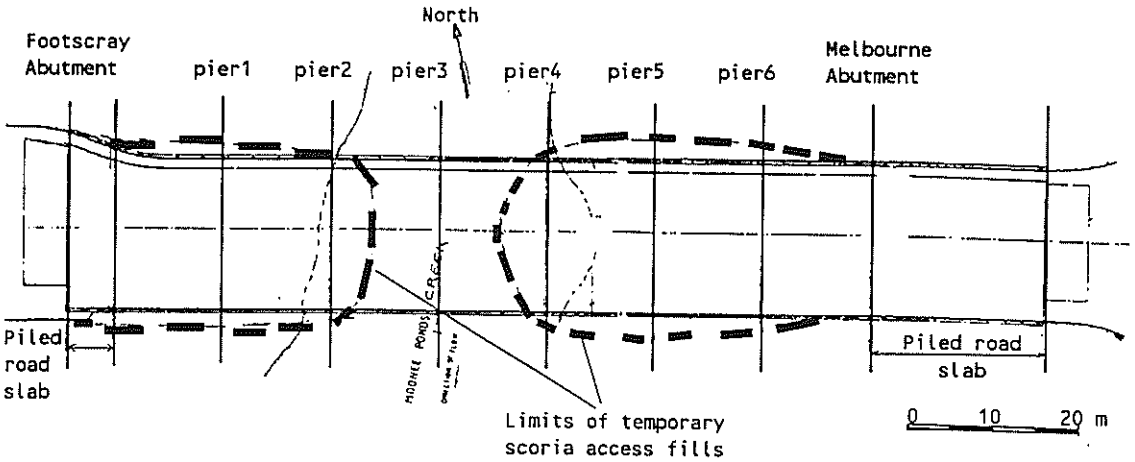

Fig. 1 Bridge site plan - Moonee Ponds Creek, Melbourne.

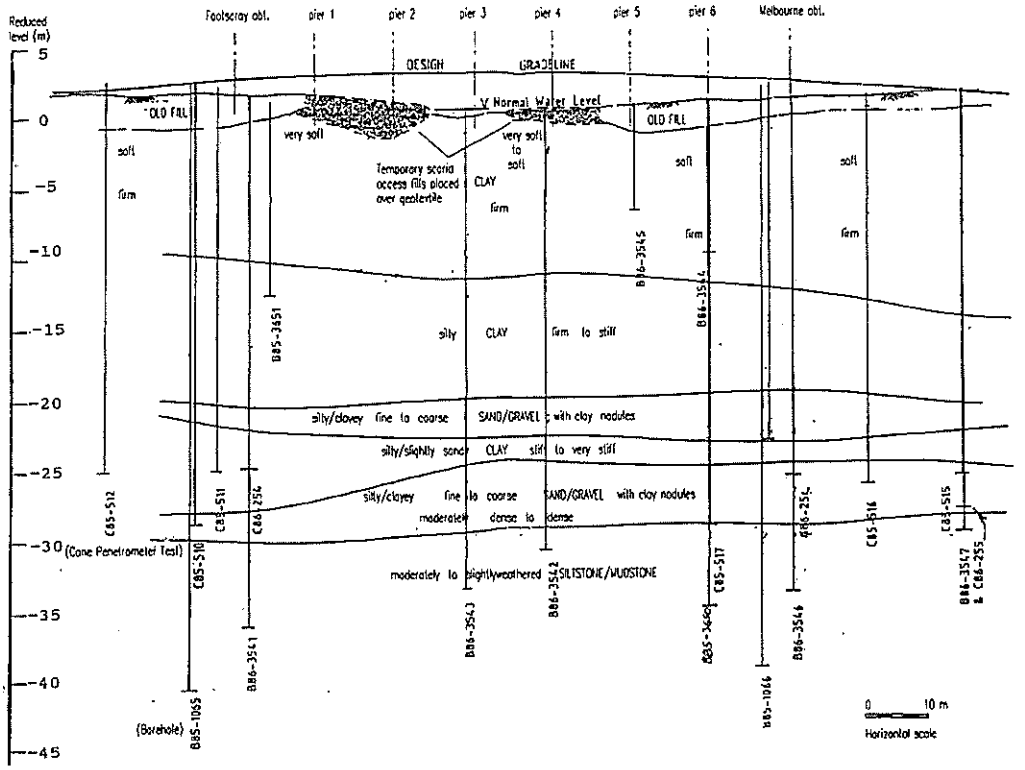

Fig. 2 Sub-surface soil profile - Moonee Ponds Creek bridge site.

of 1 m. Access filling on the Footscray side commenced about four months after that on the Melbourne side. Figure 1 shows the extent of the access fills.

Piles at piers 1 and 2 were driven immediately following access fill placement on the Footscray side, again using a geotextile reinforcing layer under the scoria. After the piling operations were finished the extent and shape of the fill were altered to try and limit the lateral soil movements. The access filling was found to be up to 3 m thick on the Footscray side of the creek.

Construction personnel were unaware of the exact volumes of scoria being placed for the access fills, although it was clear that additional material had been placed from time to time to raise the working platform above the water level. Apart from the obvious vertical settlement, the consequences of the scoria placement with respect to the effects on the piles were not fully appreciated. Following the observations of excessive pier and pile movement, subsequent investigations showed that considerable subsoil flow and displacement had occurred, presumably during placement of the fill material.

2.2 Soil Conditions

The creek bed consists of a very soft wet clay with mud flats exposed at high tide. The subsoil profile indicates very soft to firm estuarine clay to depths of up to 15 m, see Figure 2. Over the uppermost 5 m of this clay, the undrained shear strength varies from 5 to 10 kPa. This layer is weakest on the Footscray side, probably associated with the failure of a temporary site investigation access fill, placed without geotextile strengthening, about two years prior to bridge construction.

Beneath the estuarine clay are interbedded firm to stiff clays, dense sands and gravels overlying the siltstone bedrock at a depth of about 30 m. Figure 2 indicates the arrangement of the major soil layers.

2.3 Foundation Description

Reinforced concrete piles of 350 mm square section, driven about 30 m to found on siltstone, were used in rows of 10 to support the bridge piers. Six spans of 12.8 m supported the bridge and typical axial loads of 187 kN were used in design. The bending moment to cause steel yield was taken to be 130 kNm with no axial load. The concrete piers were typically 500 mm wide, 2 m high and 19 m in length with a pile centre to centre spacing of 1.96 m.

3. ANALYSIS OF PILE RESPONSE

The response of the soil was modelled as an elastic continuum, as employed by Poulos (1973), and based upon the solution of Mindlin (1946), as developed by Douglas and Davis (1964). The pile model is based upon a finite difference formulation of the fourth order differential beam equation. Combination of these two models is described in detail by Hull et al (1991) and is implemented in the computer program PALLAS (Piles And Lateral Loading AnalysiS).

Within the analysis the effect of the soil movement on the pile is accounted for, but the source generating the soil movement has no other influence. The value of the distributed load generated at the interface controls the non-linear response of the model, by the appropriate condition of pile-soil displacement compatibility or zero incremental load being imposed at the pile and soil interface.

The problem had to be simplified such that the major influences were incorporated while the analysis itself remained tractable. Firstly, the plane of the axis of the bridge was chosen as the plane in which the modelling was undertaken. Measurements of pile movements had a symmetry about the bridge axis that suggests errors from this approximation may not be severe. Secondly, the precise soil loading history and subsoil movements were not known and could only be deduced from the measured pile movements, the soil layering and strength data, and information from the inclinometer casing installed through the Footscray fill three months after placement. Representative soil profiles and loading histories were then developed in order to assess the magnitude of the likely problem, rather than attempting a precise reconstruction of the site and history. Thirdly, the influence of the group of piles was omitted, as preliminary analyses including group effects showed no significant alteration from a single pile response.

4. MODEL PARAMETERS

To enable prediction of the likely distribution of bending moment at any point in time a number of model parameters must be estimated, as well as the soil movement profile history.

For analyses of problems with large lateral soil movement, the value that is used for the limiting soil "pressure", p_u transmitted to the pile exerts a major influence on the results. This influence arises because satisfying of the equations of equilibrium for the pile actually determines the pile bending moment and shear force distributions in the regions of failed soil. The pile displacements and rotations are then determined by the stiffness response of the remaining linear soil regions. The important parameters can be seen to be the soil stiffness and the limiting "pressure" developed in the soil due to relative lateral movement of the pile. The soil stiffness is controlled by the value of Young's modulus E_s used and, like the value of p_u, is often correlated with undrained soil shear strength c_u.

4.1 Program Parameter Selection

The values of program input parameters were based upon the distribution of soil undrained shear strength inferred from both Swedish Fall-Cone (Hansbo, 1957) test results and triaxial tests on samples bored from the site, cone resistance readings (assuming $q_c/15 < c_u < q_c/25$) and previous experience at nearby sites (Poulos and Hull, 1989). It was considered appropriate to assess three possible distributions of shear strength; namely a value of 20 kPa constant with depth, a value proportional with depth (c_u = 3z kPa, where z is the depth in metres) and a case intermediate to these having a value of 5 kPa at the soil surface and 45 kPa at 15 m depth. These distributions have been designated by the letters "a","b"and "c"in the figures and are plotted in Figure 3 as functions of depth.

To account for the proximity of the soil surface the chosen failure "pressure" at the pile-soil interface incorporated a bi-linear variation of the coefficient relating p_u to c_u, starting at 2 at the surface and increasing proportionally with depth to 9 at a depth of four diameters and deeper. The distributions of p_u are also plotted in Figure 3.

Correlations of the soil Young's modulus with shear strength suggest c_u multipliers of between 200 and 1000 (Poulos and Hull 1989) and a multiplier of 500 was chosen as the most appropriate. Poisson's ratio for the soil was taken to be 0.45, but this has little effect on the results of the analysis.

A likely distribution of soil movement was more difficult to assess, as it was felt that a reversal of soil movement may have occurred because of the influence of later fill placement closer to the piles and opposite the previous fill. Readings were taken of an inclinometer between piers 1 and 2, over a period of 3 weeks in January 1989 (10 months after filling commenced, and during which no more fill was placed). The readings showed that a movement of about 7 mm occurred at the soil surface, linearly decaying to zero at a depth of 10 m. Groundline pile movements in piers 1

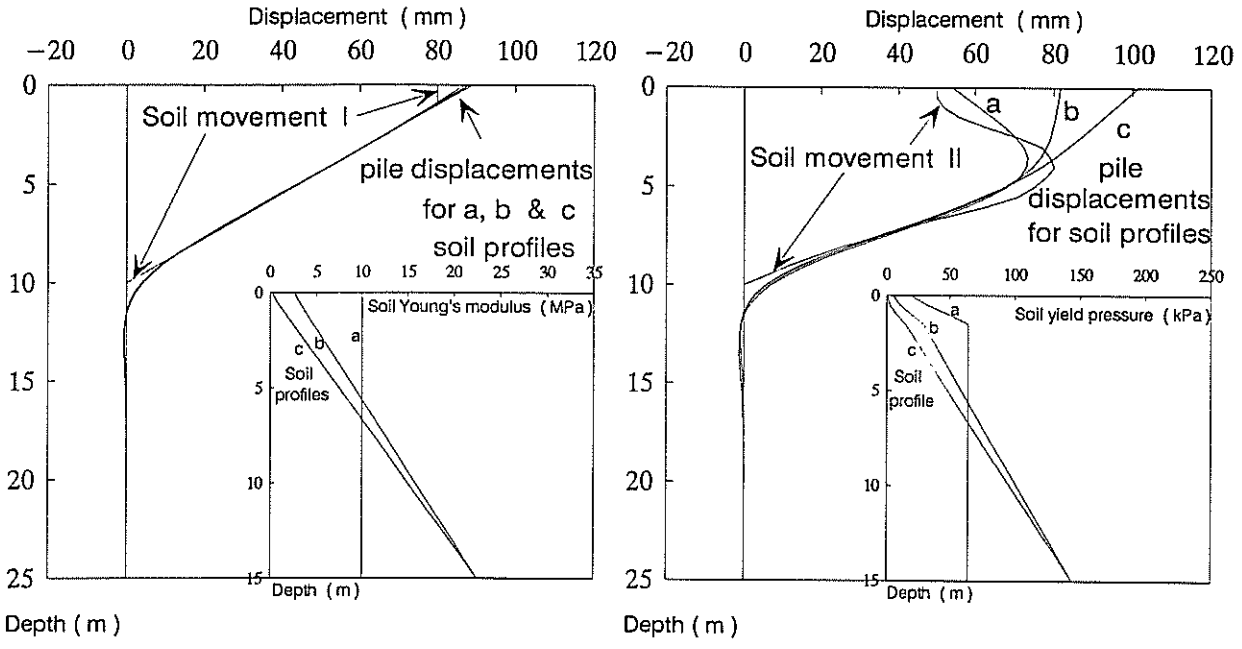

Fig. 3. Deflected shapes of piles for two soil movement profiles and three soil profiles.

and 2 were about 400 mm during the 2 months prior to installation of the inclinometer. The softer soil at the Footscray side, where piers 1 and 2 were located, and the fact that the piles at these locations were driven immediately after placement of fill on the Footscray side explains the excessive deflections they suffered. Piles in piers 3 and 4 would be expected to have experienced less lateral soil movement since; the soil was not as soft, the piles were driven over 2 months after placement of the Melbourne fill and the position of pier 3 was mid-way between the two areas of fill, where some null displacement point might be expected.

With due regard to the above, two distributions of soil movement (I and II) were adopted for the analysis of the piles, which were considered to be upper limits to the expected movements at any pier, as shown in Figure 3.

Other parameters were a pile bending stiffness, EI of 42,600 kNm^2, pile diameter of 355 mm and a modelled pile length of 20 m (the lower 10 m of the pile was in-effective, the critical length being about 6 m).

5. RESULTS

Figure 3 presents the deflected shapes of a pile in the pier for the two adopted soil movement profiles and the three undrained soil shear strength distributions. Only the second soil movement profile, which has a double curvature, causes the pile deflected shape to depart from the imposed soil movement profile. The degree of departure is then related to the properties of the soil in the upper 5 m; the stiffer and stronger soil for the first case causing the pile to more closely follow the imposed soil movement.

Both adopted soil movement profiles have a positive maximum bending moment at a depth of 10 m, where the soil movement is zero, as seen in Figure 4. But, the second soil movement profile results in larger bending moments and a wider variation with soil strength and stiffness, especially at about 4.5 m depth where a negative maximum bending moment is developed. It should be noted that all the cases produce bending moments close to, or exceeding, that required to yield the pile.

The behaviour of the real problem is most unlikely to be the result of a purely monotonic process and, to investigate a possible result of non-monotonic loading, a history of pile loading was simulated. Although employing a simpler loading than that which would have actually occurred, the results illustrate several important aspects of pile response to lateral soil movement. In Figure 5 the response of the pile to a varying imposition of the second soil movement profile (II) and using the soil profile "b" is presented as a function of time, with the major events indicated by symbols in the figure and explained in the legend.

The upper plot in Figure 5 defines the sense of the pile response and presents the movement occurring at the soil surface and the movement of the pile at the groundline as functions of time in months. The pile is seen to move more than the surface soil, and subsequently, upon reversal of the soil movements, to reach the initial pile position some time after the surface of the soil had returned to its initial position. This is a result of permanent deformations in the soil, but there is no indication from the pile deflections that the soil-pile system has reached a steady state of failure.

The values of the maximum positive and maximum negative bending moment plotted in the centre of Figure 5 show that the two maximums are essentially of equal magnitude. But also, that there is a period during the month of November in which small moments are experienced, just before the soil movements changes sense. Both curves of the maximum moments demonstrate that the pile has exceeded the yield moment, both before and after the soil movements reverse direction.

In the lower plot of Figure 5 the pile rotation at the groundline is presented. During the month of September the rotation is seen to reduce (even though the soil movement is still increasing) and is seen to be zero in mid-October

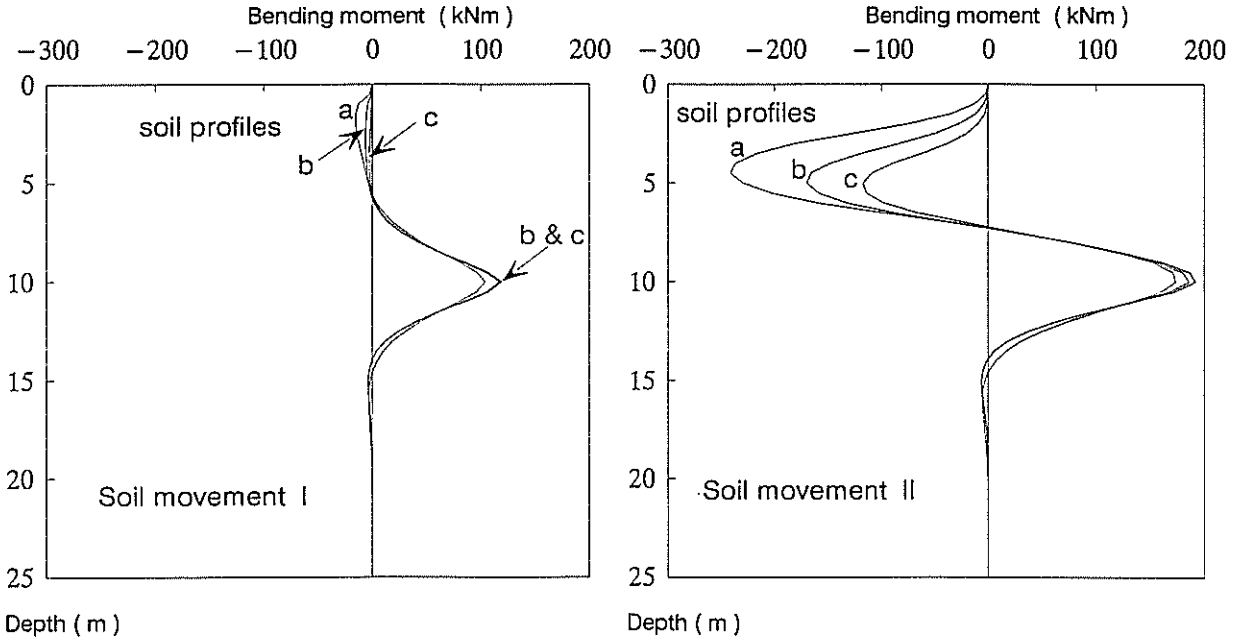

Fig. 4 Bending moment distributions for two soil movement profiles and three soil profiles.

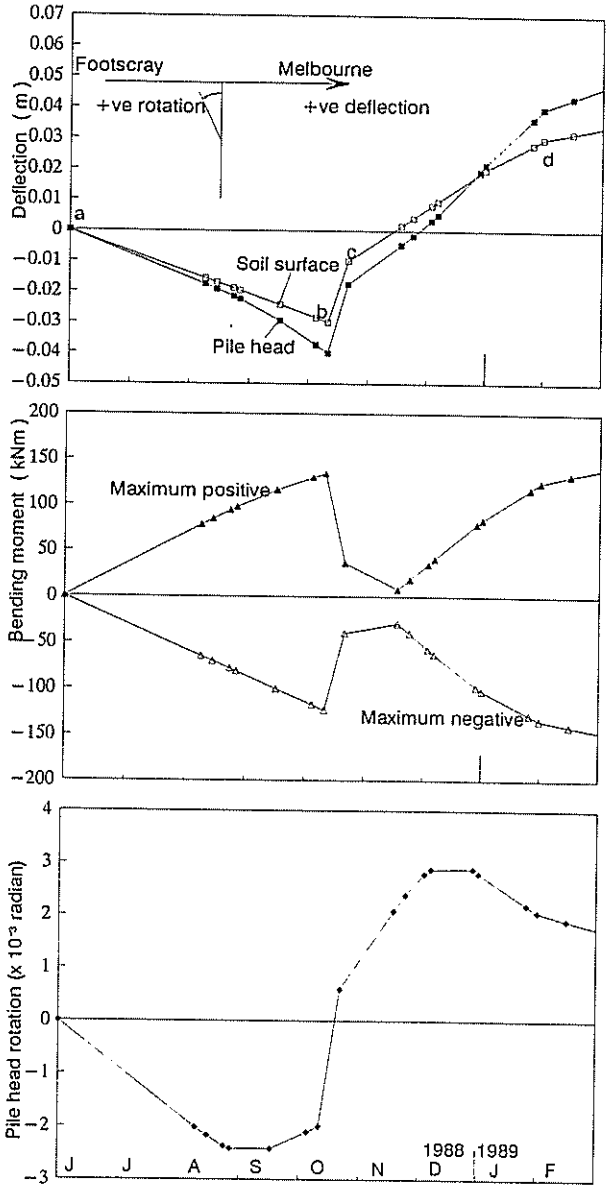

a Beginning modelling of Melbourne fill influence
b Commencement of Footscray fill
c End of main filling operation, Footscray fill
d Removal of some of the Melbourne fill

Fig. 5 Approximate modelling of the pile loading history.

(even though the soil and pile movements are non-zero). Such a reduction of rotation again occurs after December. The progressive growth down the pile of the yielded zone of soil is responsible for these unusual facets of the response.

6. CONCLUSIONS

The most critical aspect of the modelling concerned the distribution of subsoil lateral movements that had occurred after installation of the piles. Since these lateral movements were not accurately known, alternative possible distributions had to be developed taking account of the measured pile movements, subsequent inclinometer readings and soil profile data.

The analyses demonstrated that the deflections of the piles followed the subsoil movements closely, since the pile stiffness was insufficient to offer any significant restraint to the soil movement, except when the lateral soil movement distribution varied rapidly with depth, e.g. near the soil surface for the second soil movement profile. Confirmation was provided that the piles at piers 1 and 2 had probably failed in bending. The piles at piers 3 and 4 appear to be overstressed when the proposed severe soil movements are applied. However, it has been argued that the soil movement would be less severe at piers 3 and 4, and this will lead to reduced bending moments.

The computer modelling provided a valuable insight into the response of the piles to subsoil movements and greatly assisted bridge project decision making with respect to remedial actions. It was decided to replace the piles at piers 1 and 2 and to jack piers 3 and 4 back to their designed positions. Although the lateral pier deflections at piers 3 and 4 were no more than 75 mm, the eccentricity of vertical loading would have been sufficient to overstress the piles in service.

The experience with pile and pier movement at this site emphasised the need for careful consideration of the risk of the effects of temporary construction works over soft, compressible soil. The construction personnel were not aware of a developing problem or the risk associated with the unusually large amounts of scoria being used to construct the access fills.

7. ACKNOWLEDGEMENTS

The research in this paper was carried out as part of an investigation commissioned by the Roads Corporation of Victoria and is presented with the permission of Mr. R. Patterson, Chief Executive of the Roads Corporation. The views expressed are those of the Authors and do not necessarily reflect those of the Roads Corporation.

8. REFERENCES

Douglas, D.J. and Davis, E.H. (1964). "The Movement of Buried Footings due to Moment and Horizontal Load and the Movement of Anchor Plates". Géotechnique, Vol. 14, pp. 115-132.

Hansbo, S. (1957). "A new approach to the determination of the shear strength of clay by the Fall-Cone test". Swedish Geotechnical Inst. Proc. No. 14, Stockholm.

Hull, T.S., Lee, C.Y. and Poulos, H.G. (1991). "Mechanics of Pile Reinforcement for Unstable Slopes". Research Report No. 636, School of Civil and Mining Eng.,Univ. of Sydney.

Mindlin, R.D. (1946). "Force at a Point in the Interior of a Semi-Infinite Solid". Physics 7, p 195.

Poulos, H.G. (1973). "Analysis of Piles in Soil Undergoing Lateral Movement". JSMFD, ASCE, Vol. 99, SM5, pp. 391-406.

Poulos, H.G. and Hull, T.S. (1989). "The Role of Analytical Geomechanics in Foundation Engineering". Foundation Engineering Congress, ASCE, Chicago.

Behaviour of Fixed and Free Head Piles in a Laterally Sliding Soil

T.S. HULL
B.E., Ph.D.
Centre for Geotechnical Research, University of Sydney
C.Y. LEE
B.Sc. (Eng.), M.Sc. (Eng.), Ph.D.
Centre for Geotechnical Research, University of Sydney
H.G. POULOS
B.E., Ph.D., D.Sc.Eng., F.I.E.Aust., F.A.S.C.E., F.A.A.
Professor of Civil Engineering, University of Sydney

SUMMARY The response of a pile in unstable soil, undergoing sliding lateral movement from the surface to a known depth, is analysed using a numerical soil-structure interaction method capable of incorporating non-linear pile-soil interface behaviour.
The effect of head fixity and depth of slide are investigated for a simplified soil profile. Both the linear and full collapse response are modelled and the pile response is presented in terms of generated maximum bending moment and pile shear force at the level of the sliding soil base. The possibility of large pile rotations causing axial stretching of the pile, and the achievement of the yield moment of the pile, result in practical bounds to the applicability of the results.
The solutions presented for maximum bending moment can be used for the design of piles in areas of instability, and the solutions of shear force at the slide depth for the assessment of the potential improvement of slope stability due to the presence of piles.

1. INTRODUCTION

Typical practical situations in which lateral soil movements can become important include bridge pier foundations, off-shore platform piles and rows of piles in soil stabilisation works. The first two situations are examples where piles support a structure and the integrity of the piles, usually related to maximum bending moment, is important; whereas, for the stabilisation piles it is the horizontal resistance provided by the pile as a shear force at the depth of the slide that is required. For many situations the heads of piles in foundations are assumed fixed within a massive pile cap, which restricts pile head rotations. It is possible that the assumption of no rotation is not valid in practice, owing to the large pile head fixing moments that are required. In this paper, the two extreme cases of a fully fixed pile head and a completely free pile head are considered for the case of uniform lateral movement of a layer of soil. The response is investigated in terms of the generated maximum bending moment and shear force at the slide depth, and particular attention is given to the amount of slide movement associated with the attainment of ultimate strength of the pile-soil system.

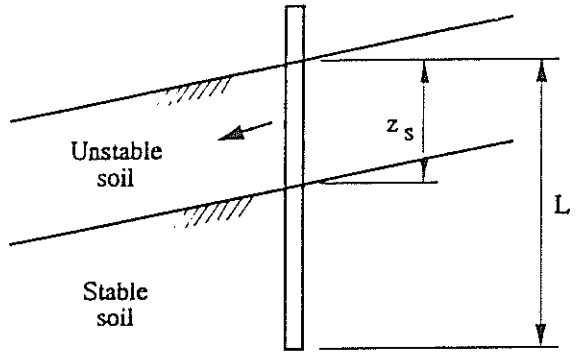

Fig. 1 Problem of a pile in laterally sliding soil.

2. MECHANISMS OF BEHAVIOUR

The problem of a pile penetrating an unstable sliding soil layer and founding within a stable soil region below, is illustrated in Figure 1. Assuming the unstable soil continues to slide and generates a limiting "pressure" p_u (i.e. $p_u d$ is the distributed loading, where d is the pile diameter) at positions along the pile, three possible modes of failure for the pile-soil system arise in which the soil fails. A fourth mode is also possible when the limited strength of the pile precludes full mobilisation of the soil strength, because a section (or sections) of the pile reach the pile yield moment. Figure 2 gives examples of the three basic modes of soil failure and one mode of pile failure, as follows:

i) Short pile failure of the soil occurs along the pile length in the stable soil when it is much shorter than the slide depth, and the pile moves with the sliding soil ("short pile" mode).
ii) Flow of soil around the pile in the sliding layer is possible for some slide depths which are much shorter than the pile length, and the pile remains effectively stationary ("flow" mode).
iii) Intermediate depths to those of the Flow and Short mode require the soil to fail along the pile in both the sliding and stable region, and have large pile rotations ("intermediate" mode).
iv) "Long" pile modes are associated with an incomplete formation of any of the three modes of soil failure, when the yield moment of the pile is reached (here the "short" mode is shown). The standard use of the term "long pile" mode assumes the full plastic moment of the pile has been attained and also that the soil has reached a limiting state of lateral bearing capacity. For the purpose of this paper the "long pile" mode is the result of terminating the analysis when the bending moment at any section first attains the yield moment.

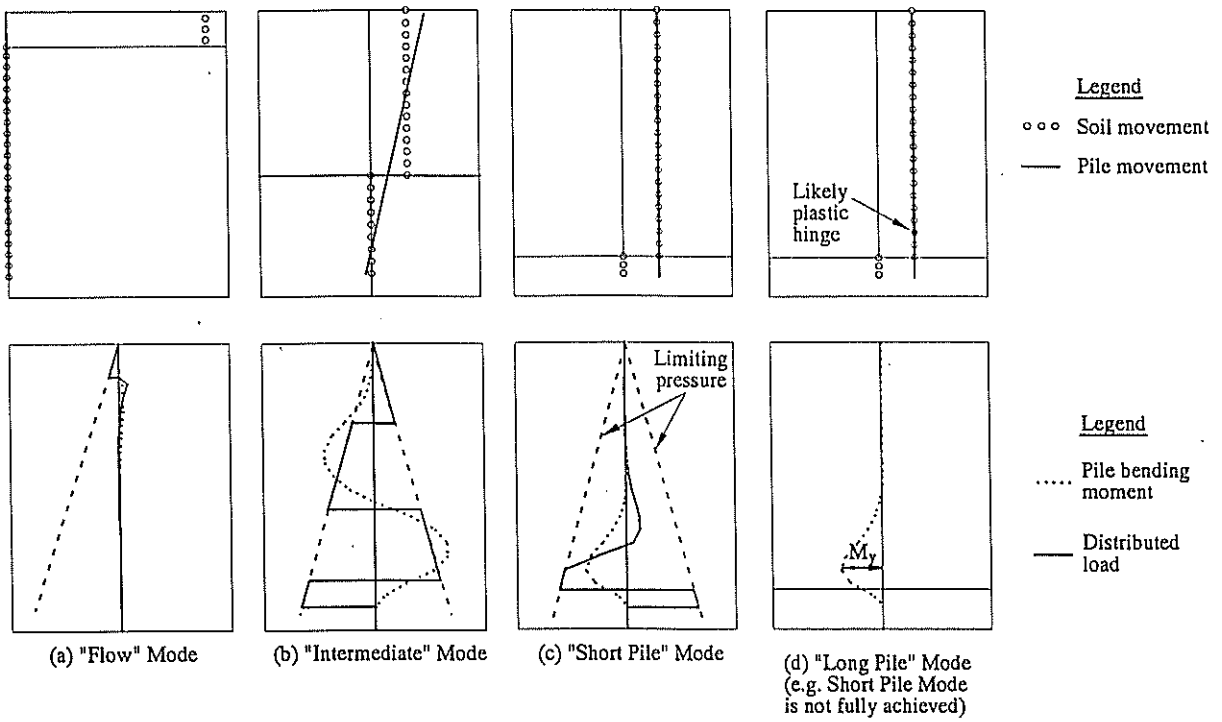

Fig. 2 Examples of distributions of deflection, bending moment and distributed load generated by sliding soil.

3. METHOD OF ANALYSIS

A modified boundary element analysis (Hull et al 1991) was employed to solve for the pile response to lateral soil movements. The analysis can model both pile head and tip loading, with a wide range of boundary conditions. An elastic continuum or spring-based model of the soil, with non-uniform properties with depth, can be specified, Hull (1987). A non-linear response is provided by an interface element that can model both strain hardening and softening responses prior to attaining the ultimate state. The source of the horizontal soil movements, as well as the generation of the shear stresses at the interface between the sliding and stable soil, are not considered beyond the effect of the soil displacing laterally. For example, the vertical movements that may accompany lateral soil displacements are not included.

4. RESULTS OF PARAMETRIC STUDY

In order to be specific, values of parameters required in the analysis were selected to be representative of realistic pile and soil conditions. The values of pile bending stiffness adopted typify reinforced concrete piles of circular section with diameters of 0.5, 1.0 and 1.5 m, or steel tube piles with the same diameters and respective thicknesses of 8, 16 and 24 mm. The pile length was held constant at 40 m. The Young's modulus of the stable soil E_s was taken as either 20 or 50 MPa, consistent with undrained soil shear strength c_u of 40 or 100 kPa for $E_s/c_u = 500$ (e.g. Davies and Budhu, 1986). The sliding soil was assigned a Young's modulus value of half that of the stable soil, to make some allowance for the increase of soil stiffness with depth which commonly occurs in natural deposits. Similarly, the limiting pile-soil "pressure" p_u in the sliding soil was given a value of half that in the stable soil (e.g. Viggiani, 1981), where $p_u = 10c_u$ was used such that $E_s/p_u = 50$.

For the three pile diameters and two values of soil stiffness analyses were carried out for different slide depths. Fixed and free head conditions were modelled.

4.1 Effect of Slide Movements

Curves for different values of slide depth, showing the development of the maximum bending moment and the bending moment at the slide depth as the slide movement increases, are presented in Figure 3. Both the fixed and free head cases for the largest diameter pile and stiffest soil are presented. For the fixed head case the head fixing moment is also shown, while for the free head case the pile rotation at the slide depth is presented.

It is clear that the pile-soil system attains a limiting state at which the generated bending moments do not change for further slide movements. This is a result of the soil lateral bearing capacity being exhausted. Unlike the bending moments, the pile rotation at the slide depth for the free head case continues to increase with slide movement, for slide depths between 36% and 85% of the pile length. This is consistent with the Intermediate mode of failure of a free head pile, where pile rotation is predicted without considering the axial stresses caused by the pile lengthening.

The free head pile reaches the soil limiting state at smaller slide movements than the fixed head pile and smaller moments are generally produced. Even so, the largest calculated maximum moments are much greater than a typical value of pile yield moment of the order of 10 MNm. Obviously, the "long" pile mode will often be observed before the limiting state of the soil occurs.

Similar statements apply for soil with a Young's modulus of 20 MPa except that a higher relative pile-soil stiffness reduces the soil movements needed to develop p_u.

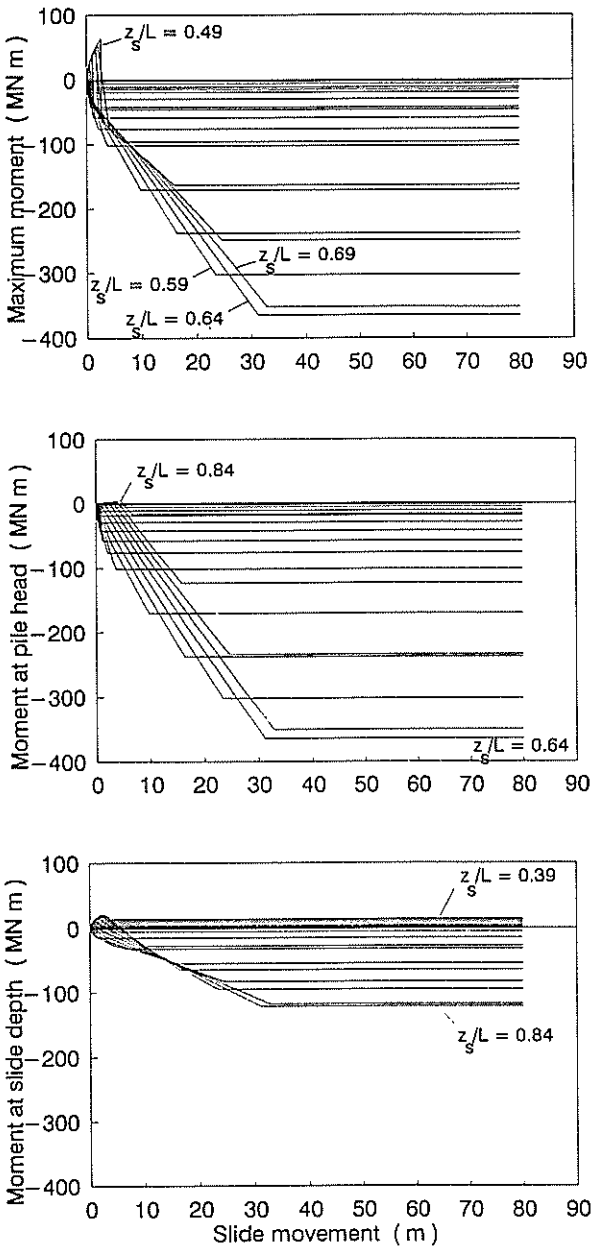

Fig. 3a Bending moment maximum, moment at head and moment at slide depth for fixed–head pile.

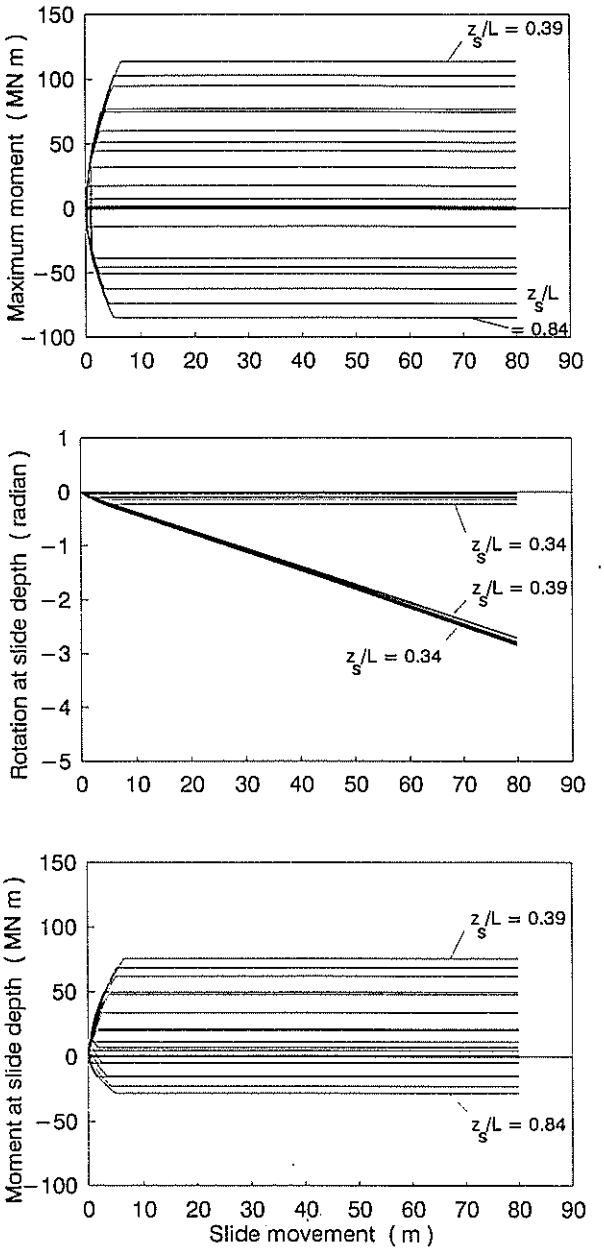

Fig. 3b Bending moment maximum and, rotation and moment at slide depth for free–head pile.

4.2 Deflected Pile Shapes

Figure 4a and 4b clearly shows the three modes of failure where the pile displaced shapes, after an extremely large soil movement of 40 m, are plotted for the stiffer soil.

For slide depths of up to 85% of the pile length the head fixity has some influence on the deflected shape, but for deeper slides the head fixity has no effect. This depth of slide corresponds to the first occurrence of the Short mode of failure (for the free head pile and without allowance for failure of the pile), in which the sliding soil carries the pile through the stable soil.

The deflected shapes of the fixed head pile for the slide depths of 13.5 and 19.5 m (and generally less than 67% of the pile length) illustrate the "flow" mode of soil failure. Whereas, the free head pile only generates the "flow" mode for the shallower depths (less than 36% of the pile length). This is consistent with an enlargement of the extent of the "flow" mode and also the extended range of the "short pile" mode to eliminate the "intermediate" mode when the pile head is fixed.

Unrealistic lengthening of the pile would be required to produce the Intermediate failure mode of the free head pile, and also the fixed head pile failure for slide depths between 50% and 75% of the pile length. However, for the small deformation assumptions of the analysis, the states achieved from the analysis are theoretically correct.

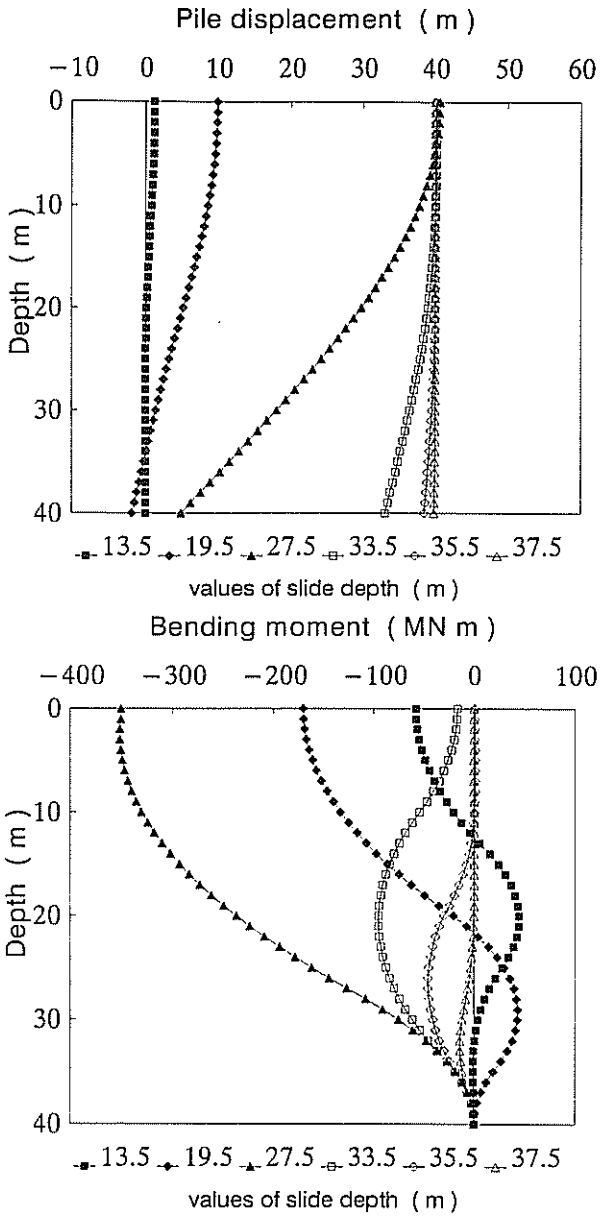

Fig.4a Fixed head pile response with Young's modulus of 50 Mpa and 1500 mm diameter pile.

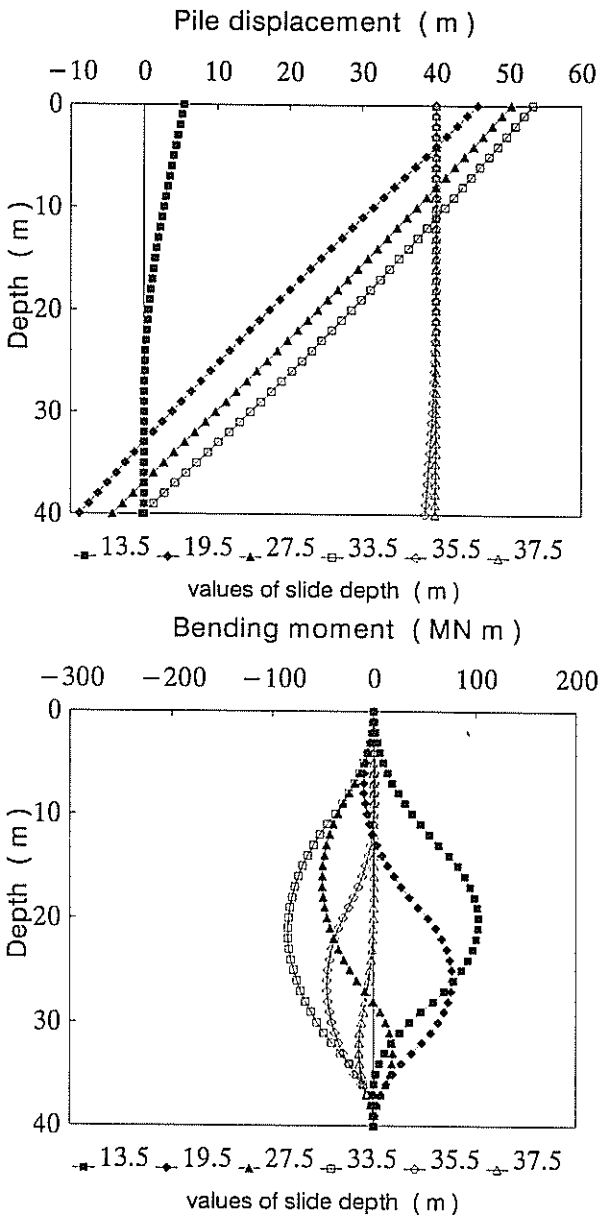

Fig.4b Free head pile response with Young's modulus of 50 Mpa and 1500 mm diameter pile.

4.3 Pile Bending Moments

For both cases of head fixity, the maximum moment must change sign when the location of the maximum moves from one position to another, as indicated by the near vertical lines near the origin of the upper graphs in Figure 3. Large negative bending moments occur at the head for the fixed head pile when the slide depth is less than 70% of the pile length. The free head pile develops much smaller negative bending moments but larger positive bending moments than the fixed head pile.

As seen in Figure 3, the bending moments at the slide depth are predominantly negative for the fixed head pile and positive for the free head pile, although the range of absolute magnitudes are similar.

Figure 4 also displays the distribution of bending moments for selected slide depths. The two curves depicting the deeper slide depths are identical for the fixed and free head piles, as expected for "short pile" modes of soil failure. The "flow" mode does not have a corresponding similarity between fixed and free head responses, because the head fixing moment actually reduces the maximum moment. However, it must be remembered that large head fixing moments may be impossible to achieve in practice.

4.4 Shear Force at Slide Depth

The shear force at the level of the slide, needed for stability calculations, is presented in Figure 5 versus the dimensionless slide depth z_s/L. The stiffer soil, three pile diameters and both head fixity conditions are considered.

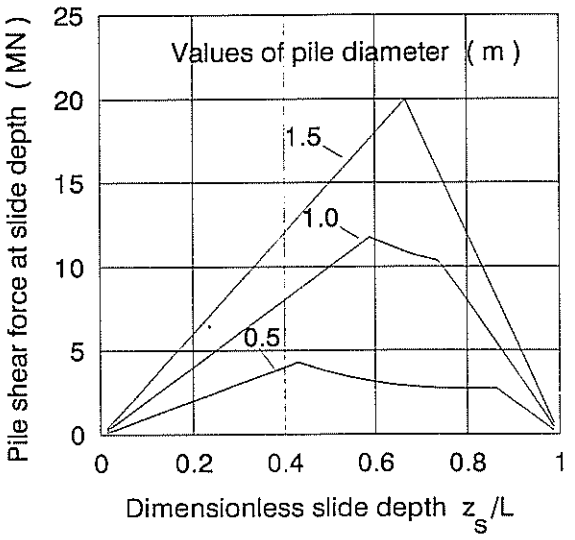

Fig. 5a Shear force developed in the pile at the depth of the slide for the fixed head pile in the stiffer soil.

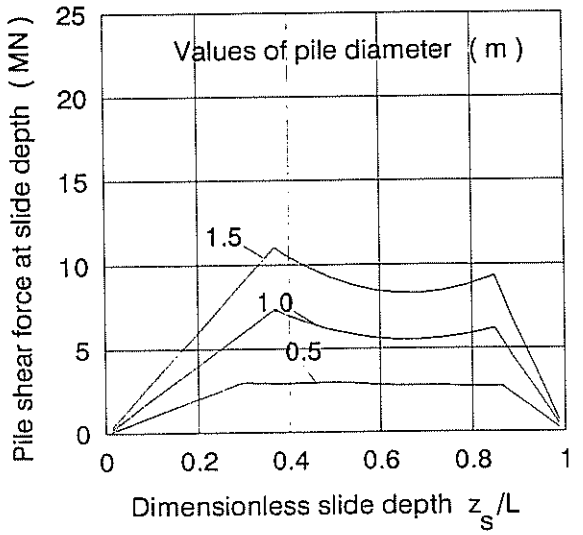

Fig. 5b Shear force developed in the pile at the depth of the slide for the free head pile in the stiffer soil.

It is clearly shown that the shear force developed during the "flow" and "short pile" modes are linearly dependent upon the slide depth and also proportional to the pile diameter. The 1.5 m diameter pile has developed complete failure of the soil (as can be seen in Figure 3) for both fixed and free head piles. Thus, the fixed head pile has a failure locus that consists of two straight lines, joining at a value of z_s of two thirds the pile length. This is a result of choosing the magnitude of p_u in the sliding soil to be half that in the stable soil.

For pile diameters 0.5 and 1.0 m the fixed head pile did not generate full soil failure at the extremely large soil movement of 80 m, and the triangular shape of the failure curves is truncated by a curved line. In Figure 5b, the free head pile failure curves are truncated by the "intermediate" mode of failure for diameters of 1.0 and 1.5 m. However, the 0.5 m diameter pile curve is truncated by both a curve for "intermediate" failure and two curves for incomplete generation of full soil failure between slide depths of 30% and 50% and between 75% and 86% of the pile length.

4.5 Limited Pile Strength

No pile will have unlimited strength to resist bending; a commonly used method to account for this is to limit the allowable extreme fibre axial stress in the pile. As a first approximation for the maximum axial stress in the pile, the rotation at the slide depth (which is generally the maximum rotation) and the bending moment at the slide depth, M_s may be used. The axial strain component corresponding to rotation of the pile, without vertical displacement of the pile, may be expressed in terms of the rotation θ as

$$\epsilon_{axial} = \frac{(1 - \cos\theta)}{\cos\theta} \qquad (1)$$

and, together with the extreme fibre stress caused by bending, the maximum stress can be written,

$$\sigma_{max} = E_p \left(\epsilon_{axial} + \frac{M_s d}{2E_p I_p} \right) \qquad (2)$$

which may be calculated for each stage of the analysis.

For a set of values of σ_{max}/E_p a plot of dimensionless shear force at the slide depth versus dimensionless slide depth is shown in Figure 6 for the 1.5 m diameter pile in the stiffest soil. Both fixed and free head boundary conditions are considered. The head fixity is seen to be relatively unimportant for the smallest presented value of dimensionless maximum axial stress, $\sigma_{max}/E_p = 0.001$, with only slide depths between 10% and 40% of the pile length predicting any benefit from fixing the pile head. This possible benefit relies upon the head fixing moment being sustainable by both the pile and the means by which the head is fixed. Figure 4a shows that a fixing moment of some 60 MNm is required at collapse when the slide depth is 34% of the pile length. But the value corresponding to the $\sigma_{max}/E_p = 0.001$ curve is 11 MNm.

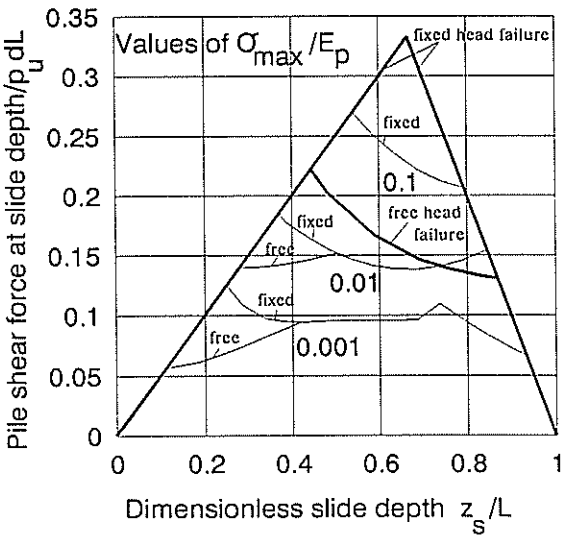

Fig. 6 Shear force developed in the pile at the depth of the slide for values of maximum fibre pile stress.

This is still greater than the pile yield moment of 10 MNm and permanent damage would occur to the pile.

5. CONCLUSIONS

The entire pile response to the "short pile" mode of failure is found to have no influence from the fixing of the pile head, because the mechanism of failure for this mode is already essentially that of a pile with head fixed in the sliding soil.

For differing head fixity the "flow" mode does not produce different values of shear at the slide depth, because the failure mechanism only involves horizontal pile-soil "pressures" (these are assumed not to change with head fixity). The head fixing moment only enlarges the range of slide depths within which "flow" type failure occurs. The response similarity does not extend to other measures of response, e.g. the deflected pile shapes and bending moment distributions are greatly influenced by head fixity.

"Intermediate" modes of soil failure, since they involve axial stretching of the pile, may not fully develop. The pile strength and/or axial pull-out strength of the pile in the soil may be insufficient to accomodate the large rotation required before this mode is produced. Previous solutions to this problem, such as Viggiani (1980), have recognised the importance of the component of maximum axial stress in the pile accompanying bending, but the techniques that were employed have no way of assessing the rotations and deflections necessary to mobilise soil and pile strengths.

The results indicate that large head fixing moments are generated, and large pile rotations are required to achieve full collapse (with a non-yielding pile). The results from the analyses therefore cast doubt upon the validity of using a small displacement formulation for the solution of such problems, without due attention to axial response. A method of considering the axial stress is presented and leads to the conclusion that the range of slide depths within which fixing the pile head is advantageous is rather limited.

6. ACKNOWLEDGEMENTS

The work in this paper was carried out as part of a project on the effect of seafloor instability on offshore foundations which was supported by a grant from the Australian Research Committee.

7. REFERENCES

Davies, T.G. and Budhu, M. (1986). "Non-Linear Analysis of Laterally Loaded Piles in Heavily Over-Consolidated Clays". Géotechnique, Vol. 36, No. 4, pp.527-538.

Hull, T.S. (1987). "The Static Behaviour of Laterally Loaded Piles". Thesis (Ph.D.) Univ. of Sydney.

Hull, T.S., Lee, C.Y. and Poulos, H.G. (1991). "Mechanics of Pile Reinforcement for Unstable Slopes". Research Report No. 636, School of Civil and Mining Eng., Univ. of Sydney.

Poulos, H.G. and Hull, T.S. (1989). "The Role of Analytical Geomechanics in Foundation Engineering". Foundation Engineering Congress, ASCE, Chicago.

Viggiani, C. (1981). "Ultimate Lateral Load on Piles used to Stabilise Landslides". Proc. 10th Int. Conf. Soil Mechs Fndn Eng, Stockholm, Vol. 3, pp. 555-560.

Analytical Predictions for Side Resistance of Piles in Rock

J.K. KODIKARA
B.Sc. (Eng.), Ph.D., M.I.E.Aust.
Research Fellow, Department of Civil Engineering and Surveying, University of Newcastle
I.W. JOHNSTON
B.Sc. (Eng.), Ph.D., F.I.E.Aust.
Associate Professor, Department of Civil Engineering, Monash University, Melbourne
C.M. HABERFIELD
B.Sc. B.E., Ph.D., M.I.E.Aust.
Lecturer, Department of Civil Engineering, Monash University, Melbourne

SUMMARY On the basis of a large number of laboratory simulation tests, an analytical model has been developed to describe the behaviour of the rough concrete/rock interface which controls the development of the side resistance of piles socketed into rock. By making a number of reasonable assumptions, the model has been used to produce some simplified design charts for the estimation of adhesion factors for piles in the Melbourne mudstone.

1. INTRODUCTION

High capacity, large diameter, bored, cast-in-situ piles are often used as a means of support for large engineering structures. When these piles are constructed in rock, the excavation process usually produces surface irregularities on the walls of the socket. Consequently, when the concrete is placed and allowed to set, the interface between the pile shaft and the surrounding rock mass takes the form of a rough concrete/rock joint.

For a number of years, the authors have been studying the behaviour of these rough concrete/rock joints and have developed a model which can describe their performance. This paper describes the basis of this model and how it has been used to produce simplified design charts for the prediction of the side shear resistance of piles in the Melbourne mudstone.

2. METHODS FOR PREDICTING SIDE RESISTANCE

Up until approximately the mid 1970s, estimations of the side resistance of piles in rock were based on crude extrapolations of clay technology. As adhesion factors were generally considered to reduce with increasing clay strength, it was assumed that for even stronger materials such as rocks, adhesion factors could be considerably lower. Consequently, it was not unusual to find values of the order of 0.05 being used in design. The adhesion factor, α, is related to the side shear resistance, τ, and the uniaxial strength of the rock, q_u, by the expression

$$\tau = \alpha q_u \qquad (1)$$

As a result of a number of independent studies conducted in various parts of the world (e.g. Horvath et al.,1980; Pells et al., 1980; Williams et al., 1980), it was established that these adhesion factors were very conservative and did not reflect the actual performance of piles in rock.

Following the publication of these many results, more relevant adhesion factors were derived (e.g. Williams and Pells, 1981; Rowe and Armitage, 1984). Figure 1 gives a typical example of this data where the adhesion factor is plotted against uniaxial compressive strength.

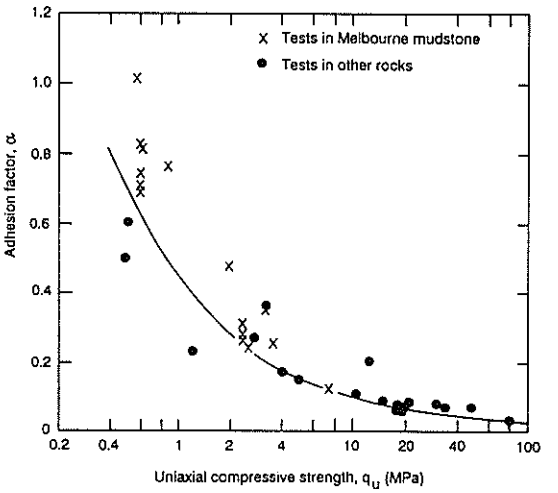

Figure 1 Typical variations of adhesion factor with uniaxial compressive strength (after Williams, et al., 1980)

The implication is that the unit side resistance in rock is a function of strength alone, whereas, it was generally known that the resistance was influenced by a large number of variables. This would account for the scatter of results shown in Figure 1, especially for the softer rocks. It follows that a method of design reflecting these factors was required.

Over recent years, there have been numerous attempts to resolve this complex problem. Some solutions have been obtained by considering the rough rock joint models which abound in the rock mechanics literature (e.g. Chiu and Dight, 1983). Alternative solutions have been derived through the use of numerical modelling techniques (e.g. Carter and Ooi, 1988). There have also been solutions based on wear theory (e.g. Leong and Randolph, 1991). Unfortunately, it would appear that all these methods involve subjectivity, require relatively complex input parameters, are empirically based or cannot reproduce the complex mechanisms that occur. It appeared then that a more direct approach was required.

3. DEVELOPMENT OF AN ANALYTICAL MODEL

It was recognised early on that any analytical model that could satisfactorily describe the very complex behaviour of a rough rock interface would require a large number of assumptions. As the success of any model would be entirely dependent on the accuracy of these assumptions, it was important that each should be verified by experimentation. This was achieved by means of a detailed programme of testing which made use of specialist constant normal stiffness direct shear equipment as described by Lam and Johnston (1982, 1989) and Johnston, Lam and Williams (1987).

It was also recognised that any attempt to model the full complexity of a random rough interface on naturally occurring rock, with all its inherent variability, would be very difficult as a first step. Therefore, the programme started with simple regular rigid triangular asperities and progressed in steps to increasingly more complex compressible interface geometries (Johnston and Haberfield, 1992). At each stage, the predictions and mechanisms predicted by the developing model were verified against the results of the tests. In addition, a synthetic soft rock of known and reproducible properties (Johnston and Choi, 1986) was used to simulate the increasingly more complex interfaces. Further details of the experimental programme may be found in Lam (1983), Johnston and Lam (1989) and Kodikara (1989).

4. THE WORKING MODEL

The working model has been developed into a computer program which uses a range of iterative procedures to calculate the distribution, magnitudes and continuity of the stresses and deformations amongst the various asperities of any chosen interface geometry. The input data required is made up of three groups of parameters as follows:-

Interface roughness:	mean asperity angle, i_m standard deviation of asperity angles, i_{sd} mean asperity height, h_m standard deviation of asperity heights, h_{sd}
Geometry:	socket length, L socket diameter, D initial normal stress on shaft, σ_{no}
Rock properties:	uniaxial compressive strength, q_u cohesion, c peak angle of friction, ϕ_p residual angle of friction, ϕ_r mass modulus, E Poisson's ratio, v uniaxial tensile strength, σ_t

The roughness characteristics of the concrete/rock interface can be determined by digitizing roughness traces of the socket wall (e.g. Chiu and Dight, 1981; Lam and Johnston, 1985). The program uses this data to set up a profile of irregular triangular asperities to represent the interface between the concrete and the rock.

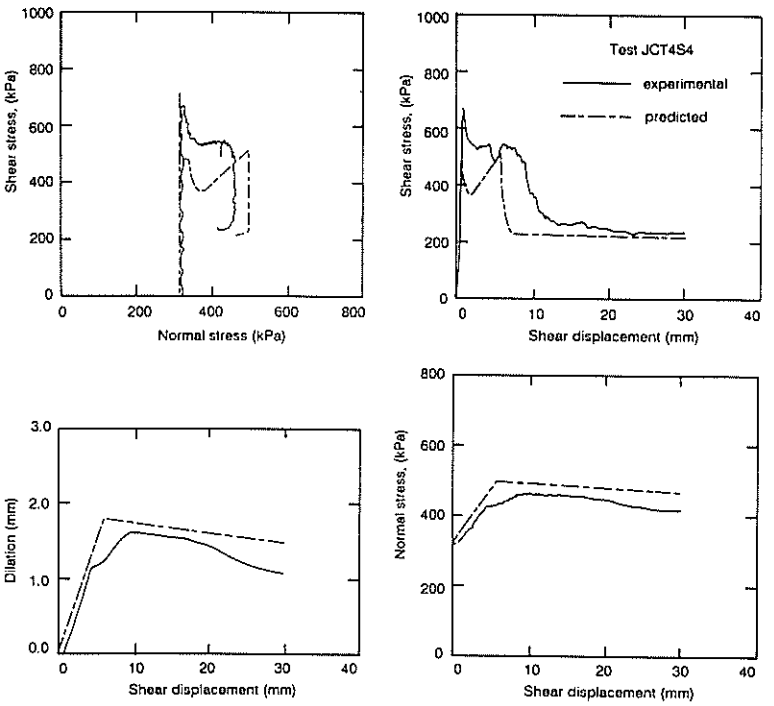

Figure 2 Comparison between predicted and experimental results for an irregular triangular interface

Triangular asperities have been adopted as they were found to avoid many of the singularities that eventuate with the point contact and localised crushing that must occur with truly random asperity shapes. Recent experimental results (Seidel, 1991) have confirmed that this simplification is reasonable.

The initial normal stress, σ_{no}, which acts on the pile shaft may be estimated from the head of concrete placed in the socket and by assuming that the ratio of horizontal to vertical stress is unity (Williams, 1980). The rock properties themselves should be determined for drained conditions (Johnston et al., 1980).

The first operation of the model is to set up the roughness profile from the input data and to calculate the compression of the asperities due to the initial normal stress. This is followed by the application of the first increment of shear displacement by sliding along the leading face of the critical asperity. Following a further process of distribution of stresses and displacements, the shear resistance for each asperity in contact is calculated. This resistance can be due to sliding on the leading face to shearing through the asperity itself. If the resistance to asperity shearing is larger than the resistance to sliding, then the sliding mechanism on that particular asperity is allowed to continue. Otherwise, a shear plane is allowed to develop through the asperity in a direction defined by the path of least resistance. This process then allows the total shear resistance to be calculated along with the final normal force, shear displacement and dilation.

Further increments of shear displacement can then be applied until the required total displacement, along with the other performance characteristics, are obtained. The output data generated by the model consists of a range of performance curves such as shown in Figure 2.

As has been pointed out by Haberfield (1987), when a rock socketed pile is loaded, the resultant socket dilation can lead to the development of radial cracks around the circumference. This has the effect of softening the pile response and, therefore, has been included in the model. It would be impractical to give all details of the current working model which has been progressively developed over several years. Instead, reference is made to Johnston and Lam (1989), Haberfield (1987), Kodikara (1989) and Kodikara et al. (1991).

5. COMPARISONS BETWEEN MODEL PREDICTIONS AND ACTUAL PERFORMANCE

Figure 2 presents a detailed comparison between the results obtained in one of the constant normal stiffness direct shear tests on an irregular triangular interface and the predictions of the model. In this comparison, the input data to describe the asperities was the actual dimensions rather than the statistical values which are used for the prediction of pile performance. The initial normal stress was 325 kPa and the normal stiffness was 90 kPa/mm. The interface was made up of three triangular asperities, each of 9.5 mm height with angles of 17.5°, 22.5° and 27.5°. The interface was machined from the synthetic mudstone of a saturated water content of about 17% which corresponded to a uniaxial compressive strength of 2.8 MPa. Full details of the tests and the materials properties used may be found in Kodikara (1989).

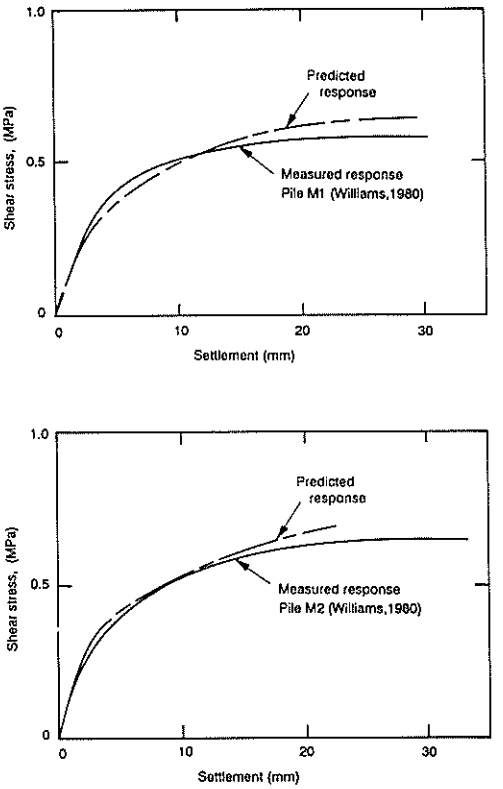

Figure 3 Comparison between predicted and measured shear load for side resistance only piles in Melbourne mudstone

Figure 3 presents comparisons between the model and two of the 1.2 m diameter side resistance only tests conducted in moderately weathered Melbourne mudstone by Williams (1980). The interface roughness data was digitized from profiles taken from the specific sockets. Additional details of these and other comparisons may be found in Haberfield (1987) and Kodikara (1989).

6. SIMPLIFIED DESIGN CHARTS FOR PILES IN MELBOURNE MUDSTONE

For any particular design problem, the model described above could be run to provide the full pile load-settlement response for the properties, geometries and characteristics involved. In this way it should be possible to examine the influence of a range of design strategies, such as varying diameter, length or socket roughness, to optimise the solution for the particular problem. However, since the program is not always available, there may be some merit in developing design charts from the model for general application. These design charts should be capable of providing some indication of performance such as the load capacity of the side component of total resistance.

As demonstrated by Kodikara (1989), in order to reduce the number of dependent variables that may influence the side resistance of a socketed pile, the adhesion factor should be expressed as a function of some dimensionless parameters. A useful representation is given by

$$\alpha = \phi\left[i_m, i_{sd}, \frac{h_{sd}}{h_m}, \frac{D}{h_m}, \frac{q_u}{\sigma_{no}}, \frac{c}{q_u}, \phi_p, \phi_r, \frac{E}{q_u}, \nu, \frac{\sigma_t}{q_u}\right] \quad (2)$$

For the Melbourne mudstone, the strength parameters (q_u, c, ϕ_p, ϕ_r, σ_t) can be correlated with saturated water content (see Johnston (1991) for a summary of these correlations), and therefore it is only necessary to specify one such dependent parameter. It is suggested that the uniaxial compressive strength is perhaps the most useful for this purpose. Also, the Poisson's ratio for the mudstone appears to be reasonably constant at about 0.3. It follows that Eq. (2) can be rewritten with only six dimensionless parameters as follows

$$\alpha = \phi\left[i_m, i_{sd}, \frac{h_{sd}}{h_m}, \frac{D}{h_m}, \frac{q_u}{\sigma_{no}}, \frac{E}{q_u}\right] \quad (3)$$

As has been demonstrated by Kodikara (1989), by considering a range of values of each of these dimensionless parameters as they apply to pile sockets in the mudstone, it is possible to generate a number of design charts. Unfortunately, for the six parameters involved, some 28 charts were required. Clearly, a further reduction in the number of dimensionless parameters of Eq. (3) is necessary for a simplified approach to design.

In practical terms, since there may be difficulties involved in determining values of i_m, i_{sd}, h_m and h_{sd} for a specific pile socket, there may be some advantage in generalising these. As discussed by Kodikara (1989), sockets in the Melbourne mudstone can be divided into three categories of wall roughness. These are

(a) smooth sockets formed by standard drilling methods in relatively homogeneous rock,

(b) medium sockets formed by standard techniques but roughened by reaming or as a result of uneven drilling pressures,

(c) rough sockets formed by regular major overbreaks or other irregularities. Hand mined sockets.

Some indication of the appearance of the sockets within these categories is given in Figure 4.

On the basis of a study of these different roughness categories for sockets in the Melbourne mudstone, it is suggested that the individual roughness parameters are as indicated in Table 1. It should be noted that a study by Kodikara (1989) showed that h_{sd} had little influence on side resistance. Further analyses of the socket roughness profiles obtained by Williams(1980) revealed that the ratio of h_{sd}/h_m was reasonably constant for all roughnesses. Therefore, this ratio was taken as 0.35 throughout. Table 1 also gives the range of the other variables (D, q_u, σ_{no} and E) which were considered applicable to the mudstone.

It was further established (Kodikara, 1989) that the range of possible values of D/h_m, had very little effect on the resulting values of adhesion factor. Therefore, the adhesion factor could be described as

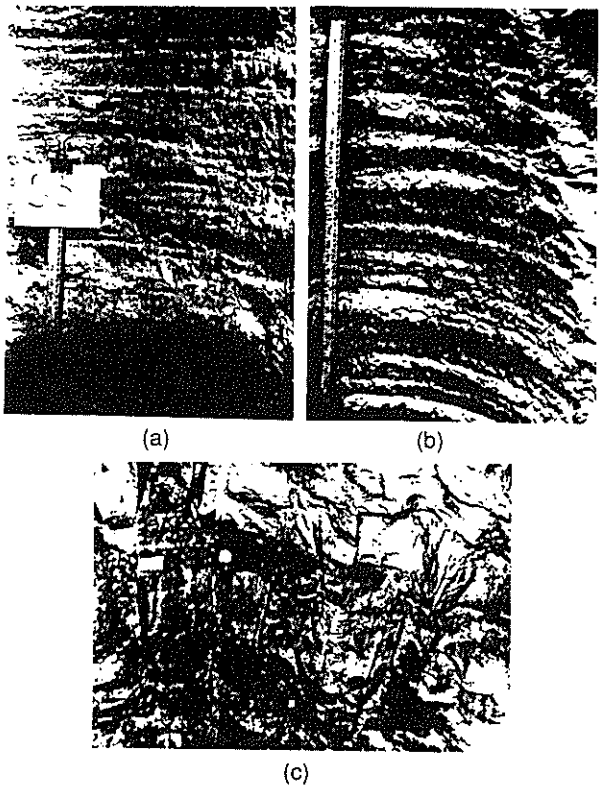

(a) (b) (c)

Figure 4 Roughness categories for sockets formed in Melbourne mudstone (a) smooth (b) medium (c) rough

$$\alpha = \phi\left[R, \frac{q_u}{\sigma_{no}}, \frac{E}{q_u}\right] \quad (4)$$

where R is the socket roughness category.

In order to produce the design data, three values of E/q_u were chosen as representing the general range of mudstone encountered. These values were 100, 200 and 300. Additionally, five values of q_u/σ_{no} were chosen and these were 5, 25, 50, 100 and 200. Therefore, for fixed values of roughness, E/q_u and q_u/σ_{no}, the model was run 200 times with random selections of i_m, i_{sd}, h_m and D within the range indicated in Table 1.

The results obtained are presented in Figure 5, with each part corresponding to a specific value of E/q_u. For a particular roughness category at a specific value of q_u/σ_{no}, the mean of the 200 results is indicated as well as the variation of $\pm$ one standard deviation about the mean.

7. DISCUSSION OF RESULTS

On the basis of the curves presented in Figure 5, it would appear that the adhesion factor for the practical range of socketed piles in the Melbourne mudstone varies between about 0.45 and 0.15. The maximum value occurs for rough sockets at high E/q_u values but at low q_u/σ_{no} values. There is a trend for the adhesion factor to increase with increasing roughness and an increasing E/q_u ratio, but to decrease with an increasing q_u/σ_{no} ratio.

TABLE 1

VARIATION OF RELEVANT PARAMETERS FOR SOCKETS IN THE MELBOURNE MUDSTONE

Parameter	Range of values for sockets in Melbourne mudstone		
	smooth	medium	rough
i_m (degrees)	10 - 12	12 - 17	17 - 30
i_{sd} (degrees)	2 - 4	4 - 6	6 - 8
h_m (mm)	1 - 4	4 - 20	20 - 80
h_{sd}/h_m	0.35		
D (m)	0.5 - 2.0		
q_u (MPa)	0. 5 - 10.0		
σ_{no} (kPa)	50 - 500		
E (MPa)	50 - 3000		

In order to compare the predictions made from the design charts with previous design curves such as is shown in Figure 1, the conditions that prevailed at the test locations of Williams (1980) were examined and estimations made of roughness, E, q_u, and σ_{no}. Using these values with the design charts of Figure 5, the range of adhesion factors that applied to the field tests were estimated and are presented in Figure 6 along with the curve previously presented in Figure 1.

According to this figure, the predictions using the simplified charts agree quite well with the field correlations of the tests conducted in rocks of relatively high uniaxial compressive strength. However, for the tests conducted in the weaker rocks (S piles), it appears that the simplified charts produce results that underestimate the correlations of Williams et al. (1980), although they do seem to agree with the correlation suggested by Horvath (1978). The reasons for this underestimation of the test results conducted in the highly weathered mudstone is not clear, but could be related to bands of much stronger sandstone known to be present in the mudstone at the site of the S pile series.

8. CONCLUSIONS

As a result of conducting a large number of constant normal stiffness direct shear tests, a mechanistic model to predict the performance of rough concrete/rock interfaces has been developed. Since these interfaces are representative of the contact between the sides of piles socketed into rock, the model can be used to predict the development of the side resistance of these piles.

While the model in the form of a computer program should be of use for the full design of side resistance of piles founded in rock, there seemed to be some merit in producing simplified design charts which would allow the prediction of the maximum pile load for a specific location.

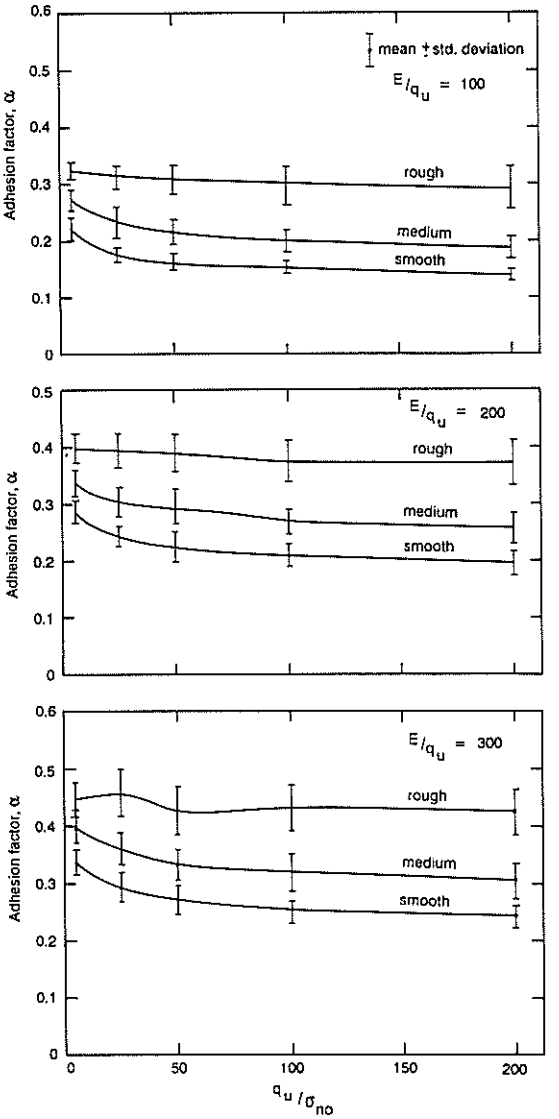

Figure 5 Simplified design charts for adhesion factor for Melbourne mudstone

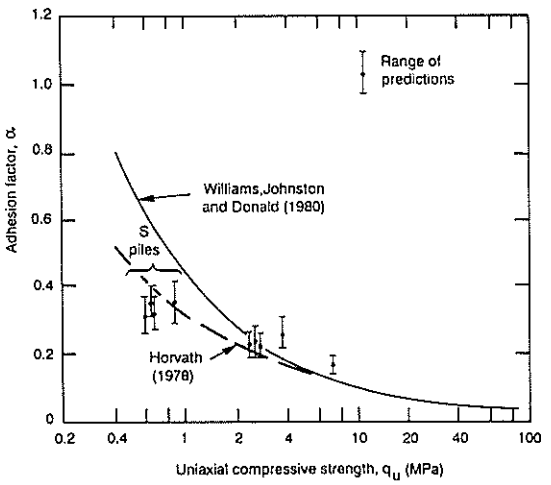

Figure 6 Comparison between predictions of performance using simplified design charts with other empirical correlations.

Therefore, by considering the range of pile dimensions and rock properties which apply to the Melbourne mudstone and by creating three typical categories of interface roughness, three simplified design charts have been developed. These charts provide an estimation of adhesion factors to cover most conditions that apply to the Melbourne mudstone.

9. REFERENCES

Carter, J.P. and Ooi, L.H. (1988). Application of a joint model to concrete-sandstone interfaces. Proc. 6th Int. Conf. on Numerical Methods in Geomech., Innsbruck, pp. 889-893.

Chiu, H.K. and Dight, P.M. (1983). Prediction of the performance of rock-socketed side-resistance-only piles using profiles. Int. Journ. Rock Mech. and Min. Sci., Vol. 20, No. 1, pp. 21-32.

Haberfield, C.M. (1987). The performance of the pressuremeter and socketed piles in weak rock. Ph.D. Thesis, Monash University, Melbourne.

Horvath, R.G. (1978). Field load test data on concrete-to-rock bond strength for drilled pier foundations, Publ. 78-07, Dept. of Civil Engng., University of Toronto.

Horvath, R.G., Kenney, T.C. and Trow, W.P. (1980). Results of tests to determine shaft resistance of rock-socketed drilled piers. Proc. Int. Conf. on Struct. Founds. on Rock, Sydney, Vol. 1, pp. 349-361, A.A. Balkema, Rotterdam.

Johnston, I.W., Williams, A.F and Chiu, H.K. (1980). Properties of soft rock relevant to socketed pile design. Proc. Int. Conf. on Struct. Founds. on Rock, Sydney, Vol. 1, pp. 55-64, A.A. Balkema, Rotterdam.

Johnston, I.W. and Choi, S.K. (1986). A synthetic soft rock for laboratory model studies. Geotechnique, Vol. 36, No. 2, pp. 251-263.

Johnston, I.W., Lam, T.S.K. and Williams, A.F. (1987). Constant normal stiffness direct shear testing for socketed pile design in weak rock. Geotechnique, Vol. 37, No. 1, pp. 83-89.

Johnston, I.W. and Lam, T.S.K. (1989). Shear behaviour of regular triangular concrete/rock joints - analysis. Journ. Geot. Engng., ASCE, Vol. 115, No. 5, pp. 711-727.

Johnston, I.W. (1991). Silurian and Lower Devonian engineering properties. To be published in Engng. Geology of the Melbourne Region, A.A. Balkema, Rotterdam.

Johnston, I.W. and Haberfield, C.M. (1992). Side resistance of piles in weak rock. To be published in Proc. Conf. on Piling Europe, London, Inst. Civil Engrs.

Kodikara, J.K. (1989). Shear behaviour of rock-concrete joints and side resistance of piles in weak rock. Ph.D. Thesis, Monash University, Melbourne.

Kodikara, J.K., Haberfield, C.M. and Johnston, I.W. (1991). An analytical model of the shear response of rough concrete/rock interfaces. Dept. Report, Dept. of Civil Engng., Monash University, Melbourne.

Lam, T.S.K. (1983). Shear behaviour of concrete-rock joints. Ph.D. Thesis, Monash University, Melbourne.

Lam, T.S.K. and Johnston, I.W. (1982). A constant normal stiffness direct shear machine. Proc. 7th S.E. Asian Geotech. Conf., Hong Kong, Vol. 1, pp. 805-820.

Lam, T.S.K. and Johnston, I.W. (1985). A scanning device to quantify joint surface roughness. Geotech. Testing Journ., Vol. 8, No. 3, pp. 117-124.

Lam, T.S.K. and Johnston, I.W. (1989). Shear behaviour of regular triangular concrete/rock joints - evaluation. Journ. Geot. Engng., ASCE., Vol. 115, No. 5, pp. 728-740.

Leong, E.C. and Randolph, M.F. (1991). Modelling sliding behaviour of rock interfaces. Proc. Int. Conf. on Computer Methods and Advances in Geomechanics, Cairns, Vol. 1, pp. 365-369, A.A. Balkema, Rotterdam.

Pells, P.J.N., Rowe, R.K. and Turner, R.M. (1980). An experimental investigation into side shear for socketed piles in sandstone. Proc. Int. Conf. on Struct. Founds on Rock, Sydney, Vol. 1, pp. 291-302, A.A. Balkema, Rotterdam.

Rowe, R.K. and Armitage, H.J. (1984). The design of piles socketed into weak rock. Report GEOT-11-84, University of Western Ontario, London, Canada.

Seidel, J.P. (1991). Unpublished research, Dept. of Civil Engng., Monash University, Melbourne.

Williams, A.F. (1980). The design and performance of piles socketed into weak rock. Ph.D. Thesis, Monash University, Melbourne.

Williams, A.F., Johnston, I.W. and Donald, I.B. (1980). The design of socketed piles in weak rock. Proc. Int. Conf. on Struct. Founds on Rock, Sydney, Vol. 1, pp. 327-347, A.A. Balkema, Rotterdam.

Williams, A.F. and Pells, P.J.N. (1981). Side resistance rock sockets in sandstone, mudstone and shale. Can. Geotech. Journ., Vol. 18, No. 4, pp. 505-513.

Stability of Retaining Walls with Compacted Backfills

S.A.S. KULATHILAKA
B.Sc.Eng. (Hons)., Ph.D.
University of Moratuwa – Sri Lanka, Formerly Graduate Scholar – Monash University
I.B. DONALD,
B.CE., M.Eng,.Sc., D.I.C., Ph.D., M.I.E.Aust
Associate Professor, Monash University – Australia

SUMMARY A new technique referred to as the "Nodal Displacement Method" - based on the Finite Element Method - was developed at Monash University for the evaluation of the stability of geotechnical structures and slopes. A compaction simulation algorithm was also developed and incorporated with an elastoplastic finite element model to simulate the compaction of the fill behind retaining walls. This paper describes the application of the nodal displacement method to evaluate the stability of retaining walls where the backfill has been compacted.

1. INTRODUCTION

In a companion paper submitted to this conference by Donald and Goh (1992), difficulties with traditional approaches to retaining wall stability are discussed and a new method, the "Nodal Displacement Method", based on finite element calculations, is presented and discussed. Donald and Goh's approach simulates backfilling behind gravity and semi-gravity walls and compares safety factors calculated from the new and traditional methods.

The essence of the Nodal Displacement Method (NDM) is that strength parameters c and $\tan \phi$ are progressively multiplied by a variable N (≥ 1) until excessive calculated deformations occur and the Safety Factor, F, is then taken as $1/N_{critical}$.

Where compaction of the backfill is required, more complex simulation algorithms are needed for satisfactory modelling of field behaviour. The present paper presents such a compaction model which leads to distributions of lateral stress on the back of the wall which are quite different from those for the case of non-compacted backfill. The compaction induced stress profiles are intended mainly for the purpose of structural design and their use in conventional stability analyses will only provide a safety factor against the initiation of movements leading to failure and not a safety factor against overall wall collapse.

More realistic assessment of wall stability may be obtained through extensions to the Nodal Displacement Method. The compaction simulation model introduces several important new variables and, in addition to factoring c and $\tan \phi$, these values must be adjusted in a sensible manner for meaningful analysis. In this paper the application of the modified method to gravity walls with compacted backfills is discussed and several examples presented. The influence of factors such as foundation stiffness is also illustrated. The stability of walls with compacted backfills is compared to those with non-compacted backfills.

2. COMPACTION SIMULATION MODEL

Broms (1972), Ingold (1979) and Seed & Duncan (1983) have proposed various models for compaction of fill behind retaining walls. The fundamental idea of Kulathilaka's (1990) model was derived from the Seed and Duncan model. Modifications made to produce a close simulation of the compaction process and the techniques employed in incorporating the model with the Elastic-Ideally Plastic Finite Element model are briefly outlined below.

Compaction effort applied at the surface by a plant is simulated by the application of a lateral stress profile at the current surface level. The compaction simulation model interpolates the compactor imposed lateral stress $\Delta\sigma_{x,c}$ for the soil element under consideration, using the depth to the Gauss points of the element.

2.1 Loading of an Element

Prior to the current compaction increment the lateral stress level of a typical soil element in the backfill will be in a K_o state (A_1), higher than K_o state (A_2) or lower than K_o state (A_3) as in Figure 1. If the initial stress state of the element is either K_o or lower than K_o, lateral stress and vertical stress will increase on a path parallel to the K_o line, while the compactor is still on the surface. If the initial stress state is higher than K_o the stress increase will follow a path of slope K_3 till it meets the K_o line and follow the K_o line thereafter.

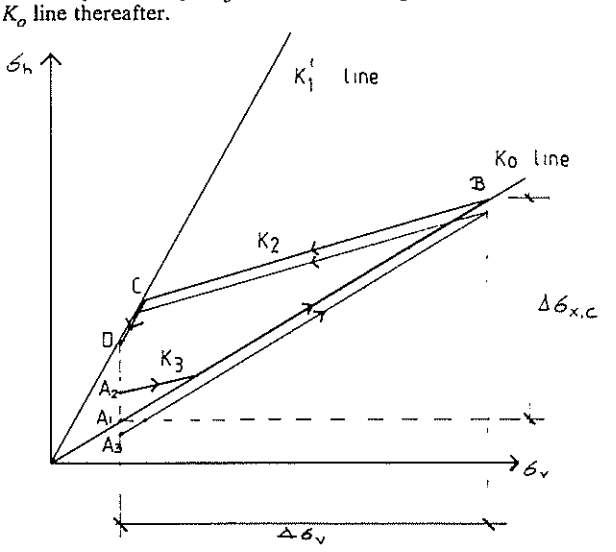

Figure 1. Basic compaction model

When the stress state is K_o or lower, the lateral stress will increase by $\Delta\sigma_{x,c}$ while the compactor is still on the surface. When the initial stress rate is higher than K_o the lateral stress state will be smaller due to the initially stiffer response. This is implemented by computing an "equivalent vertical driving stress" $\Delta\sigma_v = \Delta\sigma_{x,c}$.

2.2 Unloading Due to the Removal of the Compactor

Stress release in both the vertical and horizontal directions will take place along the K_2 line during the removal of the compactor.

If the unloading path meets the K'_1 line prior to the reduction of the vertical stress to the overburden values, unloading will follow K'_1 line thereafter. Thus an unloading path of the form "B-C-D" will be followed. The residual lateral stress increase is denoted by $\Delta\sigma_{x,r}$. The model identifies the present stress state of an element and various numerical procedures are employed to capture the turning points and to implement the stress path.

2.3 Numerical Techniques Used in the Simulation

Purely for analytical purposes, lateral stress is separated into a geostatic component ($\sigma_{x,geo}$) and a compaction induced stress component ($\sigma_{x,comp}$). The latter is obtained by adding up the compaction induced residual lateral stresses. The remaining part is taken as the geostatic stress.

By taking all the soil elements through the model, the residual lateral stress increases are computed and the total force vector on the wall is assembled. Deformations in the soil-structure system are then computed by the finite element model. The resulting stress rearrangements are then computed by the finite element model subjected to the conditions imposed by the compaction simulation algorithm. When there are stress relaxations due to wall movements, geostatic and compaction induced stress components are expected to share the reductions proportionally to their present values.

The number of passes of the compactor at a certain fill elevation is modelled in a single numerical increment. With ongoing compaction soil elements closer to the surface are expected to regain the lateral stresses relaxed through wall movements. The geostatic stress component of the element is compared with the compactor imposed stress for the element. If the latter is larger than the former, the soil element is taken to be close enough to the surface to regain the relaxed stresses.

3. POSSIBLE COMBINATIONS OF PARAMETER REDUCTION

In addition to the standard soil strength and stiffness parameters (c, ϕ, K_o *and* E), three other parameters (K'_1, K'_2 *and* K'_3), are introduced by the compaction simulation algorithm. These compaction model parameters govern the lateral stresses that could be sustained in the soil, the compaction introduced forces acting on the wall and the $\Delta\sigma_h$ vs $\Delta\sigma_v$ relationship during loading/unloading. Therefore the reduction of specific parameters by the "Nodal Factor" is more complicated than for a simple backfill case and could be performed in several ways. Extensive preliminary investigations were carried out to identify the critical variables and most appropriate method of parameter reduction.

The parameter K'_1 is a function of ϕ and controls the amount of residual compaction induced stress that can be sustained in the element. If the K'_1 values are also reduced according to the reduced ϕ value, $\phi_{red} = \tan^{-1}(N \tan \phi)$, the residual lateral stress increase due to compaction and thereby the compaction induced forces on the structure will also be reduced. This will in turn cause a reduction in wall movements. Some reduction in "lateral stress relaxation due to the wall movements" could also be expected. One series of analyses was performed where all the parameters (c, ϕ, K'_1) were reduced.

It should be borne in mind that the reduction of properties through a nodal factor is only a hypothetical phenomenon. The actual soil does not undergo any reduction in strength or stiffness. Thus the actual sustainable residual lateral stress increase due to compaction, and therefore the compaction induced forces on the structure would not change, regardless of the nodal factors used in the analyses. To be compatible, the c and ϕ values used in the stress level computations in the compaction simulation algorithm, also should not be reduced. Therefore another series of analyses was done without reducing c, ϕ and compaction model parameters in the compaction simulation algorithm. K_2 and K_3 values correspond to unloading and reloading slopes. These values, together with the K_o value, were not changed, as factoring was shown by the preliminary investigations to give erratic results.

Lateral stress increase due to compaction was found to be dependent on the direction of the movement of the compactor

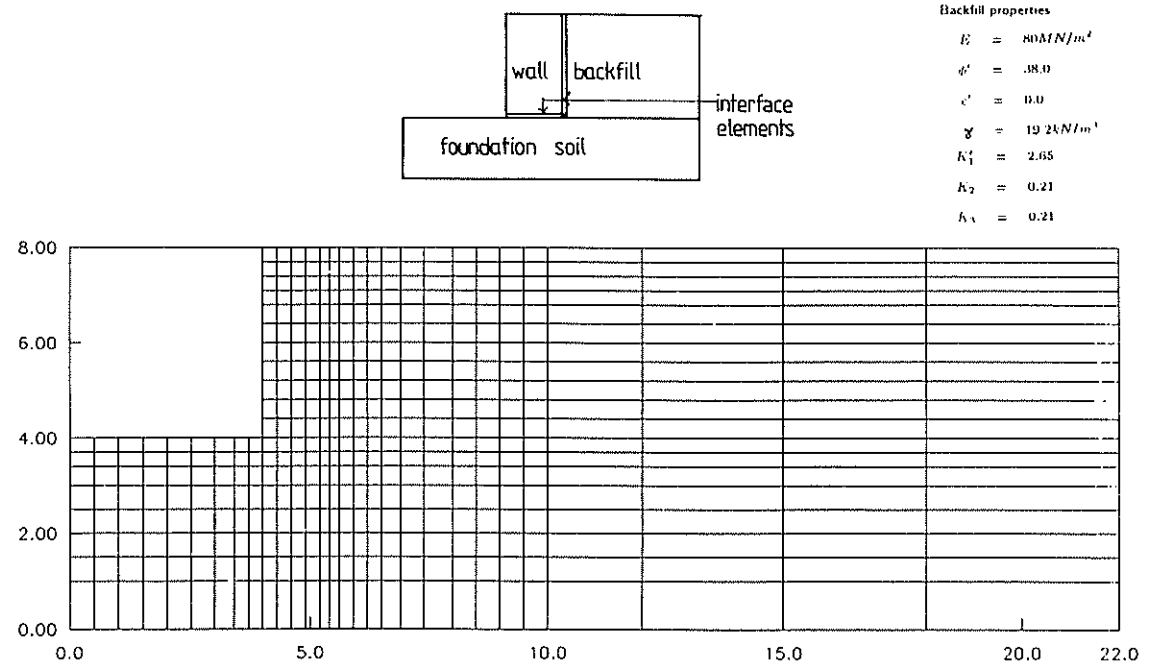

Figure 2. Finite element mesh and soil properties

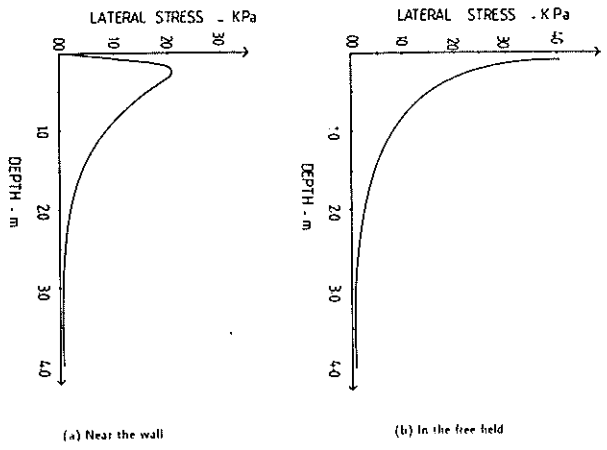

Figure 3. Compactor induced stress profiles

(D'Appolonia et al (1969)). As the intermediate principal stress is also an important parameter in the elastic ideally plastic finite element formulation, any assumption on residual stress increase parallel to the wall is also a critical factor. This aspect is discussed in detail in Kulathilaka (1990). In the examples presented in this paper, even compaction is assumed in all directions and the lateral stress increase parallel to the wall is taken to be as same as that normal to the wall.

4 EXAMPLES

The sample problem used for this analysis is a 4.0 m high gravity retaining wall with a width of 1.4 m. Backfilling behind the wall is assumed to have taken place in 11 increments, therefore there will be 11 compaction increments in addition to the compaction of the foundation layer. The geometry and FE idealization of the problem are depicted in Figure 2. All the wall/soil interfaces were modelled with one dimensional interface elements. Compactor imposed lateral stress profiles used for the examples are depicted in Figure 3. The backfill was assumed to be a cohesionless soil. Two different foundation conditions were assumed; a "stiff" foundation with a $E_{fdn}/E_{backfill}$ ratio of 4 and a "soft" foundation soil with the same modulus as the backfill. Backfill and foundation properties used are shown on the diagrams.

In some cases only the backfill properties were varied, whereas both the backfill and foundation properties were varied in other cases.

4.1 Wall on a "Stiff Foundation"

Strength and stiffness parameters of the backfill and the foundation and the compaction model parameters are reduced in three different ways with this wall on a stiff foundation. If the conventional FOS against overturning is computed with the assumption of active conditions at the back of the wall a value of 2.2 is obtained. The lateral stress profile at the back of the wall with compaction simulation is depicted in Figure 4. Using this working stress profile a FOS of 1.2 against overturning is obtained, a considerably lower value as would be expected.

4.1.1 Backfill parameters varied. Compaction model parameters kept constant. Foundation properties kept constant.

In this series only the backfill and interface strength properties were reduced. Foundation properties as well as the compaction model parameters were kept constant. The Nodal Factor, taken here as 1/N, could be increased beyond 3.4 without causing any abrupt increase in the wall displacements (Figure 5). The strong foundation soil has resisted rotation type wall movements induced

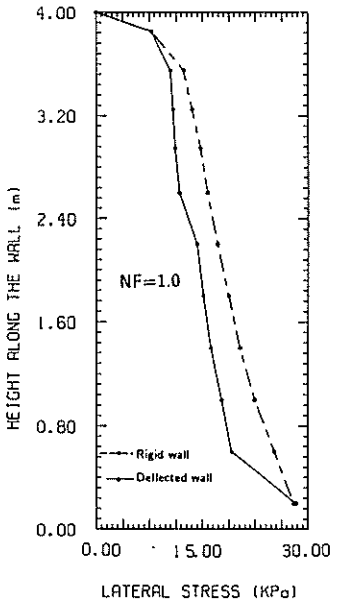

Figure 4. Lateral stresses - compacted fill

by the compaction induced nodal forces. The unchanged compaction effect (due to unchanged compaction model parameters) imposed some strengthening effect enabling larger theoretical reductions of backfill strength properties before failure.

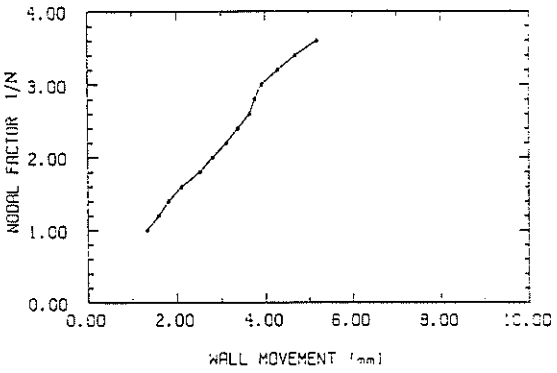

Figure 5. NDM plot - reducing backfill properties

4.1.2 Backfill and compaction model parameters varied. Foundation properties kept constant.

In this series compaction model parameters of the backfill were also reduced by the nodal factor, together with the strength and stiffness properties. Reduction of the parameter K'_1 reduced the residual compaction induced stresses and thereby reduced the strengthening effect due to compaction. After a nodal factor of 2.52 was exceeded the numerical solution did not converge. If the incremental construction process was simulated allowing high unbalanced loads when the solution was failing to converge, a large increase of displacement was calculated as depicted in Figure 6. This displacement value is not exact; nevertheless it indicates that the nodal factor of 2.52 corresponds to the inception of failure. Total displacement vectors indicate that the wall movements are predominantly horizontal and soil movements contain a very significant vertical component (Figure 7).

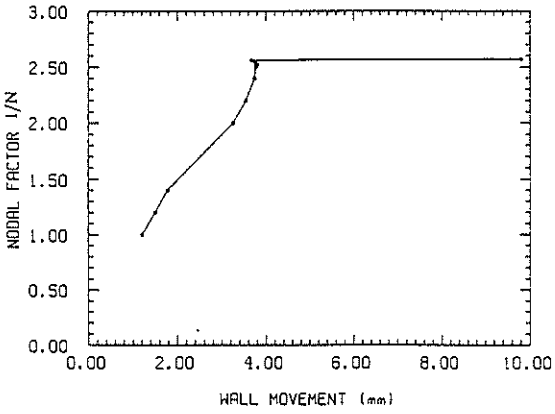

Figure 6. NDM plot- vary backfill and compaction model parameters

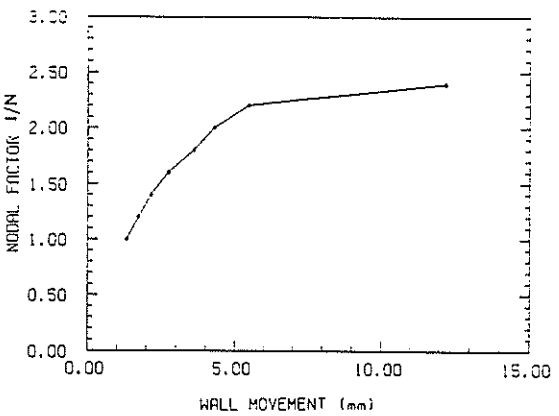

Figure 8. NDM plot - vary backfill and foundation properties

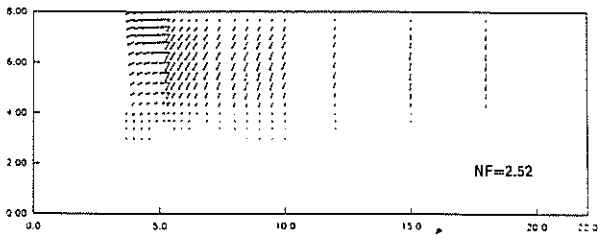

Figure 7. Total displacement vectors

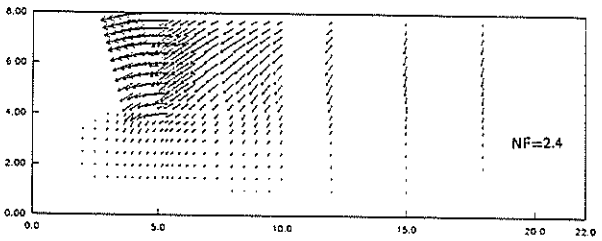

Figure 9. Total displacement vectors

4.1.3 Backfill and foundation properties varied. Compaction model parameters kept constant

In this series of examples the foundation strength and stiffness parameters are also reduced by the same nodal factor as for the backfill properties. However, the compaction model parameters were not reduced. Thus the backfill and the foundation will sustain residual compaction induced stresses as for the real soil. The compaction induced forces on the wall will be the same while the strengths are being reduced. As with the previous set the displacement at the nodal factor of 2.4 was achieved while tolerating high unbalanced loads. Thus a nodal factor of between 2.2 and 2.4 indicates the inception of failure (Figure 8). The total displacement vectors at the nodal factor of 2.4 outlined a predominantly overturning type failure (Figure 9).

4.2 Wall on a "Soft" Foundation

In these examples the wall was assumed to be founded on a soil with the same modulus as the backfill. The strength of the foundation soil was also decreased from that in the initial examples. The reduced stiffness and strength of the foundation yielded lower safety factors as illustrated by the following examples. The observations are compared with a non compacted backfilling on the same foundation.

Since the CP 2 definition of FOS on overturning does not account for foundation stiffness, this wall will also have a FOS of 2.2 against overturning (i.e. active stresses are assumed). The lateral stress distribution at the back of the wall with the compaction simulation is presented in Figure 10. Using these FE working stresses a FOS of 1.36 - marginally higher than the previous case - was obtained. This is because of the smaller lateral stresses resulting from increased wall movements.

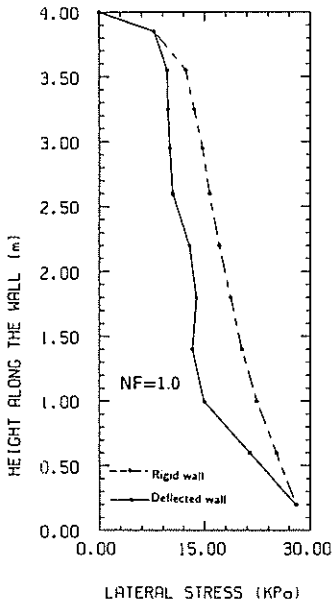

Figure 10. Lateral stresses - "soft" foundation

4.2.1 Compaction model parameters kept constant. Foundation properties kept constant.

In this series of computations only the strength properties of the backfill are reduced by the nodal factor. Neither the foundation properties nor the compaction model parameters were altered. After a nodal factor of 1.6 large movements were observed (Figure 11).

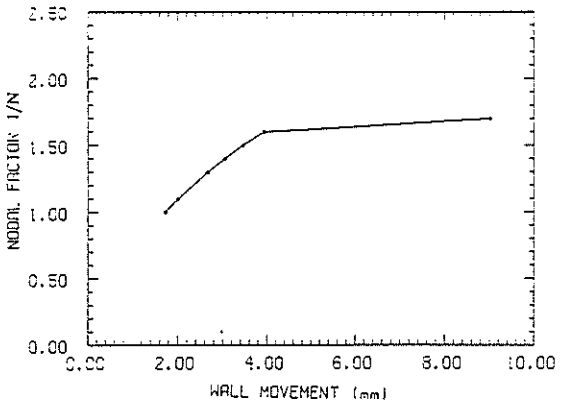

Figure 11. Soft foundation - vary backfill only

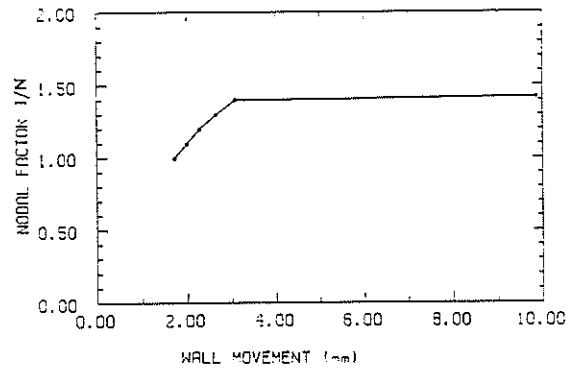

Figure 12. Vary backfill and foundation properties

4.2.2 Compaction model parameters kept constant. Foundation properties are also reduced

Foundation properties were also reduced by the nodal factor in this set of problems in addition to the backfill and interface properties. The compaction model parameters corresponding to both the foundation and the backfill were kept constant. As can be seen from Figure 12 the safety factor was 1.4 - slightly less than for the previous case.

4.3 Non-Compacted Fill on Soft Foundation

Backfilling behind the wall without compaction is simulated for the wall founded on softer soil. Founding soil was also not compacted prior to the backfilling.

The lateral stress profiles for the compacted and non compacted fill when the nodal factor is 1.0 are compared in Figure 13. Using the much smaller FE lateral stress profile of non compacted backfill a FOS against overturning of 1.78 was achieved from the CP2 analysis.

The results of the two nodal displacement method analyses with and without the reduction of foundation properties are presented in Figure 14 and Figure 15 respectively. The safety factors of 1.17 and 1.32 achieved in the two instances are much smaller than the value of 1.78 computed using FE working stresses at the back of the wall. Both safety factors are smaller than the corresponding ones for the compacted backfill. This highlights the strengthening of both the foundation and backfill due to the compaction.

It is interesting to note that for the compacted backfill the NDM safety factor was larger than that computed using the FE working stresses and for the non compacted backfill it was the other way.

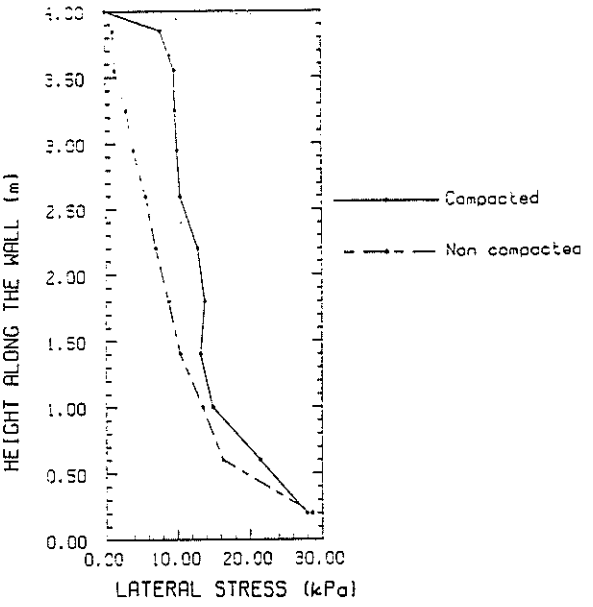

Figure 13. Lateral stress comparison

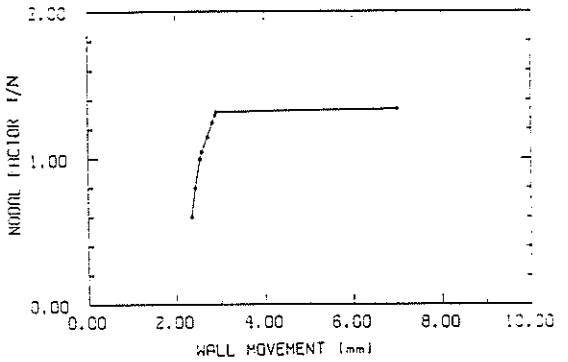

Figure 14. Non-compacted fill; vary backfill properties only.

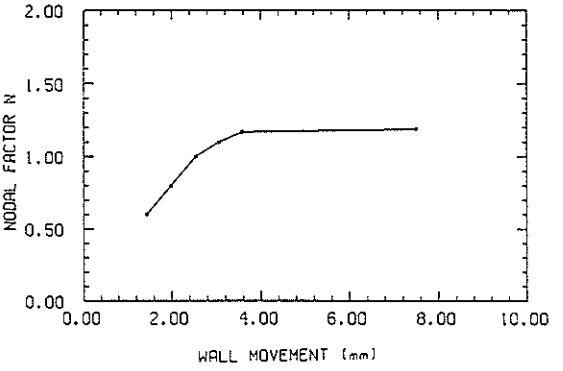

Figure 15. Vary backfill and foundation properties

5. DISCUSSION

Safety Factors or critical Nodal Factors ($=1/N_{cr}$) for a range of problems are summarised in Table I. The information is not comprehensive enough for definitive design rules to be formulated, yet some interesting trends emerge.

TABLE I

COMPARATIVE SAFETY FACTORS

Foundation Condition	Method of Evaluation	Conditions Used	FOS or $1/N_{cr}$
Stiff or Soft foundation	CP 2 (overturning)	Non Compacted fill. Use active earth pressures.	2.20
Stiff fd'n	FE stresses in CP2 def'n	Compacted fill	1.10
Stiff fd'n	Nodal Displ. Method	Only backfill strength prop. varied	> 3.4
Stiff fd'n	Nodal Displ. Method	Backfill strength and comp model prop. varied	2.52
Stiff fd'n	Nodal Displ. Method	Backfill and foundation strength prop. varied	2.30
Soft fd'n	FE stresses in CP2 def'n	Compacted fill	1.36
Soft fd'n	Nodal Displ. Method	Only backfill strength prop. varied	1.60
Soft fd'n	Nodal Displ. Method	Backfill and foundation strength prop. varied	1.40
Soft fd'n	FE stresses in CP 2 def'n	Non compacted fill. Only backfill strength prop varied	1.78
Soft fd'n	Nodal Displ. Method	Non comp. fill. Only backfill strength prop. varied	1.32
Soft fd'n	Nodal Displ. Method	Non comp. fill. Backfill and fd'n strength prop. varied	1.17

As expected, the use of F.E. calculated stresses (for N = 1, i.e. the actual field state) in conventional Code analyses leads to unrealistically low values of F. This is because the analyses make no allowance for stress release as the wall yields under the influence of the lateral stresses.

For the "stiff" foundation soil the NDM analysis with varying backfill and foundation strength gives an answer close to the CP2 analysis (2.30 cf 2.20), but this is at least partly fortuitous, as the foundation soil strength does not enter into the Code analysis. The NDM displacement vectors indicate basically overturning behaviour, which agrees with the assumption on which the CP2 value was calculated. Varying only the backfill strength yields an unrealistically high F at > 3.4 and with the present state-of-the-art of the NDM considerable engineering judgement is required to decide which parameters should be varied for any particular wall.

For the "soft" foundation soil with compacted fill a similar pattern emerges, though varying only backfill properties does not produce such a large change in F as for the stiff soil. The three values in Table I for soft foundation soil and compacted backfill are all in the range F = 1.5 ± 0.1, but the conventional CP2 value for overturning would of course remain at 2.2. For non-compacted backfill the NDM critical Nodal Factors are significantly reduced, because of the lower stress and hence lower strengths in the retained soil. It would seem on the limited evidence presented that foundation stiffness, which is ignored in conventional methods, has a major influence on the deformation pattern and hence, through displacement induced stress relaxation, on the safety factor.

6. CONCLUSIONS

Investigations have been described which demonstrate the application of the Nodal Displacement Method to calculations of the stability of retaining walls. For some situations the method yields values comparable with conventional analyses, but in other cases significant differences arise, particularly for softer foundation soils. Unlike conventional methods, the NDM does not require assumptions as to the failure mechanism and can readily model construction sequences including compaction-induced stresses. The complex wall-soil interaction effects which occur in practice are automatically allowed for and, with further refinement, the method could provide a useful alternative to existing, less than totally satisfactory design methods.

7. REFERENCES

Broms, B. (1971) "Lateral earth pressures due to compaction of cohesionless soils", Proc., 4th European Conf. on Soil Mechanics and Foundation Engineering, Budapest, pp. 373-384.

D'Appolonia, D.J., Whitman, R.V. and D'Appolonia, E. (1969) "Sand compaction with vibratory rollers", A.S.C.E. Journal of Soil Mechanics and Foundation Engineering Division, SM 1, pp. 263-264.

Donald, I.B. and Goh, A.T.C. (1992) "Determination of retaining wall stability using the finite element method", Proc., 6th A.N.Z. Conf. on Geomech, Christchurch, N.Z.

Ingold, T.S. (1979) "The effect of compaction on retaining walls", Geotechnique 29, No. 3, pp. 265-283.

Kulathilaka, S.A.S. (1990) Finite Element Analysis of Earth Retaining Structures, Ph.D. Thesis submitted to Monash University, Australia.

Kulathilaka, S.A.S. and Donald, I.B. (1991) "Finite element analysis of compaction behind retaining walls", 9th Asian Regional conf. on Soil Mech and Fdnd. Engg., Bangkok, Thailand.

Seed, R.B. and Duncan, J.M. (1983) "Soil-structure interaction effects of compaction induced stresses and deflections", Geotechnical Engineering Research Report No. UCB/GT/83-06, University of California, Berkeley, U.S.A.

Risk Associated with Construction of Large Diameter Bored Piles in Cavernous Marble

K.S.LI
B.Sc. (Eng.), Ph.D., M.I.E.(Aust)
Lecturer, Department of Civil and Maritime Engineering, University College, University of New South Wales

SUMMARY: The methods used for constructing large diameter bored piles in cavernous marble for the Light Rail Transit Development project in Hong Kong are described. The major risks and problems involved in the construction include the formation of sinkholes, collapse of soil cavities and the problem of soil piping. Techniques for minimising these risks and problems will be discussed in the paper.

1. INTRODUCTION

Marble was not discovered in Hong Kong until the late 1970s when site investigations for building developments in northwest New Territories revealed the existence of marble formations concealed by a thick cover of superficial deposits. Marble was first discovered in the Yuen Long area (1),(8), (9),(10). It was also found later in northeast New Territories in the Tolo Channel (11) and more recently in the Ma On Shan reclamation.

Cavities are present in the marble formations although the extent of cavitation varies from site to site. Very often, the cavities are small and the presence of cavities does not prelude the development of heavy foundations for tall buildings. A number of buildings, supported by driven-cast-insitu piles (8) or steel H-piles (4), have been successfully completed in the marble formations in Hong Kong.

In 1987, site investigations carried out for the Light Rail Transit (LRT) Development project in Yuen Long indicated the presence of large cavity systems in the marble bedrock at the site (2,3). Some of the cavities were believed to be connected for as far as 30m horizontally and 20m vertically, and one of the cavity systems was found to have a volume well in excess of 350m^3. Driven piles could not be used for this project because the heavy foundation loads might cause collapse of the large marble cavities. Large diameter bored piles were considered to be a suitable choice for the foundation. The bored piles were 2m in diameter and founded at levels below the large cavities. The design of the foundation

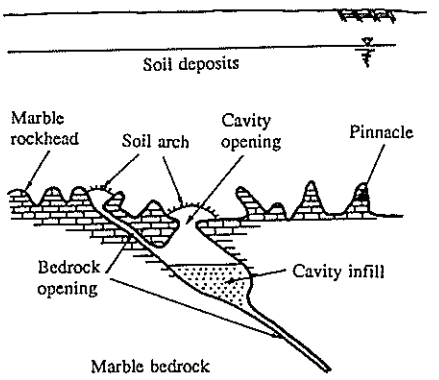

Fig.1 Features of cavernous marble

for the LRT Development has been discussed by Holmes & Keung (2) and Holmes, Keung & Li (3). This paper addresses the risks and problems associated with the construction of large diameter bored piles in cavernous marble, with special reference to the conditions in Hong Kong. Although this paper draws the experience from the LRT Development project, some of the risks and problems discussed in this paper are based on the author's assessment and do not necessarily relate to what had actually happened at the LRT site.

The geology of the LRT site is described in (2,3,7) and is similar to other marble sites in Yuen Long area described by Houghton & Wong (4). Some typical geological sections of the LRT site can be found in (7).

2. CONSTRUCTION

The LRT project was the first project in Hong Kong, and perhaps one of the very few projects of this kind in the world, involving the construction of bored piles in cavernous marble. The methods of construction used for the project have been described by Holmes, Keung & Li (3). A more detailed description is given in this section. The terminologies used in the following discussion are defined in Fig.1.

2.1 Piles with no cavity

A temporary casing is driven into the ground by a heavy-duty vibrator or by an oscillator. The soils in the casing are then removed by a grab. The casing can be extended if necessary until the marble bedrock is reached. If the pile is to be socketed only a few metres into the marble bedrock, rock excavation can be effected by chiselling. For a longer socket length, it is more efficient to use reverse circulation drilling (RCD). Efforts should be made to prevent soil piping at the bottom of the casing using a method described later in Section 3.1.

2.2 Piles with small cavities

Fig.2 shows the method of construction for a pile with a small cavity. The marble above the cavity is excavated by chiselling or RCD. When the cavity is reached, two different methods can be used.

Method A: The soft materials inside the cavity is removed and the emptied cavity is then filled with concrete. Excavation continues when the concrete has hardened. If there are more

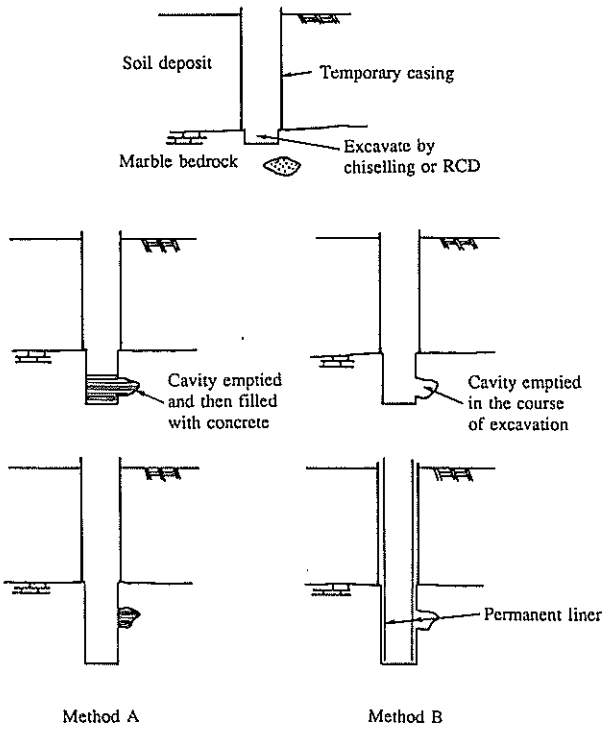

Fig.2 Piles with small cavities

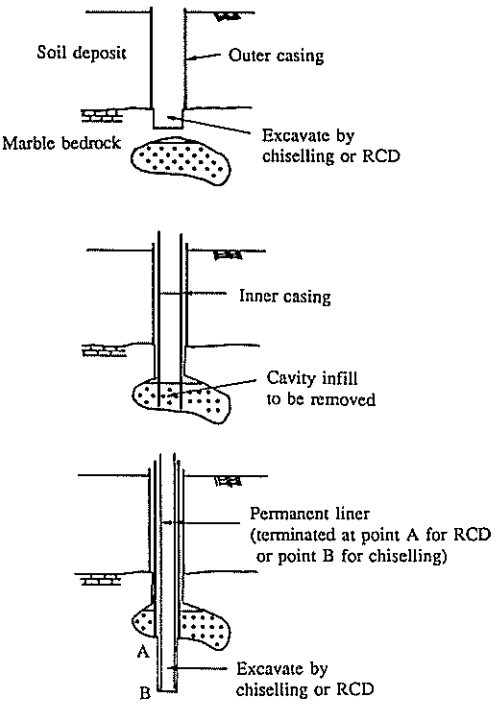

Fig.3 Piles with large cavities

than one small cavities along the pile, the same procedure can be repeated for the next cavity.

Method B: Excavation proceeds as if no cavity is present. When excavation is complete, a permanent liner is placed inside the bored hole. At the LRT site, a 2mm thick corrugated spiral tubes with a nominal diameter of 2m were used. The spiral tube would terminate at point A if a 2m diameter drill bit was used for excavation and at point B if excavation was effected by chiselling or a 2.1m diameter drill bit. Without the permanent liner, soft materials may be drawn into the bored hole from the small cavity or other sources through bedrock openings connecting the small cavity when the base of the bored hole is being cleansed by air-lifting. Despite the use of a permanent liner, this method requires a longer period of time for cleansing. For the LRT project, the cleansing process might sometimes take more than one day before the bored hole was clean enough for concreting.

2.3 Pile with large cavities

If the cavity is large, it is not economical or practical to plug the cavity with concrete. The technique of telescoping casing can be used (Fig.3). Initially, an outer casing is sunk into the ground until the marble rockhead is reached. The bottom of the outer casing should be sealed using concrete to prevent soil piping, again using the procedure described in Section 3.1. The marble above the cavity can be excavated by chiselling or RCD to create a bored hole large enough to accommodate the inner casing. On reaching the cavity, an inner casing is sunk onto the bottom of the cavity. The cavity infill materials inside the casing is then removed by grab.

At the LRT site, a 2.5m diameter outer casing was used. If the marble above the cavity was to be excavated by RCD, a 2.3m diameter drill bit would be used. This would create a sufficiently large bored hole to accommodate a 2.2m diameter inner casing.

The bottom of the inner casing should also be sealed using concrete to prevent future ingress of soft materials into the bored hole. A permanent liner has to be used for forming the pile in the cavity. The inner casing is to be extracted section by section in the course of concreting while the outer casing can be extracted when concreting is complete.

A gap between the permanent liner and the soil layer may remain when the outer casing is extracted. This gap should be backfilled with soils to prevent it from developing into a soil cavity when construction of other adjacent piles commences later.

If a large cavity is present, bursting of the permanent liner during concreting can cause very serious consequences. This can happen when the portion of the permanent liner within the large cavity loses its lateral support while the inner casing is being extracted in the course of concreting. If rupture of the permanent liner occurs, the concrete will flow quickly out of the liner to fill up the cavity, causing a very sudden and significant drop in the levels of water and concrete in the casing. At the same time, the outflow of concrete will cause a rise in the water level outside the permanent liner. The difference in water levels inside and outside the liner will result in a significant pressure on the permanent liner. If the liner is not strong enough, necking will occur and the pile will be damaged. Therefore, for long piles passing through large cavities, a strong permanent liner is strongly recommended.

In principle, piles with many large cavities can be constructed by multiple telescoping using three or more temporary casings. However, it is preferable not to construct any pile at a location with more than two large cavities because the operation of multiple telescoping is very tricky and perhaps dangerous.

2.4 General rules

The methods described above may need to be adjusted to suit particular conditions of a pile. However, there are some

general rules which apply for all situations.

As the method of construction to be adopted depends on the number and size of the cavities, it is desirable to have at least one site investigation drillhole at every pile location so that the contractor can use an appropriate construction procedure for each pile.

Piles close to each other should not be constructed at the same time whenever practicable because it will increase the risk of formation of sinkholes and lead to other serious consequences. In one instance, driving of the temporary casing by a heavy-duty vibrator caused collapse of rocks and cavity infill into the bored hole of an adjacent pile. In another instance, concrete flowed from one pile during concreting to another pile in its vicinity through the cavities connecting the two piles. The drill bit inside the second pile was totally engulfed by concrete.

When a pile is being concreted, all excavation works by RCD near to the pile must be stopped because RCD will create movements of water within the marble bedrock, washing away the cement paste of unset concrete.

Excavated rock samples should be examined frequently so that any unexpected solution features or cavities, if present, can be detected and the method of construction be changed accordingly.

3. RISKS AND PROBLEMS

3.1 Soil piping

One of the major risks of bored piling in cavernous marble is the formation of sinkholes. Soil piping is often responsible for the initiation of soil cavities and subsequent formation of sinkholes (5,6). In bored piling, soil piping can be caused by fluctuation of the water level within the casing. Positive pore-water pressures generated in response to water-level fluctuations cause dislodgment of soil particles and subsequent formation of soil cavities. Rapid circulation of water within the casing can also result in erosion of soil deposit.

Soil piping tends to start near the bottom of the casing. The size of soil cavities induced by soil piping can be very large. In one instance, about $20m^3$ of concrete was lost during concreting when the casing was slightly lifted above the marble rockhead in the course of concreting. Concrete was believed to have flowed out of the casing and filled the soil cavity outside it.

A useful and effective method to prevent soil piping is to seal the bottom of the temporary casing by concrete. On reaching the marble rockhead, a small rock socket is formed by chiselling. A small soil cavity may be created during this stage. A suitable amount of tremie concrete is then placed inside the casing. The concrete will flow out of the casing to fill up the soil cavity around it. Sometimes, the casing may need to be slightly lifted to allow an easier outflow of concrete. When concreting is complete, the casing is driven downwards before the concrete is set to ensure as tight an interface as possible between the casing and the marble bedrock. When the concrete has hardened, an impermeable annular barrier will be formed around the bottom of the casing. Excavation of rock can commence after removal of the concrete inside the casing. Sealing of casing will help minimise if not totally eliminate the problem of soil piping. The concrete inside the casing is later excavated. The forming of the initial rock socket is important to ensure that solid marble bedrock is reached, and not the pinnacles, before concreting commences. This will provide a more effective sealing.

If the problem of soil piping is ignored, the soil cavity formed near the bottom of the casing will enlarge and progress upwards along the casing until it finally collapses. Even if the soil cavities are stable at the initial stage of construction, each soil cavity in the soil profile will contribute to the risk of a large scale ground subsidence or the formation of a large sinkhole occurring at a later stage of bored piling.

Although the sealing of casing may appear to be time-consuming and costly at first thought, it is more economical in the long run when one considers the damages that may occur without this measure. The following case study is a good example to illustrate this point. For a particular pile, 18m of marble were required to be excavated before reaching the founding level. The casing was not sealed before rock excavation began. When the founding level was finally reached, a large quantity of soils suddenly oozed into the bored hole from the bottom of the casing. Luckily, the drill bit had been removed from the pile before the incident occurred. The bored hole had to be concreted in order to fill the soil cavity around the casing. The concreted section, which was in excess of 20m in length, had to be excavated to reach the founding level again. Sealing of casing also makes cleansing of the bored hole easier because a lesser amount of soils will enter the bored hole from the bottom of the casing.

3.2 Collapse of soil cavities

An increase in surface loadings during construction may cause the collapse of soil cavities formed during bored piling. In one instance, a heavy crane had sunk suddenly into the ground by about 2m due to the sudden collapse of a shallow soil cavity beneath it.

To minimise the damage caused by a sudden collapse of a soil cavity, it is useful to detect the presence of such cavities before and regularly during construction, say, by SPT tests or other types of dynamic penetrometers. If soil cavities are found, it is desirable to strengthen the ground by dynamic compaction, i.e. breaking the soil cavities before the damage is done, or filling the cavities by grouting.

The existence of a sizeable soil cavity around a pile can be indicated by the presence of a shallow depression or a vertical opening adjacent to the pile. In one instance, a 15m deep vertical opening was observed in the ground next to the temporary casing. Rapid movements of water in response to changes in the water level inside the casing can be seen around the pile. If action is not taken at this stage, a collapse of soil cavity is imminent.

Excavation for the construction of pile caps results in thinning of the soil profile and the chance of collapse of a surface soil cavity due to increased loading will be higher.

3.3 Removal of cavity infill

Removal of cavity infill from a cavity may induce an inflow of soft materials from other cavities or the soil profile through openings connected to the cavity. Although the emptying of a small cavity may not necessarily have any immediate serious consequence, it is preferable to plug an emptied cavity by tremie concrete before proceeding with further excavation. Otherwise, if more and more emptied cavities are created,

water movements in the marble bedrock will become more rapid and affect a larger area. A large-scale ground subsidence or the formation of a large sinkhole becomes more likely.

Plugging of cavities also has other advantages. It will block the openings connecting the cavity and help prevent the problem of soil piping. As more and more cavities are plugged, the cavity systems in the marble bedrock become less and less inter-connected. This will make the construction of bored pile less problematic at the later stage of construction. Ingress of soft materials from the cavity during excavation may have serious consequences because the materials may jam the chisel or drill bit in the bored hole, making its retrieval difficult. Plugging of cavities reduces this risk. It also makes cleansing of the bored hole easier because less materials will enter the bored hole through the plugged cavity. Because of the above reasons, Method A discussed in Section 2.2 is preferred to Method B for bored piles with small cavities.

Emptying of a large cavity is dangerous because it may result in loss of support and collapse of the cavity. In this case, a temporary casing will need to be driven through the infill material (Fig.3). The material encased by the casing can be removed by grab. It is desirable to seal the inner casing before proceeding with further excavation of marble so as to prevent ingress of infill materials into the bored hole.

3.4 Assessment of rock quality

The surfaces of weathered marble are pitted, and usually yellow to brown in colour, although they may sometimes have the same colour as unweathered marble. The weathered surface zone is usually thin and a thickness of 2 to 3mm is not uncommon.

When excavation is effected by chiselling, the presence of solution features in the marble bedrock can be detected quite easily by examining the rock fragments mucked out from the bored hole. However, if RCD is employed, the thin weathered surface can easily be removed by abrasion before the marble is broken up by the drill bit. As a result, it is difficult to detect the existence of solution features by examining the small marble flakes collected from the discharge hose of the reverse circulation drill. For this reason, the determination of the founding level of a bored pile cannot be based on the examination of rock samples or fragments retrieved from the bored hole. One has to rely on the site investigation information. It is important to have at least one site investigation drillhole for each pile to ensure that there is no large cavity beneath the founding level.

In judging the presence of cavities at a pile location, one should not rely solely on the drillhole log for the pile. Other site investigation data collected at nearby locations should also be considered. In one instance, the drillhole log of a particular pile did not indicate the presence of a cavity and the method of construction used was based on the assumption of no cavity. Rock samples collected at a level of about 43m below the ground surface indicated the presence of solution features at that level. The contractor ignored the implications of this finding and also the fact that the drillhole logs at adjacent locations did reveal the existence of a large cavity system close to the pile. When the pile was being concreted, about 350m^3 of concrete had flowed out of the bored hole at the level where the solution features were detected earlier during excavation. It was believed that a bedrock opening connecting to the large cavity system was present at that location.

4. CONCLUSIONS

Construction of large diameter bored piles in cavernous marble is feasible although it requires more efforts and precautions than ordinary bored piling. Many of the risks and problems associated with the construction of bored piles in cavernous marble can be minimised or solved using the methods described in the paper. It is suggested that some of the recommended construction procedures, such as sealing of casing and plugging of cavities, be stipulated in the specifications or drawings to ensure that they will be implemented by the contractor. A suitable method of measurement should also be devised so that the contractor can be suitably rewarded for implementing these procedures.

5. REFERENCES

1. Ha, T.H.C., Ng, S.K.C. and Li, Q.W. "Discovery of Carbonate Rocks in Yuen Long Area, Hong Kong", Hong Kong Baptist College Academic Journal, Vol.8, 1981, pp.129-131.

2. Holmes, D.G. and Keung, C.P.Y. "Design for Foundations in Karstic Limestone", paper presented at Conference on Karst Geology in Hong Kong, Geological Society of Hong Kong, 1990.

3. Holmes, D.G., Keung, C.P.Y. and Li, K.S. "Heavy Foundations in Karstic Limestone", Proc. Conf. on Deep Foundation Practice, Singapore, 1990, pp.105-110.

4. Houghton, D.A. and Wong, C.M. "Implications of the Karst Marble at Yuen Long for Foundation Investigation and Design", Hong Kong Engineer, June, 1990, pp.19-27.

5. Newton, J.G. "Review of Induced Sinkholes Development", Proc. 1st Multidisciplinary Conference on Sinkhole, Florida, 1984, pp.3-9.

6. Newton, J.G. and Tanner, J.M. "Case Histories of Induced Sinkholes in the Eastern United States", Proc. 2nd Multidisciplinary Conference on Sinkhole and the Environmental Impacts of Karst, Orlando, 1987, pp.15-23.

7. Pascall, D. "Cavernous Ground in Yuen Long, Hong Kong", Geotechnical Engineering, Vol.18, 1987, pp.207-221.

8. Siu, K.L. and Kwan, S.H. "Case History of a Pile Foundation in Unusual Ground in Hong Kong", Proc. 7th Southeast Asian Geotechnical Conference, Hong Kong, Vol.1, 1982, pp.423-438.

9. Siu, K.L. and Wong, K.M. "Marble and Sub-surface Karst at Yuen Long", Newsletter, Geological Society of Hong Kong, Vol.2, No.5, 1984, pp.1-7.

10. Siu, K.L. and Wong, K.M. "Concealed Marble at Yuen Long", Proc. Conf. on Geological Aspects of Site Investigation, Bulletin No.2, Geological Society of Hong Kong, 1985, pp.75-88.

11. Wong, K.M. and Ho, S. "Dolomatic Limestone in Tolo Channel", Newsletter, Geological Society of Hong Kong, Vol.4, No.4, 1986, pp.20-23.

Prediction & Measurement of Settlement of a Heavily Loaded Raft

R.J. OLDS
B.E. (Hons), M.I.E. (Aust), C.P.Eng.
Manager, Coffey Partners International Pty Ltd

NOTATION

E_u	=	undrained Young's Modulus
E'	=	drained Young's Modulus
ν_u	=	undrained Poisson's Ratio
ν'	=	drained Poisson's Ratio
q_c	=	electric cone penetrometer cone resistance
S_u	=	undrained shear strength

INTRODUCTION

In 1989 the author undertook geotechnical investigation for the raft footing of the main element of the new RCCU (Residue Catalytic Cracking Unit) project at the Shell refinery at Corio, Victoria. The site is located on deposits of deep calcareous overconsolidated clay soils of the Moorabool and Fyansford formations. Stringent settlement criteria had been specified, but, from an operational viewpoint, settlement was mainly controlled by tolerable deflections in pipework connecting to the major vessels. Total settlements and distortions had to be taken into account in the structural design of the footing.

Whilst a preliminary design for a raft footing had been prepared based on work by others, it had not been established that tolerable settlement would be achieved with a raft. Piled footing systems were therefore reviewed at an early stage.

Fieldwork involved the drilling of boreholes, pressuremeter testing, and electric cone penetrometer tests. Laboratory tests included undrained compression and classification testing. The results of these tests were used to develop a modulus profile with depth, which was used in the computer program, FOCALS, to estimate settlement at 2.5 metre centres across the 36m by 22.5 metre raft footing.

Based on the results of this analysis Shell accepted that a raft footing could be used without exceeding tolerable settlements. They proceeded with this system, saving considerable time and money compared to the piling option. Settlement monitoring since construction of the raft has allowed the accuracy of the initial predictions to be assessed, although as yet, construction is not complete.

2. THE PROJECT

The main elements of the RCCU project are the regenerator, the reactor, and the fractionator column. These three vessels are all located on a raft footing of slightly irregular, but essentially rectangular shape, and measuring 36 metres by 22.5 metres. The regenerator and reactor vessels are supported on a suspended concrete slab 12 metres above ground level. This slab is referred to as the table top, and is supported on four large columns which transfer loads to the raft. The design dead load plus live load is 97.5 MN, creating an average stress of 140 kPa on the foundation. Wind loads cause large moments and localised increased stresses on the foundation. As these vessels form the nucleus of the new refining process, a myriad of pipework interconnects the vessels with the remainder of the plant.

At the time of commencing the investigation there was considerable uncertainty about the use of a raft, as investigation by others had shown that there was no rock within 50 metres of the surface, but had not adequately defined the compressibility characteristics of the foundation to allow confident prediction that the specified settlement tolerances could be achieved.

The project was approaching the final stages of design, and it was intended foundation contracts would be awarded within two to three months of our first involvement. A preliminary design involved a uniform 1.8 metres thick raft founding at 4m depth.

3. FIELD STUDIES

Five boreholes ranging in depth from 5 metres to 50 metres had been already drilled beneath the proposed raft. The published geology of the site suggested the soils at 50 metres could continue well below the zone of influence of the raft, and previous experience in these geological units had shown these soils become extremely uniform at depth.

The fieldwork therefore concentrated on establishing a modulus profile within the four main geological units identified in published literature, and which could be inferred from the previous boreholes and samples available to observe.

Two boreholes were drilled to depths of 45m and 46m. Undisturbed samples were recovered, and pressuremeter tests carried out. Six tests were attempted using the Coffey Self Boring Pressuremeter (SBPM), but due to the presence of hard limestone gravel bands in the upper 20 metres, only two of these attempts were successful. The final attempt resulted in the shearing of the cutter and drive rod in the SBPM. Further tests were conducted in predrilled boreholes using the Coffey PMX-20 pressuremeter. Tests were conducted with at least one unload-reload cycle of applied pressure.

In addition to the drilling, seven electric cone penetrometer (ECP) tests were conducted at five locations including the two borehole locations, in an attempt to assess variations in soil stiffness across the foundation. It was originally intended that nine locations would be tested, but the gravel layers made testing extremely difficult, and the results of the testing conducted showed conditions to be relatively uniform across the foundation.

The penetrometer tests were conducted by using a dummy probe to penetrate gravel layers when the recording cone met refusal. This method caused considerable damage to equipment, breaking cones, friction sleeves, and permanently deforming several rods. Only two of the seven probes were able to penetrate past the upper 20 metres, and these terminated at 38 metres depth.

The location of the boreholes and penetrometer tests and the general arrangement of the vessels on the raft is shown on Figure 1.

4. LABORATORY TESTING

Bearing capacity was not considered likely to be a controlling factor in design of the raft, but several single stage undrained confined compressive strength tests were conducted on undisturbed samples to assist in developing a foundation model.

Due to the overconsolidated nature of the soil, confining pressures greater than the calculated vertical overburden stress were adopted for the single stage confined compression tests.

Atterberg Limits and Particle Size Distribution tests were conducted on selected samples from each of the four foundation units to assist in classification.

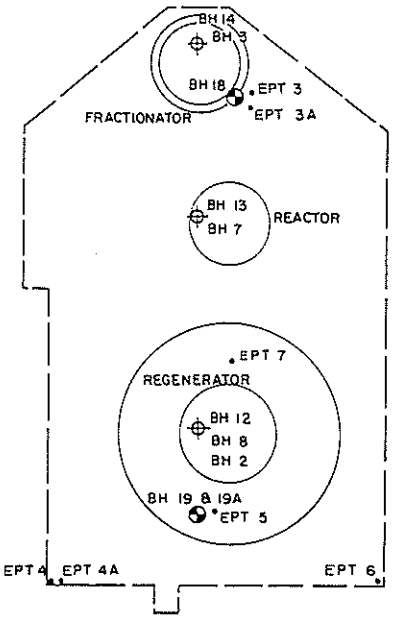

Figure 1. General arrangement of vessels on raft, borehole and EPT locations.

5. GEOTECHNICAL MODEL

5.1 Geological Units

The published geology shows the site to be located on Tertiary alluvium of the Moorabool Formation, overlying the Fyansford Formation. Each formation is described as having upper and lower units. From visual classification, and the results of the ECP tests the foundation was divided into four units as shown in Table I. These units ignored the fill layer capping the site, which was irrelevant to the study of settlement, due to the 4m founding depth proposed for the raft.

5.2 Groundwater

Groundwater was measured in slotted standpipes, at depths of between 3m and 4m below ground level. As the site was essentially level, the cause of this variation was not known, but ascribed to possible variations caused by the discontinuous gravel layers.

5.3 Pressuremeter Test Results

The pressuremeter tests were conducted in a quick manner in an attempt to restrict pore pressure dissipation during testing and hence obtain a measure of the undrained modulus of the foundation soils. Based on published evidence by Wroth (1984) in his Rankine lecture, the modulus derived from the unload/reload part of the test was used. Two Young's modulus values were derived from each test. The first value adopted

TABLE I FOUNDATION UNITS

UNIT	DEPTH (m)	DESCRIPTION	WL	Wp	Ip	% Fines
1	0 to 6	SANDY CLAY, high plasticity, grey-brown, very stiff, with layers of limestone gravel.	64	16	48	78
2	6 to 20	SILTY CLAY, high plasticity, grey and orange, very stiff with layers of limestone gravel.	55	17	38	90
3	20 to 30	SANDY SILT, low plasticity, grey, hard, calcareous.	39	29	10	74
4	> 30	SANDY SILTY CLAY, medium plasticity, grey, hard, calcareous.	44	25	19	75

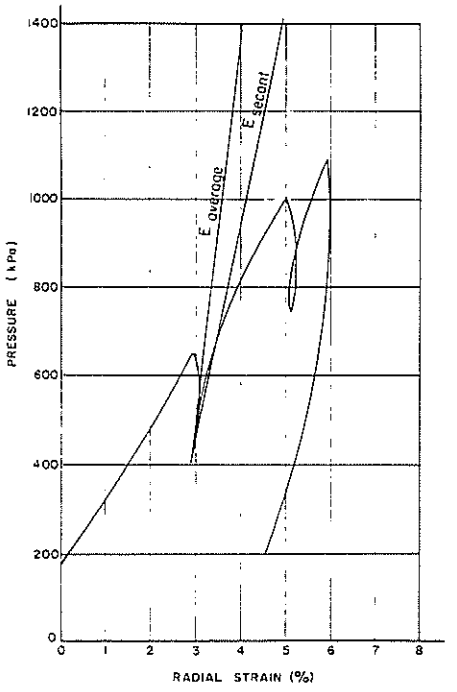

Figure 2. Typical pressuremeter test result and defined modulus values.

the average slope of the unload/reload load cycle ($E_{average}$), whilst the second value adopted the reload secant modulus between the unload and reload pressures (E_{secant}). This approach is shown schematically on Figure 2.

Twenty two pressuremeter test results were used to develop the foundation modulus model. The average and secant modulus values from these tests are shown plotted versus depth on Figure 3.

5.4 Other Test Results

Due to the amount of pressuremeter data gathered, and the reasonable consistency of this data it was not necessary to extrapolate modulus values from the indirect tests used in the investigation. The results of the ECP and the compressive strength tests were therefore not used directly in developing the foundation modulus, but the ratios E_u/q_c and E_u/S_u were calculated to check that they were within the ranges that would be expected.

The approximate ratios were as follows.

E_u/q_c = 25 to 60
E_u/S_u = 600 to 1200

The results of these tests were also plotted versus depth, to check that none of the data identified weak or compressible layers between pressuremeter test depths. A typical ECP plot is shown on Figure 4.

5.5 Design Modulus Profile

Based on the data discussed in Sections 5.3 and 5.4, undrained modulus profiles were adopted for use in the estimation of raft settlement.

Due to the importance of the structure, and the consequences of excessive settlement, it was considered that, at least in the first instance, a design modulus profile should be adopted which was judged to be reasonably conservative. The data did not show variations within the main geological units described above, but did show an increase in modulus in the Fyansford formation which occurred below about 20 metres.

Profile A, shown on Figure 3, was adopted as the design profile, as it was almost lower bound to all data. Whilst pressuremeter tests in the limestone gravel layers within the Moorabool formation showed these layers to be less compressible than the soil by a factor of about 3 to 5, it was decided not to

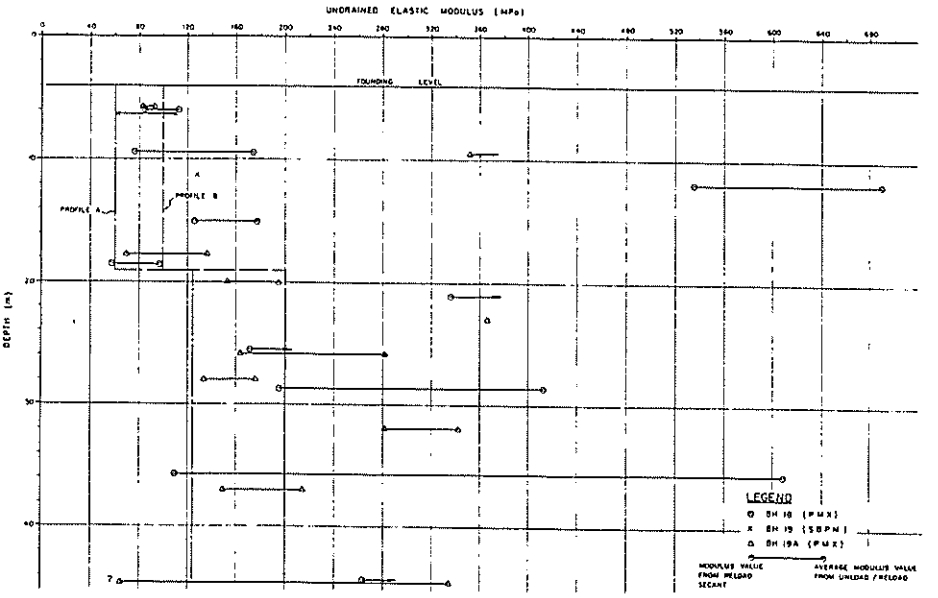

Figure 3. Undrained modulus versus depth from pressuremeter tests.

use these values to increase the mass modulus in the upper 20 metres. In addition to Profile A, a second Profile (B) was chosen as one which may predict settlement more realistically. Profile B may have been adopted if the consequences of incorrect settlement estimation were not so great.

Whilst Profiles A and B were selected from visual assessment of the data at the time of the project, a statistical assessment of the data has been made for this paper. It is interesting to compare the probability of settlement exceedance, with the ratio of the measured to predicted settlement outlined in Section 8.

The statistical assessments of both profiles A and B are presented in Table II for both layers 1 (above 20m) and 2 (below 20m). In conducting this assessment, obvious outlier results have not been included.

6. DESIGN LOADS AND SETTLEMENTS

Numerous design cases required analysis for structural design, but for the geotechnical assessment the number of load cases was simplified. The cases considered were dead load, dead load plus live load, and wind load.

At the stage of selecting design loads it was recognised that the decisions would affect the design settlement values. It was assumed that settlement under dead load would be complete by the time pipework was connected, but to offset the potential unconservative aspects of this assumption, only the main dead load of the raft plus backfill was treated as dead load. Live load was assumed to be imposed after construction was complete and pipework connected. The design live load included all true live loads plus the dead load of the vessels and ancillary structural elements on the raft. Settlement under wind load from two directions was calculated independently of other loads and added or subtracted using principles of superposition.

TABLE II
STATISTICAL ASSESSMENT
OF PRESSUREMETER RESULTS

LAYER	MODULUS	MEAN	STD DEVN.	PROFILE A		PROFILE B	
				ADOPTED E	RISK %	ADOPTED E	RISK %
1	Secant	86	27	60	40	125	93
2	Secant	199	92	100	14	200	50
1	Average	129	33	60	2	125	45
2	Average	326	126	100	4	200	16

RISK is defined as the probability that the selected modulus profile would not be achieved.
Values are E_u in MPa.

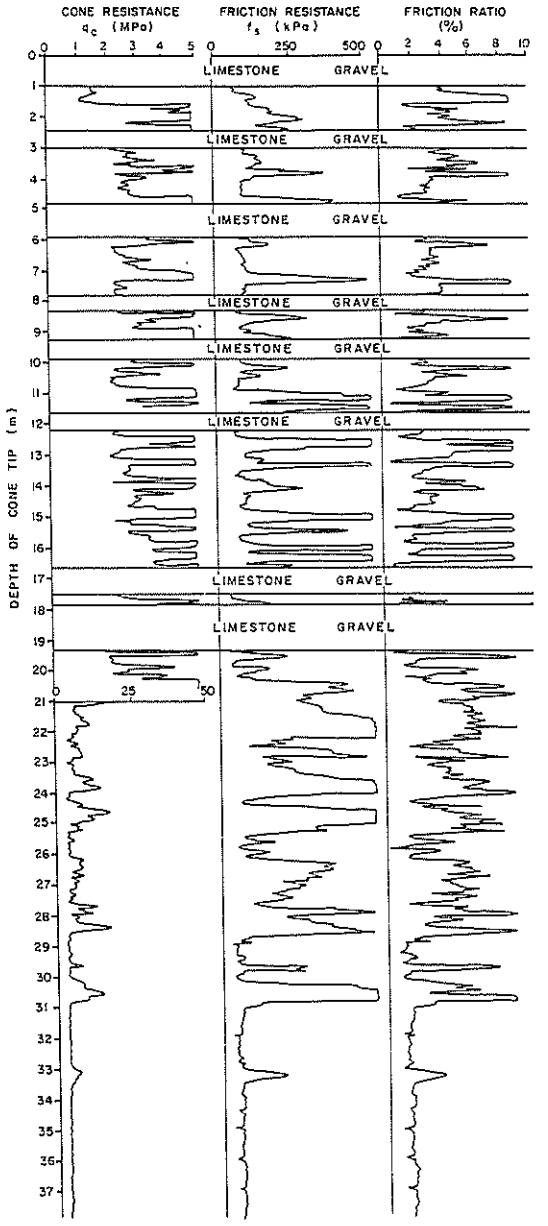

Figure 4. Typical electric cone penetrometer profile.

The raft was designed to withstand long term total and differential settlement caused by dead load plus live load, and short term deflections caused by the design three second wind gust. The pipework was designed to withstand at least the settlement caused by live load and wind load. The actual dead and live loads of the different main elements are shown in Table III.

To assess long term settlement behaviour the drained modulus of the foundation was used. No attempt was made to predict settlement-time behaviour using the conventional coefficient of consolidation as measured by oedometer, as the insitu drainage paths for excess pore pressure dissipation were assessed to be complex and incapable of being modelled in an oedometer. As the proposed construction period was relatively long (approximately 2 years), it was judged that the majority of settlement under imposed loading would be complete within that timeframe. It should be realised these were first assumptions which were reassessed at the completion of the analysis to check the validity, and the consequences of the assumption being incorrect.

The drained modulus was calculated from the undrained modulus using the theoretical equation.

$$E' = \frac{2(1+\nu')}{3} E_u \quad \ldots\ (1)$$

The adopted values of Poisson's Ratio were

$$\nu_u = 0.5$$
$$\nu' = 0.3$$

7. COMPUTER ANALYSIS

The settlement of the raft was calculated using the finite element multi layered elastic analysis program 'FOCALS' (Wardle & Fraser, 1975). Node points at 2.5m centres were adopted and the load cases as described in Section 5 analysed using the 1.8 metre thick raft. The loads and moments were applied to the raft at the nominated application points rather than spread uniformly across the raft, to identify where distortions could occur.

The results of these analyses are discussed in Section 8. These results were used only for geotechnical assessment and once it was accepted that settlements would be tolerable, the structural designers used FOCALS to conduct the numerous analyses required for structural design of the raft.

TABLE III

DEAD AND LIVE LOADS (MN)

Raft & Backfill	Columns & Tabletop	Vessels		Steel	Other
DL	DL	DL	DL & LL	DL	LL
60.25	11.95	8.17	20.13	2.76	2.45

8. ESTIMATED AND MEASURED SETTLEMENTS

The settlement estimated under the different load cases for modulus Profile B is summarised in Table IV. Due to the stiffness of the raft, predicted differential settlement was relatively small and therefore only selected points are presented in Table IV. These points correspond to the points at which settlement monitoring has been conducted, and allow direct comparison between estimated and measured settlement to date.

In summary, Profile A predicted maximum settlement of 47mm, with 29mm under raft and backfill load. The corresponding values for Profile B are 30mm and 19mm. Deflections under wind loading were within plus or minus 2mm. The maximum predicted distortion in the raft is about 0.1% for the total loading and Profile A.

In Table IV additional values are included to correspond to times at which settlement readings were taken. The two times of measured readings presented in Table IV are:-

1. at the completion of constructing the raft, the table top, and the backfilling; and

2. at the completion of constructing the three new vessels.

Case 1 is compared to the settlement prediction based on undrained conditions for the loads imposed, which is 72% of that for drained conditions based on the approach outlined in Section 6. Case 2 is compared to drained conditions under the loads for Case 1 plus undrained conditions for the vessel dead load. The average overestimation of settlements is 5.2mm (40%) with a range of 2.1mm to 8mm (17% to 73%).

The values of settlement for Profile A have not been detailed herein, but they range from 1.5 to 1.7 times those for Profile B. If the average of 1.6 is used, and multiplied by the 1.4 average value of overestimation for Profile B, an overestimation factor of 2.2 is obtained from Profile A. In other words, based on present measurements, Profile A may have a factor of safety on settlement of about 2. This value is considered reasonable for the importance of the structure and the consequences of failure. It compares to assessed probabilities of exceedance of about 3% and 25% based on average modulus values or secant modulus values respectively.

It should be recognised that settlement monitoring is continuing and that the extent of overestimation may be reduced with time. Many other factors as discussed in this paper were built into the model to establish a degree of conservatism. Whilst there was no way to establish the safety factor of 2 on settlement at the time of design, it is consistent with what might have been adopted if methods using safety factors had been used.

9. CONCLUSIONS

Pressuremeter tests have been used as the main method to develop a modulus profile for the prediction of settlement of a large heavily loaded raft footing. Different methods of test interpretation have been used and the resulting estimates compared to measurements taken during construction. Theoretical approaches in combination with assumptions have been used to distinguish between short and long term settlement. The resulting overestimates of settlement are considered reasonable given that settlements may be continuing, and given the importance of the facility and the consequences of failure.

10. ACKNOWLEDGEMENTS

The author wishes to thank the various staff members of Coffey, Shell, and Davy McKee who were involved in this project for their assistance, and Shell (Refining) Australia Pty Ltd for permission to publish the information.

11. REFERENCES

Wardle, L J & Fraser, R A (1975), Program FOCALS - Foundation on Cross Anisotropic Layered System - users' manual. Geomechanics Computer Program No 4. Melbourne: CSIRO Division of Applied Geomechanics.

Wroth, C P (1984), The Interpretation of In Situ Soil Tests. Geotechnique 34 No 4.

TABLE IV

MEASURED VERSUS
PREDICTED SETTLEMENT FOR MODULUS PROFILE B

Monitoring Point	Case 1				Case 2			
	Predicted	Measured	Difference	Ratio	Predicted	Measured	Difference	Ratio
3	13.8	9.5	4.3	1.44	2.3	15.0	5.3	1.35
4	15.5	10	5.5	1.55	22.9	15.5	7.4	1.48
5	15.5	10	5.5	1.55	22.9	16.0	6.9	1.43
6	14.6	9	5.6	1.62	21.6	14.5	7.1	1.45
7	15.5	10	5.5	1.55	22.9	16.0	6.9	1.43
8	14.6	12.5	2.1	1.17	21.6	18.5	3.1	1.17
9	12.9	9	3.9	1.43	19.0	16.0	3.0	1.19
10	12.9	10	2.9	1.29	19.0	11.0	3.0	1.73

Monitoring points 1 and 2 were destroyed in construction.
Settlement values are in mm.

The cellular raft and horizontal ground strains

J.P. PELLISSIER
B.Sc. (Eng.), M.Eng.M.S.A.I.C.E.
Project Leader, Division of Building Technology, CSIR, South Africa
A.A.B. WILLIAMS
B.Sc. (Eng.), D.I.C., Ph.D., F.S.A.I.C.E., Pr.Eng.
Consultant, Division of Building Technology, CSIR, South Africa

SUMMARY: The development of a cellular raft foundation (called the BOUCELL raft) is described and compared with the conventional slab-on-ground or stiffened raft foundation in a number of applications. The potential of the cellular raft to reduce the risk of distress to buildings caused by horizontal soil strain is discussed. Areas of application where this mechanism of horizontal soil strain should be considered, include:

- Buildings on ground to be undermined, particularly with longwall mining techniques for total extraction of coal.
- Buildings in seismically active zones where large ground motions may be involved.
- Buildings on swelling soft rock which has been weathered to considerable depth.

1. INTRODUCTION

Most of the low-rise buildings erected in South Africa are constructed with load-bearing brick walls and these walls are highly susceptible to distress in the form of cracks if they are subjected to differential movement. There has been continuous research over several decades in South Africa to develop economical foundation solutions for small structures, particularly in mass housing schemes, to cater for widespread problems caused by difficult soil conditions. Some of these natural and man-made problem soils or problem sites in South Africa include:

- **Heaving clay:** One of the major problems is that of "heaving clay" in the arid areas, or "shrinkable clay" in the seasonally more humid areas, and a number of viable solutions now exist (Williams, Pidgeon & Day, 1985).
- **Collapsing sand:** Vast areas in the more arid regions of the country are overlain by soils with a collapsible grain structure, or so-called "collapsing sand" (Schwartz, 1985). These soils can exhibit sudden differential settlement upon wetting up. They are often found to overlie a swelling clay profile, which complicates the matter further.
- **Dolomite:** There are large areas in the densely populated parts of the country that are prone to settlement on dolomite formations (Wagener, 1985).
- **Soft deposits:** In the more humid areas soft deposits, in the form of loose to very loose sand or soft clays, are encountered. Buildings constructed on these soft deposits may be subject to distress due to differential settlement.
- **Waste dumps or land fills:** With the increasing spread of urban development, the possible settlement of structures built on old waste dumps or land fills requires attention.
- **Undermining:** Where coal is mined at some depth below the surface and total extraction is employed, often with longwall mining techniques, there is considerable surface subsidence accompanied by large horizontal strains in the ground.
- **Seismic activity:** South Africa is not in a zone of high natural seismic activity (although significant events have occurred in the past), but many seismic tremors due to deep gold-mining activities cause distress in a number of areas.
- **Swelling rock:** A phenomenon not well recognised in the country as yet is the effect of deep underlying swelling rock on the performance of surface structures. In South Africa large areas of the country are underlain by such swelling rock.
- **High water table:** This is different kind of problem in the more humid areas of the country, where distress in the building consists mainly of rising damp in the walls.

From a socio-economic point of view, South Africa today faces other problems too. There is for example, a backlog in housing while mass urbanisation is taking place, and a shortage of skilled personnel capable of correctly analysing the potential effects of problem soils and sites. A need therefore exists for a foundation system that can easily be adopted as a blanket solution.

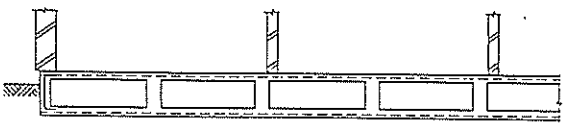

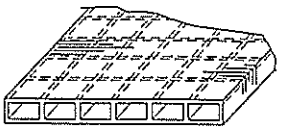

Fig.1. Cross-section of the BOUCELL cellular raft foundation

A variety of foundation and/or structural solutions has been developed, including piled foundations, stiffened rafts with articulated superstructures or methods for treating the soil to some depth (Barrett & Wrench, 1984). These methods all have advantages and disadvantages but none can be used as a solution for all problem soils.

Research and development at the Division of Building Technology of the CSIR has led to an improved cellular raft-like construction, which has been patented and is referred to as the BOUCELL raft. This cellular raft can be described as a traditional stiffened raft with an additional slab at the base (see Figure 1). Finite-element analyses comparing the stiffened raft and the cellular raft have confirmed that their structural behaviour is different.

The structural action of this cellular raft can be best described as simulating that of a composite sandwich panel. This foundation is several times stiffer, particularly in torsion, than the traditional stiffened raft with stiffening beams, because of the composite action of the top and bottom slabs with the integral webs. The advantages of the cellular raft compared with the traditional stiffened raft are discussed in more detail in Williams and Pellissier [1992] and include:

- Although dependent on geometry, the cellular raft is at least 2 to 4 times stiffer than the conventional raft in bending. Consequently, articulation joints in the superstructure can often be eliminated.
- The cellular raft shows an even greater increase in the torsional stiffness than in the bending stiffness. The result is that localised deformations are more effectively dealt with in the cellular raft, because the deformation is spread over the whole raft and is not localised as is often the case with conventional stiffened rafts.
- The cellular raft has the advantage that flexibility of architectural layout can be achieved as the webs are fairly closly spaced and the position of the internal walls is not governed by the position of the beams.
- With the cellular raft, the floor of the structure can easily be constructed above the surrounding soil, avoiding drainage problems caused by storm water or water-logged soil.

This new type of foundation is rapidly gaining ground as a blanket solution for problem soils and should be favoured in the coal mining areas, where the associated shales have weathered to become expansive clay near the surface. The potential ground movement in these areas can be fairly large - from a rise of 75 mm (caused by heaving clay) over the length of a house to a total mining subsidence of one metre, which could lead to very damaging differential movements in a house, or cause an unacceptable tilt. In such extremes the maximum horizontal displacement, expressed as a ground strain, could be 0.015 for longwall extraction of coal seams at depths of about 120 m.

In gold mining, where activities are very deep-seated, there are also effects of a seismic nature which may not reach the magnitude of major earthquakes but must be allowed for in structural design and consideration of soil/structure interaction. In this field, too, the cellular foundation could find useful application where a blanket option has advantages for a number of risks, whether from horizontal strains or motions, or vertical movements in the soil profile brought about by seismic activity. The advantages of this cellular raft foundation over the traditional stiffened raft (that is, increased stiffness in bending and torsion) apply to all the other problem soils where the vertical deformation of the soil is the overriding important factor.

This paper records the research carried out by the authors, highlighting the situation where horizontal soil strains can play an important role in the performance of the structure, and discussing the field and laboratory work carried out.

2. SEISMIC MOTIONS

2.1 Background

In South Africa very few earthquakes of medium intensity have been recorded, but between 40 and 60 tremors occur monthly in the gold mining areas (Milford and Wium, 1991). While the tremors are characterised by very high horizontal peak ground accelerations of up to 0.45 g (440 cm/s^2) with an associated ground velocity of 67 mm/s, the maximum frequency of the acceleration component is typically between 10 Hz and 50 Hz. The epicentres of these events are also relatively shallow (2 km to 4 km depth) and their effects attenuate very rapidly. Damage to residential type buildings in the mining areas has generally been limited to cracking of the plaster and brickwork, in accordance with the peak ground velocity rather than acceleration, where 10 mm/s seems to be a threshold below which there is little damage to masonry. This is a criterion often applied to acceptable ground velocities resulting from blasting with similar conditions of impact loading.

In regions subject to natural earthquakes where the strong ground motion of 0.5 g or more is random, the maximum frequency is low, say between 2Hz and 5Hz, and the disturbance is sustained for some time, perhaps up to 60 s or more. The horizontal component usually has the greatest effect on structures and according to Key (1988), "many failures occur in horizontal torsion, especially in low-rise garage-like structures that consist of a 'box' with one side omitted". Further, there seems to be evidence that the maximum ground strain at some distance from the source may be due to the secondary or slower surface waves, particularly Rayleigh waves where the horizontal component is parallel to the direction of propagation (O'Rourke, Castro and Hossain, 1984).

Horizontal displacements in low-rise buildings will be transmitted to the structure and consideration will have to be given to their dynamic response. For example, the design should reduce torsional effects, openings in walls should still permit adequate racking resistance, the roof should be light and the tops of the walls be well tied, and all connections should have adequate strength and ductility. However, the foundation will also be subject to horizontal movement and horizontal strains if the motions at two points are out of phase. The maximum soil strain, ϵ, is related to the velocity of propagation of the disturbance, C, and the peak particle velocity, V_{max}, as follows:

$$\epsilon = \frac{V_{max}}{C}$$

O'Rourke et al (1984) quoted an example of a bridge with abutments 21 m apart. If one uses values of V_{max} = 34 cm/s and C = 252 m/s (based on records from the San Fernando 1971 earthquake), the maximum differential displacement between the abutments is given as 27 mm. For a low-rise structure of similar dimensions, such as a bungalow with strip footings anchored into the ground, the displacements would have caused severe distress. In fact the ground strain of 0.13% exceeds the cracking strain of concrete (about 0.01%) and a slab-on-ground raft, anchored by stiffening beams, would have suffered.

A very good review of aseismic base isolation has been given by Kelly (1986), who points out that ground movement can be in any direction and that some mechanism to prevent movement in response to wind is needed. He mentions the

approach adopted in China for low-rise concrete block or masonry buildings, which are very stiff and heavy, and hence at high risk for earthquake damage. A thin layer of specially screened sand is laid as a separation layer under the floor beams, above a wall foundation. He goes on to say that this idea of a sliding interface as an isolation system is "an attractive one for low cost housing since it can be constructed using no more complicated technology or no more skilled labour than a conventional building".

This review reveals that dynamic ground strains in the horizontal direction at the interface of foundation and soil can be significant, and many pictures of damage show cracks through foundation slabs or roads, indicating severe soil strain far removed from actual faults. However, other effects due to soil behaviour under earthquake-induced vibrations can also cause severe distress to any structure on or near the surface.

2.2 Soil behaviour under seismic conditions

One of the most catastrophic foundation failures can be caused by liquefaction of either granular deposits or stratified formations with thin layers of fine sand or silt. If the sands tend to consolidate during shaking and drainage is impeded, pore pressures in a saturated deposit will increase and there may be a sudden drop in the shear strength of the material, leading to liquefaction. Such behaviour can occur over wide areas and originate deep within the soil profile, so no normal foundations can cope with the situation. An engineering solution to such a problem could involve explosive compaction, dynamic compaction, or vibroflotation to bring the void ratio of the deposit down to a stable value.

Even if drainage was good, sandy soils or gravels would tend to compact under sustained shaking and give rise to compaction subsidence. There is bound to be some differential settlement and some stiff foundations or rafts might be able to cope with this if the total magnitude or tilt were still acceptable.

Seismic effects could also trigger slope instability by increasing the disturbing force, or increasing the lateral pressure on retaining walls. The ground movements could also induce failure in piles at their junction with the pile cap, unless the development of lateral pressures due to embedment of the cap helps resist displacement.

On the other hand, the frictional behaviour of soil can be exploited as a measure to reduce the peak acceleration transmitted through the foundation to the superstructure. A simple base-isolation system such as the cellular raft appears to perform well over a range of frequency and amplitude (Su and Ahmadi, 1989) and an important property is that the peak deflections of the structure do not vary much with increase in ground acceleration. The concept is that during a low-intensity earthquake the structure vibrates and returns to its original position after the seismic event.

During a higher intensity earthquake the structure may slip on the friction surface, several times if necessary, before coming to rest with some residual displacement, after much of the destructive energy has dissipated.

3. HIGH-EXTRACTION COAL MINING

3.1 Background

High-extraction coal mining has the advantage that a large percentage of the available coal reserves can be recovered, but the disadvantage that it causes surface subsidence. The financial benefits of this mining technique make it a popular method world-wide, in spite of the distress it can cause in surface structures. According to Bräuner (1973) it is convenient to describe the deformation at a surface point in terms of the five components: vertical displacement or subsidence; horizontal displacement; slope of the subsidence trough; curvature (vertical) of the subsidence through; strain in the horizontal directions, which can be tensile or compressive.

Various mathematical models have been developed to predict the movement of the soil surface, but the local geology, depth, width and height of extraction have such an important effect on the subsidence profile that can develop on the surface, that each prediction model has to be calibrated for each mine. However, according to Bräuner (1973) tensile and compressive strains cause most mining damage. The main effects of these horizontal strains are tensile fractures, shear (compressive) fractures and the squeezing or buckling of structural elements.

Strains can be expressed as a percentage, or millilmetres per metre and (as used in this paper) as a dimensionless quantity. According to Bräuner (1973) the maximum strains in single troughs are from 1×10^{-3} to 10×10^{-3} and this is more than an order higher than the cracking strain of concrete and brickwork, which is about $0{,}1 \times 10^{-3}$ (or 0.01 %).

3.2 Structural requirements

A suitable foundation system should therefore either be able to resist all the horizontal forces, or allow slip to occur between the soil and the superstructure. The ribs of the conventional stiffened raft are deeply bedded into the soil and this type of foundation should therefore be designed to resist all the tensile forces, whereas the flat soffit of the cellular raft allows for a slip-surface.

The Subsidence Engineer's Handbook (1975) recommends a flexible structure where the foundation slab is cast on a polythene sheet on top of a friable layer, such as 150 mm or more of sand. However, it is questionable whether this kind of foundation would be suitable in South Africa where the coalfields are associated with highly expansive clay deposits (Pellissier 1990). These require stiff foundations to reduce the differential movement to levels that can be tolerated by the superstructure. Also, the curvature induced by near-surface coal mine extraction can be severe if hard rock overlies the mining works.

The cellular raft can be considered the optimum solution for small structures in areas with swelling surface clay, or for prevention of distress due to coal-mining subsidence, for the following reasons:

- It provides the stiffness required to reduce differential movement.
- A slip plane can easily be provided under the flat soffit.
- If the final slope of the building after undermining proves to be unacceptable the foundation normally has enough stiffness to allow the one side of the building to be jacked up to get it level again.

4. DEEP UNWORKED RESIDUAL CLAY

In Pellissier and Vogler (1990) "deep unworked residual clay" was described as deep residual swelling material ranging from stiff clay to very soft rock, where the joint structure of the original parent rock can still be seen. As discussed in the above reference and in Pellissier (1991), these materials cover a large part of the country and exhibit unique swelling properties. The swell of these materials is less affected by the overburden load, with the result that swell at 20 m depth can still affect the performance of the superstructure significantly.

In normal, shallow, surface clay the effects of horizontal swell strains are ignored as far as the design of the foundation is concerned. However, as discussed in Pellissier and Williams [1991] horizontal tensile stresses were observed in the beams of conventional stiffened rafts constructed at a swelling clay test site at Onderstepoort near Pretoria. Field evidence also indicates that the effect of horizontal swell strain caused by these deep clays can affect the performance of the building and the design of the foundation. In a discussion of the distress in a school near Springs founded on these materials, Meintjes (1991) remarked that the ratio of differential vertical displacement to differential horizontal displacement was in the range of 3/8, with the result that the one metre deep reinforced concrete ground beam failed in tension, and 20 mm tension cracks developed in it.

All the requirements discussed for mining subsidence would therefore also apply to these deep unworked residual clays.

5. CELLULAR RAFT CAPABILITIES

5.1 Theoretical assessment

The horizontal strains discussed above can be compressive or tensile and, if compressive, the perimeter of the foundation may also be subject to passive earth pressures. It is therefore advisable that the foundation be as shallow as possible to reduce the risk of distress from compressive soil strain. However, brickwork and concrete structures can normally resist compressive pressures or strains, but they are less suited to resist tensile stresses, or strains which are often larger than the cracking strain of brickwork or concrete.

An effective way of reducing the risk of distress to buildings would be to reduce the tensile soil strains transmitted to the superstructure by the foundation. Under conditions of horizontal soil strain, piled and conventional stiffened raft foundations could also experience problems, because they are firmly bedded in the soil and do not allow slip between the foundation and the soil.

However, if required, the flat soffit of the cellular raft foundation can allow slip between the soil and the foundation. As the ground deforms the horizontal component causes shearing movement underneath and along the side walls of the foundation; these frictional forces should be resisted by the raft. A certain amount of relative displacement between the raft and the soil is required to develop the maximum shear stress, which then stays constant for further relative displacement. The typical development of shear stress can be seen in Figure 2,

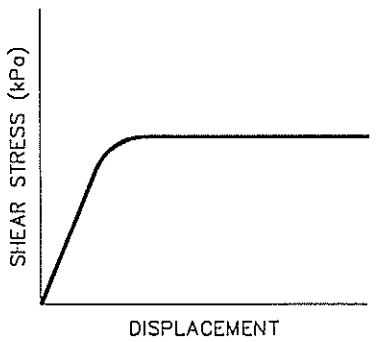

FIG.2. Relationship between friction force development and relative displacement

To analyse the transfer of frictional forces to the raft foundation the foundation may, in simple terms, be considered as a linear structure of unit width (see Figure 3) and perfectly rigid in terms of its reaction to horizontal forces applied along its length. It is also assumed that the middle of the raft will be displaced along with the ground motion (i.e. there is no relative displacement between the soil and the raft at the raft's mid-point). Away from the middle of the raft, increasingly larger relative displacement occurs between the raft and the soil. It is further assumed that the relative displacement decreases linearly towards the middle of the raft. Finally, it is also assumed that there is uniform contact-pressure distribution under the raft.

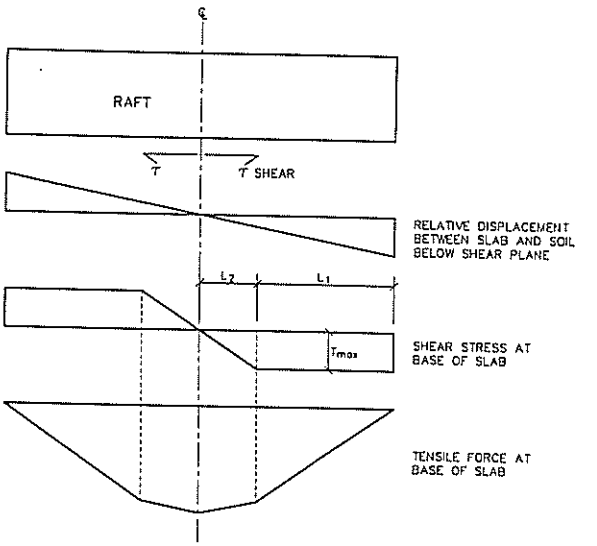

FIG.3. Friction forces acting on the underside of a raft foundation subject to horizontal tensile soil strains

The friction tensile force transmitted to the raft accumulates in its transverse section and increases bi-linearly towards the centre, and the maximum force occurs in the middle.
Based on all these assumptions Ren (1988) suggested the following equation to calculate the maximum tensile force (see Figure 3 for detail):

$$F_{max} = T_{max} \cdot L_1 + \frac{1}{2} \cdot T_{max} \cdot L_2 \qquad (1)$$

where

F_{max} = maximum tensile force in the raft due to lateral extension
T_{max} = maximum shear stress at the contact between the raft and the soil
L_1 = length over which the maximum shear stress applies
L_2 = length over which the shear stress increases linearly.

The shear strength/displacement relationship of undisturbed soils often exhibits a high peak shear strength, before dropping to a lower residual shear stress value. However, during the preparation of the flat surface for the construction of the cellular raft, a thin layer of soil would normally be disturbed under the foundation. T_{max} in equation 1 should therefore approximate the residual shear strength of the soil.

In the analysis of the shear stress build-up under a conventional stiffened raft it should be taken into account that the ribs of the raft may extend well into the soil and that the larger part of the soil remains undisturbed. Peak

shear stresses may therefore develop under a conventional raft and equation 1 should therefore be written as:

$$F_{max} = T_{res} \cdot L_1 + \frac{1}{2} \cdot T_{pek} \cdot L_2 \qquad (2)$$

where
T_{res} = residual shear strength of the soil
T_{pek} = peak shear strength of the soil.

The length over which the shear stress increases (L_2) can be calculated as follows:

$$L_2 = \frac{L_0}{\epsilon_s} \qquad (3)$$

where
L_0 = relative displacement required for maximum shear stress development
ϵ_s = horizontal ground strain as a dimensionless value.

The value of L_0 can be determined using a laboratory shear-box, and the value of the horizontal ground strain should be predicted for design purposes. It should be noted, however, that under conditions of small horizontal soil strain the maximum shear stress (T_{max} or T_{pek}) under the raft may never be mobilised.

5.2 Field and laboratory tests to investigate shear transfer

Field and laboratory simulation tests were carried out to investigate various practical conditions, as well as methods of reducing the risk of distress to buildings subject to horizontal soil strain. To investigate the transfer of stress to the bottom of the raft, three small experimental rafts were constructed at the CSIR Test Site in Pretoria and they consisted of:

- A cellular raft with plan dimensions of 2 m × 2 m, cast in situ on the flat soil surface.
- A cellular raft with plan dimensions of 2.6 m × 2.6 m, placed on top of a special slip layer. The slip layer consisted of a 3 mm rubber-bitumen layer, sandwiched between two plastic sheets.
- A conventional stiffened raft with plan dimensions of 2.6 m × 2.6 m, cast in the soil.

All the experimental rafts had a depth of 600 mm and they were loaded with concrete blocks, so that all of them had an average contact pressure of 15 kPa below the concrete slab. Since it was the development of shear stress beneath the rafts that was to be investigated, the soil at the edges of the rafts was excavated and removed to prevent passive earth pressures from developing. Hydraulic jacks were used to used to move these foundations horizontally, load cells were used to record the force required to do so, and LVDT's were used to record the movement.

The results of these tests can be seen in Figure 4. As expected, the cellular raft placed on a rubber-bitumen emulsion showed the least resistance to movement, and the conventional stiffened raft the highest. It can also be seen that shear stress development under the conventional raft showed a peak value before dropping off, while the cellular raft cast on the soil sheared at a lower shear stress, probably the residual shear strength of the soil.

The lowest coefficient of resistance was 0.44. This is, however, still higher than the ideal value of 0.2 suggested for conditions of seismic activity and an alternative product would therefore be required for these situations. A viscous type of material was sought that would offer a resistance of about 3 kPa in shearing at a velocity of 10-30 mm/s and it was hoped that a quick-breaking bituminous emulsion would be suitable, but this was not practical. A more viable option seems to be a cutback bitumen of MC 3000 grade with a viscosity of about 2000 poises for a 1 mm thickness or about 4000 poises for a 2 mm thickness. This material could then be applied between two layers of plastic sheet beneath the raft and would serve the additional purpose of providing a good damp-proof membrane.

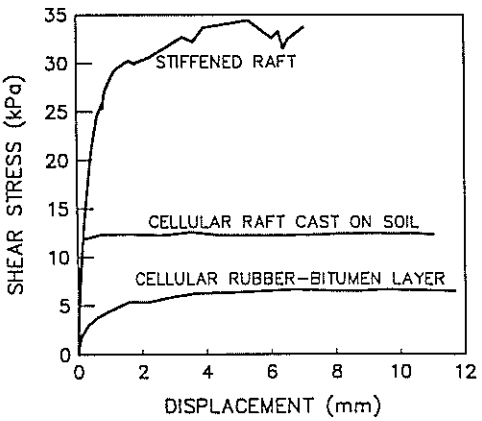

FIG.4. Results obtained from the jacking of experimental rafts

Shear-box tests simulating the field conditions were also carried out in 102 mm × 102 mm square shear boxes and in all cases vertical loads of 7.3, 15.7, 25.2 and 35.1 kPa were applied. The tests simulated the following conditions:

- Shear through the in situ soil. The natural soil does exhibit a collapse potential and, as it is difficult to simulate the in situ condition correctly, remoulded specimens were used, compacted to a density of 1 800 kg/m³ at 8 % moisture content. Further, these remoulded specimens could not model the cementation between the soil particles, with the result that the maximum shear stress was probably underpredicted.
- Concrete cast on soil. This was simulated in the shear boxes by preparing a remoulded soil specimen in the bottom half of the shear box and casting a small concrete block in the top half.
- Shear through the rubber-bitumen layer. This was simulated by preparing a remoulded specimen in the bottom half of the shear box, placing the sandwich layer of rubber-bitumen between plastic sheets and then placing a steel loading plate on top of it. Shear movement thus occurred through the sandwich layer.
- Shear between different plastic layers. Tests were also carried out to study the reduction in shear stress if several plastic sheets were placed under the raft.

The results of all these tests are given in Figure 5. The results obtained from the field test are also given in the figure and although some discrepancies exist between the field and laboratory results, the pattern of shearing resistance is clear. Note, however, that while the contact pressure below the slabs was 15 kPa, the weight of the soil between the ribs of the conventional raft contributed an

additional 9 kPa to the pressure on the shear plane at the base of the beams.

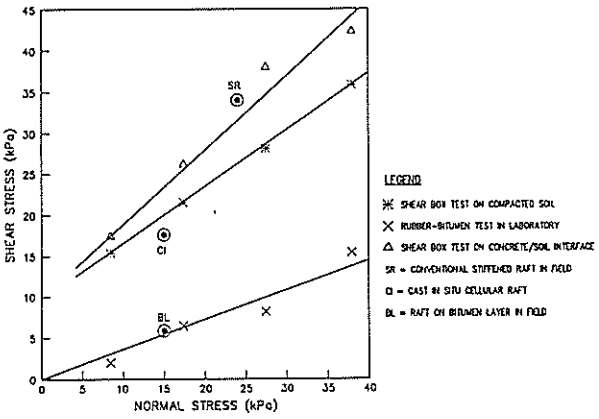

FIG.5. Laboratory shear-box test results of simulated conditions

6. DISCUSSION

Many small structures do not warrant a detailed analysis of potential structural performance under all the possible risk conditions that may be encountered during their lifetime. Further, there is often a combination of problems due to a complex soil profile, or unpredictable loading conditions. For such cicumstances an economical solution has been sought, particularly in developing regions where an absence of expertise may prevent recognition of the problems at an early stage.

The cellular raft foundation was originally conceived during a study of problems related to regional subsidence and large ground strains. The concept was then applied to the widespread difficulties encountered with heaving clays, and several successful schemes have now been completed. It was realised that it might have applications in areas of seismic activity and a few preliminary studies in the laboratory and on a test site have indicated that a base-isolation system might be developed satisfactorily. A literature survey encouraged the development of such a concept. It is not possible, however, to implement such a study on a full scale in South Africa because of the (fortunate) infrequent occurence of major seismic events to date. Further research and development in this respect seems warranted.

7. REFERENCES

Barrett, A.J. and Wrench, B.P. (1984). Impact rolling trial on "collapsing" aeolian sand. Proceedings of the Eighth Regional Conference for Africa on Soil Mechanics and Foundation Engineering, Zimbabwe, pp 177-181.

Bräuner, G. (1973). Subsidence due to underground mining. Part 2. Ground movements and mining damage. United States Department of the Interior, Bureau of Mines, Information Cicular 8572.

Key, D. (1988). Earthquake design practice for buildings. London: Thomas Telford.

Meintjes, H.A.C. (1991). Report on the investigation of cracking of Thlamoha Technical College. CSIR Report No 55022628, submitted to the Department of Education and Training of South Africa.

Milford, R.V. and Wium, D.J.W. (1991). Impact of seismic events on buildings in mining areas. The Civil Engineer in South Africa, Vol 32, No.10, October 1991.

O'Rourke, M.J. Castro, G. and Hossain, I. (1984). Horizontal soil strain due to seismic waves. Journal of Geotechnical Engineering, ASCE, Vol.110, No.9, September 1984, pp 1173-1187.

Pellissier, J.P. [1991]. Piles in deep residual clays. Paper submitted to the Tenth Regional Conference for Soil Mechanics and Foundation Engineering, Lesotho, September 1991.

Pellissier, J.P. and Vogler, U.W. (1990). A contribution to the explanation of the behaviour of swelling rock. Proceedings of the International Society of Rock Mechanics. International Symposium on Static and Dynamic Considerations in Rock Engineering, Swaziland, 10-12 September 1990, pp 241-250.

Pellissier, J.P. and Williams, A.A.B. [1991]. Development of raft foundations for small structures on heaving clay. Paper submitted to the Tenth Regional Conference for Soil Mechanics and Foundation Engineering, Lesotho, September 1991.

Ren, G. (1988). Mining subsidence prediction in relation to the stability of surface structures. Thesis submitted to the University of Nottingham for the degree Doctor of Philosophy.

Schwartz, K. (1985). Collapsible soils. The Civil Engineer in South Africa. Vol.27, No.7, pp 379-393.

Su, L. and Ahmadi, G. (1989). A comparative study of performances of various base isolation systems, Part 1: Shear beam structures. Earthquake Engineering and Structural Dynamics, Vol.18, pp 11-32.

Subsidence Engineers' Handbook (1975). National Coal Board Mining Department, London.

Wagener, F. von M. (1985). Dolomites. The Civil Engineer in South Africa, Vol.27, No.7, July 1985, pp 395-407.

Williams, A.A.B. and Pellissier, J.P. [1992]. The performance of cellular raft foundations. Paper submitted to the Seventh International Conference on Expansive Soils, Texas, USA, August 1992.

Williams, A.A.B., Pidgeon, J.T. and Day, P.W. (1985). The state of the art of problem soils in South Africa. The Civil Engineer in South Africa, Vol.27, No.7, August 1985, pp 367-377.

Class A Predictions of Pile Behaviour

H.G. POULOS
B.E., Ph.D., D.Sc. (Eng.), F.I.E.Aust., F.A.A.
Chairman, Coffey Partners International Pty Ltd.

SUMMARY Class A (before the event) predictions were made of the load-settlement behaviour of four different test piles at a site in Evanston, Illinois. The paper describes the prediction procedures adopted and the correlations employed to assess the required geotechnical parameters. Predictions are presented for the load-settlement behaviour, the distribution of load with depth and the distribution of residual load after installation of the driven piles. These are then compared with the measured behaviour of the test piles.

INTRODUCTION

Class A (before the event) predictions of the axial behaviour of four different pile types wei made in 1988. Together with a number of other predictors, the author presented these predictions at the ASCE Foundation Engineering Congress held in the United States in June 1989, after which the results of the load tests were revealed.

This paper outlines the procedures adopted by the author to predict the pile behaviour, and then compares the predicted behaviour with that observed. The main predictions were of the axial load capacities of the four pile types, at various times (2 weeks, 1 month, 1 year) after installation. However, predictions were also made of the load-settlement behaviour, the axial load distribution along each pile, and the residual load distribution in two of the piles after installation by driving.

GEOTECHNICAL DATA

The test site was located on the campus of Northwestern University in Evanston, Illinois. A considerable amount of geotechnical data was available from both insitu and laboratory tests.

A complete description of the data is presented by Finno (1989), but in summary it consisted of the following:

(1) a soil boring to a depth of 21.8m;
(2) four CPT soundings;
(3) SPT data;
(4) Menard pressuremeter tests at five depths;
(5) two dilatometer soundings;
(6) piezocone data, including three dissipation tests;
(7) data from four piezometers;
(8) pile driving data.

The laboratory data included:

(1) grain size distributions;
(2) Atterberg limits and natural water content;
(3) one dimensional consolidation data;
(4) undrained shear strength data from unconsolidated undrained tests and direct shear tests;
(5) limited stress-strain data from consolidation undrained triaxial compression and extension tests.

A summary of some of this data is given in Figure 1, which shows that there are two predominant layers within the depth of the test piles - an upper sand layer approximately 6.1 to 7.3m thick, underlain by a relatively soft clay layer which extends to about 18.3m depth. Below that depth, much stiffer layers of silty and sandy clay exist.

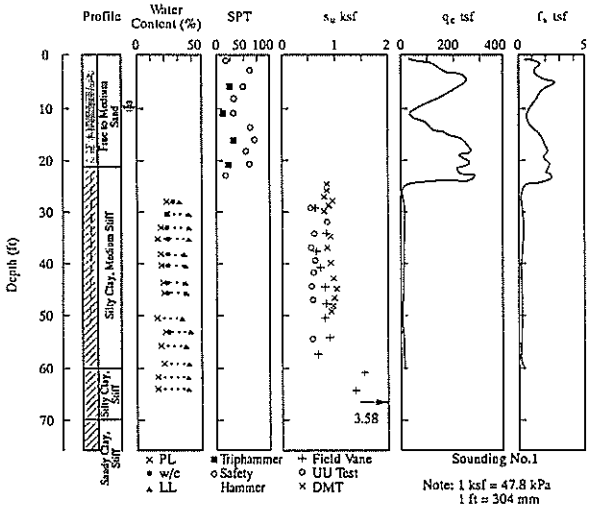

FIG.1 SUMMARY OF GEOTECHNICAL PROFILE AND DATA PROVIDED

TEST PILE DETAILS

Four piles were tested:

(1) Pile 1, a driven steel tube pile 0.457m in diameter with 9.5mm wall and 0.483m boot plate;

(2) Pile 2, a driven steel H-pile (14x73) section;

(3) Pile 3, a drilled pier constructed under slurry, having a nominal diameter of 0.61m from the surface to about 3.05m depth and a nominal diameter of 0.457m below that depth;

(4) a drilled cased pier with a nominal diameter of 0.61m to a depth of about 9.5m and 0.457m thereafter.

PREDICTION PROCEDURES

A detailed description of the author's prediction process is given elsewhere (Poulos 1989) and hence only a summary of the approach is presented here. It had been intended to employ an effective stress approach to predict the shaft resistance in the sand and clay and a total stress method to estimate base resistance in the clay. However, reliable data was lacking for a key parameter, the coefficient of earth pressure at rest, and in addition there was some doubt about the ability of refined analyses to predict accurately the stress state around both driven and bored piles after installation.

Consequently, it was decided to use one of the simplest, and least sophisticated approaches, that of correlating skin friction f_s and end bearing resistance f_b to CPT data. In the approach adopted, f_s and f_b were estimated as follows:

$$f_s = \frac{\alpha_s q_c}{N_0} R_t \qquad \ldots (1)$$

$$f_b = \alpha_b . q_c \qquad \ldots (2)$$

where q_c = measured cone resistance
α_s = soil pile factor for skin friction, depending on soil and pile type
N_0 = factor for skin friction, depending on soil type
R_t = time factor, depending on time after installation
α_b = soil-pile factor for end bearing, depending on soil time
q_c = average cone resistance above and below tip, for distance 4d above, and 4d below the pile tip.

Equations (1) and (2) were developed from a number of suggested approaches, e.g. Bustamante and Gianeselli (1982), Van Impe (1986) and Belcotec (1985). The factors α_s, α_b and N_0 are empirical and are based on correlations with load test data. Significant differences exist between recommendations from different sources, but after consideration of the available correlations, those adopted are shown in Table 1. No upper limits were placed on f_s and f_b, although in a design situation it would be appropriate to do so.

The "time factor" R_t expresses the effect on pile capacity of the dissipation of excess pore pressures developed during installation. It depends on both the overall increase in shaft resistance and the rate at which this increase occurs. For driven piles, some indication of the overall increase was obtained by comparing the undrained shear strength of the undisturbed clay and of the remoulded clay. The average ratio of these strengths was 2. Furthermore, it was felt that the correlations developed between cone resistance and shaft resistance were relevant to long term conditions, i.e. after complete dissipation of excess pore pressures. Thus, the shaft resistance immediately after driving was taken to be one half of the long term values.

The rate of development of this increase was estimated from theoretical solutions presented by Poulos and Davis (1980) and Randolph et al (1979). Taking an average value of horizontal coefficient of consolidation (from the piezocone data) of 17.5 m²/year, the values of R_t for the driven piles were found to be about 0.75, 0.85 and 1.0 for the three times under consideration.

Table 1
Factors for Determination of Shaft Friction and End Bearing from CPT Data

Pile Type	Sand	Clay	
	α_s	α_s	α_b
Driven tube (with enlarged shoe)	0.67	0.42	1.00
H-pile	0.90	0.59	0.77
Slurry pier	0.86	0.65	0.30
Cased pier	0.45	0.65	0.30

NOTES:
1. The above factors relate to long term pile load capacity.
2. For the H-pile the surface area is that of the rectangular prism enclosing the H-section.
3. For driven tube without enlarged shoe, values of α_s are 1.5 times larger than with enlarged shoe.

For the bored piles it was assumed that installation would cause little or no overall change in pore pressure, and hence it was assumed that R_t = 1, i.e. there was no significant time effect on the load capacity of the bored piles.

Predictions of the load-settlement behaviour of each pile were made using an incremental boundary element analysis of pile-soil interaction (Poulos 1979). Elastic continuum theory was used to model the soil behaviour, but at the pile-soil interface it was assumed that the response was hyperbolic. The pile was divided into 11 cylindrical shaft elements and a single pile tip element; for the bored piles an annular element at the diameter discontinuity was also allowed for.

The initial tangent Young's modulus of the soil, E_{si}, was correlated to the cone penetration resistance q_c as:

$$E_{si} = \alpha_E . q_c \qquad \ldots (3)$$

where α_E = factor depending on soil and pile type

Based on the author's limited experience, α_E was chosen to be 10 for sand and 30 for clay for the driven piles, and 7 and 21 respectively for the bored piles.

The hyperbolic factor R_f for the pile-soil interface response was taken to be 0.5 for pile shaft elements and 0.9 for the pile tip element, since it has been commonly observed that the pile tip behaviour is markedly more non-linear (and hence corresponds to a higher R_f value) than pile shaft behaviour.

To determine the residual stresses after driving of the steel tube pile and the H-pile, a static load-settlement analysis was carried out to failure (using the estimated short term shaft resistance values), followed by unloading to zero load. Poulos (1987) had indicated that the loads remaining in the pile could give a reasonable estimate of the residual loads in the pile after driving.

No attempt was made to predict pore pressure generation and dissipation around the pile as it was felt that, apart from the initial installation of the driven piles, changes in pore pressure around the piles during test loading would be small.

PREDICTED TEST PILE BEHAVIOUR

Table 2 summarises the predicted axial load capacities of the piles at the three specified times after installation.

Table 2
Predicted Pile Load Capacities

Pile	Predicted Capacity kN		
	2 weeks	1 month	1 year
Driven steel tube	846	856	872
Driven H-pile	1066	1081	1104
Slurry pier	1585	1585	1585
Cased pier	860	860	860

The following points are worthy of note:

(1) Most of the load capacity was predicted to derive from shaft resistance in the sand; the shaft and tip resistances in the clay contribute a relatively small proportion of the capacity.

(2) Because of the small contribution of the clay to the load capacity, the effects of time on pile capacity were predicted to be also relatively small.

(3) The slurry pier was predicted to have the highest capacity; a significant component of this came from the end bearing resistance of the "step" at the shaft diameter discontinuity in the sand.

For the driven piles, the residual loads were predicted from an incremental boundary element load-settlement analysis in which installation was simulated by loading the pile to failure and then unloading to zero load. The computed maximum residual load was of the order of 7 to 12% of the long term load capacity.

For the bored piers it was considered unlikely that residual loads would exceed 10% of the pile load capacity, but no attempt was made to predict detailed distributions of residual load.

For all four piles, the predicted load-settlement behaviour was substantially linear to loads well beyond 50% of the predicted ultimate load. At 50% of the ultimate load, the predicted settlements were between 1.5 and 2mm for all piles except the slurry pier, for which a settlement of about 3.5mm was predicted for loading one year after installation.

COMPARISONS BETWEEN PREDICTED AND MEASURED PERFORMANCE

A detailed account of the measured performance of the piles is given by Finno et al (1989a) while Finno et al (1989b) summarise the results of all the predictions made. The following outlines the comparisons between the measured performance and that predicted by the author.

Load Capacity

Table 3 summarises the predicted and measured axial load capacities for three times after installation. The following observations may be made:

1) For the H-pile, the pipe pile and the slurry pier, the long term capacity predictions are in fair agreement (within $\pm$15%) with the measurements.

2) For these three piles the shorter-term capacities were overestimated.

3) For the cased pier, the measured capacity was substantially in excess of that predicted by the author.

4) There were very substantial beneficial time effects with both bored piles, contrary to the author's prediction that time effects would not be significant.

5) Conversely, the observed time effects for both the driven piles were less than predicted.

Thus, while three of the predictions of long term load capacity were reasonable, the influence of time effects was quite different to that expected.

A summary of the predictions of all 24 predictors for long term capacity is shown in Table 4. It will be noted that there is a very substantial range of predicted capacities and that while the average prediction for the driven piles was quite good, the capacities of the two bored piles were generally under-predicted by a substantial margin. The author also took a small amount of comfort from the fact that his predictions were generally similar to (and in one case considerably better than) the average of the predictions.

Load-Settlement

Figures 2 and 3 compare the predicted long term load-settlement behaviour of the four piles with that predicted by the author. The piles exhibited a relatively linear load-settlement response over a considerable range of load, and the predicted behaviour mirrored this response and also gave an axial stiffness which was close to that measured. It would therefore appear that the combination of the method of analysis and the soil modulus assessed from Equation 3 gave satisfactory settlement predictions at this site. Of course, at loads approaching failure, the predictions become less satisfactory because of the shortcomings of the ultimate capacity predictions.

Pile Load Distributions

Figures 4 and 5 show the predicted and measured distributions of load at failure along the pile for the long term test. In terms of the normalised load (load divided by load at the pile head), there is fair agreement between the predicted and measured load distributions for the driven piles, except near the top of the pile. There, the predicted load is less than the measured, indicating that the predicted skin friction is larger than that actually developed.

Table 3
Comparison Between Predicted and Observed Axial Load Capacities

Pile	Load Capacity kN								
	2 Weeks			4 Weeks			43 Weeks		
	Pred	Obs[1]	Pred / Obs	Pred	Obs[1]	Pred / Obs	Pred[2]	Obs[1]	Pred / Obs
H-Pile	1066	797	1.34	1081	850	1.27	1104	1017	1.09
Pipe	846	623	1.36	856	714	1.20	872	1026	0.85
Slurry Pier	1585	1155	1.37	1585	1517	1.04	1585	1840	0.86
Cased Pier	860	1135	0.76	860	1571	0.55	860	1853	0.46

NOTES: 1 Observed values are average of values from load cell and jack
2 Predicted values are for 52 weeks

Table 4
Comparison Between Predicted and Observed Long-Term Capacities

Pile	Load Capacity kN				
	Range of 24 Predictions	Average	Standard Deviation	Author	Measured
H-Pile	610 to 1670	988	296	1104	1017
Pipe	560 to 1650	930	280	872	1026
Slurry Pier	575 to 2260	1007	409	1585	1840
Cased Pier	580 to 1330	911	213	860	1853

For the bored piles, the agreement is not particularly good, with the predicted load being greater than the measured, indicating that the predicted skin friction was less than that actually developed. The difference is particularly marked for the cased pier, for which the prediction of ultimate load was very conservative (see Table 3). The difficulty of accurately predicting the detailed performance of a pile is clearly demonstrated by these comparisons.

Residual Loads

Figures 6 and 7 compare the distributions of predicted and measured residual loads after driving in the driven steel piles. The predictions suggest relatively small compressive loads along each pile, whereas the measurements indicate tension along some or all of the pile length. However, the accuracy of these residual load measurements may be questionable (Finno et al, 1989a). Nevertheless, both the measurements and predictions indicate that the residual loads after driving are relatively small compared to the ultimate pile load capacity.

Figures 6 and 7 also show the residual loads in the piles after the completion of loading. These distributions agree more closely with the predicted residual loads, and it should be noted that the method of prediction used is in fact more relevant to the after-loading case, as it simulates loading to failure, followed by unloading to zero load.

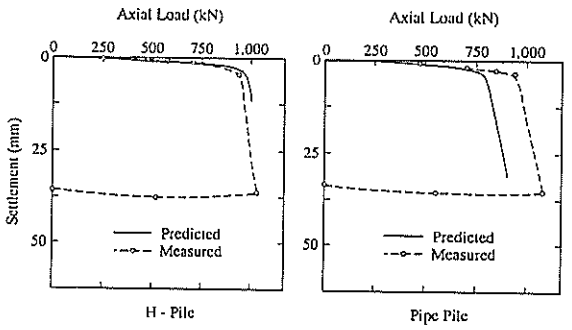

FIG.2 PREDICTED AND OBSERVED LOAD-SETTLEMENT OF DRIVEN PILES

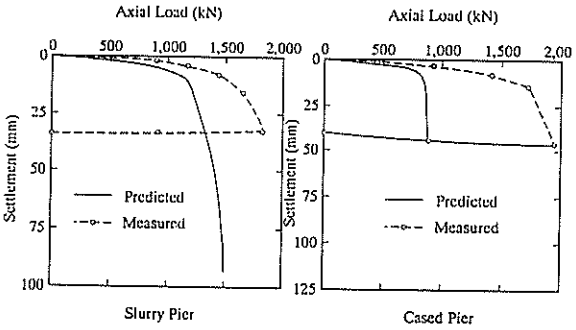

FIG.3 PREDICTED AND OBSERVED LOAD-SETTLEMENT OF BORED PILES

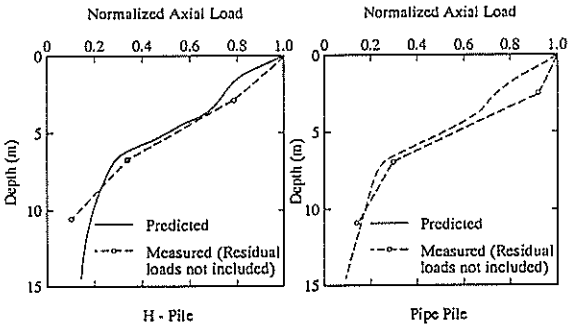

FIG.4 PREDICTED AND OBSERVED LOAD DISTRIBUTIONS AT FAILURE (Long Term)

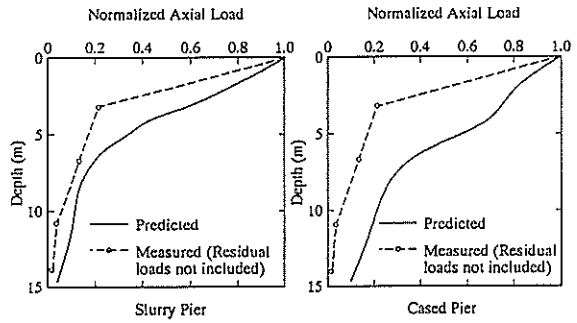

FIG.5 PREDICTED AND MEASURED LOAD DISTRIBUTIONS AT FAILURE (Long-Term)

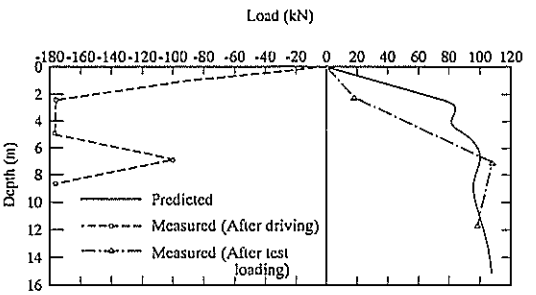

FIG.6 PREDICTED RESIDUAL LOAD DISTRIBUTION FOR DRIVEN STEEL TUBE PILE

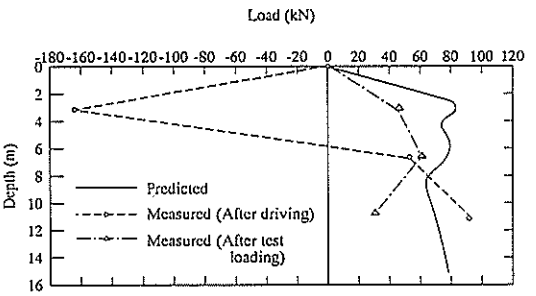

FIG.7 PREDICTED RESIDUAL LOAD DISTRIBUTION FOR DRIVEN H-PILE

CONCLUSIONS

The circumstances of this prediction exercise were more favourable than could be expected in most practical problems. There was a good definition of the subsoil profile, an abundance of geotechnical data, and loading that was well defined. Despite these favourable circumstances and the relatively straightforward nature of the problem, the Class A predictions of pile behaviour were fair only. For the driven piles, the ultimate load capacity, load-settlement behaviour and the load distribution along the piles were relatively well predicted. However, for the bored piles, the predictions of load capacity were conservative, particularly for the cased pier. For these piles, the time effects were significant, contrary to the predictions, with the load capacity increasing substantially with time. It is interesting to note that for the cased pile, all 24 predictors under-predicted the long term load capacity. A variety of prediction methods was used by the predictors, and it seems clear that the method used for prediction is likely to be of less significance than the assessment of the parameters to be input into the analysis. Certainly, the author does not believe that his predictions would have been improved by the use of more sophisticated techniques of analysis.

The difficulty of predicting both time effects and residual loads in these tests suggests that there is scope for more research aimed at a better understanding of installation and pore pressure effects on pile capacity and response.

ACKNOWLEDGMENTS

The author gratefully acknowledges the efforts of Dr. R.J. Finno in organising the prediction symposium and his generosity in supplying detailed data on the performance measurements.

REFERENCES

Belcotec (1985), Pile Foundation Problems. Belgian Geotech Vol, Ch 1, Golden Jubilee ISSMFE

Bustamante M & Gianeselli L (1982), Pile Bearing Capacity by Means of Static Penetrometer CPT, Proc 2nd Eur Symp Penetrn Testing, Vol 2, 493-500

Finno R.J. (1989), Subsurface Conditions and Pile Installation Data, Foundation Engineering Congress Test Section, Geot Spec Pub No. 23, ASCE 1-74

Finno R.J., Cosmao T. and Gitakin B. (1989a), Results of Foundation Engineering Congress Pile Load Tests, Geot Spec Pub No. 23, ASCE 338-355

Finno R.J. et al (1989b), Summary of Pile Capacity Predictions and Comparison with Observed Behaviour, Geot Spec Pub No. 23, ASCE 356-386

Poulos H.G. (1979), Settlement of Single Piles in Non-Homogeneous Soil, Jnl Geot Eng Divn, ASCE, Vol 105, No. GT5, 1979, 627-641

Poulos H.G. (1987), Analysis of Residual Stress Effects in Piles, Jnl Geot Eng, ASCE, Vol 133, No. 3, 216-229

Poulos H.G. (1989), Prediction of Axial Behaviour of Piles, Geot Spec Pub No 23, ASCE 83-95

Poulos H.G. and Davis E.H. (1980), Pile Foundation Analysis and Design, New York, John Wiley & Sons

Randolph M.F., Carter J.P. and Wroth C.P. (1979), Driven Piles in Clay, Geotechnique, Vol 29, No. 4

Van Impe W.H. (1986), Evaluation of Deformation and Bearing Capacity Parameters from Static CPT Results, 4th Int Seminar, Field Inst & Insitu Msmts, Singapore, 51-70

Study of A Case of Unsuitable Structural System on Heterogeneous Soil

M.M. REYAD
Ph.D.
Associate Professor of Soil Mech. and Found. Eng., Building Research Center, Cairo, Egypt

SUMMARY This paper presents a case story about group of residential buildings constructed in new desert area. Some Egyptian deserts have uncommon soil formation which is still not well known for many engineers. Due to insufficient investigations, the geotechnical properties of the bearing stratum were not adequately recognised specially the behaviour of the supporting soil under different stresses when it is provided with water. The result was unsuitable structural system led to severe cracks and unexpected damage in most bearing walls directly after use. The paper presents all the carried out investigations and studies to identify the problem in order to prevent any more deterioration and adopt the most convenient remedy.

1. INTRODUCTION

It is well known that Cairo, the capital of Egypt, suffers from high population intensity and lack in housing specially for low-income people. It was recommended by specialists to occupy the surrounding deserts which represent 94% of Egypt area. An industrial company decided to construct a permanent residential neighbourhood for the labourers. The chosen location lies at about 50 Km to the south west of Cairo center. The company had afforded comfortable transportation means to and from its factories.

The project was planned so that the neighbourhood consists of fifteen groups of buildings. The group consists of twelve small adjacent low-cost houses. Houses were built of a ground floor able to carry one additional floor in future. At the center there is a market, clinic, recreation area and small workshops. All buildings are surrounded by new cultivated green areas.

On January 1988, about 80% of the houses were completed and began to be occupied by the dwellers. After about six months, unexpected hair cracks began to appear in most walls. The cracks have gone wider and wider and the deterioration was very clear to human eye. The author was responsible for studying the case and solving the problem.

2. INVESTIGATIONS AND STUDIES

The study was divided into three parallel stages, i.e the state of the superstructure itself, inspection of the existing foundations and soil investigations allover the site. In the first stage all drawings and calculation sheets were revised, different in situ and laboratory tests were carried out on most concrete elements. Brick used in construction of the bearing walls as well as the joining mortar were also examined. Gypsum monitors and electronic indicators were used to measure and follow up the cracks width. Foundation inspection was done by manual excavation on both sides and around the corners of the continuous strip footings and the concrete dimensions were measured. Samples from both the concrete and the soil just under foundations level were also carefully examined.

For soil investigation purposes, 25 open test pits were dug with sufficient width to see and distinguish between the different soil formations along the sides of the excavation. The open pits stopped at depth ranging between 2.00 & 3.50 m below natural ground surface due to the appearance of hard limestone. Additional 10 mechanical borings went deeper down to depth about 10 m. The ground water table was not encountered down to the end of all borings. The samples were carefully examined and tested according to the ASTM in trusty laboratories in Cairo.

3. RESULTS AND DISCUSSIONS

3.1 The Superstructure

Houses are built according to the wall bearing system. The building consists of continuous strip footings under the brick walls which carry the reinforced concrete roof slab through reinforced beams. The test results indicated that the used bricks conform to the standard specifications but the joining mortar suffers from lack in cement content, moreover, some bricks were placed besides each other without any mortar. Concrete elements were in good condition and their strength was acceptable. The different crack indicators showed that the movement was still going on and most cracks were still going wider so that they reached 12 mm in some walls. Some cracks had a broken path around the bricks while some others had cracked the bricks themselves. Figures 1 & 2 show sketches for some cracks as examples and figure 3 shows the structural system of the houses.

3.2 The Foundations

Houses are founded on shallow foundations consist of continuous strip reinforced concrete footings on the shape of inverted T-section resting on 10 cm thick plain concrete strips under the whole length of the bearing walls as shown in figure 3. Foundations rest directly on the natural soil at depth ranging between 0.90 & 1.10 m below ground surface. They were well designed, well constructed and they were in good condition without cracks, no rust and the concrete strength was acceptable.

3.3 The Supporting Soil

Now, we are face to face with the main source of the happened troubles. The comprehensive soil investigations indicated that the upper layer, which

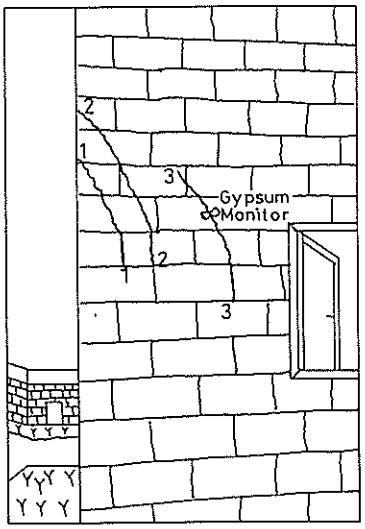

Figure 1 Cracks in an exterior wall

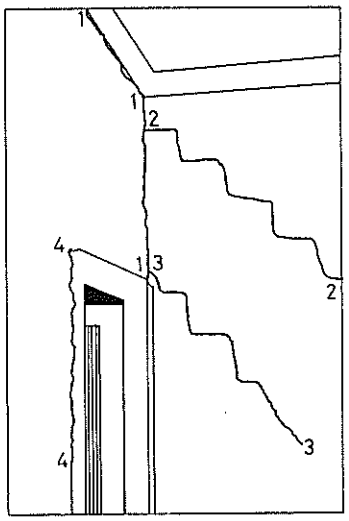

Figure 2 Cracks in an interior wall

extends at some locations down to depth 3.5 m, consists of random formation of heterogeneous soils. It contains fill, collapsible slightly cemented silty sand, expansive hard laminated silty clay, claystone and siltstone. All these kinds are found in different thicknesses, at different depths, in random succession and may lie within the area of the same building. Figure 4 shows the erratic formation of the soil in the upper layers.

As it is well known that the effect of water on such soils is so dangerous, any source of water will cause very complicated soil behaviour and the definite result will be differential movement along the continuous footings. Buildings could not tolerate or withstand the occured movement because their structural system does not afford sufficient rigidity and cracks began to appear.

The main sources of surface water were the continuous flooding of the green areas surrounding the walls, the continuous leakage of wastewater from the inspection chambers and from the separation lines between tiles in the bathrooms. As the water was still invading the soil, more and more deterioration was still taking place.

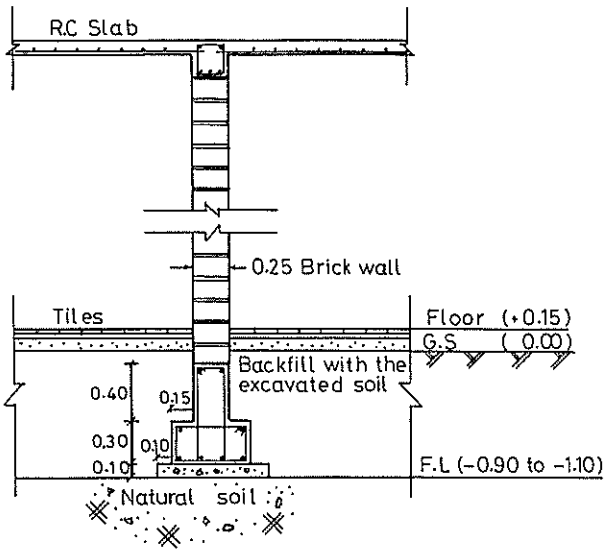

Figure 3 Typical section in interior walls and existing foundations

4. THE DECISION

The previous study shows that the mistake has two major parts. The first is that the bearing stratum consists of random combination of dangerous types of soils unsuitable to carry any type of shallow foundations directly without pretreatment and strict precautions. The second is that the adopted structural system cannot afford sufficient rigidity so that the buildings can withstand the occured differential movements without any distress.

5. PROPOSED REMEDY

The proposed remedy is divided into three stages:

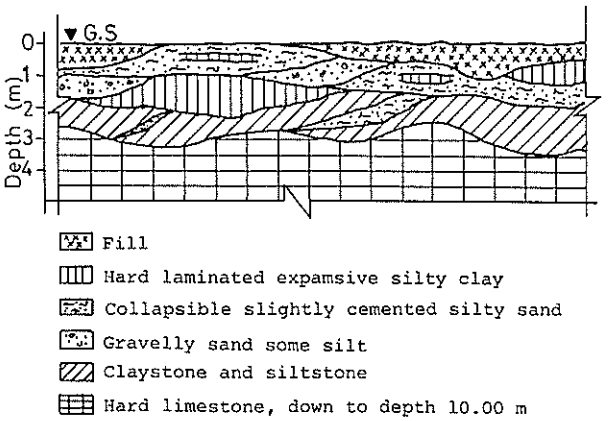

Figure 4 Typical geotechnical section in the bearing stratum

5.1 Soil Replacement

Buildings must be strongly shored up to avoid any movement. Soil is removed out at the points of intersection of the existing foundations to make excavated pits with minimum dimensions 1.50 x 1.50 m down to depth 0.95 m below the present foundation level as shown in figure 5. The bottom of excavation is regularly soaked for 72 continuous hours and the accumulated slurry is removed, then it is strongly compacted. The replacement material is gravelly sandy soil with traces of fines. It is compacted on three equiheight layers of 0.25 m each. Compaction is done at the optimum moisture content to gain minimum 95% of the maximum dry density as predetermined experimentally from the Modified Proctor Test with minimum value 1850 kg/cu.m for each layer.

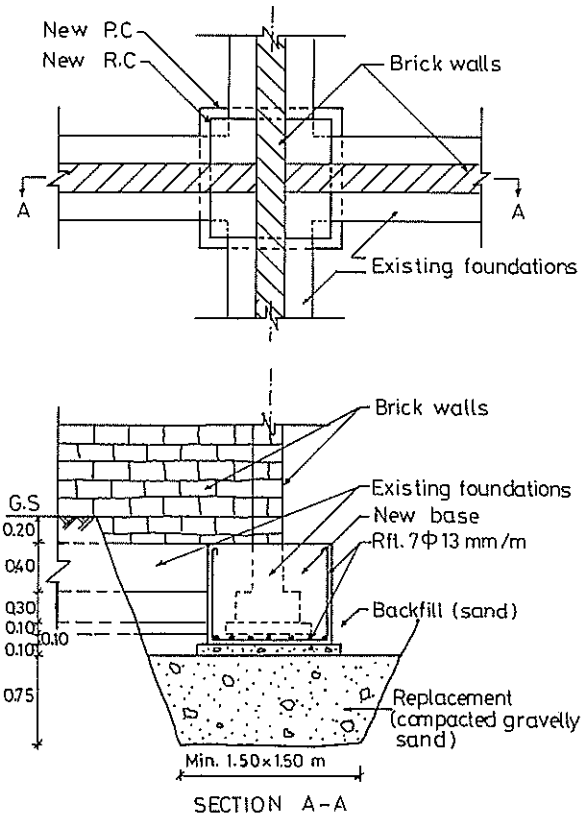

Figure 5 The proposed soil replacement and the new foundation support

5.2 Foundation Support

The new foundation support is shown in figure 5. It consists of reinforced concrete base resting on 0.10 m thick plain concrete. The reinforced concrete base has minimum dimensions 1 x 1 m and with sufficient height to surround and envelop the existing foundations at their intersections. Clean sand must be used for backfilling around foundations.

It is very important not to carry out the previously mentioned works allover the same house at the same time. The following repair works have to be done after the foundations are completely supported.

5.3 Repair Works

Thin and moderate cracks are filled with new effective filling material. Damaged walls must be removed and rebuilt again after considering the necessary safety precautions. All inspection chambers must be replaced by new chambers constructed of reinforced concrete base and walls acting as one unit and must be properly insolated. Compacted clean sand is placed under their bases and behind the side walls. Water and sewage lines must be inspected, repaired or replaced and coated by granular soil. Compacted clean sand layer with reasonable thickness must be placed under floor tiles. All buildings have to be surrounded by wide footpath with suitable outwards slope to avoid water accumulations. Grean areas must be irrigated by mechanical sprayers to avoid flooding. Maintenance works must be done regularly.

6. CONCLUSIONS AND RECOMMENDATIONS

This case reveals clearly that any shortage or lack in soil investigations leads to many troubles which waste time, effort and money to overcome. It is strongly recommended that for any new building, whatever its value or its size, soil must be thoroughly investigated allover the site. Field and laboratory tests have to be carried out carefully and the effect of water on soil behaviour under different stresses must be well recognized. The choice of suitable type of foundation and convenient structural system is very essential. Engineers must strictly apply the specifications and the code of practice during construction to avoid any future troubles.

7. REFERENCES

Hamza Associates, Consultants And Engineers, Dokky Street, Giza, Egypt.

The Analysis of Axially Loaded Piles in Layered or Non-Homogeneous Soils

J.C. SMALL
B.Sc. (Eng.), Ph.D., M.I.E.Aust., M.A.S.C.E.
Associate Professor, School of Civil and Mining Engineering, University of Sydney
C.Y. LEE
B.Sc. (Eng.), M.Sc.Eng., Ph.D.
Research Fellow, School of Civil and Mining Engineering, University of Sydney

SUMMARY A finite layer method is presented which can be used to compute the displacement of piles in layered soils or soils which have a modulus which varies with depth. Previous methods of dealing with layered soils have made use of averaging of soil properties, but the finite layer method allows a more accurate semi-analytical solution of the layered soil problem. Because the method is semi-analytic, the problem of a pile in a layered material may be solved very simply, using very little computer storage. This means that solutions may easily be obtained by the use of micro-computers. Examples of the accuracy of the method are given by comparisons with previous solutions for uniform and layered soils.

NOTATION

A_p = area of cross-section of pile
d = pile diameter
E_0 = modulus of soil at top of pile
E_1, E_2 etc. = moduli of soil layers
E_p = modulus of pile
E_s = modulus of soil
E_L = modulus of soil at level of pile tip
F = vector of transformed forces at layer interfaces; subscript i denotes the vector for layer i
I_s = influence matrix for soil
J_0, J_1 = Bessel functions of the first kind of integer order
K = pile head stiffness = load on pile/pile head deflection
K' = non-dimensional pile head stiffness
K_p = stiffness matrix for the pile
K_s = stiffness matrix for the soil
L = pile length
N = transformed stress normal to layer interface
P = vertical load on pile head
P = vector of externally applied loads
P_p = vector of loads acting on pile
P_s = vector of loads acting on soil
q = pressure acting on base of pile
Q = magnitude of ring load
r = radius
R = radius of pile
T = transformed shear stress on layer interface
u_z = vertical displacement (i.e. in z direction)
U_z, U_r = transformed displacements in vertical and radial directions
w_p = vector of vertical displacements at 'nodes' of pile
w_s = vector of vertical displacements at 'nodes' of soil
w = vector of displacements at pile 'nodes'
α = Hankel transform parameter
δ = vector of transformed displacements at layer interfaces; subscript i denotes values for layer i
ν = Poisson's ratio
ξ = ring load
ρ = vertical pile head deflection

1. INTRODUCTION

Piled foundations are commonly used to transfer structural loads onto stiffer layers of soil or to transfer loads to depths at which the soil strengths are higher. This makes the computation of the expected settlements of the piles more difficult as the modulus of the soil is either increasing with depth, or the moduli of the layers of soil through which the pile passes are different.

Solutions for the deflection of piles in layered soils or in soils for which the modulus increases with depth have been presented in recent years (Poulos and Davis (1980), Guo et al. (1987), Rajapakse (1990), El Sharnouby and Novak (1990)). However, these methods either make use of approximations or cannot deal with a soil which consists of many different layers. The exception is the method of Guo et al. which makes use of an infinite layer technique.

In this paper, a simple finite layer method is presented which can be used to compute the settlement of piles in soils which are layered or for which the modulus varies with depth. Comparisons are made with available solutions, and then some original solutions to problems involving layered soils are presented.

2. METHOD OF ANALYSIS

The method of analysis involves finding the stiffness of the soil and adding this to the stiffness of the pile. This may be done by considering the pile and the soil separately as shown in Figure 1. The pile is represented by a series of one dimensional, two noded cylindrical solid elements connected at 'nodes'. By using conventional finite element techniques (see Smith and Griffiths (1988)), a stiffness matrix can be set up for the pile. The forces which are applied at the nodes of the elements are calculated by assuming that a uniform shear loading is distributed over each pile shaft segment (which surrounds each node). For the base node, the applied force is calculated from the assumption that the pile base carries a uniformly distributed load.

The soil is assumed to be horizontally layered as is shown

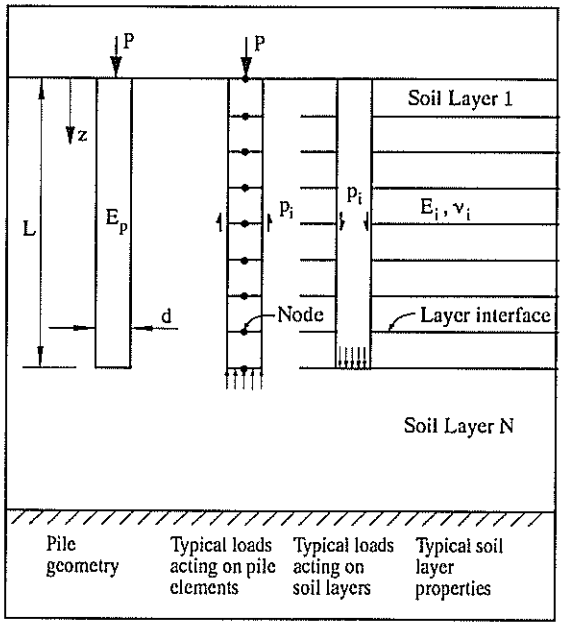

Figure 1 Pile in a layered soil

in Figure 1. This implies that the soil properties cannot change in the horizontal directions, however this is not a very severe restriction as sedimentary soils are quite often found in horizontally layered deposits. The interface forces between the pile and the soil are assumed to be applied to the soil as a series of ring loads which act at the interfaces between each soil layer. The base load of the pile is assumed to act as a uniform circular load at the layer interface which is level with the base of the pile.

We may write for the pile

$$K_p\, w_p = P_p + P \tag{1}$$

where

K_p = stiffness matrix for the pile
w_p = vector of vertical displacements at 'nodes'
P_p = vector of vertical forces at the 'nodes'
P = vector of externally applied loads

The finite layer method is used to calculate the response of the soil to the uniform pressure at the base and to the series of ring loads which are assumed to act at each soil layer interface . The accuracy of the solution method will depend on how many 'nodes' and hence soil layers are used along the pile and this aspect is examined in a later section.

By applying a unit ring load at each soil layer interface in turn (and a unit pressure at the base) and determining the deflections at all other interfaces (and at the base) we can set up an influence matrix for the soil I_s. The columns of I_s consist of the vertical displacements at all nodes due to a unit ring load with the last column containing the displacements of all nodes due to the base load.

The finite layer method has been used to solve a number of problems in geomechanics and its use is well known. The particular implementation used here is that presented by Small and Booker (1986) which makes use of integral transforms. The method of dealing with the ring loads is presented in Appendix A.

We may therefore write for the soil

$$I_s\, P_s = w_s \tag{2}$$

where

P_s = vector of the magnitudes of the ring loads and the base pressure
w_s = vector of vertical displacements at 'nodes' of the soil.

The influence matrix I_s may now be inverted to obtain the stiffness response of the soil

$$K_s\, w_s = P_s \tag{3}$$

where $K_s = I_s^{-1}$.

If there is no slip at the pile-soil interface we have the condition that the displacement of the soil and that of the pile must be equal which implies that

$$w_p = w_s. \tag{4a}$$

We must also have equilibrium of the forces acting at the interface and so

$$P_p = -P_s \tag{4b}$$

Using the conditions of equations 4a,b, we may combine equations 1 and 3 to get

$$K\, w = P. \tag{5}$$

where $K = K_p + K_s$

Equation (5) can now be solved for the displacements at the nodes along the pile w.

3. EXAMPLES

The theory presented in the previous section was firstly used to obtain solutions which could be checked against previous solutions. The first example is that of a pile in a uniform soil. This problem has been examined by El Sharnouby and Novak (1990), who looked at the effect of the number of elements used for the pile, and compared their solutions with those of several other authors.

The results of the analyses are shown in Figure 2 for floating piles in an incompressible ($\nu = 0.5$) elastic soil. The non-dimensional pile head stiffness $K' = KR/A_pE_s$ is plotted against the length to diameter ratio L/d of the pile for two pile stiffness ratios E_p/E_s = 100 and 1000 in this figure. The effect of the number of elements used in the pile by various authors (Poulos and Davis (1980), Rajapakse and Shah (1989) and Salinero (1982)) can be seen along with the present solution for 20 elements in the pile. The results calculated using the finite layer method agree most closely with those of El Sharnouby and Novak for small L/d values but agree more closely with Salinero's results for large L/d.

Figures 3a,b show similar results for end bearing piles, where the base of the pile rests on an infinitely stiff layer. The results computed using the finite layer method which are presented in this figure, were carried out using 50 elements along the pile shaft. When the piles are stiff (i.e. E_p/E_s = 1000), the finite layer results can be seen (Figure 3b) to

agree fairly closely with the results of El Sharnouby and Novak (1990).

For more compressible piles, (E_p/E_s = 100) the finite layer results agree with the results of Poulos and Davis (1980) at low L/d ratios, but agree more closely with the results of El Sharnouby and Novak (1990) at high L/d ratios (see Figure 3a). However, the finite layer results do not seem to show the same trends as any of the previous results and therefore finite element computations were carried out in order to provide an independent check on the pile head behaviour. To do this, a mesh was made up which consisted of 50 isoparametric elements along the length of the pile with two columns of elements across the radius of the pile. The program which was used was written by Balaam (1985) and is called ISOPE.

The base of the layer was chosen to be perfectly rough and rigid and the Poisson's ratio of the soil chosen to be ν_s = 0.495. The side boundary of the mesh was placed at a distance which was found to have little influence on the pile head deflection. This distance was set to be at a distance of $0.7L$ away from the pile axis for all pile lengths L analysed. This boundary was restricted from lateral (radial) movement but was allowed to move vertically (i.e. a shear free boundary).

The finite element results will also be subject to error, due to the coarseness of the mesh, the type of elements used and the positions of boundaries, however an examination of these variables has indicated that there should be little error in the calculated results with the type of elements and mesh used.

It may be seen from Figure 3a that the finite element results indicate slightly lower pile head stiffnesses than the finite layer results when E_p/E_s = 100. However the pile head stiffness as predicted by the finite element program does vary in the same way with the L/d ratio as the finite layer predictions. The finite element solutions agree well with the finite layer solutions for stiffer piles (E_p/E_s = 1000) as can be seen in Figure 3b.

Figure 4 shows results for the vertical deflection ρ of the pile head when the pile is in a soil composed of two layers with the lower layer being infinitely deep. The modulus of the upper layer is E_1, that of the lower layer is E_2 and the thickness of the upper layer is h_1. Results are compared with those of Guo et al. (1987) for two pile stiffness ratios E_p/E_s = 100 and 1000 and, as can be seen from the figure,

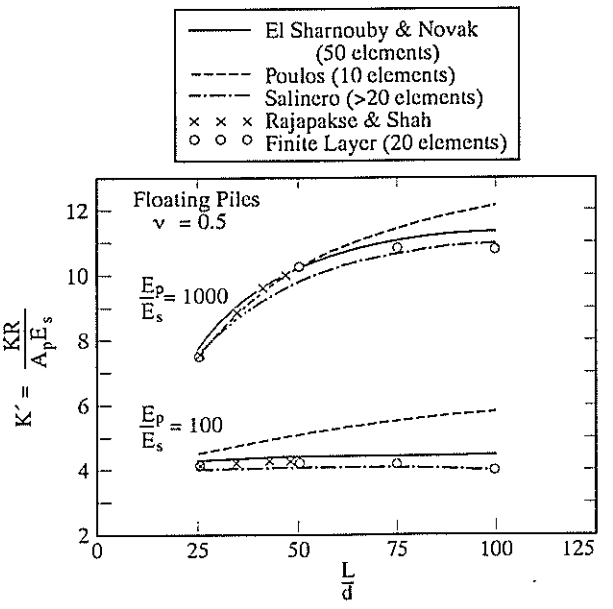

Figure 2 Dimensionless stiffness of floating piles in very deep homogeneous layer

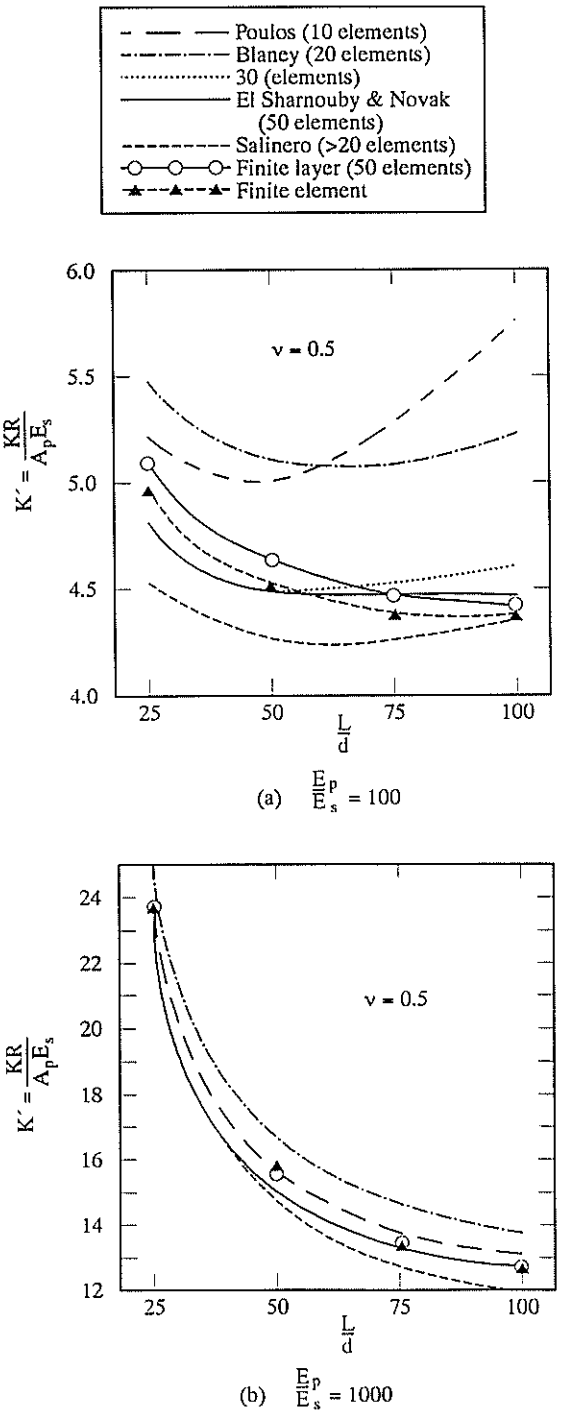

Figure 3 Dimensionless stiffness of end bearing piles in homogeneous soil

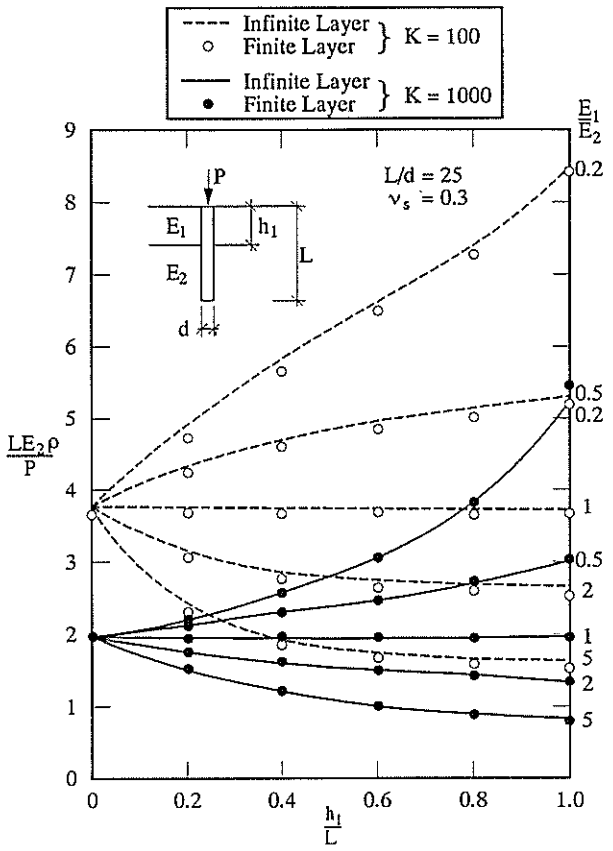

Figure 4 Settlement influence factor for pile in layered soil

very good agreement was obtained for all values of the layer stiffness ratio (E_1/E_2) that were examined.

For piles in soils for which the modulus increases with depth, the finite layer method may be applied if the appropriate modulus is assigned to each layer. The results are therefore dependent upon the number of layers used as the linear increase in modulus is treated as a stepped increase. However, if enough elements are used along the pile, reasonable accuracy can be obtained.

As an example, the problem of a pile in a soil whose modulus increases with depth was analysed. For this problem (shown schematically in the inset to Figure 5). The modulus has a value of E_0 at the top of the pile and increases at such a rate that the modulus is E_L at the base of the pile. A modulus ratio of $E_0/E_L = 0.01$ was chosen in this example.

For the case where $L/d = 25$, the computed results have been compared with those of Rajapakse (1990), Banerjee and Davis (1978) and Randolph and Wroth (1978) in Figure 5. The finite layer results agree most closely with the results of Rajapakse and Randolph and Wroth, with only a 4.2% maximum difference between the analytic solution of Rajapakse over the range of pile to soil stiffnesses (E_p/E_L) considered. To obtain this accuracy, 10 elements were used along the pile shaft and 5 below the base of the pile in the finite layer analysis.

A further example is that of a pile in a soil profile which consists of three sublayers. This problem has been considered by Poulos (1979) and Lee (1991). The problem is shown

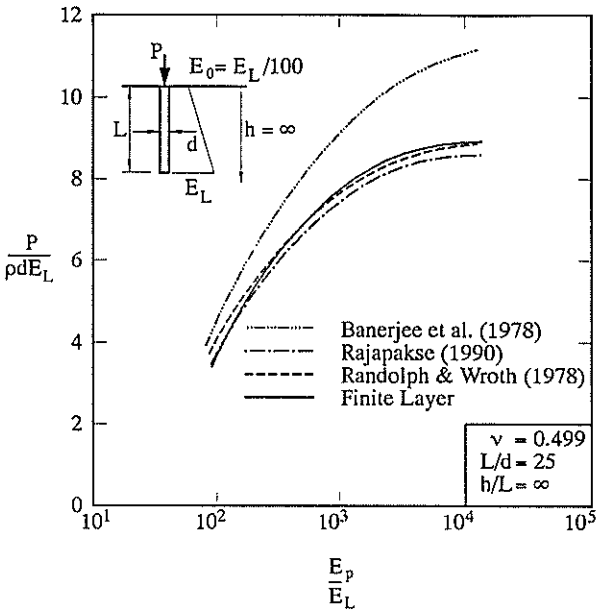

Figure 5 Settlement influence factor for pile in soil with moduulus increasing linearly with depth

schematically in Figure 6, where it may be seen that a pile of $L/d = 25$ has been driven partially into the base layer. Three cases are considered where the moduli of the various soil layers are assigned different stiffnesses as shown in the figure.

The non-dimensional settlement of the pile head $\rho d E_s/P$ is compared with results obtained previously by other authors. The results calculated using the finite layer approach are closest to the finite element solutions of Poulos (1979) with the maximum difference being only 3.86% for Case 2.

For piles bearing onto stiffer strata (where the stiffer stratum has a modulus E_b), results have been computed by Guo et al. (1987), Poulos (1980), and El Sharnouby and Novak (1990), for a pile of $L/d = 25$. The results computed by all of these methods appear to agree quite closely ((see Figure 7) for all stiffnesses of the base layer. To obtain these results, 10 elements were used in the finite layer analysis.

4. CONCLUSIONS

A method has been presented which may be used to compute the settlement of axially loaded piles in soils which are layered or for which the modulus increases with depth. The analytic method makes use of finite layer theory for computing the response of a layered soil profile to the loading imposed by the pile.

Comparisons of results computed by use of the method with results published previously show that the finite layer method is capable of producing accurate results.

5. REFERENCES

Balaam, N.P. (1985) "User's Manual - Program ISOPE", School of Civil and Mining Engineering, The University of Sydney.

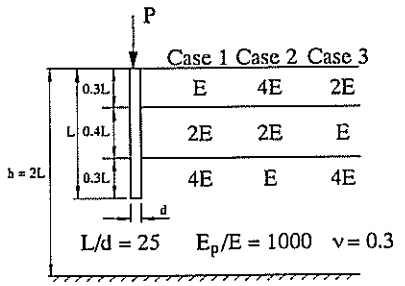

Case	Settlement Influence Factor $I_w = \frac{Ed\rho}{P}$				
	Boundary Element (Poulos, 1979)	Boundary Element Equivalent Modulus (Poulos, 1979)	Finite Element (Poulos, 1979)	Discrete Layer (Lee, 1991)	Finite Layer
1	0.0386	0.0381	0.0377	0.0361	0.0366
2	0.0330	0.0706	0.0430	0.0372	0.0414
3	0.0366	0.0391	0.0382	0.0358	0.0373

Figure 6 Settlement influence factor for pile in layered soil; results calculated by different approaches

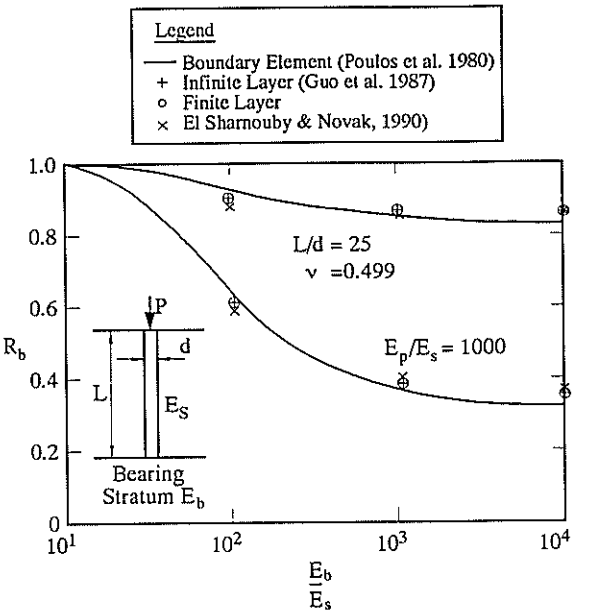

Figure 7 Effect of bearing stratum modulus on pile settlement

Banerjee, P.K. and Davis, T.G. (1978) "The Behaviour of Axially and Laterally Loaded Single Piles Embedded in Nonhomogeneous Soils", Géotechnique, Vol.28, pp.309–326.

El Sharnouby, B. and Novak, M. (1990) "Stiffness Constants and Interaction Factors for Vertical Response of Pile Groups", Canadian Geotechnical Journal, Vol.27, No.6, pp.813–822.

Blaney, G.W., Kausel, E. and Roesset, J.M. (1976) "Dynamic Stiffness of Piles", Proc. 2nd Int. Conf. on Numerical Meth. in Geomech., Blacksburg, Virginia, pp.1001–1012.

Guo, D.J., Tham, L.G. and Cheung, Y.K. (1987) "Infinite Layer for the Analysis of a Single Pile", Computers and Geotechnics, Vol.3, pp.229–249.

Lee, C.Y. (1991) "Discrete Layer Analysis of Axially Loaded Piles and Pile Groups". To appear in Computers and Geotechnics.

Poulos, H.G. (1979) "Settlement of Single Piles in Nonhomogeneous Soil", Jl. Geotech. Eng. Div., ASCE, Vol.105, pp.625–641.

Poulos, H.G. and Davis, E.H. (1980) Pile Foundation Analysis and Design, John Wiley and Sons, New York.

Rajapakse, R.K.N.D, and Shah, A.H. (1989) "Impedence Curves for an Elastic Pile", Soil Dynamics and Earthquake Engineering, Vol.8, No.3, pp.145–152.

Rajapakse, R.K.N.D (1990) "Response of Axially Loaded Elastic Pile In a Gibson Soil", Géotechnique, Vol.40, No.2, pp.237–249.

Randolph, M.F. and Wroth, C.P. (1978) "Analysis of Deformation of Vertically Loaded Piles", Jl. Geotech. Eng. Div., ASCE, Vol.104, pp.1465–1488.

Sanchez-Salinero, I. (1982) "Static and Dynamic Stiffness of Single Piles", Civil Engineering Department, University of Texas at Austin, Geotechnical Engineering Report GR82-31.

Small, J.C. and Booker, J.R. (1986) "Finite Layer Analysis of Layered Elastic Materials Using a Flexibility Approach. Part 2 – Circular and Rectangular Loadings", Int. J. Num. Meth. Engg., Vol.23, pp.959–978.

Smith, I.M. and Griffiths, D.V. (1988) Programming the Finite Element Method, Second Edition, John Wiley and Sons.

APPENDIX A

For problems involving horizontally layered materials of infinite lateral extent, solutions may easily be found by the application of the finite layer method of Small and Booker (1986). The field quantities (i.e. the displacements and stresses) are transformed by the application of Hankel transforms in the case of circular loadings. The governing equations are then solved in transform space, and finally, these solutions are inverted using numerical integration to obtain the final results.

We can write the transformed equations for the *ith* layer of soil as

$$K_i \, \delta_i = F_i \qquad (A1)$$

where

K_i = stiffness matrix for the soil layer
δ_i = vector of transformed displacements at interfaces between layers
F_i = vector of transformed stresses at the interfaces.

The form of these transformed equations is fully defined in the paper by Small and Booker (1986). In this paper, the equations are presented in the flexibility form, and so it is necessary to invert the flexibility matrix in order to obtain the stiffness matrix.

The stiffness relationship for each layer of soil as given in equation (A1) can be assembled to obtain the overall stiffness matrix for all of the soil layers. The vector of transformed stresses for the layer is given by

$$F_i = (N_p, T_p, -N_m, -T_m)^T$$

and the vector of transformed displacements by

$$\delta_i = (U_{zp}, U_{rp}, U_{zm}, U_{rm})^T \qquad (A2)$$

where the subscripts p, m denote the top (plus) and bottom (minus) of the soil layer, and N is the transform of the vertical stress, T is the transform of the shear stress, U_z is the transform of the vertical displacement and U_r is the transform of the radial displacement.

On assembling the layer matrices for all layers, the transformed interlayer displacements will add, as the displacements at the base of one layer are assumed to be the same as those at the top of the layer beneath. On the other hand, the transformed stresses will cancel, and so there will be a zero entry in the force vector at every interface except where there is a load applied (say interface ℓ), and at the top or bottom interfaces of the layered system.

We can therefore write

$$K\ \delta = F \qquad (A3)$$

where (if there are n interfaces and $n-1$ layers)

K = stiffness matrix for the layered system = $\sum_{i=1}^{n-1} K_i$
δ = $(U_{z1}, U_{r1}, U_{z2}, U_{r2}, \cdots\cdots U_{zn}, U_{rn})^T$
F = $(N_1, T_1, 0, 0, \cdots N_\ell, 0, \cdots N_n, T_n)^T$

The unknown stress transforms at the bottom of the layered system N_n, T_n can be eliminated by applying the boundary condition that the displacements there are zero (i.e. $U_{zn} = U_{rn} = 0$), or by specifying that the vertical displacement U_{zn} is zero and the shear is zero $T_n = 0$. The transformed shear and normal stresses at the top of the layered system can be set to zero as there are usually no loads on the surface.

It is therefore possible to solve the equations if the Hankel transform of the ring load can be calculated. To do this, we must be able to evaluate

$$N_\ell = \int_0^\infty r\xi J_0(\alpha r)dr \qquad (A4)$$

where ξ is a vertical ring load applied at radius R. Evaluating this integral gives

$$N_\ell = \frac{Q}{2\pi} J_0(\alpha R) \qquad (A5)$$

where Q is the magnitude of the vertical ring load.

In order to obtain the actual displacements in the layered system under the action of the ring load, we must invert the Hankel transform. For example, to obtain the vertical displacement u_z at a particular layer interface i we would have to evaluate

$$u_{zi} = \int_0^\infty \alpha U_{zi}(\alpha) J_0(\alpha R)d\alpha \qquad (A6)$$

where R is the radius of the pile at which the displacement is to be calculated.

The above integral can be evaluated numerically and, in this paper, Gaussian quadrature was used. This means that the function to be integrated needs to be evaluated at the Gauss points and this can be done simply by solving equations A3 for the particular value of the transformed ring load N_ℓ at the Gauss point α_g.

For the base of the pile, the load may be considered to be uniformly distributed over a circular region and so the transform of the base load is given by

$$N_\ell = \frac{q\ R\ J_1(\alpha R)}{\alpha} \qquad (A7)$$

where q = distributed base load
R = radius of load

Piled Bridge Abutments on Soft Clay – Experimental Data and Simple Design Methods

D.P. STEWART
B.E., Grad.I.E.Aust.
The University of Western Australia
R.J. JEWELL
B.E., M.Eng.Sc., M.I.E.Aust.
The University of Western Australia
M.F. RANDOLPH
M.A., Ph.D., M.I.E.Aust.
The University of Western Australia

SUMMARY Construction of bridge approach embankments on soft clay can result in the development of significant lateral soil movements, which impose lateral loads on the abutment piles. Estimation of these loads is highly uncertain at present. Results from two centrifuge model tests are presented and compared with predictions from several current simple design methods. Some of the factors influencing the loads induced in piles adjacent to embankments are discussed.

1. INTRODUCTION

Construction of embankments on soft clay results in the development of significant time dependent embankment settlements and movements within the soft clay. Where a bridge approach embankment is founded on soft clay, construction of the bridge itself is sometimes commenced before full settlement of the embankment has occurred. Piles supporting bridge abutments adjacent to such embankments may therefore experience significant lateral loads from horizontal soil movements, Fig. 1. These lateral loads induce bending moments and deflections in the piles which may lead to structural distress or failure of the piles or bridge structure (Leussink and Wenz, 1969; Heyman and Boersma, 1961).

Comparisons of loads predicted by various theoretical approaches with those measured in a limited number of full scale field trials have generally shown poor correlation. Hence estimation of the bending moments and deflections which will be induced in the abutment piles is uncertain. In practice, a conservative design incorporating hollow caissons to shield piles from lateral soil displacements is often adopted, or bridge construction is delayed until most of the settlement of the approach embankment has occurred.

A series of model tests have been performed on the geotechnical centrifuge at the University of Western Australia with a view to obtaining data from which a better theoretical approach may be derived. Results from two of these tests will be presented briefly and compared with several current simple design techniques.

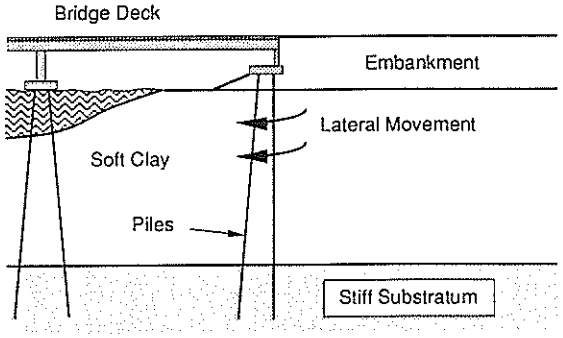

Fig. 1 Piled bridge abutment subjected to horizontal soil movements

2. CENTRIFUGE MODELLING

Geotechnical centrifuge modelling is a relatively new technique in the Australasian region, beginning with installation of a centrifuge at the University of Western Australia in 1989 (Fahey et al, 1990 and Randolph et al, 1991). The technique is well established internationally and has been used extensively for research, and as an aid to design, over about the last 20 years (Schofield, 1980).

The aim of a centrifuge test is to obtain similitude of stress and strain in model and prototype. This is achieved by accelerating a scale model, where all linear dimensions are reduced by a factor, n, to an acceleration of n gravities (g), effectively increasing the self weight by a factor n. Centrifuge models have major advantages over full scale field trials, being cheaper, well controlled, more easily and accurately instrumented and will have more uniform soil conditions in areal extent.

3. LAYOUT OF CENTRIFUGE MODELS

A number of models of piled bridge abutments on soft ground have been tested recently on the UWA centrifuge. Initially, tests were designed to replicate conditions at a proposed bridge site in Western Australia, although later tests were altered to examine a wider range of pile configurations and soil profiles. Model preparation and testing techniques for this project have been presented elsewhere (Stewart et al, 1991) and so will not be described in detail here.

The results of two tests will be presented; an 8 m thick layer of soft clay being modelled in one test, and an 18 m thick layer in the other. The configuration of the tests and layout of instrumentation is indicated on Fig. 2. For the shallow clay layer test, the undrained shear strength of the soft clay varied approximately linearly from about 13 kPa at the top to about 16 kPa at the base of the layer. In the deep layer test, the undrained shear strength varied similarly from about 13 kPa at the top to about 20 kPa at the base. The upper sections of each model had identical stress histories. In each test the soft clay layer was underlain by a very dense fine sand stratum.

Miniature model piles of brass were constructed to replicate the steel H piles (310 UC 158 sections) proposed for the prototype structure. The scaling ratio (and hence gravity level) of the models was chosen as 110 to match approximately the bending stiffness of the model and prototype piles. Each pile was strain gauged at ten levels to measure bending moment. Four instrumented piles were included in a group of 14 (two rows of seven piles) and were connected by a rigid pile cap. Two of the instrumented piles were positioned in the front row and two in the rear row.

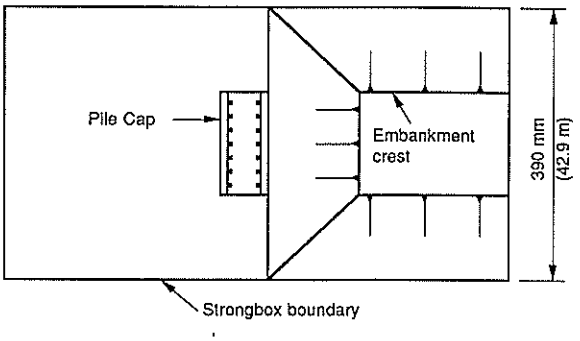

(a) Plan view

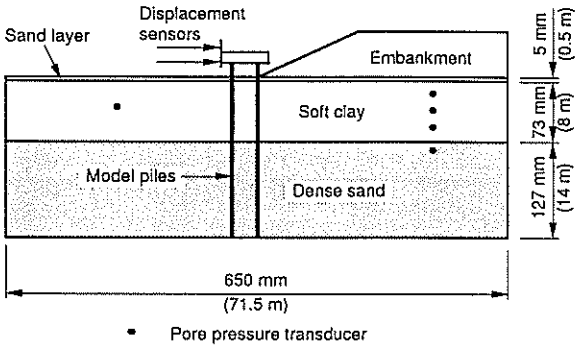

(b) Side view - shallow clay layer test

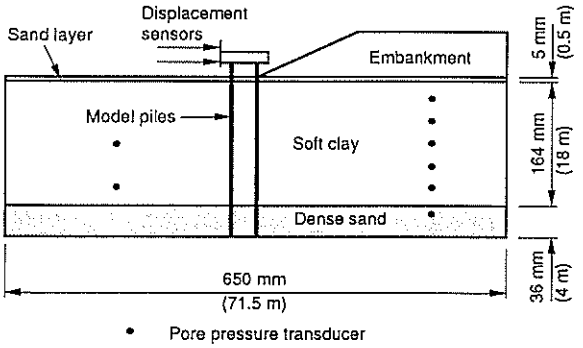

(c) Side view - deep clay layer test

Fig. 2 Centrifuge model layout

The piles were installed before the tests commenced, by pushing them fully into the sand stratum at the base of the models. This effectively fixed the piles at the base of the soft clay.

In both tests, a sand embankment was constructed in six lifts adjacent to the pile group. The embankment was built in-flight in the centrifuge by dropping sand from a hopper located directly above the model. Embankments were three-dimensional in shape, having both front and side slopes at approximately 2H : 1V, Fig. 2. The embankments were constructed to a maximum prototype height of 8 m. The dry density of the sand, as poured, was 17.5 kN/m^3.

The embankments were constructed relatively quickly during the first four stages, so that the foundation behaviour was essentially undrained. The final two stages were then added after longer time delays. Pore pressure transducers located beneath the embankments allowed pore pressure dissipation between stages to be assessed. The construction histories for the two tests were designed such that the same degree of consolidation would be achieved under each embankment at corresponding heights.

4. CENTRIFUGE TEST RESULTS

Some representative centrifuge test results are presented here in prototype units. The model bending moments have been scaled up by a factor of n^3 (110^3), and lengths and displacements by a factor of n (110). Full explanation of the scaling laws has been given by Schofield (1980).

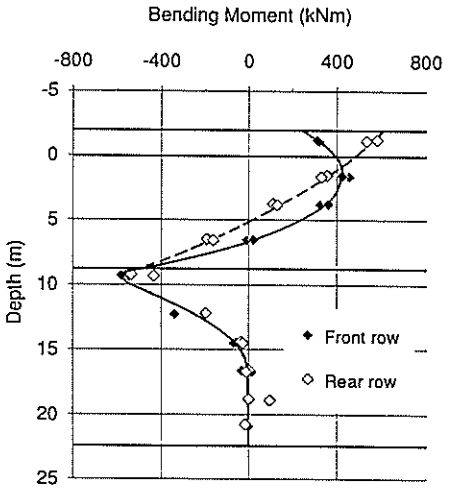

(a) Shallow clay layer test

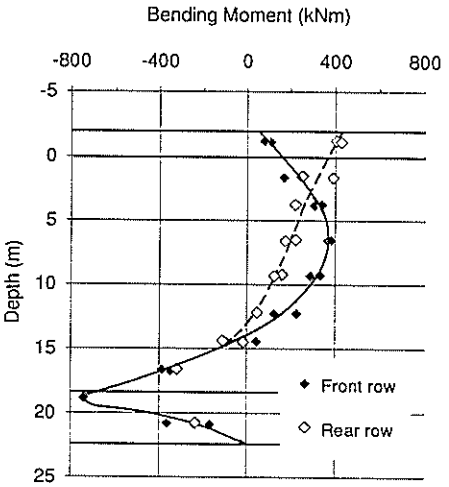

(b) Deep clay layer test

Fig. 3 Centrifuge model test results - bending moment distributions at embankment heights of 8 m.

4.1 Bending Moment Profiles

Bending moment profiles from comparable stages of the two tests are plotted on Fig. 3. In this Figure, the embankment is located on the left hand side of the piles. The general shape of the profiles are seen to be similar. For both tests the maximum bending moments were recorded at the top of the sand substratum for the front row piles. However, for the rear row piles, the maximum moment occurs at pile cap level for the shallow layer test and at the top of the sand substratum for the deep layer test.

4.2 Maximum Bending Moment

The maximum recorded bending moment for the piles in both tests is plotted against the applied embankment loading on Fig. 4. The maximum moments recorded in both tests are similar, although the rear row piles in the shallow layer test experienced significantly higher moments. The bending moments recorded during the tests were not sufficient to cause plastic deformation of the piles.

The data may be interpreted simply as a bilinear response, as shown. Inspection of the Figure suggests that for any set of data, the two lines will meet at a value of the embankment loading of about 3 to 3.5 times the undrained shear strength, s_u (taking 13 to 15 kPa as representative values). This load corresponds to a factor of safety for the embankment of between about 1.5 and 1.7 (5.14 / 3.5 and 5.14 / 3).

This observation compares well with the initiation of plastic deformation in the soil beneath a strip footing, which may be calculated from elasticity to occur at an applied load of about $3s_u$ (Poulos and Davis, 1980). The precise loading pressure which will initiate plastic deformation will depend on the initial stress state, as discussed by D'Appolonia et al (1971).

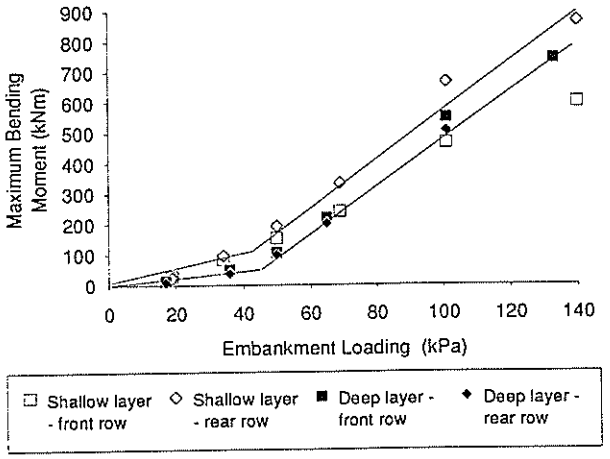

Fig. 4 Centrifuge model test results - maximum bending moments

5. CURRENT DESIGN TECHNIQUES

5.1 Pressure Based Methods

Several design techniques have been proposed based on relatively simple assumptions regarding the pressure exerted on the piles by the soft clay. These methods have all been developed from back analysis of field trials or model tests where the depth of clay was relatively small (less than 8 m) and the piles were generally relatively stiff in bending.

DeBeer and Wallays (1972) presented an empirical design method which takes into account the geometry of the embankment and the distance of the piles from the toe, Fig. 5(a). The method assumes that a uniform pressure acts on the piles over the full depth of the soft stratum. This pressure is used along with very simple assumptions regarding pile head fixity and support from stronger soil layers to estimate the maximum pile bending moment. The variation of bending moment along the pile can not be calculated.

Comparison of this simple design method with some field studies showed relatively good prediction of the maximum bending moment where the factor of safety against failure of the embankment was greater than about 1.6. This led DeBeer and Wallays to develop a second method for cases where the factor of safety is less than 1.6. In this case the most critical slip circle is drawn and the full limiting pressure ($10.5s_u$) is assumed to act on the pile above the point where the slip circle crosses the pile, Fig. 5(b).

Tschebotarioff (1973) presented design recommendations similar to the first DeBeer and Wallays method. He originally recommended that a triangular shaped lateral pressure be calculated as shown in Fig. 5(c). A revision was made to this recommendation in the light of field measurements detailed by Nicu et al (1971). In this Figure σ_z is the increase in vertical stress at the mid depth of the soft layer at the location of the piles. Tschebotarioff suggested that the lateral pressures could be ignored where the embankment loading was less than $3s_u$ (corresponding roughly to a factor of safety of 1.7).

Springman (1989) developed a relatively simple design method based on the results of some centrifuge model tests. The method predicts a parabolic shape lateral pressure acting on the piles, the magnitude of which is calculated from a complex expression approximately taking into account the average differential pile-soil movement. The method is based on a simple triangular shaped soil deformation mechanism (Bolton et al, 1991). An interactive spreadsheet is under development to assist with this analysis for single piles (Randolph and Springman, 1991). Pile groups may be analysed by applying this lateral pressure to individual piles, and then calculating the head fixing moments to yield equal deflection and zero rotation at pile cap level (Springman, 1991). Higher lateral pressures which result from the increased lateral stiffness of the pile group (compared with a single pile), are not considered.

5.2 Displacement Based Methods

Poulos (1973) presented a boundary element analysis of a single pile embedded in an elastic soil, where the soil was undergoing lateral movement. The method requires the input of a lateral soil displacement profile, and an optional limiting pressure which can act on the pile. The method accounts for continuity of the soil mass and allows varying soil properties with depth to be specified approximately. Charts have been presented showing calculated results for single piles, although pile groups could be analysed by modifying the computer program. Comparisons with some field data proved to be inconsistent, although good agreement was shown in some cases.

Bourges et al (1980) adopted a similar approach to Poulos, where a lateral soil movement profile must be specified, except the soil was represented by a series of non-linear springs (p-y curves) and soil continuity was not accounted for. The computer program allows single piles to be analysed, although may be modified to analyse pile groups.

The disadvantage of these design methods is that the results are sensitive to the lateral soil movement profile which is input. Lateral movements are difficult to predict accurately (Poulos, 1972) although recent research has shown relatively good correlations between field data and numerical analysis using complex soil models.

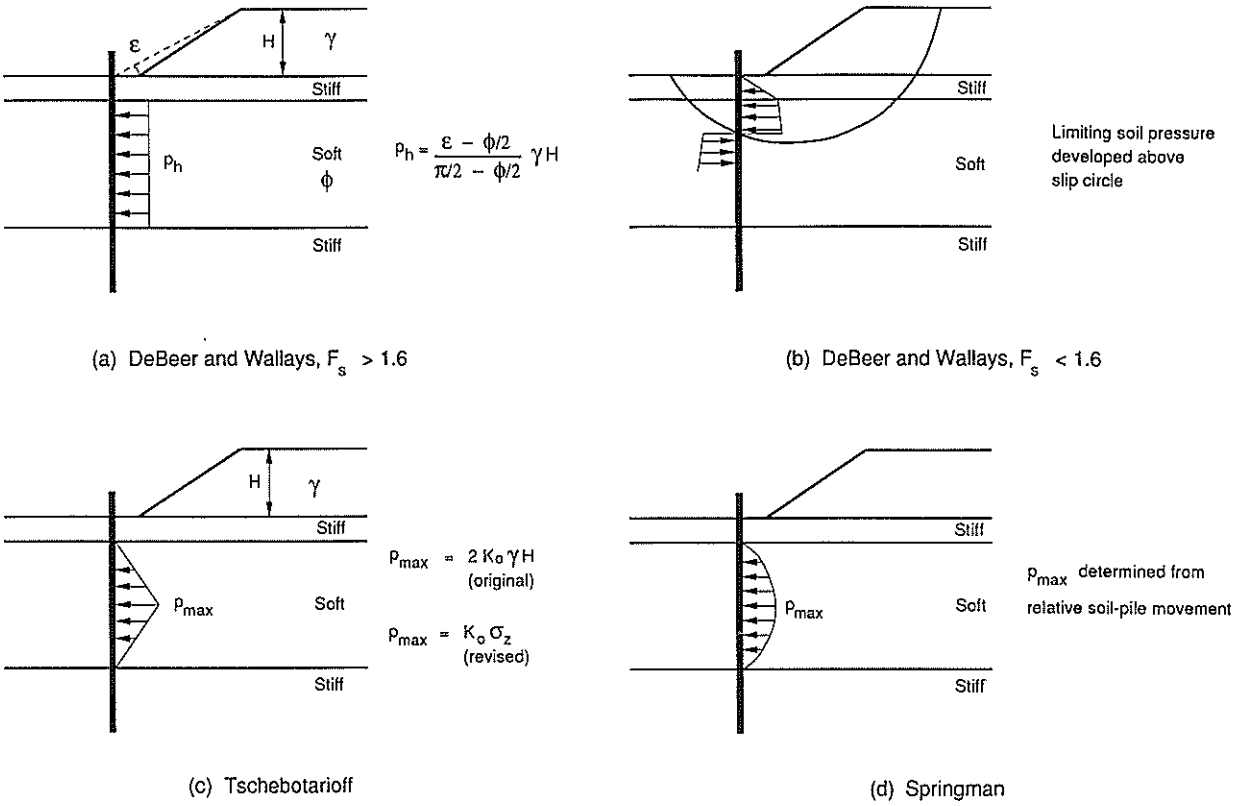

Fig. 5 Pressure based design methods

5.3 Finite Element Methods

Finite element analysis in several different forms has been conducted by various researchers. Randolph (1981) performed a site specific plane-strain analysis, where the piles were replaced by an equivalent sheet-pile wall with flexibility equal to the average of the piles and soil it replaced. The soft stratum was represented by the modified Cam Clay model, and the embankment by a pressure loading at the surface. The analysis allows pile groups to be analysed directly.

Naylor (1982) continued analyses of this form, but modelled the sheet-pile wall with link elements, thus allowing relative displacement of the soil and the wall and approximating more closely the true three dimensional behaviour around the piles. The soft stratum and embankment were represented by linear elastic models. The conclusions arising from this study were that link elements were not required in cases where the piles were quite flexible, or the soft layer was deep. A similar approach was adopted by Rowe and Poulos (1979) for the analysis of piles stabilising a slope, although an elastic-plastic soil model was used.

Carter (1982) performed a finite element analysis of a single pile at the centre of an axisymmetric mesh. An unsymmetric pressure loading was applied to the surface of the mesh, and a linear elastic soil model was used. Typical results were presented in chart form, showing the variation in bending moment with depth for various cases. The technique allows good representation of the three dimensional nature of the problem, although pile groups can not be analysed directly.

6. COMPARISON OF TEST RESULTS WITH CURRENT SIMPLE DESIGN TECHNIQUES

The centrifuge results presented earlier will be compared briefly with predictions from the three simple design methods outlined in section 5.1. The results of these analyses are shown on Fig. 6 as plots of maximum bending moment versus embankment loading. In all cases the embankment has been modelled as a plane-strain loading, which is not exactly equivalent to the centrifuge test conditions, but will provide an upper bound for the calculations.

6.1 DeBeer and Wallays

The results of the DeBeer and Wallays analysis are shown on Fig. 6 (a) as two linear sections, controlled by the factor of safety of the embankment. On Fig. 6 (b) only one section is shown, as the first method gives a higher moment than the second method. This analysis appears to compare reasonably well for the shallow layer test, but gives a gross over-estimate for the deep layer case. The predictions are not extended beyond an embankment loading of 70 kPa as this is the failure load predicted on the basis of plane-strain conditions and a totally undrained foundation response.

6.2 Tschebotarioff

Predictions from Tschebotarioff's original and revised design recommendations show inconsistent correlation with the centrifuge data. The original method compares relatively well with the shallow layer results, while the revised method compares well with the deep layer results.

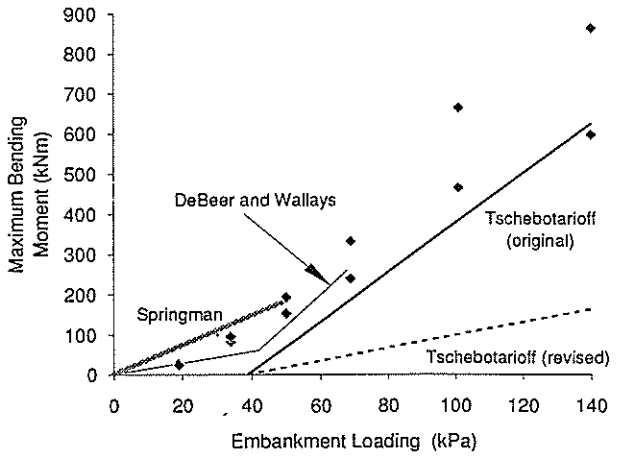

(a) Shallow clay layer

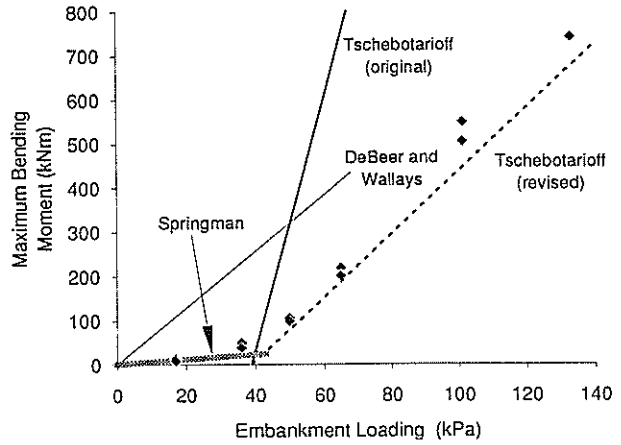

(b) Deep clay layer

Fig. 6 Comparison of centrifuge data and simple design methods

6.3 Springman

Springman's method of analysis appears to predict the initial response of both tests relatively well, although it is sensitive to the elastic modulus chosen for the soft layer. The analysis is continued up until the so-called psuedo-elastic limit proposed by Springman at a factor of safety against bearing capacity failure of 1.5. Springman does not recommend design beyond this point as higher moments are expected to develop.

The predicted bending moment distributions along the piles have not been presented. However, the shape of the predicted distributions are not entirely dissimilar from those observed in the centrifuge data. The location of the maximum bending moment along the piles was generally correct, except for the rear row piles of the shallow layer test.

7. DISCUSSION

The simple design methods which are currently available have been shown to be generally inconsistent. The DeBeer and Wallays method is cumbersome to apply and, like Tschebotarioff's analyses, is sensitive to the simple assumptions of pile fixity. Neither of these techniques accounts for the flexibility of the piles or allows the bending moment distribution to be determined.

Springman's design method appears to reproduce the initial elastic response observed in the centrifuge data, but provides no estimate of the increased moments once plastic deformation is initiated under the embankment loading. Embankments are generally designed to factors of safety during construction of about 1.3. With the use of stabilising berms this could correspond to a maximum embankment loading well in excess of $4s_u$. Since plastic deformation has been observed to commence at an embankment load of about $3s_u$, plastic deformation is likely to be of considerable influence in the behaviour of most embankments on soft clay.

It should also be noted that Springman's design method may be unsuitable for pile groups containing a large number of very flexible piles. Individual pile flexibility is accounted for in the lateral pressure calculation, however if the individual piles form a group that has relatively high lateral stiffness, the loads may be significantly underestimated.

While the problem is obviously very complex - depending upon interaction of the embankment with the soft stratum, which in turn interacts with the pile group - a relatively simple approach to design is preferable to enable initial sizing and feasibility to be examined quickly. Complex soil conditions and pile configurations could then be accounted for by a more sophisticated analysis if necessary. The methods outlined in sections 5.2 and 5.3 may be suitable for these analyses, although more work is required to confirm their suitability.

This paper has considered the behaviour of the soft stratum to be undrained, with the effects of pore pressure dissipation and embankment construction history ignored. However, the test data suggest that bending moments develop rapidly after embankment construction, and then alter little during ongoing consolidation. The effects of embankment construction rate, and the timing of pile installation during the construction period, are likely to be of greater influence and are currently under assessment.

8. CONCLUSIONS

The simple design methods which are currently available to predict bending moments in piles adjacent to embankments on soft ground have been shown to be generally inconsistent, although some aspects of the observed behaviour are accounted for.

The influence of plastic deformation within the soft stratum on the magnitude of bending moments induced in the piles has been discussed. It is concluded that the ratio of load level to undrained shear strength of the soft stratum is an essential factor, that must be taken into account when assessing the loads applied to piles by lateral soil movements beneath embankments.

A new simple design method, which will take into account the observed behaviour of model and field tests, is currently under development. It is envisaged that this method will be suitable for the majority of design situations. However, for complex problems a more sophisticated approach may be necessary, perhaps based on finite element analysis.

ACKNOWLEDGEMENTS

The work reported in this paper was funded by the Main Roads Department of Western Australia. The financial assistance of the Main Roads Department was also a major factor in the acquisition of the geotechnical centrifuge and is gratefully acknowledged. The first author is supported by a research scholarship from the University of Western Australia.

REFERENCES

Bolton M.D., H.W. Sun and S.M. Springman (1991). Foundation Displacement Mechanisms, *Ground Engineering*, 24 No. 3, April, pp 26-29.

Bourges F., R. Frank and C. Mieussens (1980). Calcul des Efforts et des Deplacements Engendres par des Poussees Laterales des Sol sur les Pieux, Note Technique du Department Sols et Fondations, LCPC.

Carter J.P. (1982). A Numerical Method for Pile Deformations due to Nearby Surface Loadings, Proc. 4th ICONMIG, Edmonton, Vol. 2, pp 811-817.

D'Appolonia D.J., H.G. Poulos and C.C. Ladd (1971). Initial Settlement of Structures on Clay, ASCE JSMFE, 97 (SM10), pp 1359-1377.

DeBeer E.E. and M. Wallays (1972). Forces Induced in Piles by Unsymmetrical Surcharges on the Soil Around the Piles, Proc. 5th ECSMFE, Madrid, Vol. 1, pp 325-332.

Fahey M., I. Finnie, P.J. Hensley, R.J. Jewell, M.F. Randolph, D.P. Stewart, K.J.L. Stone, S.H. Toh and C.S. Windsor (1990). Geotechnical Centrifuge Modelling at the University of Western Australia, *Australian Geomechanics*, December 1990.

Heyman L. & F. Boersma (1961) Bending Moments in Piles due to Lateral Earth Pressure, Proc. 5th ICSMFE, Paris,Vol. 2, pp 425-429.

Leussink H. and K.P. Wenz (1969). Storage Yard Foundations on Soft Cohesive Soils, Proc. 7th ICSMFE, Vol. 2, pp 149-155.

Naylor D.J. (1982). Finite Element Study of Embankment Loading on Piles, Report for the Department of Transport (HECB), UK.

Nicu N.D., D.R. Antes & R.S. Kessler (1971). Field Measurements on Instrumented Piles Under an Overpass Abutment, *Highway Research Record*, 354, pp 90-102.

Poulos H.G. (1972). Difficulties in Prediction of Horizontal Deformation of Foundations, ASCE JSMFE, 98 (SM 8), pp 843-848.

Poulos H.G. (1973). Analysis of Piles in Soil Undergoing Lateral Movement, ASCE JSMFE, 99 (SM 5), pp 391-406.

Poulos H.G. and E.H. Davis (1980). Elastic Solutions for Soil and Rock Mechanics, John Wiley & Sons, New York.

Randolph M.F. (1981). Pilot Study of Lateral Loading of Piles Due to Soil Movement Caused by Embankment Loading, Report for the Department of Transport (HECB), UK.

Randolph M.F., R.J. Jewell, K.J.L. Stone & T.A. Brown (1991) Establishing a New Centrifuge Facility, Proc. Centrifuge 1991, Univ. of Colorado, Ed. Hon Yim Ko, Balkema.

Randolph M.F. and S.M. Springman (1991). Analysis of Pile Response Due to External Loads and Soil Movement, Proc. ECSMFE, Florence.

Rowe R.K. and H.G. Poulos (1979). A Method for Predicting the Effect of Piles on Slope Behaviour, Proc. 3rd ICONMIG, Aachen, Vol. 3, pp 1073-1085.

Schofield A.N. (1980). Cambridge Geotechnical Centrifuge Operations, *Geotechnique*, 30, No. 3, pp 227 - 268.

Springman S.M. (1989). Lateral Loading on Piles Due to Simulated Embankment Construction, PhD thesis, Cambridge University.

Springman S.M. (1991). Analysis of the Effect of Lateral Thrust on Pile Groups Due to Surcharge Loading, Fondations Profondes, Colloque International, l'Ecole Nationale des Ponts et Chaussees, Paris, pp 293-300.

Stewart D.P., R.J. Jewell and M.F. Randolph (1991). Embankment Loading of Piled Bridge Abutments on Soft Ground, Proc. Int. Conf. on Geotechnical Engineering for Coastal Development, Yokohama, JSSMFE.

Tschebotarioff G.P. (1973). Foundations, Retaining and Earth Structures, 2nd Edition, McGraw-Hill, New York.

The Analysis of Rectangular Rafts of Finite Flexibility Subjected to Concentrated Loads

B.Q. ZHANG
B.E.
Research Student, School of Civil and Mining Engineering, University of Sydney
J.C. SMALL
B.Sc. (Eng.), Ph.D., M.I.E.Aust., M.A.S.C.E.
Associate Professor, School of Civil and Mining Engineering, University of Sydney

SUMMARY The analysis of soil-raft interaction is carried out by using the finite layer method to determine the response of the soil, and the finite element method for the analysis of the raft. The use of the finite layer method means that the three dimensional problem involved in obtaining the response of the soil to the raft loading can be reduced to a problem involving only two spatial dimensions and this greatly simplifies the solution process. Solutions are presented, in particular, for cases involving isolated or point loadings applied to the raft. Such loadings can cause the raft to deform in such a way that it lifts off the foundation, and this has to be accounted for in the analysis.

NOTATION

A_i = area of ith raft element
$\boldsymbol{a}_i$ = vector of variables at node i of element
$\boldsymbol{a}$ = $(1,\ 1,\ 1, \ldots, 1)^T$
B = breadth of raft
$\boldsymbol{B}$ = matrix relating transformed strains to transformed displacements
$\boldsymbol{b}$ = vector of z distances relative to pinned node
$\boldsymbol{c}$ = vector of x distances relative to pinned node
E = Young's modulus; subscripts r, s denote values for raft, soil
h = depth of soil layer
$\boldsymbol{I}_r$ = influence matrix for raft
$\boldsymbol{I}_s$ = influence matrix for soil
K = raft stiffness
$\boldsymbol{K}$ = stiffness matrix for soil
L = width of raft
M = overall moment applied to raft; subscripts x, z denote axis about which moment is applied
m = internal moments per unit length in raft; subscripts x, z denote direction of moment
$\boldsymbol{N}$ = vector of shape functions for element
$\boldsymbol{P}$ = vector of contact pressures acting on each element of raft
P_{tot} = total load applied to raft
p = load applied to one quarter of raft
$\bar{q}$ = average applied pressure
T = Fourier transform of loading traction
t = thickness of raft
t_y = loading traction in vertical (y) direction
U = Fourier transform of displacement; subscripts x, y, z denote displacement direction
u = displacement; subscripts $x,\ y,\ z$ denote displacement direction
$x,\ y,\ z$ = Cartesian coordinates; subscripts i denote coordinates at centre of raft element i, subscript p denotes coordinate of pinned node
Δ = differential deflection in raft
$\boldsymbol{\Delta}$ = vector of transformed displacements in soil
$\boldsymbol{\delta}_r,\ \boldsymbol{\delta}_s$ = vectors of vertical surface displacements at collocation points in the raft and soil respectively
Γ = length along surface loaded with tractions
ν = Poisson's ratio; subscripts r, s denote raft, soil
ρ = Fourier transform parameter

1. INTRODUCTION

The analysis of raft foundations has long been of interest to civil engineers and many different methods of analysis have been developed in order to predict their behaviour under loading. Plastic yielding of the soil beneath the raft has been considered in some of these methods, however interest has mainly been restricted to elastic behaviour since at working loads the behaviour of both the soil and the raft can be expected to be almost linear.

Spring models (Winkler (1867); Lee and Harrison (1970)), which are still widely used by structural engineers, have the advantage of simplicity but cannot model the real soil behaviour as there is no interaction between springs. Determination of the spring stiffnesses to be used in the Winkler model has also caused many problems, as they need to be obtained from past experience or backfigured using a plate load test. The stiffnesses obtained depend on the size of the plate used and must be modified for use with a full size structure. Elastic continuum models are therefore much preferable, and have been used by many researchers.

Analytic solutions (Gorbunov-Possadov and Serebrjanyi (1961)) or semi-analytic solutions (Brown (1969a, b), Booker and Small (1983),) tend to be restricted in their application to real problems where loadings and raft shapes can be complex. As well, they cannot deal with soils which are layered or have properties which vary with depth.

For this reason, numerical solutions were developed such as the method of Cheung and Zienkiewicz (1965) where the raft was modelled through the use of finite element techniques, while the soil was modelled as either Winkler springs or as an elastic continuum. This method was extended by Cheung and Nag (1968), by allowing lift-off or separation of

the raft and the soil and including the effects of horizontal loading. An improved method was developed by Svec and Gladwell (1973) to represent the contact pressure beneath the raft.

Other numerical solutions have been obtained by Hain and Lee (1974), who used finite elements for the analysis of the raft and treated the soil as either Winkler springs or a uniform elastic material. In order to allow the analysis of layered soils, Fraser and Wardle (1974, 1976) used integral transform techniques to obtain the response of the soil to the raft loading. This enabled analyses to be carried out for rafts of any shape on soils which were horizontally layered. Tham et al. (1988) used finite layer techniques to obtain the response of the soil and double spline elements to analyse the raft behaviour.

In this paper a method is presented in which the response of the raft is obtained from use of the finite element method, while the soil behaviour is obtained through use of a finite layer method. This allows analysis of rafts of almost any shape which are subjected to complex loading distributions. The raft can be founded on soils for which material properties vary vertically or laterally. The only restriction is that the soil properties do not vary in one lateral direction. This restriction allows a simpler analysis, yet allows enough flexibility so that the method can be used for actual engineering design. As well, problems which require contact stresses to be limited to maximum values (pseudo-failure of the soil) or to zero values (lift-off) can be accommodated.

2. THEORY

The raft and the soil are shown schematically in Figure 1 where it is assumed that the contact pressure can be represented by a series of uniform blocks of pressure. This contact pressure is chosen to be uniform over each rectangular element in the raft and to act in the vertical direction only (i.e. smooth based raft).

The solution process then involves determining the magnitudes of the contact pressures on each block so that the deflections of the raft match the deflections of the soil at certain collocation points (provided the raft does not lift away from the soil).

2.1 Analysis of Soil

In order to obtain the response of the soil to the contact pressure, it is necessary to be able to obtain the solution for an elastic soil subjected to a uniform rectangular surface loading. This is done in this paper by the use of a Fourier transform technique. The method is presented in Appendix A, which basically involves transforming all of the field variables (i.e. stresses and displacements) so that the z coordinate (Figure 1) is eliminated and a two dimensional finite element mesh may be used to solve the problem. Material properties therefore cannot vary in the z-axis direction, but can vary in the remaining axis directions. We can therefore write for the soil, (if there are n loaded regions)

$$\delta_s = I_s P \tag{1}$$

where $\delta_s = (\delta_1, \delta_2, \delta_3, \ldots, \delta_n)^T$ is the vector of vertical displacements at the collocation points, $P = (p_1, p_2, p_3, \ldots, p_n)^T$ is the vector of the contact pressures acting on each element of the raft and I_S is an $n \times n$ influence matrix for the soil, for

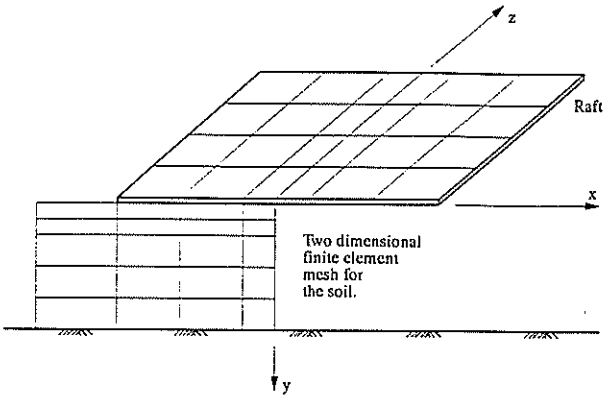

Figure 1 Raft on an elastic soil

which the ith column consists of the deflections at all of the collocation points due to the application of a unit pressure over a rectangular region i.

2.2 Analysis of Raft

The raft may be analysed in a straight-forward manner, by using finite element methods (see Zienkiewicz (1977)).

The type of element used was a four noded, 16 degree of freedom element which was developed by Bogner et al. (1965). The nodal variables a_i at a node i include the vertical displacement, w_i, the rotation in the x direction, $\left(\frac{\partial w}{\partial x}\right)_i$, the rotation in the z direction, $\left(\frac{\partial w}{\partial z}\right)_i$, and the twist $\left(\frac{\partial^2 w}{\partial x \partial z}\right)_i$ and so

$$a_i^T = \left[w_i, \left(\frac{\partial w}{\partial x}\right)_i, \left(\frac{\partial w}{\partial z}\right)_i, \left(\frac{\partial^2 w}{\partial x \partial z}\right)_i\right] \tag{2}$$

The displacements at all collocation points (which were chosen to be at the central point of each element) can be calculated in terms of the magnitudes of the uniform pressures p_j on each of the elements j of the raft, by creating an influence matrix for the raft I_r. The influence matrix for the raft, like that for the soil, consists of columns which contain the deflections at the collocation points due to unit pressures applied to each element of the raft in turn.

In order to obtain the deflections of the raft we must provide some boundary conditions and so it is necessary to 'pin' or fix the raft from displacement and rotation at some point. We must therefore introduce an unknown translation Δ, and unknown rotations θ_x and θ_z about the x and z axis directions. Hence for the raft we may write

$$\delta_r = I_r(-P) + a\Delta + b\theta_x + c\theta_z + \delta_q \tag{3}$$

where δ_q is the vector of deflections at the centre of each of the raft elements for the pinned raft under the applied loads.

2.3 Interaction Theory

In order to maintain equilibrium of the raft we must have moment equilibrium and force equilibrium. The applied moments must equal the moments due to the reaction pressure, while the total vertical load applied to the raft P_{tot} must equal the total contact pressure. Hence we have

$$\begin{bmatrix} I_s + I_r & -a & -b & -c \\ -\bar{a}^T & 0 & 0 & 0 \\ -\bar{b}^T & 0 & 0 & 0 \\ -\bar{c}^T & 0 & 0 & 0 \end{bmatrix} \begin{bmatrix} P \\ \Delta \\ \theta_x \\ \theta_z \end{bmatrix} = \begin{bmatrix} \delta_\eta \\ -P_{tot} \\ -M_x \\ -M_z \end{bmatrix} \quad (4)$$

where

$a = (1, 1, 1, \ldots, 1)^T$
$b = (z_1 - z_p,\ z_2 - z_p,\ z_3 - z_p, \ldots, z_j - z_p\ , \ldots,\ z_n - z_p)^T$
$c = (x_1 - x_p,\ x_2 - x_p,\ x_3 - x_p\ , \ldots,\ x_j - x_p\ , \ldots,\ x_n - x_p)^T$
$\bar{a}^T = (A_1,\ A_2,\ A_3\ , \ldots,\ A_j\ , \ldots,\ A_n)$
$\bar{b}^T = [A_1(z_1 - z_p),\ A_2(z_2 - z_p),\ A_3(z_3 - z_p)\ ,$
$\ldots,\ A_j(z_j - z_p)\ , \ldots,\ A_n(z_n - z_p)]$
$\bar{c}^T = [A_1(x_1 - x_p),\ A_2(x_2 - x_p),\ A_3(x_3 - x_p),$
$\ldots,\ A_j(x_j - x_p)\ , \ldots,\ A_n(x_n - x_p)]$

M_x, M_z are the applied bending moments; $x_p,\ z_p$ are the coordinates of the pinned point of the raft; A_j is the area of element j; $x_j,\ z_j$ are the coordinates of the centre of element j.

The above equations may now be solved for the contact stresses P, the translation Δ, and the rotations θ_x and θ_z of the raft. The bending and twisting moments and differential settlement of the raft can be determined by applying the contact stresses back to the raft (along with the applied loadings on the raft).

3. RESULTS

In order to verify the accuracy of the preceding theory, the problem of a rigid square raft which rests on a half-space and which is subjected to concentrated loads at the corners was analysed. Each load was represented by a square uniform loading of side $0.02L$ as shown in Figure (2), where L is the width of the raft. The applied load on a quarter of the raft is p and the average applied load is $\bar{q}$. The Poisson's ratio adopted for the raft was 0.15 and the relative raft stiffness K was chosen to be 150, where K is defined by

$$K = \frac{4E_r(1-\nu_s^2)}{3E_s(1-\nu_r^2)}\left(\frac{t}{L}\right)^3$$

Figure (3) shows the distribution of contact pressure over one quarter of the raft while the contours for moment per unit length m_x are shown in Figure (4). It may be seen that close agreement is obtained with the solutions of Brown (1978) for both the reaction, and the bending moments.

Figure (5) shows the result for settlement of a rigid rectangular raft of length L and width B by substituting point loads of equal magnitude for the concentrated loads applied over an area of $0.02L$ by $0.02L$ as shown in Figure (2). As may be expected, the results calculated by applying point loads at the corners are also very close to the solutions of Brown (1978) which were for the concentrated load case.

As the above comparisons indicate that the theory presented in this paper can be used to solve problems of soil-raft interaction accurately, some original problems were solved. The examples involve determining the distribution of differential deflection and bending moment in a rectangular raft which is supported by a single layer of finite depth and which is subjected to concentrated loads. The ratio of length L to width B of the raft was chosen to be 2 and the depth h of the layer of soil was taken to be equal to B. Poisson's ratios for

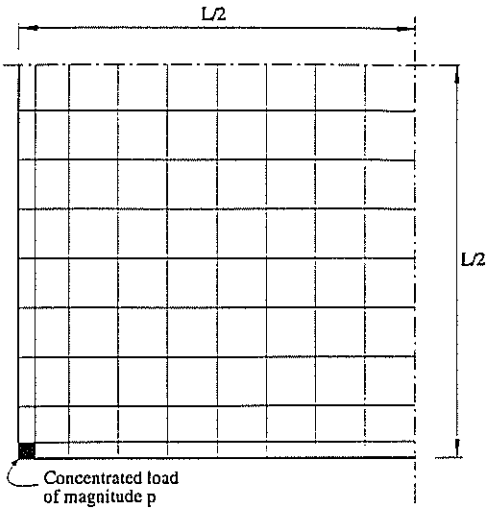

Figure 2 Concentrated load applied to square raft

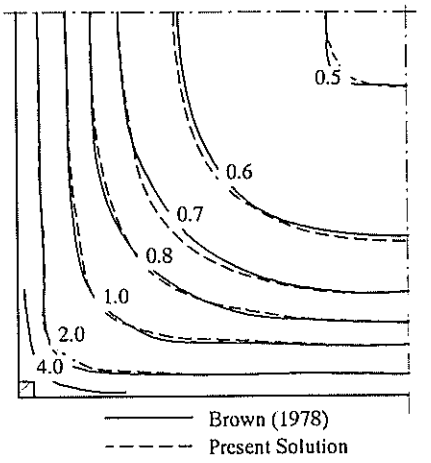

Figure 3 Contours of contact pressure $p/\bar{q}$ for rigid square raft

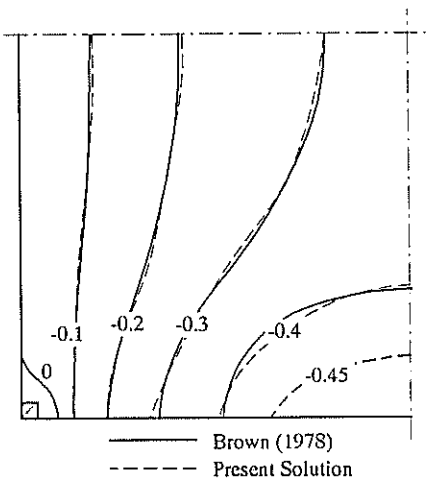

Figure 4 Contours of bending moment per unit width m_x/p for a rigid square raft

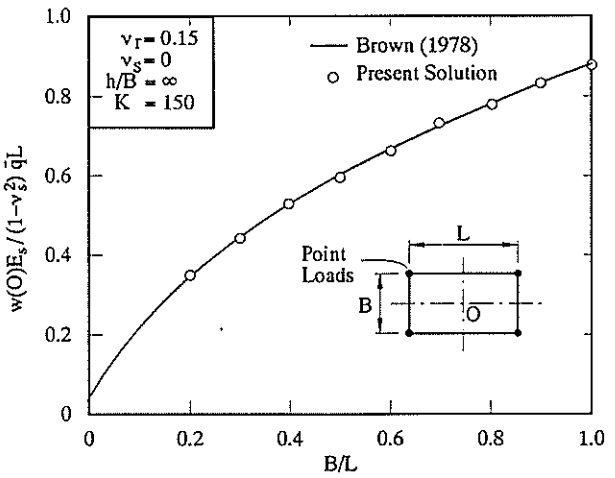

Figure 5 Settlement of symmetrically loaded rigid rectangular raft

the soil and raft were chosen to be $\nu_s = 0.3$ and $\nu_r = 0.15$. Each load was represented by a uniform loading applied over a square $0.05B \times 0.05B$. The four loading cases as shown in Figure (6) were analysed.

Differential deflection ($\Delta = w(A) - w(O)$) and maximum bending and twisting moments m_x, m_z for various stiffnesses are shown in Figures (7), (8) and (9), where the relative stiffness of the raft K is defined as follows:

$$K = \frac{E_r(1-\nu_s^2)}{E_s}\left(\frac{t}{B}\right)^3,$$

p is the load applied to one quarter of the raft and $\bar{q}$ is the average loading on the raft. The largest moment per unit length in the x direction occurs in the vicinity of the point marked X (Figure 8) while the maximum moment in the z direction occurs near the corner marked Y (Figure 9).

It was found that tensile contact pressure occurs around the centre of the raft for $K < 1$ (loading case (1)). Where tensile pressures exist, an iterative approach (see Cheung and Nag (1968)) was used to reduce the negative contact stresses to zero. A maximum of five cycles was used before a convergent solution was obtained for $K = 0.01$, the stiffness at which maximum tensile pressure areas occur.

Figure (10) shows the maximum moment in the raft for various stiffnesses for the other loading cases (2)-(4). The maximum bending moment was obtained by using the following method: (a) computing the bending moment at 6×6 Gauss points within each element; (b) selecting the maximum moment for each element; (c) comparing these maximum moment values and selecting the largest value as the maximum moment for the raft. The differential deflection (between the corner and the centre of the raft) for these three loading cases is plotted in Figure (11). The positions of the points A and O referred to in Figure 11 are identified in Figure 6. It may be seen from the figures that a more flexible raft undergoes larger differential deflection and a stiffer raft carries larger bending moments.

4. CONCLUSIONS

A method has been presented which makes use of finite layer theory in the analysis of raft foundations. The use of this theory greatly simplifies the analysis, as the three-dimensional problem is effectively reduced to one involving only two spatial dimensions. This means that solutions may be obtained through the use of two dimensional finite element meshes.

Although not all of the capabilities of the method could be demonstrated here, the examples for point or concentrated loadings show that accurate results can be obtained for rectangular rafts on uniform soil layers. Limited design charts have been provided for rectangular rafts on soil layers of finite thickness.

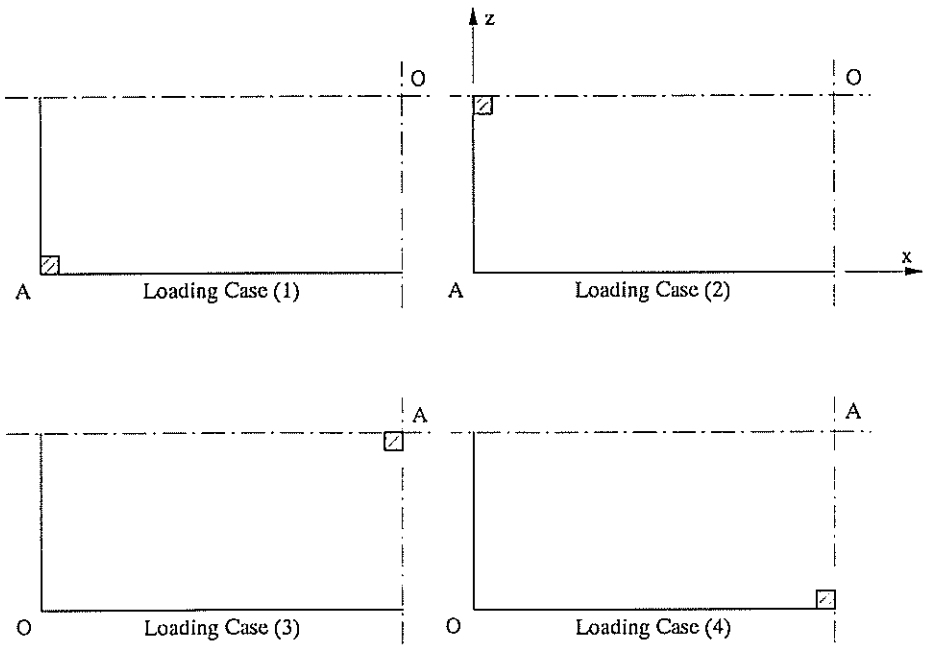

Figure 6 Concentrated loads on Rectangular raft

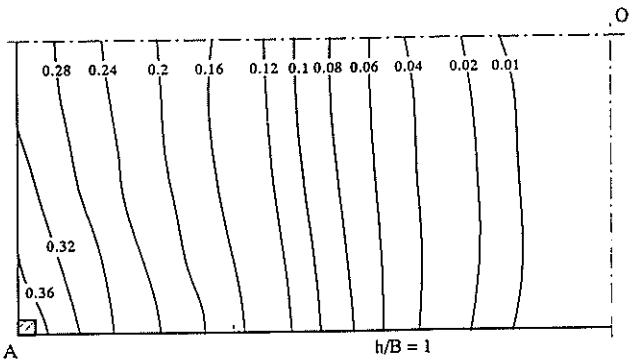

Figure 7 Contours of differential settlement $[w(A) - w(O)]G_s/\bar{q}B$ for loading case (1). K = 1.0

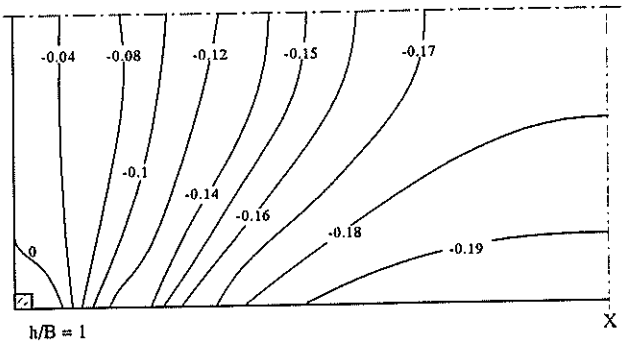

Figure 8 Contours of bending moment per unit length m_xB/pL for loading case (1). K = 1.0

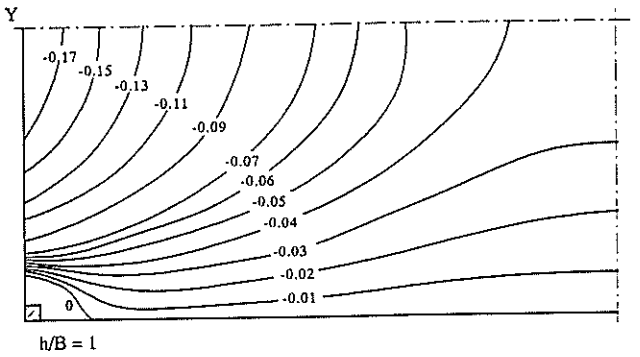

Figure 9 Contours of bending moment per unit length m_zB/pL for loading case (1). K = 1.0

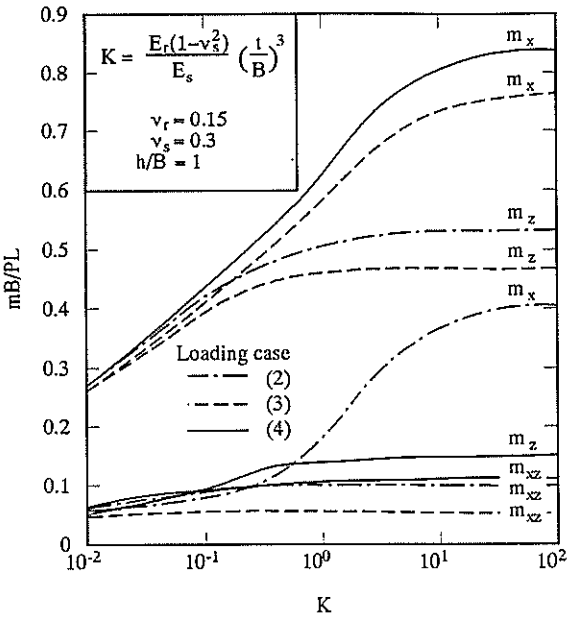

Figure 10 Maximum bending and twisting moments for rafts with concentrated loads

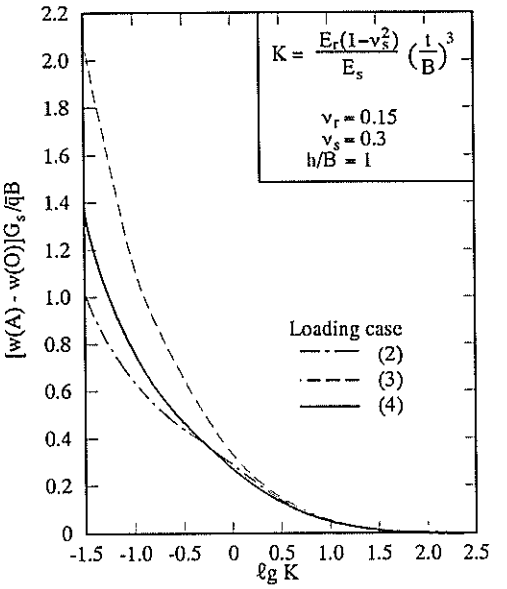

Figure 11 Differential settlement for rafts with concentrated loads

5. REFERENCES

1. Bogner, F.K., Fox, R.L. and Schmit, L.A. (1965). "The Generation of Inter-Element-Compatible Stiffness and Mass Matrices by the Use of Interpolation Formulas", Proc. Conf. Matrix Meth. Struct. Mech., 1st Wright-Patterson AFB, Ohio, (AFFDL-TR-66-80), pp.397–443.

2. Booker, J.R. and Small, J.C. (1983). "The Analysis of Liquid Storage Tanks on Deep Foundations", Int. Jl. Num. Anal. Meth. Geom., Vol.7, pp.187–207.

3. Brown, P.T. (1969a). "Numerical Analysis of Uniformly Loaded Circular Rafts on Elastic Layers of Finite Depth", Géotechnique, Vol.19, No.2, pp.301–306.

4. Brown, P.T. (1969b). "Numerical Analysis of Uniformly Loaded Circular Rafts on Deep Foundations". Géotechnique, Vol.19, No.3, pp.399–404.

5. Brown, P.T. (1978). "Stiff Rectangular Rafts Subject to Concentrated Loads", Aust. Geom. Jl., Vol.G8, No.1. pp.40–49.

6. Cheung, Y.K. and Nag, D.K. (1968), "Plates and Beams on Elastic Foundations - Linear and Non-Linear Behaviour", Géotechnique, Vol.18, pp.250–260.

7. Cheung, Y.K. and Zienkiewicz, O.C. (1965). "Plates and Tanks on Elastic Foundations - An Application of Finite Element Method", Int. Jl. Structs., Vol.1, pp.451–461.

8. Fraser, R.A. and Wardle, L.J. (1976). "Numerical Analysis of Rectangular Rafts on Layered Foundations", Géotechnique, Vol.26, No.4, pp.613–630.

9. Gorbunov-Possadov, M.I. and Serebrjanyi, R.V. (1961) "Design of Structures on Elastic Foundations", Proc. 5th Int. Conf. Soil Mech. Fdn. Engg., Vol.I, pp.643–648.

10. Hain, S.J. and Lee, I.K. (1974) "Rational Analysis of Raft Foundation", Geotech. Div., ASCE, Vol.100, GT7, pp.843–860.

11. Lee, I.K. and Harrison, H.B. (1970). "Structure and Foundation Interaction Theory", Jl. Struct. Div., ASCE, Vol.96, ST2, pp.177–198.

12. Svec, O.J. and Gladwell, G.M.L. (1973). "A Triangular Plate Bending Element for Contact Problems", Int. Jl. Solids Structs., Vol.9, pp.433–446.

13. Sneddon, I.N. (1951). Fourier Transforms, McGraw-Hill, New York.

14. Tham, L.G., Man, K.F. and Cheung, Y.K. (1988). "Analysis of Footing on Non-Homogeneous Soil by Double Spline Element", Computers and Geotechnics, Vol.5, pp.249–268.

15. Wardle, L.J. and Fraser, R.A. (1974). "Finite Element Analysis of a Plate on a Layered Cross-Anisotropic Foundation", Proc. 1st Int. Conf. Finite Element Meth. Eng., Univ. NSW, pp.565–578.

16. Winkler, E. (1867). Die Lehre von der Elastizitaz und Festigkeit, Prague.

17. Zienkiewicz, O.C. (1977). The Finite Element Method, McGraw-Hill.

Appendix A

A method for solving the displacements in an elastic soil can be developed by using a combination of Fourier transforms and finite element techniques. Suppose a uniform loading t_y which is symmetric about $z = 0$ is applied to the surface of the soil. If the soil properties do not vary in the z direction, the displacements may be transformed in the following way (see Sneddon (1951))

$$(U_x,\ U_y,\ U_z) = \frac{1}{2\pi}\int_{-\infty}^{+\infty}(u_x,\ u_y,\ u_z)\ \cos\rho z\ dz \qquad (5)$$

where $u_x,\ u_y,\ u_z$ are the displacements in the x, y, z directions respectively and $U_x,\ U_y,\ U_z$ are the Fourier transforms of these displacements. In the above equation, U_x is used for $U_x(x, y, \rho)$ and u_x for $u_x(x, y, z)$, etc.

The equivalent inverse transforms take the form

$$(u_x,\ u_y,\ u_z) = \int_{-\infty}^{+\infty}(U_x,\ U_y,\ U_z)\ \cos\rho z\ d\rho \qquad (6)$$

The transform of the loading in the vertical (y) direction is given by

$$T_y = \frac{1}{2\pi}\int_{-\infty}^{+\infty} t_y \cos\rho z\ dz \qquad (7)$$

with an equivalent inverse transform

$$t_y = \int_{-\infty}^{+\infty} T_y \cos\rho z\ d\rho \qquad (8)$$

By dividing the body into n elements and using a variational principle, the finite element equations governing the deformation of an elastic soil may be set up as follows

$$K\Delta = F \qquad (9)$$

where Δ is the vector of transformed displacements, K is the stiffness matrix and F is the force vector, defined as follows

$$\Delta = (U_{x1}, U_{y1}, U_{z1}, U_{x2}, U_{y2}, U_{z2}, \ldots, U_{xn}, U_{yn}, U_{zn})^T \qquad (10)$$

$$\begin{aligned} K &= \int_A B^T D B dV \\ F &= \int_\Gamma N^T T dS \end{aligned} \qquad (11)$$

where N is the matrix of interpolation functions which depends on the particular element adopted; A is the area of interest in the $x - y$ plane; Γ is the length along the surface loaded by tractions. The matrix B is defined by

$$B = [B_1, B_2, B_3, \ldots, B_j, \ldots, B_n] \qquad (12)$$

where

$$B_j = \begin{bmatrix} \frac{\partial N_j}{\partial x} & 0 & 0 \\ 0 & \frac{\partial N_j}{\partial y} & 0 \\ 0 & 0 & \rho N_j \\ \frac{\partial N_j}{\partial y} & \frac{\partial N_j}{\partial x} & 0 \\ 0 & -\rho N_j & \frac{\partial N_j}{\partial y} \\ -\rho N_j & 0 & \frac{\partial N_j}{\partial x} \end{bmatrix} \qquad (13)$$

Solving Equation (9) yields the transformed displacements. The actual displacements can be obtained by using a numerical inversion. For example, the displacement in the y direction u_y would be given by

$$u_y = \int_{-\infty}^{+\infty} U_y \cos\rho z\ d\rho \qquad (14)$$

This integral may be evaluated numerically by the use of Gaussian quadrature as follows

$$u_y \approx \sum_{k=1}^{m} W_k U_y(\rho_k) \cos\rho_k z \qquad (15)$$

where W_k are the Gauss weights
ρ_k are the Gauss co-ordinates
m is the total number of Gauss points

This requires that the integral in Equation (14) be truncated with the limits of integration ranging from $-R$ to $+R$ instead of $-\infty$ to $+\infty$. The required accuracy of integration can be obtained provided that R is made large enough and enough Gauss points are used.

General Report – Mining, Tunnelling and Excavations

A.G. BENNET
Associate Director, Connell Wagner (Vic) Pty Ltd

1. INTRODUCTION

Given the Conference Theme - "Geotechnical Risk, Identification, Evaluation and Solutions" and the theme of Session 3, "Mining, Tunnelling and Excavations", the twelve papers provided for reporting present a broad spectrum of endeavour and create difficulties in delivering a coherent view. Some papers even bear little relation to the theme of the Session except having incorporated the term of geotechnical risk.

At such Conferences, we should question where our skills have developed in this region, particularly in the 4 years since the conference in Sydney in 1988.

The twelve papers generally can be grouped such that two address coal mine subsidence, albeit from different perspectives, whilst two papers consider stress measurement. A further two papers consider rock mass characterisation with one considering data collection, whilst the other addresses a reliability-based method in assessment of stability and support requirements in jointed rock excavations.

Three papers address aspects of coal mining, and in particular strength criteria, peripheral fractures on the side of roadways and advanced electronic monitoring techniques.

Only one paper addresses tunnel construction, and this is primarily from an historic viewpoint since the construction was nearly 40 years ago.

The two papers on deep excavation appear to be somewhat out of context with regard to the other ten papers of this session.

2. REVIEW OF PAPERS

The paper by Villaescusa addresses the problem of rock mass characterisation. Villaescusa addresses a very specialised subject which will no doubt be of interest to those working in this field. After describing conventional techniques of rock discontinuity data collection, Villaescusa proceeds to recommend a sampling method based on a line intersection criterion due to the considerable reduction in the number of discontinuities required for subsequent mathematical analysis.

Mapping of full traces is recommendedinstead of semi-trace length sampling because of the lognormal nature of trace length distributions.

Data collection and handling has advanced significantly since the 1960's when R D Terzaghi (1965) published a method of reducing orientation bias and as well as the work by Villaescusa at the University of Queensland, a significant development by CSIRO Division of Geomechanics is SIROJOINT, a system able to determine rock mass structure automatically. CSIRO claims the system enables vital data collection concerning the structural state of the rock mass to be determined in a rapid and cost effective manner.

As with Villaescusa, Brox has drawn upon research work conducted at Imperial College, and presents an interesting approach to a quite difficult problem in the design stage using a reliability-based prediction rather than a "rule of thumb".

Brox suggests the method is becoming increasingly accepted in geotechnical engineering, and develops the concept through the identification of potentially unstable blocks. The author then proceeds to quantify potentially unstable blocks and describes in limited detail the statistical and probabilistic evaluation of stability and support requirements. In order to develop support requirements in the concept stage of a project it is admirable to attempt to develop techniques with a rational basis rather than resort to "rules of thumb", which often have an undue degree of inherent conservatism. Nevertheless the statement of Section 3.1 of this paper that "no direct consideration is given to the influence of in situ stress or the cohesive and frictional components of strength along joint surfaces" surely incorporates an intangible degree of safety.

The case studies presented by Brox represent a quantitative assessment of the method and the predicted bolt lengths for the respective cases (in Table 1) of the paper correspond reasonably with the recommended/installed lengths. However, the predicted bolt spacings for the chamber and slope differ significantly from the recommended/applied spacing but the author does not elaborate on the reasons for this divergence. It would be useful if the author had provided a justification for the statement that the reliability-based approach may be more applicable for assessing rock support requirements for rock masses that are characterised with closely spaced jointing where there is a strong likelihood of instability.

It would also be useful if the method for selecting the recommended/installed bolt lengths and spacing had been described so that the relativity of approaches could be assessed.

In the design development stage of an underground project, the understanding of the stress field and the changes liable to be induced by excavation are now generally within our grasp. Enever et al present examples of recent stress and hydraulic jacking measurements carried out by CSIRO Division of Geomechanics in three Ausrtralian states for the design of pressure tunnels. The paper highlights the stress variability associated with structural and topographic features, and their impact on tunnel lining requirements for the prevention of leakage. The paper indicates empirical design criteria for depth of cover,

incorporating topographic effects have been used successfully for many years, and the authors state direct stress measurements are necessary for modern numerical analytical methods, but the key justification for the stress measurements and hydraulic jacking tests by borehole pumping is their direct applicability.

Citing three case studies (King River, Tasmania, Boomerang Creek, NSW and Tully Millstream, Queensland) the authors present a comparison of techniques adopted.

It is significant to note that the hydraulic fracturing performed for the Tully Millstream investigation represented the first civil engineering application of the Minifrac System developed by CSIRO for 38mm diameter holes.

In summing up, it is interesting to note that the authors concluded that since at all sites topography is a major feature, they suggested geological structure has an overriding influence on stress variability, compared to topographical effects.

In contrast to the inference derived from the paper by Brox concerning stresses, Enever et al, conclude that the mapping of structural discontinuities is essential and the orientations of joint and fracture planes should be considered in conjunction with the stress field orientations, since the stress components normal to the planes are the critical factor in assessing the risk of hydraulic jacking. They furthermore conclude that hydraulic pumping of individually isolated, orientated joints is the most direct test of jacking potential.

Another paper on stress measurement has been prepared by Brox et al and relates to the first stress measurements performed in Hong Kong. A significant proportion of the paper reiterates the background behind stress measurement in rock masses and develops the methodology applied (hydraulic fracturing). Brox et al have assumed that σ_3 is vertical and apparently took measurements in a vertical borehole. Whilst the topography of the area under consideration on Tsing Yi Island is not given, it is suggested that the full stress field could usefully be determined by the hollow inclusion cell provided rock conditions permit. This would obviate the need for assumptions regarding the minor or intermediate stress orientation.

Brox et al describe their testing programme at Tsing Yi Island and indicate test results for the pressure-time and flow rate - time data were typical for Tsing Yi data. As this test programme was a first in Hong Kong, the relevance of this statement is difficult to comprehend how the data could be typical.

Those with some knowledge of the Hong Kong granites can understand the statement that the absolute magnitude of in situ stresses is not of general concern in comparison to the strength of most rocks, the relative magnitude of the minimum principal horizontal stress compared to the overburden stress is of major concern in the evaluation of the stability of large span underground excavations.

Once the rock mass characterisation and stress field have been established, strength of the mass assumes importance. Vutukuri and Hossaini have prepared a detailed paper on the statistical assessment of strength criteria for intact coal. They have re-analysed data on coal strength tests published by Hobbs (1964) and Das and Sheorey (1986). Four strength criteria have been described, namely:

- Bieniawski
- Hoek and Brown
- Johnston
- Ramamurthy

and Vutukuri and Hossaini proceed to describe their regression analysis of the triaxial test data. They state that an estimate of the axial compressive stress at failure at any confining pressure can be made if only the uniaxial compressive strength of the intact coal is known.

It is interesting to note that Vutukuri and Hossaini believe the selection of appropriate software for non-linear regression analysis is crucial in the results obtained.

Following in the sequence developed are the papers on mining and underground works. Follington and Medhurst describe a monitoring system which appears to still be in its infancy and is still subject to further development. The concept appears to be excellent in that skilled resources are far more cost effective in being able to interpret data and be relieved of tedious data gathering, often in risk prone areas.

In another field of development, CSIRO Division of Geomechanics are attempting to develop a range of intrinsically safe instrumentation that is compatible and able to address the geotechnical parameters such as convergence and support loads which affect underground coal mine management. A virtue of the system will be the ability to utilise existing mine telephone systems and be able to span up to 2 km from underground telephones.

The adoption of such systems, however, may require attention to the education of management and workforces to realise their potential. Such systems will also need to be sufficiently proven in the field, otherwise their implementation could be retarded.

Bhattacharyya and Belleza have studied the depth and degree of fracturing at the sides of pillars and continuous ribs in roadways at two underground coal mines in New South Wales. The seismic refraction technique was adopted and the end result should lead to the optimum design of pillars based on a knowledge of the support capability of the peripheral fractured zone.

In summing up, Bhattacharyya and Belleza suggested that the differences between results derived by the refraction method were lower than those by the modified uphole method and the latter were estimates. As indicated by the authors, further work in this area is essential.

The authors also suggest that the depth of the fractured zones seems to indicate a relationship with the depth of the seam below the surface. Although this statement has some backing from the work of Wilson (1972) and Barron (1978), it is perhaps too bold a conclusion from limited data.

The paper by Gordon describes the problems which beset the construction of the Homer tunnel near Milford Sound, New Zealand. With the advances in knowledge and methods of stress measurement, the ramifications of rock bursting would now be anticipated. However given that construction proceeded between 1934 and 1953 it was fortuitous that the stress levels were such that catastrophic failures did not occur, because little option on a realignment of the route appeared possible. In the paper Gordon suggests the vertical stress field, given by the gravitational component γZ where γ = unit weight of rock and Z is the depth below surface, may have been a contributing cause, but topographic and denudation effects are probably of greater significance bearing in mind the rocks traversed.

The author also suggests that the stresses were residual, largely horizontal and once released attenuated with time. It is possible that once bursting occurred no further change in the stress field occurred. However this could only be clarified by absolute stress measurement and consideration of the rock mass strength relative to these stress levels.

Two papers relating to mine subsidence have been presented and the first by Stone et al considers centrifugal modelling for total and partial extraction in the Collie field in Western Australia. The model depth considered of approximately 60m cover over the seam is relatively shallow for longwall mining. These authors suggest that to date the prediction of mining induced subsidence has relied on the use of empirical models and little or no attempt has been made to formulate predictive models based on the physical responses of geomechanical materials - soil and rock.

The tests certainly represent an initial study of the applicability of centrifuge modelling to simulate coal extraction beneath relatively soft sedimentary rock. However it should be noted that this only applies to Australian practice and other large-scale physical models for both longwall and shoftwall mining have been tested at Bellambi, NSW by ACIRL from the early 1960's. Furthermore, centrifuge modelling of mining structures is by no means new, although material similitude has been a new area of endeavour.

The greatest contribution that centrifuge testing can make in improving the understanding of subsidence mechanisms is the ability to observe crack pattern development.

The observation that more abundant cracking occurred and extended over a larger area in the longwall model compared with the Wongawilli panel model appears to bear out a similarity to the prototype experience.

The paper by Farquhar and Douglas on the other hand is an interesting case study of the effects of subsidence of old workings on a community. After a thorough search of the limited records still available of 100 year old workings, the authors have assessed the subsidence hazard in a residential area. After adopting a risk assessment, as proposed by Cole (1987), the authors determined a number of properties to be at risk in varying degrees. The authors state that the nature of geotechnical engineering, and particularly the work dealing with abandoned mines and mining subsidence, is such that the amount of data required to allow a reliable statistical analysis of the problem is seldom available or obtainable.

In discussing their Table 1, the authors claim without any appareant justification that there was a greater risk of damage to property than destruction of property and a greater risk of injury than loss of life. Whilst both statements appear logical, the methodology should be developed rather than making subjective assessments.

The final two papers allocated for this session of the Conference relate to deep excavations. The former paper by Goh et al describes the back analysis of a deep excavation in soft clay. The particular case study was the Marina Bay Station on the Singapore MRT development which was constructed by a series of coffer dams followed by submerged excavation of the soil.

The back analysis by the finite element method showed reasonable agreement with field results for deflection. The method also enabled simulation of the effects of soil properties on wall behaviour whilst alternative construction techniques were also considered.

It would be of interest to readers of this paper to know the level of the water table which prompted the decision to flood the coffer dam in order to achieve base stability.

It is also interesting to note that Goh et al advanced their analyses over those presented at the Fifth ANZ Conference in 1988 for Newton Station on the MRT system in an endeavour to develop design guidelines for deep excavations in soft Singapore clays.

The paper by Ressi di Cervia describes the use of diaphragm walls to reduce risk in deep excavation. The paper describes the method in general terms only and does not address specific geotechnical issues nor are the references adequately presented.

3. GENERAL COMMENTS

As a general observation the importance of mining geotechnics has generally been given insufficient attention by way of the number or scope of papers submitted. The contribution of underground mining, particularly to the Australian economy, is very significant and the absence of relevant papers must surely prompt questions such as:

- is the Conference a relevant venue for presentation of such papers?
- is the mining industry lacking adequate geotechnical expertise?
- are practitioners too busy to publish?
- have there been no significant advances in the technologies available to us worth reporting?

Having posed these questions it is believed the following answers apply:

- Such Conferences are the ideal vehicle for such presentations, particularly when the Conference theme is Risk, and mining exploitation does encompass an element of risk.
- The second question must be answered in the negative as some very significant work has been performed in the key production areas.
- The third question is probably answered in the affirmative. To present a paper can be an onerous task, and furthermore in the competitive world in which we practise, any mining company obtaining the technical "edge" is loathe to relinquish it to competitors.
- The fourth question is definitely answered in the negative as we see the imminent introduction of the Mark 2 Robbins Mobile Miner at Pasminco, Broken Hill, and the advances in rock cutting with road headers in stronger, more abrasive rocks such as on the Sydney Harbour Tunnel land tunnels.

4. REFERENCES

Hobbs, D.W., (1964). The strength and stress-strain characteristics of coals in triaxial compression. J. Geol. Vol. 72, pp. 214-231.

Das, M.N. and Sheorey, P.R., (1986). Triaxial strength behaviour of some Indian Coals. J., Mines Metals and Fuels, March, pp. 118-122.

Terzaghi, R.D., (1965). Sources of error in joint surveys. Geotechnique, Vol.15, pp. 287-304.

Wilson, A.H., (1972). Research into the determination of pillar size, Part 1: A hypothesis concerning pillar stability, The Mining Engineer, June 1972, pp. 409-417.

Barron, K., (1978). An air injection technique for investigating the integrity of pillars, Inst. J. Rock Mech. Min. Sci & Geom. Abstracts, Vol.15, pp. 69-76.

Cole, K., (1987). Building over abandoned shallow mines: A strategy for the engineering decisions on treatment. Ground Engineering, Vol.20, No. 4, pp. 14-30.

Subsidence Due to Abandoned Mines: Risk, Evaluation and Mitigation

F.G. BELL
B.Sc., Ph.D., C.Eng., C.Geol., F.I.M.M., F.I.Min.E., F.G.S.
Professor of Engineering Geology, University of Natal, Durban, South Africa
B. MORTIMER
B.Sc., F.G.S.
Lecturer in Engineering Geology, University of Natal, Durban, South Africa

SUMMARY. Abandoned mine workings, especially those at shallow depth, because of their potential to cause ground subsidence, often represent significant problems in urban areas where development or redevelopment is to take place. In the United Kingdom information needed to locate potential hazards due to mine-workings is available but occurs in numerous scattered locations and considerable time and effort may be involved in its collection. In recent years thematic geological maps have been produced for certain coalfield areas where workings have long since closed. These can be used as an initial aid to hazard avoidance when such areas undergo redevelopment.

Nonetheless old workings should be located prior to the development of a site, and their layout and condition determined, wherever possible. This can be accomplished by a combination of indirect and direct methods of exploration. The site then can be zoned according to the degree of risk that the workings present. This may result in buildings not being permitted in those areas of maximum risk unless the ground is stabilized beforehand. Stabilization measures may involve occupying the workings with hydraulic fill or cheap bulk grouts. In areas of less risk special foundation structures may be used.

1. INTRODUCTION

In Britain coal mining began to be carried out on a significant scale in the thirteenth century. Drifts and adits into shallow workings were usually situated at the base of quarries and open pits or along the coal outcrops in hilly country. The workings extended as far as natural drainage and ventilation permitted.

By the fourteenth century outcrop workings had largely given way to bell pits. The shafts of bell pits rarely exceeded 12.2 m in depth and their diameter was usually around 1.3 m. Extraction was carried on around the shaft until such times as roof support became impossible, another shaft was then sunk nearby.

The pillar and stall method of extraction developed in the sixteenth century. Underground workings were shallow and not extensive. In very early mining the remnant pillars were rather haphazard in size and arrangement, but with time mining became more systematic and pillars of more or less uniform shape were formed by driving intersecting roadways in the seam. Also there was a general tendency for the size of stalls to increase.

Although mining has gone on in many coalfields in Britain for several centuries, the first statutory obligation to keep mine records only dates from 1850 and it was not until 1872 that the production and retention of mine plans became compulsory.

2. PILLAR AND STALL WORKINGS AND THEIR POTENTIAL FAILURE

In pillar and stall workings pillars sustain the redistributed weight of the overburden which means that they and the rocks immediately above and below are subjected to added compression. Stress concentrations tend to be located at the edges of pillars and the intervening roof beds tend to sag. Although the intrinsic strength of coal varies, the important factors in the case of pillars are that their ultimate behaviour is a function of seam thickness to pillar width, the depth below ground and the size of the extraction area since these control the load on pillars. If a pillar fails, then the mode of failure also involves the character of the roof and floor rocks. Pillars in the centre of the mined out area are subjected to greater stress than those at the periphery. Individual pillars in dipping seams tend to be less stable than those in horizontal seams since the overburden produces a shear force on the pillar. When a structure is to be built over an area of old pillared workings the additional load on the pillars can be estimated simply by adding the weight of the appropriate part of the structure to the weight of the column of strata supported by a given pillar. This method is very conservative except when used for large concentrated loads where old workings are located at shallow depth.

Collapse in one pillar can bring about collapse in others in a sort of chain reaction because increasing loads are placed on those remaining. Slow deterioration and failure of pillars may take place after mining operations have long since ceased, although observations at shallow depth and the resistance of coal to weathering suggests that this is relatively uncommon at depths less than 30 m. Attempts, based upon statistical analysis, have been made to try and predict the maximum time required for a pillar to fail after a mine has been abandoned (Van Besien and Rockaway, 1988). They have been unsuccessful. Old pillars at shallow depth have occasionally failed near faults and they may fail if they are subjected to the effects of subsequent longwall mining. If yielding occurs in a large number of pillars, then this can bring about a shallow broad subsidence over a large surface area. The ground surface tends to displace radially inwards towards the area of maximum subsidence, thereby generating tangential compressive strain, and circumferential tension fractures frequently are developed. Such movements often develop rather suddenly, the major initial movements lasting, in some instances, for about a week. The shape of the

profile can vary appreciably with mine layout and geological conditions. Maximum profile slopes and curvatures frequently increase with increasing subsidence.

Very often pillars were robbed on retreat. Extraction of pillars during the retreat phase simulates the longwall surface condition, although it can never be assumed that all pillars have been removed. At moderate depths pillars, particularly pillar remnants, are probably crushed and the goaf (i.e., the worked out area) compacted, but at shallow depths lower crushing pressures may mean the closure is variable. Furthermore artificial supports may have been used for the extraction of thicker seams. Some of the pillars shown on mine plans may have been removed and replaced with packs and timber stacks. The stability of such temporary structures defies analysis.

Prediction of subsidence as a result of pillar failure requires accurate data regarding the layout of the mine. Such information frequently does not exist in the case of abandoned mines. On the other hand when accurate mine plans are available, the tributary method outlined by Goodman et al (1980) may be used to evaluate collapse potential. The approach adopted by Goodman et al (1980) allows zones of minimum stability in abandoned pillar and stall workings to be located. The procedure may be summarized as follows:

(1) Plot pillar locations and dimensions.
(2) Determine pillar strength (S_p) for each pillar, having regard to the unconfined compressive strength (UCS) of the rock materials and the shape and size of the pillars. This is expressed by:

$$S_p = \frac{(UCS \times N\text{-}shape \times N\text{-}size)}{FS} \quad (1)$$

where FS is a factor of safety. The N-shape factor is influenced by the width (W) and the height (H) of the pillar:

N-shape = (0.875 + 0.250 W/H)

(3) The stress (σ) on each pillar then is calculated from:

$$\sigma = \frac{(P \times A_t)}{(A_p - A_w)} \quad (2)$$

where P is the initial vertical stress at the level of the roof of the opening, A_t is the area tributary to each pillar, A_p is the cross sectional area of the total pillar, and A_w is the area of pillar lost from load carrying by virtue of weathering, loosening or overbreak.

The ratio S_p/σ gives a factor of safety for each pillar and these values are plotted on the pillar plan. Pillars which have factors of safety of less than one are considered potentially unstable and are therefore removed from the plan. Their tributary areas are reassigned to adjacent pillars and the calculation repeated. In the second calculation more pillars may be found to have failed and they may be removed for further reiteration of the calculation, if so required. Although the method requires the exact shape of individual pillars to be known, as well as the mechanical properties of the coal and overlying rocks, it nonetheless offers an approach to recognizing where the most potentially unstable areas exist so that support works can be located optimally. Previously a review of the various methods of determining pillar strength and failure was provided by Bell (1978). In addition, a survey of underground excavation failure mechanisms was given by Hoek and Brown (1980).

Even if pillars are relatively stable the surface may be affected by void migration. This can take place within a few months of or a very long period of years after mining. Void migration develops when roof rock falls into the worked out areas. When this occurs the material involved in the fall bulks, which means that migration is eventually arrested, although the bulked material never completely fills the voids. Nevertheless, the process can, at shallow depth, continue upwards to the ground surface leading to the sudden appearance of a crown hole. The factors which influence whether or not void migration will take place include the width of the unsupported span; the height of the workings; the nature of the cover rocks, particularly their shear strength and the incidence and geometry of discontinuities; the thickness and dip of the seam; the depth of overburden; and the groundwater regime.

It is frequently maintained that the maximum height of void migration is directly proportional to the thickness of seam mined and inversely proportional to the change in volume of the collapsed material. It would appear that the height of collapse is independent of the width of the excavation although it is a limiting factor. In other words the larger the span, the more likely is collapse to occur. The maximum height of migration in exceptional cases might extend to 10 times the height of the original roadway, however, it generally is 3 to 5 times the roadway height. If a competent bed occurs in the roof rocks, which is thicker than 1.75 times the span width, it will arrest the collapse. Even so voids which occur just below the surface represent just as awkward a problem.

In a recent investigation Garrard and Taylor (1988) found that the majority of void collapse height interrelationships were explained by variations in either or both the width of the working and the type of roof rock. Old workings with roofs of interbedded strata were found generally to be wider and to have collapsed to higher levels than workings in which the roofs were formed of sandstones, siltstones or mudrocks. In addition the collapse structures in polylithological sequences had significantly greater collapse height to width ratios and steeper failure surface angles than monolithological sequences. It would appear that once voids start to migrate in interbedded rocks they reach higher levels because of the rapid change between competent and incompetent beds. This perhaps destroys the coherence of the rock unit and facilitates delamination, bed separation and fracture.

Most voids are bridged when the span decreases through corbelling to an acceptable width. Walton and Cobb (1984) mentioned that three times the width of the stall appeared to be an upper limit to the extent of most void migrations in abandoned coal mines whilst Garrard and Taylor (1988) suggested that the collapse height can be obtained by multiplying the width of the workings by 2.68. However, because of the difficulty of obtaining stall dimensions in abandoned workings, the height

of void migration normally is determined from the thickness of mineral extracted and the difference in densities between the roof material in situ and when collapsed.

Exceptions, of course, do occur and void migration in excess of 20 times the seam thickness concerned has been recorded. The self-choking process may not be fulfilled in dipping seams, particularly if they are affected by copious quantities of water which can redistribute the fallen material. This can lead to the formation of supervoids and their migration to rock head, then produces large scale subsidence at ground level (Carter, 1985).

3. INVESTIGATIONS IN SUBSIDENCE AREAS

A site investigation for an important structure(s) requires the exploration and sampling of all strata likely to be significantly affected by the structural loading (Bell, 1975). The location of subsurface voids due to mineral extraction is of prime importance in this context. In other words an attempt should be made to determine the number and depth of mined horizons, the extraction ratio, the pattern of the layout, and the condition of the old workings. The sequence and type of roof rocks may provide some clue as to whether void migration has taken place and if so, its possible extent. Of particular importance is the state of the old workings, careful note should be taken of whether they are open, partially collapsed or collapsed, and the degree of fracturing and bed separation in the roof rocks should be recorded, if possible. This helps to provide an assessment of past and future collapse which is obviously very important.

The desk study includes a survey of appropriate maps, documents, records and literature. The presence on geological maps of mineral deposits which could have been mined suggests the possibility of past mining unless there is evidence to the contrary, and geological and topographic maps may show evidence of past workings such as old shafts, adits and spoil heaps. All the geological and topographic maps of the area in question, going back to the first editions, should be examined. All the same, instability problems associated with abandoned mine workings cannot necessarily rely on old mine plans. Sometimes these are early working plans which do not reflect the state of the mine at abandonment. Added to which, old mine plans are often incomplete and inaccurate. Nevertheless, such records can provide useful information relating to the extent and method of mining.

The use of remote sensing imagery and aerial photography for the detection of surface features caused by subsidence is more or less restricted to rural areas. Colour photographs may be more useful than black and white ones in the detection of past workings since they can reveal subtle changes in vegetation related to subsidence and, if there are differences in thermal emission, then infra-red (false colour) photographs should show these differences.

The reconnaissance survey involves a walk-over visit of the site to allow familiarization. Subtle variations in the topography may be observed together with evidence of past land use. If sufficient information is gathered at this stage, it may be possible to pass straight into a field investigation involving direct exploration of the ground by drilling. If this is not the case, then indirect subsurface exploration using geophysical techniques, may be undertaken.

Considerable care should be exercised at the planning stage of a geophysical survey for the location of subsurface voids because of the variable nature of the target (Cripps et al 1988). The selection of the most appropriate technique necessitates consideration of four parameters, namely, penetration, resolution, signal to noise ratio and contrast in physical properties. The size and depth of the workings, and the character of any infill control the likelihood of the workings being detected as an anomaly. With the information obtained from the desk study and the reconnaissance survey, many of the available geophysical methods can be assessed at the selection stage, using a model study, and accepted or rejected, without any requirement for field trials. Generally it is possible to detect a cavity whose depth of burial is less than twice its effective diameter. Otherwise more sophisticated surface methods or drillhole methods have to be employed. However, since the presence of a void is likely to affect the physical properties and drainage pattern of the surrounding rock mass, this can give rise to a larger anomalous zone than that produced by the void alone.

The nature of the environment around a site affects the success of geophysical surveys. For instance, traffic vibrations adversely affect the results obtained from seismic surveys, as do power lines and electricity cables in the case of electromagnetic and magnetic techniques. Of particular importance is that there should be sufficient physical property contrast between the void and the surrounding rock mass so that an anomaly can be detected.

Seismic refraction has not been used particularly often in searching for voids created by previous mining at shallow depth since such voids are often too small to be detected by this method. This is because of attenuation of seismic waves in the rock mass (Anon, 1988).

Also except for workings with a depth of cover less than 5 m, it is unlikely that resistivity profiling would detect the presence of dry pillar and stall workings. On the other hand electrical resistivity depth sounding can be applied to the location of voids where the width to depth ratio is large. Mine workings which produce an air-filled layer can often be identified on the sounding curve as an increase in apparent resistivity.

Down to a depth of 30 m terrain conductivity surveys are more effective than resistivity traversing. Conductivity values can be contoured to indicate the presence of any anomalies. Penetration into the ground achieved by electromagnetic radiation can be limited by excessive attenuation in ground of high conductivity.

Generally speaking, voids in shallow abandoned mine workings are too small and located at depths too great to be detected by normal magnetic or gravity surveys. However, the fluxgate magnetic field gradiometer permits surveys of shallow depths to be carried out since it provides a continuous recording of lateral variations in the vertical gradient of the Earth's magnetic field rather than giving the total field strength. It tends to give better definition of shallow anomalies than the proton-magnetometer. On the other hand, a proton-magnetometer can more easily detect larger and deeper features, and yields results which are more suitable for contouring. Micro-gravity meters may be successful when the voids have a significant lateral extent.

Ground probing radar appears to be capable of

detecting small subsurface cavities directly and may prove one of the most promising methods for the future. The high frequency of the system provides high resolution and characteristic traces are produced by air filled voids. Depths to voids can be determined from the two way travel times of reflected events if velocity values can be assigned to the strata above the void. The conductivity of the ground imposes the greatest limitation on the use of radar probing in site investigation as depth to which radar energy can penetrate depends upon the effective conductivity of the strata being probed. This, in turn, is governed chiefly by the water content and its salinity, and is also a function of temperature and density as well as the frequency of the electromagnetic waves being propogated.

Drilling to prove the existence of old mine workings is frequently done by open holes, which allows relatively quick probe drilling (Bell, 1986). The drillhole should be taken to a depth where any voids present are not likely to influence the performance of the structures to be erected. If a grid pattern of drillholes is used some irregularity should be introduced to avoid holes coinciding with pillar positions. The sequence should be established by taking cores in at least three drillholes. The presence of old voids is indicated by the free-fall of the drill string and the loss of flush.

One of the principal objectives of investigations of abandoned mine workings is to determine their extent and condition. Accordingly core material needs to be obtained. Double barrel sampling tubes with inner plastic liners can be used to obtain core which then can be photographed and logged, and the rock quality designation (RQD) or fracture spacing index recorded. Drilling penetration rates, water flush returns and in situ permeability tests may be used to assess the degree of fracturing. The degree of fracturing is important in that it tends to increase as old workings are approached.

Detailed mapping of galleries is best made by driving a heading from the outcrop if this is close at hand or by sinking a shaft to the level of the coal seam to obtain access to the workings. Sometimes access has been gained via old shafts. Radial holes may be drilled from the shaft to establish the dimensions of the pillars and stalls.

Below surface workings may be examined by using drillhole cameras or closed circuit television, information being recorded photographically, or on videotape, and used to assess the geometry of voids and, possibly, the percentage extraction. However, their use in flooded old workings has not proved very satisfactory. Occasionally smoke tests or dyes have been used to aid the exploration of subsurface cavities.

Most of the geophysical methods have a down-the-hole counterpart which can be used to log a hole. Crosshole techniques can be used when the depth of burial of the void is more than two or three times the diameter of the void. In interdrillhole acoustic scanning an electric sparker, designed for use in a liquid filled drillhole, produces a highly repetitive pulse. This signal is received by a hydrophone array in an adjacent drillhole, similarly occupied by liquid (McCann et al, 1975). Drillholes must be spaced closely enough to achieve the required resolution of detail. The method can be used to detect subsurface cavities, if the cavity is directly in line between two drillholes and has at least one tenth of the drillhole separation as its smallest dimension. Air filled cavities are more readily detectable than those filled with water. Crosshole seismic testing has also been used, employing two or more drillholes, to detect near-vertical subsurface anomalies. Acoustic tomography techniques are now being developed to map voids between adjacent drillholes.

4. OLD MINE WORKINGS AND HAZARD ZONING

Assessments of mining hazards has usually been on a site basis regional assessments being much less common. Nonetheless regional assessments offer planners an overview of the problems involved. This should lead to the avoidance of planners imposing unnecessarily rigorous conditions in areas where they really are not warranted.

In recent years thematic maps have been produced in Britain of both urban and rural areas with a view to benefiting planners and civil engineers concerned with land use and ground stability. Early thematic maps produced by the British Geological Survey depicted areas of undermining assumed to be within 30 m of the surface on the one hand and at depths exceeding 30 m below the surface on the other (McMillan and Browne, 1988). This 30 m depth is the subject of interpretation and is based on limited information. It assumes that bulking factors of 10 to 20 per cent will affect the strata involved in void migration. However, "safe" depth rules are often broken. Known and suspected mining areas were not differentiated. Modifications were introduced for the map of the Glasgow district so that only areas of mining shown on mine plans were represented and no areas of suspected mining were shown. No attempt was made to infer the extent of working beyond the limits defined by mine plans other than to plot relevant drillhole data. The introduction of single and multiple seam working led to the requirement that areas of shallow working (less than 30 m below rockhead) should be identified in terms of seams worked. Separate maps were prepared illustrating areas of total known mining; current mining; known mining within 30 m of rockhead, together with the locations of shafts and drillholes encountering old shallow workings; and mining for minerals other than coal and ironstone. In Fife, known and inferred old shallow mining were differentiated on the same map. Each modification has reflected an attempt to clarify the presentation of known and inferred mining. An indication of the area in which mining might be expected can be obtained by plotting all drillholes which encounter colliery spoil outside areas of workings known from abandonment plans. In areas where coal outcrops are reasonably well known, areas of suspected workings can be mapped as a separate category, although it is then necessary to assume that all workable seams have been exploited, at least in the near surface area.

In an assessment of the degree of risk due to subsidence incidents associated with abandoned mine workings in South Wales carried out by Statham et al (1987), they found that of the 388 events 64 per cent occurred in open land and so posed no threat to person or property. Twenty one per cent had occurred when people were nearby or threatened property. The remainder caused damage to highways, buildings or other property and only one of these resulted in minor injuries. In the context of the South Wales coalfield this represents a low level of hazard. Assuming that a typical incident affects an area of 5 m^2, then the probability of collapse occurring on any 25 m^2 plot is of the order of 10^{-7} per year. Even if the number of subsidence incidents which have remained undiscovered increased the above total figure by a factor of 3, then the overall risk would still be low. Statham et al

(1987) found that over 90% of the incidents occurred within 100 m of the outcrop of the coal seam concerned. They produced a development advice map for South Wales which showed two zones inside the outcrops of worked seams corresponding to migration ratio (thickness of rock cover ÷ extracted thickness) values of 6 and 10, which were expected to contain 90 per cent and 100 per cent respectively of relevant subsidence incidents. The map makes a contribution towards regional planning by taking account of a possible development constraint at an early stage and offers an early warning on the likely scale of ground investigation required at specific sites. Attempts also have been made to zone ground underlain by old mine workings in terms of its suitability for different types of foundation (Gostelow and Browne, 1986).

However, it must be borne in mind that thematic maps which attempt to portray the degree of hazard represent generalized interpretations of the data available at the time of compilation. Therefore, they cannot be interpreted too literally and areas outlined as "undermined" should not automatically be subject to planning blight. Obviously there is a tendency to assume that the limits of old mine workings represented on a map indicate the full extent of the workings but it must be borne in mind that interpretation of their location is based on scanty information and includes assumptions, some of which may be unfounded. It should be recognized that engineering problems in areas of past mining only occur if buildings are not properly planned, designed and constructed with reference to the state of undermining. Also zoning based entirely upon depth of cover above workings cannot be relied on completely, since occasionally subsidences have occurred in zones labelled "safe".

5. MEASURES TO MITIGATE SUBSIDENCE EFFECTS

Where a site which is proposed for development is underlain by shallow old mine workings there are a number of ways in which the problem can be dealt with. The first and most obvious method is to locate the proposed structure on sound ground away from the old workings or over workings proved to be stable. It is not generally sufficient to locate immediately outside the area undermined as the area of influence should be considered. In such cases the angle of influence or draw is usually taken as 25°, in other words the area of influence is defined by projecting to the surface an angle of 25° to the vertical from the periphery and depth of the workings. Such location is, of course, not always possible.

If old mine workings are at very shallow depth, then it might be feasible, by means of bulk excavation, to found on the strata beneath. This is often an economic solution, particularly at depths of up to 7 m or on sloping sites.

Where the allowable bearing capacity of the foundation materials has been reduced by mining, it may be possible to use a raft. A raft can span weaker and more deformable zones in the foundation, thus spreading the weight of the structure well outside the limits of the building. However, rafts are expensive and therefore tend to be used where no alternative exists. For low-rise buildings, up to four storeys in height, it is occasionally possible to use an external reinforced ring beam with a central lightly reinforced raft as a practical and more economic foundation.

Reinforced bored pile foundations also have been resorted to. In such instances the piles bear on a competent stratum beneath the workings. They also should be sleeved so that concrete is not lost into voids, and to avoid the development of negative skin friction if overlying strata collapse. There may be a problem with lateral stability of piles passing through collapsed zones above mine workings or through large remnant voids.

Where old mine workings are believed to pose an unacceptable hazard to development and it is impracticable to use adequate measures in design or found below their level, then the ground itself can be treated. Such treatment involves filling the voids in order to prevent void migration and pillar collapse. In exceptional cases where, for example, the mine workings are readily accessible, barriers can be constructed underground and the workings filled hydraulically with sand or pneumatically with some suitable material. Hydraulic stowing also may take place from the surface via drillholes of sufficient diameter. Pneumatic or gravity stowing often is considered where large subsurface voids have to be filled.

Grouting is generally achieved by drilling holes from the surface into the mine workings, on a systematic basis, generally on a grid pattern, and filling the remnant voids with an appropriate grout. If it has been impossible to obtain accurate details of the layout and extent of the workings, then the zone beneath the intended structure can be subjected to consolidation grouting. The grouts used in these operations commonly consist of cement, fly ash and sand mixes, economy and bulk being their important features. If the workings are still more or less continuous, then there is a risk that grout will penetrate the bounds of the zone requiring treatment. In such instances dams can be built by placing pea gravel down large diameter drillholes around the periphery of the site. When the gravel mound has been formed it is grouted. The area within this barrier is then grouted. If the old workings contain water, then a gap should be left in the dam through which the water can drain as the grout is emplaced. Pea gravel also may be used as a bulk filler where a large amount of grout is required for treatment. Alternatively foam grouts can be used.

6. CONCLUSIONS

The pillar and stall method of mining was developed in the United Kingdom in the sixteenth century to work coal, the pillars being left in place to support the roof rocks. However, because there was no legal obligation to produce and deposit mine plans prior to 1872, the presence of many old mines and their layout remains unknown. This can present a problem when structures are to be erected above old abandoned mine workings since the ground may not be capable of carrying the load safely.

A number of subsidence problems can be associated with old pillared workings. These result from either failure and collapse of the pillars or from roof collapse above the stalls with gradual migration upward of voids.

Because of these problems an extensive investigation is called for when an area above suspected shallow old mine workings is to be developed. Such investigations involve searches through old records, where available. Geophysical methods frequently have been used in an attempt to determine the nature of old workings. Unfortunately, however, they have not always been successful. Direct investigation of old workings involves drilling into them. They can then be explored by borehole camera or closed

circuit television if conditions permit. Gaining access to old workings by sinking a shaft has occasionally been resorted to.

Once the nature and extent of old mine workings has been determined the ground above can be zoned in terms of the hazard they represent. Depth below ground surface has frequently been used as the basis of hazard zoning, 30 m below surface or rockhead often being taken as the boundary between safe and questionable ground. However, exceptions to this rule of thumb have occurred.

Special foundation structures such as rafts and piles have been used in areas of shallow abandoned workings. The use of the latter, however, has been questioned. Alternatively the ground can be treated, by filling the voids, usually by grouting with bulk or foam grouts.

REFERENCES

Anon. (1988). Engineering Geophysics: Report by the Geological Society Engineering Group Working Party. Quarterly Journal Engineering Geology, Vol. 21, pp 207-271.

Bell, F.G. (1975). Site investigations in Areas of Mining Subsidence. Newnes-Butterworths, London.

Bell, F.G. (1978). Subsidence due to mining operations. In: Foundation Engineering in Difficult Ground, Bell, F.G. (Ed.), Butterworths, London, pp 322-362.

Bell, F.G. (1986). Location of abandoned workings in coal seams. Bulletin of the International Association of Engineering Geology, No 30, pp 123-132.

Carter, P.G. (1985). Case histories which break the rules. In: Mineworkings '84, Proceedings of International Conference on Construction in Areas of Abandoned Mineworkings, Edinburgh, Forde, M.C., Topping, B.H.V. and Whittington, H.W. (Eds.), Engineering Technics Press, Edinburgh, pp 20-29.

Cripps, J.C., McCann, D.M., Culshaw, M.G. and Bell, F.G. (1988). The use of geophysical methods as an aid to the detection of abandoned shallow mine workings. In: Minescape '88, Proceedings of Symposium on Mineral Extraction, Utilisation and Surface Environment, Harrogate, Institution of Mining Engineers, Doncaster, pp 281-289.

Garrard, G.E.G. and Taylor, R.K. (1988). Collapse mechanisms of shallow coal mine workings from field measurements. In: Engineering Geology of Underground Movements, Engineering Geology Special Publication No 5, Bell, F.G., Culshaw, M.G., Cripps, J.C. and Lovell, M.A. (Eds.). The Geological Society, London, pp 181-192.

Goodman, R.E., Korbay, S. and Buchignani, A. (1980). Evaluation of collapse potential over abandoned room and pillar mines. Bulletin of the Association of Engineering Geologists, Vol 17, pp 27-37.

Gostelow, T.P. and Browne, M.A.E. (1988). Engineering Geology of the Upper Forth Estuary. Report of British Geological Survey, 16, 8p.

Hoek, E.L. and Brown, E.T. (1980). Underground Excavations in Rock. Institution of Mining and Metallurgy, London.

McCann, D.M., Grainger, P. and McCann, C. (1975). Interborehole acoustic measurements and their use in engineering geology. Geophysical Prospecting, Vol 23, pp 50-59.

McMillan, A.A. and Browne, M.A.E. (1987). The use and abuse of thematic information maps. In: Planning and Engineering Geology, Engineering Geology Special Publication No 4, Culshaw, M.G., Bell, F.G. and Cripps, J.C. (Eds.), The Geological Society, London, pp 237-246.

Statham, I., Golightly, C. and Treharne, G. (1987). The thematic mapping of the abandoned mining hazard - a pilot study for the South Wales Coalfield. In: Planning and Engineering Geology, Engineering Geology Special Publication No 4, Culshaw, M.G., Bell, F.G. and Cripps, J.C. (Eds.), The Geological Society, London, pp 255-268.

Van Besien, A.C. and Rockaway, J.D. (1988). Influence of overburden on subsidence development over room and pillar coal mines. In: Engineering Geology of Underground Movements, Engineering Geology Special Publication No. 5, Bell, F.G., Culshaw, M.G., Cripps, J.C. and Lovell, M.A. (Eds.), The Geological Society, London, pp 215-220.

Walton, G. and Cobb, A.E. (1984). Mining subsidence. In: Ground Movements and Their Effects on Structures, Attewell, P.B. and Taylor, R.K. (Eds.), Surrey University Press, London, pp 216-242.

Study of Peripheral Fractured Zones at the Sides of Roadways in Underground Coal Mines in New South Wales by Seismic Methods

A.K. BHATTACHARYYA
M.Sc., Ph.D., C.Eng., P.Eng., F.Aus.I.M.M., F.I.Mine.E.,
Senior Lecturer, University of New South Wales
G.B. BELLEZA
B.S.E.M., M.E.,
Senior Engineer, Bureau of Mines and Geosciences of Philippines

SUMMARY A study of the depth and degree of fracturing at the sides of pillars and continuous ribs in roadways was conducted at two underground coal mines in New South Wales, using the seismic refraction method and a modified form of the uphole method. The equipment basically included a sledge hammer (with a device attached to provide the origin times of the generated seismic impulses), 3-component borehole geophone assemblies and a 12-channel oscillographic recorder with the facility of enhancing signals by stacking their repetitions.

In the seismic refraction method, four geophone assemblies were installed within short horizontal boreholes at approximately mid-seam height and the travel of P-waves generated along the line of the spread were recorded.

The modified uphole method recorded the travels of P-waves generated near the mouth of a longer horizontal borehole to the successively different positions of a geophone assembly within that hole.

The depths of the fractured zones were determined by analysing the time-distance plots of the travels of the P-waves. The degree of fracturing within such a zone was considered to be indicated by the ratio of the determined P-wave velocity in the fractured zone and that in the (inner) intact zone or coal specimens in the laboratory.

The depths of the fractured zones determined from the refraction method were less than the corresponding ones from the uphole method, the latter being closer to the findings of other investigators.

1. INTRODUCTION

Compressive stress fields exist below the ground surface due to the weight of the overlying rock mass and sometimes, additional tectonic causes. When an excavation is made below ground, the existing stresses are redistributed, with concentrations developing in the rock material at the peripheries of the excavations. If the stress concentrations or 'abutments' exceed the rock strength, failure or fracturing of the material occurs and the abutments shift to intact rock farther from the excavation.

In underground mines, 'pillars' i.e. large unmined blocks of the mineral deposit are often left either temporarily or permanently, to support the rock mass surrounding the excavations. A logical approach to the optimum design of pillars would require a knowledge of the support capability of their peripheral fractured zones as well as, the more intact core inside. For this reason, studies of such fractured zones were conducted at a site each in two underground coal mines in New South Wales and are outlined here.

2. SEISMIC STUDY OF PERIPHERAL FRACTURED ZONES IN PILLARS AND CONTINUOUS RIB-SIDES

The study of fractured zones at each site, was conducted in a pillar and the continuous ribside forming the opposite sides of a roadway.

Seismic methods were used for the study, because they provided comparatively simple means of determining the depths of the fractured zones as well as, the degree of fracturing therein. The methods were based on the transmission of P-waves generated by impulsive blows from a sledge hammer. S-waves could also have been used, but for the difficulty in generating them.

2.1 Seismic Recording System

The seismic recording system used, consisted of the following:

i) A 6kg sledgehammer with a triggering device attached to the shaft, for generating the P-waves and providing their origin times;

ii) 4 of 3-component geophone assembles (each containing an orthogonal configuration of 1 vertical and 2 horizontal units of 7.5Hz natural frequency, 300ohms coil impedance and 0.635 critical damping) for installation in 37mm diameter horizontal boreholes using expansion-shell anchors;

iii) ES-1200 (Nimbus Instruments, U.S.A.) battery-operated 12-channel oscillographic recorder (modified for use in 'non-gassy places' in coal mines) with the facility of stacking the repetitions of signals for enhancement;

iv) 6-core screened cables for connecting the geophone assemblies to the recorder;

v) Hollow steel rods for installing a geophone assembly within a borehole at the proper depth and orientation and subsequent retrieval.

2.2 Sites of Investigations

The investigations were conducted at the West Cliff and Coal Cliff Collieries. Both the collieries belong to Kembla Coal and Coke Pty Limited, and are located in the Southern Coalfield of New South Wales and produce predominantly high quality coking coal from the Bulli seam.

At West Cliff Colliery, the Bulli seam is 2.5 - 3m thick and lies at depths of 450-480m. The roof of the seam is usually medium grained sandstone and the floor is strong shale.

The Bulli seam at Coal Cliff Colliery is 1.5-3.5m thick and lies at depths of 350-400m. Generally, the roof of the seam is a layer of mudstone overlain by medium grained sandstone and the floor is grey shale.

The work of the investigations at the sites was mostly carried out at the weekends, when the background seismic noise from the mining activities were less.

2.3 Study of Fractured Zones at West Cliff Colliery

The location of the study at West Cliff Colliery was at one of the intake roadways of the retreating longwall panel 1. The results of the study have been detailed elsewhere (Bhattacharyya and Belleza, 1986) and are only summarised in Tables I and II.

2.4 Study of Fractured Zones at Coal Cliff Colliery

The location of the study at Coal Cliff Colliery was a pillar and the continuous ribside opposite in the 3-heading development panel 281 shown in Figure 1.

2.4.1 Application of the seismic refraction method

The positions of the geophones at the mid-seam horizon are indicated a G1-G4 in Figure 2. The position of the seismic impulses generated along the appropriate lines of gephones are denoted by the numbers 1-13. Eight repetitions of the seismic signals generated from each of those positions were recorded with stacking. The recordings were transcribed on the photo-sensitive paper using different drive speeds. The seismograms were then developed by exposing to the light of a miner's cap lamp. Later, a protective spray was applied to the paper records.

2.4.1.1 Time-distance plots of the arrivals of seismic waves and determination of their velocities

Examination of the seismograms (ignoring cross-talk) from the four geophone assemblies indicated four different arrivals. The time-distance plots of those arrivals and the velocities determined from the appropriate lines of best fit shown in Figure 3 (as an example) suggested the following:

i) velocity V_1, related to the arrival of P-waves to a geophone by the direct path;

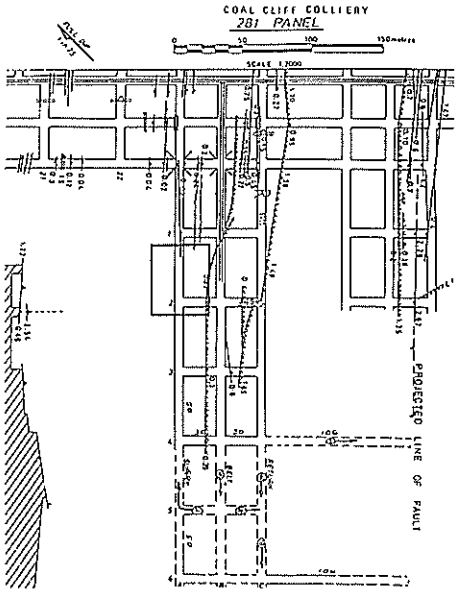

Figure 1 Part plan of the Coal Cliff Colliery showing the site of the study of peripheral fractured zones in roadways.

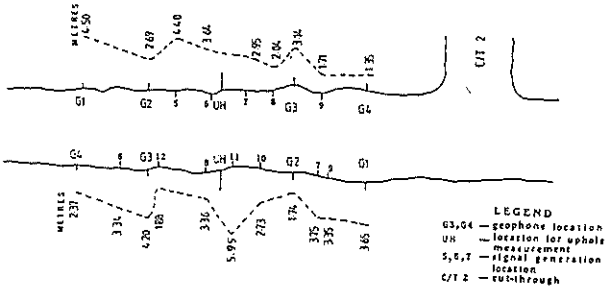

Figure 2 Positions of geophones and seismic impulses and computed mean depths of the peripheral fractured zones in the pillar and continuous rib opposite

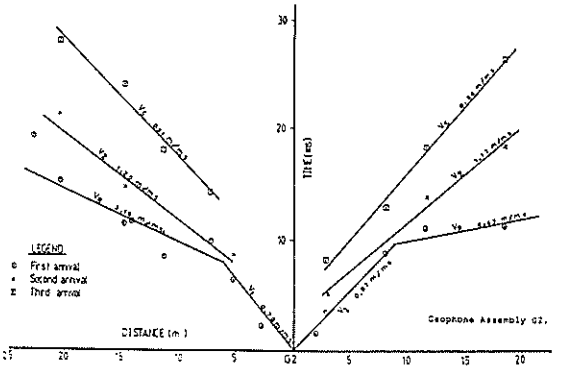

Figure 3 Time-distance plots of the arrivals of signals at geophone G2 in the continuous rib

ii) velocity V_2 related to the arrival of P-waves refracted along the interface between the fractured and the intact zones (and detected by the geophone oriented along the axis of the assembly);

iii) velocity V_R related to the arrival of P-waves refracted along the interface between the coal seam and the roof-floor;

iv) velocity V_S related to the travel of SH waves (which also originated from the hammer blows) refracted along the interface between the coal seam and the roof-floor.

The arithmetic means of the values of V_1 and the 'harmonic means' (Redpath, 1973) of the values of V_2 determined from the travels of the signals to the different geophones were used in the subsequent determinations of the depths of the fractured zones.

2.4.1.2 Determinations of the depths of fracture zones

The depth of the interface between the fractured and intact zones at a geophone position was determined by the 'intercept time' method (Redpath, 1973). The depth of the interface at a signal location was determined from the recordings of a signal by a pair of bracketing (i.e. enclosing) geophones using the 'delay time' method (Redpath, 1973).

The determined mean depths of the peripheral fractured zones in the pillar and the continuous ribside opposite are shown by the broken lines in Figure 2, and Table I.

2.4.2 Application of the modified uphole method

10m long horizontal boreholes denoted as UH in Figure 2, were drilled at the mid-seam height for the application of the uphole method. A geophone assembly was installed at successively decreasing depths within the borehole. At each depth, the seismic signal generated at a fixed position near the collar of the borehole was recorded by the geophone assembly with the stacking of eight repetitions. Seismograms of the recording was then obtained as described in section 2.4.1.

2.4.2.1 Time-distance plots of the arrivals of seismic waves and determination of their velocities

In this instance, the direct travel of the P-waves as detected by the geophone oriented along the axis of the assembly were of interest. The time-distance plots of such arrivals and the calculated velocities along the geometrically direct paths are shown in Figures 3 and 4.

2.4.2.2 Determination of the depths of fractured zones

The depths of the fractures zones along the employed particular boreholes were estimated by inspection of the determined velocities and are indicated by the dotted lines in Figures 4 and 5.

The likely sources of error in the method were: the assumption of homogeneous fractured and intact layers with constant seismic wave velocities and inadequate time resolution between close successive positions of the geophone assembly in a borehole.

TABLE I

DETERMINED DEPTHS OF PERIPHERAL FRACTURED ZONES IN ROADWAYS

Site of investigation				Seismic method used	Determined width of peripheral fractured zone (m)		Mean value of in situ velocity of P waves m/ms		Ratio V_2/V_1	Mean value of P wave velocity determined in the laboratory m/ms
Colliery	Seam	Height of mining (m)	Depth of cover (m)		Continuous ribside	Pillars	Fractured zone V_1	Intact zone V_2		
West Cliff	Bulli	2.5	450 to 480	Refraction method	4.15 ± 1.03	3.62 ± 1.01	0.86 ± 0.30	2.45 ± 0.85	2.85	1.29 ± 0.40
Coal Cliff	Bulli	2.5	350 to 400	Refraction method	3.30 ± 1.17	2.94 ± 1.12	0.85 ± 0.20	1.79 ± 0.42	2.11	
				Uphole method	6.00	4.75	1.43 ± 0.17			

2.4.1.3 Determination of the degree of fracturing

The degree of fracturing estimated by the ratios of V_2 and V_1 are shown in Table I. The likely sources of error in the method were: the assumption of homogeneous fractured and intact layers with constant seismic wave velocities, unevenness of the interface, inaccuracies in determining the plan geometry of the roadway and the proximity of the roof and floor strata of higher seismic velocities.

3. CONCLUSIONS

The results of the seismic study of the fractured zones in a pillar and the continuous ribside on the opposite sides of a roadway at the West Cliff and Coal Cliff Collieries are summarised in Tables I and II. As may be observed, the depths of the fractured zones determined by the refraction method were lower than those by the modified uphole method. The reason may partly be that the latter were just estimates as indicated in Figures 4 and 5. This aspect should be investigated further.

The depths of the fractured zones determined by the refraction method seem to indicate a relationship with the depth of the seam below the surface. This agrees with the suggestion of Wilson (1972), although the determined depths of fractured zones are lower then his as well as Barron's (1978) findings.

4. ACKNOWLEDGEMENTS

The authors express their sincerest thanks to the National Energy Research Development and Demonstration Council and Kembla Coal and Coke Pty Limited for enabling the described research to the conducted.

5. REFERENCES

1. Bhattacharyya, A.K. and Belleza, G.V. "A seismic study of peripheral fractured zones in coal pillars in an underground coal mine in New South Wales", Proceedings of the Australian Coal Science Conference, Newcastle, Vol. 1, 1986 pp 198-203.

2. Redpath, B.B. "Seismic refraction exploration for engineering site investigations". Technical Report E-73-4, U.S. Army Engineer Waterways Experiment Station Explosive Excavation Research Laboratory, Livermore, California, 1973.

3. Wilson, A.H., "Research into the determination of pillar size part 1: A hypothesis concerning pillar stability". The Mining Engineer, June, 1972, pp. 409-417.

4. Barron, K., "An air injection technique for investigating the integrity of pillars". Int. Jour. Rock Mech., Min. Sci. and Geomech. Abst., vol 15, 1978 pp. 69-76.

TABLE II

COMPARISON OF THE WIDTHS OF PERIPHERAL FRACTURED ZONES IN ROADWAYS DETERMINED BY SEISMIC METHODS WITH THOSE OF WILSON(1972) AND BARRON (1978)

Mine				Width of fracture zone (m)			
Name	Depth of cover (m)	Pillar width (m)	Pillar height (m)	Seismic Refraction Technique	Uphole method	According to Wilson (y=.0049 mh)	Barron's results (mean)
West Cliff Colliery	450-480	28	2.5	3.94± 1.03	-	5.51to 5.88	6.58± 2.63
Coal Cliff Colliery	350-400	25	2.5	3.14± 1.14	4.75to 6.00	4.29to 4.90	

A Reliability-Based Approach for the Assessment of Stability and Support Requirements in Jointed Rock Excavations

D.R. BROX
M.Sc., D.I.C., C.Eng., M.I.M.M.
Charles Haswell & Partners (Far East) Limited, Hong Kong

SUMMARY A reliability-based approach has been adopted for the assessment of stability and support requirements for three case study jointed rock excavations. The assessment of excavation stability has been based on the distributions of individual volumes of potentially unstable blocks surrounding each excavation. The assessment of support requirements has been based on the distributions of block depths and their occurrence per excavation advance. The dimensions and occurrence of potentially unstable blocks has been quantified by examining the interaction of excavation geometry with the rock mass structural patterns on 2D joint trace maps for selected section views through each rock mass. Joint trace maps have been generated using joint statistics and a simple rock mass structural model. By repetitively superimposing the respective excavation geometries on the corresponding joint trace maps it was possible to identify potentially unstable blocks according to simple geometric criteria and quantify their dimensions to construct distributions of block geometry. The probabilities of encountering individual block volumes per excavation advance have been represented on cumulative frequency distributions to provide reliability-based predictions of excavation instability. Confidence levels have been represented on cumulative frequency distributions for block depths to provide reliability-based predictions of support requirements in terms of required lengths of rock bolts to support potentially unstable blocks. Predicted rock bolt spacings have been calculated based on the number of potentially unstable blocks identified per excavation advance. A reasonably good correlation has been found to exist between the reliability-based predictions and actual and/or recommended support requirements for the three case study rock excavations that have been investigated. This approach is ideally suited for the feasibility and preliminary design stages of a project to provide estimates of support requirements for costing purposes.

1. INTRODUCTION

The assessment of stability and support requirements in jointed rock excavations is characterised with an inherent geotechnical risk due to the common variability associated with rock mass parameters and the limited information that can only be gathered during site investigations from which design decisions must be based. To deal with this inherent geotechnical risk engineers are more frequently adopting an approach that utilises stochastic methods within a probabilistic framework to recognise the uncertainty and variability associated with rock mass parameters.

This alternative and somewhat new approach has become to be known as the "reliability-based" approach and is becoming increasingly accepted in geotechnical engineering applications (Harr, 1987). By adopting a reliability-based approach the geotechnical risk can be quantified and design decisions can be made according to specified levels of certainty. The degree of conservatism associated with designs should also reduce by adopting a reliability-based approach.

Reliability-based approaches for design purposes in rock engineering have been commonly adopted for surface excavations but to a much lesser extent for underground excavations. Chan and Goodman (1983,1987) have expanded on Block Theory (Goodman and Shi, 1985) by considering joint statistics for joint spacing and continuity in order to predict support requirements. More recently, Esterhuizen and Fourie (1988) have considered the variability of joint orientation to assess the potential for wedge failure in a vertical shaft. Stacey (1989) has investigated the rockfall potential in mining stopes by considering the variability of joint spacing.

This paper presents a reliability-based approach for the assessment of stability and support requirements in jointed rock excavations. The importance of being able to predict the expected stability and support requirements prior to construction of a rock excavation is reflected upon consideration of the fundamental cost and safety aspects of a rock engineering project. Excavation stability is assessed in terms of potentially unstable block volumes and support requirements are assessed in terms of the numbers and depths of potentially unstable blocks. The distributions of both block depths and volumes are considered in the reliability-based approach (Figure 1).

The contents of this paper include a discussion on rock mass structural models in Section 3 with a description of the model used for examined case studies. Sections 4 and 5 provide brief explanations of both the statistical and probabilistic assessments of stability and support requirements. Section 6 presents limited results from assessments of three case study excavations and a discussion of these results is included in Section 7. Finally, concluding remarks on the overall limitations, applicability and further development potential of the reliability-based approach are presented.

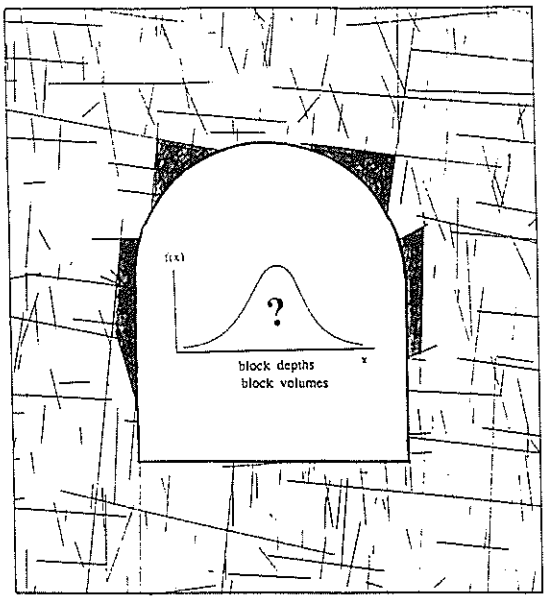

Figure 1 - Joint Trace Map and Potentially Unstable Blocks

2. ROCK MASS STRUCTURAL MODELS

2.1 Research to Date

The development of rock mass structural models was initiated for rock mechanics applications (Baecher et al.1977, Einstein and Baecher, 1983,) but more recent developments have concentrated for applications in the study of fracture flow (Dershowitz, 1984, Rouleau and Gale, 1987). The formulation of rock mass structural models has for the most part been based on the statistical characterisation of joint set parameters. Spatial interdependence between joint set parameters has been recognised through geostatistical models and the integration of these relationships has been identified as a further area for development.

Very few rock mass structural models developed to date have been utilized for assessing rock excavation stability and support requirements. Chan and Goodman (1983) developed a stochastic joint trace simulation model based on the principles of the Poisson Disk Model (Baecher et al.1977). The aim of the model was to assess support requirements in jointed rock excavations due to the presence of key blocks identified using Key Block Theory. Joint statistics for joint radii were considered however joint orientation was treated deterministically. Further refinement of this model by Chan (1984) defined measures of support requirements to characterise the number and dimension of key blocks considering the frictional properties of joints and the response of support systems.

Other rock mass structural models have been presented by McCullagh and Lang (1984) as well as Shi et al.(1985). As part of their continued research on the subject, Chan and Goodman (1987) developed a Monte Carlo procedure to be used in conjunction with the Poisson Disk Model for predicting the number and dimensions of key blocks. An investigation of the effects of excavation width, mean joint density and mean trace length on the measures of support requirements for the roof of a tunnel in a rock mass with three joint sets provided a theoretical verification of their procedure upon consideration of the results of the studies presented by McCullagh and Lang (1984).

2.2 A Simple Rock Mass Structural Model

2.2.1 Model Parameters

A simple rock mass structural model has been developed by Steffen, Robertson and Kirsten Consulting Engineers of Johannesburg, South Africa(Haines, 1983,1984). The model considers standard statistical descriptors of mean, maximum, minimum, standard deviation and a distributional form for joint dip, dip direction, dip continuity, strike continuity and spacing. The available distributional forms in the model for describing the joint set parameters are negative exponential, lognormal and normal. In general, the model simulates joints within a rock mass in three dimensions and generates two dimensional joint trace maps at selected views thereby requiring simplifying assumptions to be made on the three dimensional extent of joint bound blocks. The three dimensional form of the conceptual model is illustrated in Figure 2.

2.2.2 Generation of Rock Mass Structural Patterns

The generation process adopted in the simple rock mass structural model utilizes the Monte Carlo technique for sampling from the chosen distributional forms that represent the statistical nature of each of the joint set parameters. The first step in the generation process is the selection of the required orientation view or "slice" through the rock mass. Both joint trace map scale and plot size can be selected to conform to the purpose for which the joint trace map is intended.

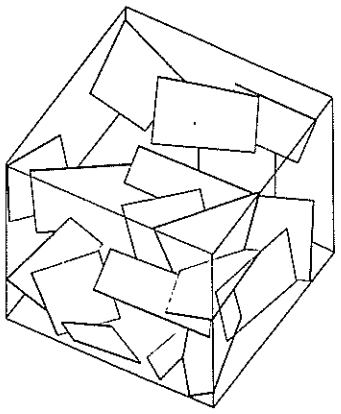

Figure 2 - 3D Conceptual Model

The generation process is based on the simulation of joints along one dimensional strips that are assembled into the 2D joint trace map for the selected view. The orientation at which the one dimensional strips are plotted are based on the mean projected orientation of each joint set for the selected view. The second step in the generation process is the calculation of the average trace length for each joint set as it would appear on the selected view. These values are determined from the distributions of apparent joint trace lengths which are automatically produced after consideration of the given ranges in the strike and dip lengths with respect to the orientation of the selected view. The direction of each plotting traverse is perpendicular to the average trace orientation of each joint set and the trace lengths plotted on the 2D map represent the external appearances of the joint planes as they would be intersected by an excavation surface. Figure 1 illustrates a complete joint trace map generated by the simple rock mass structural model with four joint sets.

3. STATISTICAL EVALUATION OF STABILITY AND SUPPORT REQUIREMENTS

3.1 Identification of Potentially Unstable Blocks

The identification of potentially unstable blocks from selected joint trace maps (Figure 1) requires the definition of representative geometric criteria. This simplified 2D approach assumes that identified potentially unstable blocks from joint trace maps are 3D joint bound blocks that will move into the excavation if not supported. In addition, no direct consideration is given to the influence of in situ stress or the cohesive or frictional components of strength along joint surfaces.

The definition of geometric criteria for the identification of potentially unstable blocks has been based on considering three different block type configurations. The three configurations have been considered irrespectively of the orientation of the excavation surfaces of interest and comprise triangular, rectangular and trapezoidal shaped blocks.

The variation in the geometry of individual blocks is inherent in the formation of potentially unstable blocks due to the interaction between the rock mass structural patterns and the excavation geometry in three dimensions. As part of the simplified 2D approach for the assessment of excavation stability and support requirements an attempt has been made to take into account of the possible variation in the geometry of individual blocks by considering the relative volumes of a unit rectangular block. From the recognition of the variable block shapes of elongate triangular wedges, rectangular blocks and irregular saw-toothed shaped polygons the volumes of blocks may be considered to vary significantly from 1/3 to the total volume of a unit rectangular block.

3.2 Quantification of Potentially Unstable Blocks

The quantification of potentially unstable blocks is conducted on a statistical basis to produce distributions for block depths, block areas and individual block volumes. Repetitive procedures including the random superimposition of excavation geometry on the joint trace map, the identification of potentially unstable blocks, the measurement and tabulation of the geometry of the blocks as well as their occurrence are required before the statistical nature of block geometry is characterized with the construction of standard histograms.

The choice and number of joint trace maps that are selected are a function of the excavation geometry but generally cross, longitudinal and plan sections are adequate. The measurement of block depths is conducted on vertical cross sections and block depth is defined as the maximum distance measured at an angle approximately perpendicular to the excavation profile. In most cases the maximum distance corresponds to the apex position of the joint bound block. Block area is measured on longitudinal and plan sections and is defined as the area completely bounded by joint traces.

The occurrence of potentially unstable blocks is characterized by the number of joint bound blocks identified in the longitudinal or plan sections. The number of blocks is further defined in relation to an excavation advance dimension such as a bench height for a chamber excavation or a blast advance round for a tunnel. The excavation advance dimension therefore defines an area on the respective selected sections for the identification of potentially unstable blocks.

The quantification of potentially unstable block volumes is based on the consideration of the histograms constructed for block depths, block areas and the block volume factor. The distribution of individual block volumes is constructed by calculating the mathematical products of the sampling of the histograms for block depths, block areas and the block volume factor. The block volume factor varies between 1/3 and unity and is considered to include the possible variation in block geometry. A diagrammatic representation of the construction of the distribution of individual potentially unstable block volumes is illustrated in Figure 3. A similar procedure is used to derive a distribution for total block volumes based on the distributions for individual block volumes and the number of potentially unstable blocks.

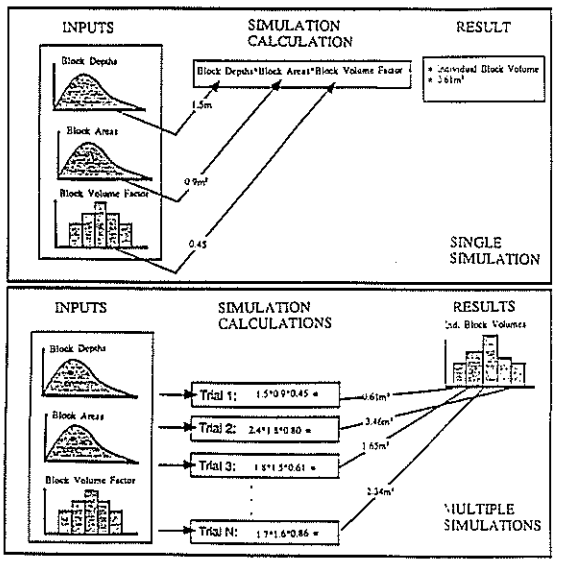

Figure 3 - Construction of Block Volume Distribution

The number of simulation calculations required using the Monte Carlo sampling technique to reasonably estimate the maximum individual potentially unstable block volume has been investigated and to be within a 20% error a total of N=5000 simulations were found to be required. The maximum individual potentially unstable block volume is of concern when it is required to specify the capacity of the rock bolts to be installed.

4. PROBABILISTIC EVALUATION OF STABILITY AND SUPPORT REQUIREMENTS

4.1 Describing Probability and Confidence Levels

The reliability-based approach to the assessment of excavation stability and support requirements is based on the characterization of the various statistical distributions describing block geometry in probabilistic terms. This characterization requires the construction of the relative cumulative frequency distributions for individual block volumes and block depths. The construction of a relative cumulative frequency distribution is a straight forward exercise from knowledge of the relative frequency histogram. From the relative cumulative frequency distribution it is also easy to determine the probabilities that a random variable will take a value less than or equal to a selected numerical value or a range of values In the context of evaluating excavation stability in terms of individual potentially unstable block volumes and support requirements in terms of block depths it is of concern to examine critical values that are not to be exceeded within a specified degree of certainty. In several engineering applications it is statistical confidence levels that can be considered for characterizing the degree of certainty in probabilistic terms.

4.2 Reliability-Based Predictions of Instability

The probabilistic assessment of excavation instability involves the consideration of the relative cumulative frequency distribution for individual block volumes. The shape of the cumulative frequency distribution for individual block volumes is a function of the respective relative frequency histogram which in turn is an unknown function of the distributional forms for block depths, block areas and the block volume factor. It has been found that if one of the distributions for block depths, block areas or block volume factor is negative exponential, then the distributional form for individual block volumes is also likely to be of this form.

The method of presenting a quantitative assessment of excavation stability is based on the examination of the probabilities of encountering potentially unstable volumes of rock as joint bound blocks. The percentage probability of encountering a particular potentially unstable volume is equal to the difference of the selected critical relative cumulative frequency percentage from 100%. The selection of critical relative cumulative frequency percentage values is somewhat arbitrary however for most engineering applications it has ben common to examine values of the random variable of interest corresponding to the 95% and 99% probabilities.

4.3 Reliability-Based Predictions of Support Requirements

The probabilistic assessment of excavation instability involves the consideration of the relative cumulative frequency distributions for block depths and block numbers. Support requirements are based solely on rock bolts with specified lengths and spacings for restraining potentially unstable blocks. The require rock bolt length is defined as being equal to the maximum block depth plus a nominal length for anchoring into solid rock behind the potentially unstable block.

The probabilistic assessment of rock bolt lengths is based on selected probabilities from the relative cumulative frequency distribution for block depths with consideration for a specified nominal anchor length. Consideration of the nominal anchor length and an overall practical rock bolt length can be accommodated and represented as an upper bound curve superimposed on the relative cumulative frequency distribution for block depths.

The probabilistic assessment of rock bolt spacings is based on selected critical probabilities from the relative cumulative frequency distribution for the number of potentially unstable blocks in relation to a specified excavation advance dimension. The selected probabilities will correspond to a particular number of potentially unstable blocks that are then addressed in relation to the exposed surface area of the excavation that is a result of the excavation advance dimension.

Rock bolt spacings are based only on square patterns and are calculated by dividing the number of potentially unstable blocks at the selected critical probability level into the surface area of excavation and then taking the square root of the resultant quotient. This spacing value can then be adjusted accordingly to a practical value. The procedure for determining rock bolt spacings assumes that only a single rock bolt is required to support a single potentially unstable block and this assumption can be verified by considering the distribution of individual block volumes.

5. CASE STUDY ROCK EXCAVATIONS

5.1 General

In order to investigate the applicability of the reliability-based approach for the assessment of stability and support requirements three case study rock excavations have been examined. The three case study rock excavations comprise a short and relatively small size tunnel, a medium size underground chamber and a small rock slope cutting. A complete reliability-based assessment of excavation stability and support requirements for each of the three case study rock excavations is beyond the presentation limitations of this paper. As such, representative aspects of each of the overall assessments for each excavation have therefore been chosen and are presented.

5.2 Rock Tunnel

The small size tunnel is situated in dolomitic rock characterized with four prominent joint sets. Joint trace maps corresponding to the cross, longitudinal and plan sections of the tunnel were generated to identify potentially unstable blocks. A distinction was made to identify block depths from both the crown and sidewall zones of the tunnel cross section. Graphical representations of crown and sidewall block depths, block areas and block numbers as histograms were constructed in order to generate a distribution for individual block volumes per 3m excavation advance.

For this case study excavation the distribution of crown block depths is presented in Figure 4 and shows that crown block depths vary between 0.3m and 5.4m with a mean block depth of 1.1m. The corresponding cumulative frequency distribution for both crown and sidewall block depths is illustrated in Figure 5. Block depths at 75%, 90%, 95% and 99% confidence levels are highlighted and reflect the significantly greater block depths for the sidewall zone as compared to the crown zone of the tunnel excavation. The length of rock bolts required corresponding to the highlighted confidence levels and including a 300mm anchor length are 1.7m, 2.3m, 2.9m and 4.2m for the crown zone and are 2.8m, 3.5m, 4.2m and 4.7m for the sidewall zone respectively.

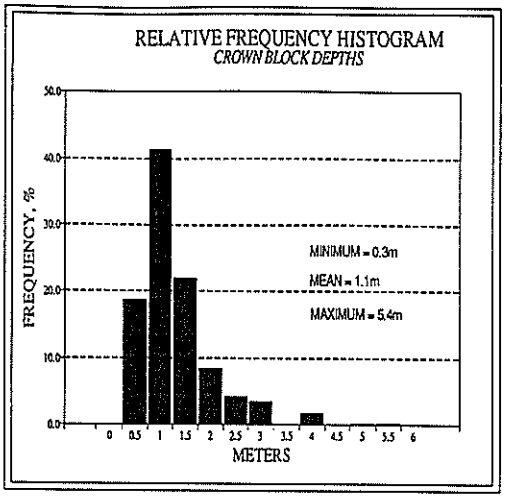

Figure 4 - Frequency Histogram for Crown Block Depths

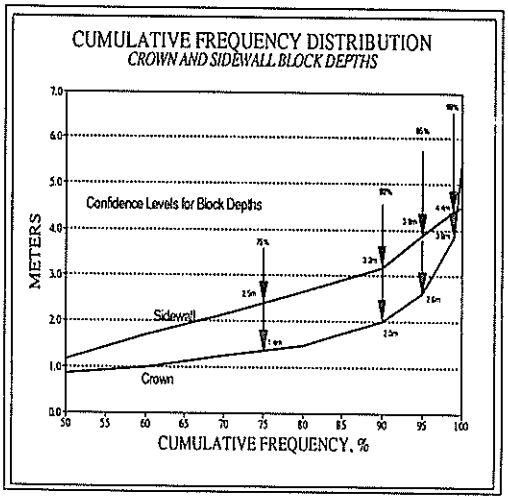

Figure 5 - CFD for Crown Block Depths

5.3 Underground Chamber

The medium size underground chamber is situated in an igneous complex of carbonatite rocks characterized with four prominent joint sets. Joint trace maps corresponding to the four walls and the plan section of the chamber were generated to identify potentially unstable blocks. Graphical representations of wall block depths, block areas and block numbers as histograms were constructed in order to generate a distribution for individual block volumes for each of the four walls per 2.5m bench excavation lift and for the roof zone per 3m excavation advance.

For this case study excavation the distribution of individual block volumes for the northeast wall is presented in Figure 6 and shows that the mean and maximum individual block volumes are 1.7m^3 and 7.3m^3 respectively. The corresponding cumulative frequency distribution for the individual block volumes of all four of the chamber walls is illustrated in Figure 7. The 25%, 10%, 5% and 1% probabilities of encountering potentially unstable block volumes per excavation advance are highlighted and reflect the significantly greater block volumes for the crown zone as compared to the four walls of the chamber excavation. At the highlighted probabilities of occurrence the individual block volumes for the crown zone correspond to 2.3m^3, 3.6m^3, 4.6m^3 and 6.8m^3 respectively. Similar cumulative frequency distributions however do exist for the four walls of the chamber excavation.

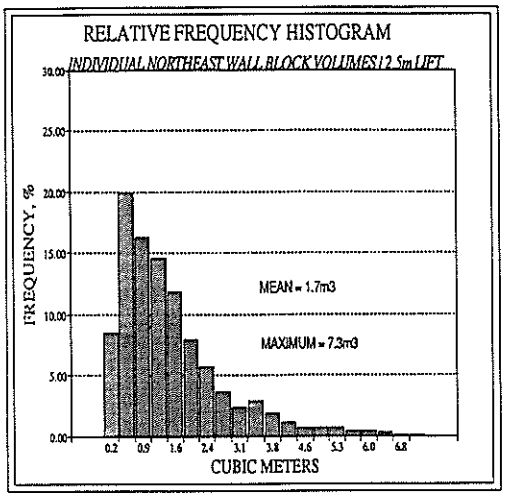

Figure 6 - Frequency Histogram for Block Volumes

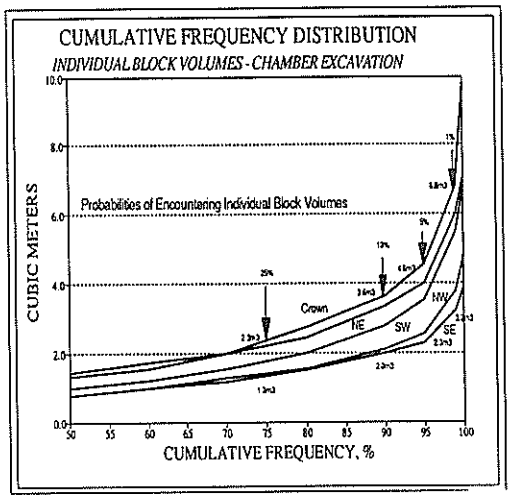

Figure 7 - CFD for Individual Block Volumes

5.4 Rock Slope

The small rock slope cutting is situated within an alternating bedded formation of quartzites and conglomerates characterized with five prominent joint sets. Joint trace maps corresponding to the cross, longitudinal and plan sections of the rock slope cutting were generated to identify potentially unstable blocks. A comparison was made to identify block depths from both 40 degree and 60 degree slope angles. Graphical representations of slope face block depths, exposed slope face block lengths,slope face block area and slope face block numbers as histograms were constructed in order to generate a distribution for individual block volumes per 20m excavation slope length.

For this case study excavation the distribution of slope face block depths for the 60 degree slope angle is presented in Figure 8 and shows that slope face block depths vary between 0.3m and 5.2m with a mean block depth of 2.0m. The corresponding cumulative frequency distribution for slope face block depths for both the 60 degree and 40 degree slope cuttings is illustrated in Figure 9. Slope face block depths at 75%, 90%, 95% and 99% confidence levels are highlighted and reflect the significantly greater slope face block depths for the 60 degree slope as compared to the 40 degree slope cutting. The length of rock bolts required corresponding to the highlighted confidence levels and including a 300mm anchor length are 2.9m, 3.9m, 4.5m and 5.3m for the 60 degree slope cutting and are 2.4m, 3.2m, 4.1m and 4.7m for the 40 degree slope cutting respectively.

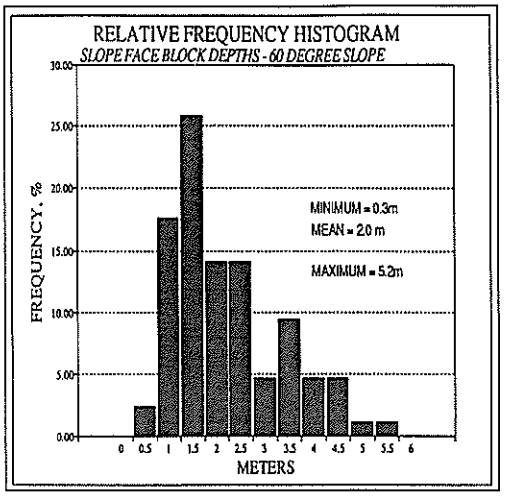

Figure 8 - Frequency Histogram for Slope Block Depths

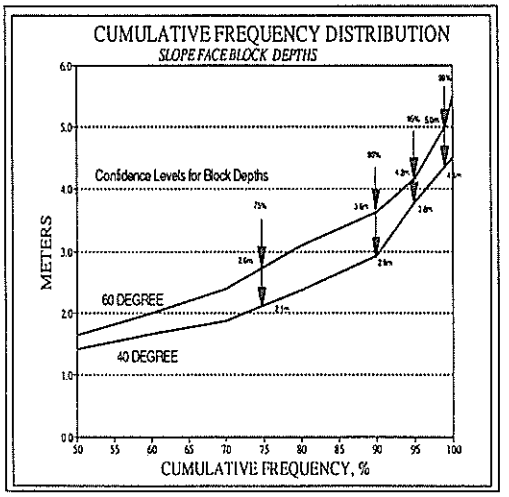

Figure 9 - CFD for Slope Block Depths

6. DISCUSSION

6.1 Reliability-Based Predictions

The reliability-based predictions for excavation stability that are represented by the relative frequency histograms and cumulative frequency distributions for individual block volumes are plausible upon consideration of the distributions for joint spacing of the joint sets for each of the case study rock excavations. As the mean joint spacings of the joint sets increased from that for the tunnel excavation to that for the rock slope cutting, so has the mean individual block volume as would be expected.

The reliability-based predictions for excavation support requirements that are represented by the relative frequency histograms and cumulative frequency distributions for block depths are also plausible upon consideration of the distributions for joint spacing for the joint sets of each of the case study rock excavations. The relatively smaller spacings of the sub-vertical joint sets corresponding to the tunnel excavation have been shown to yield overall shorter block depths for the crown section in comparison to the wider spacings of the joint sets corresponding to the chamber excavation that have yielded greater block depths for the crown section. Thus, as would be expected, wider joint spacings of sub-vertical joint sets have produced greater block depths along a horizontal excavation surface. Furthermore, the spacing of bedding structure present within a rock mass can be considered to significantly

Table I - Comparison of Predicted/Practical and Recommended/Installed Rock Bolt Lengths

	Rock Tunnel		Underground Chamber		Rock Slope	
	Crown	Sidewall	Crown	Walls	40 degrees	60 degrees
Predicted (95%)	2.9m	4.2m	2.7-3.2m	4.4m	4.1m	4.5m
Recommended/Installed	3.0m	3.0m	4.0m	3.0m	4.0m	4.0m

Table II - Comparison of Predicted/Practical and Recommended/Applied Rock Bolt Spacings

	Rock Tunnel		Underground Chamber		Rock Slope	
	Crown	Sidewall	Crown	Walls	40 degrees	60 degrees
Predicted (95%)	2.5m	2.0m	6.0m	6.5m	8.0m	6.5m
Recommended/Applied	1.5m	1.5m	1.5m	1.0m	2.5m*	2.5m*

influence the depths of potentially unstable blocks in the sidewall of an excavation. The relatively similar spacings of bedding structure for the tunnel excavation and the rock slope cutting have not surprisingly yielded similar distributions for block depths for the respective sidewall and slope face sections.

6.2 Comparison of Reliability-Based Predictions and In Situ Observations

Comparisons of the reliability-based predictions for support requirements in terms of both rock bolt lengths and spacings are made with actual and/or recommended support requirements for each of the case study rock excavations and a summary of this information is presented in Table I and II. The recommended support requirements have been generally based on consideration of rock mass classifications and rock engineering industry standards.

The predicted rock bolt lengths at the 95% confidence level are in reasonable agreement with the recommended /installed rock bolt lengths for all three case study rock excavations. The recommended rock bolt lengths for the sidewall of the tunnel and the walls of the chamber excavation correspond to rock bolt lengths at lower confidence levels as may be justified in terms of overall safety. It is noted that no major instabilities resulted in any of the case study rock excavations with the installation of the prescribed rock reinforcement.

The predicted rock bolt spacings at the 95% confidence level are in good agreement for the tunnel excavation. The rock bolt spacings at the same confidence level for the chamber excavation and the rock slope cutting correspond to spot bolting requirements in the practical sense and are not in agreement with the recommended or installed rock bolt spacings.

7. CONCLUSIONS

The good agreement seen upon the comparison of reliability-based predictions of rock bolt lengths with recommended/installed lengths for three case study rock excavations reflects the applicability of this approach, in particular for the preliminary design stage of a rock engineering project. In addition, on the basis of the assessment for the three case study rock excavations it is concluded that this approach may be more applicable for assessing rock support requirements for rock masses that are characterized with closely spacing jointing where there is a strong likelihood of instability.

The reliability-based approach has recently been adopted for the assessment of preliminary rock support requirements for a twin arrangement of 17 metre span tunnels to be sited in closely jointed granitic rock in Hong Kong.

8. ACKNOWLEDGEMENT

This paper is a summary re-draft of the MSc Dissertation completed by the Author for the Rock Engineering Group, Department of Mineral Resources Engineering, Royal School of Mines, Imperial College, London.

9. REFERENCES AND BIBLIOGRAPHY

BAECHER, G.B., LANNEY, N.A., and EINSTEIN, H.H. (1977). Statistical Description of Rock Properties and Sampling, Proc. 18th U.S. Symp. Rock Mech. Golden, CO. pp. 5CI-8.

CHAN, L.Y., and GOODMAN, R.E. (1983). Prediction of Support Requirements for Hard Rock Excavations Using Keyblock Theory and Joint Statistics, Proc. 24th U.S. Symp. Rock Mech. AEG and Texas A&M, College Station, TX. pp. 557-576.

CHAN, L. Y. (1984). Estimating Support Requirements from Simulation of Key Blocks, Proc. 25th U.S. Symp. Rock Mech., Northwestern University, Evanston, IL, pp. 857-864.

CHAN, L.Y., and GOODMAN, R.E. (1987). Predicting the Number of Dimensions of Key Blocks of an Excavation using Block Theory and Joint Statistics, Proc. 28th U.S. Symp. Rock Mech., Tucson.

DERSHOWITZ, W.S. (1984). Rock Joint Systems, PhD Thesis MIT.764pp.

EINSTEIN, H.H. and BAECHER, G.B. (1983). Probabilistic & Statistical Methods in Engineering Geology: Specific Methods & Examples, Part I: Exploration. Rock Mech. & Rock Eng. Vol. 16, pp. 39-72.

ESTERHUIZEN, G.S., and FOURIE, B.J. (1988). Reliability Based Analysis of Wedge Failure in a Vertical Shaft, Proc. 1st Reg. Conf. for Africa: Rock Mech. in Africa, South African National Group on Rock Mechanics.

GOODMAN, R.E., and SHI, G.(1985). Block Theory and its Application to Rock Engineering, Prentice-Hall, 338

HAINES, A. (1983). The Quantitative Assessment of Potential Tunnel Instability by Extrapolation of Rock Mass Discontinuity Mapping. Proc. Symp. Rock Mech. in the Design of Tunnels, SANGORM pp.1-5.

HAINES, A. (1984). The Application of Generated Rock Mass Discontinuity Patterns. Proc. 8th Reg. Conf. Africa Soil Mech & Found. Eng., Harare, pp. 13-21.

HARR, M.E. (1987). Reliability-Based Design in Civil Engineering, McGraw-Hill, 290pp.

McCULLAGH, P., and LANG, P. (1984). Stochastic Models for Rock Instability in Tunnels, J. Royal Statistical Society, Series B, Vol. 46, No. 2, pp.344-352.

ROULEAU, A., and GALE, J.E. (1985). Statistical Characterization of the Fracture System in the Stripa Granite, Sweden, Int. J. Rock Mech. & Min. Sci., Vol. 22, No. 6, pp. 353-367.

SHI, G., GOODMAN, R.E., and TINUCCI, J.P. (1985). Application of Block Theory to Simulated Joint Trace Maps, Proc. Symp. Fundamentals of Rock Joints, Sweden, Ed. Stephenson.

STACEY, T.R. (1989). Potential Rockfalls in Conventionally Supported Stopes - A Simple Probabilistic Approach, South African Inst. Min. Met., Vol.89, No. 4, pp. 111-115.

In Situ Stress Measurements Using Hydraulic Fracturing in Jointed Rock in Hong Kong

D.R. BROX
M.Sc., D.I.C., C.Eng., M.I.M.M.
Charles Haswell & Partners (Far East) Limited, Hong Kong
Dr. Ing. H. KONIETZKY
MeSy GmbH., Bochum, Federal Republic of Germany
Prof. Dr. Ing. F. RUMMEL
MeSy GmbH, Bochum, Federal Republic of Germany

SUMMARY In situ stress measurements using the hydraulic fracturing technique have been conducted in Hong Kong during the preliminary design site investigation for the Cheung Ching Tunnel as part of the Route 3 Project. Measurements were conducted in shallow boreholes completed along the eastern low rock cover section of the proposed tunnel alignment on Tsing Yi Island. The magnitude and orientation of the minimum principal horizontal stress was of concern along this critical section of tunnel where rock cover varies between 16 and 30 metres above crown level. Information concerning the in situ state of stress was significant for the evaluation of the stability of the 1.5 km long, twin arrangement of unprecedented 17 metre span tunnels. Rock mass conditions along this section of the proposed tunnel alignment are characterised with closely spaced jointing and slightly to moderately weathered granitic rock. Near consistent minimum principal horizontal stresses were measured slightly in excess of overburden stress. Results from numerical modelling of the variable topography indicate a generally good agreement with the measured stresses.

1. Introduction

The increasing number of planned underground projects in Hong Kong has led to the requirement of investigating the in situ state of stress. Engineers involved with the design and construction of underground excavations must accept that the geologic medium in which an excavation is to be sited is subjected to an unknown pre-existing stress field. Unlike the design of structures on surface where the applied stresses are known with certainty and the behaviour of the structure can be accurately predicted, the unknown pre-existing stresses must be measured if the behaviour of an excavation is to be predicted for the assessment of stability.

The purpose of conducting in situ stress measurements in Hong Kong is to define the magnitude and direction of the in situ stress field such that this information can be considered for the overall evaluation of the stability of underground excavations. This information is of particular importance when large span underground excavations are considered and the mean joint spacings are small such that the ratio of excavation span to mean joint spacing is large. Information concerning the in situ state of stress will also provide valuable research related data for the overall seismic evaluation of Hong Kong.

The first in situ stress measurements have been conducted in Hong Kong using the hydraulic fracturing technique during the preliminary design stage site investigations for the Cheung Ching Tunnel as part of the Route 3 Project(Figure 1). These measurements were conducted in closely jointed and weathered granitic rock on Tsing Yi Island. The purpose of these measurements was to investigate the minimum principal stress existing along the eastern low rock cover section of the proposed tunnel alignment for the evaluation of the stability of the 17 metre span excavations along this tunnel section.

The contents of this paper include a brief description of the components and the origin of in situ stress in Section 2. In Section 3 the four main measurement methods are discussed and in Section 4 the traditional application of the hydraulic fracturing technique in non-jointed rock is discussed. The application, testing and results of the hydraulic fracturing technique in jointed rock in Hong Kong is discussed in Section 5. A discussion of these results is presented in Section 6 and conclusions regarding the technique are presented in Section 7.

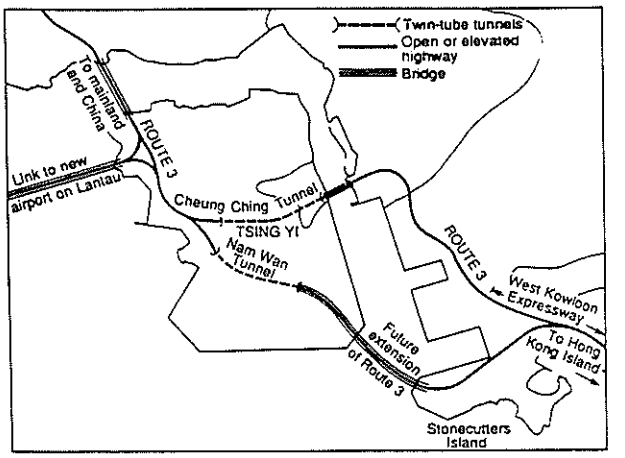

Figure 1 Cheung Ching Tunnel - Route 3 Project

2. In Situ Stresses

2.1 General

Stress is a mathematical tensor quantity that is defined by a magnitude, a direction and the plane on which it acts. Stress is a point property and the stress tensor can be represented for the unit cube in a matrix form and has six independent components as illustrated in Figure 2. There are three independent normal stress components denoted as σ_{xx}, σ_{yy}, and σ_{zz} and three independent shear stress components denoted as τ_{xy}, τ_{xz} and τ_{yz}. At a particular orientation all three shear stress components diminish and all three normal stress components reach a maximum and are then referred to as principal stresses as denoted by σ_1, σ_2 and σ_3 where σ_1 is the maximum principal stress, σ_2 is the intermediate principal stress and σ_3 is the minimum principal stress. In some cases of in situ stress measurements it may be only of interest to investigate the minimum principal stress such as for the design of pressure tunnel linings or for the evaluation of stability for large span excavations in jointed rock.

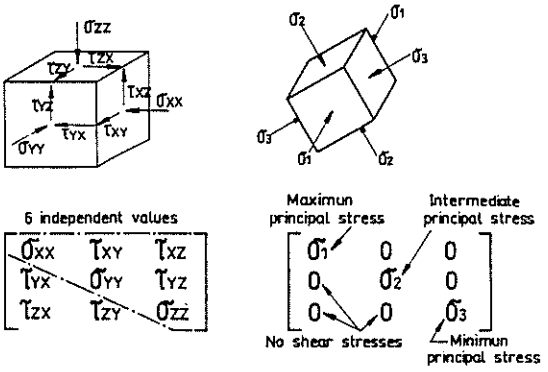

Figure 2 Stress Tensor

2.2 Origin of In Situ Stresses

The origin of in situ stresses stems from three main sources although secondary sources have also been recognised. The three main sources comprise gravitational, tectonic and residual stresses and secondary sources result from thermal and physio-chemical effects. Gravitational stresses are those stresses that are due to the weight of the superincumbent rock mass or overburden materials. Tectonic stresses are generated as a result of the relative displacements of the lithospheric plates. Residual stresses are often reffered to as locked-in stresses and are the result of pre-existing effects and are most commonly attributed due to the sudden unloading of the earth's crust by erosion and de-glaciation. The effect of glaciers in places such as Canada and the Scandinavian countries has led to high horizontal stresses at relatively shallow depths. Residual stresses are commonly associated with variable topography such as is present in Hong Kong. The measurement of in situ stresses in a region of such variable topography are likely to yield anomalous in situ stresses with high horizontal directional stresses both along major ridges and depressions.

3. In Situ Stress Measurements

3.1 General

There currently exist four main methods to measure in situ stresses as recognised by the International Society for Rock Mechanics (ISRM,1987). Different procedures and equipment as well as fundamental strategies are associated with each of these methods. Initial research into the measurement of in situ stresses in the 1960's focused on strain relief measurements assuming rock mass elasticity. Early developments in this research required that several overcoring strain relief measurements be conducted in order to determine the complete in situ state of stress. Further advances with this same work resulted in the development of a strain relief cell whereby a single test was adequate to determine the complete in situ state of stress(Leeman and Hayes, 1966). The hydraulic fracturing technique was developed as a direct measuring method in the early 1970's and is the result of the work of Hubert and Willis (1957) with early applications in the petroleum industry for the enhancement of oil well production.

Several other techniques have been developed and experimented in the attempt to measure the in situ state of stress. Some of these techniques have included large scale overcoring(Brady et al.1976) as well as alternative forms of strain relief overcoring(Hiltsher et al.1979). Only the four common methods of the ISRM are presented for the purpose of this paper.

3.2 Flat Jack

The Flat Jack method allows for the determination of a stress component parallel to and near an exposed excavation surface. The component of stress that is measured is not the virgin stress component and each measurement determines the stress only in a single direction, therefore six independent direction are required in order to determine the stress tensor.

The Flat Jack method requires the insertion of a welded flat envelope of material into a cut slot made in the side of an excavation. Prior to the cutting of the slot for the flat jack, measuring pins are installed and surveyed on either side of the slot. The component of stress acting perpendicular to the plane of the flat jack is determined as the pressure required to inflate the flat jack in order to return to the initial pin separation.

The Flat Jack method is not ideally suited for the determination of the undisturbed in situ state of stress due to practical considerations. The method however is commonly employed for the determination of stresses generated within tunnel linings long after construction for the purpose of providing design information for future excavations in a similar geological environment.

3.3 Borehole Deformation Gauge

The borehole deformation gauge method of measuring in situ stresses is based on the measurement of the changes in a borehole diameter during overcoring and has been modelled on a procedure developed by the United States Bureau of Mines (USBM). Both the deformation measurements and the elastic properties of the rock are considered in determining the 2D state of stress in the plane perpendicular to the axis of the borehole. In order to determine the complete stress tensor with this method test from three or more non-parallel boreholes must be conducted and analysed.

The distance away from an excavation for which this method can be used is only restricted by the accuracy of the overcore drilling and successful tests have been completed at distances of up to 200m. The borehole deformation gauge should be used only in relatively homogeneous rock with widely spaced jointing but can be used when boreholes are wet due to groundwater or from drilling water.

3.4 Soft Inclusion Strain Cell

Soft inclusion strain cells have been developed with 9 and 12 strain gauges in order to determine with a single test the complete stress tensor by relieving stresses through overcoring a borehole. The main problem associated with the use of strain cells are commonly related to inadequate bonding of the strain gauges to the rock.

The application of strain cells are ideally suited for homogeneous, isotropic rock where joints are widely spaced and the method is also limited by the accuracy of the overcore drilling. The determination of the components of in situ stress require the elastic properties of the rock.

3.5 Hydraulic Fracturing

The hydraulic fracturing technique can determine the three principal components of the complete in situ stress tensor using a single test with the assumption that the minimum principal stress, σ_3, is vertical along the orientation of the borehole. The technique is independent of the elastic properties of the rock and can be conducted at great depths. The technique is ideally suited for non-jointed rock or at least where the joints are widely spaced. The main problems associated with the technique are the determination of the instantaneous shut-in pressure as will be discussed later and leakage from the packer equipment.

4. Hydraulic Fracturing in Non-Jointed Rock

4.1 Measurement Procedure

Hydraulic fracturing is conducted within a sealed off section of a borehole. The sealing is commonly achieved using a double-straddle packer system consisting of two hdraulically activated rubber packers to pressurize a test interval until a fracture is created or a pre-existing fracture is re-opened within the rock material surrounding the test interval. According to the work of Hubert and Willis (1957) a hydraulic fracture will be created perpendicular to the minimum principal horizontal in situ stress. The first step in the measurement procedure is the selection of suitable test intervals upon inspection of the borehole core. Ideally, test intervals are selected where no jointing is present. Upon sealing off the selected test interval water is injected into the test interval at a controlled rate monitoring both time and test interval pressure. Once a hydraulic fracture is created the water injection is terminated and the decay in water pressure is closely monitored to examine the decay response to the moment the hydraulic fracture closes and water flow into the rock formation ceases.

The next step is the re-injection of water into the test interval to re-open the previously created hydraulic fracture. After the re-opening of the hydraulic fracture the water flow is again terminated and the pressure decay monitored. This re-opening cycle is repeated several times to confirm a consistent re-opening pressure. Figure 3 presents a typical Pressure-Time plot for a hydraulic fracture test. After a satisfactory pressure-time plot is recorded the test is complete and the double packer system is removed from the test interval. To confirm that a hydraulic fracture was created and to determine its orientation an impression packer survey of the test interval is conducted. Notable contributions for the application of hydraulic fracturing have been presented by Haimson (1974), Zoback and Pollard (1978) and Rummel et al.(1983).

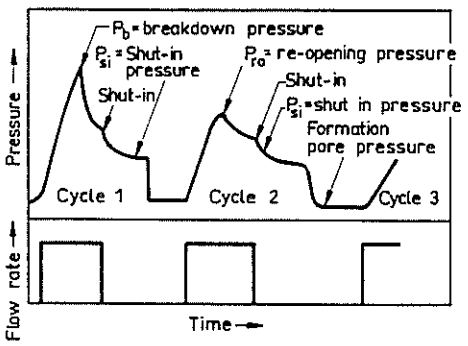

Figure 3 Typical Pressure-Time Plot

4.2 Equipment Requirements

The equipment requirements for conducting hydraulic fracturing tests are relatively simple however experienced staff are necessary to conduct the testing in order to obtain to meaningful information. Figure 4 illustrates a typical layout of the testing equipment including the double packer system, a surface readout and data acquisition unit and the impression packer survey tool. During the hydraulic fracturing test it is imperative that a surface readout of the pressure-time response is available in order to correctly monitor the behaviour of the test interval. Commonly used surface readouts include chart recorders or video displays from tape and computer disc data recording.

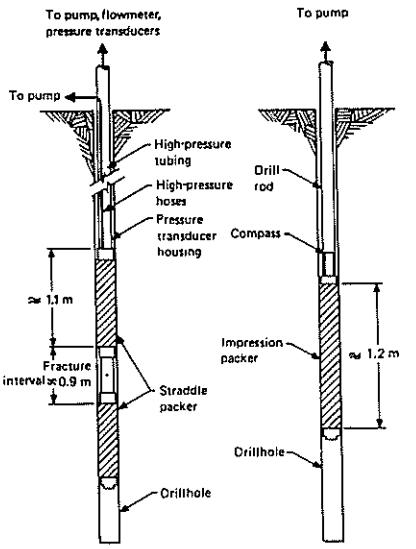

Figure 4 Testing Apparatus

4.3 Interpretation of Results

Interpretation of the results from hydraulic fracturing tests requires the identification of the breakdown pressure, P_b, the instantaneous shut-in pressure, P_{si} and the re-opening pressure, P_{ro} as highlighted on Figure 3. The breakdown pressure, P_b, is defined as that test interval pressure at which a new hydraulic fracture is created within the test interval. The instantaneous shut-in pressure, P_{si}, is defined as the test interval pressure at which the hydraulic fracture closes and water inflow into the rock mass no longer occurs. Shut-in pressures are commonly indistinct with hydraulic fracturing tests and several methods have been proposed for the determination of P_{si}. Aggson and Kim (1987) present an interesting comparison of five methods that define significantly different shut-in pressures. The re-opening pressure, P_{ro}, is defined as the test interval pressure at which the previously created hydraulic fracture is re-opened. The breakdown and re-opening pressures are clearly confirmed after repeated re-opening cycles have been completed.

In calculating the principal stress components from results of hydraulic fracturing tests it is assumed that the orientation of either the intermediate principal stress, σ_2, or the minimum principal stress, σ_3, is vertical. In the plane perpendicular to the borehole axis the stress components of interest are thus σ_h, and σ_H which are respectively the minimum and maximum principal stresses and the calculation of these components for a vertical borehole in flat lying topography are based on the following expressions:

$$\sigma_h = P_{si} \quad (1)$$

$$\sigma_H = 3P_{si} - P_b - P_o + T \text{(for initial cycle)} \quad (2)$$

$$\sigma_H = 3P_{si} - P_{ro} - P_o \text{(for re-opening cycles)} \quad (3)$$

where P_o is the initial pore water pressure in the test interval and T is the tensile strength of the rock material. For the subsequent re-opening cycles T = 0. From the above expressions, if σ_h is less than the overburden stress, σ_v, then $\sigma_h = \sigma_3$ and if σ_h is greater than σ_v, then $\sigma_h = \sigma_2$. The orientation of σ_h is perpendicular to the strike of the hydraulic fracture and σ_H is perpendicular to σ_h. The above expressions are valid for classical hydraulic fracturing in non-jointed, impermeable rock. In permeable rock formations poroelastic effects may be significant and must be considered(Detournay et al.,1989).

Hydraulic fracturing on pre-existing fractures has been investigated in detail by Cornet (1986) with the consideration of an inverse mathematical procedure for the determination of the principal stresses. Rummel (1987) has presented the calculation of stresses from hydraulic fracturing data based on fracture mechanics.

5. Hydraulic Fracturing in Jointed Rock in Hong Kong

5.1 Interpretation of Results

The interpretation of the results of hydraulic fracturing tests conducted in jointed rocks follows the same procedures as for non-jointed however the definition of the magnitudes of the breakdown pressure, P_b, the instantaneous shut-in pressure, P_{si} and the re-opening pressure, P_{ro} are not as easily selected from the pressure-time plot. The main reason for the greater difficulty in defining the characteristic pressures is due to leakage of the injected water from the test interval through joints present within the test interval. In order to define the characteristic pressures a detailed computer-based data analysis incorporating smoothing procedures with the construction of special cross-plots are commonly required(Baumgartner and Zoback, 1989). After a careful inspection of the observed hydraulic fracture orientation in the test interval in combination with the characteristic pressure values the determination of the in situ stress regime can be completed.

5.2 Testing and Results from Tsing Yi Island

A total of 25 tests were conducted in 4 boreholes at depths ranging from 8 to 50m below surface. Pressure-time data was recorded on a paper-chart recorder for continuous viewing as well as cassette tape recorder for subsequent re-processing. Test intervals were selected where either no or very few pre-existing joints were present.

An initial evaluation of the test data was conducted on site during the testing programme for comparative purposes. Out of a the total of 25 tests only 9 breakdown pressures could be confidently identified. A limited number of tests were unsuccessful due to leakage from the test interval that prevented pressure build up and thus new test intervals were selected. The detailed evaluation of all the test data was conducted after re-processing of the data at the office of MESY GmbH Bochum. Both pressure-time and logarithm plots were constructed for the determination of upper and lower bound shut-in pressures.

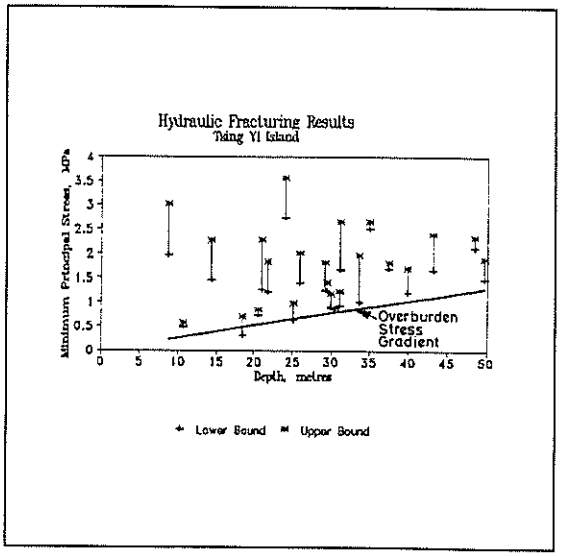

Figure 5 Tsing Yi Test Results

Test results presenting the pressure-time and flow rate-time data were typical for the Tsing Yi data. A plot of lower and upper bound minimum principal horizontal stresses versus depth for all the tests is presented in Figure 5. The results clearly indicate near consistent minimum principal horizontal stresses greater than the overburden stress. It is noted that the variability of the lower bound values is significantly less than for the upper bound values. The results of the impression packer surveys indicated an East-NorthEast orientation for the maximum principal horizontal stress, thus being sub-parallel to the proposed tunnel alignment.

5.3 Numerical Modelling

In an attempt to explain the interesting results from the hydraulic fracturing tests a numerical modelling analysis was conducted considering the variable topography of the site. The analysis was specifically aimed at investigating the variability of minimum principal horizontal stresses as determined from the different boreholes with the possible variability being a result of the topography at the site. The numerical modelling was also conducted to confirm the determined principal stress directions that were deduced from the results of the field tests. The 2D finite difference code, FLAC, was used to model the variable topography with initial stresses set using the hydraulic fracturing results from the one borehole located where the stresses were speculated to be not influenced by topography. The results of the numerical modelling analysis confirmed a general agreement to the measured stresses from the hydraulic fracturing tests. Figure 6 presents the calculated stress regime with borehole locations and Figure 7 presents a comparison of the results of the numerical modelling analysis to the measured stresses for one of the boreholes.

6. Discussion of Results

The results of the hydraulic fracturing tests indicating near consistent minimum principal horizontal stresses greater than the overburden stress are very encouraging upon consideration of the prevailing rock mass conditions. The uncertainty in determining the minimum principal horizontal stress has been represented in the form of upper and lower bound values. A non-linear variation of the minimum principal horizontal stresses was recorded for each of the four boreholes. This non-linearity can be attributed to the stress relaxation due to topography, inhomogeneous rock material properties and the influence of pre-existing joints on the prevailing stress field near the borehole.

7. Conclusions

The success of conducting hydraulic fracturing tests in closely spaced and slightly to moderate weathered granitic rock is very encouraging for the planning of further testing in similar rock mass conditions in Hong Kong. Although the absolute magnitude of in situ stresses is not of general concern in comparison to the strength of most rocks, the relative magnitude of the minimum principal horizontal stress compared to the overburden stress is of major concern for the evaluation of the stability of large span underground excavations. Hydraulic fracturing is a cost-effective method for the determination of the principal stress components versus other common methods having due regard of the rock mass conditions prevailing in Hong Kong.

8. Acknowledgements

The authors wish to acknowledge the kind approval of the Highways Department of the Government of Hong Kong for publishing this paper.

The hydraulic fracturing tests were carried out on site by Dr.Ing H. Konietzky and Dipl.Ing. Mr. P. Hegemann of MESY GmbH Bochum in consultation with the first author.

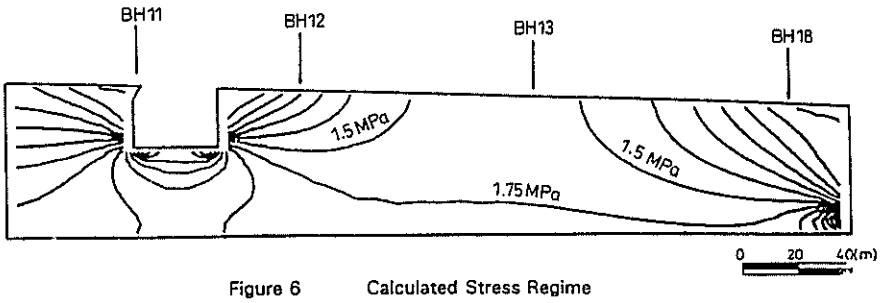

Figure 6 Calculated Stress Regime

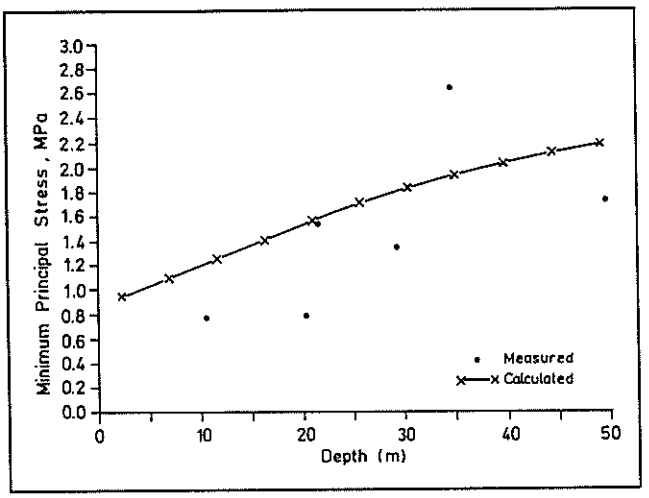

Figure 7 Comparison of Results for BH 12

9. References

AGGSON, J. R. and KIM, K.(1987). Analysis of Hydraulic Fracturing Pressure Histories: A Comparison of Five Methods Used to Identify Shut-In Pressure. Int. J. Rock. Mech. Min. Sci.& Geomech. Abstr., Vol.24, No.1, pp.75-80.

BAUMGARTNER, J. and ZOBACK, M.D.(1989). Interpretation of Hydraulic Pressure-Time Records Using Interactive Analysis Methods. Int. J. Rock. Mech. Min. Sci.& Geomech. Abstr., Vol. 26, No.6, pp.461-470.

BRADY, FRIDAY, and ALEXANDER (1976). Stress Measurement in a Bored Raise at Mt. Isa Mine.

CORNET, F.H.,(1986). Stress Determination from Hydraulic Tests on Pre-Existing Fractures - The HTPF Method, Proc. Int.
Symp. Rock. Stress and Rock Stress Measurements, Stockholm. pp.301-312.

DETOURNAY, E., CHEUNG, A.H.D., ROEGIERS, J.C., and MCLENNAN, J.D.(1989). Poroelasticity Considerations in In Situ Stress Determinations by Hydraulic Fracturing. Int. J. Rock. Mech. Min. Sci. & Geomech. Abstr., Vol. 26, No. 6., pp.507-514.

HAIMSON, B.C.(1974). A Simple Method for Estimating In Situ Stresses at Great Depth. Field Testing and Instrum. of Rock. Am.Soc. Test. and Mat., Spec. Tech. Publ. 554, pp.156-182.

HILTSHER, R., MARTNA, J. and STRINDELL, L.(1979). The Measurement of Triaxial Rock Stresses in Deep Boreholes and the Use of Stress Measurement for Design and Construction of Rock Openings. 4th IRSM Congr. Vol 2. pp. 227-234.

HUBERT, M.K. and WILLIS, D.G.(1957). Mechanics of Hydraulic Fracturing, Trans. AIME.,Vol. 210, pp. 153.

ISRM, (1987). Suggested Methods for Rock Stress Determination. Int.J.Rock.Mech.Min.Sci.&Geomech Abstr., Vol. 24., No.1, pp.53-73.

LEEMAN, E.R. and HAYES, D.J.(1966). A Technique for Determining the Complete State of Stress in Rock using a Single Borehole. Proc. First ISRM Rock Mech. Congr. Vol.II, Lisbon, pp.17-24.

RUMMEL, F., BAUMGARTNER, J. and ALHEID, H.J.(1983). Hydraulic Fracturing Stress Measurments Along the Eastern Boundary of the SW-German Block, in Hydr-Fracc. Stress Measurements, Nat. Acad. Press, Wash. D.C., pp. 3-17.

RUMMEL, F.(1987). Fracture Mechanics Approach to Hydraulic Fracturing Stress Measurements, in Fracture Mechanics of Rocks, Ed. B.K. Atkinson, Academic Press London.

ZOBACK, M.D. and POLLARD, D.D.(1978). Hydraulic Fracture Propagation and the Interpretation of Pressure-Time Records for In Situ Stress Determination. 19th U.S. Symp. Rock.Mech. pp.14-22.

Risk of Mine Related Subsidence at Ocean View

G.B. FARQUHAR
B.E., B.D., M.Sc., D.I.C., M.I.C.E., M.I.P.E.N.Z.
Senior Geotechnical Engineer, Worley Consultants Ltd
B.J. DOUGLAS
M.Sc., Ph.D.,
Principal, Barry J Douglas Geological Consultants

SUMMARY In July 1989 a subsidence pit appeared in a residential area at Ocean View above the one hundred year old abandoned Walker No. 1 Coal Mine. Subsidence hazard for the residential area was examined. The extent of the mine was assessed together with overlying ground conditions and condition of the mine. Strata overlying the mine were found to be extremely weak. Mine workings were found to be deteriorating and in an open and flooded condition. The subsidence pit was attributed to localised catastrophic collapse of the mine roof and consequent subsidence of water charged sandy gravel into the mine opening, causing the sudden collapse at the ground surface. Other similar pits were observed above nearby abandoned mines. The risk of further subsidence pits forming was assessed to be very probable. Fourteen private properties were determined to be at risk, and the degree of risk to residents and property was assessed as 'risky to some risk'. Courses of action for the Local Authority were prepared and in August 1990 the Crown accepted some liability for the situation.

1. INTRODUCTION

On the night of 12-13 July 1989, a subsidence pit formed from the sudden collapse of the ground surface in the rear yard of a residential property in John Street, Ocean View. The Local Authority commissioned an investigation to evaluate coal mine subsidence hazard above the mine.

Ocean View is a small suburban residential area on the East Otago coast 17 km south of the City of Dunedin. Coal beds extensively underlie the Ocean View district and have been worked by underground methods in several mines until as recently as 1972. The subsidence pit occurred above the one hundred year old abandoned Walker No. 1 Coal Mine.

2. SITE DESCRIPTION

Physiographically, the site primarily incorporates a raised marine terrace some 8-10 m in height. This terrace is bound immediately to the south and east by a steep, formerly wave-cut bank and a narrow coastal plain some 100 metres wide. A modified gully drains the lower part of John Street. The mine workings underlie the high terrace. Houses are situated both on the high terrace and on the low- lying land at the foot of the terrace.

3. MINING

3.1 History

Underground coal mining commenced in 1887 below the high terrace and continued until 1893 when the mine proprietor James Reid Walker abandoned the mine and recommenced mining at a new site across the valley, 200 m further east.

Although specific details on mining activities in the mine are unavailable, it is reasonable to assume it was similar to the room and rance method deployed at the same time in other Green Island Collieries (Denniston 1877). Rooms typically 3.6 - 4.3 m wide and in places 5.5 m wide, with a "comparatively slight thickness of wall or rance between each room", were worked either side of access drives. Only the centre 1.5 - 2.1 m of the seam was worked to ensure a safe mining system, even where the seam was up to 4.9 m thick.

The soft nature of the roof and floor, loose drift sands and sandy shales affected the safety of the Green Island Collieries particularly where rooms reached maximum extension (Denniston 1877). The Annual Mine Statement of 1892 and 1893 refers to the hazardous roof conditions in the old workings at the Walker No. 1 Mine, presumably in an area worked by the room and rance method.

3.2 Mine Configuration

Two original mine plans (1890 and 1902) were located but they did not portray details of the final internal configuration of the workings. Only the access and service drives were plotted, but the plans were useful in indicating the areal extent of the workings. The mine was unable to be precisely located with this information due to the lack of surveyed control points which could be positively identified. External mine features such as the air shaft and mine portal were no longer visible.

Six mine plan overlays scaled to the topographical plan were generated in an attempt to establish an accurate orientation for the mine map. On the basis of geologic and hydrologic data the mine was believed to be confined to the area beneath the high terrace and not to extend beneath the low-lying previously swampy ground. On the basis of historic and topographic features the approximate location of the mine portal was determined to be on the north facing slope of the gully now modified to form John Street. The resulting plan overlay model is shown on Figure 1.

4. SITE INVESTIGATIONS

Most of the technical information required to evaluate subsidence hazard was derived from 7 drillholes, located as shown on Figure 1. Access for drilling was restricted. An inspection was made of the exterior surfaces of buildings in the area. No indications of large scale ground settlements were detected although significant settlement of one corner of a house was observed. The Local Authority conducted

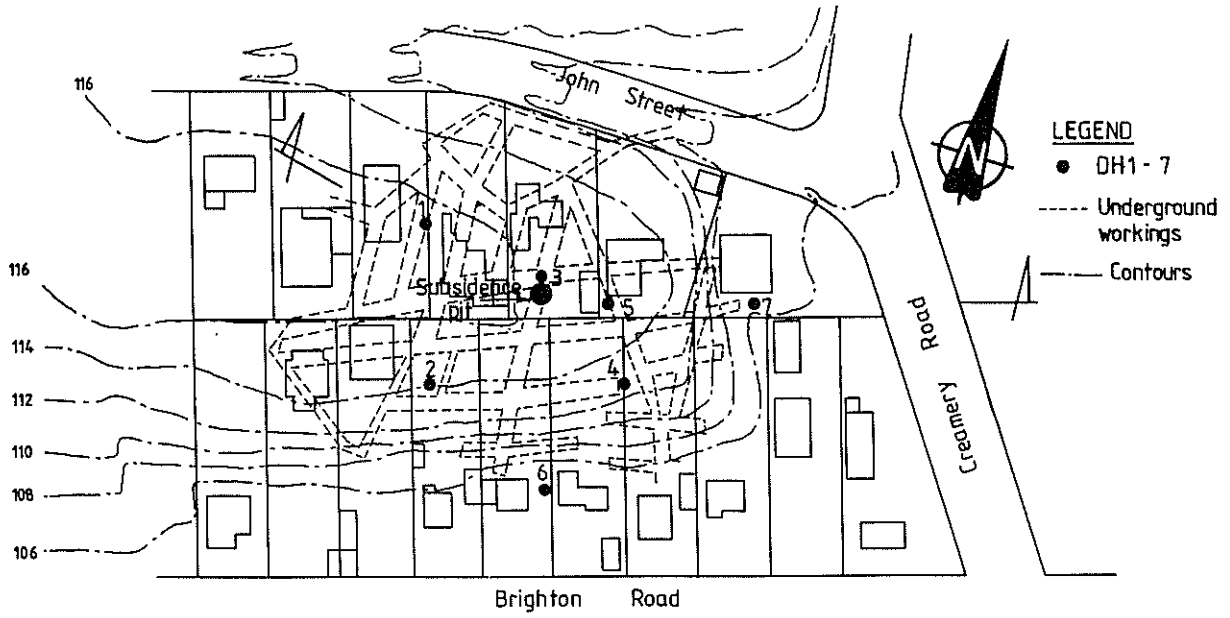

Figure 1 Site plan

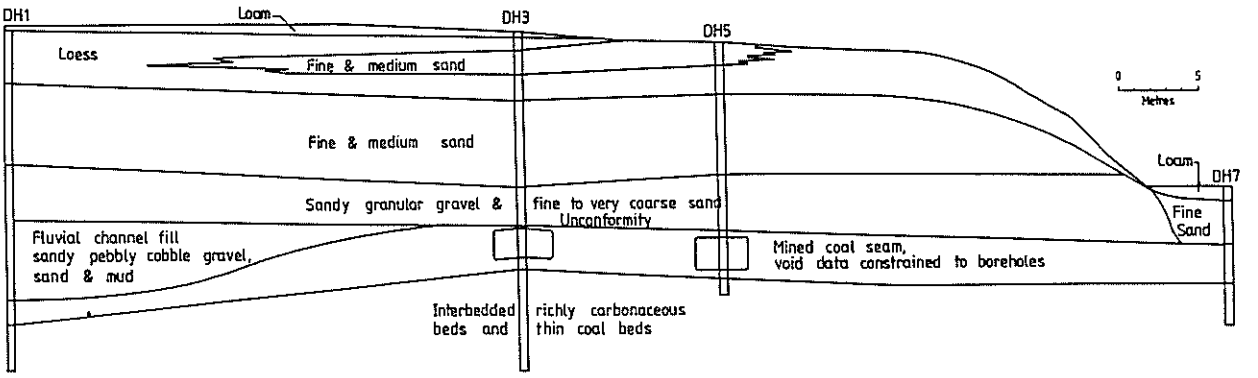

Figure 2 Geological section

a water leakage survey of pipes on John Street properties with only minor leakages being detected.

5. GROUND CONDITIONS

The ground profile in the area of the mine is depicted in Figure 2. Hillgrove Formation (Pleistocene) sediments overlie the coal bearing Taratu Formation (Upper Cretaceous). The Hillgrove Formation (9-16 m thick beneath the high terrace) consists of the following general profile:

Depth (m)	Stratum
0 - 4	Soft to stiff clay and very fine sandy mud (Loess)
1 - 9	Medium dense fine to medium sand
8 - 12	Very loose to loose sandy gravel and fine to coarse sand
12 - 16 (DH1) 8.5 - 9 (DH2)	Mud and sandy cobble gravel

These sediments unconformably overlie the Taratu Formation except to the west (DH1 & 2) where a succession of fluvial silts, sandy cobble gravels and sands, infill a channel deeply entrenched into the underlying Taratu Formation.

The Taratu Formation consists of numerous thin, laterally inconsistent fine grained carbonaceous beds of clays, silts, coal and fine sands. These sediments are extremely weak to very weak. The 1.4 - 3.6 m thick, laterally continuous, moderately strong, main coal seam occurs at or close to the top of the Formation. Beneath the high terrace the top of the coal seam varies between 11.2 and 16.0 m below ground surface. The Taratu Formation strata dip gently south eastward at 4° - 6°.

The main coal is shallowly located 3.5 - 5 m beneath the low-lying land at the foot of the high terrace. Here the sediments overlying the coal seam are predominantly loose porous fine sands.

Groundwater conditions beneath the high terrace consist of an unconfined aquifer 0.7 to 5.8 m thick occurring within the lowermost Hillgrove strata. The upper surface of the Taratu Formation defines the base of the aquifer. Groundwater level is 7.5 - 9.6 m below ground surface.

6. MINE CONDITION

Voids interpreted as excavated coal workings were intersected in 4 drillholes (DH 3, 4, 5). Drill rods fell freely into the water filled voids while drilling. In two drillholes well preserved wood, probably mine support timber or rail sleepers, were located on the coal floor.

The thickness (0.4 - 0.7 m) of typically low ash coal remaining below the floor of the worked seam, suggests that floor heave may have been a problem.

Roof or rib fall (caved) material was cored in 2 drillholes from immediately above the coal floor. In DH 3 it consisted of small coal fragments intermixed with quartz sand and well rounded granular sand (derived from Hillgrove Formation sediments). DH 3 was located immediately adjacent to the subsidence pit.

The immediate coal roof was determined to be competent, but is locally characterised by a vertical to sub-vertical cleat which might in time contribute to slabbing of the immediate roof. Water saturated conditions in the permeable strata above the worked coal seam are likely to be a significant causative factor in the deterioration of the workings. Roof strata susceptible to moisture slaking may slowly deteriorate over a long period of time before large falls develop (Krausse 1979), allowing groundwater to drain into the mine. The integrity of an entire mass of roof can be destroyed by this process (Moebs and Stateham 1986). Localised catastrophic collapse (subsidence) of the immediately overlying extremely weak, water charged sandy granular gravel sediments (of the Hillgrove Formation) will occur where significant roof failure results in the collapse of Taratu Formation strata bridging the mine roof.

7. MINE SUBSIDENCE

7.1 Characteristics

Various forms of mining result in differing effects on the strata and the ground surface. Surface subsidence related features appropriate to room and rance mining can be categorised as follows:

Subsidence pits (crown holes) are nearly circular depressions. Subsidence troughs (crown holes) are elongated depressions produced often by the coalescence of individual pits. Subsidence pits and troughs are caused by roof collapse and the ground surface may collapse suddenly.

The major mechanisms of mine deterioration in room and rance workings are roof collapse, crushing of pillars and floor heave. By far the greatest problem is roof collapse as evidenced at the Walker No. 1 Mine and nearby mines. At the cessation of mining supporting timbers would either be withdrawn or allowed to rot away allowing the roof strata to collapse into the open workings. The process of upwards collapse would continue until the workings and the collapsed ground above it were completely choke-filled with debris. Where the collapse reaches the ground surface a subsidence pit or trough (crown hole) is formed. This process is illustrated in Figure 3.

Several formulae can be found in the literature as to the maximum height of collapse that might be expected to occur. (Subsidence Engineers Handbook 1975; Healy and Head 1984). For a seam thickness of 1.2 m and a bulking factor of 15%, a conical shaped collapse could be expected to occur up to a height of 20-34 m i.e. greater than the thickness of overburden above the mine.

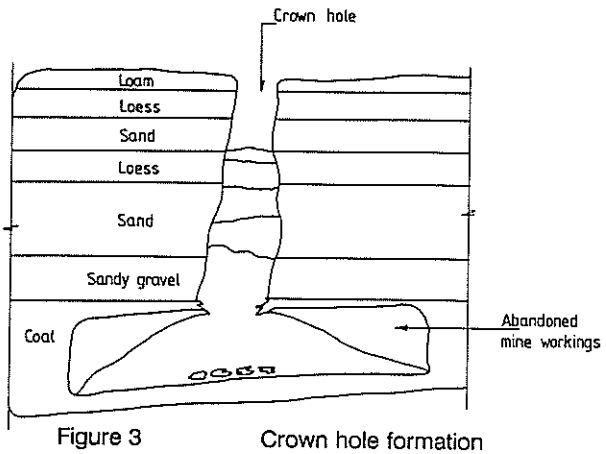

Figure 3 Crown hole formation

Dunrud and Osterwald (1980) observed that the total depth of subsidence pits may be nearly as deep as or sometimes even deeper than the height of the mine workings because collapsed material may spread laterally into the mine opening, particularly where water is present in the mine. It is believed that the surface in the John Street subsidence pit collapsed 3.5 m above flooded coal workings excavated to a height of 1.1 - 1.7 m.

7.2 The John Street Subsidence Pit

The ground surface collapsed 12 to 24 hours after an earthquake was felt in the Ocean View area. Reports and photographs indicate the surface geometry of the pit soon after collapse was circular, approximately 1.5 m wide and 3.5 m deep with vertical sidewalls. The pit widened during the succeeding months until the pit was in-filled.

7.3 Other Subsidence Features at Ocean View

Numerous subsidence pits and troughs occur 200 m to the northeast above the abandoned Walker No. 2 Mine, and 200 m to the north above the Victory Mine. The seam worked in these mines similarly occurs within the Taratu Formation. The subsidence features occur above the outer shallower workings of these mines where the overburden strata are thought to be thinnest and not capped by the relatively competent Brighton Limestone overlying the deeper workings in these areas.

Examination of aerial print photographs of the area above the Walker No. 2 Mine indicated that many of the subsidence pits and troughs currently recognisable had collapsed by 1942. One distinctive circular pit (occurring between 1976 and 1985) was located among older pits and was similar in size and shape to the John Street pit.

7.4 Subsidence and Seismicity

The John Street subsidence pit appeared within 12 to 24 hours of a magnitude 4.5 earthquake located 7.5 km offshore from Ocean View on 12 July, 1989. Considering the age and condition of the mine, the lack of competence of the overburden and temporal association of the earthquake with the appearance of the hole, it was possible that the seismic event initiated and/or accelerated the roof collapse which propagated upward over a period of hours and which was still active many days afterward. As such, the possibility of further subsidence was viewed in light of

the probability of earthquakes which would produce similar or greater intensities in the area.

During a magnitude 5.0 earthquake in 1974 no subsidence pits were reported in Ocean View. The epicentres and shallow focal depths (20 km) of the 1974 and 1989 events were similar. The most recently active nearby fault, and the one probably associated with the 1974 and 1989 events, is the Akatore Fault. The surface trace of this fault is about 3 km southeast of Ocean View. Using an estimated felt intensity for the 1989 event, the probability of occurrence of the same or greater events was assessed using information from Smith and Berryman (1983). These probabilities were used in the risk analysis.

8. RISK ASSESSMENT

8.1 Introduction

In order to assess the risk of subsidence above abandoned mines it was useful to use a framework in which to evaluate and assess risk. A suitable framework has been proposed by Cole (1987) particularly in relation to construction over abandoned shallow mines. Table I relates 'Degree of Risk' categories to 'broad-band' probabilities and is based on a ratio of 10 in both directions. The concept of 'Tolerance of Risk', i.e. an increasing expectation of less exposure to risk as the public nature of risk increases, can be introduced. In Table II the 'Degree of Risk' and 'Severity of Consequences' are combined with tolerance to give a matrix of 'acceptance' or 'expectations'. Statements are obtained from the table in the following manner:

e.g. "Impairment / of property / by subsidence damage / [is] expected by the public / [to be] unlikely".

TABLE I

DEGREE OF RISK AND PROBABILITY (AFTER COLE 1987)

Annual Probability of a Total Loss Event		
DEGREE OF RISK (Nomenclature)	TO LIFE Annual risk of fatality	TO PROPERTY Annual risk of destruction
Very risky	1 in 100	1 in 10
Risky	1 in 1,000	1 in 100
Some risk	1 in 10,000	1 in 1,000
A slight chance	1 in 100,000	1 in 10,000
Unlikely	1 in 1 million	1 in 100,000
Very unlikely	1 in 10 million	1 in 1 million
Practically impossible	1 in 100 million	1 in 10 million
	1 in 42 The overall death rate	1 in 200 The overall destruction rate

There is little doubt that readers will quibble at one or more of the statements that can be obtained from Table II and this only serves to draw attention to how one's experience of risk determines one's perception of it. Generally, it can be said that there is a difference of at least one order of magnitude between what the public will accept as degree of risk and what it will expect as degree of risk.

The nature of geotechnical engineering and particularly work dealing with abandoned mines and mining subsidence, is such that the amount of data required to allow a reliable statistical analysis of the problem is seldom available or obtainable.

8.2 Degree of Risk

The degree of risk with respect to ground subsidence above the mine was assessed by taking into consideration the following facts:

- The shallow depth of workings.
- The age of workings is old, 90 to 100 years.
- The room and rance method of mining was used and the central part of the mine is recorded as being worked out.
- Roof conditions were recorded as being poor during mining; drilling revealed that the coal roof is very thin and granular deposits directly overlie this over most of the mine.
- Coal rubble and sandy granular deposits were recovered from the floor of the mine workings. The sandy sediments probably entered the mine workings through nearby roof falls.
- The workings are presently flooded.
- Support timbers in the mine may still be in good condition.
- A subsidence pit type of collapse appeared on the night of July 12-13, 1989.
- Historical evidence of possible subsidence pits prior to subdivision of the area.
- Subsidence pits are observed to be the form of subsidence occurring above nearby mines.
- The subsidence pit collapse occurred within 12 to 24 hours after a local earthquake of probable intensity MM III to MM IV. There is a greater than 10% probability of the occurrence within 50 years of another seismic event which produces the same or greater intensity, and a 100% probability within 100 years. While seismic events may not be directly responsible for the formation of subsidence pits, they may enhance the instabilities which cause them to form.

These facts led to the conclusion that the degree of risk of further subsidence pits occurring lay between two categories; 'risky' to 'some risk'. The mine workings appeared to be still open and slowly deteriorating, and the timing and frequency of further collapses was uncertain. The existence of voids that have partly migrated towards the ground surface was considered unlikely. The loose granular nature of the overburden materials was likely to lead to the rapid migration of a void to the ground surface following a roof collapse.

Using Table I, it can be seen that there was a greater risk of destruction of property than loss of life. Similarly it could be said there was a greater risk of damage to property than destruction of property and a greater risk of injury than loss of life. The evidence of previous subsidence pits in the Ocean View area indicated typical dimensions of about 4 m diameter and 2-4 m deep i.e. not large enough for a house to completely fall into, but large enough to cause severe distress to part of a house and damage to buried services in the road reserve.

TABLE II
ACCEPTANCE OR EXPECTATION OF DEGREE OF RISK OF GIVEN CONSEQUENCE (AFTER COLE 1987)

Severity of Consequence		Degree of Risk
Impairment	Total Loss	
of life : by car, aeroplane and home accidents of property : by "Act of God" circumstances **Tolerated in special circumstances**	of life : by deep sea diving or rock climbing of property : by volcano or avalanche **Not acceptable except to a minority**	**Very risky to risky**
of life : by deafness or blindness of property : by fire **Accepted by the public**	of life : by car, aeroplane and home accidents of property : by undermining or earthquake **Tolerated by the public in special circumstances**	**Some risk to a slight chance**
of life : by sickness such as chicken pox of property : by subsidence damage **Expected by the public**	of life : by public transport accidents of property : by flooding **Accepted by the public**	**Unlikely**
of life : by sickness such as rabies of property : by radiation contamination **Demanded by the public**	of life : by fatalities in public places of property : by failure of foundations on soil **Expected by the public**	**Very unlikely**
	of life : by failure of nuclear power plant of property : by failure of foundations on rock **Demanded by the public**	**Practically Impossible**

8.3 Area of Risk

The 'area of risk' for ground subsidence is shown on Figure 4. It is derived from an overlay of the various mine models and comprises two areas:

1. Area of risk.
2. Possible extension to area at risk.

Results from the drilling on the low-lying area did not prove the absence of mine workings. Therefore a 'possible extension to the area at risk' was included. This area was identified as requiring further investigation to confirm whether mine workings extend below it.

9. REMEDIAL MEASURES

Two options were presented to the Local Authority.

(a) Not carry out remedial measures

If nothing was done, then when subsidence pits formed, they could be back-filled and damage to structures repaired. Regular survey monitoring may have helped to detect subsidence troughs. No further development in the area was recommended.

(b) Carry out remedial measures

To reduce the degree of risk from 'risky' to 'some risk', to either 'a slight chance', or 'unlikely', or 'very unlikely' required the same remedial works to be carried out whatever degree of risk was accepted, i.e. the remedial measures could not be designed to such tolerances as to differentiate between 'a slight chance' and 'very unlikely'.

Several options existed for remedial works:

1. bulk excavation and back-filling.
2. protect buildings against subsidence pits.
3. filling of mine working by grouting.

Option 1 was not considered feasible as it would have required the removal of all buildings in the area concerned. The depth of excavation, up to 17 m deep would have provided construction difficulties and the scale of such an operation would have been unacceptable in a urban setting.

Option 2 was not considered feasible because of the difficulty and expense of providing stiff foundations for the buildings in the area since most had brick veneers. Although buildings might be protected from damage caused by the formation of subsidence pits, the surrounding land would not be protected.

Option 3 was the most feasible method of preventing migration of voids and formation of subsidence pits. The existence of voids that had partly migrated towards the ground surface was considered unlikely. Because the

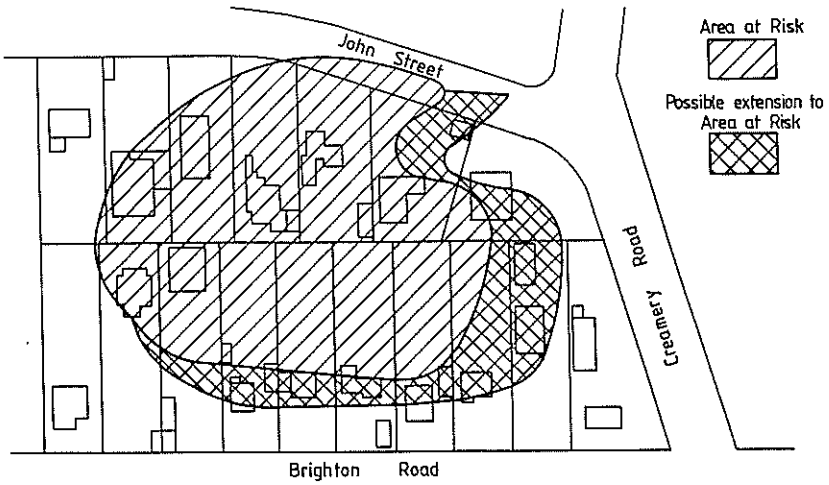

Figure 4 Areas of risk

workings were inaccessible, injection of grout would be done through drill holes. The cost of in-filling the mine by grouting was estimated as $900,000 in 1990.

In August 1990 the Crown accepted some liability for the situation and after consultation with the Local Authority and property owners, chose not to carry out remedial works. The Crown agreed to purchase the properties identified as being at risk if the owners wished to vacate, or to compensate owners wishing to remain. All the buildings on properties bought by the Crown have been demolished or relocated.

10. CONCLUSIONS

1. The ground collapse that occurred was a subsidence pit caused by the collapse of the mine roof possibly accelerated by seismic activity.

2. The degree of risk of further subsidence pits occurring above the mine was assessed to be 'risky' to 'some risk'.

3. The 'area of risk' encroached on 14 properties and part of the John Street road reserve.

4. Two options existed regarding the risk:

   - not carry out remedial works
   - carry out remedial works to reduce the degree of risk.

11. ACKNOWLEDGEMENTS

The authors wish to express their thanks to Dunedin City Council for permission to present the data from the project.

12. REFERENCES

1. Bell, F.G. (ed) (1978). Foundation Engineering in Difficult Ground, Newnes-Butterworths, p. 322-362.

2. Cole, K. (1987). "Building over abandoned shallow mines: A strategy for the engineering decisions on treatment". Ground Engineering. v. 20, no. 4, p. 14-30.

3. Denniston, R.B. (1877). "Report on Green Island Collieries, Otago". New Zealand Geological Survey reports of geological explorations, 1876-77, v. 10, p. 143-165.

4. Barry J Douglas Geological Consultants and Worley Consultants Ltd (1990). "Investigation of Mine Related Subsidence - John Street Area Ocean View". Unpublished Report to Dunedin City Council, 63 p.

5. Dunrud, C.R. and Osterwald, F.W. (1980). "Effects of coal mine subsidence in the Sheridan, Wyoming area". Geological Survey Professional paper 1164, 49 p.

6. Healy, P.R. and Head, J.M. (1984). "Construction over abandoned mine workings". Construction Industry Research and Information Association, United Kingdom, Special publication 32.

7. Krausse, H.F. and others (1979). "Engineering study of the structural geological features of the Herrin (no. 6) Coal and associated rock in Illinois". v. 2, Summary Report, Illinois State Geological Survey report prepared for Bureau of Mines Washington, Report no. Bu Mines OFR 96(1), -80, 53 p.

8. Moebs, N.N. and Stateham, R.M. (1986). "Coal Mine Roof Instability: Categories and Causes". Bureau of Mines Information Circular, 9076, United States Department of the Interior, 15 p.

9. Sames, G.P. and Laird, R.B. (1988). "Geologic conditions affecting coal mine ground control in the Western United States". Bureau of Mines Information Circular, 9172, United States Department of the Interior, 30 p.

10. Smith, W.D. and Berryman, K.R. (1983). "Revised estimates of earthquake hazard in New Zealand". Bulletin of the New Zealand National Society for Earthquake Engineering, v. 16, no. 4, p. 259-272.

11. Subsidence Engineers' Handbook (1975). National Coal Board, Mining Department, United Kingdom.

Application of advanced electronic geotechnical monitoring techniques in Australian underground coal mining

I.L. FOLLINGTON
B.Sc. (Hons), Ph.D., M.I.M.M., F.G.S.
Project Manager, CSIRO Div. of Geomechanics
T.P. MEDHURST B.E. (Hons), Grade.I.E. Aust., P.Eng.
Geotechnical Engineer CSIRO Div. of Geomechanics

SUMMARY The application of automated computer controlled instrumentation to the Australian underground coal mining industry is discussed here. The advantages of the utilisation of such advanced technology are described with specific reference to how the data provided by such systems could aid the mining engineer. The availability of this type of data could play a key role in reducing the risk that excavation instability represents to underground coal mining operations. This risk is not only to operational efficiency and profitability but also to the safety of mining personnel.

1. INTRODUCTION

The modern underground coal mine has become a technologically advanced environment with remotely controlled equipment being widely employed. In this world of "hi-tech" the geotechnical engineer is still forced to employ "low-tech" and labour intensive activities to gain any geotechnical information regarding the mining environment.

If the geotechnical engineer could retrieve his field data with the speed and efficiency that production and maintenance data can currently be accessed, then he could respond to "real time" situations instead of the all too often situation of being in the position of telling people what was going to happen after it has occurred.
Indeed, given more rapid access to data, the geotechnical engineer could move more and more into predicting instability, resulting in preventative rather than remedial action being taken. In this way the cause and not the effect could be determined reducing the risks associated with underground coal mining, resulting in the safer and more efficient extraction of underground coal.

2. GEOTECHNICAL PARAMETERS

Some of the key geotechnical parameters for which the coal mining engineer requires data include the following (1):

i/ Roof convergence - The degree and the rate at which roof convergence is taking place in any area of an underground coal mine, be it in roadways, cutthroughs, intersections or bords, is vital information. By monitoring roof convergence the stability of areas can be assessed and the potential risk of failure determined.

ii/ Pillar stability - The stability of coal pillars is fundamental to the success of any underground coal mining activity. Data concerning stress levels and the condition of existing coal pillars would be of great value in optimising pillar design.

iii/ Permanent support behaviour - The condition and effectiveness of permanent support such roof bolts, cables, rib dowels, wooden props etc requires constant monitoring to ensure that excavation stability is maintained as mining proceeds.

iv/ Powered support behaviour - The loading experienced and reaction of the proximate strata around the powered supports, as employed in both longwall mining and bord and pillar with breaker line supports, needs to be constantly monitored to safeguard personnel and maximise extraction.

v/ *In situ* stress field - The stress field in which mining takes place plays a significant part in determining the orientation and design of mining layouts. Any changes in the stress field in response to mining must be well understood if instability is to be avoided.

vi/ Goaf behaviour - The processes of goaf formation and consolidation, the caved and broken strata which remain once coal has been extracted, need to be well understood for any geological sequence if mining is to proceed safely and with minimal risk to personnel.

There are a great many additional parameters of concern to the mining engineer. More efficient collection of data regarding these and other parameters would be of great benefit to mine staff. Almost every facet of underground coal mining activity is reliant upon one or more of these

parameters in determining the degree of risk concerning the safety, efficiency and productivity of any underground coal mining operation.

3. GEOTECHNICAL MONITORING:

There are many disadvantages to the manual monitoring of geotechnical instrumentation. Computer controlled monitoring has become a comparatively widespread practice in other industries and is routinely used to gain data regarding the condition, mode of operation and efficiency of machinery and equipment.
To date this practice has not been widely adopted by the underground coal mining industry in Australia, due in part to the difficulties associated with the development of Intrinsically Safe (IS) equipment.

The complex logistics and geometry of an underground coal mine make the successful manual communication of even the simplest of geotechnical data a difficult and inefficient operation. The speed with which geotechnical data could be relayed directly to the engineer using computerised systems would allow decisions to be better based and more rapid in response to any change in conditions. However, there will alway be the need for first hand observation to accompany any geotechnical data to aid its correct interpretation.

Interruptions in the flow of geotechnical data from an operational underground coal mine can vary from hours to days or even weeks as shifts rotate, priorities change or areas become abandoned. These interruptions to the flow of geotechnical data can result in a delayed response to the onset of instability, with serious repercussions in terms of the risk to both personnel and operations.

In contrast, the uninterrupted flow of geotechnical data from computerised systems would allow new areas of understanding to be developed concerning to nature of the response of the rockmass to mining.

The dynamic nature of underground coal mining operations, relying as they do upon the continual changes in stress distribution, would be best served by a continuous geotechnical monitoring system. The availability of this type of continuous data is the key to improved geotechnical understanding leading directly to greater optimisation of excavation and support design.

The ability to be able to track the development and migration of abutment stress peaks on ribs and coal pillars would greatly assist engineers in planning future mine layouts.

Another advantage of such computerised systems would be the facility to overlay parameters and detect the inter-action between such factors as bolt performance and excavation deformation.

The repetitive nature of any geotechnical data logging activity makes it very time consuming and as a result an expensive component of any mining operation. All too often geotechnical logging activities are 'tacked' on to the duties of non-geotechnical mine personnel, who in addition do not have the time to undertake them correctly. The release of mine staff from the manual logging of instrumentation greatly reduces the cost of such geotechnical monitoring activities, making them far more cost effective.

Any form of monitoring, and in particular long term activities such as those commonly undertaken in geotechnical monitoring, requires not only accuracy but precision in terms of the readings taken. People are notoriously bad at caring out such tasks and generally suffer a high error rate. The removal of the human link in the chain greatly reduces the error rate, with the result of far higher quality data being available to the engineer.

Working in an environment as hostile as an underground coal mine invariably requires personnel to enter hazardous areas in order to retrieve geotechnical data. As a direct result of this, either mine personnel are exposed to unsafe conditions or the data is not retrieved. Computerised monitoring systems enable data to be safely retrieved from hazardous areas without the need for personnel to place themselves at risk.

Perhaps the most serious disadvantage of manual monitoring is the inevitable situation of having highly qualified and expensive mine personnel solely employed in undertaking simple and repetitive measurements. This is often the case making it difficult, for many of the reasons outlined above, to safely entrust such duties to less well qualified or more junior personnel. If these highly trained personnel were released from the tedious logging activities by the utilisation of automated systems, then they would have more time to analyse data and observe changes in conditions.

4 CSIRO ADVANCES IN INTRINSICALLY SAFE GEOTECHNICAL INSTRUMENTATION:

Rather than produce a range of independent monitoring systems, each addressing specific areas, the Division aim to develop a range of Intrinsically Safe (IS) instrumentation that is compatible and able to address the geotechnical parameters affecting underground coal mines. The Division have made a number of major technical advances towards

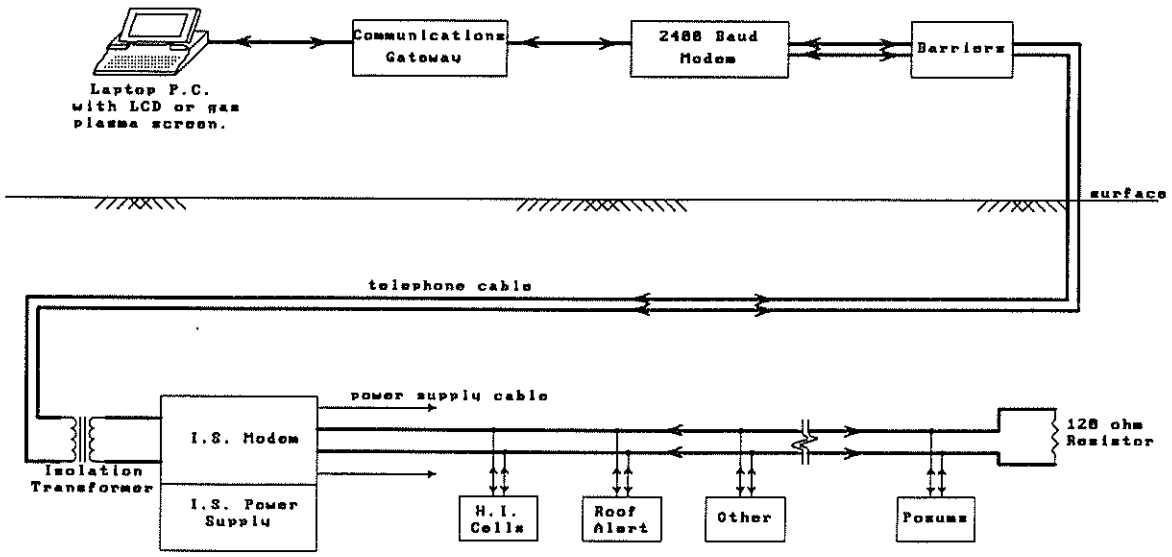

Figure 1 Schematic of Geomon - Geotechnical Monitoring System

providing sensors and monitoring systems able to address this problem.

The 'backbone' to the geotechnical monitoring system is an IS communication network, Geomon, which can link underground instrumentation directly to the surface. Geomon can link a range of geotechnical sensors from underground to a surface PC via the mine telephone system, Figure 1.

The original concept of Geomon can be generally summarised in the following six points:

- To be Intrinsically Safe
- To be a "universal" system (i.e. to have as wide a compatibility as possible)
- To utilise existing mine telephone systems
- To be able to span up to 2km from underground telephones
- To be able to monitor in real time
- To be able to interface with a standard PC

This system, together with a range of sensors which enable roof stability, stress fields and permanent and temporary support performance to be monitored, were developed under a three year National Energy Research Development and Demonstration Council funded project (2).

Roof Alert (3) is an IS sensor developed by CSIRO to monitor strata deformation. Roof Alert is an 'intelligent' extensometer with either one or two reference points. The device incorporates a programmable microchip and an internal clock which enables the rate of deformation to be determined continuously. The microchip allows the engineer to control a number of functions of the instrument including; the reading rate, the rate of deformation display, alarm levels and staging of alarms. The one reference point version, Roof Alert I, measures and displays the total strata movement between the anchor and the display head. The two anchor version, Roof Alert II, can measure and display the strata movement for two reference anchors, enabling strata movement both within and above a reinforced horizon to be determined, Figure 2.

An IS interface unit, Intermon, has been developed by CSIRO, for use with Geomon, to enable strain gauge based devices such the CSIRO Hollow Inclusion Cell to be logged remotely in the underground coal mine environment.

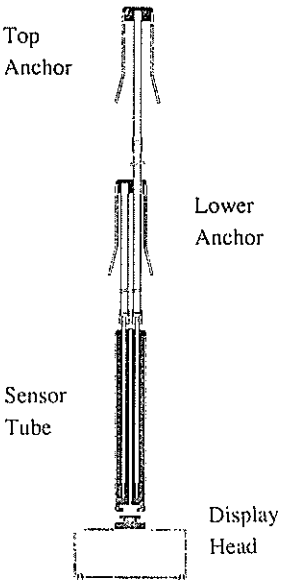

Figure 2 Mechanical Drawing of Roof Alert II

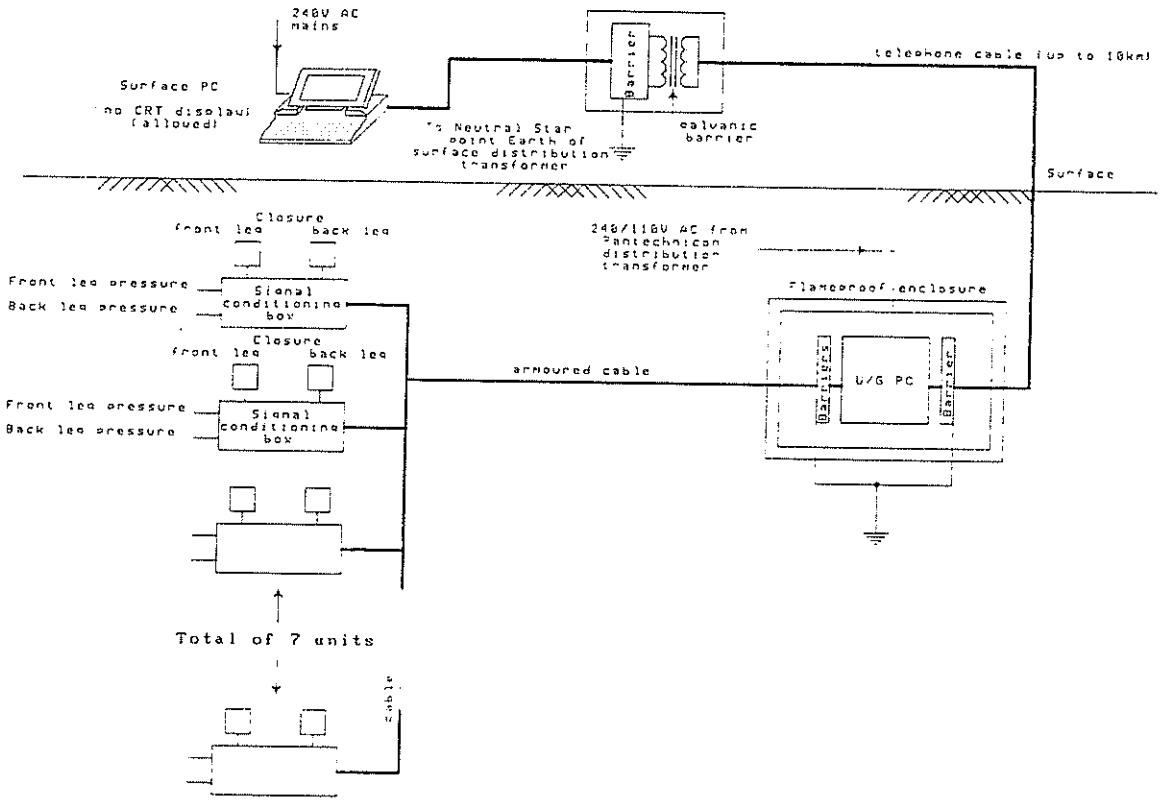

Figure 3 Schematic of Posums - Powered Support Monitoring System

Intermon can be used to monitor any strain gauge based device with a high degree of accuracy and with low drift for long periods. It would find ready application in monitoring instrumented roof bolts for example.

The Division have also developed monitoring systems under the same project which are able to monitor the behaviour of powered supports during normal mining operations, Figure 3. This type of system, when coupled with geotechnical sensors, can provide a more comprehensive 'picture' rather than piecing together of pockets of manually obtained data.

5. CONCLUSIONS AND RECOMMENDATIONS:

The use of a mine wide monitoring system such as Geomon enables geotechnical data to be gathered and processed in a way not currently available in Australia and as a result yield information to mine staff not presently available. There are many potential benefits to continuous access to information of this type, some of these are noted below.

- Once a mine wide network of geotechnical sensors were established it would be possible to identify "hotspots" in terms of instability, stress concentration, anomalous support behaviour etc. This would enable better, faster and more efficient allocation of resources to address any instability problems.

As data is collected regarding specific parameters for areas of the mine complete and detailed histories can be developed giving engineers insight into the longer term response of the rockmass to coal mining. This type of information would be particularly pertinent to coal pillar design.

The ability to track specific parameters from 'further out' will give engineers advance warning of problems enabling preventative rather than remedial action to be taken. This would greatly reduce the risk of the onset of serious instability threatening operations and personnel .

The adoption of geotechnical monitoring systems of the type described in this paper would also enable multiple parameters to be considered together resulting in improved understanding of the inter-relationship of geotechnical parameters. This improved understanding would manifest itself in improved mine layout, extraction techniques and support design.

All of the above, and the many additional benefits, would greatly contribute to reducing the risks associated with underground coal mining through the optimisation of

mining techniques and support design, increasing safety in Australian underground coal mines.

6. ACKNOWLEDGMENTS

The support of other CSIRO staff for the work described in this paper is acknowledged and into particular the efforts of Ian Hutchinson and David Hainsworth. The financial support of the National Energy Research Development and Demonstration Council is also gratefully acknowledged.

7. REFERENCES

1. Australian Coal Mining Practise. Monograph 12, AusIMM, 1986.

2. Mallett, C.W., Garritty P. and Follington I.L.(1990). Roof Strata Alert Monitoring. NERDDC, End of Project Report, Project No. 1103, Dec. 1990.

3. Follington I.L. and Hutchnison I.N. (1991) An intelligent electronic roof convergence monitoring system for underground coal mines. International Conf. on Reliability, Production and Control in Coal Mines, Wollongong, NSW, Aust., Sept. 1991.

Back Analysis of a Deep Excavation in Soft Clay

A.T.C. GOH
B.E., Ph.D., M.I.E.AUST
Lecturer, Swinburne Institute of Technology, Melbourne
K.S. WONG
B.E., M.S., Ph.D.,
Assoc Prof, Nanyang Technological University Singapore
N.PREBAHARAN
B.E., M.S.,
Graduate Student
University of Western Ontario, Canada

SUMMARY The construction of the Marina underground station and tunnels is described. The construction involved the construction of a series of cofferdams and submerged excavation of the soil. Back analysis were carried out using the finite element method in which the soil is modelled by a nonlinear, hyperbolic stress- strain relationship.

1. INTRODUCTION

One of the more complex projects in the construction of the mass rapid transit system in Singapore was the construction of the Marina Bay station and tunnels. The complexity of the site conditions made conventional excavation methods uneconomical. Consequently, an unusual method of temporary works was adopted. This involved the construction of a series of cofferdams, followed by submerged excavation of the soil. In this paper, the construction technique used and the back-analyses using the finite element method are described.

2. SITE DESCRIPTION

The site is located close to the central business district,in the southern end of Singapore. A plan view of the site is shown in Figure 1, together with a generalized soil profile of the site. With the exception of the marine inlet (Telok Ayer Basin) at the northern end, the site is covered with a recent deposit of 8m to 12m of hydraulic sandfill. Underlying the sandfill were two layers of soft marine clay, with a total thickness of between 25m and 35m. Measurments indicate that the consolidation of the marine clay due to the load from the sandfill is still not complete. The lower clay layer was underlain by the Old Alluvium which comprised of interbedded strata of dense to very dense sands and hard clays. A typical boring log of the site is shown in Figure 2.

3. CONSTRUCTION DETAILS

Apart from the difficult ground conditions, the other major constructional constraints were the construction of the station immediately below the eight lane expressway and adjacent to a four lane underpass as illustrated in Figure 1, and the requirement that the Telok Ayer Basin had to have a minimum opening of 25 m at all times to prevent pollution through stagnation and to permit storm water runoff through the basin to the sea.

The complexity of the site conditions, the tight time constraints and the required excavation to depths of the order of 15 m to 18 m, made conventional excavation methods uneconomical. The conventional strutted excavation technique would have required the use of very heavy sheetpiling or diaphragm walls, extending down to the firm Old Alluvium layer. The alternative method of ground treatment of the weak clays was also ruled out because of the large volume of soil to be treated. Consequently, an unusual method of temporary works was adopted, involving the construction of a series of cofferdams using heavy composite sheetpile sections. Base stability of the excavation was achieved by flooding the cofferdams and excavating underwater.

The construction involved the following stages as illustrated in Figure 3 :

Stage 1 - Sheetpiles were driven 2 m to 3 m into the intermediate stiff clay layer with the top protuded 2 m above the ground level. High modulus sheetpiles were used and were fabricated at the site using pairs of IBXN Frodingham sheetpile sections welded to a 610 x 305 x 149 kg/m I-beam using the submerged arc technique. The sandfill was then excavated and two levels of struts were installed, one at the ground level and the second at a depth of approximately 7 m below the ground level. Each strut comprised of battened twin I-beams, and bracings were installed between the two levels of struts.

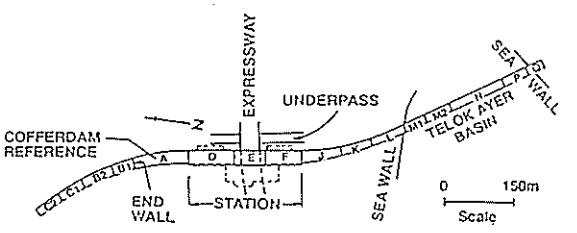

Site Plan

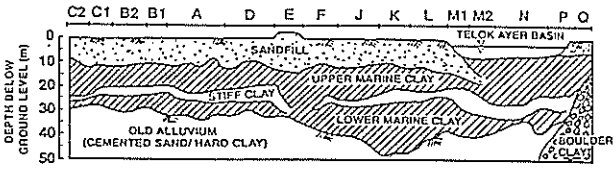

Figure 1 Site plan and generalized soil profile at Marina Bay (After Clark and Prebaharan, 1987)

Stage 2 - The cofferdam was then filled with sea water up to the top of the sheetpiles and the remaining excavation was carried out underwater using clamshells as well as waterjetting and airlifting methods. The sheetpiles were extended 2 m above the ground level in order to increase the stabilizing water pressure on the walls and the base of the excavation. The bored piles which were used to support the station and tunnels were then installed using Reverse Circulation Drilling machinery.

Stage 3 - On completion of the bored piling, the excavated formation was levelled using a layer of sand, prior to casting the 1.5 m thick unreinforced tremie concrete slab. The sand layer also served as a drainage path to pressure relief pipes which were installed prior to casting the slab. The water was then pumped out of the cofferdam under close monitoring. The station base slab and walls were then constructed, followed by the installation of the internal strut for the station walls. Partial backfilling and the removal of the lowest sheetpile strut were then carried out.

Stage 4 - The remaining permanent concrete works for the station were then constructed, followed by backfilling and removal of the remaining struts. Construction of the tunnels was similar to that of the station except that the entire construction took place below the second strut.

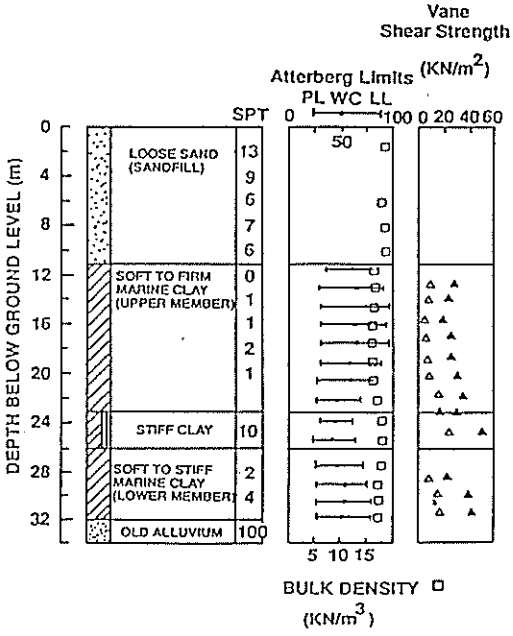

Figure 2 Typical bore log (After Clark and Prebaharan, 1987)

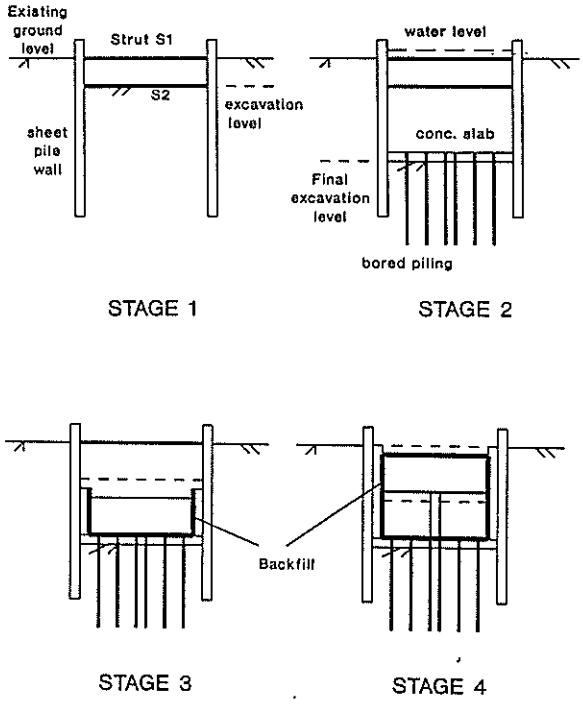

Figure 3 Construction sequence

4. METHOD OF ANALYSIS

The finite element method was employed to perform the back analysis. The plane strain finite element program essentially followed the formulations of Duncan and Chang (1977). The programme had been used successfully in other deep excavation problems in Singapore involving sheetpile walls (Broms et al., 1986) and diaphragm walls (Goh et al., 1988). In the analysis, the stage-by-stage excavation of the soil, installation of struts, flooding and dewatering were simulated. One dimensional bar and beam elements were used to model the struts, wall and other structural members, while four-noded isoparametric elements were used to model the soil. The 1.5 m thick base slab was modelled using one strut at the top and another at the bottom of the slab. The nonlinear stress-strain behaviour of the soil was approximated using the hyperbolic model developed by Duncan et al. (1980) in which the tangent modulus E_t is related to the initial tangent modulus E_i by the relationship

$$E_t = (1 - S_L R_f)^2 E_i \quad (1)$$

and

$$E_i = K.p_a.(\sigma 3/p_a)^n \quad (2)$$

where S_L is the average stress level of the soil element, R_f is the failure ratio, K is the modulus number, n is the modulus exponent, $\sigma 3$ is the minor principal stress and p_a is the atmospheric pressure. The shape of the hyperbolic curve describing the soil nonlinear stress-strain behaviour is governed by the value of R_f. Soils with low R_f values display brittle behaviour while soils with high R_f values exhibit plastic behaviour.

5. FINITE ELEMENT RESULTS

The cross-section of the mid-section of one of the cofferdams, Cofferdam D, was selected for the finite element analyses. The symmetry of the cross-sections enabled half the cross-section to be modelled. Figure 4 shows the finite element mesh used. Table 1 depicts the relevant soil parameters adopted, based on the site investigation data.

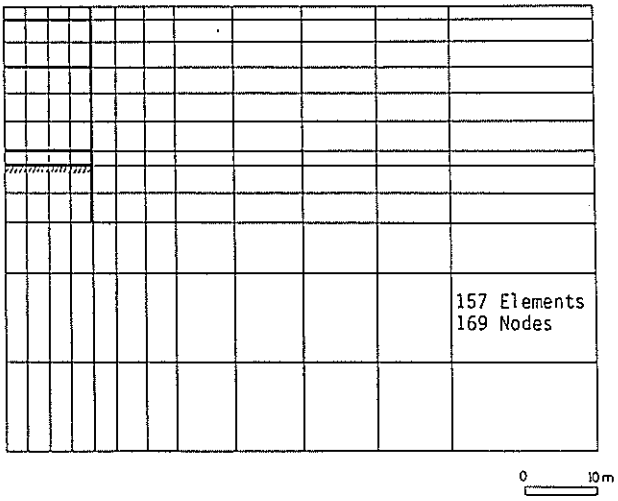

Figure 4 Finite element mesh

For the marine clay, the undrained elastic modulus/undrained shear strength ratio was taken as 300.

Table 1 Summary of soil properties

	K	n	μ	γ	R_f	c_u	Φ
Sand Fill	150	0.6	0.32	19	0.7	0	32^o
Stiff Clay	180	0	0.49	19	0.7	60	0
Old Alluvium	640	0	0.49	19	0.7	160	0
Marine Clay	$3c_u$	0	0.49	16	0.9	4.0+ 1.25z	0

μ = Poisson's ratio γ = Unit weight (kN/m^3)
c_u = undrained shear strength (kPa) Φ = friction angle
z = depth from ground surface (m)

The finite element results were compared with the actual instrumented data at two excavation stages - at the end of excavation (prior to dewatering) and at the end of dewatering. The results of the analyses showed reasonable agreement with the field results as shown in Figure 5 and Figure 6. The most critical stage of the excavation corresponded

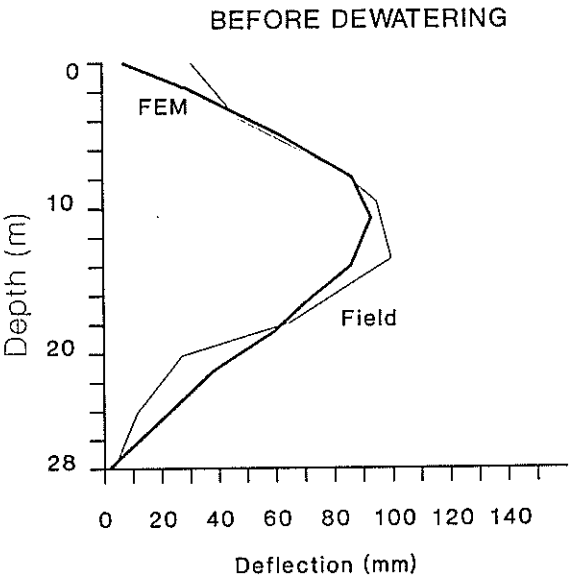

Figure 5 Comparison of field and finite element results for Cofferdam D (before dewatering)

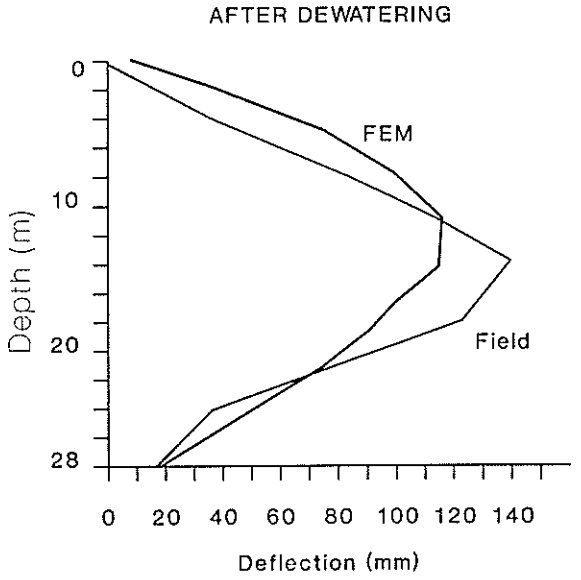

Figure 6 Comparison of field and finite element results for Cofferdam D (after dewatering)

to the end of the dry excavation stage, when the potential for basal instability was highest. This is clearly shown in Figure 7, which illustrates the computed wall deflections at 3 stages - at the end of the dry excavation, before dewatering and after dewatering. The wall deflections were largest at the end of the dry excavation. The flooding of the cofferdam reduced the wall movements during the subsequent submerged excavation. Following the dewatering, the wall again moved inwards towards the excavation.

Some parametric studies were also carried out to assess the effects of the soil properties on the wall behaviour. The properties of the marine clay were found to be the most critical. Doubling the undrained shear strength of the marine clay resulted in a reduction of the maximum wall deflection by about 28% and a decrease in the maximum bending moment by about 22%, at the end of dewatering. The effects of increasing the water level to a height of 4 m above the ground level was also investigated. This resulted in a

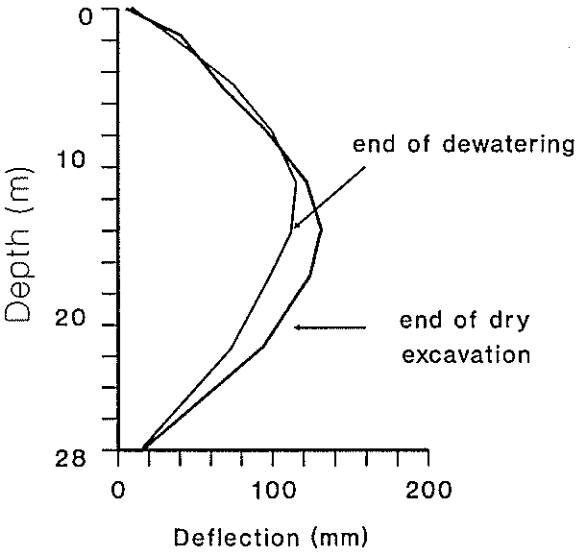

Figure 7 Computed wall deflections

reduction in the maximum wall deflection of about 8 %, at the end of excavation.

Comparisons were also carried out on the effects of alternative construction techniques. Two separate analyses were also carried out assuming conventional excavation with 6 levels of struts (at 3 m depth intervals) as shown in Figure 8. Firstly, the analysis was carried out assuming the same wall stiffness properties as the sheetpiles used in the submerged excavation technique. Secondly, the wall stiffness was increased by a factor of 10. The analysis carried out assuming the same wall stiffness properties indicated that the maximum wall deflection was about 45% larger than the deflections from the submerged excavation method case. In order to reduce the wall deflections to about the same magnitude as that obtained from the submerged excavation, the wall stiffness would have had to be increased by about 10 times, as illustrated in Figure 8.

The computed wall bending moments are shown in Figure 9 for the end of the dry excavation, after dewatering, and for the conventional excavation with 6 levels of struts. The maximum moments at the end of the dry excavation and at

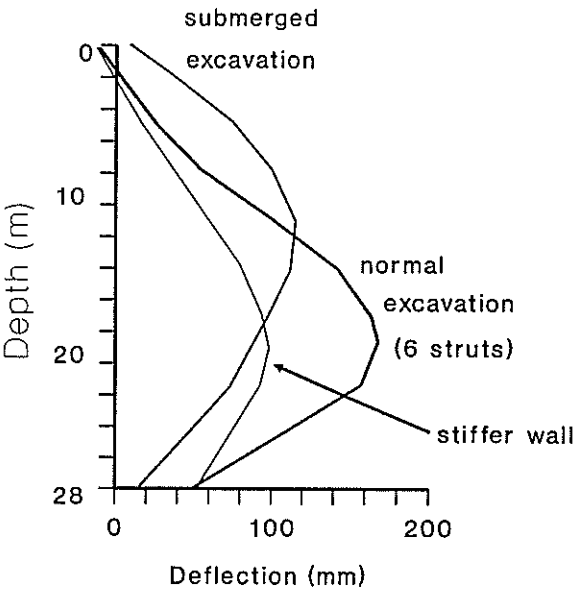

Figure 8 Comparison of wall deflections

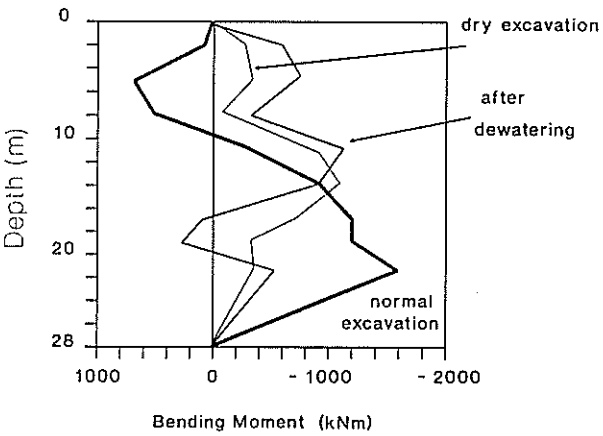

Figure 9 Computed bending moments

the end of dewatering were of the same order of magnitude. The high moments at the end of the dry excavation stage was a consequence of the large toe-in, when there was about 17 m of wall embedded below formation. About 48% larger bending moments were obtained for the conventional excavation technique in comparison with the end of dewatering stage. If the stiffer wall was used in the conventional excavation, the analysis indicated that the bending moments were about 4 times larger than the submerged excavation analysis.

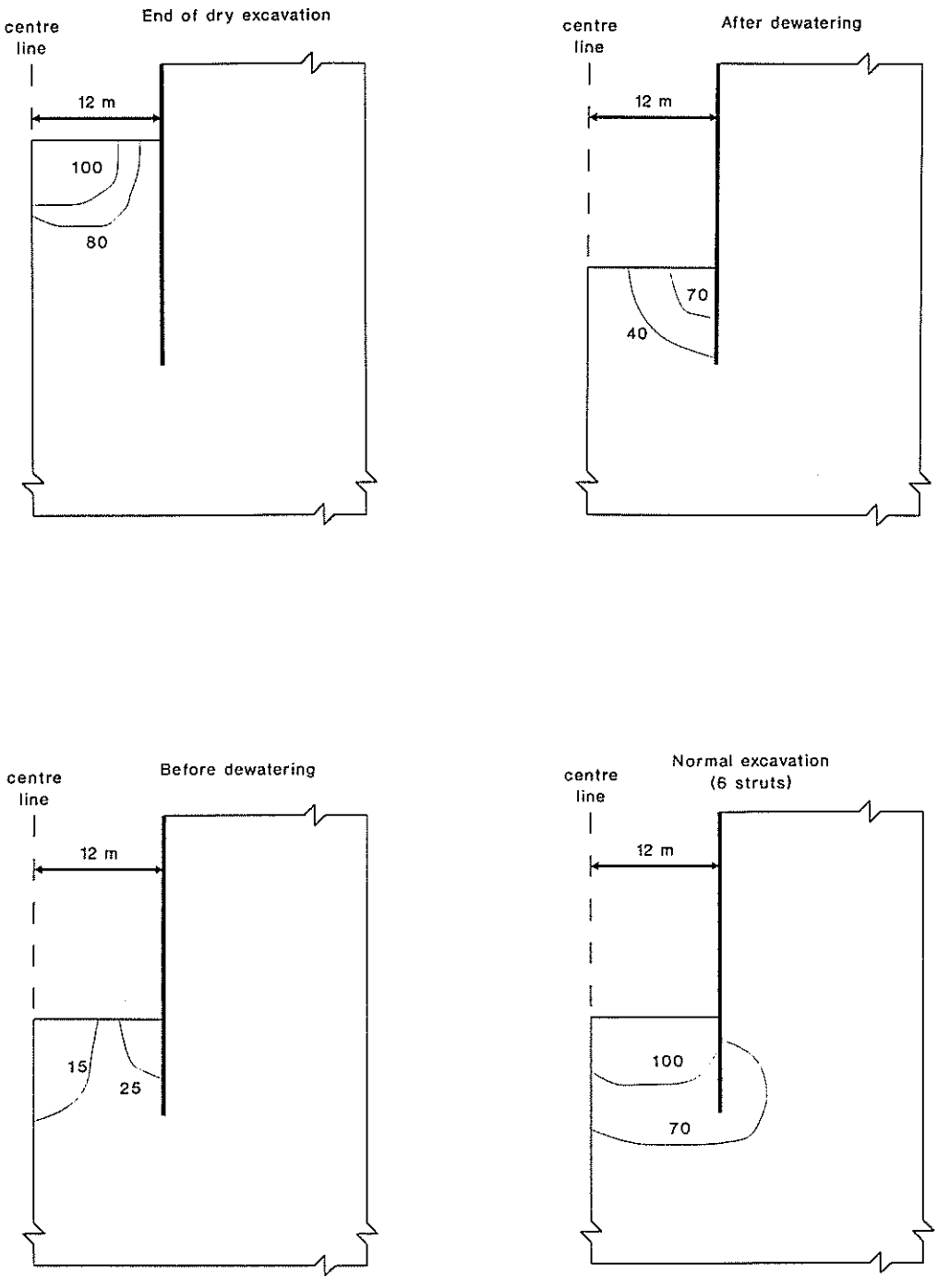

Figure 10 Stress-level contours

The stress-level contours of the soil elements in front of the wall toe for three stages of the submerged excavation analysis and the conventional excavation analysis are shown in Figure 10. The results again confirm that for the submerged excavation technique, the most critical stage occurred at the end of the dry excavation. The results indicate that some of the soil elements beneath the excavation had failed (stress-level of 100%) or were close to failure. The flooding of the excavation with water reduced the stress-levels in the soil elements beneath the excavation to less than 25%. The dewatering resulted in higher stress-levels in the soil elements but these were smaller than at the end of the dry excavation stage. This is likely to be because the construction of the 1.5 m concrete slab assisted in minimising the lateral wall movements and heave of the excavation. The analysis carried out simulating the conventional dry excavation with the same sheetpile stiffness and 6 strut levels indicated a significant portion of the soil beneath the excavation to be at failure. This lower basal stability resulted in significantly larger wall movements in comparison to the submerged excavation technique as indicated earlier in Figure 8.

6. CONCLUSIONS

Comparison of the observed behaviour with the behaviour predicted by the finite element analyses showed a reasonable agreement. The finite element method is an invaluable aid which can be used to assist in the design, particularly for complex problems for which conventional analytical solutions are unavailable. Studies can be carried out on various wall systems and effects of the variability of the soil conditions, at acceptable costs, to determine the critical factors which affect the behaviour of the wall. The wealth of field data that has been collected in the last few years from the construction of the mass rapid transit system in Singapore has provided an unique opportunity to increase understanding about the finite element method and its application to deep excavations in soft clay. This study and the previous analyses by Broms et al. (1986) and Goh et al. (1988) indicate that for deep excavation problems in Singapore, the soil non-linear stress-strain behaviour can be adequately represented by the hyperbolic model developed by Duncan et al. (1980).

7. REFERENCES

Clark, P.J. and Prebaharan, N. (1987). Marina Bay Station, Singapore, Excavation In Soft Clay. Proceedings of the 5th International Geotechnical Seminar on Case Histories in Soft Clay, Singapore. pp. 95-107.

Duncan, J.M. and Chang, C.Y. (1977). EXCAV : A Computer Program For Analysis Of Stresses And Movements In Excavations, Analysis Of Soil Movement Around A Deep Excavation. University of California, Berkeley, Department of Civil Engineering, Geotechnical Engineering Research Report No. TE77-4.

Broms, B.B., Wong, I.H. and Wong, K.S. (1988). Experience With Finite Element Analysis Of Braced Excavations In Singapore. Proceedings of the 2nd International Symposium on Numerical Methods In Geomechanics, Belgium. pp. 1-16.

Goh, A.T.C, Wong, K.S. and Burchell, A.J. (1988). Behaviour Of A Diaphragm Wall With Top-down Construction Method. Proceedings of the 5th Australia-New Zealand Conference on Geomechanics, Sydney. pp. 128-132.

Duncan, J.M., Byrne, P., Wong, K.S. and Mabry, P. (1980). Strength, Stress- strain And Bulk Modulus Parameters For Finite Element Analyses Of Stresses And Movements In Soil Masses. University of California, Berkeley, Research Report No. UCB/GT/80-01.

Residual Rock Bursting in the Homer Tunnel, Fiordland N.Z.

F.R. GORDON
B.Sc., A.O.S.M., F.AUS.I.M.M.
Principal, Gordon Geological Consultants

SUMMARY Explosive rock spalling following the excavation of the Homer Tunnel in 1953 required urgent analysis and remedial measures before public use of the tunnel was possible. The bursts were confined to areas of strong massive brittle rock located between zones of shearing and jointing. Residual stress locked in from past geological events and released by the excavation of the tunnel was assessed as the probable cause, and the rapid elimination of spalling and of rock falls over four years appeared to confirm that judgement.

The tunnel is located in an area where unusual geological events have occurred in comparatively recent time, including massive offsetting and uplift exposing deep seated crustal rocks. The stresses causing the problem are considered to have been the resultant of the uplift and the erosion of some 18kms of rock in the last 6 Million years which has left high horizontal stresses locked in while the vertical component has decreased in accordance with the present overburden thickness.

1. INTRODUCTION

The Homer Tunnel was constructed by the N.Z. Public Works Department (PWD) between 1934 and 1953 to give road access to Milford Sound. The country between Lake Te Anau and the Sound is rugged and mountainous with peaks between 1520m and 2740m with their lower slopes covered with dense bush. Profound glacial valleys up to 800m deep, now occupied by rivers, provide the route for the highway except at the divide where the Homer Tunnel penetrates a razorback ridge formed by glacial cirques between the Upper Hollyford and Cleddau valleys (Figure 1). The east or Homer portal (914m RL) was located well above the valley floor to reduce the length through bouldery scree, and the tunnel descends at a grade of 1 in 10 to the Cleddau portal, a distance of 1275.4m. Because of the lack of wharf facilities at Milford and the inaccessibility of the western portal, the tunnel was driven downgrade from the east. No seepage problems were expected. The two-way road tunnel was designed as a semi circular section 7.31m in diameter with the centre 1.52m above floor level.

2. HISTORY OF CONSTRUCTION

Details of the tunnel and the early stages of construction of a pilot heading are given in a paper by White (1947), and aspects of the enlargement are discussed by Hart (1952) and by Downer (1977). The full story of the tunnel construction and the numerous vicissitudes that occurred from water entry, isolation by snowfall, dry snow avalanches, (described in a classical paper by Smith, (1947), and from rock spalling constitutes a saga that remains to be written.

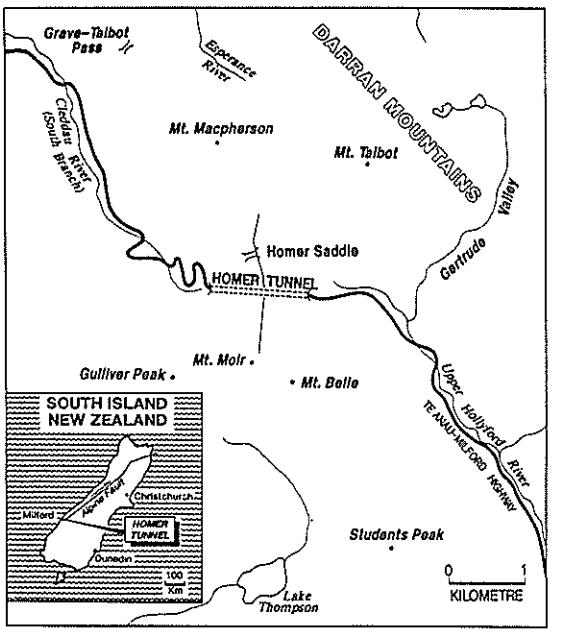

Figure 1 Locality Plan

The following is a summary of the progress of construction:-

Dec, 1934 Pick and shovel work at Homer Portal.
Jun, 1936 Rock excavation started with heading and bench.
May, 1937 Fatalities from dry snow avalanche, work ceased, 143m completed.
Nov, 1937 Downer & Co. started bottom

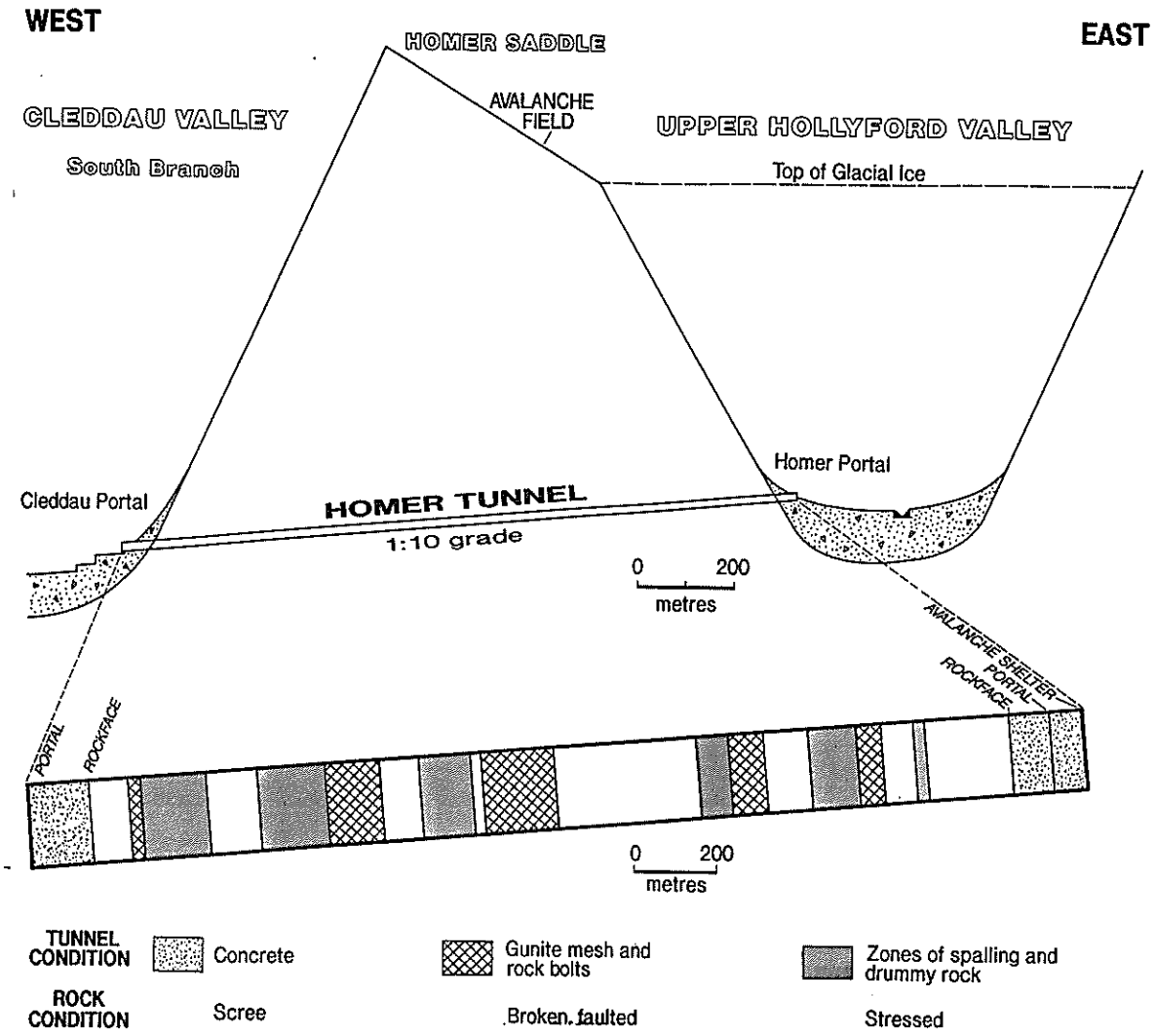

Figure 2 Long section showing rock and tunnel conditions

heading (3.96m x 2.7m).

Mar 1940 Cleddau scree penetrated, enlargement started.

Mar 1941 Ring drilling, 18 holes per ring, 0.76m apart.

Mar, 1942 Work suspended "for the duration".

Mar, 1951 Enlargement recommenced by Downer & Co. Rock spalling.

1953 Work completed.

1954 Tunnel opened to public, with winter closures.

1984 Closures minimized, avalanche warning system.

3. GEOLOGY

THe Homer Tunnel is located in the rugged Darran Mountains which are formed of the Darran Complex of leucograbbro, norite, granite, and diorite. The tunnel itself is driven in a brown biotite norite, (biotite leucogabbronorite) which often exhibits a rudely gneissoid structure, and has cataclastic properties with internal evidence of compressive stress. Numerous vertical pegmatite veins or dykes striking southwesterly and occupying tensional rents are present in the tunnel. Small dykes of dark green hornblende also occur.

The Darran Complex shows extensive areas of intrusive breccia, where new magma has invaded and split up and shattered older rock, then cooled and solidified only to be invaded and split up again. (Blattner & Coates, 1989). The igneous complex was formed between 230 and 100 million years ago beneath the continental margin of Gondwana. Late Cenozoic deformation has affected the area with horizontal offsetting of 480 kms on the Alpine Fault, and in the last 6,000,000 years the area has been gradually uplifted by some 18km, with an equivalent amount of erosion (Suggate, 1963). The last major geological event, some 20,000 years ago was glaciation, with a reshaping of the land and the emplacement of glaciers upto 800m deep. Melting of the ice occurred during the Last Interglacial, 18,000 to

13,000 years before present.

Significant tectonism and seismicity is still occurring associated with the Alpine Fault some 30kms northwestwards of the tunnel.

4. ENGINEERING GEOLOGY

4.1 Groundwater

Because the tunnel is some 400-460m below the Homer Saddle, it was not expected that there would be any problems with water. However slow water seepage was encountered along most of the length of the tunnel with flows contained in shears or faults several places, with two strong inflows of up to 7.6 l/s.

4.2 Jointing and Stability

Jointing in the tunnel walls is variable, with some massive areas devoid of joints, and other zones of close jointing, shearing and faulting in places giving zones of soft fault breccia. Several areas of horizontally jointed rock were met where roof slabbing was dangerous and required support, and timbering had to be used over about 30m of the pilot heading. The full tunnel section contained five main zones of rock breakage over about 210m where remedial works in the form of gunite, mesh and bolts had to be installed (Figure 2). The rock at the Cleddau end, over about 80m was notably weaker and more broken by jointing than elsewhere (White, 1947).

4.3 Rock Spalling in the Heading

The pilot heading encountered several zones where the rock was obviously under stress. Spalling of the rock took place with a crack like a rifle, and fragments were shot across the tunnel with considerable velocity. These effects were observed immediately following rock excavation. (White, 1947)

4.4 Problems during Tunnel Enlargement

During tunnel enlargement, the strain bursts usually began soon after a round was blasted although in some instances the explosive spalling held off for several hours, or longer (Hart, 1952). Once started, noise and spalling continued for an hour or two, and then became quiescent. In some areas periods of activity occurred several weeks after blasting and excavation had been completed. In other areas quiet spalling producing onion skins of rock occurred with the slabs falling either singly or in mass. In these areas the roof shape tended to assume the shape of an acute arch with the apex of the arch gradually getting higher as spalling continued. (Hart, 1952)

Immediately a slab spalled off, the underlying rock face was smooth and solid, yet a few hours later it sounded drummy with a new slab detaching itself, then bulging outwards, until eventually it projected from the walls with explosive force (Figure 3). The spalled slabs were tabular and lenticular, usually of dinner plate size or larger. The edges were normally thinner than the centre, and they could not be fitted back to the spalled face as the shape had changed in response to the stresses. The inner surface of the detached slab surface was partially coated with powdered rock. (Gordon, 1953)

4.5 Geotechnical Reconnaissance

A geotechnical reconnaissance of the tunnel was made in October 1953. Logging of the areas of spalling was done initially by noting areas of fresher surface in the dust-covered rock. Measurements were made of rock falls and spalls, noting the number of pieces and their size, shape and the location and position. These records were continued annually in three phases (i) at the end of the winter closure, (ii) following barring down from a mobile platform before summer opening and (iii) during summer when new falls and spalls were recorded as they were removed during maintenance. It was found that stress spalling was confined to areas of massive unjointed rock, and this applied to the locations of violent spalling that had been recorded during enlargement.

A progressive record was made of spalls, falls and drummy roof areas and this showed six areas of concentrated distress (Figure 2). These areas were upto 30m wide, and were separated by areas of jointed, faulted and sheared rock which contained the sections that had to be secured by bolting, mesh and gunite following enlargement. Parts of two of the active spalling zones in the roof were given a gunite cover immediately after excavation, and no further activity was experienced in these areas. (Hart, 1952)

The incidence of spalling from the walls and roof decreased sharply over a period of a year, and detailed monitoring was ended after four years when the spalling had practically ceased.

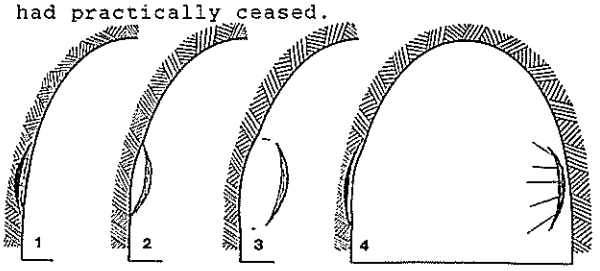

Figure 3 Explosive Rock Spalling

5. EVALUATION OF GEOTECHNICAL RISK

At the completion of the enlargement of the tunnel, the P.W.D. had to face a problem of public safety if spalling continued unabated or even intermittently. Dry snow avalanches were bad enough, but they could be avoided by closing the tunnel during the winter.

Plates of rock exploding off the walls or accumulated layers falling from the roof could possibly close the tunnel for years. The long desired road access to Milford which was a political promise close to reality had to be evaluated in terms of geotechnical risk. At the time (1953) the science of rock mechanics was in its infancy, and little was known about the tectonic history and geology of the area.

An urgent consensus of ideas on cause, risk, control or avoidance was sought. Evaluations were made by the leading engineers of the P.W.D., by the District Inspector of Mines, by an experienced, engineering geologist, H. E. Fyfe of NZ Geological Survey, and by the writer, who had just completed the geotechnical reconnaissance. A most hopeful sign was that the views of the two engineering geologists were similar, and this unprecedented situation along with the reasonable arguments that were presented about the possible causes lead to a quick but considered decision. Because of the isolation of the two periods of spalling in the pilot heading and in the full tunnel, and the obvious attenuation with time, residual stress release was considered to be responsible for the problem and the risk was therefore considered to be a short term one as the locked-in stresses had been largely released. Careful monitoring, inspection and continued barring-down were prescribed during the then winter closures and the tunnel was opened, as promised, to the public in 1954. Since that time there have been no major problems with spalling rock.

6. SHALLOW ROCK SPALLING PHENOMENA

In the marble quarries of Vermont, USA, channelling in the faces occasionally disturbed the stresses sufficiently to produce fractures with enough violence to throw the channelling machines, weighing several tonnes off their tracks. These "grassroot" stresses were considered residual. (Bain, 1931) Similarly, in the granite quarries at Barre, Vermont, residual stresses correlated to geological pressures that had acted at the close of the Tertiary, affected the excavation of blocks. (White, 1946). At Franklin Furnace Mine (N.J.) rock bursts, at the 180m level were sufficiently powerful to overturn loaded ore cars.

Skin spalling occurred at the bottom of the excavations for foundation of the Coulee Dam, almost at ground surface. Excavation had been proceeding for some depth but no satisfactory bottom was encountered as stress relief formed another loose layer of rock - rather like the skin of an onion. C.P. Berkey on acquaintance with the problem stopped further excavation and the dam was satisfactorily founded on confined (solid) rock.

Rock spalling occurrences at the Delaware Aqueduct which was part of the New York Water Supply Tunnels were noted at 160m beneath the surface, but trouble did not become continuous until a depth of over 300m was reached. Bird (in Bucky, 1942) has described various shallow rock spalling phenomena in the tunnel which were characterized by name - air slaking, working rock, springing rock, spalling rock, popping rock, and bursting rock, but he concluded that the occurrences were varying intensities of the same cause. The description of the Delaware Aqueduct rock bursting given by Bird is almost identical with the occurrences recorded at the Homer Tunnel.

At the New Victoria Dam Site on the Darling Scarp near Perth, Western Australia, spalling of fresh granite surfaces occurred some 3 to 6 weeks after the excavation of some 4-6m of weathered rock and overburden (Gordon, 1991). Spalling occurred only in massive areas, where the dominant rock structure was provided by sheet joints subparallel to the topography. Prominences or domes were favoured locations, and the detachment of the disc-shaped slabs was accompanied by audible noise. The stresses appear to be locked in or incipient sheet joints, released by excavation unloading.

7. STRESS IN ROCK MASSES - TERMINOLOGY

The actual stress at any point in a rock mass is the resultant of the stress caused by engineering activities (Induced stress), and the stresses present in the rock mass before these activities started. The latter stresses are referred to as Natural stresses, and can be conveniently divided into four:- (i) Gravitational stress which is due to the weight of superincumbent rock, (ii) Tectonic stresses due to the active present day straining of the earths crust, (iii) Latent stress which is due to other natural causes such as swelling rocks, thermal stress, topographic stress and mineralogical stress, and (iv) Residual stress. According to Denkhaus (1967), residual stresses are systems of stress in equilibrium or approaching equilibrium in the interior of a body, resulting from the whole stress history of the region. This can include past tectonic stress, geological loading from sedimentation or volcanic activity, and unloading stresses caused by erosion or denudation or by ice melting. Residual stress systems are thus a property of the rock material. Voight (1967), used an analogy of different springs in tension and compression clamped in a common yoke, a system shown diagrammatically in Figure 4.

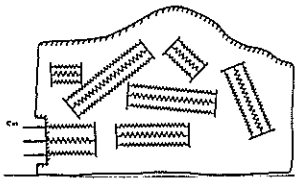

Figure 4 Residual Stress as a system of springs

Residual stress becomes important when the boundary of a stress system is cut in the course of excavation. The locked in residual stresses are released, and either gradual or violent movement occurs. Tensile straining, spitting, flaking or strain bursting at a face are manifestations of such residual energy releases.

The terminology used in this paper, illustrated in Figure 5, is expanded from that proposed by Beilenstein and Barron (1971).

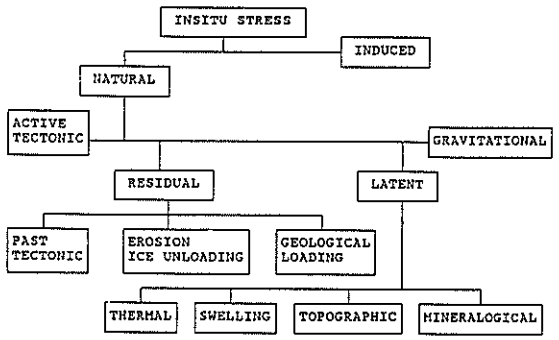

Figure 5 Terminology of Rock Stress Causes

8. POSSIBLE CAUSES OF SPALLING

All types of natural stress as indicated in Figure 5 were considered as being possible causes for the spalling in the Homer Tunnel:-

8.1 Gravitational Stress. The overburden consists of some 460m of igneous rock and seasonally the presence of snow and ice. The vertical normal stress (Oz) is assumed to be given by the unit weight of rock (Y) multiplied by the depth (Z) below the surface. Oz = YZ. The horizontal normal component of stress is given by

$$Ox = Oy = \frac{V}{1 - v} Oz$$ where V is Poissons ratio

Rock will not fail in the walls of the tunnel until the circumferential stress becomes equal to the unconfined compressive strength of the rock. Normally the circumferential stress does not exceed twice the overburden pressure (Terzaghi, 1946).

The ratio between the horizontal pressure and the vertical load depends primarily on the geological history of the rock. Anisotropy can have a considerable influence on the size and directions of local principal in situ stresses. In a folded, eroded or intruded rock mass the horizontal pressure depends in part on whether the forces have already disappeared or whether they are still stored, as in a spring, ready to be released.

8.2 Denudation may reduce the vertical stress, while the horizontal stress is reduced by a lesser amount leading to in-situ states of stress with high values of the ratio of horizontal to vertical stress, particularly at shallow depth. Voight, (1967) has presented a mechanism for unexpectedly large horizontal near-surface stress components having been locked in while the vertical component decreased as a result of denudation. An example has been given by Moye, (1959) where horizontal stress under Happy Jacks Plain in the Snowy Mountains was 10 times greater than the horizontal stress caused by the weight of the overlying rock. Such a stress is truly residual.

Suggate, (1963) estimates some 18kms of rock has been uplifted and removed by erosion in Fiordland in the last 6,000,000 years, so this mechanism is considered to be a prime candidate as the cause of the pressure problem. Several zones of horizontally jointed rock were encountered in the pilot heading where slabbing became dangerous, and roof support was urgently required.

8.3 Active tectonism is usually manifest by the accumulation of strain and its release through fault movement either as slippage or as faulting. The buildup process is marked by seismic events varying in size from micro earthquakes to moderate tremors. No seismic activity has been recorded as originating in the tunnel area, the nearest known active fault is the Alpine Fault some 30 kms to the northwest. Active tectonism is ongoing and regional so that the stresses causing the 1947 and 1953 spalling occurrences, if tectonic, should have been continuously active and would not be diminished or attenuated in time.

8.4 Past tectonic stress locked into the rock mass is a possible cause of the spalling. The current phase of activity on the Alpine Fault some 30kms to the northwest of the tunnel commenced some 20 million years ago and resulted in horizontal offsetting of 480 kms as well as vertical uplift. The area also contained many other faults active at that time. (Bishop, Blattner and Landis, 1990). Significant earthquakes now occur at about 10 year intervals.

8.5 The last disruptive intrusions of gabbros in the Darran Complex occurred some 100M years ago. The shattering effects of magma intrusion can be seen in the breccias in the surrounding areas and in the unhealed faults and in sheared areas in the tunnel. Residual stresses could be the result of incomplete rock breakage during these intrusions when it is safe to assume that not a single cubic metre of rock escaped compression and distortion. The rock mass round the tunnel has undoubtably inherited some of the stress imposed on it at great depth.

When the stresses exceeded the elastic limit of the rock a break or fault occurred. As long as the elastic limit of the rock plus the confining force of

the superincumbent load could retain these forces the stresses remained quiescent. When the tunnel was excavated the unbalanced forces had somewhere to go, and rupture and spalling occurred.

8.6 Ice Melting When melting occurred of some 800m of ice occupying the Upper Hollyford and South Cleddau Valleys the removal of the weight would have a considerable effect on rock dilatancy. The unloading forces which could be as much as 13 mPa at the bottom of the valley were almost certainly expressed as sheet joints, formed subparallel to the rock surface regardless of any structural trends in the rock mass. Sheet joints decrease in incidence with depth into the rock mass, so it is possible that residual rebound stress has been locked-in where sheeting has not broken the rock mass, which could account for stressed zones within 100m of the Homer and Cleddau portals. However the zones of spalling near the middle of the tunnel, some 500m from the valleys are more difficult to accept as resulting from ice melt unloading.

8.7 Topographic stress is caused by irregular surface topography, such as the presence of a sharp notch of a V shaped valley. Stress concentrations may even approach the strength of the rock mass. Glacial valleys are reasonably uniform in shape, and free of irregularities, and topographic stresses do not seem to be relevant except for openings excavated parallel to the steep valley walls (Brekke, 1970).

9. CONCLUSIONS

In practical terms the search for the origin and cause of the spalling phenomena in the Homer Tunnel was only of philosophical interest to the people who constructed and maintain the facility. The questions the engineers asked in 1953 were "What are the natural stresses, what is their direction and duration?" These practical questions were only partly answered at the time but enough evidence was available to say that the stresses were residual, largely horizontal, and once released attenuated with time. Even now with almost 40 years maintenance of the tunnel backed by the knowledge of four decades of advancement in rock mechanics, and with some detailed regional geological mapping finally available, it is still difficult to answer the interesting questions as to the precise origin and causes of the rock bursting. However stresses residual from the erosion of 18km of rock are the prime candidate.

10. REFERENCES

Bain, G.W., 1931. Spontaneous rock expansion. J. Geol. vol 39 pp 715-35.

Bishop D.G., Blattner, P., Landis, C.A., 1990. Miscellaneous Map of New Zealand Sheet 16 Hollyford Map (1:75,000) and notes (40p) Wellington. D.S.I.R.N.Z.

Bielenstein, H.V. and Barron, K., 1971. In-Situ Stresses. Proc. 7th Canada. Rock Mech. Symp. Edmonton. Mines Branch. Dept. Energy Min. Resour. Ottawa.

Bird, P.H., 1942. Discussion, What are the causes of rock bursts? p 21-27 in Bucky, P.B., Rock Bursts - A symposium Amer. Inst. Min. Engrs. Tech. Pub., 1468.

Blattner, P. & Coates, G. 1989. A Guide to Milford Sound. N.Z. Geological Survey Guide Book.

Brekke, T.L., 1970. A survey of large permanent underground openings in Norway. International Symposium on Large Permanent Underground Openings, Oslo, 1969, Universitforlaget.

Denkhaus, H., 1967. General Report on Theme 4 - residual stresses in rock masses. 1st International Congress I.S.R.M. Lisbon.

Downer A.F., 1977. Historical aspects of tunnelling in New Zealand. Tunnelling in New Zealand Symposium, N.Z. Geomechanics Society.

Gordon, F.R., 1953. Rock Bursting at the Homer Tunnel. Report to P.W.D. Dunedin District Commissioner of Works (Unpublished).

Gordon, F.R., 1991. Foundation conditions at the New Victoria Dam site. Report for Baulderstone Hornibrook Pty. Ltd. (Unpublished)

Hart, E.K., 1952. The Homer Tunnel enlargement with special reference to rock pressure. A.O.S.M. Thesis (unpublished)

Moye, D.G., 1959. Rock mechanics in the investigation and construction of T.1 underground power station, Snowy Mountains, Australia. Geol. Soc. America Eng. Geol. Case Histories 3 pp 13-44.

Smith, H.W., 1947. Avalanches. N.Z. Engineering vol 2 no. 5 May 1947.

Suggate, R.P., 1963. The Alpine Fault. Trans. Roy. Soc. of New Zealand. Vol. 2 No. 7, pp 105-29.

Terzaghi K, 1946. Rock tunnelling with steel supports. Commercial Shearing and Stamping Co. Ohio.

Voight, B., 1967. Correlation of large horizontal stresses in rock masses with tectonics and denudation. Theme 4 - residual stress in rock. 1st International Congress I.S.R.M. Lisbon.

White, D.U., 1947. The Homer Tunnel. N.Z. Engineering vol 2 no. 5 May 1947.

White, W.S., 1946. Rock bursts in the granite quarries at Barre, Vermont. U.S. Geol. Survey Circular 13.

Slope Stability During Blasting: A Case History

P.A. LILLY
Ph.D., F.AUS.I.M.M., M.I.E.Aust., C.P.Eng.
Managing Principal of Mining & Geotechnical Engineering, Dames & Moore, Perth
P.W. THOMPSON,
M.Sc., F.G.S.
Senior Geotechnical Engineer, Newcrest Mining Ltd

SUMMARY The paper presents a case history of the management of risk associated with blasting-induced slope instability based on blast acceleration monitoring and back analysis. Design curves showing charge weight versus distance for sensitive slopes result from the analysis.

1. INTRODUCTION

Newcrest Mining Ltd (NML) owns and operates the Telfer Gold Mine, which is located in the Great Sandy Desert of Western Australia, approximately 400km east of Port Hedland. In the part of the operation relevant to this study, a sequence of argillites and arenites dips to the east at 32° to 37° on the eastern flank of the Telfer Main Dome structure. Open pits 1A and 1B are located here. Mining in pit 1A concentrated on extraction of the Middle Vale Reef (MVR) orebody and reached an ultimate pit depth of 125m during the fourth quarter of 1990. Pit 1B produces millfeed and ore for heap-leach extraction from the mineralised sheeted-vein stockwork occurring beneath the MVR.

NML are currently mining pit 1B to a final pit depth of 95m, which involves the "push back" of the existing pit 1A footwall slope. Blasting operations in pit 1B gave rise to concern for the stability of that part of the pit 1A footwall slope which was unsupported and occurred above the haulroad (Figure 1). The integrity of the haulroad is extremely important as this provides the only access to both the underground decline portal and the then operating pit 1A, both of which provide high grade millfeed.

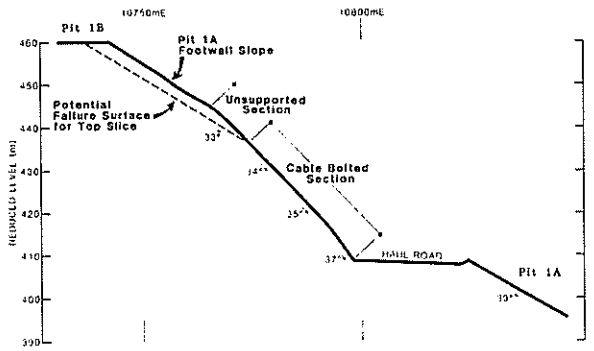

Figure 1 Typical Section Through Telfer Pit 1A Footwall Slope Section on 11670mN

Previous planar bedding plane failures onto the haul road had occurred in the pit 1A footwall slope during and after production blasts in pit 1B, although these localised failures had occurred along the northern part of the haulroad and had not presented any serious problems.

2. GEOMETRY OF THE PROBLEM

The Telfer Main Dome structure produces an increase in bedding plane dip with depth as shown on Figure 1, which also shows the geometry of the footwall slope circa May 1991. It can be seen from the figure that the pit 1A footwall slope above the haulroad had undercut bedding planes over its entire height. A slab of sandstone called the "top-slice", approximately 3m thick, had been left unbolted on the slope face, and the mass failure of this slab onto the haul road was of serious concern to the mine management as mining in pit 1B progressed downwards. In addition, there were two other major areas of concern, the first being the section of the undercut slope above the decline portal, and the second (approximately 200m from the portal) being where a ventilation raise occurred at the toe of the slope.

3. ENGINEERING GEOLOGY

3.1 Lithology and Structure

The Footwall Sandstone in which the slope was cut consists of interbedded sandstones, siltstones and claystones, with kaolinitised silt alteration products occurring throughout the rock mass and preferentially along bedding planes.

The dominant structural feature is the planar bedding. Other defect sets in the form of joints and veins are clearly visible in the Footwall Sandstone, however they tend to form release boundary surfaces to blocks sliding along bedding planes. For the purposes of this analysis, we assumed that these defects are sufficiently persistent and frequent to allow sliding to occur freely.

3.2 Density and Shear Strength Parameters

The mean density of the Footwall Sandstone is 2.34t/m^3.

Clayey and/or silty bedding planes in the footwall sandstone are known by back analysis to have very low friction (8°) and cohesion (21kPa) properties. However, the bedding plane beneath the 3m thick top slice shown on Figure 1 could not have such properties, otherwise it would have been dislodged shortly after (or during) the formation of the undercut slope.

Table I is a summary of the results of tilt tests using blocks of rock, which show a significant variation in basic friction angle. Tests 1, 2 and 8 are considered invalid due to the poor contact reported between test blocks. The remaining tests have a mean of 32° with a standard deviation of 8°.

Slope Stability During Blasting: A Case History

P.A. LILLY, PhD,FAusIMM,MIEAust, CPEng, Managing Principal of Mining & Geotechnical Engineering, Dames & Moore, Perth.
P.W. THOMPSON, MSc, FGS, Senior Geotechnical Engineer, Newcrest Mining Ltd.

TABLE I

RESULTS OF TILT TABLE TESTS

Test No.	Number of Trials	Mean Angle Required to Cause Sliding	Comments
1	4	34	POOR PLANE CONTACT (20-30%) smooth cored, silty plane. SILTSTONE.
2	4	31	
3	3	36	75% CONTACT. Undulating, smooth to rough. SILTSTONE.
4	3	39	80% CONTACT. Blocks well matched. SILTSTONE.
5	3	38	95% CONTACT. Bedding rough planar. SILTSTONE.
6	3	43	90% CONTACT. Curved, smooth, planar no infill SANDY SILTSTONE.
7	4	39	100% CONTACT. Silt infill <1mm on plane. SILTSTONE.
8	3	20	POOR CONTACT. Extremely weak. SILTSTONE.
9	3	33	Irregular, smooth plane. SILTSTONE.
10	3	27	smooth, planar bedding. SILTSTONE.
11	1	24	smooth, planar bedding. SILTSTONE.
12	3	23	smooth, planar bedding. SILTSTONE.
13	3	24	planar rough, weak. SILTSTONE.
14	3	20	Irregular rough, weak. SILTSTONE.
15	3	25	smooth, planar weak. SILTSTONE.

Profiling of the bedding planes indicated that a mean incremental friction angle of about 7° was available, while back analysis of a footwall slope failure yielded an incremental friction angle of 9°.

For the purposes of this study, therefore, a mean basic friction angle of 32° plus a mean incremental friction angle of 8° were assumed. We also assumed that the cohesion on the plane was zero.

4. BLASTING PRACTICE

4.1 Designs

Blast patterns in the floor of pit 1B are usually drilled either on a 3m by 6m pattern, or a 4m by 4.5m pattern, using 146mm diameter blast holes, to a depth of 5.5m. A typical pattern is shown on Figure 2, and shows the centre-lift design.

Most holes are charged with 24kg of ANFO, exceptions being the central line of holes, which normally contains 20kg of ANFO per hole, and the row of holes which is drilled along the crest of the pit 1A footwall slope, which is usually charged with 18kg of ANFO per hole.

Holes are primed with 400g cast primers into which down-the-hole delay detonators are inserted. Delay number normally increases away from the central line of holes (for example, Figure 2). Holes are tied in on a V pattern, with 35ms or 42ms surface delays between tied-in rows. The combination of down-the-hole and surface delays gives rise to timing contours which have smaller apical angles than that of the V tie-in.

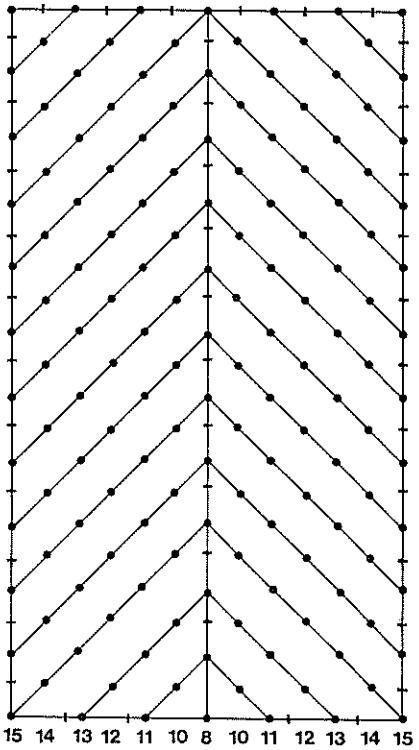

Figure 2 Typical Pit 1B Production Blast Design

4.2 Hole Timing

Figure 3 shows the frequency and cumulative frequency distributions of time between consecutive hole detonations in the blast design presented in Figure 2. This figure assumes that no scatter occurs in delay timing, and shows that approximately 40% of holes detonate within 2ms of another hole, while almost 90% of holes detonate within 10ms of another hole. Clearly a significant number of more or less instantaneous detonation events occur.

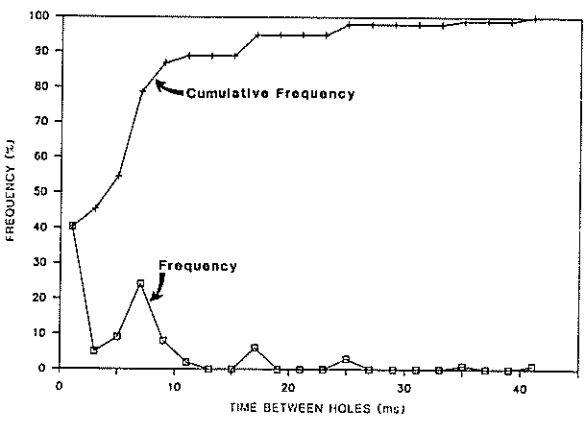

Figure 3 Time Between Detonating Holes

P.A. LILLY, PhD,FAusIMM,MIEAust, CPEng, Managing Principal of Mining & Geotechnical Engineering, Dames & Moore, Perth.
P.W. THOMPSON, MSc, FGS, Senior Geotechnical Engineer, Newcrest Mining Ltd.

5. BLAST MONITORING

5.1 Equipment

Monitoring stations (at 9 locations along the footwall slope) were constructed from angles of mild steel set at 90° and welded onto the face plates of tensioned cable bolts near the toe of the footwall ramp batter.

Bruel and Kjaer type 4370 accelerometers were mounted on studs bonded to the mounting brackets and oriented to measure vertical and horizontal components of acceleration. The accelerometers were connected to Rion Vibration meters and data recorded on a TEAC R71, 7-channel data recorder. The system was calibrated to Australian Standards before and after each measurement, limiting the estimated error to 2%.

5.2 Results and Discussion

The monitored open pit blasts were either production blasts, presplit blasts along the hangingwall batter or single hole shots designed to obtain information on individual waveforms. Presplit and single hole shots had a different acceleration response to the normal production blasts and were eliminated from statistical analysis on this basis.

Accelerations (both horizontal and vertical) from production blasts tend to correlate well with distance and total charge weight. This relationship is shown on Figure 4, in which the natural logarithm (ln) of the peak acceleration is plotted against the natural logarithm of the scaled distance, SD, where:

$$SD = \text{distance} \,.\, \text{total charge weight}^{0.5}$$

and where distance from the blast to the monitoring point is given in metres, and total charge weight is given in kilograms.

Linear regression of the data yields an equation of the form:

$$\ln(\text{acceleration}) = -1.671 \ln(SD) + 2.398$$

which has an associated correlation coefficient of -0.94. For acceleration in the units of g, this regression line reduces to:

$$\text{Acceleration (g)} = 1.1\ SD^{-1.671}$$

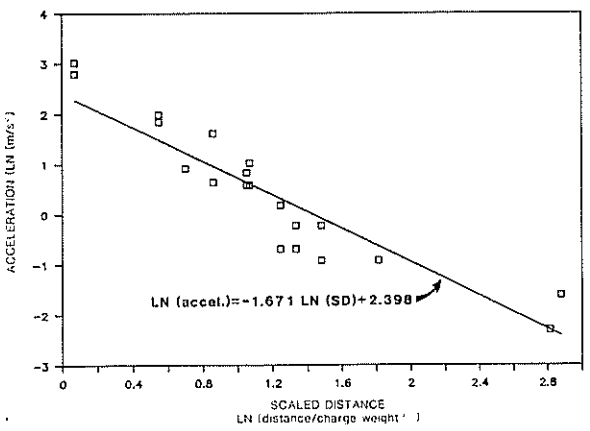

Figure 4 Production Blast Acceleration Monitoring Results

The good correlation with total charge weight (rather than charge weight per delay) is probably due to the fact that a large proportion of holes detonate within a very short time of another hole (Figure 3).

Based on an analysis of the variance of the residuals from the regression line, we expect (with 95% confidence) that a measured acceleration result will be less than:

$$\text{Acceleration (g)} = 3.1\ SD^{-1.671}$$

but greater than:

$$\text{Acceleration (g)} = 0.4\ SD^{-1.671}$$

Using these relationships, limits can be placed on the expected accelerations from a production blast.

6. SLOPE STABILITY

6.1 Historical Stability

Several failures, mainly on a small scale, had occurred in the unbolted top-slice of the footwall slope. Until May 1990, however, the locations of blasts relative to these events had not been recorded. Two subsequent events were therefore used for back analysis.

On 11 May 1990, a blast containing 374 blast holes was fired in pit 1B. During the blast, a small section of the unbolted top-slice became dislodged from the face and slid onto the haul road. The distance from the blast to the brow of the undercut portion which failed was approximately 35m.

On 14 June 1990, a blast containing 198 blast holes was fired in pit 1B. Immediately after the blast, approximately 1600bcm of material slid from the slope. The distance from the blast to the brow of the undercut portion which failed was approximately 22m.

The scaled distance relationships developed in Section 5.2 was used to estimate (by way of back-analysis) the peak acceleration acting on the failed blocks during each blast. In order to ensure that predictions tended to err on the conservative side, we used the relationship derived for the lower 95% confidence limit. This relationship suggested that accelerations were at least 2.1g and 2.7g, respectively, for the two failures discussed above.

Half-way up the dip slope above an underground mine vent raise, at a depth of approximately 80m below surface, a 100m long section of undercut bedding, approximately 10m high, has been subjected to increasing blast-induced accelerations from pit 1B for months. We estimated that accelerations of up to 6g (with a mean of 2.4g) must have occurred during blasting. Nowhere had this slope failed. Clearly significant accelerations were required to cause failures in otherwise stable sections of slope.

6.2 STABILITY ANALYSIS

6.2.1 Introduction

The pseudo-dynamic analytical method normally used to analyse slope stability is more suited to the analysis of earthquake accelerations than those from blasting. During blasting, vibration frequencies in the range 20Hz to 40Hz (depending on distance from the blast) are typical for Telfer production blasts in the footwall rocks. These are much higher than those associated with earthquakes (typically 0.5Hz to 2Hz) and, in addition, blast duration is relatively short. As a result, the use of blast acceleration data directly

P.A. LILLY, PhD,FAusIMM,MIEAust, CPEng, Managing Principal of Mining & Geotechnical Engineering, Dames & Moore, Perth.
P.W. THOMPSON, MSc, FGS, Senior Geotechnical Engineer, Newcrest Mining Ltd.

in a conventional stability analysis leads to ridiculously conservative results. We therefore only used the slope stability analytical method to estimate the form of the relationship between factor of safety and acceleration, and did not use it as a predictive tool.

6.2.2 Factor of safety versus acceleration

The results of pseudo-dynamic slope stability analyses for low frequency, long-duration acceleration pulses show that the relationship between acceleration and factor of safety has a semi-logarithmic form. However, it can be conservatively approximated by a straight line, particularly in the area of interest close to a factor of safety of 1.0.

Based on the shear strength parameters discussed in Section 3.2, the factor of safety of the unbolted top slice was estimated to be at least 1.2 under static conditions. Based on the back-analyses presented in Section 6.1, we conservatively assumed that an acceleration of at least 2g was required to cause an unbolted block to slide. Assuming a straight-line relationship, therefore, the effective factor of safety for an unbolted section of slope subjected to blast accelerations is shown on Figure 5, which also shows the equivalent curve for a slope with a static factor of safety of 1.4.

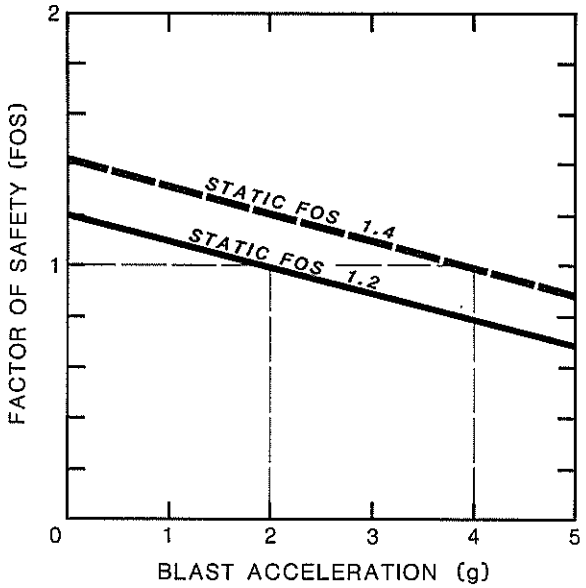

Figure 5 Assumed Factor of Safety Vs. Acceleration Relationship for Blasts

6.2.3 Portal and vent raise slopes

Based on our preliminary findings from the portal slope stability investigation, we estimated the minimum factor of safety of the undercut slope above the portal to be 1.2. Figure 5 shows the line relating factor of safety to blast acceleration at the brow for a slope having a static factor of safety of 1.2. This line indicates that, conservatively, a peak acceleration of 2g is required to cause failure in the slope. In order to reduce the risk and increase reliability, we halved this value; that is, we did not allow accelerations to exceed 1.0g in this part of the slope.

Using the upper 95% confidence limit relationship derived in Section 5.2 from measured blast accelerations we could estimate the maximum accelerations which could be expected during a blast. By re-arranging the equation, we obtained the charge weight (or number of blast holes) conservatively required a produce an acceleration of 1g for a variety of distances. Table II shows the resulting information.

TABLE II

BLAST SIZE AND MINIMUM DISTANCE ABOVE PORTAL

Charge Weight (kg)	Number of Holes	Minimum Stand-Off Distance (m)
102	4	20
410	17	40
920	38	60
1640	68	80
2550	106	100

A similar analysis was conducted for the slope above the ventilation raise. The slope was expected to have a static factor of safety of approximately 1.4 which, from Figure 5, suggests that a blast-induced acceleration of 4g could lead to failure. Thus if 2g was the maximum acceleration allowed at the brow of the undercut, then the blast sizes are conservatively estimated in Table III for a variety of distances.

TABLE III

BLAST SIZE AND MINIMUM DISTANCE ABOVE VENT RAISE

Charge Weight (kg)	Number of Holes	Minimum Stand-off Distance (m)
235	10	20
940	39	40
2120	88	60
3760	157	80
5900	246	100

7. CONCLUSIONS

Normal production blasts fired in pit 1B had relatively short, effective inter-hole delays, with up to 90% of blast holes detonating within 10ms of another hole.

Blast acceleration monitoring indicated that the relationship:

$$\text{Acceleration (g)} = K.SD^{-1.67}$$

applied, where SD = distance. Total charge weight $^{-0.5}$ and K ranged from 0.4 to 3.1 with a mean of 1.1;

Back analysis of the original, unbolted top-slice on the pit 1A footwall slope suggested that blast-induced accelerations of at least 2g were required to cause significant block failures in unbolted sections of slope.

Based on a knowledge of blast size, distance from the brow of the undercut slope and static factor of safety, the susceptibility of a section of slope to failure during blasting could be estimated.

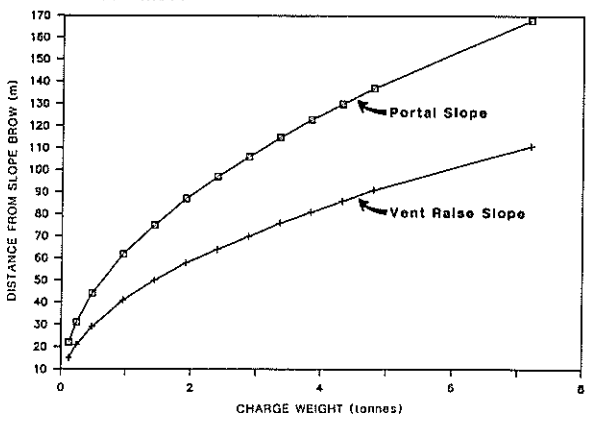

Figure 6 Charge Weight Vs. Minimum Distance for Production Blasts

Figure 6 shows the design curves used for managing the risk of blast-induced slope instability above the two most sensitive sections of the pit 1A footwall.

8.0 ACKNOWLEDGMENTS

The authors wish to thank Newcrest Mining Ltd for permission to publish this paper, and Ms Stephanie Williamson of Dames & Moore and Mr Bill Delaney of Airblast Technology for assistance with blast monitoring.

The Use of Diaghragm walls to Reduce Risk in Deep Excavation

A.L. RESSI dl CERVIA
President, ICOS Corporation of America

SUMMARY Failure in deep excavation can be divided into two main categories: - Lateral Failures, - Bottom Failures. The paper will show how the use of diaphragm walls minimizes the risk in both conditions because this construction system results in a very rigid and watertight perimeter wall that can be extended below the intended bottom of the excavation. Furthermore all construction is done from the ground level, so that when the excavation is carried out the retention system is already in place. A detailed description of application of this technique in circular structure is offered, with design considerations. A brief expla -nation of the construction method and equipment is offered to help in understanding how the stated results are achieved.

1. INTRODUCTION

Construction, as we all know is one of the riskiest industries, and its foundation segment is at the leading edge.

When we talk about risks we talk about a subject which is neither good nor bad, it is a fact, which properly understood, can be reduced (at a cost) to acceptable levels; and while there is no practical way of eliminating it, risk management consists in finding an acceptable area within the risk/cost curve where an acceptable increase in cost produces a substantial reduction in risk.

Risk in foundation construction does not only have economical implications but, unfortunately, can often be measured in human lives, and while one could make risk-reward calculations when only economic factors are involved, one cannot knowingly consider a construction system which inherently exposes human lives to danger no matter how cost effective such a system might be.

Hence, from time to time, new techniques can become prevalent, not because they are cheaper, but because they are safer. To give but just two examples: The practical disappearance of hand dug compressed air tunnelling in favour of mechanical moles and the gradual reduction of timber sheeted excavation for utilities and pits in favour of trench boxes, hydraulic shoring systems and the like.

The tendency, in essence, is to remove the worker from being in harms way as much as possible and rely on technology to make conditions safer in advance of each construction phase.

In order to illustrate how those principles come to bear in diaphragm wall construction, I shall briefly describe for those who are not familiar with the technology how the work is accomplished.

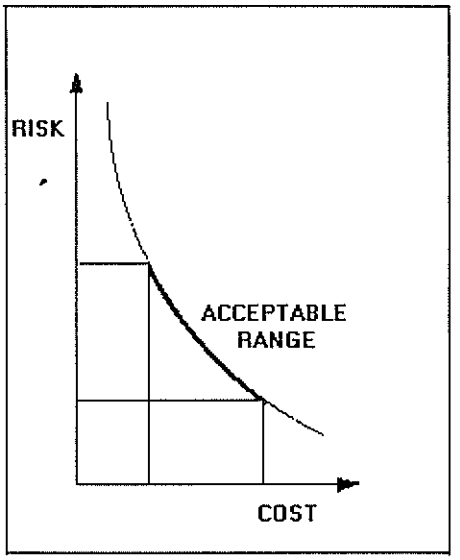

Figure 1 Risk vs Cost

2. DIAPHRAGM WALL

A diaphragm wall is an excavation in unstable soil, supported by a fluid which is constantly kept at ground level, in which a reinforcing cage is introduced, and which is later backfilled with concrete. The resulting reinforced concrete wall segment, a "panel" in the diaphragm wall lexicon, has been constructed to any practical depths (several examples in excess of 100 metres have been built) through any type of soil (ranging from soft organic to hard rock), with various planimetrical shapes (linear, cross, L.T. etc) in thickness ranging from 600 mm to 1500 mm and length of panel ranging from 2.5 to 10 metres.

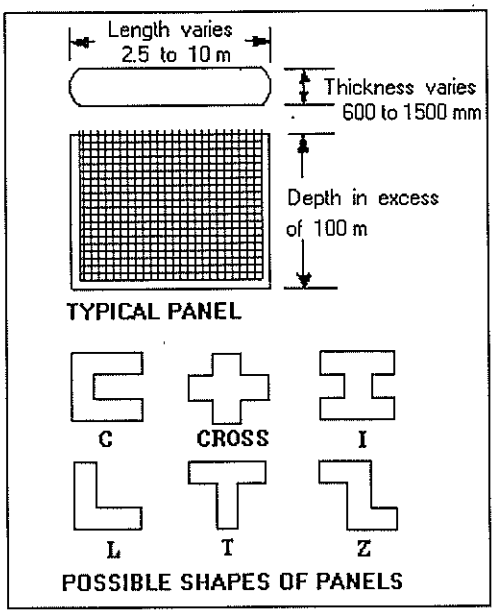

Figure 2 Diaphragm Wall

The planimetric flexibility of the wall allows for irregular contours and innovative designs and solutions.

The construction of those walls is done in the following manner:

3. GUIDE WALLS

Two guide walls are constructed at grade, fulfilling the following functions:

a. Guide the excavating tool
b. Avoid superfical ground unravelling
c. Provide support as well as vertical and horizontal bench marks for the reinforcement cage.
d. Provide reaction for the hydraulic jacks which pull the end pipes.

4. EXCAVATION

Excavation is begun between guide walls, while supporting fluid is pumped into the hole and kept always within 600 mm of the surface. The supporting fluid most commonly used is bentonite mud, although recently the use of polymers, with or without bentonite added, is gaining increasing popularity. The excavation is carried out with a variety of tools, most commonly mechanical and hydraulic clamshells. These tools provide a continuous sampling of the soil around the perimeter of the site, which is helpful in performing a safer and more economical mass excavation.

4.1 When excavation has reached the desired depth, the fluids are thoroughly desanded, stop-end pipes are positioned and a reinforcing cage, fabricated on the ground in advance, is lifted and inserted by a crane into the excavation.

4.2 High slump concrete is placed by tremie from the bottom up, displacing the fluids, and the stop-end pipes are pulled after the end of the pour to create joints with the adjacent panels.

This schematic and necessarily simplified description of the technique shows how a "panel" is constructed and gives the necessary elements to develop the consideration which are the main subjects of this paper. Obviously, a technique which has spawned an industry existing for over 40 years has branched in many directions and developed many aspects that are outside the scope of this presentation, but the bibliography gives several references which the reader can consult to deepen his or her understanding of this construction method.

4.3 Risks in Deep Excavation

Deep excavations fail by lateral failure or bottom failure. The following will discuss both failure modes and how the use of diaphragm walls is a valuable tool to minimise risks.

4.3.1 Lateral Failures

Lateral failures can in turn be divided into two main categories

a) Failure of the lateral support system
b) Failure due to loss of ground outside the excavation.

4.3.2 Failure of lateral support system

Lateral support systems are numerous, but in essence they consist of one of the following :

A Permanent or temporary systems totally installed from the ground level (e.g.diaphragm walls, sheet pile and, tangent or secant pile walls).

B Systems installed as the excavation is advanced (e.g soil nailing).

C Combination systems (e.g "H" beam and lagging).

From a safety standpoint, any system which can be totally constructed from ground level, resulting in an excavation which is protected and insulated from the surrounding area while being performed is inherently superior to a system which needs to be built as the excavation proceeds downward.

Indeed, in situations where there is a high water table that cannot be lowered economically (high flows) or practically (high settlements around the perimeter) B or C systems may not be possible. Of systems constructed from ground level precedence will go to a system which is more rigid (Diaphragm wall and tangent or secant piles vs sheet piles) as these minimise lateral movements and the need for closely spaced supports and one which also gives a better guarantee of continuity and watertightness (Diaphragm wall vs. secant or tangent pile wall).

Needless to say a perimeter wall needs to be supported in some fashion or other and here too the Diaphragm Wall offers the best advantage in the choice of the support system available. Its internal rigidity allows for the use of longer unsupported spans both horizontally and vertically, thus minimising the number of braces and/or tiebacks which cluttter or slow down the excavation. Its horizontal rigidity eliminates the need of horizontal distribution walers needed with other construction methods. The structural and planimetric characteristics of the wall allow for design where the wall (straight or built with T-sections) can act as a cantilever for high unsupported spans. Its capacity for absorbing sizable compressive loads lends itself to design solutions of circular or eliptical walls which are self-supporting and need no bracing or distribution rings during excavation. It is this particular application which epitomizes all that can be gained by using slurry walls. It is well known that, shafts, especially in difficult soils or under water and carried out to considerable depths, are complicated and potentially dangerous structures to construct. This is why structures are designed and built by the slurry wall method. A circular slurry wall offers the advantage, as do all types of slurry walls, of being in place prior to commencement of the excavation. The soil support system does not need to be continuously constructed during the excavation making both operations simpler and safer from a site management perspective.

Perhaps the most attractive feature of a slurry wall in such cases is that these structures can be designed to be fully self supporting. Once the slurry wall has been built from ground level, the excavation can proceed within the wall, completely uninterrupted, with a dewatering operation limited to pumping out only the water trapped within the volume enclosed by the shaft.

While the excavating equipment used to build slurry walls lends itself to the construction of rectilinear structures, proper planning and design can create circular structures comprised of many short straight chord elements. Such structures come very close to perfect circles and, in fact, within the thickness of the wall, a perfect circle of concrete can be delineated.

Consequently these structures can be designed as cylinders with the majority of the loads taken in compression.

The methods used to design the shafts vary and depend on the diameter and depth of the shaft as well as on the length of the chords used to approximate a circle. Obviously, the larger the shaft, the larger the compressive loads in the wall. The concrete in the walls may or may not require reinforcing for these axial loads; agin; this is primarily a function of the shaft size.

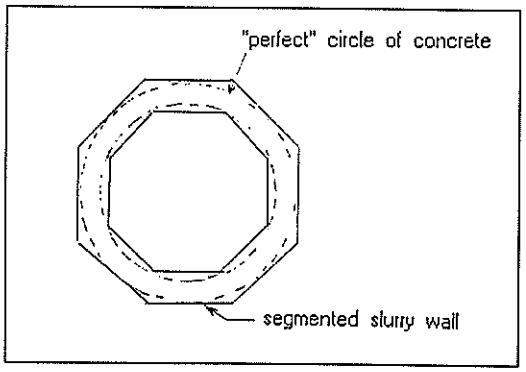

Figure 3. Circular Example

There are, essentially, two ways to place the slurry wall panel joints with respect to the chords. Either the panel joint can be located at the vertex of two chords and each chord is one slurry wall panel or, alternatively, the panel joint can be placed at the centre of a chord and each vertex is monolithic within a panel. For the second option, the chords tend to be longer as the clamshell bucket used in excavating must be able to take two "bites" in each chord. The choice of the panel joint layout again depends on the shaft size and the loads.

A perfect circle under a uniform load will act in pure compression. In a multi-sized polygon, like a slurry wall shafts bending moments develop within the chords in addition to the compressive forces. The design approach for carrying these moments depends on the location of the panel joint.

There are two approaches for a shaft with the joints at the chord vertices. Ideally, an arch can be inscribed in the panel, and the concrete designed to carry only compressive loads.

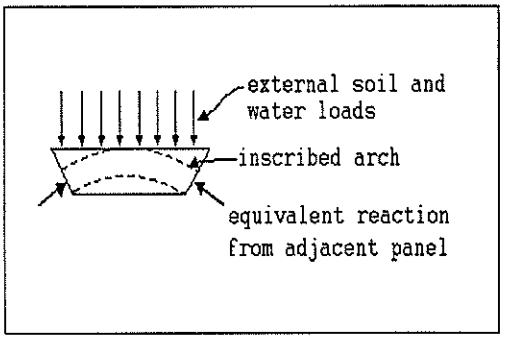

Figure 4 Shaft Joints

In such a case the stability of the panel must be considered, i.e. whether the angle at the vertex is large enough to ensure support of the panel. Alternatively, a more conservative approach will combine simple span bending moment with the axial loads, and the required reinforcing is detailed accordingly. For either approach, stability of the joint can be ensured by using wide flange sections or end stops at the joints, which become a part of the permanent wall.

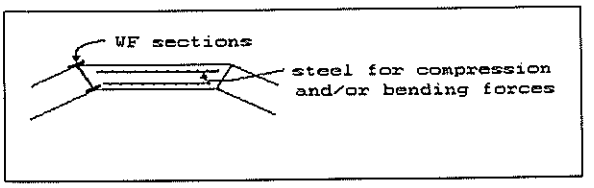

Figure 5 Panel Stability

If the panel joints are placed at the end of the chords, the analysis must consider these as pin connections. In a monolithic polygon moments develop at the vertices and at the center of the chords in the same proportion as moments in a fixed end beam.

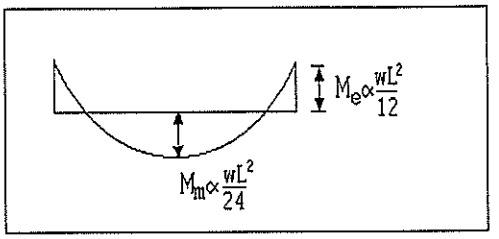

Figure 6 Panel F.E Moments

Depending on the shaft geometry, mainly the included angle of each chord, the unreinforced joint can be shown to carry a bending moment creating an equal and opposite stress to the compressive load.

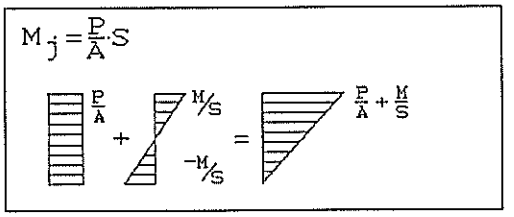

Figure 7 Joint Stresses

This moment capacity may exceed the center moment of a fixed beam, in which case it is assumed to carry only this moment (i.e 1/3 of the simple span moment). If the joint cannot carry the full one third of the simple span moment, excess moment will be redistributed to the vertex. Therefore, the vertex is designed to carry either two thirds of the simple beam moment less the capacity of the joint.

$$Mtot = \frac{wl2}{8} \qquad (1)$$

$$\text{at best } Mj = \frac{wl2}{24} \quad Mv = \frac{wl2}{12} \qquad (2)$$

and in other cases

$$Mj = \frac{P.S}{A} \quad \text{and} \quad Mv = \frac{wl2}{8} - Mj \qquad (3)$$

The reinforcing for such panels is designed to carry the combined axial load and bending moment at the vertex.

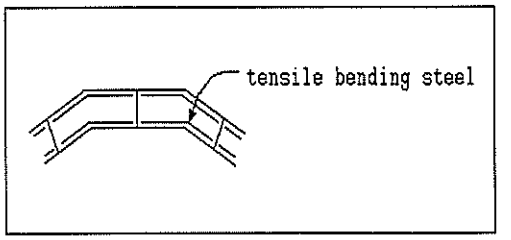

Figure 8 Reinforcing

The above description explains, on a very simple level, the design concepts of such circular structures. Detailed, three dimensional finite element computer models have been used to analyze such shafts. These models can precisely analyze the effects of unbalanced loads inside and outside the shaft due to uneven excavation and surcharges, respectively. The models can also be adapted to study the effects of verticality tolerances, i.e. if the overall structure becomes less than a "perfect" circle. These models can also allow for any vertical forces on the wall. While these models have shown slightly higher loads in some cases than those found in the rudimentary analysis outlined above, they have provided validation of these simple models. An actual design will use loads found in a computer analysis, but will detail the wall and reinforcing to carry the loads using the methods outlined above. Furthermore, comparisons of two and three dimensional models have often shown the vertical effects to be negligible, and, in fact, these structures can usually be designed fairly accurately using only two dimensions in the model. Again, the choice of the model will depend on the shaft geometry, specifically here the aspect ratio of the cylinder. A long thin cylinder can be modelled in two dimensions while a wide shallow shaft should be studied in three dimensions.

It has been shown that self supporting circular slurry walls present many advantages for constructability without presenting an overly complex design problem. These structures, by their nature, are highly indeterminate and the technique offers a safe and easy method for soil support.

Lastly, since the wall can be utilised as the permanent foundation wall, it lends itself to a top-down construction method (recently more and more popular in the U.S., Europe and the Far East) which allows for the simultaneous construction of the structure in elevation while the foundation is being excavated. Then the diaphragm wall is supported by the

permanent floor system which is constructed as the excavation proceeds.

4.3.3 Failure due to loss of ground during excavation

Deep excavations, especially in unstable soils and in the presence of high water table, are particularly sensitive to loss of ground from outside the perimeter.

Thus a system which guarantees a watertight barrier around the site avoids the need for lowering the water table, with the often concomitant result of settlement of streets, movement of adjacent buildings and damage to utilities. It also gives a better chance of preventing sudden inflows of water or material which can happen when less reliable systems, allegedly watertight, fail (e.g sheet piles jumping interlock, secant or tangent piles having a gap between them.) This is not to say a diaphragm wall cannot have defects, but it is a technique inherently safer and easier to accomplish with good standards of workmanship.

Proof of this assertion is that in many European countries and frequently in North America, building codes accept that the use of a diaphragm wall obviates the need for underpinning adjacent structures which is a requirement when other construction methods are utilised.

5. BOTTOM FAILURE

Bottom failures are caused either by "heaving" or by untreatable water-carrying seams.

Diaphragm walls can easily be designed to obviate the first problem by embedding the wall below the bottom of the excavation for a length which creates a circumscribed mass of soil of sufficient weight to avoid blow up of the bottom.

In this respect, diaphragm wall watertightness and the ability to be built in different ground conditions are advantages over other systems. The capacity, for example, of going through boulder strata to reach the required depth is a characteristic that other systems have difficulty in matching.

As far as controlling water from a "leaky" bottom formation, a diaphragm wall is no better than any other watertight barrier carried to that level, except that it is easy to incorporate grout pipes. This allows drilling and grouting below the bottom of the wall and into the water carrying formation in an easy and cost effective manner.

6. CONCLUSIONS

A diaphragm wall is an excellent way to diminish the risk of a deep excavation in difficult soil conditions, especially in the presence of a high water table. The cost of such a superior retention system is more than justified when the diaphragm wall is designed to take advantage of all its properties:

It is a permanent retention wall, incorporated into the structure.

It can be loadbearing.

It is a waterproof system.

It obviates the need for underpinning adjacent structures.

It has inherent rigidity which results in an efficient support system.

It has planimetric flexibility lending itself to imaginative design solutions.

It is apparent that such a construction technique has earned its rightful place in the "bag of tricks" of competent designers, since it provides a safe and cost effective solution to the problem of difficult deep excavations for building foundations, subway cuts, pump stations, access shafts and other underground structures.

7. REFERENCES

1. Hajnal, I. Marton, J. and Regele, Z. "Construction of Diaphragm Walls".

2. Verfel, Ing. J. "Rock Grouting and Diaphragm Wall Construction".

3. Xanthakos, P.P. "Underground Construction in Fluid Trenches".

4. Supplement to 1980 World Survey of Current Research and Development on Roads and Road Transport - The Design and Construction of Diaphragm Walls in Western Europe (1979) Sponsored by U.S. Department of Transportation Reported by International Road Federation.

Modelling Surface and Subsurface Subsidence over Coal Mines

K.J.L. STONE and R.J. JEWELL
University of Western Australia
I. MISICH
Western Collieries Ltd, Collie

SUMMARY A series of geotechnical centrifuge model tests are presented in which coal extraction at depth has been simulated and surface and subsurface movements of the overlying strata recorded. The centrifuge modelling technique and its applicability to mining problems is discussed.

1. INTRODUCTION

Historically, deep coal mining techniques had the basic philosophy of maintaining a good roof and mining conditions. Under such circumstances, subsidence effects were not significant unless collapse of the roof supports occurred. However, more modern extraction techniques - total extraction methods - rely on allowing the mine roof to collapse behind the advancing mine face. The most efficient of these techniques is longwall mining where no roof support is left behind the mined face. A slight variation of this technique is Wongawilli extraction, where pillars of coal or stooks are often left to partially support the mine roof in the vicinity of the worked face, but where the roof collapses as the face advances. The use of these modern extraction methods makes sub-surface and surface subsidence unavoidable. Such mining induced subsidence can lead to the damage of surface and sub-surface structures and services. Consequently, the prediction and minimisation of subsidence is extremely important when assessing potential and existing mineral resources.

To date, the prediction of mining induced subsidence has relied on the use of empirical models and little or no attempt has been made to formulate predictive models based on the physical response of geomechanical materials - soil and rock.

In this paper, a set of centrifuge model tests are described in which a method to simulate coal extraction at depth has been devised and surface and sub-surface movements of the overlying strata have been recorded. The method incorporates a trap-door system which replicates the total extraction of panels of coal by either Wongawilli or Longwall extraction. The centrifuge model tests have been performed on the Acutronic 661 centrifuge at the University of Western Australia. The tests represent an initial study of the applicability of centrifuge modelling to simulate coal extraction beneath relatively soft sedimentary rock.

2. CENTRIFUGE MODELLING

2.1 Introduction to Centrifuge Modelling

The centrifuge modelling technique is an effective and versatile method of producing realistic small scale model test data which can be related directly to a prototype situation. This is due to the fact that the behaviour of geotechnical materials such as soil and rock is very dependent on stress level. In a conventional model test, performed in the earth's gravitational field, it is not possible to maintain similarity with prototype situations and to ensure that the stress levels in areas of interest reach prototype values.

A geotechnical centrifuge can subject small scale models to centripetal accelerations which are many times the earth's gravitational acceleration. Under this increased acceleration field the self weight of the material being tested is increased by the same proportion by which the model dimensions have been reduced. Thus, by selecting suitable acceleration levels, it is possible to create full scale stress levels in the small scale model to ensure a correct stress level dependent response of the model.

2.2 Scaling Laws

Centrifuge scaling laws have been described extensively elsewhere (1). However, if we consider a model where the prototype dimensions have been reduced 'n' times such that $d_p/d_m = n$, where d_p and d_m are prototype and model dimensions respectively, and if 'n' is chosen as the gravity scaling factor, then the basic scaling relationships associated with centrifuge modelling are as given in Table I.

TABLE I

CENTRIFUGE SCALING RELATIONSHIPS

Parameter	Units	Scaling Relationship
Gravity	m/s^2	n
Length	m	1/n
Stress	Pa	1
Strain	%	1
Force	N	$1/n^2$
Time+	sec	$1/n^2$

+N.B.: This relationship applies to lamina flow processes such as consolidation

If a similar material is used in both the model and prototype then the similitude of stress levels at corresponding points in the model and prototype will result in a model response directly analogous to that of the prototype.

2.2.1 Scaling Considerations for Mining Applications

The centrifuge models reported herein are concerned with modelling relatively shallow mining depths - of the order of 60 metres. However, due to the limitations in size of existing model containers the required model dimensions necessary for direct scaling was not possible. Consequently the model tests were designed to be performed at half prototype scale. This necessitates that the prototype strength parameters of the overlying sediments should be reduced by a factor of two in the centrifuge model, and thus the strength to depth ratio in both model and prototype is preserved. Figure 1 summarises the prototype and corresponding model ground profiles which were used as a basis of the model tests.

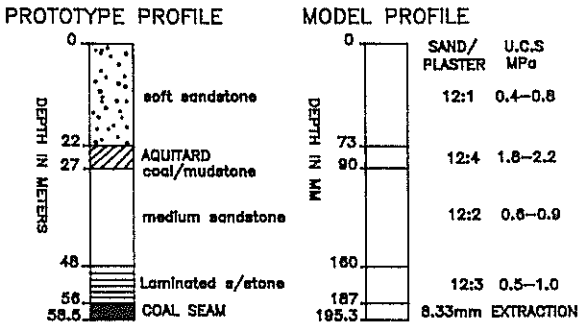

Figure 1 Approximation of model ground profile to a prototype situation.

3. CENTRIFUGE TEST PACKAGE

3.1 Actuator Assemblage for Mineral Extraction Simulation

To simulate the extraction of coal at depth, an assemblage of 18 hydraulic actuator units were designed and built. Each actuator is composed of a circular piston unit with a rectangular top cap. The plan dimensions of the top cap are 45 by 68 mm which represents a prototype area of 13 by 20 m at 150 gravities at half scale.

The actuator units are arranged three deep by six across in the centrifuge strong box to provide a simulated extraction area of 4680 square meters at prototype scale. The throw of the actuator units was set to 8.3 mm which represents an extraction height of 2.5 m at prototype scale. The strong box used for the model tests is fitted with a perspex window through which deformations of the model can be observed. Figure 2 shows a detailed drawing of a typical actuator unit and Figure 3 shows the arrangement of the actuator units in the centrifuge strong box.

The actuator units have been designed to cater for the provision of stooks by allowing pillars to remain standing to support the overlying strata as the actuator is lowered - see Figure 4. These stooks can be removed if not required - i.e for Longwall mining simulation.

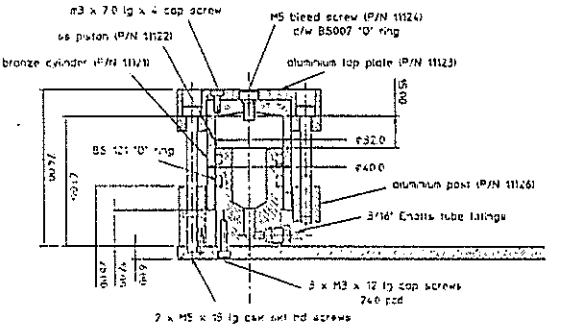

Figure 2 Assembly drawing of single actuator unit.

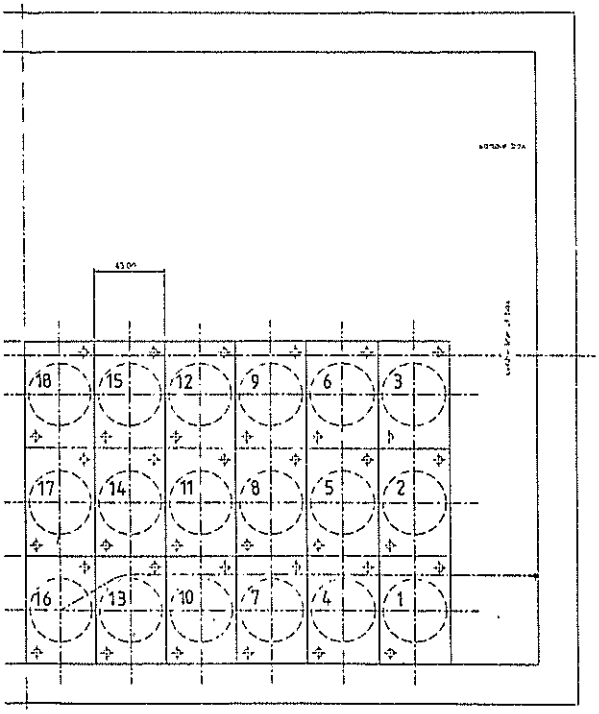

Figure 3 Plan arrangement of actuator assemblage in model container.

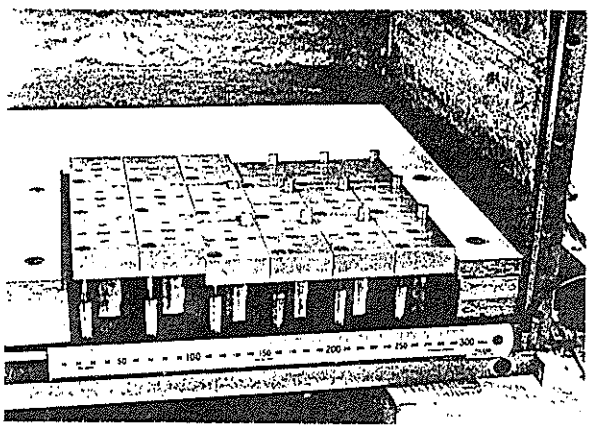

Figure 4 Actuator assemblage with stooks.

3.2 Actuator Control and Data Acquisition

Each actuator unit is connected to a miniature solenoid valve which in turn connects to a manifold on the outlet side and to a fine metering flow control valve. Thus each actuator unit can be dropped individually or collectively at controlled rates set by the orifice of the metering valve. The control of the solenoid valves is performed by a computer.

The majority of the data obtained from the model tests performed so far have been visual. Miniature CCD cameras are mounted on the package to record the sub-surface movements of the model via the perspex window and the surface disturbance of the model resulting from the dropping of the actuator units.

An imaging system has also been developed which is presently capable of monitoring the real-time motion of up to eighteen discrete points visible through the strong box window. This system is also capable of back analysing video footage of the model tests to produce displacement records of visible markers. Eventually the system will provide both strain and displacement fields of the overlying strata throughout the simulated mining process.

4. MODEL PREPARATION

4.1 Introduction

Two model tests are reported in this paper. The first test (Westcol3) was designed to simulate coal extraction by the Longwall mining style. The second test (Westcol4) was designed to simulate extraction by the Wongawilli method. This extraction technique is presently employed by Western Collieries operating the Collie Basin of Western Australia.

4.2 Tests Westcol3 and Westcol4

The model preparation of these two tests was essentially the same. The different strata were simulated using various mixtures of fine sand (250 micron average particle size) and gypsum cement. The strength of each strata was evaluated from unconfined compression tests, and by varying the mix proportions of water, sand and gypsum suitable strengths could be obtained.

One of the key elements to the success of replicating a realistic prototype situation was to develop a technique to enable the lowest strata - i.e the mine roof - to have a laminated structure - which would result in bulking of the goaf. This was achieved in the model by casting successive thin layers of gypsum/sand mixtures where each layer was allowed to dry and a small amount of dry sand was sprinkled onto the surface of the hardened mixture before the next layer was cast. The net result of this technique was to produce a 27 mm thick laminated strata with horizontal planes of weakness directly over the hydraulic actuator units.

Three more uniform gypsum/sand mixtures were then cast, in appropriate thicknesses, to represent the other layers of strata. Figure 1 shows the model profiles used in both tests, and the associated U.C.S strengths obtained for each strata. The U.C.S strengths quoted in this figure have been estimated from element tests performed on standard 76 mm diameter samples.

After the model material had been cast into the strong box the front face of the strong box was removed and a template used to spray a uniform grid of discrete marks and horizontal lines onto the model face. The surface of the models was also sprayed black to highlight any surface expressions resulting from the simulated mining.

5 MODEL TEST RESULTS

5.2 Longwall Style Extraction

The actuator units were manipulated to simulate a Longwall style extraction - i.e no stooks were provided - and the dropping order is shown in Figure 3. Two miniature CCD video cameras were employed in this test to monitor both surface deformations and deformations of the model face through the strong box window.

Video observations of the model test clearly showed that a laminated structure to the roof strata had been achieved from the model preparation process. The results of the model test are best illustrated from post-test traces of the cracking visible on the model face (Figure 5), the model surface (Figure 6) and the surface of the aquitard layer (Figure 7).

5.3 Wongawilli Style Extraction

The actuator units were dropped in the same order as for test Westcol3 (see Figure 3). Again the majority of the information obtained from the test was visual, with observations being recorded on video. Figure 8 shows the sketch of the crack pattern visible on the model face and Figures 9 and 10 show the respective crack patterns for the model surface and aquitard surface.

5.4 Comparison of Model Responses.

By comparing the traces obtained of the front faces of the models after testing, it is possible to determine slightly different responses of the two types of extraction procedure employed. For example , Figures 5 and 6 show that a large tension crack develops in the near surface almost vertically above the trailing end of the Longwall extraction. This cracked zone is much less significant in the corresponding traces for the Wongawilli extraction (see Figure 8 and 9), and is an indication that greater tensile strains had developed in the near surface in the absence of stooks at the onset of the extraction. This observation can be linked to the deformation response of the underlying strata where comparison of the cracked aquitard surfaces show a more significant deformation of the aquitard has occurred in the Longwall (Figure 7) than for the Wongawilli extraction (Figure 10). The effect of the stooks is clearly seen by the "wavey" appearance of the goaf in Figure 8 (test Westcol4) where intermittent partial support is provided to the overlying strata. The dotted lines in Figures 5 and 8 show the interface between the goaf and the overlying strata.

The degrees of subsidence resulting from the two types of extraction were obtained by comparing the pre and post-test surface and aquitard surface profiles. These data, obtained by laser transducer profiling, are best represented by the absolute settlement values at discrete points on

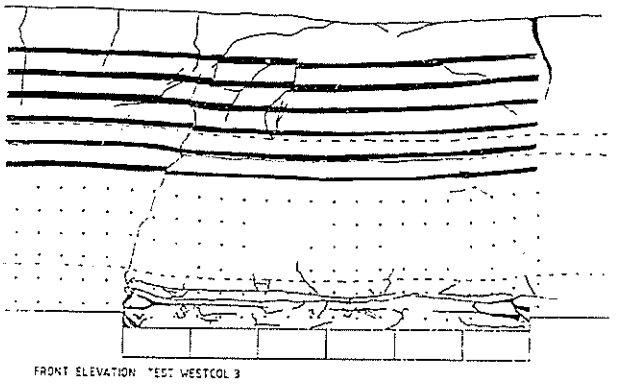

Figure 5 Trace of crack pattern on model face after test Westcol3.

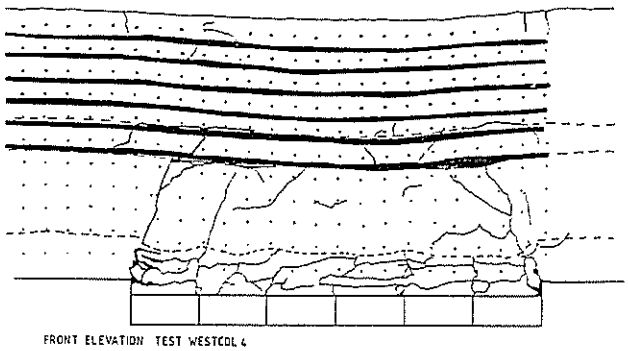

Figure 8 Trace of crack pattern on model face after test Westcol4.

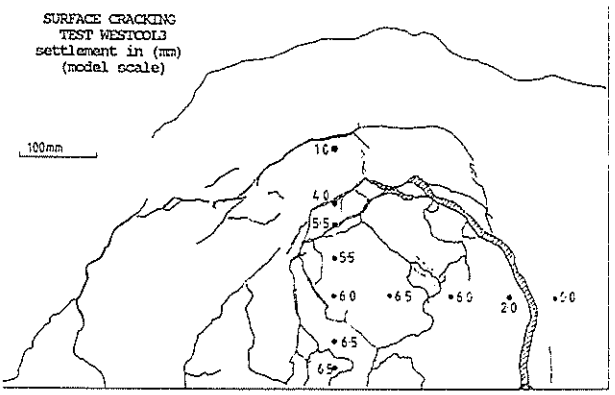

Figure 6 Trace of ground surface crack pattern after test Westcol3.

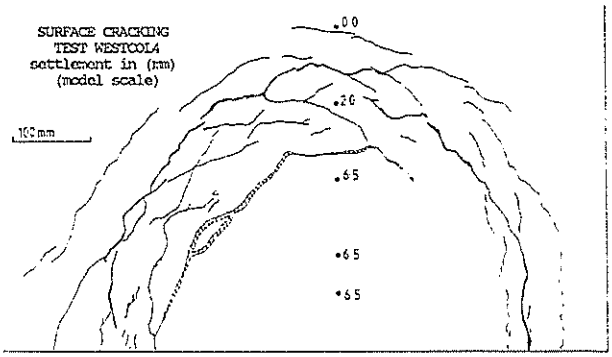

Figure 9 Trace of ground surface crack pattern after test Westcol4.

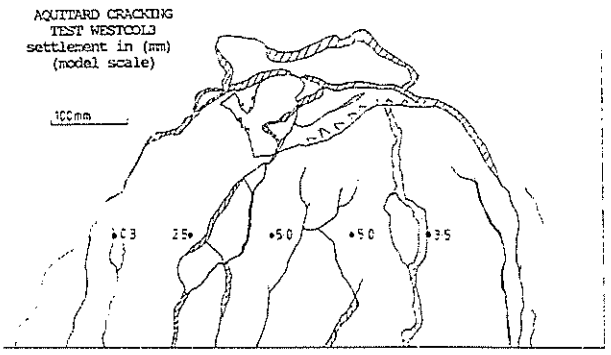

Figure 7 Trace of aquitard crack pattern after test Westcol3.

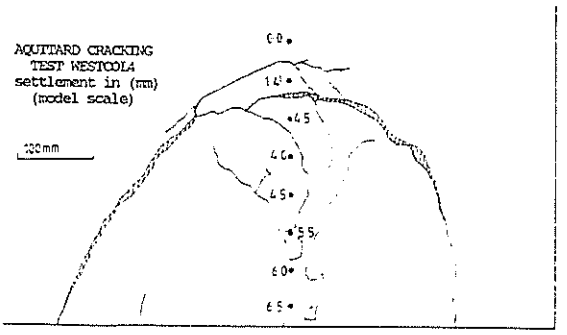

Figure 10 Trace of aquitard crack pattern after test Westcol4.

the sketches of the surface and aquitard surface crack patterns, as indicated in Figures 6 and 7 and Figures 9 and 10 for the respective Longwall and Wongawilli cases. This data show that the maximum surface and aquitard settlements recorded for both tests was fairly similar - about 70% of the extraction height. However, the traces of model face and surface crack patterns (Figures 5 and 6, and 8 and 9) illustrate that the areas affected by the extraction process is somewhat greater for the case where Longwall extraction has occurred, and although the general shape of the subsided region is similar for both tests the surface expressions (i.e visible cracks) are more pronounced for the Longwall case.

Similar observations can also be made concerning the aquitard crack patterns. In this case the differences are more pronounced with more abdundant cracking occurring and extending over a larger area in the Longwall case than in the Wongawilli case. These observations can again be attributed to the intermittent support offered by the presence of stooks in the goaf.

6. DISCUSSION AND CONCLUSIONS

The centrifuge model tests reported in this pilot study have clearly demonstrated that the centrifuge modelling technique offers a powerful tool in investigating subsidence problems resulting from mineral extraction processes in

stratified deposits. A versatile mechanical system has been developed and proof tested which enables a variety of mining methods to be studied.

Whilst only a limited amount of work has so far been undertaken on the feasibility of modelling site specific strata, it is clear that the use of artificial rock of any required strength can be reproduced by careful design of gypsum/sand/water mixtures. Model making techniques have also been developed, which indicate that as well as meeting strength criteria, the structure of the overlying strata can also be replicated. This was clearly illustrated by the laminated nature of the model mine roof in test Westcol3.

The magnitudes of the maximmm surface settlements - about 70% of the extraction height for the model tests - compare favourably with values measured in the field where the properties of the overlying strata is similar to that used in the scale model - i.e the Collie Basin of Western Australia.

7 ACKNOWLEDGEMENTS

The authors wish to thank Western Collieries Ltd and the Mineral and Energy Research Institute of Western Australia for their current and continued support of this research.

8. REFERENCES

1 Joseph P.G, Einstein H., and R.V Whitman (1987) "A literature review of geotechnical centrifuge modelling with particular emphasis on rock mechanics." Report to Air Force Service Centre, Tyndall Air Force Base, Report No. DACA88-86-D-0013.

A Review and Analysis of Rock Discontinuity Mapping Methods

E. VILLAESCUSA
B.E., M.S.
Rock Mechanics Engineer, Mount Isa Mines LTD.

SUMMARY A description of the conventional techniques of rock discontinuity data collection is presented, including a review of the biases inherent to the sampling processes. A sampling method is recommended based on practicality and also due to the mathematical inferences regarding the distributional nature of the observed discontinuity trace lengths.

1. INTRODUCTION

Some aspects of rock mass structure can be measured directly by the structural mapping of exposed faces or drill cores, or can be deduced from indirect measurements made using geophysical techniques. The geometrical properties required to characterize the rock structural geometry, and that are obtained from a typical discontinuity survey include primary set characteristics such as discontinuity orientation, trace length and spacing and secondary set characteristics such as discontinuity termination, roughness, planarity, filling material, water conditions, etc.

Geological mapping of structural data is required in the early stages of every rock characterization program. The naturally occurring data to be collected can be divided into two classes (Call et al, 1976), (1) main structures, such as faults, dykes, contacts and related features with a size of the same order of magnitude as that of the site to be characterized. The position in space, physical properties and geometrical characteristics are usually established deterministically for each of these major discontinuities. Interpretive geological cross-sections or level maps are likely to feature the position of every major structure with respect to the area of design; and (2) minor geological features, such as discontinuities, minor shears and bedding planes which represent for practical purposes an infinite population in the area of design. As a result, their geometrical characteristics and physical properties must be estimated by measurements of a representative sampled (smaller) population. Spot sampling techniques such as cell and line mapping methods are recommended to characterize this type of discontinuities.

Representative sampling, sample size, and the definition of structural domains are the most important steps in a discontinuity survey (Call et al, 1976). Structural domains are zones in which the geometrical and physical properties of the rock jointing are statistically homogenous. Geometric discontinuity set characteristics must be estimated from field measurements to obtain the experimental probability distributions to be used in the statistical characterization of the rock structure. In a statistical discontinuity sampling program, three populations are of interest: the target population, which is the three-dimensional distribution of discontinuities at some depth in the rock mass; the exposed population or sets of discontinuities intersecting outcrops, borings or excavation walls; and the sample, or collection of discontinuities whose properties are actually measured (Call et al, 1976). It must be clear that not every discontinuity in the target population or rock mass has an equal chance of appearing in an outcrop of excavation wall, and that not each of those that do appear, has an equal opportunity of appearing in the sample.

Rock discontinuity properties are three-dimensional entities, but observations of rock structure are usually one-dimensional (as in bore holes) or at best two-dimensional, when the observations are gathered from outcrops or excavation walls. Unfortunately, even a complete two-dimensional description of the rock structure is sometimes difficult to establish due to the limited sizes of exposures where the discontinuities are mapped, and to difficulties of access along the different orientations, which are required to establish the rock discontinuity anisotropies.

Several methods are available to determine the discontinuity set characteristics including line sampling (Call, 1972), semi-trace length sampling (Cruden, 1977; Priest and Hudson, 1981) and cell mapping techniques (Mathis, 1988). In the present case the critical differences between the methods will be described, including inferences about the statistical analysis of the discontinuity trace length characteristics from each of the line sampling methods.

2. CELL MAPPING

This is a form of areal sampling or two-dimensional mapping in which an area interception criterion is established in order to collect the field data. Rectangular or square windows, which are called "cells" are defined along the excavation walls. A statistical value based on the properties of the discontinuities found within the boundaries is assigned to each cell. We begin by visually defining individual discontinuity sets within the cell boundaries; this process requires the grouping by eye of a family of discontinuities with similar orientational

properties in order to form a geological design set. For each discontinuity set we record the orientation and locations of all the discontinuities within the cell boundaries. The number of end points contained within the window is recorded for each discontinuity observed. Mathis (1988) has developed a quicker sampling method, in which the discontinuity properties are sampled from a reduced number of observations that appear to represent the mean values for each individual set. Imaginary lines, perpendicular to each discontinuity set, are used to calculate the average apparent discontinuity spacing. Estimates of the observed number of discontinuity trace centres per cell and the average sampled trace length can also be calculated (see Figure 1). Pahl (1981), Laslett (1982) and Kulatilake and Wu (1984) have presented methods to estimate the two-dimensional average values of the discontinuity trace length from areal sampling techniques.

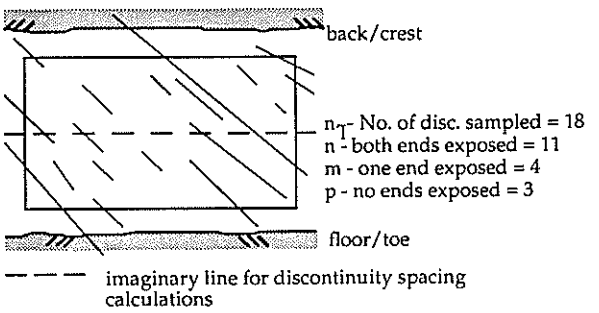

Figure 1 Typical cell mapping procedures

This method is time consuming compared with line sampling. It is evident from Figure 1 that only four discontinuities would be sampled along a horizontal line through the cell, while eighteen discontinuities would be sampled using the cell mapping procedure.

3. SEMI-TRACE LENGTH MAPPING

The semi-trace length sampling concept was first introduced by Cruden (1977) in his analysis of discontinuity size, and later used by Priest and Hudson (1981). The mapping scheme consists of sampling only the discontinuity trace segment appearing above the sampling line (see Figure 2).

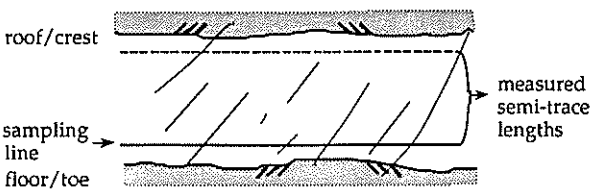

semi-trace length measurements are restricted to the portion above the sampling line

Figure 2 Semi-trace length sampling

Semi-trace length sampling is also a two-dimensional mapping technique, which uses an intersection criterion to determine whether or not a particular discontinuity will be included in the sample (Mathis, 1988). However, mathematical analysis regarding the distributional estimation of the observed discontinuity trace length distributions indicate that semi-trace length data appears to be insensitive to changes in the underlying uncensored trace length distribution, as discussed by Warburton, (1980) and Laslett, (1982) and presented in Section 6.

4. LINE MAPPING

This is a systematic, one-dimensional spot sampling technique, which can be extended to two-dimensions if the line is located inside a sampling window. The method consists of stretching a measuring tape along the exposed face and recording the measurements and features of interest of every discontinuity that intersects the tape. Ideally, the sample sites would be randomly selected at three equal-length, mutually orthogonal directions. Any discontinuity ignored by one line, because of its orientation, would be sampled preferentially by one or both of the other lines. In practice, however, the sites are determined by availability and accessibility of rock exposures. Experience has shown that approximately 2 days are required to choose an appropriate mapping site, establish the line, and record the data required. Mapping should be done preferentially, in clean (washed) or newly exposed rock surfaces, which allows for a better exposure of the discontinuity geometry. Vertical sampling lines are very important in the sampling process, but sometimes difficult to obtain due to the absence of vertical development within the area of interest. A recommended compromise is to use several randomly located, short ladder-based, lines within the drives or face walls where heights greater than 4m are available.

The length of the line is normally extended until a prerequisite number of observations is obtained. Savely (1972) determined that at least 60 observations are required to stereographically define the discontinuity sets found along a particular sampling line. Experience also suggests that at least 40 observations per discontinuity set are required in order to construct experimental histograms and provide a sound statistical data base of the discontinuity set characteristics such as discontinuity spacing, trace length and discontinuity orientation (Villaescusa, 1991). Priest and Hudson, (1981) presented a method to calculate the number of observations required to estimate the precision of the mean discontinuity spacing value for a negative exponential distribution. Forty observations will estimate the underlying mean within 20% at the 80% confidence level. The required number of observations increases very rapidly as the estimation error is decreased. In practice, however, depending on the complexity of rock jointing (a rock mass generally contains between three to six discontinuity sets) and the number of sampling lines used (a line samples some discontinuity sets preferentially), between 200 and 300 observations should be made at each structural domain for design.

If geostatistical inferences of discontinuity spacing or discontinuity linear density are to be made the sampling line should be at least 40m long in order to obtain reliable variograms, with significant ranges of influence (Villaescusa and Brown, 1990). Lastly, we must be careful to not group data from different rock types or across major discontinuities, unless we have

previously established structural domains for design.

In the present case a new rigorous line sampling scheme has been developed. A standard procedure such as that described by Call et al, (1976) was modified in order to gather data suitable for three-dimensional computer modelling of the discontinuity network and to correct for sampling biases (Villaescusa, 1991). The data collected is more suitable for rock fragmentation (blasting) predictions, than for slope stability or rock reinforcement analyses, but additional discontinuity set characteristics such as discontinuity overlap, minimum dip, etc., can be recorded if required. The new sampling scheme was developed to be compatible with the mathematical corrections for edge effects brought about by the finiteness of a sampling window on the observed data developed by Laslett (1982). Discontinuities are observed through a convex window, as in cell mapping, with a line transect drawn inside the convex window, and only those traces which cross the line are recorded (see Figure 3).

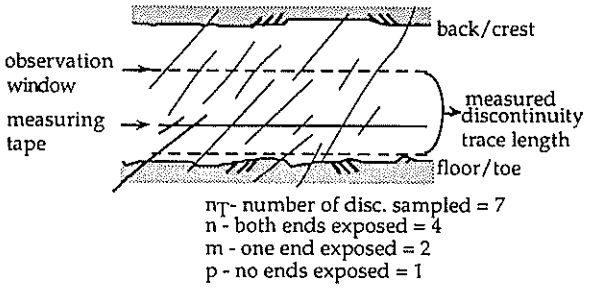

Figure 3 Line sampling of rock discontinuities

At each selected mapping site a window is drawn and a measuring tape is stretched across the window to record every discontinuity intersecting the tape. The information is recorded on a tabular data sheet suitable for subsequent computer analysis (see Figure 4).

The dimensions of the observation window should be kept constant at each site, since data from different lines is usually grouped together. Basic information at each site should include the number, location, elevation, bearing and plunge of the reference line, the dip and dip direction of the rock exposure and the censoring levels of the convex window (up and down). A mnemonic system compatible with the notation used by the local geologists, should be implemented to identify different rock types and discontinuity filling material at each site (Call et al, 1976). Discontinuity characteristics to be measured in the survey include;

1. **Distance,** along the tape where the discontinuity intersects the line. Discontinuity spacings are calculated from the intercept distances, the mean discontinuity set orientation and the orientation of the sampling line. Numerically, the individual apparent spacing values are defined by sorting the discontinuities by individual sets down the sampling line and subtracting the distances between adjacent discontinuities of the same set.

2. **End points,** of the discontinuities intersecting the tape. When the discontinuities are observed through a convex window, three sets of observations are obtained: discontinuities totally contained (2 trace end-points observable), discontinuities intersecting only one of the window boundaries (1 trace end-point observable), and finally discontinuities transecting the window (0 trace end-points observable).

3. **Type of structure,** such as discontinuity, vein, fault, bedding, shear, contact, or blast induced fracture.

4. **Dip/Dip Direction,** of discontinuities intersecting the tape.

5. **Rock type,** recorded in the mnemonic code as described above.

Line No: _____ North: _____ Bench face/wall dip: _____ Page: _____ of _____
Bearing: _____ East: _____ Bench face/wall dip dir: _____ By: _____
Plunge: _____ Censoring levels (m): up _____ down _____ Date: _____
Elev: _____ Location: _____ Start: _____ Finish: _____

LOCATION		STRUCTURE					GEOMETRY							REMARKS
									Above		Trace Length	Below		
Dist(m)	Endpoints	Type	Dip Dir	Dip	Rock		Rough	Plan	T1	T2	(m)	T1	T2	

NOTATION USED:

Endpoint Locations		Structure Type				Roughness		Planarity		T1 (Termination)		T2	
0	transecting	J	joint	B	bedding	R	rough	P	planar	AJ	another joint	L	low angle (<20°)
1	intersecting	V	vein	S	shear	S	smooth	W	wavy	IR	intact rock	H	high angle (<20°)
2	contained	F	fault	C	contact	SL	slickensided	I	irregular	FC	floor censored	UN	unknown
		BX	blast induced							RC	roof censored		

Figure 4 Data collection sheet for line sampling of rock discontinuities

6. **Roughness**, a qualitative measure of the small (2 cm or less) asperities on the discontinuity surface (Call et al, 1976). Rough, smooth and slickensided categories are used.

7. **Planarity**, a qualitative indication of the geometrical nature of the discontinuities. Planar, wavy and irregular are the categories used.

8.**Trace Length**, measured as seen in the rock face. A trace is the maximum measurable length of the resulting intersection between a discontinuity and a planar excavation in rock.

9. **Termination**, as observed in the top and the bottom of the discontinuity in the dip direction (Call et al, 1976), but only if the discontinuity is contained; otherwise, termination could be artificially created ("unobservable") by the dimensions of the observation window or the excavation geometry. A discontinuity termination which is "unobservable" on the top is said to be "roof censored" regardless of the cause of censoring. Likewise, a discontinuity termination which is "unobservable" on the bottom is called "floor censored". Discontinuities can terminate either against another discontinuity or in intact rock. Call et al, (1976) introduced the concept of high (>20°) and low (<20°) angle termination against other discontinuities; when this happens, observations suggest that one of the discontinuities will propagate further along a common direction (see Figure 5).

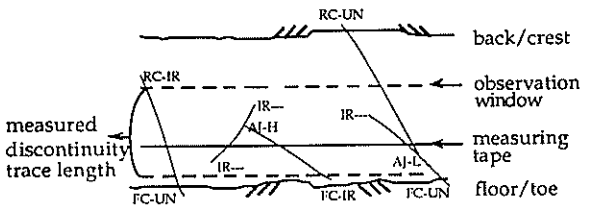

Figure 5 Types of discontinuity termination

10. **Remarks**, used to describe characteristics such as discontinuity aperture, thickness of filled discontinuities, and observed water conditions.

5. MAPPING BIASES

Geological mapping of rock discontinuities introduces four main biases into the sampled data, namely orientation, size, truncation and censoring. Carefully defined sampling or correction procedures are essential to eliminate or minimize these effects. At each site, at least three different directions of mapping should be chosen to reduce the orientation bias introduced when discontinuities striking parallel to a surveying line are sampled to a lesser degree than discontinuities striking normal to the sampling direction (Terzaghi, 1965). Furthermore, a quantitative correction of this bias as described by Priest (1985) can be implemented during data analysis.

Size bias in discontinuity sampling occurs at two levels. At the first level, larger discontinuities are more likely to intersect an outcrop or excavation wall than smaller discontinuities. At the second level, the likelihood that a sampling line intersects a discontinuity trace is directly proportional to the length of the trace (Baecher and Lanney, 1978). A method based on mathematical stereology (Warburton, 1980) can be used to correct the first level bias and the second level bias can be corrected using a method developed by Laslett (1982). The line sampling method presented here collects the raw field data in a manner compatible with Laslett's method and subsequent corrections of both biases can be implemented (see Villaescusa, 1991).

In data collection, a decision is made to disregard any discontinuity with a trace length smaller than an arbitrary cut-off. Also, the dimension of the artificial window imposed on the rock discontinuities limits the mappable size of the observed structures. As a result, the sampled trace length distributions are both truncated and censored. Truncation occurs when trace length values below a certain threshold are not recorded. Censoring occurs when the observed length of a trace is shortened due to the edge effect of the observation (artificial or not) window (i.e. when one or both ends of the trace are not visible). Censored traces provide only a lower bound estimate of their length. Censoring is a property of the sample, whereas truncation is a property of the distribution (Kendall & Stuart, 1973).

The walls of an underground excavation or an open cut bench face are rarely smooth or planar, especially when the openings are created by traditional drill-blast-scale techniques. Even in cases in which overbreak is negligible, hole deviation alone will control the conditions or geometry of the final excavated walls. As pointed out by Mathis (1988), the excavation process will expose discontinuities which would normally be hidden behind the plane of mapping (see Figure 6), leading to over-estimation of parameters such as observed trace length, discontinuity density and also a reduction in the discontinuity orientation bias. Under these conditions the mapping surface could be compared to a stereological thick section and appropriate corrections to the sampled data, such as those described by Weibel (1980) can be implemented.

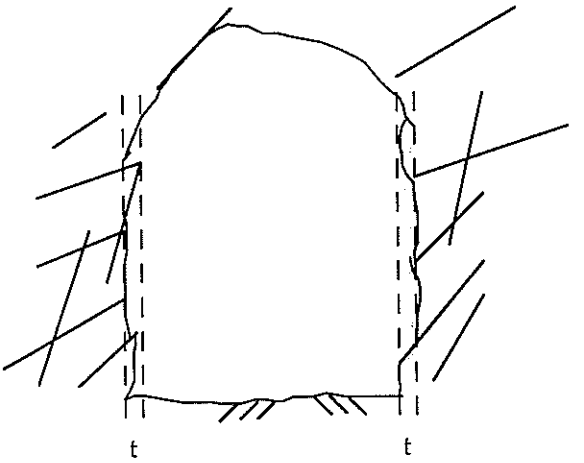

Figure 6 Actual mapping surfaces after blasting and scaling showing finite section thickness t . (After Mathis, 1988)

6. JOINT TRACE LENGTH ANALYSIS

The most widely used method of estimating discontinuity size is based on measurements of trace length exposures in outcrops and underground or open cut excavation walls. The traces are lines formed by the intersections of the discontinuities with the excavations in rock. Sampled trace lengths (from areal or line sampling) and semi-trace lengths are both truncated and censored as described before. Truncation can be corrected using a method suggested by Warburton (1980) whereas censoring can be corrected using a method developed by Laslett (1982). However, censoring is harder to correct because the analysis must consider the two-dimensional point proccess of the trace centres in the sampling wall.

Observed joint traces are separated into three classes, depending of the number of visible end-points (0,1 or 2). Baecher (1980) presented a likelihoood function for the progressively censored two-dimensional density function of joint trace length, based on life testing methods (Epstein, 1960). However, analysis by Warburton (1980) and Laslett (1982) has shown that life testing methods do not appropiately take into account the point process of the trace centres in the window of observation. Laslett (1982) has given maximum likelihood estimators for areal and line sampling of traces in two-dimensions which correctly predict the parametres of the underlying uncensored trace length distributions.

The advantage of semi-trace length sampling is that the uncensored distribution of trace segments lengths can be estimated from the censored sample data using life-testing methods, without involving the point process of the discontinuity trace centres (Priest and Hudson, 1981). The problem is that uncensored semi-trace length and uncensored full trace lengths generally have different distributional forms (Warburton, 1980). If a Poisson line segment model applies, the observed semi-trace lengths come from the following distribution (Cox, 1959)

$$H(L) = \int_0^L \frac{[1-F(Z)]\,dZ}{\mu L} \qquad (1)$$

where F(Z) is the underlying cummulative distribution of trace lengths and μL is the mean trace length. Therefore H(L), the observed semi-trace length distribution, is a monotonic decreasing distribution which is not sensitive to any changes in the uncensored underlying trace length distribution.

Experimental results from areal and line sampling (Roleau, 1984; Massoud, 1987 and Villaescusa, 1991) suggest a lognormal nature for the observed full trace length distributions. Mathematical analysis by Cox (1959) suggests that if a Poisson line segment model applies, the observed full trace lengths come from the following distribution

$$G(L) = \int_0^L \frac{Z\,F(Z)\,dZ}{\mu L} \qquad (2)$$

where F(Z) is the underlying cummulative distribution of trace lengths and μL is the mean trace length. Therefore G(L), the observed trace length distribution from line sampling should never appear remotely exponential.

7. CONCLUSIONS

Conventional rock discontinuity mapping methods use a line or an areal intersection criterion in order to establish a statistically representative sample of the rock mass structural properties. Mathematical corrections of mapping biases are available for cell and line mapping methods. However, from a practical point of view, a line intersection criterion is preferred to an areal intersection criterion, due to the considerable reduction in the number of discontinuities required for the subsequent mathematical analysis regarding the determination of the distributional properties of the discontinuity set characteristics. Mapping of full traces is recommended instead of semi-trace length sampling, since the observed semi-trace length distributions are monotonic decreasing functions which will never reproduce the actual lognormal nature of the underlying trace length distributions.

8. REFERENCES

Baecher, G.B. and Lanney, N.A. (1978). Trace length biases in joint surveys. Proc. 19th U.S. Symp. Rock Mech. Mackay School of Mines, pp. 56-65.

Baecher, G.B. (1980). Progressively censored sampling of rock joint traces. Mathematical Geology. Vol 12, No. 1., pp. 33-40.

Call, R.D. Analysis of geologic structure for open pit slope design. Thesis (PhD) University of Arizona, Tucson.

Call, R.D., Savely, J.P. and Nicholas, D.E. (1976). Estimation of joint set characteristics from surface mapping data. In Monograph on Rock Mech. Appl. in Mining, W.A. Hustrulid (Ed.). AIME, NewYork. pp. 65-73.

Cox, D.R. (1959). Some sampling problems in technology. In New Developments in Survey Sampling. N. Johnson and H. Smith (Eds.). Wiley and Sons, NewYork. pp. 507-513.

Cruden, D.M. (1977). Describing the size of discontinuities. Int. J. Rock Mech. Min. Sci. & Geomech. Abstr. Vol. 14., pp. 133-137.

Epstein, B. (1960). Estimation from life test data. Technometrics. Vol. 3, pp. 107-109.

Kendall, M.G. and Stuart, A. (1973). The advanced theory of statistics. Hafner, New York.

Kulatilake, P.H.S.W. and Wu, T.H. (1984). The density of discontinuity traces in sampling windows. Tech. Note. Int. J. Rock Mech. Min. Sci. & Geomech. Abstr. Vol. 21., pp. 345-347.

Laslett, G.M. (1982). Censoring and edge effects in areal and line transect sampling of rock joint traces. Mathematical Geology. Vol. 14, No. 2., pp. 125-139.

Massoud, H. (1987). Modelisation de la petite fracturation pour les techniques de la geostatistique. Thesis (PhD) Ecole Nationale Superieure des Mines des Paris.

Mathis, J.I. (1988). Development and verification of a three-dimensional rock joint model. Thesis (PhD) Luleå University of Technology.

Pahl, P.J. (1981). Estimating the mean trace length of discontinuity traces. Int. J. Rock Mech. Min. Sci. & Geomech. Abstr. Vol. 18., pp. 221-228.

Priest, S.D. and Hudson, J.A. (1981). Estimating discontinuity spacing and trace length using scanline surveys. Int. J. Rock Mech. Min. Sci. & Geomech. Abstr. Vol. 18., pp. 183-197.

Priest, S.D. (1985). Hemispherical projections methods in rock mechanics. Allen & Unwin, London.

Roleau, A. (1984). Statistical characterization and numerical simulation of a fracture system - Application to groundwater flow in the Stripa granite. Thesis (PhD) University of Waterloo, Ontario.

Savely, J.P. (1972). Orientation and engineering properties of jointing in the Sierrita Pit, Arizona. Thesis (MS) University of Arizona, Tucson.

Villaescusa, E. and Brown, E.T. (1990). Characterizing joint spatial correlation using geostatistical methods. Proc. Int. Symp. on Rock Joints. Loen, Norway. pp. 115-122.

Villaescusa, E. (1991). A Three-dimensional model of rock jointing. Thesis (PhD) University of Queensland, Brisbane.

Warburton, P.M. (1980). A stereological interpretation of joint trace data. Int. J. Rock Mech. Min. Sci. & Geomech. Abstr. Vol. 17., pp. 181-190.

Weibel, E.R. (1980). Stereological Methods. Academic Press, London.

Assessment of Applicability of Four Empirical Strength Criteria for Intact Coal

V.S. VUTUKURI
M.S.
Senior Lecturer, Department of Mining Engineering, University of New South Wales
S.M.F. HOUSSAINI
M.E.
Post-graduate Student, Department of Mining Engineering, University of New South Wales

SUMMARY The applicability of four empirical strength criteria, namely, Bieniawski, Hoek and Brown, Johnston and Ramamurthy has been assessed for intact coal by using the published triaxial test data. For nonlinear regression analysis, the PC package FFIT has been selected. The best fit has been found by minimising the sum of the squares of the relative errors between the function and the data points. Although unique values of the constants in all criteria have been determined with good coefficients of determination ranging from 0.83 to 0.86 for overall data, a wide variation has been noticed in the values of the constants when individual data sets have been analysed. A strong negative correlation has been observed between B in Bieniawski's criterion and uniaxial compressive strength, σ_c (coefficient of determination, $r^2 = 0.86$), m in Hoek and Brown's criterion and σ_c ($r^2 = 0.71$) and B in Ramamurthy's criterion and σ_c ($r^2 = 0.88$). The following empirical strength equation best describes the triaxial strength test data analysed for intact coal:-

$$\frac{\sigma_1}{\sigma_c} = 1 + B\left(\frac{\sigma_3}{\sigma_c}\right)^{0.6}$$

where σ_1 = axial compressive stress at failure, MPa;
σ_3 = confining pressure, MPa;
σ_c = uniaxial compressive strength, MPa; and
$B = 7.2075 - 1.7263\,(log\ \sigma_c)^2$.

An estimate of the axial compressive stress at failure at any confining pressure can be made if only the uniaxial compressive strength of the intact coal is known.

1. INTRODUCTION

The estimation of the triaxial strength of coal is essential in the design of pillars in underground coal mines. The size of pillars determined should allow maximum coal recovery while maintaining overall stability.

The theoretical triaxial strength criteria based on the actual mechanism of fracture do not fit the experimental results properly and to overcome this problem, many empirical criteria have been formulated for rocks. The strength criteria can be written in terms of either

(1) principal stresses, σ_1 and σ_3 at failure such as

$$\sigma_1 = \sigma_c + a\,\sigma_3^{\,b} \qquad (1)$$

or

(2) normalised principal stresses at failure obtained by dividing the principal stresses, σ_1 and σ_3 at failure by the relevant uniaxial compressive strength, σ_c such as

$$\frac{\sigma_1}{\sigma_c} = 1 + B\left(\frac{\sigma_3}{\sigma_c}\right)^{\alpha} \qquad (2)$$

In equations (1) and (2), a, b, B and α are constants.

Equation (1) was proposed by Murrell (1965) whereas equation (2) was proposed by Bieniawski (1974a). Equation (2) permits the direct comparison of a number of tests on the same plot. A typical relationship between σ_1 and σ_3 or $\frac{\sigma_1}{\sigma_c}$ and $\frac{\sigma_3}{\sigma_c}$ at failure for coals is a nonlinear one.

Four empirical strength criteria proposed by Bieniawski (1974a), Hoek and Brown (1980a, b), Johnston (1985) and Ramamurthy (1986) have been selected to assess their applicability for intact coal by using the published triaxial test data. These authors have not analysed data for coal and the appropriate values for constants are not available for the same.

2. SUMMARY OF THE FOUR CRITERIA

2.1 Bieniawski's Criterion

The criterion proposed by Bieniawski (1974a) is:-

$$\frac{\sigma_1}{\sigma_c} = 1 + B\left(\frac{\sigma_3}{\sigma_c}\right)^{\alpha} \qquad (3)$$

where B = 3.0 for siltstone and mudstone;
= 4.0 for sandstone;
= 4.5 for quartzite; and
= 5.0 for norite and
α = 0.75 for all rock types.

Yudhbir, Lemanza and Prinzl (1983) modified the Bieniawski's criterion and proposed the following equation:-

$$\frac{\sigma_1}{\sigma_c} = A + B\left(\frac{\sigma_3}{\sigma_c}\right)^{\alpha} \quad (4)$$

where A = 1 for intact rocks;
= 0.0176 $Q^{0.65}$
where Q = NGI rating for rock mass.
B = 2.0 for tuff, shale and limestone;
= 3.0 for siltstone and mudstone;
= 4.0 for sandstone and quartzite; and
= 5.0 for norite and granite and
α = 0.65 for all rock types.

The details of NGI rock mass classification are given by Barton, Lien and Lunde (1974).

2.2 Hoek and Brown's Criterion

The criterion proposed by Hoek and Brown (1980a, b) is:-

$$\frac{\sigma_1}{\sigma_c} = \frac{\sigma_3}{\sigma_c} + \left(s + m\frac{\sigma_3}{\sigma_c}\right)^{0.5} \quad (5)$$

where m and s are material constants. σ_c is the uniaxial compressive strength of the intact rock i.e. of a laboratory size specimen (say a 50 mm diameter by 100 mm long core) which is free from discontinuities such as joints or bedding planes. For intact rocks, s = 1 and m depends on rock type as follows:-

7 for dolomite, limestone and marble;
10 for mudstone, siltstone, shale and slate (normal to cleavage);
15 for sandstone and quartzite;
17 for andesite, dolerite, diabase and rhyolite; and
25 for amphibolite, gabbro, gneiss, granite, norite and quartz-diorite.

They also suggested approximate relationships between the constants m and s and the rock mass ratings developed by Bieniawski (1974b) and Barton et al. (1974) and the latest recommendations were given separately for disturbed and undisturbed rock masses (Hoek and Brown, 1988).

Substitution of $\sigma_1 = 0$ in equation (5), and solution of the resulting quadratic equation for σ_3, gives the uniaxial tensile strength of a rock, σ_t as:-

$$\sigma_3 = \sigma_t = \frac{1}{2}\sigma_c\left[m - \left(m^2 + 4\right)^{0.5}\right] \quad (6)$$

2.3 Johnston's Criterion

The criterion proposed by Johnston (1985) is:-

$$\frac{\sigma_1}{\sigma_c} = \left[\left(\frac{M}{B}\right)\left(\frac{\sigma_3}{\sigma_c}\right) + 1\right]^{B} \quad (7)$$

where M and B are constants. These constants depend upon σ_c as follows:-

$$M = 2.065 + k\,(log\ \sigma_c)^2$$

$$B = 1 - 0.0172\,(log\ \sigma_c)^2$$

where k = 0.170 for dolomite, limestone and marble;
= 0.231 for mudstone, shale, slate and clay;
= 0.270 for sandstone and quartzite;
= 0.659 for amphibolite, gabbro, gneiss, granite, norite and grano-diorite; and
= 0.276 for all rock types combined (overall)

and

σ_c = uniaxial compressive strength, kPa.

When $\sigma_1 = 0$, σ_3 becomes tensile strength, σ_t and

$$\frac{M}{B} = -\frac{\sigma_c}{\sigma_t}$$

This is the only criterion which suggests that the values of the constants are not only dependent on rock type but also on uniaxial compressive strength of the rock.

The equation (7) has also been proposed by Sheorey, Biswas and Choubey (1989).

2.4 Ramamurthy's Criterion

The criterion proposed by Ramamurthy (1986) is:-

$$\frac{\sigma_1}{\sigma_3} = 1 + B\left(\frac{\sigma_c}{\sigma_3}\right)^{\alpha} \quad (8)$$

where B and α are constants.

The constant α was found to be between 0.75 and 0.85 and an average of value 0.8 was suggested for all rock types. He proposed the following values for B:-

1.8 for siltstone, clay, tuff and loess;
2.2 for shale, slate, mudstone, claystone and sandstone;
2.4 for limestone, anhydrite and rocksalt;
2.6 for quartzite, andesite, diorite, norite, liprite and basalt;
2.8 for marble and dolomite; and
3.0 for granite and charnockite.

This criterion is only applicable for all values of $\sigma_3 > 0$.

3. REGRESSION ANALYSIS OF TRIAXIAL TEST DATA

Regression models can be classified as:-

1. Linear - Simple
- Multiple
2. Nonlinear.

In simple linear regression model, the term "simple" implies a single regressor variable, x, and the term "linear" implies linear in x.

$$y = \beta_0 + \beta_1 x + \varepsilon \quad (9)$$

where y = measured response variable;
β_0 = intercept;
β_1 = slope; and
ε = model error.

In multiple linear regression model, the term "multiple" implies multiple (more than one) regressor variables, x_1, x_2, ..., x_n,

and the term "linear" implies linear in regressor variables, $x_1, x_2, \ldots\ldots, x_n$.

$$y = \beta_0 + \beta_1 x_1 + \ldots\ldots\ldots\ldots + \beta_n x_n + \varepsilon \qquad (10)$$

where $\beta_0, \beta_1, \beta_2, \ldots\ldots, \beta_n$ are the parameters that specify the nature of the relationship.

The regressor variables or the response variable are not necessarily in natural units. They may be transformations (log, square root, etc).

In a nonlinear regression model, at least one of the parameters enters the model in a nonlinear way.

$$y = a + b^{-c\,x} + \varepsilon \qquad (11)$$

3.1 Estimation of Regression Coefficients

To find the best-fitting curve to match the plotted data, the sum of the squares of the errors between the data and the function evaluated with the parameter values is minimised. Although this procedure is widely used, relative errors can be quite high for low values of regressor variable. To overcome this difficulty, the sum of the squares of the relative errors can be minimised.

3.2 Example

The following triaxial test data refers to Uchitdih coal (Das and Sheorey, 1986). The value of m in Hoek and Brown's criterion is to be determined for this data assuming $s = 1$.

Minor principal stress, MPa	Major principal stress, MPa
0	35.3
7	76.8
15	99.0
25	124.3
35	147.5
45	161.5
60	169.3
70	187.4

Hoek and Brown's criterion is nonlinear. Unless appropriate software is available for nonlinear regression, it is not feasible to do the analysis by the use of a calculator. Hoek and Brown (1980a) recommended the following transformation to make it a simple linear model to determine the appropriate values for the parameters by the use of a calculator:-

$$(\sigma_1 - \sigma_3)^2 = \sigma_c^2 + m\,\sigma_c\,\sigma_3 \qquad (12)$$

Equation (12) is of the form

$$y = a + b\,x \qquad (13)$$

where $y = (\sigma_1 - \sigma_3)^2$;
$x = \sigma_3$;
$a = \sigma_c^2$;and
$b = m\,\sigma_c$.

x and y are known and a and b can be estimated by simple linear regression analysis by the use of a calculator.

It must be mentioned here that linearisation of a nonlinear model does not produce an equivalent model. A full discussion on regression analysis is given by Myers (1990).

By simple linear regression analysis, σ_c has been found to be 64.52 MPa (test value - 35.3 MPa) and m to be 2.51. Sheorey et al. (1989) also reported that σ_c estimated from simple linear regression after transformation has been significantly higher than the test value.

By nonlinear regression analysis through the minimisation of the sum of the squares of the errors, σ_c has been found to be 51.94 MPa and m to be 3.92. For this analysis, the PC package for statistical analysis, SPSS/PC+ has been used. "Eureka: The Solver" can also be used but limited to about 20 data points.

By nonlinear regression analysis through the minimisation of the sum of the squares of the relative errors, σ_c has been found to be 37.55 MPa and m to be 7.24. For this analysis, the PC package FFIT has been used (Hoyer, 1989).

The results of analysis of relative errors (in percentage) from the three methods of regression analysis are given in TABLE I. Figure 1 gives the three curves found from the three methods of regression analysis. From this example, it has been concluded that FFIT program serves well for nonlinear regression analysis of triaxial test data and it has been used for all analyses.

TABLE I

RESULTS OF ANALYSIS OF RELATIVE ERRORS IN % FROM THREE METHODS OF REGRESSION ANALYSIS

	Simple linear regression analysis after transformation	Nonlinear regression analysis using SPSS/PC+	Nonlinear regression analysis using FFIT
Mean	10.504	10.868	9.233
Std dev	14.244	8.724	5.647
Minimum	2.894	4.924	0.191
Maximum	45.287	32.037	18.963
Range	42.392	27.113	18.772

4. DATA FOR ANALYSIS

In order to examine the applicability of the four empirical criteria selected, the triaxial strength data for coals from two publications (Hobbs, 1964 and Das and Sheorey, 1986) have been used. The uniaxial compressive strength ranges from 2.2 to 51.4 MPa. Twenty six sets of data are available for analysis.

In these tests, the specimens used were of two sizes, 5.1 cm long by 2.5 cm diameter (Hobbs, 1964) and 4.2 cm long by 2.8 cm diameter (Das and Sheorey, 1986). For practical purposes, both sizes can be considered to be the same. For analysis, these coal specimens have been considered to be intact.

Coal, in general, contains three dominant planes of weakness, the bedding planes and the two families of cleat planes, the three families being orthogonal to one another. Hobbs (1964) reported the results which were similar for two orientations.

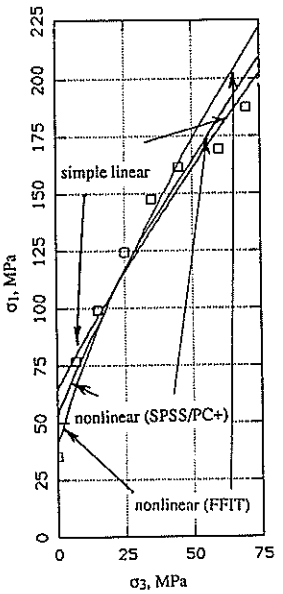

Figure 1 Plot of triaxial test data for Uchitdih coal and regression lines from 3 different regression models.

Although laboratory size coal specimens do contain planes of weakness, they can be considered to be intact. For example, if the criterion by Yudhbir et al. (1983) is used to describe coal strength behaviour, parameter A has to be near 1. From the analysis of coal test data, A has been found to be between 0.9959 and 1.0152.

Two of the criteria selected, namely, Hoek and Brown and Johnston, have been suggested to describe results in the "brittle" range only i.e. $\frac{\sigma_1}{\sigma_3} > 3.4$ (Mogi, 1966). However, Das and Sheorey (1986) concluded that the triaxial behaviour of coal did not become significantly ductile above the brittle limit. Hence, all the triaxial test data have been included in the analysis.

5. ANALYSIS

5.1 Bieniawski's Criterion

A plot of $\frac{\sigma_1}{\sigma_c}$ versus $\frac{\sigma_3}{\sigma_c}$ for all data along with the regression curve is shown in Figure 2. The values for B and α have been determined to be 3.90 and 0.7445 respectively. These values are in the range suggested by Bieniawski (1974a). The coefficient of determination has been found to be 0.857. The analysis of relative errors has indicated that 18.2% of the calculated values fall within 5% relative error, 27.9% within 10% and 40.3% within 15%. The details of this analysis are as follows:-

Mean - 22.891
Standard deviation - 19.767
Minimum - 0.181
Maximum - 103.112
Range - 102. 931

Analysis of individual data sets has given a range of values for B from 2.2910 to 6.8326 and for α from 0.4117 to 0.8687.

Analysis of these values in conjunction with the σ_c has indicated that there is a significant correlation between B and σ_c (Figure 3) and practically no correlation between α and σ_c. The relationship between B and σ_c is as follows:-

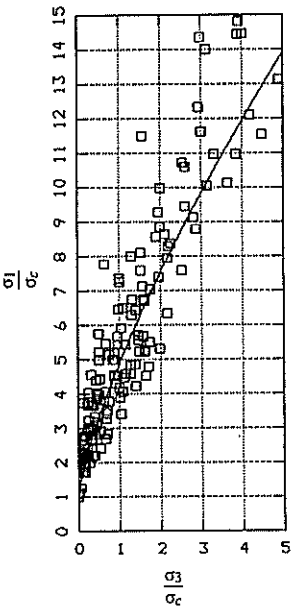

Figure 2 Plot of $\frac{\sigma_1}{\sigma_c}$ versus $\frac{\sigma_3}{\sigma_c}$ for all data along with regression line according to Bieniawski's criterion.

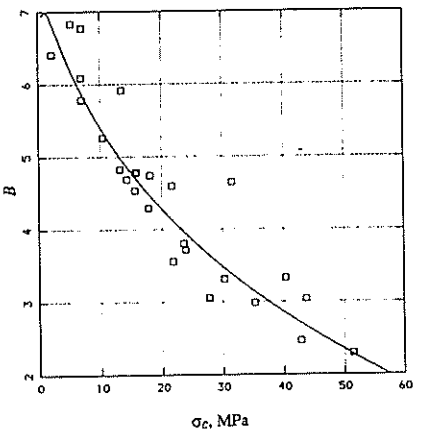

Figure 3 Plot of B versus σ_c for Bieniawski's criterion.

$$B = 7.0266 - 1.6228\ (log\ \sigma_c)^2 \qquad (14)$$

The coefficient of determination for this regression has been found to be 0.864.

Using the above equation for calculating B and the average value of 0.6 for α, axial stresses at failure, σ_1 and relative errors have been calculated and analysis of them has given that 39.6% of the calculated axial stresses fall within 5% relative error, 63.6% within 10% and 83.1% within 15%. The details of this analysis are as follows:-

Mean - 8.890
Standard deviation - 8.111
Minimum - 0.126
Maximum - 42.418
Range - 42.292

Taking α as 0.6, the values for parameter B have been recalculated for all the individual data sets. From this analysis, B has been found to be between 2.0663 and 7.7150 and the relationship between B and σ_c has been found to be as follows:-

$$B = 7.2075 - 1.7263\ (log\ \sigma_c)^2 \qquad (15)$$

The coefficient of determination for this regression has been found to be 0.910.

Using equation (15) for calculating B and 0.6 for α, axial stresses at failure, σ_1 and relative errors have been calculated and analysis of them has given that 52.6% of the calculated axial stresses fall within 5% relative error, 82.5% within 10% and 91.6% within 15%. The details of this analysis are as follows:-

Mean - 6.250
Standard deviation - 6.123
Minimum - 0.003
Maximum - 31.715
Range - 31.712

5.2 Hoek and Brown's Criterion

The value for m has been determined to be 14.55. This value is in the range suggested by Hoek and Brown (1980a). The coefficient of determination has been found to be 0.847. Analysis of individual data sets has given a range of values from 5.3795 to 50.190 for m. Analysis of these values along with the σ_c has indicated that there is a significant correlation between them (Figure 4). The relationship between them has been found to be as follows:-

$$m = 35.512 - 10.764\ (log\ \sigma_c)^2 \qquad (16)$$

The coefficient of determination for this regression has been found to be 0.7000.

Using equation (16) for calculating m, axial stresses at failure, σ_1 and relative errors have been calculated and analysis of them has given that 27.9% of the calculated axial stresses fall within 5% relative error, 51.3% within 10% and 69.5% within 15%. The details of this analysis are as follows:-

Mean - 13.427
Standard deviation - 12.381
Minimum - 0.142
Maximum - 66.562
Range - 66.420

5.3 Johnston's Criterion

The values for M and B have been determined to be 6.8889 and 0.6562 respectively. The coefficient of determination has been found to be 0.826. Analysis of individual data sets has given a range of values for M from 5.26 to 67.48 and for B from 0.33 to 0.78. However, no good correlation has been found either between M and σ_c or between B and σ_c as suggested by Johnston (1985).

5.4 Ramamurthy's Criterion

The values for B and α have been determined to be 3.955 and 0.6256 respectively. These values are in the range suggested by Ramamurthy (1986). The coefficient of determination has been found to be 0.868.

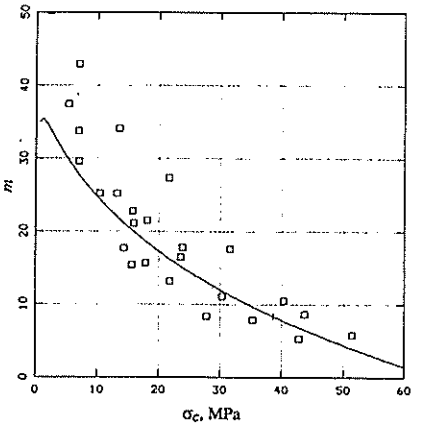

Figure 4 Plot of m versus σ_c for Hoek and Brown's criterion.

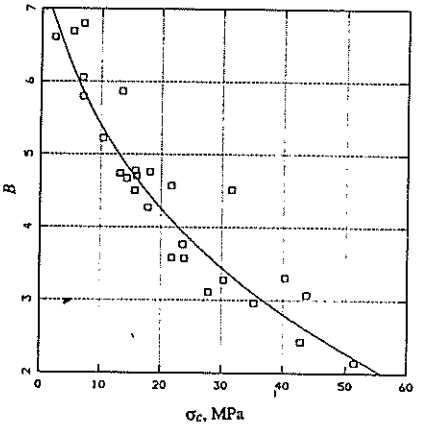

Figure 5 Plot of B versus σ_c for Ramamurthy's criterion.

Analysis of individual data sets has given a range of values for B from 2.15 to 6.80 and for α from 0.47 to 0.82. Analysis of these values in conjunction with the σ_c has indicated that there is a significant correlation between B and σ_c (Figure 5) and practically no correlation between α and σ_c . The relationship between B and σ_c has been found to be as follows:-

$$B = 7.0601 - 1.6579\ (log\ \sigma_c)^2 \qquad (17)$$

The coefficient of determination for this regression has been found to be 0.878.

Using equation (17) for calculating B and the average value of 0.667 for α, axial stresses at failure, σ_1 and relative errors have been calculated and analysis of them has given that 39.6% of the calculated axial stresses fall within 5% relative error, 62.3% within 10% and 76.6% within 15%. The details of this analysis are as follows:-

Mean - 11.214
Standard deviation - 14.319
Minimum - 0.132
Maximum - 122.222
Range - 122.090

Taking α as 0.67, the values for parameter B have been recalculated for all the individual data sets. From this analysis, B has been found to be between 2.5805 and 9.1073 and the relationship between B and σ_c has been found to be as follows:-

$$B = 7.1551 - 1.6311\ (log\ \sigma_c)^2 \qquad (18)$$

The coefficient of determination for this regression has been found to be 0.839.

Using equation (18) for calculating B and 0.67 for α, axial stresses at failure, σ_1 and relative errors have been calculated and analysis of them has given that 36.4% of the calculated axial stresses fall within 5% relative error, 63.0% within 10% and 81.2% within 15%. The details of this analysis are as follows:-

Mean - 10.458
Standard deviation - 12.130
Minimum - 0
Maximum - 103. 390
Range - 103.390

6. CONCLUSIONS

The selection of appropriate software for nonlinear regression analysis is crucial in the results obtained. The PC package FFIT has been found to be most appropriate for nonlinear regression analysis of triaxial test data. Out of the four criteria selected, Bieniawski's criterion with variable B (equation (15)) and a constant α of 0.6 appears to be the most appropriate one for coal. Ramamurthy's criterion with variable B (equation (18)) and a constant α of 0.67 comes next. There is very good correlation between parameter B of Bieniawski's criterion and parameter B of Ramamurthy's criterion (Figure 6). The relationship is as follows:-

$$B_B = 0.1244 + B_R \qquad (19)$$

where B_B = parameter B in Bieniawski's criterion and
B_R = parameter B in Ramamurthy's criterion.

The index of determination for this regression has been found to be 0.997.

The value of B depends upon σ_c which in turn depends upon material and structural characteristics and experimental conditions. Since there is not much difference in α, B can be taken approximately as a measure indicating the effect of σ_3 on σ_1. The lower the uniaxial compressive strength, the higher is the pressure sensitivity of triaxial strength at low confining pressure.

An estimate of the triaxial strength of coal can be made by means of the Bieniawski's criterion but with a variable B dependent upon σ_c (equation (15)) and a constant α of 0.6, that has an accuracy sufficient for practical purposes. The only parameter required for this criterion is the uniaxial compressive strength which can be determined simply.

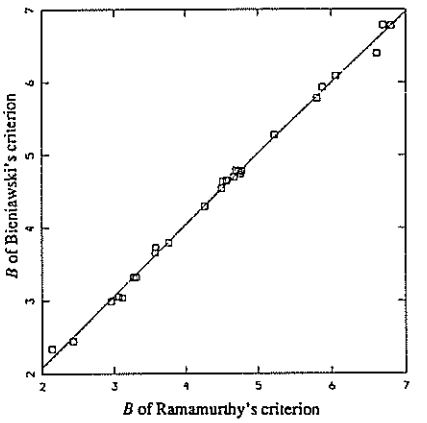

Figure 6 Plot of B of Bieniawski's criterion verus B of Ramamurthy's criterion

7. REFERENCES

Barton, N., Lien, R. and Lunde, J. (1974). Engineering classification of rock masses for the design of tunnel support. Rock Mech. Vol. No. 6 No. 4 pp. 189-239.

Bieniawski, Z. T. (1974a). Estimating the strength of rock materials. J. S. Afr. Inst. Min. Metall. Vol. No. 74 No. 8 March pp. 312-20.

Bieniawski, Z. T. (1974b). Geomechanics classification of rock masses and its application in tunnelling. Proc. 3rd Cong. Int. Soc. Rock Mech. Denver Vol. No. 2 Part A pp. 27-32.

Das, M. N. and Sheorey, P. R. (1986). Triaxial strength behaviour of some Indian coals. J. Mines, Metals and Fuels. March pp. 118-22.

Hobbs, D. W. (1964). The strength and the stress-strain characteristics of coal in triaxial compression. J. Geol. Vol. No. 72 pp. 214-31.

Hoek, E. and Brown, E. T. (1980a). Underground excavations in rock. London. Instn. Min. Metall.

Hoek, E. and Brown, E. T. (1980b). Empirical strength criterion for rock masses. J. Geotech. Engng. Div. ASCE. Vol. No. 106 No. GT9 pp. 1013-35.

Hoek, E. and Brown, E. T. (1988). The Hoek-Brown failure criterion - a 1988 update. Proc. 15th Can. Rock Mech. Symp. Univ. of Toronto. pp. 31-38.

Hoyer, D. I. (1989). FFIT. Cherrybrook NSW. David I. Hoyer.

Johnston, I. W. (1985). Strength of intact geomechanical materials. J. Geotech. Engg. Vol. No. 111 No. 6 June pp. 730-49.

Mogi, K. (1966). Pressure dependence of rock strength and transition from brittle fracture to ductile flow. Bull. Earthquake Res. Inst. Tokyo Univ. Vol. No. 44 pp. 215-32.

Murrell, S. A. F. (1965). The effect of triaxial stress systems on the strength of rock at atmospheric temperatures. Geophys. J. Roy. Astr. Soc. Vol. No. 10 pp. 231-81.

Myers, R. H. (1990). Classical and modern regression with applications. 2nd ed. Boston. PWS-KENT Publishing Company.

Ramamurthy, T. (1986). Stability of rock mass. Indian Geotech. J. Vol. No. 16 No. 1 Jan. pp. 1 - 74.

Sheorey, P. R., Biswas, A. K. and Choubey, V. D. (1989). An empirical failure criterion for rocks and jointed rock masses. Engg. Geol. Vol. No. 26 No. 2 Jan. pp. 141-59.

Yudhbir, Lemanza, W. and Prinzl, F. (1983). An empirical failure criterion for rock masses. Proc. 5th Cong. Int. Soc. Rock Mech. Melbourne. Vol. No. 1 pp. B1-8.

General Report, Session 4: Soil Properties and Testing

D.McG. ELDER
B.E.(Hons.), Ph.D., M.I.P.E.N.Z., M.A.P.E.N.S.
Jacques, Whitford & Associates Ltd, Halifax, Canada
N.J. TRAYLEN
B.E.(Hons.), M.I.P.E.N.Z.
Soils & Foundations Ltd, Christchurch

1. INTRODUCTION

In the first keynote address to the "Fifth Australia-New Zealand Conference on Geomechanics - *Prediction vs Performance*", Duncan (1988) reminded us that

> "The art of geotechnical engineering consists partly in deciding...what allowances should be made for the possibility that something will go wrong".

Duncan proposed nine categories of reasons why problems occur with predictions. Six of these relate directly to assumptions about soil properties and test results:

1. Unrecognised geologic details
2. (Un)disturbed samples
3. Unrepresentative samples
4. No tests, or no analyses
5. Wishful thinking
6. Variations in conditions

Identification and evaluation of risks associated with determination of soil properties is clearly an appropriate and continuing theme from the last Australia-New Zealand conference. From analysis of case histories of geotechnical problems and failures in each of these categories, Duncan concluded that

> "...Even under the most ideal circumstances we must cope with some degree of uncertainty regarding performance, due to our inevitable uncertainties regarding site conditions, and the behaviour of the materials with which we work.
>
> ...If the consequence of wrong prediction is added cost no larger than the cost to build more conservatively in the first place, the consequences of wrong prediction are minimal, and it is appropriate to risk the consequence of being wrong for the economy of being right. At the opposite extreme, where the possible consequence of being wrong is loss of human life and repair costs much higher than the costs of first construction, a conservative approach based on the worst assumptions is appropriate."

These risks relate to the consequences of unconservative design. Unfortunately, the decision process for a geotechnical engineer faced with providing design recommendations from a paucity of good quality data is rarely so simple. This is primarily because there is an additional risk which is often given little rigorous examination, yet cannot be treated superficially by the geotechnical engineer. This is the risk that through insufficient understanding of the relevant geotechnical factors a design will be overly conservative and lead to unnecessary expense.

Structures generally do not fail through conservative design. Nevertheless, the economic risk remains real. In fact it would be rare to find a geotechnical engineer who has not experienced each of three common situations:

- a professional engineer chose on a particular project to carry out all geotechnical-related design without reference to the geotechnical engineer, probably by employing very conservative design assumptions and almost certainly with minimal or no geotechnical testing

- the same professional engineer on another project accused the geotechnical engineer, with little or no basis, of being too conservative in making design recommendations

- a project which did not proceed due to the cost of actions recommended by the geotechnical engineer

Typical examples in the author's experience of where these situations occur regularly are remedial measures prior to building on unstable ground, and piled foundations for buildings. None of the three situations above has consequences which are life-threatening or might lead to expensive remedial measures at a later stage. Yet each involves risk-based decisions, which are most likely to involve a lack of detailed knowledge of soil conditions and properties. Improved understanding of soil properties therefore remains a key element of risk identification and evaluation, prior to determining solutions.

2. MEASURING SOIL PARAMETERS

In his General Report on "Geotechnical Testing" at the fifth Australia-New Zealand conference, Fahey (1988) suggested that some soil parameters cannot be reliably measured in the laboratory, although "reliably and consistently" might be a fairer qualification. Fahey highlights four groups of major parameters in particular (numbers of relevant papers in this session are noted in brackets for each category):

- coefficient of consolidation, c_v or c_h (0 papers)
- stiffness of natural sands (3)

- density, and angles of friction/dilation, of natural sands (2)
- *in situ* horizontal stress (or K_0) (0)

In the authors opinion, hydraulic conductivity should be added as a separate item to any list of this type, even though it is also incorporated in c_v and c_h. (1)

At the design stage the alternative to laboratory testing for measurement of soil parameters is *in situ* testing. There are few *in situ* tests able to quantify these soil properties with a high degree of reliability and consistency, yet at a cost reasonable for most typical projects. It is usually necessary to rely on widespread but cruder *in situ* tests. These are therefore the parameters associated with greatest uncertainty in many design situations.

Although accurate determination of soil parameters is difficult at the design stage, it is often possible to quantify these parameters quite accurately by back-analysis, when performance monitoring has been carried out.

Of the 21 papers submitted in time for review, 18 were based on laboratory testing and only three presented results of field testing. Disappointment over the comparative lack of interest in analysing and reporting *in situ* test results expressed by Fahey in his equivalent 1988 session report is reiterated here. Even more disappointing is that no paper dealt in any detail with back-analysis of soil properties from performance monitoring. Although "back-analysis *per se* is not guaranteed to provide any more accurate values of fundamental soil parameters than local point measurements" (Fahey, 1988) "this is the procedure which, in principle, leads to the most reliable assessment of geotechnical design parameters" (Jamiolkowski et al, 1985).

The usefulness of back-analysis as a tool for determining soil parameters is illustrated by analysis of settlements measured for a number of buildings in Christchurch ranging from 6 to 23 storeys high, on shallow footing or raft foundations (Traylen, 1987; Soils & Foundations, 1988-90).

Full investigation was carried out on all sites, and included testpits, boreholes, standard penetration testing, cone penetration testing, plate load testing, and extensive laboratory analysis including consolidation testing. Design settlements were estimated using a variety of methods as appropriate for each foundation type and subsurface profile. In determining appropriate values of soil compressibility for cohesive soils, greater reliance was placed on laboratory consolidation test results, but all other data were taken into account by using published correlations between secondary parameters (e.g. CPT values) and compressibility. For granular soils, established correlations were the primary means of estimating compressibility.

Settlements were monitored during and following construction by precise levelling. The range of predicted mean settlements using a number of appropriate methods in each case, and the range of actual settlements measured at different locations across each structure are shown in Table 1.

Table 1. Settlements for 3 Christchurch Buildings

BUILDING	Predicted settlement	Actual settlement	Actual / Predicted
1	60 - 100 mm	30 - 40 mm	0.4 - 0.5
2	60 - 130 mm	40 - 60 mm	0.4 - 0.6
3	30 - 50 mm	8 - 12 mm	0.25

In each case above, and for several other buildings in Christchurch not reported above, the average actual settlement measured was only quarter to half the settlement predicted using common conventional methods. Detailed back-analysis shows that mean compressibilities for Christchurch soils - alluvial gravels, sands and silts - are typically and consistently less than half the values commonly reported elsewhere for soils with similar classification, SPT, CPT resistance, etc. Further analysis indicates several factors contribute to the poor predictive performance of these existing correlations:

1. Reported correlations between compressibility and both SPT and CPT values (corrected) are generally linear whereas the correlations developed for Christchurch soils are highly non-linear. The authors suspect that this is likely to be the case for other soils, but is generally unrecognized or unreported. (A notable exception to this is Burland & Burbidge's method, which suggests a logarithmic relationship between SPT N and compressibility).

   Using non-linear relationships of similar form for different soil types, good correlations between SPT, CPT values and compressibility can be developed for all Christchurch soils from silts to gravels. Settlements can often be predicted to within $\pm$ 20-30% using SPT, CPT test results and these correlations.

2. Precise soil grading (particle size distribution), grain angularity, and other semi-geologic factors such as depositional environment probably account for the difference between established correlations and those developed for Christchurch. These are likely to be similarly important elsewhere and account for a considerable part of the unreliability often encountered when using semi-empirical methods to estimate settlements on granular soils.

   Establishment of site-specific correlations by back-analysis can eliminate much of this unreliability.

This example shows the importance of back-analysis as a technique for determining soil properties. It is unfortunate that this analysis is carried out far too rarely, probably because there is generally little direct remuneration to the practising geotechnical engineer for doing this work once construction is complete.

The benefit however is clear - and again the example above of Christchurch soil can be used to illustrate this. Many older buildings in the city have piled foundations. However since the work above was carried out by the authors, for a number of significant structures in Christchurch which in the past would have been piled, piles have not been

recommended by the authors as necessary to control static settlements. Both the risk of unexpected excess settlements, and the risk of unwarranted conservatism, have been substantially reduced.

3. SESSION PAPERS

The papers received for this session may be categorised in a number of different ways: by soil property discussed, by method of soil property determination, by soil type or by areas of risk considered. The papers cover a wide range of general topics and there are few common themes. In some cases, alternative paper groupings to those used could be equally appropriate - for example, three papers dealt specifically with cemented calcareous sands. However for discussion purposes papers are loosely separated into the categories below, which combine general subject themes with the overall conference theme of risk identification, evaluation and solution. Numbers of papers are noted in brackets:

- Improvement of design predictions (3)
- *In situ* properties, correlations and natural variability (4)
- Advances in soil testing methods (6)
- Fundamental behaviour (8)

3.1 Improvement of Design Predictions

Poulos and Al-Douri carried out model tests on jacked piles in calcareous sands to study the influence of density on shaft friction under static and dynamic loading. This is a continuation of the studies relating to problems with low capacities of jacked piles used around Australia in foundations for offshore structures. These sands were from the site of the North Rankin platform. Medium-dense and dense states were investigated using two sizes of test vessel, of 300mm and 600mm diameter; boundary conditions probably affected test results for the smaller vessel.

They conclude that skin friction, elastic modulus and jacking resistance increase with soil density and overburden pressure, but that skin friction under static loading is less than that during jacking. Cyclic loading "degrades" skin friction, and the degradation becomes more severe with increasing soil density or overburden pressure, and with increasing cyclic displacement.

The results provide a significant contribution to the understanding of pile capacities in these soils.

The paper by Ervin and Kurzeme relates directly to the aspect of risk discussed above, that of balancing the risk of failure against the risk of unnecessary conservatism in design. They carried out plate load testing to estimate bearing capacities and increased settlements beneath footings on gravelly soils which were expected to experience load increases up to 30% following building refurbishment. This is an interesting application of the test, particularly as the existing building was used to provide a reaction.

A comment on the possibility that the upward reaction on the building might have reduced the existing stress beneath adjacent footings, and thereby reduced the magnitude of measured deflections, would be interesting. The authors hope that settlement monitoring was undertaken to verify the predictions of soil properties made by this method.

Vuong analyses different models for prediction of the resilient modulus, required to predict the life of granular pavement. Resilient moduli were determined for basecourse crushed rock in repeated load triaxial tests. Lives predicted using the program NONCIRCL ranged from 0.3 to 3 times the corresponding NAASRA design lives, demonstrating the risks inherent in selecting a particular model for design.

3.2 *In Situ* Properties, Correlations and Natural Variability

Particular properties of natural soils, and the risks associated with random sampling being unrepresentative of natural variability, were the subject of the four papers in this category.

Mostyn and Waters carried out detailed investigation and a comprehensive program of laboratory testing for a site in Sydney to determine the natural variability of the shrink-swell index, which is used to estimate maximum ground surface movement. They conclude that to classify a site to even a low degree of confidence at least two to three tests, together with good geotechnical logging of a borehole, are required. The inclusion of good logging may reduce the number of shrink-swell tests required to characterise a site by a factor of three or more.

This is a good example of a case where better, rather than more, testing is desirable to reduce risks associated with natural soil variability.

Natural properties of clays in the Adelaide city area are reported in companion papers by Jaksa and Kagwa, and Kagwa and Jaksa. They use data compiled from many sources for most significant investigations in the city since the mid 1960s.

In the first paper, they use reported values for *in situ* bulk density and moisture content, and assume values of specific gravity, to show that the degree of saturation generally exceeds 95%. Previously these soils have been treated as unsaturated.

It is not clear why they state reservations about the accuracy of laboratory measured values of G_s, since the test is straightforward and relatively simple. Furthermore they conclude that since the degree of saturation exceeds 95% then effective and total stresses are equal. This requires further examination before such a conclusion can be safely drawn. The suggestion that the measurement of air contents of 0 to 5% is attributable to air entering the fissure system during testing and sampling implies that the true *in situ* degree of saturation is probable 100%, although the groundwater table is known to be 20 to 30m below ground level.

In their second paper, Kaggwa and Jaksa calculate *in situ* effective stresses assuming that negative pore pressures are present, and relate undrained shear strength and elastic

modulus to these. However they conclude that normalised values of s_u and E_u are within expected ranges for typical over-consolidated clays regardless of the pore pressures. They do not refute the common view that for residential buildings, soil shrinkage and swelling remain the dominant factors for footing design.

Natural soil variability is also discussed by El-Sohby et al who examined the silica/sesquioxide ratio, which is an indicator of "soil genesis and environmental setting" in Egyptian clayey deposits around the Nile valley. They note that chemical weathering significantly modifies physical and geotechnical properties.

3.3 Advances in Soil Testing Methods

Further advances in the ability to study pile capacities in calcareous sands around Australia are presented by Parkin et al who describe adaptions to the Monash double-walled calibration chamber made to accommodate the driving and cyclic load testing of model piles. Some problems in soil preparation and testing were apparent. They infer from the absence of plugging during driving that the pile clearance criterion (2D) is adequate. Crushing during pull testing probably caused shear strength to decrease substantially up the shaft, but they acknowledge that more work is required before the shear stress can be adequately predicted using CPT data.

Moore et al confirm previous findings that free-field vibration measurements may be affected by interaction between the ground and the mountings. They analyse theoretically the effects of different mountings. Results are supported in most cases by geophysical tests but some discrepancies occurred for reasons that are not understood. Embedded rods, rather than surface plates, appeared to give best estimates of ground vibrations.

The basecourse triaxial apparatus, capable of accepting samples up to 250mm diameter and 625mm high, is a useful research device but impractical for routine basecourse evaluation. An alternative, the "simple shear compactor" developed at the University of Auckland, is discussed by Pender et al. The original machine has been upgraded and automated. Various aggregates were tested and results verify the usefulness of the method, which uses a smaller quantity of material than the triaxial cell and has a very simple sample preparation procedure. The device provides a rapid means of categorising basecourse aggregates.

In companion papers, Brown and Abdel-Latif evaluate the effect of insertion on results of the screw plate test, which is used to determine soil compressibility without some of the disadvantages of the flat plate loading test. The two papers deal with the test in sand and clay using miniature laboratory testing.

In loose sand at low effective stresses, the effect of insertion appears to be minimal and to predict the soil modulus well. Scatter is greater in clays, but insertion appears to have minimal effect for overconsolidation ratios less than 5. For higher values of OCR the pressure increases beneath the screw plate during insertion, resulting in overestimation of E and c_v. A similar method for reducing disturbance when insertion is carried out with a threaded rod is proposed for both cases, but is not substantiated by further test results.

Yetton and Bell analyse the Pinhole Test, which was originally developed by Sherard et al (1976) to estimate the piping resistance of core material for dams. It has subsequently been modified and used to assess soil erodibility, particularly for Banks Peninsula loess in New Zealand. Sherard et al proposed the test result be used as a dispersion index. Although the most widespread use of the term "dispersion" indicates clay mineral deflocculation, Sherard et al redefined the term to mean colloidal erodibility.

Yetton (1986) showed that the pinhole test is a very unreliable measure of dispersion in its original and most common sense. Yetton and Bell propose that the test be retained, but used to define erodibility alone. While high erodibility may indicate the presence of dispersive clay minerals, erodibility is controlled by a number of soil properties, of which dispersion is only one. They propose a relatively quick and simple classification procedure to assign an erodibility category based on the head at which sustained erosion first occurs.

The authors suggest that rather than using the upstream head as the key indicator, it may be sensible to use the hydraulic gradient across the sample. This dimensionless form would allow use of different sized test samples, and direct comparison with field situations. Thus a soil which eroded at 100mm head in the test (i=2) would also be expected to erode rapidly in a field situation if the hydraulic gradient were close to 2 through a path of preferred flow (e.g. a fissure or interface between two soils). This would allow a factor of safety against erosion to be calculated directly, and used in design.

Dispersion and erosion are extremely important concepts, particularly in the design of water-containing earth structures. Yetton and Bell highlight a discrepancy in the interpretation of a common test which could increase the risk of failure due to a design being based on incorrect assumptions. Their suggested reinterpretation is logical and should be adopted, after consideration of the suggestion made above.

3.4 Fundamental Behaviour

Eight papers deal with fundamental behaviour and properties of soils. The first five deal with stiffness and yielding of various soils following particular loading (stress path) conditions.

Allman et al report results from the continuing studies to explain clay soil behaviour in the critical state framework. The state boundary, or yield surface (stress state) marks the transition in behaviour from high to low stiffness. The shape of this surface away from the p' axis is difficult to define accurately by conventional undrained triaxial tests since stress paths do not necessarily reach, then precisely follow, the state boundary surface.

Allman et al carried out drained testing constrained to follow specific stress paths in triaxial compression and extension. They demonstrate that, as predicted, extension tests on 1-dimensionally consolidated samples do not identify the state boundary surface, which is however closely predicted by the modified Cam-clay model.

Chu et al also consider soil yielding, in their investigation into strain-softening of dense Sydney sand. They carried out strain path triaxial and multiaxial tests and identified three principal types of strain-softening behaviour. Depending upon the test type and the strain path followed, strain-softening may occur due to non-homogeneous deformation, as a path-dependent material behaviour, or due to shear bands which occur in response to 3-dimensional loading. This study is a useful contribution to understanding the constitutive behaviour of granular media.

Three papers consider the response of soils to cyclic and dynamic loading. Zhao et al continue the theme of calcareous sand behaviour discussed earlier, investigating the effect of stress level and frequency on the number of cycles to failure. Both a stress path triaxial cell, and a conventional triaxial cell with dynamic deviator load capacity, were used and sand from the north Rankin site (see Poulos and Al-Douri, above) was artificially cemented by mixing with gypsum cement.

The cementing contributed a significant part of the static strength and rapid post-peak strength loss occurred at high cement ratios. However about 10^6 cycles were required to cause 50% strength loss. Elastic modulus, pore pressure and axial strain responses were independent of load cycle frequency, but the duration of peak load application, and hence the cyclic frequency, significantly affected the number of cycles to failure.

Although it is dangerous to generalize based on specific tests on a particular soil, it is interesting to note that it is often assumed dynamic soil properties are relatively independent of cyclic frequency. This is certainly the case in earthquake analyses, although earthquake frequencies are commonly $>>1$ Hz, whereas wave loadings are typically closer to 10 Hz. Without detailed behavioural information on local soils, it is necessary to use general correlations based on overseas soils when performing dynamic site response analyses.

Pender et al employ the assumption of frequency independence at earthquake frequencies in investigating the change in shear modulus and damping with strain amplitude for Auckland clays and Tauranga volcanic ash. Recent earthquake data has indicated enhanced site response may occur in soils exhibiting elastic behaviour and minimal damping over an extended range of strains. Most tests were carried out at frequencies 0.2 Hz on 75mm diameter triaxial samples. Pore pressures were measured at the sample midheight using miniature transducers.

They conclude that for Auckland clays the number of cycles has relatively little effect on the stiffness and damping behaviour. The effect of strain amplitude is adequately described by conventional models. Degradation of these soils under earthquake loading is unlikely to be significant.

The Tauranga ash soil behaved more like a sand during cyclic loading, despite having index properties similar to the Auckland clay. It experienced rapid build-up in pore-pressure during cyclic loading, with a consequent decrease in stiffness. Damping did not increase with strain amplitude.

Larkin and Chan investigated dynamic behaviour of volcanic soils from the New Zealand central volcanic plateau using the dynamic torsion test, and compared results to the "overseas" models discussed also by Pender et al. They concluded that dynamic properties - normalised shear modulus and damping - of these soils generally do not deviate significantly from trends described by the commonly used models. A number of slight differences in behaviour were noted which could be incorporated into future analyses.

Seismic response analysis is very sensitive to the dynamic properties used. It is important to evaluate properties of local soils specifically, wherever possible, and to perform sensitivity analyses to indicate the degree of reliability which can be placed on the results.

Wesley presents results of residual strength measurements carried out in the ring shear apparatus on some New Zealand soils, and also analyses data with respect to overseas correlations. Comprehensive reporting of soil classifications and index properties means that these results can be widely used, although inclusion of particle size gradings would have been beneficial.

Results for "normal" soils are consistent with those found overseas and commonly used correlations between residual friction angle, and plasticity index or clay fraction, appear reasonably valid. However the scatter in data is large, and indicates - as might be expected - that a multiple correlation with both plasticity index and clay fraction is likely to be more reliable than either alone. In this respect, it would have been useful to attempt correlation with the parameter

$$(CF)^2.LL.PI$$

which was shown by Collotta et al (1989) to predict the residual friction angle with considerably less uncertainty.

Wesley shows that residual friction angles for volcanic ash soils are considerably higher than for normal soils with comparable clay fraction and plasticity index. The alternative correlation proposed above is unlikely to perform better for these soils.

Two papers deal with soil properties unrelated to any discussed in this section. Indraratna and Husin evaluate methods for predicting the swell potential of clay shales in Thailand, which have caused instability and failure of diversion channel linings. They investigate correlations among swell potential, plasticity index, clay fraction and activity for a soil from the Mae Moh area, but considerable scatter is evident and suggests that other controlling parameters should be investigated further.

Airey assesses the effect of stress history and void ratio on hydraulic conductivity of a remoulded Sydney clay with water and kerosene. Dramatic increases in hydraulic conductivity have previously been noted when pollutants, particularly liquid hydrocarbons, contact soils. It is concluded that the relationship between hydraulic conductivity and void ratio is best determined using normally consolidated soils.

Kerosene required increased hydraulic gradient for initiation of flow, and exhibited a lower hydraulic conductivity. Possible factors affecting this behaviour are discussed, and surfactants are postulated as a cause of increased flow under certain conditions. However considerable further work is required, using a range of other permeants, before general conclusions can be drawn.

4. CONCLUSIONS

Of the twenty one papers reviewed for this session, all but two discussed work carried out in research institutions. This is probably not surprising since the laboratory facilities required to carry out research on fundamental soil behaviour are primarily located in these institutions. However it is unfortunate that greater effort is not being made by practising geotechnical engineers and geologists to investigate and report information on general soil behaviour.

As discussed earlier, laboratory testing is only one of three general methods for determining soil properties. *In situ* testing, and back-analysis of performance monitoring results, are equally valid and important. Until back analysis in particular has been used to verify assumptions made about soil behaviour, the state of the art must be concluded to have some distance to advance.

Pollutant Migration through Clay

D.W. Airey
M.A., Ph.D.
Lecturer, University of Sydney

SUMMARY Tests have been performed on a remoulded clay to establish the variation of its hydraulic conductivity with stress history and void ratio. The hydraulic conductivity has been determined by both direct and indirect methods, and a comparison of these methods is presented. Finally, a pollutant, kerosene, was forced through the samples and the hydraulic conductivity determined. No flow of the kerosene was detected until a breakthrough pressure, dependent on the void ratio, was exceeded. Thereafter, the hydraulic conductivity was almost linearly related to the flow rate.

1. INTRODUCTION

Clayey soil barriers are widely used to contain water, chemicals and potentially harmful pollutants from municipal and toxic waste facilities because of their low hydraulic conductivities. However, their suitability for this purpose is the subject of increasing research as it has been demonstrated (eg. Mesri and Olsen, 1971, Fernandez and Quigley, 1985) that dramatic increases in hydraulic conductivity are possible when clayey soils are mixed with some pollutants, and in particular with liquid hydrocarbons. These increases occur because the thickness of the diffuse double layer that surrounds the clay particles is reduced, a consequence of the relatively low dielectric constants of the organic chemicals compared with water, effectively increasing the pore space between the particles. The reduction in double layer thickness can also be accompanied by volume reduction so that there is a possibility that cracks and preferential flow paths may develop in the soil. The risks of chemical processes affecting the integrity of clay barriers has led in many parts of the world to their prohibition as the principal barrier for containing toxic wastes.

Tests conducted in different apparatus to investigate the effects of liquid hydrocarbons on the hydraulic conductivity have given apparently conflicting results (Foreman and Daniel, 1986); in a rigid walled permeameter the hydraulic conductivity increased 1000 times when heptane, an immiscible liquid hydrocarbon, replaced water as the permeant, whereas in a flexible wall permeameter no flow was observed up to hydraulic gradients of 300. As neither apparatus represents the field conditions exactly there has been considerable debate as to which type of permeameter apparatus should be used to investigate the chemical effects. The tests described in this paper have been performed in an hydraulic oedometer apparatus. Apparatus of this type have been concluded by some authors (eg. Mitchell and Madsen, 1987) to be the most flexible and useful for estimating the chemical effects on the soil structure.

This paper describes the results of a series of tests to investigate the hydraulic conductivity of a natural clay from Sydney. A comparison is made of direct and indirect determinations of the hydraulic conductivity, using water as the permeant, from conventional and hydraulic oedometer cells. In addition the hydraulic oedometer has been used to determine the hydraulic conductivity of the soil using kerosene as the permeant.

2. NOTATION

In this paper the constant, k, relating the average flow velocity, v, to the hydraulic gradient, i, in Darcy's law

$$v = k\, i$$

will be referred to as the hydraulic conductivity. This constant is dependent on both the density, γ, and the viscosity, μ, of the flowing fluid. The intrinsic permeability, K, where

$$K = k\, \mu/\gamma$$

is independent of the fluid properties, that is K is a property of the porous medium alone. In this paper K will be referred to as the permeability of the soil.

3. SOIL AND FLUID PROPERTIES

Only remoulded soil samples have been used in the tests described below. The natural soil was first air dried and pulverised before being passed, dry, through a 425 micron sieve. Only the soil (about 75% of the total) that passed through this sieve has been used in the tests and in determining the soil properties described below. It is believed that if the soil had been wet sieved more than 90% would have passed 425 microns. The particle size distribution, obtained using a laser particle size analyser, is shown in Figure 1. It can be seen that the largest particle size was only 20 microns. X-ray diffraction analysis indicated that the soil was composed predominantly of kaolin, with approximately 20% quartz, and trace amounts of montmorillionite and illite. When dried the soil had a ubiquitous brown stain that is believed to be amorphous iron oxi-hydrate. This iron compound was precipitated on exposure to air during drying, as when the natural soil was freshly cut it had a greyish colour.

The soil had the following properties: Liquid Limit = 53, Plastic Limit = 26 and Plasticity Index = 27.

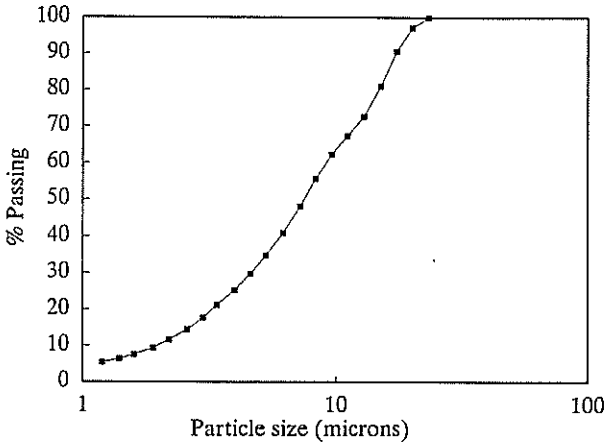

Figure 1. Particle size distribution

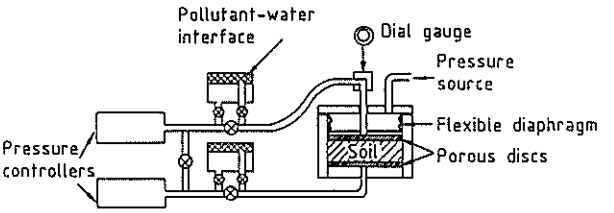

Figure 2. Hydraulic oedometer apparatus

The kerosene had the following properties: Specific gravity approximately 0.8, and Viscosity = 3.6 centipoise.

4. APPARATUS

Two types of oedometer have been used in these experiments:
(a) a small conventional oedometer cell with diameter 34 mm and initial sample height 12 mm. In this oedometer no control of the drainage was possible and only load and settlement readings could be obtained.
(b) an hydraulic oedometer with sample dimensions 75 mm diameter by 19 mm high. In this oedometer a back pressure could be applied to the sample and direct measurements of the hydraulic conductivity could be obtained. Two GDS pressure controllers (Menzies, 1988) were used to provide the back pressure and measure the volume changes during consolidation and hydraulic conductivity testing. The arrangement of the apparatus is shown in Figure 2. The settlement was measured by a dial gauge, and the vertical stress was provided by a separate pressure source. Also shown in Figure 2 are two pollutant-water interfaces that were used only when pumping kerosene through the soil. In each interface a layer of the less dense kerosene was placed above a layer of water. As the two fluids were immiscible this arrangement prevented any kerosene from entering the pressure controllers. Attempts to use membranes between the water and the kerosene were unsuccessful because the kerosene rapidly attacked the rubber compounds used and resulted in leaks from the interfaces.

5. EXPERIMENTAL PROCEDURE

The air dried and pulverised soil passing the 425 μm sieve was mixed with distilled de-aired water at a moisture content close to the liquid limit, and placed in a compaction mould. A vertical stress was applied, and increased in stages up to a maximum of 40 kN/m^2 for the hydraulic oedometer samples and 96 kN/m^2 for the conventional oedometer samples. Samples were removed from the compaction moulds and trimmed to fit the required oedometer.

For the conventional oedometer the vertical stress was increased in stages up to 580 kN/m^2 and then reduced to zero. For each stage the variation of settlement with time was recorded.

For the hydraulic oedometer a small vertical stress of 20 kN/m^2 was applied and then, keeping the vertical effective stress constant, the back pressure was increased to approximately 500 kN/m^2 to ensure full saturation. The vertical effective stress was increased in stages (see Table 1), with for each stage the changes of settlement and volume change with time recorded. For each stage after consolidation was complete, water was pumped through the samples to directly determine the hydraulic conductivity. The final operation in the first three tests was to pump kerosene through the soil. In test AR2 kerosene was pumped through the soil after the fifth stage at an effective vertical stress of 50 kN/m^2. This was followed by consolidation to a vertical effective stress of 400 kN/m^2 and further kerosene permeation.

Table I. Stress histories used for hydraulic oedometer tests

Test No.	Vertical Effective Stress (kN/m^2)
DG1	20-50-480-50
DG2	20-50-200-50
AR1	20-50-200-600-200-50
AR2	20-50-100-200-100-50-400

Two methods were used to determine the hydraulic conductivity: either one pressure controller could be set to provide a constant flow rate, the other being held at a constant pressure, and the pressure difference recorded, or each controller could be set at a different pressure and the flow rate recorded, with in both cases the tests continuing until equal flow rates were measured by the two controllers. No significant differences could be detected between the two methods.

The hydraulic conductivity could then be determined from

$$k = \frac{Q\,H\,\gamma_w}{A\,\Delta p} \qquad (1)$$

where Q = flow rate
A = Area of the sample
H = Sample height
Δp = pressure difference
γ_w = Unit weight of water

Before each conductivity measurement the two pressure controllers were connected together so that any difference in their readings could be determined and corrected for, and the accuracy of the pressure readings was of the same order as their resolution of 1 kN/m^2. The accuracy of the volume change readings (resolution 1 mm^3) was affected by small temperature variations (+/-1°C) in the temperature controlled laboratory. The resulting volume changes were significant at low flow rates, especially when using the kerosene-water interfaces because of their additional fluid volume, and have been allowed for by running the tests over more than 24 hours to get a reliable average. For a few stages different flow rates (between 0.5 and 7 mm^3/min) were used to check on the validity of Darcy's law, and when water was the permeant only very slight differences in hydraulic conductivity were measured.

In addition to direct measurements of the hydraulic conductivity indirect measurements were obtained from the consolidation responses. In conventional analyses of one-dimensional consolidation the coefficient of consolidation, c_v is deduced from a plot of settlement against either the square root or the logarithm of time. For both of these methods a curve fitting procedure is used (eg.Lambe, 1951) to determine t_{90} and t_{50} respectively. This allows c_v to be deduced as

$$c_v = \frac{0.848\,H^2}{t_{90}} \qquad (2)$$

and then the hydraulic conductivity can be calculated from

$$k = c_v\,m_v\,\gamma_w \qquad (3)$$

where m_v = volume compressibility
γ_w = unit weight of water

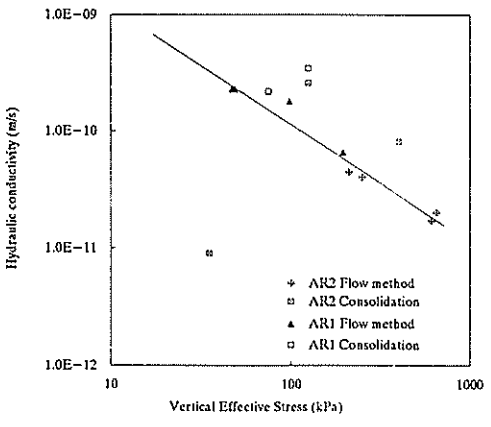

Figure 3. Relation between hydraulic conductivity and vertical effective stress during loading

6. RESULTS

Figure 3 shows a comparison of the hydraulic conductivities determined by the direct flow method and from the consolidation data plotted against vertical stress for the loading stages of tests AR1 and AR2. Results from the consolidation phases have been plotted against the mean effective vertical stress for that phase. The hydraulic conductivities determined by the direct flow method in both tests are in good agreement and can be described by a linear relation in this log-log plot. Values of the hydraulic conductivity determined from the consolidation responses appeared to be slightly higher, in these and other tests, for all but the initial stages. In all the tests the consolidation method gave a low estimate of the hydraulic conductivity for the first load increment. This occurred because the shape of the consolidation curve did not match the expected theoretical response, a result of the sample disturbance on installation into the oedometer. For test AR1 the direct flow method gave a conductivity of 3×10^{-8} m/s at a vertical effective stress of 50 kN/m^2, two orders of magnitude higher than the other values shown in Figure 3. This is believed to have been caused by leakage along the sidewalls of the oedometer, again the result of disturbance during sampling. During unloading the consolidation responses did not correspond closely with the expected theoretical response and the estimated hydraulic conductivities were up to two orders of magnitude lower than those obtained from the direct flow method. Based on these results it appears that the consolidation method can only be relied on to provide good estimates of the hydraulic conductivity for normally consolidated soils.

Figure 4 shows the hydraulic conductivities determined by the direct flow method (loading and unloading) and the indirect consolidation method (loading only) plotted against void ratio for all the tests. Although there is some scatter in this figure there is generally good agreement between the hydraulic conductivities estimated by the different methods. The scatter is not unexpected because in both methods differences in void ratio and hence hydraulic conductivity occur across the samples as a result of effective stress variations. The simple consolidation theory assumes that the hydraulic conductivity and compressibility remain constant during a load increment, whereas in practise they will be changing continuously.

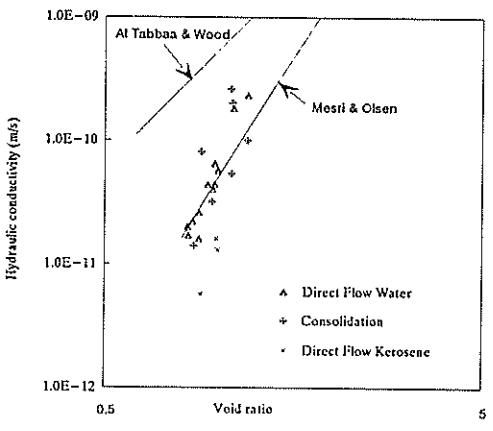

Figure 4. Relations between void ratio and hydraulic conductivity for kaolinitic clays

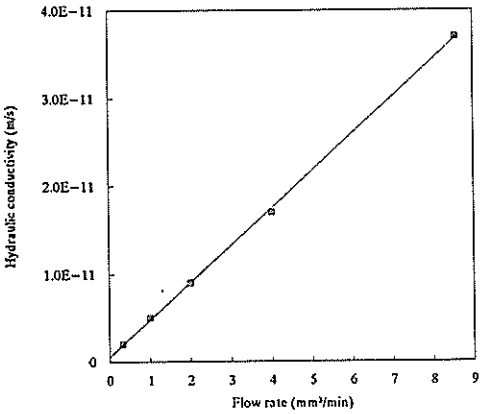

Figure 5. Relation between hydraulic conductivity and flow rate during kerosene permeation

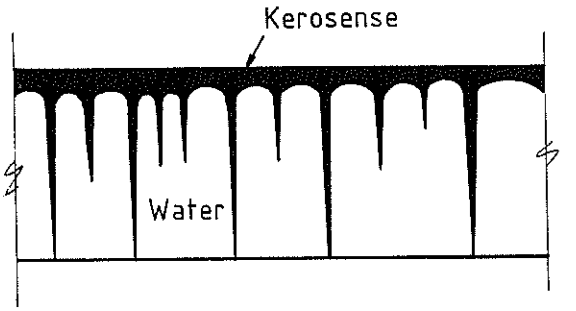

Figure 7. Sample section showing kerosene distribution

As expected the data show that the relation between hydraulic conductivity and void ratio is unaffected by the stress history of the soil, and can be described by a linear relation in this log-log plot. Similar results, also shown on Figure 4, have been obtained for other kaolinitic clays (Al Tabbaa and Wood, 1990, Mesri and Olsen, 1971). It can be seen that the results are practically identical to those reported by Mesri and Olsen.

Also shown on Figure 4 are values of the hydraulic conductivity obtained when pumping kerosene through the samples at a flow rate of 1 mm^3/min. These limited data appear to show that when kerosene is pumped through the water saturated soil the hydraulic conductivity is reduced. However, the hydraulic conductivity has been found to depend on the flow rate. For test AR2 at an effective vertical stress of 400 kN/m^2 the hydraulic conductivity increased almost linearly with the flow rate, for flow rates between 0.33 and 8.6 mm^3/min as shown in Figure 5. At this void ratio with water as the permeant an hydraulic conductivity of 3×10^{-11}m/s was expected, slightly lower than the value at the maximum flow rate using kerosene.

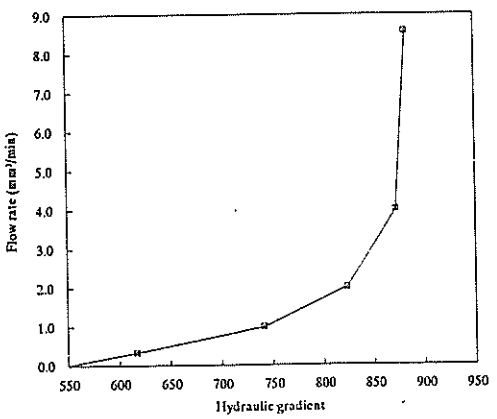

Figure 6. Relation between hydraulic gradient and flow rate during kerosene permeation

An important difference between the flows of kerosene and water was that no flow occurred for the kerosene until a breakthrough pressure was reached when the hydraulic gradient was sufficient to overcome the capillary pressures in the pores. Figure 6 shows the relation between the hydraulic gradient and flow rate which can be extrapolated to estimate the breakthrough gradient as approximately 550 for this 17 mm thick sample.

In the first test, DG1, the kerosene was pumped from the top to the bottom of the sample, and was able to pick up some black material from the flexible rubber membrane used to apply the vertical pressure. When the sample was sectioned at the end of the test a black stain in the soil enabled the presence of kerosene to be detected. It was observed that the kerosene had fingered its way through the soil (see Figure 7) and that the kerosene had only entered a small portion of the soil pores. Tests in which several pore volumes of two other immiscible liquid hydrocarbons were pumped through clays (Fernandez and Quigley, 1985) also resulted in only 5 to 10% of the pore water being replaced. In the subsequent tests the kerosene was pumped from the bottom of the oedometer so that the reaction with the rubber membrane would not affect the hydraulic conductivity, however, it was found that the hydraulic conductivity with respect to the kerosene was practically identical, that is the presence of the black material had no apparent affect.

In test AR2 after passing more than one pore volume of kerosene through the sample at an effective vertical stress of 50 kN/m^2 the vertical stress was increased by 350 kN/m^2 and the sample allowed to consolidate. The hydraulic conductivity determined indirectly from the consolidation response was 7×10^{-11} m/s. This was close to the value expected for the water saturated soil, and was further evidence that only a small amount of the pore space had been filled with kerosene. Further permeation with kerosene followed with significant reductions in hydraulic conductivity, and increases in the breakthrough pressure. The hydraulic gradient required for flow increased from approximately 150 to 550 as the void ratio decreased from 1.02 to 0.91.

7. DISCUSSION

Attempts were made to investigate the hydraulic conductivity of the natural soil, but these were unsuccessful because the samples could not be trimmed to fit the oedometers without cracking. Because the cracks would have a significant effect on the hydraulic conductivity it was decided to use only remoulded samples. However, when the soil was dried out iron that was originally in the ground water precipitated and turned the initially grey soil a reddish brown colour. On remoulding the samples the iron did not return to solution and this may have affected the hydraulic conductivities, and the values may therefore not be representative of the natural soil.

The flow of two or more immiscible fluids through porous media (rocks) is of considerable interest to petroleum engineers and has received much study (eg. Dullien, 1979). It has been shown that as an immiscible fluid such as kerosene enters a water saturated soil it has to overcome the capillary pressures at the fluid-water interface in the pores. As the capillary pressure is dependent on the pore size the fluid moves preferentially into larger pores creating the fingering type pattern shown in Figure 7. As the pressure of the fluid increases eventually breakthrough will occur and thereafter the fluid will flow only through the channels that have broken through. Some of the fluid will be left in non-conducting channels that do not influence the flow behaviour. By increasing the pressure head further, more water will be replaced by the fluid and the number of flow channels will be increased. Similar processes appear to have occurred as the kerosene was pumped through the clay samples used in these tests.

It has been found (eg. Dullien, 1979) that under conditions of steady flow the immiscible fluids flow independently of each other, with neither fluid influencing the flow behaviour of the other, and that this behaviour can be described by an extended form of Darcy's Law. For each fluid phase j:

$$v_j = \left(\frac{K_{ej}\, \gamma_j}{\mu_j} \right) i \qquad (4)$$

where v_j is defined by Q_j/A, and K_{ej} is the effective permeability of the fluid j. The effective permeabilities will thus depend on the saturation, or proportion of the pore space occupied by each phase. It is customary to express these effective permeabilities as fractions of the permeability K using:

$$K_e = K\, K_r$$

where K_r is called the relative permeability. This should take values between 0 and 1 depending on the saturation of the particular phase of interest.

The amount of kerosene pumped into the sample before breakthrough was approximately 5% of the pore fluid, so that a low relative permeability might be expected. However, the relative permeabilities varied between 0.43 at the lowest flow rate and 7.8 at the highest. High relative permeabilities, up to 2.5, have also been reported (Dullien, 1979) when viscous oils have been pumped through water saturated clayey rocks. It has been suggested that the water which is bound to the clay particles is not easily displaced by the oil (this has been demonstrated by Fernandez and Quigley, 1985), and has a "lubricating" effect, so that the kerosene behaves as if it has a viscosity lower than its bulk value. Since the bulk viscosity is used in the extended Darcy's law this will predict much smaller flows than are actually observed.

The hydraulic conductivity has been found to depend on the flow rate. A similar flow rate dependence has been reported (Quigley, 1989) from tests in which cyclohexane was pumped through a clayey soil. These observations suggest that the extended Darcy's law may not be valid when kerosene is pumped through the clay. However, the relative permeability can be expected to increase as the flow rate increases because the increased pressure head will force more kerosene into the soil increasing the kerosene saturation. The relative permeability in the extended Darcy's law is only constant for a fixed saturation.

It has been suggested (Fernandez and Quigley,1985) that the changes to the double layer thickness dominate the effects of viscosity and bulk density. If this is true then the extended Darcy's law will not be applicable as the permeability will be changing as kerosene displaces the water. The high relative permeabilities measured in these tests are indicative of chemical effects, but further tests are required to investigate the applicability of the extended Darcy's law. Alternatively, as suggested by Quigley, 1989 the kerosene may be forced along macropore channels or micro-fissures that expand or contract in proportion to the pressure head.

The results presented are in general agreement with those of other investigators who have forced insoluble liquid hydrocarbons through clayey soils. The hydraulic conductivity does not increase much beyond that of water, and significant breakthrough pressures are required to overcome the capillary pressures in the pores. However, it has been shown (Quigley, 1989) that the presence of small amounts of surfactant, as would be likely in any waste dump, can reduce the breakthrough pressure significantly so that this can not be relied on to contain insoluble liquid hydrocarbons.

7. CONCLUSIONS

The hydraulic conductivities determined from the direct flow method and indirectly from the consolidation response showed good agreement for the normally consolidated clay. The consolidation response gave poor predictions of the hydraulic conductivity on unloading and for the initial loading stage. Sidewall leakage can cause the direct flow method to indicate high hydraulic conductivities in the initial stages of the tests.

For clays the relation between hydraulic conductivity and void ratio can best be determined from tests on normally consolidated soil.

Significant hydraulic gradients were required to make the kerosene flow through the clay, and when flow did occur the hydraulic conductivity was less than for water. The hydraulic conductivity increased almost linearly with the flow rate.

ACKNOWLEDGMENT

Some of the tests were performed by David Duff and Paul Gorman as part of an undergraduate thesis. The assistance of Antonio Reyno and Dennis Nobbs is also gratefully acknowledged.

REFERENCES

Al-Tabbaa,A. and Wood,D.M.(1986) Some measurements of the permeability of kaolin. Geotechnique.

Dullien,F.A.L.(1979) Porous Media, Fluid Transport and Pore Structure. Academic Press

Fernandez,F. and Quigley,R.M.(1985) Hydraulic conductivity of natural clays permeated with simple liquid hydrocarbons. Can. Geotech. J. 22, 205-214.

Foreman,D.E. and Daniel,D.E.(1986) Permeation of compacted clay with organic chemicals. Proc ASCE, Vol 112, No 7, 669-681

Lambe,T.W.(1951) Soil Testing for Engineers. John Wiley & Sons

Mesri,G. and Olsen,R.E.(1971) Mechanisms controlling the permeability of clays. Clay and Clay Minerals, 19, 151-158.

Menzies,B.K.(1988) A computer controlled hydraulic triaxial testing system. Advanced triaxial testing of soil and rock. ASTM STP 977, 82-94.

Mitchell,J.K. and Madsen,F.T.(1987) Chemical effects on clay hydraulic conductivity. In Geotechnical Practice for Waste Disposal, ASCE Geot.Spec.Publ. No 13, 87-116.

Quigley,R.M.(1989) Pollution Migration, Waste Dumps & Groundwater. Part 1, Centre for Geotechnical Research, Sydney University.

Stress Path Tests to Investigate Yielding of K_o Consolidated Soil

M.A. ALLMAN
B.E., Ph.D.
Research Assistant, Geotechnical Engineering Research Centre, City University, London
J.H. ATKINSON
B.Sc., A.G.G.I., M.Sc., D.I.C., Ph.D., M.A., F.I.C.E., C.Eng., F.G.S.
Professor of Soil Mechanics, GERC, City University, London
D.O. JORDAN
Dip.Civ.Eng,., D.I.C., M.Eng.Sc., Dip.Ed.
Lecturer, Department of Civil & Building Engineering, Victoria University of Technology, Melbourne

SUMMARY

During loading of foundations or excavation for slopes and retaining walls soil states generally move towards a state boundary surface. If the state reaches this surface the soil stiffness will decrease significantly and ground movements will increase. Hence, the location of the surface, and assessment of the risk that states will reach the surface, form an important part of soil testing and geotechnical analysis. For one-dimensionally consolidated soils conventional methods, based on stress paths obtained from undrained compression and extension tests, are unsuitable for this purpose. An alternative method, described in the Paper, is to carry out drained stress path probing tests and then to normalise the data to take account of the variation in water content. A set of test results obtained from stress path tests on one-dimensionally reconsolidated reconstituted samples gave a well defined state boundary surface similar to that corresponding to modified Cam-clay.

1. INTRODUCTION

An essential feature of soil behaviour is the observation that stiffness is considerably greater when a soil is overconsolidated than when it is normally consolidated. However, as an overconsolidated soil is loaded it will, sooner or later, reach a state where it again becomes normally consolidated and strains will begin to accelerate as the stiffness decreases. Consequently, in a geotechnical design it is necessary to locate the states at which the changes of stiffness occur. This is particularly important for lightly overconsolidated soils where the change of stiffness may occur after the application of a relatively small load (Atkinson and Sallfors, 1991). For one-dimensional consolidation and swelling in oedometer tests stiffness begins to decrease at the normal consolidation line but for triaxial states it is necessary to take account of the shear stresses as well as the mean normal stresses. Then the change of stiffness occurs when the state reaches a surface usually known as the state boundary surface (Schofield and Wroth, 1968; Atkinson and Bransby, 1978).

A general state boundary surface is illustrated in Figure 1. The axes are the deviator stress $q' = (\sigma'_a - \sigma'_r)$, the mean normal stress $p' = 1/3\ (\sigma'_a + 2\sigma'_r)$ and the specific volume $v = 1 + e$ where e is the voids ratio. In Figure 1(b) the line BCF is a normal consolidation line and in Figure 1(a) the two arcs through F and B are sections of the state boundary surface corresponding to the two swelling and reconsolidation lines AB and DF.

Figure 1(a) also shows two identical loading paths AC and DE. The state at A is lightly overconsolidated and it reaches the state boundary surface at B; the state at D is heavily overconsolidated and, for the same loading path, the state does not reach the boundary surface. For the state initially at A the overall strains are dominated by those along BC after the state has reached the boundary surface. Consequently the initial stage of any geotechnical analysis of ground movements should locate the state boundary surface and assess whether the loading will cause the soil state to reach the surface.

The state boundary surface is a boundary to all possible states: so, in Figure 1(b) it is not possible for soil to reach states outside (i.e. above) the normal consolidation line BCF. In Critical State Soil Mechanics (Schofield and Wroth, 1968) the state

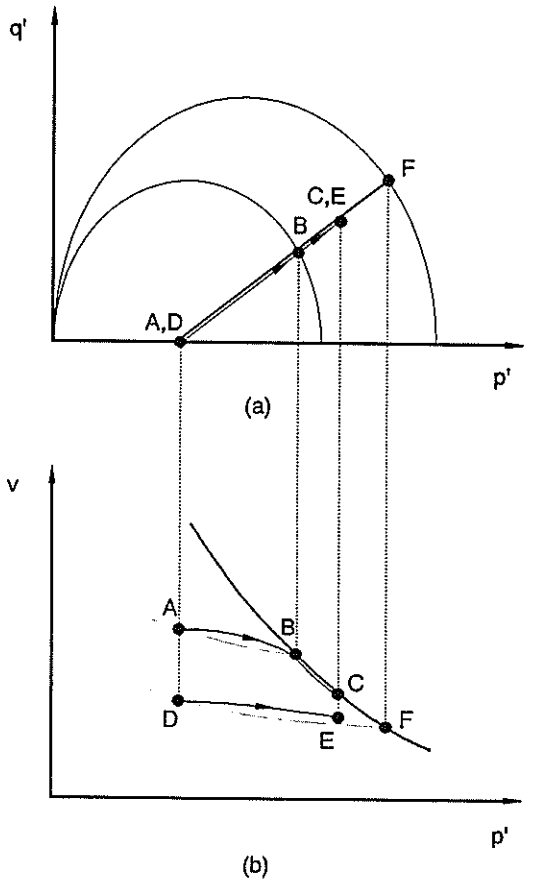

Figure 1 State paths for soil loading related to the state boundary surface

boundary surface is also a yield surface so that for states along AB and DE the strains are taken to be elastic. However, it is now evident that this is too simple a view of soil behaviour as there are significant inelastic strains at states inside the boundary surface (Atkinson et al, 1990). Nevertheless the state boundary surface is important as it locates states where stiffness decreases significantly and, as such, it is necessary to discover its position in a laboratory testing programme.

2. CURRENT EXPERIMENTAL METHODS TO LOCATE THE STATE BOUNDARY SURFACE

The two methods commonly used to identify parts of the state boundary surface are:

a) the examination of the change of stiffness during drained compression tests (eg. Parry and Nadarajah, 1973), and

b) the examination of the effective stress path in undrained tests (eg. Atkinson et al, 1987).

Method a) is illustrated in Figure 2 which shows the results of a test in which a soil was first K_o compressed and swelled and then isotropically (constant q') compressed. The soil is a silty clay and the K_o and isotropic consolidation lines shown in Figure 2 are from other data. During the K_o compression test the stress was held constant for a time and additional volume changes occurred largely due to creep. Although both sets of data certainly reach the appropriate normal consolidation lines it is not easy to define the precise points at which the states first reach the state boundary surface. This is the familiar problem of identification of the preconsolidation pressure from the results of one-dimensional tests for which a number of empirical methods have been proposed (eg. Casagrande, 1936).

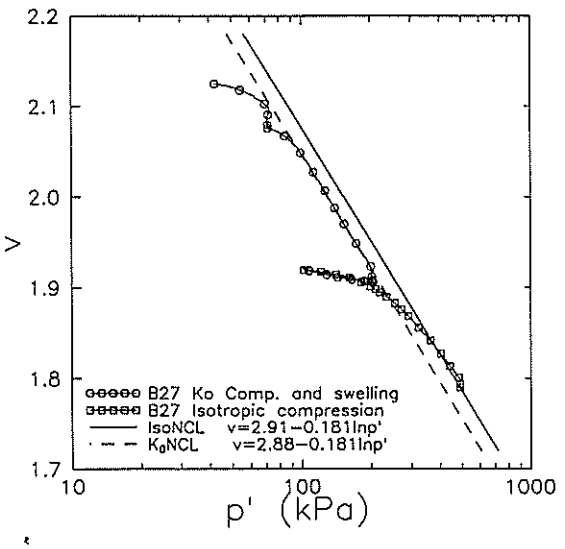

Figure 2 Location of the state boundary surface from drained compression tests

Method b) is illustrated in Figure 3 which shows the results of an undrained compression test (B51) and an undrained extension test (B52) on a K_o consolidated soil. This method presumes that all undrained effective stress paths for normally consolidated samples follow the state boundary surface. While this is reasonable for isotropically normally consolidated samples it is by no means certain that the effective stress path for an undrained extension test (test B52 in Figure 3) will follow the boundary surface. This question was discussed by Atkinson (1989) who suggested that, since the deviator stress was reduced, the undrained stress path for an extension test would be more likely to move inside the boundary surface and follow an elastic wall (Schofield and Wroth, 1968).

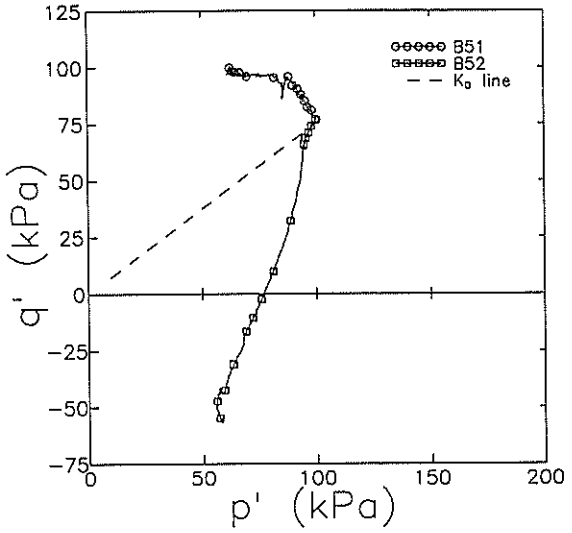

Figure 3 Location of the state boundary surface from undrained triaxial tests

Both of the current methods for locating the state boundary surface for a soil entail difficulties. These are due, firstly, to soil yielding inside the boundary surface which means that there is no clear yield point to be found in any stress-strain curve and, secondly, to the observation that effective stress paths for undrained tests may not necessarily remain on the boundary surface, particularly for extension tests on anisotropically consolidated samples.

An alternative method for locating the state boundary surface from laboratory tests might recognise that the surface represents the outer boundary surface of all possible states of a soil and so any test to examine the surface should certainly follow paths which probe outwards. The difficult three-dimensional geometry of the surface (in q':p':v space) may be simplified by normalising the test data to take account of the changing specific volume during drained tests (Atkinson and Bransby, 1978).

3. NORMALISATION OF SOIL TEST DATA

In Figure 1(a) the sections of the state boundary surface are geometrically similar and so they may be scaled, or normalised, by dividing q' and p' by a suitable pressure which depends on the current specific volume. Figure 4(b) shows a state at S which has a current state v_s and p'_s: the stress corresponding to v_s on the critical state line is p'_c, on the K_o normal consolidation line is p'_K and on the isotropic normal consolidation line is p'_e and any one of these may be used as normalising parameters. (The one used most often is the equivalent pressure p'_e).

The choice of which parameter to use for normalisation depends largely on the data available. For the present work, which was carried out on soils which were one-dimensionally consolidated, the appropriate choice is p'_K (the equivalent pressure on the K_o normal consolidation line at the same specific volume as that at the current state S). Figure 4(a) illustrates the same state boundary surface as that shown in Figure 1 normalised with respect to p'_K and taken into the extension region for negative values of

q'. (For simplicity of illustration the surface is shown as symmetrical about the p'/p'_K axis). In Figure 4(a) the critical state line and the isotropic and K_o normal consolidation lines become single points and all curved sections, like those in Figure 1, reduce to a single curve. The K_0 normal consolidation line is at $p'/p'_K = 1.0$.

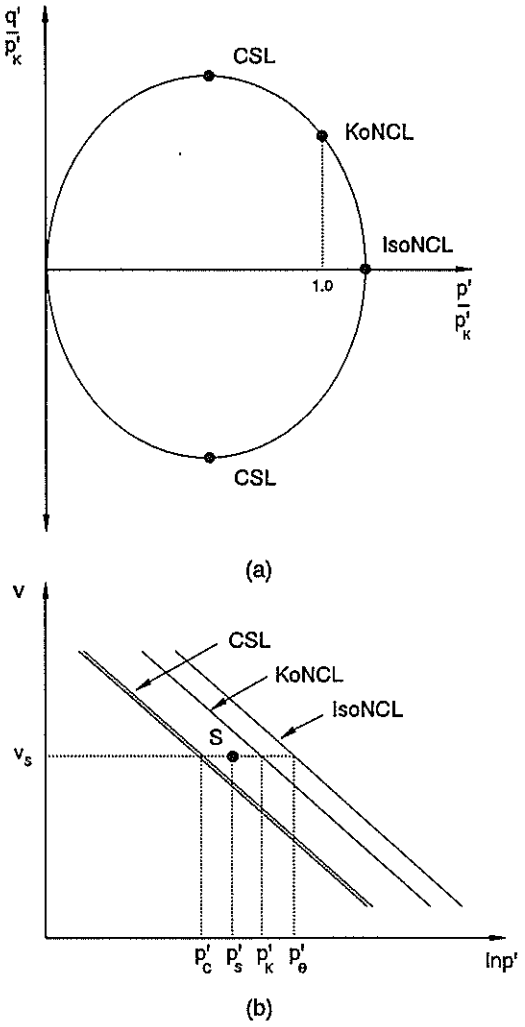

Figure 4 Normalisation of soil test data

The importance of the normalised state boundary surface shown in Figure 4 is that the state of an overconsolidated soil will lie inside the surface during a loading path which may involve any changes of the deviator and mean normal stresses. When the state reaches the boundary surface it will remain on the surface, unless the loading path is reversed in which case the path moves back inside the surface.

This feature provides a convenient method for locating the surface. Soil samples may be overconsolidated to states inside the surface and then loaded, drained, along paths which move outwards so that they are certain to intersect and then follow the boundary surface. After normalisation the test data will uniquely identify the position and shape of the boundary surface.

4. LABORATORY TESTS

A series of laboratory tests was carried out on reconstituted samples of soil from the UK soft clay test bed site at Bothkennar near the Firth of Forth in Scotland. Descriptions of the geology and the principal engineering characteristics of this soil were given by Hawkins et al (1989). The tests formed part of a major investigation into the stiffness and strength of intact and reconstituted samples of the Bothkennar soils carried out for the SERC (Science and Engineering Research Council). The particular tests described in this Paper were intended specifically to investigate the position of the state boundary surface on the wet side of critical, ie. the Roscoe surface (Atkinson and Bransby, 1978), for reconstituted and one-dimensionally lightly overconsolidated samples.

Samples for testing were prepared by one-dimensional consolidation of a slurry mixed to a water content of approximately 1.25 times the liquid limit. After initial consolidation in a thick wall cylinder to a vertical effective stress of either 50 or 100 kPa the samples were transferred to a hydraulic triaxial cell for further consolidation and testing. The triaxial cell was computer controlled using systems like those described by Atkinson, Evans and Scott (1985) so that the axial stress (or strain), the radial stress (or strain) and the pore pressure (or volume) could each be controlled, and varied, independently.

Samples were one-dimensionally consolidated to the point A in Figure 5 and three samples were then swelled to the points B_1 to B_3 where the overconsolidation ratio ($R_o = p'_m/p'$) was 2.0. All the samples were then loaded, drained, along the paths shown in Figure 5. Also shown in Figure 5 are lines given by $q' = Mp'$ corresponding to ultimate failure at the critical state with $M_c = 1.45$ and $M_e = 1.0$ for compression and extension respectively. These were obtained from other tests and correspond to a critical state friction angle $\phi' = 36^0$ for both compression and extension.

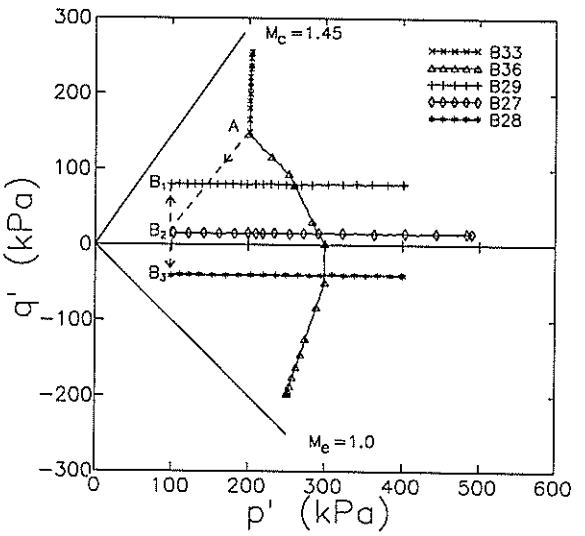

Figure 5 Paths followed during stress path probing tests

5. DISCUSSION AND CONCLUSIONS

Figure 6 shows the state paths for the tests illustrated in Figure 5 normalised with respect to the equivalent pressure p'_K on the one-dimensional normal consolidation line (see Figure 4(b)). Also shown on Figure 6 is the state path for test B52 which was a conventional undrained extension test.

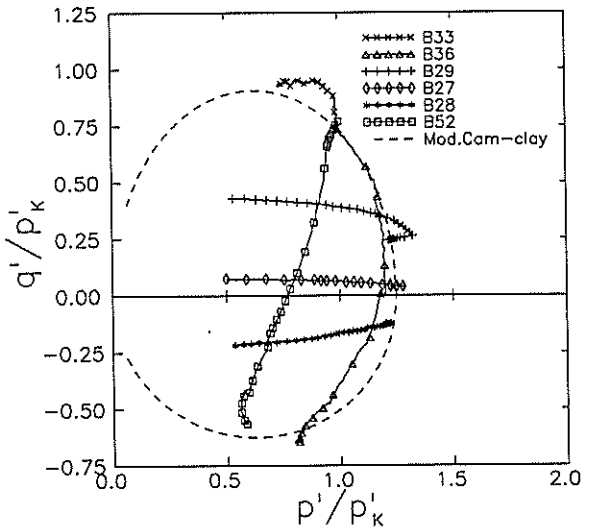

Figure 6 Stress paths from Figure 5 after normalisation

In Figure 6 the state paths for tests B33 and B36 define a state boundary surface and the paths for tests B27, B28 and B29 reach this surface part-way through the loading path and thereafter remain close to the boundary surface. In contrast the state path for the undrained extension test B52 lies well inside the boundary surface defined by the drained probing tests.

The broken lines in Figure 6 correspond to the state boundary surface for modified Cam-clay (Roscoe and Burland, 1968) with different values M_c = 1.45 and M_e = 1.0 for compression and extension respectively.

These data demonstrate that stress paths obtained from conventional extension tests on one-dimensionally consolidated samples do not identify the state boundary surface. Tests in which the state path is deliberately directed outwards from the current boundary surface, or which are directed to intersect the surface, can locate the boundary surface when the test data are correctly normalised to take account of the changing water content during the drained tests. For the reconstituted and one-dimensionally reconsolidated soil tested in the present work the experimentally determined state boundary surface is closely approximated by the surface given by modified Cam-clay making allowance for different values of the critical state strength parameter M for compression and extension. Similar results were obtained from tests on reconstituted samples of Thames alluvium by Pickles (1989) and on reconstituted samples of Pisa clay by Berardi et al (1991).

From a practical point of view soil stiffness will decrease significantly once the state reaches the boundary surface. It is, therefore, necessary to locate the position of the surface for general states of compression and extension to assess the risk that states of soils in the ground in different parts of a loaded soil structure may reach the boundary surface.

6. ACKNOWLEDGMENTS

The work described in this Paper was sponsored by the Science and Engineering Research Council and was carried out in the Geotechnical Engineering Research Centre at City University, London. The third Author was a visitor at City University while on study leave from the Victoria University of Technology, Melbourne.

7. REFERENCES

1. Atkinson, J.H. (1989). Closure to discussion on Atkinson, J.H., Richardson, D. and Robinson, P.J. Compression and Extension of K_o Normally Consolidated Clay. American Society of Civil Engineers, Jnl. of Geot. Eng. Vol. 115, No. 8, pp. 1175-1179.

2. Atkinson, J.H. and Bransby, P.L. (1978). The Mechanics of Soils. McGraw-Hill: London.

3. Atkinson, J.H., Evans, J.S. and Scott, C.R. (1985). Developments in stress path testing equipment. Ground Engineering, Vol. 18, No. 1, pp. 15-22.

4. Atkinson, J.H., Richardson, D. and Stallebrass, S.E. (1990). Effect of recent stress history on the stiffness of overconsolidated soil. Geotechnique. Vol. 40, No. 4, pp. 531-540.

5. Atkinson, J.H., Richardson, D. and Robinson, P.J. (1987). Compression and extension of K_o normally consolidated clay. American Society of Civil Engineers. Jnl. of Geot. Eng. Vol. 113, No. 12, pp. 1468-1482.

6. Atkinson, J.H. and Sallfors, G. (1991). Experimental determination of soil properties. General Report to Session 1. Proc. 10th European Conf. Soil Mech. and Foundn. Eng., Florence, Vol.3, pp. 915-956.

7. Berardi, G., Caroti, L., Giunta, G., Jamiolkowski, M. and Lancelotta, R. (1991). Stiffness of granular soils from field performance. Proc. 10th European Conf. Soil Mech. and Foundn. Eng., Florence. Vol.1, pp. 7-10.

8. Casagrande, A. (1936). The determination of the preconsolidation load and its practical significance. Proc. 1st Int. Conf. Soil Mech. and Foundn. Eng. p. 60.

9. Hawkins, A.B., Larnach, W.J., Lloyd, I.M. and Nash, D.F.T. (1989). Selecting the location and the initial investigation of the SERC soft clay test bed site. Q. Jnl. Eng. Geol. Vol 22:4 pp. 281-316.

10. Parry, R.H.G. and Nadarajah, V. (1973). A volumetric yield locus for lightly overconsolidated clays. Geotechnique, Vol. 23, No. 3, pp. 450-453.

11. Pickles, A.R. (1989). The application of critical state soil mechanics to predict ground deformations below an embankment constructed on soft alluvium. Ph.D. Thesis, City University, London.

12. Roscoe, K.H. and Burland, J.B. (1968). On the generalised stress-strain behaviour of 'wet' clay. Engineering Plasticity (J. Heyman and F.A. Leckie, eds). Cambridge University Press, pp. 535-609.

13. Schofield, A.N. and Wroth, C.P. (1968). Critical State Soil Mechanics. McGraw-Hill, London.

Screw Plate Insertion Disturbance in Sand

P.T. BROWN
B.Sc., B.E., Ph.D., M.I.E.Aust.
Research Associate, University of Sydney
M.F. ABDEL-LATIF
B.Sc., M.Eng.Sc.
Post Graduate Student, University of Sydney

SUMMARY Laboratory tests in clean dry sand using an embedded screw plate and a screw plate inserted under the control of a threaded rod having the same pitch as the screw plate are described. The values of Young's modulus obtained from these tests are compared in order to estimate the effects of insertion disturbance on the results.

1. INTRODUCTION

The flat plate loading test is widely used for in-situ determination of soil compressibility in materials such as sands which cannot readily be sampled without altering the soil properties. As discussed in Brown and Abdel-Latif (1992), when carried out at the bottom of a borehole, there may be problems with the flat plate loading test in obtaining satisfactory bedding of the plate, and errors in modulus due to the stress relief of the soil just beneath the bottom of the borehole.

The screw plate test is designed to eliminate these two disadvantages of the flat plate. However when the insertion of the screw plate is carried out under the control of a threaded rod having the same pitch as the screw plate, with the aim of achieving perfect contact between the screw plate and the soil, there is a pressure increase beneath the plate during insertion. Such a pressure increase may increase both the mechanical disturbance and the stress disturbance due to insertion and both effects are likely to change the values of modulus obtained from screw plate tests.

The purpose of the two series of tests described in this paper was to determine the nature of the screw plate insertion disturbance, and its effect on values of modulus obtained in normally consolidated clean dry sand at various relative densities and subject to a range of surcharge pressures, by comparison with values obtained from tests using an embedded screw plate.

2. DESCRIPTION OF TESTS

Two series of tests were carried out in dry Sydney sand using a screw plate 30 mm diameter, 1.5 mm thick, with a pitch of 4.2 mm mounted on a 6 mm diameter shaft. The first series was carried out in a container 450 mm diameter and 650 mm deep, similar to that shown in Fig. 1 of Brown and Abdel-Latif (1992) except that no provision for drainage was required. In these tests the torque required for screw plate insertion under the control of a threaded rod with the same pitch as the screw plate, and the resulting thrust developed beneath the screw plate, were measured. The torque was measured by means of a spring balance at the end of the torque arm. The thrust was measured by means of a strain-gauged disc and strain bridge, so that the displacement of the measurement system would be small and would cause a minimal reduction in the development of thrust. For the lower levels of thrust the strain-gauged disc displacement was 1.0 mm/kN and for the larger thrusts the displacement of the thicker disc was 0.4 mm/kN.

The second series of tests was carried out in a similar container 320 mm diameter and 340 mm deep. In these tests a screw plate was embedded at a depth of 150 mm during the process of sand raining, or a screw plate was inserted by rotation to a depth of 150 mm, and then the screw plate was loaded continuously and the load and displacement were measured and recorded automatically, to provide results from which the initial modulus could be obtained. The geometry of the tests is shown in Fig. 1.

In the case of the inserted screw plate, any thrust built up during insertion was released before commencement of the modulus test. Calculation of the modulus involved allowance for the bending of the screw plate (Brown, 1991).

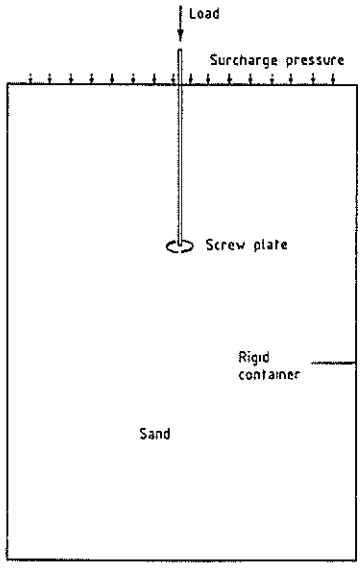

Figure 1. The geometry of the tests.

Tests were carried out at relative densities of about 15%, 65% and 85% (based on $\gamma_{min}=14.1$ kN/m^3 and $\gamma_{max}=16.2$ kN/m^3), with surcharge pressures (σ_v) ranging from 35 kPa to 200 kPa. However tests were not carried out with the inserted screw plate for the higher densities at the higher surcharge pressures for fear of breaking the screw plate.

3. THRUST TEST RESULTS

The variation of torque and thrust with depth for a screw plate inserted from the surface of the sand is shown by the lower pair of curves in Fig. 2. It will be seen that both torque and thrust increase quite rapidly with depth until they reach a maximum and then decrease slightly.

If the thrust pressure exerted by the plate is assumed to be uniform, and a friction angle of 15° between the smooth steel screw plate and the sand is assumed, (Standards Australia, 1990), a Mohr circle construction shows that the sand immediately beneath the plate is in a state of failure by the end of the first revolution of the screw plate. It seemed probable that a zone of failed sand formed beneath the screw plate and expanded with further insertion until the failure zone had reached the upper surface of the sand. This idea is supported by the results of an additional test in which insertion was commenced after the screw plate had been embedded at a depth of 100 mm. The results from this test are shown as the upper curves in Fig. 2, and it will be seen that the values of thrust are much higher than occurred in the case of insertion from the surface.

The values of thrust arising during insertion were found to increase with both sand density and surcharge pressure, as well as with the depth at which insertion commenced. In the case of insertion beneath the bottom of a borehole, because of the diffence in shape of the geometrical boundary, the actual values of thrust which arise may differ from those measured in these tests. Also the measured values of thrust are probably influenced by the proximity of the side walls of the container. However

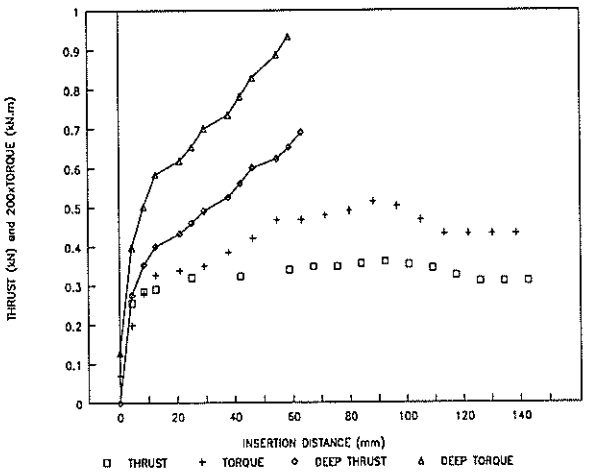

Figure 2. Thrust and torque during screw plate insertion into medium density sand with σ_v = 100 kPa.

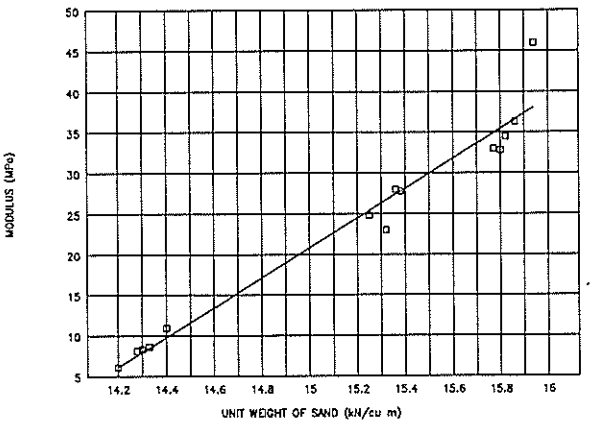

Figure 3. Values of modulus using a buried screw plate and σ_v = 35 kPa.

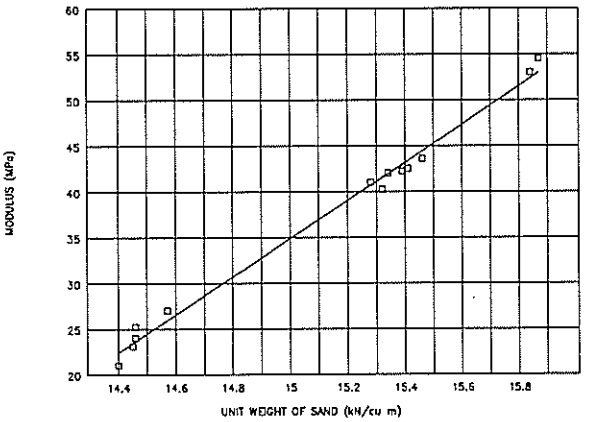

Figure 4. Values of modulus using a buried screw plate and σ_v = 100 kPa.

these tests indicate that significant thrusts may be built up and then released before the modulus test, so that the sand immediately beneath the screw plate will have been sheared, compressed and unloaded before the modulus test is carried out.

4. MODULUS TEST RESULTS

Fig. 3 shows the values of initial modulus obtained from tests carried out using an embedded screw plate for a range of sand densities and a surcharge pressure of 35 kPa. The two important features of this diagram are the very significant variation of modulus with sand density, and the small scatter of the results about the fitted regression line. The latter indicates that the tests were carried out with little variation of results due to random effects. Fig. 4 shows the corresponding results from tests with a surface surcharge pressure of 100 kPa. In this case the rate of change of modulus with unit weight is the same as in Fig. 3 although it is less obvious, and the results show a similar small scatter about the regression line.

The results shown in these two figures have been adopted as the best available values of initial modulus for Sydney sand from plate loading tests. An attempt was made to carry out flat plate loading tests using embedded discs, but it was not found possible to overcome the problems of providing a flat bearing surface without altering the properties of the sand.

Fig. 5 shows the values of initial modulus obtained from tests using an inserted screw plate and a surcharge pressure of 35 kPa, together with the regression line previously shown in Fig. 3 for an embedded screw plate. It will be seen that the values of modulus obtained from the inserted screw plate are in some cases quite conservative, being only about 60% of those obtained with the embedded screw plate. Fig. 6 shows the corresponding results of modulus tests carried out using an inserted screw plate and a surcharge pressure of 100 kPa, together with the regression line previously shown in Fig. 4 for an embedded screw plate. It can be seen that the modulus values obtained from the inserted screw plate tests range from about 70% to 110% of those obtained with the embedded screw plate.

5. DISCUSSION OF RESULTS

It seems probable that the sand, both above the screw plate and a small distance below the screw plate, has been very extensively sheared and is in the critical state. The actual density of the sand in each region will depend on the pressure conditions applying at the time of shearing, but dilation and reduction in density will certainly occur with the medium and dense sand.

The other effect which must influence the results is that the vertical stress beneath the screw plate, induced by the insertion process, particularly just below the plate, will cause an increase in horizontal stress which will not be released when the screw plate is released at the end of the insertion. Thus the sand beneath the screw plate is subject to higher horizontal stresses as a result of the insertion. Higher all-round stresses are known to cause an increase in modulus, but higher differences in horizontal and vertical stress may cause a decrease in modulus, so the resulting effect is uncertain.

6. CONCLUSIONS

Laboratory tests using a miniature screw plate show that when a screw plate is inserted into the sand under the control of a threaded rod having the same pitch as the screw plate, there may be considerable thrust developed beneath the screw plate.

In the case of loose sand at a surcharge pressure of 35 kPa, corresponding to depths of 2 - 3 m., the effect of the insertion disturbance on the values of modulus obtained appears to be negligible but may be appreciable in the case of greater depths and denser sands. However most of the values of modulus obtained were accurate or conservative, though some values were up to 10% high.

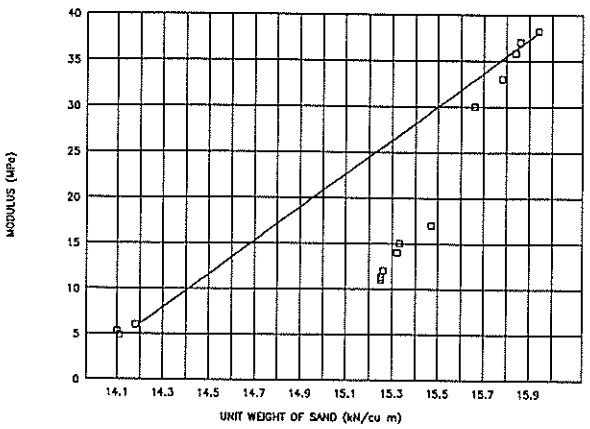

Figure 5. Comparison of modulus values for σ_v = 35 kPa.

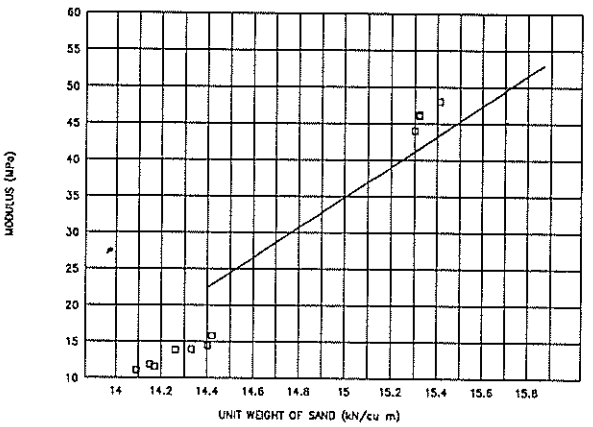

Figure 6. Comparison of modulus values for σ_v = 100 kPa.

The effect of insertion disturbance could probably be reduced by allowing the screw plate to enter the soil free of control by the threaded rod until near the desired test depth, and engaging the threaded rod only for the final revolution in order to ensure good contact with the soil.

The insertion disturbance effects discussed appear to arise from dilation and hence will probably be reduced by the presence of silt in the sand.

7. REFERENCES

Brown, P.T. (1991). The Bending of a Screw Plate, submitted to ASTM Geotechnical Testing Journal.

Brown, P.T. and Abdel-Latif, M.F. (1992). Screw Plate Insertion Disturbance in Clay. Proceedings of the Sixth Australia-New Zealand Conference on Geomechanics.

Standards Australia (1990). Australian Standard AS 3774-1990 Loads on bulk solids containers.

Screw Plate Insertion Disturbance in Clay

P.T. BROWN
B.Sc., B.E., Ph.D., M.I.E.Aust
Research Associate, University of Sydney
M.F. ABDEL-LATIF
B.Sc., M.Eng.Sc.
Post Graduate Student, University of Sydney

SUMMARY Laboratory tests in clay using an embedded flat plate and screw plate, and a screw plate inserted under the control of a threaded rod having the same pitch as the screw plate are described. The values of Young's modulus and coefficient of consolidation obtained from these tests are compared in order to estimate the effects of insertion disturbance on the results.

1. INTRODUCTION

The flat plate loading test has long been a popular method for in-situ determination of soil compressibility, but this form of test has two disadvantages. Firstly there are difficulties in obtaining perfect contact between the plate and the soil. Secondly, when it is necessary to determine soil properties at a depth greater than the diameter of the plate, the test must be carried out at the bottom of a borehole, and the soil immediately beneath the plate will have undergone complete vertical stress relief due to the excavation of the borehole. This stress relief can only be approximately reversed by pre-loading the plate since the unloading is uniform, but the loading due to the rigid plate is small at the centre and very large at the edges.

The screw plate test provides a means of carrying out a similar compressibility test, while avoiding these two disadvantages of the flat plate. This test is carried out with a helical plate inserted into the soil by rotation. If the progress of the screw plate is controlled by means of a threaded rod whose pitch is the same as the pitch of the screw plate, the contact between the soil and the plate will be excellent, although there may be some pressure increase beneath the plate during insertion. However if the screw plate is permitted to enter the clay at a smaller rate of entry per revolution than its pitch, good contact between the plate and soil appears unlikely, and the resulting values of modulus at small loads will be too low.

If the screw plate is inserted to a depth of one hole diameter below the bottom of the borehole, the soil beneath the screw plate will have undergone virtually no stress relief, although the cylinder of soil above the screw plate will have been sliced during the insertion process. However with plastic clays there appears to a considerable rejoining at these cuts.

The purpose of the series of tests described in this paper was to obtain an indication of the effect of the screw plate insertion disturbance on values obtained for undrained modulus, drained modulus and coefficient of consolidation in kaolin with over-consolidation ratios of 5 and 10, by comparison with values obtained from tests using an embedded flat plate.

2. DESCRIPTION OF TESTS

A series of laboratory tests were carried out in kaolin consolidated from a slurry in a container 300 mm diameter, similar to that described by Poulos et al (1976) and shown in Fig.1. The resulting clay bed was 86 mm deep and tests were carried out with 30 mm diameter plates on 6 mm diameter shafts at a depth of 43 mm. Although the kaolin was relatively permeable, the reduction in permeability caused by the increase in effective stress at the top and bottom boundaries, from which drainage occurred, caused a slowing of consolidation such that about a month was required to obtain full consolidation at the centre of the container. Consolidation was monitored by plotting the amount of water expelled from the clay against log time.

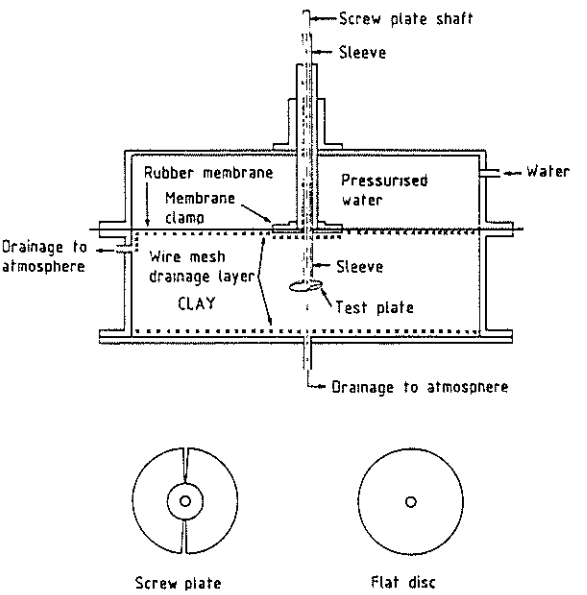

Figure 1. The laboratory test equipment

Tests were carried out with a flat disc and a screw plate, both of which were embedded in the slurry prior to consolidation, and with a screw plate which was inserted by rotation from the clay surface after consolidation was complete. The entry rate of the inserted screw plate was controlled by a threaded rod whose pitch was the same as that of the screw plate, in order to ensure good contact between the soil and the plate. These types of test were chosen so that the effect of screw plate shape could be assessed by comparison of the values of modulus from the buried disc and buried screw plate tests. Also the effect of insertion disturbance could be assessed by comparison of the values of modulus from the buried and inserted screw plate tests.

The first series of tests was carried out in kaolin with an over-consolidation ratio of 5, obtained by consolidation at 250 kPa, followed by unloading to 50 kPa, and the second series of tests was carried out with an over-consolidation ratio of 10, by consolidating at 400 kPa and unloading to 40 kPa.

Each test consisted of application of an increment of dead loading which was maintained until consolidation appeared to be almost complete. In the case of the inserted screw plate, there was a time delay of at least 20 minutes between completing insertion and application of the first load increment, so that all excess pore pressures generated by the insertion process should have dissipated before the start of the modulus test.

Values of displacement of the plates were measured by means of a displacement transducer and recorded in a computer at intervals of about 0.2 seconds initially, increasing to intervals of about 100 seconds at the end of a test lasting 20 minutes. In many cases, a second load increment was applied, which gave similar results to those from the first load increment. The load increments used were 1 to 2 Kg in order to ensure that the soil behaviour was as close to elastic as possible, however the resulting immediate settlements were typically only about 0.003 mm, which may have led to some inaccuracies in displacement measurement.

The first stage of interpretation of the results consisted of trial and error selection of three parameters, namely immediate settlement reading, total final settlement reading and time factor ($F=c_v/a^2$) for conversion of measured time (t) to the dimensionless time factor ($T=c_vt/a^2$). The values of these parameters were then used to convert the readings into values of degree of settlement (U) and dimensionless time factor (T), which were plotted on a computer screen for comparison with the corresponding theoretical values given by Small and Booker (1987) for a rigid disc embedded in a deep soil layer.

The second stage of the interpretation was conversion of the values of immediate and total final settlement to values of Young's modulus for a very deep soil layer, using an assumed value of drained Poisson's ratio of 0.3. In the case of the disc, the equation used is that given by Selvadurai (1979), and included in Selvadurai and Nicholas (1979), for a fully bonded embedded disc of finite stiffness subject to a uniform load over a zone at the centre of the plate. In the case of the screw plates, values of modulus were obtained from curves produced by finite element analysis of bending of the screw plate (Brown, 1991). Finally the values of modulus were corrected for proximity of the boundaries using results from finite element analysis of a stiff embedded plate.

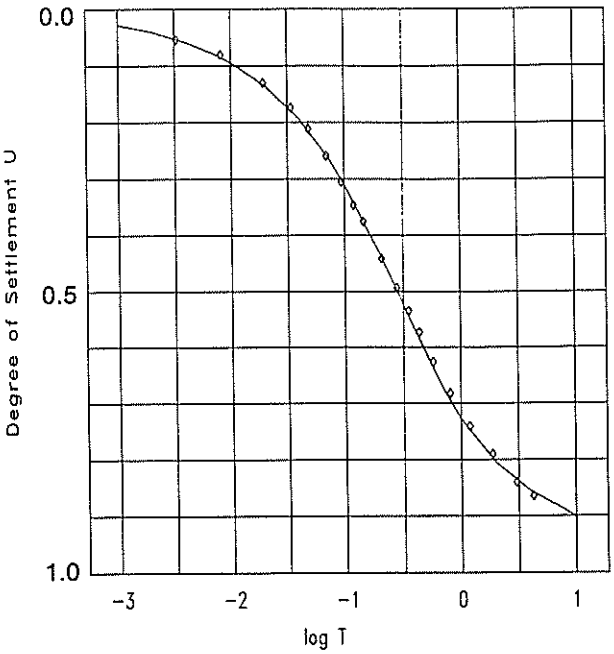

Figure 2. Settlement-time curve for well-consolidated clay

Values of c_v were obtained from the values of $F=c_v/a^2$ where a is the radius of the plate.

A typical successful screw plate test curve is shown in Fig. 2, with the theoretical curve to which it was fitted. When the clay at the centre of the container was not fully consolidated, the subsequent test showed settlement behaviour similar to that for a normally consolidated clay as shown in Fig 3.

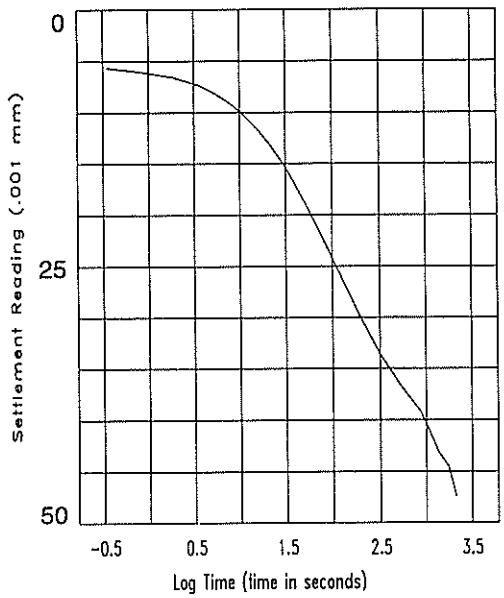

Figure 3. Settlement-time curve for incomplete consolidation

3. TEST RESULTS

The values of modulus and coefficient of consolidation obtained from the tests are shown in Table I. No allowance was made for the proximity of the top, bottom and side boundaries in the calculation of coefficient of consolidation, since in this case it is likely to have an insignificant effect, due to the fact that the dissipation of excess pore pressure is from the zone of positive pressure beneath the plate to the zone of negative pressure above the plate, and little of this dissipation occurs far from the plate.

It will be seen that there is considerable scatter in the results, but nevertheless it seems possible to draw some useful conclusions. While the values of undrained and drained modulus for the disc at OCR=5 are larger than those for the screw plate, the difference is probably not statistically significant due to the small number of values available, and hence it appears that the insertion disturbance of the screw plate is of no more than limited importance. For OCR=5, the values of c_v are somewhat larger for the disc than for the screw plate, whereas one would expect that if the two slots at the cutting edges of the screw plate had any effect it would be to increase the apparent c_v, so we can assume that the slots have no significant effect on the rate of consolidation.

When OCR=10, comparison of the values of undrained modulus from the two forms of screw plate test suggest that there may be a significant effect due to insertion disturbance. However the values of drained modulus and c_v are so much larger in the case of the inserted screw plate that it appears probable that there is a significant difference caused by insertion disturbance.

Since the change in modulus is an increase, it is unlikely to have been caused by the slicing of the clay above the screw plate.

Field testing experience shows that the penetration of the cutting edges of the screw plate causes a pressure increase immediately below the screw plate, and this is likely to be greater for the stiffer clay having OCR=10 than the more compressible clay with OCR=5. If we suppose that for OCR=10 the pressure beneath the screw plate reached 600 kPa compared with the previous consolidation pressure of 400 kPa, when this pressure was released prior to commencement of the modulus test, the OCR would have increased to 15, which could be the cause of the apparent changes in E' and c_v.

TABLE I

TEST RESULTS

Test type	Test Number	Over-Consolidation Ratio	Undrained Young's Modulus MPa	Drained Young's Modulus MPa	Coefficient of Consolidation mm^2/min
Flat disc buried	1	5	90	19	121
	2		90	38	176
	3		59	9	74
	4		56	24	200
Screw plate buried	5	5	51	8.0	68
	6		22	8.1	108
	7		42	9.0	81
	8		39	7.5	119
Screw plate inserted	9	5	59	12.1	68
	10		33	10.8	94
	11		33	9.1	162
	12		55	11.0	95
	13		49	8.8	61
Flat disc buried	14	10	89	15.2	81
	15		49	13.4	53
Screw plate buried	16	10	38	10.2	108
	17		31	4.7	63
Screw plate inserted	18	10	59	33	405
	19		72	46	1188
	20		54	46	256
Oedometer	21	5	-	-	109
	22	10	-	-	87

Values of c_v obtained from oedometer tests on 25 mm thick specimens of the same kaolin as used for the tests described above, are 109 mm^2/min for OCR=5, and 87 mm_2/min for OCR=10. The specimens were compressed to this length during pre-consolidation and were not cut to this length, thus avoiding smearing of the ends. These results provide some confirmation of the conclusion that the values of c_v for OCR=5 have not been significantly affected by the insertion, but that for OCR=10 the effect of insertion is significant.

4. CONCLUSIONS

Tests giving values of Young's modulus and coefficient of consolidation for clay, using embedded flat plates and screw plates, and inserted screw plates have been described and compared.

Despite scatter in the results, it appears that screw plate insertion has little effect on the results when OCR=5, but that the effects are significant when OCR=10.

It seems likely that the increase in OCR from 5 to 10 has caused the pressure increase beneath the screw plate during insertion to become very much higher and so cause a further increase in over-consolidation ratio, thus increasing values of modulus and c_v.

This effect could probably be avoided by allowing the screw plate to enter the soil free of control by the threaded rod until near the desired test depth, and engaging the threaded rod only for the final revolution so as to ensure good contact with the soil.

5. REFERENCES

Brown, P.T. (1991). The Bending of a Screw Plate, submitted to ASTM Geotechnical Testing Journal.

Poulos, H.G., de Ambrosis, L.P. and Davis, E.H. (1976). Method of Calculating Long-Term Creep Settlements. Journal of Geotechnical Engineering Division, A.S.C.E., Vol. 102, No. GT7, pp. 787-804.

Selvadurai, A.P.S. (1979). An Energy Estimate of the Flexural Behaviour of a circular Foundation Embedded in an Isotropic Elastic Medium, International Journal for Numerical and Analytical Methods in Geomechanics, Vol.3, pp. 285-300.

Selvadurai, A.P.S. and Nicholas, T.J. (1979). A Theoretical Assessment of the Screw Plate Test. Proceedings of the Third International Conference on Numerical Methods in Geomechanics, Aachen, pp.1245-1252.

Small, J.C. and Booker, J.R. (1987). The Time-Deflection Behaviour of a Rigid Under-Reamed Anchor in a Deep Clay Layer, International Journal for Numerical and Analytical Methods in Geomechanics, Vol. 11, pp. 269-281.

Strain Softening of a Granular Soil in Triaxial and Multi-Axial Testing

J. CHU
B.E., Ph.D., Former Research Student
S-C. R. LO
B.Sc., Ph.D., C.Eng., M.I.C.E., M.I.Struct.E., M.I.E.Aust., M.H.K.I.E.
Senior Lecturer
I.K. LEE
B.C.E., M.Eng.Sc., Ph.D., F.I.E.Aust., M.A.S.C.E.
Professor and Head of Department, Department of Civil and Maritime Engineering, University College, University of New South Wales, Australian Defence Force Academy, Canberra

SUMMARY An intensive research program was carried out to investigate the strain softening behaviour of a dense granular soil. Strain path testing technique was developed and adopted for the study. Both strain softening observed from triaxial and multi-axial tests were reported. The factors affecting the occurrence of strain softening were discussed.

1 INTRODUCTION

Strain softening of soils has been credited as one of the causes for some geotechnical failures (Skempton, 1948, 1970, 1985; Morgenstern, 1977). Despite of the intensive studies over the past decades, the mechanism of strain softening has not been well understood. In the early studies of Skempton (1948), Hoeg (1972), and Lo and Lee (1973), strain softening was referred to as the phenomenon of decreasing deviatoric stress after the peak value is reached, as observed in conventional triaxial compression (CTC) tests. Such a type of response was regarded as a true material property of a soil element. However, recent experimental studies with improved testing techniques have revealed that strain softening observed in CTC tests may be mainly a result of the non-homogeneous deformation rather than a material behaviour (Hettler and Vardoulakis, 1984). Based on such observations, the adequacy of regarding strain softening observed in CTC tests as a material behaviour has been questioned (Read and Hegemier, 1984).

An intensive research program for investigating the strain softening behaviour of dense granular soils has been conducted in the authors' institution over the last few years. As the stress-strain responses of a soil element are highly path dependent, the strain softening behaviour needs to be studied along a wide range of paths. To achieve the research objectives, strain path testing technique was developed and adopted for the study of strain softening response of dense granular soils. The control of strain path may prove to be a better alternative to the control of stress path as, upon onset of strain softening, the latter approach may 'force' a sample into an inadmissible state. Strain path control can be achieved by controlling the strain increment ratio, thus allowing the decrease in stresses associated with strain softening to develop freely.

The studies of strain softening behaviour of granular soils have been carried out under both axisymmetric and three dimensional conditions. The former was achieved by triaxial testing and the later by multi-axial testing. Four types of strain softening were observed in the studies. Some of the experimental findings will be presented in this paper.

To facilitate the discussion, it is essential to give a precise definition of strain softening. Among the various existing definitions of strain softening, Valanis' definition was adopted in the present studies (Valanis, 1985). Mathematically, Valanis' definition can be written as:

$$d\sigma'_{ij}d\epsilon_{ij} < 0 \qquad (1)$$

Note that the stresses and strains measured from a test can be used directly in Inequality (1) without refering to a certain consittutive model. The rationale for the adoption of Valanis' definition is detailed in Chu, Lo, and Lee (1991). This definition is given in incremental forms, hence, it is dependent on the current direction of the stress and strain increment vectors only. Therefore, the definition is particularly suitable for investigating, experimentally, strain softening response along a wide range of stress/strain paths.

The stress and strain parameters used in this paper are defined as below:

$$R = \sigma'_1/\sigma'_3$$
$$p' = \frac{1}{3}(\sigma'_1 + \sigma'_2 + \sigma'_3)$$
$$q = \frac{1}{\sqrt{2}}[(\sigma_1 - \sigma_2)^2 + (\sigma_2 - \sigma_3)^2 + (\sigma_3 - \sigma_1)^2]^{\frac{1}{2}}$$
$$\epsilon_v = \epsilon_1 + \epsilon_2 + \epsilon_3$$
$$\epsilon_s = \frac{\sqrt{2}}{3}[(\epsilon_1 - \epsilon_2)^2 + (\epsilon_2 - \epsilon_3)^2 + (\epsilon_3 - \epsilon_1)^2]^{\frac{1}{2}}$$
$$\mu = \frac{2\sigma'_2 - \sigma'_3 - \sigma'_1}{\sigma'_1 - \sigma'_3}$$
$$\nu = \frac{2d\epsilon_2 - d\epsilon_3 - d\epsilon_1}{d\epsilon_1 - d\epsilon_3}$$

in which p', q, ϵ_v and ϵ_s are the generalized mean stress, deviatoric stress, volumetric strain and deviatoric strain, respectively. μ is Lode stress parameter and ν is the Lode strain parameter. For a test commencing from an isotropic compression state, p'_0 is used to represent the initial effective isotropic confining stress. Under an initial anisotropic compression state, σ'_{20} and σ'_{30} are used for the initial effective stress conditions.

Using the stress and strain parameters defined as above, Inequality (1) can be re-written as:

$$dp'd\epsilon_v + \beta dq d\epsilon_s < 0 \qquad (2)$$

where:

$$\beta = \frac{(3 + \mu\nu)}{\sqrt{(3 + \mu^2)(3 + \nu^2)}} \qquad (2a)$$

Under some special conditions, Inequality (2) degenerates into $dq < 0$, which is consistent with the intuitive expectation of strain softening (Chu, 1991). Inequality (2) can be regarded as a generalization of $dq < 0$ for more complicated loading conditions.

2 STRAIN PATH TESTING TECHNIQUE

2.1 Testing Arrangement

A triaxial cell with internal load cell and LVDTs was used for testing a nominated 100 mm height and 100 mm diameter sample. The test arrangement for triaxial testing

TABLE I

TEST CONDITIONS

Test	H/D	Free-end	Grease	t/d_{50}	Dp/D	Platen condition
#1	2	No	-	-	1	NS
#2	1	Yes	ordinary	0.85	1.10	NS
#3	1	Yes	HVS	0.85	1.10	NS
#4	1	Yes	HVS	2.0	1.15	PM

H = height of sample
D = diameter of sample
t = thickness of latex disc
d_{50} = grain size
D_p = diameter of enlarged platen
NS = no specification
PM = polished to mirror finish
HVS = high vacuum silicone grease

has been detailed in Chu, Lo, and Lee (1991). The multi-axial tests were conducted with a new multi-axial cell (Chu, 1991). This cell can shear a 100 mm by 88 mm by 88 mm sample to a large strain without introducing apparent non-homogeneous deformations. Therefore, the multi-axial cell is particularly suitable for studying the strain softening behaviour of soils. The test arrangement for multi-axial testing is shown in Fig. 1. For three-dimensional loading, the major principal stresses was applied by a compression machine, the minor principal stress by hydrostatic pressure of cell fluid, and the intermediate principal stress by a pair of 'composite boundary' loading platens. It is the use of a pair of 'composite boundary' loading platens that enables the sample to be sheared to a large strain. The basic design of the new multi-axial cell was introduced by Lo (1985) and Lee et al (1988). Further improvement and calibration were contained in Chu (1991). Computerized control and data-logger systems were used to control a stress/strain path and to sample data automatically.

In all the triaxial and multi-axial tests, free-ends with enlarged platen was adopted. The bedding and membrane penetration errors were reduced by liquid rubber technique (Lo, Chu, and Lee, 1989). A digital pressure/volume controller (DPVC) was used to control/measure the volume change of the sample. The principle and the accuracy of a DPVC in soil testing have been discussed by Menzies (1987) and Lo and Chu (1991).

2.2 Strain Path Testing Technique

In both triaxial and multi-axial tests, a strain path was specified by the principal strain increment ratio, $d\epsilon_v/d\epsilon_1$. Such a strain path can be imposed on a sample by controlling the volume change of the sample via a DPVC in accordance with the measured axial deformation. During a test, the strain increment ratio can either be maintained constant, or varied in accordance with certain pre-determined relationship. The minor principal total stress (the cell pressure) was maintained constant during a test. However, the control of volume change leads to a change in pore pressure, thus a change in the minor principal effective stress. The implementation of strain path testing is detailed in Chu and Lo (1991).

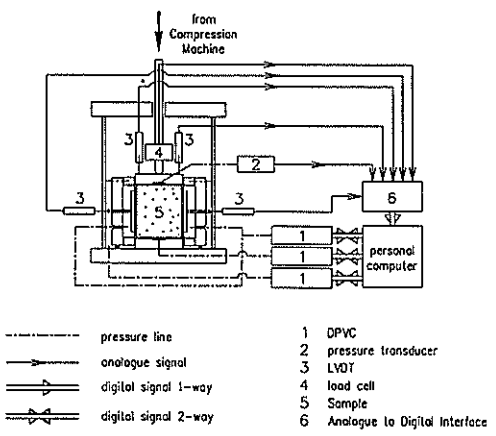

Figure 1 Test Arrangement

2.3 Material Tested

The material tested was Sydney sand, a uniformly graded quartz sand with the mean grain size of 0.3 mm. The dry sand was re-constituted into saturated samples of 100 mm diameter by 100 mm height. The procedure for the preparation of sample was detailed in Lo and Lee (1990). The void ratio of the samples ranged from 0.599 to 0.621.

3 TEST RESULTS

3.1 Compression Tests

To investigate whether the strain softening in a drained CTC test is mainly influenced by the boundary conditions, four drained CTC tests with different boundary conditions were performed. The test conditions of the four tests are detailed in Table 1. Among them, test #4 had the best quality of free-ends. Hence the end restraint in test #4 was most effectively reduced. The stress-strain curves of the four tests are presented in Fig. 2, in which R_f represents the stress ratio at failure. Fig. 2 clearly shows that the rate of 'softening' in a drained CTC test is considerably affected by the extent of reducing the end restraint. Thus, the strain softening observed in a drained CTC test is not a material property but a result of non-homogenous deformation. If the correct technique is used, strain softening can be significantly delayed and the deviatoric stress will keep at its maximum value without 'softening' to a large strain, as in test #4. However, it was impossible to avoid any deviation from a perfect test condition, hence non-homogeneous deformation eventually occurred in test #4 when $\epsilon_s > 16\%$, which caused 'softening'. The above finding is in agreement with the studies of Hettler and Vardoulakis (1984)

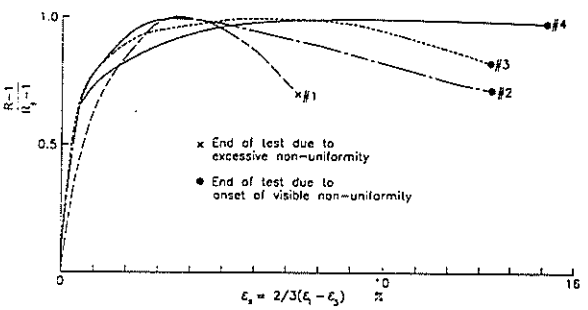

Figure 2 CTC Tests with Different Conditions

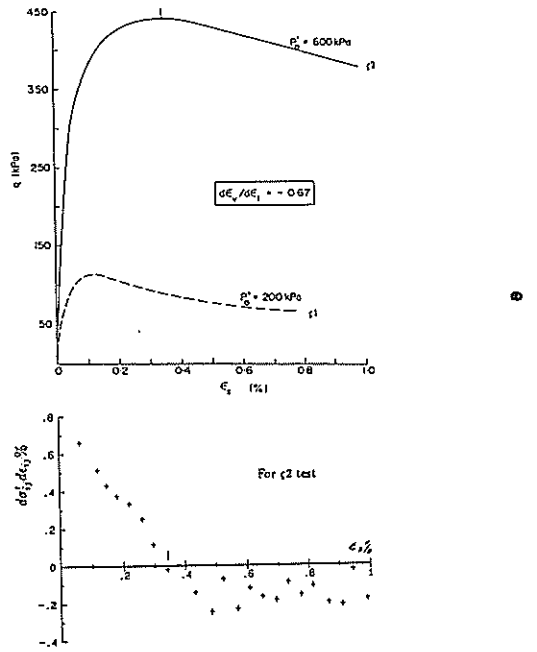

Figure 3 Pre-failure Strain Softening

and Read and Hegemier (1984). It also implies that if the correct testing technique is not used in a CTC test, the measured post-failure behaviour can be considerably in error !

Repeating test #4 using a multi-axial cell with $\sigma'_2 = \sigma'_3 =$ 300 kPa resulted in the similar response as in Fig. 2 for test #4 (Chu, 1991).

3.2 Strain Path Tests

Two types of strain path tests will be presented in this paper. A Type-A strain path test sheared a sample with a constant strain increment ratio from an isotropically consolidated state, whereas in a Type-B test, strain path control was only imposed in the post-failure region, that is, after failure state was attained. The test results of the two different types of tests will be presented separately in the following.

Type-A:

The results of two triaxial strain path tests are presented in Figs. 3(a). A strain increment ratio of $d\epsilon_v/d\epsilon_1 = -0.67$ was used for both tests. The two tests were commenced from an initial effective confining stresses of $p'_0 = 200$ kPa and 600 kPa respectively. The variation of $d\sigma'_{ij}d\epsilon_{ij}$ with the deviatoric strain is plotted in Fig. 3(b) for test $\varsigma 2$. It can be seen by comparing Fig.3(a) with Fig. 3(b) that the sign of $d\sigma'_{ij}d\epsilon_{ij}$ became negative in the region of $dq < 0$. According to Inequality (1), strain softening occurred in $dq < 0$ region for test $\varsigma 2$. Same conclusion can be reached for test $\varsigma 1$. When strain softening occurred, the strain levels were less than 0.5%. For such a small strain, non-homogeneous deformation was not observed and unlikely to occur. Therefore, it was concluded that the observed strain softening is a material behaviour.

The effective stress paths resulting from tests $\varsigma 1$ and $\varsigma 2$ are shown in Fig. 4(a). The failure curve determined by drained triaxial $d\sigma'_3 = 0$ tests is also plotted in Fig. 4(a). Since strain softening occurs prior to failure, it can be called pre-failure strain softening. The effective stress paths of other three Type-A tests are given in Fig. 4(b). These three tests were conducted with the same strain increment ratio of $d\epsilon_v/d\epsilon_1 = -0.11$ but commenced from different

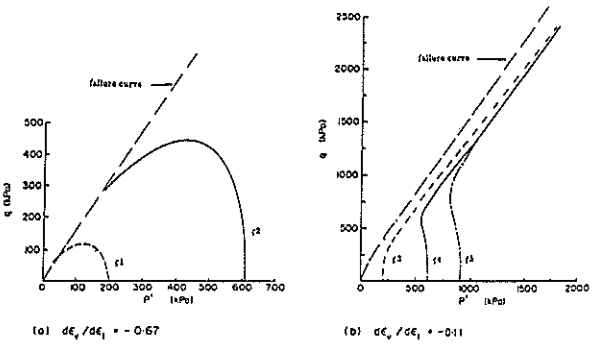

Figure 4 Effective Stress paths of Strain Path Tests

initial effective confining stresses of $p'_0 = 200$, 600, and 900 kPa, respectively.

The effective stress paths of two Type-A multi-axial strain path tests are given in Fig. 5. The strain increment ratio, $d\epsilon_v/d\epsilon_1$, was −1.2 for test M28 and −0.67 for test M26. The strain path control for both tests were commenced at the initial effective confining stresses of $\sigma'_{20} = 450$ kPa and $\sigma'_{30} = 300$ kPa. By checking the stress-strain data with Inequality (1), it was shown consistently that strain softening occurred in the $dq < 0$ region for the above two tests. Shear bands and other non-homogeneous deformation were not observed in the region of DF for test M28. Therefore, the strain softening occurred in this test was a material behaviour. In Fig. 5, points F and B were failure points as identified by Lade's failure criterion (Lade, 1977) for test M28 and M26 respectivelly. The adequacy of modelling the three-dimensional failure behaviour of dense Sydney sand by Lade's failure criterion was discussed in Chu (1991). Thus, the strain softening occurring in test M28 was also a pre-failure strain softening. On the other hand, strain hardening was manifested in test M26 all the way to failure. After failure point B, shear bands were observed, which caused strain softening in the region BC. Since the strain softening occurring in the region BC is associated with shear bands, it is called banding softening. The occurrence of banding softening will be further discussed in the next section.

Type-B:

The typical stress-strain curves of two Type-B triaxial strain path tests, $s1$ and $s2$, are presented in Fig. 6. Both tests were sheared to failure along a drained $d\sigma'_3 = 0$ path with $p'_0 = 300$ kPa. Along this path, the strain increment ratio manifested at the failure was $d\epsilon_v/d\epsilon_1 = -0.54$. When failure was reached, strain paths of $d\epsilon_v/d\epsilon_1 = -0.67$ and $d\epsilon_v/d\epsilon_1 = -0.25$ were imposed on the two samples in tests $s1$ and $s2$ respectively in the post-failure region. With different strain path control, different stress-strain behaviour

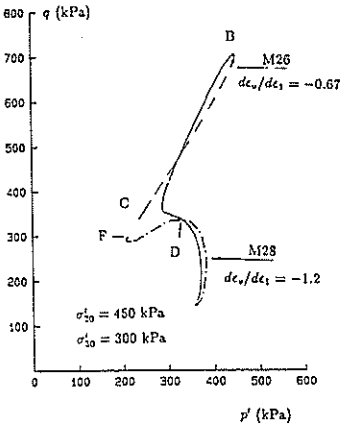

Figure 5 Multi-axial Strain Path Tests

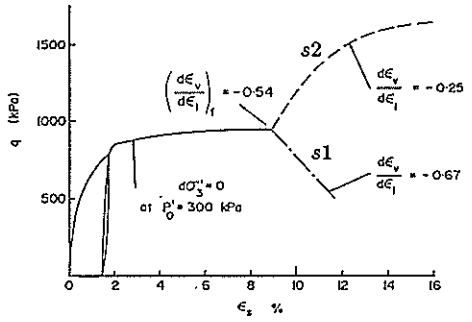

Figure 6 Post-failure Strain Softening

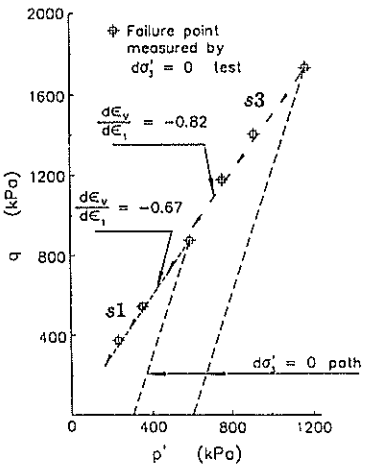

Figure 7 Post-failure Effective Stress Paths

was observed from the two tests in the post-failure region. For test $s2$, strain hardening was manifested, while softening was resulted in test $s1$. Strain softening was identified according to the definition of Inequality (1). It again shows that strain softening occurs in the region of $dq < 0$. This kind of strain softening is called post-failure strain softening as it occurs in the post-failure region. When strain softening occurred, non-homogeneous deformation was not observed. Thus, it was a material property. The effective stress path for test $s1$ is given in Fig. 7. The effective stress path resulting from another Type-B test, $s3$, is also shown in Fig. 7, together with a number of failure points determined by drained triaxial $d\sigma_3' = 0$ tests. Test $s3$ was conducted by following the same procedure as test $s1$. The sample in this test was sheared by a drained $d\sigma_3' = 0$ path with $p_0' = 600$ kPa to failure and then by strain path of $d\epsilon_v/d\epsilon_1 = -0.82$ in the post-failure region. It can be seen from Fig. 7 that the effective stress paths of the two Type-B tests coincide with the failure curve during post-failure softening. Such a behaviour is representative of other test conducted and reported in (Chu, Lo, and Lee, 1991).

The stress-strain curves of two Type-B multi-axial post-failure tests are shown in Fig. 8. These tests were conducted by shearing the sample to failure along a drained $d\sigma_2' = 0$ and $d\sigma_3' = 0$ but $\sigma_2' \neq \sigma_3'$ path and then imposing a strain path of $d\epsilon_v/d\epsilon_1 = -1.2$. Failure points A and A' in Fig. 8 were detected by Lade's failure criterion. The initial effective confining stresses used for the two tests were $\sigma_{20}' = 450$ kPa & $\sigma_{30}' = 300$ kPa and $\sigma_{20}' = 300$ kPa & $\sigma_{30}' = 200$ kPa respectively. Immediately after imposing the strain path control from the failure point, strain softening as identified by Inequality (1) occurred. However, unlike the post-failure strain softening observed in Type-B triaxial tests, non-homogeneous deformation in the form of shear band was observed soon after the strain path control commenced from the failure, that is, banding softening occurred. Although at the very beginning the observed strain softening may still be a material response to the imposed strain increment ratio, studies indicate that under three-dimensional conditions, the behaviour in the post-failure region is dominated by banding softening (Chu, 1991).

4 DISCUSSIONS OF TEST RESULTS

4.1 Classification of Strain Softening

The strain softening behaviour presented above may be classified into four types. The strain softening due to the end-restriant is one type. 'Softening' observed from CTC tests is a typical example of this type of strain softening. Softening may also be induced by the inevitable deviation from the ideal test condition, such as the slight initial inhomogenity of a sample. This is the second type of strain softening. It needs to be particularly emphasized that the above two types of 'strain softening' cannot be regarded as a true material property.

The pre-failure strain softening occurring along a strain path (under either axisymmetric or three-dimensional conditions) and the post-failure strain softening under axisymmetric conditions are the third type of strain softening. These type of softening is a true material behaviour as they reflect the response of dense granular soil to the imposed strain path. The banding softening observed in the multi-axial strain path tests is the fourth type of strain softening. Although the banding softening is associated with the development of shear bands in the post-failure region, it is different from the first type of softening. Under $\sigma_2' \neq \sigma_3'$ conditions banding softening inevitably occurs in the post-failure region irrespective of what kind of pre-failure path is used (Chu, 1991). Therefore, the occurrence of banding softening is mainly a response of the tested sample to the imposed $\sigma_2' \neq \sigma_3'$ stress state.

4.2 Factors Affecting the Occurrence of True Strain Softening

The occurrence of pre-failure strain softening depends on the strain increment ratio of the path followed. It can be seen from Figs. 3 and 4 that strain softening occurs for tests with $d\epsilon_v/d\epsilon_1 = -0.67$ but not for tests with $d\epsilon_v/d\epsilon_1 = -0.11$. Similar observation is also established for multi-axial strain path tests, as shown in Fig. 5. These indicate that the lower the strain increment ratio $d\epsilon_v/d\epsilon_1$, the larger the tendency for pre-failure strain softening to occur provided the other conditions are the same. The pre-failure strain softening is also affected by the initial effective confining stress. Under axisymmetric conditions, the influence of both $d\epsilon_v/d\epsilon_1$ and p_0' can be shown in Fig. 9 (Chu, Lo, and Lee, 1991).

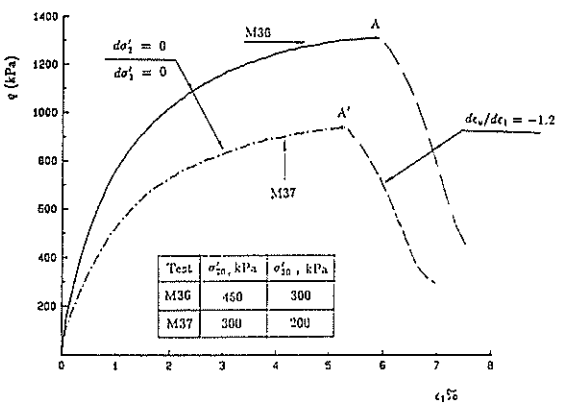

Figure 8 Multi-axial Post-failure Strain Softening

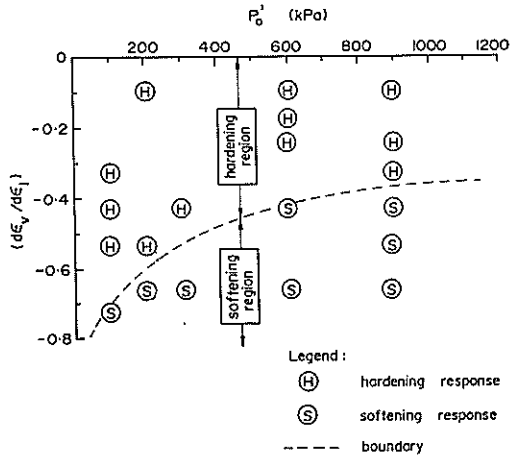

Figure 9 Response Boundary of Pre-failure Softening

The occurrence of post-failure strain softening is related to the relative magnitude of the strain increment ratio to the ratio manifested at failure, as can be seen from Fig. 6. The strain increment ratio manifested at the failure along the drained $\sigma_3' = 300$ kPa path was $(d\epsilon_v/d\epsilon_1)_f = -0.54$. When a strain increment ratio of $d\epsilon_v/d\epsilon_1 = -0.67$ was imposed for test $s1$ in the post-failure region, strain softening occurred. On the other hand, strain hardening occurred for test $s2$ with $d\epsilon_v/d\epsilon_1 = -0.25$. Therefore, the conditions for the occurrence of post-failure strain softening can be mathematically expressed as:

$$\left(\frac{d\epsilon_v}{d\epsilon_1}\right)_f - \left(\frac{d\epsilon_v}{d\epsilon_1}\right)_i \begin{cases} > 0, & \text{softening;} \\ = 0, & \text{perfectly plastic;} \\ < 0, & \text{hardening.} \end{cases} \qquad (3)$$

in which $(d\epsilon_v/d\epsilon_1)_i$ represents the strain increment ratio imposed in the post-failure region. The perfectly plastic behaviour refers to as the stress-strain behaviour observed from test #4 of Fig. 2.

The factors affecting the occurrence of banding softening may be complicated. However, it was established by the experiments that there are two necessary conditions for the occurrence of banding softening. First, the stress state has to reach failure, which can be seen from test M26 of Fig. 5 and tests M36 and M37 of Fig. 9. Second, the stress state must be in $\sigma_2' \neq \sigma_3'$ condition, as banding softening does not occur for multi-axial tests conducted with $\sigma_2' = \sigma_3'$ condition (Chu, 1991).

5 CONCLUSIONS

The strain softening behaviour of a granular soil observed in triaxial and multi-axial tests was presented in this paper. Strain path testing technique was developed for studying the strain softening behaviour of soils. Three types of strain softening behaviour were identified and studied.

The studies verified that strain softening observed from CTC tests and multi-axial $\sigma_2' = \sigma_3'$ tests is not a material property but a result of non-homogeneous deformation.

Along a constant $d\epsilon_v/d\epsilon_1$ path, strain softening can occur as a material behaviour in either the pre-failure region or the post-failure region for $\sigma_2' = \sigma_3'$. Under such conditions, strain softening is a path dependent behaviour. The occurrence of pre-failure softening is affected by the strain increment ratio imposed. The smaller the strain increment ratio the greater the tendency for pre-failure strain softening to occur. The occurrence of post-failure strain softening on the other hand, depends on the strain increment ratio imposed in the post-failure region relative to the ratio manifested at failure, as mathematically expressed in Eqn. (3).

Under axisymmetric conditions, the effective stress paths resulting from post-failure strain softening behaviour coincide with the failure curve determined by drained $d\sigma_3' = 0$ tests.

Banding softening is related to shear bands which occur as a response of three-dimensional loading. The present studies indicate that banding softening can only occur in the post-failure region under three-dimensional stress state of $\sigma_2' \neq \sigma_3'$.

6 ACKNOWLEDGEMENT

The study reported in this paper forms part of a research program on the constitutive behaviour of granular medium conducted in the Department of Civil and Maritime Engineering, University College, University of New South Wales, Canberra. The support from members of the Department involved in the project is gratefully acknowledged.

7 REFERENCES

Chu, J. (1991). Strain softening behaviour of granular soils under strain path tsting. PhD. thesis, Univ. College, Univ. New South Wales.

Chu, J. and Lo, S-C. R. (1991). On the implementation of strain path testing. Proc. 10th European Conf. Soil Mech. Found. Eng., Florence, Vol. 1, pp. 53-56.

Chu, J., Lo, S-C. R., and, Lee, I. K. (1991). Strain softening behaviour of a dense granular soil in strain path testing. Accepted by J. Geot. Eng., ASCE.

Hettler, A. and Vardoulakis, I. (1984). Behaviour of dry sand tested in a large triaxial apparatus. Geotechnique, Vol. 34, pp. 183-198.

Hoeg, K. (1972). Finite element analysis of strain-softening clay. J. Soil Mech. Found., ASCE, Vol. 98, No. SM1, pp. 43-58.

Lee, I. K., et al (1988). The response of Shanghai clay in multi-axial tests. Proc. 5th ANZ Conf. on Geomech., Sydney, pp. 155-158.

Lade, P. V. (1977). Elasto-plastic stress-strain theory for cohesionless soil with curved yield surfaces. Int. J. Solids Str., Vol. 13, pp. 1019-1035.

Lo, S-C. R. (1985) Constitutive relationships of granular soils. PhD. thesis, Univ. New South wales.

Lo, S-C. R. and Chu, J. (1991). Measurement of K_0 by triaxial strain path testing. Soils and Founds., Vol. 31, No. 2.

Lo, S-C. R., Chu, J., and Lee, I. K. (1989). A technique for reducing membrane penetration and bedding errors. Geot. Testing J., ASTM, Vol. 12 No. 4, pp. 311-316.

Lo, S-C. R., and Lee, I. K. (1990). Response of a granular soil along constant stress increment ratio path. J. Geot. Engng., ASCE, Vol. 116, No. 3, pp. 355-376.

Lo, K. Y. and Lee, C. F. (1973). Stress analysis and slope stability in strain-softening materials. Geotechnique, Vol. 23, pp. 1-11.

Menzies, B.K. (1987). A computer controlled hydraulic testing system. Proc. ASTM Symp. on Advanced Triaxial Testing, pp. 82-94.

Morgenston, N. R. (1977). Slopes and excavations in heavily over-consolidated clays: State-of-the-Art report, Proc. 9th Int. Conf. on Soil Mech. Found. Eng., Tokyo, Vol. 2, pp. 547-604.

Provest, J.-H. and Hoeg, K. (1975). Soil mechanics and plasticity analysis of strain softening. Geotechnique, Vol. 25, pp. 279-297.

Read, H. E. and Hegemier, G. A. (1984). Strain softening of rock, soil and concrete – a review article. Mechanics of Materials, Vol. 3, pp. 271-294.

Skempton, A. W. (1948). The rate of softening of stiff fissured clays with special reference to London clays. Proc. 2nd Int. Conf. Soil Mech. Found. Eng., Rotterdam, Vol. 2, pp. 50-53.

Skempton, A. W. (1970). First time slides in over consolidated clays. Geotechnique, Vol. 20, pp. 320-324.

Skempton, A. W. (1985). Residual strength of clays in landslides, folded strata and laboratory, Geotechnique, Vol. 35, pp. 3-18.

Valanis, K. C. (1985). On the uniqueness of solution of the initial value problem in strain softening materials. J. Appl. Mech., ASME, Vol. 52, pp. 649-653.

Some Engineering Implications of Chemical Weathering of Soil Formations At Nile Valley Boundaries

MOHAMED A. EL-SOHBY
Professor, Faculty of Engineering, Al-Azhar University Nasr City, Cairo, Egypt
S. OSSAMA MAZEN
Senior Researcher, General Organization for Housing, Building and Planning Research Dokki, Cairo
MAHMOUD I. ABOUSHOOK
Associate Prof. Faculty of Engineering, Al-Azhar University, Nasr City, Cairo

SUMMARY Analysis of result, of silica sesquioxide ratio of clayey deposit in Egypt showed that there are significant variations in the values of this ratio depending upon whether the soil is in side or outside the Nile Valley. It is observed that the clayey deposits outside the Nile Valley (desert region) are poorly developped eventhough they are quit old compared to inside the Nile Valley. These changes could be attributed to genesis of soil deposits. The alluvial formations of the Nile Valley have been enriched by lateric soil carried down by the Nile River from tropical zone of Abyssinia. Furthermore it was found that the morphological conditions affected the silica/sesquioxide ratio indicating differential weathering between east and west desert formations. Also the results indicated that chemical weathering modified geotechnical properties significantly.

1. INTRODUCTION:

The extent to which different types or soils have been chemically weathered may be expressed by the ratio or the silica remaining in the soil to the amount or iron oxide and aluminium oxide that has accumulated(margnien 1966). This is known as the silica/sesquioxide ratio (Margnien,1966 correia, 1967; Gidigasu, 1971 and Tuncer and Lohnes, 1977).

Lateritic soils occurs extensively in tropical zones of the world as defined by (Hadu,1975 and Massed et al.,1985).Although Egypt lies outside the tropical zone, observations of silica/sesquioxide ratio or clayey deposits occuring in the flood plain of the Nile Delta indicated lateritic origin of these deposits (El-Sohby et al., 1988). This was shownby the signiricant variation in the silica/sesquioxide ratio between the deposits of the Nile Delta and thoseof its boundaries. This may be due to the enrichment of the alluvial formations of the Nile by soil deposits carried by the Nile River from the tropical zone or Abyssinia.This agrees with Novias_ Ferreiva, 1985 who stated that lateritic soils may be somtimes carried out by erosion process to low levels to form recent alluvium.

The objective or the present work is to conrirm the previous findings. Therefore, sections across the Nile were taken at different locations in Egypt in Nile Valley and the boundaries. Their geotechnical, chemical and mineralogical properties were determined. Then the silica/sesquioxide ratio was taken as a basis for the identification and the evaluation of chemical weathering and chracterstics.

2. MATERIAL INVESTIGATED

Soil for study were taken from five sections across the Nile (See Fig 1). The First section (A)is in the Nile Delta. The second section (B) is in Cairo area. The third section (C) is in Fayoum in the south west or Cairo. The fourth location (D) is in Assuit at a distance of 500 Kilometers south of Cairo. The Firth location(E) is in Asswan at a distance of 1000 kilometers south or Cairo.

From each location two groups of samples were taken. The first group represents The Nile deposits (A,B,C,D,E), The second group representes the desert boundaries. Eastern bounderies are represented by Ae, Be & Ee whereas western bowdaries are represented by Aw,Bw,Cw,Dw,Ew.

In the present work, the clay or the second group is termed desert clay.This is to dirrerentate it from the alluvial Nile clay and to emphasize the effect of arid climate conditions of the region.

3. EXPERIMENTAL WORK

The program or study of the present work included chemical analysis and Geotechnical laboratory testing of soil samples.Complete chemical analysis was carried out on all soil samples for the determination of chemical constituents. Geotechnical laboratory testing was done for the determination or grain size distribution, bulk unit weight, initial moisture content, Atterberg limits and specific gravity. Furthermore, X-ray dirrerection analysis was performed on soil samples for the determination of predominant clay minerals.

All the results of chemical, engineering and mineralogical properties are summarized in Table (1). They represent soil deposits from The Nile Valley and from eastern and western desert boundaries.

4. RESULTS AND DISCUSSION

From the obtained results we observ the following:

a. Comparison of values of silica/ sesquioxide ratio of all samples in all

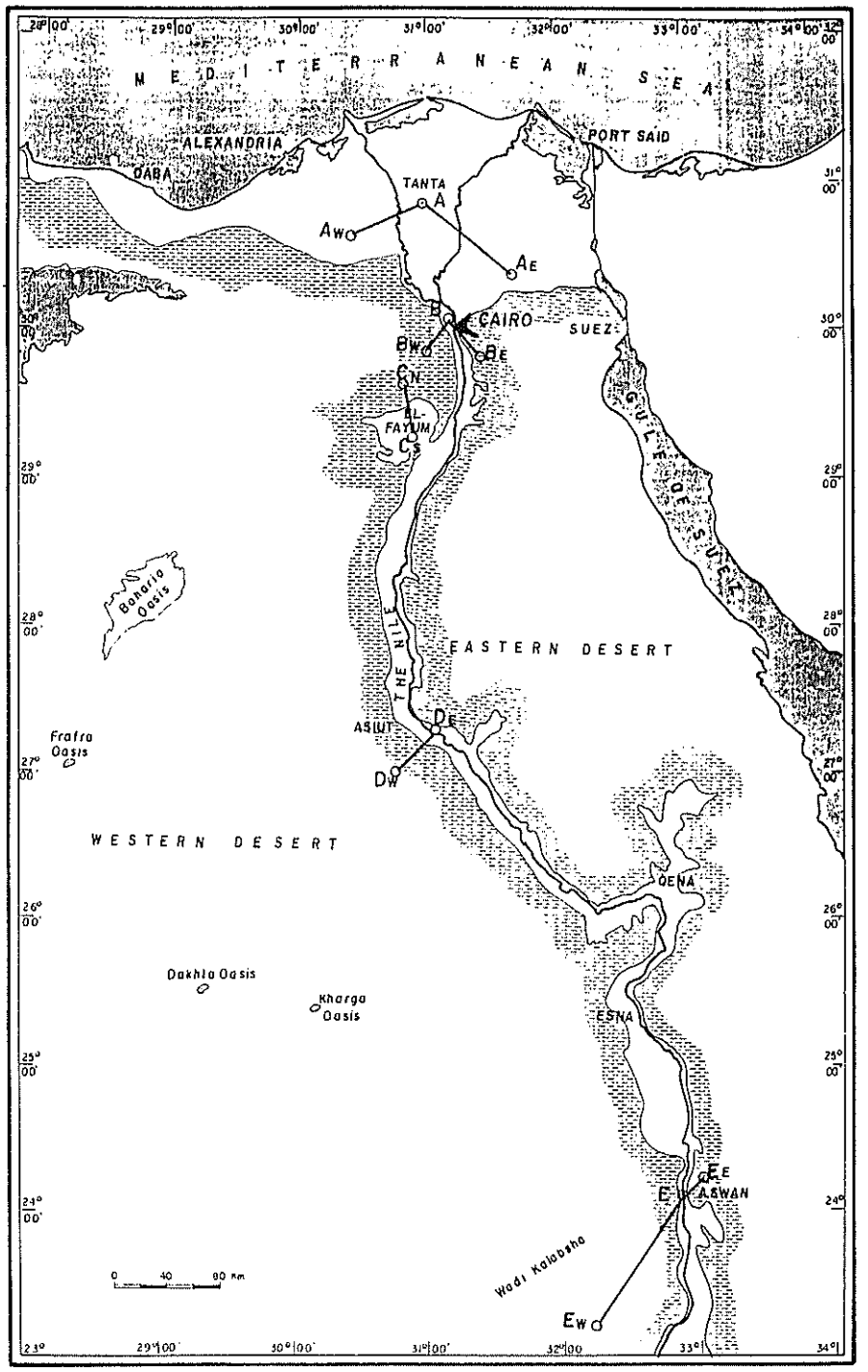

Figure 1 Location map

Table I
Geological, Mineralogical, Chemical and Geotechnical Properties of Investigated Soil

Location and Section	Type Classification		Geological, Mineralogical & Chemical Propertion			Geotechnical Properties				
			Age	Predminants Clay Mls	R	ω	γ_d KN/m3	S_r %	W_L	I_p
Nile Delta (A)	Nile Clay	A	Holecence	M-I-K	1.52	34.	15.7	100	67.	32
	Eastern Boundary Clay	Ae	Pliestocene	M-K-I	1.90	5.	19.5	35	72	35
	Western Boundary Clay	Aw	Pliestocene	I-M-I	1.49	8.	18.5	47	67	30
Cairo (B)	Nile Clay	B	Holecence	M-I-K	1.54	32.	15.	100	60	29
	Eastern Boundary Clay	Be	Eocene	M-K-I	2.40	4.5	19.	28	82	35
	Western Boundary Clay	Bw	Eocene	K-M-I	1.60	9.5	18.	51	70	30
Fayoum (C)	Nile Clay	C	Recent	M-I-K	1.50	33.	16.	100	65	31
	Western Boundary Clay	Cw	Eocene	M-I-I	1.70	8.0	19.5	37	92	45
Assiut (D)	Nile Clay	D	Recent	M-I-K	1.50	3.1	15.5	100	52	22
	Western Boundary Clay	Dw	Eocene	M-K-I	1.75	9.0	20.	69	75	32
Aswan (E)	Nile Clay	E,	Pliestocene	M-I-K	1.50	29.5	14.8	97	62	30
	Eastern Boundary Clay	Ee	Cretaceous	M-K-I	2.20	3.5	21.	33	92	40
	Western Boundary Clay	Ew	Cretaceous	K-M-I	1.30	10.0	19.	62.5	72	37

* . The depth of the sample ranges between: 2-3m
M= . Montmorillonite
K= Kaolinite
I= Illite
R= Silica/sesquioxide ratio= $\frac{Sio\ 2}{Fe2O3 + A12O3}$

studied sections indicate that this ratio is generally higher in case of desert clay compared to Nile Clay. The differences of the silica/sesquioxide ratio or these two groups of soils can be attributed to the origin of deposit. It may confirm that the Nile clay is most probably transported from the tropical zone in Abyssinia. Whereas the desert clay of the boundaries is old geological formations or Egypt.

b. The values or silica/sesquioxide ratio of the western desert clay are lower than those of the eastern desert clay as well as the predominance of kaolinite mineral in the western desert clay compared to the eastern desert clay. This can be due to the difference in morphological conditions between the western desert and the eastern desert.

c. At the site of Wadi kalabsha in western deset of Asswan, the value of the silica/sesquioxide ratio of soil on the western bowndaries is 1.30 (a value very close to the Nile clay). This low value can be explained in the light of geological history which attributed to sedimentary environment. Attia, 1955 indicated that the deposition of the soil in the western boundary at Asswan had taken place in lagoon and delta conditions. The predominance of kaolinite mineral in the clayey deposit or the Aswan western boundary confirm this point.

d. Physical and geotechnical properties of tested soils indicated:
1) a relatively high liquid limit, high plasticity, high dry unit weight of the desert clay compared to Nile clay.
2) a relatively high water content, high degree of saturation of the Nile clay compared to the desert clay.

5. CONCLUSIONS

1. The present study consisted of various sections representing the Nile Valley and its bounderies to confirm the effect of chemical weathering on different soil charactaristics.

2. Egyptian clayey soils were classified into two groups the first, denoted Nile clay represent Nile delta and its valley and the second denoted desert clay represent the boundaries.

3. Comparison between the silica/sesquioxide ratio of the two groups indicated that this ratio is generally higner in case or desert clays compared to the Nile clays except the western desert in Aswan location at Wadi Kalabsha which was on ancient delta during the createceous geological age.

4. For soil formation in Egypt, the silica/sesquioxide ratio can be an indicator or soil genesis and enviromental setting. It can differntiate between soil transported by the Nile from abayssinia and other formations.

5. The silica/sesquioxid ratio are relatively low in the western clayey desert compared to the eastern clayey desert. Also the kaolinite clay mineral is the predominant clay mineral in western clayey desert compared to eastern clayey desert.

6. Chemical weathering modified physical and geotechnical properties significantly.

6. REFERENCES

Attia, M. I. (1954). Deposits in the Nile Valley and the delta. Geol. Survey Egypt, Cairo, pp. 3-7.

Attia, M.I.(1955). Topography, geology and iron-one deposits of the district east of Aswan.Geol.Survey Egypt. Cairo, pp. 78-80

Correia, J. A. (1967). Some results or chemical analysis of laterites. 4th Reg. conf. for African on Soil Mech. and Found. Engng, Cape Town, pp. 37-51.

El-Sohby,M.A.;Mazan,S.O.and Aboushook, M.I. (1988). Some observations on the silica/ sesquioxides ratio of two groups of Egyptian soils. Proc. of the 2nd Int. conf. on Geomechanics in Tropical soils, Singapore, volume 2,pp. 521-524.

Gidigasu,M.D. (1971).The importance of soil genesis in engineering classification of Ghana soils. Engineering Geology, Vol. 5, pp. 117-161.

Madu, R. M. (1975). Some Nigerian residual soils their characteristics and relative road building properties on a group basis. 6th Reg. conf. for African on soil Mech. and Found. Engng. Durban. south Africa. pp. 121-139.

Maignion,(1966).Compte rendue de rechercnes sur les laterites. UNESCO. Paris.

Massad, F., Samara, V. and Barros, J.M.C. (1985). Engineering properties of two layers of lateritic soils from SAO paulo city, Brazil. 1st Int conf.on Geomechanics in Tropical.Lateritic and Saprolitic soils, Brazil, Vol. 1, pp. 331-343.

Novias Ferreira, H.(1985). Characterization, identification and classification of tropical lateritic and saprofication of tropical lateritic and saprolitic for geotecnical purposes. 1st conf. on Geomechanics in tropical. Lateritic saprofitic soils, Brazil, Vol. 3, pp. 139-170.

Tuncer, E. R., and Lohnes,R. A. (1977). an engineering classification for certain basalt derived lateritic soils. Engineering Geology,Vol.11,pp. 319-339.

Evaluation of Tertiary Age Gravel Deposits Using Plate Load Tests

M.C.ERVIN
B.E. (Civil), M.Eng.Sc., F.I.E.Aust.
Associate, Golder Associates Pty Ltd
M. KURZEME
B.E. (Civil), Ph.D., M.I.E.Aust.
Principal, Golder Associates Pty Ltd

SUMMARY Plate load testing has been carried out to assess settlement characteristics of a gravel deposit present beneath the footings of an existing buidling. Applied stresses of up to 1500 kPa were applied, with Youngs Moduli of in excess of 300 MPa measured. As a result of these tests, settlements due to increased footing loads resulting from refurbishment of the building could be confidently predicted.

1. INTRODUCTION

Planning for refurbishment of an eight storey building, with a single basement level, indicated the applied loads on the existing footings would increase by up to about 30 percent. The resulting applied bearing pressure would exceed the design value adopted when the building was constructed. As a consequence additional geotechnical investigations were undertaken.

The original foundation investigation for the building indicated that its footings would be expected to found on weathered siltstone. However, the subsequent investigation undertaken for the refurbishment showed that some footings were founded on several metres of gravelly soil. The response of these soils under the increased loads was uncertain and further more detailed testing was ordered.

Plate load testing was considered to be the most appropriate method of assessing the deformation properties of the gravelly soils. These tests were performed at several locations within the basement of the building and the test results were used to evaluate the strength and Youngs Modulus of the gravelly soils.

It was concluded that the ultimate bearing capacity of the gravelly soil was in excess of the maximum pressure of 1500 kPa applied during the plate load tests. For estimating the likely settlement of the footings under the effect of the proposed increase in loads, a design Youngs Modulus of 300 MPa was adopted for both the gravelly soil and the weathered siltstone.

2. STRUCTURAL CONSIDERATIONS

The existing building is an eight storey reinforced concrete structure with a single basement level. The columns are located on an 8.5 m by 8.5 m grid, and are supported on pad footings and an edge beam. The pad footings are typically about three metres square and are founded about 1.3 m below the basement floor slab.

The footings were designed using an allowable bearing pressure of 500 kPa for pad footings and 400 kPa for strip footings, when founded on highly weathered siltstone. The bearing pressures imposed by the footings, under the original building loads, were estimated to be in the range of 360 kPa to 470 kPa. After the refurbishment the imposed bearing pressures are expected to be in the range of 420 kPa to 625 kPa. The highest pressure is 25% above the previous design allowable bearing pressure. The increased footings loads were expected to cause settlement of the affected footings, resulting in differential settlement between these footings and other footings not subjected to an increase in load. This differential settlement would impose additional movements and shears in the existing superstructure, the magnitude of which would be dependent on the magnitude of the settlements. It therefore was important the settlement characteristics of the founding soils were established.

3. FOUNDATION INVESTIGATION

The foundation investigation performed before construction of the building involved drilling of four boreholes to depths ranging from 7.3 m to 12.5 m below street level. The locations of these boreholes is shown on Figure 1. The boreholes were advanced by continuous flight solid augers through the soils, and by continuous diamond coring through the weathered rock. Standard penetration tests were performed in the soils.

The subsequent investigation for the refurbishment involved drilling of nine boreholes, and the excavation of four test pits, through the basement floor slab. The locations of these boreholes and the test pits are also shown in Figure 1.

The boreholes were advanced to depths ranging from 1.55 to 7.65 m below the basement floor level, which is about 3 m below street level. It was expected from the design drawings that all footings would be founded on weathered siltstone, with the difference in depth between the design and actual founding levels made up in low strength concrete. Consequently, continuous coring was adopted as the drilling method. The first three boreholes were drilled through the footings, and revealed that at these locations the footings were founded on clayey gravels and gravelly clays. Other drilling methods were then attempted, but it was not possible to obtain undisturbed samples of these materials, or to evaluate their strength by downhole testing. Core recovery in the underlying variably weathered mudstone was also difficult due to the highly fractured nature of this rock. Varying thicknesses (up to four metres) of clayey gravels and gravelly clays were encountered in four of the other six boreholes, which were drilled through the basement floor slab. It therefore was unclear how many of the footings were founding on mudstone and how many on these soils.

Four test pits were then excavated to obtain a better assessment of the clayey gravels and gravelly clays, than was possible from the boreholes. The pits were excavated adjacent to pad or strip footings, at the locations shown in Figure 1, to establish the founding depth of the footings.

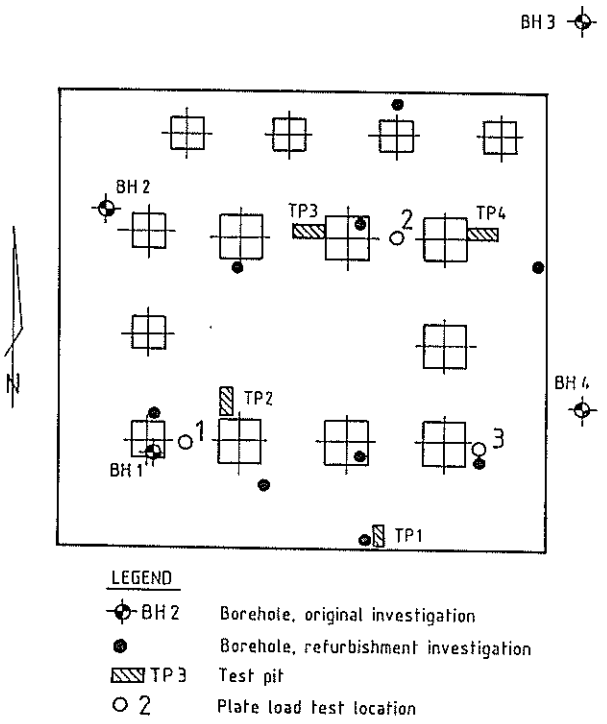

Figure 1 Site Plan

4. FOUNDATION CONDITIONS

The sequence encountered below the basement floor slab generally consisted of a minor thickness of fill immediately below the slab, over dense clayey sand, and clayey gravel, or very stiff and hard gravelly clay, overlying extremely weathered and highly weathered mudstone. The depth to the mudstone ranged from zero to 5.7 m below the basement floor level. The depth was generally greater along the north south axis of the building reducing to zero along the eastern and western sides of the building.

The geological mapsheet of the area indicates that the general area of the site is located on Silurian Age sedimentary rock, consisting of calcareous shale, limestone, sandstone and tuff. This is overlain in parts by Tertiary age gravels and sands. The soil and rock encountered in the boreholes was consistent with the geological map indications.

The footings were exposed to the founding level in three of the test pits. The strip footing exposed in Test Pit 1 was founded on clayey gravel at a depth of 1.25 m below the basement floor level. The pad footing in Test Pit 2 was founded on extremely weathered mudstone at a depth of 1.25 m, and the pad footing in Test Pit 3 was founded on gravelly clay at a depth of 1.30 m. It was not possible to obtain undisturbed samples of these founding materials using conventional sampling methods, and hence it was not possible to evaluate the strength or compressiblity of these materials by laboratory testing. In-situ testing within the boreholes using a pressuremeter also was not possible, as the boreholes could not be drilled in the gravelly materials to the close tolerances necessary for pressuremeter testing. Hence it was concluded that the only practical means of quantitatively evaluating the strength and compressiblity of the gravelly soils was by plate load testing in the bottom of the test pits.

5. METHOD OF PLATE LOAD TESTING

When planning the plate load testing it was considered that the tests should be carried out up to a pressure equal to three times the original design bearing pressure of 500 kPa to allow a check on whether a factor of safety of 3 on bearing capacity was exceeded. A loading system capable of allowing an applied pressure of 1500 kPa on a 500 mm diameter plate was therefore proposed. This also allowed the pressure-displacement behaviour of the founding soils to be monitored well beyond the planned increase in applied bearing pressure.

Three test locations were selected, based upon the variability in the founding conditions observed during the geotechnical investigation. The test locations are shown on Figure 1. The basis for selecting these locations was:-

- Test Location 1
  Extremely to highly weathered mudstone present at founding depth. Footing response on this material expected to be different to that on gravels. Desirable to have data on the deformation characteristics of the mudstone, to allow size effects to be considered when extrapolating from the 500 mm dia. plate to the prototype footings (up to 3.3 m square). Testing carried out at founding level, 1.35 metres below existing basement floor level.

- Test Location 2
  Founding soils predominantly gravelly clay/clayey gravel. Testing of this material at both founding level and at about two metres depth carried out. Tests at two levels proposed to allow any marked change in property with increasing depth to be observed, and therefore included in the subsequent analysis.

- Test Location 3
  The borehole near this test location indicated sandy clay soil present at founding depth. As this material was judged likely to have differing engineering properties to the gravelly clay it was considered prudent to test this material also. Testing at two levels, as for Test Location 2 was carried out.

Space restrictions within the basement precluded providing the required 300 kN reaction with kentledge, and ground anchors would have been difficult to install with the available headspace. It therefore was decided to use the existing building superstructure for reaction.

The design, fabrication and installation of the reaction system was arranged by the Structural Consultant. The adopted system comprised two 610UB101 beams spanning between column locations, then propped against the floor slab above, at the column location. The beams were supported about 600 mm above basement floor level, and a jacking column then suspended from beneath these beams, and extending down to the level of the top of the proposed jack. This arrangement is schematically shown on Figure 2.

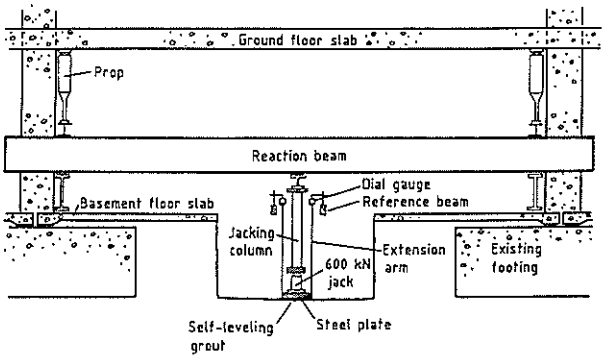

Figure 2 Plate Load Testing Arrangement

Three 25 mm thick steel plates were used to transfer the load to the soil. These plates were successively 500, 400 and 300 mm in diameter. Where necessary a 175 mm diameter spacer plate was also used.

Prior to assembling the test plates and jack, the test area surface was excavated to the required depth and made as level as practical. To provide a smooth and level surface on which to seat the 500 mm diameter plate, a thin layer of self levelling grout, 505 mm in diameter, was cast on the ground surface and allowed to harden prior to the test being carried out. The use of this self levelling grout proved to be extremely convenient, and allowed the subsequent testing to be successfully carried out without apparent seating errors. The grout used was HILTI CA1c80F, a fast setting two part epoxy. However, in the cool temperature prevailing in the basement of the building, the grout still had to be warmed by radiators and blow heaters to accelerate the setting. Up to about 4 hours was required. However, the resulting prepared surface was smooth and flat, making subsequent set up of the testing equipment relatively easy.

Vertical displacement during loading was measured by dial indicator gauges, mounted on simply supported timber reference beams, 3.6 m long. Measurement was made at four locations equally spaced around the lowest plate. To facilitate measurement at floor surface level extension rods were mounted the plate. Figure 2 also shows this arrangement.

The loading sequence adopted for the tests was as follows.

Load Cycle 1:- 0 to 165 kPa to 0. Assumed to be a seating cycle, with zero displacement for the test taken as that on completion of this cycle.

Load Cycle 2:- 0 to 500 kPa to 165 kPa. This was intended to simulate the initial loading of the building footings. The applied pressure of 500 kPa held for 10 minutes to observe any creep.

Load Cycle 3:- 165 kPa to 665 kPa to 165 kPa. This provided data on the anticipated response of the footings under increased load. The applied pressure of 665 kPa was held for 30 minutes and creep settlement observed.

Load Cycle 4:- 165 kPa to 1500 kPa to 165 kPa. To obtain the pressure-displacement behaviour beyond the anticipated design pressure and to allow an assessment of the available bearing capacity of the materials being tested.

During each load cycle, the pressures were incrementally applied using a calibrated hand operated jack.

6. TEST RESULTS

The results of the tests are summarised in Table 1, with the results of tests 2A and 2B also presented graphically as Figure 3. These two test results are typical of the other three, and illustrate how the use of the high strength self levelling grout almost eliminated seating effects.

Upon completion of each test, a sample of the material from immediately beneath the test location was taken. The results of laboratory index testing carried out on thee samples are presented in Table 2.

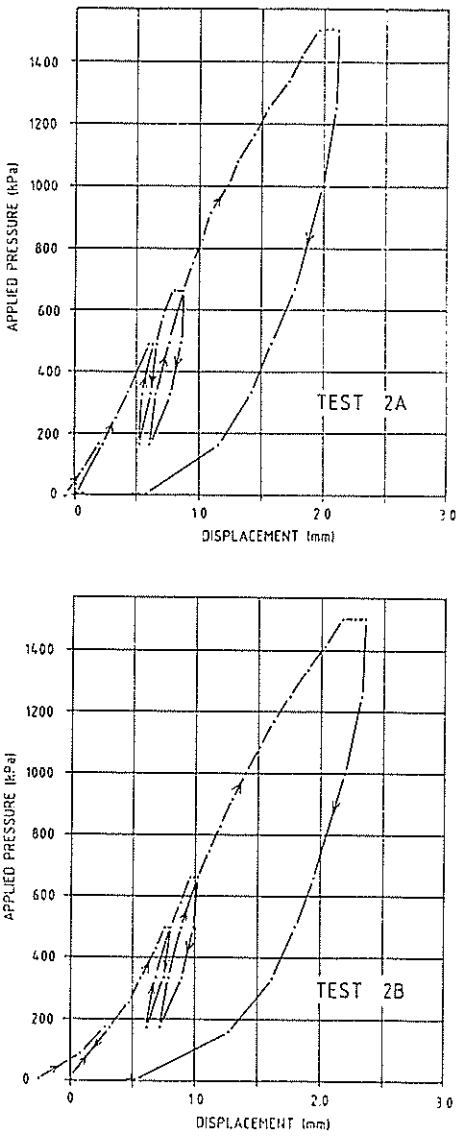

Figure 3 Pressure-Displacement Response

TABLE 1

RESULTS OF PLATE LOAD TESTS

Test No.	1	2A	2B	3A	3B
Depth below basement floor (m)	1.38	1.37	2.01	1.36	2.02
Initial Displacement at 500 kPa (mm)	0.50	0.60	0.78	0.84	0.72
665 kPa (mm)	0.70	0.82	0.98	1.05	0.85
1500 kPa (mm)	1.76	1.97	2.16	2.34	1.93
Creep over 30 mins @ 665 kPa (mm)	0.08	0.05	0.05	0.05	0.01
Creep over 10 mins @ 1500 kPa (mm)	0.13	0.15	0.18	0.16	0.16

TABLE 2

LABORATORY TEST RESULTS

Test No.	1	2A	2B	3A	3B
Particle Size					
% passing 75 mm	-	94	100	100	100
% passing 19 mm	-	59	90	91	99
% passing 2.36 mm	-	34	77	50	93
% passing 75 μm	-	22	17	12	18
Atterberg Limits					
Liquid Limit	-	34	40	36	31
Plasticity Index	-	18	25	20	17
Moisture Content	17.4	9.4	9.5	8.8	8.6
Material Classification	HW Siltstone	Clayey Gravel (GC)	Clayey Gravelly Sand (SC)	Clayey Sandy Gravel (GC)	Clayey Sand (SC)

These test data have been used to calculate the Youngs Modulus of the founding materials, assuming a rigid circular plate acting on the surface of a semi-infinite elastic material of constant modulus (Perloff 1975). However, the plate load testing was actually performed within a pit, about 1.5 m wide, rather than on the surface. Approximate solutions for circular plates acting below the surface (Pells, 1983), indicate that the "true" Youngs Modulus is unlikely to differ by more than 10 per cent from the values calculated by the adopted method.

The Youngs Modulus calculated for several of the load cycles in each of the tests, and over pressure ranges relevant to the building performance, are presented in Table 3.

To check on long term creep effects, the displacement observed whilst the applied pressure was held constant for 30 minutes at 665 kPa was plotted against log of time, a common means of evaluating creep. For the tests carried out, the creep rate with respect to log of time was found to be decreasing and after about 15 minutes creep had virtually ceased. It therefore was concluded long term creep effects will be small and can be satisfactorily accounted for by adoption of secant modulus values.

TABLE 3

YOUNG'S MODULUS VALUES

Load Cycle	Pressure Range (kPa)	Youngs Modulus (MPa) Test 1	Test 2A	Test 2B	Test 3A	Test 3B
2	165-500	360	315	285	250	320
3	165-500	1530	875	585	645	585
3+	500-665	560	360	380	380	470
3*	500-665	320	280	290	290	470
4	330-665	875	535	510	470	525

\+ Initial loading modulus value
* Secant Modulus value

7. ESTIMATE OF FOOTING SETTLEMENT

Each of the tests indicated similar deformation properties for the various materials tested. The test results also indicated the ultimate bearing capacity of the soils and weathered rock encountered at this site appears to be well in excess of 1500 kPa for the adopted 500 mm dia. loaded area.

Direct application of the results of the plate load tests to an elastic analysis of predicted footing movement was considered appropriate. For design purposes, a Youngs Modulus of 300 MPa was adopted, and considered to be uniform with depth. Using his value, it was predicted the maximum likely additional settlement of any footing under the refurbishment loads would be about 2 mm.

Because this predicted settlement was small, no attempt was made to refine the estimate to allow for probable increased stiffness with depth, due to reduced weathering of the basement rock.

8. CONCLUSIONS

Investigation of gravelly soils to obtain strength and compressibility data is difficult using routinely adopted methods of investigation. As a consequence, conservative bearing values and estimates of settlement are frequently recommended. At this site it was necessary to be able to predict with confidence the likely settlement under planned increased in load of existing footings founded on up to several metres of predominantly gravelly soil.

Plate load testing was successfully used to obtain deformation properties of these gravelly soils. This testing had to be performed within the existing basement of the building and using relatively high applied loads. The use of the existing building as reaction for the test, and the use of the fast setting self levelling grout to prepare the test surface, are considered to have been significant factors in allowing the tests to be successfully performed.

The tests showed the Tertiary Age gravel deposits present at the site are of low compressiblity, similar to that of highly weathered siltstone.

REFERENCES

Pells, P.J.N. (1983), "Plate Load Tests on Soil and Rock", in In-Situ Testing for Geotechnical Investigations, Ed. Ervin, M.C., pp 73-86, Balkema, Rotterdam.

Perloff, W.H. (1975), "Pressure Distribution and Settlement", in Foundation Engineering Handbook, Ed. Winterkorn & Fang, p 150, Van Nostrand Reinhold.

Evaluation of Swelling of an Expansive Clay Shale from Mae Moh, Thailand

B. INDRARATNA
B.Sc.(Hons), A.C.G.I., M.Sc.(London), D.I.C., Ph.D.(Alberta)
Lecturer, University of Wollongong, NSW, Australia
M.R.B. HUSIN
B.Sc.(Wales), M.Eng.(AIT)
Formerly Graduate Student, Asian Institute of Technology, Bangkok, Thailand

SUMMARY The instability problems and some failures of diversion channel linings in Nothern Thailand have been caused by the presence of expansive clay shales. The clay shale found in the vicinity of the Mae Moh diversion channel is a fine-grained, fissured material. Its considerable clay fraction is responsible for adverse engineering properties such as swelling, slaking, creep and strain-weakening, all of which contribute to the progressive reduction in strength. The purpose of the investigation conducted on the Mae Moh diversion channel was to identify and classify the expansive nature of the clay shale. A discussion of various methods in predicting the swell potential of an expansive clay shale is presented, with particular reference to the oedometer based results.

1. INTRODUCTION

This paper describes about the results of some laboratory tests conducted on block samples of an expansive clay shale obtained from the right bank of the Mae Moh diversion channel in Thailand. The swelling nature of this clay shale presents slope stability problems along the diversion channel. Several types of tests were conducted to investigate the properties of the clay shale. The tests were conducted primarily using the oedometer, the triaxial apparatus, the hydraulically pressurized consolidometer and the pressure membrane apparatus. Three different types of samples, namely the undisturbed, the remoulded and the pressurized samples were used. This was done to study the change in properties with regards to the different methods of specimen preparation in the laboratory condition. Only the oedometer results are discussed within the scope of this paper.

2. PROPERTIES OF MATERIAL

2.1 Particle Size Distribution

The particle size distribution of the tested clay shale is shown in Fig. 1. The silt and clay fractions are 50% and 20% by weight, respectively. The clay size fraction is 30%, which makes the activity of the crushed (pulverized) clay in the order of 0.6, according to the definition proposed by Skempton (1953). His suggestion indicates that this clay shale was probably subjected to normal climatic weathering and deposited in fresh water with illite and kaolinite as major fine grained minerals. The subsequent sedimentary process has resulted in the genesis of clay shale.

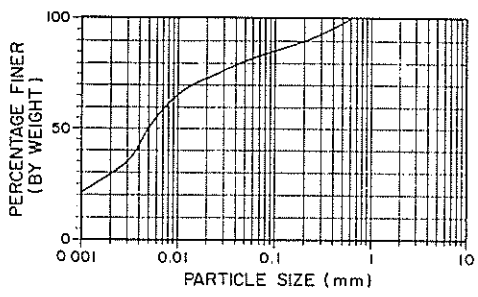

Figure 1 Particle size distribution of clay shale

2.2 Optical Microscope Test

The Becke line test showed that the fringe blur of some minerals moves out indicating that the refractive index is less than that of Canada Balsam (1.537). Birefringence was moderate and the relief was low. This observation suggests the presence of montmorillonite in the smectite group. The value between the maximum and minimum vibrational directions of montmorillonite $(n_\mu - n_\alpha)$ was 0.021. The Becke Line test also showed that the fringe blur moved in indicating that the refractive index was more than that of the Canada Balsam. This further suggested the presence of illite which is the predominant mineral component of the clay shale.

According to Jiang and Peacor (1990) mixed layers of illite/smectite can occur in a variety of weathering, sedimentary, digenetic, metamorphic and hydrothermal environments. They also confirmed the prograde transition of illite to smectite during burial digenesis and very low grade metamorphism and alteration associated with hydrothermal activity. These observations suggest that this transformation may have resulted in this particular clay shale becoming more expansive with age.

3. TEST RESULTS

3.1 Free Swell Test

The free swell of this clay shale was 1.8. According to Sritharan & Rao (1988) this can be classified as a clay of medium expansivity. It is of importance to note that the free swell procedure is not designed to provide the actual magnitude of swelling under field conditions, but for the purpose of identification only. The free swell test is primarily introduced to gauge the expansivity of the clay fraction rather than providing a specific quantification.

3.2 Double Oedometer (DB) Test

The upper bound for the swelling pressure determined from the Double Oedometer test is approximately 1000 kPa (Fig. 2). The initial void ratio when both specimens were at 25 kPa loading was higher of the saturated sample (0.66) than of the dry sample (0.57). Figure 3 shows that the final compression is about 50% higher for the specimen that was loaded in the wet state than the specimen which

was loaded in the dry state. The compression was found to be about the same (proportional ratio) for each stage of loading. The samples tested were almost identical in terms of initial dry density (16.5 kN/m^3), initial moisture content (14%) as well as the initial degree of saturation (62%).

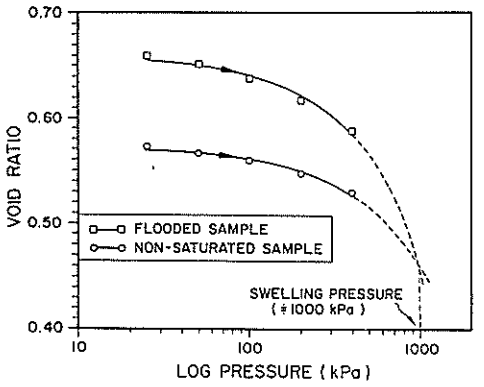

Figure 2 Variation of void ratio with pressure from double oedometer test

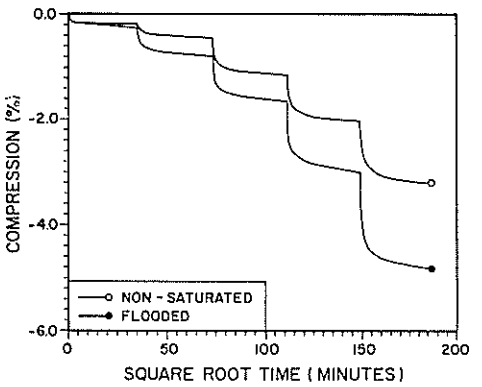

Figure 3 Variation of compression with square root time from double oedometer test

The swelling pressure from double oedometer test was found to be higher than that determined from the other oedometer methods. This is due to the fact that the pressure taken as the swelling pressure is not that which is required to bring the sample to its original height as in the swell consolidation and different pressures oedometer tests. Instead, it is the pressure required to bring the sample to its height after being compressed in the dry state by a pressure equal to the swelling pressure. Weston (1980) stated that the main drawback of this test is that the method is based on the assumption that the swell is independent of the stress or moisture path. According to his findings, the measured swell in the laboratory is about twice that found in the field.

3.3 Swell Consolidation Oedometer (SC) Test

The swelling pressure determined from this test was found to be approximately 400 kPa (Fig. 4). The maximum percentage swelling recorded when the sample was placed under a light load of 6.25 kPa was 0.48%. From the consolidation curve section it is observed that the sample is brought back to a height less than its original height under a load of 400 kPa. The initial values of void ratio, moisture content and degree of saturation are 0.58, 14% and 63%, respectively.

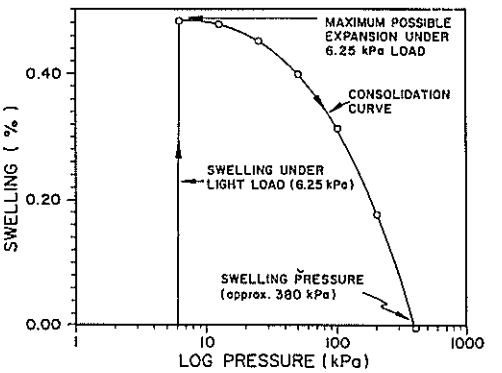

Figure 4 Variation of swelling with log pressure from swell consolidation oedometer test

This method simulates the condition in which the clay shale is allowed to absorb water and swell first before loading. This might not be a good representation of the actual conditions in the Mae Moh diversion channel before it comes into service. By swelling the clay shale before loading, it instigated a higher pressure required to compress the pre-swelled sample than the samples in the Different Pressures Oedometer Method. The higher load required to bring the specimen to its original height can be attributed to the additional energy needed to expel the absorbed water

3.4 Different Pressures Oedometer Method (DPM)

Figure 5 illustrates that the swelling pressure determined from this test is approximately 350 kPa, which is close to that determined by the swell consolidation test. The maximum swelling recorded when the samples were placed under loads of 6.25 kPa, 50 kPa and 200 kPa were 0.48%, 0.34% and 0.13%, respectively, whereas at a load of 400 kPa the sample was compressed by 0.03% of its original height. From the constructed curve joining all the maximum swell positions on the consolidation curve section, it is clear that the sample is brought back to a height less than its original height under a load of 400 kPa.

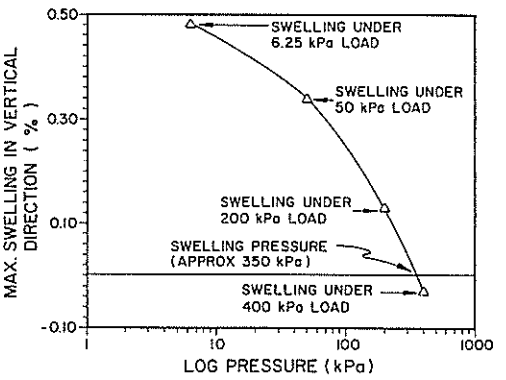

Figure 5 Results of different pressures oedometer method

This method simulates the condition in which the clay shale is loaded before it is allowed to absorb water and swell. This represents more closely the actual conditions in the Mae Moh diversion channel before it comes into service. By loading the clay shale before it is allowed to swell, a lower pressure is required to compress the samples in

contrast to the case of swell consolidation oedometer test. Therefore, this test has an advantage over the swell consolidation and double oedometer tests for the determination of swelling pressure. The loading-wetting events in this method follow the same sequence as in the field, where the loads are first applied to the unsaturated soil undergoing compression before it comes in contact with water. This test is carried out on the assumption that all the samples tested are identical.

3.5 Huder Amberg Oedometer (HA) Test

The swelling pressure determined from Huder-Amberg oedometer test is approximately 350 kPa (Fig. 6). The ability of the sample to swell under a load of 400 kPa suggests that the swelling pressure might be greater than 400 kPa, but the test curves intersect at a lower pressure and that this value is considered to be the swelling pressure. This test has an advantage because it takes into consideration the disturbance of the soil and tries to normalize the differences during the introduction of a second loading cycle. Figure 6 clearly indicates that there is a certain degree of disturbance from the first and second loading. The unloading curves show that the initial disturbance was compensated for after the second loading, judging from the similarity in void ratios at the same levels of loading.

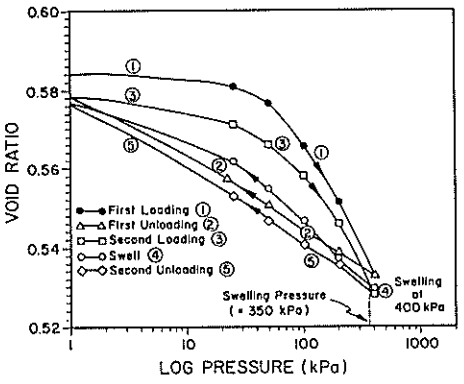

Figure 6 Variation of void ratio with pressure from Huder-Amberg oedometer test method

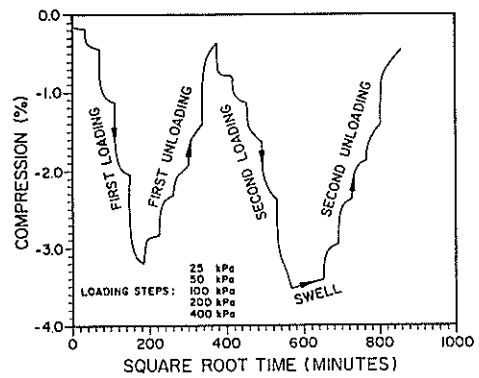

Figure 7 Variation of compression with square root time from Huder-Amberg oedometer test method

Figure 7 illustrates the compression induced by different loading and unloading conditions. The maximum swelling recorded when the sample was placed under a maximum load of 400 kPa was 0.112%. For the Huder-Amberg test, the values of the initial void ratio, moisture content and degree of saturation are 0.58, 14% and 61%, respectively. Witke (1980), in his study of tunnels situated in gypsum keuper (a swelling rock), concluded that the Huder-Amberg oedometer test results proved useful and gave reliable swelling pressure estimations. He also suggested that this test can be conducted reliably for the determination of swelling pressure. The final unloading curve in Fig. 7 can be approximated to a straight line in the semi-logarithmic plot and this result is in accordance with the results discussed by Witke (1980).

3.6 Variable Density Oedometer Test

The void ratios of samples compacted at different initial dry densities under specific loads is illustrated in Fig. 8. For the sample compacted at an initial dry density of 13.5 kN/m^3 (R1), the final void ratio (0.935) was lower than the initial void ratio (0.941). However, the final void ratios of the samples R2, R3, R4 and R5 indicate final void ratios greater than their initial void ratios. This is a result of the increased initial dry densities for samples R2-R5. Figure 9 shows that the swell under a load of 25 kPa is generally higher for samples compacted at a higher initial dry density. As expected, samples with lower initial dry densities are more compressive than those compacted at higher initial dry densities. The compression index, C_c, appears to decrease with the increasing initial dry density. The swelling index, C_s, of the sample R1 (lowest dry density) is quite high (0.118), while that of the other samples is rather consistent and converges to approximately 0.027. The magnitudes of C_c and C_s were based on the void ratios corresponding to the loading pressures of 200 kPa and 400 kPa for each test.

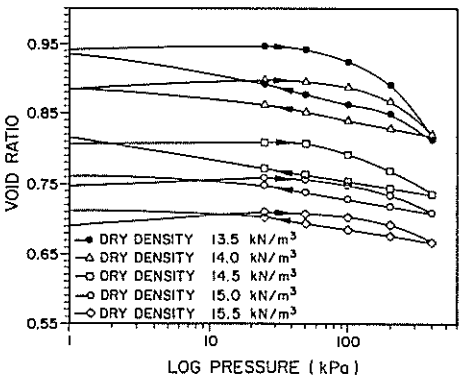

Figure 8 Results of variable density oedometer test

The test on remoulded clay shale was carried out to determine the variation of the compression index, swell index and the ratio C_s/C_c for the samples with different initial dry densities. The samples were initially saturated at a constant volume in order to overcome the swelling tendency of remoulded samples. The shape of the rebound curve is related to the unbending and slippage at particle contacts (Cepeda, 1987). The ratio C_s/C_c (0.19-0.46) shows that the material is a relatively active clay. Furthermore, the test results obtained for the Mae

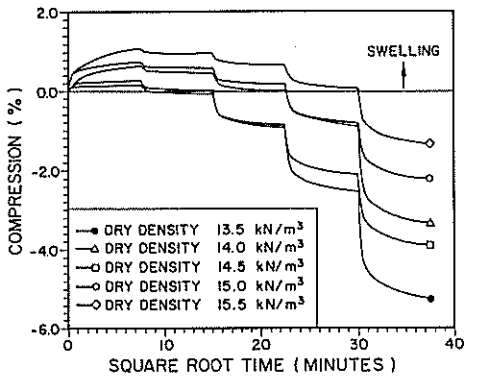

Figure 9 Variation of compression with square root time from variable density oedometer test

Moh clay shale are in accordance with the findings of Cepeda (1987) who has proposed the relationship: C_s = 0.0008 to 0.003 LL for reconstituted as well as fresh shale. This test may be used to simulate the field conditions whereby expansion could be quantified for the case when the cementation of the clay shale was suddenly destroyed, and saturation allowed under heavy load prior to subsequent unloading (Husin, 1991).

3.7 Pressure Membrane Oedometer Test

The variation of void ratios with applied pressure for samples remoulded at different air pressures is shown in Fig. 10. The initial void ratio of the sample subjected to a pressure of 300 kPa (3 bars) was greater than that of the sample subjected to a pressure of 1200 kPa (12 bars). The final void ratio of the samples ranges from 0.97 to 1.03. The range of ultimate compression was between 8.7% to 10.7% as shown in Fig. 11. The compression index, C_c, for all the specimens is approximately 0.26. The swelling index, C_s, is approximately 0.032 for the samples subjected to applied pressures of 300 kPa and 600 kPa and is 0.017 for the sample subjected to an applied pressure of 1200 kPa. The ratio C_s/C_c is found to be about 0.12 for the samples pressurized at 300 kPa and 600 kPa and 0.07 for the sample subjected to a pressure of 1200 kPa. The test showed that the compressibility may not be directly related to the suction $(u_a - u_w)$ at moderate applied pressures. The compression indices (0.26 and 0.28) and swelling indices (0.030 and 0.034) are about the same for the samples pressurized at 300 kPa and 600 kPa, respectively. While the compression index for the sample pressurized at 1200 kPa is similar to that of the samples pressurized at lower air pressures. Its swelling index seems to be smaller (0.017). This indicates that the swelling potential decreases as the applied air pressure, hence suction head increases. The ratio of C_s/C_c ranges from 0.07 to 0.12.

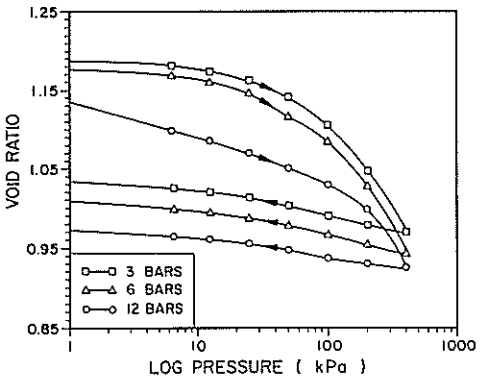

Figure 10 Results of oedometer test on samples prepared in the pressure membrane apparatus

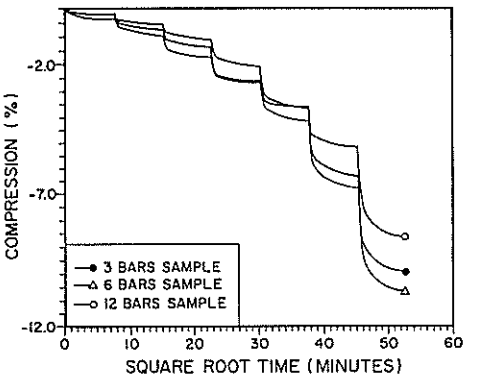

Figure 11 Variation of compression with square root time from pressure membrane test

4. RELATIONSHIP BETWEEN SWELL POTENTIAL AND SOIL PROPERTIES

A large number of undisturbed samples were collected and their free swelling behaviour was evaluated. These tests were conducted with the aid of the Electricity Generating Authority of Thailand. The Atterberg limits of the clay shale material and the particle size distribution (clay %) were considered as the basic governing properties. The plasticity index (PI) and the activity of the clay shale were determined for this wide array of undisturbed specimens. Figure 12 represents % swell against the plasticity index. Although the results indicate significant scatter, two relationships (linear and non-linear) based on regression analysis can be proposed, where % swell increases with the plasticity index. Figure 13 illustrates the variation of clay shale activity with the % clay size, according to the USBR swell classification chart. The Mae Moh clay shale indicates % swell mainly in the region 3-10%, hence its degree of expansion can be classified as medium-high.

5. CONCLUSIONS

The experimental results showed that the clay shale was highly cemented. The material contained some active and expansive minerals (smectite group) which contributed to its moderate expansive behaviour. Consequently, the construction of the Mae Moh diversion channel required careful planning, as slope instability was introduced by the swelling nature of these clay shales.

The swelling pressure was about 400 kPa for the majority of the tests conducted. The free swell type of oedometer tests have a limitation in that it allows volume changes and incorporates hysteresis into the estimation of the in situ

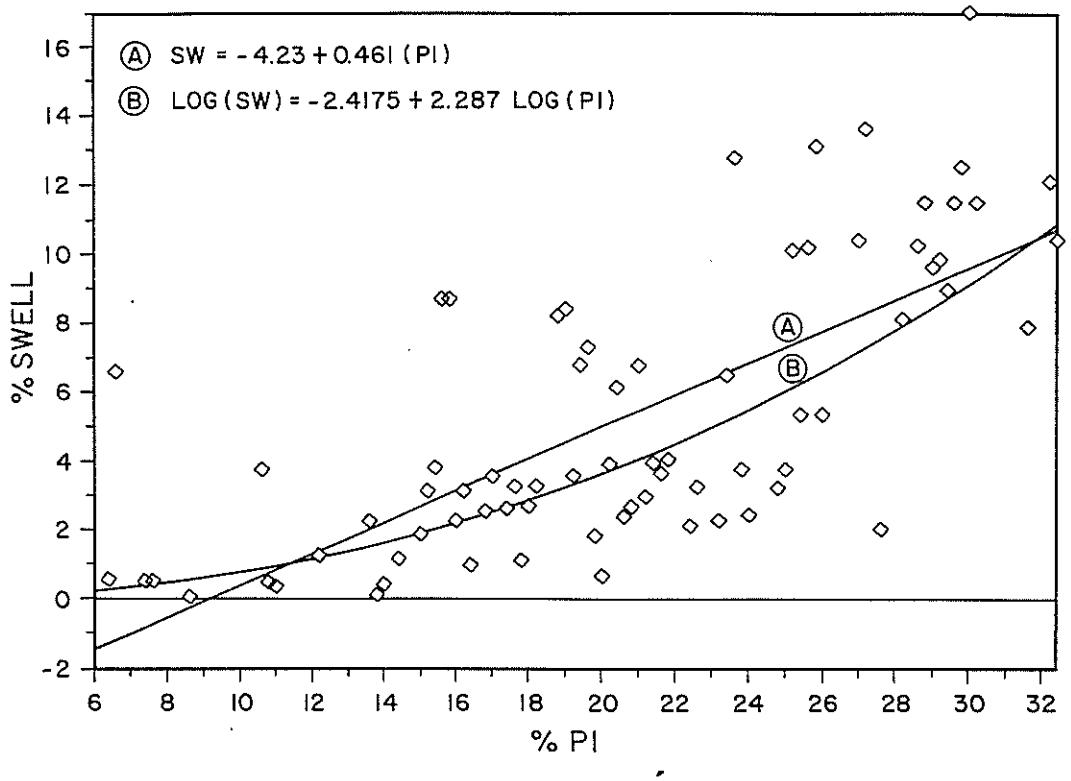

Figure 12 Variation of percentage swell with plasticity index

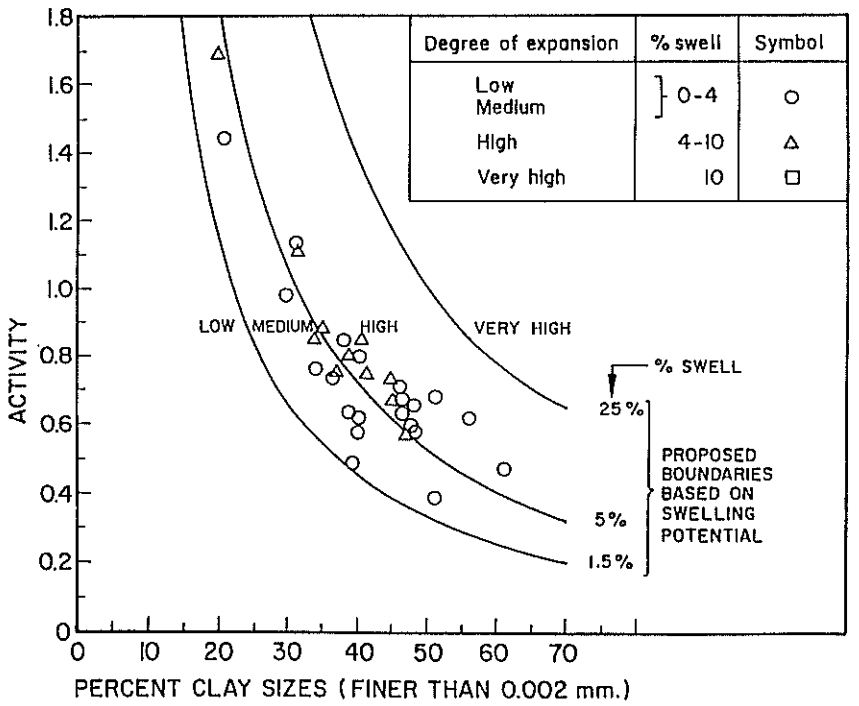

Figure 13 Variation of clay shale activity with percentage of clay size

stress state. The Huder-Amberg test was found to be the best test for measuring the swelling pressure. A rather high expansion was recorded when the sample was tested in its unconfined state. Although not discussed in detail in this paper, a low expansion was observed (less than 1%) when the sample was placed under a light load of 6.25 kPa and allowed to swell only in the vertical direction. Moreover, differential swelling was also observed in the sub-parallel directions. Therefore, the swelling of the clay shale was possibly due to the mineral orientation as well as the horizontally bedded fissures (Husin, 1991).

In the field conditions, the problem of the variation in soil properties (vertically as well as horizontally) exists, particularly at the layer boundaries. The studies of a particular swelling soil which is interbeded between non swelling soils such as sand or silt proves to be even more complicated when an attempt is made to relate the laboratory results to the field conditions. The presence of the non-swelling soil layers will reduce or even arrest the swelling of the composite layer.

5. ACKNOWLEDGEMENTS

The authors are particularly grateful to Mr. Saman Wijewardena for his assistance during the preparation of this paper. Funding provided by the Canadian International Development Agency during the course of this project is also appreciated.

6. REFERENCES

1 Cepeda, A. "An Experimental Investigation of the Engineering Behaviour of Natural Shales", PhD. Thesis, University of Illinois, Urbana-Champain, 1987.

2 Husin, M.R.B. "Engineering Behaviour of Clay Shale in the Mae Moh Diversion Canal", MEng. Thesis, Asian Institute of Technology, Bangkok, 1991.

3 Jiang, W.T. and Peacor, D.R. "Transmissiom and Analytical Electron Microscope Study of Mixed-layer Illite/Smectite Formed as an Apparent Replacement Product of Diagenetic Illite", Journal of Clay Minerals, 1990, pp. 449-468.

4 Skempton, A.W. "The Colloidal Activity of Clays", Proc. of the 3rd ICSMFE. Switzerland, 1953, pp. 57-61.

5 Sritharan, A. and Rao, S.M. "A Scientific Basis for the use of Index Tests in Identification of Expansive Soils", Technical Note, ASTM, 1988, pp. 208-211.

6 Weston, D.J. "Expansive Roadbed Treatment for Southern Africa", Proc. of the 4th Int. Conf. on Expansive Soils, Denver, Colorado, 1980, pp. 339-360.

7 Witke, W "Fundamentals for the Design and Construction of Tunnels in Swelling Rocks", Proc. of the 4th Congress of the ISRM Conf., Montreaux, Switzerland.

Normalised Shear Strength and Compressibility Characteristics of Adelaide Expansive Clay

W.S. KAGGWA
B.Sc.(Eng.)., M.Eng.Sc., Ph.D., M.I.E.Aust.
Lecturer in Civil Engineering, The University of Adelaide, Australia
M.B. JAKSA
B.E., M.I.E.Aust.
Lecturer in Civil Engineering, The University of Adelaide, Australia

SUMMARY The available data on the undrained shear strength and compressibility of Adelaide clays is presented, particularly for the Keswick Clay. Analyses which take into account the soil suction in the soil mass (in-situ negative pore pressures) are used to relate the undrained shear strength and Young's modulus determined from field and laboratory tests to the effective stress state in the soil. It is shown that in spite of the wide variations in the values of undrained shear strength and compressibility characteristics of Keswick Clay, which are attributable to the variable effective stress state within the soil mass and also the inherent variability of the clay, the normalised values fall within ranges typical of over-consolidated clays acted upon by positive pore pressures.

1. INTRODUCTION

Expansive clay soils occur extensively in the Adelaide metropolitan area and surrounding suburbs, as shown in Fig.1. The clays are typically stiff and appear to be over-consolidated, with high values of total suction in situ. Extensive data is available on the index properties of the clays, natural moisture content including seasonal variations, soil suction and their shrink-swell characteristics. However, less data is available on the shear strength and compressibility characteristics of these clays. In addition, this data is mainly for undrained or short-term conditions.

The authors have assembled a large data base on the shear strength and compressibility of the expansive Keswick and Hindmarsh Clays from the Adelaide metropolitan area, the in situ moisture content, dry density, and total soil suction. This paper analyses the data for Keswick Clay, determined from field and laboratory tests, in order to derive common variations with depth and the influence of the effective stress state. The data base is, however, not exhaustive, and the data for the sand layer is not included in this paper.

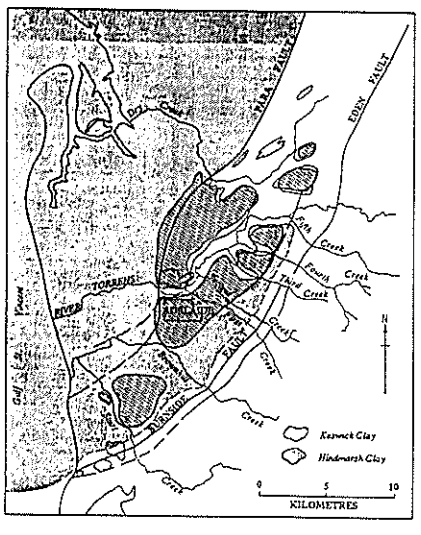

Fig. 1: Distribution of expansive clays around Adelaide

2. DESCRIPTION AND PROPERTIES OF EXPANSIVE CLAYS

A typical soil profile in the Adelaide metropolitan area consists of fill or recent deposits up to 2 metres, underlain by a layer of a highly expansive clay known as Keswick Clay, of variable thickness (typically 5 to 8 metres thick). There is a sand layer, typically 4 to 6 metres underneath, followed by another expansive clay layer, known as Hindmarsh Clay, which can be up to 5 metres in thickness. This clay layer is underlain by Hallet Cove Sandstone. The general water table is located within this sandstone layer. Occasional perched water tables are found in the Keswick Clay layer. The investigations at the South Australian Department of Mines and Energy by Sheard and Bowman (1987a,b) provide clear definitions of the two clay layers. The analyses reported in the present paper are limited to the upper Keswick Clay, with indicative data for the Hindmarsh Clay included wherever possible.

Generally, the particle size distribution curves show that average percentage of clay, silt, and sand are 65%, 20% and 15%, respectively. The clay soils have been described as highly plastic, reactive, and over-consolidated with a classification CH according to the Unified Soil Classification System. The predominant clay minerals are illite (50%) and kaolin (20%) and montmorillonite less than 20%. The specific gravity falls within the range G_S = 2.68 - 2.77. The in situ water content, dry density and degree of saturation are discussed in a companion paper by Jaksa and Kaggwa (1992) in the proceedings of this conference. Extensive data on the description and properties of the clay soils is available and the summary by Cox (1970) presents the basic information.

The variations of the dry density, moisture content and total soil suction with depth are shown in Fig.2. It can be seen that the dry density, moisture content and total soil suction all vary widely for a given depth below the ground surface. This is likely due to (a) the natural variability of geological materials in situ, (b) the highly fissured nature of the clay, resulting in moisture flow mainly along the fissures rather than through the entire soil mass, (c) the effects of sampling disturbance, and (d) the seasonal variations for samples taken closer to the ground surface. This large scatter in the soil

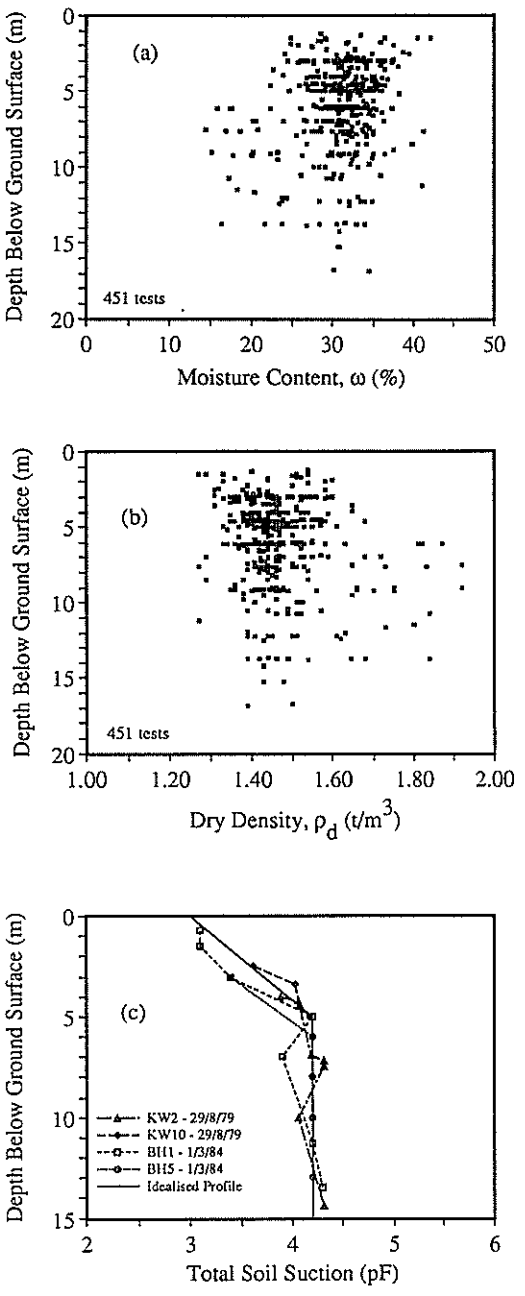

Fig. 2: Variation of moisture content, dry density and total soil suction with depth

state parameters has led many consulting geotechnical engineers to rely solely on field measurements relevant to the site under investigation.

Experience from investigations of the shear strength and compressibility of Adelaide clays has shown that for the case of residential buildings, shear strength and compressibility characteristics of the clays are not a controlling factor in the design of footings (see for example Pile and McInnes, 1984), but rather that the swelling and shrinkage of the soil due to moisture changes is the major factor. As a result, estimates of the shear strength and compressibility of the clays have been based on either past experience, results of pocket penetrometer or cone penetration tests, or unconsolidated undrained (UU) triaxial tests. Because of fissuring in the clays, laboratory tests have largely been used to confirm the results of field tests.

Detailed investigations have been carried out for large commercial building projects, with stratigraphy, field tests such as cone penetration, pressuremeter and screw plate load (SPLT) tests, and laboratory tests being performed. Isotropically consolidated triaxial tests using the in situ (total) stress, followed by shearing under undrained conditions (CIU), have been used to check the values estimated from field tests. In many UU tests, 3-stage shearing has been used, but there is uncertainty whether the excess pore pressures within the soil specimen dissipate before the commencement of the second and third shearing stages. The results of the in situ tests and laboratory tests show that at any given location, the undrained shear strength increases with depth for the upper Keswick Clay, with the ratio $(s_u/\sigma_{vo}) = 1.0$ to 1.5, where s_u is the undrained shear strength and σ_{vo} is the overburden pressure (total vertical stress). However, a slight decrease in undrained shear strength with depth has been obtained for the lower Hindmarsh Clay layer.

The compressibility of the clay samples has been determined from results of field tests especially plate loading, screw plate, and pressuremeter, tests. In the laboratory, the oedometer consolidation and shrink-swell tests have been widely used. It does not appear that the deviator stress versus axial strain response obtained from the triaxial test has been widely used to determine the value of Young's modulus under undrained or drained conditions. Thus, some of the data presented in this paper is based on analyses of the test results by the authors.

3. SUMMARY OF RESULTS FROM FIELD TESTS

In the field, the total horizontal stress is typically higher than the total vertical stress. The results of strength and compressibility measurements from field and laboratory tests are summarised in this section. It should be remembered that the computed in situ shear strength depends on the effective normal stresses within the soil mass and the drainage conditions during the test.

3.1 Undrained Shear Strength

Estimates of the undrained shear strength based on field tests including self-boring pressuremeter (SBPT) tests, cone penetration tests, and screw plate load (SPLT) tests, are shown in Fig. 3. The variation of undrained shear strength with depth below the ground surface for the three field test methods shows that the screw plate test results have the widest scatter, followed by the cone penetration test. The SBPT test results have the least scatter. The lowest undrained shear strength can be approximated by the ratio $(s_u/\gamma_w z) = 1.8$, where γ_w is the unit weight of water and z is the depth below ground surface. The highest values are given by the ratio $(s_u/\gamma_w z) = 5.0$, with a maximum undrained shear strength of 250 kPa for the Keswick Clay. The large variation in the undrained shear strength near the ground surface can be attributed to variations in moisture content (and total soil suction) caused by water infiltration during

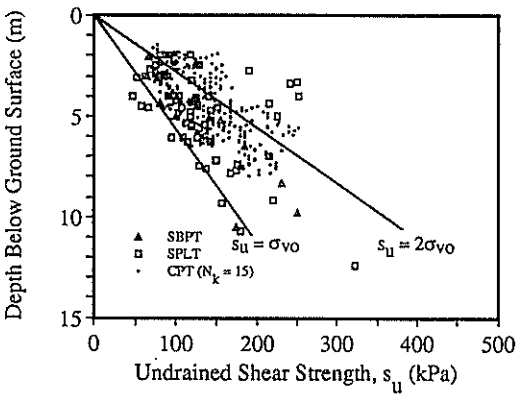

Fig. 3: Variation of field-determined shear strength with depth

winter, and evaporation during summer, with the active zone extending to a depth of about 5 metres.

3.2 Compressibility

The undrained Young's modulus has been estimated from the pressure versus radial strain during the pressuremeter test and the immediate load-settlement curve of the screw plate load tests, using the small strain linear portion of the curves. The variation of the initial tangent modulus, E_{ui}, with depth is shown in Fig. 4. As in the case of the undrained shear strength, the screw-plate test results show the most scatter. In general, the SBPT test results suggest that E_{ui} (horizontal) increases with depth whereas no general trend can be inferred from the screw-plate test results. The lower value of E_{ui} (horizontal) can be expressed by the ratio $(E_{ui}/\gamma_w z) = 300$ whereas the upper value, which would be applicable to intact clay and clay at low moisture content, can be expressed by the ratio $(E_{ui}/\gamma_w z) = 2000$. Thus, there is a variation of an order of magnitude of the undrained Young's modulus. It would also appear that values of E_{ui} greater than 100 MPa should not be used.

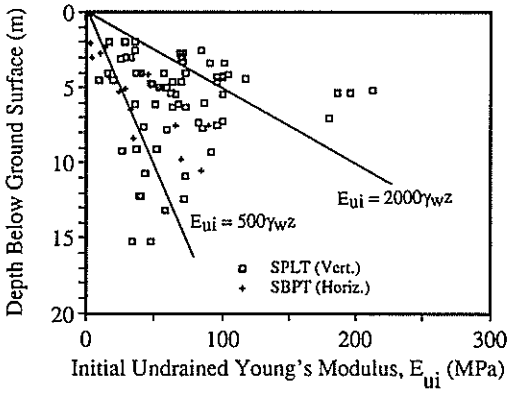

Fig. 4: Variation of field-determined undrained Young's modulus with depth

It is not advisable to use the initial tangent modulus when designing foundations except where the imposed loads are low. For typical loading conditions where the factor of safety against bearing capacity failure is between 2 and 3, the above moduli would have to be reduced by factors of 3 to 5, in order to estimate the expected foundation settlements.

4. SUMMARY OF TRIAXIAL TEST RESULTS

In the case of laboratory triaxial tests, the measured shear strength is affected by factors such as soil disturbance, in particular stress relief during soil preparation prior to re-consolidation, and the use of distilled water as the pore fluid, which causes swelling of the expansive clay.

4.1 Shear Strength of "Undisturbed" Samples

The laboratory shear strength tests that are most widely used are the unconsolidated undrained (UU) triaxial tests in which a confining pressure equal to the estimated overburden pressure is applied to the specimen. In a few cases, "consolidated quick" triaxial tests have been performed. This test involves saturation of the clay (by applying a back pressure at low effective confining pressure), isotropic consolidation with the effective all-round pressure equal to the overburden pressure (total stress), followed by shearing under undrained conditions. Fig. 5 shows the variation of undrained shear strength with the initial moisture content of the soil specimen. It can be seen in Fig. 5 that there is a wide scatter between the lower and upper values of undrained shear strength (the ratio $(s_u)_{min}/(s_u)_{max}$ varies from 2 at high moisture contents, to 4 at low moisture contents, where the subscripts min and max denote minimum and maximum values, respectively. Thus, the moisture content of the soil specimen should not be used alone as the basis for estimating the undrained shear strength.

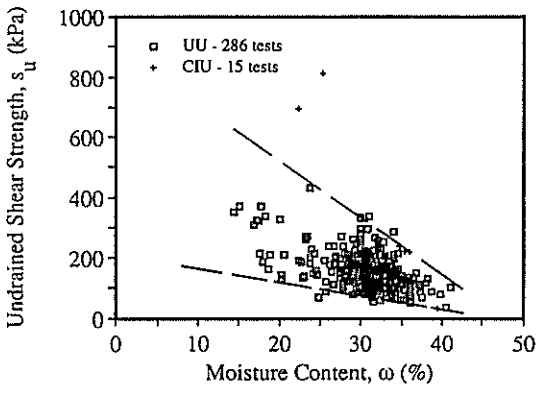

Fig. 5: Variation of laboratory-determined shear strength with moisture content

Fig. 6 shows the variation of undrained shear strength s_u, with confining pressure on undrained shear strength. In the UU tests, there appears to be a maximum value of undrained shear strength approximately equal to 300 kPa. The low values of s_u (less than 60 kPa) have been attributed to failures along fissures. The results from CIU tests indicate an increase in s_u with consolidation pressure, with some scatter though much less than that for UU tests.

Fig. 7 shows a plot of peak stress difference $q = (\sigma_1 - \sigma_3)$ versus mean normal effective stress $p' = (\sigma_1' + 2\sigma_3')/3$, from the CIU tests. The effective shear strength of Keswick Clay can be expressed by the Mohr-Coulomb strength parameters $c' = 0$ and a friction angle $\phi' = 18°$ to $21°$. The angle of internal friction, ϕ', falls within the expected range of values reported in previous investigations (for example Richards and Kurzeme, 1973).

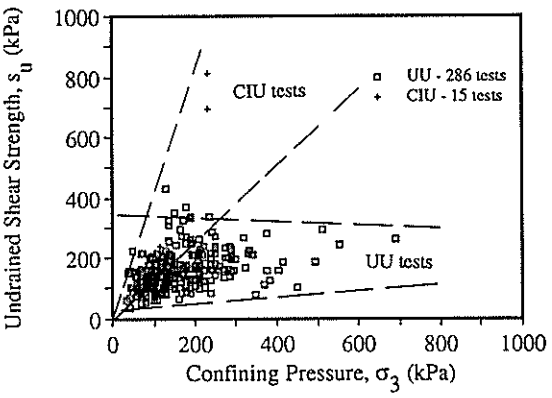

Fig. 6: Variation of laboratory shear strength with consolidation pressure

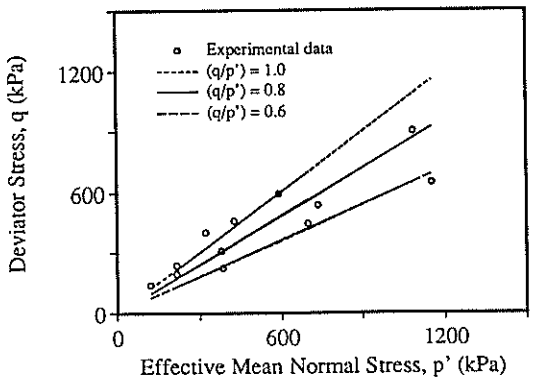

Fig. 7: Peak and Residual strength envelopes in p' - q stress space

4.2 Compressibility

The value of undrained Young's modulus at a fraction of the failure deviator stress has been computed from the deviator stress versus axial strain response. Fig. 8 shows the variation of the undrained Young's modulus corresponding to 50% of failure deviator stress, E_{u50}, versus the isotropic consolidation pressure, p_o'. There is a wide scatter probably due to soil disturbance and the natural soil variability as the boreholes were taken along a line of 900 metres. The ratio E_{u50}/p_o varies between 75 and 200, with an average of 120. Compared to the results of in-situ tests, the initial tangent modulus E_{ui}, is between 4 to 10 times higher than E_{u50}.

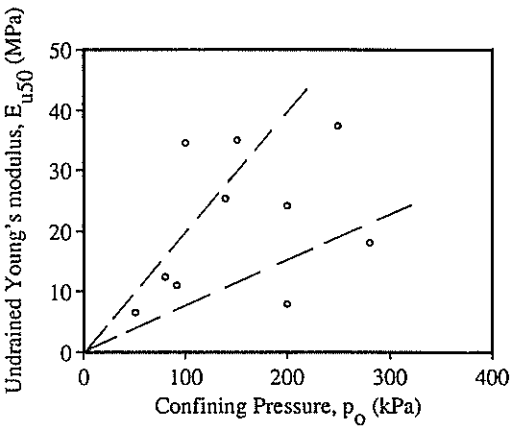

Fig. 8: Variation of Young's modulus with confining pressure

5. INTERPRETATION OF TEST RESULTS

5.1 In-situ Earth Pressure Coefficient K_o

The earth pressure coefficient K_o, $(\sigma_{ho}'/\sigma_{vo}')$, has been estimated using the total horizontal stress estimated from pressuremeter tests, the total vertical stress based on overburden pressure, and total soil suction estimated from the psychrometer test.

The results of pressuremeter tests consistently indicate that the total horizontal stresses in the Adelaide clays are greater than the estimates of total vertical stresses based upon the overburden pressures. It is assumed that the values of total soil suction, measured using the psychrometer, are representative of the negative pore pressures acting within the clay mass.

The earth pressure coefficient K_o can be determined from the relation:

$$K_o = \frac{\sigma'_{ho}}{\sigma'_{vo}} = \frac{\sigma_{ho} - u_o}{\sigma_{vo} - u_o} = \frac{K - \alpha}{1 - \alpha} \qquad (1)$$

where

σ_{ho}, σ_{vo} = total horizontal and vertical in-situ stresses, respectively

σ'_{ho}, σ'_{vo} = effective horizontal and vertical in-situ stresses, respectively, and
u_o = in-situ pore pressure.
$K = \sigma_{ho} / \sigma_{vo}$ the ratio of total stresses
$\alpha = u_o / \sigma_{vo}$ the pore pressure ratio

Based on the results of consolidated undrained triaxial tests where the excess pore pressures are negligible, even at failure, (Skempton and Bishop's parameter $\bar{A} = \Delta u / \Delta(\sigma_1 - \sigma_3) \leq \pm 2\%$), it is assumed that during the pressuremeter test, the negative pore pressures remain unchanged.

In using Eqn.1, u_o can be estimated from the equivalent total soil suction p" (the sum of matrix suction $p"_m$, and solute suction $p"_s$), from the values of pF determined using the psychrometer tests. Aitchison (1965) presented an equation for estimating the equivalent negative pore pressure u_o, which can be written as follows:

$$u_o = \chi_m p"_m + \chi_s p"_s \quad (2)$$

where

$$p"_m = -0.0981(10^{pF_m}) \text{ in kPa} \quad (3)$$

and

$$p"_s = -0.0981(10^{pF_s}) \text{ in kPa} \quad (4)$$

$p"_m$ is the difference between air pressure and water pressure, $p"_s$ is the solute or osmotic suction, χ_m and χ_s are factors which lie within the range 0 to 1. Because the clay is very close to full saturation in situ, termed quasi-saturated (see Jaksa and Kaggwa, 1992 and Kaggwa, 1992), and the common practice of using distilled water as the pore fluid in laboratory tests, it is assumed as a first approximation that $\chi_m = \chi_s = 1$. This approximation is being investigated by the authors, using a modified triaxial base pedestal, ensuring that the pore water within the specimen is isolated from the distilled water used in the back pressure system.

The results of pressuremeter tests and psychrometer tests (from the Adelaide Subway Project, 1979, and the Commonwealth Centre Project, 1984) have been used to determine the variation of K_o with depth, which is shown in Fig. 9. It can be seen that in general, the earth pressure coefficient at rest decreases from about $K_o = 1.45$ at a depth of 2 m below the ground surface, to $K_o = 1.05$ at a depth of about 4 m below the ground surface. For depths between 5 m and 10 m, the average value of $K_o = 1.20$. It should be noted that the effects of seasonal variations in surface temperature and moisture are less pronounced as the depth below the ground surface increases, and are insignificant at depths greater than 5 m.

The above values of the coefficient of earth pressure, K_o are to be expected in an over-consolidated clay. The over-consolidation ratios in laboratory specimens would therefore be expected to be much higher for the typical consolidation pressures based on overburden pressure.

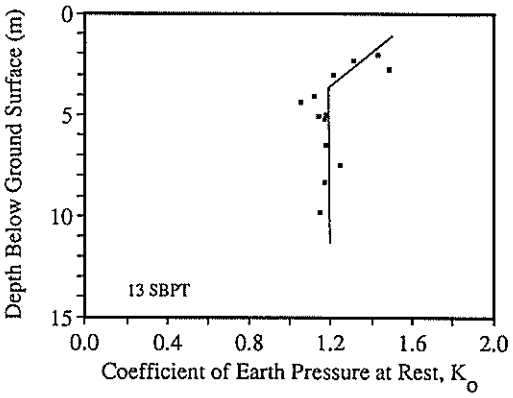

Fig. 9: Variation of predicted in-situ K_o with depth

5.2 Normalised Undrained Shear Strength

Due to the semi-arid climate in Adelaide, the clays have been subjected to cycles of wetting and drying. As the clay dried, large negative pore pressures were generated, leading to high normal effective stresses, and during wetting the negative pore pressures dissipated, leading to lower normal effective stresses. This is the main cause of overconsolidation, and the in-situ normal effective stresses are less than the maximum stresses to which the clay has been subjected during the stress history. It is uncertain whether the overconsolidation ratio is related directly to the highest normal effective stresses or to some intermediate value. The reason for this uncertainty can be appreciated from a consideration of the changes in void ratio which accompany the drying and wetting processes.

Fig. 10 shows a plot of the undrained shear strength ratio (s_u/σ'_{vo}) (where σ'_{vo} is the effective in-situ vertical stress) versus depth below the ground surface based on SBPM tests. This ratio properly takes into account the effects of soil suction. The range of values of the ratio (s_u/σ'_{vo}) is between 0.1 and 0.2.

The results presented by Wroth and Houlsby (1985) show that the undrained shear stress ratio increases as the overconsolidation ratio increases. Values of (s_u/p'_o) for isotropically consolidated triaxial specimens of clay range from 0.25 and 0.3 for normally consolidated specimens, to 0.5 and 0.6 for isotropic overconsolidation ratio (p'_{max}/p'_o) = 3, where p' is the mean normal effective isotropic consolidation pressure and the subscript max denotes the maximum value to which the specimen is subjected prior to triaxial testing using a consolidation pressure p'_o.

5.3 Normalised Young's Modulus

The values of undrained Young's modulus obtained from the interpretation of pressuremeter and screw plate load tests have been normalised with respect to the effective vertical stress σ'_{vo} and plotted against depth below the surface of the Keswick Clay layer in Fig. 11. The ratio (E_{ui}/σ'_{vo}) falls within the range 10 to 50.

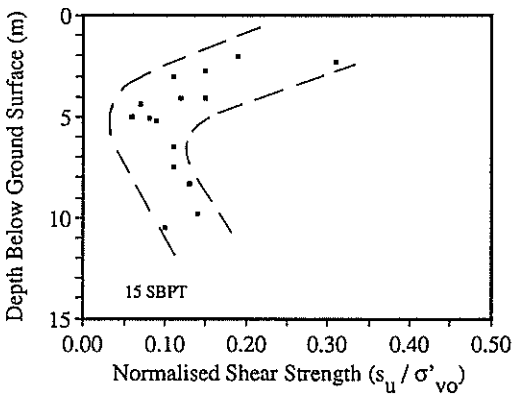

Fig. 10: Normalised shear strength ratio (s_u/σ'_{vo}) versus depth

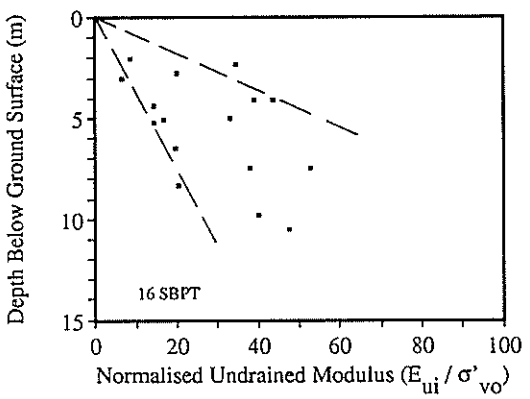

Fig. 11: Normalised undrained Young's modulus (E_{ui}/σ'_{vo}) versus depth

On the basis of Fig. 10 and Fig. 11, the ratio of E_{ui}/s_u lies within the range 100 to 250. As pointed out earlier, the undrained Young's modulus for use in design calculations E_u, would be typically 3 to 5 times less than the initial Young's modulus. Thus the ratio (E_u/s_u) would be within the range of 20 to 80, which is comparable to values obtained for most overconsolidated clays.

6. CONCLUSIONS

Although Keswick Clay is subjected to negative pore pressures in-situ, the normalised undrained shear strength and Young's modulus, with respect to the in-situ vertical effective stress, fall within the expected range of typical over-consolidated clays subjected to positive pore pressures. Provided the in-situ effective stress state within the clay mass can be properly estimated, and in particular the negative pore pressures, then experience from other clays can be used to estimate the undrained shear strength and Young's modulus for use in the preliminary design of foundations.

7. ACKNOWLEDGEMENTS

This paper is part of a research programme into the behaviour of Adelaide expansive clay soils, made possible through a grant from the Australian Research Council. This financial assistance is acknowledged. The authors are grateful to the many geotechnical engineering firms in Adelaide who allowed them access to their investigation reports that have been used in compiling the strength and compressibility characteristics of Keswick Clay.

8. REFERENCES

Cox, J.B. "A Review of the Geotechnical Characteristics of the Soils in the Adelaide City Area", Symposium on Soils and Earth Structures in Arid Climates, IE Aust, Adelaide, 1970.

Jaksa, M.B. and Kaggwa, W.S. "Estimation of Degree of Saturation of Adelaide Expansive Clay Soils", 6th ANZ Conf., Christchurch, February, 1992.

Kaggwa, W.S. "On In-Situ Stresses, Soil Suction, Shear Strength and K_o of Hindmarsh Formation Clay", Civil Engg Trans. IE Aust. submitted for publication, 1992.

Pile, K.C. and McInnes, D.B. "Laboratory Technology for Measuring Properties of Expansive Clays" 5th Int Conf on Expansive Soils, Adelaide, May, 1984, pp. 85 - 93.

Richards, B.G. and Kurzeme, M. "Observations of Earth Pressures on a Retaining Wall at Gouger St. Mail Exchange, Adelaide", Aust. Geomechanics Journal, Vol. G3, No.1, 1973.

Sheard, M.J. and Bowman, G.M. "Definition of the Keswick Clay, Adelaide/Golden Grove Embayment, Para and Eden Blocks, South Australia", Geol Surv. of S. Aust. Q. Geol Notes, No. 103, July, 1987, pp.4 - 9.

Sheard, M.J. and Bowman, G.M. "Redefinition of the Upper Boundary of the Hindmarsh Clay, Adelaide Plains Sub-Basin and Adelaide/Golden Grove Embayment", Geol. Surv. of S. Aust., Q. Geol Notes, No. 103, July, 1987, pp. 9 - 16.

Wroth, C.P. and Houlsby, G.T. "Soil Mechanics - Property Characterisation and Analysis Procedures", Theme Lecture No.1, Proc. 11th ICSMFE, Vol.1, 1985, pp.1-55.

Degree of Saturation of the Keswick Clay Within the Adelaide City Area Above the General Groundwater Table

M.B. JAKSA
B.E., M.I.E.Aust.
Tutor and Post Graduate Student, University of Adelaide, Australia
W.S. KAGGWA
B.Sc.(Eng.)., M.Eng.Sc., Ph.D., M.I.E.Aust.
Lecturer , The University of Adelaide, Australia

SUMMARY The available data on in-situ bulk density and moisture content, and the specific gravity of solids of the Keswick Clay within the Adelaide city area are examined. It is shown that for clay samples located at depths above the general water table the degree of saturation is typically greater than 95%, whereas these soils have been previously treated as unsaturated, and as a consequence, the in-situ effective stresses equated to the total stresses.

The paper also presents an evaluation of the sensitivity of the degree of saturation to the average value of specific gravity of the clay particles, using estimates from laboratory measurements and those based on crystal structure and mineral composition.

1. INTRODUCTION

Traditionally, the degree of saturation, S_r, is obtained from the measured moisture content, ω, and dry density, ρ_d, tabulated values of the density of water, ρ_w (usually assumed constant at 1000 kg/m^3) and the value of the specific gravity of the solids, G_s via the relationship shown in Equation (1), below.

$$S_r = \frac{\omega G_s \rho_d}{(G_s \rho_w)-\rho_d} \qquad (1)$$

For a soil mass, G_s varies over a small range; typically 2.60 to 2.80.

In coarse grained, and inert fine grained soils, the moisture in the voids has no influence on the size of the particles. In expansive clays, however, the size of the particles, and hence the volume of the soil mass, is dependent on its moisture content. For example, the clay mineral montmorillonite can increase its thickness many times due to the influence of moisture. The swelling nature of these clays makes it very difficult to perform accurate laboratory tests to determine G_s.

It has been recognised that the expansive clays found in the Adelaide city area exist with little or no air voids over a wide range of moisture contents.

This paper highlights the importance of the assumed value G_s on the computed S_r, and shows that when dealing with expansive clays, sensitivity analyses are a practical means of estimating S_r. In addition to this, a method is suggested for evaluating G_s based on the proportions of clay minerals present in the soil mass.

2. KESWICK CLAY WITHIN THE ADELAIDE CITY AREA

This paper, and its companion paper, Kaggwa and Jaksa (1992), will focus on a region of the city of Adelaide, described previously by others (eg. Cox, 1970 and Selby and Lindsay, 1982) as the *Adelaide city area*, which contains the central business district of Adelaide, as well as the suburb of North Adelaide.

The majority of this Adelaide city area, and a significant portion of the metropolitan area of Adelaide, is underlain by very expansive clays known as the Keswick and Hindmarsh clays. Until recently, the Keswick and Hindmarsh Clays were grouped into the one formation, namely the Hindmarsh Clay. This formation consisted of: an *upper clay layer* of high plasticity and extreme reactivity, (USC classification CH) which can be described as a heavily fissured, very stiff to hard, grey-green mottled clay; a *middle sand member*, a grey and brown dense, clayey coarse sand; and a *lower clay layer* similar in appearance and behaviour to the more recent upper clay layer. The formation is thought to have been deposited in the Pleistocene and is typically 10 to 25 metres in total thickness.

Sheard and Bowman (1987a,b) found that a disconformity exists between the upper clay layer and the underlying middle sand member. As a result, Sheard and Bowman renamed the upper clay layer; the *Keswick Clay*, and the middle sand member and the lower clay layer; the *Hindmarsh Clay*. The middle sand member marker bed is absent in some parts of the Adelaide city area and here the boundary between the Keswick and Hindmarsh Clays is difficult to establish. Figure 1 shows the distribution of these clays in the vicinity of the city of Adelaide.

Within the Adelaide city Area, the groundwater table generally occurs between 20 and 30 metres below the ground surface in the *Hallett Cove Sandstone*; a permeable formation which immediately underlies the Hindmarsh Clay. A perched water table has been encountered sporadically within the upper three metres of the Keswick Clay, and is thought to be due to drainage troughs associated with the formation of gilgai (Selby and Lindsay, 1982). Occasionally, a perched water table has been encountered in the sand member of the Hindmarsh Clay, but tends to affect only the upper few centimetres of the underlying clay (lower clay layer).

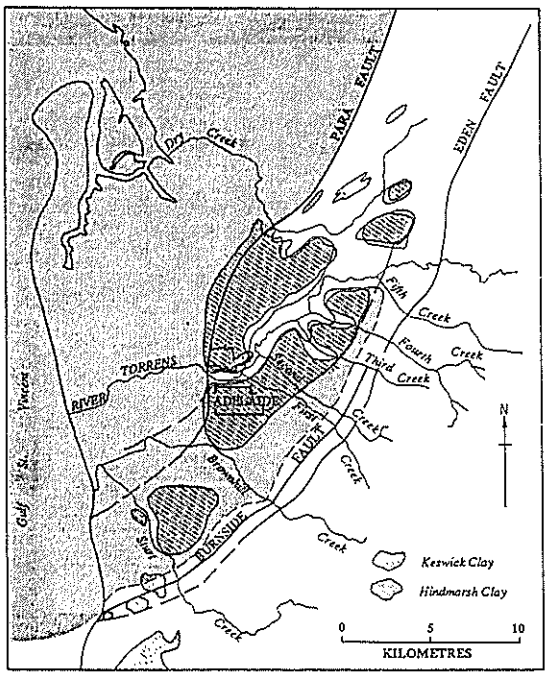

Figure 1. Distribution of the Keswick and Hindmarsh Clays in the Vicinity of the City of Adelaide.

A large data base of geotechnical properties of the Keswick and Hindmarsh Clays has been compiled by the authors from a number of consulting engineering firms and government institutions. These data included the majority of site investigations within the Adelaide city area, approximately 160 in all, since the mid 1960's. This paper makes use of this data base to investigate the degree of saturation of the Keswick Clay.

2.1 Review of Published Data

In his detailed and significant paper, Cox (1970) compiled geotechnical properties of the Keswick and Hindmarsh Clays from 20 site investigations within the Adelaide city area. He compared the properties of these clays, the Keswick Clay in particular, to the well known London Clay and found striking similarities between them. Among the many properties that Cox investigated, he presented a relationship between the dry density, ρ_d, of the Keswick Clay and its moisture content, ω. A unique relationship between ρ_d and ω can be obtained by assuming a constant specific gravity of solids, G_s. Cox's relationship, together with the results of experimentally determined values of ρ_d and ω, are reproduced in Figure 2. Cox assumed a constant value for G_s of 2.70, which was the mean of three laboratory tests carried out on samples of Keswick Clay. The results of these tests, however, were not published. As can be seen from Figure 2, the majority of test results lie between the 95% and 100% degree of saturation lines. He suggested that the 0% to 5% air which was measured could be attributed to air entering the fissure system during sampling and testing. Cox calculated that, for a fissure spacing of 25 mm, the fissures need open only 0.0025 mm to give a degree of saturation of 95%. Similar calculations carried out by the authors, suggest a fissure opening of 0.25 mm.

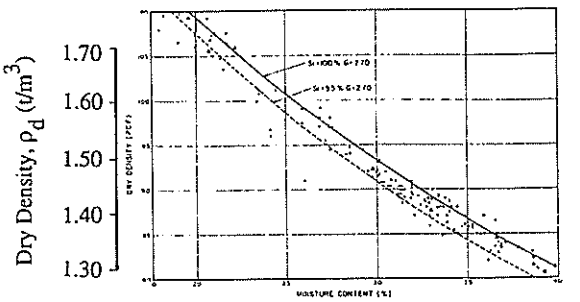

Figure 2. Relationship between Moisture Content, Dry Density and Degree of Saturation for Keswick Clay (after Cox, 1970)

3. SUMMARY OF IN-SITU DRY DENSITY AND MOISTURE CONTENT

Figure 3 shows the variations of the moisture content, ω, and dry density, ρ_d, of the Keswick Clay with depth below ground surface of 451 separate test results from the compiled data base. As is clearly evident, there appears to be no correlation between either of these measured quantities and depth.

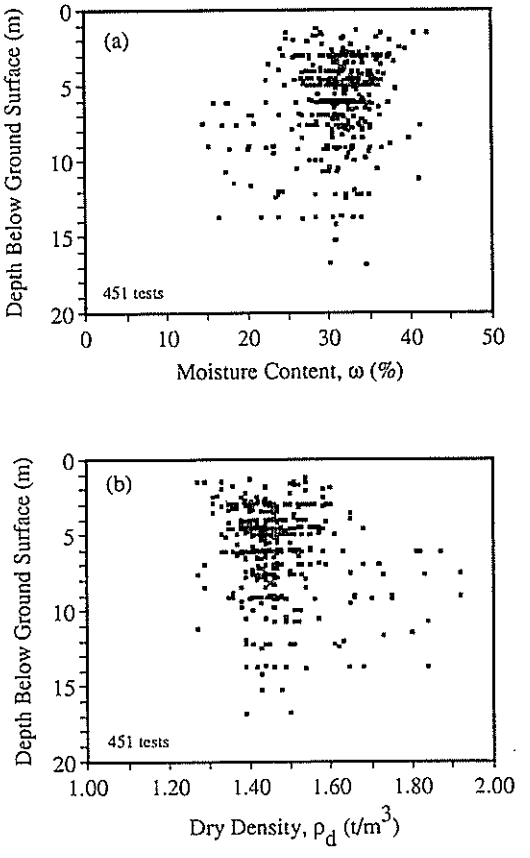

Figure 3. Relationships between Moisture Content and Dry Density of Keswick Clay with Depth Below Ground Surface.

The relationship between the measured values of dry density and moisture content is shown in Figure 4. Superimposed on this graph are the 80%, 90% and 100% degree of saturation lines based on a G_s of 2.70 as quoted by Cox(1970). As can be seen from Figure 4, there is a strong correlation to a constant degree of saturation. Many of the test results, however, plot above the 100% saturation line which is physically not possible. Two reasons are suggested for this. Firstly, the test results, obtained from many different testing laboratories, may not have been accurately determined. Secondly, and more likely, the specific gravity of solids, G_s, as published by Cox may be lower than the *true* mean of the soil particles. These two postulations will be treated in turn.

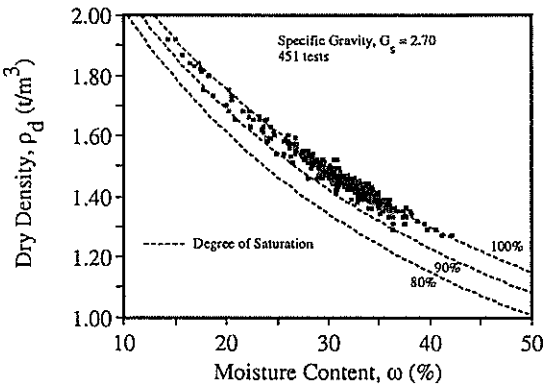

Figure 4. Relationship between ω, ρ_d and S_r for Keswick Clay for G_s = 2.70

4. SENSITIVITY OF S_r TO THE REPORTED ρ_d AND ω

It is possible to determine whether the accuracy of the laboratory tests contribute to the variation in S_r by comparing the reported test results to those determined by assuming S_r = 100% and substituting into Equation (1). Figure 5 shows the relationship between the reported moisture content, ω, and that evaluated by expression (1) and using S_r = 100%, G_s = 2.70 and the reported ρ_d. Figure 6 shows a similar relationship between the reported dry density, ρ_d, and that derived by assuming S_r = 100%. Superimposed on both of these figures is the line where the reported value equals that obtained by assuming saturation. The spread of results about these lines suggests that it is unlikely that the reported test results greatly contribute to the calculated S_r. As a result, it is likely that the G_s suggested by Cox(1970) is lower than the *true* mean G_s of the Keswick Clay. The sensitivity of G_s on the degree of saturation of the Keswick Clay will be treated in the following section.

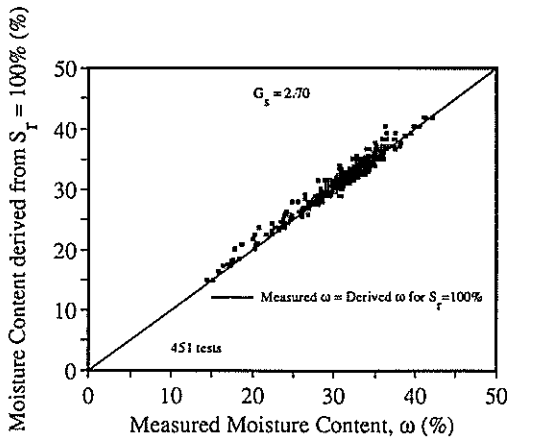

Figure 5. Relationship between Reported Moisture Content and the Moisture Content Calculated assuming Saturation.

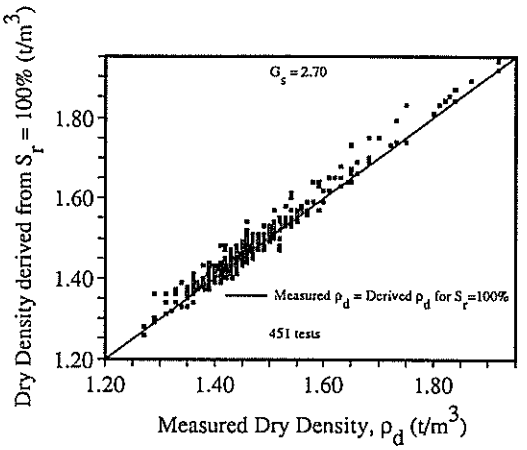

Figure 6. Relationship between Reported Dry Density and the Dry Density Calculated assuming Saturation.

5. SENSITIVITY OF S_r TO THE ASSUMED VALUE OF G_s

One could postulate, as Cox(1970) inferred, that the bulk of the Keswick Clay within the Adelaide city area is saturated. Should this be the case, the value of G_s can be back-calculated, from the expression (1), using the measured quantities of ρ_d and ω and setting S_r = 100%. Figure 7 presents the histogram and statistical parameters of the back-calculated values of G_s. The variation in G_s is due mainly to

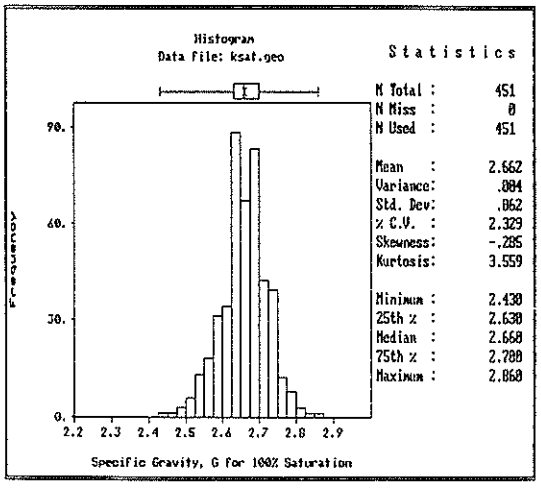

Figure 7. Histogram of Back-Calculated G_s of Keswick Clay assuming Saturation.

the fact that it is unlikely that all of the Keswick Clay is saturated and hence by assuming S_r = 100% the back-calculated G_s is under-estimating its *true* value. Secondly, while the Keswick Clay is relatively homogeneous throughout the Adelaide city area, there are regions where the clay becomes quite sandy, especially in the vicinity of the Hindmarsh Clay sand member and in the proximity of the River Torrens. This natural variability would also contribute to the variation of G_s.

Whilst this back-calculation of G_s for S_r = 100% is a useful technique for estimating the likely ranges of G_s, this procedure does not provide a true average of the specific gravity because of the likelihood that some of the Keswick Clay is not completely saturated.

One would expect, that due to the influence of variations in seasonal moisture ingress and egress caused by transpiration, rainfall, irrigation and evaporation, the degree of saturation for depths less than 3 to 5 metres below the ground surface to be less than 100%, and below this, to tend toward 100%. Figure 8 shows the variation of S_r with depth below the ground surface. It appears, from this figure, that no such conclusion can be drawn. Thus the use of a single value of G_s to represent the entire Keswick Clay is misleading. Since the Keswick Clay does not exhibit free moisture it is classified as being *quasi-saturated.*

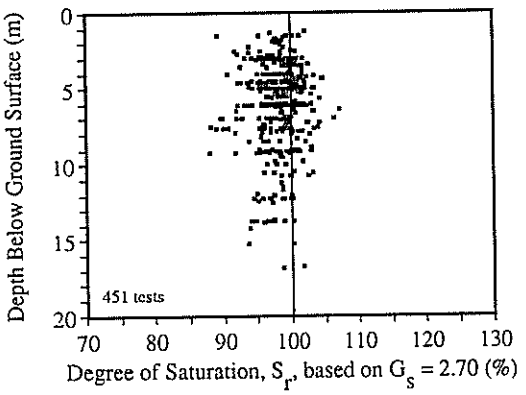

Figure 8. Relationship between Degree of Saturation for Keswick Clay and Depth Below Ground Surface.

Table I presents the results of a sensitivity analysis based on varying the assumed value of G_s from 2.70 to 2.80 so as to reduce the number of test results that have a calculated degree of saturation greater than 100% for the 451 test results obtained from the data base. The degree of saturation was evaluated using Equation (1). While an assumed G_s of 2.80 gives only two results with an S_r greater than 100%, it is unlikely that the mean value of G_s for Keswick Clay would be as high as this. Values of 2.73 - 2.77, on the other hand, give credible degrees of saturation. Figures 9, 10 and 11 show the relationship between ρ_d and ω with degree of saturation lines based on assumed values of G_s of 2.73, 2.75 and 2.77, respectively. These assumed values of G_s provide sensible degrees of saturation for the laboratory tested samples.

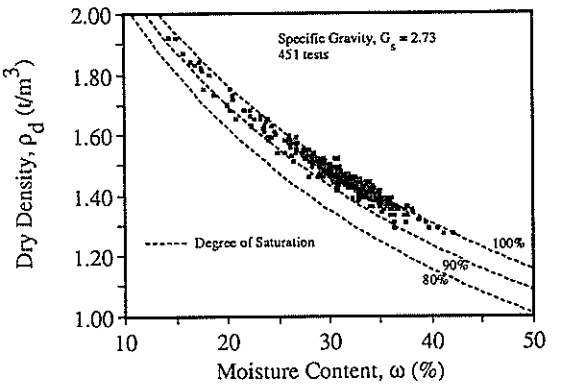

Figure 9. Relationship between ω, ρ_d and S_r for Keswick Clay for G_s = 2.73

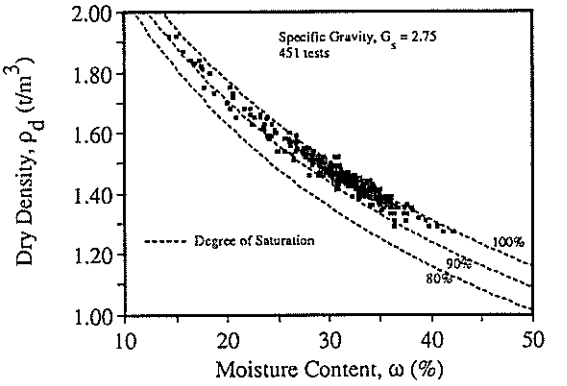

Figure 10. Relationship between ω, ρ_d and S_r for Keswick Clay for G_s = 2.75

TABLE I. RESULTS OF SENSITIVITY ANALYSIS OF DEGREE OF SATURATION FOR VARIOUS G_s

Specific Gravity, G_s	No. of values where S_r >100%	Mean (%)	Standard Deviation (%)	Minimum S_r (%)	Maximum S_r (%)
2.70	64 of 451 (14%)	98.24	2.84	88.83	107.12
2.73	25 of 451 (6%)	96.96	2.84	86.29	105.63
2.75	**13 of 451 (3%)**	**96.15**	**2.84**	**85.18**	**104.67**
2.77	6 of 451 (1%)	95.35	2.84	84.11	103.74
2.80	2 of 451 (0.5%)	94.59	2.84	83.10	102.85

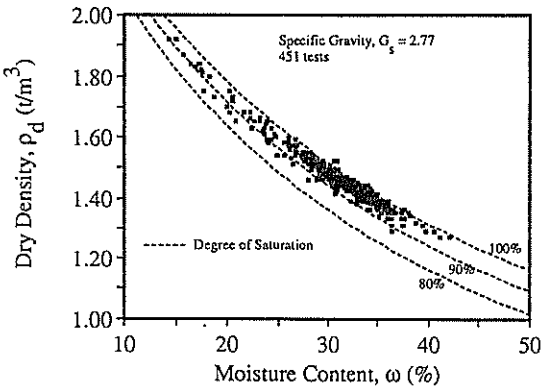

Figure 11. Relationship between ω, ρ_d and S_r for Keswick Clay for G_s = 2.77

6. ESTIMATION OF G_s BASED ON MINERALOGY OF CLAY PARTICLES

Few laboratory tests have been carried out to determine the G_s of the Keswick Clay. In the extensive data compilation carried out by the authors no such test results were found. It is likely that this is due to the fact the G_s published by Cox(1970) has been universally accepted throughout the geotechnical community in South Australia.

As discussed previously, it is difficult to determine the specific gravity of solids of a reactive clay. Table II shows the wide range of specific gravities of solids of reactive clay minerals as reported by a number of sources.

A more appropriate technique for estimating G_s is to use the mineralogy of the soil mass. Lambe and Whitman(1969) published a set of specific gravities of clay minerals based on theoretical calculations of the clay crystal structure. These are shown in Table II.

Cox reported that x-ray diffraction tests performed on the Keswick Clay from one site investigation within the Adelaide city area, found that the clay contained "greater than 50% illite, greater than 20% kaolinite, and generally less than 20% montmorillonite". These were found to be in similar proportions to that of the London Clay.

It is proposed, that to estimate G_s of a reactive clay, the following expression be adopted:

$$G_s^* = \sum_{i=1}^{n} p_i (G_s)_i \qquad (2)$$

where:

G_s^* is the average specific gravity of solids based on the mineralogy of the soil mass,

p_i is the proportion of the i^{th} mineral present in the soil mass,

$(G_s)_i$ is the specific gravity of solids of the i^{th} mineral, calculated from the crystal structure, and

n is the number of significant mineral types present in the soil mass.

Performing this calculation based on the proportions detailed above and the specific gravities shown in Table II, the estimated G_s is between 2.74 and 2.77, which compares well with the results obtained from the sensitivity analyses presented earlier.

7. IMPLICATIONS FOR ANALYSES

Keswick Clay is essentially saturated and hence effective stresses will differ from total stresses. High total suctions have been measured within the Keswick Clay, and as a result, effective stresses should be based on negative pore pressures and total stresses. Hence the calculated coefficient of earth pressure at rest, K_o, will be much lower than currently used. The evaluation of effective stresses and K_o is treated in detail in the companion paper Kaggwa and Jaksa (1992).

8. CONCLUSIONS

A large number of laboratory test results of dry density, ρ_d and moisture content, ω, have been examined, and their relationship presented. It has been found that the majority of the Keswick Clay is saturated or very close to being saturated.

The value of the specific gravity of solids, G_s, of the Keswick Clay has been re-examined. Using sensitivity analyses and statistical procedures, it is suggested that a more appropriate value of the mean of G_s for the Keswick Clay is 2.75 ± 0.02. This more precise evaluation of G_s will enable errors associated with geotechnical design, and their inherent probability of failure, to be reduced.

A technique for estimating the G_s of reactive clays, based on their mineralogical composition, has been proposed which provides a practical alternative to carrying out often difficult laboratory testing.

TABLE II. PUBLISHED SPECIFIC GRAVITIES OF CLAY MINERALS

	Specific Gravities, G_s				
Clay	Lambe & Whitman		Mitchell	Sowers	Bowles
Mineral	Crystal Structure	Measured	Measured	Measured	Measured
Illite	**2.84**	2.60 - 2.86	2.6 - 3.0	2.2 - 2.6	2.60
Kaolinite	**2.61**	2.62 - 2.66	2.60 - 2.68	2.2 - 2.6	2.60 - 2.63
Montmorillonite	**2.74**	2.75 - 2.78	2.35 - 2.7	2.2 - 2.6	2.40

9. ACKNOWLEDGEMENTS

The authors wish to acknowledge the valuable contribution of the following organisations for providing access to their site investigation reports and test results:

Coffey Partners International Pty. Ltd., Connell Wagner (SA) Pty. Ltd., Hosking Oborn Freeman and Fox Pty. Ltd., Kinhill Engineers Pty. Ltd., Koukourou and Partners, PPK Consultants Pty. Ltd., SACON, and Woodburn Fitzhardinge Geotechnical.

10. REFERENCES

Bowles, J.E. (1968). *Foundation Analysis and Design*, McGraw-Hill Book Co., New York, 659 p.

Cox, J. B. (1970). A Review of the Geotechnical Characteristics of the Soils in the Adelaide City Area. *Proceedings of Symposium on Soils and Earth Structures in Arid Climates*, I.E.Aust. and Aust. Geomech. Soc., Adelaide, pp. 72-86.

Kaggwa, W.S. and Jaksa, M.B. (1992). Normalised Shear Strength and Compressibility Characteristics of Adelaide Expansive Clay. *Proceedings 6th Australia New Zealand Conf. on Geomechanics*, Christchurch.

Lambe, T. W. and Whitman, R. V. (1969). *Soil Mechanics*, John Wiley & Sons Inc., New York, 553p.

Mitchell, J.K. (1976). *Fundamentals of Soil Behaviour*. John Wiley & Sons, Inc., New York, 422p.

Selby, J. and Lindsay, J. M. (1982). *Engineering Geology of the Adelaide City Area*, Dept. Mines & Energy, Bull. 51, 94p.

Sheard, M. J. and Bowman, G. M. (1987a). Definition of Keswick Clay: Adelaide/Golden Grove Embayment, Para and Eden Blocks, South Australia. *Q. geol. Notes, geol. Surv. S. Aust.*, 103, pp. 4-9.

Sheard, M. J. and Bowman, G. M. (1987b). Redefinition of the Upper Boundary of the Hindmarsh Clay: Adelaide Plains Sub-Basin and Adelaide/Golden Grove Embayment. *Q. geol. Notes, geol. Surv. S. Aust.*, 103, pp. 9-16.

Sowers, G.F. (1979). *Introductory Soil Mechanics and Foundations: Geotechnical Engineering*, MacMillan Publishing Co., New York, 4th ed., 621 p.

The Dynamic Response of Volcanic Soils

T.J. LARKIN
B.E., Ph.D., A.M.A.S.C.E.
Senior Lecturer, Department of Civil Engineering, University of Auckland
S.Y. CHAN
M.E.
Site Engineer, Binney and Partners Ltd, London, England

1. INTRODUCTION

This paper concerns the measurement of dynamic properties of some volcanic soils found in The New Zealand central volcanic plateau. Large areas of the central North Island are covered with this material or material of a similar type. The dynamic properties of this soil are important in predicting the response of this material to earthquake loading. There is a paucity of data on the dynamic properties of volcanic soils in New Zealand. This creates uncertainties in the use of analytical methods to calculate seismically induced ground motion.

Many of the analyses performed in New Zealand use overseas data to estimate the dynamic properties. The results of site response analyses are particularly sensitive to the shear modulus - strain relationship as was shown by Larkin and Donovan (1). Thus it is of some importance that for reliable results of theoretical analyses dynamic properties actually measured from volcanic soils are used as the basis for constitutive models used in site response analyses. Many analyses predict amplification of the bedrock motion, sometimes by a large amount, thus the depth and properties of the near surface soils are of considerable importance in this area of work.

A study of the dynamic properties of two volcanic soils was undertaken using the dynamic torsion test equipment at the University of Auckland. Details of these two soils are given in Tables 1 and 2.

Table II Properties of Volcanic Soils.

	Atterberg Limits			Particle size (%)		
Sample name	PL	LL	PI	Clay Fraction	Silt Fraction	Sand Fraction
Rotorua	44	62	18	8	25	66
Rerewhakaaitu	33	51	18	18	57	25

The soils tested were obtained from a construction site in the Whakarewarewa State Forest Park from depths of 3m to 4m. The samples have been categorised into two types, known as Rotorua and Rerewhakaitu ash. The Table above shows the soils have low plasticity index (18%) and are classified as MH in the plasticity chart of Casagrande. The Rotorua ash samples contain coarser particles than the Rerewhakaaitu ash and from visual observation the Rotorua ash is described as sandy silt while the Rerewhakaaitu ash is clayey silt.

The principle objective of the testing programme was to obtain dynamic properties of saturated ash soils as a function of shear strain at various effective confining pressures. This data may then be compared with the overseas data base used as a basis for the dynamic properties of soils in earthquake analyses. The laboratory confining pressures ranged from 25kPa to 150kPa.

Table I Properties of Volcanic Soils.

SAMPLE NAME	SAMPLE DESCRIPTION	WATER CONTENT (%)		BULK DENSITY (kg/m³)		VOID RATIO		Sr (%)		SOLID DENSITY (kg/m³)
		Before	After	Before	After	Before	After	Before	After	
Rerewhakaaitu 1	grey brown clayey silt	61.7	55.6	1479.2	1516.7	L7	L5	90	90	2466.1
Rerewhakaaitu 2	grey brown clayey silt	54.9	64.0	1533.0	1563.2	L5	L6	91	99	
Rotorua 1	yellow brown sandy silt with soft pumice pebbles and organic roots.	51.6	66.3	1429.1	1545.5	L6	L6	80	100	2412.8
Rotorua 2	yellow brown sandy silt with soft pumice pebbles and organic roots	50.2	62.2	1355.6	1487.3	L7	L6	73	92	
Rotorua 3	yellow brown sandy silt with soft pumice pebbles and organic roots.	44.6	65.1	1313.7	1552.3	L7	L6	65	100	

A detailed description of the free vibration torsion test equipment and the testing and analysis technique is contained in Chan(2). This work describes the enhanced system of date collection and analysis and the experimental results presented here.

2. DYNAMIC TEST RESULTS

A series of free vibration torsion tests were performed on the volcanic ash soils whose properties are shown in Tables 1 and 2. The unprocessed data takes the form of torsional displacement of the sample as a function of time. This data was then processed to compute shear modulus and damping curves. Examples of the results of this process are shown in Figure 1 and Figure 2. These results show the strongly nonlinear nature of the soil response with the shear modulus decreasing with increasing shear strain after a constant modulus response (low strain plateau) in the very low strain range. The equivalent viscous damping factor increases with increasing strain to peak values of approximately 20%. These general trends are in line with the international body of literature on the results of dynamic tests on soils, although some features of these results on volcanic soils differ from overseas data, as will be discussed later.

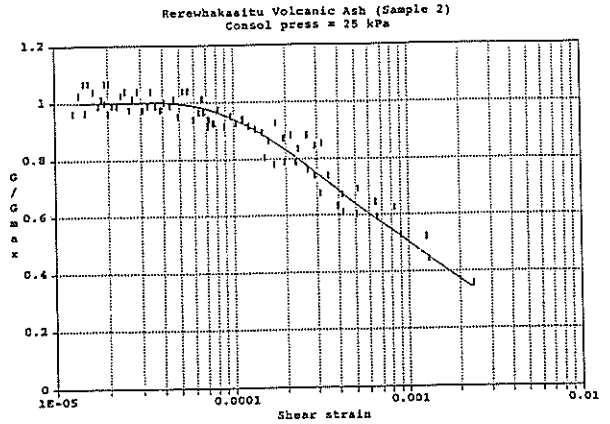

Figure 1. Typical variation of shear modulus with shear strain.

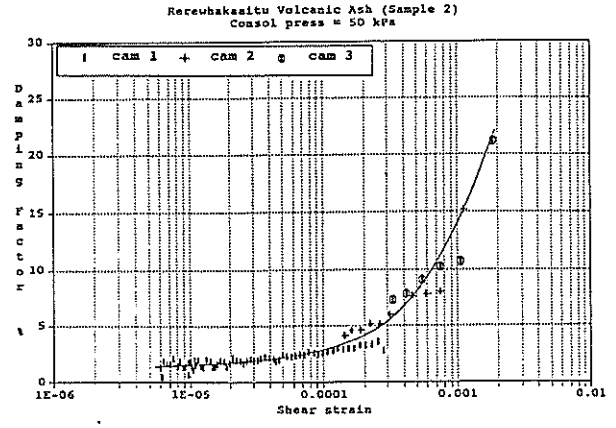

Figure 2. Typical variation of damping factor with shear strain.

A series of tests at different confining pressures were carried out on the two volcanic soils. The results of these tests are summarised in Table 3 where values of the low strain shear modulus, G_{max}, and damping factor, D_{min}, are shown for five different cell pressures, along with the low strain shear wave velocity.

These results show that the low strain shear modulus and damping ratio are stress dependent and hence in any soil profile are a function of the depth, with higher confining stress resulting in higher shear moduli and lower damping. This variation in dynamic properties with confining stress is shown in Figure 3 and Figure 4. The value of shear modulus is sensitive to the stress level while the damping factor is very insensitive for the soils tested. Within the stress range tested the shear modulus is approximately a linear function of the confining stress.

2.1 Comparison of test results with other investigators.

The purpose of summarising data on shear modulus and damping curves is to provide useful guidelines on the form of the relationship for typical soils. This information can be used for preliminary investigations or when no other data will be available. In this study the volcanic ash test results are compared with recent papers of summarised data for clays and sands. Sun et al (3) concentrated on clays while Seed et al (4) collected various data for sands and gravelly soils.

2.1.1 Shear modulus curves.

A summary of the shear modulus curves of the two volcanic soils tested is shown in Figure 5. Generally speaking the following features may be identified:

(1) Rotorua curves (bold lines) are flatter than Rerewhakaaitu. This is expected since Rotorua samples are more sandy, and is consistent with the general trend that curves for sands are flatter than for clays.

(2) For both Rotorua and Rerewhakaaitu samples, the G/G_{max} curves essentially move to the left, as the confining pressure increase. However, the change

Table III Variation of Properties with Confining Stress.

	Rerewhakaaitu			Rotorua		
Confining pressure (kPa)	G (MPa)	V_s (m/s)	D_{min} (%)	G (MPa)	V_s (m/s)	D_{min} (%)
25	11.3	84.9	1.7	-	-	-
50	15.0	98.0	1.7	23.7	123.8	1.3
75	19.0	111.9	1.5	-	-	-
100	23.4	124.3	1.3	40	164	-
150	34.0	149.8	1.0	42.8	166.0	1.3

is not very significant. This is consistent with other reports for clays and sands. Sun et al (3) state that the influence of confining pressure is generally small for clays with plasticity indices exceeding 25 and for shear strains less than 0.01. For sands, studies by Hardin & Drnevich (5), Shibata & Soelarno (6) and Iwasaki et al (7) show that G/G_{max} curves are slightly influenced by the confining pressure.

2.1.2 Damping curves

Figure 6 summarizes the damping curves for the Rotorua and Rerewhakaaitu samples. The damping curves are essentially independent of the confining pressure, which is consistent with various reports for clays and sands. Sun et al (3) reports that damping curves for clays have not significantly deviated from the range indicated by Seed & Idriss (8), implying that confining pressure has a limited influence on damping characteristics of clays. For sands, Seed et al (4) state that at pressures greater than 500 psf (24 kPa), the effect of confining pressure is small compared with the effect of shear strain.

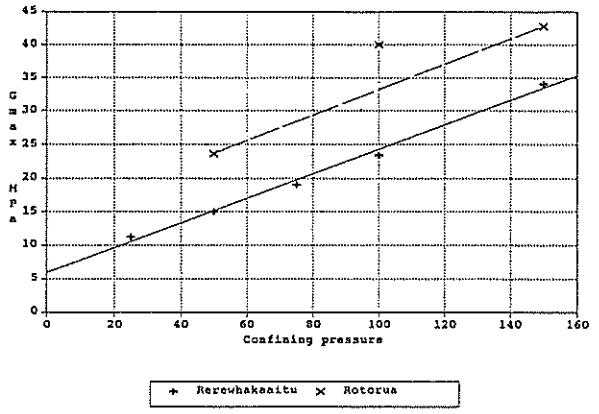

Figure 3. G_{max} variation with effective confining pressure.

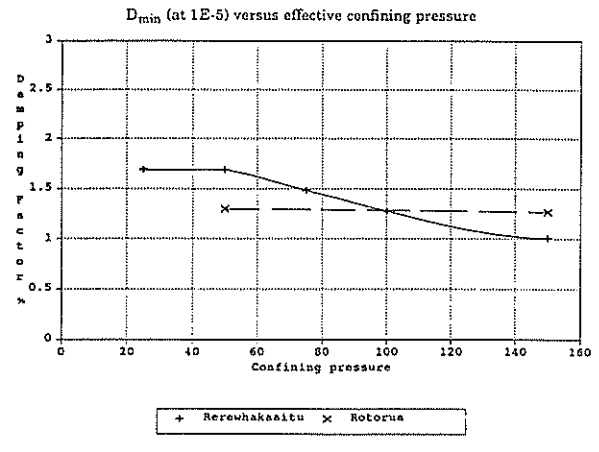

Figure 4. D_{min} versus effective confining pressure.

2.2 Volcanic ash Compared with clays.

2.2.1 Normalized shear modulus curves.

Sun et al (3) conclude that normalized shear modulus curves for clays are most significantly influenced by the plasticity index (PI). Figure 7, after Zen and Higuchi,(9) provides a useful guide on the form of normalized shear modulus curves with respect to shear strain and PI. In addition, void ratio may be a significant secondary factor to be considered in selecting a normalized shear modulus curve for analysis purposes. In this study, the void ratios are essentially unchanged with confining pressure and hence its effect is insignificant.

Figure 7 compares G/G_{max} curves between volcanic ash samples and clays Zen and Higuchi, (9). Because the volcanic ash samples have a PI of 18, it is expected that their curves lie near the PI boundary of 20. Between strains of $7*10^{-5}$ and $2*10^{-3}$ the volcanic ash curves essentially lie near the PI=20 boundary, and hence close

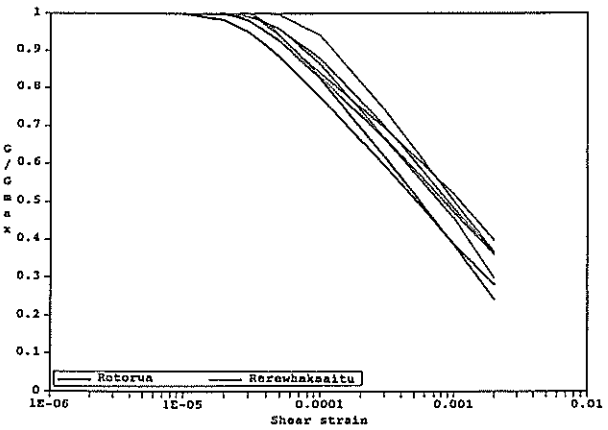

Figure 5. Normalised shear modulus curves for Volcanic Soils.

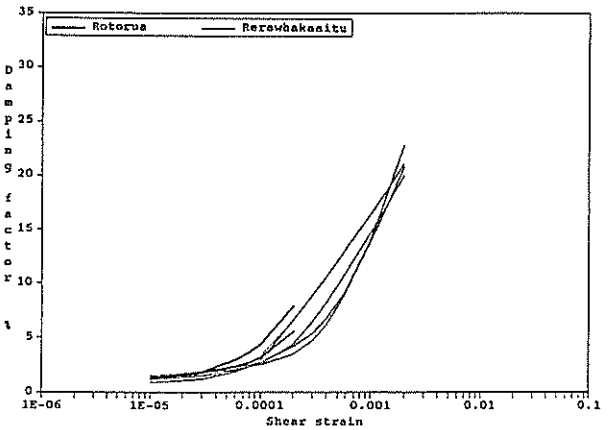

Figure 6. Damping curves for volcanic soils.

comparison is evident. At smaller strains ($<7*10^{-5}$), two differences are observed.

(1) The volcanic ash curves have a more extended G/G_{max} plateau ($G/G_{max}= 1$). This 'elastic' behaviour is maintained to strains of 1 to $5*10^{-5}$.

(2) The volcanic ash curves rapidly drop away from the plateau, starting between strains of $1*10^{-5}$ and $1*10^{-4}$. This is in contrast with the more gradual decay of the PI boundaries.

In summary, although the volcanic ash G/G_{max} curves are consistent with the proposed curves of Zen and Higuchi (9) for a wide range of strain, there is a potential for volcanic ash curves to deviate from Zen and Higuchi's curves at smaller strains.

2.2.2 Damping curves

Reported values for the damping curves of clays have not significantly changed from the boundaries indicated by Seed and Idriss in 1970. Figure 8 depicts the comparison between volcanic ash curves and Seed & Idriss (8). There are three observations.

(1) At low strains (<0.0001) volcanic ash curves have low damping values and are positioned at the lower boundary of Seed & Idriss (8).

(2) At higher strains (>0.0001), volcanic ash curves show a steep gradient and hence, the curves travel from the lower boundary at low strains to the higher boundary at higher strains.

(3) The volcanic ash curves essentially lie within the boundaries of Seed & Idriss (8). Judging from the gradient of the volcanic ash curves, it appears that the damping can be significantly higher than Seed & Idriss at high strains (>0.002) but this is still to be experimentally verified.

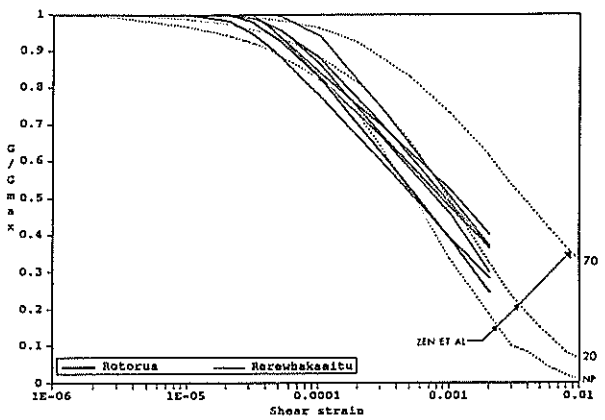

Figure 7. Comparison of G/G_{max} for volcanic ash and clays.

2.3 Volcanic ash compared with sands and gravelly soils.

2.3.1 Normalized shear modulus curves.

Seed et al (4) report that the boundaries indicated by Seed & Idriss (8) are generally representative of most sands. The curve for gravels may be a little flatter than that for sands.

Figure 9 compares volcanic ash curves and boundaries of Seed & Idriss (8). The following are observed:

(1) The volcanic ash curves have more extended G/G_{max} plateaus.

(2) Similar to the comparison with clays, the volcanic ash curves exhibit a sudden and rapid decay (between $1*10^{-5}$ and $1*10^{-4}$) as opposed to the more gradual decay of the boundaries for sands.

(3) The volcanic ash curves are not located near the mean curve for sands. Instead, they generally lie near the upper boundary. Hence, the volcanic ash curves do not closely compare with the mean curve of Seed & Idriss (8).

2.3.2 Damping curves.

Seed at al (4) concludes that damping ratios for sands and gravels are very similar. Figure 10 compares volcanic ash damping curves and the boundaries suggested by Seed et al (4). The observations are similar to those noted for volcanic ash versus clays. It is interesting to note that at low strains (<0.0001), volcanic ash curves consistently lie near the lower boundary for both sands and clays.

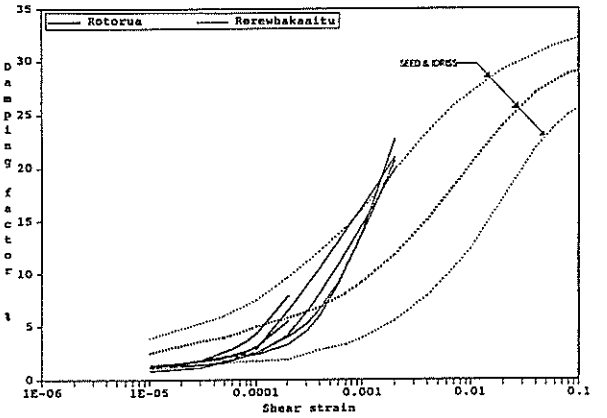

Figure 8. Comparison of damping curves for volcanic ash and clays.

2.4 Comparison of volcanic ash and residual Waitematas.

This comparison is initiated in an attempt to see if volcanic ash curves are significantly different from some known curves of local soils, obtained using the same equipment. Parton(10) and Larkin and Taylor(11) obtained curves for saturated residual Waitematas while

Plested(12) obtained results related to unsaturated residual Waitematas. It was found that the volcanic soils responded similarly to unsaturated Waitematas as far as shear modulus was concerned while the damping factors showed little correlation.

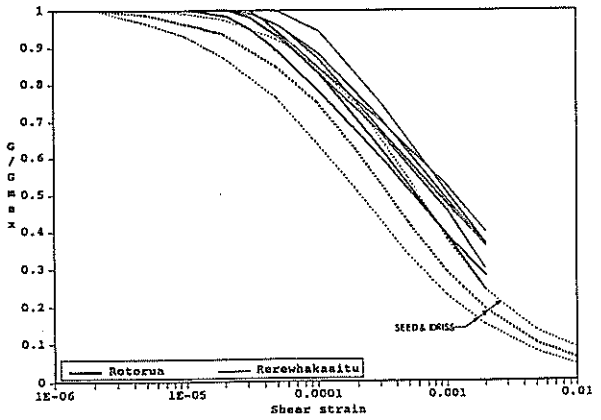

Figure 9. Comparison of G/G_{max} for volcanic ash and sands.

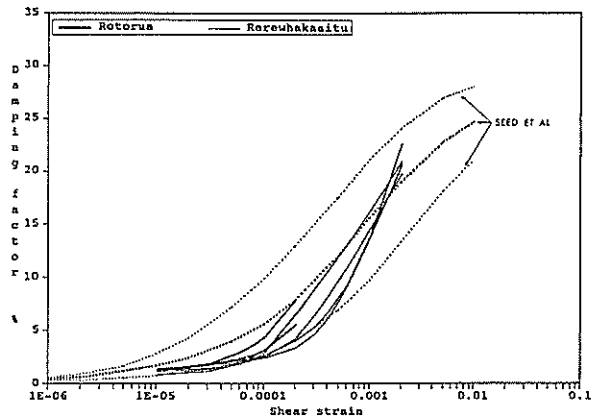

Figure 10. Comparison of damping curves for volcanic ash and sands.

3. SENSITIVITY OF SOIL RESPONSE ANALYSES TO DYNAMIC SOIL PROPERTIES.

The evaluation of dynamic soil properties is one of the key parameters used in theoretical seismic site response studies. This section of work investigates the sensitivity of computed results to variation in dynamic soil properties, especially with respect to volcanic soils. A comparison is made between the calculated earthquake response of a 30 metre layer of volcanic soil using the internationally used data base for sands and nonplastic silts, Seed and Idriss(8) and the data base formed from the measured properties presented in this paper.

The overseas data base for sands is shown in Figure 9 and in the absence of other information may be the source of the dynamic properties used in an analysis. This data base uses a value of G_{max} that is proportional to the square root of depth, where as the experimental data shows essentially a linear variation in G_{max} with depth, see Figure 3. Thus the maximum shear wave velocity at the

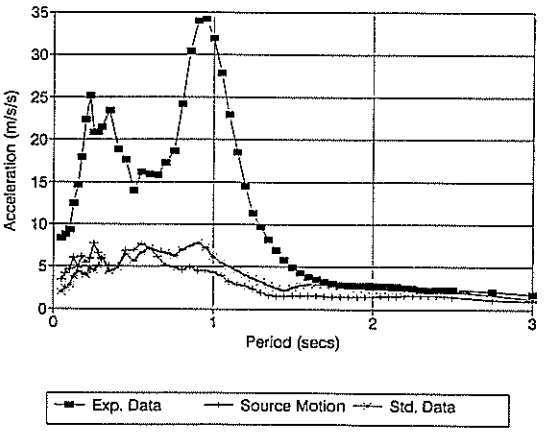

Figure 11. Comparison of Surface Response Spectra.

soil/bedrock interface predicted for the volcanic soil on the basis of the experimental work presented here is 146 m/s, while that obtained using the data set of Seed and Idriss is 262 m/s. This significant factor along with a different relationship between shear modulus and shear strain form the differences in the analyses. The overseas data base was used with an estimation of the relative density of the soil of 70%.

The 30m profile was analysed using a method of nonlinear analyses described by Larkin (13) using the computer program DENSOR. The earthquake used had a peak bedrock acceleration of 0.3g. Figure 11 shows the ground surface response spectra computed using the two data bases as input for the constitutive relationship for the soil. The figure shows the very marked difference in the spectra obtained from the two analyses. The surface response using the experimental data from this study is up to four times that using the existing standard data base established for sands. Very different conclusions and design constraints would result from the analyses. This example illustrates the sensitivity of dynamic analyses to the soil property data and highlights the need for much care and investigation of alternatives when performing theoretical seismic soil response analyses. The divergence of results is caused mostly by the difference in the way G_{max} varies as a function of the overburden stress, but the results are also sensitive to the shape of shear modulus curve.

4. CONCLUSIONS

Normalized shear modulus and damping curves for the volcanic ash samples did not significantly deviate from the general trend of proposed 'standard' curves for clays and sands. It is concluded that the volcanic ash modulus curves fit well with the 'standard' curves for clays while the damping curves fit slightly better with sands. When compared with some limited data of local Waitemata soils, the volcanic ash modulus curves showed similar behaviour to unsaturated Waitematas while the damping curves did not indicate any observable trend.

The above comparisons have also revealed certain characteristics of the volcanic ash curves which are different to the 'standard' curves of clays and sands.

The following conclusions are for the volcanic ash samples

(1) The G/G_{max} and damping curves are essentially independent of confining pressure.

(2) Volcanic ash G/G_{max} curves fit reasonably well with summarized G/G_{max} curves for clays. In contrast, they do not fit well with sands because they are much higher than the mean curve.

(3) Volcanic ash damping curves fit slightly better with sands than clays in the sense that the curves are relatively closer to the mean curve for sands for most parts of the strain range.

(4) The volcanic ash G/G_{max} curves show similar behaviour with unsaturated Waitematas. Saturated Waitematas, on the other hand, are located to the right, indicating a more gradual attenuation. No trend was observed for the damping curves. Further data is needed to confirm these results.

(5) The volcanic ash G/G_{max} curves contain longer low strain plateaus, reaching $5*10^{-5}$. In addition, the attenuation from the plateau are sudden and rapid - this occurs between strains of $1*10^{-5}$ and $1*10^{-4}$.

(6) The volcanic ash damping curves indicate low damping factors at low strains ($<1*10^{-4}$), steep curve gradients at higher strains ($>1*10^{-4}$) and damping values which are possibly significantly higher than the mean curves of clays and sands for strains greater than 0.002.

The results of a seismic analysis of a layer of volcanic ash soil is shown to be very sensitive to the dynamic soil properties used. Care must be taken in selecting such properties and a number of analyses performed to gauge the spread of results and the sensitivity to the data.

REFERENCES

1. LARKIN,T.J. and DONOVAN N.C.(1979). "Sensitivity of Computed Nonlinear Effective Stress Soil Response to Shear Modulus Relationships", Proc Second US National Conference on Earthquake Engineering, Stanford, August, pp. 573-582.

2. CHAN, S.Y. (1990) Measurement of Dynamic Properties of Some Volcanic Ash Soils., M.E.Thesis Department of Civil Engineering, University of Auckland.

3. SUN et al (1988) Dynamic Moduli and Damping Ratios for Cohesive Soils, Report No. UCB/EERC-88/15, University of California, Berkeley, August.

4. SEED et al (1986) "Moduli and Damping Factors for Dynamic Analyses of Cohesionless Soils". J.Geotechnical Eng., ASCE, Vol.112, No.11, pp. 1016-1032.

5. HARDIN, B.O. and DRNEVICH, V.P. (1972). "Shear Modulus and Damping in Soils : Design Equations and Curves." J.Soil Mechs and Found Div, ASCE, 98(7), pp. 667-692.

6. SHIBATA,T and SOELARNO, D.S. (1975). "Stress-strain Characteristics of Sands Under Cyclic Loading". Proc Japanese Society of Civil Engineers, No.239.

7. IWASAKI, T, et al (1976). "Dynamic Shear Deformation Properties of Sands for Wide Strain Range." Report of Civil Engineering Institute, No.1085, Ministry of Construction, Tokyo, Japan.

8. SEED, H.B. and IDRIS, I.M. (1970). Soil Moduli and Damping Factors for Dynamic Response Analysis, Report No. UCB/EERC-70/10, University of California, Berkeley.

9. ZEN,K and HIGUCHI, Y (1984). "Prediction of Vibratory Shear Modulus and Damping Ratio for Cohesive Soils". Proc Eighth International Conf on Earthquake Engineering, San Francisco, July, Vol.3, pp.23-30.

10. PARTON,I.M. (1972). Site Response to Earthquakes with reference to the Application of Microtremor Measurements, PhD thesis, University of Auckland.

11. LARKIN, T.J. and TAYLOR, P.W. (1977). Comparison of Downhole and Laboratory S Wave Velocities, Canadian Geotechnical Journal, Vol.16, pp. 152-162.

12. PLESTED, M.L. (1985). In situ Investigation of Shear Waves in Soil Media, PhD thesis, University of Auckland, School of Engineering Report No. 378.

13. LARKIN, T.J. (1979). "DENSOR - A Computer Program for Seismic Response Analysis of Nonlinear Horizontal Soil Layers", Report No. 51508-6, Norwegian Geotechnical Institute, Oslo, Norway.

Mountings for Measurement of Ground Vibrations

P.J. MOORE
B.E., M.S., Sc.D., M.I.E.Aust.
Reader in Civil Engineering, University of Melbourne
J.R. STYLES
B.E., M.Eng.Sc.
Senior Lecturer in Civil Engineering, University of Melbourne
A.CHANG
B.E.
Post Graduate Student, University of Melbourne

SUMMARY Studies have shown that mountings which support vibration transducers for free field vibration measurement may interact with the ground in such a way as to reduce the accuracy of vibration measurement particularly for high frequency vibrations. These theoretical studies form the basis for assessment of the accuracy of the vibration measurements in the field using different mountings. Geophysical surveys have been carried out at a field site to establish the ground geometry and the stiffness characteristics of the ground. Comparisons were made between the observed vibration amplitudes measured on different mountings placed on or just below the surface of the ground. The mountings used were either plates (surface mounted) or rods (varying depth of embedment), an accelerometer being attached to the upper surface of the mounting in each case. The source of vibration used was an electromagnetic vibrator which generated sinusoidal steady state vibrations. Study of the experimental data shows an approximate measure of agreement with theoretical predictions for some series of measurements, but for other measurements there was relatively little agreement for reasons that are not understood at this stage.

1. INTRODUCTION

With respect to the measurement of vibration amplitudes at the ground surface, much attention has centered on the transducers themselves and their characteristics (eg. Bradley and Eller (1961), Richart et al (1970) and Hanna (1985)). Relatively less attention has been given to the mounting of transducers. Brown (1971), for example, describes measurements of ground vibrations caused by construction equipment and by blasting operations. The transducers were mounted on a block of aluminium but no further details were provided. More recently Grant (1983) described an investigation in which he concluded that the measured ground motion can be considerably influenced by the performance of the mounting. He found that mounting shape, size, material type and method of installation all played prominent roles.

Regarding the measurement of ground vibrations from blasting operations, Dowding (1985) has mentioned that the type of mounting is least critical when the maximum particle accelerations are less than 0.3g. For greater accelerations he suggests that the mounting should be partially or completely buried if the ground surface consists of soil. These recommendations are quite inadequate.

Regarding earthquake vibrations, Crouse et al (1984) have commented on the desirability of satisfying two criteria:

(a) the base dimensions of the mounting are much smaller than the wavelengths of the seismic waves and

(b) the natural frequencies of the mounting are much greater than the seismic wave frequencies.

While these criteria are necessary for the accurate measurement of ground vibrations, they must be quantified to be useful in practice.

A theoretical examination into the performance of mountings for measurement of free field vertical and horizontal vibrations has been carried out by Moore (1986, 1988). This work showed how the magnitude of the error in the measurement of vibration amplitude depends upon the vibration frequency, the mounting geometry, the ground rigidity and the natural frequency of the mounting.

2. TRANSMISSIBILITY

The precision with which the vibration transducer correctly measures the ground vibration amplitude may be indicated by means of the displacement transmissibility (T_D). For a vertical sinusoidal ground vibration of amplitude Z_0, the displacement transmissibility is given by

$$T_D = \frac{A_Z}{Z_0} = \frac{[1 + (2D\ \omega/\omega_z)^2]^{1/2}}{[(1 - (\omega/\omega_z)^2)^2 + (2D\ \omega/\omega_z)^2]^{1/2}} \qquad (1)$$

where ω = frequency of ground vibration

ω_z = vertical natural frequency of the mounting (+ transducer) on the ground surface

= $(k_z/m)^{1/2}$

k_z = vertical stiffness of mounting on the ground

m = total mass of unit (mounting + transducer)

D = damping ratio

A_z = amplitude of vibration as measured by the transducer.

The damping ratio for many transducers is either in the vicinity of zero or around 0.7. The types of transducers mostly used by the authors are Brüel & Kjaer piezoelectric accelerometers. As stated by Serridge and Licht (1986) the damping ratios for these instruments are very low. In the following discussion the damping ratio will be taken as zero.

From equation (1) it is clear that the transducer will provide increasingly accurate measures of the amplitude of ground motion as the displacement transmissibility more closely approaches unity. As illustrated in Fig. 1, this is best achieved at low values of the frequency ratio. For example Fig. 1 shows that for zero damping and provided the frequency of ground motion is no greater than 30% of the natural frequency (f_n) the maximum error in the measurement of ground motion amplitude is 10%. Fig. 1 also shows that the errors in amplitude measurement may become quite large when the frequency of ground motion is greater than 50% of the natural frequency of the mounting unless considerable damping is present in the system.

3. INSTRUMENTATION AND EQUIPMENT

In order to determine experimentally the magnitudes of errors in free field vibration amplitude measurements at different frequencies of ground motion, a program of field testing was commenced. This involved using vertically mounted transducers and various plate and rod mountings covering a range of sizes. The plate mountings were made of timber, aluminium or steel and varied in diameter from 100mm to 400mm and in mass from 140g to 126kg. The rods were made of steel and varied from 10mm to 80mm in diameter and from 50mm to 200mm in length. The transducer used was a Brüel & Kjaer piezoelectric accelerometer type 4370. This was used in conjunction with a Brüel & Kjaer Charge Amplifier type 2635 which produces an output voltage proportional to the charge coming from the accelerometer.

The source of vibrations was provided by a Ling dynamic System Model 409 electromagnetic shaker. This shaker has an operating frequency range from 5Hz to 9kHz, and a maximum thrust of 196N. The shaker was attached to a steel footing placed on the ground surface. A transducer was attached to this footing to monitor the vibrations transmitted into the ground. The mass-spring resonance within the shaker occurred at 30Hz so this frequency was avoided in field testing. For most of the field testing the displacement amplitude of the shaker footing was kept at 2μm.

The signal generating system for the shaker was a Hewlett Packard Model 2000 wide range oscillator. For the field testing all of the electrical equipment was run off a portable petrol driven generator.

After passing through the charge amplifier, the signal generated by the transducer was fed into a Hewlett Packard (Model HP 3566OA) dynamic signal analyser for provision of the final output.

4. FIELD TESTING

Testing was carried out at Lyndhurst near Melbourne, the site consisting of a deposit of siliceous dune sand of fine to medium grain size. The dynamic moduli at the testing site were evaluated by means of a number of seismic refraction surveys.

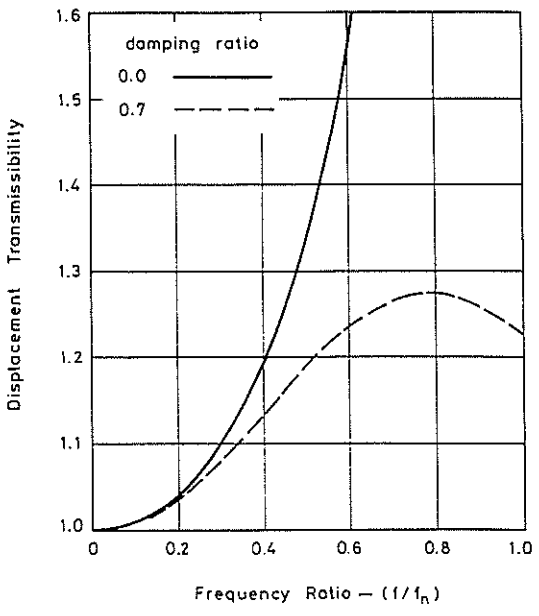

Fig. 1 Effect of Damping on Displacement Transmissibility

The geophones were placed collinearly in the ground and observations of first arrival times were made with forward and reverse shots. The results of two tests in the same general area with geophones spread over a distance of 45m are shown in Figs. 2 and 3. The results indicated that the P wave velocities varied slightly from test to test and that there was a small increase in velocity with depth. Overall it was concluded that there existed a surface layer of sand at least 5m in thickness with a shear modulus that was within the range of 27MPa to 33MPa. In calculating the shear modulus the Poisson's Ratio was assumed to be 0.3 and the soil density was measured at 1.9t/m^3.

Vibration amplitude measurements were carried out with the different mountings over a frequency range of 40 to 260 hertz. In most cases the mountings were located 1m from the shaker. Results for the timber mountings are shown in Fig. 4. No definite trends are apparent from this data. Since the calculated natural frequencies for these mountings (see Table 1) are relatively high the plotted data would appear to indicate the typical scatter of results to be expected at low frequency ratios with the ground motion being generally within the range of 5 to 10 x 10^{-8}m.

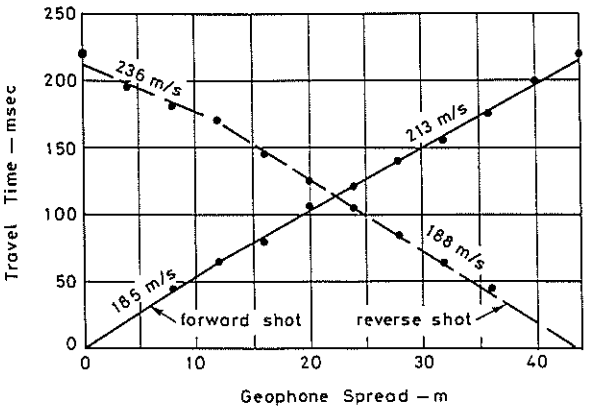

Fig. 2 First Spread Seismic Refraction
- Lyndhurst Site

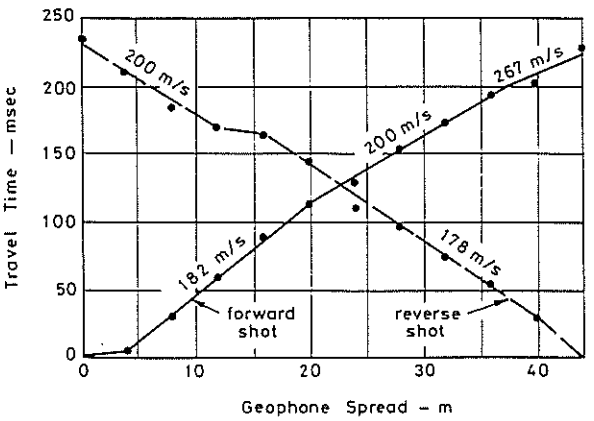

Fig. 3 Second spread Seismic Refraction
- Lyndhurst Site

TABLE 1

Natural Frequencies for Timber Mountings

Diameter (mm)	Mass (kg)	Natural Frequency (hertz)	
		G = 27MPa	G = 33MPa
100	0.14	1180	1310
200	0.48	900	1000
400	1.7	670	740

Fig. 5 shows results of vibration measurements taken with aluminium mountings. At low frequencies the amplitudes are of a similar magnitude to those obtained with the timber mountings. At the high frequency end of the observation range there appears to be a noticeable difference between the amplitudes measured with different size mountings. The larger mountings generate the larger observed amplitudes and, as shown in Table 2, this is consistent with the calculated decreases in natural frequency.

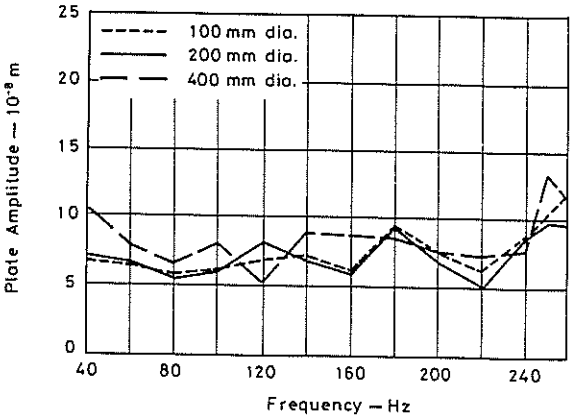

Fig. 4 Vibration Measurements with Timber Mountings

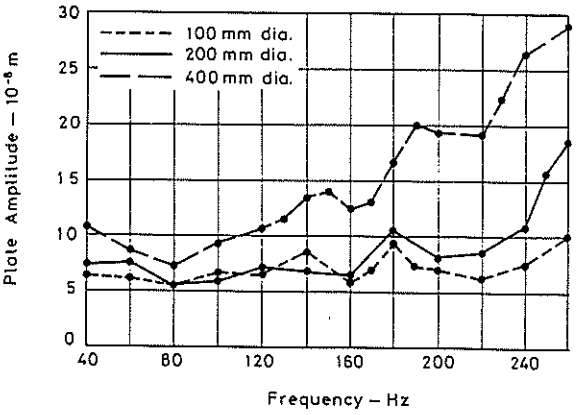

Fig. 5 Vibration Measurements with Aluminium Mountings

TABLE 2

Natural Frequencies for Aluminium Mountings

Diameter (mm)	Mass (kg)	Natural Frequency (hertz)	
		G = 27MPa	G = 33MPa
100	0.50	630	690
200	2.56	390	430
400	10.00	280	310

Figs. 6 and 7 show results of amplitude observations with mountings of different diameters and different total mass. With these observations actual peaks occur with the measured amplitudes. Based on the earlier discussion in this paper and on Fig. 1 those peaks would be expected to occur at or slightly below the natural frequency. As may be seen from the calculated natural frequencies in Table 3, such a level of agreement is only approximate.

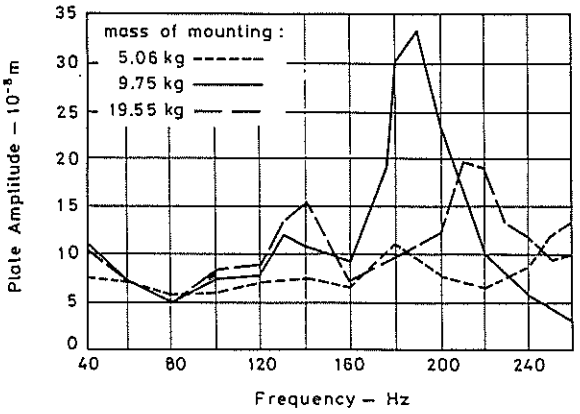

Fig. 6 Vibration Measurements with Steel Mountings - 200mm dia.

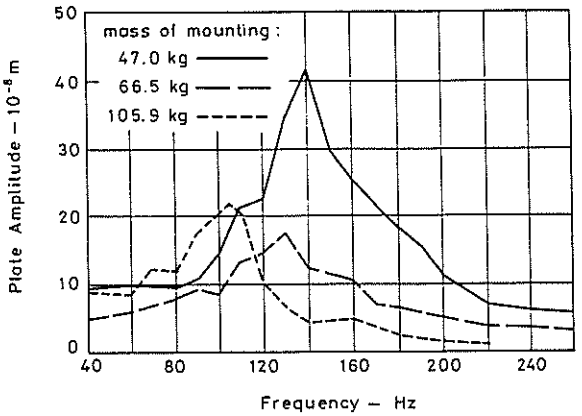

Fig. 7 Vibration Measurements with Steel Mountings - 400mm dia.

TABLE 3

Natural Frequencies for Steel Mountings

Diameter (mm)	Mass (kg)	Natural Frequency (hertz)	
		G = 27MPa	G = 33MPa
200	5.06	280	310
200	9.75	200	220
200	19.55	140	160
400	47.0	130	140
400	66.5	110	120
400	105.9	90	100

Fig. 8 shows the amplitude results obtained with steel rod mountings. At the high frequency end of the measuring range there appears to be a trend towards increased measured amplitudes as the rod length decreases. From Table 4 it is seen that the natural frequency increases as the rod length decreases. Additionally the natural frequencies are quite high in comparison with the frequencies used for the observations. It is considered that the measured amplitudes should provide a reasonable estimate of the ground motion and the reason for the apparent trend mentioned above is not known.

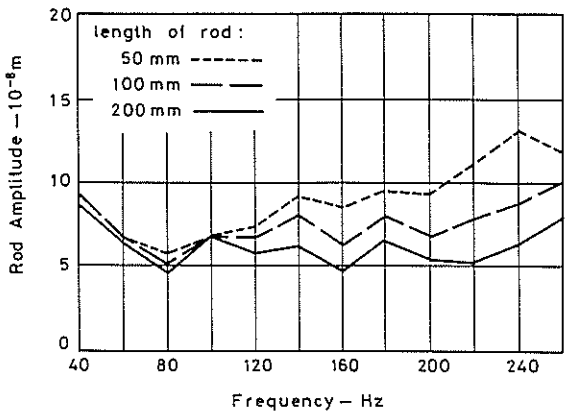

Fig. 8 Vibration Measurements with Steel Rods - 10mm dia.

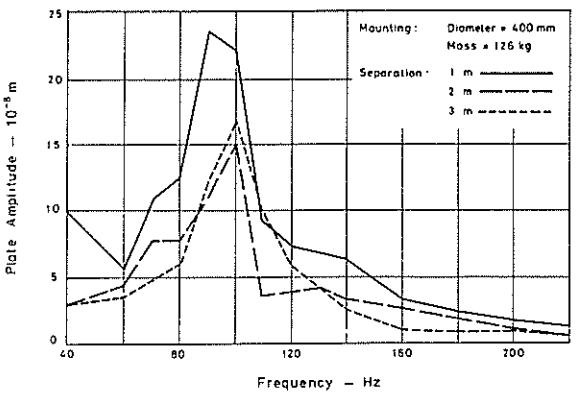

Fig. 9 Effect of Separation on Vibration Measurements

TABLE 4

Natural Frequencies for 10mm Dia. Rod Mountings

Length (mm)	Mass (g)	Natural Frequency (hertz)
50	25	2100
100	52	2000
200	108	1900

The effect of separation between the measurement point and the source of vibrations is illustrated in Fig. 9. The calculated natural frequency for this mounting is between 80 and 90 hertz so the observed peaks in the amplitude plots occur at slightly higher frequencies than would be predicted. This may be caused by increased stiffness of the ground resulting from the high confining pressure arising from this heavily loaded mounting. The expected decrease in observed vibration amplitude with increasing separation is only partially supported by these observations.

Fig. 10 shows comparisons between calculated and observed amplitude ratios for one particular mounting. The observed amplitude ratio is the ratio between the observed amplitude of the plate mounting and the observed average amplitude of the rod mountings, the latter being assumed to provide a reasonable estimate of the ground motion. The calculated amplitude ratios are based on the two estimates of natural frequency the curves

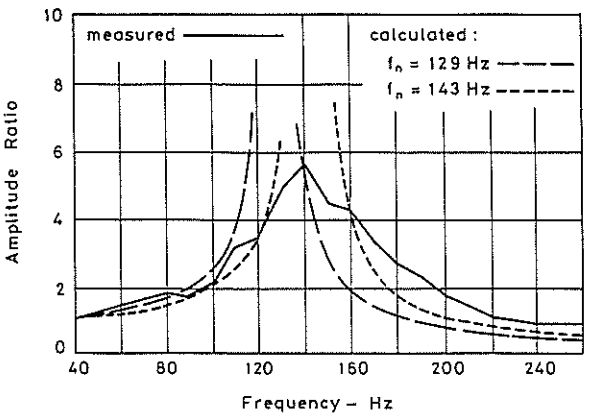

Fig. 10 Calculated and Observed Amplitude Ratios for 400mm dia. 47kg Mounting.

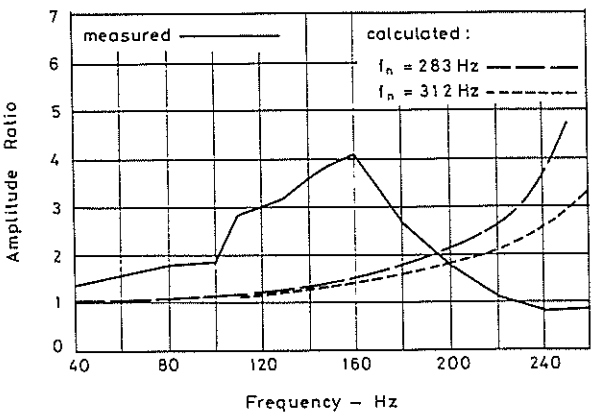

Fig. 11 Calculated and Observed Amplitude Ratios for 400mm dia. 9.8kg Mounting

plotted corresponding to zero damping. If allowance is made for damping which is clearly present in the observations then approximate agreement between calculated and observed amplitude ratios is evident. For some observations however this is not the case as illustrated in Fig. 11. The observed peak in the amplitude ratio in this case is significantly lower than the calculated peak for reasons which have yet to be understood.

5. CONCLUSIONS

For the majority of the vibration amplitudes observed at a field site, there is approximate agreement with theoretical predictions. The errors in vibration amplitude measurement tended to increase as the natural frequency for the mounting used, more closely approached the ground vibration frequency. In spite of the observed scatter in results the vibrations observed with the rod mountings appeared to provide the best overall estimate of the vibration levels in the ground.

6. REFERENCES

Bradley, W. and Eller, E.E. (1961), "Introduction to Shock and Vibration Measurements", Ch. 12 of Shock and Vibration Handbook, C.M. Harris and C.E. Crede, editors, Vol. I, pp. 12.1 - 12.24, McGraw Hill Book Co., New York.

Brown, L.M. (1971), "Measurements of Vibrations caused by Construction Equipment and Blasting", Dept. of Highways, Ontario, Report No. RR 172.

Crouse, C.B., Liang, G.C. and Martin, G.R. (1984), "Amplification of Earthquake Motions Recorded at an Accelerograph Station", Proc. 8th World Conf. on Earthquake Engineering, Vol. 2, pp 55-62.

Dowding, C.H., (1985), Blast vibration Monitoring and Control, Prentice-Hall Inc. New Jersey.

Grant, J.R.T. (1983), "Investigation into Transducer - Ground Coupling Techniques for Surface Blast Vibration Measurement", M.Eng.Sc. thesis, Faculty of Engineering, James Cook University of North Queensland.

Hanna, T.H. (1985), Field Instrumentation in Geotechnical Engineering, Trans Tech Publications, Federal Republic of Germany.

Moore, P.J. (1986), "Measurement of Vertical Ground Vibrations", Proc. of In-Situ '86, Use of In Situ Tests in Geotechnical Engineering, Blacksburg, Virginia, ASCE Geotechnical Special Publication No. 6, p 840-853.

Moore, P.J. (1988), "Performance of Mountings for Horizontal Ground Vibration Measurements", Fifth Aust.-N.Z. Conf. on Geomechanics, Sydney, pp 427-431.

Richart, F.E., Hall, J.R. and Woods, R.D., (1970), Vibration of Soils and Foundations, Prentice-Hall Inc, New Jersey.

Serridge, M. and Licht, T.R. (1986) Piezoelectric Accelerometer and Vibration Preamplifier Handbook. Brüel and Kjaer, Denmark.

Small Scale Variability of Reactive Soils in Western Sydney

G.R. MOSTYN
B.E., M.Eng.Sc., B.A., M.I.E.Aust.
Senior Lecturer, University of New South Wales, Kensington, N.S.W., Australia
M. WATERS
B.Sc., B.E., Grad.I.E.Aust.
Engineer, Dames & Moore, North Sydney, N.S.W., Australia

SUMMARY The Australian Standards AS2870 deal with the design of slabs and footings for residential construction, several methods of site classification are countenanced by these standards. One such method is the estimation of the maximum ground surface movement (y_s) and this is often based on shrink-swell index (I_{ss}) test results. The standard provides no guidance on the number of tests that should be completed. The paper describes a detailed site investigation on one site in western Sydney aimed at determining the small scale variability of the shrink-swell index. The site was selected with a view to minimising this variability. A comprehensive programme of laboratory testing was completed on samples obtained during the site investigation. The results of this programme were then analysed to determine the variability across the site. The results indicate that the variability is such that a single shrink-swell test result can be a very poor indicator of site reactivity even for this "low variability" site. In general at least two to three tests are required to classify a site with even low confidence. A detailed geotechnical log increases the value of test results almost three fold. For the site with relatively low variability two or three tests and a detailed log result in a site classification which is also relatively low in variability.

1 INTRODUCTION

Soils may be considered reactive or expansive if they undergo significant volume changes as the degree of saturation changes. Large variations of soil moisture conditions in the Australian environment mean that when reactive soils are present, they can have a severe effect on overlying light weight structures. Australian geotechnical practice has adopted methods to deal with reactive soils that are relatively sophisticated compared with those adopted in many other parts of the world.

As more information has become available, it has become apparent that the variability of these soils must be taken into account in site characterisation. The variability occurs over all scales including that of a typical Australian residential allotment even when conditions would appear to indicate that soil behaviour should be reasonably uniform (Moss and Bone, 1988).

This variability results in the extent of the site investigation required being uncertain as there is a conflict between cost and extent. This paper presents the results of an investigation to establish the least variation in reactivity that might be expected over a typical residential site. It also attempts to define the site investigation that would be adequate to establish representative values of surface movement.

2 AUSTRALIAN PRACTICE

The first Australian Standard that covered design of footings and slabs over reactive soils was released in 1986 (Standards Australia, 1986). This standard has been complimented by a commentary and map and subsequently revised and split into two parts (Standards Australia, 1988a, 1988b, 1988c and 1990). The potential for surface movement depends on two factors: (i) the potential for moisture change and (ii) the soil profile. The approach adopted in the Australian standards is to classify the site rather than the soil, in this manner both of the above two factors can be taken into account.

The various standards describe differing methods to classify a site, the language varies between standards and it is not always clear exactly what was intended by the drafting committee. Nevertheless three methods of classification are appropriate for reactive clay sites, these are:

* Visual assessment and interpretation of performance of existing buildings.
* Soil profile identification and classification from established data.
* Computation of predicted surface movement, y_s.

In general the determination of the predicted surface movement depends on (i) soil sampling and testing to provide Instability Indices for the soils encountered, and (ii) information on the design change in soil suction versus depth. The Instability Index, I_{pt}, is defined as the percent vertical strain per unit change in suction (in pF units), it is therefore like a modulus but is not constant. The standards provide a range of methods of determining I_{pt} by testing undisturbed samples. The standards also provide a set of recommended suction versus depth profiles for various places within Australia. Thus given an appropriate site investigation it is possible to predict the surface movement on a site and therefore to classify the site.

The standards do not give any indication of the scope of site investigation considered appropriate to classify a site. In a given area, for example Sydney, the site classification is almost entirely dependent on the value or values obtained for the Instability Index. With this in mind it was decided to investigate the variability of this property.

3 SITE SELECTION

It was intended to investigate the variability of the Instability Index for a given soil profile and therefore it was desirable for the selected site to satisfy as many of the following criteria as possible:

* Soil behaviour typical of the reactivities encountered in western Sydney. Thus this required an expected Moderate reactivity (i.e. Class M site).
* Low expected variability across the site so that the underlying variability could be established. Thus preferable sites would be flat with expected consistent subsurface conditions and away from the boundaries of profile units shown on available maps.
* Information already available regarding soil reactivity. Thus if possible sites that had been established by the CSIRO in Blacktown City would be ideal.
* Easy access for investigation, thus a co-operative owner, easy physical access and a minimum of subsurface services would be ideal.

Five sites were chosen from those detailed in Coffey and Partners (1985) and Moss and Bone (1988) and from discussions with the Government Architects Branch. Preliminary site visits were then completed.

There are two map series that may be used to assist with profile identification in the Sydney Region. The first is the Soil Associations of the County of Cumberland map, first published in the early 1960s by the N.S.W. Department of Agriculture and re-issued by Standards Australia (1988b). This map was intended for agricultural purposes but was indicated by the 1986 Standard to be useful for site classification. The second is a series of Soil Landscape maps published recently by the Soil Conservation Service (Chapman & Murphy, 1989; Bannerman & Hazelton, 1990). These maps were used to assess the potential for lateral variation across the site, and it was thus considered desirable to find a site which was well within a given unit on both series of maps and thus not near any map unit boundaries.

On the basis of the site visits, review of the maps and other information available for each site, it was decided that a site at Plumpton Park was almost ideal. This site was selected.

4 SITE DESCRIPTION

The selected site had many advantages for this investigation, amongst these were:

* The site was in the Cumberland Soil Association and the Blacktown Soil Landscape Unit and away from the boundaries of these map units. These are very extensive units which are typical of western Sydney and are expected to be Moderately reactive.
* The site was very flat with no large trees and no obvious activity by man except having been cleared some time ago. Thus access was easy and no subsurface services were expected.
* The site was apparently owned by the Blacktown City Council and awaiting future subdivision, so permission could be obtained to complete a site investigation.
* Immediately adjacent to the chosen site was a Ground Movement Station (not currently operating) and there was considerable data already available about the subsurface soils and their reactivity. In fact Coffey and Partners (1985) had estimated the surface movement at the site as between 32 and 36mm, i.e. Class M.

5 FIELD WORK

The field work consisted of three simple stages:

* A site visit was completed as part of the site selection process. The surface features of the site were recorded during this visit.
* Seven boreholes were augered on the site on the 12th July 1990. These bores were located on the two arms of an "L" shaped pattern, one arm extending north along the slope and the other east down the gentle slope. Holes were located at the intersection of the two arms and at 5 and 30 m along each arm, two holes were redrilled for better logging and to provide some redundant samples. Undisturbed samples were obtained almost continuously for the first 2 metres. In general samples were started at 0.15, 0.60, 1.10 and 1.60m depths.
* Three test pits were excavated with a backhoe on the 8th August 1990, these enabled some large disturbed samples to be obtained and for the profile to be better established.

6 LABORATORY WORK

In general shrink-swell tests were completed on each of the samples. Sometimes more than one test could be completed on a sample and other times more than one shrink or swell stage could be completed.

These tests were completed in accordance with the methods outlined in the Draft Australian Standard DR89116 "Methods of testing soils for engineering purposes - Method G1.3: Soil reactivity tests". The test basically consists of obtaining two undisturbed sub-samples and measuring the shrink strain, ε_{sh}, from in-situ conditions on one and the swell strain, ε_{sw}, from in-situ conditions under a light surcharge on the other. A shrink-swell index, I_{ss}, is then determined from assumed values of the change in soil suction and ratio between the slope of the shrink (unrestrained) and swell (restrained) strain versus moisture content relationship.

A limited program of laboratory suction measurements was completed using psychrometer and filter paper techniques. Finally classification testing was undertaken, this included linear shrinkage, Atterberg limits and particle size analyses.

7 FACTUAL RESULTS

The soil profile is shown on Figure 1, and consists of:

* A clayey silt topsoil to a depth of between 0.2 and 0.3 metres, overlying
* A mottled red-brown and grey silty clay of intermediate plasticity with shale and siltstone fragments to 70mm and rare ironstone bands, this is layer 2 and 3 on Figure 1. This graded at approximately 1 metre depth to
* A grey silty clay of intermediate plasticity with rock fragments to 200mm diameter, which inturn graded to
* Grey siltstone at between 1.8 and 2.8 m depth.

The profile was relatively consistent across the area investigated, the depths at which one layer changes into an-

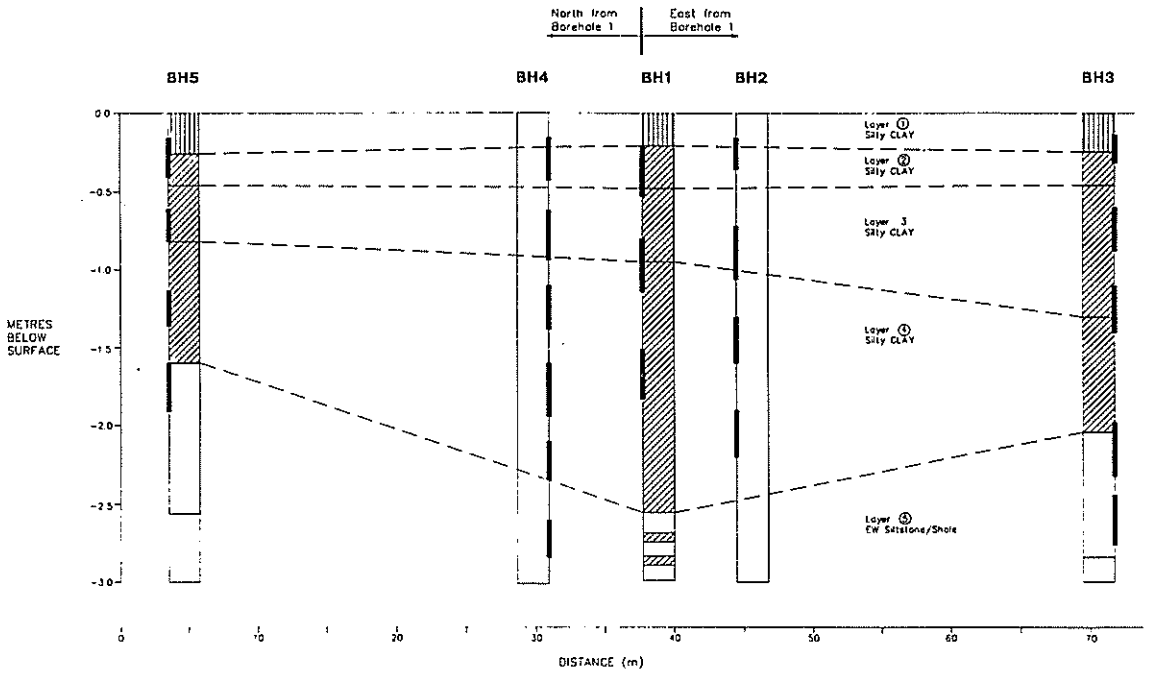

Figure 1 Geotechnical section through the site investigation

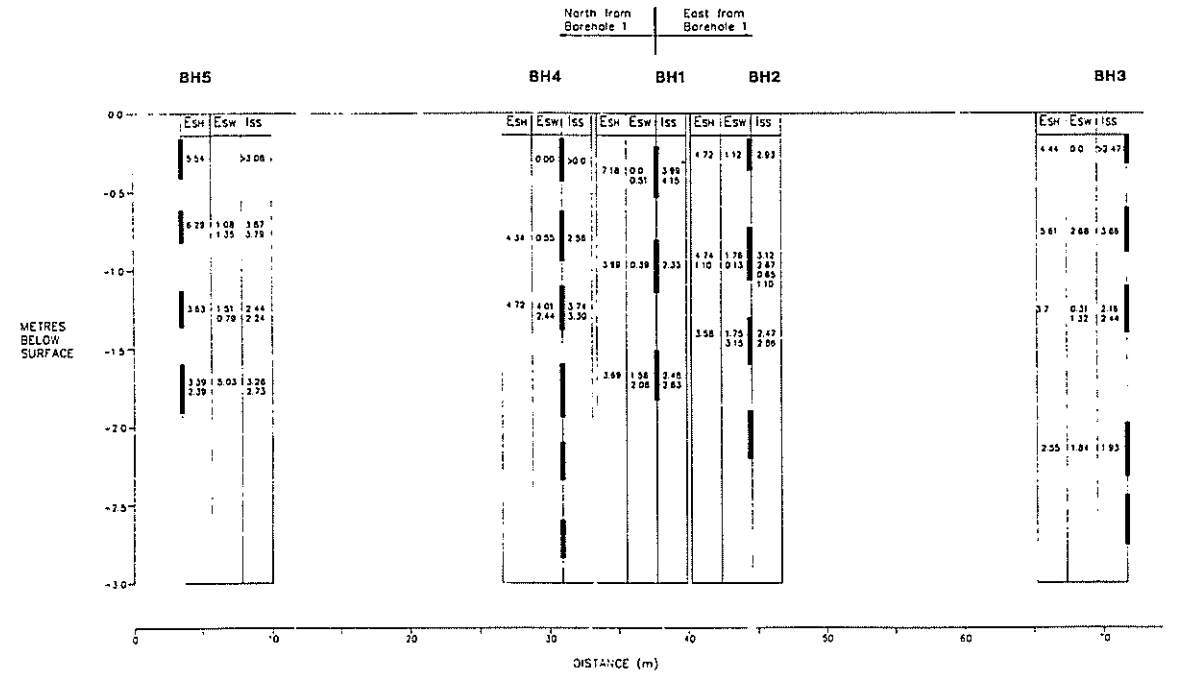

Figure 2 Summary of factual data

other are a little arbitrary as all boundaries were gradational.

The results of the shrink-swell tests are presented on Figure 2, this shows all ε_{sh}, ε_{sw} and I_{ss} results. Where two shrink or swell stages were completed on a sample, these have been combined to produce more than one I_{ss}. In all 28 results for I_{ss} were determined.

8 ANALYSIS OF RESULTS

There are a number of approaches that can be adopted to determine site reactivity given the 28 I_{ss} results obtained from 5 boreholes. These different approaches and the implications are discussed in the following sections.

8.1 Single Test

In some site investigations a single shrink-swell test may

be completed and used to characterise the site reactivity. The results of this current investigation can be used to simulate 28 single test investigations on the basis that any one of the samples or tests may have been undertaken to characterise the site. For this series of tests the mean I_{ss} was 2.69% with a standard deviation of 0.97%. This is equivalent to an average y_s of 41.4mm in the Sydney region and the site would be classed on the average as (low) Class H, i.e. virtually on the boundary with Class M.

If it is assumed that I_{ss} is normally distributed, which is not unreasonable, then a single shrink-swell test would result in the site being classified as Class S 7.6% of the time, Class M 39% of the time, Class H 51% of the time and even Class E 2.7% of the time. Similar values are determined if the percentages are estimated simply from the raw data. The conclusions do not alter very much even if the obviously unreliable result from BH 4 at 0.15m of 0% and the deep result from BH 3 at 2.5m are ignored. In which case the percentages are 3.4, 36, 59 and 2.0 respectively.

The above indicates that there is considerable variability associated with the use of only one shrink-swell test even on this site which was selected because it was expected to have low variability.

A more reasonable assessment of a one test site classification may be based on the 17 results obtained from between 0.6 and 1.3m depth, i.e. below the topsoil and above the level at which suction changes are small. These tests have a mean of 2.68% and a standard deviation of 0.91% and thus the site classifications obtained would be Class S 6.4%, Class M 40%, Class H 51% and Class E 2.0%. These are almost identical to those discussed above.

8.2 Single Borehole

The information can be viewed as five separate boreholes, from each of which several shrink-swell test results have been obtained. In this case the site could be classified from each of these boreholes by a number of different methods. Firstly the shrink-swell behaviour of the soil at any depth could be taken as that obtained from the sample nearest to it, i.e. boundaries to each layer are taken as the mid-point between each pair of samples. This may be the approach adopted if the borehole had not been carefully logged. The classifications of the site obtained using this method are given in the "mid-point" row of Table I.

An alternate is to use the borehole information and engineering judgement to decide the extent of each layer, the result of this method is given in the "geotechnical" row of Table I. Finally it is usual practice to remove the topsoil prior to constructing a residential slab, in this situation the suction changes that are applicable to the site are those occuring over the depth of influence below the topsoil, results of this method, adopting geotechnically based layers, are given in the "topsoil removed" row of Table I.

From the above it is apparent that in this case the mid-point method (mean 46.4mm, s.d. 6.43mm) over estimates the thickness of the reactive soils compared with the geotechnical assessment (mean 38.6mm, s.d. 3.78mm) and therefore over estimates the site reactivity. In addition it is clear that removing the topsoil can have a large influence on the expected surface movement (mean 54.4mm, s.d. 6.35mm) and should be taken into account when classifying a site.

TABLE I
SURFACE MOVEMENT BY BOREHOLE PROFILE

Method	BH 1	BH 2	BH 3	BH 4	BH 5
Midpoint	51	45	42	36	48
Geotechnical	37	40	33	40	43
Topsoil removed	46	62	51	59	54

Surface movement in mm

With the midpoint method layer thickness is purely a function of sample location and as would therefore be expected results in considerably larger scatter than the geotechnical assessment of layering. This indicates the importance of accurately logging the borehole and not just using it as a means of obtaining samples. It can be seen that multiple tests in a single borehole produces relatively low variability in the resulting site classifications.

8.3 Multiple Tests

One potential method of classifying the site would be to undertake more than one shrink-swell test and adopt the mean I_{ss} to characterise the site. An approximate idea of the classifications that would result from repeated such investigations can be obtained by random sampling from the existing test base (ignoring the two outriders). Table II shows the frequency that would be obtained for each class for varying numbers of tests.

TABLE II
FREQUENCY OF VARIOUS CLASSIFICATIONS

No of tests	Site classification			
	S	M	H	E
1	3.4	36	59	2.0
2	-	36	64	-
3	-	32	68	-
5	-	28	72	-
10	-	20	80	-

8.4 Variability

One useful way of assessing the relative merits of different site investigation procedures is to determine how often a particular method would predict the surface movement, y_s, to within, say, plus or minus 5mm of the mean as this is roughly half a class. Following this criterion, the following results are obtained:

Method	Percentage y_s within ± 5mm
Single test	30
Midpoint	56
Geotechnical	81
Two tests	42
Three tests	50
Five tests	61
Ten tests	78

As can be seen from the above:

* A single test results in a very poor classification.
* Three to five tests represents a significant improvement in reducing the variability but at a cost.
* The variability for the midpoint method (which used about five test results for each hole) and for random sampling using five tests is about the same.
* The simple measure of completing a detailed log of a borehole results in the same increase in accuracy of classification as almost trebling the number of tests completed (i.e. in this case the midpoint method is equivalent to about four tests, while the geotechnical method is equivalent to greater than 10 tests).

9 RECOMMENDATIONS AND CONCLUSIONS

The investigation indicated that if a single test is undertaken there is very large variability in the resulting site classification even on this site which was selected because of its expected low variability. Other sites which were not as geotechnically uniform would presumably show considerably more variability.

The best method of classifying a site based on shrink-swell test results is to accurately log a borehole and complete a few, at least two and three is considerably better, tests and then determine y_s from these results. It should be noted that the extra information obtained from a detailed log means that this is not the same as just completing three tests on a site and taking the mean I_{ss} to characterise the site. In fact this approach yields the same level of confidence in the classification as randomly completing over 10 shrink-swell tests. In addition detailed logging will alert the investigator to the presence of fill on the site, which is known to cause many problems with reactive soils in Sydney.

10 ACKNOWLEDGEMENTS

The authors would like to acknowledge the financial assistance given by Mr Don Katauskas and the technical assistance of Mr Bruce Walker both of Jeffery & Katauskas, Sydney.

11 REFERENCES

1. Bannerman, S.M. and Hazelton, P.A. (1990) "Soil Landscapes of the Penrith 1:100 000 Sheet" Soil Conservation Service of New South Wales, Sydney (and accompanying map).

2. Chapman, G.A. and Murphy, C.L. (1989) "Soil Landscapes of the Sydney 1:100 000 Sheet" Soil Conservation Service of New South Wales, Sydney (and accompanying map).

3. Coffey and Partners Pty Ltd (1985) "Sydney Swelling Soils Study - Analysis of Data" Report No. S7032/2-AD prepared for the N.S.W. Builders Licensing Board (Unpublished).

4. Moss, D. and Bone, L. (1988) "Reactive Clays in the Sydney Region" Final Year Project, School of Civil Engineering, University of New South Wales, Sydney (Unpublished).

5. Standards Association of Australia (1986) "AS2870-1986 Residential Slabs and Footings" SAA, Sydney.

6. Standards Association of Australia (1988a) "AS2870 Supplement 1-1988 Commentary - Residential Slabs and Footings" SAA, Sydney.

7. Standards Association of Australia (1988b) "AS2870 Supplement 2-1988 Soil Associations of the County of Cumberland Map (Sheets 1 to 3) - Residential Slabs and Footings" SAA, Sydney.

8. Standards Association of Australia (1988c) "AS2870.1-1988 Residential Slabs and Footings, Part 1: Construction" SAA, Sydney.

9. Standards Association of Australia (1989) "DR89116 Methods of Testing Soils for Engineering Purposes - Method G1.3: Soil Reactivity Tests" SAA, Sydney.

10. Standards Australia (1990) "AS2870.2-1990 Residential Slabs and Footings, Part 2: Guide to Design by Engineering Principles" Standards Australia, Sydney.

Model Pile Testing in Calcareous Sand and Silt in a Laboratory Calibration Chamber

A.K. PARKIN
Ph.D., M.I.E.Aust.
Senior Lecturer in Civil Engineering, Monash University
C.P. TAN
Ph.D., M.I.E.Aust.
Research Scientist, CSIRO Division of Geomechanics, Melbourne
Y.W. YEE
M.Eng.Sc.
Geotechnical Engineer, Ove Arup & Partner, Kuala Lumpur

SUMMARY This paper describes adaptations made to the Monash double-walled calibration chamber in order to study pile installation techiques and dynamic performance in a selection of saturated calcareous sands and silts, for application to structures in Bass Strait, Australia.

1. INTRODUCTION

In carbonate sands, such as those found in the hydrocarbon producing areas of Bass Strait, Australia, conventional driven piles have been found to provide extremely low uplift capacity (10-15 kPa), attributable to particle crushing (Angemeer et al., 1973). Whilst grouted insert piles have generally performed well in such materials, giving adhesions of > 400 kPa (Hyden et al., 1988), their installation is slow and expensive.

Because initial developments in the technology of the driven grouted pile (DGP) showed promise of a more economic solution (Nauroy et al., 1988), a programme of development was undertaken by Esso Australia Ltd. at a variety of scales for application to platforms in Bass Strait. This paper reports on one component of this study, undertaken jointly by CSIRO Division of Geomechanics and Monash University, and based on modifications to a large CPT calibration chamber to accommodate the driving and cyclic load testing of model piles.

2. THE MONASH CPT CALIBRATION CHAMBER

The Monash Calibration Chamber is one of a family of six chambers of similar construction, designed specifically for the study of the CPT in samples of clean dry sand, and described in various places (e.g. Veismanis, 1974; Chapman, 1980, Belotti et al., 1982, etc.). In essence, the equipment consists of a large triaxial sample, 1.2m high by 1.8m high, enclosed in rubber membranes and compressed by a lateral water jacket and a base piston (Fig. 2). The exterior cell wall is of cavity construction to facilitate the imposition of K_o lateral restraint or the measurement of lateral volume change. . A hinged reaction frame (not shown) provides restraint to hold the cell together, whilst also mounting an electro-mechanical drive system for the CPT on the sample axis.

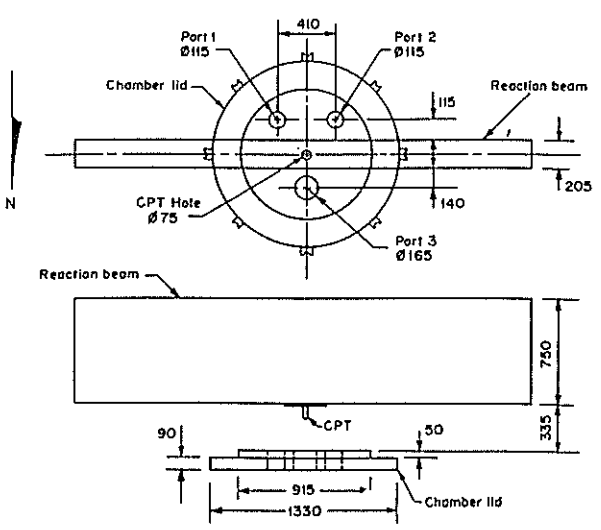

Fig. 1 Test pile layout and lid modifications

In normal use, sample formation is by raining from a stationary sand spreader that is lifted over the top of the chamber (with the reaction frame tilted away). The Monash equipment, which originates in a design from the Norwegian Geotechnical Institute (Parkin and Lunne, 1982), allows very homogeneous samples to be prepared at a range of relative density (50-100%) by controlling the rate of deposition through screen plates of various sizes. However, samples of lower D_r are much less uniform

3. EQUIPMENT DEVELOPMENT FOR MODEL PILE TESTING

3.1 Calibration Chamber and Reaction Beam

Because of the rather narrow profile of the reaction beam, it was possible to devise a test arrangement wherein three model piles could be tested in a single chamber sample of sand, whilst allowing a CPT test to be performed on the sample centreline. The resulting arrangement (Fig. 1) provided for two 100mm piles to be driven on one side of the beam and one 150mm pile on the other, with each pile having a minimum clearance of 2D from the others and from the sample boundary (ignoring the CPT). The necessary access holes were bored through the chamber lid and the underlying 40mm plywood sample platen, each being provided with a split collar for pile guidance and a bolted cover when not in use. Seals (consisting of O-rings and rubber gaskets) were provided at each position between the lid and platen to allow the cavity to be evacuated (for sealing the main membrane).

Mountings for a 25 t Instron jack were welded onto the sides of the reaction beam to service each of the pile locations, with the jack being rotated around these positions as required. In the case of Port 3 (150mm pile), the position was already occupied by the drive unit for the CPT, which therefore had to be transferred to a hinged table. The jack was connected to piles via a positive coupling (for 2-way loading) that incorporated two load cells as well as making allowance for misalignment.

3.2 Sand Spreader

Because the calcareous materials to be used in this study were particularly dusty, the existing sand spreader was modified to provide a complete dust seal. This included sealing the slideway for the

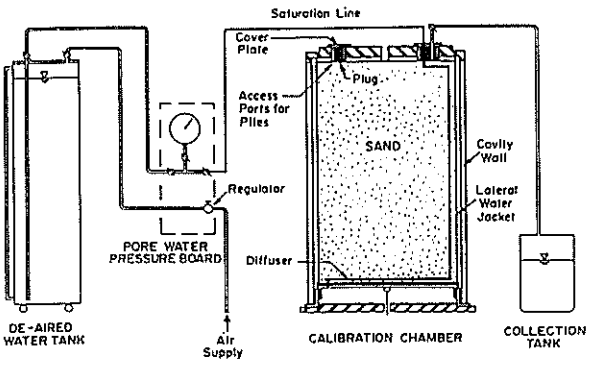

Fig. 2 The Monash calibration chamber

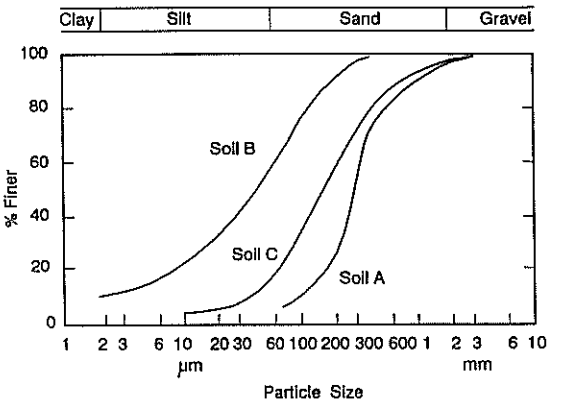

Fig. 3 Particle size distributions

shutter assembly and conversion of the perspex under-barred to steel. However, it was more difficult to extend these provisions to the lifting mechanism for the travelling screen unit, and it was judged that this could be eliminated without serious effect.

3.3 Saturation Arrangements

Whilst the sand spreader can only place samples of very dry sand, substantially saturated samples were required for the pile investigation. Unlike the quasi-static cone test, it was necessary to be able to model dynamic driving and cyclic load conditions, as well as to provide a realistic environment for grouting operations. In the system adopted, de-aired water was fed from saturation water tank at a low pressure, entering the sample through one of the pile ports (Fig. 2) before discharging through a spiral diffuser of perforated pipe at the sample base. Excess water was collected from the top and measured for the purpose of calculating sample saturation, the flushing continuing until the effluent water was judged to be reasonably free of entrained air.

4. MATERIALS

The investigation used three different materials, designated A, B and C, all highly calcareous and ranging from a medium sand through to a sandy silt (Fig. 3). Soil A was recovered from the Kingfish B area of Bass Strait, and consisted largely of coral and shell fragments, whilst Soil C was obtained from an on-shore deposit of calcarenite at a test site in South Australia. Both soils were air dried and passed through a 4.75mm sieve, but Soil C contained a proportion of cohesive lumps that needed to be broken down by hand. By contrast, Soil B was produced by finely grinding 1.5 m^3 of Soil A to a grading representative of another Bass Strait site. However, as might be expected, this processing failed to preserve the porous nature of the particles, which is clearly evident in the density limits (Table I) as well as other effects reported later.

5. TEST SAMPLE FORMATION

As samples were required to simulate in-situ formations, target void ratios were specified, but beyond this there was little to predict how these very silty materials would respond to usual methods of sample formation. However, it was clear that they would have to be dense as the base piston had a very limited stroke (67mm or 3.7%) to accommodate all the volume change from saturation, consolidation and the driving of three piles.

Preliminary trials indicated that a 10mm screen plate would be most appropriate for the coarser sands, but, during full-scale placement, flow from the sand spreader was found to be reluctant (because of fines-induced cohesion) unless assisted by a concrete vibrator. For the first sample of Soil A (CH 1), the void ratio of 1.38 (D_r = 28%) was appreciably over target (1.20), but this could not be corrected by the use of a finer screen as flow would have ceased altogether. Soil C, although finer than Soil A was also rained in the first instance (CH 2A), but produced a sample of such low density that the volume changes on saturation/consolidation caused the rubber membranes to be torn from the base piston. Several weeks were lost, and the replacement sample (CH 2B) had to be placed wet by stamping (because of the impracticality of drying in time), by which a void ratio of 1.33 was achieved.

For Soil B, being much finer again, it was quite clear that new methods were required, and that these would have to limit consolidation settlement to the smallest possible amount. A sample mixed to field water content (at field void ratio of 0.95) was found to be near-liquid and quite unsuitable for placement, indicating that the ground material was a poor analogue of a natural calcareous silt. The soil was therefore pre-mixed in a paddle mixer at w = 18% (approx. optimum), being the minimum water content at which the soil could be worked and brought to saturation during compaction (as evidenced by laitance formation on top).

Because of the time required to grind a sufficient quantity of Soil B, it was not possible to form a full sample therewith. Hence the lower 0.7m of CH 3 was built up from moist (w = 35%) Soil A (where it was below the reach of test piles) and covered with Terram fabric before completion of sample construction with Soil B. Mixed soil was delivered by bucket and compacted by stamping, with gyratory floating found to be an effective way of finishing each layer. Because of the considerable forces of compaction transferred to the sample former, it was found to be necessary to fill the external water jacket at the same rate as the sample, in order to provide lateral support. The void ratios achieved were 0.52 (cf. 0.95 in-situ) and 1.00 in Soils B and A respectively.

Unlike other samples formed in the dry, it could not be expected that this sample, being saturated, would derive sufficient support from the water jacket to allow removal of the sample former and placement of the top platen. Therefore suction was applied to the base diffuser for five days, until a suction of 40 kPa was reached on a pore-pressure transducer installed near the Soil A/Soil B interface. During this time, a substantial volume of water was collected in the water trap of the vacuum pump and the sample surface settled 15mm (made up by dry soil placed on top).

After seating and sealing the plywood top platen (which required the application of > 23mm Hg vacuum for the full duration of a chamber test), samples were consolidated to a prescribed test condition. Whilst it is common practice to use K_o consolidation for chamber samples, this was not possible here because of the limitation on piston travel. Instead the lateral pressure was first raised in stages to about 60% of the required value, after which the vertical pressure was raised and consolidation then completed at K = 1. However, a K_o condition was imposed whilst a CPT test was conducted, and maintained during the driving of piles.

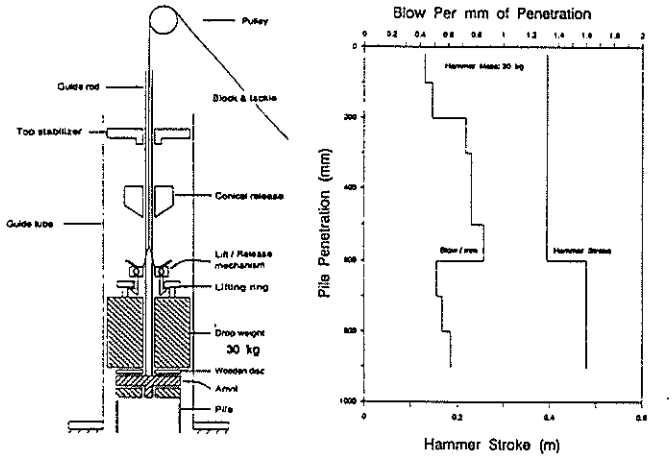

Fig. 4. Pile driving equipment and typical record

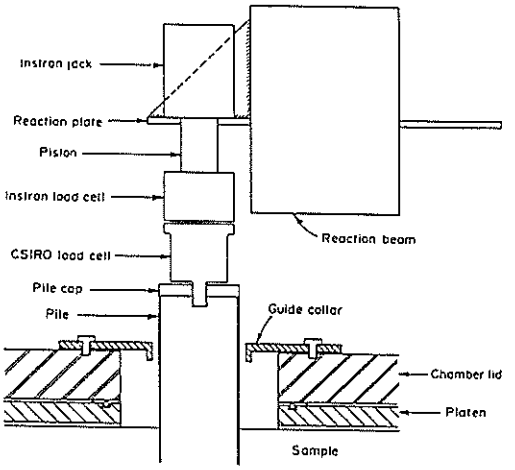

Fig. 5. Pile loading arrangement

6. PILE TESTING PROGRAMME

6.1 Model Piles and Driving System

Test piles were fabricated from steel tube of 100 and 150mm OD, with 5mm wall and a 26° external bevel on the leading edge. All piles were 1.3m long, allowing for 0.9m embedment, and were provided with a steel top cap with a central screwed hole. Piles were fitted with external strain gauges at six levels and grout ports at three levels. For installation, a pile-driving system was attached, consisting essentially of a 20kg donut hammer sliding on a guide rod that screwed into the pile cap (Fig. 4). An external tube attached to the jack reaction plate provided directional guidance to the pile.

When the embedded piezometers (at 0.55 and 1.00m depth) indicated a satisfactory dissipation of excess pore-pressures arising from consolidation and CPT testing, the selected pile port was opened and pile driving commenced under K_o conditions. For this phase, one of the uppermost strain gauges was connected to a high speed logger for stress measurement at the instant of impact. During driving in the two natural sands (A and C), the lateral pressure fell steadily from its initial value (280 kPa) to about 200 kPa after some 0.5m penetration, evidently due to particle crushing and consolidation induced by dynamic driving stresses. Whilst even greater reductions may occur in-situ, this was felt to be a prudent minimum for the model situation so that driving was interrupted at this point while the pressure was raised to 225 kPa. Pressure loss during driving was much less for Soil B because of its greater density and less compressible particles.

Table 1 - Physical Properties of Soils

Soil	G	ρ min (t/m^3)	ρ (t/m^3)
A	2.71	1.07	1.34
B	2.71	1.45	1.74
C	2.68	1.03	1.34

Table II - CPT Results

Test	Soil	σ_3 (kPa)	q_c(MPa)	f_s(kPa)	F.R.
CH1	A	275	7.8	69	0.88
CH4	A	267	7.55	66	0.88
CH2B	C/A	272	6.35	63	0.99
CH3	B/A	280	12.7	126	0.99

On reaching prescribed depth, the height of the internal soil plug was plumbed through the pile cap, after which the jacking system was installed and connected to the pile head (Fig. 5). The pile testing sequence then consisted of an initial static pull test (at a displacement rate of 1mm/min up to peak), followed by grout injection through the pile wall (after relaxation to zero load), with a sequence of reversing cyclic load applied thereafter. However, only the pull tests are reported here.

6.2 Test Results

CPT tests across the four samples recorded here showed significant differences arising from both material variations and the manner of sample formation (Fig. 6). For the pluviated samples of Soil A (CH 1 and 4), tip resistance clearly reflects density variations during the three "pours" required to form the sample, the humps being associated with interfaces where the soil appears to have been enriched with fines (unlike clean sands). By contrast, the sample of Soil C (which was formed by stamping wet sand, following the collapse of sample CH 2A) showed a tip resistance that clearly reflects variations in initial moisture content, as sampled during placement. Whilst the same method of placement was used for Soil B (CH 3), the degree of control is clearly better as a result of the material being mixed from dry to a controlled water content. Here, a plateau is attained at about 12 MPa before coming under the influence of the fabric interface. Numerical results, as summarised in Table II, show a friction ratio increasing somewhat in the more silty materials (as it should) and a significantly greater strength in the dense and less crushable Soil B.

Although the dynamic resistance increased throughout pile driving, the nominal average skin friction (obtained from pile head force and embedded area) dropped rapidly with penetration, evidently as a result of particle crushing on the interface, Fig. 7 being typical (as also observed by Poulos, 1988). By plumbing the pile core, it was apparent that there had been negligible plugging, with the soil plug occupying 70% of the embedded volume for the sandy materials and 110% for the silty Soil B (due to its greater density). From the size of the soil plugs, it follows that base resistance during driving was not great and that remoulding of the external soil had been negligible. Therefore, it is probable that a clearance of 2D between piles is sufficient to ensure their independent action in such materials.

On pull testing, the load displacement curves show a significantly greater capacity for the larger 150mm pile, as would be expected, but elsewhere capacity appears to decrease in the finer materials (Fig. 8; also Table III). From the strain gauge output at maximum load, pile load-depth relationships were derived and plotted against a normalised depth z/L (Figs. 9 and 10). On the basis of fig. 7 and the inferred

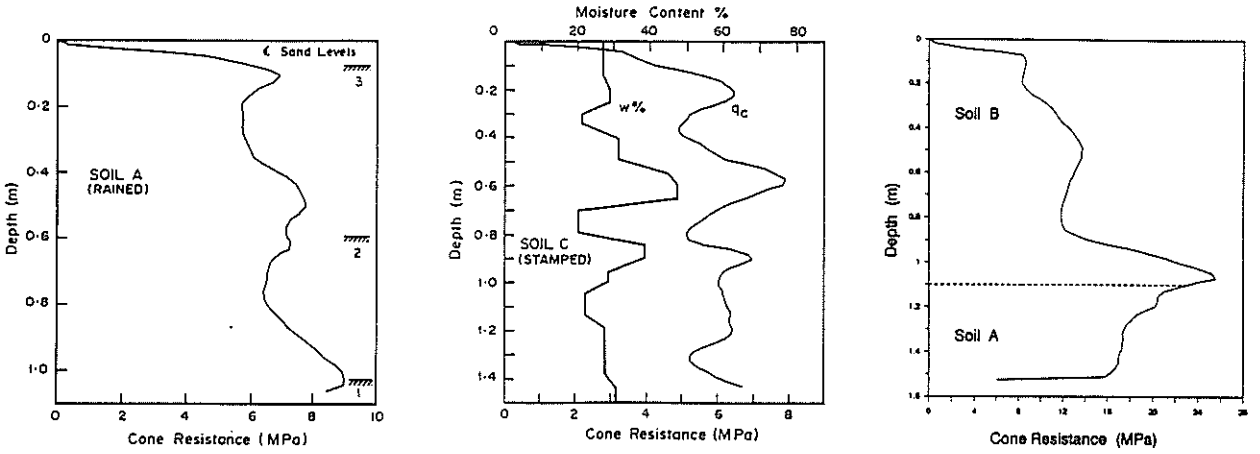

Fig. 6. Penetrometer test profiles, Samples CH 1, CH 2B and CH 3

crushing along the pile shaft, these curves should be concave upward, commencing from zero load at the toe, but this is true of only one test (P2CH 1). For test P1CH 4, total capacity is appropriate to pile diameter, but there is a substantial base load which has no explanation. For Soils C and B (Fig. 10), the scatter of plotted points is such that regression analysis cannot be trusted to indicate an appropriate curve form, but a significant base load is again apparent.

From the regressed curves of Fig. 9 and similar hand-fitted curves on Fig. 10, plots of shear stress v. depth were prepared (although P1 CH 4 must be regarded as uncertain because of the indicated base load). The resulting curves indicate a shear stress decreasing by > 50% over about 6D from the base for all materials, a result which does not accord with elastic theory (Randolph, 1988). It is also possible to approximate each of these distributions with a straight line, yielding an average skin friction as tabulated in Table III. These values appear to decrease with fineness, but interpretation is hampered by uncertainty in P1CH 4 and a rather higher cell pressure in P2CH 1.

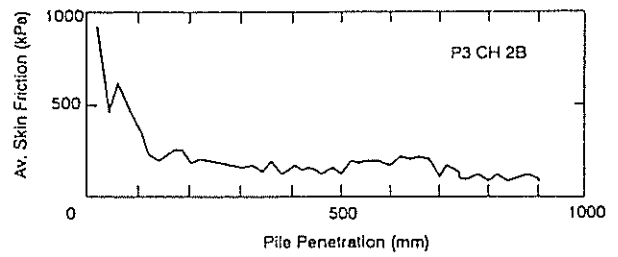

Fig. 7. Nominal average skin friction on driving

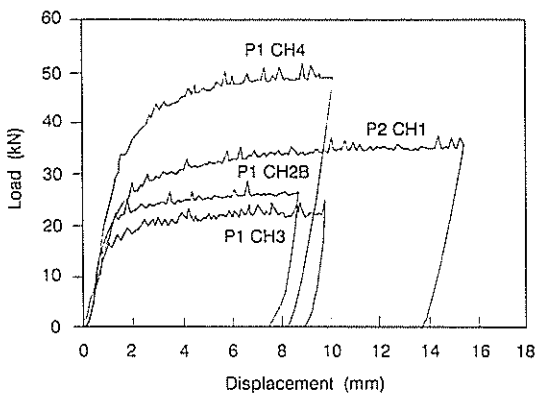

Fig. 8 Load displacement curves, pull tests

In order for it to be possible to predict these developed shear stresses from a CPT test, it is necessary for a full displacement device to be compared with one of near zero displacement in highly crushable soils. If τ_{av} can be considered representative, then τ_{av}/f_s varies from about 2 (CH 1) to 0.4 (CH 3), for reasons which are not clear at this stage, but which may reflect greater arching capacity in the dense silty Soil B.

Table III Summary, Pile Pull Tests

Pile No. Nom. O.D. (mm)	Driven Length (mm)	Soil Type	Init. Void Ratio	σ_3 (kPa)	Peak Load (kN)	τ_{av} (kPa)	Peak Displ (mm)
P2 CH 1 (100)	770	A	1.38	300	35	135	14.6
P1 CH 2B (100)	870	C	1.33	225	25.5	70	7.8
P1 CH 4 (150)	830	A	1.34	225	47	75	10.0
P1 CH 3 (100)	905	B	0.51	220	22	55	10.0

7. CONCLUSIONS

Whilst it has been possible to modify a large sand calibration chamber to conduct load tests on model piles driven into a range of calcareous sediments, these developments severely taxed the equipment and required rapid development of new techniques. Sample formation by raining was found to be barely possible, but the premix-stamping procedure for silty soils appears to be as good as any of the alternatives. It was shown that Soil B, produced by grinding, was not a good analogue of a calcareous silt, but may model some aspects acceptably. There was little evidence of plugging on driving, from which it was inferred that the pile clearance criterion was adequate. Pull testing indicated a shear stress decreasing substantially up the shaft due to crushing, but interpretation is subject to some uncertainty due to apparent base loadings. More work will be required in order to predict developed shear stress from CPT data.

8. ACKNOWLEDGEMENTS

This, and parallel papers (Parkin et al., 1990; Tan et al., 1990; Parkin, 1991) reports on a study undertaken jointly by CSIRO Division of Geomechanics and Monash University under contract to Exxon Production Research Company (USA), as agent of Esso Australia Ltd.

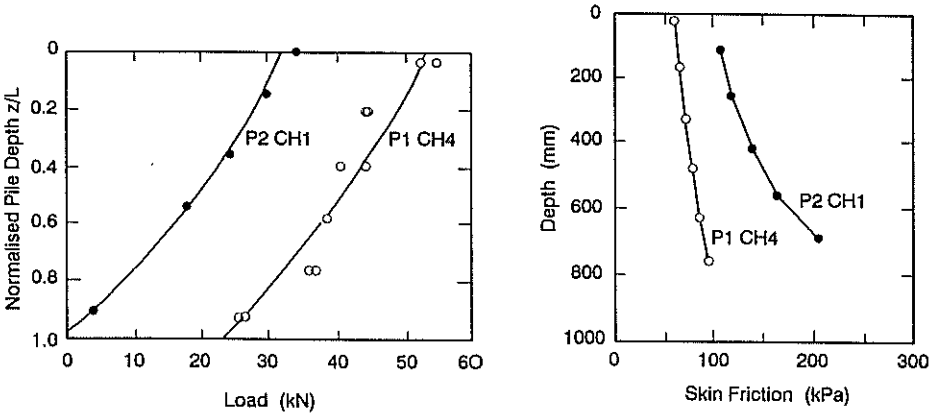

Fig. 9 Distributions of load and skin friction at peak Soil A

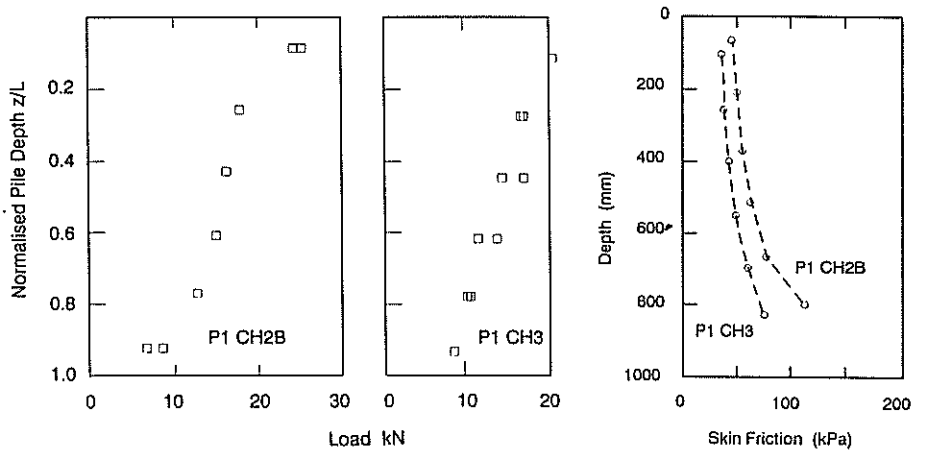

Fig. 10 Distributions of load and skin friction at peak, Soils B and C

and BHP Petroleum Ltd. The permission of these companies to publish is gratefully acknowledged. Particular recognition is accorded to Dr. T. W. Dunnavant (EPR) who conceived and supervised the project, and Mr. D. R. Willoughby as principal for CSIRO. Mr. C. Powell (Monash) provided advanced technical services. Other contributions came from Messrs J. M. Hulett (EPR), A. M. Hyden (EAL) and S. Anderson (Wolohan Grill and Partners).

9. REFERENCES

Angemeer, J., Carlson, E.D. and Klick, J.H. (1973). Techniques and results of offshore pile load testing in calcareous soils. Proceedings, 5th Annual Offshire Technology Conference, Paper OTC 1894 (Houston), Vol. 2, pp 677-692.

Bellotti, R., Bizzi, G. and Ghionna, V. (1982). Design, construction and use of calibration chamber. Proceedings, 2nd European Symp. on Penetration Testing (ESOPT II) (Amsterdam) Vol. 2, pp 439-446.

Chapman, G.A. (1980). Interpretation of friction cone penetrometer tests in sand. Ph.D. Thesis, Monash University, Australia.

Hyden, A.M., Hulett, J.M., Murff, J.D. and Abbs, A.F. (1988). Design practice for grouted piles in Bass Strait calcareous soils, Proceedings, Int. Conf. on Calcareous Sediments (Perth), Vol. 1, pp 297-304.

Nauroy, J.F., Brucy, F. and Le Tirant, P. (1988). Skin friction of piles in calcareous sands. Proceedings Int. Conf. on Calcareous Sediments, Perth, Vol. 1, pp 239-244

Parkin, A.K. (1991).Chamber testing of piles in calcareous sand and silt. Proceedings, 1st Int. Symp. on Calibration Chamber Testing (ISOCCT), (Potsdam, N.Y.) (in press).

Parkin, A.K. and Lunne, T. (1982). Boundary effects in the laboratory calibration of a cone penetrometer for sand. Proceedings, 2nd European Symp. on Penetration Testing (ESOPT II) (Amsterdam), Vol. 2, pp 761-768.

Parkin, A.K., Yee, Y.W., Tan, C.P. and Willoughby, D.R. (1990). Driven model piles tested in calcareous sand in a large calibration chamber. Proceedings, 22nd Annual Offshore Technology Conference, Paper OTC 6242 (Houston), Vol. 1, pp 389-397.

Poulos, H.G. (1988). The mechanics of calcareous sediments. Jaeger Memorial Lecture to 5th Australia-New Zealand Conf. on Geomechanics. (Sydney). Australian Geomechanics (August 1988), pp 8-41.

Randolph, M.F. (1988). Evaluation of grouted insert pile performance. Proceedings, Int. Conf. on Calcareous Sediments (Perth), Vol. 2, pp 617-626.

Tan, C.P., Parkin, A.K. and Yee, Y.W. (1990). Monotonic testing of a model pile driven in a calcareous sandy silt. Proceedings 22nd Offshore Technology Conference, Paper OTC 6242 (Houston), Vol. 1, pp 399-404.

Veismanis, A. (1974). Laborabory investigation of electrical friction cone penetrometers in sand. Proceedings, European Symp. on Penetration Testing (ESOPT) (Stockholm), Vol. 2.2, pp 407-419

Cyclic Undrained Stiffness of Stiff Clay and Volcanic Ash

M.J. PENDER
B.E.(Hons)., Ph.D., M.I.P.E.N.Z., M.A.S.C.E.
Professor of Geotechnical Engineering, University of Auckland
G.C. DUSKE
N.Z.C.E.
Senior Technical Officer, University of Auckland
R.J. PEPLOE
B.E., M.E.
Geotechnical Engineer, Tonkin and Taylor Ltd, Auckland

SUMMARY: This paper will present results of strain and stress controlled cyclic undrained triaxial tests on specimens of Auckland clays and on volcanic ash specimens from Tauranga. The change in shear modulus and damping with strain amplitude over a range of ±0.1% to ±2% will be presented. Most of the tests were done at frequencies of 0.2 Hertz. In addition monitoring of the pore pressure change, which were measured at mid-height of the specimen, will be discussed.

1. INTRODUCTION

The cyclic undrained stiffness of soils is important in the prediction of the response of a site to earthquake excitation. It is also important for consideration of dynamic soil structure interaction both for footing and raft foundations and for the cyclic lateral stiffness of pile foundations. It is well established that the cyclic behaviour is very dependent on shear strain amplitude (γ). Two parameters are commonly used to characterise the soil properties, these are apparent shear modulus (G) and equivalent viscous damping ratio (D) both of which are defined in Fig. 1. As the shear strain amplitude increases the apparent shear modulus decreases and the damping ratio increases. It has long been established that the values of these properties are independent of cyclic frequency, at least in the range of interest of interest in earthquake engineering, Taylor (1971).

This paper presents some cyclic stiffness and damping data for clays from two sites in Auckland and a volcanic ash from a site in Tauranga which demonstrate the effect of strain amplitude. The intention of the tests reported was to investigate the rate of decrease in G with increasing strain amplitude and the effect of the number of cycles. It is concluded that degradation is unlikely to be significant for the Auckland clays but that the volcanic ash behaves more like a sand than a cohesive soil in that it exhibits a substantial increase in pore water pressure and a degradation of stiffness during undrained cyclic loading.

The current understanding of the undrained cyclic properties of soil has evolved over the last two or three decades. An early source of information is the report of Seed and Idriss (1970). Using data available in the late 60's this proposed that one G - γ relation and one D - γ relation are representative of the behaviour of clays, a similar pair of relations was thought to be appropriate to the properties of sand. The current understanding is a little more complex in that the G - γ relation for clays is now thought to be a function of plasticity index, Sun et al (1988), the form of their relation is presented in Fig. 2. These curves have become important in understanding site effects which were a most significant part of the response of the local soils to the Mexico City earthquake in 1985 and the soils in Oakland during the Loma Prieta earthquake of 1989. Damping ratio values for clays may also be a function of plasticity index but to date no definite proposal has emerged and the scatter of the data is about the same as presented by Seed and Idriss in 1970, this range of damping values is presented in Fig. 3.

The ordinate in Fig. 2 is the ratio G/G_{max}. The G_{max} used to normalise the strain dependent shear modulus is the value observed at very small strain amplitudes. This is the shear modulus associated with the passage of elastic shear waves, it has been found that for shear strains of the order of about 10^{-4} to 10^{-3} % most soils behave elastically. It is well known that G_{max} is a function of the void ratio of the soil and the square root of the mean principal effective stress. This square root relation will be used in the paper to correct for the change in stiffness of the volcanic ash as the pore water pressure increases.

Apparent Shear Modulus: G = slope AA'

Equivalent Viscous Damping Ratio:

D = Area of loop / (4π area of Δ OAB)

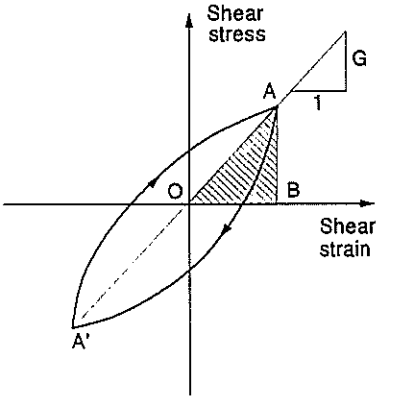

Figure 1 Definitions of the apparent shear modulus and equivalent viscous damping ratio.

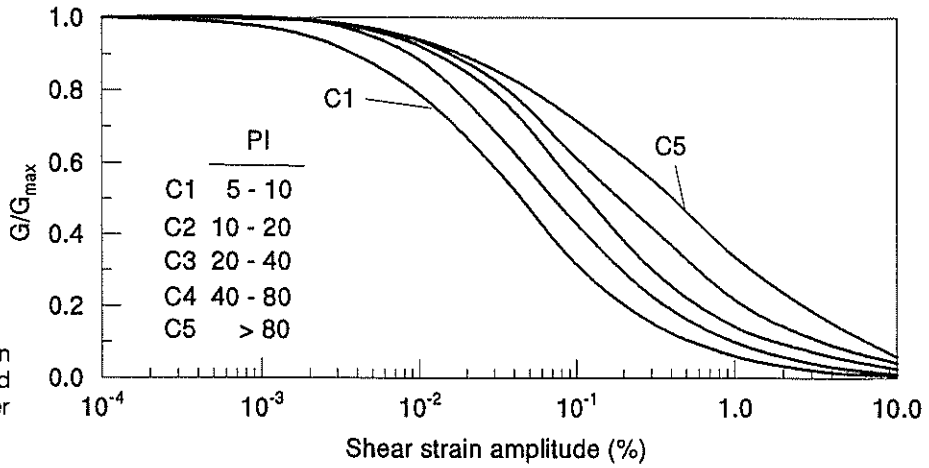

Figure 2 Relation between apparent shear modulus and strain amplitude for clays (after Sun et al (1988)).

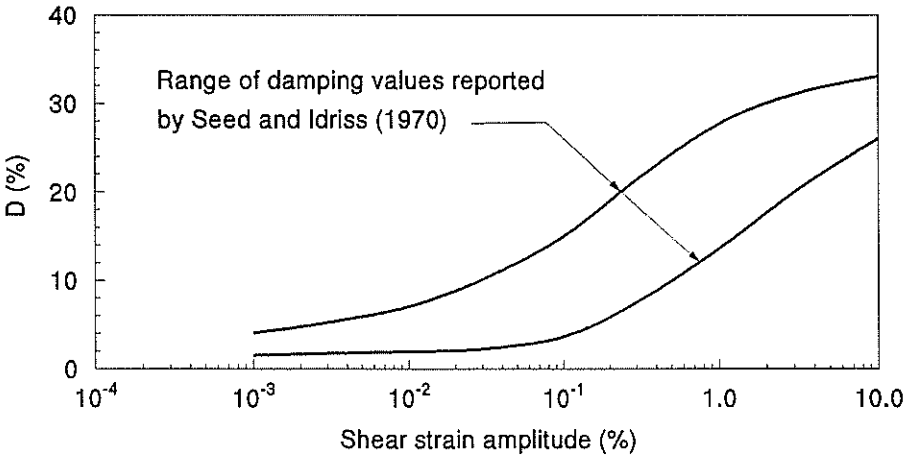

Figure 3 Range of damping values observed for clays (after Seed and Idriss (1970)).

2. TEST PROCEDURE

The soil specimens were cut from block samples 200mm high and by 203mm in diameter. These were recovered from the site by pushing a steel sampling tube into a prepared surface at the site. The tubes are fitted with a removable cutting shoe and driving head. After pushing into the soil the sampling tubes are recovered by hand digging, the cutting shoe and the driving head removed, and the ends sealed with rubber sheeting held in place with clamped endcaps. The samples are stored in the laboratory until the time of testing when the block is extruded from the tube in a hydraulic press and the sample cut into four with a wire saw. In this way four 75mm diameter by 150mm tall specimens are obtained from each sample.

A back pressure of 700 kPa was used to ensure saturation of the specimens. The frequency of cycling was 0.2 Hz. The majority of the tests were strain controlled but a few stress controlled tests are also reported. The strain controlled apparatus was originally designed by Taylor and Bacchus (1969). The pore pressure response in the soil was monitored during the tests using a miniature pressure transducer mounted at mid-height of the specimen.

Strain control was applied externally to the triaxial cell so any bedding errors would introduce errors in the measurement of the shear modulus. Consolidation of the specimen was assumed to take care of any such potential problems. The data was gathered using a personal computer (AT clone) fitted with an analogue to digital card. This was capable of recording four channels of data at a rate of several thousand cycles per second. For each loading cycle 30 data sets were recorded and each phase of the test continued typically for 40 cycles. The computer software was able to record the transducer readings as well as plot the load deformation loops to the computer screen during the tests. Subsequent to the test more detailed processing of the data was done. In finding the apparent shear modulus for each loop, which from Fig. 1 is a secant modulus, the end points need to be identified. Some refinement was applied to the data at the turning points before the G and D values were calculated.

The test procedure for each specimen, after back pressure saturation and consolidation, was to start with the smallest strain amplitude desired (in the case of a strain controlled test) or the smallest cyclic shear stress (for a stress controlled test), and apply the first 40 or so cycles and pause to process the data etc. The next strain amplitude was set and another series of 40 or so cycles then applied. Generally there was no reconsolidation of the specimens between tests at different strain amplitudes. The only exceptions being at the end of the testing of the volcanic ash where the strain amplitude was decreased for the last two loading phases and consolidation to dissipate the excess pore water pressure was allowed prior to the final loading phase.

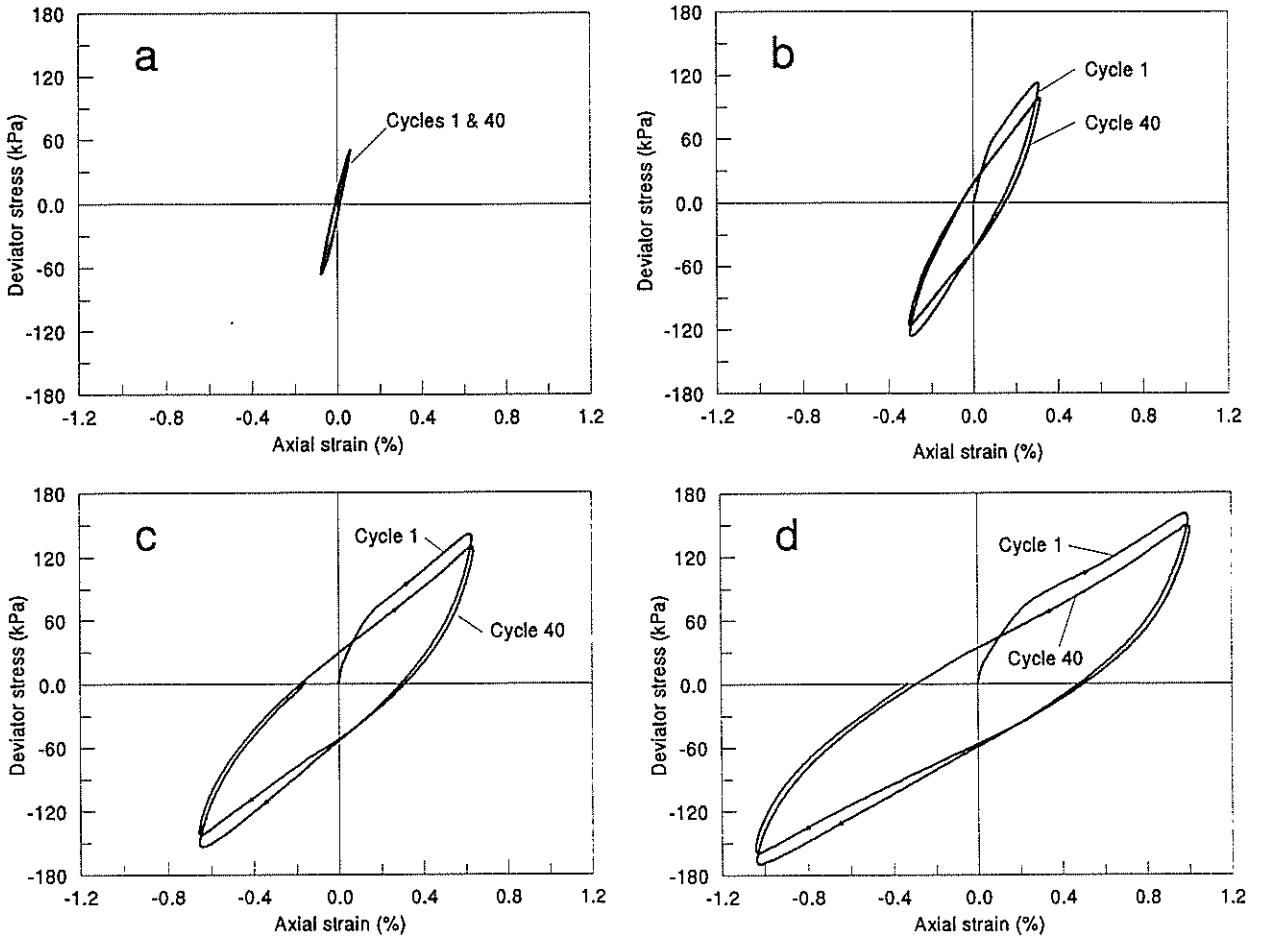

Figure 4 Stress strain loops from strain controlled tests on Auckland clay. (a) strain amplitude 0.07%, (b) strain amplitude 0.32%, (c) strain amplitude 0.64%, (d) strain amplitude 1.03%.

3. AUCKLAND CLAYS

Two clay samples from Auckland were tested, one from Sunset Rd. on the North Shore and the other from a subdivision at Manurewa. The water content of the specimens after back pressure saturation and hydrostatic consolidation to effective confining pressures in the range 100 to 200kPa was about 40%. The plasticity index of the clays was in the 30 - 40% range and the liquidity index was about 0.1. The undrained shear strength of the clays, determined with a laboratory vane, was about 75 to 100kPa. Strengths of this order and the liquidity index suggest that the clay would behave as a heavily overconsolidated material. Clays with roughly this range of properties are one of the characteristic materials found in the Auckland area.

Some typical stress strain loops for the Auckland clays are plotted (to the same scale) in Fig. 4a to d. The shear stress plotted is the deviator stress, $\sigma_1 - \sigma_3$, and the strain is the axial strain of the specimen (using this set of axes the slopes of the lines between the ends of the loops in Figs. 4 and 7 are three times the value of G). It is apparent from Fig. 4 how the apparent shear modulus decreases with increasing strain amplitude whilst the damping ratio increases. In addition it is evident that there is some degradation of the shear modulus as the number of cycles increases. This is barely perceptible for the small cyclic shear strains in Fig. 4a but becomes more apparent as the strain amplitude increases. At the end of some several hundred cycles of undrained cyclic loading a small increase in pore water pressure, of the order of 20kPa, was noted. This is not altogether surprising as static undrained shearing of a stiff clay would not generate large increases in pore water pressure. Since the number of cycles of undrained loading applied to the clay specimens was much greater than that expected in an earthquake and, as the rise in pore water pressure was small, the slight degradation in stiffness can be considered as a fatigue phenomenon.

In Fig. 5 the effect of strain amplitude on the apparent shear modulus for the first few cycles of each loading stage is plotted along with part of the C2 and C3 clay curves from Fig. 2. If the apparent shear modulus at the end of the 40 cycles for each loading stage is plotted the points lie just beneath those in the figure. As has been explained above the curves in Fig. 2 are normalised with respect to the small strain shear modulus of the soil, a value that was not determined for the Auckland clays. The assumption made to circumvent the lack of this piece of information was to take the shear modulus result for the smallest strain amplitude and attach it to the C2 clay curve. These points are labelled starting points in the figure. Having made this assumption it is of interest that the apparent shear modulus plots for the Auckland clays

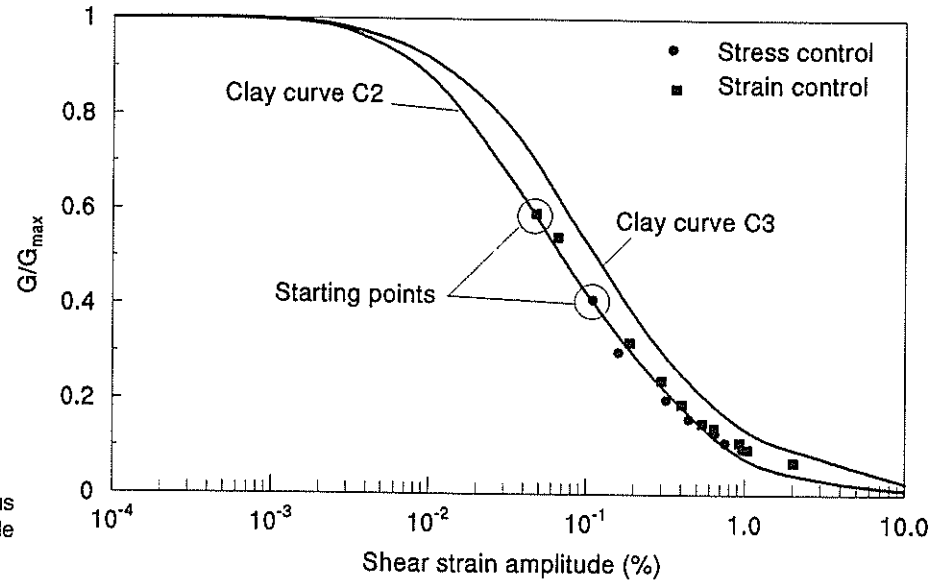

Figure 5 Shear modulus variation with strain amplitude for the Auckland clays.

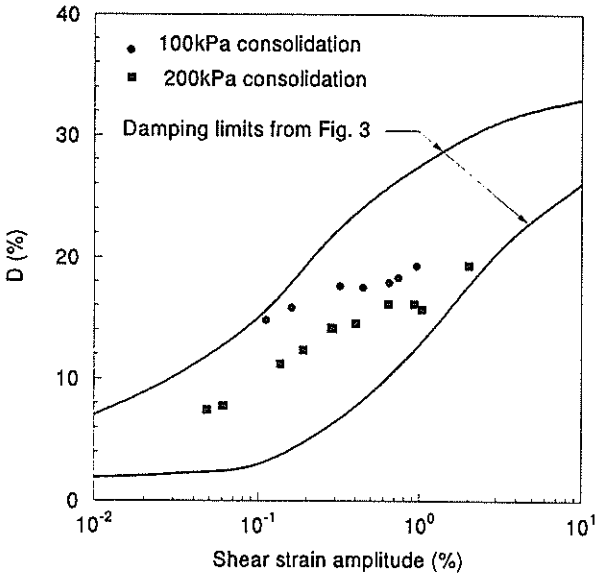

Figure 6 Damping values for the Auckland clays.

follow the trend of the C2 and C3 clay curves which cover the plasticity index of the clay. As the increase in pore pressure was small during the course of the tests no correction was applied to the apparent shear modulus values to account for changes in effective stress.

In Fig. 6 the damping values of the clays are plotted along with part of the range of damping values from Fig. 3. The results for the Auckland clays lie within the range reported by Seed and Idriss (1970).

4. TAURANGA VOLCANIC ASH

A specimen of volcanic ash from Tauranga was subject to cyclic undrained loading. The ash had a natural water content of 62%, a plasticity index of 25%, a liquidity index of 0.6 and an undrained shear strength similar to that of the Auckland clays.

Figure 7 shows the effect of strain amplitude on the cyclic stiffness of the volcanic ash soil. Two sets of results are given for strain controlled tests and two for stress controlled tests. In the strain controlled tests the shear modulus decreases as the number of cycles increases and this is manifested with a decrease in the shear stress at the extremity of the loop, Figs. 7a and 7b give examples of this which are very similar to the behaviour seen in Fig. 4. In the case of stress controlled cycling the decrease in apparent shear modulus with increasing number of cycles is accompanied with an increasing range of shear strain for the loops, Figs. 7c and 7d give examples of this. In the case of the loops plotted in Fig. 7d there is a very rapid degradation in stiffness which is due in part to the large cyclic shear stresses applied to the specimen and also to the generation of pore water pressure discussed below. The specimen for which results are plotted in Fig. 7c and d was consolidated to an effective consolidation pressure of 100kPa whereas the specimen for Fig. 7a and b was initially consolidated to 200kPa.

Unlike the Auckland clays the volcanic ash soils demonstrated a considerable generation of excess pore water pressure during the cyclic loading. After several hundred cycles of undrained loading the pore water pressure had risen to 85% of the initial effective consolidation pressure. In this way the cyclic response of the ash is similar to that of saturated sand. The increase in pore water pressure must have been at least a contributor to the decrease in the shear modulus of the ash. Thus there may be two mechanisms leading to the decrease in the shear modulus of the ash with increasing numbers of cycles - degradation (a type of fatigue as with the clays) and the decrease in effective confining stress because of the rise in pore water pressure.

In Fig. 8 the variation of the apparent shear modulus with strain amplitude is plotted for the tests on the volcanic ash. Part of clay curve C2 is plotted for comparison and the first strain amplitude result is attached to the curve in the same manner as has been described above for the clay. Also in Fig. 8 the strain controlled results are supplemented with those for the stress controlled tests on the ash and the apparent shear modulus values are "corrected" for the decrease in effective stress caused by

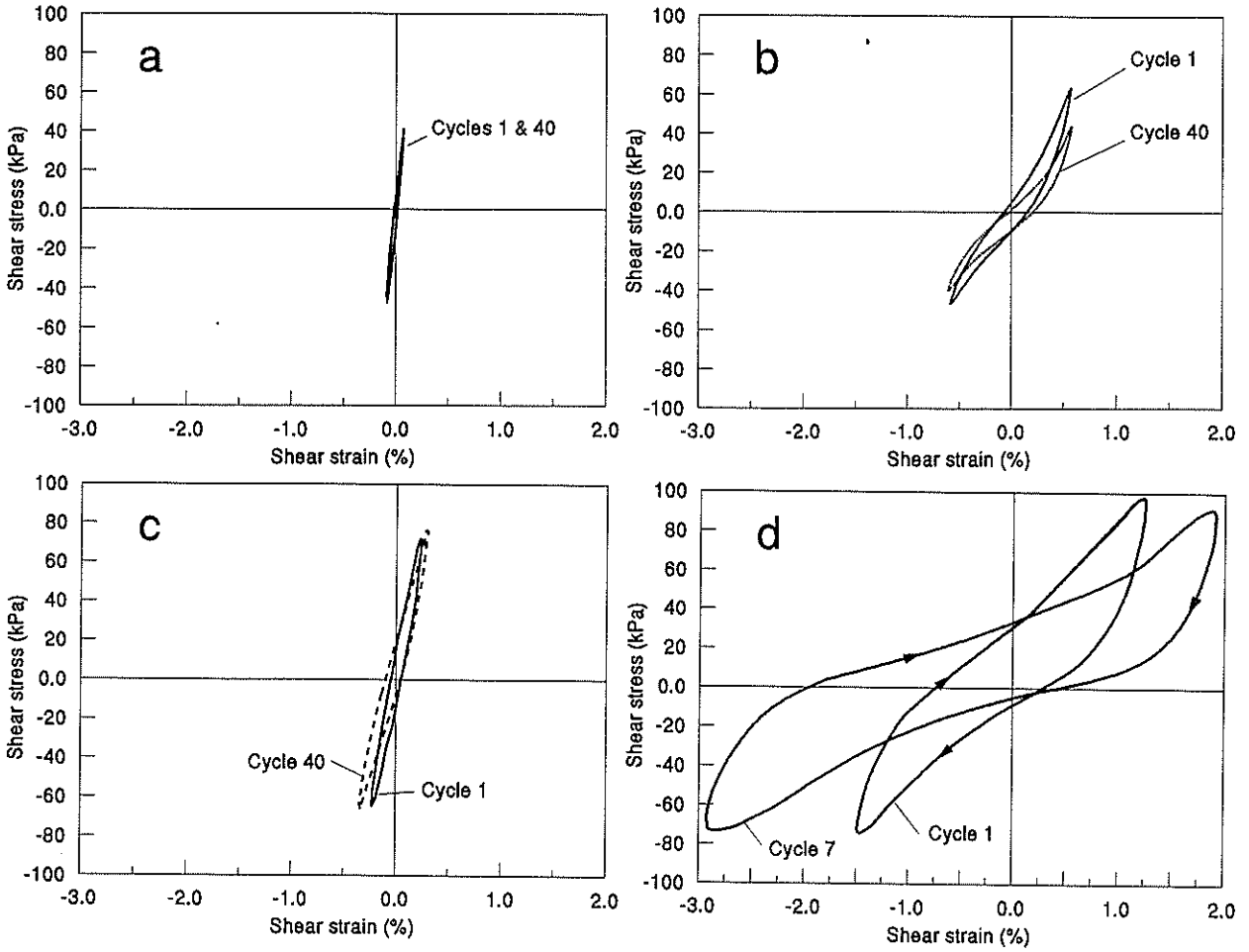

Figure 7 Stress strain loops for tests on volcanic ash. Strain controlled tests at 200kPa consolidation pressure; (a) strain amplitude 0.09%, (b) strain amplitude 0.60%. Stress controlled tests at 100kPa consolidation pressure, (c) and (d).

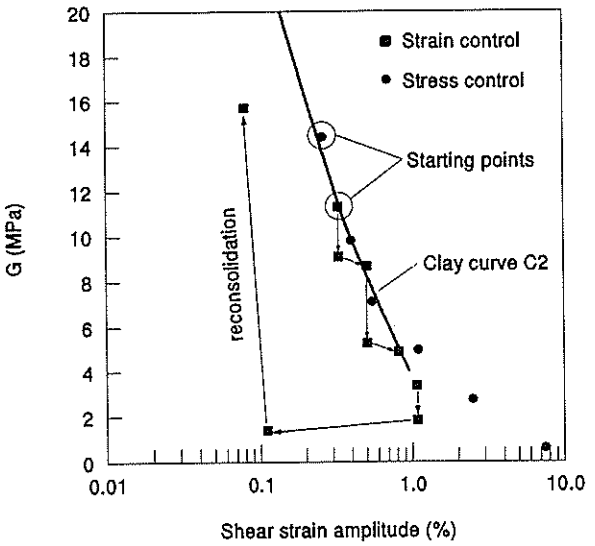

Figure 8 Shear modulus variation with strain amplitude for the volcanic ash, G_{max} corrected to account for the decrease in effective stress.

the increase in pore water pressure. This is done with the square root relation between small strain shear modulus and effective confining pressure mentioned in the introduction. At the end of one of the tests on the ash the effect of decreasing the strain amplitude was investigated. Firstly a decrease to 0.11% , whilst the large excess pore pressure is still within the soil, and then a further reduction to 0.08% after reconsolidation back to an effective stress of 200kPa. It is apparent that the reconsolidation does not allow the ash to regain the stiffness at the commencement of the cyclic loading. Thus several hundred cycles of undrained cyclic loading of the ash causes a permanent degradation in the shear stiffness of the soil.

Figure 9 plots the damping data for the volcanic ash. It is apparent that for the early stages of the cyclic loading the damping behaviour is within the ranges shown in Fig. 3 but as the number of load cycles increases and the strain amplitude is increased the damping does not increase as expected. Possibly this is a consequence of degradation of the internal structure of the ash reflected by the degradation in shear stiffness and increase in pore water pressure.

5. DISCUSSION

The cyclic loading results for the Auckland clays indicate that for the larger strain range the G - γ and D - γ curves in Figs. 2 and 3 are applicable. Although an assumption was needed to locate the results on the particular curve in

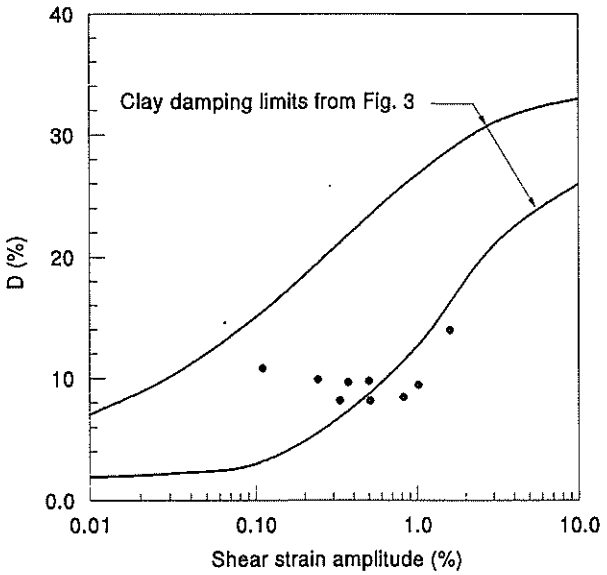

Figure 9 Damping values for the volcanic ash.

Fig. 5 the slope of the relation follows closely those in Fig. 2, thus even if the location of the curve for the Auckland clays in the G - γ plot is in doubt it is apparent that the rate of decrease in apparent shear modulus with increasing strain amplitude is the same as the curves in Fig. 2. It is of interest that the stiffness and damping do not seem to be greatly affected by the number of cycles of loading even though the total number of load cycles was several hundred by the end of the test and well beyond the number expected in an earthquake. Although there is some degradation in stiffness this is small and occurs at the higher strain ranges. Finally there is a negligible change in pore water pressure in the clay for each cycle. These features of the clay mean that the estimation of site response or calculations of soil structure interaction during earthquake loading can be based on levels of shear strain only and does not require changes to incorporate degradation with the number of cycles or with changes in effective stress following the generation of pore water pressure.

The test results for the volcanic soil indicate a sensitivity to cyclic loading much greater than that of the clay. During the cycling the pore water pressure increases and the stiffness of the ash decreases as can be seen with the stress strain loops in Fig. 7, these changes occur in a few tens of cycles. In this way the volcanic ash has more in common with the cyclic behaviour of a saturated sand than with the cyclic behaviour of the Auckland clay, although, on the basis of soil classification data, one would expect the ash to be more closely allied with the clay. Similarly, at small cyclic strains, the damping in the ash starts with values to be expected from Fig. 3 but the damping does not increase as expected as the strain amplitude increases. Finally when one of the ash specimens was reconsolidated after the pore water pressure had increased to 85% of the effective confining pressure and further cyclic loading conducted at small shear strains the initial stiffness was not recovered. These aspects of the volcanic ash behaviour suggest that the soil has a sensitive structure that is degraded by successive cycles of loading. This means that the estimation of the response of the material to earthquake excitation is, in principle, more complex than that of the Auckland clays. The liquidity index may be a useful parameter for categorising the likely pore pressure response of cohesive soils under cyclic loading. The liquidity index, calculated using the water content of the specimens after back pressure saturation and consolidation, was about 0.1 for the Auckland clays and 0.6 for the Tauranga ash.

The assumption used to locate the initial test result on the G/G_{max} relations presented in Fig. 2 is the most doubtful part of the procedures followed in this paper. A direct measurement of the small strain stiffness of the soil would be a useful addition to the test procedure. At present the installation of bender elements, Dyrik and Madshus (1985), in the top and bottom platens of the triaxial apparatus is being considered. In defence of the of the procedure of simply attaching the data points to the appropriate curve in Fig. 2 the free vibration torsional test results of Larkin and Chan (1992), presented to this conference, support the assumption that the G - γ relation for NZ volcanic soil is very similar to the clay curves. For the Auckland clays similar free vibration torsional tests by Plested (1985) indicate that the form of the curves follows those in Fig. 2.

6. CONCLUSIONS

The following conclusions are reached from the results presented herein:

(i) The stiffness and damping of the Auckland clays was not greatly affected by the number of cycles. This means that earthquake response calculations can be attempted with properties that depend only on shear strain amplitude, i.e. they can be based on a total stress method of calculation.

(ii) For the Tauranga volcanic soil the resistance to cyclic loading was more complex as a rapid build up in pore water pressure, with a consequent loss in stiffness, was observed. Also the damping available did not increase with strain amplitude.

(iii) The results of Fig. 6 suggest that the Auckland clays have damping properties which are adequately described by Fig. 3. Figure 5 shows that the rate of change of apparent shear modulus with strain amplitude for the Auckland clays follows closely that of curves C2 and C3 in Fig. 2. This is an important conclusion as recent earthquake data has coupled enhanced site response, such as occurred at Mexico City in 1985 and in Oakland in 1989, with soils having an extended range of strains over which the behaviour is elastic with a G - γ relation to the right of the C5 curve in Fig. 2.

7. ACKNOWLEDGEMENTS

The work reported in this paper was supported in part by the Structures Committee of the Road Research Unit of the former National Roads Board. The project number was 138601 and the support is gratefully acknowledged.

Dr. L. D. Wesley and Dr. T. J. Larkin, both of the Civil Engineering Department of the University of Auckland, provided helpful comments on the paper. In addition Dr.

Wesley kindly supplied the index data for the soils tested and suggested that the liquidity index might be a useful parameter for categorising the cyclic response of soils.

8. REFERENCES

1. Dyrik, R and Madhus, C. (1985) Lab measurements of G_{max} using bender elements. Proc. of the conference on: Advances in the art of testing soils in cyclic conditions, sponsored by the Geotechnical Engineering Division of the ASCE and held in conjunction with the 1985 ASCE convention held in Detroit.

2. Larkin, T. J. and Chan, S. Y (1992) The dynamic response of volcanic soils, Proc. 6th, Australia NZ conference on Geomechanics, Christchurch.

3. Plested, M. L. (1985) In situ investigation of shear waves in soil media. University of Auckland School of Engineering Report No. 378.

4. Seed, H. B. and Idriss, I. M. (1970) Soil moduli and damping factors for dynamic response analysis. Earthquake Engineering Research Centre, University of California, Berkeley. Report No. EERC 70-10.

5. Sun, J. I., Golesorkhi, R. and Seed, H. B. (1988) Dynamic moduli and damping ratios for cohesive soils, Earthquake Engineering Research Centre, University of California, Berkeley, Report No. UCB/EERC-88/15.

6. Taylor, P. W. (1971) The properties of soils under dynamic stress conditions with applications to the design of foundations in seismic areas, Report No. 79, Civil Engineering Department, University of Auckland.

7. Taylor, P. W. and Bacchus, D. R. (1969) Dynamic cyclic strain tests on a clay, Proc. 7th. International Conference on Soil Mechanics and Foundation Engineering, Mexico City, Vol. 1, pp. 401-409.

Simple Shear Compaction of Basecourse Aggregates

M.J. PENDER
B.E.(Hons), Ph.D., M.I.P.E.N.Z., M.A.S.C.E.
Professor of Geotechnical Engineering, University of Auckland
R.J. PEPLOE
B.E., M.E.
Geotechnical Engineer, Tonkin and Taylor Ltd, Auckland
G.C. DUSKE
N.Z.C.E.
Senior Technical Officer, University of Auckland

SUMMARY: This paper will report on a research project in which the densification and stiffness of basecourse aggregate were measured during cyclic simple shearing. Good quality greywacke and basalt aggregates and a lesser quality argillite aggregate from the Auckland region were tested. The intention of the simple shear compaction device is to provide a rapid means of categorising various basecourse aggregates. The differences between the good quality basecourse materials and the lesser quality argillite is readily apparent from the test results.

1. INTRODUCTION

Characterisation of basecourse aggregates is difficult in that the materials contain large particles so determination of mechanical properties requires large specimens and large pieces of apparatus. Earlier projects concerned with the characterisation of roading basecourse at the University of Auckland used a triaxial apparatus capable of accepting specimens 250mm in diameter and 625 mm high, Toan (1976). These specimens are difficult to handle and also difficult to prepare, requiring a separate compactor and about 1 man-day of effort just to prepare the specimen. The net effect of this is that the basecourse triaxial is a useful piece of research equipment but hardly likely to be used for routine evaluation of prospective basecourse materials. In this paper a method of characterisation of basecourse materials which uses a smaller quantity of material and has a very simple specimen preparation procedure is discussed. This is the so-called simple shear compactor originally developed at the University of Auckland following the ideas of Dr. G. R. Martin. The initial work was reported by Maurice (1977). This paper describes and summarises the results of an extensive series of tests on various aggregates from Auckland using an updated version of the machine having a more versatile control system than the original and also an automated data gathering system.

The data presented below provide a comparison between the stiffness properties of greywacke, basalt and argillite and the densification of the aggregate with increasing numbers of cycles. This data can be obtained relatively easily with the simple shear compactor and in particular it provides a ready means for comparing the likely performance of various aggregates. The apparatus could be used to gauge the performance of a hitherto unused aggregate by doing parallel tests on the new aggregate and comparing with the results of a similar suite of tests on an aggregate of known field performance.

2. APPARATUS

The objective was to develop a device that could subject a basecourse specimen to cyclic simple shear and monitor shear stiffness and change in volume as functions of shear strain amplitude and normal stress.

The simple shear compactor consists of an assembly of "floating" steel confining plates each 10mm thick. There are 10 of these giving a total specicmen thickness of 100mm The plan dimensions of the specimen are 250mm by 250mm. The top of the specimen is fixed in position whilst the shear force (or displacement) is applied to the base of the specimen. The shear force and displacement is applied through a servo controlled hydraulic system. Normal stress is also applied to the specimen through a servo controlled hydraulic system. Control of the servo systems and the recording of the deformation of the specimen is done by PC computer fitted with analogue to digital (for recording output from force and displacement transducers) and digital to analogue (for control of the servo valves) facilities. The system is able to apply several hundred thousand loading cycles unattended. Both shear strain and shear stress controlled testing is possible with the apparatus, however it was found that the system works better under strain control. The majority of the tests were done at 3 cycles per second, although some preliminary testing confirmed that the results were not affected by loading frequency.

Friction at the base and between the confining plates are important factors in the performance of the device. The roller bearings between hardened steel plates were shown to have negligible friction under the normal loads applied to the specimens under test. Friction between the confining rings was investigated and also found to have negligible effect on the measured basecourse properties. Initial tests revealed that as well as the simple shear deformation the specimen exhibited a rocking deformation which became more significant as the shear strain amplitude increased. This undesireable deformation was prevented by restraining vertical motion of the ends of the top platen, the additional component of vertical load was measured and included as part of the normal load on the specimen.

Specimen preparation involved removing the coarse fraction (> 25mm) from the basecourse and simply placing a weighed amount into the apparatus. Because of

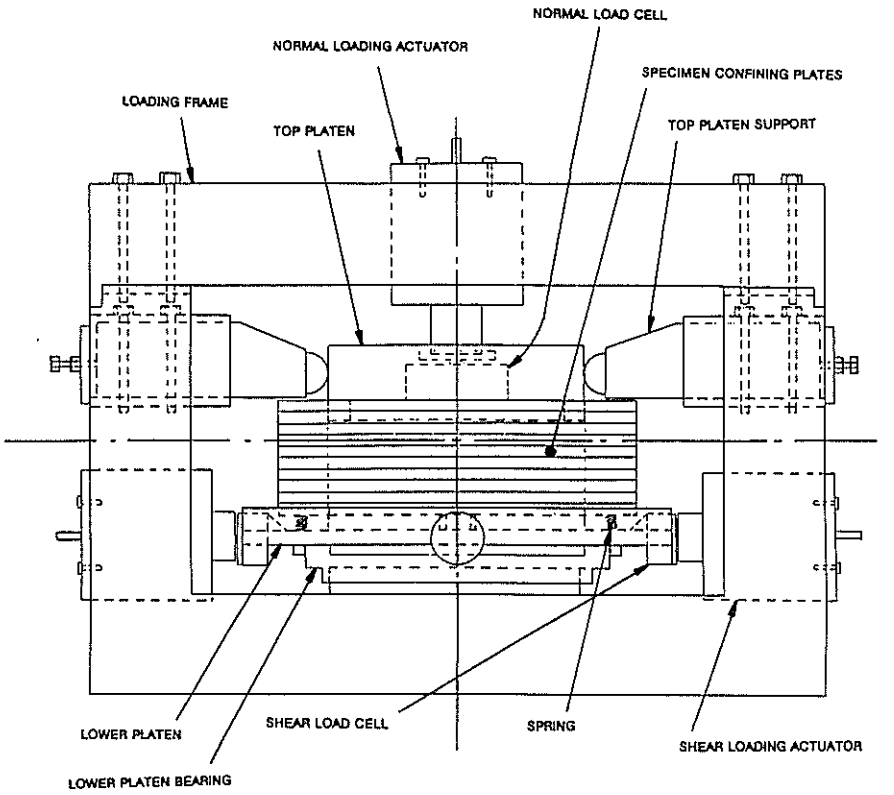

Figure 1 Simple shear compactor.

the design of the device there is no facility for saturating the material to be tested. The basalt and greywacke specimens were placed at a moisture content of 4%. The argillite showed a great affinity for water and was placed in the device at a water content of 10%.

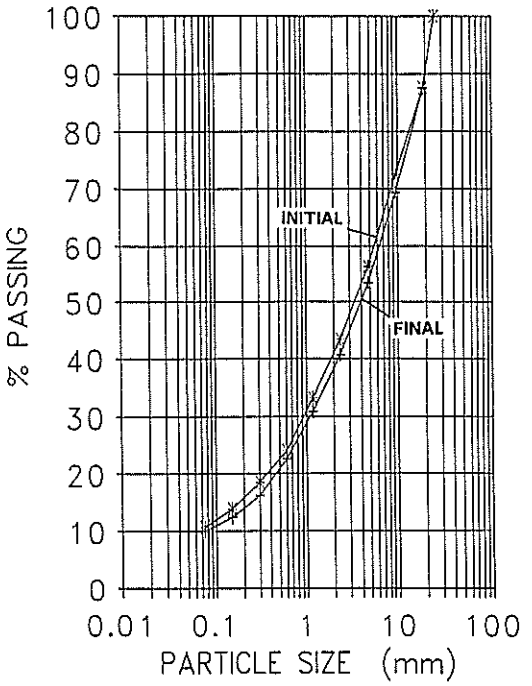

Figure 2 Particle size distribution for the argillite basecourse (before and after testing).

3. TEST RESULTS

Basecourse materials available in Auckland, greywacke, basalt and argillite, were tested. The grading curves for the greywacke and argillite complied with the M/4 specification. The grading for the argillite did not satisfy the M/4 curve, it is plotted on the curve marked "initial" in Fig. 2.

A range of tests at various confining pressures showed that the stiffness of the basecourse increased approximately linearly with normal pressure. This observation was not unexpected and will not be discussed further in this paper.

The change in density was characterised with the Dry Density Ratio, a parameter which reflects the increase in density during the cyclic loading. It is calculated by converting the settlement of the top platen to the current density of the specimen. The Dry Density Ratio is then the ratio of the current density to the initial density of the specimen. The shear modulus is the secant modulus calculated by taking the slope of the line joining the ends of each stress strain loop.

3.1 Strain controlled tests

Figure 3 shows the increase in density during strain controlled cyclic loading of the basalt, the shear strain amplitudes for the various tests are given in Table I. It is apparent that, for the range of shear strain amplitudes investigated, the density increases at a faster rate for the larger shear strain amplitudes. For the test with a shear strain amplitude of 0.27% there was still a noticeable increase in density after 500,000 cycles. The rate of density increase was much less, but still finite, for the 0.02% shear strain amplitude after 500,000 cycles.

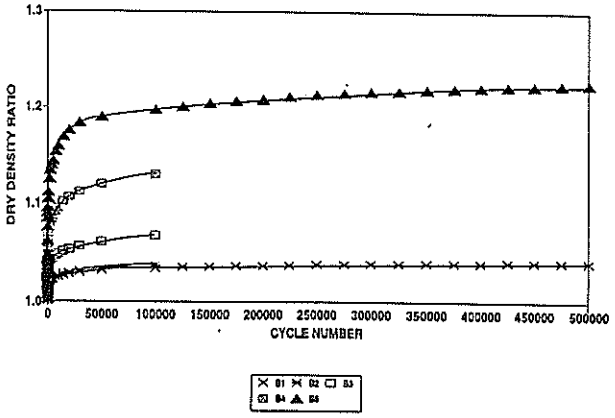

Figure 3 Increase in density of basalt as a function of shear strain amplitude.

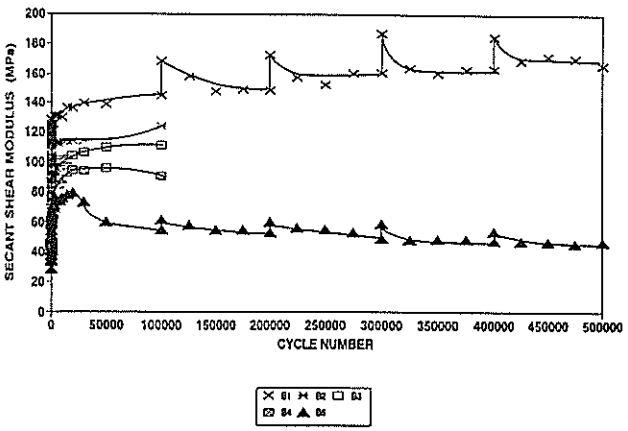

Figure 4 Effect of shear strain amplitude and number of cycles on basecourse shear stiffness.

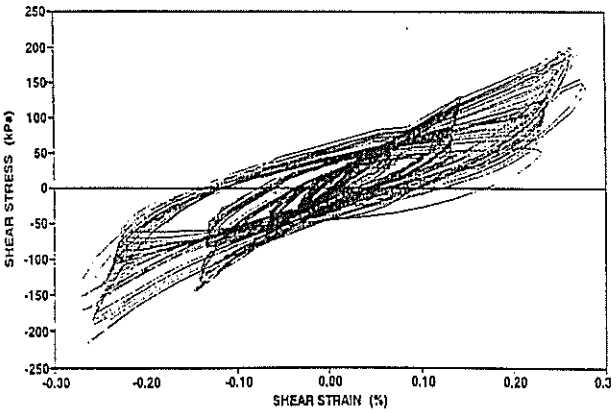

Figure 5 Shear stress shear strain loops for tests on the basalt.

Table I: Shear strain amplitudes for the tests on basalt in Figs. 3 - 5.

Test number	Shear strain amplitude %
B1	0.024
B2	0.033
B3	0.067
B4	0.145
B5	0.273

The effect of the 500,000 cycles on the secant shear modulus is shown in Fig. 4. The tests were done over a five day period with stages of 100,000 cycles each day. Between stages the specimens were rested overnight. It is clear from the figure that the stiffness is higher at the recommencement of cycling, this being more significant at small strain amplitudes. Also of significance, possibly greater, is the fact that for the higher shear strain amplitude, 0.273%, there is a decrease in the cyclic shear stiffness for cycle numbers in excess of about 20,000, this decrease occurs despite the fact that the density of the basecourse material is still increasing.

In Fig. 5 some stress strain loops for various cycles are presented. These show the hysteretic nature of the stress-strain loops and how the shape of the loop changes with cycle numbers.

In Figs. 6 and 7 the results for one specimen of basalt subject to stage loading for a total of 450,000 cycles is presented. Each stage consisted of 50,000 cycles at a set strain amplitude, the values for the various stages are set out Table II. In Fig. 6 the progressive increase in density with increasing cycle numbers is evident but with a marked decrease in the rate of increase between 300,000 and 400,000 cycles. The explanation for this is seen in Table II where there is a decrease in the strain amplitude, this appears to have an overconsolidation effect and virtually no increase in density is observed during this part of the test, once the previous maximum strain amplitude is exceeded the densification process continues. In Fig. 7 the effect is presented more clearly by plotting dry density ratio against shear strain amplitude.

3.2 Stress controlled tests

In Fig. 8 the results of stress controlled tests on argillite are presented. The diagram shows a fatigue phenomenon for the larger shear stress amplitudes with a progressive and quite rapid increase in the shear strain amplitude, i.e. a progressive decrease in the shear modulus of the basecourse specimen. On the other hand for the low levels of shear stress amplitude the argillite settles down to a stable stiffness with no apparent degradation after 50,000 cycles. Figure 9 plots data obtained from strain controlled tests on argillite. There are three different levels of cyclic shear stress as set out in Table III. The drop in the shear modulus after a small number of cycles at larger strain amplitudes is the strain controlled equivalent to the increase in shear strain amplitude in the stress controlled tests. This indicates deterioration or damage to the basecourse specimen. The curve labelled "final" in Fig. 2 is the particle size distribution of the argillite after the large strain tests, the initial distribution is also shown in Fig. 2. It is apparent that there has been slight particle breakdown. Similar comparisons attempted for the greywacke and basalt did not reveal any change in grading.

3.3 Comparative results for the three aggregates

Figures 10 and 11 present data after 100,000 cycles of strain controlled loading on the three aggregates, the dry density ratio and the shear modulus are plotted against the shear strain amplitude of the tests. Figure 10 shows that the greywacke is a little more resistant to densification

Table II: Shear stain amplitudes for the various stages of the test illustrated in Figs. 6 and 7.

Test number	Shear strain amplitude %
ST1#1	0.024
ST1#2	0.033
ST1#3	0.068
ST1#4	0.103
ST1#5	0.141
ST1#6	0.178
ST1#7	0.070
ST1#8	0.145
ST1#9	0.215

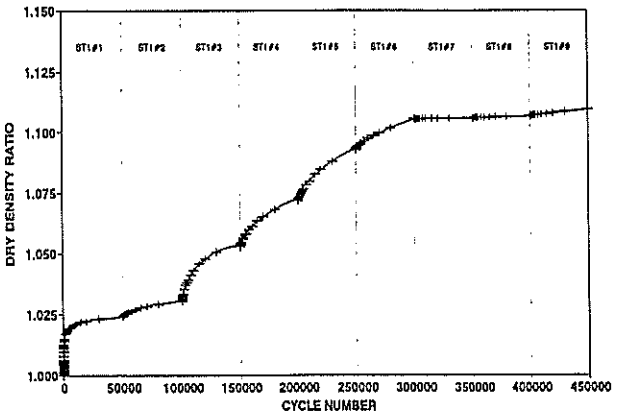

Figure 6 Dry density ratio for the stage testing on basalt.

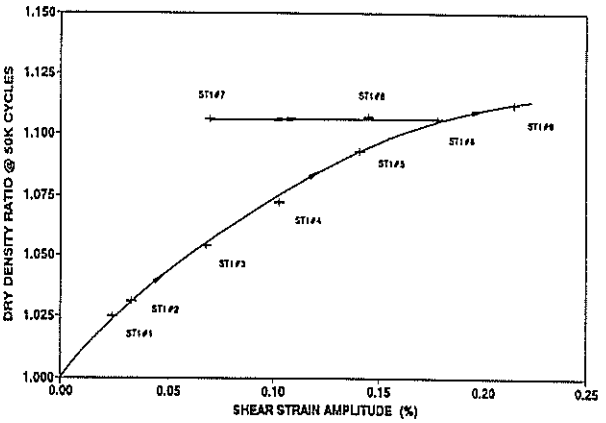

Figure 7 Effect of reduction of shear strain amplitude on dry density ratio.

than the basalt and argillite. Figure 11 shows that the argillite has inferior shear stiffness behaviour with numbers of cycles in comparison to the basalt and greywacke.

4. DISCUSSION

Section 3 presents a representative sample from a large amount of data reported by Peploe (1991). The speed with which a basecourse specimen can be set up in the apparatus and tested makes the device attractive for comparing different aggregates.

Empirical observations of pavement performance usually relate deterioration to the presence of water in and

Table III: Shear strain amplitude for the tests on argillite in Fig. 9

Test number	Shear strain amplitude %
A1	0.034
A2	0.148
A3	0.312

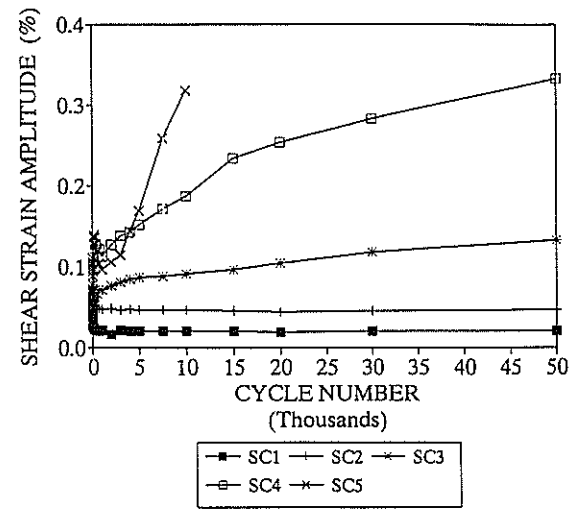

Figure 8 Stress controlled tests on argillite basecourse.

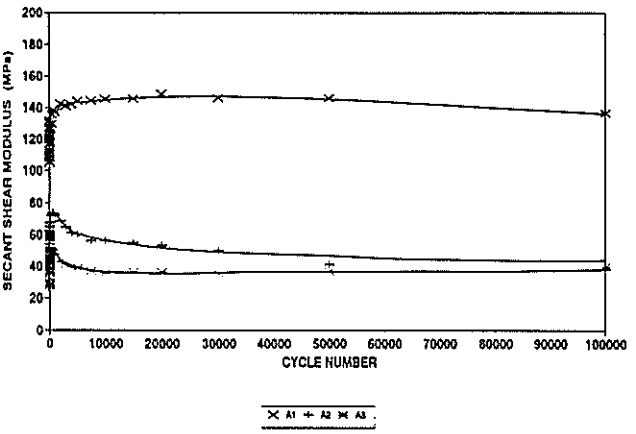

Figure 9 Strain controlled tests on argillite basecourse.

perhaps saturation of the basecourse. It would be desirable to perform compaction tests on saturated specimens. The present design of the apparatus precludes this and installing and sealing a tough membrane between the specimen and the confining plates would require modification of the apparatus.

Figure 7 presents the most interesting data with respect to the construction of pavements. It suggests that if vigorous shear straining is applied to the basecourse during compaction and then the operational shear strains during the pavement life are less than those at compaction the basecourse will perform with a large value of the shear modulus. Figure 8 shows that if the cyclic shear stress is less than a threshold value the basecourse will deform in a stable manner with no, or very small, accumulation of

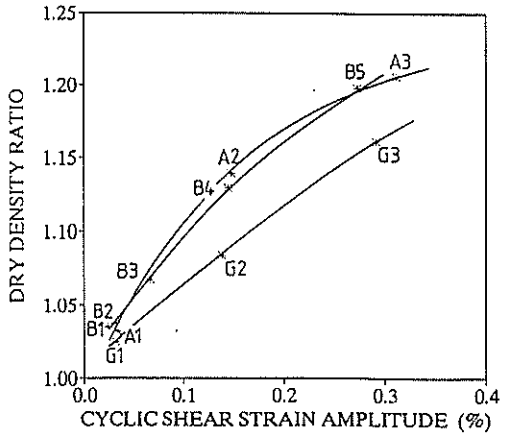

Figure 10 Comparison of the densification of the three types of aggregate at 100,000 cycles.

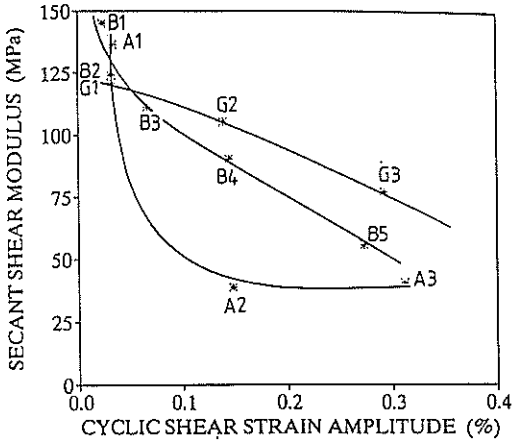

Figure 11 Comparison of the shear modulus of the three types of aggregate at 100,000 cycles.

strain. These two observations have the potential to lead to a pavement design method.

5. CONCLUSIONS

The simple shear compactor provides a means of categorising basecourse materials. In comparison with tests in the triaxial apparatus, which require a considerably larger specimen and much more time in preparation, the simple shear compaction test is attractive. At the present state of development the greatest limitation of the device is probably the lack of facility to test the basecourse specimen in a saturated condition.

The test results illustrate the effect of shear strain amplitude on density and shear modulus. They show that a threshold stress exists beneath which the basecourse shakes down to a fixed shear modulus. Further investigation of this concept might lead to developments in the design of pavements.

The tests confirm the well known fact that greywacke and basalt are superior aggregates to argillite. A small amount of particle breakdown was observed with the argillite but no perceptible change was found for the basalt and argillite.

6. ACKNOWLEDGEMENT

The work reported in this paper was supported in part by the Pavements Committee of the Road Research Unit of the former New Zealand National Roads Board. The project number was BC/60 and the support is gratefully acknowledged.

7. REFERENCES

1. Maurice, R. J. (1977) The development of a simple shear compactor for basecourse studies. M. E. thesis Civil Engineering Department, University of Auckland.

2. Peploe, R. J. (1991) Simple shear compaction of basecourse aggregates. PhD thesis Civil Engineering Department, University of Auckland.

3. Toan, D. V. (1976) Effects of basecourse saturation on basecourse performance. Report No. 125 University of Auckland School of Engineering.

Influence of Soil Density on Pile Skin Friction in Calcareous Sediments

H.G. POULOS
B.E., Ph.D., D.Sc.Eng., F.I.E.Aust., F.A.S.C.E., F.A.A.
Professor of Civil Engineering, University of Sydney
R.H. AL-DOURI
B.Sc.E., M.Eng.Sc., M.I.E.Aust.
Post Graduate Student, University of Sydney

SUMMARY Model tests on jacked piles in calcareous sand have been performed to study the influence of density on the shaft friction under static and cyclic loading.
Two types of test vessel have been used, in which dense and medium dense samples of New North Rankin calcareous sand have been consolidated under various overburden pressures. Model instrumented piles have been jacked into the sand samples and a study made of the influence of the sand density on the following aspects:
a) the jacking force required to install the pile
b) the skin friction and soil modulus for static loading
c) the degradation of skin friction under cyclic loading
d) the skin friction of the soil following the cyclic loading.
It has been found that the initial density of the sand has a significant effect on all these aspects.

INTRODUCTION

Previous experience from laboratory and field tests shows that the low capacity of jacked piles in calcareous sand can cause problems in the design of foundation for offshore structures. Dramatic evidence of such problems materialized in 1982 when some driven piles at the site of the North Rankin platform on the north west shelf of Australia dropped as much as 60m (about 50% of design length) under their own weight. Such experiences have stimulated subsequent investigators to perform laboratory work under a range of test boundary conditions, in order to reach a better understanding of the behaviour of piles and to develop means for making a reasonable estimation of pile capacity under both static and cyclic loading conditions. Several programs of model and field testing of piles in calcareous soils have been undertaken in the last decade (eg. Nauroy and Le Tirant, 1983; Poulos and Chan, 1986; Poulos and Lee, 1988), but a number of aspects of pile behaviour still require further investigation. One of these aspects is the influence of the density of the calcareous soil on pile response under axial loading.

This paper presents the results of static and cyclic loading tests on model piles jacked into calcareous sand samples with different initial densities, and under various overburden pressures. The following aspects of behaviour have been studied:

a) the jacking force required to install the pile
b) the skin friction and soil modulus for static loading
c) the degradation of skin friction during cyclic loading
d) the skin friction of the soil following the cyclic loading

PROPERTIES OF CALCAREOUS SAND

The calcareous sand used in the tests was obtained from the site of the North Rankin gas platform on the North West shelf of Western Australia. The grading curve is shown in Figure 1 and this soil can

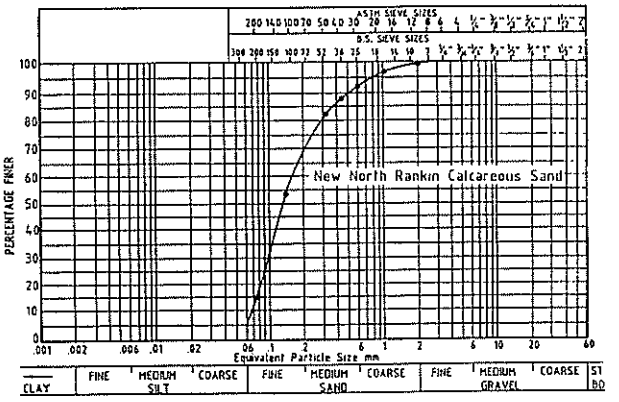

FIG 1 GRADING CURVE FOR CALCAREOUS SAND

be considered to be a well graded carbonate sand of mainly bioclastic and pelletal origin. The minimum and maximum dry densities of the test samples were 9.6 kN/m^3 and 13 kN/m^3. Microscopic examinations conducted on the calcareous sand showed that it contained a diverse range of particles with a high incidence of intra-particle voids, thin-wall particles and rod-like particles (Allman 1988). The angular nature of particles of this calcareous sand lead to a high friction angle and a high void ratio, and consequent high compressibility (Hull et al, 1988). The latter reference gives typical values of parameters for calcareous sand, as shown in Table 1.

APPARATUS AND TEST PROCEDURE

Two different sizes of test vessel were employed in this study, to gain a better understanding of the influence of the boundary condition of the test vessel (ie. the friction between the soil and the vessel wall) on the behaviour of the pile. The details of the large

TABLE 1. Physical Properties of New North Rankin Calcareous Sands tested (Hull et al 1988)

Cu =d10/d60	Fineness Modulus	Carbonate Content (%)	Max. Dry Density (kN/cu.m)	Min. Dry Density (kN/cu.m)
2.27	1.85	94	12.1	8.64

vessel and associated apparatus are shown diagrammatically in Figure 2. Both vessels were similar and in each case, it was possible to employ three alternative base conditions:

1. Rigid base: the test vessel base was a thick steel plate. This was commonly used for model pile tests in soil consolidated by a pressure applied only at the top.

2. Semi-Rigid base: in this case the soil was separated by a rubber membrane from the underlying pressurised water, which was deaired and confined in the bottom chamber. Again the soil was consolidated by an applied pressure at the top only.

3. Pressure Controlled base: This base was as for the second case, except that pressure was also applied at the bottom. In this case the soil was subjected to equal pressure at the top and base boundaries.

The tests described in this paper were obtained primarily using the rigid base and semi-rigid base conditions. The influence of the base condition was found to be relatively small, but is discussed in detail by Al-Douri (1992).

The main difference between the two vessels was that the small one had a diameter half that of the larger vessel. The large pressure vessel was mounted on a trolley which could be moved across the loading frame, permitting the model pile to be positioned for testing easily, while the small vessel was fixed on the base of the loading frame after it was positioned. The inside walls of both vessels were lined by a stainless steel sheet to reduce the friction between these walls and the sand.

The model pile was fabricated from 25mm external diameter aluminium tube, with a 3mm wall thickness. The pile was instrumented inside at 5 sections along the aluminium shaft. In each section, four electrical resistance strain gauges (forming a full Wheatstone Bridge circuit) were installed to enable measurement of the axial pile loads.

Installation and loading tests were performed by means of a loading machine of 15kN capacity. The applied load and the force along the pile were measured by a calibrated proving ring and strain gauges. The pile head displacement was measured by a displacement transducer (LVDT). All these measurements were recorded using a micro-computer connected to a data acquisition system.

The sand bed was prepared by raining sand into each vessel using a special device (Al-Douri et al 1990). The adopted procedure of raining sand produced a uniform bed of soil and enabled control of the density, with "loose" and "medium dense" sand samples being produced depending on the height of sand raining. The corresponding range of dry unit weight was 9.6 kN/m^3 to 10.5kN/m^3.

Dense samples were prepared by the same method as the medium dense, except that after raining, the soil was vibrated by two vibrators attached to the large

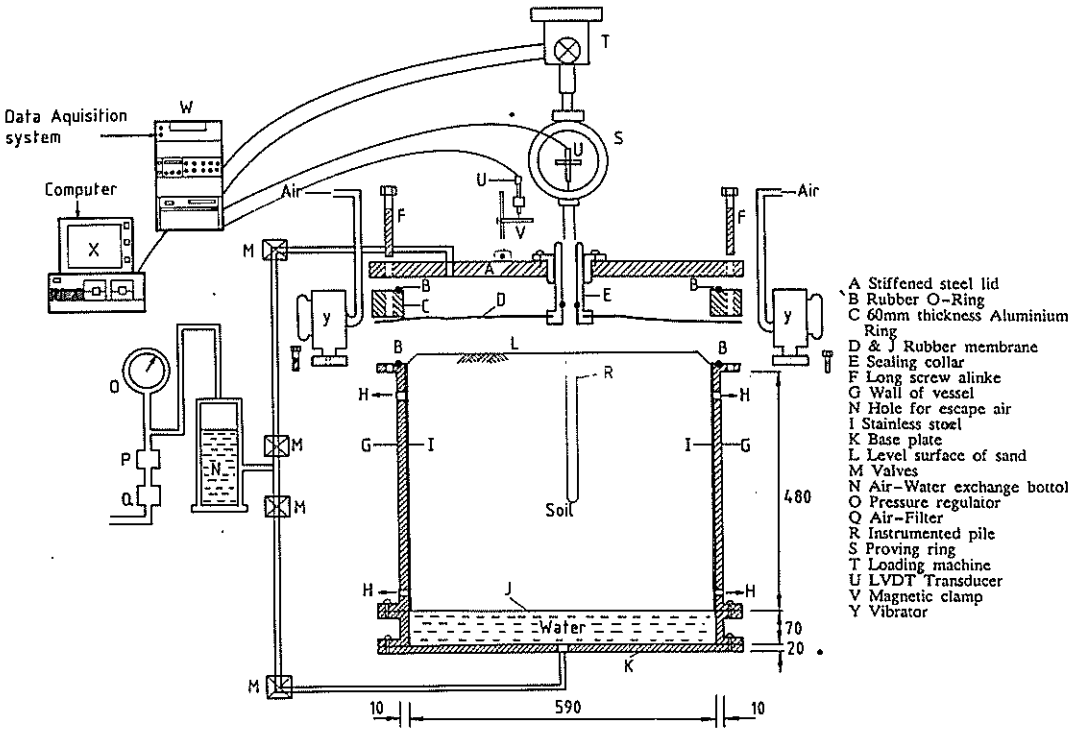

FIG. 2 DIAGRAMMATIC VIEW OF TEST SETUP

test vessel and by one on the small vessel. A unit weight greater than 10.5 kN/m^3 was obtained, the actual value depending on the time of vibration. After placement of the sand, a uniform overburden pressure was applied and the soil was allowed to consolidate for a period of at least 36 hours.

At the completion of consolidation, the pile was jacked into the sand bed using a loading machine. Readings of force and displacement were taken, and the strain gauges were monitored to determine the distribution of force along the pile at various stages of the jacking process. The applied load was recorded at a specified intervals until the pile reached its final penetration of about 290mm. After jacking, the pile was left unloaded for more than three hours until the readings of the strain gauges had stabilized. After taking the final set of residual load readings, the pile was attached to the loading machine and tested.

Each test generally consisted of three stages:

1. An initial static loading, in tension, to 10% of pile diameter, which was assumed to be failure (Kulhawy and Carter 1988).
2. A cyclic loading of the pile between pre-determined amplitudes of displacement for between 50 to 100 cycles.
3. The final static loading, to failure, to investigate the influence of cyclic loading on the performance of the pile.

The rate of displacement was constant for all the tests at 0.4mm per minute to avoid rate of loading effects on the pile capacity response. Two series of tests were performed on piles in medium dense and dense soils, using large and small test vessels, and the results are presented below.

RESULTS

A total of 30 tensile static and cyclic tests were performed on jacked model piles using both small and large vessels. The initial density and the overburden pressure applied in the tests are shown in Table 2, which also summarizes some of the key measurements of pile behaviour.

Behaviour During Jacking

Figure 3 shows a typical result for the behaviour of an instrumented pile during jacking in dense and medium-dense samples under three different overburden pressures.

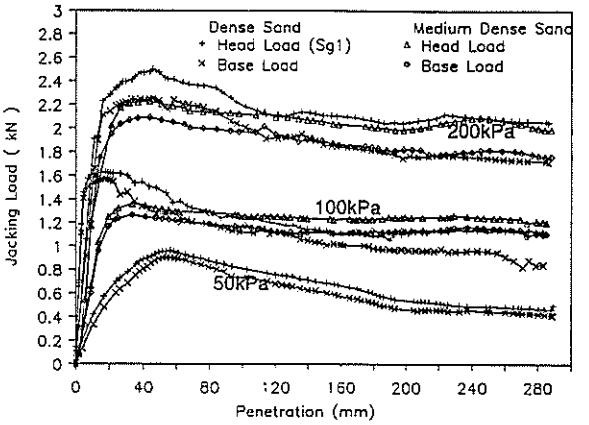

Figure 3. Head and Base Loads Versus Pile Pentration For Different Densities and Overburden Pressure

TABLE 2. Summary of Tests Carried out in Both Small and Large Test Vessels

Vessel Type	Vertical Pressure kPa	Density Range kN/cu.m	No. of Tests	Average Maximum E.B.C * During Jacking kPa	Average Maximum Friction During Jacking kPa	Average Maximum Friction During Testing kPa
Small	100	9.7-9.9	2	3400	22.1	9.5
	100	10.9-11.6	2	3528	32.0	15.4
	200	10.2-10.4	2	4945	34.8	22.5
	200	11-12	3	7478	47.8	36.1
Large	50	10.2	1	1854	12.7	4.0
	75	9.9	1	2489	13.6	4.6
	100	9.7-10.1	6	2857	18.3	8.3
	100	11-12	4	3356	28.6	14.2
	150	9.7-10.0	2	3315	21.2	12.0
	200	9.9-10.1	4	4151	27.6	16.9
	200	10.5-11.1	3	4866	33.8	25.9

* E.B.C = End-Bearing Capacity

The jacking force versus penetration for both densities increased to a peak and then decreased towards an ultimate value. The peak load was well defined for dense sand samples. The "strain- softening" behaviour appears to be more pronounced for the low overburden pressure of 50kPa than for the higher overburden pressures of 100kPa and 200kPa. The maximum values of head load and end bearing capacity for dense samples were higher than those for the medium dense samples, as can be seen from the values summarized in Table 2.

Figures 4a and 4b show the influence of soil density on the peak skin friction and end bearing resistance, normalized with respect to overburden pressure, during jacking of the piles. Both increase with increasing density as would be expected. The results are consistent with those of Poulos and Chua (1985), who observed that, for shallow foundations, the bearing capacity increased with increasing relative

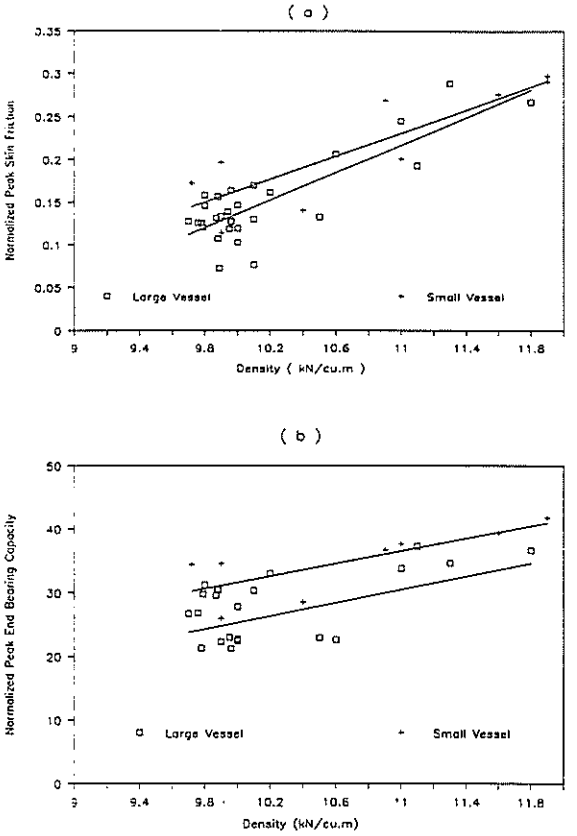

Figure 4. The Influence of Soil Density on Normalized Peak Skin Friction and End Bearing Capacity During Jacking

density of the silica and calcareous sands. However, there was a distinct tendency for the results obtained from the tests in the small vessel to be higher than those from large vessel. This reflects the greater influence of side restraint in the small vessel, especially on the skin friction.

Results of Static Loading Tests

Figure 5 shows typical relationships between load and deflection during tensile loading for dense and medium-dense sand subjected to 100 kPa and 200 kPa overburden pressure. For dense sand, the tensile load increased to a peak at about 0.5 mm deflection and then dropped to an ultimate value. In the case of the

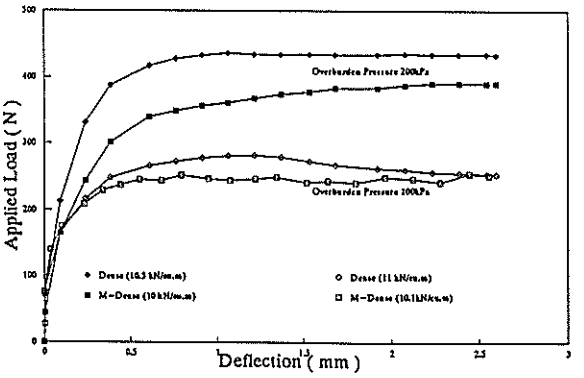

Figure 5. Load-Deflection Curves During Static Loading for Different Densities and Overburden Pressures

medium-dense sand, the load increased to a maximum value, with little evidence of a subsequent reduction.

Figure 6 plots the peak skin friction f_s as a function of applied overburden pressure σ'_{vo}, and reveals a reasonably linear relationship. The values of f_s are lower than those for piles in silica sands. Expressing the normalized static skin friction as f_s/σ'_{vo}, Figure 7 shows the influence of density on f_s/σ'_{vo} obtained from tests using both small and large vessels. The normalized skin friction in both cases increases with increasing density, but the values from small vessel tests tend to be greater than those from the large vessel, again apparently reflecting the influence of lateral restraint. The values of normalized

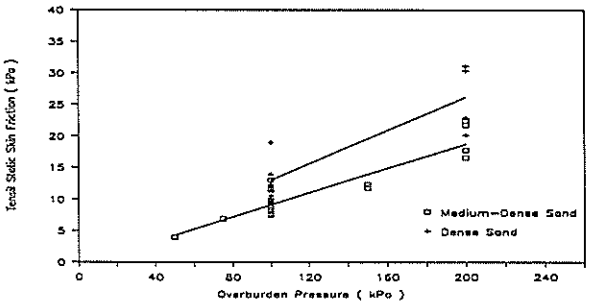

Figure 6. The Influence of Overburden Pressure on Static Skin Friction For Medium-Dense and Dense Sands

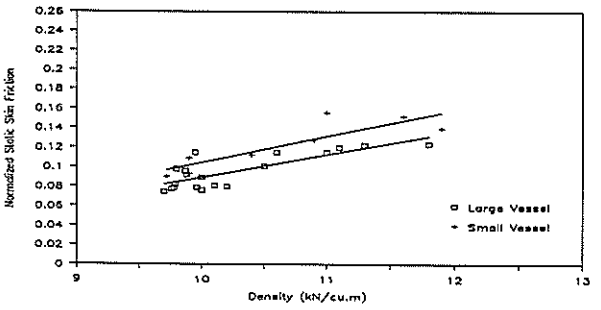

Figure 7. The Influence of Soil Density on the Normalized Static Skin Friction Using Both Large and Small Vessels

skin friction in Figure 7 are lower than those recorded during jacking (Figure 4a), but the reason for this difference is not clear at the present time.
From the load-settlement behaviour, the initial slope may be used with the elastic theory of Randolph and Wroth (1978) to backfigure the equivalent Young's modulus of soil.

Figure 8 shows the initial tangent soil modulus E_t' versus effective overburden pressure for both medium-dense sand and dense sand. The value of E_t' increases as σ_{vo}' increases, and is substantially greater for the dense sand than for the medium-dense sand. Corresponding values of Young's modulus E_{50}', for a load level of 50% of ultimate, are shown in Figure 9. Again E_{50}' increases with increasing overburden pressure in both medium-dense sand and dense sand, and is smaller than the tangent value E_t'. The E_{50}' values from the present tests are similar to those

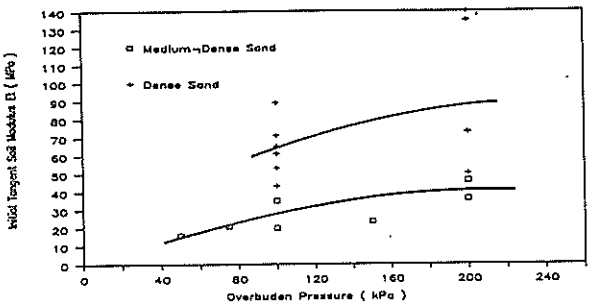

Figure 8. Effect of Overburden Pressure on Initial Tangent Soil Modulus for Medium-Dense and Dense Sands

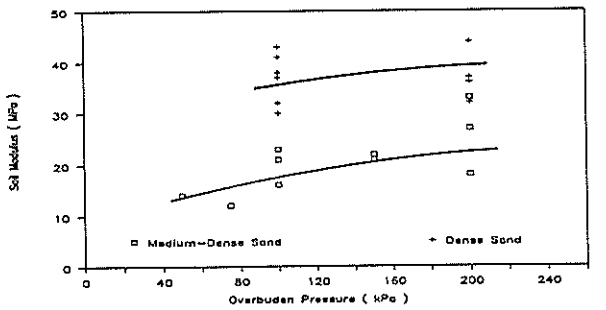

Figure 9. Effect of Overburden Pressure on the Static Young's Modulus "E50" for Medium-Dense and Dense Sands

obtained by Allman (1988) using a vessel similar to the small vessel used here.

Results of Cyclic Loading Tests

The skin friction degradation factor D_f is defined as the ratio of post-cyclic skin friction f_c to the peak static skin friction f_s. The influence of density on the magnitude of degradation factor is demonstrated in Figure 10. Figure 10a shows the relationship between the D_f and number of cycles in both medium-dense sand and dense sand for a given σ_{vo}' = 100kPa and a cyclic displacement $\pm\rho_c$ = 1.25mm. Figure 10b shows the same relationship in Figure 10a for σ_{vo}' = 200kPa and a cyclic displacement $\pm\rho_c$ = 2.5mm. For all tests, the highest rate of degradation occurs in the first 10 cycles and then the rate reduces. The value of D_f for medium-dense sand is greater than that for dense sand indicating that cyclic degradation is more severe for dense sand. The results of Allman (1988) on a jacked pile in dense calcareous sand are also shown in Figure 10b, and are consistent with the present results.

The variation of D_f with effective overburden pressure illustrated in Figure 11. The value of D_f decreases as σ_{vo}' increases for both sand densities. These results differ from some earlier tests (Chan 1986) in which the degradation factor appeared to be more or less independent of σ_{vo}'. Chan's tests were carried out on a different calcareous soil (from Bass Strait).

The influence of cyclic displacement on the value of D_f for medium-dense sand under σ_{vo}' = 100kPa and σ_{vo}' = 200kPa is shown in Figure 12. As found in previous tests, the value of D_f increases as $\pm\rho_c$ increases. The values of D_f for cyclic displacements of 0.5mm and 0.25mm are similar to those obtained from jacked piles in calcareous sand by Chan (1986).

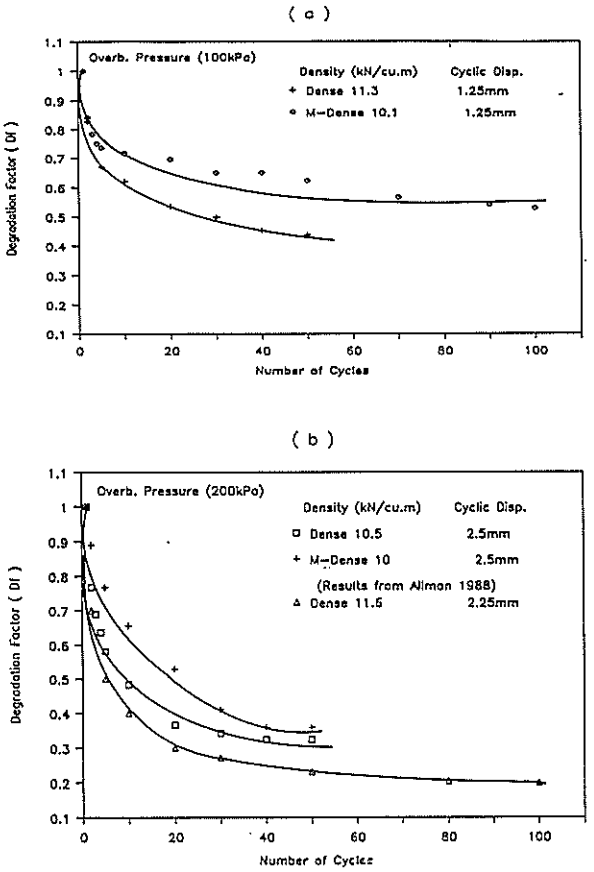

Figure 10. Degradation Factor Versus Number of Cycles

It is noteworthy that low values of D_f (0.6 or less) can occur for $\pm\rho_c$ in excess of about $\pm$ 0.5 mm, ie. cyclic loading can cause a severe loss of skin friction. However, the cyclic degradation for jacked piles is not as severe as for the grouted model piles tested by Lee and Poulos (1990), for which degradation factors of less than 0.1 were obtained.

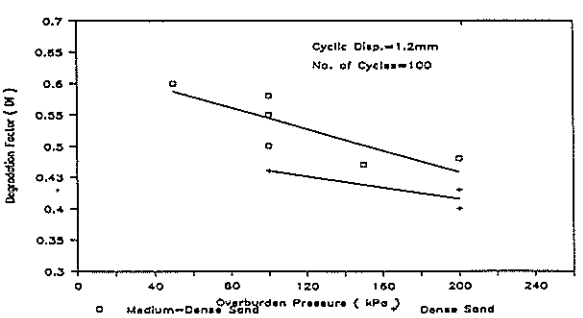

Figure 11. Degradation Factor Versus Overburden Pressure for Medium-Dense and Dense Sands

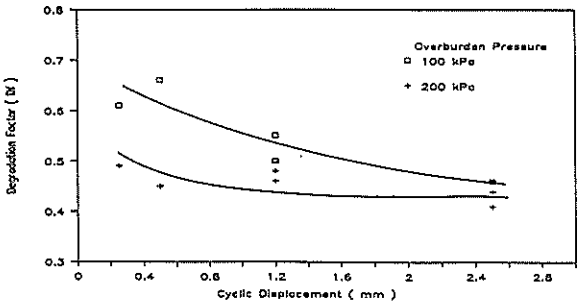

Figure 12. Degradation Factor Versus Cyclic Displacement for Medium-Dense Sands Under 100 and 200 kPa

CONCLUSIONS

Model tests on jacked piles in calcareous sand have been carried out to investigate the influence of initial soil density on the resistance during jacking, the static skin friction and soil stiffness, and the degradation of skin friction under cyclic loading. Tests were carried out for two different density states ("medium-dense" and "dense") in two different sizes of test vessel.

The tests carried out in the smaller test vessel show generally higher values of skin resistance, indicating that the results of these tests may be influenced by the side-wall restraint of the vessel.
The following conclusion have been drawn from the tests:

1) the jacking resistance increases as the initial soil density increases, with both the end-bearing and shaft resistance increasing

2) the jacking resistance increases as the overburden pressure increases

3) both skin friction and soil Young's Modulus increase with increasing soil density and increasing overburden pressure

4) the skin friction developed under static loading conditions is less than that developed during jacking.

5) under cyclic loading, the skin friction tends to "degrade". Degradation becomes more severe as the soil density increases.

6) degradation of skin friction becomes more severe as the cyclic displacement increases and as the overburden pressure increases.

It is believed that the results of these tests are of value in the design of driven piles in calcareous sediments.

ACKNOWLEDGEMENTS

The work described in the paper forms part of a research project on the mechanics of calcareous soil, which is supported by a grant from the Australian Research Committee. The authors gratefully acknowledge the assistance of Dr. T.S. Hull and Dr. C.Y. Lee with several aspects of the experimental work, and Mr. R. Barker who supervised construction of the experimental apparatus.

REFERENCES

Al-Douri R. H., Hull T. S. and Poulos H. G. (1990). Preparation and Measurement of Uniform Sand Beds in The Laboratory. Research Report No. R609, School of Civil and Mining Eng., The University of Sydney.

Al-Douri R.H. (1992). The Behaviour of Jacked Piles in Calcareous Sand. PhD Thesis, The university of Sydney.

Allman M.A. (1988). The Behaviour of Piles in Cemented Calcareous Soils. PhD Thesis, University of Sydney.

Chan K.F. (1986) Behaviour of Model Piles in Calcareous Sand. M.Eng. Sc. Thesis, The University of Sydney.

Hull T. S., Poulos H. G. and Alehossein H. (1988). The Static Behaviour of Various Calcareous Sediments. Proc. Int. Conf. on Calc. Sediments., Perth, Australia, Vol. 1, pp. 87-96.

Kulhawy F.H. and Carter J.P. (1988). The Design of Drilled Shaft Foundations, Short Course Lecture Notes. Civil and Mining Eng. Foundn. C.G.R., The University of Sydney.

Lee C.Y. and Poulos H.G. (1990). Experimental Investigatiions of Axial Capacity of Model Grouted Piles in Marine Calcareous Sediments. Research Report No. R618, School of Civil and Mining Eng. Sydney University.

Nauroy, J.F. and Le Tirant, P. (1983). Model Tests of Piles in Calcareous Sands. ASCE Spec. Conf. on Geot. Practice in Offshore Eng. Austin, pp. 356-369.

Poulos H.G. and Chan, K.F. (1988). Tests on Model Instrumented Piles in Calcareous Soil. Proc. Int. Conf. on Calc. Sediments, Perth, Australia, Vol. 1. pp. 245-254.

Poulos H.G. and Chau E.W. (1985). Bearing Capacity of Foundations on Calcareous Sand. Proc. 11th Int. Conf. Soil Mechs. Foudn. Eng., pp. San Francisco, Vol. 3, 1619-1622.

Poulos H.G. and Lee C.Y. (1988). Model Tests on Grouted Piles in Calcareous Sediments. Proc. Int. Conf. on Calc. Sediments, Perth, Australia, Vol. 1, pp. 255-260.

Randolph M.F. and Wroth C.P. (1978). Analyses of Deformation of Vertically Loaded Piles. Jnl. Geot. Eng., ASCE, Vol. 104, No. GT12, pp. 1465-1488.

Some Residual Strength Measurements on New Zealand Soils

L.D. WESLEY
M.E., M.Sc.(Eng.), Ph.D., M.I.P.E.N.Z.
Senior Lecturer, Civil Engineering Department, University of Auckland

SUMMARY

The results of residual strength measurements on some New Zealand soils are presented. The soils tested consisted mainly of weathered Waitemata sandstones, weathered volcanic ash, Pleistocene material, and Onerahi Chaos. The results show that while most soils conform to the pattern of behaviour of overseas soils, the range of ϕ'_r values within any group is large. The volcanic ash soils show consistently high ϕ'_r values and do not conform to conventional soil behaviour.

1. INTRODUCTION

The residual strength of soils is important in geotechnical engineering in relation to the stability of existing land slides and the stability of deposits which contain shear surfaces or similar discontinuities. It is also of importance in understanding or evaluating the risk of progressive failure in certain materials. In this paper the results of a series of residual strength measurements on a number of New Zealand soils are presented.

2. TEST PROCEDURES

The tests have been carried out in a Bromhead ring shear apparatus (Bromhead, 1979). This device is much simpler than the original ring shear apparatus described by Bishop et al (1971); the most important difference between the two devices is in the constraints placed upon the location of the shear surface within the ring sample. The design of the original apparatus is such that the shear surface forms at the centre of the samples with approximately equal thicknesses of soil above and below the shear plane. In the Bromhead apparatus, the shear surface invariably forms close to the top of the sample, and in most cases appears to be right at the interface with the upper platen. Despite this important difference, the test results from the two devices appear to be very similar (Bromhead, 1979).

The tests have been carried out at a rotation rate of 0.024 or 0.12°/min; this corresponds to displacement rates of 0.018 and 0.09mm/min. These rates were chosen for convenience; the higher rate was generally used during working hours, and the lower rate outside these times. While this rate is slightly faster than displacement rates normally used in ring shear tests, the influence on measured strengths is negligible (Skempton 1985). The normal stress range used in the tests was from 25kPa to 500kPa.

The actual procedure for setting up the samples and conducting the tests was to first adjust the water content of the soil so that it was a little wetter than the plastic limit, and then to press it into the annular slot in the apparatus. Loads were then added to consolidate the sample to the maximum normal stress to be used in the test, and then unloaded to the minimum stress to be applied. The test was then carried out using a sequence of increasing normal stresses. By using this procedure the amount of soil lost by "squeezing" out through the small gap at the edge of the upper platen was minimised.

In addition to the ring shear tests, measurements were made of natural water content, Attenberg limits and particle size.

3. SOILS TESTED

The samples tested came from the upper half of the North Island and belonged mainly to the following geological groups:

Weathered Waitemata series sandstone and siltstone
Weathered Pleistocene deposits in the Auckland area
Weathered volcanic ash
Weathered Onerahi Chaos sandstone or siltstone.

No attempt has been made to systematically obtain representative samples from each of these groups; tests have simply been carried out as time and samples have been available. Nearly all the samples used were obtained as part of site investigations for other purposes, and no claim is made that they are necessarily typical or representative of the geological groups they come from.

The location of the samples, together with descriptions and geological origin, is given in Table 1. Also included among the volcanic ash samples are four samples from Indonesia. This has been done partly because of an interest in volcanic ash soils on the part of the writer, and partly to check some residual strength measurements made earlier on these soils (Wesley, 1977). These earlier measurements on samples from Indonesia gave ϕ'_r values in the range of

TABLE 1. SAMPLE DETAILS AND TEST RESULTS

Sample No	Location	Description		Natural Water Content %	Atterberg Limits			Particle Size		Residual Angle ϕ'_r
		Soil Type	Geological Origin		LL	PL	PI	<.06	<.002	
1	Symonds St, Auckland	Stiff grey clay	Waitemata Siltstone	-	77	40	37	92	35	19.3
2	"	Pale yellow silt	"	43.0	52	33	19	56	20	27.5
3	"	Hard grey clay	"	51.5	89	29	60	98	45	14.0
4	"	Firm yellow clay	"	51.9	80	40	40	93	52	20
5	Redoubt Rd, Manukau	Grey clay	"	51.2	97	47	50	92	59	9.9
6	Takapuna	Highly plastic grey clay	"	46.8	118	35	83	100	76	7.4
7	Sunset Rd, North Shore	Pale yellow clay	"	45.9	89	39	50	87	57	13.1
8	Omata 1 New Plymouth	Pale brown clayey silt	Volcanic ash	99.6	108	72	36	82	41	24.5
9	" 2	"	"		103	60	43			31.0
10	" 3	"	"	-	151	83	68	100	f	18.1
11	Morrinsville 1	Pale brown clayey silt	"	51.7	115	68	36	66	28	28.0
12	" 2	"	"	71.0	113	67	46	65	f	34
13	Mangamahoe Dam New Plymouth	Pale yellow clayey silt	"	72.4	93	84	9	65	22	35
14	Minden, Tauranga	Light brown clayey silt	"	47.6	54	33	21	65	39	26
15	Ruahihi,Tauranga 1	Orange brown silty clay	"	90.5	104	74	30	56	f	35
16	" 2	Orange silty clay	"	137.8	140	84	56	45	f	37
17	Darajat,Indonesia 1	Brown silty clay	"	162.0	183	112	71	96	77(f)	35
18	" 2	"	"	166.5	197	120	77	100	f	31
19	" 3	"	"	153.3	183	140	43	100	f	37
20	Kamojang,Indonesia	Yellowish brown silty clay	"	135.6	175	133	42	100	f	36
21	Takapuna	Highly plastic grey clay	Pleistocene deposits	38.9	129	40	89	99	91	8.1
22	Takapuna	Greyish white clay	"	42.1	89	42	47	100	72	10.0
23	Takapuna	Grey clay	"	-	39	20	19	83	40	25.6
24	angarei	Yellow clay	Onerahi chaos	56.4	88	43	45	98	52	15.9
25	hangarei	Hard grey clay	"	-	64	29	35	90	30	13
26	Bay of Plenty (Wirihana Quarry)	Yellowish brown silty clay	Weathered ignumbrite	46.9	71	40	31	78	34	23.5
27	Bay of Plenty (Camerons Quarry)	Brown silty clay	Weathered greywacke	25.2	38	28	10	58	13	25.0

f indicates flocculation during sedimentation.

24° to 39°; these were from samples with clay contents in the range of 65% to 83% where ϕ'_r values would typically be less than 10°.

Two of the weathered Waitemata series samples, Nos 5 and 6, were taken from clearly identified shear zones where slipping had taken place at some time in the past. Investigations were being carried out at both these sites because of stability concerns associated with these shear zones.

4. TEST RESULTS

The results of the tests are summarised in Table 1 and presented graphically in the figures that follow. The values of ϕ'_r have been calculated for an effective normal stress of 200kPa and an assumed cohesion intercept of zero. This stress level is thus a little lower than the mid range value of the normal stresses used in the tests.

It is clear from Table 1 that the soils tested cover a fairly wide range of soil types. Plasticity indicies range from 9 (Sample 13) to 89 (Sample 21) and clay fractions from 13% (Sample 27) to 91% (Samples 21). It should be noted that clay fractions for some of the volcanic ash samples are not given; this is due to flocculation occurring during the sedimentation process, a phenomenon not uncommon with such soils.

The position occupied by the soils on the plasticity chart is shown in Fig.1. On the basis of their relative distribution, the soils divide themselves into two groups, namely the non volcanic ash soils ("normal" soils) and the volcanic ash soils. The former group tend to lie close to the A-line, in accordance with conventional soil behaviour, while the volcanic ash soils lie well below the A-line in a zone typical of such soils (Wesley 1974). This natural division of the soils into two distinct groups will be used as a basis for presenting the results of the ring shear tests.

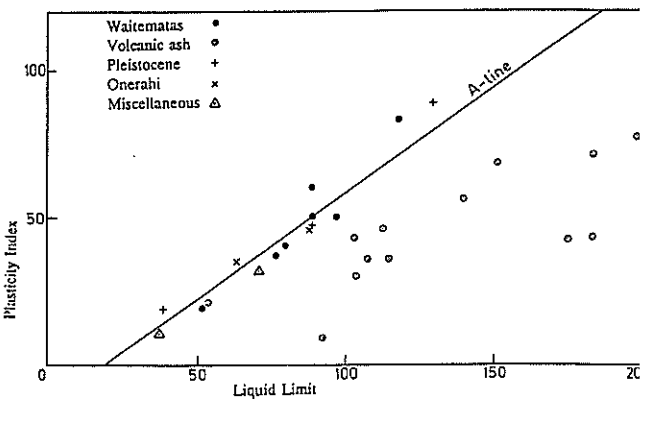

Fig 1 Position on Plasticity Chart

A typical result for tests on the non volcanic ash soils is shown in Fig.2. These soils all tended to behave in a conventional manner, as described for example by Lupini et al (1981) or Skempton (1985). The strength envelope is slightly curved, so that the value of τ/σ_n is somewhat higher at lower stress levels and then falls to an approximately constant value at higher stress levels. The values of shearing resistance at any particular stress level tend to be quite constant, especially for the high plasticity materials which have low ϕ'_r values. For the low plasticity materials the residual strength tends to be rather less constant and varies somewhat at any particular stress level. This variation, however, is still very small, and has an almost negligible effect on the ϕ'_r value. Tests were carried out on some soils in this group using a sequence of both increasing and decreasing normal stress; it was found that almost identical readings were obtained in each case.

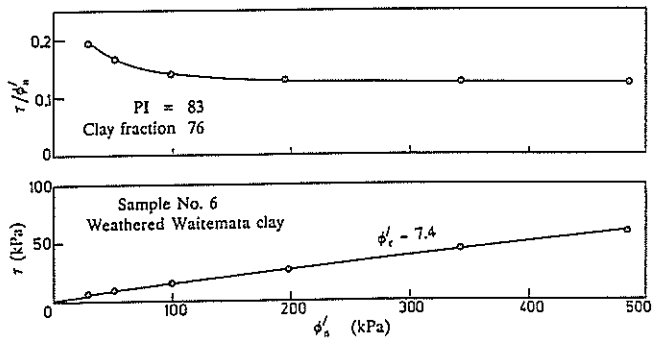

Fig 2 Ring shear result from Sample 6

For the volcanic ash group, a typical result is shown in Fig.3. With these soils, the residual strength was generally high but was less well defined as readings tended to fluctuate considerably at each normal stress. Also, when tests were carried out using both increasing stress and decreasing stress sequences, there tended to be significant variations in the readings. However there did not appear to be a consistent pattern to these variations. The result in Fig.3 shows the ϕ'_r value to be generally lower for the unloading sequence than for loading, but this was not a uniform pattern in all tests.

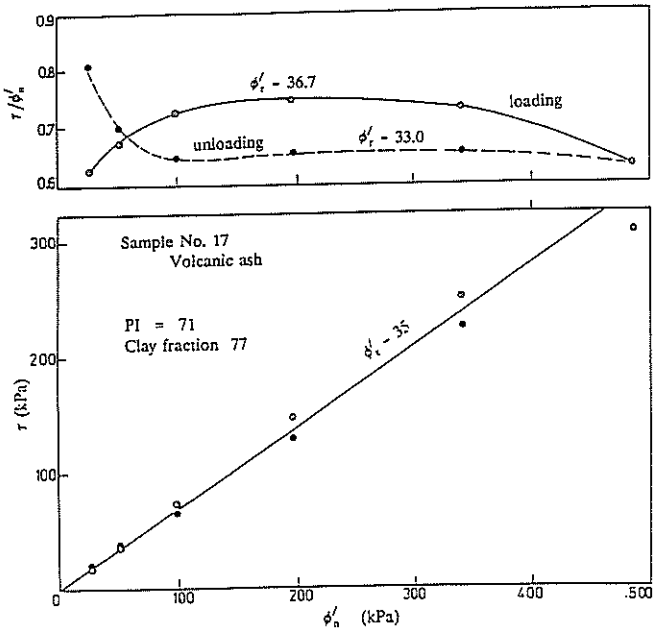

Fig 3 Ring shear result from Sample 17

In Fig.4 the residual strength values are plotted against plasticity index; this is done separately for the two soil groups. Also shown on these graphs is a line which represents the approximate upper limit of ϕ'_r values obtained from sedimentary soils overseas. This line (and the similar line in Fig.5) has been deduced from the data summarised by Lupini et al (1981). This line is not a well defined line (nor is the lower limit line) and is introduced here only for the purpose of comparing results from New Zealand soils with those obtained overseas (mainly in the United Kingdom). The behaviour of the non volcanic ash soils appears to generally conform to "normal" soil behaviour, while that of the volcanic ash samples is quite different.

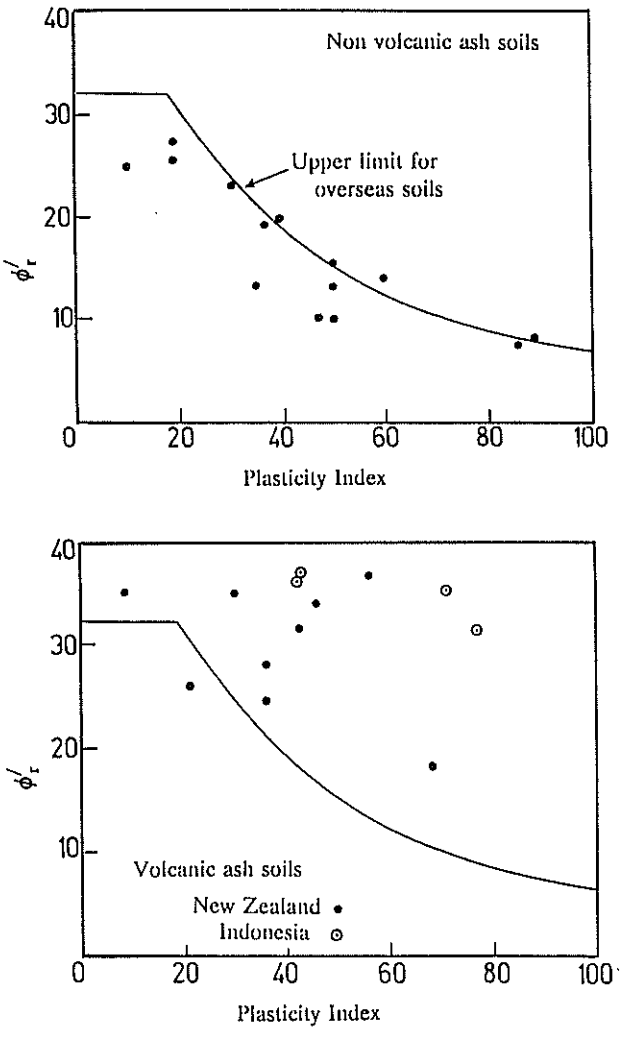

Fig 4 ϕ'_r versus Plasticity Index

The ϕ'_r values from the volcanic ash samples are much higher than for "normal" soils, and do not appear to be related to plasticity index. The highest ϕ'_r values are from Indonesian samples, which are believed to have higher allophane contents than the New Zealand ash samples.

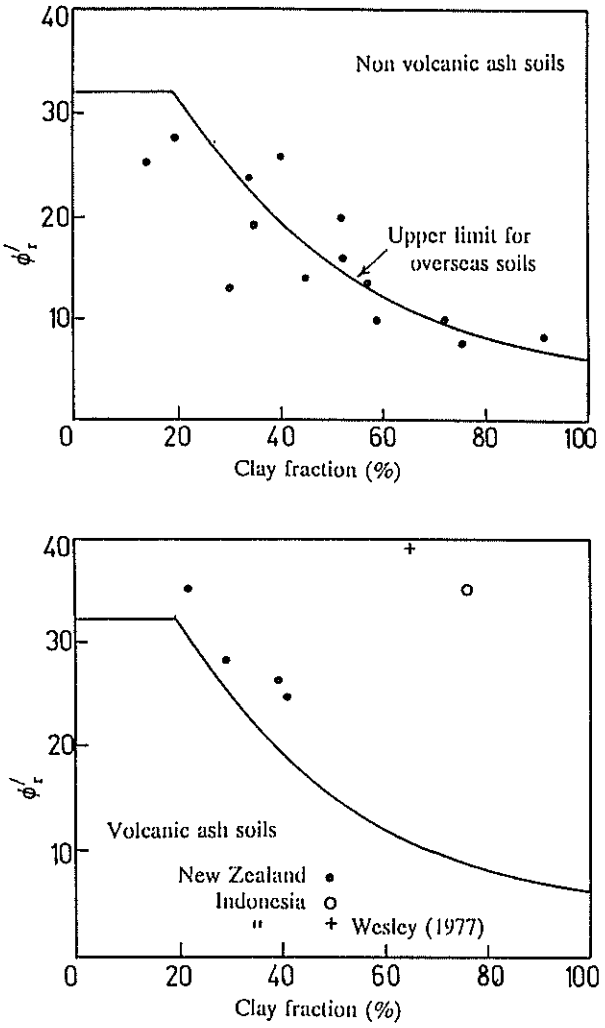

Fig. 5 ϕ'_r versus clay fraction

In Fig.5, the results are re-plotted against clay fraction using a similar format to Fig.4. This emphasises similar trends to those shown in Fig.4, although the plot of ϕ'_r against clay fraction for the non volcanic ash soils shows greater scatter than the similar plot against P.I. Also, a number of points be significantly above the upper limit line.

5. DISCUSSION OF RESULTS

5.1 Normal (Non Volcanic Ash) Soils.

Not surprisingly, the behaviour of these soils conforms fairly well to that of overseas soils, as summarised by Lupini et al (19081). Perhaps the most significant feature to emerge from the tests is the wide range of values obtained within particular soils groups. For examples, in the Waitemata series samples, values of ϕ'_r ranged from 7.4° to 27.5°. In the Pleistocene materials, the ϕ'_r values ranged from 8.1° to 25.6°. However, this range of values is not surprising in view of the similar wide range in P.I. values and clay fractions.

As mentioned earlier, two of the Waitemata samples were from pre-existing shear zones, which were associated with stability concerns at their respective sites. The very low ϕ'_r values from these samples (7.4° and 9.9°) are a salutary reminder that zones of very low strength materials can be found within what are otherwise quite competent materials. Geotechnical engineers are sometimes tempted (or forced) to adopt "typical" values for properties of commonly occurring materials such as weathered Waitemata clays; this is no doubt unavoidable to some extent but the results presented here highlight the risks associated with this approach. Regardless of whether such an approach is adopted, or a detailed investigation carried out, there is still the risk that the detailed investigation may not identify these low strength zones.

It will be apparent to the reader that the number of tests for soil groups other than the Waitematas is too few to be able to draw any general conclusions.

5.2 Volcanic Ash Soils

The ϕ'_r values from the soils are unusual, firstly because they are very high and secondly because they do not appear to be related to either plasticity index or clay fraction. The reason for this is not known exactly, but appears to be due to the unusual characteristics of the amorphous clay mineral allophane. There is something about this material which gives it high frictional resistance when sheared, and the absence of plate-like particles presumably means that particle reorientation leading to lower frictional resistance does not occur in these soils. As mentioned above, the measured shearing resistance in the ring shear tests tended to vary somewhat at any particular normal stress. The precise reason for this is not known, although it is believed to be due to the nature of the shear surface which forms during the test. In tests on volcanic ash samples carried out in the Imperial College ring shear apparatus, it was observed that a number of shear planes developed, and shearing probably switched from plane to plane in a random manner, with associated variations in readings. This is in contrast to sedimentary clays where the formation of a shear surface results in a drop in strength and thus a natural tendency for only one plane to form.

6. CONCLUSION

The main points of interest which emerge from this study are as follows:

1. Apart from the volcanic ash samples, the behaviour of the soils in ring shear tests is similar to that recorded overseas with sedimentary soils.

2. The range of ϕ'_r values is very large, even within a particular geological soil group.

3. Very low ϕ'_r values obtained from two samples of Waitemata series clays emphasise the risk that local low strength zones may exist within what are otherwise quite competent materials.

4. Results from the volcanic ash samples are very distinctive; the ϕ'_r values are very high and do not appear to be related to either plasticity index or clay fraction.

7. ACKNOWLEDGEMENTS

Thanks are due to Tonkin and Taylor Ltd., Consulting Engineers of Auckland, and to Dr Warwick Prebble of Auckland University for making available some of the samples included in this study.

REFERENCES

Bromhead E.N. (1979) A simple ring shear apparatus Ground Engineering July, 1979, pp 40-44.

Bishop A.W., Green G.E., Garga V.K., Andresen A and Brown J.D. (1971). A new ring shear apparatus and its application to the measurement of residual strength. Geotechnique 21,4, pp 273-328.

Lupini J.F., Skinner A.E. and Vaughan P.R. (1981). The drained residual strength of cohesive soils. Geotechnique 31,2, pp 181-213.

Skempton A.W. (1985). Residual strength of clays in landslides, folded strata, and the laboratory. Geotechnique 35,1, pp 3-18.

Wesley L.D. (1977). Shear strength properties of halloysite and allophane clays in Java, Indonesia. Geotechnique 27,2, pp 125-136.

Risks in Using Materials Data Obtained from Repeated Load Triaxial Tests in Pavement Design and Analysis

B. VUONG
B.E., M.E.Sc.
Research Scientist, Australian Road Research Board

SUMMARY To design and to analyse granular pavements requires resilient moduli and Poisson's ratios for the granular base and sub-grade materials concerned. They can be obtained from repeated load triaxial tests. A typical basecourse crushed rock was tested using a range of cyclic and static confining pressures and the resilient moduli were derived and fitted to available models for resilient modulus. One of the models was found to produce comparable constants for both test types and, therefore, could provide a basis for correcting the moduli obtained from different methods of applying confining pressure. All the models were used in the program NONCIRL to predict the lives of some typical granular pavements selected from the NAASRA Pavement Design Guide. The predicted lives range from 0.3 to 3 times the NAASRA design lives and this indicates that the risks associated with the use of different characterisation models in pavement design and analysis are significant.

1. INTRODUCTION

The recent widespread acceptance of new mechanistic pavement design procedures, such as those adopted in the 1987 NAASRA Guide to the Structural Design of Road Pavements (1), has led to a need for improved material characterisation techniques for all classes of pavement materials, particularly for unbound granular materials and subgrades. At the National Workshop on Resilient Modulus Testing of Unbound Pavement Materials and Subgrades organised by the Australian Pavement Research Group (APRG) in South Australia, in February 1991 (2), there were consensus statements that the repeated load triaxial test with either cyclic or static confining pressure can be used to determine material resilient modulus and Poisson's ratio, which are used as input parameters in the mechanistic pavement design. However, as the two test types could produce different modulus values at the same stress levels (3, 4, 5, 6), their application to pavement design and analysis could produce different end results.

This paper describes the results for a typical base crushed rock determined by the two test types. Some available non-linear material models are used to fit the results and then incorporated in the program NONCIRL (7) to predict pavement lives for some typical granular pavements selected from the NAASRA Guide. Comparisons of pavement lives calculated with NONCIRL to those estimated by the NAASRA Guide enable identification of the risk associated with the use of different test types and different characterisation models in pavement design and analysis.

2. THE DESIGNED PAVEMENTS

Granular pavement structures as designed according to the NAASRA Guide consist of a thin sprayed chip seal surfacing of about 20 mm, a base layer and a sub-base layer laying on the subgrade. The predicted pavement life calculated using the NAASRA subgrade strain criterion is expressed as:

$$N = (8511/\varepsilon_V)^{7.14} \qquad (1)$$

where N is the number of Equivalent Standard Axles (ESA) and ε_V the critical subgrade strain at top of the subgrade calculated with the program CIRCLY (8), using the standard loading configuration as described in the NAASRA Guide.

Altogether 9 granular pavements were designed for three subgrade types (namely CBR3, CBR5 and CBR10, respectively) and for three design traffics (namely 10^5, 10^6 and 10^7 ESAs, respectively). The NAASRA Design Chart (Figure 8.4 in the 1987 NAASRA Guide) was used for selecting the total thicknesses of the base and sub-base layers of the 9 granular pavements, which are given in Table I.

TABLE I

PAVEMENTS ADOPTED IN THE STUDY.

Pav No	CBR	Total thickness (mm)	Design life (ESA)
1	3	400	10^5
2	3	520	10^6
3	3	640	10^7
4	5	300	10^5
5	5	390	10^6
6	5	480	10^7
7	10	200	10^5
8	10	260	10^6
9	10	320	10^7

3. CHARACTERISATION OF THE GRANULAR BASE/SUB-BASE MATERIAL

3.1. Testing methods

Four samples of a typical basecourse crushed rock, each with specified density of 2.20 t/m^3 and moisture content of 4 %, were prepared for repeated load triaxial testing to provide data for examining the difference in resilient modulus produced by the two test types.

For the samples 1 and 2, each sample was tested in accordance with the SHRP Protocol P46 testing procedure (9) using static confining pressures (σ_3) in the range of 20 kPa to 68 kPa and vertical/radial stress ratios (σ_1/σ_3) in the range of 2 to 10.

After the above test series, the same sample was subjected to another test series using cyclic confining pressures in the range of 20 kPa to 120 kPa and with stress ratios in the range of 2 to 10, as suggested in the ARRB testing procedures (10).

The samples 3 and 4 were tested in the reversing order, i.e. to start with the test series with cyclic confining pressures and then following with the test series with static confining pressures. The emphasis was to show the negligible effects of loading history on the resilient moduli derived in the tests.

The difference between the stress paths of the two test types can be seen in Figure 1, where they are plotted in the stress space of total stress, $\theta = (\sigma_1 + 2.\ \sigma_3)$, and deviator stress, $q = (\sigma_1 - \sigma_3)$. As shown in Figure 1, the two test types have the same peak total stress and deviator stress, but different initial static total stresses and different cyclic total stresses.

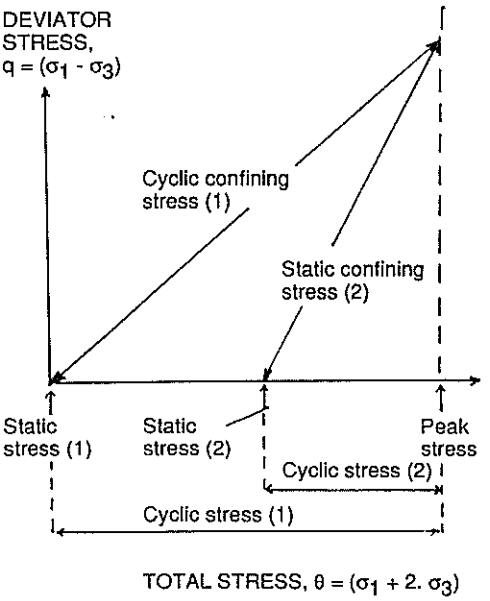

Figure 1 Stress paths for the two repeated load triaxial test types

3.2. Test results

The resilient modulus (E_r) and Poisson's ratio (ν_r) were calculated using the generalised Hooke's law as:

$$E_r=(\sigma_{1r}-\sigma_{3r}).(\sigma_{1r}+2.\sigma_{3r})/(\varepsilon_{1r}.(\sigma_{1r}+\sigma_{3r})-2.\varepsilon_{3r1}.\sigma_{3r}) \quad (2)$$

$$\nu_r = (\varepsilon_{1r}.\sigma_{3r}-\varepsilon_{3r}.\sigma_{1r})/(\varepsilon_{1r}.(\sigma_{1r}+\sigma_{3r})-2.\varepsilon_{3r1}.\sigma_{3r}) \quad (3)$$

where σ_{1r} and σ_{3r} are the cyclic vertical and radial stresses, respectively; and ε_{3r} and ε_{1r} are the measured radial and vertical resilient strains, respectively.

In the test with static confining pressure, $\sigma_{3r} = 0$, the above equations are simplified as:

$$E_r = \sigma_{1r}/\varepsilon_{1r} = q_r/\varepsilon_{1r} \quad (4)$$

$$\nu_r = -\varepsilon_{3r}/\varepsilon_{1r} \quad (5)$$

The moduli obtained from a typical test are plotted against peak mean stresses, $\sigma_m = \theta/3$, as shown in Figure 2. The results indicate that, for the same peak mean stresses, the

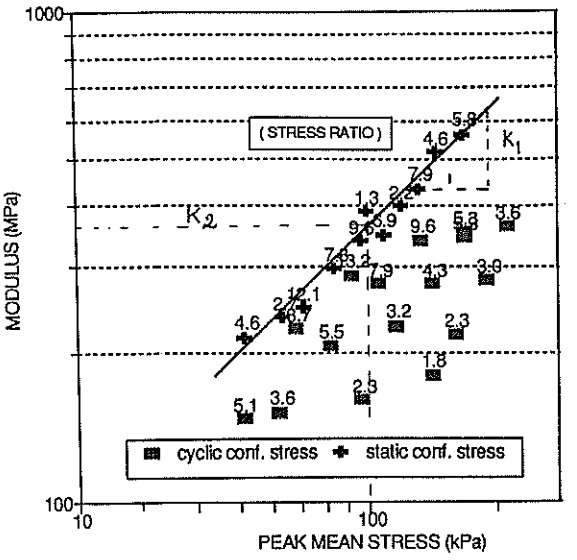

Figure 2 Typical results fitted with chacraterisation Model 1 (Sample No. 3)

modulus obtained from the tests with static confining pressure are generally higher than those obtained from the tests with cyclic confining pressures.

3.3. Characterisation models for granular materials

There have been many characterisation models developed for different granular base materials using different testing techniques (3, 4, 5, 11). They are often expressed as functions of some common stress parameters, such as confining stress, σ_3, deviator stress, $q = \sigma_1 - \sigma_3$, total stress, $\theta = \sigma_1+2.\sigma_3$, mean stress, $\sigma_m = \theta/3$, and stress ratio = σ_1/σ_3. This study considers four models, which are closely fitted to the test results, as described below.

3.3.1 Model 1: Modulus Vs peak mean stress (for tests with constant confining pressure)

Past studies of resilient response of granular material using the method of applying static confining pressure (11) reported that the resilient modulus is a function of the peak total stress; i.e.

$$E_r = K_2.\theta^{K1} \quad (6)$$

To allow K_2 to have the same unit as E_r (MPa), Equation 6 can be expressed in another form of

$$E_r = K_2.(\sigma_m/\sigma_{Ref})^{K1} \quad (7)$$

where $\sigma_m = \theta/3$ is the peak mean stress and σ_{Ref} is the reference stress of 100 kPa.

Typical results fitted by Model 1 are shown in Figure 2. Average values of K_1 and K_2 obtained from all the tests are 0.70 and 340 MPa.

3.3.2. Model 2: Modulus Vs peak mean stress and stress ratio (for tests with cyclic confining pressure)

Studies for various granular materials carried out at ARRB using the test with cyclic confining pressure (12, 13, 14, 15) reported that the resilient modulus is a function of both peak mean stress and stress ratio (σ_1/σ_3).

In this case, the model has the same form as that of Equation 7 and with the same value for K_1, but K_2 is a function of peak stress ratio (σ_1/σ_3), i.e

$$K_2 = K_{2max} - S_1.\{Log7 - Log(\sigma_1/\sigma_3)\} \quad (8)$$
for $(\sigma_1/\sigma_3)<7$

$$K_2 = K_{2max} \quad (9)$$
for $(\sigma_1/\sigma_3)\geq 7$

Typical results fitted by Model 2 are shown in Figure 3. Average values of K_{2max} and S_1 obtained from all the tests are 270 and 230 MPa, respectively.

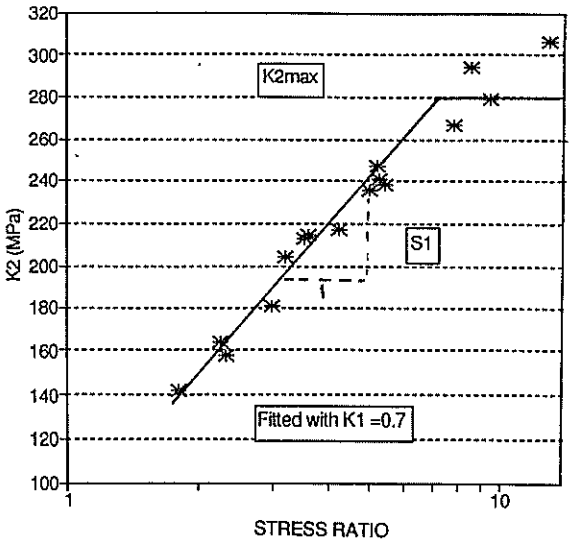

Figure 3 Typical results fitted with chacraterisation Model 2 (Sample No. 3)

3.3.3. Model 3: Modulus Vs average mean stress (for both test types)

Vuong (6) also reported that the two test types could produce comparable moduli at the same average mean stress, $\sigma_{mAve.} = (\sigma_{mstatic} + \sigma_{mpeak})/2$, providing that the peak stress ratios (σ_1/σ_3) in tests with cyclic confining pressures are greater than 5. The relationship is expressed as

$$E_r = K_3.(\sigma_{m\ Ave.}/\sigma_{Ref})^{K1} \quad (10)$$

Typical results fitted by Model 3 are shown in Figure 4. Average value for K_3 obtained from all the tests is 430 MPa.

3.3.4. Model 4: Modulus Vs average mean stress and stress ratio (for tests with cyclic confining pressure)

To fit more closely the results obtained from tests with cyclic confining pressure, the parameter K_3 in Equation 10 is expressed as a function of peak stress ratio (σ_1/σ_3), i.e.

$$K_3 = K_{3max} - S_2.\{Log7 - Log(\sigma_1/\sigma_3)\} \quad (11)$$
for $(\sigma_1/\sigma_3)<7$

$$K_3 = K_{3max} \quad (12)$$
for $(\sigma_1/\sigma_3)\geq 7$

Typical results fitted by Model 4 are shown in Figure 5. Average value for K_{3max} is the same as the average value for K_3 in Model 3, whereas the average value for S_2 obtained from all the tests is 360 MPa

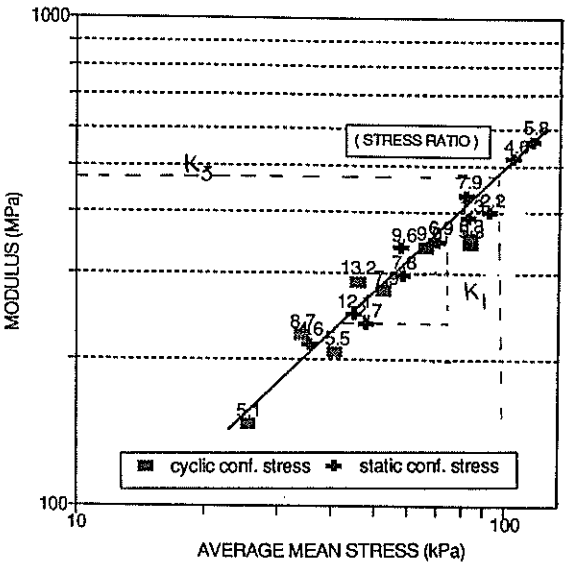

Figure 4 Typical results fitted with chacraterisation Model 3 (Sample No. 3)

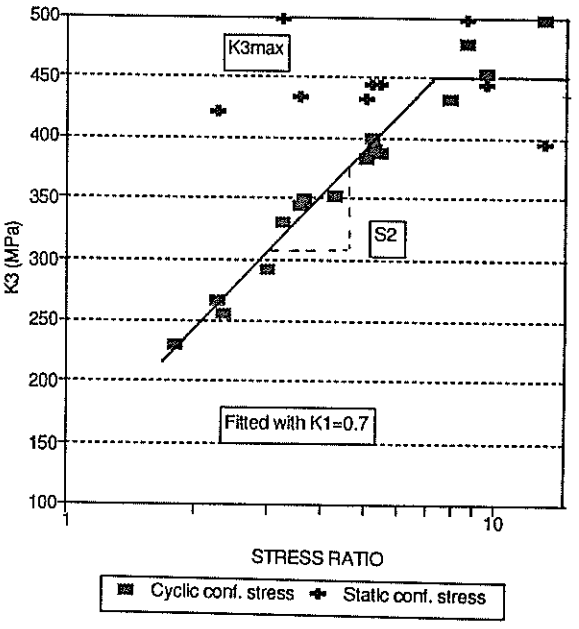

Figure 5 Typical results fitted with chacraterisation Model 4 (Sample No. 3)

4. CHARACTERISATION OF THE SUBGRADES

In the NAASRA Guide, the subgrade materials are assumed to be elastic and cross-anisotropic of Ev/Eh=2.0 and the vertical modulus of a subgrade can be determined from the empirical relationship of

$$Ev = 10.CBR \quad (13)$$

However, Vuong (13, 14, 15) reported that resilient modulus of subgrades can reduce with increasing deviator stresses. Generally the subgrade modulus can be expressed as:

$$E_r = E_{max} (1 - q/q_{ref})^p \quad (14)$$

and

$$E_r \geq E_{min} = E_{max}/4 \quad (15)$$

where q is the deviator stress; q_{ref} is the reference stress of 300 kPa; and E_{max} and p are the material constants

Vuong (16) also suggested typical E_{max} values of 32 MPa, 61 MPa and 145 MPa for the subgrades of CBR 3, 5 and 10, respectively, and a typical p value of 2. The Poisson's ratio for the subgrade is assumed to be a constant of 0.45.

5. STRUCTURAL ANALYSIS USING NONCIRL

5.1 Brief description of NONCIRL

In order to carry out structural analyses of flexible pavements, the NAASRA Guide uses a computer program CIRCLY (8), which is based on linear elastic layer theories. To make this program more versatile, it has been modified to NONCIRL (7) for analysing pavements having non-linear material characteristics. NONCIRL uses CIRCLY in the iterative process to calculate layer moduli of pavement layers and subgrades for given modulus-stress relationships. It also considers correction for tensile stresses in unbound layers and for overburden static pressures.

The computing process used in NONCIRL has the flow chart shown in Figure 6.

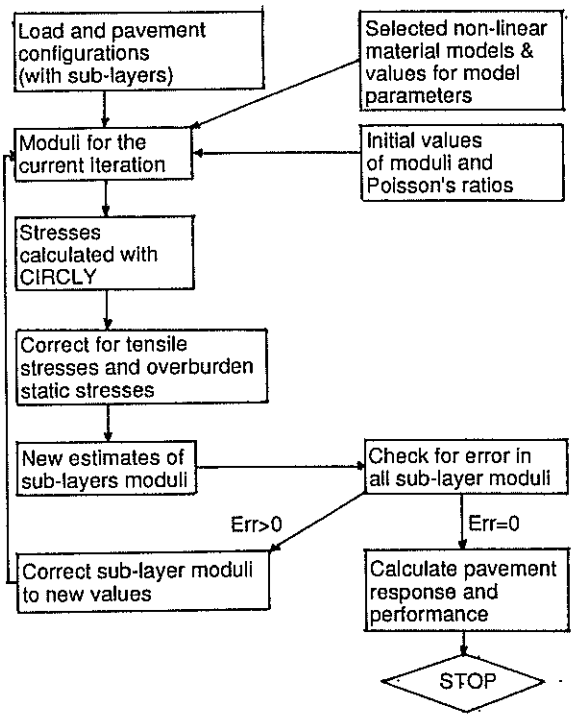

Figure 6 Flow chart for calculation of elastic moduli for materials having stress-dependent characteristics using NONCIRL.

To calculate the modulus values, E_r, for the final main analysis, a number of iterations were performed with E_r being calculated and updated based on the existing peak mean stress, average mean stress and peak stress ratio for each sub-layer. These are also checked for tensile stresses.

In the program, the cyclic stresses are the stresses induced from the applied wheel load; whereas the static stresses are the earth pressures at rest, which are assumed to be the same as the overburden pressure, i.e.

$$\sigma_{1s} = \sigma_{3s} = g.H \quad (16)$$

where g is the specific density of the material (in kN/m^3) and H is the depth to the point where the stresses are calculated.

Equilibrium is also checked after each iteration using the following measure of error in the calculated sub-layer moduli:

$$\text{Error} = \textbf{SUM} (E_i - E_{i-1})^2/E_i^2 \quad (17)$$

where E_i and E_{i-1} are the sub-layer moduli for the current and previous iterations, respectively.

5.2 Pavement and loading configurations

The granular layers and the subgrade were divided into sub-layers and the modulus of each sub-layer was then calculated accordingly to maximum stresses at the middle of the sub-layers, usually occurring at the vertical loading axis through the loading centre or through the centre of the loading group. The number of sub-layers of the base and sub-base layers for the nine pavements were 4, 5, 6, 4, 5, 6, 4, 4 and 4, respectively; whereas the subgrade was divided into 4 sub-layers having thicknesses of 250 mm, 350 mm, 500 mm and a semi-infinite bottom layer.

The Equivalent Standard Axle load (ESA) applies a uniform pressure of 550 kPa applied on two circular areas, each with an radius (R) of 0.107 m and a spacing between the loading centres of 0.330 m.

5.3. Analyses using different characterisation models for unbound materials

As shown in section 3, it is uncertain which testing method and material model for unbound material would be appropriate for use in NONCIRL. To show the risks associated with the use of different test types and different characterisation models in pavement design and analysis, five analyses were considered:

(a) Analysis 1 (AN1): This analysis uses Model 1 for the base material and assumes that the material is weightless and can have tensile stress. The purpose of this analysis is to demonstrate that the above assumptions can significantly affect the results.
(b) Analysis 2 (AN2): This analysis uses Model 1 for the base material and assumes that the material has a unit weight of 22.5 kN/m^3 and that tensile stress is unable to develop in the material. These assumptions are more realistic than those used in AN1.
(c) Analysis 3 (AN3): This analysis uses Model 2 for the base material and the same assumptions as made in AN2.
(d) Analysis 4 (AN4): This analysis uses Model 3 for the base material and the same assumptions as made in AN2.
(e) Analysis 5 (AN5): This analysis uses Model 4 for the base material and the same assumptions as made in AN2.

All analyses used Equation 14 for subgrade modulus and a typical value of E_v/E_h of 2 for all granular and subgrade sub-layers (E_v is vertical modulus and E_h is horizontal modulus) as suggested by the NAASRA Guide.

The input parameters for the material models for the base material and the subgrades are given in section 3 and section 4, respectively.

6. COMPARISON OF MODULI

The percentage differences between the calculated moduli for the five analyses and the NAASRA estimates, for a typical pavement, are plotted in Figure 7 for examination. In this case the NAASRA estimates for the 6 granular sub-layers, from top to bottom, are 500, 340, 232, 158, 108, 73 Mpa, respectively.

As shown in Figure 7, all analyses produced different moduli as compared to those estimated by the NAASRA Guide. The results also show that the analysis AN1 produced the lowest moduli, particularly at depths below 100 mm, because it assumed weightless materials and allowed tension in the base sub-layers and hence reduced significantly the peak stresses and sub-layer moduli.

By considering the overburden pressures and by correcting tensile stresses in the granular sub-layers, the analysis AN2 produced much higher moduli than those estimated by AN1.

The analysis AN3 (characterisation Model 2) produced very conservative estimates for all sub-layers as compared to those estimated by AN2 (characterisation Model 1). This reflects the difference in the constant K_2 in the models determined by the two test types.

The analyses AN4 and AN5 produced similar estimates of moduli for all sub-layers, except the top sub-layer. This indicates that the characterisation Model 3 and Model 4 could provide a basis for correcting the moduli obtained from different methods of applying confining pressure.

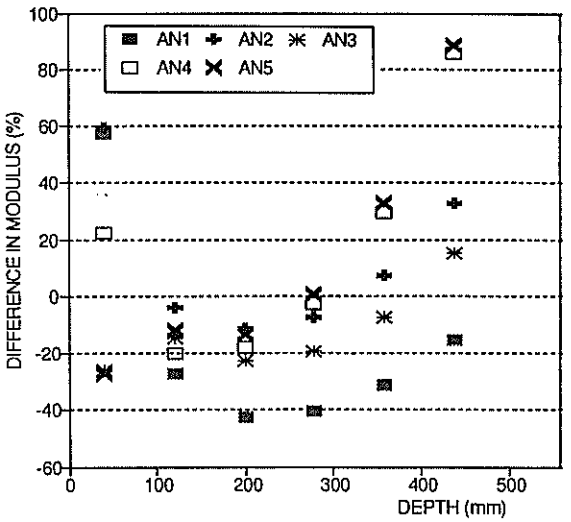

Figure 7 Percentage difference in modulus as compared with NAASRA estimates

7. COMPARISON OF CRITICAL STRAINS AND PAVEMENT LIVES

Pavement life is defined in the NAASRA Guide as a function of the maximum vertical compressive strain on the top of the subgrade (see Equation 1). The vertical strains at the top of the subgrade estimated by the five analyses are tabulated in Table II. It should be noted that the critical maximum vertical strains can occur at either the vertical axis through the load centre or the vertical axis through the centre of the loading group.

The pavement lives estimated by the five analyses are given in Table III. They vary from 0.3 to 3 times the NAASRA design lives and this indicates that the risks associated with the use of different characterisation models in pavement analysis and design are significant.

The results also indicate that the analyses AN1 and AN3 produced more conservative predictions than other analyses; whereas the analysis AN2 could involve higher risk by producing high design lives for all pavements. The analyses AN4 and AN5 produced less conservative predictions, except for pavements with very thick basecourse layers (Eg. pavements 2 and 3).

8. SUMMARY AND CONCLUSIONS

Resilient modulus testing of the typical base crushed rock were carried out using two repeated load triaxial test types (i.e. with constant and cyclic confining pressures) and the resilient moduli were derived and fitted to available models for resilient modulus. It was found that the constant (K_2) of the 'modulus-peak mean stress' model (Model 1) is different for different test types and this indicates that the effects of static confining pressure on the model constant may be significant.

It was also found that the 'modulus-average mean stress' model (Model 3) produced the same constants (K_3) for both test types (providing that stress ratios in the test with cyclic confining pressure are greater than 6). This model can provide a basis for correcting the moduli obtained from different methods of applying confining pressure.

K_2 and K_3 were also expressed as a function of stress ratio in order to fit more closely the test results obtained from tests with cyclic confining stress (Model 2 and Model 4).

The characterisation models were used in the program NONCIRL to calculate sub-layer moduli for their stress dependent characteristics and to predict pavement lives for nine typical granular pavements. It was found that besides the effect of different characterisation models determined from the repeated load triaxial tests, pavement analysis should take into account the effect of no-tension in the base layers and the effect of earth pressure at rest.

For the pavements studied, the pavement lives calculated with NONCIRL for different characterisation models ranged from 0.3 to 3 times the NAASRA design lives. This indicates that the risks associated with the use of different characterisation models in pavement analysis and design are significant.

Although the results in this study supported the use of the 'modulus-average mean stress' models (Model 3 and Model 4) for reducing the difference in the predicted pavement lives, the differences between the two models are still very high for some pavement configurations. In addition, this study does not take into account experimental errors involved in the tests. Therefore, there is scope for further studies to identify the risks involved in applying the repeated load triaxial tests into practice and to minimise them, particularly in the area of evaluating the performance of new and marginal materials.

9. REFERENCES:

[1] NATIONAL ASSOCIATION OF AUSTRALIAN STATE ROAD AUTHORITIES (1987). Pavement Design - A Guide to the Structural Design of Road Pavements. NAASRA, Sydney.

[2] APRG (1991). Summary report on recommendations of acceptable test procedures and equipment requirements for determination of input parameters for mechanistic pavement design. APRG National Workshop on Resilient Modulus Testing, Adelaide, Feb. 1991.

[3] Brown, S.F and Hyde, A.F.L. (1975). The significance of cyclic confining stress in repeated load triaxial testing of granular material. Transportation Research Record TRR No. 537, pp. 49-58.

TABLE II

VERTICAL STRAINS ON TOP OF SUBGRADE CALCULATED WITH NONCIRL

VERTICAL STRAIN CALCULATED AT TOP OF THE SUBGRADE (microstrain)										
Pav. No.		1	2	3	4	5	6	7	8	9
Depth (mm)		400	520	640	300	390	480	200	260	320
AN1	R=0mm	2000	1351	964	1805	1284	946	1401	1100	873
	R=165m	1801	1221	887	1707	1155	846	1720	1136	820
AN2	R=0mm	1600	1123	818	1557	1147	861	1299	1041	836
	R=165m	1455	1020	755	1485	1037	773	1592	1080	788
AN3	R=0mm	1895	1304	940	1816	1316	979	1465	1164	931
	R=165m	1722	1179	863	1760	1192	875	1901	1246	891
AN4	R=0mm	1619	1088	764	1638	1182	870	1376	1100	878
	R=165m	1471	987	704	1570	1069	780	1728	1155	832
AN5	R=0mm	1751	1156	807	1763	1252	916	1461	1153	918
	R=165m	1595	1047	742	1711	1136	820	1901	1237	880

Grey shade = maximum critical strain

TABLE III

PAVEMENT LIVES CALCULATED WITH DIFFERENT CHARACTERISATION MODELS

RATIO OF 'CALCULATED LIFE/NAASRA ESTIMATED LIFE'									
Pav. No.	1	2	3	4	5	6	7	8	9
NAASRA estimate (10,000 ESAs)	10	100	1000	10	100	1000	10	100	1000
AN1	0.31	0.51	0.57	0.64	0.73	0.65	0.91	1.76	1.15
AN2	1.52	1.91	1.83	1.85	1.64	1.27	1.58	2.52	1.58
AN3	0.45	0.66	0.68	0.62	0.61	0.51	0.44	0.91	0.73
AN4	1.40	2.39	2.97	1.29	1.32	1.18	0.88	1.56	1.11
AN5	0.80	1.55	2.01	0.76	0.88	0.82	0.44	0.96	0.80

[4] Nataamadja, A. (1989). Variability of pavement material parameters under repeated loading. Thesis (Ph.D.), Monash University, Australia.

[5] Vuong, B (1991). Resilient modulus testing and applications at ARRB. APRG National Workshop on Resilient Modulus Testing, Adelaide, Feb. 1991.

[6] Parkin, A.K. (1991). Modulus testing of large specimens at Monash. APRG National Workshop on Resilient Modulus Testing, Adelaide, Feb. 1991.

[7] Vuong, B. (1991). NONCIRL - A program for structural analysis of pavements having non-linear material characteristics - Technical Note. Australian Road Research Board Report RI91-014.

[8] Wardle, ,L.J. (1979). Program CIRCLY User's Manual. CSRIO Div. Applied Geomechanics, Melbourne.

[9] SHRP (1989) - SHRP Interim Protocol P46 - Resilient Modulus of Unbound Granular Base/Subbase Materials and Subgrade Soils.

[10] Vuong, B. (1987). The ARRB test procedures for characterizing dynamic stress-strain properties of granular basecourse materials. Australian Road Research Board Report WD-403-11.

[11] Barksdale, R.D. (1975). Test procedures for characterising dynamic stress-strain properties of pavement materials. Special Report 162, Transportation Research Board, Washington

[12] Vuong, B. (1985). Permanent deformation and resilient behaviour of a Victorian crushed rock using the repeated load triaxial test. Australian Road Research Board AIR 403-6.

[13] Vuong, B. (1986). Mechanical response properties of road materials obtained from a pavement test section at Rooty Hill, New South Wales. Australian Road Research Board AIR 403-7.

[14] Vuong, B. (1986). Mechanical response properties of road materials obtained from the ALF pavement test section at Somersby, New South Wales. Australian Road Research Board AIR 403-8.

[15] Vuong, B. (1987). Mechanical response properties of road materials obtained from the ALF pavement test section at Benalla, Victoria. Australian Road Research Board AIR 403-10.

[16] Vuong, B (1991). Determination of material design parameters for various subgrade types. APRG

Suggested Revision of the Pinhole Test Erosion Classes

M.D. YETTON
B.Sc., M.Sc.(Hons) (Engineering Geology)
Manager, Soils & Foundations Ltd, Christchurch
D.H. BELL
B.Sc.(Hons)
Senior Lecturer, University of Canterbury, Christchurch

SUMMARY The Pinhole Test as developed by Sherard et al (1976a) is an excellent test of erodibility in fine grained soils. However it is not a reliable measure of dispersion, which is just one of a number of processes which can contribute to erodibility in soils. In view of this we suggest the test classes to which samples are assigned following testing be revised to remove the dispersive - non-dispersive implication inherent in the original classification.

1. INTRODUCTION

A common laboratory test method used in erodibility analysis is the pinhole test, as developed by Sherard et al (1976a). The test was originally proposed for recompacted fine grained soils and found particular application in the testing of piping resistance in potential core material for earth dams. Evans (1977) modified the method to test undisturbed insitu samples of Banks Peninsula loess and the pinhole test has been used to assess insitu soil erodibility in this material since that time (see for example Wilms, 1979; Saul, 1979; Evans & Bell, 1981; Schafer & Trangmar, 1981; Crampton, 1985; Yetton, 1986; Bell et al, 1986). Yetton (1990) discusses the relevance of the test in subsurface erosion investigation.

The test procedure is briefly as follows. Water under head flows through a 1 mm pinhole in an undisturbed soil sample and the degree of erosion enlargement of the pinhole is assessed. The head is increased in increments from 50 mm to 1000 mm, and each head is sustained for 10 minutes. The total test time is between 10 and 40 minutes, depending on the erodibility of the soil tested.

The original test class classification of Sherard et al (1976a) was based on colour of the eroding water and rate of water flow, and two basic classes of D and ND were suggested defining dispersive and non-dispersive behaviour.

Advantages of the test include:

(1) The comparatively realistic modelling of subsoil erosion conditions;

(2) The ability to test both insitu undisturbed and recompacted samples;

(3) Fast test time;

(4) Reproducible results;

(5) The equipment is simple and takes up little space in the laboratory.

2. ERODIBILITY AND DISPERSION

An erodible material is defined here as a rock or soil which undergoes the particle by particle removal of grains, aggregates or flocs through the action of flowing water. Erosion occurs when the shear stresses induced by the fluid flow, either on or in the soil, are great enough to cause the removal of these particles (see Arulanandan & Perry, 1983).

The fundamental properties controlling the erodibility of fine grained soils are soil grain size, cohesion and soil propensity to undergo slaking and dispersion. Intuitively it could reasonably be expected that soil erosion is dependant on the interaction of these various properties rather than on any single property.

The term "dispersion" was originally introduced to the literature as a pseudonym for clay mineral deflocculation and many authors define and use the term in this manner (Emerson, 1967; Ryker, 1977; Holmgren & Flanagan, 1977; Bell, 1978; Liggins, 1979; Schafer, 1982).

Sherard et al (1976a) redefine the term dispersion to mean "colloidal erodibility" and propose the pinhole test result be used as a dispersion index. Thus if the water running through the sample under the lowest test head erodes the sample and carries a cloudy coloured suspension, and this suspension does not settle out over the 10 to 15 minutes of testing, then the sample is classified as dispersive (D1 or D2). Samples in which only limited erosion has occurred, with little or no cloudiness, are prefixed by ND (non-dispersive) and by various number grades depending on the head required to initiate erosion (ND1-4).

3. DIFFICULTIES IN USING THE TEST TO MEASURE DISPERSION

Results from a number of studies of different soil types suggest the pinhole test is not a reliable indicator of dispersion defined in the most widely used sense (i.e. clay mineral deflocculation).

Sherard et al (1976b) in a comparison between various dispersion test methods after developing the pinhole test, noted a discrepancy between the crumb test for dispersion and the pinhole test. The crumb test for dispersion consists of immersing a crumb of soil in a beaker of water and observing the extent of the colloidal halo, and was first introduced by Emerson (1967). Sherard et al (1976b) found about 40% of the crumb samples which displayed non-dispersive clay mineral behaviour were classified as "dispersive" by the Pinhole Test.

An examination of existing data available for undisturbed samples of Banks Peninsula loess also indicates a poor correlation between dispersion measured by the crumb test and pinhole "dispersion" (see Figure 1). If dispersion was the only variable being measured by erosion in the pinhole test a straight line relationship could be reasonably expected. In Figure 1 no such relationship is apparent.

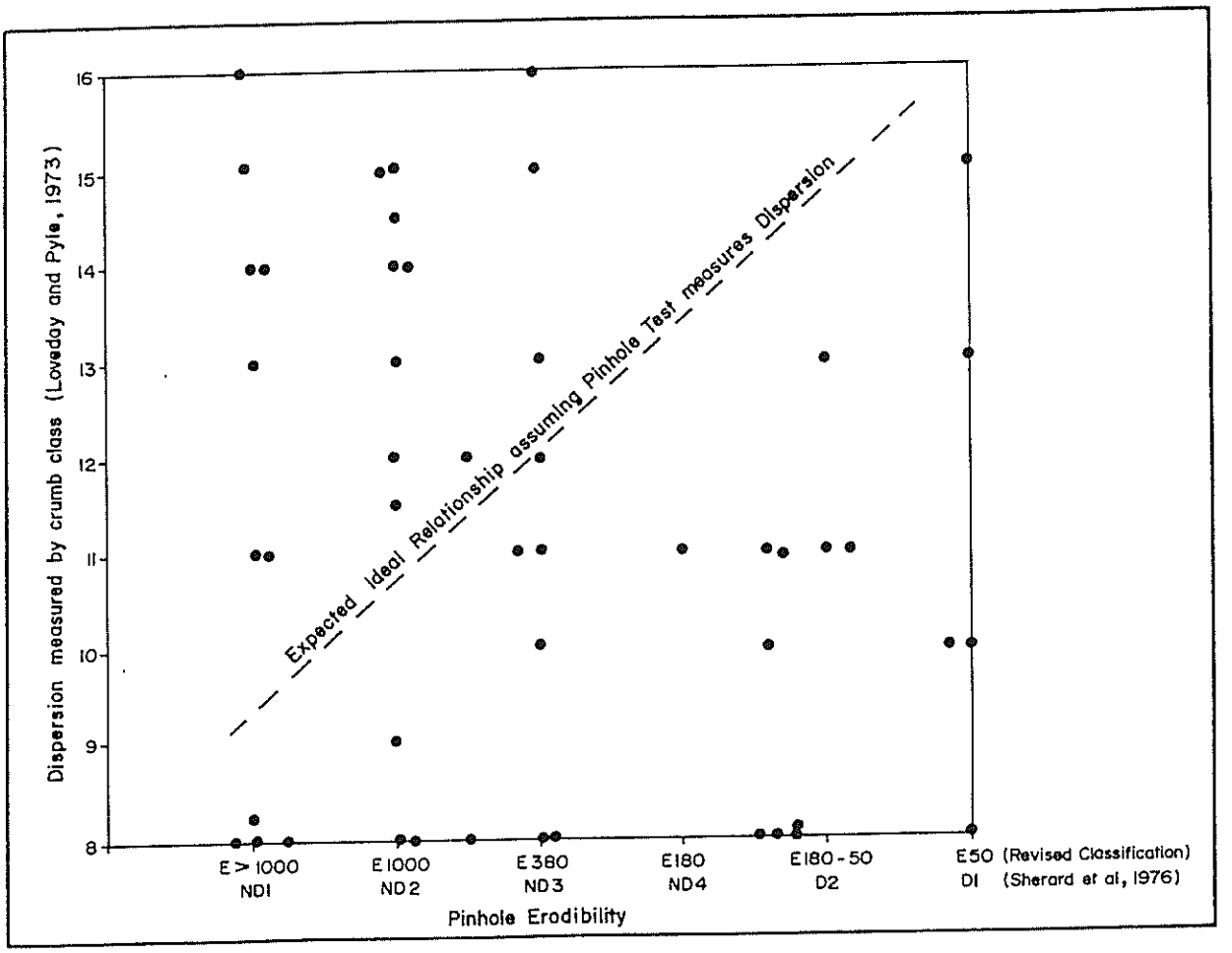

FIGURE 1: The relationship between pinhole test results and dispersion (measured by the crumb test) for 47 samples of Banks Peninsula Loess (data from Yetton 1986; Crampton 1985 and Saul 1979)

To further highlight this discrepancy a sample of loess was cleaned of the clay sized fraction which ensured a crumb of the resulting sandy silt showed no dispersion (colloidal cloudiness) in the crumb test. When this sample of sandy silt was pinhole tested it proved to be the most erodible material tested in the writers' experience, and thus the corresponding Sherard et al (1976a) classification class was Dispersive 1 (D1).

Other tests for dispersion fail to correlate with the pinhole test results. Schafer & Trangmar (1981) present a comparison of data for recompacted loess from Banks Peninsula and adjacent areas. In their study they compared pinhole test results with the porewater analysis and the SCS dispersion tests (refer Sherard et al, 1976b for details of these test methods). Schafer & Trangmar conclude that although there was reasonable correlation, in many cases neither the SCS test nor the porewater analysis method, correlate completely with the pinhole test.

More recently Craft and Acciardi (1984) noted discrepancies between the pinhole test results and the pore water analysis test for dispersion of sampled soils (see Figure 2). Once again materials classified as non-dispersive by the pore water test were classified "dispersive" by the pinhole test. Figure 2 also shows the results of Goldsmith and Smith (1985), who found clayey silts from the Auckland region to be dispersive as measured by both the porewater analysis method and the SCS test, yet were classified as non-dispersive (ND1) by the pinhole test.

The results outlined above confirm that although the pinhole test measures erodibility, it is not always an accurate indicator of dispersion. While in some soils, high erodibility may indicate the presence of dispersive clay minerals, in most soils high erodibility is the result of the interaction of a number of key soil properties, only one of which is dispersion.

4. RECOMMENDED MODIFICATIONS TO THE PINHOLE TEST CLASSIFICATION

The conclusions above do not invalidate the pinhole test as an effective measure of erodibility, rather they suggest a reclassification of the pinhole test result classes is required to remove the dispersive - non-dispersive implication inherent in the original.

Minor modifications of the pinhole test classification have been suggested by Evans (1977) and Bell (1981). These changes both emphasise the extent of erosion under the various heads as the principal criteria separating the classes. The degree of water cloudiness is less important. The D - ND terminology of Sherard et al (1976a) is retained. Schafer & Trangmar (1981) define a quantitative "erosion index" based on the volume increase in the pinhole size as calculated from the volume of eroded soil in the test water. Scaling equations adjust the index for different pinhole diameters and flow rates. This is an improvement on the original classification as it removes the dispersive - non-dispersive distinction, however the collection, evaporation and weighing of sediment in the test water, along with the calculations required, are all time-consuming.

A relatively quick and simple classification procedure, outlined briefly below and in more detail in the appendix, is proposed here for use. During the test the usual record is kept of water discharge per unit time which is plotted up as a graph at the test

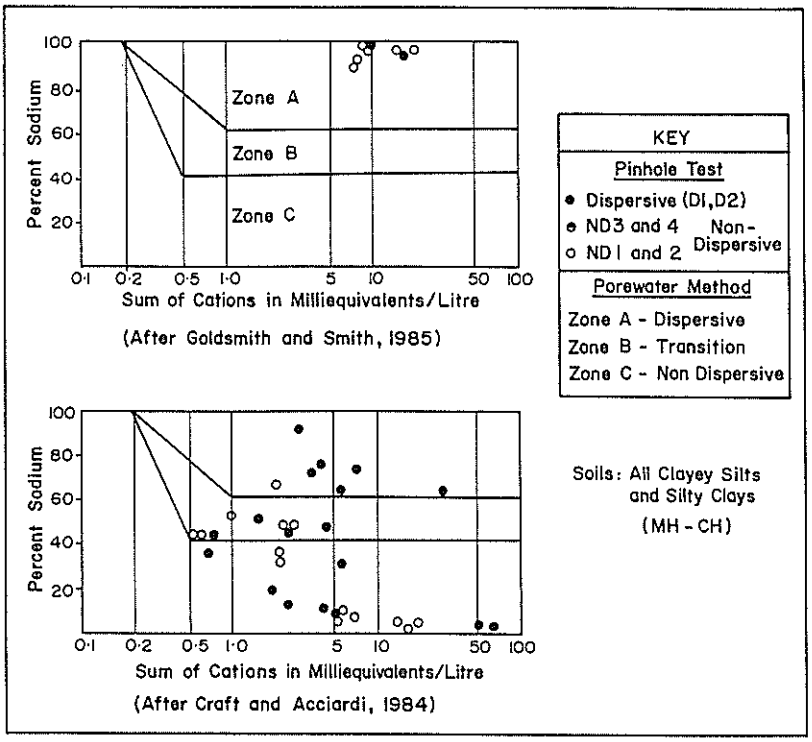

FIGURE 2: Discrepancies between the pinhole test results and the Porewater Analysis method of dispersion testing

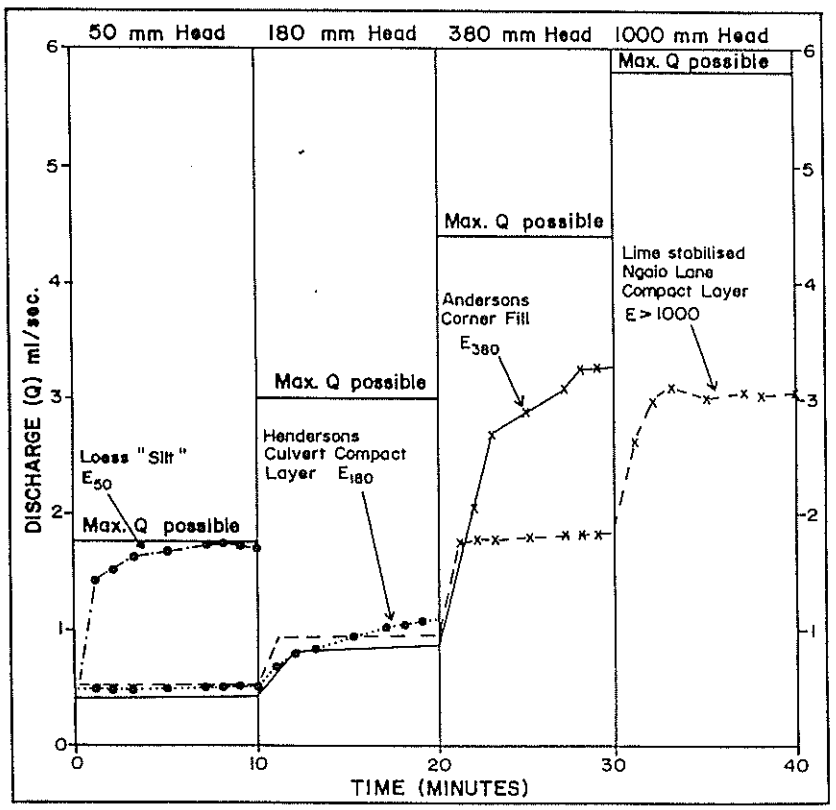

FIGURE 3: Examples of suggested erodibility classification classes (data from Yetton, 1986)

completion. From this graph the head at which sustained erosion first occurs is established. This is first defined as the head which produces a progressive increase in discharge over three or more minutes (see examples in Figure 3). An erosion category is then assigned according to this head i.e. for 50 mm head = E_{50}, for 180 mm head = E_{180}, etc. If significant erosion first occurs at a low head, but only becomes sustained at the next higher head, then intermediate classes can be used i.e. $E_{180-380}$.

Although "E" by convention is the symbol for the modulus of elasticity in soil and rock mechanics, we consider it is unlikely to be confused with erodibility by virtue of the subscript and the quite different context in which this test would normally be used.

The general correlation of Sherard's classes with those proposed in this new classification is as follows:

D1	=	E_{50}
D2	=	E_{180-50}
ND4	=	E_{180}
ND3	=	E_{380}
ND2	=	E_{1000}
ND1	=	$E_{>1000}$

In principle the gradient of the discharge - time graph during the period of sustained erosion could be quantified and used to further refine the separation of sample erosion characteristics should this ever be required.

5. CONCLUSION

While the pinhole test as originally proposed by Sherard et al (1976a) is an excellent test of erodibility in fine-grained soils, it is not a reliable indicator of dispersion. This does not invalidate the test but does indicate the need for reclassification of the test result classes. We suggest a simple system based on the head at which sustained erosion first occurs.

6. ACKNOWLEDGEMENTS

Useful discussions relating to the topic were held with P. Glassey, N. Crampton and I. McCahon. Diagrams are by Lee Leonard and typing by Julie Howard.

7. REFERENCES

Arulandan, K. and Perry, E.B. (1983) "Erosion in Relation to Filter Design Criteria in Earth Dams", J. of Geotechn. Engng Divn ASCE, Vol. 109, No. 5, pp 682-698.

Bell, D.H.; Glassey, P.J. and Yetton, M.D. (1986) "Chemical Stabilisation of Dispersive Loessial Soils, Banks Peninsula, Canterbury, New Zealand", Proceedings of the 5th Congress of the International Association of Engineering Geology, Buenos Aires, Argentina, October 1986.

Bell, D.H. (1982b) "Chemical Stabilisation of Dispersive Soils", Paper No. 112 presented to NZIE Annual Conference in Christchurch on 10 February 1982.

Bell, D.J. (1982a) "Port Hills Erosion Control and Chemical Stability of Loess", unpublished FT Guide, Trip 6 NZIE Annual Conf., Christchurch 1982.

Bell, D.H. (1981) "Dispersive Loessial Soils of the Port Hills, Christchurch", paper presented at Conf. on Geomechanics and Urban Planning, Palmerston North, N.Z.

Bell, D.H. (1978) "The Engineering Geology of Banks Peninsula Loess", paper presented at Seminar on Slope Stability, Univ. of Canterbury.

Craft, C.D. and Acciardi, R.G. (1984) "Failure of Porewater Analysis for Dispersion", J. Geotech. Engng Divn ASCE, Vol. 110, No. 4, pp 459-473.

Crampton, N.A. (1985) "Engineering Geological Aspects of the Lyttelton - Woolston LPG Pipeline", Unpub. MSc. Univ. of Canterbury, 241 pp.

Emerson, W.W. (1967) "A Classification of Soil Aggregates Based on their Coherence in Water", Aust. J. of Soil Res. S47.

Evans, G.L. (1977) "Erosion Tests on Loess Silt, Banks Peninsula", Proc. 9th ICSMFE Tokyo, Vol. 2, pp 63-69.

Evans, G.L. and Bell, D.H. (1981) "Chemical Stabilisation of Loess, New Zealand", Proc. Xth Int. Conf. Soil Mech. and Found. Engng, Stockholm, June 1981, pp 649-658.

Goldsmith, P.R. and Smith, E.H. (1985) "Tunnelling Soils in South Auckland, New Zealand", Eng. Geol., Vol. 22, pp 1-11.

Holmgren, G.G. and Flanagan, C.P. (1977) "Factors Affecting Spontaneous Dispersion of Soil Materials as Evidenced by the Crumb Test", in Disp. Clays, Related Piping and Erosion in Geotechnical Projects, ASTM STP 623. J.L. Sherard and R.S. Decker, Eds. Am. Soc. Testing and Materials, 1977, pp 370-389.

Liggins, J.B. (1979) "The Dispersive Soil Problem", paper presented to Tech. Session on Disp. Soils, 17th AGM, Adelaide, Australia.

Ryker, N.J. (1977) "Encountering Dispersive Clays on Soil Conservation Service Projects in Oklahoma", Disp. Clays, Related Piping and Erosion in Geotechnical Projects, ASTM STP 623. J.L. Sherard and R.S. Decker, Eds. Am. Soc. Testing and Materials, 1977.

Saul, G.J. (1979) "Comparison of Dispersive Properties of Port Hills Loess with Particle Arrangement", Rep. for Geomechanics 3, BE (Civil), Univ. of Canterbury, 13p.

Schafer, G.J. (1982) "Identification of Dispersive Soils", paper presented to IPENZ Ann. Conf., Christchurch, N.Z.

Schafer, G.J. (1978) "Pinhole Test for Dispersive Soil - Suggested Change", J. Geotech. Engng Divn ASCE, Vol. GT6, pp 760-765.

Schafer, G.J. and Trangmar, B.B. (1981) "Some Factors Affecting Tunnel Gully Erosion", Proc. of Xth Int. Conf. Soil Mech. and Found. Engng, Stockholm, June 1981, pp 481-486.

Sherard, J.L.; Dunnigan, L.P.; Decker, R.S. (1976a) "Pinhole Test for Identifying Dispersive Soils" J. Geotech. Engng Divn, ASCE, Vol. 102, pp 69-85.

Sherard, J.L.; Dunnigan, L.P.; Decker, R.S. (1976b) "Identification and Nature of Dispersive Soils" J. Geotechn. Engng Divn, ASCE, Vol. 102, No. GT4.

Wilms, T.R. (1979) "An Investigation into Aspect Related Erosion Forms in a Valley in the Port Hills, Banks Peninsula", M.Agr. Thesis, Lincoln College.

Yetton, M.D. (1986) "Investigation and Remedial Methods for Subsurface Erosion Control in Banks Peninsula Loess", Unpub. MSc. Thesis, Univ. of Canterbury, 231p.

APPENDIX: RECOMMENDED TEST PROCEDURE AND CLASSIFICATION SYSTEM

Procedure

An undisturbed tube sample of soil (normally 35 mm diameter) is obtained in the field and kept at insitu moisture content until testing is performed.

The tube sample is trimmed to a standard length of 50 mm and a truncated conical depression is countersunk in the centre top of the sample.

A hole is drilled through the entire 50 mm sample centred in this conical depression. By using a 1 mm diameter surgical needle in a light drill press, a hole only slightly larger than 1 mm is normally obtained.

The sample is then set up in the apparatus (refer Figure 4) and water passes through the sample pinhole under increasing increments of head (50 mm, 180 mm, 380 mm, and 1000 mm), each maintained for a 10 minute period.

N.B. The plastic nipple in the apparatus, which is centred in the countersunk depression and leads into the sample pinhole should be at least 1.5 mm in diameter.

The water emerging from the sample pinhole is collected in a graduated cylinder and the water volume at 1, 2, 3, 5, 7, 8, 9, and 10 minutes recorded at each head.

The classification of pinhole erodibility is based on the measured flow rate (Q) averaged over each minute.

Notes

Although the test normally runs over 40 minutes, a rough check can be kept of the flow rates for any obvious acceleration in flow during the test. Where erosion clearly exceeds the criteria below, the test can be halted.

The test equipment should be run without a sample at some stage before or after the test to obtain the maximum possible flow under the various heads. This is essentially a function of the diameter of the hole in the plastic nipple and providing the same nipple is maintained in the equipment, this check need only occur periodically.

The maximum possible flow rate for each head without sample restriction is required to insure that any observed levelling off in increase in flow rate reflects sample characteristics and not the capacity of the equipment. This can be a particular problem in highly erodible material.

Classification

From the record of water volume over time the average flow rate (in ml/sec) is calculated for each minute period.

A graph is prepared with flow rate (Q) on the y axis and time (minutes) on the x axis. Vertical lines marking the 10 minute head changes, and the maximum flow rates possible without restriction by the sample, are shown on this.

The data is plotted and the points connected by straight lines. Ignoring the first minute after each head change, the head at which sustained erosion first occurs and continues over three or more minutes is noted. Sustained erosion is defined as that which produces a significant progressive increase in flow rate greater than 0.1 ml/sec over a three minute period.

The head determined above is subscripted to "E" e.g. E_{50}, E_{180} etc.

Note

If significant erosion first occurs at a low head, but only becomes sustained at the next higher head, then intermediate erosion classes can be adopted e.g. $E_{180\text{-}380}$.

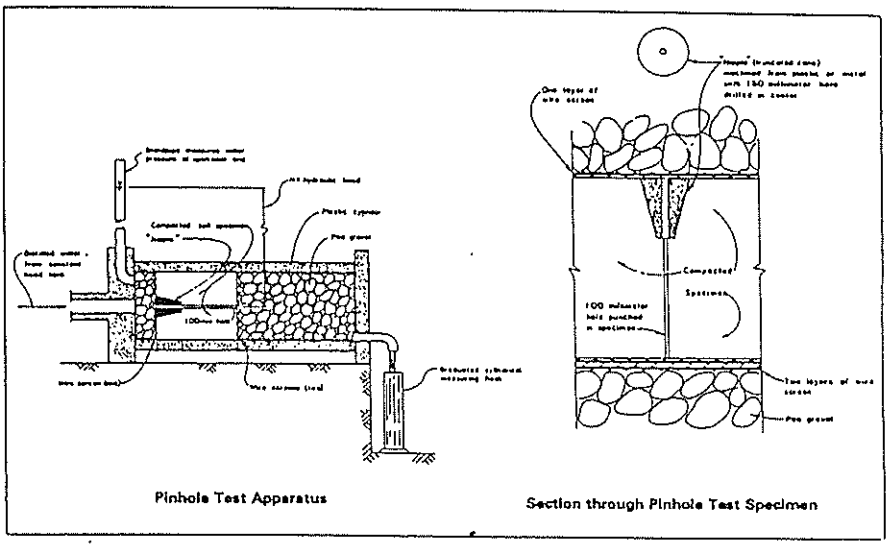

FIGURE 4: Pinhole erosion test apparatus and section through test specimen (from Sherard et al, 1976a)

Settlement Determination on Sand

G.S. YOUNG
B.E., M.Eng.Sc., M.I.E.Aust.
Associate, Arup Geotechnics Pty Ltd, Sydney
A.B. PHILLIPS
B.Sc.(Eng.), Ph.D., M.I.E.Aust., M.I.C.E.
Director, Arup Geotechnics Pty Ltd, Sydney
P.T. BROWN
B.Sc., B.E. Ph.D., M.I.E.Aust.
Research Associate, University of Sydney

SUMMARY Settlements of alluvial sands on a site in Sydney were predicted using an elastic method. Moduli were determined from standard penetration test blow counts. Rather than use published correlations, a limited number of in situ screw plate tests were undertaken at depth in a borehole to relate elastic modulus to blow count. Settlements were monitored as construction proceeded and were found to be in good agreement with predictions.

1. INTRODUCTION

Located in Sydney's historic Hunters Hill, the 12 hectare Pulpit Point site (Fig. 1), formerly the Mobil Oil Terminal, is located partly on a sandstone peninsula extending into Sydney Harbour and partly on fill placed over alluvium. During 1990 it was developed as a residential estate of 132 luxury dwellings and 32 vacant blocks. In order to provide building platforms and access roads, considerable reshaping of the site was required.

Site investigations, mainly in connection with environmental studies, had been undertaken at various times prior to development. The available information was correlated and additional investigation undertaken to determine the properties and thicknesses of the fill, alluvial and residual soils found

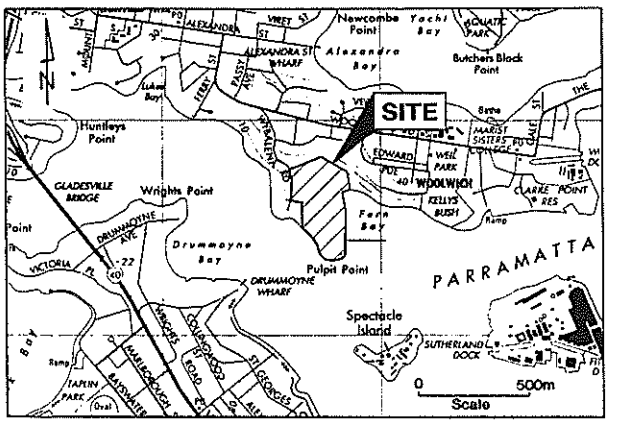

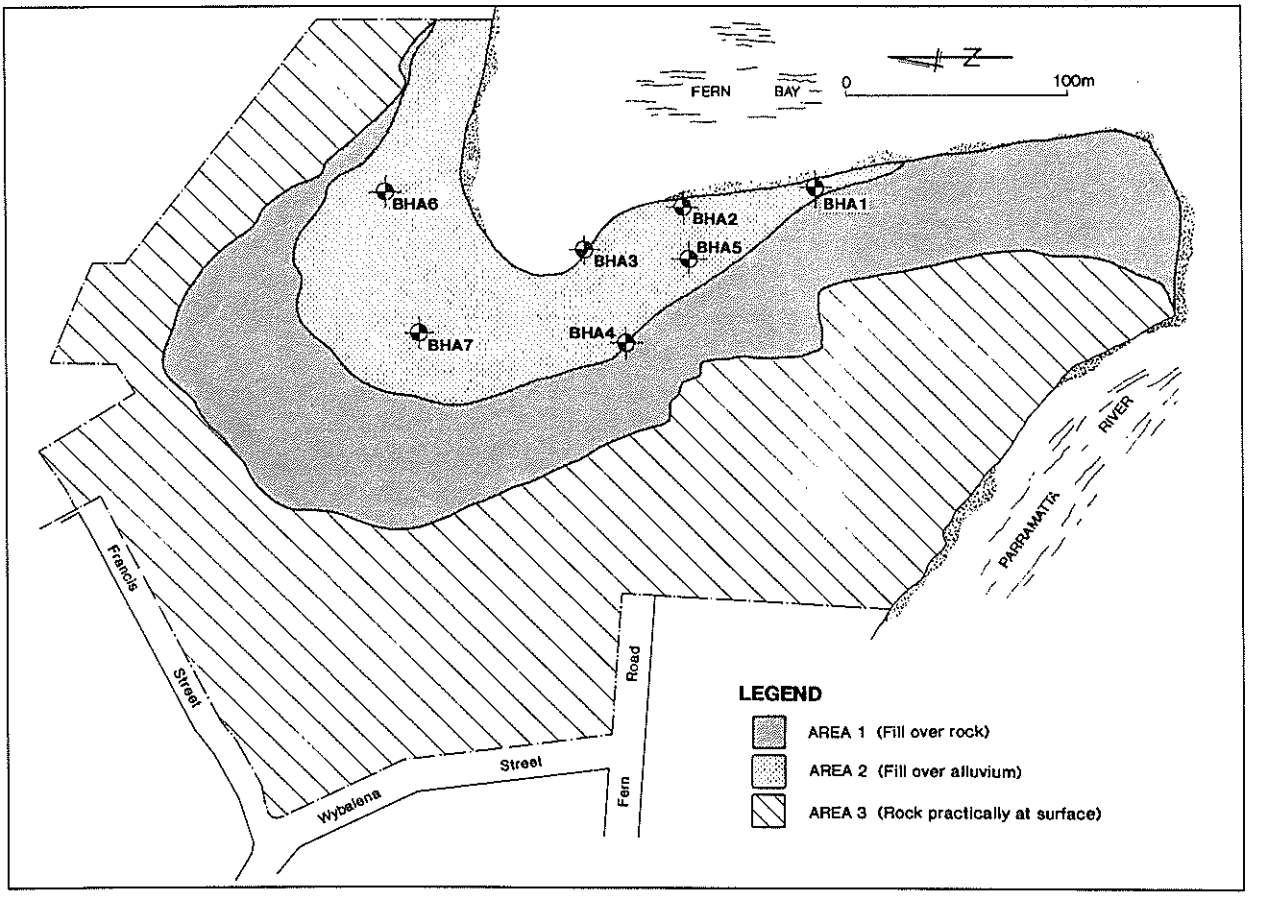

over the lower areas of the site, as well as depth to bedrock and its strength.

Over 2 m of new fill was placed over old fill and alluvium in one part of the site (Area 2 on Fig. 2), to provide a level platform for the construction of a community centre and an open area. The community centre was one of the few light weight, single storey buildings on site and high level foundations were preferred. However, because of the variation of rock level around the site, it was also one of the few buildings to be constructed over as much as 15 m of alluvium. A prediction of alluvium settlement was required for foundation design and to determine the effect on services.

Considerable scatter of site data and lack of precise methods for estimating settlements of a thick layer of compressible material made selection of shallow footings for an extensive single storey building too large a risk to take. To improve the accuracy of settlement predictions and reduce the risk inherent in selecting high level foundations, a small number of in situ screw plate tests were correlated with SPT data. The resulting Young's moduli were higher than would otherwise have been adopted and were shown to be appropriate by monitoring settlements of a trial fill.

2. SITE HISTORY

Prior to the current development, Pulpit Point was a major local centre for petroleum and associated products. Significant changes to the natural landscape had taken place to allow for the positioning of large chemical and oil storage tanks. A wide flat area fronting Fern Bay had been created by cut and fill in the sandstone bedrock and reclaiming some of the harbour by the placement of fill over alluvium.

Over a long period of time small amounts of leakage and spillage of petrochemicals had led to pollution of the fill and upper alluvial soils on the site. A total cleanup was undertaken involving the removal of large volumes of polluted soils and their replacement with clean fill.

3. SITE INVESTIGATION

A site investigation was carried out comprising 7 boreholes (Fig. 2) in addition to earlier holes that had been drilled prior to the cleanup operations.

Apart from defining the variable succession of fill, alluvium and rock on the site, one of the main aims of the investigation was to predict settlements in Area 2. The method adopted was to drill several boreholes and carry out in situ testing and sampling at regular intervals. Screw plate tests were performed in one borehole selected to be typical of the area, in order to correlate standard penetration test (SPT) results with in situ Young's modulus.

4. CORRELATION OF IN SITU TEST RESULTS

Fill, alluvial deposits and residual soil overlay rock at depths of up to 15 m.

Due to the sandy nature of the alluvial and residual materials, SPTs were the main form of in situ testing. Results are shown plotted against depth on Figure 3. A general trend of linear increase with depth is apparent. It is noted that reported SPT results were not corrected for overburden pressure.

In addition, five screw plate tests were carried out at depths of 2.28, 2.52, 3.65, 6.47 and 8.0 m beneath the ground surface using the device described in Appendix A. The first two tests were found to have been carried out in fill, so the results were ignored for the purposes of correlation.

The values of Young's modulus calculated from the three tests in alluvium were 0.9, 13.5 and 79.1 MPa respectively. These results are plotted against depth on Figure 4 with the curve showing the assumed form of variation of modulus between the measurement points.

To make more general use of the values of modulus from the screw plate tests, they were correlated directly against the

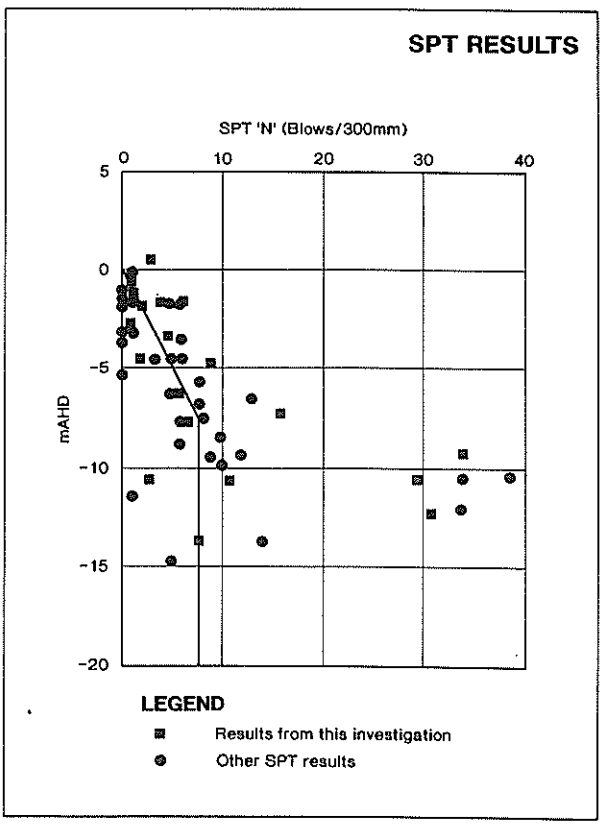

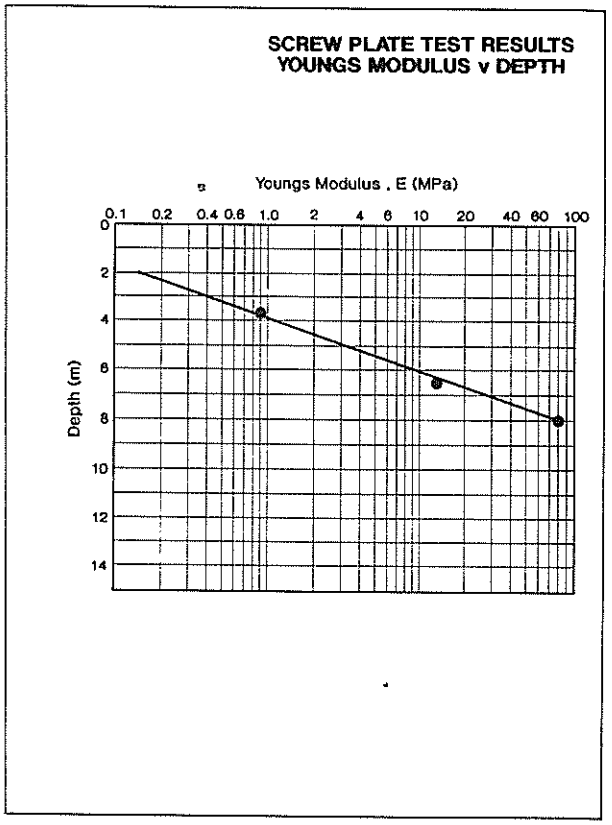

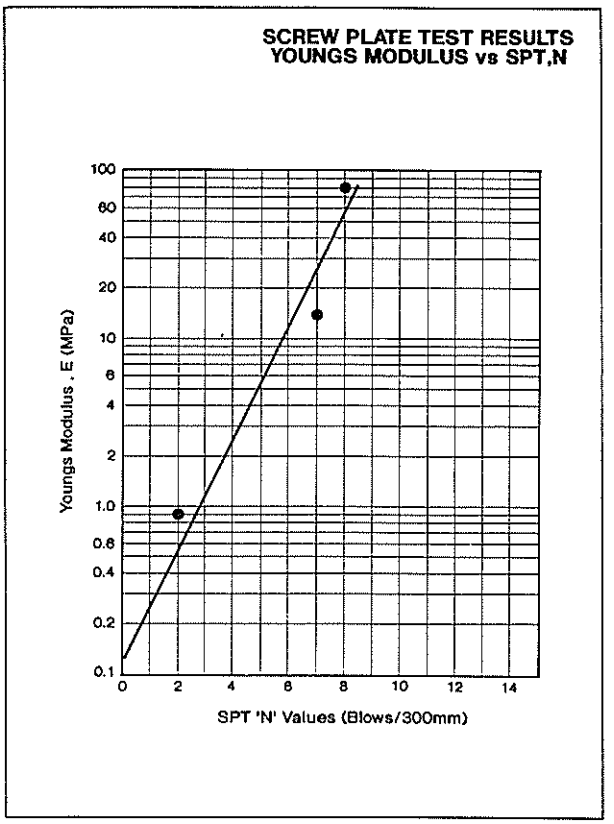

SPT N values from a borehole 2 m away, to produce the curve of SPT versus modulus (Fig. 5). To smooth scatter in the data a design line, as shown on Figure 3, was adopted to represent the N values in the alluvium.

It will be noted that young's modulus increases rapidly with SPT blow count in a non-linear fashion. This was an unexpected result.

5. SETTLEMENT ASSESSMENT

Surface settlements were determined under the applied fill load using OASYS computer program VDISP. This allows horizontal soil layers with a varing soil modulus to be analysed using a Mindlin's approach. Individual settlement predictions were made at different locations by calculating the central settlement of a 50 m square loaded area.

6. MEASURED SETTLEMENTS

Following the site cleanup, a total of 25 settlement plates were placed on top of the alluvium throughout the area where large settlements were expected. This number of plates was installed because it was expected that a percentage would be damaged during the earthworks. Clean fill was subsequently placed on the site to depths up to 3 m and level readings on the settlement plates were taken weekly. Of the total of 25, only eight plates appeared to be undamaged by the time filling was complete. The measured and predicted settlements on these eight plates are compared on Table 1. Settlements appeared to be virtually instantaneous.

On the whole predicted settlements were very close to the observed actual settlements. Significant over-prediction of settlements only occurred in the case of Settlement Plates 10 and 12. A possible explanation for these differences could be an over-estimation of the depth to rock for the calculations as the depth to rock was interpolated from the widely separated borehole information. The only under-prediction was for Plate 14 and amounted to about 5%.

TABLE I
COMPARISON OF MEASURED AND PREDICTED SETTLEMENTS

Settlement Plate	Measured Settlement	Predicted Settlement
	mm	mm
7	105	110
10	65	100
12	80	130
14	190	180
15	165	180
16	150	155
19	100	110
20	100	100

7. CONCLUSION

The comparison of predicted and measured settlements using a site investigation which consists of a large number of economical standard penetration tests, combined with a small number of in situ screw plate tests to "calibrate" the conversion of SPT results to values of modulus, is a very cost efficient method for enabling settlement predictions of satisfactory accuracy. This enables the accuracy of settlement predictions to be improved markedly and the level of risk reduced.

In this particular case Young's modulus have a non-linear relationship to SPT blow count, but the measured settlements appear to justify its adoption. This may not be a general rule and it is recommended that the relationship sould not be used for other sites.

APPENDIX A

Screw Plate Tests

The screw plate test is a means of carrying out an in situ determination of soil compressibility in a borehole to large depths. The screw plate used consists of two half flights of a helix, with the two cutting edges at the same level, and is shown in Figure 6 (photo) and the inset in Figure 7 (drawing of drill rig). Two cutting

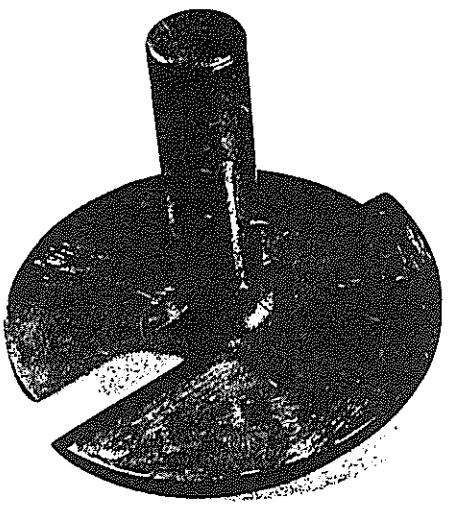

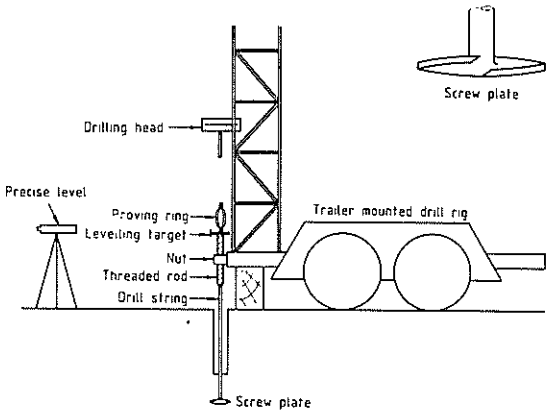

edges are used in order to avoid the unbalanced torque from one cutting edge which tends to make the screw plate wander during insertion. The screw plate is 100 mm diameter, 5.5 mm thick and has a pitch of 20 mm per revolution.

Insertion of the screw plate is controlled by a threaded rod whose pitch is also 20 mm per revolution, which forces the screw plate to enter the soil at exactly the pitch of the helix, and so ensures good contact between the plate and soil.

Test Procedure

A mud-filled hole of 120 mm diameter is first drilled to a depth about 200 mm less than the depth at which it was intended to carry out the test. Then the drill bit is withdrawn and the screw plate is attached to the end of the drill string, and lowered to the bottom of the hole. The threaded rod is attached to the top of the drill string, and the nut on the threaded rod is bolted onto the drill rig. Then the threaded rod is rotated through ten revolutions to bring the screw plate 200 mm below the bottom of the hole, unless the torque required for insertion reached 5 kg/m in which case insertion is discontinued in order to avoid the possibility of damage to the screw plate by excessive bending.

The nut on the threaded rod is then detached from the drill rig and consequently the weight of the drill string is applied to the screw plate. The proving ring and levelling target shown in Figure 7 are attached to the top of the drill string and load increments are applied by the drilling head using the hydraulic system of the drill rig, and measured by means of the proving ring. Displacements are measured by means of a precise level to an accuracy of a few hundredths of a millimetre, using a level placed about 4 m from the borehole in order to minimise interaction of the loading system with the displacement measurement system. A minimum of four load increments are applied in order to demonstrate by their consistency that the measurements are satisfactory. A typical load displacement curve is shown in Figure 8.

Interpretation

The interpretation of the measurements involves correction of the

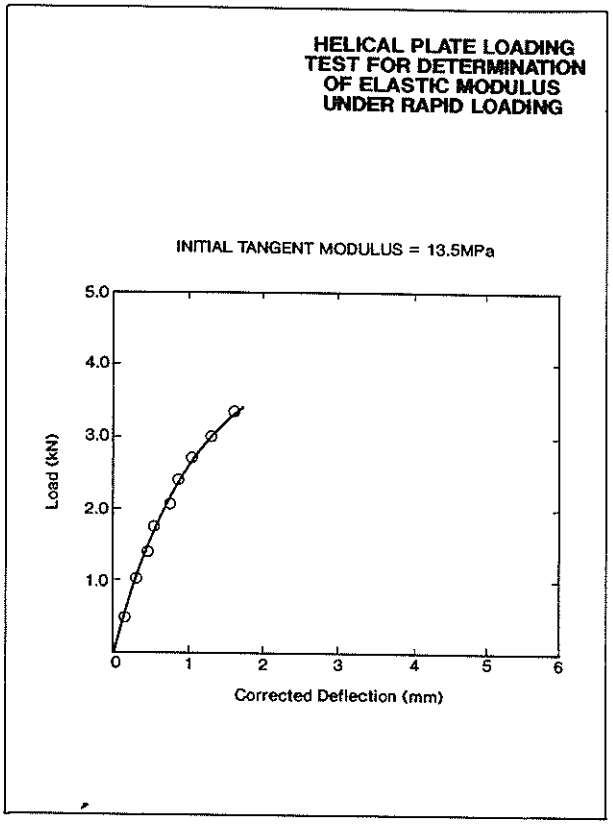

displacement readings for the axial shortening of the drill rods, which had been determined by laboratory compression tests on the rods. Correction for bending of the screw plate is made possible by the results of a finite element analysis. The corrected displacement is then substituted in the equation

$$\frac{wE}{pa} = \frac{\pi(3-4\nu)(1+\nu)}{16(1-\nu)}$$

derived by Collins (1962), for a rigid circular plate in full bonded contact with the soil, where w is the displacement, E is the Young's modulus, p is the average loading pressure applied to the plate, a is the radius of the plate and ν is the Poisson's ratio of the soil.

REFERENCE

Collins, W.D. (1962). Some Axially Symetric Stress Distributions in Elastic Solids Containing Penny Shaped Cracks. I. Cracks in an Inifinite Solid and a Thick Plate. Proc. of the Roval Society, Series A, Volume 203, pp. 359 - 386.

Fatigue Failure of a Cemented Sand

M.M. ZHAO
B.E.
Research Assistant, University of Sydney
J.T. HUANG
B.E., M.E.
Research Student, University of Sydney
D.W. AIREY
M.A., Ph.D.
Lecturer, University of Sydney

SUMMARY A series of monotonic and cyclic undrained triaxial tests have been performed on an artificially cemented carbonate sand. The effects of the stress level and frequency on the number of cycles to failure have been investigated. It has been found that the number of cycles to failure increases with frequency for a given stress level, and that the time for which the load is applied is more important than the number of cycles of loading. The test results have been used to produce fatigue S - N curves with fatigue failures occurring at stress levels as low as 60% of the static peak strength.

1. INTRODUCTION

The foundations of many offshore structures around the coast of Australia are located in moderately cemented calcareous soils, and they rely to varying extents on the strength provided by the cementation for their stability. Due to the actions of wind and waves these foundations are subjected to significant cyclic loads during storms for relatively small numbers of cycles, and to larger numbers of smaller cyclic loads at other times. It is widely acknowledged that large cyclic loads cause a significant reduction in strength but the effects of large numbers of smaller amplitude loads is uncertain.

Previous studies of the fatigue response of cemented soils have been primarily concerned with establishing the behaviour of such materials for road bases (eg. Pretorious and Monismith, 1972). These tests have shown that the tensile strength can reduce to 60% of its static value at 10^6 cycles, but the applicability of these results to soil elements subjected to significant compressive loads beneath foundations is unclear. Results have been presented (Airey and Fahey, 1991) for naturally cemented calcarenite samples which suggest that a more rapid drop off in strength can occur under compressive cyclic stresses. However, the naturally cemented calcarenite samples obtained from the North-West Shelf showed significant variations in their cementation over short distances making it difficult to estimate an appropriate static strength, and hence to interpret the results.

In this paper the results of cyclic "fatigue" undrained triaxial tests on artificially cemented calcareous samples are presented. The technique for preparing uniform and repeatable cemented samples is briefly discussed and the results of some conventional undrained triaxial tests on the cemented soil are presented. The cyclic tests have been performed at frequencies between 0.1 and 10 Hz and the effects of frequency on the response are reported.

2. SAMPLE PREPARATION

To avoid the difficulties caused by the variability of naturally cemented samples carefully manufactured artificially cemented sand samples have been used. This has the additional benefit that the variability that is inherent in any fatigue testing programme should be minimised. An uncemented carbonate sand (dredged from the North Rankin A site) has been mixed with gypsum cement and water and one-dimensionally compressed in a mould to a pre-determined dry density. This procedure has been used to produce samples with cement contents up to 20% and a range of densities from 12.5 to 19 kN/m^3. Full details of the sample preparation procedure have been described elsewhere (Huang and Airey, 1991). It has been demonstrated that this procedure can produce repeatable samples having uniform densities and strengths. For the combinations of density and cement content used in the tests described below, the peak strength in unconfined compression and triaxial tests has been found to vary by +/- 2%.

To reduce the number of variables for the fatigue tests only samples with a nominal density of 13 kN/m^3 and a cement content of 20% have been used. This combination of density and cement content has been selected because the behaviour of the cemented soil has similarities to that of the weaker moderately cemented material at the North Rankin site.

3. TEST PROCEDURE

Tests have been performed in two triaxial apparatuses. The static tests have been performed in a stress path triaxial cell similar to that described by Menzies (1988). The cyclic tests have been performed in a conventional triaxial apparatus with the deviator load provided by an MTS hydraulic actuator. To check that the different apparatuses did not affect the results static tests have been performed in each and have produced practically identical results. For both apparatuses microcomputers have been used for data acquisition and test control.

The following procedure has been used for all the tests. The samples were set-up in the apparatus enclosed within two membranes to prevent leaks from holes created by the angular soil particles and with drainage through porous discs at each end of the sample. For the uncemented samples there was sufficient suction to keep them intact

during this process. A small confining stress was applied and then the back pressure was increased, keeping the effective stresses constant, to approximately 600 kPa. The samples were left overnight, or longer if the B value was still less than 0.96, to ensure saturation. The samples were then consolidated in stages to the required confining stress. In the monotonic tests the samples were sheared to failure at an axial strain rate of 5%/hour.

All the cyclic tests were one-way tests with the deviator stress q ($=\sigma_1-\sigma_3$) being cycled between a peak value and a small positive minimum value, typically 20 kPa. The deviator stress was ramped up to the mean value in 1 minute before commencing the cyclic loading. A sinusoidal load waveform was used for all the tests. Data were recorded continuously up to the mean deviator stress, but thereafter readings were only recorded for selected cycles. During cyclic loading the data acquisition rate was chosen so that at least 40 readings per channel per cycle were recorded, a total of 160 readings per cycle.

Limitations of the hydraulic system have meant that large displacement amplitudes could not be applied at high frequencies. Tests at a frequency of 10 Hz have therefore been limited to the smaller deviator stress amplitudes, and in a few tests the load dropped off when the displacements increased as failure approached. This is discussed further below.

4. STATIC TESTS

Figure 1 shows the undrained stress-strain responses, and Figure 2 the associated pore pressure changes, from monotonic tests to failure for a range of confining stresses. In these tests the samples had all been prepared to the same nominal density 13 kN/m^3 and cement content 20%. These figures show the effects of increasing the confining stress are to increase the peak strength and to significantly increase the pore pressures at failure. The detail of the post-peak behaviour was found to depend on the shape of the rupture pattern developed, but in all tests the samples approached a unique ultimate stress ratio, and the same ultimate deviator stress. The similarity of the ultimate conditions was expected because all the samples had very similar densities. It is normally expected that increasing the confining stress causes a change from a brittle to a more ductile response, but in these undrained tests the samples became more brittle; the strain to the peak remained approximately constant, and the post-peak drop in strength increased.

As one of the effects of cyclic loading is expected to be the breakdown of the cementation it is interesting to investigate the effects of different cement contents on the undrained behaviour. Figure 3 shows the stress, strain responses from undrained tests conducted at a confining stress of 300 kN/m^2 with cement contents of 0, 5 and 20%. The associated pore pressure changes are shown in Figure 4. These figures show results typical of cemented

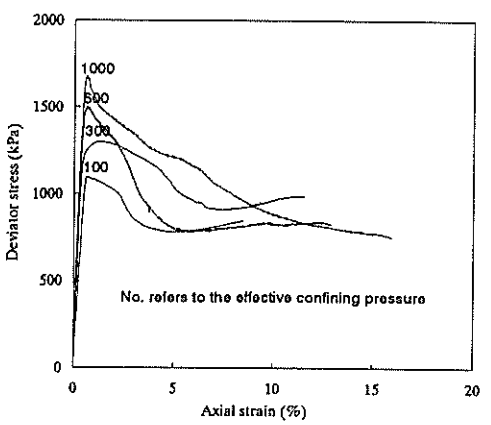

Figure 1. Effect of effective confining stress

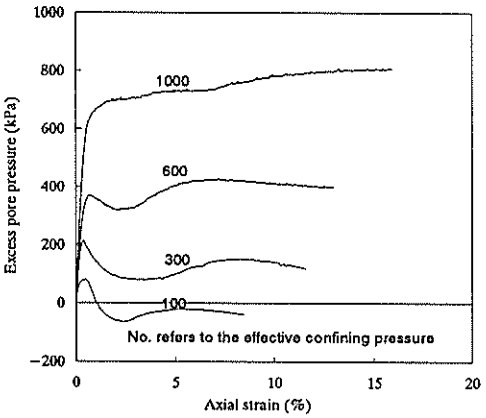

Figure 2. Effect of effective confining stress

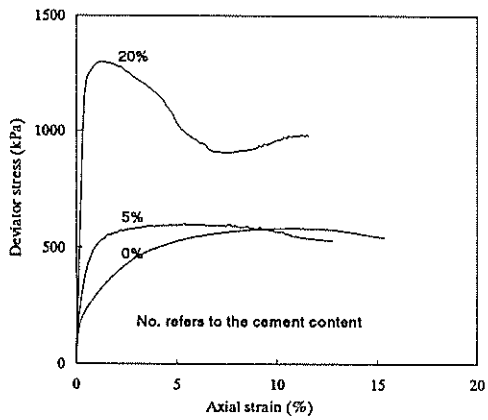

Figure 3. Effects of varying cement content

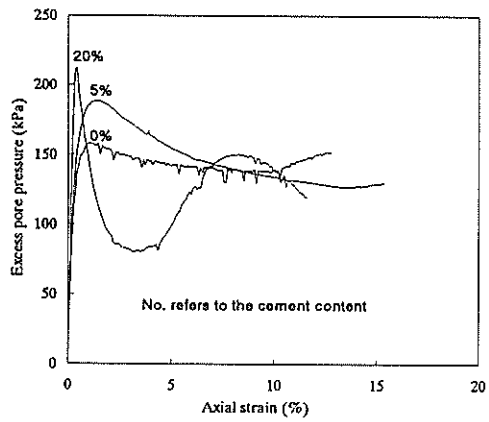

Figure 4. Effects of varying cement content

soils; as the cement content increases the peak strength increases, the initial stiffness increases, and the strain to the peak decreases. For this density and confining stress the peak strength varies from 550 kPa with no cement to 1270 kPa with 20 % cement. Clearly there is a possibility for a loss of strength should cyclic loading cause a breakdown in the cementation. It should be noted that the increase in cement content not only increased the peak strength but also the frictional strength of the soil, as the ultimate stress ratio was found to increase from 1.55 to 1.85.

5. CYCLIC TESTS

All the samples used for the cyclic tests were prepared with a nominal dry density of 13 kN/m^3 and a cement content of 20%, and they were all isotropically consolidated to a mean effective stress of 300 kN/m^2 before starting the cyclic phase of the tests. In the cyclic tests two parameters have been varied; the frequency of loading, and the stress level S where S has been defined as the ratio of the peak deviator stress in a cyclic test to the peak deviator stress in a static test.

Figure 5 shows the deviator stress, axial strain response for a test conducted at a frequency of 0.1 Hz with S = 0.76. The response from a typical monotonic test is also shown for comparison. In each cycle there was an accumulation of axial strain the rate of which at first decreased and then increased as failure was approached. In this test failure, in the sense that the peak deviator stress could not be reached, occurred after 1310 cycles. However, because the hydraulic system could not provide the required load as the deformations increased the sample was able to support significant loads for a further 100 cycles. The point at which failure occurred was therefore dependent, to some extent, on the capacity of the hydraulic system. Although similar behaviour occurred in other tests the uncertainty in the number of cycles at failure was always less than 100 cycles. The variation of the peak pore pressure with the peak axial strain for this test during cycling loading is shown in Figure 6. Comparison with the monotonic test response, also shown in Figure 6, indicates that much greater pore pressures are generated in the cyclic test. It can be seen from Figure 5 that failure appears to occur when the cyclic curve meets the monotonic post peak response, however, the greater pore pressures in the cyclic test suggest that the cause of failure is more complex.

The rates of development of axial strain and pore pressure with numbers of cycles were found to be strongly dependent on the frequency of loading. However, the relation between the mean pore pressure and the mean axial strain, shown in Figure 7, was similar in all the tests and apparently independent of frequency. For all the tests the mean strain at failure was approximately 1% and no significant trend with stress level ($0.6 < S < 0.9$) could be detected. The effect of the pore pressure increase was to move the effective stress state to the left in a deviator stress, mean effective stress p'($=(\sigma_1'+2\sigma_3')/3$) plot and closer to the failure envelope determined from the static

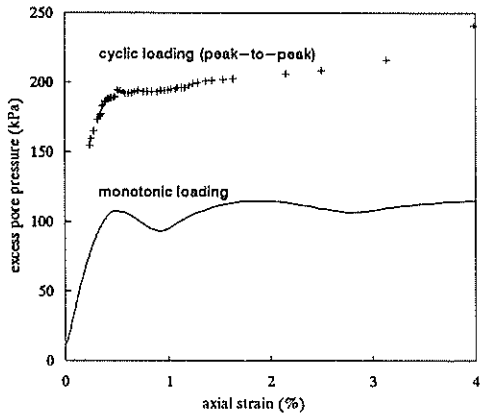

Figure 6. Comparison of static and cyclic pore pressure responses

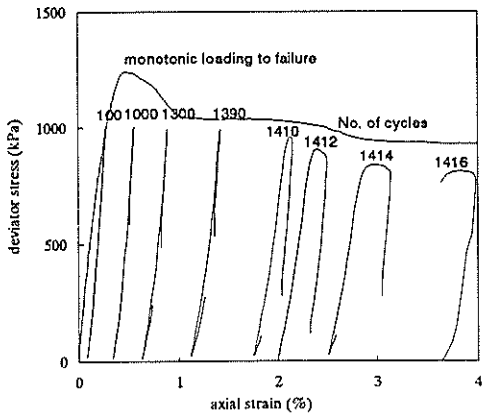

Figure 5. Comparison of static and cyclic stress, strain responses

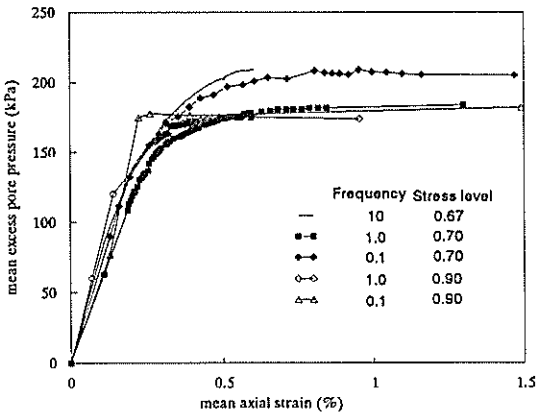

Figure 7. Mean pore pressure versus mean axial strain during cyclic tests

tests. Figure 8 shows the failure locus determined for the static tests in a deviator stress, mean effective stress plot. The peak effective stress states at failure for the cyclic tests lie close to the monotonic failure envelope, especially at high stress levels, suggesting that the cyclic loading has had only a minor effect on the cementation strength. Nevertheless, some breakdown of the cementation must have occurred for the pore pressure and axial strain to build up.

Figure 9 shows the relation between the frequency and the number of cycles to failure normalised by the number of cycles to failure at 0.1 Hz for three different stress levels (S = 0.7, 0.76, 0.9). Only one point is shown at 10 Hz (S=0.67), because the limitations of the hydraulic jack prevented higher stress levels from being applied at this frequency. Further the test at 10 Hz was stopped before failure occurred which has been indicated by the arrow in Figure 9. This plot shows a clear trend for the number of cycles at failure to increase with increasing frequency, with no apparent effect of the stress level. Although this plot is based on very limited data the similarity of the trend at three different stress levels suggests that this is a significant result. The figure shows that an order of magnitude increase in the frequency results in an order of magnitude increase in the number of cycles to failure. This suggests that the time for which the peak stress is applied in a cycle is more important than the number of cycles, and that the apparent frequency effects are in fact due to creep or viscous effects. A similar frequency dependency has been reported (Attewell and Farmer, 1973) for fatigue tests on rocks.

Figure 10 shows the relation between the secant Young's modulus during cycling and the peak-to-peak axial strain. It was found that the shear modulus remained practically constant throughout the cyclic tests. The results show a trend of decreasing modulus with increasing strain, and there appears to be a slight frequency effect with lower moduli being measured at lower frequencies for a given strain amplitude. For the static tests the modulus could not be measured at axial strains below 0.2% because of uncertainties about the stress-strain response related to the seating of the ram. Over the range for which it could be measured, indicated in the Figure, the modulus appeared to be constant, and close to the lowest value measured in the cyclic tests. These results confirm the observations of many researchers (eg. Atkinson and Sallfors, 1991) that the influence of strain rate on modulus is relatively small.

The results from the fatigue tests may be summarised in the form of an S-N curve (see Figure 11) relating the numbers of cycles at failure to the stress level. Figure 11 shows that all the data lie within a reasonably narrow

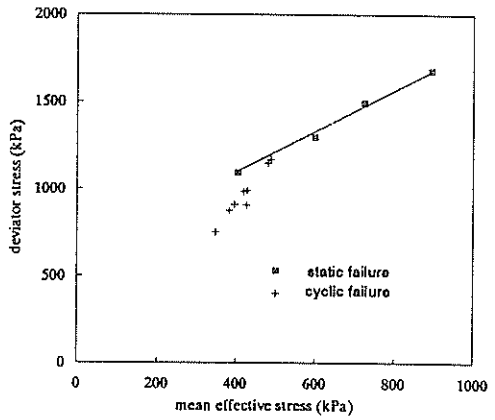

Figure 8. Failure conditions in static and cyclic tests

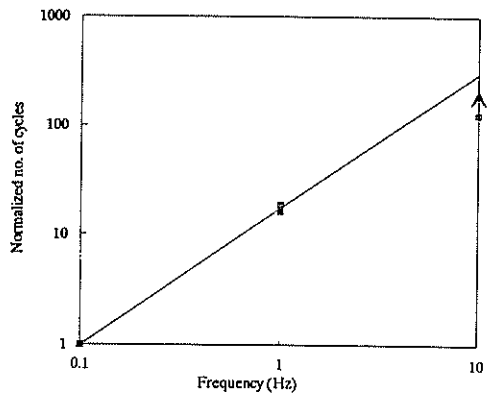

Figure 9. Effect of frequency on the number of cycles to failure

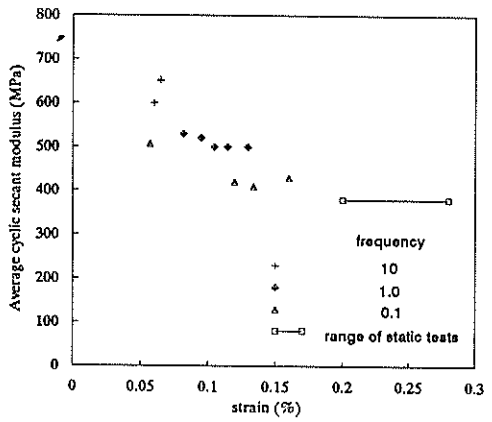

Figure 10. Young's moduli from static and cyclic tests

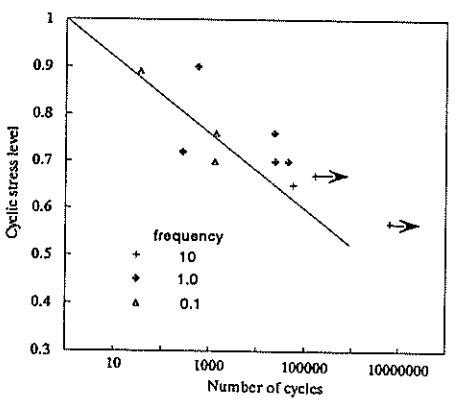

Figure 11. Fatigue S-N curve, stress level versus number of cycles to failure

band despite the range of frequencies used, and the effects of this on the number of cycles to failure discussed above. Two of the tests at 10 Hz, indicated by the arrows, were stopped before failure but in both tests mean strains of more than 0.6% had accumulated so that the samples must have been close to failure at the end of the tests. A tentative S-N line has been drawn through the results obtained from the tests at 0.1 Hz which indicates that failure at a stress level of 0.5 might occur at 10^6 cycles. However, insufficient data have so far been obtained to have much confidence in this result.

6. DISCUSSION

The results indicate that the number of cycles to failure is strongly dependent on the loading frequency. However, the frequency independence of the pore pressure, axial strain responses and the similarity of the modulus values at different frequencies suggest that it is not the frequency *per se* but the time for which the load is applied that is important. The small increase in modulus with frequency is consistent with the view that the time for which the load is applied is important, as at lower frequencies more strain will result.

The frequency dependency of the results has important implications for all cyclic tests and in particular for tests designed to investigate the fatigue limits at numbers of cycles of the order of 10^8, the order of the total number of waves subjected to an offshore structure in 30 years. Ideally all tests should be performed at frequencies similar to those experienced by the soil in the ground, which for the wave loading of offshore structures is about 0.1 Hz. The time involved in applying large numbers of cycles at this frequency makes such an approach impractical, but because of the frequency dependency of the results there is nothing to be gained by performing the tests at higher frequencies. It thus appears impractical to investigate the fatigue response beyond 10^6 cycles which at 0.1 Hz would take 115 days.

In metal fatigue it has been found that at high stress levels creep is an important mechanism, and the frequency of loading is important, while at lower stress levels the fatigue response is almost independent of frequency. If such a trend were also to apply for the cemented sand then higher frequencies could be used for the lower stress levels. However, for the stress levels used ($S > 0.67$) there is no evidence of a trend suggesting that the frequency effects diminish as the stress level decreases. Work is continuing to investigate this point.

It is evident from these results that cyclic loading can cause fatigue type failures of cemented sands and that there can be a significant and dramatic loss of strength when this occurs. If the S-N curve in Figure 11 is extrapolated to 10^8 cycles then failure is predicted at a stress level of 0.35. If fatigue failures were to occur at such low stress levels the long term stability of offshore foundations would be cause for concern. However, in practice it is expected that there will be a threshold below which no degradation of the soil and no fatigue failures will occur. Further, the applicability of undrained tests for large numbers of cycles is uncertain as in the ground drainage will occur, and for uncemented soils this usually results in an increase in strength.

7. CONCLUSIONS

For the particular cemented soil and confining stress used in these tests the cementation was responsible for a significant part of the static strength, and there was a relatively rapid post-peak loss of strength.

Fatigue tests demonstrate that the samples are susceptible to a dramatic loss of strength. However, cycles of the order of 10^6 are required for the strength to drop below 50% of its peak value.

The frequency has a significant effect on the number of cycles to failure at any given stress level. The time for which the peak load is applied is important, and therefore there is no benefit to be gained from performing tests at 10 Hz to investigate the in-situ response where the loading frequency is 0.1 Hz.

The Young's modulus and pore pressure, axial strain responses were both found to be independent of frequency.

ACKNOWLEDGEMENT

The research into the behaviour of cemented soils has been made possible by support from a Sydney University Research Grant and from the Australian Research Council.

REFERENCES

Airey,D.W. and Fahey,M.(1991) Cyclic response of Calcareous soil from the North-West Shelf of Australia, Geotechnique 41, No. 1, 101-121.

Atkinson,J.H. and Sallfors,G.(1991) Experimental determination of stress-strain-time characteristics in laboratory and in-situ tests. Proc X ECSMFE, Vol 3, 915-955.

Attewell,P.B. and Farmer,I.W.(1973) Fatigue behaviour of rock, Int.J.Rock Mech.Min.Sci., 10, 1-9.

Huang,J.T. and Airey,D.W.(1991) Manufacture and Index testing of a cemented carbonate sand. Research Report R631, School of Civil and Mining Engineering, Sydney University.

Menzies,B.K.(1988) A computer controlled hydraulic triaxial testing system. Advanced triaxial testing of soil and rock. ASTM STP 977, 82-94.

Pretorius,P.C. and Monismith,C.L.(1972) Fatigue crack formation and propagation in pavements containing soil-cement bases. Highway Research Record, Vol 407, 102-115.

General Report: Analytical and Probabilistic Methods

J.P. CARTER
Professor of Civil Engineering, University of Sydney, N.S.W. 2006, Australia

SUMMARY This General Report reviews the papers allocated to the session on Analytical and Probabilistic Methods. It also gives a brief review of the other important developments in these areas that have taken place recently. The methods of analysis covered include finite element, boundary element and distinct element techniques, stochastic methods, limit states approach, and risk assessment in rock engineering.

1. INTRODUCTION

Computers have now become so prevalent that their use in geomechanics is no longer confined to research laboratories. Many practicing geotechnical engineers are now using them routinely in their daily work and have done so for most of the past decade. The availability of relatively cheap personal computers and work stations has made possible the solution of a host of different tasks in geotechnical engineering, including laboratory data logging, spreadsheet analysis, and even the solution of complicated boundary and initial value problems, that a generation ago would have remained unsolved or at best would have required drastic simplification, idealisation and approximation.

Difficult non-linear and time dependent problems, i.e. problems that are deterministic in nature, can now be solved using numerical methods. Furthermore, sophisticated stochastic analysis can also be performed routinely and cheaply using the computational power of modern computers.

Has this ready access to computational power resulted in improvements in our understanding of our geotechnical problems, greater confidence in our solutions to these practical problems, and more reliable predictions of behaviour? Has the practice of geotechnical engineering been generally enhanced because of the greater levels of sophistication that may now be included in our analytical and probabilistic tools?

One of the objectives of this paper is to address these broad questions by briefly reviewing recent developments in the fields of analytical and probabilistic methods in geotechnics. A second and important aim of the paper is to summarise and review the findings of the twelve papers submitted to this conference that have been grouped together in this category. Where relevant, their part in advancing our knowledge in this area will be stressed.

The areas of analytical and probabilistic techniques are extremely diverse. To report on the many developments would be a lengthy task and one that is inappropriate for this conference. For this reason this paper will deal with only the most recent developments (particularly those taking place over the past two years), and the treatment will be necessarily selective, reflecting the writer's own interests and familiarity with the literature.

2. PAPERS IN THIS SESSION

The summary of the papers presented in this session will indicate the theoretical concepts that have been discussed and the practical problems to which these theories have been applied.

Twelve papers have been grouped under the general heading of Analytical and Probabilistic Methods. At least four may be described as dealing mainly with deterministic methods of analysis, one describes an expert system, two deal with the application of grey system theory and fuzzy mathematics to geotechnical problems, one describes an entirely new concept for the analytical assessment of risk in rock engineering, and the remainder elaborate on probabilistic techniques. The applications include piles, slopes, footings, dams and sub-surface exploration. This break down into sub-categories is summarised in Table I.

3. FINITE ELEMENT METHODS

The finite element method is now accepted as a valuable analysis tool in geotechnical engineering. However, its use is still confined to research tasks and the more challenging and sophisticated technical problems in the geotechnical profession, and perhaps that is as it should be. The method has the advantage of being able to model the complex geometry and the variety of different materials which occur in real engineering problems, as well as having the ability to incorporate the complex constitutive behaviour of soils and rocks, and being able to model, at least approximately, the actual construction process and loading history.

A review of the literature over the recent past indicates that the solution of large three-dimensional problems has become much more common in geomechanics, e.g. Brown and Shie (1990a, 1990b), Lee and Rowe (1990a, 1990b), Lai and Booker (1991), obviously reflecting the availability of relatively cheap computing power. The economies to be gained by coupling together finite element and boundary element schemes have also been exploited for problems of this nature, e.g. Duddeck (1991), Beer (1983). A number of papers on this theme may be found in the

TABLE I

CLASSIFICATION OF SESSION PAPERS

Authors	Method					Application					
	Deter-ministic	Proba-bilistic	Grey/ Fuzzy	Expert System	New	Slopes	Dams	Foot-ings	Piles	Explo-ration	Seismic
Assadi and Sloan	✓					✓					
Budkowska & Grzesiak	✓							✓			
Chen	✓					✓					
Styles, Moore & Gupta	✓										✓
Li		✓				✓					
Lo, Li & Lee		✓							✓		
St. George		✓				✓					
Williams & Zou		✓				✓					
Chowdhury, Zhang & Li			✓			?					
Xiao & Carter			✓			✓					
Goh				✓						✓	
Hudson, Sheng & Arnold					✓		✓				

proceedings of the Sixth International Conference on Numerical Methods in Geomechanics (Beer, Booker and Carter, 1991), held in Cairns in May 1991.

Of the papers reviewed in this session, only those presented by Assadi and Sloan (1992), Budkowska and Grzesiak (1992) and Williams and Zou (1992) make use of the finite element technique.

3.1 Deterministic Finite Element Analysis

The paper by **Sloan and Assadi** describes a relatively new finite element formulation that can be used to obtain rigorous limit solutions for collapse loads in geotechnical problems. This represents a significant advance and presents the profession with a valuable new computational tool. Reliable estimates of collapse loads may now be obtained to problems involving very complicated geometry and boundary conditions. In their paper the authors have described the procedure and presented limit solutions for the collapse of slopes in cohesive-frictional soils, i.e. in materials that obey the Mohr-Coulomb strength criterion and deform plastically according to an associated flow rule. This analysis demonstrates the power and versatility of the finite element technique, and illustrates how it can help to obtain very useful solutions to practical problems. No doubt the limit analysis has many applications in the geotechnical field, as well as in other branches of engineering mechanics (e.g. in the yield line theory of structural analysis).

Presumably the finite element procedure presented in the paper by Assadi and Sloan could also be applied to materials obeying other failure criteria, e.g. the Hoek-Brown strength criterion for intact and jointed rock, as long as a suitable multi-linear approximation to the strength criterion can be found. It is also noted that their method, based on the bound theorems of plasticity, is strictly applicable only to materials deforming with an associated plastic flow rule. For many frictional soils the associated flow rule overestimates the influence of dilatancy and therefore the volume changes that will occur in the soil as it fails. Perhaps it may be useful if some guidance could be given about the validity and applicability of these solutions to obtaining approximate estimates of collapse loads in materials deforming with a non-associated flow rule, e.g. a frictional soil at critical state deforming without volume change.

A specific question that the authors may wish to address concerns Figure 9 of their paper. This figure shows stability bounds for a 45 degree slope in purely cohesive material. Two extreme points on each bound have been joined by a straight line. An explanation of why linear interpolation between these extremes is valid would be helpful. Furthermore, in Figures 10 and 11 of their paper the upper and lower bounds diverge increasingly as the friction angle increases, and therefore the true collapse load is more difficult to estimate. Why does this occur, and what would be required to bracket more tightly the collapse loads at higher friction angles? Finally, can the same technique be used to analyse the stability of jointed rock masses, where the strength of the discontinuities may have an overriding influence on the strength of the mass?

In the paper by **Budkowska and Grzesiak** a scheme is presented for the finite element simulation of the time dependent behaviour of a pavement structure containing cracks. The time dependence enters the problem because the soil and pavement courses have been modelled as viscoelastic materials. A relatively simplistic viscoelasticity has been assumed, in which only deviatoric creep occurs, i.e. there is no volumetric creep. Some detail of the mathematical formulation is provided. While the approach for this idealised problem is valid, in the writer's opinion the solution of the problem using Laplace transforms together with the finite layer techniques, e.g. Booker and Small (1985), would have been more economical.

In the paper some significance is given to the role of cracks in the pavement and underlying layers in determining the overall response to surface loading. No detail is given about how the cracks were modelled. As the analysis was also axi-symmetric, presumably so also were the cracks, i.e. they are ring cracks concentric with the centre of the circular loading on the surface. Surely this is an extreme idealisation and one that would rarely be encountered in practice.

In Figures 3 to 10 of this paper the horizontal axis is labelled as 't' for time. It is likely that this axis is mis-labelled and should actually be radial distance from the centre of the loaded region. This point requires clarification.

3.2 Probabilistic Finite Element Analysis

The stochastic finite element method can be used to determine the range of responses of soil or rock masses where some of the input parameters are uncertain and have been assigned assumed distributions. This procedure is being used increasingly in geotechnical engineering where much uncertainty accompanies the selection of typical soil parameters and loads, e.g. Drumm et al, 1990.

One of the concerns of the paper by **Williams and Zou** is the application of the stochastic finite element method to the analysis of the stability of coal mine spoil piles. In particular, the finite element procedure has been used to make a prediction of the stresses in the spoil pile. These predictions have then been used as input to a stability analysis based on the approximate limit equilibrium techniques. Specifically, the finite element results have been used to identify the probable location of the critical slip surface. Because the stress predictions are based on soil properties with specified statistics, the computed stresses also have associated probability distributions.

The use of the finite element method in this way begs certain questions. Because the analysis presented by Williams and Zou allowed for non-linear material behaviour, why was it necessary subsequently to analyse the stability of the spoil pile using limit equilibrium techniques? Could the finite element solutions themselves indicate the degree of risk or even the overall factor of safety for the slope? On the question of the finite element analysis, it is unclear from the paper how the loading was applied to the spoil pile. Was gravity "switched on" in the analysis, or was the appropriate sequence of spoil pile construction modelled. This question may be important, as the final response of the spoil pile will be dependent, to some degree, on the loading sequence, and therefore it may be important to follow this sequence as accurately as possible. The paper by Williams and Zou deals with wider issues than just finite element analysis, and these will be addressed later in this review.

4. BOUNDARY ELEMENT METHODS

The boundary element method has grown in stature during the past decade. It now rivals the finite element method for use in geomechanics. Its major application to date has been in the analysis of underground openings and thus it has received much attention by practitioners in the field of rock mechanics. It also has particular application to the analysis of piles and pile groups, e.g. Chin and Poulos (1991), the dynamic behaviour of foundations, e.g. Alarcon Cano and Dominguez (1989), and the analysis of excavations in anisotropic, jointed rock, e.g. Carter and Alehossein (1990).

The past five years or so has seen the merger of the finite and boundary element techniques in the one computational procedure. There are now several software packages available commercially for coupled BE-FE analysis in geomechanics. Since this is a topical subject, and one in which there is considerable research effort currently being expended, it is surprising that there are no papers in this session that concern the boundary element methods.

5. DISTINCT ELEMENT METHODS

Research into the development of the distinct element technique and its application in geomechanics has accelerated over the last few years. It is now feasible to solve three dimensional problems with this technique, e.g. Ghaboussi and Barbosa (1990). It is interesting that there are no papers on this topic submitted to this session of the conference as several software packages employing the distinct element methods are now available commercially.

6. EXPERT SYSTEMS

Until recently the majority of computer applications that have been developed in the geotechnical field have been numeric and deterministic. Their main function has been to relieve engineers of the need for carrying out manually repetitive, and sometimes quite sophisticated mathematical calculations.

It has been recognised for some time that much of geotechnical practice involves the application of deductive reasoning, often in the absence of precise calculation. Sometimes important design decisions have to be based on knowledge gained by experience.

With the emergence of expert system technology, geotechnical engineers now face the prospect of capturing this empirical-type knowledge in a suitable knowledge base, from where it may be retrieved by appropriate interrogation procedures.

Recently, the development of expert systems designed specifically for use in geotechnical practice have been described in the literature, e.g. Wong, Poulos and Thorne (1989). In this conference the paper by **Goh** (1992) describes an expert system for sub-surface exploration. This system has been designed to provide "advice on a sub-surface exploration program for a particular site". Embedded in the knowledge base is information from selected textbooks, codes of practice, design manuals, and information gleaned from interviews with "expert" practitioners.

Several questions arise in relation to expert systems in general and these are relevant to the system described in Goh's paper. Much effort is obviously required to develop this type of design tool. However, the user should also be concerned with establishing the validity of the system's conclusions and recommendations. As far as the writer is aware, there exist no well established procedures for validating particular expert systems. This is an area that requires further exploration.

With regard to the expert system described by Goh for site exploration, it would appear that some information about the soil profile is required *a priori*, before a recommendation can be made by the system about the depth of planned exploration. This feature of the system requires clarification.

7. FUZZY MATHEMATICS AND GREY SYSTEM THEORY

In the last few decades theoretical methods have been developed to deal with uncertainty in real systems. The use of stochastic techniques in geotechnical engineering is now well established. However, there are alternatives to probabilistic methods such as the grey system theory and fuzzy mathematics. Special mathematical theories have been developed to describe systems which are inexact or indistinct, e.g. Zadeh (1965, 1975). Much of the adaptation of these theories to geotechnical problems has taken place recently, e.g. Nguyen (1985), Boissonnade (1986), Xiao and Zhou (1987), Sakurai and Shimizu (1987), and Xiao and Yu (1990). Some of these methods are directly applicable to the issue of risk assessment in geotechnical works.

In this conference, papers by **Xiao, Carter and Yu** (1992) and **Chowdhury, Zhang and Li** (1992) fall into this category. Xiao *et al* describe the use of fuzzy mathematics for the description of typical geotechnical parameters and then demonstrate the use of the theory for the prediction of the stability factor for planar sliding of rock slopes. Detail is provided on how to describe fundamental properties as fuzzy numbers, e.g. the strength parameters of a rock mass. This includes a description of how to assign appropriate weights to different measures of the same parameter, according to the perceived levels of reliability that should be associated with each measure. It would appear that the major attraction of this technique is that it is unnecessary to assume that the uncertainty of the parameter must be described by a normal or some other statistical distribution. The use of fuzzy mathematics is akin to the use of linguistic variables to describe the physical system and its stability.

In the paper by **Chowdhury, Zhang and Li** the use of grey system theory to interpret and then to extrapolate field observations is described. The authors point out that a procedure such as this is useful for updating risk assessment during construction, i.e. as some real data becomes available. Such a process would help planning and redesign where necessary. An example problem is considered (presumably a hypothetical one), in which measurements of pore water pressures in a slope are observed, and then the theory is applied to produce an extrapolation in time, i.e. a prediction of the subsequent pore water pressures based on the observations to date. The paper contains insufficient detail of the method to allow the reader to follow the exact sequence of calculations required for the example problem. It is also unclear whether the example problem may have an inbuilt trend to which this extrapolation technique is well suited. It would be worthwhile knowing for what problems this method is well suited and what are its limitations. Furthermore, the application to a real problem would also provide a better test of the technique. Nevertheless, it would seem that the technique proposed in this paper merits further investigation.

8. COUPLED PROBLEMS

One of the great benefits of the increased computing power that has become readily available is that researchers are now turning to some important problems in geotechnics, problems that in previous times had proved too challenging and dependent on much computing power for their solution. One important class of problems that has come under scrutiny recently is that which involves the coupling together of two or more physical and perhaps chemical processes.

Of course, coupled problems are not new in geomechanics. One problem studied extensively since the beginnings of soil mechanics has been the consolidation of soil, in which a solid deformation process is coupled to the flow of a pore fluid.

Recently, problems such as the coupling of heat flow, stress-deformation and even pore fluid flow have been examined and solutions to practical problems have been obtained, e.g. Savvidou and Booker (1989), Booker and Savvidou (1985), Britto, *et al* (1989), Smith (1990). The basic formulation for these problems and the solutions to various boundary value problems have application to the storage of hot radioactive waste in "stable" geological deposits, and also to mining at depth in hot rocks.

Another problem of this type involves the analysis of contaminant migration through soil and fissured rock, e.g. Rowe and Booker (1989, 1990). These problems involve fluid flow, advection and dispersion of pollutants throughout the medium. The new solutions that are being obtained are invaluable for designers of landfills and other domestic and hazardous waste storage facilities. Of course, information about the basic physical (and chemical) properties of the soils and rocks is an essential input to these mathematical models. Comprehensive and complementary experimental studies are also underway at present to measure these key parameters, e.g. Quigley *et al* (1987).

9. CONSTITUTIVE MODELLING

Research work has been underway for some time now into the development of appropriate constitutive models describing the stress-strain behaviour of soils and rocks. Numerous conferences and publications have been devoted to this topic. There are many reported instances in the literature where quite sophisticated non-linear, elastoplastic soil models have been applied to practical problems.

The topics in this category that have received recent interest include the analysis of shear band formation, e.g. Vardoulakis *et al* (1988), and the application of Cosserat theory to soil and rock problems, e.g. Mühlhaus (1986). The full potential of these theories has yet to be realised but they may help improve our understanding of deformation and collapse mechanisms in soil and rock.

10. SLOPE STABILITY ANALYSIS

Judging by the number of papers in this conference dealing with slope stability, it can be inferred that this is still a topical subject, and one with a number of unresolved issues.

The perennial (and deterministic) problem of reliably locating the critical failure surface in soil slopes continues to receive attention. The paper by **Chen** (1992) in this conference is concerned with this problem. Chen describes his experience in this area and discusses several key issues including: the importance of using a non-linear failure envelope for cohesionless soils, the determination of the global minimum factor of safety by a random search approach, comparison of results obtained using the simplified Bishop method and the Morgenstern-Price method, and the important issue of the verification of the results of limit equilibrium techniques with closed form solutions. The paper ends with some useful conclusions including the comforting recommendation that for slopes where geological heterogeneity and discontinuities do not dominate, the simplified Bishop method generally produces satisfactory results.

The paper by **Williams and Zou** has been discussed previously in relation to stochastic finite element analysis. However, the paper also contains the results of wedge analysis of the spoil pile stability. These deterministic, limit equilibrium analyses have been carried using the techniques and computer codes developed by Donald and Giam (1989). The results have been compared to those obtained from the dynamic programming method coupled to the results of the stochastic finite element stress analysis. This comparison showed that good agreement between the methods was possible for the location of the critical slip surfaces. However, there was some disagreement in the minimum factors of safety predicted by the two methods. This begs the question of which method should be relied upon in design.

In the paper by Williams and Zou selected values of the strength parameters are provided. In particular, relatively large mean values have been adopted for the cohesion intercepts of the spoil pile material and the floor material. Presumably an effective stress analysis was performed. It would be instructive to learn to what physical source such large cohesions may be attributed.

10.1 Reliability Methods for Slopes

Most of the recent attention of researchers in the area of slope stability has focussed on replacing the classical and deterministic factor of safety approach by methods which hopefully can deal with uncertainty in a meaningful fashion. The concept of reliability analysis is now being pursued actively. The papers by **Li** (1992) and **St. George** (1992) to this conference address this issue.

Li has developed an efficient point estimate method (PEM) for calculating the reliability index of slopes. The paper also contains a useful discussion of the merits of the PEM and goes to some length to discredit the alternative single random variable (SRV) approach. The presentation of this argument is particularly noteworthy and it asserts that the use of the SRV approach, that apparently is common in practice, results in a gross overestimation of the probability of failure of slopes. This occurs largely because the SRV approach ignores the reduction in the variance of the key soil properties that will occur with spatial averaging, such as along a potential failure surface. An example involving the undrained failure of a slope in clay provides a useful insight into this problem. Authors claimed by Li to have used the "erroneous" SRV approach may wish to respond to these criticisms.

Li goes on to develop his point estimate method after noting the shortcomings of existing PEMs, including that due to Rosenblueth (1975, 1981). The reliability index for the slope is defined as:

$$\beta = \frac{\mu_F}{\sigma_F} \qquad (1)$$

where μ_F and σ_F are respectively the mean and standard deviation of the factor of safety. The obvious strength of Li's method for determining β is the avoidance of a multitude of calculations of the factor of safety, corresponding to the large number of possible combinations of the random variables, such as the soil strength parameters and unit weights. Li's paper sets out the method but contains only one numerical example. The application of the PEM to more problems of practical interest will be welcome.

In the paper presented by **St. George**, a reliability approach has also been followed and the sensitivity of predictions to the input data has been examined. Unlike Li, St. George has selected the first order second moment method (FOSM) for the analysis of the reliability index for slopes. He presents examples taken from extensive case studies of failures in opencast mines in the United Kingdom. The limit equilibrium technique employed to compute the factors of safety was that due to Janbu.

A number of interesting observations are made in the paper by St. George. He warns that "it is unreasonable to expect the techniques of risk analysis and statistics to resolve problems which cannot be formally answered, and as such are not introduced directly into the analysis". He goes on to draw an important distinction between "subjective uncertainties" that arise from a lack of knowledge, and "objective uncertainties" that are related to measured statistical or probabilistic information. St. George states that the major uncertainties in slope stability analysis arise:

i) because there may be natural heterogeneity in the shear strength of geological materials,
ii) when structural features such as discontinuities control the failure,
iii) because of the presence of water (and pore water pressures) in the slope, and
iv) from uncertainties about the appropriateness of the limit equilibrium models.

These key issues are examined at length in the paper. The point is also made that these uncertainties are compounded by the sampling and testing techniques that are used to gather information about the geological materials. However, the point is well made that it is only possible to account for those uncertainties which are measurable, unless a judgement factor is also included in the reliability analysis.

The paper concludes that for two-dimensional problems the probability of failure is sensitive to changes in the modelling error and variations in the water table. Spatial and parameter correlations have less influence on the probability of failure. For three dimensional problems, the uncertainty of the resistance that can be provided at the side margins of the moving mass has an important influence on the probability of failure.

11. LIMIT STATE APPROACHES

Lo, Li and Lee (1992) present a review of the probabilistic theory for the limit state method, and give interesting background information about the use of the limit states approach in the new draft Australian code for piling. The paper includes a description of procedures recommended in the code for the determination of partial safety factors in the limit state format. This paper and the draft code form part of a concerted effort to bring codes of practice for geotechnical engineering into line with approaches used elsewhere, such as in structural engineering. The argument advanced in favour of the limit states approach is that it generally gives better control over the reliability of design.

This paper points out that the uncertainties involved in pile design are different to those involved in structural design, and therefore the approach used for the formulation of the limit state piling code is different from those used in structural codes.

One of the strengths of this paper is the clear exposition of the various levels of probabilistic analysis that are available and the discussion of which levels are suitable to piling practice. This information may be well known in structural engineering, but the writer suspects that generally this is not the case in geotechnical engineering, so that the present paper is both timely and informative. The paper reminds us that in piling practice the foundation engineer has some control over the estimates of reliability. For example, he can obtain more reliable estimates of the soil parameters by carrying out more extensive site investigation, or he can reduce uncertainty by carrying out pile load tests. How such measures can be incorporated into a quantitative risk assessment is explained clearly in the paper by the use of examples. The paper concludes that a consistent level of reliability is possible in pile design, provided the strength reduction factor is properly correlated with the confidence level of the design by a thorough statistical analysis of the available and relevant data. Many practitioners await the release of this draft standard.

12. SEISMIC RISK ANALYSIS

The premise of the paper to this conference by **Styles, Moore and Gupta** (1992) is that structural damage from an earthquake will be minimised if the natural frequencies of the elements of a building are separated from the frequency of the excitation, i.e. if resonance is not allowed to occur. The paper discusses the individual elements of a building, including its footing and the superstructure, and provides estimates of the natural frequencies of these components. Simple, but approximate closed-form expressions for the natural frequencies are provided.

While the issue of resonance is important, it should be borne in mind that damage to structures can also take place without resonance occurring, as the authors appear to acknowledge in their introduction. The prediction of other quantities, such as the dynamic response of the structure, is also important.

The issues addressed in this paper have been explored elsewhere, e.g. see Novak (1974a, 1974b), Novak and El Hifnawy (1983, 1984), Roesset (1980), where it has been shown that the natural frequencies of buildings are affected by the type and stiffness of the foundation. The problem of predicting the overall response of the building to seismic excitation is complex, and should also include the influence of damping, both within the soil as radiation and material damping, and in the structure. The stiffness and damping constants for foundations actually depend on frequency, but it is often possible to choose constant values which are representative for the region of the dominant frequency. It has been demonstrated by Novak and El Hifnawy (1984) that the flexibility of the foundation may have a profound effect on the response of buildings to seismic excitation. Both the absolute and relative effect of different foundations vary with soil stiffness. Piles usually yield higher natural frequencies but lower damping than other types of foundations. The depth of the soil layer may also be important. With a finite soil layer, a significant loss of geometric damping occurs and this results in larger building displacements.

13. NEW DEVELOPMENTS

The remaining paper assigned to this section is by **Hudson, Sheng and Arnold** (1992) and it presents a new approach to the assessment of risk in rock engineering. The paper identifies the need for a coherent approach for the identification of parameters which are significant in any rock engineering activity. It then proposes one possible approach. This involves the use of a "rock mechanics interaction matrix" to identify the relative significance of factors such as: the overall environment including geology and climate, the quality of the intact rock, the nature of the discontinuities in the rock mass, the ground water conditions, the proposed construction procedures, etc. It is asserted that an important feature of the matrix approach is that the interactions between parameters can be used as an indication of which parameters and mechanisms are critical before, during and after the construction of a project. Unfortunately, no detail about how this is done is given in the paper. We are promised this detail in later publications. The paper goes on to describe rock mechanics aspects of the Fei-Tsui Dam in Taiwan. This includes a description of the measures used to improve the shear strength of the rock mass, which included cleaning of the discontinuities and replacement of the infill material with cement grout. The paper contains little in the way of mathematical analysis.

14. CONCLUSIONS

The availability of increased computing power continues to encourage the development of numerical tools in geotechnical engineering.

This paper has reviewed recent developments in the fields of analytical and probabilistic methods in geotechnical engineering, with particular reference to the papers presented under this heading in the conference.

It appears that there is a growing awareness of the need to use the analytical tools in the assessment of the reliability of geotechnical works. It is also evident that slope stability problems are still the focus of much attention in the literature. However, recent activity in this area seems to be aimed at risk assessment rather than deterministic methods of analysing slope stability problems.

15. REFERENCES

1. Alarcon, E, Cano, J.J. and Dominguez, J. (1989) Boundary Element Approach to the Dynamic Stiffness Functions of Circular Foundations, Int. J. Numer. Analytical Methods Geomechanics, Vol. 13, No. 6, pp. 645-664.

2. Assadi, A. and Sloan, S.W. (1992) Stability of Slopes in Cohesive-Frictional Soil, Proc. 6th ANZ Conference on Geomechanics, Christchurch, NZ.

3. Beer, G. (1983) Finite Element, Boundary Element and Coupled Analysis of Unbounded Problems in Elastostatics, Int. J. Numer. Methods in Engineering, Vol. 19, pp. 567-580.

4. Beer, G., Booker, J.R. and Carter, J.P. (1991) Computer Methods and Advances in Geomechanics, Vols 1 and 2, A.A. Balkema, Rotterdam.

5. Boissonnade, A.C. (1986) Identification of Fuzzy Systems in Civil Engineering, Proc. Int. Symposium on Fuzzy Mathematics in Earthquake Research, Seismological Press, Beijing, pp. 48-71.

6. Booker, J.R. and Savvidou, C. (1984) Consolidation Around a Spherical Heat Source, International Journal of Solids and Structures, Vol. 20, pp. 1079-1090.

7. Booker, J.R. and Small, J.C. (1985) Finite Layer Analysis of Settlement, Creep and Consolidation Using Micro-computers, Proc. 5th Int. Conf. on Numerical Methods in Geomechanics, Nagoya, Japan, A.A. Balkema, Rotterdam, Vol. 1, pp. 3-18.

8. Britto, A.M., Savvidou, C., Maddocks, D.V., Gunn, M.J. and Booker, J.R. (1989) Numerical and Centrifuge Modelling of Coupled Heat Flow and Consolidation Around Hot Cylinders Buried in Clay, Geotechnique, Vol. 39, No. 1, pp. 13-25.

9. Brown, D.A. and Shie, C.-F. (1990a) Three Dimensional Finite Element Model of Laterally Loaded Piles, Computers and Geotechnics, Vol. 1, No. 3, pp. 59-80.

10. Brown, D.A. and Shie, C.-F. (1990b) Numerical Experiments into Group Effects on the Response of Piles to Lateral Loading, Computers and Geotechnics, Vol. 10, No. 3, pp 211-230.

11. Budkowska, B. B. and Grzesiak, W. (1992) Numerical Simulation of the Time-Dependent Stratified Viscoelastic Soil Medium with Cracks, Proc. 6th ANZ Conference on Geomechanics, Christchurch, NZ.

12. Carter, J.P. and Alehossein, H. (1990) Analysis of Tunnel Distortion due to an Open Excavation in Jointed Rock, Computers and Geotechnics, Vol. 9, No. 3, pp. 209-232.

13. Chin, J.T. and Poulos, H.G. (1991) Axially Loaded Vertical Piles and Pile Groups in Layered Soil, Int. J. Numer. Analytical Methods Geomechanics, Vol. 15, No. 7, pp. 497-512.

14. Chowdhury, R.N, Zhang, S. and Li, J. (1992) Geotechnical Risk and the Use of Grey System Theory, Proc. 6th ANZ Conf. on Geomechanics, Christchurch, NZ.

15. Donald, I. and Giam, S.K. (1989) Improved Comprehensive Equilibrium Stability Analysis, Civil Engineering Research Report No. 1/1989, Monash University.

16. Duddeck, H. (1991) Application of Numerical Analysis for Tunnelling, Int. J. Numer. Analytical Methods Geomechanics, Vol. 15, No. 4, pp. 223-240.

17. Drumm, E.C., Bennett, R.M. and Oakley, G.J. (1990) Probabilistic Response of Laterally Loaded Piers by Three-point Approximation, Int. J. Numer. Analytical Methods Geomechanics, Vol. 14, No. 7, pp. 499-508.

18. Ghaboussi, J. and Barbosa, R. (1990) Three-dimensional Discrete Element Method for Granular Materials, Int. J. Numer. Analytical Methods Geomechanics, Vol. 14, No. 7, pp. 451-472.

19. Hudson, J.A., Sheng, J. and Arnold, P.N. (1992) Rock Engineering Risk Assessment through Critical Mechanism and Parameter Evaluation, Proc. 6th ANZ Conference on Geomechanics, Christchurch, NZ.

20. Lai, J. and Booker, J.R. (1991) A Residual Force Finite Element Approach to Soil-Structure Interaction Analysis, Int. J. Numer. Analytical Methods Geomechanics, Vol. 15, No. 3, pp. 181-204.

21. Lee, K.M. and Rowe, K.R. (1990a) Finite Element Modelling of the Three-dimensional Ground Deformations Due to Tunnelling in Soft Cohesive Soils: Part 1 - Method of Analysis, Computers and Geotechnics, Vol. 10, No. 2, pp. 87-110.

22. Lee, K.M. and Rowe, K.R. (1990b) Finite Element Modelling of the Three-dimensional Ground Deformations Due to Tunnelling in Soft Cohesive Soils: Part 2 - Results, Computers and Geotechnics, Vol. 10, No. 2, pp. 111-138.

23. Li, K.S. (1992) A Point Estimate Method for Calculating the Reliability Index of Slopes, Proc. 6th ANZ Conference on Geomechanics, Christchurch, NZ.

24. Lo, S-.C.R., Li, K.S. and Lee, I.K.L. (1992) Limit State Design of Pile Foundations: A Probabilistic Appraisal, Proc. 6th ANZ Conference on Geomechanics, Christchurch, NZ.

25. Mühlhaus, H-B. (1986) Shear Band Analysis in Granular Material by Cosserat Theory, Ingenier Archiv, Vol. 56, pp. 383-388 (In German).

26. Novak, M. (1974a) Effect of Soil on Structural Response to Wind and Earthquake, Earthquake Engineering and Structural Dynamics, Vol. 3, No. 1, pp. 79-96.

27. Novak, M. (1974b) Dynamic Stiffness and Damping of Piles, Canadian Geotechnical Journal, Vol. II, pp. 574-598.

28. Novak, M. and El Hifnawy, L. (1983) Effect of Soil-Structure Interaction on Damping of Structures, Earthquake Engineering and Structural Dynamics, Vol. 11, pp. 595-621.

29. Novak, M. and El Hifnawy, L. (1984) Effect of Foundation Flexibility on Dynamic Behaviour of Buildings, Proc. 8th World Conf. on Earthquake Engineering, Vol. III, Prentice-Hall Inc., New Jersey, pp. 721-728.

30. Nguyen, V.U. (1985) Some Fuzzy Set Applications in Mining Geomechanics, Int. J. Rock Mechanics, Mining Sciences and Geomechanics Abstracts, Vol. 22, No. 6, pp. 369-379.

31. Quigley, R.M., Fernandez, F., Yanful, E., Helgason, T., Margaritis, A., and Whitby, J.L. (1987) Hydraulic Conductivity of Contaminated Natural Clay Directly Below a Domestic Landfill, Canadian Geotechnical Journal, Vol. 24, No. 3, pp. 377-383.

32. Roesset, J.M. (1980) Stiffness and Damping Coefficients of Foundations, Proc. Session on Dynamic Response of Pile Foundations: Analytical Aspect, ASCE National Convention, Florida, pp. 1-30.

33. Rosenblueth, E. (1975) Point Estimates of Probability Moments, Proc. Nat. Acad. Sci. Mathematics, Vol. 72, No. 10, pp. 3812-3814.

34. Rosenblueth, E. (1981) Point Estimates for Probability, Applied Mathematical Modelling, Vol. 5, pp. 329-335.

35. Rowe, R.K. and Booker, J.R. (1989) A Semi-analytic Model for Contaminant Migration in a Regular Two- or Three-dimensional Fractured Network: Conservative Contaminants, Int. J. Numer. Analytical Methods Geomechanics, Vol. 13, No. 5, pp. 531-550.

36. Rowe, R.K. and Booker, J.R. (1990) Contaminant Migration in a Regular Two- or Three-dimensional Fractured Network: Reactive Contaminants, Int. J. Numer. Analytical Methods Geomechanics, Vol. 14, No. 6, pp. 401-426.

37. Sakurai, S. and Shimizu, N. (1987) Assessment of Rock Slope Stability by Fuzzy Set Theory, Proc. 6th Int. Cong. on Rock Mechanics, ISRM, Montreal, A.A. Balkema, Rotterdam, Vol. 2, pp. 503-506.

38. Savvidou, C. and Booker, J.R. (1989) Consolidation Around a Heat Source Buried Deep in a Porous Thermoelastic Medium with Anisotropic Flow Properties, Int. J. Numer. Analytical Methods Geomechanics, Vol. 13, pp. 75-90.

39. Smith, D.W. (1990) Boundary Element Analysis of Heat Flow and Consolidation for Geotechnical Applications, Ph.D. Thesis, University of Sydney.

40. St. George, J.D. (1992) Reliability Analysis of Failed Slopes, a Back Analysis View of the Sensitivity to Input Parameters, Proc. 6th ANZ Conference on Geomechanics, Christchurch, NZ.

41. Vardoulakis, I., Sulem, J. and Guenot, A. (1988) Borehole Instabilities as Bifurcation Phenomena, Int. J. Rock Mech. Min. Sci. and Geomech. Abstracts, Vol. 25, No. 3, pp. 158-170.

42. Williams, D.J. and Zou, J-.Z. (1992) Location of Critical Slip Surfaces in Coal Mine Spoil Piles, Proc. 6th ANZ Conference on Geomechanics, Christchurch, NZ.

43. Wong, K.C., Poulos, H.G. and Thorne, C. (1989) Site Classification by Expert Systems, Computers and Geotechnics, Vol. 8, No. 2, pp. 133-174.

44. Xiao, B., Carter, J.P. and Yu, X. (1992) Some Applications of Fuzzy Mathematics to Rock Engineering and Slope Stability, Proc. 6th ANZ Conference on Geomechanics, Christchurch, NZ.

45. Xiao, B. and Zhou, C. (1987) Discussion on Fuzzy Mathematics Used for Slope Stability, J. of Yunnan Metallurgy, No. 4, pp. 5-10. (In Chinese)

46. Xiao, B. and Yu, X. (1990) Fuzzy Limit Equilibrium Analysis for Slope Stability, J. Nonferrous Metals (Quarterly), No. 3, pp. 1-5 (In Chinese)

47. Zadeh, L.A. (1965) Fuzzy Sets, Information and Control, Vol. 8, pp. 338-358.

48. Zadeh, L.A. (1975) Calculation of Fuzzy Restriction in Fuzzy Sets and Their Application to Cognitive and Decision Processes, Academic Press, New York.

Stability of Slopes in Cohesive-Frictional Soil

A. ASSADI
M.Sc., Ph.D.
Res. Assoc., Dept. of Civ. Engrg. and Surveying, Univ. of Newcastle, Australia
S.W. SLOAN
M.Sc., Ph.D.
Sr. Lect., Dept. of Civ. Engrg. and Surveying, Univ. of Newcastle, Australia

SUMMARY This paper examines the drained stability of slopes in cohesive-frictional soil. Plane strain conditions are assumed and active failure is achieved by increasing either the unit weight of the material or the boundary pressure applied at the top surface. Two numerical methods are described which are based on the limit theorems of classical plasticity and a finite element discretisation. These methods give solutions which are rogorous upper and lower bounds on the exact collapse load.In the lower bound procedure, statically admissible stress fields are computed by using an internal linear approximation to the Mohr-Coulomb yield criterion. Conversely, in the upper bound procedure, kinematically admissible velocity fields are computed using an external approximation to the Mohr-Coulomb yield criterion. Both of the methods lead to large linear programming problems. The results show that the true collapse load is bracketted within two reasonable bounds which are tighter than existing analytical solutions.

1. INTRODUCTION

The plane strain slope problem to be considered is shown in Figure 1. The soil is modelled as a Mohr-Coulomb material with a uniform effective cohesion c, friction angle ϕ and unit weight γ . Collapse of the slope may occur in a variety of ways. For a fixed slope height H, collapse may be triggered by increasing either surcharge σ_s or the unit weight γ. The drained stability of the slope is thus conveniently described by the dimensionless load parameters $\gamma H/c$ and σ_s/c.

This paper describes the application of two numerical techniques to yield sharp bounds on $\gamma H/c$ or σ_s/c for drained conditions. The numerical schemes are based on a finite element formulation of the plastic limit theorems and lead to large linear programming problems. Safe estimates for the value of $\gamma H/c$ or σ_s/c may be obtained using the lower bound theorem of classical plasticity which states that any statically admissible stress field will provide a lower bound on the true limit load. Unsafe estimates for the value of $\gamma H/c$ or σ_s/c can be deduced from the upper bound theorem which states that any kinematically admissible velocity field will provide an upper bound on the true limit load. The exact value of $\gamma H/c$ or σ_s/c may thus be bounded from above and below but the bounds must be sufficiently tight to be of practical use.

One of the first to propose the lower bound theorem as a linear programming problem was Lysmer (1). Similar methods have also been described by Anderheggen and Knopfel (2), Bottero et al. (3), Sloan (4) and Assadi and Sloan (5). A key development, due to Pastor (6), was the introduction of extension elements which permit statically admissible stress fields to be extended to semi-infinite domains. Another important improvement, due to Sloan (7), was the development of an active set algorithm, which fully exploits sparsity and uses a steepest edge search to locate the optimal solution rapidly.

One of the earliest investigations of a numerical formulation for the upper bound theorem may be found in Anderheggen and Knopfel (2). Bottero et al. (3) included the effects of

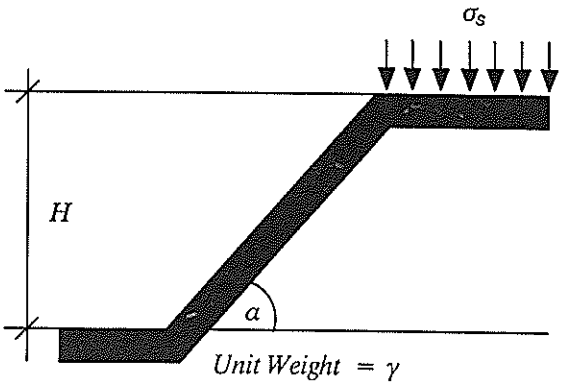

Figure 1 Plane strain slope

velocity discontinuities and applied the method to a variety of soil mechanics problems. Sloan (8) proposed a formulation based on duality theory and used the steepest edge active set algorithm to solve the resulting linear programming problem efficiently. The upper bound method, like the lower bound method, typically leads to very large optimisation problems involving several thousand variables and constraints, and it is essential to exploit the extreme sparsity of the constraint matrix to the full.

2. FINITE ELEMENT FORMULATION OF THE LOWER BOUND THEOREM

2.1 Elements for Lower Bound Limit Analysis

The sign conventions for stresses, with compression taken as positive, are shown in Figure 2. The formulation employs three types of elements as shown in Figure 3. The stresses vary linearly within each element according to

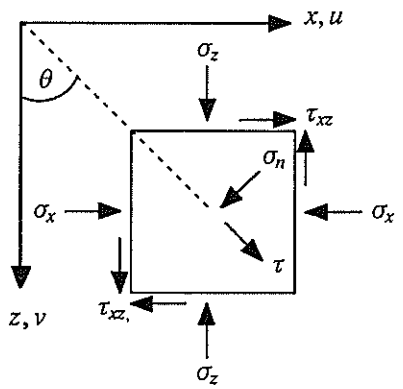

Figure 2 Sign convention for velocities and stresses

$$\sigma_x = \sum_{i=1}^{i=3} N_i \sigma_{xi} \;\; ; \;\; \sigma_z = \sum_{i=1}^{i=3} N_i \sigma_{zi} \;\; ; \;\; \tau_{xz} = \sum_{i=1}^{i=3} N_i \tau_{xzi} \quad (1)$$

where N_i are linear shape functions and σ_{xi}, σ_{zi},τ_{xzi} are the nodal stresses. The triangular and rectangular extension elements, which enable a statically admissible stress field to be extended within a semi-infinite domain, are based on the same linear expansion as the simple three noded triangle.

Stress discontinuities are permitted to occur at all edges that are shared by adjacent elements.

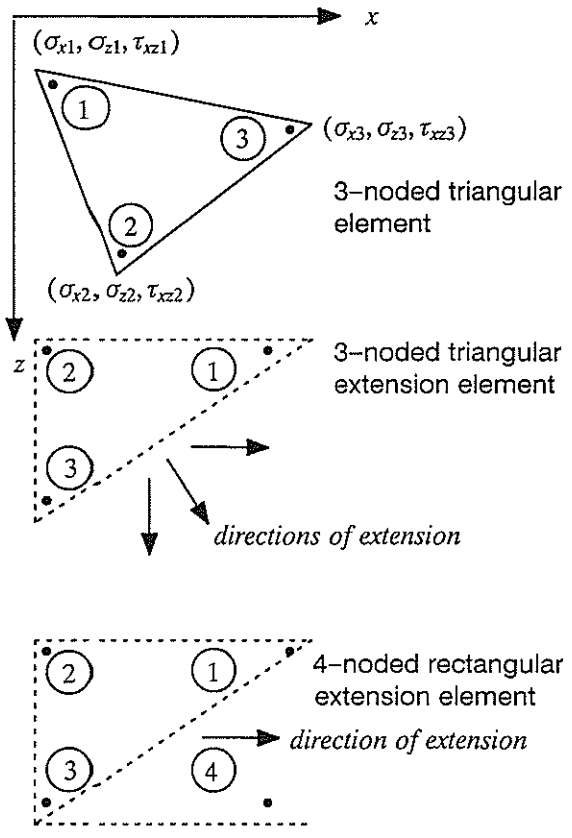

Figure 3 Elements for lower bound limit analysis

2.2 Statically admissible stress field

In order to be statically admissible, and thus provide a rigorous lower bound on the collapse load, the stresses must be in equilibrium, satisfy the stress boundary conditions, and nowhere violate the yield criterion. These conditions are treated as linear constraints which are expressed in terms of the unknown nodal stresses and body forces. The collapse load is described by an objective function which is either a function of the unknown normal boundary stresses or the unknown body forces.

2.3 Equilibrium Conditions

Under plane strain conditions the equilibrium equations may be written as

$$\frac{\partial \sigma_x}{\partial x} + \frac{\partial \tau_{xz}}{\partial z} = 0 \quad ; \quad \frac{\partial \sigma_z}{\partial z} + \frac{\partial \tau_{xz}}{\partial x} = \gamma \quad (2)$$

Differentiating equation (1) and inserting in equation (2), two linear constraints are obtained

$$\mathbf{a}_1 \quad \mathbf{x} \quad = \quad \mathbf{b}_1 \quad (3)$$

with $\mathbf{a}_1$ a constant matrix, $\mathbf{x} = \{\sigma_{x1}, \sigma_{z1}, \tau_{xz1},...,\sigma_{x3}, \sigma_{z3}, \tau_{xz3}\}^T$ and $\mathbf{b}_1 = \{0, \gamma\}^T$.

For each rectangular extension element, three additional linear equalities(one for each component of stress) are necessary to extend the linear stress distribution to the fourth node. These have the matrix form of

$$\mathbf{a}_2 \quad \mathbf{x} \quad = \quad \mathbf{b}_2 \quad (4)$$

where $\mathbf{x} = \{\sigma_{x1}, \sigma_{z1}, \tau_{xz1},...,\sigma_{x4}, \sigma_{z4}, \tau_{xz4}\}^T$ and $\mathbf{b}_2 = \{0,0,0,0\}^T$.

A stress discontinuity is statically admissible if all pairs of nodes on opposite sides of the discontinuity have equal shear and normal stresses. This will give rise to four equality constraints and may be written in terms of the nodal stresses according to

$$\mathbf{a}_3 \quad \mathbf{x} \quad = \quad \mathbf{b}_3 \quad (5)$$

where $\mathbf{a}_3$ is a constant matrix, $\mathbf{x} = \{\sigma_{x1}, \sigma_{z1}, \tau_{xz1},...,\sigma_{x4}, \sigma_{z4}, \tau_{xz4}\}^T$ and $\mathbf{b}_3 = \{0,0,0,0\}^T$.

2.4 Stress Boundary Conditions

The prescribed stress boundary conditions on the external faces of the domain, may be treated as equality constraints on the nodal stresses. If an edge is defined by the nodes (1,2), and the stresses at these nodes are prescribed to be (σ_{n1}, τ_1) and (σ_{n2}, τ_2), then substitution into the stress transformation equations leads to four equality constraints of the form

$$\mathbf{a}_4 \quad \mathbf{x} \quad = \quad \mathbf{b}_4 \quad (6)$$

where
$\mathbf{a}_4$ is a constant matrix, $\mathbf{x} = \{\sigma_{x1}, \sigma_{z1}, \tau_{xz1}, \sigma_{x2}, \sigma_{z2}, \tau_{xz2}\}^T$ and $\mathbf{b}_4 = \{\sigma_{n1}, \tau_1, \sigma_{n2}, \tau_2\}^T$.

Equations (3), (4), (5) and (6) ensure that the stress field satisfies equilibrium and the boundary conditions and the remaining step is to enforce linear constraints to satisfy the yield conditions.

2.5 Internal Linear Approximation to Yield Criterion

Under plane strain loading, the Mohr-Coulomb yield criterion may be written as

$$F = (\sigma_x - \sigma_z)^2 + (2\tau_{xz})^2 - ((\sigma_x + \sigma_z)\sin\phi + 2c\cos\phi)^2 \quad (7)$$

and we require that $F \leq 0$.

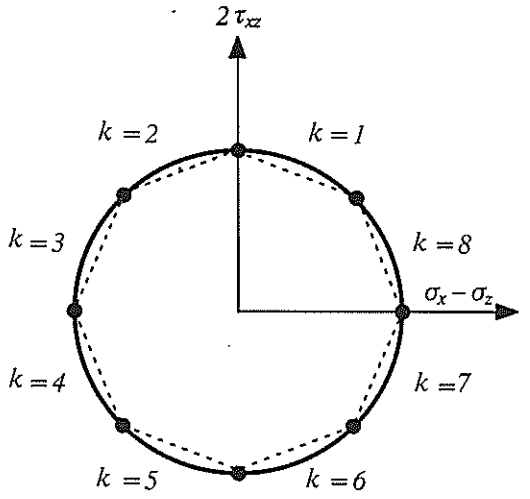

Figure 4 Internal linearization of Mohr-Coulomb yield criterion

In terms of the quantities $(\sigma_x - \sigma_z)$ and $2\tau_{xz}$, this function plots as a circle of radius $((\sigma_x+\sigma_z)\sin\phi+2c\cos\phi)$ as shown in figure 4. Since this type of constraint is nonlinear, it is replaced by an inscribed polygon with p sides of equal length. With reference to Figure 4, which shows an eight-sided approximation, the linearised yield criterion is given by

$$F_k = A_k\sigma_x + B_k\sigma_z + C_k\tau_{xz} - 2c\cos\phi\cos(\pi/p) \leq 0 \quad (8)$$

where
$A_k = \cos(2\pi k/p) - \sin\phi\cos(\pi/p), B_k = -\cos(2\pi k/p) - \sin\phi\cos(\pi/p), C_k = 2\sin(2\pi k/p)$ and k ranges from 1 to p. The above equation needs to be enforced at each node of each triangular element. For each rectangular extension element the inequality constraints $F_{k1} \leq F_{k2}$, $F_{k2} \leq 0$ and $F_{k3} \leq 0$ have to be imposed. In each three-noded triangular extension element we need to apply the constraints $F_{k1} \leq F_{k2}$, $F_{k3} \leq F_{k2}$ and $F_{k2} \leq 0$. In general terms, the linearised yield criterion generates inequalities of the form

$$\mathbf{a}_5 \quad \mathbf{x} \quad \leq \quad \mathbf{b}_5 \quad (9)$$

where $\mathbf{a}_5$ is comprised of the coefficients A_k, B_k, C_k, $\mathbf{x} = \{\sigma_{xi}, \sigma_{zi}, \tau_{xzi}\}^T$ and $\mathbf{b}_5 = 2c\cos\phi\cos(\pi/p)\{1, 1, ..., 1\}^T$.

2.6 Objective Function

To isolate the particular stress field which optimises the collapse load, an objective function has to be defined. The objective function can be expressed as an integral of the form

$$Q = \int_s \sigma_n ds \quad (10)$$

where Q is the collapse load per unit thickness and σ_n is the normal stress acting over some part of the external boundary. For each segment on the boundary, we have

$$Q = (L/2)(\sigma_{n1} + \sigma_{n2}) \quad (11)$$

where L is the length of the segment and $(\sigma_{n1}, \sigma_{n2})$ are the normal stresses at each of its ends. Q may be expressed in terms of the cartesian nodal stresses of Figure 2 according to

$$Q \quad = \quad \mathbf{c}^T \quad \mathbf{x} \quad (12)$$

where the coefficients c are functions of the length and orientation of the boundary edge, and $\mathbf{x} = \{\sigma_{x1}, \sigma_{z1}, \tau_{xz1}, \sigma_{x2}, \sigma_{z2}, \tau_{xz2}\}^T$.

2.7 Computation of Lower Bound Collapse Load

Once the various coefficients are assembled, the problem of finding a statically admissible stress field, which maximises the collapse load over a specified area, may be written as

$$\begin{aligned} &\textit{Minimise} && -\mathbf{C}^T\mathbf{X} \\ &\textit{Subject to} && \mathbf{A}_1\mathbf{X} = \mathbf{B}_1 \\ & && \mathbf{A}_2\mathbf{X} = \mathbf{B}_2 \\ & && \mathbf{A}_3\mathbf{X} = \mathbf{B}_3 \\ & && \mathbf{A}_4\mathbf{X} = \mathbf{B}_4 \\ & && \mathbf{A}_5\mathbf{X} \leq \mathbf{B}_5 \end{aligned} \quad (13)$$

where $\mathbf{X}$ is the global vector of unknown stresses and $\mathbf{C}^T\mathbf{X}$ corresponds to the collapse load.

3. FINITE ELEMENT FORMULATION OF THE UPPER BOUND THEOREM

3.1 Elements for Upper Bound Limit Analysis

The triangular element which is used to model the velocity field is shown in Figure 5. The velocities vary linearly within each element according to

$$u = \sum_{i=1}^{i=3} N_i u_i \quad ; \quad v = \sum_{i=1}^{i=3} N_i v_i \quad (14)$$

where N_i are linear shape functions and (u_i, v_i) are the nodal velocities in the x and z directions respectively. A kinematically admissible velocity field must satisfy the flow rule and the velocity boundary conditions.

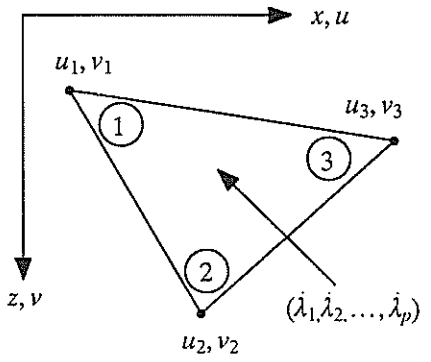

Figure 5 Element for upper bound limit analysis

3.2 Flow Rule Equations

For plane strain deformation, the flow rule equations are given by

$$\dot{\varepsilon}_x = \dot{\lambda}\frac{\partial F}{\partial \sigma_x} \; ; \; \dot{\varepsilon}_z = \dot{\lambda}\frac{\partial F}{\partial \sigma_z} \; ; \; \dot{\gamma}_{xz} = \dot{\lambda}\frac{\partial F}{\partial \tau_{xz}} \qquad (15)$$

where $\dot{\lambda} \geq 0$ is a plastic multiplier rate and compressive strains are taken as positive.

To remove the stress terms from the flow rule equations, and thus provide a linear relationship between the unknown velocities and plastic multiplier rates, an external linear approximation to the Mohr-Coulomb yield criterion is needed.

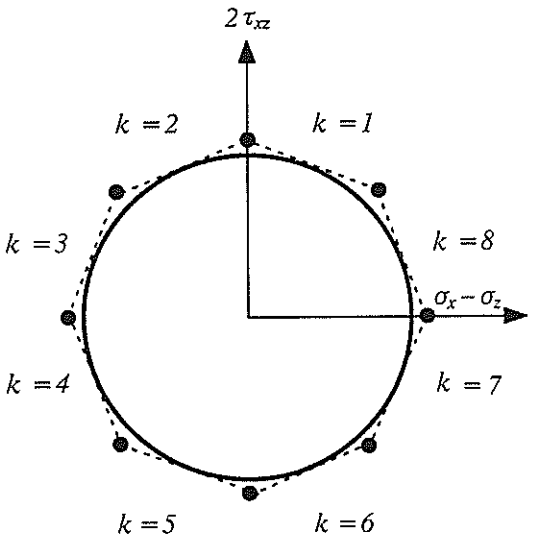

Figure 6 External linearization of Mohr–Coulomb yield criterion

3.3 External Linear Approximation to Yield Criterion

An eight-sided approximation is shown in Figure 6. This polygon has p sides of equal length and the linearised yield condition may be written as

$$F_k = A_k\sigma_x + B_k\sigma_z + C_k\tau_{xz} - 2c\cos\phi = 0 \qquad (16)$$

where
$A_k = \cos(2\pi k/p) - \sin\phi$, $B_k = -\cos(2\pi k/p) - \sin\phi$, $C_k = 2\sin(2\pi k/p)$ and k ranges from 1 to p. Differentiating equation (14) and using equations (15) and (16) furnishes the flow rule equations as

$$\begin{aligned}
&\sum_{i=1}^{i=3}\frac{\partial N_i}{\partial x}u_i + \sum_{k=1}^{k=p}\dot{\lambda}_k A_k = 0 \\
&\sum_{i=1}^{i=3}\frac{\partial N_i}{\partial z}v_i + \sum_{k=1}^{k=p}\dot{\lambda}_k B_k = 0 \quad \dot{\lambda}_k \geq 0 \qquad (17)\\
&\sum_{i=1}^{i=3}\frac{\partial N_i}{\partial x}v_i + \sum_{i=1}^{i=3}\frac{\partial N_i}{\partial z}u_i + \sum_{k=1}^{k=p}\dot{\lambda}_k C_k = 0
\end{aligned}$$

These relations may be expressed in the general form of

$$\mathbf{a}_{11}\mathbf{x}_1 + \mathbf{a}_{12}\mathbf{x}_2 \;=\; \mathbf{b}_1 \qquad (18)$$

where $\mathbf{a}_{11}$ and $\mathbf{a}_{12}$ are matrices of constants, $\mathbf{b}_1 = \{0,0,0\}^T$, $\mathbf{x}_1 = \{u_1, v_1, u_2, v_2, u_3, v_3\}^T$, and $\mathbf{x}_2 = \{\dot{\lambda}_1, ..., \dot{\lambda}_p\}^T$.

3.4 Velocity Discontinuity

For each velocity discontinuity one inequality constraint is required to ensure that the power dissipated along the discontinuity is nonnegative. The sign of each discontinuity,s, refers to the sense of the tangential jump in the velocity, u_t, and is defined so that $\mid u_t \mid = su_t$, where $s = \pm 1$ and is specified as data. The constraint $su_t \geq 0$, may be written as

$$\mathbf{a}_2 \;\; \mathbf{x}_1 \;\; \leq \;\; \mathbf{b}_2 \qquad (19)$$

where $\mathbf{a}_2$ is a function of the discontinuity orientation and direction of sliding s, $\mathbf{x}_1 = \{u_1, v_1, u_2, v_2\}^T$ and $\mathbf{b}_2 = 0$.

To satisfy the flow rule condition in a discontinuity an equality constraint is enforced to ensure that the angle between the discontinuity and the direction of the velocity jump is equal to ϕ. This may be expressed as

$$\mathbf{a}_3 \;\; \mathbf{x}_1 \;\; = \;\; \mathbf{b}_3 \qquad (20)$$

in which $\mathbf{a}_3$ is a function of the discontinuity orientation, direction of sliding and ϕ, $\mathbf{x}_1 = \{u_1, v_1, u_2, v_2\}^T$ and $\mathbf{b}_3 = 0$.

3.5 Velocity Boundary Conditions

The boundary conditions on the velocities give rise to constraints of the general form

$$\mathbf{a}_4 \;\; \mathbf{x}_1 \;\; = \;\; \mathbf{b}_4 \qquad (21)$$

where $\mathbf{a}_4$ is a matrix of constants, $\mathbf{x}_1 = \{u_i, v_i\}^T$ for node i and $\mathbf{b}_4$ is a vector of prescribed values.

3.6 Computation of Upper Bound Collapse Load

Once the various coefficients are assembled the problem of finding a kinematically admissible velocity field, which minimises the total dissipated power, may be expressed as

$$\begin{aligned}
&\textit{Minimise} && \mathbf{C}_1^T\,\mathbf{X}_1 + \mathbf{C}_2^T\,\mathbf{X}_2 \\
&\textit{Subject to} && \mathbf{A}_{11}\,\mathbf{X}_1 + \mathbf{A}_{12}\,\mathbf{X}_2 = \mathbf{B}_1 \\
& && \mathbf{A}_2\,\mathbf{X}_1 \leq \mathbf{B}_2 \\
& && \mathbf{A}_3\,\mathbf{X}_1 = \mathbf{B}_3 \\
& && \mathbf{A}_4\,\mathbf{X}_1 = \mathbf{B}_4 \\
& && \mathbf{X}_2 \geq 0
\end{aligned} \qquad (22)$$

where $\mathbf{X}_1$ is the global vector of unknown velocities, $\mathbf{X}_2$ is the global vector of unknown plastic multiplier rates, $\mathbf{C}_1^T\,\mathbf{X}_1$ is the power dissipated by plastic shearing in the velocity discontinuities, and $\mathbf{C}_2^T\,\mathbf{X}_2$ is the power dissipated by plastic deformation in the triangles. A detailed analysis of various strategies for solving this type of optimisation problem efficiently may be found in Sloan (8). We note in passing that equation (22) may be solved very efficiently by applying the steepest edge active set algorithm to its dual.

4. RESULTS

A typical lower bound mesh, for $\alpha = 45$, $\sigma_s/c = 0$ and $\phi = 20$ is shown in Figure 7. The grid has 1170 nodes, 356 triangles, 2 triangular extension elements, 24 rectangular extension elements and 562 stress discontinuities and was

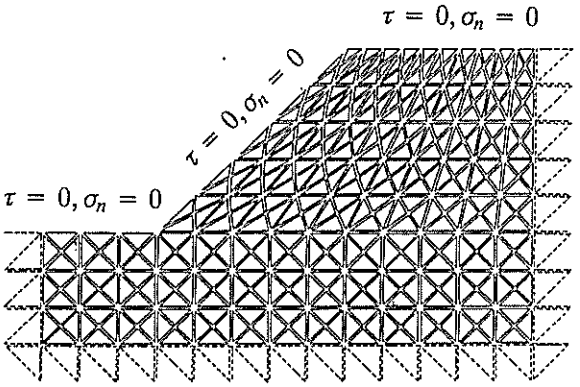

Figure 7 Lower bound mesh for nonvertical slope with $\alpha = 45$, $\sigma_s/c = 0$ and $\phi = 20$

adopted after experimenting with a wide variety of arrangements. The configuration of the extension elements ensures that the stress field can be extended throughout the semi-infinite domain of the problem, without violating equilibrium, the stress boundary conditions or the yield criterion, and thus provides a rigorous lower bound on the collapse load. To perform the lower bound computation, we first prescribe values for H, α,σ_s,c, and ϕ and then solve equation (13) to find a statically admissible stress field which maximises a uniform unit weight for the slope. For a 12-sided approximation to the Mohr-Coulomb yield surface, the mesh of Figure 7 gives a lower bound of $\gamma H/c = 15.74$.

A typical upper bound mesh, also for the case of $\alpha = 45$, $\sigma_s/c = 0$ and $\phi = 20$ is shown in Figure 8. The grid has two vertical and two horizontal discontinuities and the boundary conditions are as shown. Overall, there are 391 nodes and 620 triangles. To compute an upper bound for $\gamma H/c$, we first select values for H, α,σ_s,c, and ϕ and then solve equation (22) to find a kinematically admissible velocity field which minimises a uniform unit weight for the section. For the mesh of Figure 8, with a 12-sided approximation to the yield surface and the same properties as before, the upper bound method furnishes a value for $\gamma H/c$ of 18.30.

Figure 9 shows the stability bounds for a slope with $\alpha = 45$ and $\phi = 0$ in which two extreme points on each bound have been connected by a straight line.

Figures 10 and 11 illustrate a complete summary of the stability bounds for $\alpha = 90$ and a range of ϕ from 0 to 50.

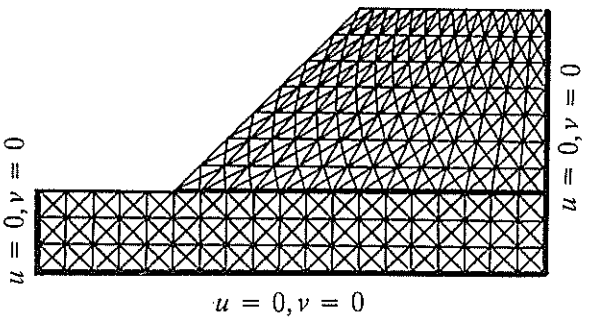

Figure 8 Upper bound mesh for nonvertical slope with $\alpha = 45$, $\sigma_s/c = 0$ and $\phi = 20$

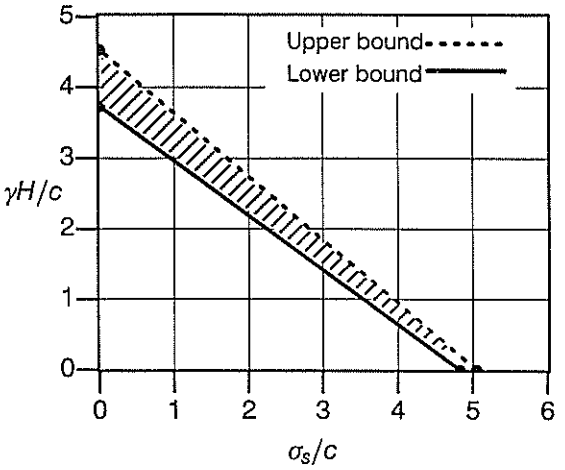

Figure 9 Stability bounds for nonvertical slope problem with $\alpha = 45$ and $\phi = 0$

5. CONCLUSIONS

The drained stability of a slope, under conditions of plane strain, has been investigated. Rigorous bounds on $\gamma H/c$ and σ_s/c using numerical formulation of the limit theorems, have enabled the exact solution to be bracketted within quite close bounds for a range of slope geometries.

6. ACKNOWLEDGEMENTS

The research reported in this paper is funded by a grant from the Australian Research Council. The authors are thankful for this support.

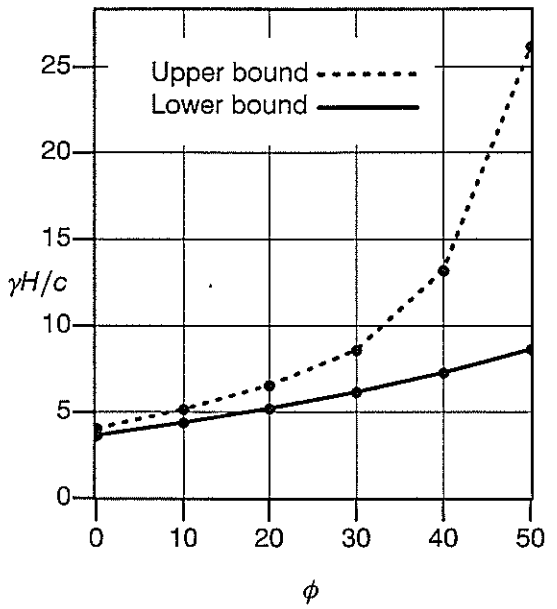

Figure 10 Stability bounds for vertical slope with $\sigma_s/c = 0$

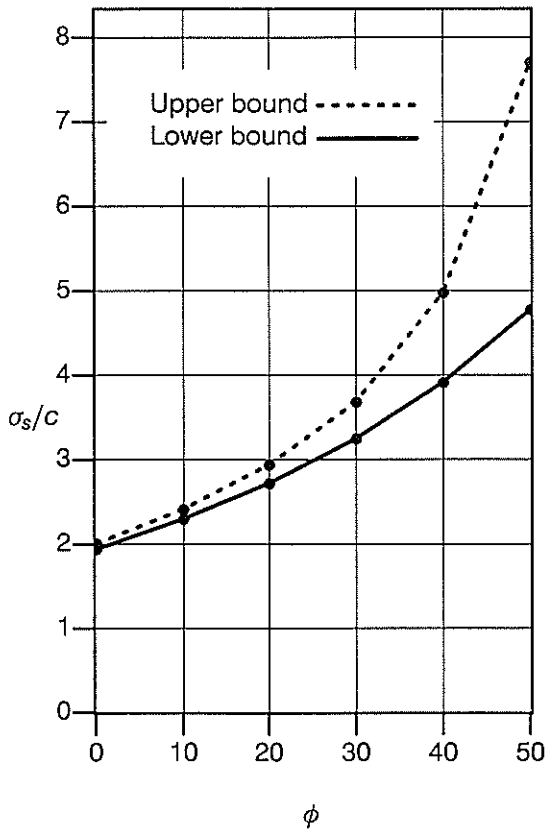

Figure 11 Stability bounds for vertical slope with $\gamma H/c = 0$

7. REFERENCES

1. Lysmer,J. "Limit Analysis of Plane problems in Soil Mechanics", Journal of Soil Mechanics and Foundation Division,A.S.C.E.,Vol. 96,SM4,1311-1334, 1970.

2. Anderheggen,E.,Knopfel,H. "Finite Element Limit Analysis Using Linear Programming", International Journal of Solids and Structures,No. 8, 1413-1431, 1972.

3. Bottero,A.,Negre,R.,Pastor,J.,Turgeman,S. "Finite Element Method and Limit Analysis Theory for Soil Mechanics Problems", Computer Methods in Applied Mechanics and Engineering,No. 22, 131-149, 1980.

4. Sloan,S.W. "Lower Bound Limit Analysis Using Finite Elements and Linear Programming", International Journal for Numerical and Analytical Methods in Geomechanics, No. 12, 61-77, 1988.

5. Assadi,A.,Sloan,S.W. "Undrained Stability of A Shallow Square Tunnel", Journal of Geotechnical Engineering A.S.C.E., Vol. 117, No. 8, 1152-1173, 1991.

6. Pastor,J. "Limit Analysis :Numerical Determination of Complete Statical Solutions-Application to Vertical Cut", Journal de Mechanique Appliquee(in French),No. 2, 167-196, 1978.

7. Sloan,S.W. " A Steepest Edge Active Set Algorithm for Solving Sparse Linear Programming Problems", International Journal for Numerical Methods in Engineering, No. 26, 2671-2685, 1988.

8. Sloan,S.W. "Upper Bound Limit Analysis Using Finite Elements and Linear Programming", International Journal for Numerical and Analytical Methods in Geomechanics, No. 13, 263-282.

Numerical Simulation of the Time-Dependent Stratified Viscoelastic Soil Medium with Cracks

B.B. BUDKOWSKA
M.S.C.E., Ph.D.
Associate Professor of Civil and Environmental Engineering Department, University of Windsor, Ontario, Canada
W. GRZESIAK
M.S.C.E., Ph.D.
Assistant Professor, Civil Engineering Department, Gdansk Technical University, Poland

SUMMARY The paper contains the numerical analysis of viscoelastic stratified half space with cracks filled out by air. The cracks are of different type, size and location. The employed constitutive model assumes the proportionality relationship between the spherical components of stress and strain tensor and viscoelasticity law between deviators. With respect to time variables the recurrent integral method is applied, while with respect to spatial variables – the finite element is employed.
In order to analyze the effect of cracks on the displacement and stress field, the computer program was prepared and some numerical examples are investigated. The conclusions connected with risk induced by the variably located cracks are drawn on the basis of numerical results.

1. INTRODUCTION

It is well known fact, that granular materials like soil exhibit time dependent behaviour. This property can be analyzed in the scope of the theory of viscoelasticity. The most common way of the investigation of the temporal properties of the medium is through the application of the time dependent material characteristics like Young modulus E, bulk modulus K or shear modulus G.
In this paper the viscoelastic homogeneous and nonhomogeneous half space of layered type with cracks are subjected to the analysis. The applied load is uniformly distributed over the circular area and simulates the load transferred by the wheel of the heavy vehicle.

2. FORMULATION OF THE PROBLEM

We will consider the nonhomogeneous medium of layered type with cracks filled by air. Each layer of the medium is assumed to be isotropic. This fact enables one to split the stress–strain relationship into two independent parts, that is volumetric and deviatoric. It is commonly recognized fact in analysis of granular materials to relate the spherical components of stress–strain tensor to the proportionality law. Mathematically, it can be expressed as:

$$\sigma_{kk} = 3K\epsilon_{kk} \qquad (1)$$

where
K –is the bulk modulus,
σ_{kk}, ϵ_{kk} –stand for spherical components of stress and strain tensor respectively.

In the paper, it is assumed that the bulk modulus is constant. The time dependent properties of the medium are connected to the deviatoric components of stress and strain tensor. At the constitutive level the integral approach available in the framework of the theory of viscoelasticity is employed. Thus the following type of relationship between deviators is taken to the analysis:

$$t_{ij}(t) = \int_0^t E_1\,(t-\tau)\,\dot{e}_{ij}\,(\tau)\,d\tau \qquad (2)$$

where
t_{ij}, $\dot{e}_{ij}$ –are the stress and strain rate deviator tensors respectively,
E_1 –denotes the relaxation function.

Dot over e_{ij} means the differentiation with respect to time. It is assumed, that time dependent behaviour of granular materials [1,2,3,5,6,8] will be simulated by means of the three parametric standard model. In consequence the explicit form of the relaxation described by eq. (2) is taken as:

$$t_{ij}(t) = 2\{[E_L + (E_S - E_L)e^{-\beta t}]e_{ij}(0) + \int_0^t (E_L + (E_S - E_L)e^{-\beta(t-\tau)}\,\dot{e}_{ij}(\tau)d\tau] \qquad (3)$$

where the meaning of E_L and E_S is indicated in Fig. 1 and β is the inverse of the retardation time.
The function which appears in equation (3) is the relaxation function and according to the definition represents the time dependent stress induced by uniformly applied state of deformation. The inverted relation to the equation (3) gives the creep function.

$$e_{ij}(t) = \frac{1}{2E_L} + [\frac{1}{2E_S} - \frac{1}{2E_L}]e^{\beta \frac{E_L}{E_S} t}\,t_{ij}(0) + \int_0^t (\frac{1}{2E_L} + (\frac{1}{2E_S} + \frac{1}{2E_L})e^{\beta \frac{E_L}{E_S}(t-\tau)}\dot{t}_{ij}(0)d\tau \qquad (4)$$

where $J_1(t)$ shown in Fig. 1 is the creep function which

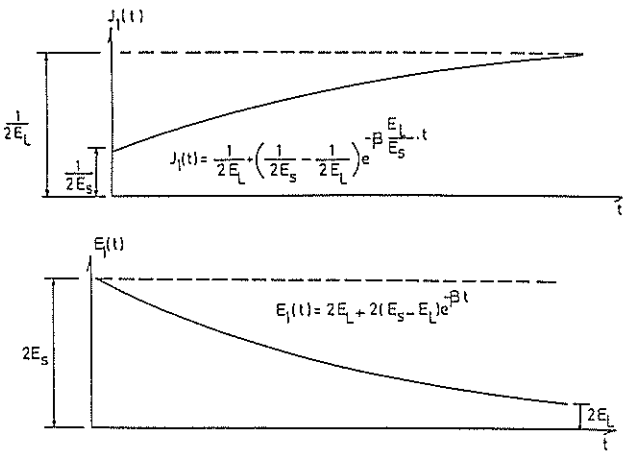

Fig. 1. Creep and relaxation function for the applied model

by definition describes the time dependent deformation induced by the uniformly applied state of stress. In analogy to the theory of elasticity, the relations (2) and (3) involve the time dependent shear modulus, while the temporal function of equation (4) represents the compliance of shear modulus. The analyzed functions connected with the applied model are shown in Fig. 1.

From Fig. 1, it is seen, that constitutive model has finite value of shear modulus at t = + 0 and decreases to finite value at t = infinity. It means that the applied model preserves finite value of stress never reaching zero. The analysis of deformation reveals, that with elapsing time, the deformation tends to the finite, stable value. Consequently, it means that the applied model involved to the behaviour of deviatoric stress–strain components has features of solid.
Combining the equation (1) with (3), after some regrouping, the following constitutive equation is used to the further analysis.

$$\sigma_{ij}(t) = K\,\epsilon_{kk}\,\delta_{ij} + 2\{[E_L + (E_S - E_L)\,e^{-\beta t}]e_{ij}(0) + \int_0^t [E_L + (E_S - E_L)e^{-\beta(t-\tau)}]\dot{e}_{ij}(\tau)\,d\tau\} \quad (5)$$

where
δ_{ij} –is the Kronecker symbol,
σ_{ij} –stands for the stress components.

3. THE DISCRETE FORM OF THE TEMPORAL BEHAVIOUR OF THE MODEL

Since the time dependent relationship is connected with the deviators of stress and strain, we will refer to the equation (3), which for arbitrary time instant t_n is written as follows:

$$t_{ij}(t_n) = 2[E_L\,e_{ij}(t_n) + (E_S - E_L)e^{-\beta t_n}\,e_{ij}(0) + \int_0^{t_n} (E_S - E_L)e^{-\beta(t_n-\tau)}\dot{e}_{ij}(\tau)\,d\tau] \quad (6)$$

According to recurrent formulation, assuming the correctness of the relationship (6) – the analogous relation for the next time instant t_{n+1} has the form:

$$t_{ij}(t_{n+1}) = 2\{[E_L\,e_{ij}(t_{n+1}) + (E_S - E_L)e^{-\beta t_{n+1}}\,e_{ij}(0) + \int_0^{t_n} (E_S - E_L)e^{-\beta(t_{n+1}-\tau)}\dot{e}_{ij}(\tau)\,d\tau\}\,d\tau \quad (7)$$

where t_{n+1} is translated by Δt with respect to the time instant t_n.

Comparing the relationships (6) and (7), we wish to formulate the temporally discrete formula for arbitrary time instant which involves:
a) previous time instant,
b) current time instant,
c) increment of time.

Thus, after some regrouping, the equation (7) can be written as follows:

$$t_{ij}(t_{n+1}) = 2\{E_L\,e_{ij}(t_{n+1}) + e^{-\beta\Delta t}[e_{ij}(0)(E_S - E_L)e^{-\beta t_n} + \int_0^{t_n} (E_S - E_L)e^{-\beta(t_n-\tau)}\,\dot{e}_{ij}(\tau)d\tau] + \int_{t_n}^{t_{n+1}} (E_S - E_L)e^{-\beta(t_{n+1}-\tau)}\,\dot{e}_{ij}(\tau)\,d\tau\} \quad (8)$$

It is worth to notice, that the last integral has finite value and is equal to:

$$\Delta I_n = (E_S - E_L)\,\frac{1 - e^{-\beta\Delta t}}{\beta(t_{n+1} - t_n)}\,[e_{ij}(t_{n+1}) - e_{ij}(t_n)]$$

The glance at the equation (8) enables one to notice terms which have some physical interpretation. Namely, the first term represents the current deformation, the second one contained within square bracket denotes the history of deformation, and the last term of finite value defines the increment of history of deformation.

The first integral from zero to t_{n+1} can be precisely evaluated on the basis of formula (8) in the following way:

$$t_{ij}(t_{n+1}) = 2[E_L\,e_{ij}(t_{n+1}) + I_{n+1}] \quad (9)$$

where

$$I_{n+1} = e^{-\beta\Delta t}\,I_n + \Delta I_n \quad (10)$$

The above described algorithm combined with equation (1), gives the following formula which constitutes the discrete form of the applied constitutive equation.

$$\sigma_{ij}(t_{n+1}) = \sigma_{kk}\,K\,\delta_{ij} + 2\{E_L\,e_{ij}(t_{n+1}) + (E_S - E_L)\,\frac{1 - e^{-\beta\Delta t}}{\beta(t_{n+1} - t_n)}\,(e_{ij}(t_{n+1}) - e_{ij}(t_n) + e^{-\beta\Delta t}\,(e_{ij}(0)(E_S - E_L)e^{-\beta t_n} + \int_0^{t_n} (E_S - E_L)e^{-\beta(t_n-\tau)}\dot{e}_{ij}(\tau)\,d\tau\} \quad (11)$$

4. NUMERICAL FORMULATION WITH RESPECT TO SPATIAL VARIABLES

To analyze the described problem with respect to spatial variables the finite element method (FEM) is implemented [4,7,9]. Combination of the recurrent integral method with respect to temporal variables and FEM with respect to spatial variables leads to the following discrete matrix equation valid for arbitrary type of the finite element:

$$\{[K]^E + [K]^V\,[E_L + (E_S - E_L)\,\frac{1 - e^{-\beta\Delta t}}{\beta(t_{n+1} - t_n)}]\}\{V_{n+1}\} = \{P_{n+1}\} - [K]^V\{e^{-\beta\Delta t}\,I_n + (E_S - E_L)\,\frac{1 - e^{-\beta\Delta t}}{\beta(t_{n+1} - t_n)}\}\{V_n\} \quad (12)$$

where
$[K]^E$, $[K]^V$ –are the stiffness matrices connected with elastic and viscous properties respectively,
$\{V_{n+1}\}$, $\{V_n\}$ –are the displacement vectors related to t_{n+1} and t_n time instants respectively.

After determination of the displacement field, the stress components are computed in accordance with the following formula:

$$\sigma(t_{n+1}) = [D]^E\,[B]\,\{V_{n+1}\} + [D]^V\,[B]\,[E_L\{V_{n+1}\} + e^{-\beta\Delta t}I_n + (E_S - E_L)\,\frac{1 - e^{-\beta\Delta t}}{\beta(t_{n+1} - t_n)}\,[\{V_{n+1}\} - \{V_n\}]] \quad (13)$$

where

$[D]^E$, $[D]^V$ – are the material matrices connected with elastic and viscous properties respectively,
$[B]$ – stands for the deformation matrix.

5. NUMERICAL EXAMPLES

The described constitutive model which employs with respect to time variables the recurrent integral method and with respect to spatial variables the FEM is used in the analysis of some problems of practical importance.

The geometry, boundary conditions, location of cracks are shown in Fig. 2. The finite element mesh consists of the eight noded isoparametric quadrilateral elements.

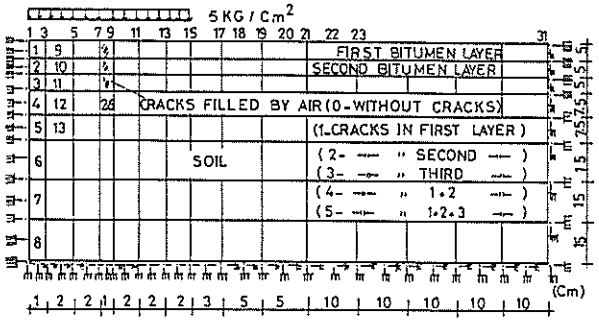

Fig. 2. Geometry, finite element mesh, load and boundary conditions.

The time dependent analysis involves also two special cases, that is the time instant $t = +0$ and $t =$ infinity. Regarding the effect of the location of the cracks on the temporal displacement and stress fields the following cases are analyzed:

1) –homogeneous medium with cracks of different location (notation of schemes 4H0 and 8H0),

2) –homogeneous medium with cracks of different location (notation of schemes 8H1 ÷ 8H5),

3) –nonhomogeneous medium of layered type without cracks (one layer of bitumen and soil – notation of schemes – 8N0),

4) –nonhomogeneous medium of layered type with cracks (one layer of bitumen and soil – notation of schemes 8NS1 ÷ 8NS5),

5) –nonhomogenous medium of layered type without cracks (double layer of bitumen and soil – notation of schemes 8N0D)

6) –nonhomogeneous medium of layered type with cracks (double layer of bitumen and soil – notation of schemes – 8ND1 ÷ 8ND5)

The first number in the notation of schemes defines the number of nodes connected with the FE used in the analysis. The location of the cracks in the scheme is denoted by the last number in the notation of schemes. That is: single crack in the top layer – as 1, single crack in the second layer (from the top) – as 2, single crack in the third layer – as 3, double crack, in the top two layers – as 4, the triple crack in the top three layers – as 5. The location of the cracks is indicated in Fig. 2. For all cases described above, the common value of the time step $\Delta t = 100$ is used in numerical computations.
In order to compare the accuracy of the results, the four noded isoparametric element is used. The comparative investigations are done for the homogeneous medium in the absence of cracks and in presence of cracks. The obtained results in terms of the displacement and stress fields almost coincide. Some of the results in terms of the temporal displacement field are presented in Figs. (3 ÷ 10). The comparison of the displacements for different media for the first and the tenth time steps are shown in Fig. 11. The temporal diagrams of stresses for different analyzed cases are shown in Figs. (12 ÷ 14). The temporal variability of stress components is computed for the element denoted as 28 located at the tip of the crack (below the crack).

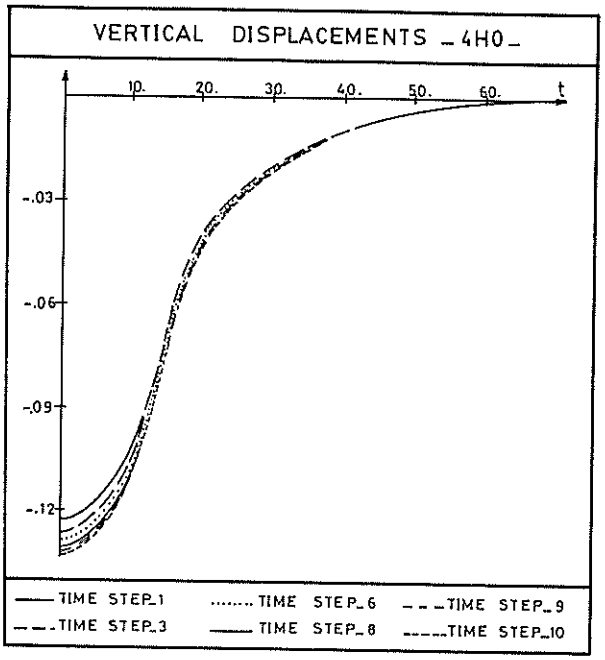

Fig. 3. The vertical displacements for the homogeneous medium without cracks for indicated time steps (4 noded FE).

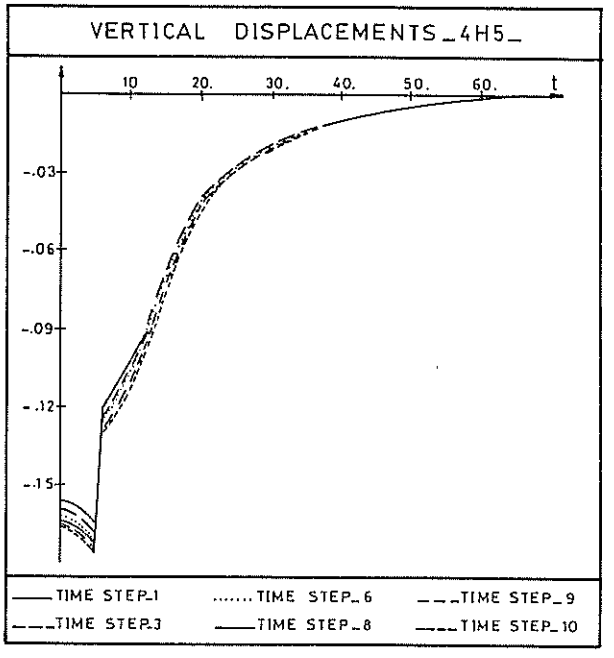

Fig. 4. The vertical displacements for the homogeneous medium with cracks located in top three layers for indicated time steps (4 noded FE).

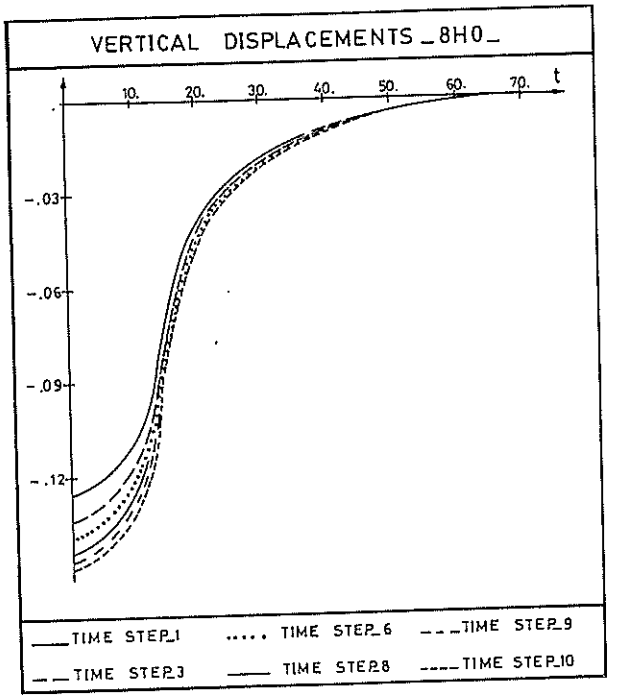

Fig. 5. The vertical displacements of homogeneous medium without cracks for indicated time steps (8 noded FE).

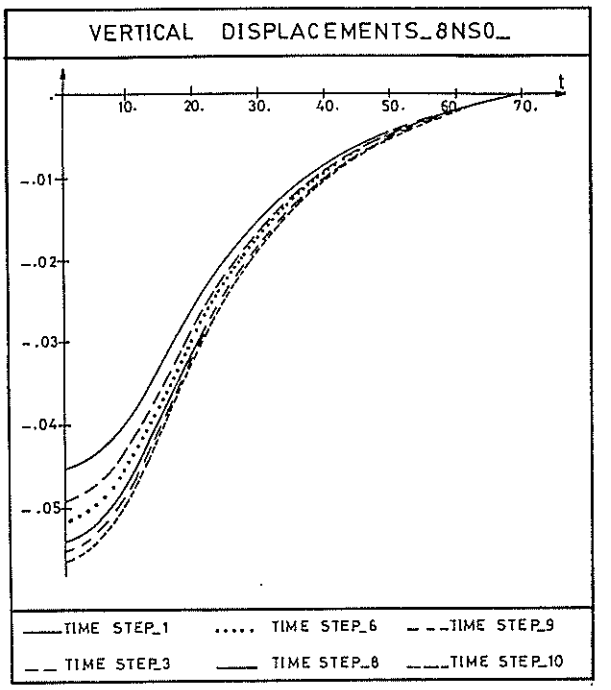

Fig. 7. The vertical displacements for nonhomogeneous medium (one layer of bitumen and soil) without cracks for indicated time steps (8 noded FE).

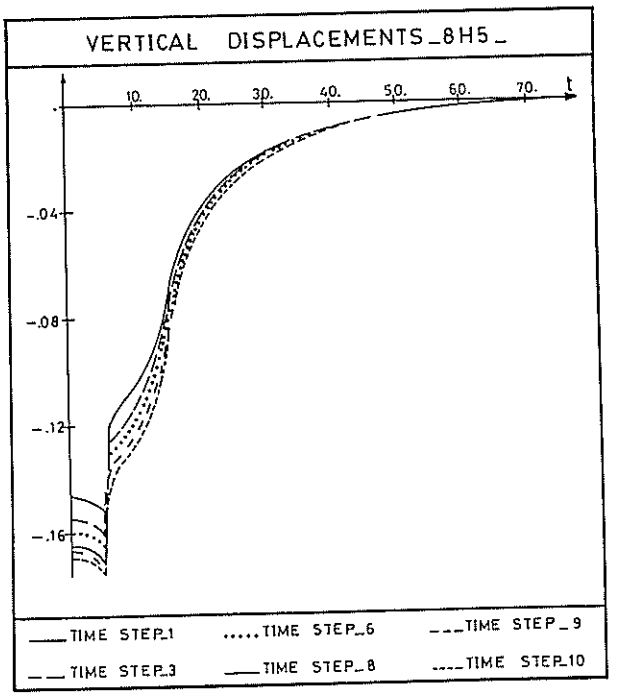

Fig. 6. The vertical displacements of homogeneous medium with cracks located in the top three layers for indicated time steps (8 noded FE).

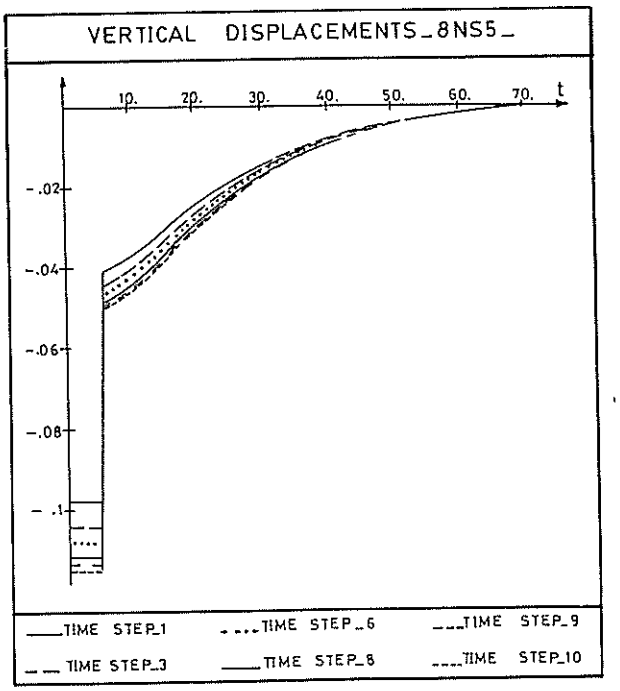

Fig. 8. The vertical displacements for nonhomogeneous medium (one layer of bitumen and soil) with cracks in the top three layers for indicated time steps (8 noded FE).

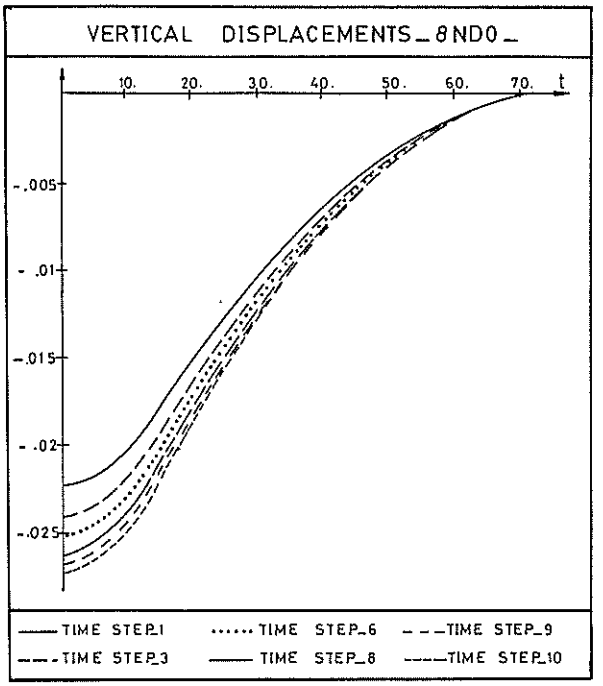

Fig. 9. The vertical displacements for nonhomogeneous medium (two layer of bitumen and soil) without cracks for indicated time steps (8 noded FE).

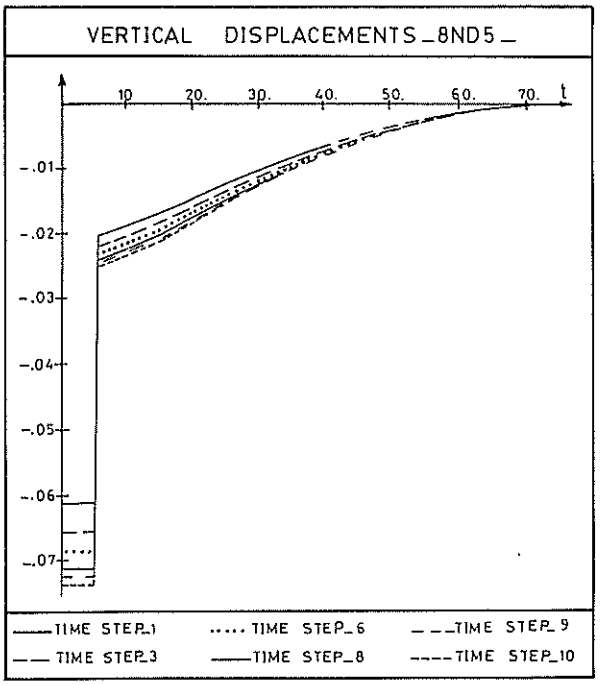

Fig. 10. The vertical displacements for nonhomogeneous medium (two layers of bitumen and soil) with cracks in the top three layers for indicated time steps (8 noded FE).

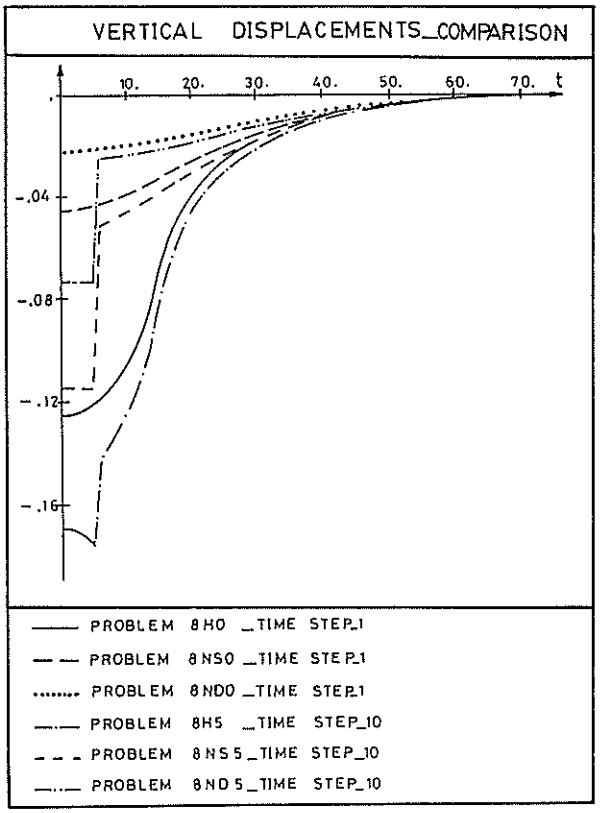

Fig. 11. The comparative distributions o vertical displacements for indicate time steps (8 noded FE).

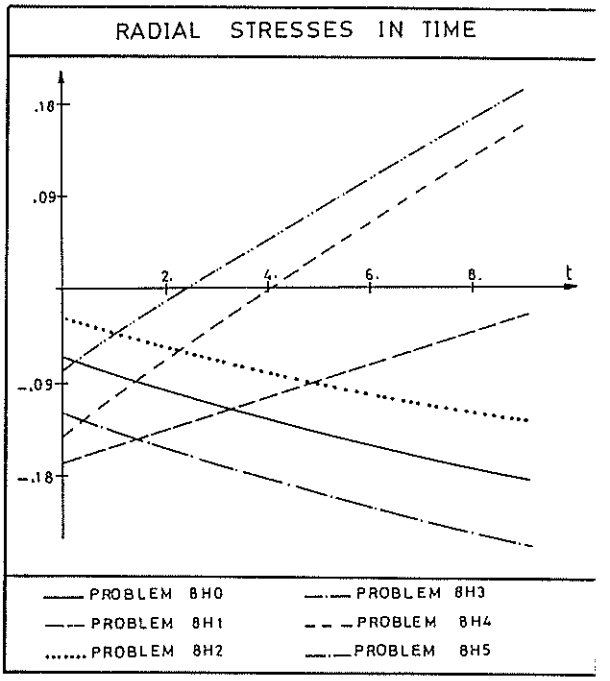

Fig. 12. The temporal radial stress distributio for indicated cases of the analysi (el.nr. 28, 8 noded FE - middl Gaussian point).

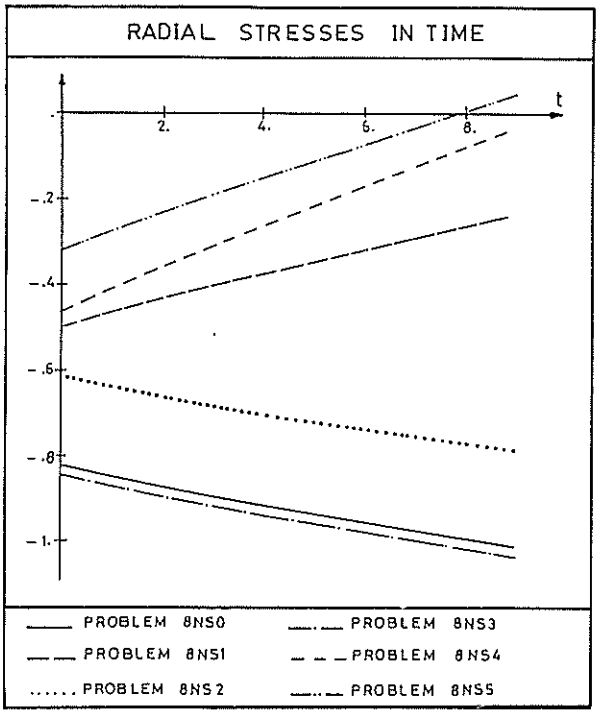

Fig. 13. The temporal radial stress distribution for indicated cases of the analysis (el.nr.28, 8 noded FE – middle Gaussian point).

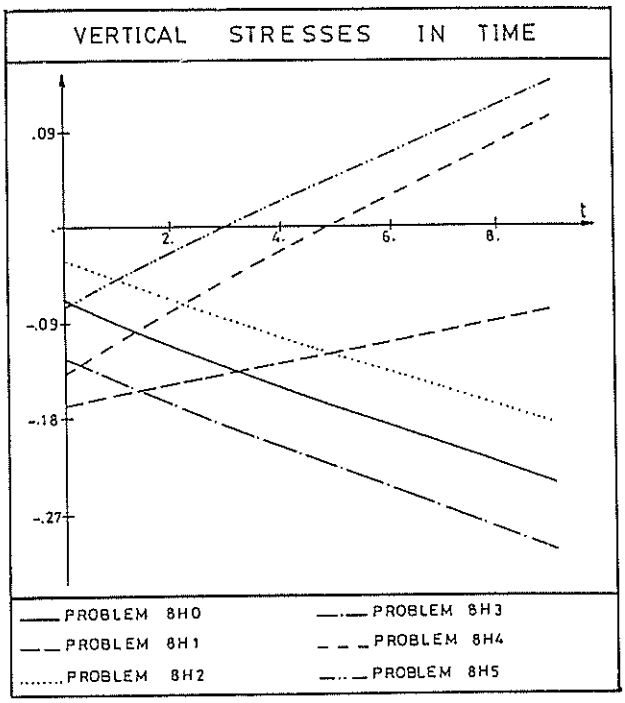

Fig. 14. The temporal vertical stress distribution for indicated cases of the analysis (el.nr.28, 8 noded FE – middle Gaussian point).

6. CONCLUSIONS AND FINAL REMARKS

In the paper the viscoelastic homogeneous and nonhomogeneous medium with variably located cracks are subjected to the analysis. The problem employs the simple type of constitutive model for which the volumetric components of stress and strain tensor are related to the proportionality law, while the time dependent properties are connected to deviatoric components. The temporal discrete analysis employs the recurrent integral method, while with respect to spatial variables the FEM is used. The applicability of the described model to the investigation of the effect of cracks on the displacement and stress field is analyzed on the basis of some examples of practical importance. The obtained results form the basis to the following conclusions:

1) The main factor which effects significantly the magnitude of the vertical displacements is due to the thickness of the bitumen layers.
   For comparison: The equivalent displacements of the homogeneous medium are three times larger than the analogous displacements of nonhomogeneous medium which consists of single layer of bitumen and the soil medium. The equivalent displacements of the homogeneous medium are six times larger than the analogous displacements of the nonhomogeneous medium which consists of double layer of bitumen and the soil medium.
2) The presence of the inner cracks (covered by the top layer) – located, in second and third layer has no substantial influence on the magnitudes and the shapes of the deflection surface.
3) A basic change in the shape as well as magnitude of the deflection of the top surface takes place when the cracks start to appear from the top surface. In this case a sharp jump producing discontinuity of the deflection surface is observed in the closest vicinity of the cracks. The magnitude of the displacement jump depends heavily on the depth of the cracks. From this fact it follows, that the application of the load in the vicinity of the top cracks highly increases the risk of failure of the medium through the large discontinuous deformations.
4) The analysis of stress field for investigated cases indicates that for homogeneous materials all stress components increase with time. For the media with cracks the radial σ_x and vertical σ_z stress components have tendency to decrease.

7. ACKNOWLEDGEMENTS

The financial support of Natural Sciences and Engineering Research Council of Canada under grant number OGP 110262 is gratefully acknowledged.

8. REFERENCES

1. Athanasopoulos, G.A., Richard, F.E, (1983). Effect of creep on shear modulus of clays, *J. Geotech. Eng.*, Vol. 109, pp. 1217–1232.
2. Budkowska, B.B., Grzesiak, W. Simulation of sub–pavement cracks in layered viscoelastic medium, *Int. J. Computers and Geotechnics*, (to appear).
3. Budkowska, B.B., Fu, Q., (1988). Some aspects of numerical analysis of creep in layered granular medium, *Int. J. Computers and Geotechnics*, Vol. 5, pp. 285–306.
4. Budkowska, B.B., Fu, Q. Analytical determination of the optimal strain and stress points for the displacement model of the finite element method, *Computers and Structures, An International Journal*, (in press).
5. Eringen, A.C., (1967). *Mechanics of continua*, John Wiley & Sons, New York.
6. Flugge, W., (1967). *Viscoelasticity*, Blaisdell Publishing Company.
7. Hughes, T.J.R., (1987). *The finite element method*, Prentice–Hall, Inc., New Jersey.
8. Sekiguchi, H., (1977). Rheological characteristics of clay, *Proc. 9th ICSMFF*, Vol. 1, pp. 289–292.
9. Zienkiewicz, O.C., (1977). *The finite element method*, McGraw–Hill Company (UK).

Experience with the Search of Minimum Factor of Safety of Slopes

Z. CHEN
Ph.D.
Senior Engineer, Institute of Water Conservancy and Hydroelectric Power Research, China

SUMMARY:This paper discusses the various problems which should be properly dealt with in the calculations of the minimum factors of safety by the methods of optimization.

1. INTRODUCTION

While a computerized solution of factor of safety for a given slip surface of a slope has been a design routine, the search for the minimum factor of safety still remains, by and large, a *computer aided manual* performance. During the past decade, many researchers have found that the methods of optimization can be employed to minimize the factor of safety. The simplex method, complex method, alternative variable method, Powell's method, Davidon – Fletcher – Powell method and the steepest descent method have been employed. (Nguyen,1985, Sun, 1982, Celestino and Duncan, 1987, Chen and Shao, 1988, Chen, 1991). It can be predicted that a computerized solution of minimum factor of safety will also become a design routine in the near future.

Understanding that transferring research findings to practice requires the accumulation of experience, the author wishes to discuss the following topics that he feels of practical interests: (1) comparisons of calculated results by using different approaches such as the Bishop's simplified method versus Morgenstern-Price method, broken line versus smooth curve slip surfaces. etc.; (2) the importance of using non–linear failure envelope for cohesionless materials; (3) determination of the global minimum factor of safety by a random search approach; and (4) Verification of the results by closed form solutions.

2. THE METHODS OF OPTIMIZATION AS APPLIED TO SLOPE STABILITY ANALYSIS

2.1 The Scheme of a Searching Procedure

The problem of minimizing an objective function

$$F = F(\mathbf{Z}) \tag{1}$$

with respect to the variable vector $\mathbf{Z}$, which represents a set of variables

$$\mathbf{Z} = (z_1, z_2, \cdots, z_n)^T \tag{2}$$

can be readily solved by using various methods of optimization, whose principles are covered by a variety of textbooks(e. g. Fox, 1971, Walsh, 1975, Nennis, et. al., 1983). The numerical procedure starts from an initial estimate $\mathbf{Z}^0$ and terminates at $\mathbf{Z}^m$ at which F acquires its minimum, denoted by F_m.

In slope stability analysis, F is the value of factor of safety, while $\mathbf{Z}$ represents the information by which a slip surface can be uniquely defined.

A circular slip surface can be defined by X_c , Y_c ,and D_s , where X_c , Y_c are the coordinates of the center, and D_s , the depth of the circle which is defined as the ordinate value of the horizontal tangent to the circle (refer to Fig.4). (1) becomes

$$F = F(X_c,\ Y_c,\ D_s) \tag{3}$$

A slip surface of generalized shape is generally simulated by a set of nodal points. Each pair of the contiguous ones are connected by either a straight line or a curve. (Li and White, 1987; Chen and Shao, 1988). Curves are generated with the aid of the spline functions. In this case, $\mathbf{Z}$ represents coordinates of the nodal points, $x_1, y_1, x_2, y_2, \ldots, x_n, y_n$, and (1) becomes

$$F = F(x_1, y_1, x_2, y_2, \cdots, x_n, y_n) \tag{4}$$

For details, refer to Chen and Shao (1988).

A latest updating aimed at reducing the degree of freedom includes replacing $x_1, y_1, x_2, y_2, \ldots, x_n, y_n$ by the relative coordinates $b_1, b_2, \cdots, b_n$. b_i is defined as the distance between the ith nodal point of a slip surface during the course of optimization and that of the slip surface taken as the initial estimate (refer to Fig. 1). Each nodal point is assigned a direction of movement, α_i . In these directions the nodal points move from their initial positions $A_1, A_2, \ldots, A_n$ to $B_1, B_2, \ldots, B_n$, the ones which define the critical slip surface.Since

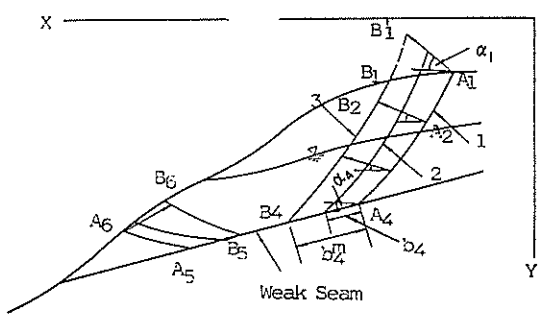

Figure 1 Slips surface of generalized shape: 1. the initial estimate $\mathbf{Z}^0$; 2. a slip surface during the process of optimization $\mathbf{Z}$; 3. the critical slip surface $\mathbf{Z}^m$.

$$Z_i = Z_i^o + \Delta Z_i = \begin{Bmatrix} x_i^o \\ y_i^o \end{Bmatrix} + b_i \begin{Bmatrix} cos\alpha_i \\ sin\alpha_i \end{Bmatrix} \quad (5)$$

(1) becomes

$$F = F(b_1, b_2, \cdots, b_n) \quad (6)$$

This means that α_i's do not appear as variables in $\mathbf{Z}$. Experience has shown that the difference of the results obtained by different assigned values of α_i is insignificant if the corresponding nodal points are connected by smooth curves.

2.2 Comparisons of Different Patterns for Discretizing Slip Surfaces

Most researchers connect nodal points by straight lines. The author found that for soil slopes whose materials are virtually homogeneous, a slip surface simulated by smooth curves can be more effective. Fig. 2 shows an example in which the slip surface was discretized by four nodal points. The value of F_m for the slip surface of broken line shape was 1.483 while that for the slip surface of smooth curve shape was 1.372. This means that more nodal points are needed for the broken line pattern to obtain the true minimum factor of safety.

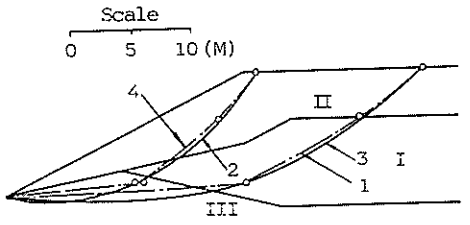

Figure 2 An example showing the difference between the minimum factors of safety obtained by the straight line and the curve pattern.

Dotted lines : the slip surfaces generated by the straight line pattern, 1: $F_o = 1.952$, 4: $F_m = 1.483$

Solid lines : the slip surfaces generated by the the curve pattern,*3*: $F_o = 1.767$; 2:$F_m = 1.372$.

TABLE I. Geotechnical Properties of the Materials (Fig. 2, Fig. 3, Fig. 7 and Fig. 8)

Soil layer	Density ρ (g/cm^3)	Shear strength parameters	
		φ(deg)	C(kpa)
I	2.0	38	0
II	2.0	23	5.3
III	2.0	20	7.2

2.3 Comparisons of Different Methods for Stability Analysis

Fig. 3 gives the calculated results using: (1) a circular slip surface and the Bishop's simplified method and ;(2) a slip surface generated by four nodal points with the smooth curve pattern and Morgenstern – Price Method (extended by Chen and Morgenstern,1983). It can be found that the two approaches yielded virtually the same results. It suggests that although the Bishop's simplified method does not allow a complete force equilibrium, it is applicable to slopes whose failure mode is not controlled by geological heterogeneity or / and discontinuities, from the viewpoints of both the value of F_m and the location of the critical slip surfaces.

For cases where non – circular slip surfaces must be used, the methods satisfying complete equilibrium should be priorities. This argument comes from the inherent shortcomings of the methods that satisfy only force equilibrium conditions. The author's experience has confirmed Duncan and Wright's (1980) statements that these methods may give factor of safety within 15%, sometimes even more, of those satisfying complete equlibrium.

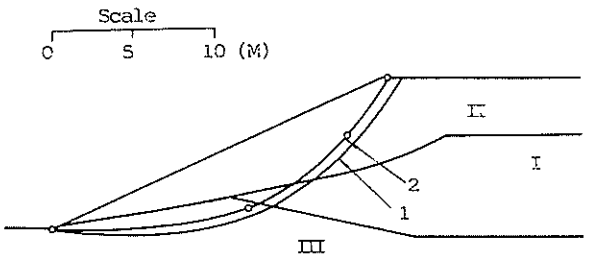

Figure 3 An example showing the difference between the minimum factors of safety obtained by the simplified and rigorous analytical methods. For the circular critical slip surface 1, $F_m = 1.384$; for the non–circular slip surface 2, $F_m = 1.372$.

3. STABILITY ANALYSIS FOR GRANULAR MATERIALS

Granular materials are generally regarded as cohesionless, i. e., the cohesion c equals zero. Experience has shown that for a slope composed of uniform material of this sort, the computation always yields a very shallow critical slip surfaces, such as the slip surface 1 in Fig.4 The calculated $F_m = 1.113$ is actually the value of a factor of safety of an infinitive slope. The fact that no meaningful critical slip surface can be created is not only less pleasing but also unrealistic. Researchers (De Mello, 1977, Charles, 1984) have found that the failure envelope of granular materials, especially compacted rockfills, always exhibit significant curvature particularly at low and medium stresses. The higher strength at low stress will prevent a shallow slip surface from being critical. The stability analysis using nonlinear failure envelope is obviously more relevant.

The nonlinear failure criterion proposed by De Mello(1977) is described by the relationship of the form

$$\tau_f = A(\sigma')^b \quad (7)$$

where τ_f *and* σ' are shear strength and effective normal stresses respectively, and A, B, the material parameters.

An alternative proposed by Duncan et. al. is expressed as:

$$\varphi' = \varphi_o - \Delta\varphi log\ (\sigma'_3 / P_a) \qquad (8)$$

Where φ' is the effective friction angle; φ_o , $\Delta\varphi$, material properties, and σ'_3 , P_a , the minor effective principle stress and the atmospheric pressure respectively.

The nonlinear stability analysis for a slip surface generally involves the following steps: (1) perform the conventional stability analysis using the assumed parameters of linear failure criterion, and determine the normal effective stresses σ' on the failure surface; (2) determine τ_f by (7) or (8) for each slice based on the calculated value of σ', or σ'_3 , (3) assign $c' = \tau_f$ and $\varphi' = 0$ for the corresponding slice, (4) perform the stability analysis again for the same slip surface and find the factor of safety. The normal effective stresses calculated in step (1) are generally not sensitive to the assumed values of linear parameters. Therefore, iterations are generally not necessary.

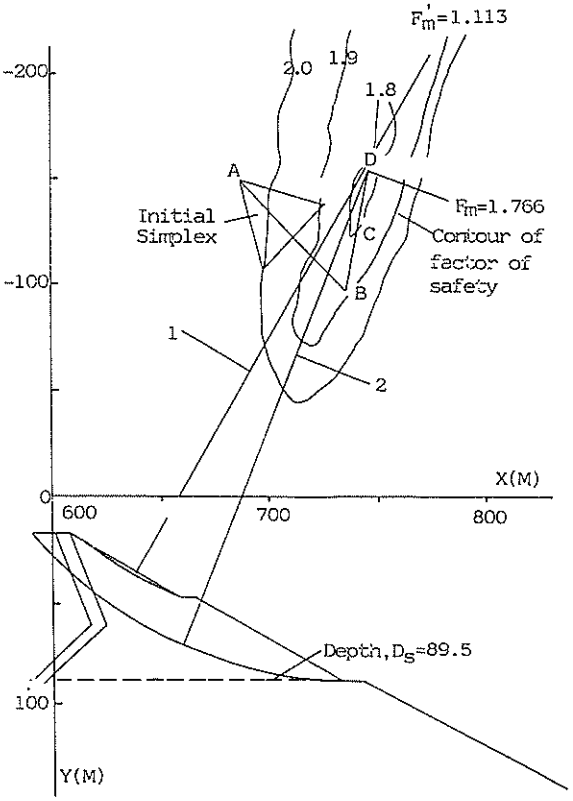

Figure 4 The critical slip surfaces 1: using linear strength parameters, $c = 0$, $\varphi' = 40°$; 2: using nonlinear strength parameters proposed by Duncan (1978), $\varphi_o = 45°$, $\Delta\varphi = 5°$.

The calculated critical slip surface using nonlinear failure envelope for the example shown in Fig.4 has a moderate depth and seems to be reasonable. Fig.4 shows the contour of factors of safety with respect to X_c , Y_c, and a fixed depth D_s = 89.5. The searching for F_m corresponding to that depth by simplex method started from an intial simplex, passed through B and C, and eventually terminated at D, at which F_m = 1.766.Fig. 5 shows the results calculated by taking X_c , Y_c, D_s all as variables. The three trials used different initial estimates, whose locations deviated from each other appreciably (Fig. 5a), and resulted in virtually the same critical slip surfaces and the associated minimum factors of safety.

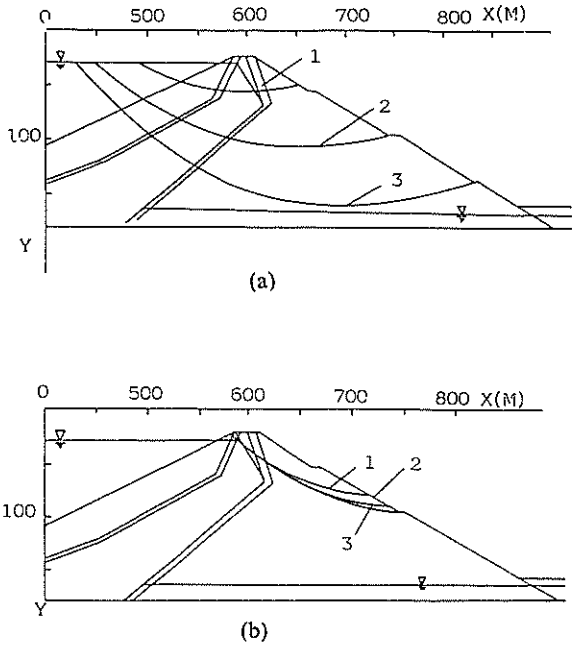

Figure 5 Comparisons of critical slipe surfaces using different initial estimates (refer to Table II), (a) three initial estimates; (b) the corresponding critical slipe surface.

TABLE II. The Nonlinear Analysis for F_m using Different F_o for the Example Shown in Fig. 5

Number of trials	F_o	F_m
1	2.396	1.764
2	2.725	1.759
3	2.594	1.800

Charles(1984) presents a chart, shown in Fig. 6, for rapid assessment of rockfill slope stabilty. The minimum factors of safety calculated by the author using the approach described previously are represented by the circles in the same figure. It can be found that the two sets of results, which are obtained independently, agree with each other remarkably.

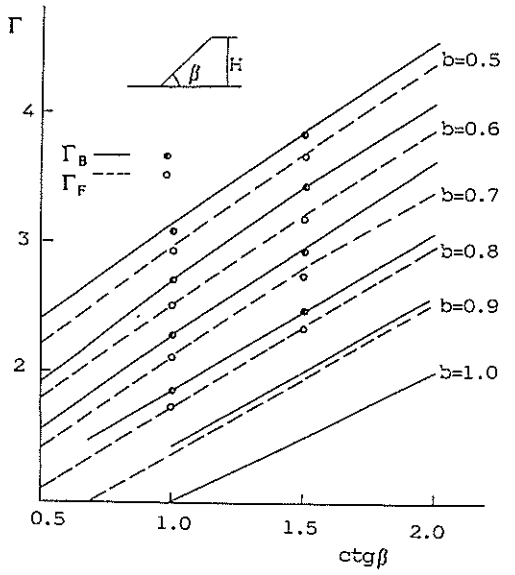

Figure 6 Comparisons of the calculated results with the chart provided by Charles and Soares (1984).

NOTE: The circles represent the author's calculations. $\Gamma = F(\gamma H)^{(1-b)} / A$. Subscripts B and F refer to the values of Γ associated with the Bishop's simplified method and Fellenuis method respectively.

4. SEARCH FOR THE GLOBAL MINIMUM FACTOR OF SAFETY

In spite of the successful applications of the methods described herein, experience also showed that the algorithm sometimes suffered from premature termination at which the solution was actually not a global minimum. This always happens when: (1) the problem involves too many degrees of freedom; (2) the initial estimate is set too far away from the critical slip surface; and (3) the slope profile contains too many different zones. All these circumstances can be related to the problem of finding the global minimum of an optimization problem. Fig.7 shows an example in which the slip surface 1 was used as an initial estimate, the calculation terminated with the slip surface 3 while the global minimun had already been known to be the slip surface 2. However the computation will succeed on any of the following occassions: (1) if the slope profile is uniform; (2) if the slip surface 1 is set close to the critical slip surface 2; and (3) if less nodal points with a discretization pattern using curves are employed.

To overcome the difficulties in finding the convergent solution of the global minimum factor of safety, a random search method has been developed. The purpose of the random search is to find an initial estimate that is close enough to the global minimum. For a slope under investigation, a search area that possibly contains the critical slip surface is defined. Several hundred, or thousand, slip surfaces are randomly generated in this area. Their corresponding factors of safety are compared and the one that is associated with the minimum factor of safety is retained as the initial estimate. Fig. 8 shows the slip surface used as the initial estimate selected among 45 random trials in the search area. This initial estimate is so close to the critical slip surface that no difficulties in finding F_m would ever be expected.

Modern statistics has permitted the production of very nice sequences of random numbers which are mutually independent, uniform, and non–repetitive. With the aid of

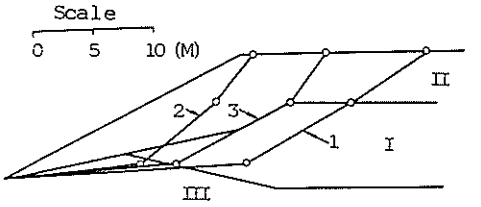

Figure 7 Example displaying the unsuccessful searrches for minimum factor of safety. Slip surfaces: 1. The initila estimate $F_o = 1.951$. 2. The known critical slip surface, $F_m = 1.484$. 3. The slip surface at which the calculation terminates. $F = 1.511$.

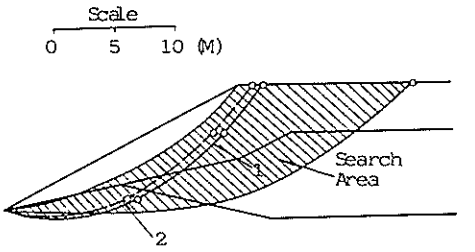

Figure 8 The random search. Slip surfaces 1: the initial estimate selected among 45 randomly created slip surfaces, $F_o = 1.384$; 2: the critical slip surface, $F_m = 1.372$.

these random numbers, one will be able to scan the space containing the variable vectors uniformly with high density and to roughly locate the global minimum. As a matter of fact, the random search itself can be used to find the critical slip surface, as proposed by Boutrup et. al. (1980) and Siegel et. al. (1981). However, very large number of random searches will be needed when the degree of freedom is relatively large. Combining random search and optimization analysis can be more effective than either purely stochastic or purely analytic approach.

Other topics concerning the generation of random slip surfaces, the determination of appropriate times of random searches and the use of simplified analytical stability methods in random search will be covered elsewhere due to the limited space available.

5 COMPARISONS BETWEEN THEORETICAL AND NUMERICAL RESULTS

To justify the results obtained by the methods of optimization, Chen and Shao (1988) have given a test example in which the value of F_m and the associated critical slip surface of a frictionless, weightless slope subjected to a uniform load were compared with those provided by the Prandtl solution. Two more sophisticated examples are given here to demonstrate the feasibility of the methods described herein. Their closed form solutions have been given by Sokolovski (1965).

5.1 Test Example 1 : Stability Analysis of a Uniform Frictionless Slope

This example differs from the Prandtl solution in its nonzero unit weight of the slope materials. For the analysis decribed in Fig. 9, the upper two nodal points were connected by a straight line while the others were connected by curves. Morgenstern – Price method was employed. It can be seen that both the value of F_m and the location of the associated critical slip surface agree well with those given by the closed form solution.

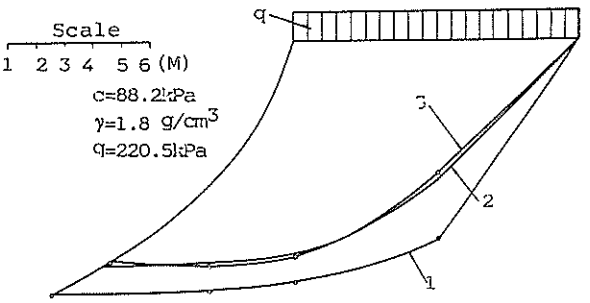

Figure 9 Analysis of a frictionless slope. Slip surfaces 1: initially estimated, $F_o = 1.101$; 2: critical by theory; 3: critical by calculation, $F_m = 1.009$.

5.2 Test Example 2 : Stability Analysis of a Uniform Weightless Slope

This example, shown in Fig. 10, represents another more generalized case where the material exhibits nonzero values for both friction angle and cohesion, but the material is assumed to be weightless. Again, the upper two nodal points were connected by a straight line while the others were connected by curves. The value of F_m and the location of the associated critical slip surface calculated by the optimization procedure also show little deviation from those known by the theory.

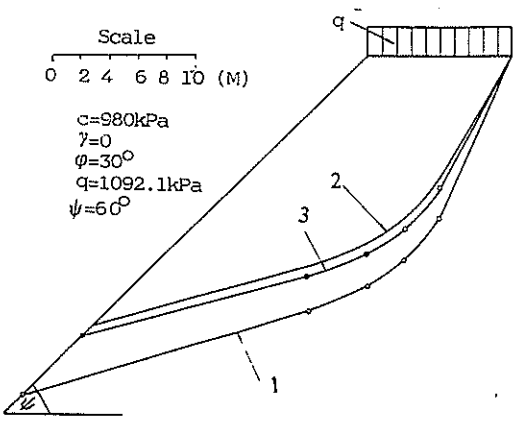

Figure10. Analysis of a weightless slope with both friction and cohesion. Slip surfaces 1: initially estimated, $F_o = 1.110$; 2: critical by theory; 3: critical by calculation, $F_m = 0.970$.

6. CONCLUSIONS

The numerical approach to searching for the minimum factor of safety has been used by the author in tens of projects in China since its development (Chen and Shao, 1988). Experience has shown that its successful applications to practical problems depend on a robust and friendly computer program and an understanding of the problems that could possibly arise in the particular slope investigated. The main points of this paper can be summarized as follows:

(1) For soil slopes where geological heterogeneity and discontinuities are not dominating, using circular slip surfaces and the Bishop's simplified method generally produces results as good as any more rigorous approach does. This argument is justified by both the values of minimum factors of safety and the locations of the critical slip surfaces. Since the circular slip surface pattern, which involves only three degrees of freedom, always provides rapid convergent solutions, its applications to this sort of slope are recommended.

(2) The need for slip surfaces of generalized shape arises when the slope profile is geologically heterogeneous, containing weak zones or discontinuities. When performing the calculation for this sort of problems, one should be always mindful that the increase in the degrees of freedom will increase the computing time and the convergence difficulties considerably. The smoothly curved part of the slip surface should be simulated by splines rather a broken line since it requires more nodal points than a curve to produce equally good simulation.

(3) An important updating aimed at facilitating the evaluation of the global minimum employs a random search technique. This approach allows a rough determination of the location of the critical slip surface. An initial estimate set in that location will approach the critical slip surface rapidly by the methods of optimizations. The technique has proved to be very powerful in finding the global minimum factor of safety.

(4) For slopes composed of uniform compacted granular materials, the use of linear strength parameters with zero cohesion always produces a very shallow critical slip surface which is not only physically meaningless but also unrealistic considering the higher shear strength the material generally exhibits at lower normal stresses. The results using nonlinear strength envelope presented in this paper gave physically reasonable critical slip surfaces. They are consistent with those obtained by Charles and Soares(1984).

(5) The computation results of the two test examples that possess closed form solutions have furnished convincing evidence that the searching technique described herein provides not only practically feasible but also theoretically reliable solutions to stability problems.

7. ACKNOWLEDGEMENTS

The financial support for this research project comes from the National Natural Science Foundation of China.

8. REFERENCES

Boutrup, A. W. and Lovell, C. W. (1980). Search technique in slope stability analysis. Engineering Geology.Vol. 16, pp. 51–61.

Cellelstino, T. B. and Duncan, J. M. (1981). Simplified search for non–circular slip surface. Proceedings, 10th International Symposium on Soil Mechanics and Foundation Engineering.Stockholm. Vol.3 pp–391–394.

Charles, J. A. and Soares, M. M. (1984). Stability of Compacted rockfill slopes. Geotechnique. Vol. 34, pp. 61–70.

Chen, Z. and Morgenstern, N. R. (1983). Extensions to the generalized method of slices for stability analysis. Canadian Geotechnical Journal.Vol. 20, pp. 735–748.

Chen, Z. and Shao, C. (1988). Evaluation of minimum factor of safety in slope stability analysis. Canadian Geotechnical Journal. Vol. 25, pp. 735–748.

Chen, Z. (1991). Updating the limit equilibrium method and its applications.Thesis(Ph. D.) Tsinghua University.

De Mello, V. F. B. (1977). Reflection on design decision of practical significance to embankment dam construction. Geotechnique.Vol. 27. pp. 281–354.

Duncan, J. M., et. al. (1978). Strength, stress and bulk modulus parameters for finite element analysis of stresses and movements in soils. Report No. VCB / GT / 78–02, University of California, Berkeley.

Duncan, J. M. and Wright, S. G. (1980). The accuracy of equilibrium methods of slope stability analysis. Proceedings, 3rd International Conference on Landslide,Delhi, Vol. 1, pp.247 – 254.

Fox, R. L.(1971). Optimization methods for engineers. Addison – Wesley Publishing Company, Massachusetts.

Li, K. S. and White, W. (1987). Rapid evaluation of the critical slip surface in slope stability problems. International Journal for Numerical and Analytical Methods in Geomechanics. Vol. 11. pp.449–473.

Nennis, Jr., J. E. and Schnabel, (1983). Numerical methods for unconstrained optimization and nonlinear equations. Prentice – Hall, Inc., Engleword Cliffs, New Jersey.

Nguyen, V. U. (1985). Determination of critical slope failure surface. ASCE Journal of Geotechnical Engineering. Vol. 111. pp. 238–250.

Siegel, R. A.; Kovacs, W. D. and Lovell, C. W. (1981) Random surface generation in stability analysis, ASCE Journal of Geotechnical Engineering.Vol. 109, pp. 996 – 1002.

Sokolovski, V. V. (1965). Statics of granular media.Pergamon Press, New York.

Sun, J. S. (1984). The numerical analysis of strip partition method. Chinese Journal of Geotechnical Engineering. Vol. 6, pp. 1–12 (In Chinese).

Walsh, G. R. (1975). Methods of optimization.John – Wiley and Sons, London.

Geotechnical Risk and the Use of Grey Extrapolation Technique

R.N. CHOWDHURY
F.I.E.Aust.
A. Professor, University of Wollongong, Wollongong, NSW, Australia
S. ZHANG
Lecturer, Ballarat University of College, Ballarat, Victoria, Australia
J. LI
Postgraduate Student, University of South Australia, Adelaide, Australia

SUMMARY This paper is concerned with an aspect of the assessment of geotechnical risk with particular reference to observational data and its interpretation. The use of a grey prediction model (grey extrapolation technique) is discussed. This is part of what is known as the grey system theory which is concerned with systems subject to uncertainty. An illustrative example concerned with data on pore pressure equilibrium in an excavated slope of overconsolidated clay has been presented.

1. ASSESSMENT OF GEOTECHNICAL RISK

Assessment of geotechnical risk is often an important task for engineers involved in a project. Such an assessment is often made before the project is undertaken. During the planning and design stages, geotechnical and other data must be collected, organised and analysed carefully to develop an appreciation of the factors which influence geotechnical performance and the adequacy of that performance during the life of the project. A judgement can then be made about geotechnical risk on the basis of available information, completed analyses and on the basis of previous experience on similar projects or on other projects with some similar aspects to the new proposed project.

Judgements made during the planning and design stages are not final. Considerable information may become available during the construction phase of a project. Based on this new or additional information, it is very useful to update the judgements made previously. In particular, observational data about stresses, strains, displacements or pore water pressures may highlight some gaps in analyses made previously. It may also be necessary to revise some of the assumptions on which the analyses were based. More improtantly, observational data may either validate or invalidate the geotechnical models adopted for different elements of the project or for different stages of the same element of the project. Consequently, assessment of geotechnical risk must continue during the execution of the project.

2. OBSERVATIONAL PROCEDURES BEYOND CONSTRUCTION STAGE

In significant geotechnical projects it is considered necessary to continue the observational approach beyond the construction stage. There are two main reasons for this. Firstly, it is an acknowledgement of the uncertainties in relation to geotechnical prediction and performance. Both systematic and random uncertainties are associated with the adopted values of geotechnical parameters such as shear strength and deformation parameters, pore water pressures and in situ stresses. In particular, spatial variability of these parameters is often not known except perhaps qualitatively. There are also uncertainties concerning loads and, in particular, dynamic loads associated with random events such as earthquakes. The influence of such events on geotechnical parameters also involves considerable uncertainty. Finally, there are uncertainties related to geotechnical models which have been adopted for analyses. Considering all these factors, it is only logical that geotechnical engineers should invest in instrumentation and other observational procedures for performance monitoring beyond the construction stage of a project.

The second main reason for continued observational approaches on a project after its completion is that long-term performance is often quite different from the end-of-construction performance. For example, as is now well recognised, excavated slopes in saturated overconsolidated clays usually have their highest factor of safety at the end of construction. This is because the unloading process of excavation generates excess negative porewater pressures in the zone adjacent to an excavation. Consequently, there is an increase in shear strength which partly compensates for the increased shear stresses associated with the excavation process. However, these negative excess pore water pressures are 'transient' and must, therefore, dissipate in the long-term. The long-term pore water pressures are significantly higher and the shear strength associated with these equilibrium pore water pressures is, therefore, significantly lower than that at the end of construction. On the other hand, the shear stresses are more or less the same as at the end of construction. Therefore, the factor of safety in the long-term can be significantly lower than that in the short-term. Many years or decades may pass before the pore water pressures rise to equilibrium values. The modelling of the rate of pore water pressure equilibration is not easy and, in any case, significant uncertainty would be associated with a predictive process. Consequently, the installation of permanent devices such as piezometers is advisable. Based on the actually measured pore water pressures, the geotechnical risk associated with an excavation can be updated. Moreover, the rate of change of risk can also be interpreted on the basis of such observational data.

3. AIM AND SCOPE OF THIS PAPER

The main aim of this paper is to introduce briefly an approach which can be used for interpretation of observational data as well as its extrapolation. This approach is part of what has been called "Grey System Theory" and may be called the "Grey Extrapolation Technique". After a brief introduction to this technique, its relevance to geotechnical risk assessment is considered. for this purpose an illustrative example is considered which relates to long-term pore water pressure equilibration after an excavation is made in overconsolidated soil. This is the type of problem which has already been introduced in the previous section of this paper.

The application of the grey system theory to settlement prediction was considered in a previous paper and excellent performance of the method was shown for that type of problem (Zhang et al, 1991).

The grey extrapolation technique may also be used for problems involving the variation of more than one parameter. There are many geotechnical situations in which it is desirable to consider the variation of multiple parameters. However, the use of the grey extrapolation technique for such problems is outside the scope of this paper. The research work is not so well advanced at this stage.

Analysis of data relating to a major case history of progressive slope failure associated with reservoir filling and rainfall infiltration has just been undertaken and the results will be published at a subsequent date.

3.1 Grey System Theory

The grey system theory was proposed by Deng (1982, 1985) and is concerned with the analysis and interpretation of uncertain information. A system which is completely unknown may be denoted as a 'black' system and one which is fully known as a 'white' system. Most systems are, however, neither fully unknown nor fully known and, therefore, may be denoted as 'grey' systems. In general, all geotechnical engineering systems can be regarded as 'grey' since the quality of data is never perfect, the quantity of data may be insufficient and since the relationships between parameters or between parameters and performance are never known exactly or completely.

Grey system theory includes the development of system models and system analysis, grey forecasting, grey decision-making and grey control. From the original data, a generating data model is established. System analysis involves the analysis of correlation between various factors influencing a problem and the identification of the importance of each factor . The tendency of one or more factors to vary together is assessed in grey system theory. Forecasting may include the prediction of the time of occurrence of a particular value of a variable and the occurrence of an unusual or catastrophic event. Decision-making is concerned with the identification of an optimal strategy based on given criteria. The execution of a strategy is called 'control' and grey control is primarily concerned with the control of grey parameters in a system.

Grey system theory can be applied to diverse fields such as economics and meteorology and its relevance to geomechanics must be considered on the basis of experience. In an earlier paper (Zhang et al, 1991) settlement prediction based as grey system theory was shown to be both reliable and accurate. In the present paper, the method is used for prediction of pore water pressures with time based on observational data.

As in the preious paper (Zhang et al, 1991) only the prediction technique of the methodology is used in the present paper.

Grey prediction technique is based on the accumulation trend of random data. The intrinsic characteristics of a grey system can, in general, be modelled using differential equations. However, in this paper only a simple one-parameter random model (or one-dimensional random model) is used.

4. TECHNIQUES FOR ENHANCING DATA INTERPRETATION

4.1 Accumulation Operations

The first step is to determine the accumulation trend of random variables. Considering m random variables x(1), x(2) .... x(m). The first order accumulation operation is performed as follows:

$$\begin{aligned} x^1(1) &= x(1) \\ x^1(2) &= x^1(1) + x(2) \\ x^1(3) &= x^1(2) + x(3) \\ &\cdots\cdots \\ x^1(m) &= x^1(m-1) + x(m) \end{aligned} \qquad (1)$$

The variables x(1), x(2), x(3) .... etc could also be the values of a single parameter at different times. In many cases it is found to be useful to consider the incremental changes in a parameter which varies with time. This is also discussed in a subsequent section.

This is an accumulation operation of the first order. An accumulation operation of the nth order will relate $x^n(1)$ to $x^{n-1}(1)$, $x^n(2)$ to $x^n(1)$ and $x^{n-1}(2)$ and so on as shown below:

$$\begin{aligned} x^n(1) &= x^{n-1}(1) \\ x^n(2) &= x^n(1) + x^{n-1}(2) \\ &\cdots\cdots \\ x^n(m) &= x^n(m-1) + x^{n-1}(m) \end{aligned} \qquad (2)$$

Initially the data may be quite random. With the first accumulation operation, the randomness of the data is reduced and with each subsequent accumulation operation randomness decreases further. Thus the cumulatively generated data can be plotted as a smooth curve with a clearly evident trend. Often one or two accumulation operations may be sufficient and higher order operations are, therefore, unnecessary.

4.2 Inverse Accumulation Operations

Another type of operation is the inverse accumulation operation. For example, starting from the accumulation data of nth order given in Eq. (2), the first order inverse accumulation operation is shown below:

$$\begin{aligned} Inv^1[x^n(1)] &= x^{n-1}(1) \\ Inv^1[x^n(2)] &= x^n(2) - x^n(1) = x^{n-1}(2) \\ &\cdots\cdots \\ Inv^1[x^n(m)] &= x^n(m) - x^n(m-1) = x^{n-1}(m) \end{aligned} \qquad (3)$$

If the inverse accumulation operation is carried out to the nth order, the original data are obtained. Thus

$$\begin{aligned} Inv^1[x^n(1)] &= x(1) \\ Inv^1[x^n(2)] &= x(2) \end{aligned} \qquad (4)$$

5. GREY PREDICTION MODEL

A simple differential equation to model the accumulation trend of Eq. (1) is

$$\frac{dx^1}{dt} + Ax^1 = u \qquad (5)$$

in which the variable x^1 is a function of time t; A and u are constants to be determined.

The incremental changes in the variable are first obtained from the raw data. The accumulation operations are carried out from this incremental data. A variable like x^1 is the value obtained after the first such operation.

A solution may easily be obtained for this differential equation considering a continuous case. Similarly, a solution can be obtained for a discrete case.

For a continuous case the solution is

$$x^1(t) = [x(1) - u/A]\, e^{-At} + u/A \qquad (6)$$

For a higher order accumulation operation (nth order) the equation becomes.:

$$x^n(t) = [x^{n-1}(1) - u/A]\, e^{-At} + u/A \qquad (7)$$

The constant A and u are determined from a matrix operation as discussed elsewhere (Zhang et al, 1991). The elements of the component matrices are the original data and the data generated from accumulation operations.

Table 1
Variation of r_u with time

No.	1	2	3	4	5	6	7	8	9	10	11	12	13	14	15	16	17	18	19	20
Time (years)	0.5	1	1.5	2	2.5	3	3.5	4	4.5	5	6	7	8	9	10	11	12	13	14	15
r_u	0.05	0.11	0.17	0.21	0.24	0.26	0.27	0.28	0.28	0.28	0.29	0.28	0.29	0.28	0.29	0.29	0.29	0.30	0.29	0.30

6. ILLUSTRATIVE EAMPLE

6.1 Statement of the Problem

At the site of an excavated slope pore water pressures have been monitored over a period of 15 years. The value of r_u, the pore water pressure ratio, at a significant location is shown in Table 1.

The following calculations are required

(a) Based on observed data over the first four years (8 data points), what would have been the predicted value of r_u after the passage of 15, 27 and 35 years. What would have been the final equilibrium value?

(b) Based on observed data over the first six years (11 data points), what would have been the predicted value of r_u after the passage of 15, 27 and 35 years? What would have been the final equilibrium value.

(c) Considering all the data, what is the predicted value of r_u after 27 years? What are the predicted values after 35 and 65 years? What is the final equilibrium value?

6.2 Results of Analyses

The grey extrapolation technique was based on the grey prediction model discussed in the previous section. The incremental approach worked very well and the results are shown in Tables 2, 3 and 4.

Table 2
Calculated Values of r_u based on the first eight data points (4 years data)

Year	Calculated Value	Observed Value
15	0.3182	0.30
27	0.3183	-
35	0.3183	-
Final	0.3183	-

Table 3
Calculated Values of r_u based on the first eleven data points (6 years)

Year	Calculated Value	Observed Value
15	0.30067	0.30
27	0.30070	-
35	0.30070	-
Final	0.30070	-

Table 4
Calculated Values of r_u based on the whole data set, twenty data points (15 years)

Year	Calculated Value of r_u
27	0.2976
35	0.2976
65	0.2976
Final	0.2976

It should be noted that the particular model chosen in this case works only with the use of incremental changes in the observed variable. These incremental changes should be used as the basis for the accumulation operations. Some calculations were, of course, made with the raw data. These preliminary calculations showed that the calculated value of r_u increases significantly with time without levelling out at any time. Such results are obviously unreasonable and incorrect for the type of problem under consideration.

The calculation procedure of the model was developed in such a way that it is not necessary to use equal time steps. Therefore, data concerning a variable recorded at irregular time intervals can be used for analysis.

7. DISCUSSION AND CONCLUSIONS

For pore water pressures is an excavated slope of saturated overconsolidated clay, the main trend is always an increase in the pore water pressure. It is well known that the rate of this movement towards equilibrium of pore water pressure decreases with time. There are, however, many other factors and mainly climatic factors which may influence this trend. Therefore, the changes occurring may not appear to follow a regular and smooth curve during the equilibration period. In this type of problem, the use of a numerical technique for extrapolation is of significant interest. Purely theoretical predictions are not easy to make and may not provide accurate estimates because of the various uncertainties involved. In the present case, the use of grey extrapolation technique based on incremental changes in the observed data proved to be successful. The use of the technique based on the raw data proved to be unsuccessful.

It is interesting to note that even with only 8 data points (covering a 4 year period) the predicted value is reasonably close to the observed value after 15 years. Moreover, there is insignificant change after the 15 year period which appears to be quite reasonable on the basis of the available data.

As the number of data points considered in the prediction model increases, so does the accuracy of the prediction. With 11 data points (covering 6 years) the value of r_u after 15 years is almost identical to the observed value.

The results are encouraging and indicate that more complex applications of grey systems theory should be considered in geomechanics. The geotechnical risk associated with major projects should be considered using the grey prediction technique to analyse observational data. Such an approach would indeed facilitate the assessment of risk associated with the reactivation of major landslides and with the development of major dam-reservoir systems. At present, the authors are investigating the development of the technique for geotechnical risk involving multiple factors. In particular, a case history involving a major project is being considered for which significant observational data are available.

8. REFERENCES

1. Deng, J 1982. "Control problems of grey systems", System and Control Letters, Vol. 1 No. 5, p. 288-294.

2. Deng, J 1985. The Grey Control Systems 422 pp (in Chinese)

3. Zhang, S, Li, J and Chowdhury, R N, 1991. "A New Approach Based on Grey System Theory for Settlement Prediction", Proceedings Int. Conf. of the Int. Assoc. for Computer Methods and Advances in Geomechanics, Cairns, Queensland, Australia, May 6-10, 1991, pp. 211-216.

Explore – An Expert System for Subsurface Exploration

A.T.C. GOH
B.E., Ph.D., M.I.E.Aust.
Lecturer, Swinburne Institute of Technology, Melbourne

SUMMARY Expert systems are computer programs that are capable of incorparating empirical and qualitative knowledge. Because many geomechanics solutions require judgement and rules of thumb, there is potential that expert systems can be utilised to assist the geotechnical engineer in the decision making process. In this paper, an overview of expert systems is presented. The methodology involved in building a geotechnical expert system for subsurface exploration is then described.

1. INTRODUCTION

The majority of the computer applications that have been developed in the field of geotechnical engineering have been numeric and deterministic in nature. They essentially assist engineers to perform tasks that require mathematical and repetitive calculations. However, the geomechanics solution process usually involves more than just quantitative reasoning. Qualitative and experienced-based knowledge are often essential components in the decision making process. The encapsulation of this empirical-type knowledge and reasoning process through the application of expert systems technology represents an additional tool that can be utilised to assist the geotechnical engineer.

In order to investigate the usefulness of expert systems for geotechnical engineering applications, a pilot system was developed to solve a typical geotechnical problem, namely that of providing advice on a subsurface exploration program for a particular site. In this paper, an overview of expert systems is presented. First, the basic concepts and architecture of expert systems are introduced. The methodology involved in the development of the expert system EXPLORE is then described and suggestions made about future directions.

2. WHAT ARE EXPERT SYSTEMS ?

Expert systems can be described as "computer programs that use logical relationships to incorporate knowledge and experience about a specific problem area to perform specialised tasks that typically require human judgement" (Palmer 1987). Some researchers (eg. Blockley 1982) prefer to use the term knowledge-based systems to expert systems in order to emphasize that expert system programs are intended to act as assistance tools rather than replace the experts.

There are two essential features of expert systems. Firstly, in an expert system, the knowledge-base is separated from the control mechanism. A knowledge-base is a collection of rules, facts, database and computational procedures. The control mechanism, commonly called the inference engine, determines when, what and how rules, facts etc. stored in the knowledge-base are fired or executed. This separation of the knowledge-base from the control strategy is one of the greatest strengths of expert systems because it allows engineers to concentrate on building up the knowledge-base (by amending, adding or deleting rules and facts) without worrying about how it will affect the control strategy. While conventional programs may contain some components of judgement and rules of thumb, they are usually implemented in numeric terms, which makes enhancement and amplification of the knowledge difficult.

Secondly, knowledge-based expert systems , like experts, are "transparent" (Fenves 1986) in that they are capable of inspecting their knowledge and reasoning process and produce explanations or justifications of their reasoning. This means that a user is able to know during run-time why a certain question is being asked, and how a certain conclusion has been arrived at. The general architecture of an expert system is illustrated in Figure 1.

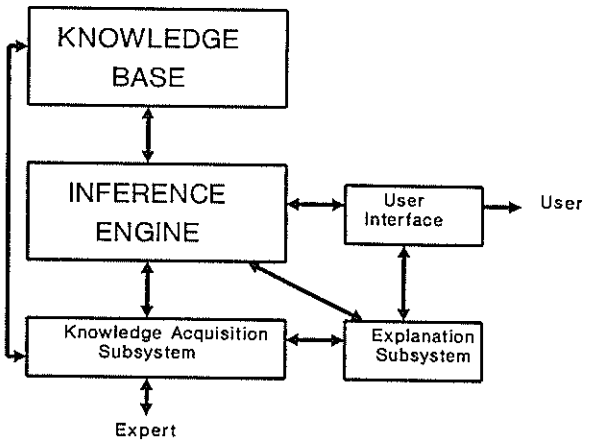

Figure 1 Expert system architecture.

The most common method of representing knowledge in the knowledge-base is through the use of production rules. These have an IF condition THEN action format. For example

IF {condition 1}
AND {condition 2} OR {condition 3}

THEN {conclusion 1}
AND {conclusion 2}

This can be interpreted to mean : IF the set of conditions is true, THEN draw these conclusions. If all the conditions in the rule are true, then the rule is said to fire.
The following are some sample rules :

Rule : Foundation type

IF bearing stress is less than allowable bearing pressure

THEN foundation type is shallow foundation

Rule : Uniform soil conditions

IF soil condition is uniform
AND number of storeys is greater than 2

THEN minimum number of boreholes is 4

There are two major search strategies used in inference mechanisms, namely backward chaining and forward chaining. In backward chaining, the system starts at a goal and works backwards in an attempt to find a solution. In forward chaining, the reverse occurs. The system begins with data and proceeds to fire rules in order to see where they lead.

A review of the main features of some commercial expert system development tools, commonly called shells, has been described by Sharpe et al (1989). The increasing popularity of using knowledge-based systems among engineers is due in part to the availability of inexpensive, microcomputer based expert system shells. This has allowed the engineer to become effective knowledge engineers, thereby eliminating the need to "marry" an expert with a knowledge engineer to complete the expert system.

Todate, much of the research in expert systems applications in civil engineering have been concentrated in the area of structural engineering. A good summary of these are outlined by Allen (1987). It is recognised, however, that among all civil engineering disciplines, geotechnical engineering problems lend themselves best for expert systems solutions because many geotechnical solutions are based on judgements and "rules of thumbs" yardsticks synthesized from experiences. It is ironical, therefore, that compared to structural engineering, expert systems have yet to make any significant impact in geotechnical engineering. This apparent dichotomy could be explained from an inherent distrust of computer solutions in an experiential discipline. Yet it is precisely because geotechnical engineering is a discipline where qualitative and experience-based knowledge has almost no substitutes that expert systems can be harnessed to maximum advantage. Some recent examples of expert systems in geotechnical engineering include pile foundation design (Wong et al 1989), retaining wall selection (Hutchinson 1985), classification of soils from cone penetration data (Mullarkey 1985), and lateral pile design (Goh and Koo 1990).

3. BUILDING THE EXPERT SYSTEM

The following steps were taken to develop a user-friendly expert system EXPLORE for providing advice on the number and spacing of boreholes, the depth of the boreholes and the recommended types of tests to be carried out at a particular building site.

- Selecting the inference engine;
- Knowledge acquisition; and
- Building the knowledge base.

3.1 Selection Of Inference Engine

In order to cut down the development time, an expert system shell was selected, rather than using LISP or PROLOG, or other high level programming lauguages such as BASIC and PASCAL. The expert system shell CRYSTAL (1987) which is a backward chaining rule-based system was used in the development of the expert system. The shell runs on IBM-compatible personal computers. This shell was adopted mainly because of its availability and is user-friendly. It provides excellent graphics displays, multiple windows, multiple-choice menus and is capable of capturing graphics created using other graphics programs. The knowledge in CRYSTAL can be kept in separate knowledge bases which can be loaded into main memory as and when required. Its ability to interface with external programs, databases and spreadsheets enhances its potential for future expansion of EXPLORE.

3.2 Knowledge Acquisition

The next step was the knowledge acquisition - a process of gathering, transferring and transforming problem solving expertise from "experts" into rules, facts and questions. The main factors affecting the selection of the number and spacing of boreholes, the depth of boreholes and the types of testing was investigated. The main source of information was obtained from surveying geotechnical textbooks (eg. Clayton et al 1982; Das 1984; Johnson & Kavanagh 1968, Weltman & Head 1983), codes of practice (SAA Site Investigation Code 1981; Victorian Building Regulations 1983) and manuals (Canadian Foundation Engineering Manual 1987; NAVFAC Design Manual 1982). Interviews with two experienced engineers were another source of information.

The next step was the organisation of the knowledge. An object network as shown in Figure 2 was used to reduce the overall problem into a series of sub-problems. The depth of exploration is dependent on the foundation type selected and the structural loading. The selection of the foundation type is in turn dependent on the subsoil conditions, the function of the structure and the structural loading. The spacing of the boreholes is related to the function

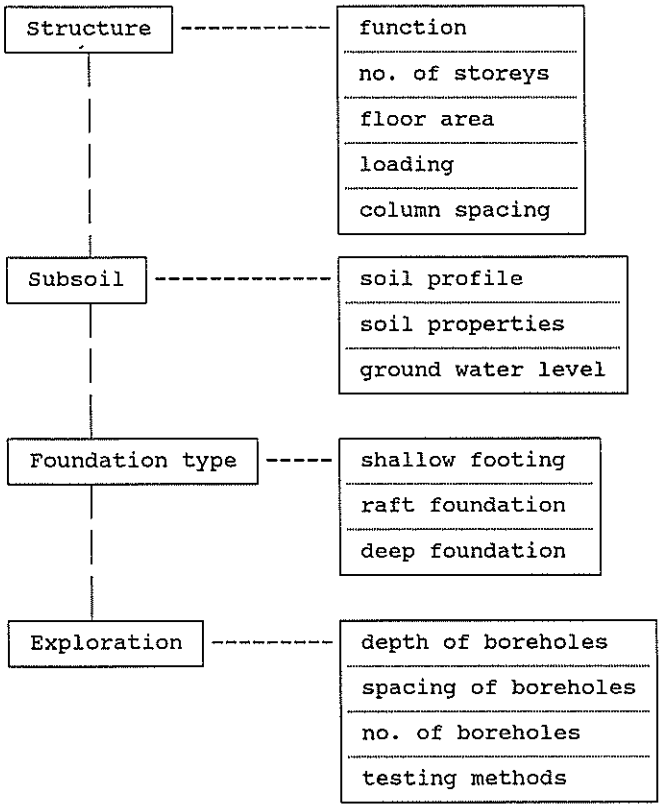

Figure 2 Object network

of the structure and the complexity of the subsoil conditions. The testing methods are mainly dependent on the subsoil conditions. The knowledge acquisition was the most serious bottleneck in the development of EXPLORE.

3.3 Building The Knowledge Base

The knowledge was then transformed into rules, questions and facts using CRYSTAL's English-like language. The rules were expressed in the form "if ... then ... " as mentioned previously. The general structure of the expert system is shown in Figure 3. The expert system consisted of 127 rules and 265 commands. For reasons of brevity, the detailed structure and listing of the knowledge-base is not presented in this paper. To achieve the objective of a highly interactive system, a series of input screens have been designed. The user is required to respond to a series of questions about the structure and the subsoil conditions. Figure 4 shows two typical input screens. EXPLORE was developed to be used at a fairly early stage in the planning of the project, where available data about the ground and loading conditions may be limited. For example, the user is asked to input the number of storeys of the structure in order to estimate the loads acting on the foundation system. Information about the estimated allowable bearing pressure of the subsoil is also required in order to determine whether shallow foundations are adequate, or piling is required. CRSTAL's environment takes care of the explanation component of the expert system. The user is able to query the system at run-time for an explanation for the train of logic behind the queries and results. Help screens such as that illustrated in Figure 5, obtained from the Victorian Building Regulations (1983), were also incorporated to assist the engineer if required.

For residential and commercial buildings, the total load acting on the foundation system was determined by assuming that the average (dead and live load) pressure per storey was 10 kPa. In estimating the bearing stress, information is required on either the number of columns or the effective area over which the column load acts. For industrial buildings, because of the variability of loading conditions in different industries, the user was required to input the maximum column load and the number of columns.

Figure 6 shows a condensed version of the flow chart for determining the depth of exploration. The bearing stress is determined from the structural information provided. A comparison is then made with the soil allowable bearing pressure. If the allowable bearing pressure is exceeded, then the use of piling is recommended. If the allowable bearing pressure is not exceeded, then shallow foundations are recommended. However, the user is also given the option of selecting piling instead. A raft foundation is recommended if the bearing area exceeds half the total floor area of the building. Based on the type of foundation selected and the depth of the foundation, the depth of

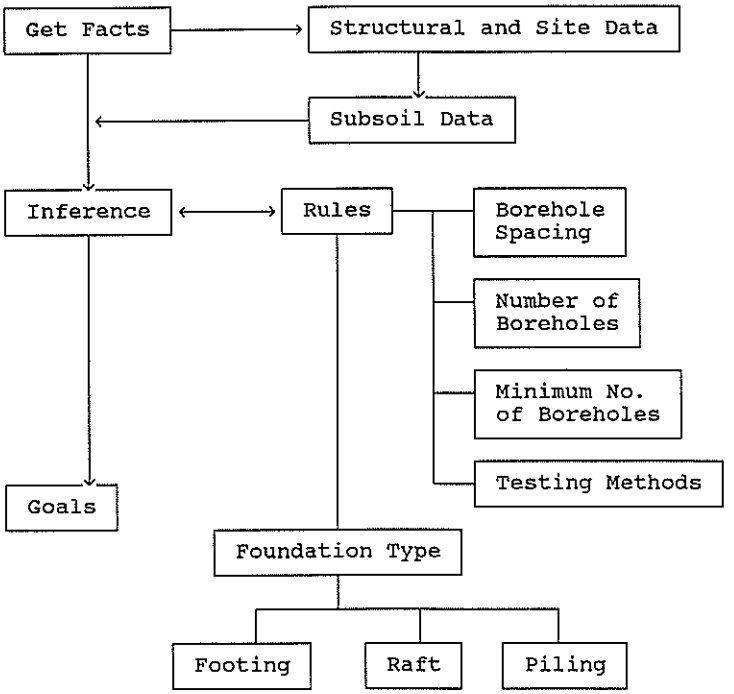

Figure 3 General structure of EXPLORE.

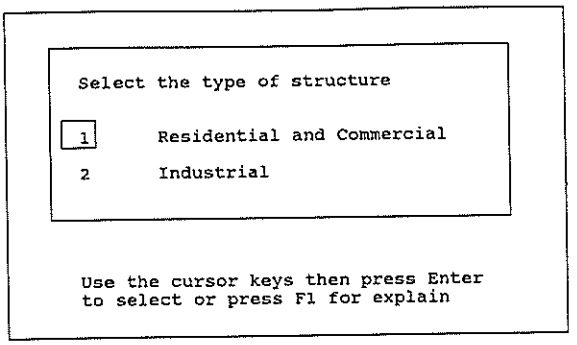

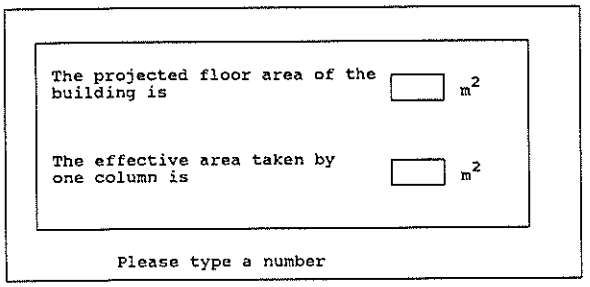

Figure 4 Typical input screens.

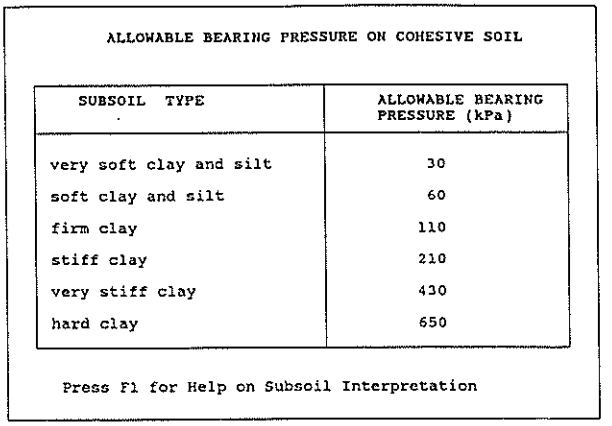

Figure 5 Typical Help screen.

exploration is determined by calculating the depth at which the applied vertical stress is less than 10% of the effective overburden stress at that depth, using the formulations of Boussinesq.

Table 1 shows the guidelines used for determining the borehole spacing and consequently the number of boreholes. A typical output screen of the recommendations of EXPLORE is shown in Figure 7. The recommended types of testing to be carried out were based on the guidelines in the SAA Site Investigation Code (1981).

3.4 Validation

Validation of the expert system was carried out through a limited number of case study comparisons. Good correla-

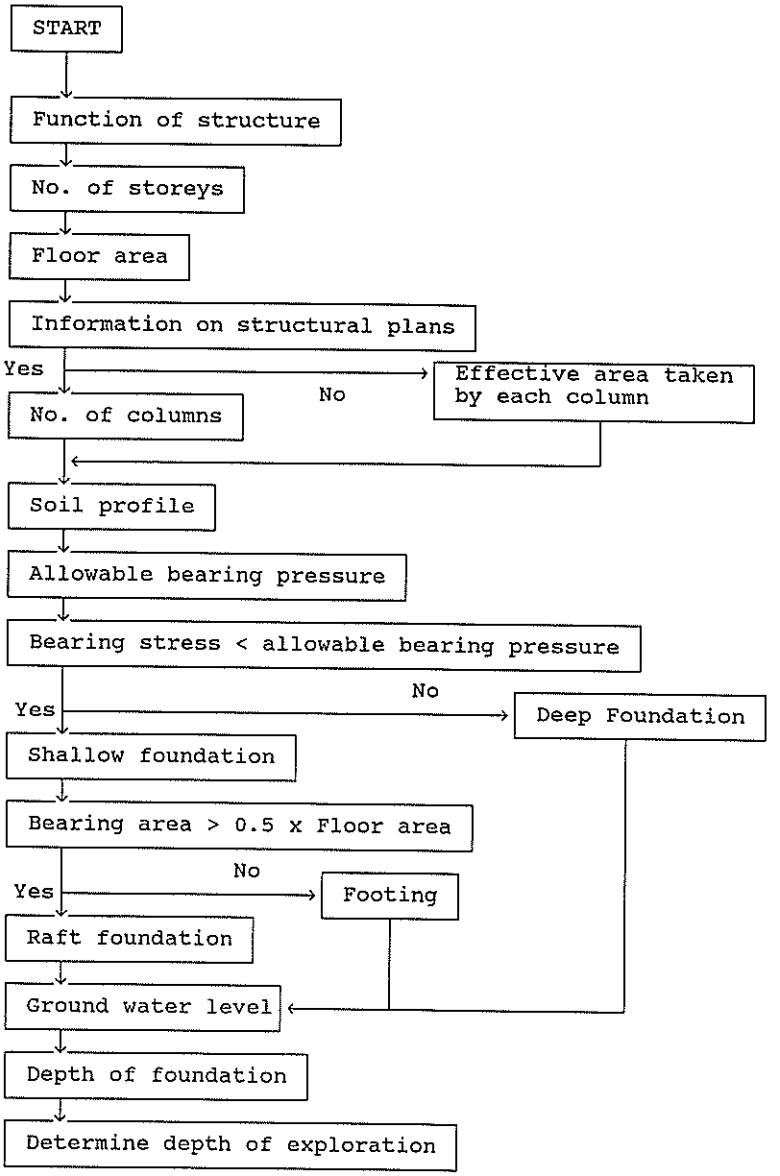

Figure 6 Flow chart for exploration depth.

Table 1 Borehole spacing guidelines.

	Uniform soil profile		Complex soil profile	
	one borehole per	Min. no. boreholes	one borehole per	Min. no. boreholes
Multistorey	100 m^2	4	50 m^2	5
One/two storey	250 m^2	2	150 m^2	3
Industrial	200 m^2	4	150 m^2	5

BUILDING TYPE	RESIDENTIAL
NO. OF STOREYS	4
FLOOR AREA	150.0 m^2
NO. OF COLUMNS	10
BEARING STRESS	50.0 kN/m^2
SOIL ALL. BEARING PRESS.	217 kN/m^2
SOIL TYPE	COHESIVE
FOUNDATION TYPE	SHALLOW
FOOTING DEPTH	1.0 m
WATER TABLE	2.0 m
DEPTH OF EXPLORATION	6.8 m
NO. OF BOREHOLES	4

Figure 7 Typical output screen.

tions were obtained between the EXPLORE recommendations and the actual procedures employed, in the case of the recommended number of boreholes. However, a comparison with actual borelogs indicated that EXPLORE tended to recommend slightly larger depths of exploration, for the cases analysed for the regions around Melbourne comprising residual soils and weathered rocks. In these cases, the borelogs indicated shallower boreholes in comparison to EXPLORE. This was because sampling was terminated because of refusal. The expert system provides recommendations as to the depth to which sampling is to be carried out. It is unable to take into consideration the fact that sampling may cease because bedrock is encountered at shallower depths. Further validation of the expert system is currently being carried out.

3.5 Limitations

The current version of EXPLORE is limited to planning of building sites. The scope of the system can be expanded to cover various other geomechanical structures such as embankments, bridge abutments, roads, retaining walls etc. In the selection of the appropriate foundation system, the effects of the foundation system on adjacent sites and the effects from adjacent sites have not been taken into consideration. In addition, the effects of foundation settlement have not been taken into account. As with most existing expert systems, EXPLORE is unable to learn by itself from existing case studies. With further developments in machine learning, it is envisaged that this is one area for further research.

4. DISCUSSION

Although conventional programming techniques could have been used to develop a similar interactive program, this would have required a significantly greater computational effort in order to make it user friendly, in comparison to expert system shells. Only limited knowledge, no more than that required to learn to use a spreadsheet, is required to learn to use an expert system shell. The structure of the expert system in which the knowledge base is separated from the inference engine, and the use of natural language processing also enables expert systems to be more easily modified/expanded if the original developer is unavailable.

Because geotechnical engineering is a field where experiential knowledge has almost no substitute, there is a need for preserving and disseminating this knowledge. The architecture of expert systems which permits interactive dialogue and explanation is a powerful tool which has potential applications in training inexperienced engineers. As pointed out by Santamarina and Chameau (1987), expert systems facilitate the development of a repository of cases that can be used to study these cases, ask for explanations and justifications and even ask "what if".

5. CONCLUSIONS

The objectives of this paper were to provide an overview of expert systems and to describe the methodology involved in developing the expert system EXPLORE. Expert systems are useful tools which can be utilised to assist geotechnical engineers and train young engineers. The tools necessary to develop geotechnical expert systems are available and can be used to improve on the state of geotechnical engineering practice.

6. REFERENCES

Allen, R.H. (1987). Expert systems in structural engineering ; works in progress. Journal of Computing in Civil Engineering, ASCE. Vol.1, No.4, pp. 312-319.

Blockley, D.I. (1982). Fuzzy systems in civil engineering. In Approximate reasoning in decision analysis. ed. Gupta M.M. and Sanchez E. North Holland. pp. 103-115.

Canadian Foundation Engineering Manual (1987). Canadian Geotechnical Society, 2nd ed.

Clayton, C.R.I, Simons, N.E. and Matthews, M.C. (1982). Site investigation. Granada Publishing.

CRYSTAL (1987). User Manual. Intelligent Environments, UK.

Das, B.M. (1984). Principles of foundation engineering. PWS Publishers.

Fenves, S.J. (1986). What is an expert system ?. Proc. ASCE Symp. on Expert Systems in Civil Engineering. ed. Kostem C.N. and Maher, M.L. pp. 1-6.

Goh, A.T.C. and Koo, K.T. (1990). An expert system for laterally loaded piles. Proc. Int. Conf. on Structural Engineering and Computation, Beijing, China.

Hutchinson, P.J. (1985). An expert system for the selection of earth retaining structures. Master's thesis, University of Sydney.

Johnson, S.M. and Kavanagh T.C. (1968). The design of foundations for buildings. McGraw-Hill.

Mullarkey, P.W. (1985). CONE- An expert system for interpretation of geotechnical characterisation data from cone penetrometer. PhD thesis, Carnegie-Mellon Univ., Pittsburg.

NAVFAC Design Manual DM7.1 (1982). Dept. of the Navy, Naval Facilities Engineering Command, USA.

Palmer, R.N. (1987). Editorial. Journal of Computing in Civil Engineering, ASCE, vol.1, No.4, pp. 224.

Santamarina, J.C. and Chameau, J.L. (1987). Expert systems for geotechnical engineers. Journal of Computing in Civil Engineering, ASCE, Vol.1, No.4, pp. 241-252.

Sharpe, R., Marksjo, B. and Ho, F. (1989). Wind loading and building code expert systems. Proc. Australasian Conf. on Expert Systems in Engineering, Architecture and Construction, Sydney, pp. 223-242.

SAA Site Investigation Code (1981). Standards Association of Australia.

Victorian Building Regulations (1983). State Government of Victoria.

Weltman, A.J. and Head, J.M. (1983). Site investigation manual. CIRIA Special Publication 25.

Wong, K.C., Poulos, H.G. and Thorne, C.P. (1989). Expert systems in geotechnical engineering. Proc. Australasian Conf. on Expert Systems in Engineering, Architecture and Construction, Sydney, pp. 63-79.

Rock Engineering Risk Assessment through Critical Mechanism and Parameter Evaluation

J.A. HUDSON
B.Sc., Ph.D., D.Sc., C.Eng., M.I.C.E., F.I.M.M.
Professor of Engineering Rock Mechanics, Imperial College of Science, Technology & Medicine, University of London, UK
J.SHENG
B.Sc., Ph.D.
Associate Professor, Department of Civil Engineering, National Central University, Taiwan
P.N. ARNOLD
B.Sc., M.Sc., D.I.C., F.G.S.
Post-Graduate Student, Imperial College of Science, Technology & Medicine, University of London, UK

1. INTRODUCTION

There is currently a need in rock engineering for a coherent approach which allows the identification of the important parameters and mechanisms for any rock engineering activity - based on the project's objectives. A new methodology is being developed which enables, through a comprehensive listing of all major geotechnical parameters, the establishment of the interactive mechanisms associated with these parameters and also a method for prioritizing the mechanisms and parameters based on the 'cause' and 'effect' values and the assessment of instability scenarios (1,2). The appraisal is directed to the objective(s) of the project. This technique is demonstrated by use of rock interaction matrices where the cause and effect of parameter interactions can be used as an indication of the critical mechanisms and parameters before, during and after construction.

Essentially the 'cause' refers to the influence that a parameter has on the engineering system; whereas, the 'effect' refers to the influence that the system has on the parameter. The methodology is briefly referred to here and will be expanded in future papers. The principles of the technique are illustrated with repect to some of the rock treatment methods applied in the construction of the Fei-Tsui Dam in Taiwan (3).

2. USE OF THE INTERACTION MATRIX APPROACH

The interaction matrix is the running theme through a three-tier approach that is being developed to assist in the design, construction, and monitoring for all rock engineering. The three tiers are
a) REMIT - Rock Engineering Mechanisms Information Technology (in the language of systems, this component consists of morphological and cascading systems, ie the basic structure of the system with interlinking),
b) RESP - Rock Engineering System Performance (consisting of a process-response system with generic induced perturbations, ie studying the responses governed by the natural rock mass process and effects induced by engineering), and
c) ONSE - Objective-based Network Sequence Evaluation (consisting of the system pathways governed by the project engineering, ie the specific engineering work required to achieve the objective).

Within any engineered rock mass there will usually be a number of key parameters, from the rock mass, the site environment and the engineering project, which will dominate the performance of the engineered rock mass to the detriment of the engineering objectives. The key parameters can only be determined by identifying the mechanisms and the sequence of interactions which take place to create instability. We use the interaction matrix for this purpose.

Many interaction matrices have been developed by the senior author, and we can only demonstrate part of one here to give the general idea (see Figure 1). In this sub-matrix, of a larger slope stability assessment matrix, we show just three of the main parameters in the black boxes along the leading diagonal. The information in Box ij illustrates one example of the interaction of the parameter in Box ii on the parameter in Box jj.

We can now develop coding methods to enable this interaction matrix to be used for quantitative assessment of parameter significance, dominance, and indeed system risk. The general principle is shown in Figure 2. If the actual construction procedure is placed in the last box, ie Box nn, then the right hand column of the matrix illustrates the design factors, and the lower row of the matrix illustrates the effects of engineering.

As mentioned, the actual use of the total REMIT/RESPONSE system will be explained in future publications; here we simply illustrate how a key parameter can be identified in a complex sytem of parameters, interactions, inputs, outputs, and responses - all governed by mechanical and hydrological canonical ensembles.

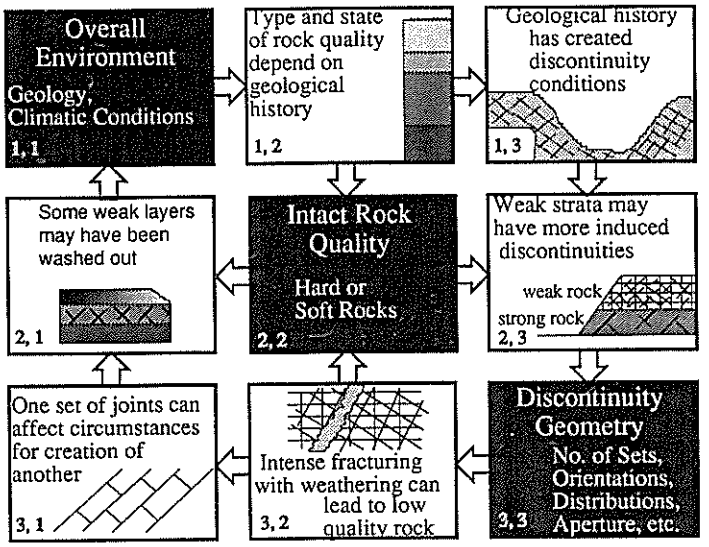

Figure 1 Interaction matrix for slope stability (this is a sub-matrix of a much larger array).

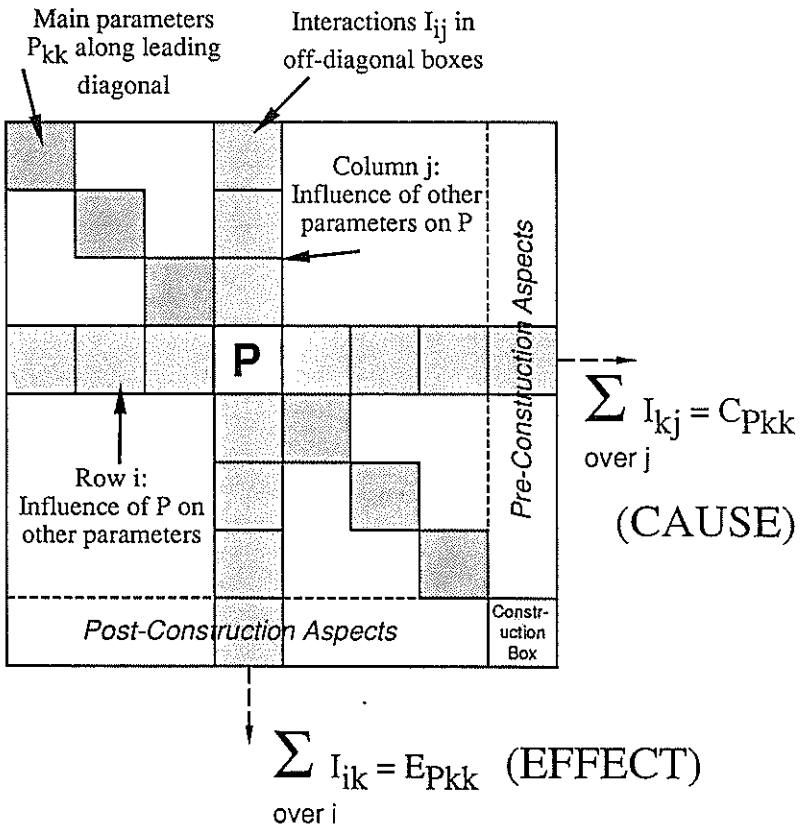

Figure 2 Generic interaction matrix.

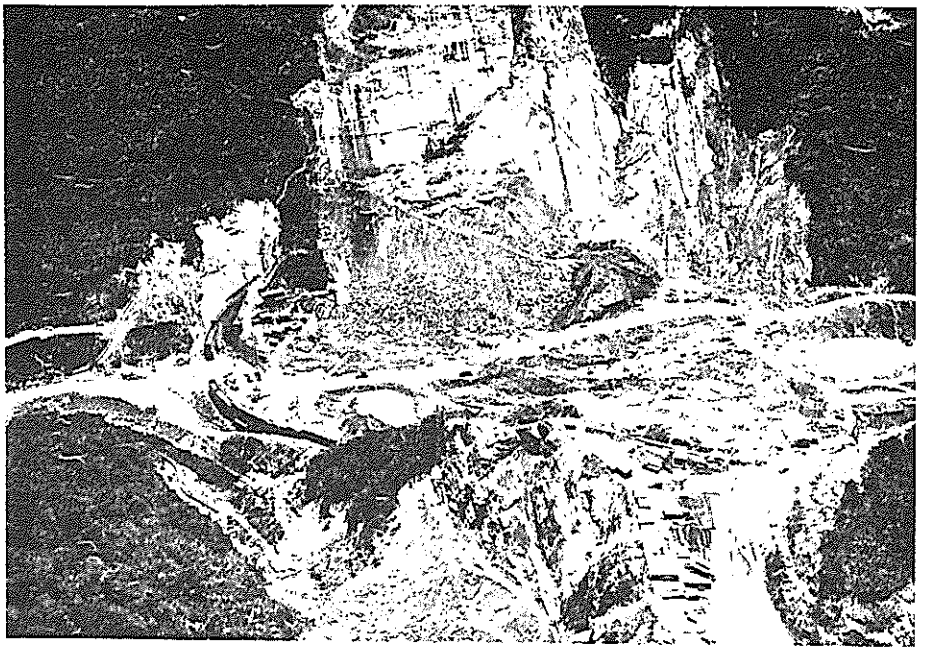

Figure 3 Excavation of the Fei-Tsui Dam.

3. FEI-TSUI DAM IN TAIWAN

Thus, in order to illustrate the way in which such a system may operate, we have chosen to consider some key aspects of the Fei-Tsui dam in Taiwan. Naturally, in this limited presentation, we cannot consider the dam construction comprehensively, but we can illustrate our methodology with reference to certain key aspects that were encountered.

3.1 Overall Site Conditions

The Fei-Tsui dam is a wide V-shaped concrete dam 122.5m in height and 510m in length along the top of the dam. Massive sandstone and siltstone of Oligocene age form the foundation of the dam site. The strike of bedding is generally parallel to the river with a dip of 40 degrees towards the right bank. This leaves the left abutment dip -slope and the right scarp slope. Although the sandstone and siltstone are strong, clay bedding seams vary from less than 1cm to about 15cm in thickness and form unfavourable weak planes. Additionally, moderately developed joints are detected in the area and stress relief may complicate the situation. The excavation is illustrated in Figure 3 and the completed dam is shown in Figure 4.

Typhoons and earthquakes are two natural factors in the area. Although other factors such as north-east monsoons, south-west monsoons and extra topical storms affect the rainfall over the reservoir area, typhoons produce the maximum rainfall every year. The maximum precipitated water of 2.5gm/cm2 was recorded in 1963 and 1969. Earthquakes in northern Taiwan are mainly caused by the subduction of the Philippine sea plate beneath the Eurasia plate. Magnitudes of 4 are common and could exceed 7 on the Reichter scale; a peak ground accelleration of 0.25g horizontal and 0.15g vertical is used for the basic earthquake design criteria.

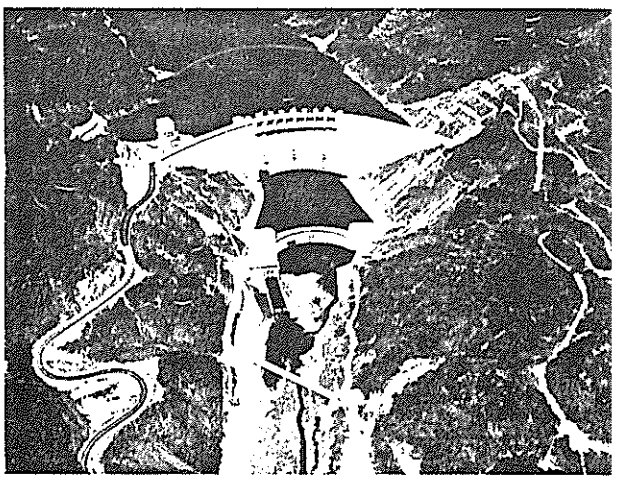

Figure 4 The completed Fei-Tsui Dam.

3.2 Major Concerns Relating Fei-Tsui Dam

Since the dam is located only 30km south of the densely populated Taipei City, the perception of dam stability is important to the public as well as the project engineers. From the rock mechanics point of view, the rock mass shear strength at the dam site plays an important role as far as the stability problem is concerned. In practice, there is little that the engineers can do to improve the quality of the intact rock, and that leaves the engineering effort directed towards the improvement of the discontinuity mechanical properties. Also, the discontinuity geometry, which includes factors such as number of sets, orientation, distributions, aperture etc, demands a thorough investigation.

3.3 Leading Diagonal Terms for Interaction Matrix

Various aspects of the dam design will require consideration of different parameters. However, if we concentrate on the stability of the abutments, we can list out twelve leading diagonal terms for the interaction matrix which represent the main aspects used in the compilation of a 12x12 interaction matrix for this part of the dam. These are given below with illustrative components of the terms.

These are

1,1 - Overall Environment
Geology, climate, seismic risk, previous instability

2,2 - Intact Rock Quality
Strong, weak, weathering susceptibility.

3,3 - Discontinuity Geometry
Sets, orientations, apertures, roughnesses.

4,4 - Discontinuity Mechanical Properties
Stiffness, cohesion, friction.

5,5 - Rock Mass Properties
Deformability, strength, failure.

6,6 - *In Situ* Rock Stress
Principal stress magnitudes and directions.

7,7 - Hydraulic Conditions
Permeability.

8,8 - Slope Orientation and Locations
Dip, dip direction, position.

9,9 - Slope Dimensions
Height, width, local and overall.

10,10 - Proximate Engineering Disturbances
Adjacent blasting.

11,11 - Support/ Maintenance
Bolts, cables, grouting, pre/post construction.

12,12 - Construction
Excavation method, sequencing.

These twelve leading diagonal terms can be used to create a total 12x12 matrix which will have 144-12=132 interaction terms (4). To illustrate the type of information that this produces, in Figure 1 we illustrated a 3x3 part of the 12x12 main matrix.

3.4 Important Aspects of the Fei-Tsui Dam

In a short paper we cannot discuss the significance of all the 132 potential interactions, and indeed the matrix might need to be enlarged. We can, however, point to some of the interesting interactions to illustrate our methodology.

Some of the leading diagonal parameters are fixed and some are not. Essentially parameters 1,1 to 7,7 are functions of the rock mass and site, whereas parameters 8,8 to 12,12 are functions of the engineering. In fact, the slope orientation, location and dimensions are more or less fixed because of the dam considerations. However, we do have the opportunity to vary some of the parameters as follows.

1,1 Overall Environment - cannot be altered
2,2 Intact Rock Quality - cannot be altered
3,3 Discontinuity Geometry - cannot be altered
4,4 Discontinuity Mechanical Properties - can be altered.
5,5 Rock Mass Properties - can be altered
6,6 *In Situ* Rock Stress - cannot be altered
7,7 Hydraulic Conditions - can be altered
8,8 Slope Orientation/location - essentially fixed
9,9 Slope Dimensions - essentially fixed
10,10 Proximate Engineering Disturbances - can be modified
11,11 Support / Maintenance - can be modified
12,12 Construction - can be modified.

Because of the perception that the dam should be safe and also because of the real geotechnical importance of the discontinuities and given the constraints listed above, one finds that many of the potential instability mechanisms can be avoided if attention is placed on the discontinuity mechanical properties, leading diagonal term 4,4.

3.5 Alteration of Discontinuity Mechanical Properties

A very elegant method was used on site to essentially eliminate all of the mechanisms associated with the row and column interactions for the leading diagonal term 4,4 - in fact, this amounts to 22 separate mechanisms associated with the mechanical properties associated with the discontinuities. In other words, if it is possible to enhance the mechanical properties of the discontinuities so they are commensurate with the proximate rock, then they will be effectively mechanically inert.

On site, this was achieved by use of a water jet and water knife to wash out the discontinuity fill which was mainly clay, rock fragments and weathered rock. When the aperture of the discontinuity was larger than 10mm, a water jet was used between two parallel adits approximately 12m apart. When the aperture of

the discontinuity was smaller than 10mm, a water knife and water drill were used with the water drill hole spacing at about 200mm. The water jet operated at a pressure of 200kg/cm2; the water knife and water drill operated at a pressure of 2400kg/cm2.

Naturally, this discontinuity treatment programme required the initial excavation of a series of access tunnels and working adits in the dam-loaded zone. A typical discontinuity is shown in Figure 5; a 'halfway stage in the washing-out is shown in Figure 6; and the cleaned, open discontinuity shown in Figure 7.

This programme was extensively planned to allow for the idiosyncrasies of the left and right abutment and the below river bed zone. The washed and cleaned discontinuities were then backfilled with non-shrinking cement mortar and paste grouted under pressure, with checks to ensure that the discontinuity had been completely filled. Tests on the shear strength showed that the treated discontinuities had good average strengths with a cohesion value of above 3.1MN/m2 and a friction value of 38 degrees. The grouting access tunnels and boreholes were also backfilled with concrete.

3.6 Effect of Treating the Discontinuities

If now, we consider the deleterious mechanisms that have been minimised or eliminated by this treatment, we have the following by consideration of row 4 and column 4 in the total 12x12 matrix.

Matrix row 4 interactions

4,1	Treated discontinuities lead to better overall environment.
4,2	Joint movement inhibited, less effect on intact rock.
4,3	Strong joints inhibit formation of new joints.
4,4	Discontinuity mechanical properties - enhanced by treatment described.
4,5	Stiffer discontinuities give better rock mass properties.
4,6	Treated discontinuities have less effect on the *in situ* stress.
4,7	Filled discontinuities inhibit water flow.
4,8	Stronger discontinuities give safer slopes.
4,9	Increased cohesion allows higher slopes
4,10	Stronger joints allow closer proximate disturbance.
4,11	Treated joints require less support and maintenance.
4,12	Stronger joints allow greater flexibility during construction.

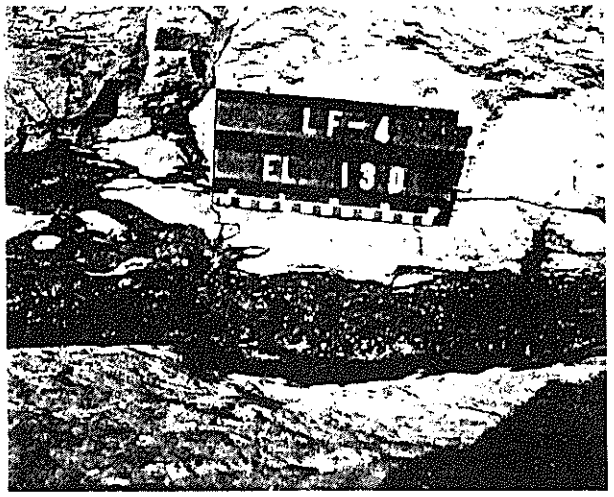

Figure 5 Typical clay filled discontinuities in the rock mass

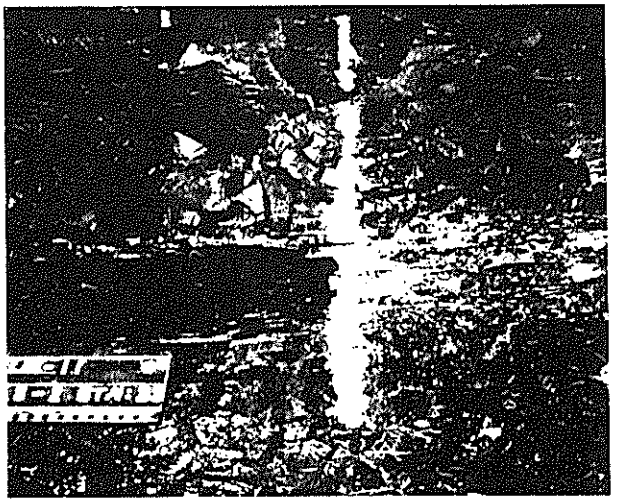

Figure 6 Washing out the clay in the discontinuity

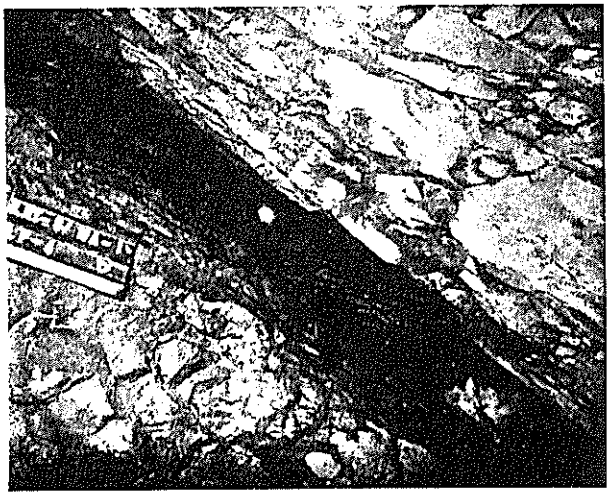

Figure 7 The 'cleaned' discontinuity

Matrix column 4 interactions

1,4	The overall environment has less effect on the discontinuities.
2,4	Weak intact rock has less effect on discontinuities.
3,4	Number of effective discontinuities reduced.
4,4	Discontinuity mechanical properties enhanced
5,4	Discontinuities less affected by mass behaviour.
6,4	Discontinuities less affected by *in situ* stress.
7,4	Discontinuities less affected by water flow.
8,4	Position of slope will not affect discontinuities
9,4	Discontinuities not susceptible to high slope effects.
10,4	Discontinuities less affected by blasting.
11,4	Less support required.
12,4	Many construction problems minimised.

We have discussed the interaction matrix row and column associated with just one parameter. Naturally, in a full application of this system, we would consider all the possibilities, and indeed the significance of both the parameters and the interactive mechanisms in the context of geotechnical risk. Moreover, this would be a continuing process, from the start of site investigation right through to the monitoring and remedial action phase.

4. CONCLUSIONS

In this paper, we have had the opportunity to briefly present the results of an on-going, long-term, research programme aimed at developing a structured approach to all rock engineering. This methodology has the acronym REMIT/RESPONSE. *Inter alia*, this allows direct identification of geotechnical parameter significance, the assessment of sub-system risk, and the consequential overall system risk - as linked to critical parameters and mechanisms by using the interaction matrix described. We illustrated how this methodology can operate via one specific case example. The research will continue to make the evaluation of risk more explicit.

5. ACKNOWLEDGEMENTS

The authors are very grateful to the RET-SER Engineering Agency for providing all the photographs presented in this paper. The research that led to the development of these ideas has occurred over many years and has been partially supported by both the US & UK Governments.

6. REFERENCES

1. Hudson J. A., "Rock Engineering Mechanisms Information Technology (REMIT): Part I - The Basic Method" Proceedings of the 7th International Congress on Rock Mechanics, Aachen, Germany, 1991.

2. Arnold P. N., Hudson J. A. & Tamai A. "Rock Engineering Mechanisms Information Technology (REMIT): Part II - Illustrative Case Examples" Proceedings of the 7th International Congress on Rock Mechanics, Aachen, Germany, 1991.

3. Feitsui Reservoir Administration Bureau, Taiwan Power Company, Sinotech Engineering Consultants Inc, RET-SER Engineering Agency, "Feitsui Reservoir Project", ASCE International Convention, San Francisco, 53p, 1990.

4. Hudson J. A., "Atlas of Rock Engineering Mechanisms: Part II - Slopes" Rock Mechanics Information Service, Imperial College, London 1991.

A Point Estimate Method for Calculating the Reliability Index of Slopes

K.S. LI
B.Sc. (Eng.), Ph.D., M.I.E.(Aust)
Lecturer, Department of Civil and Maritime Engineering, University College, University of New South Wales

SUMMARY: A point estimate method is developed for calculating the reliability index of slopes. The new point estimate method has the same order of accuracy as Rosenblueth's method which is commonly used for geotechnical reliability analysis, but the proposed method is much more efficient.

1. INTRODUCTION

In current probabilistic approaches to slope analysis, the safety of a slope is usually measured by the reliability index β which is defined as

$$\beta=\frac{\mu_F}{\sigma_F} \tag{1}$$

where μ_F and σ_F are respectively the mean value and standard deviation of the factor of safety F. The usual approach for calculating μ_F and σ_F is based on the Taylor's series expansion about the mean values of the random variables (1). This method requires the calculation of derivatives of F. Very often, difficulties arise in obtaining these derivatives because the factor of safety function $F(\underline{X})$, where X is the collection of random input parameters, is either too complex or it cannot be expressed in an explicit mathematical form (e.g. $F(X)$ may represent a program which computes the factor of safety of a slope for a given set of input parameters X). In this case, it would be convenient to use a point estimate method (PEM) which does not require the calculation of derivatives.

This paper reviews the existing point estimate methods and proposes a new PEM which is much more efficient than the PEM developed by Rosenblueth (25),(26) commonly used for probabilistic analysis of slopes.

2. PROBABILISTIC MODELLING OF SOIL PROPERTIES

Before reviewing the existing PEMs, it is necessary to discuss the existing approaches to probabilistic modelling of soil properties because the misuse of PEM in some of the existing publications on probabilistic analysis of slopes is related to incorrect modelling of soil properties. In probabilistic analysis of slopes, an approach exists in which the random variation of a soil property within the soil profile is represented by one single random variable (19),(20),(21),(22),(24),(29),(30). This approach is referred to as the single-random-variable (SRV) approach in the present paper. As illustrated in Fig.1(a), the SRV approach implies that all realisations of the soil property are the same at all location, although the exact magnitude of the realisation remains random based on this model. As pointed by the author in many occasions (6),(10),(12),(13), this approach is erroneous because if the model is correct, the actual magnitude of the soil property at all locations within the soil profile can be determined with absolute certainty by measuring the value of the soil property using one sample

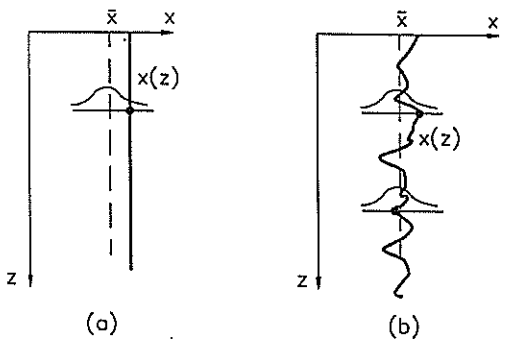

Fig.1 Probabilistic modelling of soil profile

taken anywhere within the profile. Unfortunately, the SRV approach is still being used for probabilistic analysis of slopes.

A more realistic approach is to model a soil profile as a random field as shown in Fig.1(b). In this model, the values of the soil property at different locations are treated as separate random variables. Although the concept of random field has been used for a long time in mining engineering (18), it has only been introduced to soil engineering in the early 1970s, notably by Cornell (3), Lumb (16),(17) and by Vanmarcke (28).

The use of the SRV approach will result in a gross overestimation of the failure probability of slopes (8),(12), (13),(15) because it ignores the variance reduction due to spatial averaging. This can be discerned by a simple example of a homogeneous cohesive slope with a planar slip surface. The shear resistance R along the slip surface of length L can be expressed as $R=L\cdot c_L$ where c_L is the spatial average of the undrained shear strength c_u along the slip surface. It is assumed that c_u has a constant mean trend versus depth as shown in Fig.1.

If the SRV approach is used, c_L is equal to c_u because the undrained shear strength has the same magnitude everywhere within the soil profile. Therefore $\mathrm{var}\{c_L\}=\sigma^2$ where σ^2 is the variance of c_u. In reality, the variation of c_u is similar to that shown in Fig.1(b). A low value of c_u at one location is compensated by a high value at another location along the slip surface. As a result, the variability of the spatial average is less than that of the point property due to the compensating

effect. The variance of c_L can be expressed as $\sigma^2 \cdot \Gamma^2(L)$ where $\Gamma^2(L)$ is the variance reduction factor which can be approximated by δ/L (28). δ is the scale of fluctuation. It is a measure of the spatial extent within which a soil property exhibits a strong autocorrelation.

In the SRV approach, soil properties are assumed to be perfectly correlated because the values of a soil property are the same at all locations within the soil profile. This corresponds to an infinitely large scale of fluctuation. In practice, the scale of fluctuation is typically of the order of a few metres (14). Therefore, the variance reduction due to spatial averaging is very significant. For instance, if δ=2m, the variance reduction factor for a 10m long slip surface is about 0.2. The variance of the spatial average is therefore only one-fifth of the value based on the SRV approach.

The SRV approach grossly overestimates the variability of spatial averages of soil properties, giving an unrealistically high failure probability. For instance, Matsuo & Kuroda (19) reported failure probabilities of slopes of the order of 20 to 40% for the typical range of factor of safety of 1.2 to 1.4.

The random field model which gives a more realistic prediction of failure probability of a slope is now well accepted by many researchers as a useful model for probabilistic modelling of soil profiles (1),(8),(12),(15),(31). Unfortunately, the SRV approach is still being used by soil engineers who are unaware of the random field model or by some researchers who ignore the development of the more realistic albeit slightly more difficult random field model. The continued use of the SRV approach gives practitioners, such as Peck (23), the feeling that the discipline of geotechnical reliability has not reached maturity because the high failure probability predicted by this approach is obviously incompatible with the observed frequency of failures.

2. POINT ESTIMATE METHODS

Point estimate methods refer to those methods which enable the statistical moments of a random function $f(\mathbf{X})$ to be calculated using the values of $f(\mathbf{X})$ at a specific set of values of $\mathbf{X}$. An accurate and efficient PEM has been developed by Evans (4),(5), and also discussed in (11) and (16), for functions with independent random variables. Although Evans' method is accurate, it is of limited use in geotechnical reliability analysis because soil properties are spatially autocorrelated and therefore not statistically independent.

Rosenblueth (25),(26) developed a 2-point PEM for correlated random variables in which the joint probability density of $\mathbf{X}$ is assumed to be concentrated at points in the 2^n hyperquadrants of the space defined by $\mathbf{X}$. The expected value of $f(\mathbf{X})$ is obtained by summing the product of $f(\mathbf{X})$ and the probability content of $\mathbf{X}$ for all $\mathbf{X}$ in the 2^n hyperquadrants. Rosenblueth's method involves 2^n evaluations of $f(\mathbf{X})$. As the number of evaluations increases exponentially with n, the method becomes impracticable when n is large.

Rosenblueth's method is commonly used for probabilistic analysis of slopes by researchers who adopt the SRV approach (20),(21),(22). If the SRV approach is used, the number of random variables will be small and so will be the number of evaluations of F required for the implementation of Rosenblueth's method. However, if one accepts the fact that soil profiles should be modelled as random fields, the number of random variables involved in slope stability analysis will be very large. Consider a slope which is analysed by the method of slices. If the soil properties are modelled as random fields, the spatial averages of strength parameters c', $\tan\phi'$ and the soil density γ for each slice should be modelled as separate random variables, giving a least $3n$ random variables for n slices. If there are 10 slices, the use of Rosenblueth's 2-point method will then require at least 2^{30} or 1704 million evaluations of F. This is hardly feasible in practice.

3. A NEW POINT ESTIMATE METHOD

A new PEM has recently been developed by Li (7). The new PEM has the same order of accuracy as Rosenblueth's 2-point for multivariate functions, but it is more efficient. It enables the reliability index of a slope to be calculated using a much smaller number of evaluations of F. The formulation of the new PEM presented herein is different to that described in Li (7), but the final result is the same.

Given the first- and second-order statistical moments of the random variables, an exact expected value can only be obtained if $f(\mathbf{X})$ is of at most a quadratic polynomial which can be expressed in the following general form.

$$f(\mathbf{X}) = f(\boldsymbol{\mu}) + \sum_i a_i(x_i-\mu_i) + \sum_i b_i \cdot (x_i-\mu_i)^2 + \sum_{ij} c_{ij}(x_i-\mu_i)\cdot(x_j-\mu_j) \tag{2}$$

where μ_i is the mean value of x_i and $\boldsymbol{\mu}=(\mu_1,\mu_2,..,\mu_n)$ for a function of n variables. Taking expectation on both sides of (2), we obtain

$$\mathrm{E}[f(\mathbf{X})] = f(\boldsymbol{\mu}) + \sum_i b_i \cdot \sigma_i^2 + \sum_{ij} c_{ij} \cdot \sigma_i \cdot \sigma_j \cdot \rho_{ij} \tag{3}$$

where σ_i is standard deviation of x_i and ρ_{ij} is the correlation coefficient between x_i and x_j.

Define $f(..,\pm1,..,\pm1,..)=f(..,\mu_i\pm\sigma_i,..,\mu_j\pm\sigma_j,..)$, it can be proved that

$$f(\boldsymbol{\mu}) + \sum_i b_i \cdot \sigma_i^2 = \frac{1}{2^n}\sum_{p=0}^{1}\sum_{q=0}^{1}\cdots\sum_{s=0}^{1} f((-1)^p,..,(-1)^q,..,(-1)^s) \tag{4}$$

$$c_{ij}\cdot\sigma_i\cdot\sigma_j = \frac{1}{2^n}\sum_{p=0}^{1}\cdot\underbrace{\sum_{q=0}^{1}}_{i\text{th term}}\cdot\underbrace{\sum_{r=0}^{1}}_{j\text{th term}}\cdot\sum_{s=0}^{1}\eta\cdot f((-1)^p,..,(-1)^q,..,(-1)^r,..,(-1)^s) \tag{5}$$

where η=1 if $q+r$ is even and η=−1 if $q+r$ is odd. Substitution of (4) and (5) into (3) yields the 2-point estimates developed by Rosenblueth (25) for multivariate functions. The procedure described in (4) and (5) is not an efficient way for obtaining the different terms in (3). It requires a total of 2^n evaluations of $f(\mathbf{X})$. A more efficient PEM can be obtained using the following procedure.

Define $f_i(x_i)=f(\mu_1,..,\mu_{i-1},x_i,\mu_{i+1},..,\mu_n)$. According to (2), $f_i(x_i)$ can be expressed as:

$$f_i(x_i) = f(\boldsymbol{\mu}) + a_i\cdot(x_i-\mu_i) + b_i\cdot(x_i-\mu_i)^2 \tag{6}$$

Since $f_i(x_i)$ is a quadratic function in x_i, application of the 2-point estimate developed by Rosenblueth (25) for a univariate function to (6) will yield the exact expectation of $f_i(x_i)$. Therefore,

$$\mathrm{E}[f_i(x_i)] = \frac{1}{2}[f_i(x_i^+) + f_i(x_i^-)] = f(\boldsymbol{\mu}) + b_i\cdot\sigma_i^2 \tag{7}$$

where $x_i^+=\mu_i+\sigma_i$, $x_i^-=\mu_i-\sigma_i$. Summing (7) for all i, we obtain

$$f(\mu)+\sum_i b_i\cdot\sigma_i^2=(1-n)\cdot f(\mu)+\frac{1}{2}\sum_i [f_i(x_i^+)+f_i(x_i^-)] \qquad (8)$$

Eq.(8) gives the first two terms on the right hand side of (5). To obtain the last term of (3), it is necessary to calculate the coefficient c_{ij}. It can be easily proven that $c_{ij}=\partial^2 f(\mathbf{X})/\partial x_i\partial x_j$ for a quadratic function. This derivative can be obtained by the following finite difference formula.

$$c_{ij}=\frac{f_{ij}(x_i^+,x_j^+)-f_i(x_i^+)-f_j(x_j^+)+f(\mu)}{\sigma_i\cdot\sigma_j} \qquad (9)$$

where $f_{ij}(x_i^+,x_j^+)=f(\mu_1,..,\mu_{i-1},x_i^+,..,\mu_{j-1},x_j^+,..,\mu_n)$. By substituting the results of (8) and (9) into (3), the following formula is obtained.

$$E\{f(X)\}=(1-\frac{3n}{2}+\frac{\rho}{2})\cdot f(\mu)+\frac{1}{2}\sum_i [(3-2\cdot\rho_i)\cdot f_i(x_i^+)+f_i(x_i^-)] +\sum_{i<j} f_{ij}(x_i^+,x_j^+)\cdot\rho_{ij} \qquad (10)$$

where $\rho_i=\Sigma_j\,\rho_{ij}$, $\rho=\Sigma_i\,\rho_i$ and $\rho_{ii}=1$ by definition. Eq.(10) only requires $(n^2+3n+2)/2$ evaluations of $f(\mathbf{X})$ as compared to 2^n evaluations for Rosenblueth's 2-point PEM. The proposed PEM is more efficient than Rosenblueth's method for $n>3$ and is much more so when n is large. If the random variables are independent, Eq.(10) can be simplified to the following PEM which only requires $2n+1$ evaluations of $f(\mathbf{X})$.

$$E\{f(\mathbf{X})\}=(1-n)\cdot f(\mu)+\frac{1}{2}\sum_i [f_i(x_i^+)+f_i(x_i^-)] \qquad (11)$$

If the calculation of $f(\mathbf{X})$ is time consuming, it is preferable to transform the random variables $\mathbf{X}$ into a new set of uncorrelated random variables, say $\mathbf{Z}$, by means of an orthogonal transformation. In this case, the expected value of $f(\mathbf{X})$ can be obtained by applying (11) to the function in the transformed parameter space $\mathbf{Z}$ (8).

5. ILLUSTRATIVE EXAMPLE

The example used in this study is shown in Fig.2. Both the SRV approach and the random field model are used. The mean value of F can be calculated using the proposed PEM by taking $f(\mathbf{X})=F$. Similarly, the variance and hence the standard deviation of F can be obtained by taking $f(\mathbf{X})=(F-\mu_F)^2$. The reliability indices obtained from these two approaches are compared.

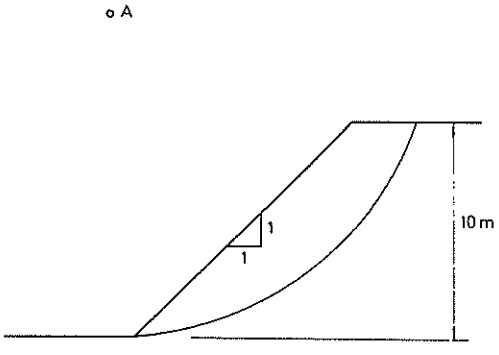

Fig.2 Details of illustrative example

The input parameters are shown in the following table. For simplicity the cross-correlation of soil properties is neglected, i.e. cov{c',tanϕ'}=0 and so on.

Soil property	mean value	coeff. of variation
c'	8 kPa	20%
tanϕ'	tan30°	10%
γ	18 kN/m^3	5%

When using the random field model, the following autocorrelation function is assumed for all the soil properties.

$$\rho(\tau_x,\tau_y)=e^{-0.4\cdot(\tau_x+\tau_y)}$$

where τ_x and τ_y are respectively the lag distances in the horizontal and vertical directions in metres. An approximate Morgenstern and Price's method based on the condition of overall moment equilibrium is used, assuming a constant interslice function and a value of $\lambda=0.6$. The moment is taken about point A in Fig.2. The method of analysis is described in detail elsewhere (12),(13),(15).

The reliability indices based on the SRV approach and the random field model are 1.882 and 3.144 respectively. The SRV approach gives a much lower reliability index of the slope. This shows clearly the importance of using the correct approach for modelling the spatial variability of soil properties. The reliability index based on the SRV approach can also be obtained using Rosenblueth's method due to the small number of variables involved. The result is 1.880 which is very close to the value obtained from the proposed PEM. This is to be expected because the PEM based on (10) has the same order of accuracy as Rosenblueth's method.

6. CONCLUSIONS

The limitations of the existing point estimate methods are discussed. It is observed that the commonly used 2-point PEM developed by Rosenblueth is too efficient for use in geotechnical reliability analysis. A more efficient point estimate method is proposed for calculating the reliability of slopes.

7. REFERENCES

1. Alonso, E.E. "Risk Analysis of Slopes and its Application to Slopes in Canadian Sensitive Clays", Geotechnique, Vol.26, pp.453-482.

2. Benjamin, J.R. and Cornell, C.A. "Probability, Statistics and Decision for Civil Engineers", NY:McGraw Hill, 1970.

3. Cornell, C.A. "First-order Uncertainty Analysis of Soils Deformation and Stability", Proc. 1st Intl. Conf. Application of Statistics and Probability in Structural and Soil Engineering, Hong Kong, 1971, pp.129-144.

4. Evans, D.H. "An Application of Numerical Integration Technique to Statistical Tolerancing", Technometics, Vol.9, 1967, pp.41-446.

5. Evans, D.H. "An Application of Numerical Integration Technique to Statistical Tolerancing III - General Distributions", Technometics, Vol.14, 1972, pp.25-35.

6. Li, K.S. "Fallacies of Current Probabilistic Approaches to Progressive Slope Failure", Proc. 6th Intl. Conf. Application of Statistics and Probability in Structural and Soil Engineering, Mexico, 1991.

7. Li, K.S. "A Point Estimate Method for Calculating Statistical Moments", Research Report, Dept. of Civil and Maritime Engineering, University College, UNSW, 1991.

8. Li, K.S. "Reliability Index for Probabilistic Slope Analysis", Research Report, Dept. of Civil and Maritime Engineering, University College, UNSW, 1991.

9. Li, K.S. "Point Estimate Methods in Probabilistic Analysis", Research Report, Dept. of Civil and Maritime Engineering, University College, UNSW, 1991.

10. Li, K.S. "Point Estimate Methods in Geotechnics", Proc. Asian Pacific Conf. on Computational Mechanics, Hong Kong, 1991.

11. Li, K.S. and Lumb, P. "Reliability Analysis by Numerical Integration and Curve Fitting", Structural Safety, Vol.3, 1985, pp.29-36.

12. Li, K.S. and Lumb, P. "Probabilistic Design of Slopes", Canadian Geotechnical Journal, Vol.24, 1987, pp.520-535.

13. Li, K.S. and White, W. "Reliability Index of Slopes", Proc. 5th Intl. Conf. on Application of Statistics and Probability in Soil and Structural Engineering, Vol.2, 1987, pp.755-762.

14. Li, K.S. and White, W. "Probabilistic Characterization of Soil Profiles", Research Report, Dept. of Civil and Maritime Engineering, University College, UNSW, 1987.

15. Li, K.S. and White, W. "Probabilistic Approaches to Slope Design", Research Report, Dept. of Civil and Maritime Engineering, University College, UNSW, 1987.

16. Lumb, P. "Application of Statistics in Soil Engineering", in I.K.Lee (ed.) Soil Mechanics - New Horizons, 1974, pp.44-111.

17. Lumb, P. "Spatial Variability of Soil Properties", Proc 2nd Intl. Conf. on Application of Statistics and Probability in Soil and Structural Engineering, pp.397-421.

18. Matheron, G. "Principles of Geostatistics", Economic Geology, Vol.58, 1963, pp.1246-1266.

19. Matsuo, M. & Kuroda, K. "Probabilistic Approach to Design of Embankments", Soils and Foundations, Vol.14, 1974, pp.1-17.

20. McGuffey, V., A-Grivas, D., Iori, J. and Kyfor, Z. "Conventional and Probabilistic Embankment Design", J. Geo. Eng., ASCE, Vol.108, 1982, pp.1246-1254.

21. Moon, A.T. "Probabilistic Slope Stability Analysis Using Rosenblueth's Method", Unpublished Report 1984/53, Tasmania Department of Mines, 1984, 16p.

22. Nguyen, V.U. and Chowdhury, R.N. "Simulation for Risk Analysis with Correlated Variables", Geotechnique, Vol.35, 1985, pp.47-58.

23. Peck, R.B. "The Selection of Soil Parameters for the Design of Foundations", Sociedad Mexicana de Mecanica de Suelos, 1975.

24. Priest, S.D. and Brown, E.T. "Probabilistic Stability Analysis of Variable Rock Slopes", Trans. Inst. Min. & Metallurgy (Sec. A: Mining Industry), Vol.92, 1983, pp.A1-A12.

25. Rosenblueth, E. "Point Estimates for Probability Moments", Proc. Nat. Acad. Sci. Mathematics, Vol.72, No.10, 1975, pp.3812-3814.

26. Rosenblueth, E. "Point Estimates for Probability", Applied Mathematical Modelling, Vol.5, 1981, pp.329-335.

27. Tobutt, D.C. and Richards, E.A. "The Reliability of Earth Slopes", Int. J. Num. Analy. Methods in Geomech., Vol.3, 1979, pp.323-354.

28. Vanmarcke, E.H. "Probabilistic Modeling of Soil Profiles", J. Geo. Eng., ASCE, vol.103, 1977, pp.1227-1246.

29. Wolff, T.F. "Embankment Reliability Versus Factor of Safety: Before and After Slide Repair", Int. J. Num. and Analy. Methods in Geomech., Vol.15, 1991, pp.41-50.

30. Young, D.S. "A Generalized Probabilistic Approach for Slope Analysis", J. Mining Eng., Vol.3, 1985, pp.215-228.

31. Yucemen, M.S. and Al-Homond, A.S. "Probabilistic Three-Dimensional Analysis of Slopes", Structural Safety, Vol.9, 1990, pp.1-20.

Limit State Design of Pile Foundations: A Probabilistic Appraisal

S-C.R. LO
B.Sc.(Eng.), Ph.D., M.I.E.Aust.
Senior Lecturer, University College, University of New South Wales
K.S. LI
B.Sc.(Eng.), Ph.D., M.I.E.Aust.
Lecturer, University College, University of New South Wales
I.K. LEE
B.C.E., M.Eng.Sc., Ph.D., F.I.E.Aust
Professor of Civil Engineering, University College, University of New South Wales

SUMMARY: A draft revised Australian piling code has recently been issued for public comment. In the draft piling code, a limit state approach is used for the design of pile foundations. The purpose of this paper is to review the probabilistic theory for the limit state method. The procedure for determining the partial safety factor in the limit state design format is described and the implementation of the limit state design format is discussed with reference to the draft piling code.

1. INTRODUCTION

The concept of overall factor of safety is traditionally used in pile design. Such a design philosophy was enshrined in Australia by the original Australian Piling Code AS2159-1978. However, there is a strongly supported trend towards the use of limit state design in which a series of partial safety factors are used in lieu of the overall factor of safety. It is generally believed that a well formulated limit state design code can give better control on the reliability of design. Most structural design codes are now based on limit state design.

One can argue that limit state procedures should also be used for pile design. Indeed, the draft unified European code on geotechnical design (Euro 7) has already adopted the limit state method for geotechnical design. A committee was appointed by Standards Australia in 1988 to revise the current Australian Piling Code and the draft consequent code, issued for public comment in August 1991, will hereafter be called the draft piling code. To improve the control on reliability level of pile designs and maintain consistency with the recently introduced structural design codes (AS3600, AS4100), a decision was made to adopt the limit state method in the draft revised piling code. The partial factors for loadings recommended in the draft code are based largely on the structural design code AS3600 whereas the partial factors for the resistance of the pile, expressed as strength reduction factors, were deduced mainly from calibration with the existing piling code AS2159.

The characteristics of the uncertainties involved in pile design are different from those involved in structural design. The approach used for the formulation of the limit state piling code may need to be different from those in structural codes. At present, study on the limit state design of pile foundations is very limited. More research is urgently needed for a probabilistic appraisal of the limit state approach.

The objective of this paper is to discuss the use of limit state method for pile design based on rigorous probability theory. Special reference is made to the draft Australian Piling Code. Parametric studies are performed to examine the effectiveness of the limit state method in the control of the reliability level of pile design.

2. LIMIT STATES AND PERFORMANCE FUNCTION

A pile foundation is designed to satisfy certain requirements such as the ability to support the structure without failure and excessive settlement. Each of these requirements is called a 'limit state'. A failure is interpreted as the violation of a limit state. Here, failure is interpreted in the most general sense. If the limit state is related to settlement, a failure is said to occur if the settlement is excessive. The paper will focus on the ultimate resistance of pile foundations.

The safety-failure state of a pile foundation can be described by a performance function $G(\mathbf{X})$ where $\mathbf{X}$ is the collection of input parameters. The performance function is defined in such a way that failure is implied by the condition of $G(\mathbf{X})<0$ and safety by $G(\mathbf{X})>0$. The hypersurface defined by $G(\mathbf{X})=0$ is termed the limit state boundary.

3. LEVELS OF PROBABILISTIC ANALYSIS

Probabilistic analysis can be classified into three different levels depending on the rigour and level of sophistication of the analysis. To discuss the difference between the three levels of analyses, we will use a single pile as an illustrative example. If the ultimate capacity of the pile is R and the applied loading (or actions) is S, the performance function can be written as

$$G(\mathbf{X})=R-S \tag{1}$$

It is assumed that R and S are independent random variables. The mean value, standard deviation and coefficient of variation (COV) of R are denoted respectively by μ_R, σ_R and V_R. Similar notations are used for S and all other random variables discussed later.

3.1 Level 3 methods

A Level 3 analysis is the most complete method of risk analysis in which all the random variables are represented by their joint probability density function and the failure probability is evaluated directly by integrating the probability density function over the failure domain $G(\mathbf{X})<0$ as indicated in Fig.1. In foundation engineering, the joint probability density function of the random input parameters is seldom known and a Level 3 analysis cannot be performed in practice.

3.2 Level 2 methods

Define the centroid of the random variables to be the point $\mu=(\mu_1,\mu_2,..,\mu_n)$ where μ_i is the mean value of the ith random

variable. If the centroid is farther away from the limit state boundary, the probability of failure, which is numerically equal to the volume ABCD under the probability density function as shown in Fig.1, will become smaller. Therefore, the minimum distance between the centroid and the failure boundary can be used as a measure of the safety level of the design. Intuitively, the minimum distance can be defined in the parameter space X. However, such a definition will not give rise to a consistent measure of reliability. Consider two designs with the same minimum distance OP from the limit state boundary as shown in Fig.2(a) & (b). The variability of R and S is higher for the design in Fig.2(a) than for the second design in Fig.2(b). Obviously, the first design has a higher failure probability even though the centroids are both at the same distance from the failure boundary for two designs. To obtain a consistent measure of risk, Hasofer & Lind (1) suggested that the variables be transformed to the uncorrelated standardised parameter space Z as shown in Fig.2(c). In this case, the minimum distance OD in Fig.2(c) is independent of the variability of the input parameters and can therefore be used as a consistent measure of the safety level of the design. The distance OD is defined as the reliability index β and is now commonly used both in structural and geotechnical reliability analyses as a measure of the reliability level of a system. If the random variables are normally distributed, the failure probability P_f can be related to the reliability index by the following relationship (2).

$$P_f=\Phi(-\beta) \tag{2}$$

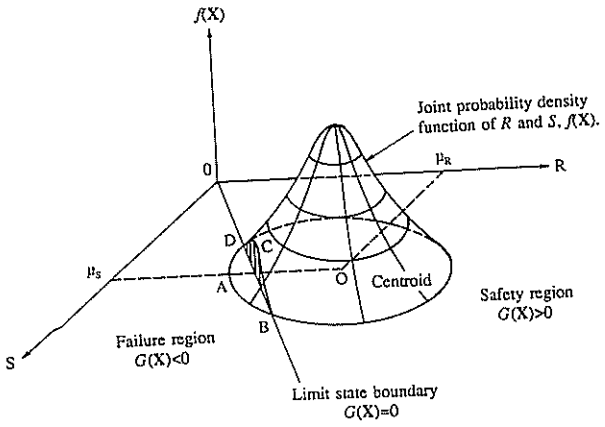

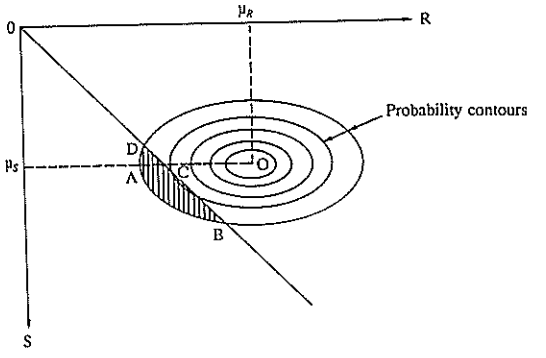

Fig.1 Joint probability density function of R and S

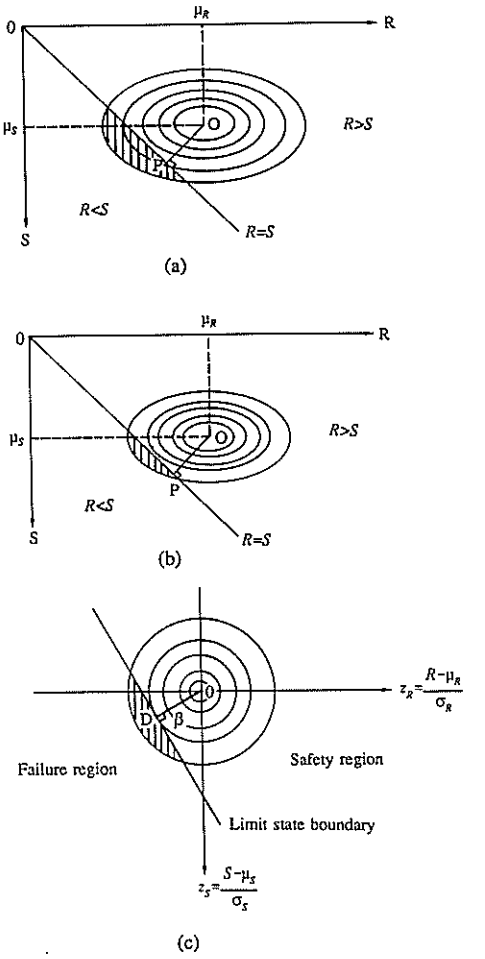

Fig.2 Level 2 design

A probabilistic analysis based on the concept of reliability index is referred to as a Level 2 method. The value of β can be calculated using the first- and second-order statistical moments (i.e. mean values, variances and covariances) of the input parameters. These quantities can be estimated from the soil data in pile designs.

3.3 Level 1 methods

Level 1 methods include the traditional overall factor-of-safety (FOS) approach and the limit state method. At present, geotechnical designs are based almost exclusively on the overall FOS approach. A pile design is deemed to be sufficiently safe if the factor of safety, defined by the following equation, is larger than a specified minimum FOS, F_{min}.

$$F=\frac{R'}{S'} \tag{3}$$

where R' and S' are the nominal ultimate capacity and applied load determined by the designer. The procedure is equivalent to checking that the factored or allowable ultimate capacity of the pile, $R_{all}=R'/F_{min}$, is greater than the nominal load S'. Conceptually, safety analysis is effected by ensuring that the

checking point $X_d=(R_{all},S')$ satisfy the following inequality.

$$G(X_d)=G(R_{all},S')\geq 0 \qquad (4)$$

The procedure for calculating the nominal load S' is usually well defined in structural codes. However, the procedure for determining the nominal value of R is less well defined in geotechnical codes. Risk-averse geotechnical engineers tend to choose a more conservative value of R'. The minimum overall factor of safety for pile design is sometimes stipulated in foundation codes. However, the choice of F_{min} is largely based on experience rather than rigorous statistical analysis.

Due to the limitations of the overall FOS approach, there is a trend towards the use of the limit state method which can produce a more uniform level of safety for geotechnical designs. In this method, the checking point has the form $X_d=(R^*,S^*)=(\gamma_R R',\gamma_S S')$ where R^* and S^* are called the design values of R and S; γ_R and γ_S are respectively the strength reduction factor and load factor and are collectively called the partial safety factors. Safety analysis is effected by checking that the following inequality is satisfied.

$$G(\gamma_R R',\gamma_S S')\geq 0 \text{ or } \gamma_R R'\geq\gamma_S S' \qquad (5)$$

An alternative format of the form $\gamma_R R(x_i/\gamma_i)$ where x_i is an input soil parameter and γ_i is the partial safety factor on soil parameters can also be used for the design value R^*. However, the format in (5) is preferred because the relationship between the resistance R and the soil parameters is sometimes not known. An example of this is the skin friction factor 'F' for piles in sands which in an unknown function of many soil parameters.

Although the limit state method is not as effective as the Level 2 method in controlling the reliability level of foundation designs, the safety checking procedure is much simpler and welcomed by practising engineers. Furthermore, by carefully selecting the partial safety factors, the reliability level can be controlled to within reasonably narrow limits.

4. LIMIT STATE METHOD

In this section, the limit state method is examined in more detail. Referring to Fig.2(c), it can be noted that point D is a stationary point. If this point is chosen to be the checking point, the reliability index β will be least sensitive to small variations in the variability of the input parameters. Therefore, a suitable choice for the checking point X_d in the X-space will be the point corresponding to the stationary point D in the Z-space. The design values corresponding to this checking point are given as (2):

$$R^*=\gamma_R R'=\mu_R(1+\alpha_R\beta V_R) \qquad (6)$$

$$S^*=\gamma_S S'=\mu_S(1+\alpha_S\beta V_S) \qquad (7)$$

α_R and α_S are the direction cosines of checking point D in the Z-space. Re-writing the nominal values as $R'=\delta_R\mu_R$ and $S'=\delta_S\mu_S$ where δ_R and δ_S are coefficients, the partial safety factors can be obtained from the following equations according to (6) and (7).

$$\gamma_R=(1+\alpha_R\beta V_R)/\delta_R \qquad (8)$$

$$\gamma_S=(1+\alpha_S\beta V_S)/\delta_S \qquad (9)$$

Usually, the nominal ultimate capacity R' is chosen to be smaller than the mean value i.e. $\delta_R<1$ while a value higher than the mean value is adopted for the nominal load i.e. $\delta_S>1$. According to (8) and (9), the partial safety factors γ_R and γ_S depend on the variability of the input parameters if the reliability index has to be maintained at an absolutely constant level . To keep the limit state design format reasonably simple, some simplifications must be made. Two options are available. In the first option, the partial safety factors are maintained constant. In the second option, variable partial safety factors are used.

The first option is acceptable if the variability of input parameters is relatively constant for all design situations, as in structural designs. In pile designs, the foundation engineer usually has some control over the reliability of the input parameters. He can obtain more reliable estimates of the soil parameters by carrying out more extensive site investigation and soil testing. Alternatively, he can reduce the uncertainty of the design method by performing pile load tests. Therefore, V_R can vary over a range of values depending on the efforts spent in reducing the level of uncertainty in the design. Because of this, the use of a constant strength reduction factor will not be effective in controlling the reliability level of pile designs. The partial safety factors can be obtained by calibration. The procedure is best illustrated by examples.

4.1 Example 1

In this example, the partial safety factors in (6) and (7) are obtained by calibration using the following parameters.

$$V_R=0.25 \qquad V_S=0.2 \qquad \beta=3$$

A reliability index of 3 is consistent with the reliability level of structural design. The nominal values are taken to be the mean values of the random variables, i.e. $\delta_R=\delta_S=1$. Based on these information, the following results can be obtained using the procedure described elsewhere (3).

$$\alpha_R=-0.983 \qquad \alpha_S=0.186 \qquad \gamma_R=0.263 \qquad \gamma_S=1.112$$

The reliability index based on the above two options are compared. In the first option, the partial safety factors obtained from the above calibration are maintained constant for all designs. In the second option, a variable strength reduction factor is used. As discussed earlier, the stationary point in the Z-space is not sensitive to small changes in the variability of the design parameters, the value of α_R can be assumed to be constant for practical purposes. Using the value of α_R obtained from the above calibration procedure, the following relationship based on (8) can be used to determine the strength reduction factor for any given value of V_R.

$$\phi=(1+\alpha_R\beta V_R)/\delta_R=1-2.95 V_R \qquad (10)$$

Table 1 Variation of reliability index with V_R

V_R	0.15	0.2	0.25	0.3
β	2.76 (4.85)	2.96 (3.71)	3.00* (3.00)*	2.98 (2.51)

* Results from calibration

Table 1 compares the results for the two options. The values in brackets are the results based on a constant strength reduction factor. It can be observed that the use of a variable

strength reduction factor gives a much better control of the reliability level.

4.2 Example 2

In practice, R and S may consist of more than one component. The ultimate capacity is the sum of the shaft resistance R_F and bearing resistance R_B and the applied load may consist of dead load S_D and live load S_L. Therefore, a more general model for ultimate failure of a pile can be written as follows.

$$G(\mathrm{X})=R-S=R_F+R_B-S_D-S_L \tag{11}$$

The limit state format for the design loading can be expressed as $\gamma\cdot(S_D'+S_L')$ or $\gamma_D\cdot S_D'+\gamma_L\cdot S_L'$, where γ, γ_D and γ_L are load factors. The second format is commonly used in structural codes and it is logical to follow the same format in geotechnical codes. For a particular type of structures, the variability and relative magnitude of the different components of S usually vary within a fairly narrow range. Therefore, the use of constant load factors are usually adequate.

Similarly, the limit state format for the design resistance can be written as $\gamma_R\cdot(R_F'+R_B')$ or $\gamma_F\cdot R_F'+\gamma_B R_B'$ where γ, γ_F and γ_B are strength reduction factors. As discussed earlier, the variability of the resistance can vary over a range of values. Furthermore, the relative magnitude of R_F and R_B can also vary significantly. For instance, the resistance of floating piles in sand is dominated by R_F and that of piles founded on a hard stratum is controlled by R_B. A variable strength reduction factor is therefore required to control the reliability level to a reasonably constant level. The following two formats are examined in more detail.

Format A:

$$\gamma_R\cdot R'\geq\gamma_D\cdot S_D'+\gamma_L\cdot S_L' \quad \text{or} \quad \gamma_R\cdot(R_F'+R_B')\geq\gamma_D\cdot S_D'+\gamma_L\cdot S_L' \tag{12}$$

Format B:

$$\gamma_F\cdot R_F'+\gamma_B\cdot R_B'\geq\gamma_D\cdot S_D'+\gamma_L\cdot S_L' \tag{13}$$

To examine the effectiveness of these two formats in controlling the reliability level, a sensitivity analysis is performed. Both formats are calibrated using the following parameters.

V_F=0.15 V_B=0.3 V_D=0.05 V_L=0.3

$\mu_F/(\mu_F+\mu_B)$=0.5 $\mu_L/(\mu_D+\mu_L)$=0.3 β=3

$R_F'=\mu_F$ $R_B'=\mu_B$ $S_D'=\mu_D$ $S_L'=\mu_L$

where V_F and μ_F denotes respectively the COV and mean value of R_F and so on. Again, the stationary point in the **Z**-space is chosen to be the checking point in the calibration. Once the direction cosines of the checking point are determined, the variable strength reduction factor for Format A can be determined using an equation identical to (8). The COV of R can be calculated using the following relationship.

$$V_R=\sqrt{r^2\cdot V_F^2+(1-r)^2\cdot V_B^2} \tag{14}$$

where $r=\mu_F/(\mu_F+\mu_B)$. If Format B is used, the strength reduction factor are determined from the following equations.

$$\gamma_F=1+\alpha_F\cdot\beta\cdot V_F \tag{15}$$

$$\gamma_B=1+\alpha_B\cdot\beta\cdot V_B \tag{16}$$

where α_F and α_B are the direction cosines for R_F and R_B obtained from calibration.

Fig.3 shows the sensitivity of the reliability index to changes in the ratio of $r=\mu_F/(\mu_F+\mu_B)$. Format A tends to give a better control of the reliability than Format B. A sensitivity analysis has also been performed to examine the variation of β with changes in the variability of R_F and R_B and the results are shown in Fig.4 for the two extreme cases of r=0 and r=1. Again, Format A is less sensitive to changes in V_F and V_B. In summary, Format A outmatches Format B. The former is adopted in the draft piling code.

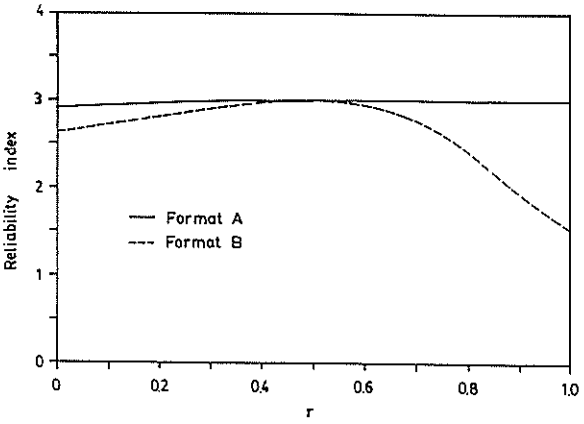

Fig.3 Variation of β with r

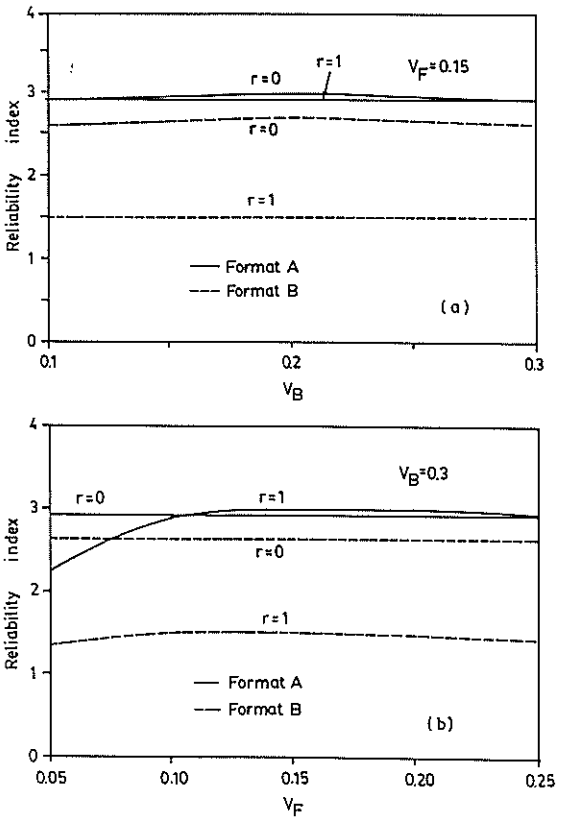

Fig.4 Variation of β with (a) V_B and (b) V_F

5. DISCUSSION

Since the above examples are based on assumed, although reasonable, values of input parameters, the partial safety factors presented in those examples should be taken as recommended values at this stage. However, the conclusions drawn from these examples should remain valid in relative terms.

The value of V_S=0.2 used in Example 1 is considered to be typical of conventional foundation loadings which are dominated by the dead load component and the value of V_R=0.25 also represents a typical level of confidence in pile design. The partial safety factors obtained from the calibration corresponds to an overall factor of safety of $F=\gamma_S/\gamma_R$=1.112/0.267=4.2. This value may seems to be high compared with that traditionally used. The discrepancy is mainly due to the fact that foundation designs are usually based on a nominal value of R' less than the mean value. For instance, the adhesion factor recommended in the current (1978) Australian piling code for piles in cohesive soils is based on more or less the lower bound values of the observed data. As a result, the nominal value R' based on this conservative estimate of adhesion factor will be significantly less than the mean value of R. δ_R is therefore less than unity and the minimum overall factor of safety based on a conservative nominal value will naturally be smaller in magnitude. This illustrates the important point that the partial safety factor will be influenced by the choice of nominal values.

Both Examples 1 and 2 clearly illustrate the need for using a variable strength reduction factor in pile design. This design philosophy has been stated although in an implicit manner in the current Australian piling code AS2159-1978 (and other foundation codes such as the British Code CP2004) because the designer is allowed to use a lower overall factor of safety depending on his judgement on the confidence level of the pile design. In the draft piling code, the designer is allowed to use a variable strength reduction factor depending on the level of certainty of the design parameters.

Example 2 suggests that it is not necessary and indeed not desirable to use separate strength reduction factors for the shaft and base resistance. The use of a single strength reduction factor is sufficient to give effective control on the reliability level provided a variable 'weighted' COV is used for V_R using (14). However, the requirement of linking the variable strength reduction factor to the variability of V_F, V_B and the ratio r is not evident in the draft piling code. From a theoretical standpoint, the level of confidence should ideally be quantified in terms of the variability of the ultimate resistance V_R. The probabilistic procedure for determining the variability of the shaft resistance V_F and that of the base resistance V_B is now well established (4),(5). The overall variability of the ultimate resistance can be obtained easily using (14). However, foundation engineers with little training in probabilistic analysis may still prefer to use a deterministic procedure for pile design. An alternative to expressing the level of confidence directly in terms of V_R will be to provide a series of tables from which the designer can obtain the confidence level for any particular type of pile design. For instance, using typical values of V_B and V_F for one type of pile design, the value of V_R and hence the confidence level can be directly related to the ratio of r using (14). A table can then be prepared to relate r to the confidence level for that particular type of pile design.

The current Australian piling code AS2159-1978 uses a lumped nominal load for design i.e. equal load factors are applied to various load components. For normal foundation loads which are dominated by the dead load, the use of equal load factors may be adequate. However, when the foundation loads are dominated by other environmental loads such as wind loads which tend to be more variable, the use of separately factored nominal loads (a format which is used in the draft piling code) will be necessary for good control of reliability level. Fig.5 shows the ratio of load factors for live load and dead load required to achieve a reliability index of 3 for different combinations of V_L and ratio of $\mu_L/(\mu_D+\mu_L)$. As the variability of live load and proportional of live load increase, a higher ratio of γ_L/γ_D is required. Hence, if γ_L/γ_D is to be maintained constant for simplicity, a 'average' ratio greater than unity is required.

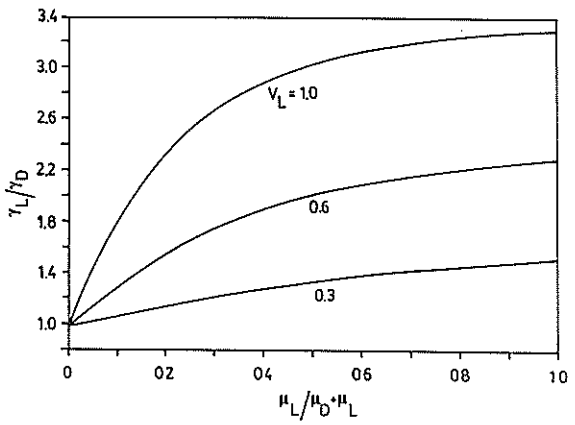

Fig.5 Variation of β with $\mu_L/(\mu_D+\mu_L)$

6. CONCLUSIONS

The probabilistic theory for the limit state method is reviewed. The partial safety factor in the limit state design can be deduced from a Level 2 probabilistic analysis using parameters that can be estimated from geotechnical data. It is observed that the use of a variable strength reduction factor is required to give effective control of the reliability level of pile designs. The limit state method provides formal procedure whereby the uncertainties involved in the design can be taken into account in the analysis. If more reliable data or design methods are used, the limit state method will allow a higher strength reduction factor and hence a less 'conservative' design.

The limit state format used by the draft piling code outmatches other limit state formats examined. A very consistent reliability level can be achieved provided that the strength reduction factor is properly correlated with the 'confidence level' of the design by a thorough statistical analysis of the relevant database. The range of dead to live load ratio for which a particular limit state format is applicable also needs to be specified.

To achieve a consistent reliability level, the confidence level of the pile capacity has to be assessed from the confidence levels of the shaft resistance and base resistance using a weighted averaging procedure as described mathematically by (14) which takes into account the relative magnitude of shaft resistance and base resistance. Such a procedure is not present in the draft piling code.

Further improvement in the control of reliability level can be achieved by using partial load factors which depend on the live to dead load ratio and characteristics of the live load.

The paper is a preliminary study on the limit state design of pile foundations. Further studies are needed and pursued by the authors.

7. ACKNOWLEDGMENT

This project forms part of a continuing research program at the Department of Civil and Maritime Engineering, University College, University of New South Wales on the application of probabilistic methods in geotechnical engineering.

8. REFERENCES

1. Hasofer, A.M. and Lind, N.C. "Exact and Invariant Second Moment Code Format", J. of Eng. Mech. ASCE, Vol.100, 1974, pp.111-121.

2. Leporati, E. "The assessment of Structural Safety", Research Studies Press, 1979.

3. Li, K.S., Lo, S-C.R. and Lee, I.K. "A Preliminary Study on Limit State Design of Pile Foundations", Research Report, Department of Civil & Maritime Engineering, University College, University of New South Wales, 1991.

4. Li, K.S., White, W., Chu,J. and Zhao, M.M. "Probabilistic Modelling of Soil Profiles and its Application in the Analysis of Pile Foundations", Chinese Journal of Geotechnical Engineering, Vol.11, No.6, 1990, pp.120-128.

5. Tang,W.H. "Uncertainties in Offshore Axial Pile Capacity", Foundation Engineering: Current Principles and Practices, ASCE, Vol.2, 1989, pp.833-847.

Reliability Analysis of Failed Slopes, a Back Analysis View of the Sensitivity to Input Parameters

J.D. ST GEORGE
B.Sc., M.Sc., A.R.S.M., M.I.M.M.
Senior Lecturer, Department of Mining Engineering, University of Auckland

1. INTRODUCTION

In probabilistic analyses the uncertainties associated with the problem are included within the framework of the analysis, therefore the risks associated with the consequences of various strategies can be evaluated in terms of selected design criteria. Extensive literature on the probability of failure related to slope analysis has been published, mostly confined to theoretical development with few trial or hypothetical slopes investigated. Those studies which have been reported require a great deal of statistical data for a full analysis and generally represent slopes which have a very low failure probability. In this work slope failures from surface coal mines are back analysed using a reliability approach.

A probabilistic model has been developed which is capable of incorporating variations in shear strength, modelling errors and watertable. The variability of the shear strength parameters were considered to be a combination of spatially correlated variations and independent components. A further refinement to include 3-D effects from end resistance and variance reduction along the failure length, provided a means of estimating the probability of failure for different lengths and volumes. These could then be compared to actual failure volumes. This paper presents a background to the techniques and the basis for the model, it then reviews the case studies and investigates the sensitivity to input variables with respect to the failure analysis.

2. UNCERTAINTIES IN SLOPE ANALYSIS

There are many variables that enter into slope analyses and with a probabilistic approach, the uncertainties associated with these variables need to be quantified and included in the analysis. Subjective uncertainties, from a lack of knowledge or information, necessitate the use of deductive reasoning and therefore will never be totally eliminated. They are usually allowed for by conservative, flexible design procedures and the observational approach advocated in many engineering projects. It would be unreasonable to expect the techniques of risk analysis and statistics to resolve problems which cannot be formally answered, and as such are not introduced directly into the analysis. Objective uncertainties which can be recognized and to some extent be quantified, are related to measured statistical or probabilistic information. The major uncertainties in a slope stability analysis arise from the natural heterogeneity in the shear strength (c and ϕ) of geological materials, structural controls on failure, water conditions and model assumptions. These are further compounded by sampling and testing techniques. Minor variations from inaccurate measurements of slope geometries and variability in material properties (i.e. density and permeability) are not treated separately as they do not influence the stability analysis to the same extent. The main contribution to these uncertainties are discussed in the following sections.

2.1. Variability in Shear Strength

Within so-called homogeneous geological units the shear strength is known to vary widely from point to point. No amount of testing can fully characterise the nature of this heterogeneity, and therefore some probabilistic uncertainty will always remain. The variability in shear strength, in most cases, is dependent on location and as such is spatially correlated. This regionalised behaviour implies that points in close proximity are strongly correlated as would be reasonable to expect from the natural processes involved in their formation or in the method of placement for man-made slopes. The correlation will diminish as the distance between points becomes larger, until the covariance between points is zero. This spatial dependence has other implications that are introduced later in the analysis. The sampling and test results present a different problem in that they contain inferential uncertainties. These are quantifiable and can be reduced to an arbitrary level by increasing the sample size. However they will also introduce bias errors for the following reasons.

During the recovery and preparation process, it is unavoidable to prevent some mechanical disturbance to the sample. Stress conditions on the boundary will change as a result of removal from the in situ stress field and little is known about the induced stresses caused by sampling. The results from laboratory shear or triaxial tests are used to predict the behaviour of a slip surface many orders of magnitude larger. The influence of macro effects or scaling remain essentially unsampled. The testing techniques present inherent differences between actual conditions and the simulated laboratory test. These problems may be partially avoided by testing large scale samples in situ, however it is difficult to exercise full control over the test environment in the field and this contributes to the overall uncertainty.

2.2. Water Conditions within Slope

Most uncertainties concerned with determining the watertable or pore pressures within a slope are from a lack of information and are therefore subjective.

The prediction of the water pressures within the slope from very limited information usually involves gross, order or magnitude assumptions about infiltration rates, position of aquifers, aquicludes, flow, permeabilities, and presence of perched aquifers or artesian conditions. Water pressures estimated from measuring sites within a slope will have a statistical uncertainty from the interpolation between measuring stations. Meteorological data introduces more variables into the problem.

2.3. Structural Controls on Failure

When the geometry of a slope failure is governed by structural features (discontinuities), for example wedge failures in rock slopes, an uncertainty is introduced at the level of the mechanism. This is because there will be variability in the dips, dip directions, spacing and length of discontinuities controlling the failure as well as those errors associated with the measurement of these parameters. With enough information there are techniques which allow for the mechanisms to be modelled probabilistically quite successfully. Unfortunately the field data is seldom available in the areas of interest and extrapolation of structural data is problematic and in itself stochastic.

2.4. Model uncertainty

Further uncertainty arises from the simplifying assumptions made in the analytical model. Therefore, even if all input parameters to a particular model were known exactly, there would be an uncertainty associated with the output. From the very nature of the simplifying assumptions in the analytical models, part of these uncertainties are biased. In the absence of any significant data the design engineer may have to make a subjective estimate for the model uncertainty.

It is apparent from the above comments that in risk assessment of a slope failure, it is only possible to model those uncertainties that are measurable, unless some 'judgement factor' is included. The risks are expressed in the form of a probability or reliability, which can then be applied to design decisions. The objective uncertainties relate to two fundamental areas in slope analysis, firstly the failure mechanism and secondly to the analysis - input parameters and calculation process. The true variation of input parameters can never be determined completely since any sampling will only be partial and the unknown inaccuracies present in testing techniques can not be quantified. This lack of information particularly in respect to the shear strength and watertable will require the use of deductive reasoning to resolve. In this paper no attempt has been made to examine the effects of structural controls on the failure mechanisms since no quantitative data was available for the case studies. The uncertainties associated with the variability in shear strength, water conditions and modelling error have been investigated within a probabilistic slope analysis.

3. MODEL DEVELOPMENT

The first stage of a probability based slope analysis is to quantify the possibility of failure, the second being to rationalise the consequence of failure. The probability of failure P(Slope failure) is denoted by P_f. The procedures for analysing slope failures are the same as in ordinary deterministic methods - limiting equilibrium, stress-deformation or plasticity models. Because of the generally sparse information available, the simplicity and wide acceptance in deterministic analyses of limiting equilibrium or slice techniques, these are favoured for probabilistic analyses. Using the factor of safety F defined as the ratio of resisting (R) to mobilising (S) forces or moments, the probability of failure is defined as $P(F < 1.0)$ or $P(R < S)$.

Initially a distinction is required between the failure probability of one specific failure surface and the slope as a whole. The P_f may refer to a specific location along the slope, for one cross section and the analysis is confined to two dimensional plane strain failures in that section. Alternatively a complete length of slope or a geologically homogeneous unit is treated as one entity, the P_f applying to the whole section. In a homogeneous material free from structural controls, there are an infinite number of kinematically possible failure surfaces for any given cross section. These will represent the family of curves, circular, log spiral or non-linear, each contributing to the overall P_f. Cornell (1971) argued that these potential failure surfaces represented components of a series system and since many of these surfaces would be in close proximity, their probabilities would be highly correlated. The overall system reliability would therefore be close to the surface with the highest P_f. Alonso (1976) has shown by a case study of circular failure in a homogeneous material that the surface with the highest P_f corresponds to that with the minimum factor of safety F. More recently Sharp (1982) and Chowdhury and Zhang (1988) have demonstrated that this is only true for certain statistical parameters.

The probability of sliding represents in a single figure the frequency of conditions that cause a particular slope geometry to fail, as a proportion of all possible conditions. In order to calculate this probability either the full distribution of the random input variables or their moments are required. These are then combined in an appropriate probability model, taking account of modelling errors, to produce the distribution of failure conditions, or its moments.

Second moment analysis has been favoured in place of full distribution methods, because no assumptions are required regarding the distributions of the input variables. Two techniques are commonly referred to in the literature: these are point estimates and the first-order second moment method (FOSM). In the latter method it is possible to model the spatial variability and the covariance between the shear strength parameters, as demonstrated by Alonso (1976) and therefore this method was preferred. To analyse failure geometries of any shape, the simplified Janbu method, Janbu(1973) was formulated in a FOSM approach. Approximations of the mean and variance of the factor of safety are determined from first-order expansion terms of a Taylor series. Full details of the equations are given in St George (1991). In all second moment methods it is necessary to assume some distributional form of the factor of safety or safety margin to calculate a probability of failure. It is convenient to assume a normal distribution and calculate probabilities from standard tables. For comparative purposes the reliability index β is a useful parameter, defined from the mean and standard deviation of the factor of safety by

$$\beta = \frac{\bar{F}_s - 1}{\sigma_F} \qquad \ldots.(1)$$

To incorporate the spatial variability of the shear strength it is necessary to calculate the covariance between points within the slip surface. This requires some correlation function to be defined. An approach from the theory of regionalised variables was developed to estimate this covariance. Firstly the spatial behaviour must be characterised. This information is contained in the form of a variogram which is the compliment to the covariance function. Normally the process involves fitting parameters for a number of general models to the field data and then selecting the most appropriate model. Since it was the intention here to investigate the influence of spatial variability a general model was selected and the parameters were varied. The exponential variogram model was chosen because it has a convenient mathematical form and is a monotonically increasing function with a sill (C). This sill represents the independent variance and occurs when point spacing exceeds the range of influence (a). A nugget effect C_o is included which accounts for the non-spatial contribution to the overall variance. The general form of the exponential function variogram is

$$\gamma(h) = C_o + C(1 - e^{-h/a}) \qquad \ldots.(2)$$

If either a = 0 or C = 0, the model reduces to the spatially uncorrelated component C_o.

A quasi 3-D approach developed by Vanmarcke (1977b) incorporates the spatial variability along the slope together with the resistance at the lateral margins of the potential failure and produces a 3-D probability of failure. This approach has a lot of appeal since it only requires the mean and variance from the 2-D plane strain solutions and variance reduction function, end resistance and failure length (b) to find the 3-D P_{fb}. The variance reduction function Γ^2 takes into account the spatial variability along the slope. To make this consistent with the spatial model in 2-D, a function was chosen which modelled the same characteristic behaviour as the exponential variogram. Vanmarcke (1977a) has shown that the reduction function $\Gamma(b)$ defined as

$$\Gamma(b) = \begin{cases} 1 & b \le \delta \\ \left(\frac{\delta}{b}\right)^{\frac{1}{2}} & b \ge \delta \end{cases} \qquad \ldots.(3)$$

provides a close approximation to the exponential correlation function if δ the scale of fluctuation is equal to twice the range.

In order to calculate the resistance at the ends of the failure, assumptions regarding the strength and stress conditions are required. It is inevitable that these will only be approximate, and depend on localized conditions. Initially the stress distribution on the lateral margins is assumed to result from active earth pressures and the resisting forces at each end may be calculated using the shear strength. A lateral release factor (α) is proposed which takes into account structural and geometrical effects on release. The total end resistance is determined from $Re = \alpha_1 Re_1 + \alpha_2 Re_2$ where the subscripts refers to each end of the failure. Spatial variability of the lateral margins was neglected as its contribution to the overall variance would be small.

The contribution to the total resistance from the strength of the lateral margins is usually ignored in conventional 2-D analyses because the resulting F is conservative. In the 3-D probabilistic model, as the failure width (b) increases the contribution from the lateral margins as a proportion of the total resistance, will reduce. At the limit for long slope widths the 3-D safety factor F_b will be equivalent to the plane strain 2-D F. Also as the failure width (b) increases, the variance of the 3-D factor of safety is attenuating from the unit width variation. Therefore provided F > 1.0, short failure widths will have low 3-D probabilities of failure P_{fb} due to a high F_b from the end resistance and the P_{fb} for long failures will also be small due to the low variance in F_b. This variance reduction concept is applicable whether or not the variables are spatially correlated. Vanmarcke (1977b) derived a critical width b_c for a cylindrical failure area which minimises the reliability index and consequently maximises P_{fb}. Using the reduction function in equation (3), the critical width b_c is approximated by

$$b_c = \frac{F}{F - 1} d_o \qquad \ldots.(4)$$

Where d_o is a function of end section geometry and the failure surface and F is the plane strain factor of safety. For these assumptions b_c is independent of the rate of variance reduction.

Both the 2-D and 3-D probabilistic models have been programmed in Fortran 77. Besides the slope and failure surface geometries the input parameters are as follows:

Shear strength:	Mean and standard deviation of c and ϕ for each material and lateral margins.
Spatial:	Sill C, nugget effect C_o and range of influence a

Failure width b
Lateral release factor α
Model error
Coefficient of watertable variation

The results from each analysis produced a 2-D F and a 3-D F_b with their respective reliability indices and probabilities of failure, making the assumption of a normal distribution. The critical failure width defined in equation (4) was also calculated, approximating d_o from the ratio of section area to length of failure arc. The variance reduction parameter, the scale of fluctuation, was set at 2a, although deviations from this can be made during program execution.

4. CASE STUDIES

The majority of cases for this work were taken from an extensive study of failures in UK opencast mines, conducted by the Department of Mining Engineering, University of Nottingham. A review of this work is presented by Stead (1984). The failures recorded by Chandler (1974) were included as a control to test the algorithms but as no failure lengths were recorded, these cases were not included in the 3-D analyses. All the case studies have been recorded on a database system and are identified by a group code and number. The groupings are made according to the material on the failure surface and are listed in Table I. Individual failures are referenced by the group code and number, e.g. LIAS_301 and SEAT_79.

Each group is representative of a particular geologic material and should display reasonably consistent properties. The material properties from each group were taken from published test results. The standard deviation for these parameters was obtained by comparing the range of the data with a coefficient of variation of 40% for cohesion and 20% for ϕ, the lower value was used in the analysis.

Reliability Analysis of Failed Slopes, a Back Analysis View of the Sensitivity to Input Parameters.
J.D. ST GEORGE

Table I

Case Studies Under Material Grouping

Group	Code	Number	Description
Lias Clay	LIAS	8	Brecciated and unbrecciated clay.
Loosewall	LWCC	14	Backfill materials - circular failure mechanisms only.
Loosewall	LWBP	11	Biplanar failures with basal materials having weaker strength than backfill.
Seatearth	SEAT	17	Majority of failure plane within seatearth material.
Clayband	CLBD	13	Failure plane confined to bedding features with high clay content.

5. ANALYSIS

The sensitivity of the input variables was initially studied in 2-D taking the observed failure geometries, thereby removing this uncertainty from the analyses. The parameters which were independent of the variability in shear strength, i.e. model error and watertable, were investigated first.

Model error: This term is added to the overall variance and will therefore increase the P_f (P_f < 50%). Figure 1 is a plot of P_f versus model error for two Lias Clay failures showing the expected increase in P_f as the model error becomes more significant. For the remainder of this work the error was kept constant at 5%. This is consistent with the expected accuracy of limit equilibrium methods.

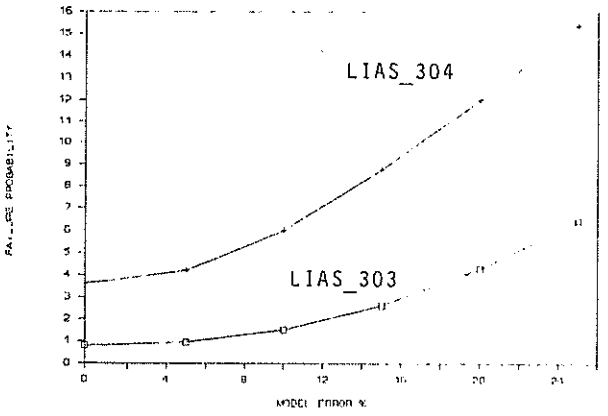

Figure 1 Sensitivity to model error

Watertable: It has been assumed that on the scale of the cross sections, the watertable or pore pressures are completely correlated. The variations are therefore just additive on the overall variance and have a similar effect on the P_f as model error. The upper and lower estimates for the phreatic surface were made on the basis that they covered all probable conditions consistent with slope observations and any measurements. A dry or fully drained slope would represent the lower limit. The upper limit is less reliable to estimate although a fully saturated slope would represent a maximum watertable in the absence of artesian conditions. The same Lias Clay cases show, in Figure 2, the effect of changing the coefficient of variation of watertable on P_f.

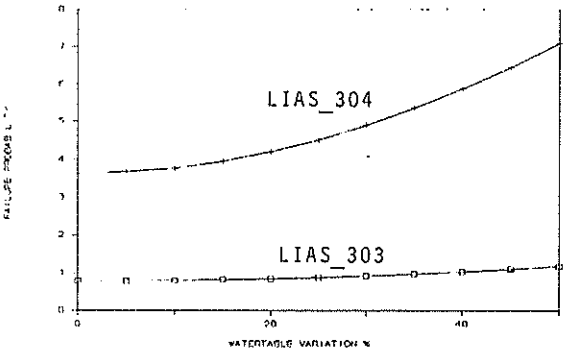

Figure 2 Sensitivity to watertable variations

The variability in the shear strength is related to the individual variance of c and ϕ, their spatial correlation and the correlation between them. Intuitively the presence of spatial correlation will cause a reduction in the overall variance for the shear strength. In order to study this effect, different ranges or autocorrelation distances (5-200m) were compared to the completely uncorrelated P_f. It was found that the size of failure influenced the behaviour of P_f with respect to the range of influence. For the large failures the P_f decreased initially on increasing the range until some minimum point was achieved. Then gradually increased asymptotically to the uncorrelated value. For the small scale failures this effect was probably masked (a < 5) as they only showed an increase towards the uncorrelated values. The P_f is plotted against the range of influence (a) in Figure 3, for the large (LWCC_104) and small (LWCC_129) failures.

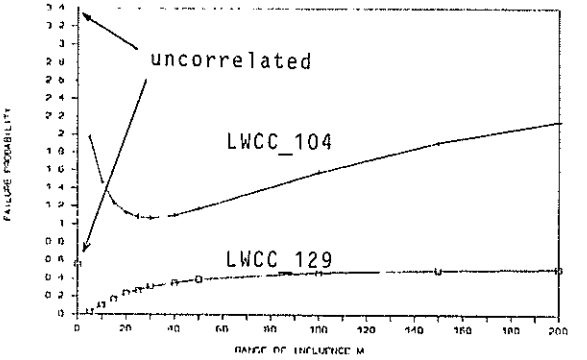

Figure 3 Effect of range of influence on P_f

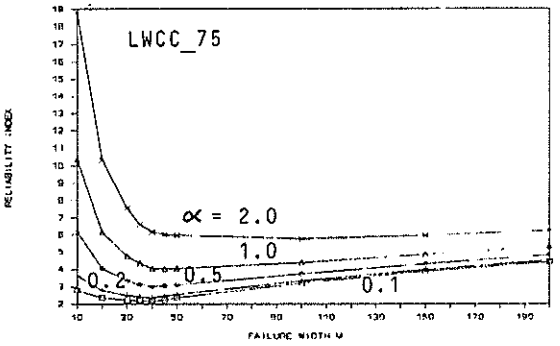

Figure 4 Effect of lateral release on β

Correlation between the shear strength parameters c and ϕ was investigated by varying the correlation coefficient from -1 to +1. The changes in P_f were very small and, as expected, positive correlation contributed to an increase, negative correlation a decrease in P_f.

Extending the analysis to 3-D introduces the lateral release factor (α), variance reduction function and the scale of fluctuation. The resistance on the lateral margins also requires a shear strength value. In case studies where failure through the lateral margins occurs in essentially intact material, a strength representative of that material was used e.g. loosewall slopes. For rock slopes where intact strength is high, release occurs along discontinuities and a uniform strength of ϕ=30° c=0kPa was assumed. Then α measures the relative strength of release to this standard value. The lateral release factor directly affects the 3-D factor of safety F_b and in the limit as failure width $b \to \infty$, F_b converges to F.

The form of the reduction function and scale of fluctuation have been chosen to be consistent with the 2-D spatial behaviour and therefore the 3-D model will be essentially controlled by the range of influence (a). By holding the range constant, the effect of variations in end resistance, on P_{fb}, can be observed. This is achieved by varying the lateral release factor with both ends of the failure having the same α. Figure 4 shows the reliability index (β) plotted against failure width (b) at different lateral release factors for case study LWCC_75. As can be seen the critical failure width b_c defining a minimum β (maximum P_{fb}) is dependent on the lateral release factor. The critical failure widths becoming shorter with reducing end resistance, as would be expected. It clearly shows the influence α has on the reliability index. At the observed failure width for the slope (100m), β changes from 3.2 (α=0.1) to 5.7 (α=2.0). This effect will be amplified for rock slopes where strength differences between intact rock and discontinuities are high. Other factors such as slope curvature helping release also appear to be important in these cases.

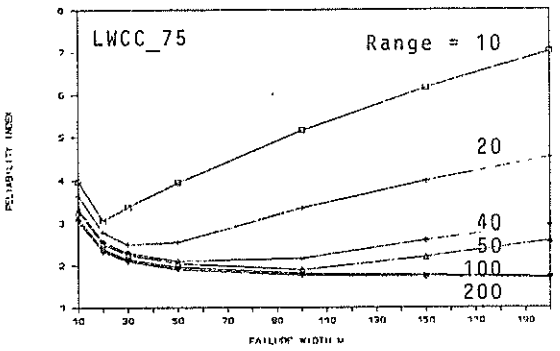

Figure 5 Effect of range of influence on β

By holding the lateral release factor constant (α=0.2), the effect of spatial correlation on the reliability index is investigated. Figure 5 shows a plot of failure width versus reliability index for different ranges of influence (a) for the same case study. It clearly demonstrates that the minimum β is also dependent on the range. The critical failure width b_c calculated using equation (4) was compared to the actual failure widths and have been plotted as a ratio in Figure 6. Three cases are not included due to excessive predicted failure lengths: the largest being 2741m for an actual failure length of 150m, and those cases with F < 1, b_c is undefined. A further indication of failure length was obtained from examining the cross section length L_{xs} of the failures. It was noted the majority of actual failures were within $1 < L_{xs} < 3$. Failure lengths longer than $3L_{xs}$ were attributed to being essentially multiple events. There was only one failure noticeably shorter than L_{xs} and this was caused by over steepening at the toe, along a portion of the slope.

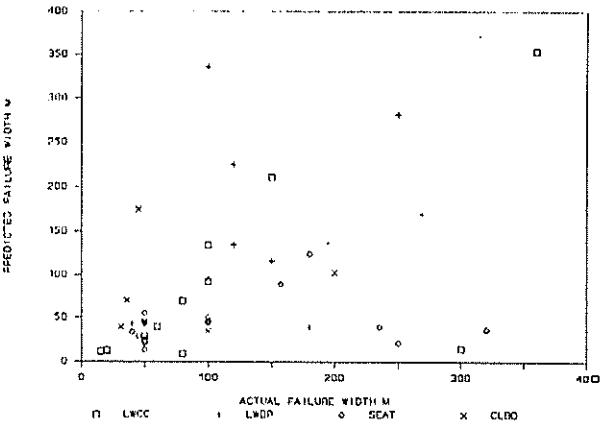

Figure 6 Actual vs predicted failure widths

In order to use the 3-D P_{fb} in a predictive analysis the slopes were re-examined without regard to the actual failure plane. The loosewall cases were all analysed in this way and compared to the actual failures. Two failure modes were investigated circular and biplanar. The critical circular slip surfaces with the minimum 2-D F were located by standard search routines and this was then compared to the lowest F from the biplanar analysis. The dip of the pavement was assumed known, with a strength of c=0kPa and ϕ=16°. The lowest overall F defined the failure geometry; then the critical failure width b_c and L_{xs} were calculated for this cross section if $L_{xs} < b_c < 3L_{xs}$; b_c was taken as the failure length, otherwise L_{xs} was used. The P_{fb} was calculated for this failure width. The spatial variability was modelled with a range of 100m. The lateral release factor, in all cases, was set to 1, since side release would occur through spoil material. The results are presented together with the actual failure widths and volumes in Table II. Also included are time to failure and water rating for the slopes. The cases are listed in ascending order of probability and it is evident the very low P_{fb} values have a delayed failure and/or water has been an important component. The predicted failure widths and volumes deviated considerably from the observed which is perhaps indicative of the lowest 2-D F not producing the maximum 3-D P_{fb}. All those failures with a P_{fb} > 5% water appears to be a significant factor, except for LWBP_83 where no information was available. The two cases with P_{fb} much greater than 50% (LWCC_169 and LWBP_183) were examples of extremes. LWCC_169 had a slope angle of 60° to a height of 33m while LWBP_183 was cut at 40° to a height of 80m on an 8° dipping pavement. Even with optimistic strength parameters both these cases

TABLE 2

Failure Probabilities for Loosewall Case Studies

Code	Probability of Failure P_{fb}	Predicted Volume x10³m³	Predicted Width m	Actual Volume x10³m³	Actual Width m	Time Factor	Water Factor
LWCC_79	6.4×10^{-5}	67	87	6	60	4	3
LWBP_17	3.1×10^{-3}	38	80	176	180	2	4
LWBP_44	2.5×10^{-2}	1009	244	500	250	4	3
LWCC_192	3.5×10^{-2}	6	37	13	50	4	1
LWBP_144	5.1×10^{-2}	36	83	50	150	3	3
LWCC_129	6.6×10^{-2}	1	17	0	15	2	0
LWCC_172	8.9×10^{-2}	3	30	5	80	2	2
LWCC_219	0.16	30	64	28	80	3	3
LWCC_69	0.18	4	32	30	300	2	1
LWCC_152	0.33	1	22	1	50	2	0
LWCC_239	0.72	1	19	1	20	3	3
LWBP_217	0.72	303	129	368	120	2	1
LWBP_201	0.77	67	108	87	120	3	4
LWCC_75	1.12	36	91	51	100	1	1
LWCC_199	3.38	28	78	36	100	2	2
LWBP_150	4.77	11	41	5	100	4	0
LWBP_155	8.24	9	39	21	90	2	4
LWBP_83	20.90	2	39	2	40	2	0
LWBP_177	31.80	210	148	728	150	1	3
LWCC_104	50.20	247	145	135	360	4	3
LWCC_169	82.30	8	42	8	25	3	3
LWBP_183	99.80	188	125	466	200	3	3

Time Factor	
0	No details
1	< 1 week
2	1 week - 1 month
3	1 - 3 months
4	3 - 6 months

Water Factor	
0	No details
1	Dry/fully drained
2	Slight seepage/rainfall
3	Heavy seepage/rainfall
4	Artesian conditions

have 2-D F below 1 for dry conditions. The other case with $P_{fb} > 50\%$, LWCC_104 had a submerged toe due to the formation of a sump, this would explain the long time to failure since the dry P_{fb} for same geometry was 5.1×10^{-1}. For case studies with P_{fb} above 5×10^{-2} and below 5%, there is reasonable concordance between measured and predicted volumes and failure widths. One notable exception is for LWCC_69 where the observed failure width is a factor of 10 greater than predicted.

6. CONCLUSIONS

From the 2-D analysis it was noted how the P_f was sensitive to changes in model error and watertable variations. The effect of spatial and parameter correlation had a lesser influence on P_f, however the behaviour of P_f, with respect to spatial variability, was found to be dependent on the scale of failure. The most significant infuence on the 3-D P_{fb} was the resistance of the lateral margins and clearly this represents an area were more research could be carried out. The form of the variance reduction function altered P_{fb} and also affected the so-called critical failure width where the minimum ß is defined. The retrospective analysis of the loosewall failures produced mixed results. Those cases with very low P_{fb} did not measure up in terms of failure geometries, widths and volumes with the observed failures. However there was good agreement between volume and failure width for most of the other cases and this might provide a means of estimating potential failure volumes. As the 3-D P_{fb} is sensitive to lateral release, the presence of weak planes or slope curvature will greatly reduce the probability of failure, particularly for rock slopes. The critical failure width would become less important since the potential failures would be positional, related to release features on the slope.

7. REFERENCES

Alonso E. (1976) Risk Analysis of Slopes and its Application to Slopes in Canadian Sensitive Clays, Geotechnique, 26, No 3, 453-472.

Chandler, R.J. (1974) Lias Clay: The long-term stability of cutting slopes, Geotechnique, 24, No 1, 21-38.

Chowdhury R.N. and Zhang S. (1988) Prediction of Critical Slip Surfaces, 5th Australia-New Zealand Conf on Geomechanics, Sydney, 451-455.

Cornell C.A. (1971) First Order Uncertainty Analysis of Soils Deformation and Stability, Proc 1st ICASP-SSE, Hong Kong.

Janbu N. (1973) Soil Stability Computations, Embankment Dam Engineering, Casagrande Volume, Wiley, New York, 47-87.

Sharp K.D. (1982) Development of a Model for Probabilistic Slope Stability Analysis and Application to a Tailings Dam, PhD Thesis, University of Utah.

Stead D. (1984) An Evaluation of the Factors Governing the Stability of Surface Coal Mine Slopes. PhD Nottingham University.

St George J.D. (1991) Probabilistic Methods Applied to Slope Stability Analysis, unpublished PhD thesis, Auckland University.

Vanmarcke E.H. (1977a) Probabilistic Modelling of Soil Profiles, J of Geotech Engng Div ASCE, 103, GT11, 1237-1246.

Vanmarcke E.H. (1977b) Reliability of Earth Slopes, J of Geotech Engng Div ASCE, 103, GT11, 1247-1266.

Resonance Avoidance in Seismic Design

J.R. STYLES
B.E., M.Eng.Sc.
Senior Lecturer in Civil Engineering, University of Melbourne
P.J. MOORE
B.E., M.S., Sc.D., M.I.E.Aust.
Reader in Civil Engineering, University of Melbourne
R.K. GUPTA
M.E., Ph.D., M.I.E.Aust.
Research Fellow, University of Melbourne

SUMMARY In seismic design, the minimization of structural damage from an earthquake is assisted if positive steps for resonance avoidance for buildings and building elements are taken. Resonance avoidance refers to lack of coincidence between the dominant ground frequencies and the natural frquencies of building elements. This paper examines the assessment of dominant ground frequencies and natural frequencies of buidings, foundations, floors, beams and columns. Some approaches to modifying the natural frequencies of buildings and building elements to avoid possible resonance are discussed.

1. INTRODUCTION

Damage to buildings or building components from earthquakes is caused when the materials of construction cannot withstand the stresses imposed by the ground motions. A necessary but clearly insufficient condition that must be satisfied if damage is to be minimised is that the natural frequencies of buildings or building components should be separated from the dominant ground motion frequencies in the earthquake.

An increasing amount of information is now becoming available regarding the magnitudes of the dominant ground frequencies at particular sites. For many sites the dominant frequencies lie between 1 and 5 hertz. With overlying alluvium it is possible, in the absence of records, to estimate the dominant ground frequencies from a knowledge of the stiffness and depth of the alluvium. Calculations indicate that the fundamental natural frequency of the ground in cases where the alluvium becomes stiffer with depth is likely to be greater than 1 hertz. Lower natural ground frequencies may occur with soft alluvium of constant stiffness.

Expressions for natural frequencies of whole buildings in terms of building height show that it is likely that coincidence between the natural frequencies of some buildings and the ground will occur. If this information can be made site specific then useful guidance on undesirable building heights may be obtained.

With raft and footing foundations resonance effects may be encountered particularly with soft ground. The foundation natural frequency rises as the ground becomes stiffer and it may be varied by altering the foundation dimensions and foundation loads.

Natural frequencies of floors may also fall within the range of commonly encountered dominant ground frequencies from earthquakes. Some control may be exercised over the natural frequencies of floors by varying the floor dimensions and support conditions at the edges.

Compared with other building components, beams and columns are less likely to suffer from resonance effects since the natural frequencies of these components are often much greater than the dominant ground frequencies.

2. DOMINANT GROUND FREQUENCIES

In the absence of records the dominant ground frequency at a site may be estimated from the calculated natural frequency of ground response resulting from the deep seated movement of the underlying strata. for the case of a homogeneous stratum overlying the basal rock the fundamental natural frequency (f_n) is given by (Richart et al, 1970)

$$f_n = v_S/4L \text{ hertz} \qquad (1)$$

where v_S = shear wave velocity of the stratum
L = stratum thickness

Fig. 1 illustrates that natural frequencies may be less than 1 hertz for large layer thicknesses of soft to medium ground overlying the rock. For non-homogeneous ground for which the shear modulus increases with depth, Moore (1987) has shown that the fundamental natural frequency depends dominantly on layer thickness (L) and rate of increase of shear modulus with depth (m). The shear modulus (G_z) at any depth (z) is represented by

$$G_z = G_o + mz \qquad (2)$$

where G_o = shear modulus at ground surface

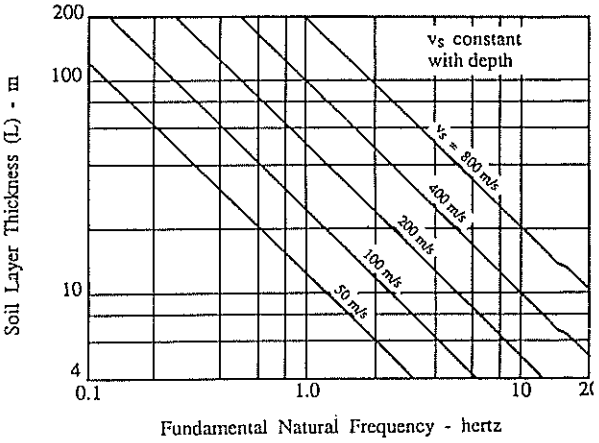

Fig. 1 Natural Frequency for Constant Shear Modulus Case

Fig. 2 indicates the effect of parameter m on the natural frequency. It may also be shown for particular values of G_o and m that the natural frequency increases as the layer thickness decreases.

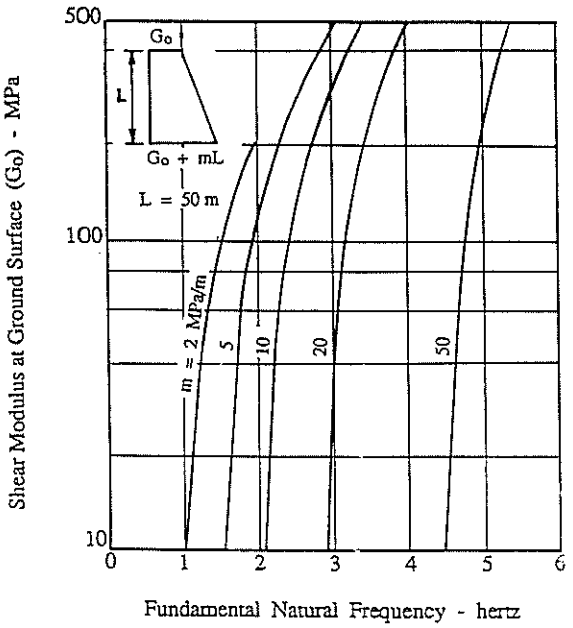

Fig. 2 Effect of Shear Modulus on Natural Frequency

3. NATURAL FREQUENCIES OF BUILDINGS

A number of simple empirical formulae have been proposed for the estimation of the natural frequency of a building for the fundamental transverse mode (mode 1) of vibration. Anderson et al (1952) have examined the popular formula for the fundamental period (T) of vibration

$$T = K\,H/D^{1/2} \text{ sec} \qquad (3)$$

where H = building height (m), and
D = depth of building (m) parallel to the direction of vibration

Based upon a large number of observations by the authors and by Salvadori and Heer (1960) it appears that the constant K should be approximately 0.1. Housner and Brady (1963) examined a number of formulae, among the simplest being

$$T = 0.1\,N \text{ sec} \qquad (4)$$

for rigid frame buildings, and

$$T = (0.5N^{1/2} - 0.4) \text{ sec} \qquad (5)$$

for steel frame buildings, where N = number of floors in the building.

More recently, Ellis (1980) has examined the accuracy of some of these simple formulae and he proposed that a slightly better expression for natural frequency (f_n) is

$$f_n = 46/H \text{ hertz} \qquad (6)$$

While errors of ±50% were not uncommon in the prediction of natural frequency, he found that simple formulae, such as equation (6), were likely to be as accurate as computer based predictions.

4. RESPONSE OF FOUNDATIONS

In examining the response of shallow footing and raft foundations to horizontal ground vibrations the ground is often idealized as an elastic solid with the stiffness being given as (Bycroft, 1956)

$$k = 32\,(1-\upsilon)\,Gr/(7-8\upsilon) \qquad (7)$$

where G and υ are the shear modulus and Poisson's ratio for the ground
r is the radius of the footing

An alternative and perhaps more relevant expression for rectangular footings is that quoted by Barkan (1962)

$$k = 2(1+\upsilon)\,G\beta_x\,(BL)^{1/2} \qquad (8)$$

where β_x is a factor depending on foundation shape.
B and L are footing dimensions

For square footings (B x B) equation (8) simplifies to

$$k = 2.4\,GB \qquad (9)$$

for a Poisson's ratio of 0.25

From equation (9) the natural frequency of horizontal vibration for the footing may be derived to yield

$$f_n = 0.8\,(G/\sigma B)^{1/2} \qquad (10)$$

where σ is the average bearing pressure acting on the footing.

Fig. 3 illustrates the way in which the natural frequency decreases as the bearing pressure increases or as the footing size increases. If normal foundation engineering design practice is followed then the bearing pressure should increase as the ground becomes stiffer. This can be allowed for by specifying a linear relationship between G and σ. If this is incorporated into equation (10) then it is obvious that the natural frequency becomes dependent on the width of the foundation only. This is shown in Fig. 4 for a typical range of foundation soils that are likely to be encountered. Fig. 4 indicates that the likely range of natural frequencies for shallow foundations is somewhat narrower than might be inferred from a study of Fig. 3.

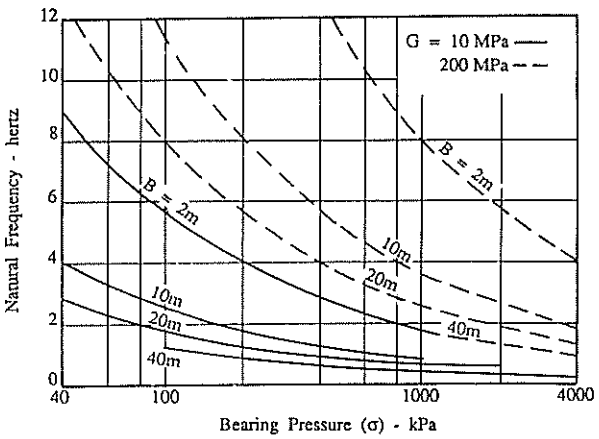

Fig. 3 Effect of Bearing Pressure and Footing Width on Natural Frequency

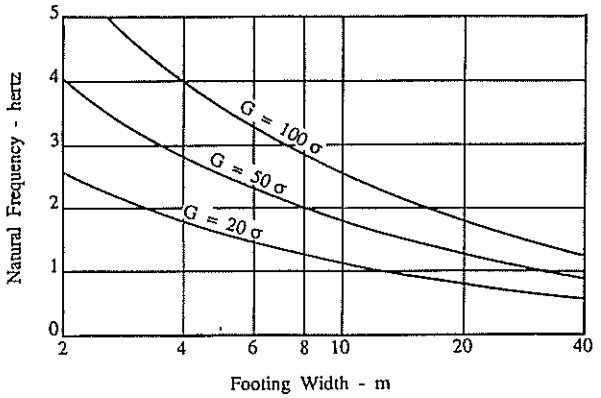

Fig. 4 Effect of Footing Width on Natural Frequency
- Shear Modulus/Bearing Pressure Relationships Included

For lightly loaded stiffened slabs, common in residential development, the use of equation (8) to evaluate horiontal soil stiffness may lead to a significant inderestimate of the natural frequency of the footing. As for vertical and torsional modes of vibration the horizontal stiffness increases as the depth to a rigid stratum underlying the elastic layer decreases.

Fig. 5, which was derived from a three-dimensinal finite element analysis, shows the effect of layer thickness on the natural frequency for a slab designed in accordance with Australian Standard 2870: Residential Slabs and Footings - the slab type chosen was for articulated full masonry construction placed on a moderetely reactive clay site.

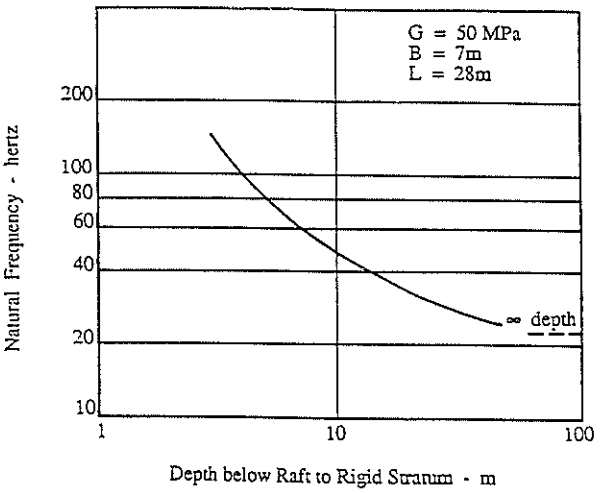

Fig. 5 Influence of Depth to Rigid Stratum
on Natural Frequency of Raft Footing

5. RESPONSE OF SLABS, BEAMS AND COLUMNS

Where a simple element is to be analysed or designed, tabulations of natural frequency for various support conditions and geometry are available for both beams and plates (eg. Stokey, 1976). An example of such a tabulation is given in Table 1. Where more information than the frequency of the first mode of vibration for a beam is required, approximate solutions, precise solutions involving frequency functions (e.g. Kohoutek, 1985) or finite element approaches need to be considered.

TABLE 1

FUNDAMENTAL NATURAL FREQUENCIES
FOR RECTANGULAR PLATES (from Stokey, 1976)

b, a; s s s s	b/a	1.0	2.0	∞
	$\omega_n/(D/\rho h a^4)^{1/2}$	19.74	12.34	9.87
b, a; c c c c	b/a	1.0	2.0	∞
	$\omega_n/(D/\rho h a^4)^{1/2}$	35.98	24.57	22.37

D = $Eh^3/12(1-\upsilon^2)$ s = simply supported edge
h = plate thickness c = clampled edge
ρ = plate density a,b = length, width of plate

A complete analysis for natural frequencies and related deformations of a multi-storey building will usually require a three-dimensional finite element study. Factors which need to be considered include:

(a) Aspect Ratio (length : width) - particularly when large, dominant deformation under seismic loading is in the length direction;

(b) Column/Beam Panel in-fill material - if rigid in-fill (brick) is integrated with the beams/columns, natural frequency of the building increases;

(c) Rigidity of connexions;

(d) Rigidity of base and rotational stiffness of foundation;

(e) Disposition of lift and stair cores - particularly if eccentric will promote a torsional rather than lateral sway mode of vibration.

The response of a five-storey reinforced concrete framed building is given as an example of the stiffening effect of brick in-fill.

Overall Dimensions (L x W x H) (m)	54.1	22.2	18.4
Floors cast integrally with frame			
All connexions assumed rigid			
Natural Frequency (f_{n1}, f_{n2}, f_{n3}) (H_Z)			
Considering Brick In-fill	2.24,	2.45,	2.62
Ignoring Brick In-fill	1.91,	2.19,	2.55

6. CONCLUDING REMARKS

For shallow footing and raft foundations located on deep deposits of soft to medium stiff soil, the natural frequency of the footing may coincide with the fundamental frequency of the soil deposit. The natural frequency of the footing decreases as the footing width increases.

It is unlikely that the natural frequencies of individual beams and columns in a building would coincide with dominant natural frequencies experienced in an earthquake. However, for some buildings, coincidence between the natural frequency for the building as a whole and the ground motion will occur. The fundamental natural frequency for whole buildings can be estimated approximately using simple empirical formulae.

7. REFERENCES

Anderson, A.W. et al (1952). Lateral Forces of Earthquake and Wind. Trans. ASCE 117: pp 716-780.

Bycroft, G.N. (1956). Forced Vibrations on a Rigid Circular Plate on a Semi-Infinite Elastic Space and on an Elastic Stratum. Phil. Trans. Roy. Soc. of London, Series A, Vol. 248, pp 327-368.

Barkan, D.D. (1962). Dynamics of Bases and Foundations. McGraw Hill Book Co.

Ellis, B.R. (1980). An assessment of the accuracy of predicitng the fundamental natural frequencies of buildings and the implications concerning the dynamic analysis of structures. Proc. Inst. Civ. Engrs. Vol. 70 (Part 2): pp 763-776.

Housner, G.H. and Brady, A.G. (1963). Natural periods of vibrations of buildings. Proc. ASCE. Eng. Mechanics Div. 89 (EM4): pp 31-65

Kohoutek, R. (1985). Analysis of Beams and Frames. Analysis and Design of Foundations for Vibraitons. P.J. Moore (Editor). Rotterdam. Balkema.

Moore, P.J. (1987). Some Geotechnical Aspects of Seismic Response. Environmental Geotechnics and Problematic and Soils and Rocks. A.S. Balasubramaniam et al, (Editors). Rotterdam. Balkema.

Richart, F.E., Hall, J.R. and Woods, R.D. (1970). Vibrations of Soils and Foundations. Prentice-Hall Inc., New Jersey.

Salvadori, M.G. and Heer, E. (1960). Periods of Framed Buildings for Earthquake Analysis. Proc. ASCE. Struct. Div. 86 (ST12): pp 59-71.

Stokey, W.F. (1976). Vibrations of systems having distributed mass and elasticicty. Shock and Vibration Handbook. C.M. Harris and C.E. Crede (Editors). New York. McGraw Hill.

Location of Critical Slip Surfaces in Coal Mine Spoil Piles

D.J. WILLIAMS
B.E., Ph.D., M.I.E.Aust.
Senior Lecturer in Civil Engineering, The University of Queensland
J.-Z. ZOU
B.E., M.E.
Research Student, The University of Queensland

SUMMARY By their very nature, coal mine spoil piles are at considerable risk of instability. The stresses within a coal mine spoil pile of a particular geometry are calculated using the stochastic finite element method, which allows for the observed variability of the spoil material properties. Various base spoil strengths are adopted to demonstrate the sensitivity of the results to conditions in this critical region. Using the calculated stresses, an improved dynamic programming method is used to locate the critical slip surface within the spoil pile, and hence determine the minimum factor of safety, for each set of spoil material strengths. The minimum factors of safety obtained are compared with those determined using a generalised limit equilibrium wedge analysis employing a pattern search optimisation procedure. Possible improvements to the stochastic finite element based improved dynamic programming method are discussed.

1. INTRODUCTION

In Australia, the spoil removed to expose coal during surface mining is conventionally loose dumped from a dragline bucket in spoil piles within the already mined pit. Since the spoil is free to ravel at about its angle of repose (of the order of 37 $^{\circ}$ to the horizontal) and water softened material can occur at the base, there is a considerable risk of spoil pile instability. Investigations by others (1, for example) of the failure of coal mine spoil piles have revealed that the failures are characterised by a deep-seated, essentially two-wedge mechanism, in which the pit floor region forms the base of the lower wedge, and the upper wedge extends behind the latest spoil pile crest. The failures extend to the pit floor region either because of water softened spoil at that location, or because of the presence of a weak seam within the floor material. In this paper, failure confined to the spoil only will be considered, and pore water pressures are absent from the spoil pile.

The precise location of the critical slip surface within a spoil pile is best determined by some optimisation procedure. One such procedure is the dynamic programming method. In this method, the distribution of stresses within the spoil pile is required. This may be provided by finite element calculations, which allow a constitutive model for the spoil material to be incorporated into the solution. The geotechnical properties of spoil material vary considerably, and this was allowed for by employing a stochastic finite element method (2). Definition of the variability of the spoil material properties was based on a simple statistical analysis of spoil property data collected from coal mines in the Bowen Basin Coalfields in Central Queensland. The geometry of the spoil pile can also vary markedly. However, for the purposes of the paper a particular spoil pile geometry was adopted. In the stochastic finite element calculations, various values for the strength parameters at the critical base of the spoil pile were considered to demonstrate the sensitivity of the solution to conditions at the spoil base.

Use of the dynamic programming method requires the definition of a grid of state points which overlaps the potential slip region. The state points are arranged in a series of stages. An improved dynamic programming method was used, in which possible slip surfaces, which must pass between state points, may pass both between and along stages. In the conventional dynamic programming method, slip surfaces may only pass between stages (3). Allowing possible slip surfaces to pass both between and along stages has the potential to provide greater accuracy for a given spacing of state points. The critical slip surface is that which gives the minimum factor of safety.

The results obtained using the improved dynamic programming method are compared with the results obtained using a generalised limit equilibrium wedge analysis employing a pattern search optimisation procedure (4). The accuracy of and possible improvements to the stochastic finite element based improved dynamic programming method are discussed.

2. SPOIL PILE GEOMETRY

Although the geometry of spoil piles varies greatly, depending among other factors on the depth to coal, the lithology and breakdown potential of the spoil, the mining methods employed and the dip of the coal seam, a fixed geometry was adopted for the purposes of this paper. It was based on that analysed by Richards (5), as used by Williams and Zou previously (2), and is shown in Figure 1. It involves a spoil pile 76.5 m high, with a slope face angle of 34.5 $^{\circ}$ and a base slope angle of 3.4 $^{\circ}$. Behind the leading face is a series of 20 m high crests with 37 $^{\circ}$slopes. The height of the spoil pile is about the maximum achieved by spoil piles, and it has a relatively steep face angle, so that it represents somewhat of a worst case. The spoil pile is assumed to be located on strong floor material, so that any failure would occur entirely within the spoil. Pore water pressures are absent from the spoil pile.

3. MATERIAL PROPERTIES

3.1 Results of Statistical Analyses of Collected Spoil Property Data

Spoil materials produced by the surface mining of coal in the Bowen Basin Coalfields of Central

Queensland comprise soil and uncemented "superficials", and coal measures overburden and interburden rocks. Data on the density ρ and strength of these materials were collected from records of spoil pile failure investigations carried out at Goonyella and Riverside Mines, and from records of laboratory and in situ testing of spoil materials from these mines.

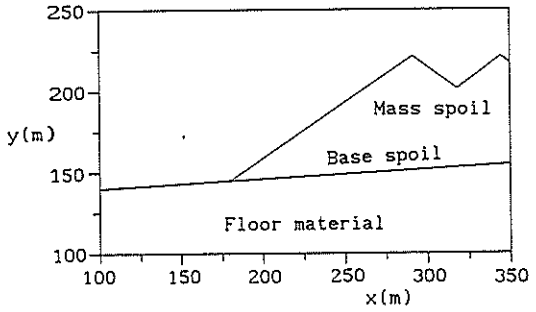

Figure 1 Adopted spoil pile geometry

Borehole samples taken from basal failure zones show the existence, in some cases, of a band of highly saturated softened spoil at the pit floor/spoil interface. Therefore, it is appropriate to consider data on the base spoil strength separately from spoil mass strength data.

The available strength data was based on the confined triaxial testing of a range of spoil materials, under various test conditions. The data exhibited a large variability, but it was not possible to separate the data according to lithology and the potential for material breakdown, nor according to test conditions. In practice, little attempt is made to selectively place spoil of different strength in order to optimise stability, apart from some selective placement of good quality spoil at the critical base of the pile. The available spoil strength data comprised values of mass and base cohesion (c_m and c_b, respectively), and values of mass and base friction angle (ϕ_m and ϕ_b, respectively).

The statistical analyses of the spoil density and strength data were carried out using a commercially available computer package SAS. The results of the analyses are summarised in Table I.

TABLE I

RESULTS OF STATISTICAL ANALYSES OF COLLECTED SPOIL DENSITY AND STRENGTH DATA

Spoil property	Data set size	Mean μ	Standard deviation σ
ρ ($Mg.m^{-3}$)	61	1.86	0.22
c_m (kPa)	62	73.1	77.7
ϕ_m ($^\circ$)	62	28.1	10.8
c_b (kPa)	87	121.8	83.1
ϕ_b ($^\circ$)	87	8.0	4.0

The standard deviations given in Table I show that the cohesion data are widely scattered in both absolute and percentage terms. The scatter of the density and ϕ_m data is small, while the scatter of the ϕ_b data, although large in percentage terms, is only moderate in absolute terms.

All of the spoil properties other than c_m may reasonably be approximated as being normally distributed. The distribution of c_m is somewhat better approximated by an exponential or log-normal distribution. However, for the purposes of the paper, all spoil properties were assumed to be normally distributed. In the ensuing analyses, three sets of spoil strengths were considered. In the first, the spoil strengths given in Table I were adopted. In the second, zero cohesion (mean and standard deviation) was assigned for the base spoil, and in the third zero friction angle (mean and standard deviation) was assigned to the base spoil, with the other strengths unchanged from those given in Table I. Assigning zero friction angle to the base spoil may be thought of as representing undrained failure at the base.

3.2 Other Material Properties

To apply the stochastic finite element method, values for a number of other properties are required. These properties include the strength of the floor material, the Young's moduli of the spoil and floor materials, and the Poissons ratio of the spoil and floor materials. Mean values for the cohesion and friction angle of the floor material were taken to be 625 kPa and 28°, respectively, after Richards (5). Mean values for the Young's modulus of the floor material beneath the spoil, mass spoil material, and base spoil material were estimated from modulus data given in Richards (5) to be 154 MPa, 28 MPa and 19 MPa, respectively. A value of 0.3 was assumed for the Poissons ratio of all materials. No data were available on the distributions of these properties, and zero standard deviations were adopted.

4. STOCHASTIC FINITE ELEMENT METHOD

4.1 Introduction

The stochastic finite element method (SFEM) is an extension of the conventional finite element method (FEM) to reliability analysis. The SFEM uses as input the probability distributions of the spoil material properties, rather than the deterministic values used in the conventional FEM. The probability distributions of the stresses and displacements within a body are then calculated by approximate methods as outlined in Williams and Zou (2). For this paper use was made of a SFEM program developed from a general purpose finite element program written by Owen (6). The program can be used for reliability analyses of problems that involve elasto-plastic work-hardening material behaviour. This represents an advance on available SFEM programs which cater for elastic material behaviour only.

4.2 Application of SFEM to Spoil Pile Stability Analysis

Since the probability distributions of the spoil material properties have been approximated as normal, they are defined by the means and standard deviations of the spoil material properties, and these are used as input to the SFEM program. The program then calculates the means of the stresses and displacements, and their standard deviations, throughout the spoil pile. The stresses are used as input in the application of the improved dynamic programming method.

The SFEM program also compares the calculated stresses with the adopted yield criterion, to give the probability of failure and factor of safety locally. The location of high values of the local probability of failure or low values of the local factor of safety within the spoil pile indicates

the probable location of the critical slip surface. This is used as a basis for selecting the appropriate location for the state point grid used in the improved dynamic programming method.

As described in Williams and Zou (2), the spoil pile geometry shown in Figure 1 was represented by a finite element mesh comprising 74 eight-noded iso-parametric plane strain elements. It was assumed that the spoil material and underlying floor material would behave as if they were fully drained. They were therefore modelled as single phase materials, with only two degrees of freedom (the horizontal and vertical components of displacement) assigned to each node. Both the horizontal and vertical nodal displacements were constrained to zero at the base of the mesh. The horizontal displacement component only was constrained to zero at the vertical boundaries of the mesh. The strength properties of the spoil at the base of the pile, different from that of the spoil mass, were modelled by assigning different strength properties to a 1 m thick layer at the spoil pile base.

Both the spoil and floor materials were modelled as isotropic materials, characterised by linear elastic behaviour until the yield point, which was defined by the Mohr-Coulomb criterion. Beyond yield, the material was allowed to undergo work-hardening defined by a hardening parameter equal to one tenth of the relevant Young's modulus, following the approach taken by Owen (6). The incorporation of work-hardening was necessary to ensure a convergent solution in cases close to failure.

4.3 Results of SFEM Analyses

For the purposes of calculating local probabilities of failure and factors of safety, the Mohr-Coulomb yield criterion was used in a performance function, as detailed in Williams and Zou (2). Contours of the local probability of failure for the three sets of spoil strengths considered were presented as Figures 2, 3 and 4 in (2), and will not be repeated here. They served as a basis for selecting the appropriate location for the state point grid used in the improved dynamic programming method.

5. IMPROVED DYNAMIC PROGRAMMING METHOD

5.1 Introduction

Dynamic programming has been developed as a numerical algorithm for the rapid optimisation of sequential multi-stage decision problems (3, 7). Such problems are characterised by two features. Firstly, that at any stage the system may exist in any one of a finite number of states and, secondly, that it is required to find the mimimum system "cost". The minimum cost depends on the trajectory between stages and is defined as the sum of the costs incurred on passing between adjacent stages. The problem of determining the critical slip surface and hence mimimum factor of safety of a slope may readily be formulated in this manner. In this paper, an improved dynamic programming method (IDPM) is employed, in which possible slip surfaces can pass both between and along stages.

The application of the dynamic programming method requires that it be coupled with an appropriate analysis for the solution of the problem in question. Baker (3) described a procedure for applying the dynamic programming method, coupled with Spencer's limit equilibrium method of slope stability analysis, to locate the critical slip surface and hence determine the mimimum factor of safety. Yamagami and Ueta (8) applied the dynamic programming method, coupled with an expression for the factor of safety, to search for critical slip surfaces in finite element stress fields. In this paper, the IDPM is coupled with an expression for the factor of safety in which the stresses are obtained from stochastic finite element calculations. The IDPM is described briefly and used to locate the critical slip surface and hence determine the minimum factor of safety of a coal mine spoil pile, for three different sets of strength parameters.

5.2 Equations for Factor of Safety and Incorporation into Dynamic Programming

Similar to the approach taken by Yamagami and Ueta (8), the overall factor of safety for a particular slip surface (such as curve AB in Figure 2) can be defined as

$$F_s = \frac{\int_A^B \tau_f . dx}{\int_A^B \tau . dx} = \frac{\sum_{i=1}^{n} \tau_{f_i} . \delta l_i}{\sum_{i=1}^{n} \tau_i . \delta l_i} \qquad (1)$$

where τ is the mobilised shear stress at any point along the slip surface AB, τ_f is the shear strength of the material at that point, x is the horizontal co-ordinate, n is the number of stages along the slip surface, and δl_i is the length of the ith stage.

Dynamic programming is applicable only to "additive" integration functions or summations (3), which are merely numerical approximations to linear functions. Since the expression for the factor of safety given by equation (1) involves a ratio of integration functions or summations, it is not additive as required. This can be resolved using the principles of variational calculus, by introducing an auxiliary functional G_F defined by the following expression.

$$G_F = \sum_{i=1}^{n} (\tau_{f_i} - F_s . \tau_i) . \delta l_i \qquad (2)$$

Equation (2) is an additive function to which dynamic programming may be applied. Baker (3) showed that by minimising G_F, the minimum value for F_s would be obtained.

For the ith stage on a particular slip surface, the following expressions for τ_{fi} and τ_i can be written.

$$\tau_{f_i} = c + \sigma_s . \tan\phi \qquad (3)$$

$$\tau_i = \frac{(\sigma_1 - \sigma_3)}{2} . \sin(2\beta) \qquad (4)$$

where c is the cohesion and ϕ the friction angle of the material comprising the slope, σ_s is the stress acting normal to the slip surface over the ith stage, and σ_1 and σ_3 are the major and minor principle stresses at the slip surface over the ith stage, respectively. Equation (3) is the Mohr-Coulomb yield criterion. The stress σ_s and the angle β are given by the following expressions.

$$\sigma_s = \frac{(\sigma_1 + \sigma_3)}{2} + \frac{(\sigma_1 - \sigma_3)}{2} . \cos(2\beta) \qquad (5)$$

$$\beta = \alpha - \vartheta + \frac{\pi}{2} \qquad (6)$$

where α is the angle the base of the ith stage makes with the horizontal, and θ is the angle σ_1 makes with the horizontal.

In optimising equation (2) for each slip surface selected within the defined grid of state points, a value for F_s is first assumed. During the optimisation process, equation (1) is used to calculate a value for F_s and the result compared with the assumed value. The assumed value for F_s is updated and the process continued until some convergence criterion (such as the assumed and calculated values of F_s agreeing to within 0.01) is reached.

5.3 Brief Description of IDPM

The region of possible slip surfaces is selected using the results of stochastic finite element calculations as a basis. Within this region a grid of state points is arranged comprising n stages, with j state points along the ith stage line (such a grid is shown in Figure 2). Each state point, represented by S(i,j), has a certain value for its state parameter (or stress state). For state points outside the slope, the state parameter is zero. The state parameters for state points within the slope are based on the results of stochastic finite element calculations. The "cost" between any two state points can be calculated based on their separation distance and the difference in value of their state parameter. The minimum cost between the initial state point S(1,1) and any state point S(i,j) is defined by the optimal value function H(i,j).

There is a restriction in the application of dynamic programming that all trajectories pass through fixed end points, which implies that H(1,1) and H(n+1,1) have one value each. Provided that these fixed end points are located outside the slope, where the state parameter is zero, this restriction is of no practical concern.

For a given slope geometry, given slope material properties, and a defined region of possible slip surfaces, the following summarises the IDPM procedure for locating the critical slip surface and determining the corresponding minimum factor of safety.

1. The optimal value function of the starting point (state point S(1,1) or point A in Figure 2) is initialised to zero, that is

$$H(1,1) = 0 \qquad (7)$$

2. A value is assumed for the optimal value function of the ending point (state point S(N+1,1) or point B in Figure 2). Then, based on the recurrence relation derived from Bellman's (7) optimisation principle, the optimal value function for each state point of each stage line may be calculated (3). In this step, the optimal value functions for all possible paths from each stage point, both between and along stages, are calculated.

3. The optimal value function of the ending point is minimised.

4. The critical slip surface is traced back through the possible slip surface region, based on the calculated minimum optimal value functions, and hence the minimum factor of safety determined.

According to Giam and Donald (9), in a perfect state point grid the stage lines should be perpendicular to the critical slip surface. However, the one state point grid must suffice for all possible slip surfaces. As the critical slip surface is the most important, a check should be made that it intersects the stage lines approximately at right angles everywhere. The benefits of the IDPM over the conventional dynamic programming method, in which possible slip surfaces can only pass between stage points on adjacent stages, becomes more marked the more acute the angle between the slip surface and the stage lines.

5.4 Application of IDPM to Spoil Pile Stability Analysis

Based on the results of the SFEM analyses, the state point grid shown in Figure 2 was selected. The state points were arranged in a series of stages, with stages on average 2 m apart and state points within each stage on average 0.55 m apart. This gave a state point grid about one order of magnitude finer than that used for the same spoil pile geometry by Williams and Zou (2). For convenience in setting up the geometry of the state point grid, which was generated automatically, it extends beyond the slope boundary. All state points outside the spoil pile are assigned zero state parameters. The stress state at each state point within the spoil pile represents the local stress state of its surrounding area, and was assigned the stress calculated for the finite element Gauss point nearest to the particular state point. Possible slip surfaces are formed by connecting fixed points A and B (Figure 2), outside the slope, via intermediate state points. The only state points of any consequence are those located within the slope. It can be seen that the slip surface intersects the stage lines approximately at right angles everywhere.

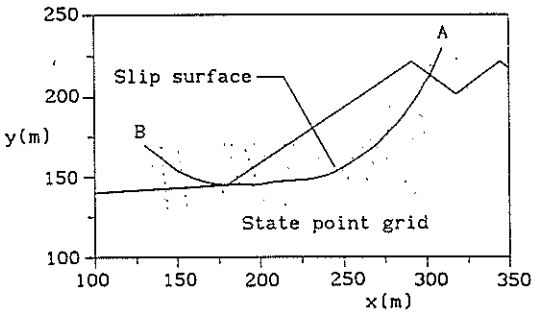

Figure 2 Selected state point grid showing slip surface AB

5.5 Results of IDPM Analyses

The results of the stochastic finite element based IDPM analyses are shown in Figures 3, 4 and 5, for the mean spoil strengths given in Table I, zero base spoil cohesion and zero base spoil friction angle, respectively. Figures 3 to 5 show the locations of the critical slip surface and the values of the minimum factor of safety obtained.

6. GENERALISED WEDGE ANALYSIS

6.1 Introduction

The generalised limit equilibrium wedge analysis program GWEDGEM, described in Donald and Giam (4), was used for the purposes of comparison with the results obtained using the SFEM and IDPM. In GWEDGEM, both force and moment equilibrium are fully satisfied and the failure mechanism is kinematically admissible. That is, the sliding

wedges may move without causing gaps or overlaps. Inclined internal interfaces are allowed and the critical inclination is searched for. Various multi-variable unconstrained search routines are available within the program for locating the critical slip surface for a given problem. The mechanism may have any multi-linear shape, although two to nine wedges are usually sufficient. The method is applicable to general stability problems, and has been shown (4, 10) to be superior to available limit equilibrium methods employing vertical slices, where the critical slip surface is non-circular.

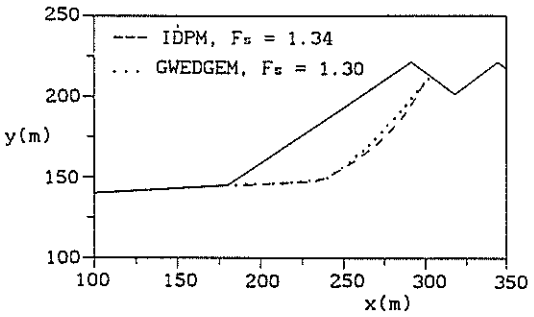

Figure 3 Critical slip surfaces and minimum factors of safety F_s for mean spoil strengths

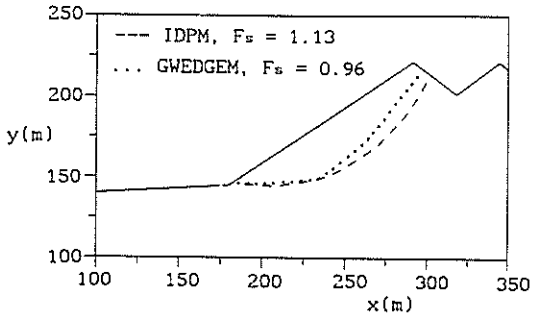

Figure 4 Critical slip surfaces and minimum factors of safety F_s for zero base spoil cohesion

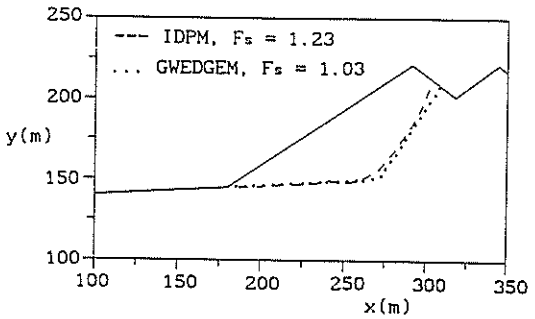

Figure 5 Critical slip surfaces and minimum factors of safety F_s for zero base spoil friction angle

In view of the relatively tight curvature of the critical slip surface, nine wedge mechanisms were selected. The pattern search option was adopted as the optimisation procedure for the determination of the critical slip surface for the three sets of strength parameters. The pattern search procedure was found by Giam and Donald (9) to be one of the best options available within GWEDGEM. It can successfully handle a wide range of slope stability problems, the number of slip surfaces needed to be considered to arrive at the minimum factor of safety is not excessive, and it is computationally efficient.

6.2 Results of GWEDGEM Analyses

The results of the limit equilibrium based GWEDGEM analyses are shown together with the results of the corresponding IDPM analyses in Figures 3, 4 and 5. Figures 3 to 5 show the locations of the critical slip surface and the values of the minimum factor of safety obtained.

7. DISCUSSION

The minimum factors of safety F_s obtained from the two analyses used in this paper, and from earlier IDPM analyses for the same spoil pile geometry and spoil material properties by Williams and Zou (2), are compared in Table II.

TABLE II

COMPARISON OF CALCULATED MINIMUM FACTORS OF SAFETY

Spoil strengths	Minimum F_s		
	IDPM		GWEDGEM
	(2)	Current	
Mean strengths	1.79	1.34	1.30
Zero base cohesion	1.16	1.13	0.96
Zero base friction	1.42	1.23	1.03

7.1 Effect of State Point Grid Spacing

The disparity between the minimum F_s calculated in the current IPDM analyses and those reported in (2), are due to the state point grid spacing being about an order of magnitude finer in the current analyses. The inadequacy of this spacing was evident from the jagged critical slip surfaces which were obtained.

Figures 3 to 5 show the critical slip surfaces obtained to be reasonably smooth, and the minimum F_s obtained were substantially reduced. Using the mean base spoil strengths, the finer spacing resulted in a 34 % reduction in the calculated minimum F_s. For zero base spoil cohesion the reduction was only 3 %, while for zero base friction angle the reduction was 15 %. It appears that the higher the overall strength of the base spoil, the finer the state point grid spacing required to achieve acceptable accuracy, particularly where the resistance at the base is mainly cohesive. Where the resistance at the base is mainly frictional, a relatively coarse state point grid appears adequate.

7.2 Effect of Base Spoil Strength

The minimum F_s values determined in the current IDPM and GWEDGEM analyses both demonstrate the critical part played by the strength of the spoil at the base of the pile in providing stability. The GWEDGEM results show that removing either the base spoil cohesive or frictional resistances reduces the minimum F_s value to about unity. Considering the relative orders of magnitude of the two strength components, base frictional resistance has a relatively larger effect than does base cohesion.

Figures 3 to 5 show that while the removal of base spoil cohesion has little effect on the location of the critical slip surface, the removal of base spoil frictional resistance lengthens the basal

plane and steepens the back slope of the critical slip surface considerably. This has the effect of involving a greater volume of spoil in a potential failure.

7.3 Comparison of Current IDPM and GWEDGEM Results

Figures 3 to 5 show that the current IDPM and GWEDGEM analyses give similar locations for the critical slip surfaces. For the mean spoil strengths, the two analyses gave comparable minimum F_s values. However, for zero base spoil cohesion and zero base spoil friction angle, the GWEDGEM analyses gave considerably lower minimum F_s values (about unity) than the IDPM analyses.

These results appear to be mainly attributable to the effect of work-hardening in the SFEM. Since the mean spoil strengths gave a minimum F_s value well above unity, little of the spoil pile material would have yielded and subsequently work-hardened. Hence, similar minimum F_s values were obtained by the two analyses. A separate analysis with no work-hardening in the SFEM gave an almost unchanged minimum F_s value of 1.33 for the mean spoil strengths. However, the other two sets of spoil strengths brought the minimum F_s value close to unity. Under these conditions, a considerable amount of the spoil material in the vicinity of the slip surface would have yielded and the effect of the imposed work-hardening was to raise the apparent minimum F_s value. Attempted SFEM analyses without work-hardening failed to converge for these two cases.

7.4 Possible Improvements to IDPM Analysis

Refinement of the work-hardening function in the SFEM is required to avoid it causing an excessive rise in the minimum factor of safety, particularly when the minimum value approaches unity. Further investigation is warranted of the state point grid spacing required for different spoil pile geometries and spoil material strengths. Refinement of the way in which state point stresses are determined from finite element calculations is warranted. Yamagami and Ueta (8) found that there could be a significant difference in the minimum factor of safety obtained depending on how state point stresses were approximated.

8. CONCLUSIONS

The coupling of numerical optimisation techniques with stability analyses or computed stress fields has been the subject of a number of papers over the last decade. This paper adds another variant, with the use of the stochastic finite element method to calculate the stress field, and the use of an improved dynamic programming method to locate the critical slip surface. This advance is aimed at allowing for the constitutive behaviour and variability of geomaterials and improving computational efficiency.

As advances are made there is a continual need to check the results produced against more proven methods. The critical slip surface and corresponding minimum factor of safety for a coal mine spoil pile has been obtained using the new method for three sets of spoil material strengths. The results obtained have been compared with those of a proven generalised limit equilibrium based wedge analysis employing a pattern search optimisation procedure. The comparison showed good agreement in the location of the critical slip surfaces, but showed some disagreement in the minimum factors of safety obtained. Reasons for this have been suggested, highlighting features of the new method which warrant further attention.

9. ACKNOWLEDGEMENTS

The authors are indebted to the late Peter Giam and to Ian Donald for providing access to the program GWEDGEM. The co-operation of BHP-Utah Coal Limited in providing access to records of spoil density and strength data from Goonyella and Riverside Mines is gratefully acknowledged. During the course of the research work on which this paper is based, the second named author was partially supported by a National Energy Research Development and Demonstration Council grant.

10. REFERENCES

1. Boyd, G.L., Komdeur, W. and Richards, B.G. (1978). Open strip pitwall instability at Goonyella Mine - causes and effects. Proc. Aust. I.M.M. Conf., North Queensland, pp. 139-157.

2. Williams D.J. and Zou J.-Z. (1991). Stochastic finite element analysis of coal mine spoil pile stability. Proc. Int. Conf. of Assoc. for Computer Methods and Advances in Geomechanics, Cairns, Vol. 2, pp. 1411-1416.

3. Baker, R. (1980). Determination of the critical slip surface in slope stability computations. Int. J. for Numerical and Analytical Methods in Geomechanics, Vol. 4, pp. 333-359.

4. Donald, I.B. and Giam, S.K. (1989a). Improved comprehensive equilibrium stability analysis. Civil Engineering Research Report No. 1/1989, Monash Univ.

5. Richards, B.G. (1982). The finite element analysis of mine spoil slopes using slip elements to simulate strain softening yield behaviour. Civil Eng. Trans., I.E.Aust., Vol. CE24, No. 1, pp. 69-76.

6. Owen, D.R.J. (1980). Finite elements in plasticity. Pineridge Press Limited.

7. Bellman, R. (1957). Dynamic programming. Princeton Univ. Press.

8. Yamagami, T. and Ueta, Y. (1988). Search for critical slip lines in finite element stress fields by dynamic programming. Proc. Sixth Int. Conf. on Numerical Methods in Geomechanics, Innsbruck, pp. 1335-1352.

9. Giam, S.K. and Donald, I.B. (1989). Appropriate optimisation techniques for failure surface determination in geotechnical stability analysis. Civil Engineering Research Report No. 3/1989, Monash Univ.

10. Donald, I.B. and Giam, S.K. (1989b). Slope stability programs review. ACADS Publication No. U256.

Some Applications of Fuzzy Mathematics to Rock Engineering and Slope Stability

BO XIAO
B.S., M.E.
Post Graduate Student, University of Sydney
J.P. CARTER
B.E., Ph.D., F.I.E.Aust.
Professor of Civil Engineering, University of Sydney
XUEFU YU
B.E.
Professor of Mining Engineering, University of Science and Technology Beijing

SUMMARY In this paper, the basic concepts of fuzzy mathematics are described and applied to several important problems in rock engineering. A method is presented for determining the fuzzy values of typical rock mass parameters. The limit equilibrium method is used as the basis for calculation of the stability factor for a rock slope and fuzzy arithmetical operations are required to evaluate this factor because the parameters used in the calculation are considered to be indistinct. The techniques presented in the paper are illustrated by typical example calculations.

1. INTRODUCTION

Many methods of analysis have been formulated to allow quantification of the degree of stability of structural systems. In rock slope engineering the predominant technique is the limit equilibrium method. However, most of these analyses are strictly deterministic in context, i.e. they assume that the structure and its environment are deterministic quantities. In most of these analyses, a criterion for structural stability is generally established. Suppose a state parameter K is defined as a function of uncorrelated random variables $x_1, x_2, \ldots, x_n$, all of which have an influence on structural stability. The equation

$$K(x_1, x_2, \ldots, x_n) = 0 \tag{1}$$

is called the limit state condition. For example, if we consider the simple problem of a sliding block and assume that K is a function of a resistance force R and a sliding force S, both acting in the direction of sliding, then the limit state equation can be written as

$$K(R,S) = R - S = 0 \tag{2}$$

Thus the structure will be stable when $K \geq 0$ and, conversely, failure will occur when $K < 0$.

Although this is essentially a deterministic representation of stability, some parameters involved in the calculation may be "inexact" or "indistinct", in that their precise values may be difficult to determine. In other words, uncertainties exist in most aspects of structural stability, particularly when such problems occur in nature. Loads, environmental factors, material properties, and structural dimensions are usually difficult to predict due to lack of sufficient data. Furthermore, knowledge of the full complexity of the problem is often imperfect, i.e. some of the mechanisms that control stability may be poorly understood, which gives rise to additional uncertainty.

The ratio of the resisting force to the sliding force along the failure plane is called the stability factor. Thus this conventional stability factor, which is obtained from appropriate calculation, can be considered to be "fuzzy", e.g. although the calculated value of a stability factor may be greater than one, there is a finite probability that its true value may be less than one. It is because of this "fuzziness" that the stability number should not be called a safety factor.

It is worthwhile to pursue a method of analysis which can adequately describe the "fuzziness" for this and other problems in rock engineering. Fuzzy mathematics (Zadeh, 1965) has provided a potential tool for solving many real engineering problems and to date it has been used successfully on a number of important practical problems (e.g. Nguyen, 1985; Boissonnade, 1986; Xiao & Zhou, 1987; Kacewicz, 1987; Sakurai & Shimizu, 1987; Xiao & Yu, 1989; 1990).

In this paper the basic techniques of fuzzy mathematics are described. The method is used to evaluate the stability of rock slopes where potential failures are determined in each case by a single joint plane on which sliding of a rock block may occur. The use of the method to describe the fuzziness of one of the rock mass strength parameters is also illustrated.

2. BASIC CONCEPTS OF FUZZY MATHEMATICS

In this section some basic definitions and some of the important concepts of fuzzy mathematics are presented for completeness. More details are discussed by Zadeh (1965, 1975). Where appropriate, the important concepts are illustrated by examples.

2.1 Definition of a Fuzzy Set

A fuzzy set of objects x is defined as a set of ordered pairs, i.e.

$$I = \{ \mu(x) , x \} \tag{3}$$

where $\mu(x)$ is termed the "grade of membership of x in I". $\mu(x)$ may only take values in the closed interval [0,1]. For example, in structural problems, if stability is almost certain to occur, then $\mu(K)$ is equal to 1. This means that the membership function $\mu(K)$ can be regarded as a linguistic variable. In reality, there are many cases in which the transition from membership to non-membership of an object in a set is gradual rather than

abrupt. For such cases the grade of membership of x in I is represented by values of $\mu_I(x)$ in the range from 0 to 1. If the fuzzy set I contains a finite number of members, then it can also be expressed as:

$$I = \mu_I(x_1)/x_1 \cup \mu_I(x_2)/x_2 \cup \ldots \ldots \cup \mu_I(x_n)/x_n = \int \mu_I(x)/x \quad (4)$$

The symbol $\cup$ is used to represent the union operation, and the symbol / denotes the correspondence between an object in the set and its membership function. $\int$ is used here to represent all relationships between elements of the fuzzy set I and their degrees of membership. $\int$ is **not** used here to denote integration.

2.2 Fuzzy Number

A fuzzy number is a quantity that is characterised by a distribution (either discrete or continuous) of possible values. For example, consider the case where the cohesion c of a rock mass can be regarded as a fuzzy number, which is expressed as

$$c = 0.8/95 \cup 1.0/100 \cup 0.7/105.$$

In loose terms, this is the same as stating that c is "approximately 100". More formally, the above expression means that the cohesion has several possible discrete values, viz. a value of 100 with a membership grade of 1.0, a value of 95 with a grade of 0.8, and value of 105 with a grade of 0.7. Thus the membership function expresses the likelihood that the parameter has the nominated value.

2.3 Extension Principle

One of the basic ideas of fuzzy set theory, which provides a general extension of nonfuzzy mathematical concepts to fuzzy environments, is the extension principle. Consider a function f that provides a mapping of the real number x onto y, i.e. $f: x \rightarrow y$. This mapping concept can also be applied to fuzzy numbers, i.e. if I is fuzzy number, then $f: I \rightarrow f(I)$. This is called an "extension" of the mapping f.

From the extension principle, two inferences may be obtained and these are discussed below.

2.4 Inference 1

If C is a constant, then

$$C * \int \mu_I(x)/x = \int \mu_I(x)/C * x \quad (5)$$

where * denotes one of the arithmetical operations of multiplication, addition, division or subtraction. In other words, the first inference of the extension principle is that any arithmetic operation on a fuzzy set implies that the same operation is carried out on all elements of the set, but the values of the membership function for the newly formed set are the same as those of the original set.

2.5 Inference 2

If f is a relationship or a monotonic function that provides a mapping from x to y and I is a fuzzy set expressed as

$$I = \int \mu_I(x)/x \quad (6)$$

then

$$f(\int \mu_I(x)/x) = \int \mu_I(x)/f(x) \quad (7)$$

This equation states that the image of I under the relationship f can be deduced from the knowledge of the images of x under f.

2.6 Theorem

If I, J and K are three fuzzy numbers and their membership functions are μ_I, μ_J and μ_K respectively, and if $K = I * J$ is the result of an arithmetic operation on the fuzzy numbers I and J, then the membership function of K is given by

$$\mu_K(z) = \bigvee (\mu_I(x) \wedge \mu_J(y)) \quad (8)$$

where $\vee$ is the symbol used to indicate that the maximum should be selected from all possible values of the membership function, and $\wedge$ is the symbol used to indicate that the minimum should be selected from the possible values. Zero must not be a possible value of the fuzzy number J whenever * represents the operation of division.

Example

An example is now presented to illustrate some of the definitions and concepts discussed above. Suppose fuzzy numbers I and J are given as follows

$$I = 0.7/3 \cup 1.0/2 \cup 0.8/1$$

$$J = 0.9/3 \cup 0.6/2$$

then the operation of addition of these two fuzzy numbers can be represented as

$$\begin{aligned} I + J &= (0.7 \wedge 0.9)/(3+3) \cup (1.0 \wedge 0.9)/(2+3) \cup \\ &\quad (0.8 \wedge 0.9)/(1+3) \cup (0.7 \wedge 0.6)/(2+3) \cup \\ &\quad (1.0 \wedge 0.6)/(2+2) \cup (0.8 \wedge 0.6)/(2+1) \\ &= 0.7/6 \cup (0.9 \vee 0.6)/5 \cup (0.8 \vee 0.6)/4 \cup 0.6/3 \\ &= 0.7/6 \cup 0.9/5 \cup 0.8/4 \cup 0.6/3 \end{aligned}$$

3. DETERMINATION OF FUZZY PARAMETERS

One of the most difficult problems in applying the above techniques in practice involves determining the membership function for the parameters that are considered to be fuzzy. This problem arises in most applications, including the stability analysis of rock slopes. In this case the parameters which are important include those defining the geometry of the rock slope, its geological features such as jointing and bedding planes, and the shear strength of the planar features upon which rock blocks may slide. Data defining these "properties" are usually determined from field observation and laboratory testing or are estimated on the basis of experience. Discrete measurements or estimates of the important parameters are usually provided and more than one measurement of each parameter may be available. Since the data which are

obtained from testing or observation may take a wide range of values, it is convenient first to normalise the primary data before proceeding to the determination of the membership function. Furthermore, it may be possible to measure or determine values for the design parameters in a variety of different ways. It is therefore desirable to have a rational means of assigning weights to the parameter values, based upon their method of determination. Suitable processes for normalising the data and for rationally selecting the weighting factors are considered below.

3.1 Normalisation of Data

Let $X = \{x_1', x_2', \ldots, x_m'\}$, where X is a set of data to be normalised. Normalisation of the data is carried out according to the following formula

$$x_i'' = \frac{x_i' - \overline{x'}}{s} \tag{9}$$

where the mean of sample X containing m values is given by

$$\overline{x'} = (\frac{1}{m}) \sum_{i=1}^{m} x_i' \tag{10}$$

and its standard deviation is

$$s = \sqrt{\frac{1}{m}\sum_{i=1}^{m} (x_i' - \overline{x'})^2} \tag{11}$$

If normalised data is required in the range [0,1], the extreme value standardisation formula may be employed, i.e.

$$x_i = \frac{x_i'' - Min(x_i'')}{Max(x_i'') - Min(x_i'')} \tag{12}$$

where $Max\{x_i''\}$ and $Min\{x_i''\}$ denote the maximum and minimum values, respectively, of the set of values x_i''.

Example

Suppose there are five measurements of the one parameter, i.e. $x_1' = 12.2, x_2' = 7.5, x_3' = 7.0, x_4' = 6.7$, and $x_5' = 6.1$. The mean and standard deviation of this set of data can be computed from equations (10) and (11) as 7.9 and 2.2, respectively. The values of x_i'' are computed using equation (9), i.e. $x_1'' = 1.95$, $x_2'' = 0.18$, $x_3'' = -0.41$, $x_4'' = -0.55$ and $x_5'' = -0.82$. Hence, the sample data can be normalised onto the closed interval [0,1] using equation (12) to give: $x_1 = 1$, $x_2 = 0.23$, $x_3 = 0.15, x_4 = 0.1$ and $x_5 = 0$.

3.2 Weighting Factors

In many practical problems it may be possible to obtain estimates of any one design parameter by a variety of means. As mentioned above, it is desirable to have a rational means of determining weights to be assigned to each of the measurements, according to the "reliability" of each of the different methods of assessment. If one method is more important or known to be more reliable than others, then it should be assigned a large weight. Conversely, if sometimes a method is known to produce doubtful or even spurious results, it should be assigned a low weight. A method for determining the weighting coefficients is now described.

If there are n measurements of a given parameter, then the $n \times n$ matrix V of influence coefficients is first established, i.e.

$$V = \begin{bmatrix} V_{11} & V_{12} & \cdots & V_{1n} \\ V_{21} & V_{22} & \cdots & V_{2n} \\ \cdots & \cdots & \cdots & \cdots \\ V_{n1} & V_{n2} & \cdots & V_{nn} \end{bmatrix} \tag{13}$$

where the relative importance of the measurement or estimate m_i compared to m_j is quantified by the influence coefficient V_{ij}. Suggested values for V_{ij} are shown in Table I.

TABLE I

INFLUENCE COEFFICIENTS

Description	Values of V_{ij}
m_i is as important as m_j	1
m_i is only slightly more important than m_j	3
m_i is obviously important than m_j	5
m_i is much more important than m_j	7
m_i is overwhelmingly important than m_j	9

Note: Intermediate values of the influence coefficient may be defined, i.e. 2, 4, 6 or 8, as appropriate. If m_i is less important than m_j, then the reciprocals of the values of V_{ij} shown in Table I are used in the matrix V, i.e. $V_{ji} = 1/V_{ij}$ for $i \neq j$ and $V_{ii} = 1$.

Finally, the weight assigned to the factor m_i is defined by a weighting coefficient w_i, i.e.

$$w_i = \frac{\overline{w_i}}{\sum_{i=1}^{n} \overline{w_i}} \tag{14}$$

where

$$\overline{w_i} = \left[\prod_{j=1}^{n} V_{ij} \right]^{1/n} \tag{15}$$

Values of w_i will always be between 0 and 1 and the sum of the weights w_i will always be 1.

3.3 Membership Function

There exist many functions that could be used to define the membership of a fuzzy number. In this paper, the form of the membership function for problems in rock mechanics is suggested by the normal distribution used in probability theory. An important difference here is that the membership function is "weighted" according to the method by which the fuzzy parameter was determined. Accordingly, the membership function of the fuzzy parameter x_i is suggested as follows

$$\mu(x_i) = e^{-\xi \frac{(\bar{x} - x_i)^2}{w_i}} \tag{16}$$

where the mean of the values is determined by

$$\bar{x} = \frac{1}{n} \sum_{i=1}^{n} x_i \tag{17}$$

TABLE II

ROCK MASS PARAMETERS AND CSIR ROCK MASS RATINGS FOR MARBLE
(After China Nonferrous Metal Company and Daye Nonferrous Metal Company)

Parameters	c_i MPa	σ_c MPa	RQD	i	Condition of Joints	Ground water	Joint orient-ation
Values	19	79.4	70%	7	-	-	-
CSIR ratings	-	7	13	10	20	7	-15

Note: c_i is the cohesive strength of the intact rock,
σ_c is the uniaxial compressive strength of specimen,
RQD is a measure of the drill core quality,
i is the intensity of jointing, measured as the number of joints per metre.

and ξ is called "resolution number" whose value determines the "width" or "scale" of the membership distribution.

In general, a design parameter P can be expressed as a fuzzy number, as follows

$$P = \mu(x_1)/x_1 \cup \mu(x_2)/x_2 \cup \ldots \cup \mu(x_n)/x_n \quad (18)$$

There is thus some ambiguity about the value of P, and $x_1, x_2, \ldots, x_n$ are all possible values.

4. ILLUSTRATIVE EXAMPLES

To illustrate the use of the techniques described above, two different types of example are considered. In the first, the parameters that are commonly used to characterise the mechanical behaviour of a rock mass are discussed. In particular, a method to determine fuzzy values of cohesive strength of a rock mass are presented. In the second example, the problem of rock slope stability is addressed.

4.1 Example 1

In any discussion of rock parameters, it is important to distinguish characteristics of a specimen of intact rock from the properties of the rock mass as a whole. It is well known that the behaviour of the rock mass depends on the rock substance, the discontinuities as well as the presence of water and the existing in situ stress regime. At present, there are a number of methods which are used for determining rock mass strength properties on the basis of the strength of the intact rock material measured in the laboratory. For a given rock mass, different methods will result in different estimates of strength properties of the mass. Hence, in accordance with the concepts presented above, these parameters can be considered to be "fuzzy". As an example, it is possible to represent the cohesion of a rock mass by a fuzzy number, and procedures for doing this are presented below.

Consider a marble rock mass for which both field and laboratory data are available (China Nonferrous Metal company et al, 1987), as shown in Table II.

Using these data, at least four methods can be employed to estimate the cohesion of the rock mass which is denoted by c_m. These methods are described below.

(a) The CSIR geomechanics classification scheme for jointed rock masses (Hoek & Brown, 1980) may be used to provide an estimate of the rock mass cohesion. The data in Table II indicate that the overall rock mass rating (RMR) is 42, and so the rock mass can be described as Class III. For this class of rock mass the CSIR scheme suggests that the cohesion is likely to be in the range 150 - 200 kPa. For the present purpose a value of c_{m1} = 180 kPa has been selected as representative.

(b) The empirical strength criterion suggested by Hoek and Brown (1980), may be used to describe the strength of the rock mass, i.e.

$$\sigma_1 = \sigma_3 + \sqrt{m\sigma_c\sigma_3 + s\sigma_c^2} \quad (19)$$

Where σ_1 is the major principal stress, σ_3 is the minor principal stress applied to the specimen and m and s are constants which depend upon the properties of the rock and upon the extent to which it has been fractured before being subjected to the stresses σ_1 and σ_3,

As mentioned above, the total rating of the rock mass is 42. Hoek and Brown (1980) have suggested an approximate relationship between rock mass quality and the empirical strength constants. Based on this relationship the constants m and s are estimated as m=0.5 and s=0.0001.

Using the data in Table II, and the values of m and s deduced above, Mohr circles of stress corresponding to failure may be drawn. Hence the cohesion of the rock mass, applicable over the normal stress range from 0 to 10 MPa, can be determined graphically by fitting a straight line envelope to the failure circles. Following this procedure a value of c_{m2} = 220 kPa can be obtained.

(c) Hubbert et al (1960) have suggested a correlation between the intensity of rock jointing and the cohesion of the rock mass. This correlation is presented in Figure 1, where the ratio of rock mass cohesion, c_m, to the cohesion of the intact rock, c_i, is plotted against i, the "intensity" of the jointing. Based on this relationship and using the values of c_i and i presented above, a value for the rock mass cohesion is estimated as c_{m3} = 608 kPa.

(d) China Nonferrous Metal Company and the Daye Nonferrous Metal Company (1987) have deduced from

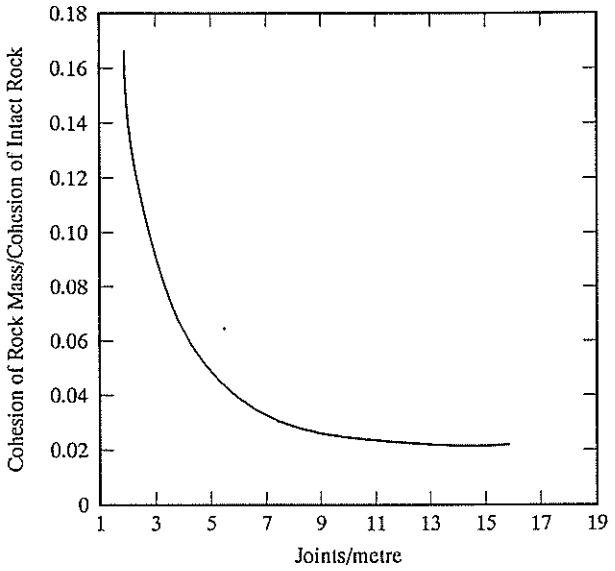

Figure 1 Relationship between joint spacing and cohesion of rock mass (after Hubbert et al)

their experience that a value of c_m may also be estimated from the formula

$$c_m = \frac{c_l}{(i+25)} \tag{20}$$

For the rock mass in question, equation (20) provides an estimate of $c_{m4} = 594$ kPa.

Each of these four estimates of the rock mass cohesion can be normalised onto the interval [0,1], using equations (10)-(13), to give: $c_{m1} = 0$, $c_{m2} = 0.094$, $c_{m3} = 1.0$ and $c_{m4} = 0.967$.

In this example, the first method for determining c_m is considered only slightly more important than the second, and much more important than the third, and obviously more important than the fourth. The matrix V, ranking the relative influence of each method, is established on the basis of Table I as follows:

$$V = \begin{bmatrix} 1 & 3 & 7 & 5 \\ 1/3 & 1 & 4 & 3 \\ 1/7 & 1/4 & 1 & 2 \\ 1/5 & 1/3 & 1/2 & 1 \end{bmatrix} \tag{21}$$

The weighting coefficients for each method can be obtained from equation (15), as $w_1 = 0.576, w_2 = 0.254$, $w_3 = 0.093$ and $w_4 = 0.077$.

Based on experience, it is suggested that a reasonable value of the resolution number ξ is 0.2 for this case. It should be noted, however, that a rational means for determining appropriate values of ξ for other types of problem have not been developed. This matter requires further research.

Substituting the normalised data, the weighting coefficients and the resolution number into equation (17), the membership grades of the fuzzy number c_m are obtained as $\mu(c_{m1}) = 0.94$, $\mu(c_{m2}) = 0.81$, $\mu(c_{m3}) = 0.60$ and $\mu(c_{m4}) = 0.59$. Therefore, the fuzzy number c_m can be expressed as follows:

$c_m = 0.81/180 \bigcup 0.94/220 \bigcup 0.6/608 \bigcup 0.59/594$ kPa

4.2 Example 2

Consider now the problem of the sliding of a rock block on a planar sliding surface, as shown in Figure 2. H is the height of the slope, γ is the unit weight of rock mass, θ is the slope angle and β is the inclination of the potential failure plane. Gravity acts in the vertical direction. The shear strength of the planar interface is described by the Mohr-Coulomb criterion with a cohesive component of the shear strength c and friction angle φ.

Under the action of gravity, the sliding force per unit width acting along the failure plane is obtained from simple statics as:

$$F_s = \frac{LH\gamma}{2}(\cos\beta - \frac{\sin\beta}{\tan\theta})\sin\beta \tag{22}$$

where L is the length of failure plane.

The force resisting this sliding can be shown to be:

$$F_r = \frac{LH\gamma}{2}(\cos\beta - \frac{\sin\beta}{\tan\theta})\cos\beta\tan\phi + Lc \tag{23}$$

The slope stability factor is conventionally expressed as:

$$K = \frac{F_r}{F_s} = \frac{2c}{\gamma H(\cos\beta - \frac{\sin\beta}{\tan\theta})\sin\beta} + \frac{\tan\phi}{\tan\beta} \tag{24}$$

In this example, the parameters c, ϕ and β are all regarded as fuzzy numbers. They are defined as follows:

$c = 1/100 \bigcup 0.7/105$ kPa
$\phi = 1/35° \bigcup 0.8/37°$
$\beta = 1/45° \bigcup 0.5/43°$

The remaining parameters defining this problem are assumed to have "crisp" (non-fuzzy) values, i.e.

$$\gamma = 20 \text{ kN/m}^3, \quad H = 40 \text{ m}, \quad \theta = 60°$$

The stability factor may be calculated from equation (24), using Inferences 1, 2 and the theorem presented previously to perform the appropriate arithmetic operations on the fuzzy numbers. These operations give the fuzzy stability factor as:

$$K = 0.5/1.7 \bigcup 0.5/1.8 \bigcup 1.0/1.9 \bigcup 0.8/2.0 \bigcup 0.5/2.1 \bigcup 0.5/2.2$$

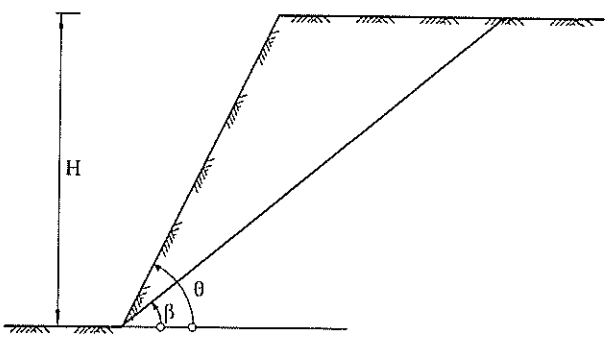

Figure 2 Geometry of the slope

TABLE III

QUALITATIVE DESCRIPTION
OF THE MEMBERSHIP FUNCTION

Class	Value of Membership Function	Meaning
1	$\mu(K) = 0$	Certainly will not occur
2	$0 < \mu(K) \leq 0.1$	Very unlikely to occur
3	$0.1 < \mu(K) \leq 0.3$	Seldom occurs
4	$0.3 < \mu(K) \leq 0.5$	Could occur
5	$0.5 < \mu(K) \leq 0.7$	Likely to occur
6	$0.7 < \mu(K) \leq 0.9$	Very likely to occur
7	$0.9 < \mu(K) \leq 1.0$	Will almost certainly occur

In order to describe the possible distribution of the stability factor K, Table III provides suggested meanings that are to be associated with selected values of the membership function for K.

The relationship between K and its membership function is shown in Figure 3. This figure indicates that a stability factor of 1.9 has a value of the membership function equal to 1. According to Table III, this outcome can be described qualitatively as "will almost certainly occur". A value of the factor equal to 2.0 is "very likely to occur" and other values of the stability factor, viz. 1.7 to 1.8 and 2.1 to 2.2 "could occur".

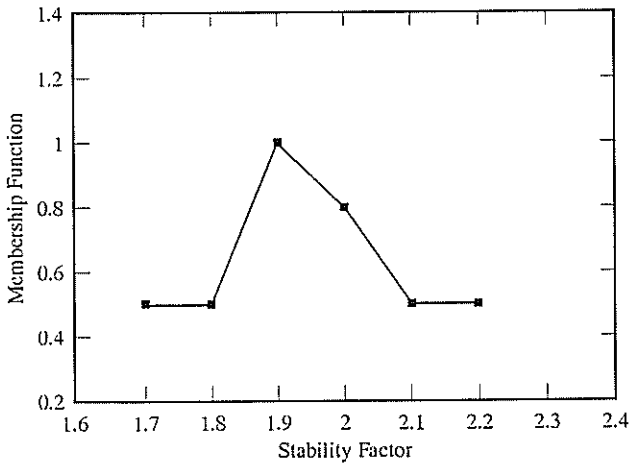

Figure 3 Fuzzy stability factor

5. CONCLUSION

The methods presented in this paper can be used not only to establish a model for describing complex or imperfect systems, but can also make full use of human ability to handle imprecise and vague information.

The procedures required to determine the fuzzy number in rock engineering and the fuzzy stability factor for a rock slope have been presented, together with the essential background theory of fuzzy mathematics.

6. ACKNOWLEDGMENTS

Partial support for this work was provided in the form of Research Scholarships awarded to the first author by the Centre for Geotechnical Research at the University of Sydney and by the China State Education Commission. Support for some of this work was also provided by the Australian Research Council.

7. REFERENCES

China Nonferrous Metal Company and Daye Nonferrous Metal Company, Hubai China (1987) The Slope Stability and Selection of Reinforcement Design at Tonglu Mine. Research Report, pp. 12-24. (In Chinese)

Bienianwski, Z.T. (1979) The Geomechanics Classification in Rock Engineering Applications. Proc. 4th Int. Cong. on Rock Mech., ISRM, Montreux, Vol. 2, A.A.Balkema, Rotterdam, pp. 41-48.

Boissonnade, A.C. (1986) Identification of Fuzzy Systems in Civil Engineering. Proc. Int. Symposium on Fuzzy Math. in Earthquake Researches. Seismological Press, Beijing. pp. 48-71.

Hoek, E. and Brown E.T. (1980) Underground Excavations in Rock. Institute of Mining and Metallurgy, London.

Hubbert, M.K. and Rubey, W.W. (1960) Role of Fluid Pressure in Mechanics of Overthrust Fault. Bull. Geol. Soc. Amer. 70 and 71.

Kacewicz, M. (1987) Fuzzy slope stability method, Math. Geol., V.19, No. 8, pp. 757-767.

Nguyen, V. U. (1985) Some Fuzzy Set Applications in Mining Geomechanics, Int. Jour. of Rock Mech. Min. Sci. & Geomech. Abstr., Vol. 22, No. 6, pp. 369-379.

Sakurai, S. and Shimizu, N. (1987) Assessment of Rock Slope Stability by Fuzzy Set Theory, Proc. 6th Int. Cong. on Rock Mech., ISRM, Montreal, A.A.Balkema, Rotterdam, Vol.2, pp. 503-506

Xiao, B. and Zhou, C. (1987) Discussion on Fuzzy Mathematics Used for Slope Stability, Jour. of Yunnan Metallurgy, No. 4, pp. 5-10. (In Chinese)

Xiao, B. and Yu, X. (1989) Survey of Numerical Methods for Slope Engineering. Jour. of Mine Technology. No. 5, pp. 13-16. (In Chinese)

Xiao, B. and Yu, X. (1990) Fuzzy Limit Equilibrium Analysis for Slope Stability. Jour. of Nonferrous Metals (Quarterly), No. 3, pp. 1-5. (In Chinese)

Zadeh, L.A. (1965) Fuzzy Sets, Information and Control, Vol. 8, pp. 338-358.

Zadeh, L.A. (1975) Calculation of Fuzzy Restriction in Fuzzy Sets and Their Application to Cognitive and Decision Processes, Academic Press, New York.

Finite Element Analysis of Pressuremeter Tests in Soil

H.S.YU
M.Sc., D.I.C., D.Phil.
Lecturer, University of Newcastle, Australia

SUMMARY. A finite element analysis is carried out for the self-boring pressuremeter tests in clay. The main objective of this study is to quantify possible effects of finite length of the pressuremeter on soil parameters derived from the tests. It has been concluded that serious overestimation of the strength parameters of clay may be deduced by applying the Gibson and Anderson method to field pressuremeter tests. A new interpretation procedure is therefore proposed to eliminate effects due to the simple assumptions used in the conventional interpretation method.

1. INTRODUCTION

In the early stage of development of pressuremeters, the results of pressuremeter tests were interpreted by means of empirical expressions to give parameters for design such as allowable bearing capacity factors and moduli for allowable settlement. The first fundamental interpretation of an expansion test was published by Gibson and Anderson (1961) in which the pressuremeter was considered to be infinitely long so that the deformation of the surrounding soil was assumed to be in conditions of axial symmetry and plane strain. The interpretation was developed for both undrained expansion tests in clay and expansion tests in cohesionless soils, for which the soil is assumed to behave elastically until failure occurs at a constant effective stress ratio and with no volume change.

As far as the undrained expansion is concerned, Palmer (1972) has also developed a method which can be used to interpret pressuremeter tests without a prerequisite assumption of stress-strain relationship for the soil being tested. However this approach has been found to be very sensitive to the disturbance of the soil caused by installation, and the resulting uncertainty about the reference strain. By comparison, it is generally accepted that the original Gibson and Anderson analysis is preferable in deriving undrained shear strength as recommended by Mair and Wood (1987). Although the Gibson and Anderson analysis has been widely used to interpret self-boring pressuremeter tests in clay, it is also recognised that it often leads to overestimation of undrained strength.

The literature contains several well-documented reports of tests on clays with the self-boring pressuremeter. Results indicate important disagreement with the results of good laboratory tests or other in-situ tests. It is the Authors belief that these disagreements may be largely due to the influence of the finite length of the pressuremeter. Although the analyses assume an infinitely long pressuremeter, a typical length to diameter ratio is about six. Yu (1990) has recently carried out a comprehensive study of the influence of finite length for various pressuremter tests in both clay and sand. In his study, a two-dimensional finite element analysis was used to simulate pressuremeter tests, which are then back-analysed using the conventional cavity expansion solutions. This paper will concentrate on the influence of finite length for self-boring pressuremeter tests in clay. The pressuremeter tests are analysed using a novel two-dimensional finite element formulation, which is particularly suitable for axisymmetric problems (Yu, 1991; Yu et. al., 1991).

2. NUMERICAL MODELLING OF PRESSUREMETER TESTS

In this paper, the self-boring pressuremeter was assumed to be installed deep into the ground without any disturbance and the initial soil stress state was assumed unchanged by the installation of the pressuremeter. To isolate effects due to the finite length of the pressuremeter from possible numerical errors due to the non-linear solution algorithm, a calibration calculation with an infinitely long pressuremeter was carried out for each pressuremeter test with a finite length of probe. Figure 1 shows a mesh for real pressuremeter calculations which consists of 288 modified 6 node triangular elements and the mesh with a plane strain condition in the vertical direction was used to model infinitely long pressuremeters. Care was taken in designing these meshes so that possible regions with higher stress gradients have a higher density of elements. The pressuremeter membrane was modelled by 6 elements and boundary conditions used in calculations are shown in Figure 1.

A fixed ratio of the total height of mesh to half length of the pressuremeter has been used and different length to diameter ratios are obtained by multiplying the vertical coordinate of all meshes by a certain factor. The material behaviour of the infinite medium was simulated by a correcting layer for which the continuum properties and the correcting layer properties are related by an elastic solution (Yu, 1990).

3. ANALYSIS OF PRESSUREMETER TESTS

3.1 Parameters for the Analysis

In order to quantify the effects due to the finite length of pressuremeter probes, numerical simulations of self-boring pressuremeter tests in clay have been carried out using the axisymmetric finite element method developed by the author (Yu, 1991). The soil mass has been idealised as an

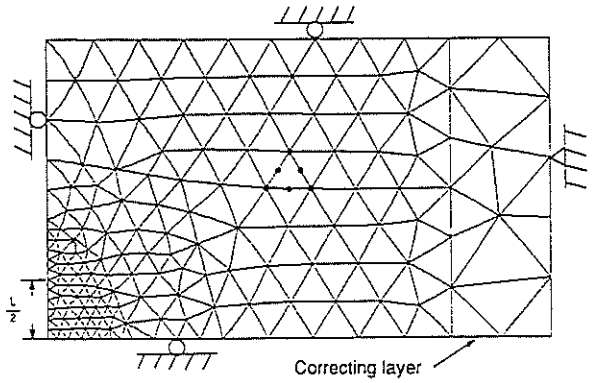

Figure 1: Finite element mesh used for simulation of pressuremeter tests

elastic-perfectly plastic medium which obeys the von Mises yield criterion and deforms under constant volume conditions. Pressure controlled 'quick' expansion tests were simulated and each test was continued to a cavity strain $\epsilon = 10\%$ for centre of pressuremeter membrane. Effects due to finite stiffness of membrane are ignored in this study.

Table 1 summarises all values of the key parameters varied in the numerical simulations. An isotropic initial stress state with zero value for all stress components was assumed.

Table 1 Numerical tests of self-boring pressuremeter in clay

$\frac{I_r}{\frac{L}{2}}$	50	100	200	300	500
4	F8	F12	F16	F20	F4
6	F7	F11	F15	F19	F3
8	F6	F10	F14	F18	F2
∞	F5	F9	F13	F17	F1

Figure 2 shows a typical set of results of numerical simulations of the self-boring pressuremeter test in clay. The pressure-expansion curve from each numerical simulation was interpreted as if it were derived from a real field test, using the standard technique proposed by Gibson and Anderson. The shear modulus G has been derived from the initial pressure-expansion curve over the range $\psi = 0 \rightarrow s_u$, which is the elastic range for the Tresca material. For the von Mises material used in this study, the elastic range is expected to be even larger than that for the Tresca model. With respect to determination of shear strength, two approaches were recommended by Mair and Wood (1987). The plot of ψ against $\ln \epsilon_v$ is usually used to define s_u, which can either be estimated from the slope of the curve or the extrapolated limit pressure at $\frac{V-V_0}{V} = 1$. As pointed out by Mair and Wood, strengths obtained with the limit pressure method appear to be less sensitive to the assumed reference conditions, and hence less sensitive to disturbance associated with installation of the pressuremeter. Both of these approaches have been used to derive undrained shear strength from the expansion curve for comparisons. In order to investigate possible effects of using different volumetric strain definitions, two different ways of deriving it namely, $\epsilon_v = 2\ln(\frac{a}{a_0}), \epsilon_v = \ln(\frac{V}{V_0})$ were used, where a, a_0 are the current and initial radius of the middle point of the pressuremeter membrane and V, V_0 are the current and initial pressuremeter volumes respectively. A least squares method was used to find the slope in deriving the shear strength.

Two different strain ranges measured by strain magnitude of the middle point of the membrane (i.e. $\epsilon_c = 2 \rightarrow 5\%$ and $\epsilon_c = 2 \rightarrow 10\%$) were chosen for deducing the undrained shear strength so that the analysis may be objective and possible effects due to different strain ranges used for deriving the undrained shear strength could be quantified.

When the undrained shear strength is estimated from the limit pressure by extrapolation, the so-called Menard limit pressure is used for interpretation. The Menard limit pressure is defined as the pressure at which $\frac{V}{V_0} = 2$, corresponding to $\frac{a}{a_0} = \sqrt{2}$. The choice of Menard limit pressure instead of the true limit pressure at which $\frac{V}{V_0} = \infty$ allows the interpretation to be made using the two different volumetric strain definitions described earlier. In determining the effects due to finite length of pressuremeters, we need to investigate the ratio of limit pressures of pressuremeter tests with an infinitely long probe and those with a finite length. The following expression was assumed:

$$\psi_{lm} = s_u^l(1 + \ln(\frac{G}{s_u^l})) \qquad (1)$$

where ψ_{lm} denotes the Menard limit pressure, which is found by extrapolating the expansion curve in the range $\epsilon_c = 5 \rightarrow 10\%$, and s_u^l represents the undrained shear strength corresponding to the Menard limit pressure. After obtaining ψ_{lm} for each pressuremeter test, equation (1) can be used to derive s_u^l using a Newton-Raphson solution scheme.

3.2 Numerical Results

The derived undrained shear strengths for each pressuremeter test are summarised in Table 2 and Table 3. Table 4 shows the derived shear moduli. For all the cases, $s_{utc} = 1.0$ is used which corresponds to a plane strain undrained shear

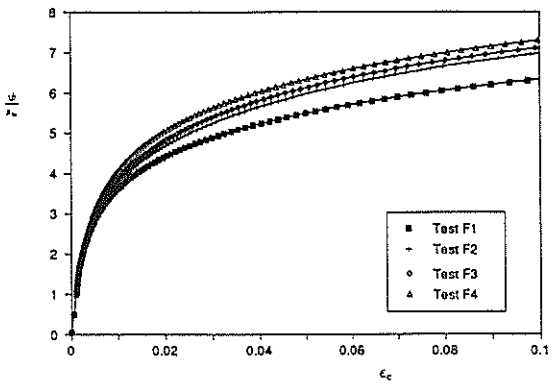

Figure 2: A typical set of results for numerical simulations of the self-boring pressuremeter test in clay

strength of $\frac{2}{\sqrt{3}}$. The derived values of plane strain undrained shear strength from the numerical analyses of the pressuremeter tests with an infinitely long probe are found to be in good agreement with the actual shear strength used in the analysis. The maximum error is found to be less than about 2%. This evidence suggests that the performance of the numerical method used in the analysis is very satisfactory. It is also necessary to note that in Table 4 the actual values of shear moduli used in the analysis are equal to the values of rigidity index (i.e. $I_r = \frac{G}{s_{utc}}$) listed in the Table because a value of unity for s_{utc} is used in the calculation.

Table 2 The derived shear strength for self-boring pressuremeter test in clay using loading slope

$\frac{L}{D}$	I_r	50		100		200		300		500	
	ϵ_c	2 – 5%	2 – 10%	2 – 5%	2 – 10%	2 – 5%	2 – 10%	2 – 5%	2 – 10%	2 – 5%	2 – 10%
4	s_{uv}	1.3227	1.3506	1.3546	1.3673	1.3625	1.3686	1.3582	1.3653	1.3563	1.3627
	s_{uc}	1.3434	1.4057	1.4312	1.4553	1.4530	1.4430	1.4307	1.4172	1.3947	1.3884
6	s_{uv}	1.2692	1.3055	1.3141	1.3330	1.3390	1.3583	1.3518	1.3668	1.3624	1.3705
	s_{uc}	1.2514	1.3077	1.3297	1.3777	1.4042	1.4309	1.4264	1.4358	1.4269	1.4217
8	s_{uv}	1.2329	1.2776	1.2883	1.3017	1.3046	1.3328	1.3261	1.3510	1.3478	1.3648
	s_{uc}	1.2144	1.2582	1.2648	1.3123	1.3404	1.3842	1.3798	1.4130	1.4125	1.4264
∞	s_{uv}	1.1488	1.1707	1.1676	1.1777	1.1666	1.1787	1.1689	1.1793	1.1697	1.1814
	s_{uc}	1.1555	1.1744	1.1664	1.1769	1.1666	1.1784	1.1686	1.1790	1.1695	1.1812

In general it can be seen that the use of conventional one dimensional cavity expansion theory to pressuremeter tests with finite length of probes tends to overestimate both shear strength and shear moduli. When the volumetric strain is defined by twice central strain of the membrane, the overestimation of shear moduli was found to be negligible even for the pressuremeter tests with a length/diameter ratio of 4. Significant overprediction of shear moduli was observed, however, when the volumetric strain is calculated from the actual volume of the pressuremeter membrane. As far as undrained shear strength is concerned, the numerical results suggest that the overestimation due to the finite length/diameter ratio, using the approach of deriving undrained shear strength from the slope of logarithmic plot of expansion curve, largely depends on the rigidity index of the soil. The rigidity index is defined as ratio of shear modulus to undrained shear strength. By comparison, it is interesting to note that the effect on undrained shear strength due to pressuremeter geometry, using the approach of deducing undrained shear strength from the limit pressure, are relatively independent of the rigidity index. The following sections are devoted to examining the variation of the length/diameter ratio effects with different parameters for the pressuremeter tests.

Table 3 The derived shear strength for self-boring pressuremeter test in clay using limit pressure

$\frac{L}{D}$	I_r	50	100	200	300	500
4	s^l_{uv}	1.2857	1.3099	1.3096	1.3091	1.3104
	s^l_{uc}	1.2689	1.3045	1.3022	1.3005	1.3073
6	s^l_{uv}	1.2270	1.2478	1.2692	1.2734	1.2808
	s^l_{uc}	1.1938	1.2303	1.2545	1.2598	1.2762
8	s^l_{uv}	1.1690	1.2057	1.2363	1.2395	1.2483
	s^l_{uc}	1.1363	1.1779	1.2072	1.2260	1.2483
∞	s^l_{uv}	1.0395	1.0491	1.0798	1.0844	1.0938
	s^l_{uc}	1.0474	1.0491	1.0745	1.0844	1.0923

Table 4 The derived shear moduli for self-boring pressuremeter test in clay

$\frac{L}{D}$	I_r	50	100	200	300	500
4	G_v	58.5628	116.8647	233.4681	350.0718	583.2787
	G_c	49.8962	99.5284	198.7926	298.0567	496.5849
6	G_v	55.0649	109.8705	219.4812	329.0920	548.3132
	G_c	48.9956	97.7274	195.1905	292.6537	487.5797
8	G_v	53.4678	106.6770	213.0952	319.5133	532.3491
	G_c	48.8132	97.36259	194.4609	291.5592	485.7556
∞	G_v	48.1071	95.9503	191.6364	287.3225	478.6946
	G_c	48.5762	96.8885	193.5128	290.1371	483.3856

3.3 Effects of Length to Diameter Ratio

The effects of length to diameter ratio on derived soil properties may be examined in detail by considering the case where the rigidity index is equal to 100. The ratio of derived parameters from pressuremeter tests with an infinitely long membrane to derived parameters from pressuremeter tests with a finite length of membrane was used to measure the effects of finite length.

The variation of the effects on stiffness, due to the finite length of pressuremeter probe, with length to diameter ratio is shown in Figure 3. It can be seen that the membrane end effects for the case when volumetric strain is calculated from the volume of the pressuremeter are more significant than the case when volumetric strain is assumed to be twice the central strain of the membrane. For the pressuremeter tests with a length to diameter ratio of 6, the overestimation of shear modulus is about 13% when the volumetric strain is calculated from volume of pressuremeter.

As far as the shear strength is concerned, different ways of deriving the strength were distinguished. The variation of the effects due to finite length of pressuremeter with length to diameter ratio is shown in Figure 4 to Figure 5 for different ways of calculating the volumetric strain. It can be seen that the effects of finite length of the pressuremeter increases when the length to diameter ratio decreases.

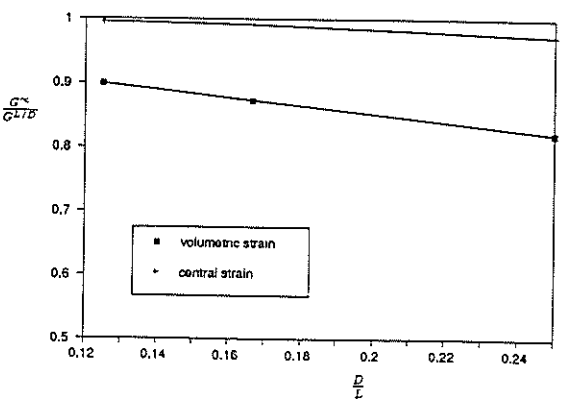

Figure 3: Effects on shear modulus due to length to diameter ratio

3.4 Effects of Soil Rigidity Index

Five different values of rigidity index, denoted by I_r, have been used in the numerical calculations so that the possible effects due to variation of rigidity index on the derived soil properties may be fully quantified. To isolate the effects of rigidity index from the effects due to different length to diameter ratios, the case when the length to diameter ratio is equal to 6 was chosen to highlight the importance of rigidity index.

From Table 4, it is easily noticed that the variation of effects on shear modulus, due to the finite length of pressuremeter probes, with rigidity index is very small, and could be neglected in practice.

The numerical results of the effect on undrained strength due to finite length of pressuremeters for the case when length to diameter ratio is equal to 6 are shown in Figure 6 to Figure 7 for two different ways of deriving the volumetric strain used in the analysis. It can be seen that the ratio of the derived undrained shear strength for pressuremeter tests with an infinitely long probe to the derived shear strength for the pressuremeter tests with a length to diameter ratio of 6 is less than unity for all cases.

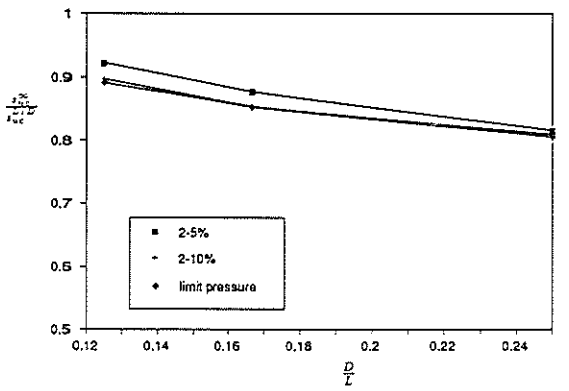

Figure 4: Effects on strength due to finite length using central strain

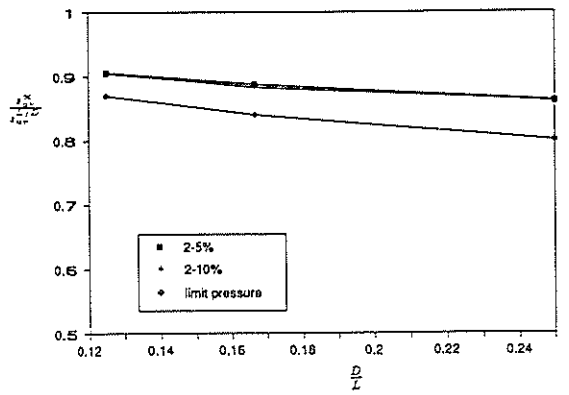

Figure 5: Effects on strength due to finite length using volumetric strain

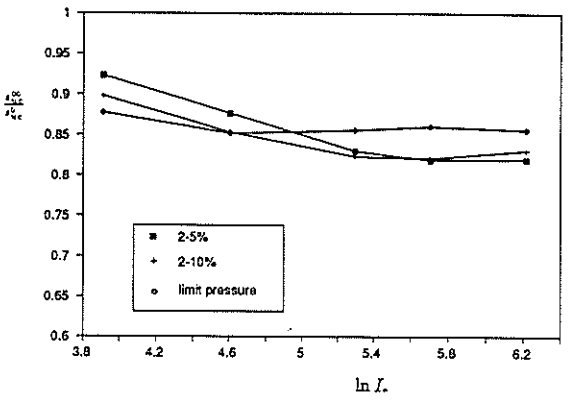

Figure 6: Variation of finite length effects on strength with rigidity index using central strain

It suggests that the use of the conventional one dimensional interpretation method for the real pressuremeter tests with a finite length tends to overestimate the 'true' undrained shear strength. It is interesting to see that the effects due to finite length are relatively independent of the rigidity index if the undrained shear strength is derived from the limit pressure. The average overestimation of undrained shear strength for this case is about 15%. For the case when the undrained shear strength is deduced from the slope of pressuremeter expansion curve, the finite length effects increase with the rigidity index.

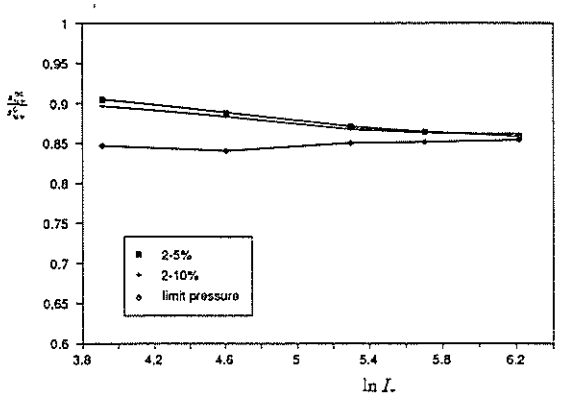

Figure 7: Variation of finite length effects on strength with rigidity index using volumetric strain

4. RECOMMENDED INTERPRETATION PROCEDURE

The analysis presented above has illustrated clearly the danger of applying an undrained shear strength profile obtained from self-boring pressuremeter tests using the conventional Gibson and Anderson method. By using the numerical results, a correction may be made to the pressuremeter test results to account for the finite length effects.

A value of 6 for length to diameter ratio may be used to represent the geometry of the self-boring pressuremeter which has been widely used in practice (e.g. the Cambridge self-boring pressuremeter). Hence only numerical results for the pressuremeter tests with a length to diameter ratio of 6 are considered in the following discussion. Of course, the same argument may be used for self-boring pressuremeter tests with a different length to diameter ratio.

For self-boring pressuremeter tests in clay, the effects on derived undrained shear strength due to the finite length of the probe depends on the approach used to derive the undrained shear strength. As was mentioned earlier, when the undrained shear strength is estimated from the limit pressure, the finite length effect is relatively independent of the rigidity index and the average overestimation of the undrained shear strength was found to be about 15%. This suggests that when the undrained shear strength is obtained from the limit pressure approach, the finite length effects may be accounted for by multiplying the derived strength by a factor of 0.85.

On the other hand, if the undrained shear strength is estimated from the pressuremeter expansion slope, it is necessary to distinguish the two different strain definitions used in presenting the pressuremeter expansion curve. When the undrained shear strength is obtained from the plot of pressure against the volumetric strain, the following expression may be used to represent the finite length effects on the derived strength:

$$\frac{s_{uv}^{\infty}}{s_{uv}^{6}} = 0.971 - 0.0185 \ln I_r \qquad (2)$$

If the undrained shear strength is estimated from the plot of pressure against the membrane central strain, the finite length effect was found to be slightly dependent on the strain ranges used in the interpretation. In general, the use of the membrane central strain could lead to a slightly more overestimation of the undrained strength due to finite length of pressuremeters.

Equation (2) may be used to improve the conventional Gibson and Anderson method in deriving the undrained shear strength from the pressuremeter test results.

With respect to the shear modulus, it was found that the effect on shear modulus due to finite length is negligible when the shear modulus is derived from the initial curve in the plot of pressure against membrane central strain. However, if the plot of pressure against volumetric strain is used to estimate the shear modulus, the finite length effect was found to be quite significant. The overestimation of the shear modulus due to the finite length may go up to 13%. It suggests that the derived shear modulus from the plot of pressure against volumetric strain for the pressuremeter test results needs to be multiplied by 0.87 in order to eliminate the effect due to pressuremeter geometry.

5. CONCLUSION

One of the major advantages of the pressuremeter test is the possibility of evaluating accurate soil parameters from the test data. In the past a simplified one-dimensional cavity expansion theory has been used to reduce the pressuremeter test data to give design parameters. The cavity expansion theory involves important assumptions about the material behaviour and pressuremeter geometry. In this paper, the two-dimensional finite element formulation was used to assess the effects of pressuremeter geometry on derived soil parameters.

For the self-boring pressuremeter tests in clay, it was found that use of the conventional Gibson and Anderson method for the field pressuremeter test tends to overestimate the undrained shear strength and shear modulus. It is interesting to note that the overestimation of the shear modulus, when derived from the plot of the pressure against central membrane strain, is negligible. As far as the shear strength is concerned, the numerical results suggest strong dependence of the finite length effects on rigidity index when the undrained shear strength is derived from the loading slope. By contrast, when using the limit pressure to obtain the undrained shear strength, the finite length effects have been found to be relatively independent of the rigidity index of the soil.

Based on numerical results, an improved procedure for obtaining soil parameters from pressuremeter tests in clay has been proposed to eliminate effects of using the simple assumptions in the conventional interpretation methods.

6. ACKNOWLEDGEMENT

The work presented in this paper was carried out while the author was a research student at the University of Oxford. The author wishes to thank Professor G.T. Houlsby for his useful supervision.

7. REFERENCES

Gibson, R.E. and Anderson, W.F.(1961). In-situ measurement of soil properties with the pressuremeter. *Civ. Engng. Publi. Wks. Rev.*, 56:615-618.

Mair, R.J. and Wood, D.M.(1987). *Pressuremeter testing - Methods and interpretation.* Butterworths, London.

Palmer, A.C.(1972). Undrained plane strain expansion of a cylindrical cavity in clays. *Geotechnique*, 22:451-457.

Yu, H.S.(1990). *Cavity expansion theory and its application to the analysis of pressuremeters.* D.Phil. Thesis, Oxford University, England.

Yu, H.S.(1991). Rational Displacement Interpolation Function for Axisymmetric Finite Element Analysis of Nearly Incompressible Materials. *Finite Elements in Analysis and Design (in press).*

Yu, H.S., Houlsby, G.T. and Burd, J.H.(1991). A novel isoparametric finite element displacement formulation for axisymmetric analysis of nearly incompressible materials. *Int. J. Num. Meth. Eng. (in press).*

General Report – Slope Stability and Seismic Hazard

B.W. RIDDOLLS
Riddolls Consultants Ltd, Queenstown, N.Z.
I.R. BROWN
Ian R. Brown and Associates Ltd, Wellington, N.Z.

1. INTRODUCTION

This paper gives an overview of the eleven papers allocated to this session of the conference. They cover a broad range of topics, and have been arbitrarily grouped as follows:

- Slope Stability
  - Hazard / Risk Assessment and Zoning
  - Failure Mechanisms and Analysis
  - Stabilisation
- Seismic Hazard

No "State-of-the-art" reviews have been attempted; emphasis is on highlighting the main points made in each paper, especially any which could form the basis for generating Session discussion.

2. SLOPE STABILITY

2.1 Hazard/Risk Assessment and Zoning

2.1.1 Assessing geotechnical risk of instability between adjacent mining operations.

Dunbavan and Boyd[1] describe a case study involving a 60m highwall failure located at the boundary between two different coal mining operations in the New South Wales Northern Coalfield. Adverse geological structure had not been appreciated at the time of establishing a boundary mining agreement.

A probabilistic approach to stability analysis was adopted to help define mining limits and assess future risk.

Previous instability had occurred along a mylonitic weak zone at the base of a coal seam (p), one of a four seam sequence dipping out of the highwall at moderate angles; groundwater was observed to be perched on the seam. Strength parameters were evaluated both in the laboratory and by back analysis, the latter giving field roughness and waviness effects.

To reflect variations in ground conditions both across and along the highwall, stability analyses included a probabilistic approach (Point Estimate Method) to give a probability distribution for the factor of safety at each cross section. Failure surfaces through two seams were assessed separately. The factor of Safety was assumed to be a function of three variables involving shear resistance and groundwater. For a particular highwall profile and location, the average Factor of safety was calculated for the probability distributions of the three selected variables.

For risk assessment, because groundwater level was shown to vary with time, the probability distribution of the factor of safety was based on variables relevant in a 1000 year storm event. To establish mining limits, the point estimate method was used to determine highwall locations that met design criteria. Risk of slope failure was then calculated using probability of occurrence of groundwater levels resulting from the 1000 year storm event. The quantitative risk assessment was applied to both failure surfaces, involving either partial or complete highwall failure. The differences in risk were found to be helpful in evaluating the consequences of slope instability. Quantification of risk also provided an opportunity to value the cost of insuring against losses.

The case history is a useful illustration of alternative approaches of assessing risk, and relating these to financial aspects.

2.1.2 Rock slope instability zoning with kinematic and morphological factors

Glawe and Hudson[2] describe a study of both the kinematic (i.e. movement) and morphological characteristics of an unstable slope in Austria. It involved sliding of a 40m thick jointed limestone plateau forming mass on an 8m sequence of weaker sediments.

Activity was monitored by both surface surveys and locally on individual blocks by precise instrumentation.

Differing rates of movement are compared with morphological characteristics of the disintegrating limestone slab which vary according to extent of downslope displacement and block diminution; 5 zones were distinguished.

Potential failure mechanisms were examined by means of modelling (finite element) of individual blocks to identify likely areas of stress concentration and displacement. This indicated the development of a tensile zone within the lower parts of the limestone behind the free face which could have initiated the disintegration of the stiff slab into single blocks.

The study highlights the merits of a combined approach to stability assessment.

2.1.3 Landslide Risk Zoning

The paper by Fell[3] describes risk zoning schemes that have been developed and used in various parts of eastern Australia. It includes discussion on confusion over terminology (i.e. hazard and risk), and the influence on a scheme of the user, liability, and insurance matters. Confusion over the meaning of the terms "hazard" and "risk" is attributed to their interchangeability in common usage, both essentially implying chance (of loss etc.). Following Hunt[4], the author adopts the definitions:

Hazard - refers to the slope failure itself and probability of occurrence.

Risk - refers to the consequences of failure on human activities.

The various landslide risk zoning schemes described relate to particular areas, the majority being based on a widely accepted risk classification for slope instability developed originally for the Sydney basin by the Sydney group of the Australian Geomechanics Society. This classification uses criteria that are a mixture of hazard, i.e. probability of occurrence, risk, i.e. the implications of failure, and method i.e. statements of evidence of potential for loss of life. It includes "Implications for development" including extent of geotechnical investigations required.

In the Lake Macquarrie City Council area of New South Wales, a zoning of geotechnical conditions affecting stability forms the basis for screening for requirement for assessment in terms of the AGS risk classification. Zones not requiring such assessment would thus tend to have less investigation or development costs.

In a landslide zonation of the Shire of Lillydale, Victoria, the AGS risk classification was applied, slightly modified to fewer classes, due to limited availability of information, with amendments to assessment requirements, and giving supplementary information on both extent and probability of damage, and development controls. The zonation has provided a basis for the Shire to implement controls without reference to a geotechnical assessment.

The study identified the Montrose Debris slide area, which occurred on the western slope of Mt Dandenong in 1891, and is now developed for housing. This area was the subject of more detailed zonation work, including evaluation of potential debris flow characteristics, qualification of probable size, recurrence and damage/injury potential, and development control alternatives.

The paper concludes by advocating standards of hazard and risk terminology, and discusses some limitation of the AGS classification ensuing from its use, including the impact of high risk categorization on property values, and conservative assessments from practitioners, owing to lack of landslide insurance in Australia. Such insurance cover is perceived to allow for more "economic zoning" in New Zealand and the UK. The lack of insurance or compensation funding in Australia is also mentioned in relation to whether people should remain in areas where the probability of injury or loss of life is greatest.

The paper raises many issues worthy of further discussion, not least of which is clarification of "hazard and risk" definitions. We believe adoption of those such as given in IPENZ "Engineering Risk"[5] would help reduce confusion i.e.:

Hazard - A condition or situation which has the potential to create or increase harm.....

Risk - The probability that a potential hazard will be realised .....

2.2 Failure Mechanisms & Analysis

2.2.1 Landslide and uplift of river bed

The paper by Mehrotra et al.[6] describes a major landslide event in Garwhal Himalaya, India, which occurred after 36 hours of continuous heavy rain. At the toe, the landslide resulted in some 8m of uplift of the bed of the Tal River over a distance of 250m, causing it to change its course.

Bedrock consists of Eocene shales and sandstones. In the slide area, the shales are fractured and moderately to highly weathered, and the sandstones hard and massive. The landslide involved the weathered shale and included movement along the interface with the sandstone.

Analysed numerically as a rotational failure, results showed such slope conditions to be highly unstable with only marginal increase in pore pressure, common during the monsoon.

2.2.2 Stability analysis in stiff fissured clay

Moon[7] presents a case study where geotechnical risk has been minimised by an improved understanding of the site geology, and by detailed observation and monitoring during construction. The presence of closely

spaced slickensided and/or polished defects in stiff soils around a coastal project were recognised following a slope failure. The paper outlines the development of understanding of site geology, the nature of soil defects, and material properties. Of particular interest is the generalised slope model used in the project, which enabled a rapid assessment of approximate factor of safety to be made, using a stability chart. The charts took into account the depth and thickness of the layer containing defects, and the dip and continuity of the defects.

2.2.3 Effect of autocorrelation on probability of failure

Mostyn and Soo[8] have used five case studies of slope stability analyses that have been published in the literature to investigate the effect of autocorrelation on the probability of failure. In this paper, the authors are concerned with autocorrelation of strength parameters c and ø, i.e. the correlation of each parameter with itself in space. The authors state that autocorrelation is reflected in the fact that the property of a soil within a particular layer will vary in space, but the value of this property at two points close together is likely to be similar, while the values for points remote from each other are likely to be independent of each other.

We do not believe that the last part of this statement should be true. One of the purposes of site investigations is to define the geometry of a slope stability problem so that regions or zones can be identified where values for material properties are likely to be homogeneous; if the values of properties for points remote from each other are shown to be independent of each other, then it would seem that there is a basic problem with definition of the site geometry. The authors have found that using their assumptions regarding autocorrelation in the five case studies, there are significant reductions in the computed probabilities of failure. Despite considerable amount of research that has been carried out over the years on probabilistic slope stability analyses, we do not see this approach widely used in engineering practice.

The paper by Mostyn and Soo adds to the literature on this topic, but we believe it is unlikely that their results will alter the reluctance of practising engineers to adopt probabilistic analyses.

2.2.4 Assessing effects of earthquakes on slopes

Sinclair's[9] paper proposes a simple method for assessing the reduction in factor of safety of a slope due to an earthquake, or of estimating the yield acceleration at which deformation might occur. The method depends on the slope angle and the factor of safety of the slope immediately prior to the earthquake. Sinclair's procedure will no doubt be helpful for slope assessments where more rigorous analysis is not required. He has been clear in stating the limitations of using the method. Although the method of analysis is simple, this is only true if the factor of safety of the slope prior to the earthquake is known. To arrive at an accurate static factor of safety in most cases will probably require a stability analysis. Once a model is set up on a computer, then it can be used to carry out a more rigorous analysis of the effects of earthquake loading, which means there may be little advantage in using a simplified method.

2.3 Stabilisation

Saul, Anderson and Graham[10] describe various investigation techniques and remedial measures on Beanpole Corner landslide, repeated movement of which has adversely affected the North Island main trunk railway line near Wellington. It comprises a shallow (*ca* 10m) colluvial mass overlying greywacke. Movement and rainfall data together suggested instability occurred when the 3-month average rainfall exceeded 100mm.

Back analysis was used to determine strength parameters for the assessment of remedial work options, based on both dry and wet conditions, the latter being adopted for final design. Slope trimming was chosen as the main stabilisation measure rather than drainage owing to uncertainties in the relationship between movement and groundwater pressure. Earthworks involved removal of most of the slide mass.

The slope is close to a major active fault; seismic stability is an interesting problem not covered in this paper.

3. SEISMIC HAZARD

3.1.1 Assessment of strong motion

Williams[11] has taken strong ground motion intensity data from the 1989 Newcastle (Australia) earthquake, and used these to estimate site amplification. The results of this work show that at low levels of bedrock acceleration, soft soil sites can have amplification factors of up to 9. Williams has put the Newcastle experience in context with other earthquake studies, in particular the site effects observed at Mexico City (1985) and Loma Prieta (1989). These two well documented earthquakes have given geotechnical engineers much valuable data, and it is likely that when the complete macroseismic database from Newcastle becomes available and more complete analyses are carried out then this earthquake will contribute to our knowledge of soft site effects.

Although it is useful to be able to generalise on the earthquake response of sites, as more is learned about this phenomenon, it is clear that there can be special site factors which make each site and case study unique. The Newcastle setting is quite different from both Loma Prieta and Mexico City, so it will not be unexpected if further analyses of intensity data from Newcastle produce results which do not agree with these other case histories.

3.1.2 Economic solutions to mitigate geotechnical risks

Brahaharan and Vessey[12] describe an approach to mitigating geotechnical risk that includes taking account of benefit/cost ratios to determine acceptable levels of ground improvement.

The project is a facility comprising pre-sedimentation ponds and treatment plant for water taken from the Waipawa River to supply Gisborne City, New Zealand. It is founded on alluvial deposits of saturated loose silty sand and soft silty clay that make the facility susceptible to settlement and liquefaction in an area of high seismic risk.

Ground improvement by pre-loading, dynamic compaction or a combination were considered for the two main components to minimise the risk of damage. In economic analysis for the pre-sedimentation ponds, ground improvement was shown to be uneconomic, compared with their values, and therefore prudent only to design them to minimise damage.

In the case of the main plant, where the value considerably exceeded the cost of ground improvement, economic analysis included assessment of the expected cost of damage from liquefaction in relation to probability of occurrence of seismic events of differing intensities. Damage ratios, i.e. cost of damage as a ratio of value of the structure, were then determined for seismic events both with and without ground improvements, to give the cost of damage for various levels of seismic event.

Benefit/cost ratios for the cost of damage compared with that for ground improvement showed potentially large savings in settlement damage costs through preloading of the site, and this option was carried out.

3.1.3 Seismic stability of a wharf

Jennings and Thompson[13] describe investigations carried out to assess seismic stability of a reclamation at Port of Tauranga. They considered two levels of earthquake loading, Operating Level Earthquake, and Contingency Level Earthquake, corresponding to design peak ground accelerations of 0.2g and 0.36g respectively. Five methods for investigation of liquefaction potential were applied to the site, and each method indicated liquefaction would occur in soils behind the wharf under the Operating Level Earthquake. Given the nature of the soils, and their expected behaviour under earthquake loading, the stability of the rock buttressed slope under the wharf was assessed, and slope displacements under the critical acceleration were estimated.

The paper also describes the analysis carried out to assess whether collapse behaviour, or flow slides could develop after liquefaction of soils around the wharf. The authors conclude that displacement behaviour of structures under seismic loading is difficult to assess. This is especially true for complex foundation conditions as described at Tauranga. The authors have shown how systematic work can lead to rational analysis of the problem, and have described a design solution that satisfies the seismic design philosophy and criteria adopted.

4. REFERENCES

1. Dunbavan, M. and Boyd, G. "Assessing geotechnical risk of instability between adjacent mining operations: case study". Proceedings 6th Australia New Zealand Conference on Geomechanics, Christchurch.

2. Glawe, V. and Hudson, J.A. "Rock Slope instability with kinematic and morphological factors". *Ibid.*

3. Fell, R. "Some landslide risk zoning schemes in use in Eastern Australia and their application."*Ibid.*

4. Hunt, R.E. 1984: "Geotechnical Engineering Investigation Manual". McGraw Hill

5. Institution of Professional Engineers New Zealand, 1984. "Engineering Risk." Report of President's task committee on professional practice and risk.

6. Mehrotra, G.S., Gupta, A. and Sarkar, S. "Landslide and uplift of river bed in Tal Valley, Garwhal, Himalaya". Proceedings 6th Australia New Zealand Conference on Geomechanics, Christchurch.

7. Moon, A.T. Stability analysis in stiff fissured clay at Ruby Bay, Queensland." *Ibid.*

8. Mostyn, G. and Soo, S. "The effect of autocorrelation on the probability of failure of slopes." *Ibid.*

9. Sinclair, T.J.E. "A simple method for assessing the effects of earthquakes on slopes". *Ibid.*

10. Saul, G.J., Anderson, C.K. and Graham, C.J. "Beanpole Corner Landslide stabilisation." *Ibid.*

11. Williams, D.J. "Assessment of strong motion during 1989 Newcastle earthquake." *Ibid.*

12. Brabhaharan, P. and Vessey, J.V. "Development of economical solutions to mitigate geotechnical risks." *Ibid.*

13. Jennings, D.N. and Thompson, G.S. "Seismic stability of the Sulphur Point Wharf". *Ibid.*

Development of Economical Solutions to Mitigate Geotechnical Risks: Waipaoa Water Treatment Augmentation Plant

P. BRABHAHARAN
B.Sc.Eng.(Hons.), M.Sc.Eng., M.I.C.E., M.I.M.M., C.Eng., M.I.E.Aust. C.P.Eng. R.Eng.
Senior Geotechnical Engineer, Works Consultancy Services Limited
J.V. VESSEY
B.E.(Civil), B.A.(Economics), M.I.P.E.N.Z., R.Eng.
Principal Consultant, Works Consultancy Services Limited

SUMMARY A case study of the Waipaoa Treatment Plant is presented to illustrate the use of engineering and economic evaluation to assess geotechnical and seismic risks, and develop economical solutions to civil engineering projects. At the Waipaoa Site, geotechnical assessment identified a high risk of damage to the main plant due to settlements, and a moderate risk of damage due to liquefaction during large earthquake events. An economic evaluation provided the likely financial benefits from ground improvement measures to mitigate these risks, and enabled a comparison of the capital expenditure and the likely costs during the life of the facility. This enabled the Client to decide on the level of risk mitigation appropriate for the facility, and provided a basis for the design of the treatment plant and ground improvement measures.

1. INTRODUCTION

Recent advances in geotechnical and seismic engineering enable engineers to identify and develop solutions to mitigate risks which were previously considered unavoidable. However these risks, particularly geotechnical seismic risks are difficult to assess with any certainty, and may involve expensive engineering solutions. Therefore, engineers and clients require some method of deciding on the level of risk mitigation appropriate for their particular project.

This paper illustrates the use of recent developments in geotechnical and seismic engineering, and economic evaluation to provide a basis for clients to decide on the level of risk mitigation appropriate for their facility. This can then be used to develop solutions which are sound, cost effective and commercially viable.

The Waipaoa water treatment augmentation plant is located on the east bank of Waipaoa River, about 10 km northwest of Gisborne City in New Zealand, and will augment the water supply to Gisborne particularly during the drier summer months. The plant consists of a river intake sump, presedimentation ponds, and the main plant.

The main plant includes clarifiers, filters, a clear water tank and an operations building, see Figure 1.

It's location on alluvial deposits generally comprising of loose silty sand to soft silty clay makes the facility susceptible to large settlements and earthquake induced liquefaction. The assessment of settlement and liquefaction risks, development of engineering solutions to mitigate these risks, and the use of economic evaluation to select economically viable solutions are presented.

2. GROUND CONDITIONS

Ground investigations comprising boreholes and Static Cone Penetration Tests (CPT) were carried out followed by laboratory soil classification tests, and one dimensional consolidation tests.

In the presedimentation pond area, the soils are predominantly loose silty sands to a depth of about 12 m, with soft clayey silts below this depth. Standard Penetration Test (SPT) N-values vary from about 3 at 2 m depth, increasing to about 10 at 25 m depth. Groundwater levels were 2 m to 5 m below surface during the investigations in the summer.

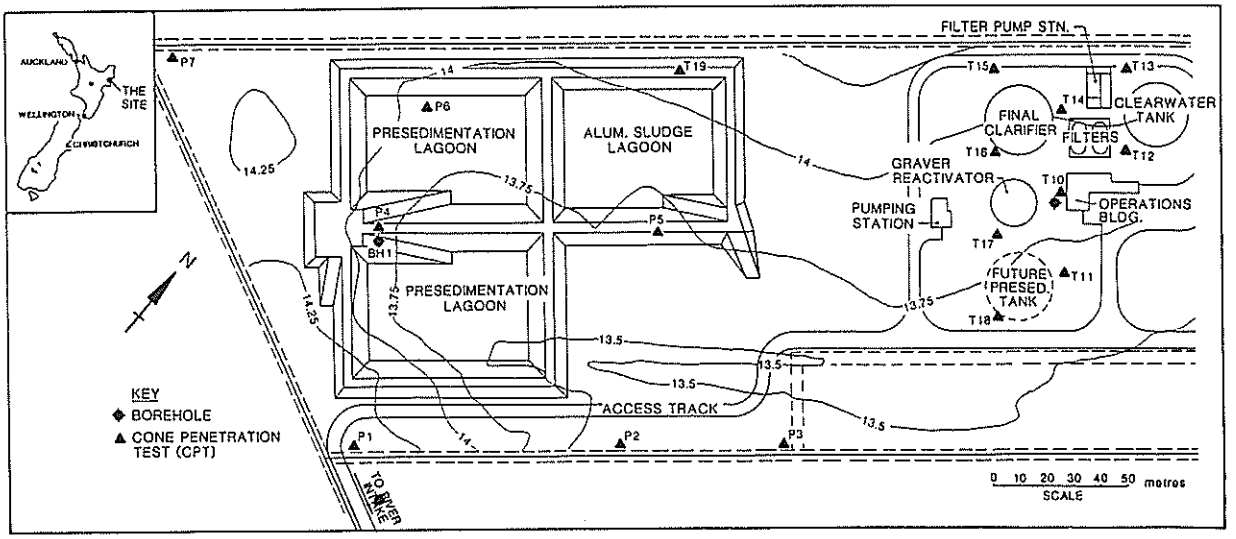

Figure 1 Location Plan

Figure 2 shows the ground conditions at the main plant area, where the soils are more fine grained than at the presedimentation pond site. The soils are predominantly soft clayey and sandy silts to a depth of about 12 m, below which the soils become silty clay and clayey silt. There are a number of silty sand horizons which are continuous over the site. SPT N-values vary from about 2 near the ground surface to about 10 at 25 m depth. CPT cone resistance (q_c) values vary from about 0.3 MPa at 3 m depth increasing to about 1.2 MPa at 30 m depth. The groundwater levels at the main plant area vary between about 0 m and 3 m below ground surface.

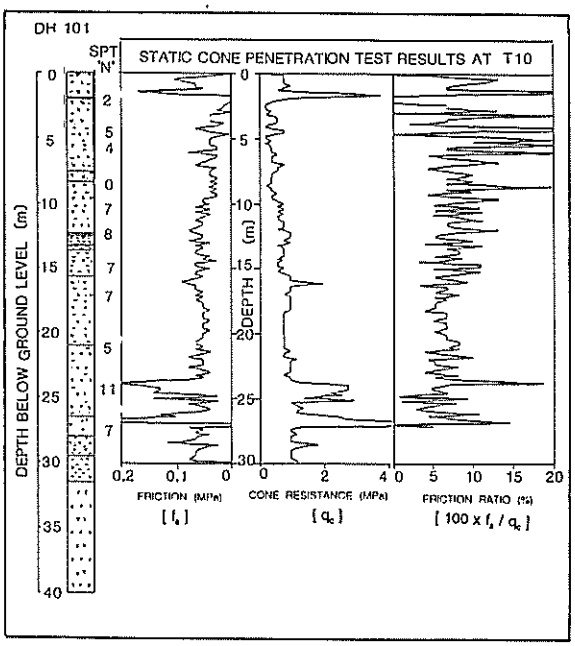

Figure 2 Ground Conditions at Waipaoa Main Plant Area

3. SEISMICITY

Waipaoa is situated in a region of New Zealand with high seismic risk. The return periods, magnitudes and peak ground accelerations for earthquakes of Modified Mercalli intensities ranging from VI to X have been estimated from Matuschka (1980), Smith and Berryman (1986), and Smith (1990), and are shown in Table I.

TABLE I
SEISMICITY OF THE WAIPAOA SITE

RETURN PERIOD (YEARS)	INTENSITY (MODIFIED MERCALLI)	MAGNITUDE (RICHTER)	PEAK GROUND ACCELERATION
9	VI	6.5	0.14 g
45	VII	7.0	0.21 g
140	VIII	7.5	0.31 g
410	IX	8.0	0.46 g
1729	X	8.5	> 0.5 g

4. SETTLEMENTS

The geotechnical investigations showed the soils at the Waipaoa site to be compressible. Six consolidation tests carried out on soils recovered during drilling gave coefficients of volume compressibility (m_v) ranging from about 0.33 m^2/MN near ground surface to about 0.15 m^2/MN at 35 m depth.

The coefficient of secondary compression (C_α) assessed from the consolidation tests is about 0.0022. The soils at Waipaoa site are of medium to high compressibility and extend to depths exceeding 40 m, giving a potential for large settlements of the treatment plant structures under their imposed loads.

In the main plant area, the tanks are partially set into the ground, to reduce the net bearing pressure on the ground. Primary consolidation settlements of up to 200 mm and secondary compression settlements of up to 150 mm were estimated for the 18 m to 25 m diameter main plant tanks. These could result in differential settlements of the order of 150 mm across or between the tanks.

In view of the high compressibility of the soils, the presedimentation ponds were designed with earth bunds which are more flexible than concrete or steel structures. The ponds are also partially set into the ground to minimise the net bearing pressures and hence the settlements.

5. LIQUEFACTION

The Waipaoa site is susceptible to liquefaction, because it has high groundwater levels, loose sandy silt/silty sand, and potential for large earthquake events. The particle size distribution of the soils at the Waipaoa Site is shown on Figure 3, together with the grading envelopes for soils which liquefy (Tsuchida, 1971). The particle size distribution of the soils from Waipaoa range from soils which "very easily liquefy" to soils which are finer than those considered to liquefy (Tsuchida, 1971). Recent research has indicated that liquefaction of soils with a significant silt content can occur, although these were previously considered resistant to liquefaction.

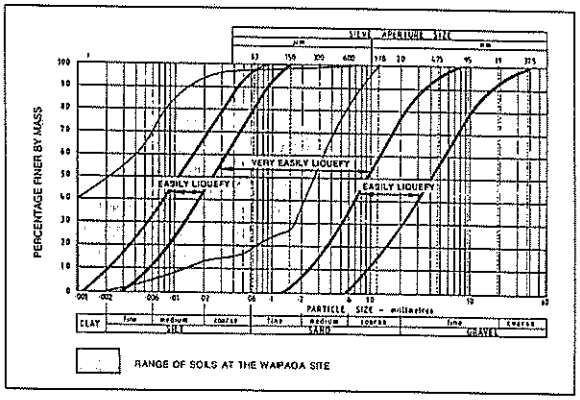

Figure 3 Particle Size Distribution of Waipaoa Soils

Seed et al (1984) have developed an empirical correlation to assess the liquefaction susceptibility of soils with fines. The fines content is defined as the total percentage of silt and clay size particles. Figure 4 shows the intensity of ground motion at the site represented by the stress ratio [τ_{av}/σ'_o] against the corrected SPT N-value for the Waipaoa site, where τ_{av} is the average peak shear stress and σ'_o is the effective overburden stress evaluated at a depth under consideration. The figure shows the stress ratio for an earthquake event giving a peak ground acceleration of 0.24 g and the corrected SPT N-value for the Waipaoa site in comparison with the empirical criteria for liquefaction presented by Seed et al.(1984). This comparison shows that the soils at Waipaoa are susceptible to liquefaction.

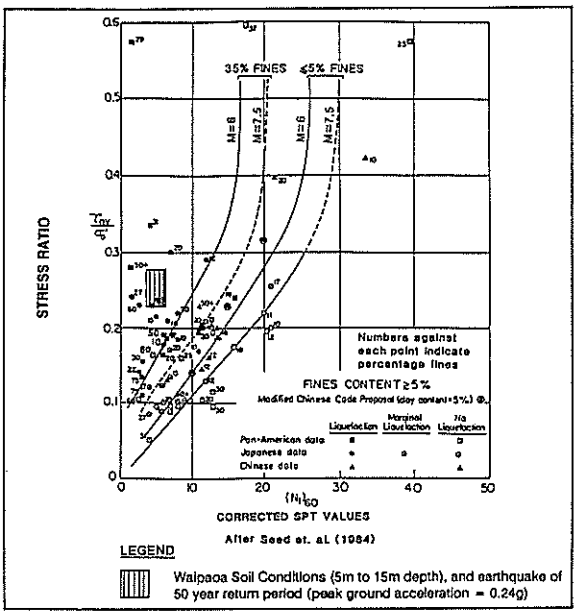

Figure 4 Liquefaction from Stress Ratio-SPT Relationship

Arulanandan et al (1986) have presented information on soils in Ying Kou City in China that liquefied and gave surface expression during the Magnitude 7.3 (Richter) Haicheng earthquake in 1975. The Ying Kou City experience shows that even soils with 40% to 90 % fines which have low SPT N-values can liquefy. Table II shows a comparison of the soil properties and the potential seismic events at Waipaoa, with the soil properties in Ying Kou City and the 1975 Haicheng earthquake. The soils at both sites have large moisture contents and liquidity indices, indicating a loose soil structure. The comparison shows remarkable similarities between the two sites, suggesting the soils at Waipaoa to be susceptible to liquefaction.

TABLE II
PARAMETERS INFLUENCING LIQUEFACTION AT YING KOU CITY AND WAIPAOA SITES

PARAMETER INFLUENCING LIQUEFACTION	YING KOU CITY 1975 HAICHENG EARTHQUAKE	WAIPAOA SITE
Earthquake - magnitude - ground acceleration	 7.3 0.1 - 0.15 g	 up to 8 up to 0.55 g
Groundwater - depth below ground level	1 - 2 m	0 - 3 m
Moisture Content	24 - 35%	22 - 42%
Fines Content	40 - 90%	5 - 90%
Plasticity Index	6 - 14	9 - 27
Liquidity Index	0.5 - 2.3	0.3 - 1.5
SPT 'N' (weak layers)	3 - 5	0 - 7
Cone Resistance q_c	0.3 - 5.9 MPa	0.2 - 1.2 MPa

The Waipaoa site has the conditions necessary for liquefaction, and empirical correlations reported in the research literature indicate the soils at Waipaoa to be susceptible to liquefaction, although they have a high percentage of fines. The soils will actually liquefy only if sufficient porewater pressures can develop during a seismic event.

Dynamic triaxial tests on samples of sand and silt from the Waipaoa main plant site was carried out at different stress ratios, to directly assess their susceptibility to pore pressure development, and hence liquefaction. There is insufficient test data to define the relationship between the stress ratio and the number of cycles of dynamic excitation for initial liquefaction. However, an assessment using the trend from research literature (National Research Council, 1985) and the laboratory test data show that earthquake events giving a peak ground acceleration of about 0.24 g or more could cause liquefaction at the Waipaoa main plant site.

The consequences of liquefaction are important in assessing the potential loss due to damage caused by an earthquake event. At the Waipaoa main plant site, liquefaction could cause loss of bearing capacity resulting in tilting of the tanks, or settlements of the order of 400 mm which can cause significant damage. The partially buried tanks proposed could float out of the ground when the surrounding ground liquefies, causing significant damage similar to that observed in Whakatane during the 1988 Edgecumbe earthquake in New Zealand (Jennings et al, 1988).

6. RISK MITIGATION

To reduce the risk of damage to the treatment plant due to settlements caused by compression of the soils, and earthquake induced liquefaction, special foundation measures or treatment were considered to be necessary. The structures could have been founded on deep pile foundations bearing on an unliquefiable dense stratum of low compressibility. However, as the soft to firm and compressible soils extend to a depth more than 40 m, piles would have been long making the piled foundation option expensive. Ground improvement could be used to mitigate the risk. Two methods, preloading and dynamic compaction were considered to provide the most practical and effective solutions at a reasonable cost.

Preloading the site with a 4 m high earthfill embankment for a period of about six months would reduce post-construction settlements to an acceptable level and reduce the risk of settlement damage. However, preloading would not appreciably reduce the risk of damage due to liquefaction. Dynamic compaction would reduce the liquefaction susceptibility of the soils, and thus mitigate the risk of damage due to earthquake events. It could also reduce the compressibility of the soils to a maximum depth of 15 m. Since the tanks at Waipaoa are up to 25 m diameter, their depth of influence is much greater than 15 m. Therefore, dynamic compaction alone would not sufficiently reduce the risk of settlement damage. A combination of dynamic compaction and preloading would minimise the risk of damage due to settlements and earthquake induced liquefaction.

7. ECONOMIC ANALYSIS

An economic analysis of financial benefits from risk mitigation measures for the Waipaoa Treatment Plant was carried out. The value of the treatment plant and the cost of ground improvement for risk mitigation is shown on Table III.

7.1 Presedimentation Ponds

For the presedimentation ponds, the cost of risk mitigation measures is $ 0.42 million for dynamic compaction of the soils, and $ 0.25 million for preloading the area. The total cost of $ 0.67 million is very high compared to the $ 0.8 million value of the ponds. This clearly shows that ground improvement would be uneconomical for the presedimentation ponds, and a detailed economic analysis was not necessary. It was therefore decided to design the ponds to minimise damage rather than carry out expensive ground improvement.

TABLE III
COST OF RISK MITIGATION OPTIONS

TREATMENT PLANT COMPONENT	VALUE OF SCHEME	COST OF RISK MITIGATION BY GROUND IMPROVEMENT		
		PRELOADING	DYNAMIC COMPACTION	PRELOADING AND DYNAMIC COMPACTION
	$ MILLION			
Main Treatment Plant	6.0	0.28	0.32	0.60
Presedimentation Ponds	0.8	0.25	0.42	0.67

7.2 Main Plant

The value of the Main Plant structures is $ 6 million, and the cost of ground improvement by preloading and by dynamic compaction are $ 0.28 million and $ 0.32 million respectively. A detailed economic analysis was considered appropriate to assess the economic benefits from ground improvement. The aim of the economic analysis is to determine the optimum level of risk mitigation. Ground improvement is not economically prudent unless the expected reduction in damages exceed the actual cost of carrying out the improvement.

7.2.1 Settlement damage

Without ground improvement, settlement of the treatment plant would certainly have occurred. However, there is a probability associated with settlement damage, due to the uncertainties in the assessment of the amount of settlement. This probability together with the assessed cost of reinstating the structures damaged due to settlement, was used to assess the total damage cost if no ground improvement was undertaken. Similarly, the damage cost with each option was calculated assuming the reduction in settlement likely to be achieved, and the probability of the ground improvement being effective.

It was considered likely that most of the damage to the treatment plant due to settlement of the structures would occur during the first year after construction, because the presence of laterally extensive sand layers would assist drainage and accelerate consolidation.

7.2.2 Seismic damage

The expected cost of damage can be estimated from the integral of the Damage cost v Probability of occurrence curve (Ministry of Works and Development, 1983). For seismic induced damage from ground shaking and liquefaction, this curve can be derived by combining the probability of occurrence and the expected damage costs for seismic events of different intensities, as illustrated in Figure 5.

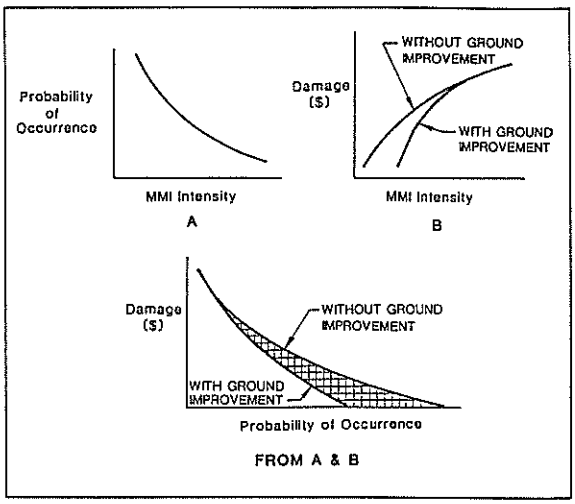

Figure 5 Derivation of Seismic Damage Costs

The expected saving in damage cost resulting from ground improvement is given by the cross hatched area between the curves representing the damage costs, with and without ground improvement. The expected savings in damage costs (given by the annual damage costs discounted over the life of the facility) was then compared with the cost of the ground improvement to ascertain the economic benefits from varying levels of risk mitigation.

For the Waipaoa treatment plant, the expected damage costs were estimated from the probability of damage and the damage ratios estimated generally in accordance with the recommendations of the Applied Technology Council (1985). The damage ratio is the cost of damage as a ratio of the value of a structure. The probability of damage was assessed using the geotechnical assessments, and engineering judgement. Whilst this is not an accurate assessment, the results give sufficient accuracy to make decisions on the appropriate level of risk mitigation. The damage ratios for seismic induced liquefaction damage estimated for the Main Plant area at Waipaoa are shown in Table IV.

The estimated damage ratios together with the value of the main plant give the damage costs for various levels of seismic events. Similarly, the estimated damage costs can also be estimated assuming that ground improvement is carried out.

7.2.3 Discussion

The present value of the savings in damage costs for the different ground improvement options were calculated as discussed above, and are given in Table V.

TABLE IV
DAMAGE RATIOS FOR SEISMIC EVENTS WITH AND WITHOUT GROUND IMPROVEMENT

SEISMIC EVENT			DAMAGE RATIO (MAIN PLANT)			
MODIFIED MERCALLI INTENSITY	RETURN PERIOD (YEARS)	PROBABILITY OF EVENT/ YEAR	NO GROUND IMPROVEMENT	PRELOADING	DYNAMIC COMPACTION	PRELOADING AND DYNAMIC COMPACTION
VI	9	0.1111	-	-	-	-
VII	45	0.0222	0.15	0.10	0.03	0.03
VIII	140	0.0071	0.35	0.30	0.1	0.1
IX	410	0.0024	0.55	0.50	0.3	0.3
X	1729	0.0006	0.8	0.75	0.5	0.5
>X	-	-	1.0	1.0	1.0	1.0

TABLE V
PRESENT VALUE OF DAMAGE COST AND SAVINGS FROM GROUND IMPROVEMENT OPTIONS

OPTION	DAMAGE COST		TOTAL DAMAGE COST	SAVINGS IN DAMAGE COST
	SETTLEMENT	SEISMIC		
	$ MILLION			
No Ground Improvement	1.40	0.72	2.12	-
Preloading	0.30	0.56	0.86	1.26
Dynamic Compaction	0.75	0.21	0.96	1.16
Preloading & Dynamic Compaction	0.23	0.21	0.44	1.68

This table shows the cost of damage from settlements and from seismic events, the total damage costs and the savings in damage costs which could be achieved by different ground improvement options. Table VI shows a comparison of the savings in the total cost of damage from settlements and seismic events with the actual cost of undertaking the ground improvement measures to mitigate the risk. The benefit cost ratios for these options are also given in the table.

TABLE VI
BENEFIT / COST RATIO OF GROUND IMPROVEMENT

	COST OF RISK MITIGATION	SAVINGS IN DAMAGE COST	BENEFIT /COST RATIO	INCREMENTAL BENEFIT/COST RATIO FOR MITIGATION IN ADDITION TO PRELOADING
	$ MILLION			
Preloading	0.28	1.26	4.5	-
Dynamic Compaction	0.32	1.16	3.6	-
Preloading & Dynamic Compaction	0.60	1.68	2.8	1.3

For the main plant area, potentially large savings in damage costs can be achieved through ground improvement. By preloading the site to reduce settlement damage, a reduction in damage costs of about $ 1.26 million can be expected for an initial remedial works cost of $ 0.28 million, representing a benefit / cost ratio of 4.5, see Table VI. While dynamic compaction also offers a good overall benefit for the cost of the work, it actually offers less benefit at a higher initial cost compared to preloading.

The combined option of using both preloading and dynamic compaction would reduce the risk of both settlement damage and liquefaction damage giving potential savings of $ 1.68 million for an initial mitigation cost of $ 0.6 million. This gives a benefit / cost ratio of 2.8 which is a good return on investment. However, the incremental cost of $ 0.32 million over the cost of preloading, nets savings in damage costs of only about $ 0.42 million representing an incremental benefit / cost ratio of 1.3. There is a possibility that a damaging earthquake may never occur during the life of the plant. Therefore given the low incremental benefit / cost ratio and the uncertainty of ever achieving the savings in damage costs, it is difficult to justify additional expenditure on risk mitigation by dynamic compaction.

It should be noted that the client is building the Waipaoa water treatment augmentation plant only to supplement the water supply to Gisborne City during the dry summer months. Therefore, no account was taken in the economic analysis of the disruption to the water supply to Gisborne City as a result of any damage which will put the treatment plant out of operation. Further, since the failures would not be catastrophic, it is unlikely that there would be any risk to human life. If there was a risk to human life, then economical considerations may be outweighed by the need to save lives.

8. DESIGN ADOPTED

On the basis of the economic analysis, the client decided to reduce the risk of damage due to settlements by preloading the main plant site, and accept the risk of liquefaction induced damage. Also since the capital cost of the presedimentation ponds is small in comparison to the cost of risk mitigation, the Client decided not to carry out ground improvement at the presedimentation ponds site.

Preloading of the main plant area has been successfully carried out, and construction of the main treatment plant is currently underway.

9. CONCLUSIONS

The Waipaoa site is a difficult construction site with deep alluvial deposits comprising soft silts and loose sand layers, with high groundwater levels. The site investigations at an early stage showed that the ground conditions were poor and there was a risk of damaging settlements and earthquake induced liquefaction. The likely settlements were estimated based on information from the investigations. Since the soils contained fine grained silts, the risk of liquefaction was not clear and required special laboratory tests and a detailed geotechnical assessment using information from recent research literature. This enabled the risk of liquefaction to be assessed. Risk mitigation measures were chosen based on the information from the geotechnical appraisal.

The economic analysis enabled an assessment of the financial benefits from the risk mitigation measures. This gave a clear basis on which the Client made an informed judgement as to the level of risk mitigation to be adopted for the project. This method can be applied to any project, although it is recognised that additional factors such as risk to life and disruption may need to be considered in addition to the economic benefits from reduced structural damage.

10. ACKNOWLEDGEMENTS

The authors wish to acknowledge the permission to publish this paper from the Gisborne District Council for whom the work was carried out. The contribution and assistance of many colleagues in Works Consultancy Services Limited who worked on the Waipaoa project is also acknowledged.

11. REFERENCES

Applied Technology Council (1985). Earthquake damage evaluation data for California. ATC-13. California.

Arulanandan, K., Yogachandran, C., Meegoda, N.J., Ying, L., and Zhauji, S. (1986). Comparison of the SPT, CPT, SV and electrical methods of evaluating earthquake induced liquefaction susceptibility in Ying Kou City during the Haicheng earthquake. Proc. Specialist Conf. on Use of In situ Tests in Geotechnical Engrg, Virginia Tech, Blacksburg, Virginia June 23-25, 1986. Edited by Samuel P Clemence, Geotechnical Special Publication no. 6 ASCE, New York. pp. 389-415.

Jennings, D.N., Edwards, M.C., and Franks, C.R. (1988). Some observations of sand liquefaction in the 2 March 1987 Edgecumbe (New Zealand) earthquake. Proc. 5th ANZ Geomech. Conf. Sydney, 22-23 August 1988. pp. 602-607.

Matuschka, T. (1980). Assessment of seismic hazards in New Zealand. School of Engineering Report No. 222, University of Auckland. May 1990, Auckland.

Ministry of Works and Development (1983). Guide for the economic evaluation of engineering projects. Civil Engineering Division. CDP 817/C : 1983. Wellington.

National Research Council (1985). Liquefaction of soils during earthquakes. Committee on earthquake engineering. National Academy Press. Washington.

Seed, H.B., Tokimatsu, K., Harder. L.F. and Chung, R.M. (1984). The influence of SPT procedures in soil liquefaction resistance evaluations. Report No. UBC/EERC-84/15. Earthquake Engineering Research Centre. California.

Smith, W.D. (1990). Earthquake Hazard in New Zealand : Some implications of the Edgecumbe earthquake, March 1987. Bulletin NZ National Society for Earthquake Engrg. Vol. 23, No. 3, September 1990. pp. 211-219.

Smith, W.D. and Berryman, K.R. (1986). Earthquake hazard in New Zealand : inferences from seismology and geology. Royal Society of New Zealand. Bulletin 24. pp. 223-243.

Tsuchida, H. (1971) Estimation of liquefaction potential of sandy soils. Proceedings of the Third Joint Meeting, US-Japan Panel on Wind and Seismic Effects. UJNR. May 1971.

Assessing Geotechnical Risk of Instability between Adjacent Mining Operations – A Case Study

M. DUNBAVAN
Ph.D., M.A.G.S.
Supervising Engineer, In-Situ Processes, BHP Engineering
G. BOYD
M.Sc., M.A.I.M.M., M.A.G.S., M.G.S.A.
Managing Director, Boyd Mining Pty Ltd

1. INTRODUCTION

Instability of a 60 m highwall excavated to a common boundary between two adjoining but separately owned coal mining operations in the NSW northern coalfields represented potential for significant economic loss for both parties. On the one hand, the failure threatened an arterial coal haulroad located adjacent to the boundary in one lease, whilst on the other, the possibility of reserves sterilisation due to a restriction of mining limits became apparent.

A lack of appreciation of the geological structure along the boundary at the time of establishing a boundary mining agreement resulted in failure of the first of 4 x 300 m long mining blocks located against the boundary. To develop acceptable guidelines for establishing safe mining limits, a joint investigation into the cause(s) of failure was commissioned.

To more usefully define mining limits, it was agreed a probabilistic approach to stability analyses be adopted from which the risk of boundary highwall failure was to be assessed.

This approach allowed operators to better understand, in relative terms, the magnitude of risk embodied in the mining limits analysed. The quantification of risk also represented an opportunity to value the cost of insuring against losses incurred by inadvertent failure.

2. BOUNDARY HIGHWALL INSTABILITY

2.1 History of Failures

Instability first occurred in March 1989 during stripping to the base of the upper overburden, exposing P Seam. Pit limits at the time of first instability are shown in Figure 1, with the toe of the (basal) B Seam 110 m west of the lease boundary, and the toe of the P Seam layer 90 m west of the same boundary. Movement was concentrated at the roof of T coal horizon or above, with a scarp ultimately forming behind the planned highwall crest.

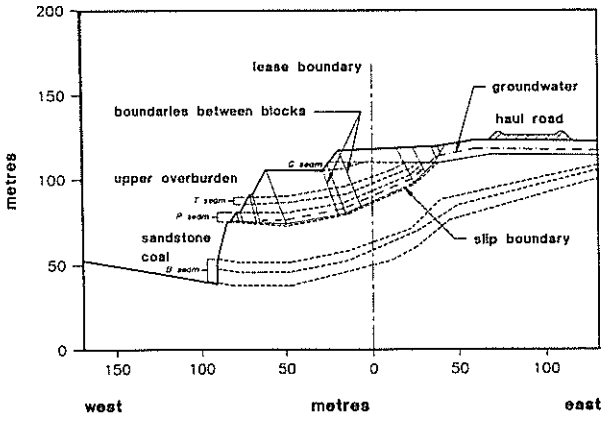

Figure 1 Lease boundary geology and structure

With further extraction along the boundary, slip of the upper overburden occurred during excavation of a bench to a level just above the roof to the T Seam. To reduce the hazard to mining operations from continued rock movement, the slope above bench level was dozed parallel to bedding at an angle of approximately 35°. During excavation of the next bench, movement occurred along the base of the P Seam initially in the northern portion of the panel when the toe of the slope was only 20 m west of the lease boundary (see Figure 1). Movement was accompanied by significant floor heave indicating the failure surface lay in the floor beneath P Seam. Movement in the slope extended over the full length of the panel, but movement along the base of P Seam diminished to zero at the southern panel limit, where the toe of the seam was located at 50 m west of the boundary. The scarp of the failure developed at its current day position at 90 m east of the lease boundary (see Figure 1).

2.2 Failure Path

Measurement and observation of the slope deformation suggests a non-linear displacement at the base of the P Seam. Exposure of the P Seam floor sequence revealed the failure path corresponded to a mylonite of crushed carbonaceous siltstone with subordinate silt and clay some 100 mm in thickness.

The failure path, confined to the mylonite followed the dip of the beds at the base of the P Seam horizon. Variation in dip along the failure path caused discrete blocks to form, with subsequent displacement and rotation resulting in the deformation clearly observable in the failed slope.

At the head of the failure, a sub-vertical scarp developed over a visible depth of 3 m to 4 m. Subsidence of blocks in front of the scarp showed only minor rotation, suggesting the final (i.e. current) scarp location resulted from local instability at the head of the failure, and not due to the primary failure mechanism.

The mylonite at the base of the P Seam occurs commonly in exploration drilling records from both sides of the boundary. It is a natural geological feature associated with past tectonism, and is considered a feature of sub-regional extent, and certainly occurs throughout the high dip zone along the common lease boundary.

3. GEOTECHNICAL CONDITIONS - LEASE BOUNDARY

3.1 Geology

The upper horizon (above the base of the P Seam) consists of thinly interbedded argillaceous sandstone, siltstone and carbonaceous siltstone and claystone carrying up to three mineable coal seams (P, T and G in ascending order).

Low grade regional metamorphism associated with tectonic folding and faulting has developed a shale sequence in fine grained sequences. The induration arising from metamorphism has left all fine grained sediments as hard, brittle and highly competent rocks with slaking potential, but not prone to dispersion.

Due to rock competence, the depth of weathering is shallow, with

the residual soil zone confined to a depth of 2 m or less. The moderate to slightly weathered zone, comprising iron stained joint surfaces, extends to a maximum depth of 15 m.

Significant intrusion of the T and P Seams by dolerite has affected coal quality, and on occasion has formed minor clay seams representing decomposed sill material. However, the mylonite below the P Seam horizon appears free of intrusive, and development of silt and clay in the mylonite is thought to represent products of degradation of the mylonite, probably due to groundwater percolation.

3.2 Structure

Detailed mapping about the failed highwall revealed a total of eight parallel reverse faults dipping 80° west, and resulting in a total displacement of approximately 2 m (west blocks up). The largest displacement on any one fault measured 0.8 m.

The faults lie in the western limb of an anticlinal structure, the axis of which occurs 150 m east of the common boundary. Bedding dips were measured to peak at 45°, with the interval of steepest dips averaging 31°. This compares to an average of 16° measured from a computer model of the anticline.

Seepage was observed to originate from bedding structures, suggesting a degree of openness along both bedding and jointing. However, no slickensided nor polished surfaces were ascribed to bedding, partings or joints, which conforms with general observations in both pits.

Jointing is close spaced (0.5 m to 1.5 m) and from past mining experience, has caused little to nil instability in excavated highwalls along the boundary.

3.3 Groundwater/Rainfall Observations

Four geotechnical holes were completed as single or multi-level piezometers.

Groundwater was recorded in two piezometers, the first completed at the base of P Seam where a level of 0.5 m above base was observed, and the second completed at the base of the deeper B Seams where a level of 1 m above base was recorded.

The groundwater observed at the base of the P Seam is perched, indicating incomplete hydraulic connection down through the sequence.

Rainfall records indicate that during March 1989 when first failure of the highwall occurred, a total of 115.6 mm of rain fell, 50 mm of which occurred in the one wet weather spell over three days, with 30 mm recorded in one of the days. April, May and June of 1989 recorded high non-seasonal rainfalls of 139.2 mm, 122.4 mm and 113.5 mm. These compare to a 10 year average for the same months of 72.24 mm, 46.62 mm and 36.76 mm.

The mining of the next panel and subsequent failure during August/September 1989 was preceded and accompanied by very low rainfall, 5.4 mm and 12.4 mm respectively compared to a ten year average of 44.91 mm and 45.07 mm respectively for the same months. It is speculated that the highwall rainfall in March, April, May and June caused a significant rise in groundwater levels, declining but still significant during the mining of the next panel. Observations at the face during overburden excavation indicated dry conditions and the slope after failure remained dry.

3.4 Material Properties

The final selection of design parameters was based on back analysis of the major highwall failure and independent laboratory testing of rock mass defects, including the P Seam mylonite, by respective consultants.

3.4.1 Back analysis

Back analysis of a reconstruction of the failure in the previous panel suggested with zero groundwater loading, and zero cohesion, a friction angle of 17.5° equated to a unit factor of safety. Computations were completed assuming the following parameters:

. Upper overburden: $C = 0$, $\phi = 25°$, $\delta = 25$ kN/m^3
. Puxtress mylonite: $\delta = 20$ kN/m^3
. Fractured coal: $C = 15$ kPa, $\phi = 36°$, $\delta = 15$ kN/m^3

The Sarma method of analysis was used, which permits use of non-linear and user defined surfaces of deformation. Surfaces observed and reconstructed from all information available were thus included and modelled.

3.4.2 Laboratory testing

Independent laboratory strength testing of the Puxtrees mylonite indicated:

- peak shear strength corresponding to C = 0 to 28 kPa, friction = 28°;
- residual shear strength corresponding to C = 0 to 27 kPa, friction = 17.5° to 19.0°.

The laboratory results thus agreed well with lower bound strength parameters determined by back analysis. However, it must be appreciated that back analysis yields parameters representing the effect of all processes acting in the slope affecting stability, and not just failure plane strength.

3.4.3 Expected parameters

Laboratory strength results show the frictional strength of the P Seam mylonite varied between 17.5° and 28°. The roughness of the surfaces in the mylonite zone and undulating trend of bedding surfaces, interrupted by small displacement faults, render it unlikely that a state of residual strength existed throughout the mylonite at the time of failure.

Further manipulation of the back analysis model indicated a most likely average frictional strength of approximately 21° (and zero cohesion) under an average groundwater head of 2 m.

Agreed strength parameters of other rock mass zones and structures for the design of Panel E8 are summarised in Table I. Mean parameters (as tabulated) were used in back analysis of the major highwall failure.

TABLE I
DESIGN VALUES FOR GEOMECHANICAL PROPERTIES

Rock Group	Unit Weight (kN/m^3)	Cohesion (kPa)		Friction Angle (deg)	
		Mean	Std. Dev.	Mean	Std. Dev.
Upper overburden (above P seam)	25	0	0	25	2
P seam mylonite	20	0	0	21	2
Sandstone (below P seam)	25	0	0	35	2.5
B seam shale	25	0	0	30	2.5

4. ANALYTICAL METHODS

4.1 Approach

The development of a slip mechanism in the overburden is dominated by geological structure. Variations in structure, mainly changes in dip of discontinuities, will result in different factors of safety at different locations in the slope. Any design approach has to address this variation and the method of stability analysis should be able to represent the effects of structure (joints, bedding planes and shear zones) on the slip mechanism.

Variation of structure was addressed by analysing six highwall cross sections for a slope strike length of approximately 450 m. The locations of cross sections were chosen to represent

different structural regimes and were placed as close as practicable to boreholes to reduce reliance on interpolated geological data.

For stability analysis, a two dimensional method was adequate in representing broad geological features and the proposed terrace mining method for overburden removal. Sarma's limit equilibrium method was selected from a range of methods applicable to non-circular slip mechanisms. The main advantages of Sarma's method for this case were use of a non-circular slip boundary and specification of non-vertical block interfaces within the sliding mass together with shear resistance on those interfaces. Figure 1 illustrates a typical cross section with the slip mechanism used for slope design.

As well as significant changes in geological structure between cross sections, ground conditions also vary within each cross section. Even if detailed measurements were obtained from field or laboratory tests, data represent only point values from a large three dimensional volume. A probabilistic approach was adopted to represent variation in ground conditions. The Point Estimate Method was used in conjunction with Sarma's method of stability analysis and estimated probability distributions for ground conditions to produce a probability distribution for the factor of safety at each cross section.

4.2 Design Assumptions

The main assumptions required for the slope design were:

- existing geological data were representative of the major structural features in the area under study;
- geomechanical property values were normally distributed and the selected values were representative of ground conditions;
- the location of the slip boundary was dominated by the mylonite at the base of P seam for one case and by the fractured zone in B seam for the second case;
- the presence of groundwater in P seam is transient and dependent on infiltration from storms. The six hour storm produced the worst conditions due to slope drainage for longer storm durations. Similar conditions were assumed for slip through B seam;
- two dimensional slope stability analysis was representative of field conditions and three dimensional wedge slips did not affect slope stability.

4.3 Ground Condition

4.3.1 Geomechanical properties

The drilling records and existing excavations showed a complex series of coal seams, interburden rocks and dolerite intrusions comprised the strata exposed during mining. Exact replication of these strata in a numerical model for stability was not feasible. Thus, the strata were grouped into four major rock types for the purposes of stability analysis. The selection of values for geomechanical properties was based on the application of those values in Sarma's method of stability analysis in conjunction with the point estimate method. Table I lists the rock groups and geomechanical properties used in design calculations.

4.3.2 Groundwater levels

No significant seepage or water levels in piezometers had been observed in the upper overburden. B seam at the base of the slope appeared to be the main aquifer in the region. Seepage from the coal was steady, but no major flows were observed which might indicate elevated groundwater conditions in the pit slope. The assumption of transient groundwater conditions in the upper overburden was supported by some observations of seepage from excavated faces, but only after rain had recently fallen.

The highly fractured upper rock mass could allow rainfall infiltration to move rapidly through the mass to build a saturated zone starting from the base of P seam above the competent sandstone unit. Because of the likely rapid infiltration rate and the many discontinuities along which water could exit from the rock mass, a six hour duration storm was selected as producing the worst groundwater conditions. The derivation of relevant rainfall characteristics is described in a later section.

For a six hour storm event, the infiltration was estimated to be 40 mm depth of water/m^2 for a 1,000 year average recurrence interval event. Using estimates of void ratio due to rock mass discontinuities and discounting absorption into the rock material, this infiltration corresponded to a 2 m head above the P seam mylonite. This level was adopted as an average value together with a standard deviation of 1 m head.

4.4 External Loads

Experience at the site had shown no measurable effects on slope stability from either overburden blasting or natural seismicity. The truck and shovel operations are based on successive excavation of 15 m to 20 m high terraces from west to east. Overburden shots are relatively small compared with those used in conventional dragline operations. Shots have a maximum burden of 20 m and are usually fixed with two free faces.

Loading applied by machinery (large trucks and occasionally a dragline) is small in comparison with the weight of the rock mass as well as being transient. The rock mass properties do not favour brittle failure. The main impact of a significant highwall slip would be loss of haul road access for machinery rather than danger to a particular machine or operator.

4.5 Probability Distribution for the Factor of Safety

The two cases, slip boundaries through P seam and B seam, were assessed independently. The P seam case was expected to be the one controlling final highwall design because of previous instability. However, the changing geological structure and more severe consequences of slip developing through B seam shale meant that this case could not be ignored. For each case the factor of safety was assumed to be a function of three variables.

For slip through P seam these were shear resistance of the P seam mylonite, shear resistance of the upper overburden and position of transient groundwater in P seam due to a 1,000 year ARI storm' event; and for B seam were shear resistance of the B seam shale, shear resistance of the sandstone and position of transient groundwater in B seam due to a 1,000 year ARI storm event.

The point estimate method requires 2^n evaluations where n is the number of variables (eight for three variables), for estimation of the probability distribution of the dependent variable, in this exercise the factor of safety. From the eight values, the mean and standard deviation were calculated using standard statistical formulae. Thus, for a particular highwall profile and location, the average factor of safety could be calculated for the probability distributions of the three selected variables. The standard deviation of the factor of safety was used to calculate the probability that the factor of safety may be less than 1.0.

5. RISK ASSESSMENT

5.1 Time Dependency

The absence of any thick clay bands and the relatively shallow depth of weathering led to the assumption that geomechanical properties relevant to highwall design would be independent of time. Excavation of slopes certainly changes stress conditions in the remaining rock mass. Some relaxation (that is, a time dependent effect) may occur as stresses are redistributed, however this effect was expected to be minor. The majority of the discontinuities within the rock mass was rough and no significant deterioration within the mine life was expected.

The remaining variable considered in highwall design was groundwater level, which certainly varies with time. The highly fractured condition of the upper overburden and relatively thin soil cover may have made that part of the overburden susceptible to rapid infiltration of rainfall runoff with subsequent transient rises in groundwater level. The absence of persistent

seepage from exposed rock faces and the lack of water in standpipes installed to different depths indicated negligible groundwater storage in the upper overburden. Thus, the groundwater levels were assumed to depend on storm events, the severity of which can be expressed as a function of time, namely the average recurrence interval (ARI).

Rainfall infiltration characteristics were estimated using a technique developed by the U.S. Department of Agriculture Soil Conservation Service. This technique is based on prediction of direct runoff from a specified depth of rainfall, given classification of the soil as one of four major hydrological groups together with an estimate of antecedent moisture condition (AMC).

The infiltration analysis was undertaken for a wide population of storm events. Design storm data were derived from information published in "Australian Rainfall and Runoff" (The Institution of Engineers, Australia, 1987). Values for precipitation as a function of storm duration were calculated for ARIs between 1 and 100 years. Because of the apparently high permeability of the rock mass, a storm duration of six hours was adopted as that creating the most adverse variation in groundwater conditions. This was a subjective assessment because no data were available for analysis. Extending the storm data to a 1,000 year ARI, the infiltration was equivalent to 40 mm depth of water per square metre surface area for a six hour duration storm.

Assuming that all infiltration moved rapidly down through the rock mass with no seepage, and that the material below the suspected slip boundaries was impervious, the 40 mm infiltration was estimated to produce a 2 m rise in groundwater level. The uncertainty in this estimate was high and a probability distribution for the height of the rise was chosen subjectively. The distribution was assumed normal with an average of 2 m and a standard deviation of 1 m. This distribution was not time dependent and the only time dependence resulted from the use of the 1,000 year ARI storm event.

5.2 Risk of Slope Failure

The probability distribution for the factor of safety was based on variables which were relevant for the occurrence of a 1,000 year ARI storm event. The risk of slope failure during mine operations is equal to the combined probability that the factor of safety will be less than unity and the probability of the 1,000 year ARI event occurring during the operating period (a value of 0.015 for 15 years operation). Values for this risk are given in the following section.

6. APPLICATION

6.1 Establishing Limits of Mining

The usual criteria for slope design include minimum values for the factor of safety under various loading conditions and combinations of material property values. The variability of the properties and conditions which influence the factor of safety significantly reduced confidence in the idea of using only the factor of safety as the design criterion. The adoption of a probabilistic approach was described earlier. The application of the results from the analyses is the topic of this section.

Engineers from both mines and the regulatory authority agreed that the minimum average factor of safety for slip in the upper overburden should be 1.3 and that for a slip in the entire overburden should be 1.5. This judgement was made before any information on the probability distribution of the factor of safety was available. For the selected cross sections within the design area, the highwall location to meet the above criteria was determined by trial and error using average geomechanical properties and groundwater conditions.

Slip in the upper overburden was the controlling factor. The use of average values in the first part of the calculation was convenient, but did not give a statistically acceptable average value for the factor of safety. This was obtained from the point estimate method. If the slope location did not meet the design criteria when this calculation was completed, the location was revised until criteria were met.

The risk of slope failure was then calculated using the time dependent probability of the occurrence of groundwater levels due to a 1,000 year ARI storm. The following table gives results of calculations for different cross sections.

TABLE II
RESULTS FROM PROBABILISTIC STABILITY ANALYSIS

Section	Upper Overburden			Entire Overburden		
	Ave FS	Pr FS<1.0	Risk	Ave FS	Pr FS<1.0	Risk
A	1.45	0.002	3×10^{-3}	1.84	10^{-6}	1.5×10^{-6}
B	1.36	0.004	6×10^{-3}	1.84	10^{-6}	1.5×10^{-6}
C	1.36	0.004	6×10^{-3}	1.78	10^{-7}	1.5×10^{-8}
D	1.36	0.004	6×10^{-3}	1.84	10^{-8}	1.5×10^{-10}
E,F	1.30	0.010	1.5×10^{-4}	1.76	10^{-7}	1.5×10^{-8}

The combination of values of factor of safety and the risk of failure were found by mine staff to be helpful in discussing the consequences of slope instability. For example, the consequences of instability of the entire overburden were much greater than those for the upper overburden, but the likelihood of the former occurring was less by at least 1,000 fold. The use of quantitative risk may be extended to estimating the financial risk (or liability) to which each mining operation was exposed. Slip in the upper overburden would render a haulroad on the adjacent lease unserviceable. The restoration cost would involve both earthworks to relocate the haulroad and the cost differential in producing coal until the haulroad was restored. The liability is the restoration cost times the risk of failure. With risks less than 10^{-4}, costs of tens of millions of dollars correspond to liabilities of thousands of dollars.

6.2 Monitoring Sub-surface Conditions and Displacements

Without resorting to complex (and expensive) instrumentation systems, the performance of the slope design and design assumptions may be assessed from groundwater levels and rock mass movement. Standpipe piezometers were installed in several boreholes. Screens were open to T, P and B seams and standing water levels were measured regularly. To correlate changes in water level with storm rainfall, an automatic data logger was installed in the field and connected to a tipping bucket rain gauge and water level sensors in the standpipes.

In the six months since installation, rainfall has been sparse and the district is a declared drought area. The water levels in the standpipes have consistently fallen during this period and showed no transient response to rainfall.

Monitoring of rock mass movement by conventional surveying methods has resulted in a very useful database for assessing design performance. Movement toward the excavation has been recorded since the commencement of overburden removal. Initially, the displacement rates increased and decreased sharply as a layer of overburden was removed adjacent to a monitoring station. As mining progressed, the displacement rates decreased in magnitude but persisted for a much longer period. This may be compared with the rate of change of momentum of the rock mass, in that deeper mining affected a larger rock mass which accelerated more slowly than smaller masses, but also decelerated more slowly.

The trend of displacement rate at the end of overburden removal was continuously decreasing. Although some extension cracks had appeared across the haulroad behind the highwall crest, the road remained serviceable. Displacement monitoring is being maintained.

Effects of Regional Geology on the Seismic Hazard in Christchurch, New Zealand

D.McG. ELDER
B.E.(Civil), Ph.D., M.I.P.E.N.Z.
Soils & Foundations Ltd, N.Z.
I.F. McCAHON
B.E.(Civil), M.I.P.E.N.Z.
Soils & Foundations Ltd, N.Z.
M.D. YETTON
B.Sc., M.Sc.(Geol)
Soils & Foundations Ltd, N.Z.

SUMMARY A detailed seismic hazard assessment has been carried out for Christchurch, New Zealand. A seismicity model has been developed for the central South Island. The effects of very deep alluvial soils beneath the city have been evaluated. The overall seismic hazard is considerably greater than has previously been thought.

1. INTRODUCTION

Several comprehensive seismic hazard assessments have previously been carried out for New Zealand (e.g. Smith & Berryman, 1983; Matuschka et al, 1985). Although these studies were necessarily on a coarse scale and took only nominal account of regional geology-related factors such as fault seismicity or attenuation pattern variations, they have often been used to estimate the earthquake hazard at Christchurch.

Evidence from recent geologic studies indicates that a number of fault zones in the central South Island, including the Alpine Fault and others in North Canterbury, have the potential to generate larger earthquakes than has previously been assumed (e.g. Cowan & Pettinga, 1990). In addition, seismic hazard assessments for specific sites in Christchurch, employing all available geotechnical information for those sites (Soils & Foundations, 1988) suggest that earthquake effects in some areas of the city would be considerably stronger than at comparable epicentral distances from similar earthquakes in other areas of New Zealand. Brown et al (1991) confirmed the severity of the earthquake hazard for the city from a qualitative evaluation of Christchurch geology.

Examination of these recent research results highlighted the urgent need for a comprehensive evaluation of the seismic hazard in Christchurch. The results of this evaluation are reported in detail by Elder, McCahon & Yetton (1991).

Damage to structures at a given epicentral distance during a particular earthquake varies with ground conditions at different locations. Ground shaking is usually most severe on geologically recent, loose or soft sedimentary deposits. Notable examples of earthquakes where strong localised magnification occurred on these types of soils are the 1985 Mexico City earthquake and the 1989 Loma Prieta (San Francisco) earthquake.

In general the effects of an earthquake with magnitude M = 8.1 at 400 km epicentral distance (i.e. Mexico City during the 1985 earthquake) could also be generated by a smaller earthquake with M = 7.0 at 100 - 150 km or M = 7.5 at 50 - 100 km. A number of fault zones in the central South Island would satisfy these criteria for generation of effects at Christchurch. Furthermore, the Alpine Fault, within 125 km of Christchurch at its nearest point, and relatively quiescent during the past 150 years, is estimated to have experienced at least four large earthquakes ($M \geq 8$) at intervals of about 500 - 550 years. The last such event was about 550 years ago.

The quaternary alluvial deposits of loose, cohesionless soils beneath Christchurch are stiffer (but far deeper) than the soft clays beneath critically affected areas of Mexico City. In many places these soils are similar to the loose sands and silts in the Marina District of San Francisco. This great depth of uncemented soils beneath Christchurch (up to 1 km) enhances the potential for amplification of incident seismic waves due to impedance mismatches and constructive interference at soil strata boundaries.

The expected amplification of effects at Christchurch is supported by past observations. During a number of historical earthquakes, higher intensities have been reported at Christchurch than at other locations equidistant from the epicentre but on bedrock or shallow soils (Elder, McCahon & Yetton, 1991). Dibble et al (1980) concluded from historical evidence that intensities at Christchurch were, **on average**, 0.9 MM units higher than at Lyttelton and 1.6 MM units higher than at Akaroa. In some parts of the city intensities were more than 2 MM units higher than on Banks Peninsula.

Studies by Dibble et al (1980) and Davis & Berrill (1988) showed that Christchurch can expect significant frequency-dependent amplification of spectral accelerations. These would not be accounted for adequately either by the allowance for 'soft soil' effects made in the current New Zealand Design Loadings Code, or by existing spectral generation models.

2. ANALYSIS TECHNIQUES

Seismic hazard analysis requires use of a seismicity model to describe the rate of occurrence of earthquakes of different magnitude in each source region, and an attenuation model to describe the ground shaking effect produced at a site away from the source. Some attenuation models allow for variable site geology by using simplified groupings of ground characteristics, however to accurately predict effects at specific sites it is generally necessary to employ separate, additional analyses.

The seismic hazard analysis for New Zealand reported by Smith & Berryman (1983) estimated intensities using three different attenuation models for different areas of the country. No site-specific effects were included in the model, which predicted return periods at Christchurch:

Intensity (MM units)	Return Period
VI	14 years
VII	48 years
VIII	160 years
IX	600 years

The study reported by Matuschka et al (1985) estimated spectral accelerations throughout the country using a modified version of the attenuation model proposed by Katayama (1982). A slightly different attenuation model was used for each of four Ground Class conditions to make some allowance for site geology. Spectral accelerations predicted at Christchurch for structure natural period T = 0.2 seconds (close to peak structural response for the attenuation models used) were:

a_s	Return Period
0.3g	50 years
0.45g	150 years
0.8g	450 years
1.0g	1000 years

In this study a general source-to-site attenuation model was used to predict the bedrock motion beneath the deep alluvium at Christchurch, then a separate deep soil response model was employed to determine the variable effects throughout Christchurch caused by spatial soil inhomogeneity in the deep alluvium.

3. SEISMICITY MODEL

The seismicity model developed to describe the rate and magnitude of earthquake occurrence in source regions through the central-northern South Island has the mathematical form:

$$N = a_4[10^{b(4-M)} - 10^{b(4-Mmax)}] \quad (1)$$

where N is the annual number of earthquakes per given area with magnitude $\geq$ M, a_4 is the annual number of earthquakes with magnitude $\geq$ 4, b is a constant and M_{max} is a constraining maximum magnitude. M_{max}, a_4 and b are determined for each characteristic source region. Details of the model are described elsewhere (Elder, McCahon & Yetton, 1991; 1992).

The model bears similarities to that of Smith & Berryman (1983), but a number of significant modifications have been made to improve the accuracy of prediction at Christchurch:

- seven small, new seismicity zones have been employed in north and offshore Canterbury with boundary delineations suggested by recent geologic, tectonic and seismicity evidence

- the seismicity parameter *b*, often assumed to be close to 1.0, is decreased to 0.5-0.8 in some smaller zones to fit seismicity data. These smaller values are consistent with recommendations for medium to large earthquakes on individual faults, or in small, tightly constrained fault zones (e.g. Schwartz & Coppersmith (1986).

- parameters for the Alpine Fault region have been significantly adjusted to best reflect available geologic evidence for large earthquakes

- maximum magnitudes M_{max} have been reduced in regions where very large earthquakes are considered unlikely

4. INTENSITIES PREDICTED AT CHRISTCHURCH

The intensity attenuation model developed by Smith (1978a,b) has been refined to allow for variable directions of energy propagation consistent with tectonic features in the South Island (Elder et al, 1991). To simplify computation, a functional relationship has been developed among magnitude, distance and intensity.

This attenuation relationship is used with the source seismicity model described above to estimate exceedance probabilities for different intensities at Christchurch, for "average ground" conditions. The "continuous" intensity predicted by the model converts to the "Modified Mercalli" intensity by simple truncation (e.g. I=7.3 gives MM VII).

For medium intensities at Christchurch ($6 \leq I \leq 8$) the inferred seismic hazard at Christchurch is contributed to almost evenly by seismicity zones and known faults within 100 km of the city. At higher intensities very large earthquakes in more distant seismicity zones begin to dominate.

Intensities recorded near Christchurch during a number of historical earthquakes were investigated to assess the likely effect of the deep, loose cohesionless soils beneath the city. Isoseismal pattern distortions for a number of these suggest amplification of intensities above levels recorded at Banks Peninsula, where sites are on shallow soil or bedrock. Intensities recorded in Christchurch and on Banks Peninsula are compared in Figure 1 for nineteen historical earthquakes.

For three of these earthquakes, the mean intensities felt at Christchurch were up to one MM unit lower than those felt on Banks Peninsula. For six earthquakes the mean intensities were the same, while for the remaining ten the mean intensities at Christchurch were up to three MM units higher than those reported on Banks Peninsula.

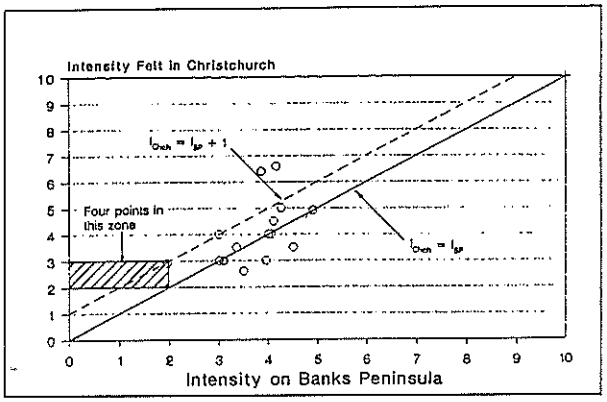

Figure 1. Comparison of Felt Intensities at Christchurch and on Banks Peninsula

Scatter in the comparison is expected due to the different reporting locations for different earthquakes, and variable epicentral distances. However some intensity amplification on Banks Peninsula may also occur due to geometric focusing, or in valleys where deeper soil deposits also coincide with greater population. Although the correlation is not strong, it appears reasonable to assume that intensities felt at Christchurch are, on average, at least 0-1 MM units higher than those for "average ground" at equivalent epicentral distances elsewhere in the country.

Return periods predicted for different intensities at Christchurch, allowing for ground amplification effects, are shown in Figure 2. Intensities predicted by Smith & Berryman (1983) for "average ground" are shown for comparison.

The effect of improving the seismicity model is to decrease the intensities predicted for "average ground" at Christchurch below those predicted by Smith & Berryman for return periods <20 years or >500 years. Intensities with return periods 20-300 years are higher than those predicted by Smith & Berryman.

However intensities at Christchurch are amplified on average by about 1 MM unit above those on "average ground" and then significantly exceed Smith & Berryman's predictions at all return periods. These results suggest that Christchurch is likely to experience medium to high shaking intensities at least as frequently as Wellington. Only for very long return periods (>> 1,000 years) is the predicted intensity higher for Wellington.

5. ACCELERATION RESPONSE SPECTRA

Acceleration response spectra are predicted for "bedrock conditions" at Christchurch using the source seismicity model and the attenuation model of Katayama (1982). A number of modifications proposed for New Zealand conditions (e.g. McVerry, 1986) have been examined in detail (Elder et al, 1991). We consider that at present the justification for their use in New Zealand is not apparent either on the basis of the original data presented, or from analysis of other data. The original Katayama model is consequently used without modification as the best available at present for New Zealand geological conditions.

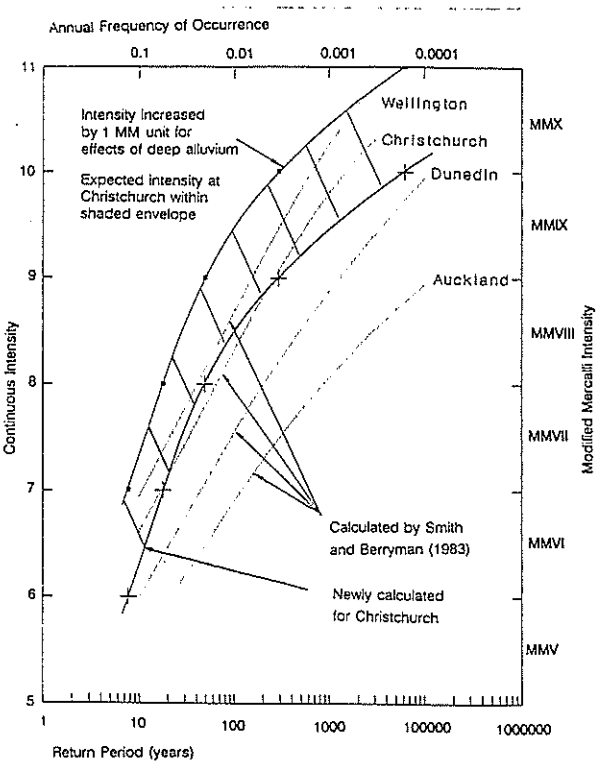

Figure 2. Return Periods for Different Intensities at Christchurch

Analysis of the maximum likely earthquake magnitude in each seismicity zone, and distances from Christchurch, suggests that the most severe effects at the city can not be clearly attributed to any one fault or seismicity zone. Instead, similar effects could be caused by medium sized earthquakes very close to the city; by large, slightly more distant earthquakes or by very large, distant earthquakes. This deterministic approach is useful in comparing the types of acceleration response spectra likely to be generated at Christchurch by each type of earthquake. These typical maximum earthquakes in each seismicity zone may be represented by three examples:

1. M=7.0, r=25km eg. Porters Pass zone - Ashley section; Canterbury Plains zone; Pegasus zone
2. M=7.3, r=50km eg. Porters Pass tectonic zone; Banks Peninsula zone
3. M=8.1, r=150km eg. Alpine Fault

Acceleration response spectra at Christchurch for each of these three earthquakes are shown in Figure 3.

The three spectra shown in Figure 3 are very similar. This confirms that no one or group of zones dominates a deterministic analysis for Christchurch. It also supports previous findings (e.g. Mulholland, 1982) that a relatively uniform spectral shape can be assumed throughout New Zealand, independent of location or return period.

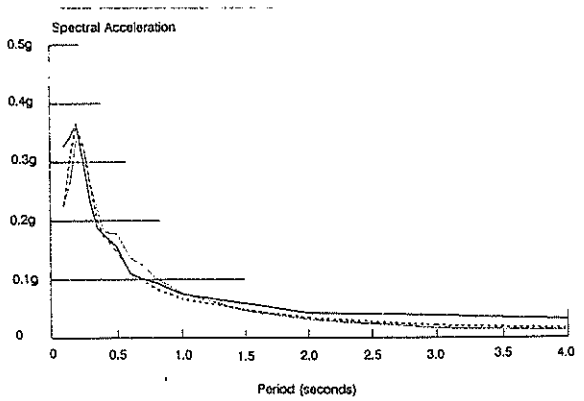

Figure 3. Typical acceleration response spectra for bedrock at Christchurch.

The consequence of assuming a constant shape for bedrock acceleration spectra at Christchurch is that exceedance probabilities/return periods calculated for accelerations at one natural period (e.g. the period corresponding to peak acceleration) also apply to other accelerations scaled from this value. This simplifies analysis considerably.

Exceedance probabilities are predicted at Christchurch for various peak bedrock spectral accelerations (assumed at natural period T=0.2 seconds). Following the analysis of Berrill (1985) a probability enhancement factor B_z=1.6 is calculated for the Canterbury region and applied to accelerations. Probabilities for low peak spectral accelerations ($a_s \leq 0.15g$) are dominated by small to medium local earthquakes while those for high accelerations ($a_s \geq 0.45g$) are dominated by large earthquakes on the Alpine Fault.

As discussed above for intensities, the incident accelerations at bedrock will be considerably modified as they propagate upwards through the loose, cohesionless alluvium to the ground surface. Four separate effects are possible:

- Amplification due to geometric focusing by non-planar basement geology
- Amplification due to impedance mismatch between bedrock and overlying soil
- Constructive and destructive interference between incident and reflected waves in layered soils
- Attenuation due to dissipation in soft soils, particularly of high frequency components

The first effect above is expected to be negligible compared to the other three beneath Christchurch, and is not considered in this study.

A three dimensional model of the geology beneath the city was constructed from a database of over 20,000 borelogs, to depths up to 500m, compiled by Soils & Foundations Limited (Elder et al, 1991). Results of seismic profiling reported by Kirkaldie & Thomas (1963) and by Dibble et al (1980) were also used to estimate soil types and the bedrock interface at greater depths. The method of analysis is described by Elder et al (1991a).

Response spectra at the ground surface in Christchurch were calculated at each point on a 500m grid across the city.

The effects of the deep alluvium are generally threefold:

- Removal of short period spectral accelerations by hysteretic damping
- Marked increase in peak spectral accelerations across most of the city
- Shift in spectral shape towards the longer period end of the spectrum, with peak accelerations occurring at natural periods 0.5 - 1.5 seconds

The spectral shape at any location depends strongly on the soil profile at that location, but modifications to acceleration response spectra are considerably greater than those expected if the current New Zealand Loadings Code were used to predict these effects. Although the deep soil effects influence the overall spectral magnitudes and shapes, three general shapes can be differentiated and are dependent most strongly on soil types within 20m of the ground surface. Examples of these acceleration response spectra are shown in Figure 4. Almost all calculated spectra can be placed into one of these three groups.

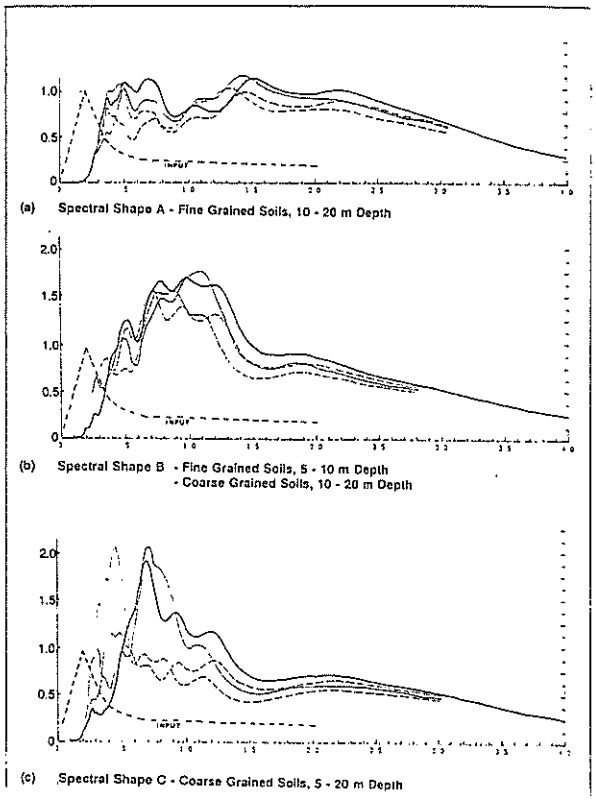

Figure 4. Acceleration Response Spectra at the Ground Surface in Christchurch

Using the soil profile criteria defining the three spectral shape groups in Figure 4, and the 3-dimensional geological model defined at each node on the 500m grid, the city is subdivided into microzones for seismic response

prediction. The peak spectral acceleration at the ground surface increases above the bedrock acceleration on average by about 20%, but by up to 100% in many parts of the city.

Return periods predicted for different spectral accelerations at Christchurch are shown in Figure 5. At all return periods, spectral accelerations predicted for Christchurch in this detailed, site specific study considerably exceed those previously expected. For a return period 150 years, peak spectral accelerations are likely to be 0.55g - 0.9g. The national study by Matuschka et al (1985) indicates a peak spectral acceleration about 0.45g at this return period. The amplification predicted is more pronounced for smaller earthquakes at shorter return periods, but slightly less marked for larger events.

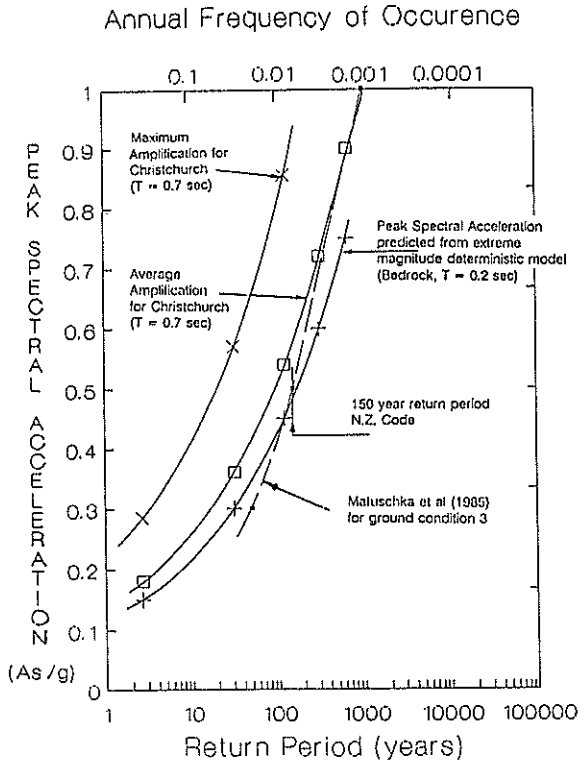

Figure 5. Return Periods for Amplified Peak Spectral Accelerations at Christchurch.

6. CONCLUSIONS

Analysis of data from historical earthquakes suggests that Christchurch regularly experiences earthquake effects considerably more severe than is generally thought. This is due to higher levels of active seismicity near the city, and the amplification effects of deep, loose, cohesionless alluvium up to 1 km deep beneath the city.

Detailed evaluation of historical and instrumental seismicity together with tectonic studies of active faulting zones, around Christchurch and in central/north Canterbury, provides evidence that the recent quiescence of major seismic activity within 150 km of Christchurch is an anomaly. The city can expect to generally experience earthquake effects in the medium strength range about as frequently as Wellington. This regularity of seismic shaking was observed in the first 70 years of the city's history; it is only since 1930 that Christchurch has not experienced significant effects from a large earthquake.

A 3-dimensional geological profile has been constructed for the alluvium beneath the city, based on a compilation of over 20,000 soil records and results of seismic surveys. Analysis of likely earthquake effect amplification has been carried out on a 500m grid across the city.

Intensities in Christchurch are likely to be magnified by up to 2 MM units above those intensities which would be felt at comparable epicentral distances on bedrock, and by at least one MM unit above intensities felt on "average ground".

Spectral response accelerations in Christchurch may be up to twice those for equivalent sites on bedrock. The natural period at peak acceleration response is likely to be 0.5 - 1.5 seconds. This shifts acceleration response spectra for the city well outside those spectra derived in the current New Zealand Loadings Code.

Probabilistic assessment for both intensities and spectral accelerations predicts that the hazard from events with return periods less than 150 - 300 years is considerably greater than suggested by previous studies. At longer return periods the hazard is also increased, but less markedly.

The consequences of these findings for specific hazards in Christchurch are discussed in companion papers. Yetton et al (1992) consider the potential for seismically triggered landslides in and around Christchurch. McCahon et al (1992) analyse liquefaction potential for the city using the same 500m grid employed in this study.

ACKNOWLEDGEMENTS

The research carried out in this study was funded by the New Zealand Earthquake and War Damage Commission. Dr. R.O. Davis, of the University of Canterbury, assisted with deep alluvium modelling. A number of organizations provided information and data, and many people assisted in reviewing the work. Staff at Soils & Foundations Limited, Christchurch carried out much of the data compilation, analysis and figure preparation. The assistance of all these people is gratefully acknowledged.

REFERENCES

Berrill, J.B. (1985) "Distribution of Scatter in New Zealand Accelerograph Data", Bulletin NZNSEE, Vol. 18, No. 2, pp. 151-164.

Brown, L.J., Beetham, R.D., Elder, D.McG, Weeber, J.H (1991) "Christchurch Geology and its relevance to Earthquake Hazard". Submitted to Bulletin NZNSEE.

Cowan, H.A. and Pettinga, J.R. (1990) "Seismic Hazards in the Canterbury Civil Defence Region", Report prepared for Canterbury United Council.

Davis, R.O. and Berrill, J.B. (1988) "Design Earthquake Response Spectra for the Telecom Site, Hereford Street, Christchurch", Unpublished Report to Soils & Foundations (1973) Ltd.

Dibble, R.R.; Ansell, J.H.; and Berrill, J.B. (1980) "Report on a study of seismic risk for B.P. New Zealand Ltd. sites at Woolston and Lyttelton", Unpublished Report to B.P. New Zealand Ltd.

Elder, D.M., McCahon, I.F., Yetton, M.D. (1991) "The Earthquake Hazard in Christchurch". Report to the New Zealand Earthquake and War Damage Commission.

Elder, D.M., McCahon, I.F., Yetton, M.D., Davis, R.O. (1991) "Potential Modification of Structural Response Spectra by Deep Sediments under Christchurch, New Zealand" Pacific Conference on Earthquake Engineering, Auckland, New Zealand.

Elder, D.M., McCahon, I.F., Yetton, M.D. (In Prep.) "The Earthquake Hazard in Christchurch.

Katayama, T. (1982) "An Engineering Prediction Model of Acceleration Response Spectra and its Application to Seismic hazard Mapping", Earthquake Engineering and Structural Design, 10, pp. 149-163.

Kirkaldy, P.H.S. and Thomas, E.G. (1963) Final Report on a seismic survey in the Canterbury Plains area of New Zealand. BP Shell & Todd Petroleum Development Ltd Geological/Geophysical Report 27 (unpublished).

Matuschka, T., Berryman, K.R., O'Leary, A.J., McVerry, G.H., Mulholland, W.M. and Skinner, R.I. (1985) "New Zealand Seismic Analysis", Bulletin N.Z. Soc. Earthq. Eng., Vol. 18, No. 4, pp. 313-322.

McCahon, I.F., Elder, D.M., Yetton, M.D. (1992) "Seismic Liquefaction Potential in Christchurch, New Zealand" Sixth Australia-New Zealand Geomechanics Conference, Christchurch, New Zealand

McVerry, G.H. (1986) "Uncertainties in Attenuation Relations for new Zealand Seismic Hazard Analysis", Bulletin NZNSEE, Vol. 19, No. 1, pp 28-39.

Mulholland, W.M. (1982) "Estimation of design earthquake motions for New Zealand", University of Canterbury, Department of Civil Engineering, Report 82/9.

Schwartz, D.P. and Coppersmith, K.J. (1986) in "Active Tectonics: Studies in Geophysics". National Academy Press, pp 224, 225.

Smith, W.D. (1978a) "Spatial distribution of felt intensities for New Zealand earthquakes", N.Z. Journal of Geology and Geophysics 21, pp. 293-311.

Smith, W.D. (1978b) "earthquake risk in New Zealand: statistical Estimates", N.Z. Journal of Geology and Geophysics 21, pp. 313-327.

Smith, W.D. and Berryman, K. (1983) "Revised Estimates of Earthquake Hazard in New Zealand", Bulletin NZNSEE, Vol. 16, No. 4 pp. 259-272.

Soils & Foundations (1988) "New Telephone Exchange, Christchurch - Geotechnical Report", Unpublished Report to Telecom N.Z. Ltd.

Yetton, M.D., Elder, D.McG., McCahon, I.F. (1992) "The Potential for Seismically Triggered Mass Movement in Christchurch" Sixth Australia-New Zealand Geomechanics Conference, Christchurch, New Zealand.

Some landslide risk zoning schemes in use in Eastern Australia and their application

R. Fell
B.E., M.Eng.Sc., F.I.E.Aust.
School of Civil Engineering, University of New South Wales, Sydney, Australia

ABSTRACT Landslide risk zoning schemes in use in Eastern Australia have developed with mixed terminology to describe the probability and the consequences of landsliding. The terms "hazard" and "risk" have been interchanged. The zoning schemes have also been influenced by the lack of insurance to cover damage due to landsliding, and have generally made inadequate allowance for the situation where loss of life is possible. It is suggested that some standardisation of terms and approach is needed, and steps taken to introduce landslide insurance.

1 INTRODUCTION

Since 1984, the author has been involved in the development of several landslide risk zoning schemes in New South Wales and Victoria. These are:

- Joint author of the Australian Geomechanics Society "Classification of Risk of Slope Instability" (Walker et al, 1985)
- Project leader for geotechnical zoning studies of the Lake Macquarie City Council area (Newcastle, NSW) in 1984 (Coffey and Partners, 1984, Fell and Flentje, 1991 and Flentje, 1991).
- Review consultant (with D.H. Stapledon) of landslip risk assessment, Mooroolbark (in the Shire of Lillydale), Victoria (Coffey and Partners, 1987)
- Review consultant (with M. Ervin) for classification of risk of slope instability in the Shire of Lillydale, Victoria (Coffey Partners International, 1990)
- Project team member for development of guidelines for management of lands subject to landsliding in the Richmond and Tweed River catchments, NSW (MacGregor, McManus and Fell, 1990 and MacGregor and McManus, 1992)
- Review consultant (with D.H. Stapledon) for classification of landslide risk due to debris flow in the Montrose area (Shire of Lillydale), Victoria.

This involvement has seen a development of the approach taken to landslide risk zoning in these studies, all of which (except the Richmond-Tweed study) are in urban areas, and involve relatively large scale mapping. It has also highlighted the confusion in terminology used in such studies, the influence of the user (often a council) on the scheme, and the influence of liability and insurance matters.

The paper sets out to share some of these experiences, and discusses future directions such schemes might take.

2 DEFINITIONS OF HAZARD AND RISK

The terms "hazard" and "risk" are poorly defined in landslide zoning schemes. This is possibly forseeable, because when one refers to the Oxford Pocket Dictionary one finds the following:

	Hazard	—	chance, danger, risk
and	Risk	—	chance of bad consequences, exposure to chance of injury or loss

ie. that the terms are interchangeable.

The concepts of hazard and risk are well developed in dam engineering, and are used in selection of design floods for spillways and other features. ANCOLD (1983) give the following definitions:

Hazard	—	relates to the potential damage or loss of life in the event of a dam failure, or misoperation of the dam or its facilities
Risk	—	relates to an evaluation of the probability of failure accuracy.

ANCOLD (1983) gives three grades of hazard which are based on US Corp of Engineers criteria:

"Low" hazard

Rural areas where no residences are threatened and economic loss downstream would be minimal, such as farm buildings, limited damage to agricultural land, minor roads, etc

"Significant" hazard

Rural areas where a few residences would be threatened and economic loss would be appreciable, including possible damage to secondary roads, minor railways, or relatively important public utilities

"High" hazard

Where more than a few residences would be threatened, or where loss of human life is liable to be more than a few persons, or where economic loss would be appreciable, such as possible serious damage to extensive community, industrial, commercial or agricultural facilities, highways, primary roads, main railways, important public utilities.

Varnes (1984), in a UNESCO review of principles and practice of landslide hazard zonation, cautions

that the terms hazard and risk do not have universally similar meanings and proposes that the United Nations Organisation UNDRO (Office of the United Nations Disaster Relief Coordinator) and UNESCO definitions be used. These are:

Natural hazard (H) means the probability of occurrence within a specified period of time and within a given area of a potentially damaging phenomenon

Vulnerability (V) means the degree of loss to a given element or set of elements at risk (see below) resulting from the occurrence of a natural phenomenon of a given magnitude. It is expressed on a scale from 0 (no damage) to 1 (total loss)

Specific risk (R_S) means the expected degree of loss due particular natural phenomenon. It may be expressed by the product of H times V

Elements at risk (E) means the population, properties, economic activities including public services, etc at risk in a given area

Total risk (R_t) means the expected number of lives lost, persons injured, damage to property, or disruption of economic activity due to a particular natural phenomenon, and is therefore the product of specific risk (R_S) and elements at risk (E). Thus:

$$R_t = (E)(R_S) = (E)(HxV)$$

The terms hazard and risk are interchanged compared to the ANCOLD (1983) definitions. Varnes does not, however, define what low, medium, high etc total risk would be.

Hunt (1984), who discusses rating of hazard and risk in some detail, gives the following definitions:

Hazard — refers to the slope failure itself in terms of its potential magnitude and probability of occurrence

Risk — refers to the consequences of failure on human activities.

These are consistent with Varnes (1984) definitions.

Magnitude is further defined in terms of the volume of material which may fail, the velocity of movement during failure, and the land area which may be affected. Risk is related to property damage and potential for loss of life. The degree of hazard and risk is classified as shown in Table 1.

For the purposes of discussion, the Hunt definitions will be adopted for the remainder of this paper.

3 AUSTRALIAN LANDSLIDE ZONING SCHEMES

In 1985 the Sydney Group of the Australian Geomechanics Society established a subcommittee to develop a risk classification for slope instability in the Sydney basin, and to provide guidelines for hillside construction. The classification was not a zoning scheme, but it was expected that most practitioners would adopt the risk classification when working in the Sydney basin (including Sydney, Newcastle, Gosford, Wollongong). Table 2 presents the risk classification.

It should be noted that:

- the classification was developed for the whole of the Sydney basin, which includes a diverse range

Table 1. Landslide hazard and risk degree (Hunt, 1984).

HAZARD DEGREE	RISK DEGREE
No Hazard: A slope is not likely to undergo failure under any forseeable circumstances.	The rating basis for risk is the type of project and the consequences of failure. No Risk: The slope failure will not affect human activities.
Low Hazard: A slope may undergo total failure (as compared with partial failure) under extremely adverse conditions which have a low probability of occurrence (for examples, a 1000-year storm or a high-magnitude earthquake in an area of low seismicity), or the potential failure volume and area affected are small even though the probability of occurrence is high.	Low Risk: An inconvenience easily corrected, not directly endangering lives or property, such as a single block of rock of small size causing blockage of a small portion of roadway and easily avoided and removed.
Moderate Hazard: A slope probably will fail under severe conditions which can be expected to occur at some future time, and a relatively large volume of material is likely to be involved. Movement will be relatively slow and the area affected will include the failure zone and a limited zone downslope (moderate displacement).	Moderate Risk: A more severe inconvenience, corrected with some effort, but not usually directly endangering lives or structures when it occurs, such as a debris slide entering one lane of a roadway and causing partial closure for a brief period until it is removed.
High Hazard: A slope is almost certain to undergo total failure in the near future under normal adverse conditions and will involve a large to very large volume of materials, or a slope may fail under severe conditions (moderate probability), but the potential volume and area affected are enormous, and the velocity of movement very high.	High Risk: Complete loss of a roadway or important structure, or complete closure of a roadway for some period of time, but lives are not necessarily endangered during the failure. Very High Risk: Lives are endangered at the time of failure by, for example, the destruction of inhabited structures or a railroad when there is no time for a warning.

Table 2. Australian Geomechanics Society Sydney Group classification of risk of slope instability (Walker et al, 1985).

RISK OF INSTABILITY	EXPLANATION	IMPLICATIONS FOR DEVELOPMENT
VERY HIGH	Evidence of active or past landslips or rockface failure; extensive instability may occur.	Unsuitable for development unless major geotechnical work can satisfactorily improve the stability. Extensive geotechnical investigation necessary. Risk after development may be higher than usually accepted.
HIGH	Evidence of active soil creep or minor slips or rockface instability; significant instability may occur during and after extreme climatic conditions.	Development restrictions and/or geotechnical works required. Geotechnical investigation necessary. Risk after development may be higher than usually accepted.
MEDIUM	Evidence of possible soil creep or a steep soil covered slope; significant instability can be expected if the development does not have due regard for the site conditions.	Development restrictions may be required. Engineering practices suitable to hillside construction necessary. Geotechnical investigation may be needed. Risk after development generally no higher than usually accepted.
LOW	No evidence of instability observed; instability not expected unless major site changes occur.	Good engineering practices suitable for hillside construction required. Risk after development normally acceptable.
VERY LOW	Typically shallow soil cover with flat to gently sloping topography.	Good engineering practices should be followed.

Table 3. Lake Macquarie City Council geotechnical zoning (Fell and Flentje, 1991).

ZONE	DESCRIPTION
NEWCASTLE COAL MEASURE SEQUENCE	
ZONE T1 >15° slopes COAL & CLAYSTONES	Steep slopes, greater than 15°, with known coal seams and/or tuffaceous claystones present that may affect the site.
ZONE T2 >15° slopes NO COAL or CLAYSTONES	Steep slopes, greater than 15°, without known coal seams and/or tuffaceous claystones present that may affect the site.
ZONE T3 5° - 15° slopes COAL & CLAYSTONES	Moderate slopes, between 5° and 15°, with known coal seams and/or tuffaceous claystones present that may affect the site.
ZONE T4 5° - 15° NO COAL or CLAYSTONES	Moderate slopes, usually between 5° and 15°, without known coal seams and/or claystones present that may affect the site.
ZONE T5 <5° slopes COAL & CLAYSTONE	Gentle slopes, less than 5°, with known coal seams and/or tuffaceous claystones present that are not expected to affect the site.
NARRABEEN GROUP	
ZONE T1A >15° slopes CLAYSTONES	Steep slopes, greater than 15°, with known or inferred claystones-shale intervals present that may affect the site.
ZONE T2A >15° slopes NO CLAYSTONES	Steep slopes, greater than 15°, without known or inferred claystones-shale intervals present that may affect the site.
ZONE T3A 5° - 15° slopes CLAYSTONES	Moderate to gentle slopes, between 5° and 15°, with known or inferred claystones-shale intervals present that may affect the site.

of sedimentary rock environments, including shale, sandstone, interbedded siltstone and sandstone, and coal measure rocks
- the "risk" classification explanations are a mixture of hazard, ie. probability of occurrence, risk, ie. the implications of failure, and method, ie. statements of evidence of instability
- there is no mention of potential for loss of life.

The AGS classification has been widely accepted by practitioners and councils. Some practitioners have modified the classification to remove the "very low" classification, partly motivated by concern of professional liability. The classification has been instrumental in educating councils to the concept of risk classification, and has led to a reduction in demands to pronounce a site "stable", with all the associated legal implications.

3.2 Lake Macquarie City Council geotechnical zoning

In 1984 Lake Macquarie City Council implemented a geotechnical zoning scheme, based on a study by Coffey and Partners (1984). This followed several landslide incidents, which resulted in significant cost to Council in investigations and remedial works. The zoning was revised in 1991 (Fell and Flentje, 1991 and Flentje, 1991) to account for additional geotechnical information available from 600 consultant's reports to Council, and elsewhere prepared from 1984 to 1991. The Council area is underlain by the Newcastle Coal Measures and Narrabeen group sedimentary rocks. Much of the instability in the area relates to the presence of tuffaceous claystone, and/or coal seams. Table 3 summarizes the recommended 1991 zoning classifications.

It has been recommended that the AGS risk classification be adopted for all sites requiring assessment. Assessment will be required
- for all zones when new subdivisions are being developed
- for zones T1, T2, T3, T1A, T2A and T3A when building applications and minor subdivisions are being assessed. This is necessary because conditions alter locally and require individual assessment.

For zone T4, Council officer's inspection only is recommended, with good construction practice for hillside development to be followed (based on the table in Walker et al but with some quantification on depths of cuts and heights of fills). Unless major site changes are proposed, zone T5 is to be developed following "normal engineering practices". As part of the 1991 study detailed geological maps at 1:4000 scale (some 1:10,000 and 1:25,000) have been prepared, to show the location of coal seams. These will be made available to practitioners, and will be a valuable guide to areas of potential instability, given the strong relationship between instability and the presence of claystone and nearby coal seams. The slope boundaries were delineated on experience of instability, but it should be noted that large scale instability is often associated with low slope angles — 6° to 10°.

The LMCC geotechnical zoning is not strictly a landslide hazard/risk zoning, except in so far as zones T4 and T5 are concerned. It is left to the practitioner assessing the site to classify the hazard/risk. Efforts to convince Council and local consultants that a clearer definition between hazard and risk was desirable were unsuccessful, because they felt that the AGS classification was working satisfactorily.

3.3 Shire of Lillydale landslip risk classifications

In 1987 the Shire of Lillydale had a relatively small area in Mooroolbark assessed for landslide/hazard risk by Coffey and Partners Pty Ltd (1987).

This study was in a subdivision, and the area was zoned into very high, high, medium and low risk according to the AGS classification. The area was underlain largely by basalt, and there was evidence of instability in some areas. Arising out of this, and a study in 1988 of freehold land in the Upper Yarra and Dandenong Ranges (Coffey and Partners, 1988), the Council engaged Coffey and Partners to zone the whole of their Shire. This is reported in Coffey Partners International Pty Ltd (1990) and Lillydale Council (1990), and in Olds and Wilson (1992).

The hazard/risk classification was based on the AGS classification, but modified to exclude very high and very low categories because it was impracticable to differentiate them from high and low respectively with the limited amount of detailed investigation being used. It was also amended to describe the likelihood of landsliding, and the damage potential. The risk classification, development controls and damage potential are shown in Table 4.

The zone boundaries were based on geology (which included basalt, volcanics, and sedimentary), slope angle, evidence of instability, and geomorphologic and geologic similarity to known unstable areas. Low and medium risk areas were differentiated into Lb (basalt) and L (other) and M1, M2, based on geology and slope angle.

Development controls and site assessment procedures were developed and made available to the public in Shire of Lillydale (1990). These are summarised in Table 5.

The building development controls were based on those in Walker et al (1985), with quantification on heights of cuts and fills, and some amplification on disposal of waste water. It can be seen that in this classification, "risk (explanation)" is equivalent to Hunt's (1984) "hazard degree", and "damage potential" is equivalent to "risk degree".

It is a genuine zoning scheme, in that it allows routine controls to be implemented for a large part of the Shire without reference to a geotechnical assessment, and even then, imposes quite tight control on development.

The descriptive terms are general and probability is not quantified, which is not unreasonable given the large area involved and the intensity of investigation possible. The classification does not specifically refer to potential for loss of life, but this was identified in two areas, one of which has been further studied — ie. the Montrose debris slide area which is discussed below.

Table 4. Shire of Lillydale landslide risk and damage potential classification (Coffey and Partners International, 1990 and Lillydale Shire Council, 1990).

Risk Zone	Explanation	Damage Potential	
		Extent	Probability
Exempt	Instability is improbable		
Low	Landslip is very unlikely	}	
Low-basalt	Landslip is very unlikely but caution is warranted	} Slight	Very low
Medium 1	Landslip is unlikely	} Slight	Low
Medium 2	Landslip is unlikely but higher risk than M1	} Moderate	Very low
High	There is some risk of landslip	} Severe	High
		} Large severe	Moderate

Table 5. Shire of Lillydale landslide risk zones, assessment and development methods.

Risk Zone	Assessment Requirements	Development Controls
Exempt	No stability assessment	Good engineering practice
Low	Confirm risk classification at same time as classification of site reactivity	Good hillside practice
Low-basalt	Assessment by geotechnical practitioner	Good hillside practice
Medium 1	Confirm risk classification at same time as classification of site reactivity	Good hillside practice
Medium 2	Geotechnical assessment and where necessary, geotechnical investigations	Minimum Good hillside practice
High	Detailed geotechnical studies, visual assessment alone insufficient	No building development until risk downgraded by investigation and/ or remedial works

3.4 Richmond and Tweed River catchments, guidelines for management of lands subjected to landsliding.

This study, which is reported in MacGregor, McManus and Fell (1990) and MacGregor and McManus (1992) is different to the others in that rural areas are involved, and the objectives were to develop guidelines for implementation by Soil Conservation Service of NSW officers. It is also significantly different in that being rural land, the objective is not to produce an environment with "zero" risk of landsliding, but rather to limit it to ensure farming is not disrupted, land is not degraded with respect to its farming potential, and that erosion which could cause river siltation is controlled.

3.5 Shire of Lillydale — debris flow risk zoning at Montrose

As part of the study discussed in section 3.3, it was recognised that a large debris flow or avalanche had occurred off the western slope of Mt Dandenong in 1891. This had flowed about 1km from the base of the mountain. The area is now partly developed as suburban housing. It was realised that if such an event was to occur now, there was a high probability that lives would be lost. Coffey Partners International were engaged to carry out further investigations of the area and to prepare a zoning classification of debris flow hazard/risk. This is described in Coffey Partners International (1991) and Moon, Olds and Wilson (1992).

The study involved some significant features additional to that for the general landslip classification study for Lillydale Shire described in section 3.3. These included:

- delineation of potential source areas for debris, flow paths and deposition zones
- quantification of the size of potential debris flows, the probability of occurrence and, to a lesser extent, the damage potential
- consideration of development control alternatives.

Figure 1 shows part of the zoning map of the area. Tables 6, 7 and 8 the risk zones, assumed recurrence interval, and the damage potential.

Because of the intensity of the investigations carried out, there are no "assessment requirements" relating to debris flow, but the area is covered by the landslip risk zones described in Table 5, so will also be classified in that respect. The Coffey Partners International (1991) report presents a matrix of development control options, giving varying degrees of conservatism which the Council may adopt. This includes reference to the possible need to evacuate some areas, allow no further development, restrict development, and inform the residents of the risk.

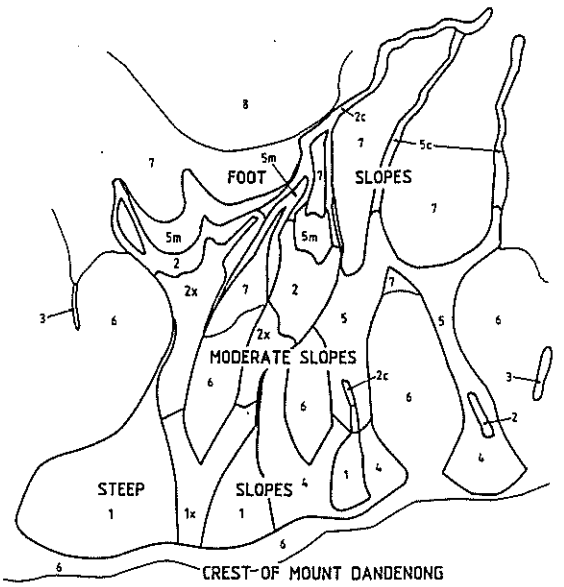

Figure 1. Part of debris flow risk zoning at Montrose (adapted from Coffey Partners International (1991).

At the time of writing this paper the author had not been requested to review the final report (although earlier drafts had been reviewed), and Lillydale Council had not decided which option to adopt.

It will be noted that considerable judgement has to be exercised in such a zoning study:

- to determine the magnitude of likely debris flow volumes
- to determine flow paths and distances
- assessing the recurrence intervals of events (in this case a historic event assisted, as did evidence of instability in the source areas).

However, the outcome is a zoning which allows rational decision making based on the best available methods and data.

4 DISCUSSION

There are some issues which arise from these reports:

a) There is a need to reach some standard terminology on what is meant by hazard and risk. It is the author's view that it will be necessary to adopt a dual scheme, similar to Hunt (1984), which uses hazard degree to describe the probability and magnitude of the event, and risk degree to describe the likely impact on human activities if the landslide occurred, or the Lillydale zoning approach which uses risk category to describe the probability and magnitude of the event, and damage potential to describe the likely impact on human activities if the landslide occurred.

   It is the author's view that hazard and risk are interchangeable words in many person's minds, so any adopted standard should only include one of them. This would favour use of "hazard" (quantified where practicable), and "damage potential" (also quantified where practicable). The preference for the term hazard rather than risk is to maintain some link to Varnes (1984) UNESCO definitions. The other option would be to adopt Varnes (1984) definitions, but define limits for very low, low, medium, high, very high, natural hazard and total risk.

b) The AGS classification has been useful for what it was developed for, but it is the author's view (and the author was a joint author of the AGS classification), that the "risk of instability" is an unfortunate mix of the terms hazard and risk. The AGS classification fails to quantify the probability or magnitude of sliding or the damage potential. It also fails to consider the potential for loss of life. It has also been used outside the geological environment for which it was developed.

c) Whichever scheme is used, there are significant implications to the practitioners developing the zoning, the councils who are usually required to implement the zoning, and the public. Classification of a site as a high risk, or very high risk of instability, in the AGS system (or the equivalent terms in other zonings) has an immediate impact on property values, even though landsliding may have a low probability of occurrence, and may not be severly damaging when it occurs. The lack of insurance for landsliding in Australia forces conservative decisions and statements to be made by practitioners, so as to avoid the risk of being sued. Insurance cover is available in some countries, including the United Kingdom and New Zealand, and this allows for more economic zoning to be adopted.

Table 6. Montrose debris flow study, description of debris flow risk zones (adapted from Coffey Parters International, 1991).

Zone Number	Risk Category	Description of Risk Zone
1	High	Steep slopes where landslips may occur, some of which may become debris flows. Initiation and transportation zone for a high risk design debris flood (high risk event).
1X	High X	Subdivision of Zone 1 to include Modern (post European) disturbed ground of 10,000m^3 or greater. Initiation and transportation zone for a High X risk design debris flow (high X risk event).
2	High	Likely extent of deposition area for a High risk event originating in Zone 1.
2X	High X	Subdivision of Zone 2 to indicate likely extent of deposition for a high X risk event originating in Zone 1X.
2C	High	Gullies downstream of Zone 2 where debris may be deposited by the high risk event. Large parts of Zones 2C will also be affected by a high X risk event.
3	High	Gullies where parts of the gully floor are steep (greater than 40% slope) and parts of the immediate catchment are very steep (greater than 50% slope). Debris torrents may affect the sections of gully covered by Zone 3.
4	Medium	Medium risk equivalent of Zone 1.
5	Medium	Medium risk equivalent of Zone 2.
5C	Medium	Medium risk equivalent of Zone 2C and some downslope margins away from gullies.
5M	Medium	Marginal area to Zones 2 and 2C. Medium risk because of difficulty of predicting extent of deposits resulting from high risk events. This difficulty includes the uncertainty associated with assessing the proportion of debris flowing down particular gullies and with assessing the extent of fringe areas. Zone 5M also takes into account the medium risk of larger than design debris flows occurring in the Zone 1 or Zone 1X areas.
6	Low	Low risk equivalent of Zone 1.
7	Low	Low risk equivalent of Zone 2. Extended to include all areas of flatter slopes in which deposits of colluvium or alluvium could occur.
8A	Low	Foothills not included in Zone 7, where steeper slopes occur.
8B	Very low	Foothills or alluvial flats not included in Zone 7 or 8A.
9	Very low	Crestal ridge of the Dandenongs.

Table 7. Montrose debris flow study, assumed recurrence intervals for design debris flows (adapted from Coffey Partners International, 1991).

Risk Category	Assumed Recurrence Interval (years)	Assumed Probability of Occurrence in 50 year period (%)
High X	1 in 100 to 1 in 300	15 to 39
High	1 in 100 to 1 in 1,000	5 to 39
Medium	1 in 1,000 to 1 in 10,000	0.5 to 5
Low	greater than 1 in 10,000	less than 0.5
Very low	greater than 1 in 100,000	less than 0.05

Table 8. Montrose debris flow study, potential damage, injury and death in the flow path of the design debris flows if they occur (adapted from Coffey Partners International, 1991).

Zone Numbers	Damage Potential
1,1X,4,6,8A	Loss of life and serious injury possible. Destruction of buildings could occur.
2,2X,5,5M,7	Loss of life and serious injury possible. Destruction of buildings could occur in or close to gullies and in upper parts of zones. Buildings may survive in fringe areas.
2C,5C,3	Loss of life and serious injury possible. Destruction of buildings could occur in gullies. Buildings on the edge of gullies could deflect flow and survive. Severe flooding could occur at the margins and downstream of these zones.
8B,9	Not assessed as these zones are not likely to be affected by debris flows.

The zoning of the town of Ventnor on the Isle of Wight is an excellent example of what can be done if insurance cover is available. The town of 30,000 persons is virtually all on landslide affected land, but it has been possible to subzone the area to reflect the damage potential. This is described in Hutchinson (1991), Lee et al (1991) and other papers from the same conference.

d) There is a need for strong development controls, and funding for compensation for affected houseowners in areas with a high probability of being affected by death threatening landslides (such as those at Montrose). It is the author's view that Table 8 does not adequately convey the potential to loss of life. Debris slides in zones 1, 1X, 2 and 2X at least, would probably (not possibly) result in loss of life and injury. Whether persons should be allowed to remain living in such areas which have an assessed probability of occurrence of 5% to 39% in the next 50 years is questionable, and influenced by the lack of insurance or compensation funding.

ACKNOWLEDGEMENTS

The author has been fortunate to have worked with Lillydale and Lake Macquarie Councils, and the Soil Conservation Service of NSW, on the projects described. The cooperation of the consultants involved in the projects is acknowledged, as is the friendly cooperation of review panel colleagues David Stapledon and Max Ervin, and project team members Philip Flentje, Patrick MacGregor and Kevin McManus.

REFERENCES

Coffey and Partners Pty Ltd (1984). Lake Macquarie City Council. Geotechnical Zoning Study. Report No S7341-1-A3.

Coffey and Partners Pty Ltd (1987). Landslip risk - Mooroolbark. Report M1224/5.

Coffey Partners International Pty Ltd (1990). Slope stability review within the Shire of Lillydale. Report No M2027/1-AD.

Coffey Partners International Pty Ltd (1991). Study of debris flow and other landslips, Montrose, Victoria. Report M2120/1-AJ.

Fell, R. and Flentje, P. (1991). Lake Macquarie City Council. Geotechnical Zoning Study. Unisearch Limited , Report A 14082-01.

Flentje, P. (1991). Geotechnical zoning study of Lake Macquarie City. M.App.Sc. Thesis (in preparation).

Hunt, R.E. (1984). Geotechnical Engineering Investigation Manual. McGraw-Hill.

Hutchinson, J.N. (1991). Keynote paper. The landslides forming the South Wight undercliff of the Isle of Wight , in Slope Stability Engineering Developments and Applications. The Institution of Civil Engineers.

Lee, E.M., Moore, R., Brunsden, D. and Burt, D. (1991). Strategies for managing the landsliding complex at Ventnor, Isle of Wight, in Slope Stability Engineering Developments and Applications. The Institution of Civil Engineers.

MacGregor, J.P. McManus, K.J.. and Fell, R. (1990). Management of protected lands subject to mass movement in the Richmond River catchment. Unisearch Limited Report for Soil Conservation Service of NSW.

MacGregor, J.P. and McManus, K.J. (1992). Management of lands subject to mass movement, in Sixth ISL, Christchurch, New Zealand, February.

Moon, A.T., Olds, R.J. and Wilson, R.A. (1992). Debris flow risk zoning at Montrose, Victoria, Sixth ISL, Christchurch, New Zealand, February.

Olds, R.J. and Wilson, R.A. (1992). Landslip risk zoning and development controls in the Shire of Lillydale, Victoria, in Sixth ISL, Christchurch, New Zealand, February.

Shire of Lillydale (1990). Development in areas of possible slope instability. Resident Information Guide.

Varnes, D.J. (1984). Landslide hazard zonation, a review of principles and practice. UNESCO.

Walker, B.F., Dale, M., Fell, R., Jeffery, R., Leventhal, A., McMahon, M., Mostyn, G. and Phillips, A. (1985). Geotechnical risks associated with hillside development.

Rock Slope Instability Zoning with Kinematic and Morphological Factors

U. GLAWE
(M.Sc., Dipl.-Geol.)
Department of Applied Geology, Schlossgarten 5, 8520 Erlangen, Germany
J.A. HUDSON
(Professor of Rock Mechanics)
Department of Mineral Resources Engineering, Imperial College of Science, Technology and Medicine, London SW7 2BP, UK

1. INTRODUCTION

In this paper, a natural rock slope is analyzed using a combination of geological and engineering approaches. The movement of the individual parts of the slope has been monitored since 1987. The objective of the work was to study the stability of the slope and the associated mechanisms utilizing this integrated approach. A particular feature was the kinematic and morphological zoning procedures, which further highlights the geological and geotechnical combination.

In the next two Sections, we describe the site conditions and the monitoring systems that we used. This is followed by a presentation of the movements that were detected and the consequential idea of kinematic and morphological instability zoning. Further work was conducted in modelling the blocks using FE-analyses to assist in understanding the fundamental mechanisms that are operating and the associated parameters.

Finally, as a result of the various factors that have been discussed, we summarize the crucial geotechnical parameters and make comments concerning the assessment of risk for a natural system.

2. SITE CONDITIONS

The research area, which is shown in fig. 1, is located in the Carinthian Alps in Austria in a region which has experienced several large scale landslides - which have had a deleterious effect on proximate roads.

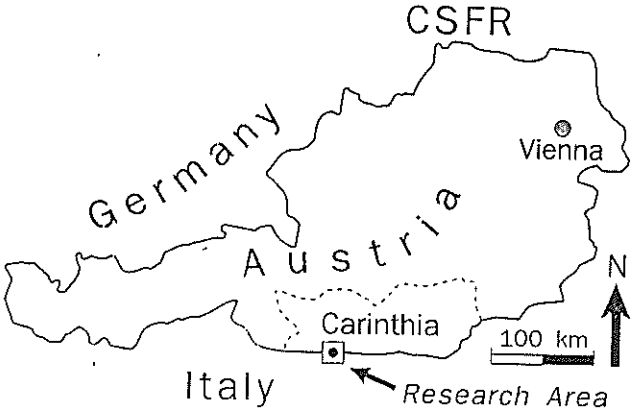

Fig. 1 Location of research area

In fig. 2, we present a schematic cross section of the "Tressdorfer Hoehe", a plateau-shaped mountain. It should be noted, that the surface topography and isolated limestone blocks are essentially the final stage of a disintegration process that has been operative since the last Ice Age, i.e. over the last ten thousand years.

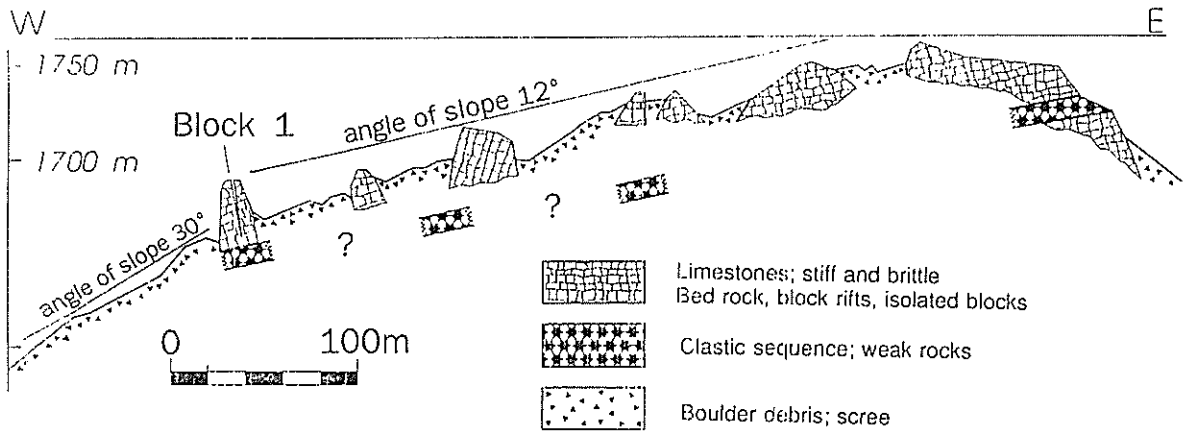

Fig. 2 Geological and morphological section through study area

The limestone slab at the mountain top disintegrated in a series of blocks, which are now moving and are potentially subject to sudden toppling. The stiffer cap-rock of which the blocks are composed overlies a stiff basement seperated by a weak foundation interlayer (fig. 3).

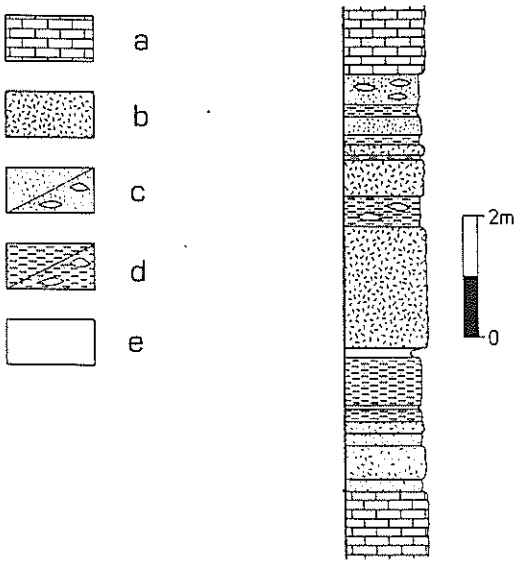

Fig. 3 Geological section of the weak interlayer. (a and b) limestone; (c) sandstone/with clay lenses; (d) siltstone/with clay lenses; (e) claystone

The geometry of the blocks in question is dominated by the main joint sets, which are shown in fig. 4. The NNE- and the ESE-dipping joint sets are opened during failure at the upper scarp (see fig. 2), whilst the SW-dipping sets are opened at the slope edge. The frequencies of the three joint vary from 0.1 to 1m: in some cases, the jointing can be widely spaced because of the existence of reef in the Lower Permian limestone.

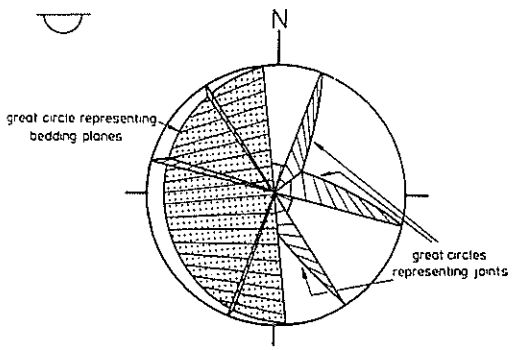

Fig. 4 Discontinuity pattern in study area bedrock

3. MONITORING SYSTEMS

A variety of monitoring devices were used for both the area of interest as a whole and for individual analyses of specific kinematic problems that were addressed. On the wider scale, a precise geodetical survey was undertaken starting in 1989 and is on-going. In Fig. 5, the vectors of absolute displacements and the error ellipses are shown. The geodetic net consists of two fixed pillars, from which 28 optical targets within the block field are monitored. To separate translational and rotational components of the displacements of individual blocks, at least three targets were positioned on the major blocks. The relative displacements between individual blocks were recorded using quasi-continuous readings of extensometers and other displacement indicators.

Some of these instruments were one electronic fixed clinometer, twelve location plinths for tiltmeters, four Moire-indicators, 120 locations for the tape extensometer measurements. Additionally, precipitation, rock and air temperatures are monitored continuously. An example of an instrumentation complex is shown in fig. 6. The pivot of a tilting block (1A) can be established from the configuration of the instrumentation set-up. In fact, the configuration of all the instrumentation was established for optimal interpretation of the slope's kinematics.

4. DETECTED MOVEMENTS

In fig. 7-10, we illustrate examples of the type of measurements that were made from the very large number of data recorded. In fig. 7, the within-crack temperature is shown over a three month period. It can be clearly seen that the variation is extremly small - within one fifth of a degree - and hence will not affect the displacement readings significantly. In the same tension crack close to the upper scarp, precise extensometer measurements were conducted simultaneously . The results are shown in fig. 8. The dominant trend is a quasi-linear increase of crack aperture totalling one tenth of a millimeter over the same three month period.

Fig. 9 shows displacement readings over a much longer period from June 88 to July 90, taken in a crack close to the slope edge (see also fig. 2). These readings exhibit an almost linear trend over the 120mm recorded. The seasonal influences are detectable within these data. Finally, in fig. 10, we show a scaled up three month portion of the curve in fig. 9. On this curve, individual influences such as heavy rainfall are manifested. It is important to note that such detail is below the resolution of the geodetic survey; indeed, this was the motivation for the two phase displacement recording approach. Also, in anticipation of the need to detect such small displacements for zoning purposes the instrumentation was clearly necessary.

In the next section, we will be discussing the indicators for decoding the measured displacements.

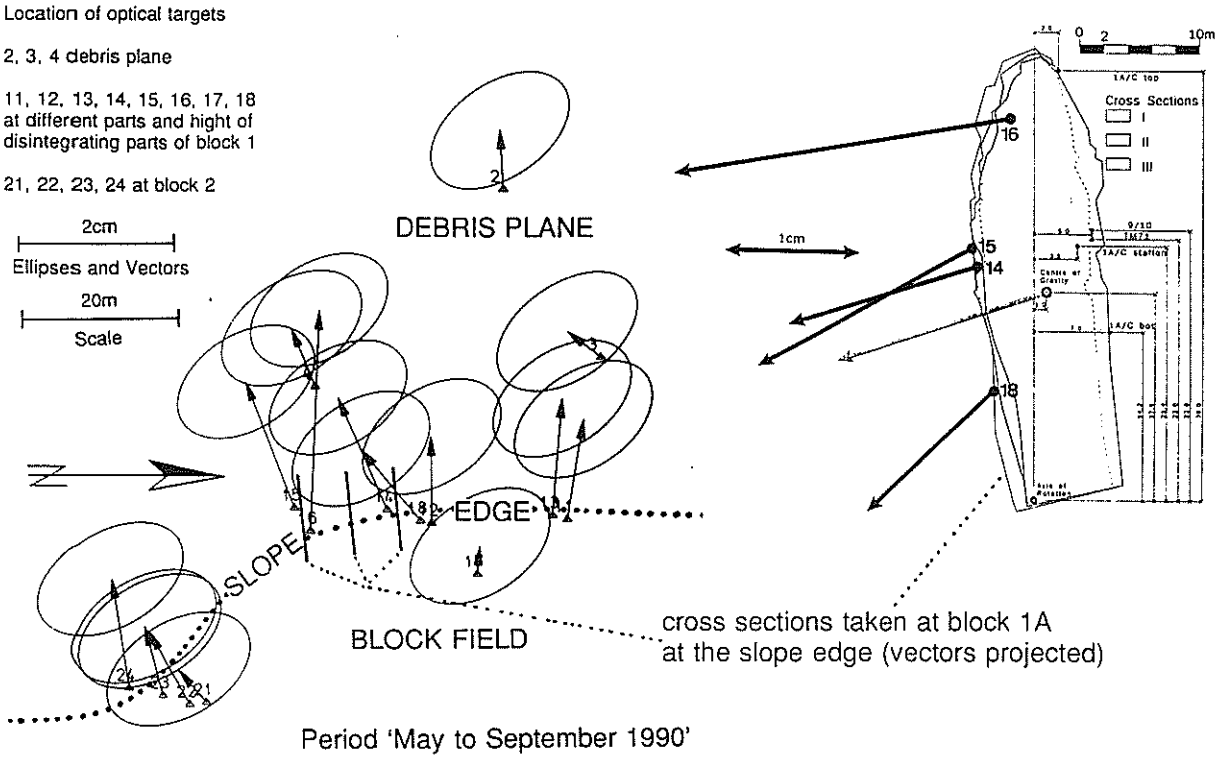

Fig. 5 Results of geodetic measurements in the area of the slope edge

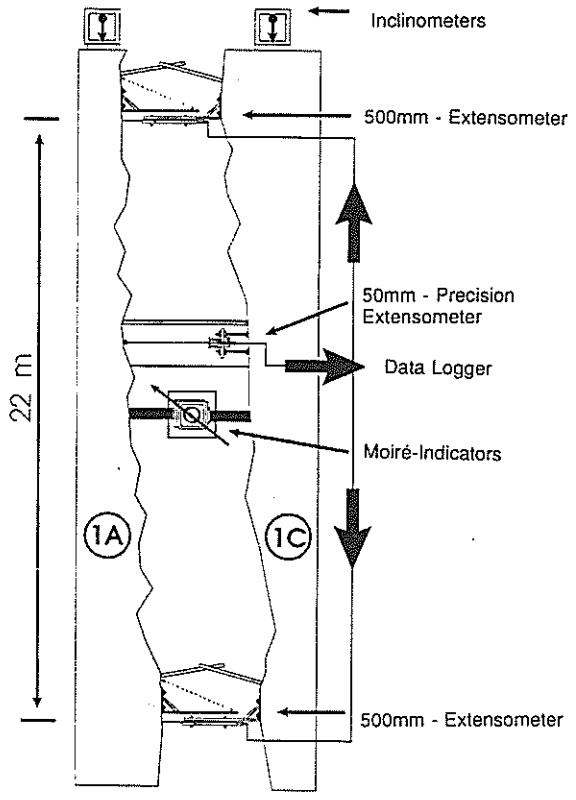

Fig. 6 Instrumentation complex used for continuous monitoring of the path of a block pivot

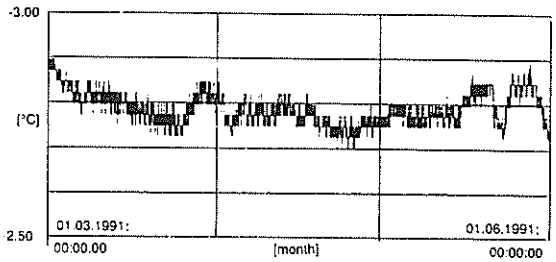

Fig. 7 Within-tension crack temperature measurements close to the upper scarp

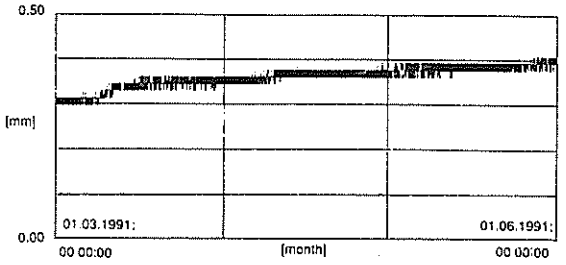

Fig. 8 Precision extensometer measurements in the tension crack close to the upper scarp (see Fig. 7)

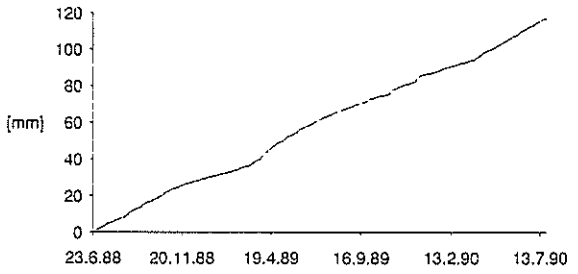

Fig. 9 Precision extensometer measurements in a tension crack close to the slope edge

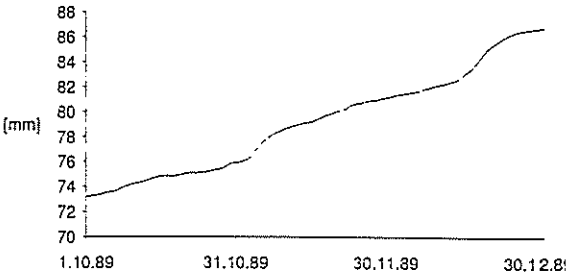

Fig. 10 Scaled-up portion of curve in Fig. 9

A crucial contribution to this interpretation was the use of tiltmeters, indicating the degree to which each block is rotating. This information is an essential pre-cursor to mechanism interpretation.

5. KINEMATIC AND MORPHOLOGICAL INSTABILITY ZONING

Utilizing this procedure for interpreting the displacements, we found that the movements could be conveniently characterized by the factors listed in the table in fig. 11. These can be classified as 'kinematic' characteristics and 'morphological' characteristics, as they apply to the various rock regions from the bed rock right through the completly disintegrated rock mass of the debris plane. We have also provided some guidance on the approximate block sizes in the centra column of the table.

This procedure was implemented to produce the instability zone plane shown in fig. 12. This is clearly leading to the possibility of a risk assessment map for the area. Of course, a total mechanical analysis is not possible because of the complexity of the circumstances: this is why the observational and interpretative approach was used. However, we can gain great advantage by modelling some basic mechanisms of individual parts of the slope, especially being able to take into account the relatively soft foundation layer beneath the blocks. Some of this research is presented in the next Section.

	KINEMATIC CHARACTERISTICS (results of monitoring)	CUBE OF BLOCKS	MORPHOLOGICAL CHARACTERISTICS
BED ROCK	No movement detectable	not defined	insignificant changes in slope angles at the top region; three joint sets and bedding planes; no open cracks or other instability criteria, Karst
BLOCK RIFTS	creep with low rate (<mm/a); toppling and external influences on the kinematics not detectable	< 150.000m^3	trench and ridge structures; lateral disintegration of block rifts (tension cracks), local depressions; opening of two joint sets
BLOCK FIELD	creep with significant rate (cm/a); toppling and seasonal external influences detectable	< 50.000m^3	isolated blocks and pinnacles, different amount of rotation indicated by dip of bedding planes, block shapes controlled by the two opened joint sets
SLOPE EDGE	creep with high rate (<dm/a); seasonal and transient external influence significant; sudden toppling failure; rock falls	< 25.000m^3	convex slope edge; opening of the third joint set; significant amount of rotation indicated by dip of bedding planes
DEBRIS PLANE	differing amounts of displacement (mm/a to cm/a), no seasonal or transient external influences detectable	< 100m^3	uniform dip of slope, individual boulders of intact rock

Fig. 11 Table of kinematic and morphological characteristics

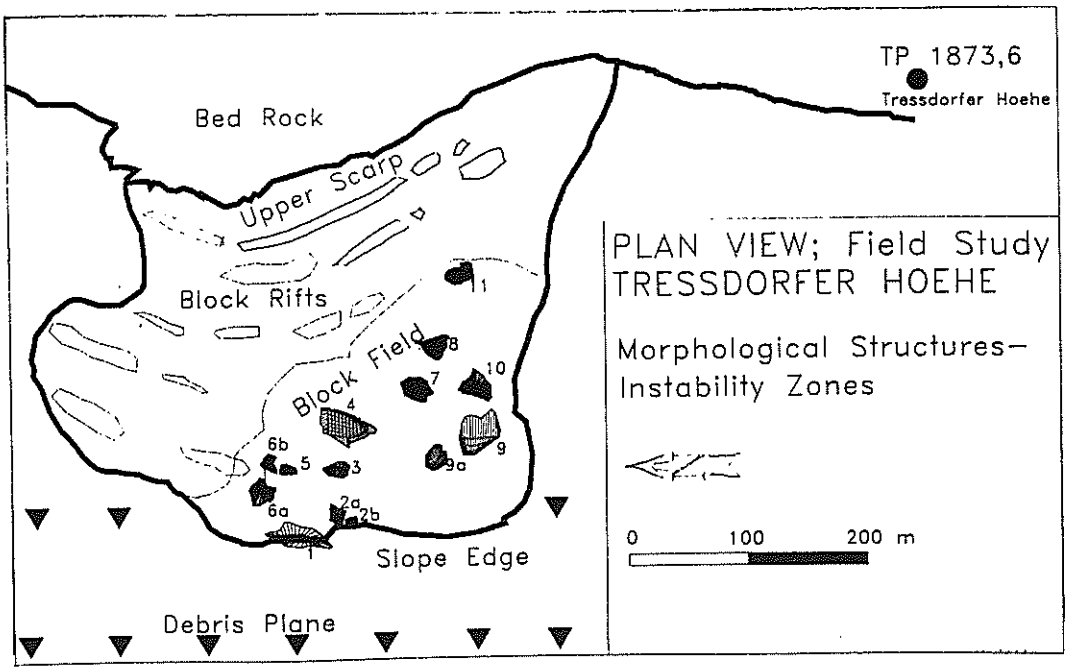

Fig. 12

6. RESULTING POTENTIAL FAILURE MECHANISMS

The field conditions for block 1A and for the presently developed upper scarp were idealized as shown in fig. 13, the dip of the overall slope being 12 degrees. The thickness of the weak strata and the stiff cap-rock are eight metres and fourty metres, respectively.

Results from the FE-analyses are shown in fig. 14: these include the horizontal stresses at the slab margin and the deformed mesh resulting from gravitational loading. It is realized that the rock disintegrated earlier while gravity was acting, but these results are useful to indicate the likely areas of high stress and displacement and hence failure mechanisms.

The failure criterion allowed for post-yield plasticity. The analysis indicated that increasing plasticity of the weak layer led to the development of a tensile zone within the lower parts of the cap-rock behind the free face, which possibly initiated the disintegration of the

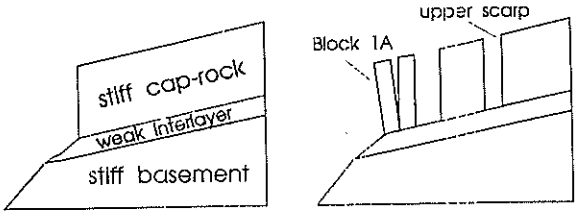

Fig. 13 Idealized field conditions for FE modelling

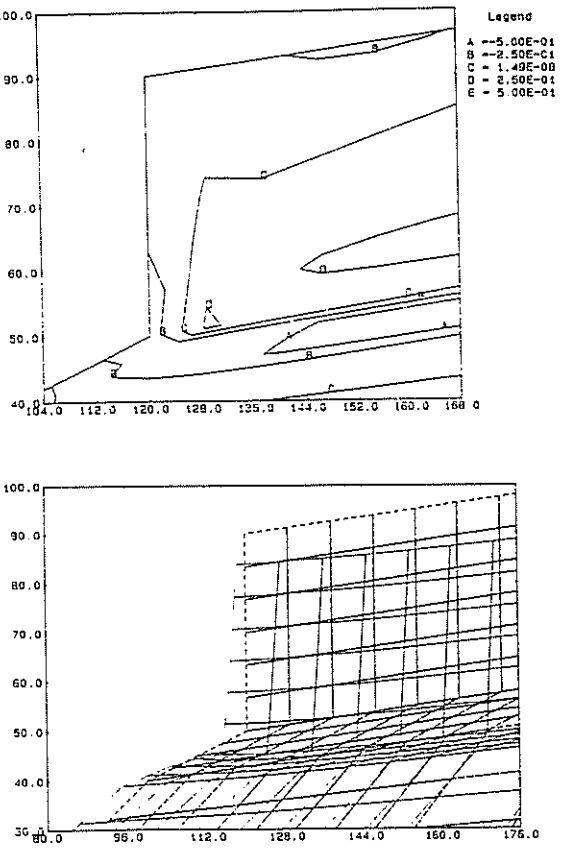

Fig. 14 Illustrative FE modelling results for stress and displacement

stiff slab into single blocks. This failure mechanism appears to exist at the present upper face.

These analyses also indicated, via the stress distribution of individual blocks, that 'shear outs' at the blocks are appear to be highly unlikely - because the deviatoric stresses do not exceed 2.0MPa. This is another indication of the value of such analyses in indicating likely and unlikely failure mechanisms - within the context of the types of instabilities being discussed here.

Because of the restriction on the length of this presentation, we cannot demonstrate all the analyses and results, but we hope that the limited presentation here will have highlighted our basic philosophy and methodology in approaching this very complex natural instability.

7. CRUCIAL GEOTECHNICAL PARAMETERS

As a result of the work described here, we have been able to identify the important geotechnical parameters and mechanisms associated with this specific problem. In this table we have included such factors as block geometry and the various types of displacement indicators. Thus, our interpretation of geotechnical parameters includes all those factors which are necessary to solve the geotechnical problem - whether these be mechanical, geometrical or geological.

In fig 15, we include a table of these parameters as they relate to the toppling mechanisms discussed earlier. These can be used directly as we have demonstrated in this paper to monitor potential instability. They could also be used in a tailored risk assessment methodology, via a semi-quantitative classification scheme, especially to indicate relative block instability risk priority.

8. CONCLUSIONS

In this paper, we have described the study of a particular natural instability. The techniques were specifically directed towards analyzing the potential risk of slope instability at the case study location "Tressdorfer Hoehe", and were tailored accordingly. However, we would like to emphasize that the methodology has a very general applicability in assessing geotechnical risk. In the complex circumstances encounted, simple models are inadequate and complex models are not viable because the input is insufficient. Thus, an intermediate approach has to be adopted, which integrates the observational techniques with trend interpretation and identification of the critical geotechnical parameters. As we have mentioned, a series of blocks such as those analyzed could be classified according to their relative risk - which is often what is required in remedial measures when constraints are imposed by limited financial resources.

	GEOTECHNICAL PARAMETERS AND INSTABILITY INDICATORS	CONSEQUENTIAL RISK	GEOTECHNICAL APPROACH
WEAK SEQUENCE	mechanical properties of rock mass and intact rock	bearing capacity failure, development of shear zone results in secondary block toppling	laboratory testing, continuous monitoring of pivot (tiltmeters, extensometers), geodetic monitoring
	geometry (dip, thickness)		
CAP-ROCK AND INDIVIDUAL BLOCKS	block (pinnacle) geometry	single block toppling	field study and monitoring of path (depth) of pivot
	strength of rock mass	disintegration of bed-rock, shear off at block toe, sudden failure	laboratory testing, FE- and DE-analyses
	discontinuity orientation, spacing and shear strength	secondary failure (plane, block) in toppling blocks, decrease of block toppling factor of safety	field study, monitoring of block tilting
	rate of tilting	indicator only	
	degree of external influences	sudden toppling failure induced by joint water pressure (for potential toppling blocks $F \sim 1/z_w^3$)	continuous, precise monitoring of external factors, block tilting and tension crack aperture

Fig. 15 Table of significant parameters for block instability zoning and block instability risk assessment

Seismic Stability of the Sulphur Point Wharf

D.N. JENNINGS
WORKS Consultancy Services, Hamilton
G.S. THOMPSON
Port of Tauranga Ltd, Mt Maunganui

ABSTRACT: The Sulphur Point Wharf development is a major expansion of the Port of Tauranga Ltd's port facilities in Tauranga Harbour involving an area of some 60 hectares. Initial development of the reclaimed site involves the construction of some 600 metres of wharf with a design dredge depth of 14.5 metres.

The Tauranga Harbour consists of deep deposits of predominantly sands interspersed with layers of silts and fine gravels. The wharf structure consists of a reinforced concrete deck supported on driven precast prestressed concrete piles. The sands at the site which form the marginal slope under the open piled wharf structure are protected with rock buttressing.

This paper describes the seismic design philosophy developed for the wharf structures and the design criteria adopted. "Operating" and "contingency" design earthquakes are defined together with performance expectations relative to the design life of the facility. The features and considerations associated with the assessment of seismic stability in the geotechnical engineering design process are presented.

Initial investigations at Sulphur Point indicated that the recent sands did have a liquefaction potential. Site investigations and the evaluation of soil properties with respect to seismic shaking is described. Extensive piezo cone penetrometer testing together with static and dynamic triaxial testing of undisturbed piston samples has enabled the behaviour of the soils to be assessed. Insitu geophysical testing including shearwave velocity measurement is described.

The wharf structure/soil interaction associated with the marginal slope and soil behaviour have been addressed in the design process. Wharf stability and estimated deformation behaviour under the operating and contingency design earthquakes is presented.

1. INTRODUCTION

The Port of Tauranga is a major port facility located in the Bay of Plenty area of the North Island of New Zealand (Figure 1). Wharf construction has concentrated on the Mount Maunganui side of the harbour since development of the port commenced in 1950. Presently there is some 2000m of concrete wharf at Mount Maunganui providing a nominal 11 berths.

To enable further expansion of the Port of Tauranga the development of facilities at Sulphur Point on the Tauranga side of the harbour has been initiated. The construction of 600m of wharf and associated land facilities involving an area of some 60 hectares is now well advanced.

Works Consultancy Services Ltd has assisted the Port of Tauranga Ltd with the development of the wharf design philosophy, site investigations and the geotechnical evaluation of the site. Assistance and advice has been provided by Works Consultancy Services Ltd on geotechnical design aspects.

Sulphur Point has been developed with extensive reclamation utilising sands dredged from the harbour. The extensive deposits of recent sediments in the Tauranga Harbour at Sulphur Point present a significant challenge for the development of the site. This paper describes the seismic design consideration for the development of Sulphur Point. Stability of the wharf structures is discussed.

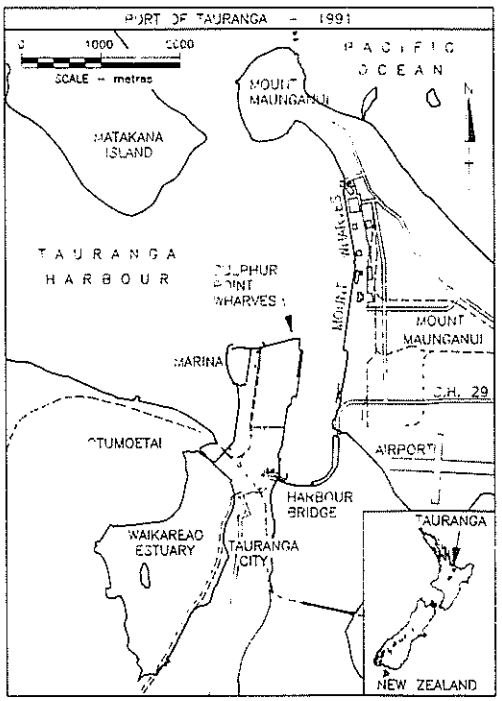

Figure 1 : Location Plan

2. SEISMIC DESIGN CRITERIA

A design philosophy for the Sulphur Point development was adopted which reflected the operational requirements of the Port of Tauranga Ltd. Aspects considered included:

- seismic hazard
- seismic design philosophy
- geotechnical aspects
- structural aspects
- performance requirements
- design life

For the Sulphur Point facilities two levels of earthquake design loading were adopted. The two levels have been described as the operating level earthquake and the contingency level earthquake.

Operating Level Earthquake: This loading was assessed to have a probability of exceedence of 50% during the 50 year design life of the facility. As a result of this event it is expected that minor repairable damage would be experienced and the facility would remain operational.

Contingency Level Earthquake: This more severe loading was assessed to have a probability of exceedence of 10% during the 50 year design life. In the case of this event extensive damage would be expected but the facility would be resistant to collapse.

Seismic design parameters adopted for the design [based on Matuschka *et al* (1985)]are summarised in Table 1.

3. GEOLOGY

The Port of Tauranga is located in the Tauranga Harbour, a drowned Pleistocene river basin. The basement to the basin consists of a number of volcanic rock units formed principally in the time interval 1 to 6 million years before present day (Houghton and Hegan, 1980). Soft, weakly consolidated fluvatile and estuarine sediments (the Tauranga Formation) consisting of deep deposits of predominantly sands (often pumiceous) interspersed with shells, layers of silts and occasional layers of fine gravels.

Investigations have shown this description to be typical of the Sulphur Point site where borehole K1 encountered these materials to a depth of 49.5m. The soils have been broadly grouped:

Upper materials	Recent beach sands
Lower materials	Older alluvial silts, sands and gravels

The interface between the soil groups typically varied between RL -12m and RL -18m.

4. SOIL PROPERTIES

A variety of investigations were carried out for the wharf development including:

- boreholes (both washdrilled and cored)
- standard penetration tests (SPT)
- piezo cone penetration tests (uCPT)
- geophysical profiles
- seismic shear wave velocities
- laboratory tests (grading, classification, static and dynamic triaxial tests)

Samples for triaxial testing were recovered by thin walled piston sampler. Excellent samples were recovered and sampling from the HQ3 triple barrel coring was also remarkably effective.

The location of tests along the wharf structure are indicated on Figure 2.

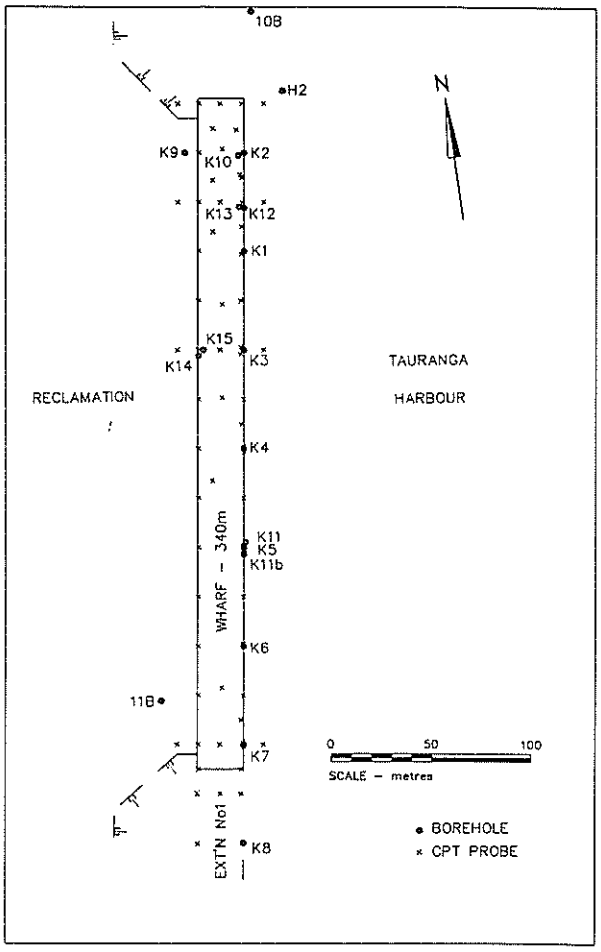

Figure 2 : Location of Tests

Event	Probability of Exceedence during design life	Return Period (t_r)	Peak Spectral Acceleration	Design Peak Ground Acceleration	Magnitude M
Operating Level	0.50	70 years	0.5g	0.20g	6.5
Contingency Level	0.10	450 years	0.9g	0.36g	7.5

Table 1 : Seismic Design Parameters

Typical soil data at location K3 are presented in Figure 3.

A feature of the sands identified at Sulphur Point was their relatively sharp grain profiles. This was particularly noticeable where the sands contained significant volcanic glass.

5. LIQUEFACTION POTENTIAL

Liquefaction is a situation where cohesionless soils lose their shear strength through the generation of pore water pressures when subjected to (earthquake) shaking. There are a number of techniques for evaluating the liquefaction potential for cohesional soils. Based on the site investigation data available these techniques were applied to the Sulphur Point soils.

5.1 Grading Criteria

The data, plotted in Figure 4, indicates that the upper SANDS (ie down to RL -12m to RL -18m) consistently satisfy the grading criteria for easily liquefiable sands (Iwasaki, 1986). The fines content increases in the lower soils and this will provide a higher resistance to liquefaction.

5.2 CPT Evaluation

An evaluation of the level ground liquefaction potential of the soils at the site based on CPT cone resistance, q_c, data has been made using the approach presented by Franklin (1986) based on an evaluation of q_{c1} (where q_{c1} is the limiting cone resistance at 100 kPa overburden stress). Liquefaction potential has been assessed for the case behind the wharf, ie formation level RL +4.5m and the limiting CPT values are shown on Figure 3.

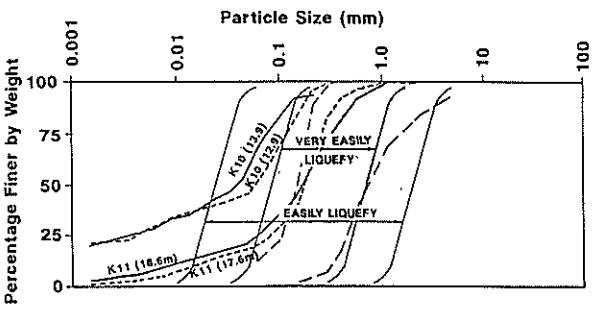

Figure 4 : Soil Particle Size

From this appraisal it is apparent that:

i) For the operating earthquake there are layers which are weak and will experience liquefaction to a depth of RL -15m (cf K7).

ii) For the contingency earthquake the CPT evaluation indicates that liquefaction will be extensive and extends to a depth in excess of RL -25m.

5.3 SPT Evaluation

The SPT results indicate similar liquefaction potential to that derived from the CPT data. However there is large scatter in the SPT results and this complicates the interpretation and raises concerns over the reliability of the data and the method of interpretation (Martin, 1991).

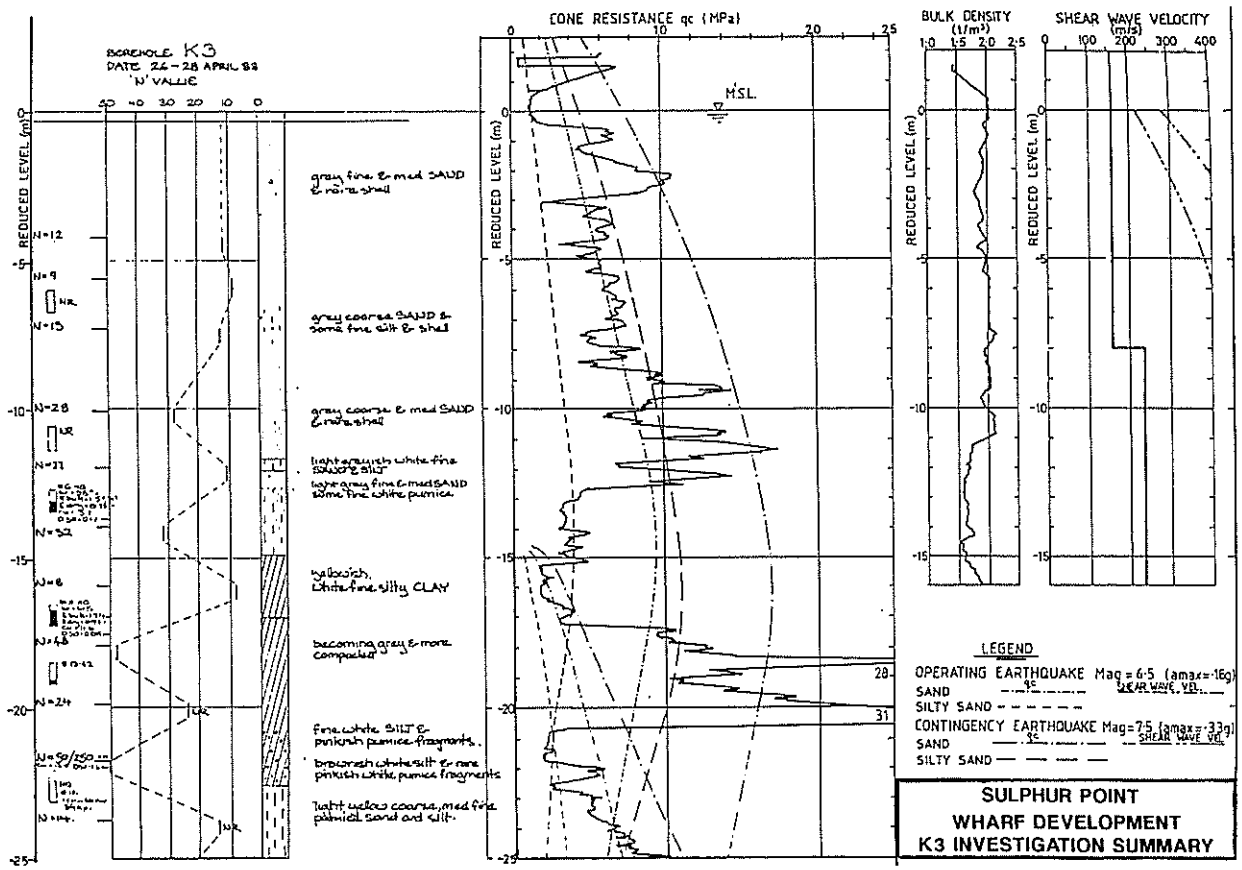

Figure 3 : Typical Soil Data

5.4 Shear Wave Data

Typical shear wave velocity for sands ranges are presented in Table 2. The data from Sulphur Point was consistent with this and typical results are shown on Figure 3.

Material Type and Age	Shear Wave Velocity, Vs
Very recent non-compacted sands	90-200 m/s
Other Holocene sands (<10,000 yrs)	150-300 m/s
Pleistocene sands (>10,000 yrs)	180-450 m/s

Table 2 : Typical Ranges of Vs in Standard Sands (after NRC, 1985)

From laboratory testing it has been found that there is a threshold shear strain, γc, of 0.01% below which there is no excess pore water pressure generated (Dobry, 1985 and NRC, 1985). Using this approach shear wave velocities have been calculated for a threshold strain of 0.01% for the operating and contingency earthquakes as illustrated in Figure 4.

From an assessment of the shear wave velocity data in Figure 3 it is observed that there is an extensive pore pressure generating potential at various levels under both the operating earthquake and the contingency earthquake.

5.5 Dynamic Triaxial Data

Dynamic triaxial isotropically consolidated tests were undertaken on a range of soil types obtained by piston sampling. The pore pressure response is summarised on Figure 5.

The pore pressure response is consistent with that expected from the literature. The recent beach sands are more susceptible to liquefaction than the recent silty sands.

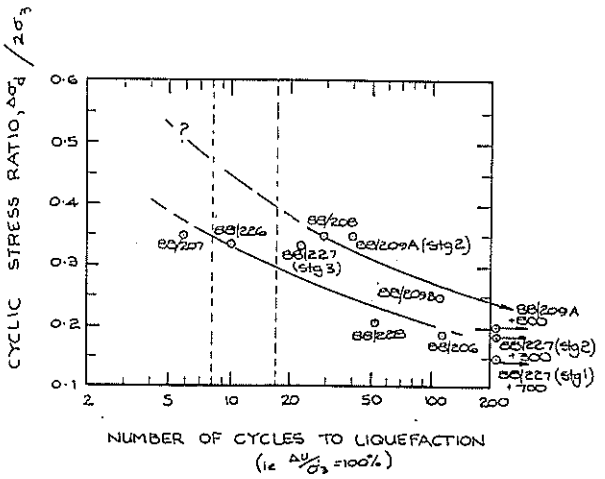

Figure 5 : Dynamic Triaxial Data

From the dynamic triaxial pore pressure response data presented on Figure 5 factors of safety against liquefaction have been calculated:

a) Operating earthquake:

$$FS = \frac{\text{Test strength at 8 cycles}}{\text{Design shear stress}}$$

$$= \frac{0.35}{0.33} = 1.06$$

b) Contingency earthquake:

$$FS = \frac{\text{Test strength at 15 cycles}}{\text{Design shear stress}}$$

$$= \frac{0.28}{0.60} = 0.47 < 1.0$$

The dynamic triaxial data is consistent with the other observations. It indicates that performance under the operating design earthquake will be marginal and significant liquefaction will occur for the contingency design earthquake.

5.6 Discussion

From the evaluation of the investigations data presented in the previous sections it is observed that the soils at Sulphur Point do have a level ground liquefaction potential.

Under the operating earthquake it is observed (CPT data) that some layers of material behind the wharf have a liquefaction potential whereas under the contingency earthquake liquefaction potential is extensive.

6. WHARF STRUCTURE FORM

A variety of wharf structures were considered for the Sulphur Point site., The traditional suspended concrete deck supported by concrete piles, with raked piles providing lateral load resistance, was discarded in favour of the preferred ductile structure (Figure 6).

Vertical prestressed concrete piles are detailed for ductility and during earthquake loading the wharf is restrained in position by the sloping marginal embankment. The marginal embankment is excavated and then lined with rock fill for protection and reinforcement. The displacement performance of the wharf is dependent on the behaviour of the slope.

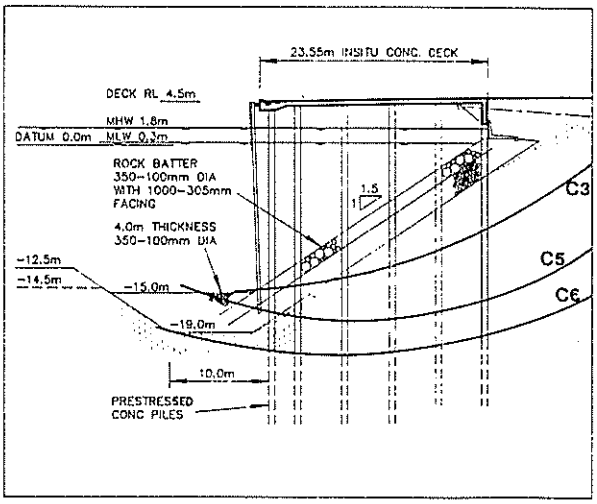

Figure 6 : Wharf Structure

Tie backs have been used to increase the lateral stiffness of the wharf against service loads arising from shipping.

A tied back sheet pile wharf option was appraised in detail. However there were technical and cost problems coping with the liquefied soil pressures during earthquake loading both in terms of sheet pile strength and deadman design for walls with dredged depths of 14.5m alongside.

7. WHARF STRUCTURE STABILITY

The stability of the rock buttressed slope and its associated stability under seismic loading was assessed. The stability of the rock slope was considered for two situations:

i) Stability under seismic loading without increased pore pressure.
ii) Post seismic stability with increased pore pressures.

The stability of the slope is complicated by the presence of the piles which will provide dowel action and some strengthening. For the purposes of the preliminary appraisal the piles were ignored.

The stability analysis indicated:

i) The critical acceleration for the rock slope assuming a $\phi = 36°$ for the sands is approximately 0.07g (ie the horizontal acceleration to reduce the stability to Factor of Safety = 1.0).

With this critical acceleration slope displacements have been estimated [Bracegirdle (1980)] as follows:

- operating earthquake-displacement $\approx$ 0.05m
- contingency earthquake-displacement $\approx$ 0.2m (assuming no increase in pore pressures)

ii) A pore pressure rise of approximately 50% in the slope materials reduces the stability to a factor of safety of less than 1. In this situation load is transferred to the piles and full dowel action would be developed. The need for a more detailed study to address this was identified.

8. COLLAPSE STABILITY

8.1 Procedure

While it is accepted that, provided the dynamic loading is severe enough, all sands can experience a 100% pore pressure ratio only "loose" sands will suffer large displacements. This large displacement behaviour associated with very low undrained (residual) shear strength is the catastrophic failure (flow slides) usually associated with liquefaction (Casagrande, 1975). Moderately dense to dense sands exhibit "cyclic mobility", ie only very small strains develop before shearing and dilatancy cause a reduction in the pore water pressure which represents a recovery of the effective stress.

It is difficult to quantify the actual soil behaviour and whether or not collapse behaviour will develop. Poulos *et al* (1985) presents a procedure for evaluating the stability of a soil mass subject to shear stress, such as a slope or embankments. This procedure provides a rational basis for determining the post liquefaction stability of the wharf structure based on the soil characteristics.

Poulos *et al* (1985) describes the calculation of a factor of safety against liquefaction, F_L, (ie factor of safety against catastrophic instability) as:

$$F_L = \frac{\text{Undrained steady-state shear strength}}{\text{Shear stress required to maintain static equilibrium}}$$

$$= \frac{Su}{\tau_d}$$

Using limit equilibrium stability analyses the driving shear stress, τ_d, can be easily computed. Values in the range $\tau_d = 19$ to 31 kPa have been calculated for the Sulphur Point Wharf.

The undrained steady state shear strength (Su) is considered to be a function of void ratio only (Poulos *et al*, 1985). (This reflects the observation that under severe loading and displacement all soil structure is destroyed and the void ratio is the fundamental property.) The critical step in the procedure for liquefaction evaluation is the determination of the insitu void ratio and the correction of laboratory-measured undrained steady state strengths to take into account changes in void ratio of the soil during sampling and testing. In the case of Sulphur Point a wide range of insitu void ratios exist and no definitive measurements of insitu void ratio have been made. It is considered that sample disturbance associated with the thin walled piston samples was minimal and the samples are representative of the insitu void ratios.

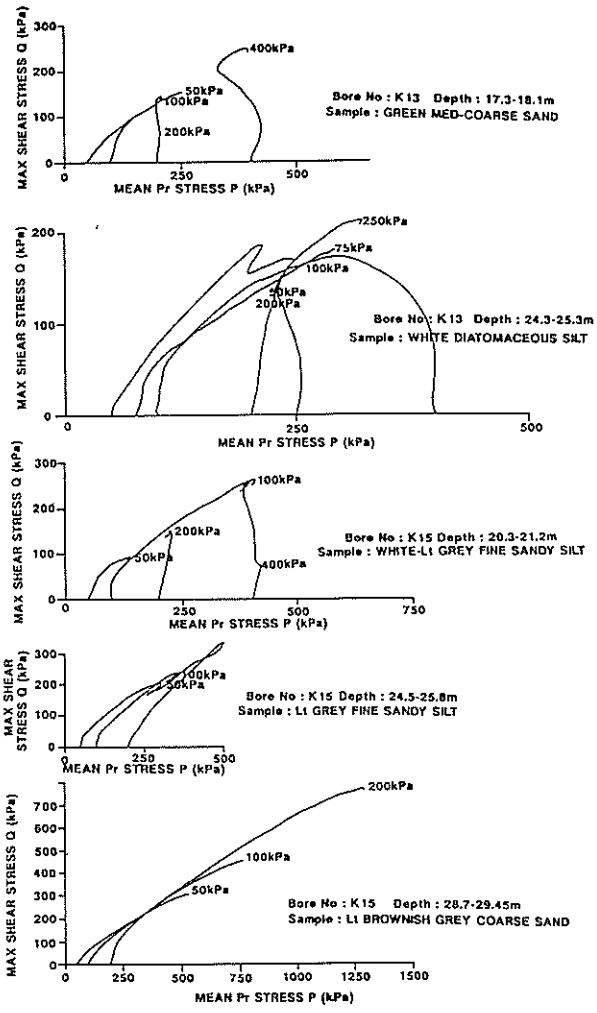

Figure 7 : Triaxial Strength Data

Bore No.	RL (m)	Depth (m)	Description	Void Ratio e	Undrained Strength Su
K13	-14.8 to -15.6	17.3-18.1	Grey green med-course pumiceous sand	1.25 to 1.99	>100 kPa
K13	-22.4 to -22.8	24.9-25.3	White diatomaceous silt	1.95 to 3.89	>100 kPa
K15	-18.3 to -18.2	20.3-21.2	White-light grey fine sandy silt	1.23 to 1.40	≈100 kPa
K15	-21.5 to -22.8	24.5-25.8	Light grey fine sandy silt	1.38 to 1.42	≈150 kPa
K15	-25.7 to -26.45	28.7-29.45	Light brownish grey coarse sand, some gravel	0.55 to 0.67	>300 kPa

Table 3 : Triaxial Undrained Strength

The sample of silt (K12, depth approximately 25m) which was tested by dynamic triaxial testing was also subjected to static undrained triaxial loading with the 42% residual dynamic pore pressure. This sample indicated an undrained strength of some 80 kPa.

8.2 "Undrained Strength" of the Sulphur Point Soils

From conventional consolidated undrained triaxial tests the steady state "undrained" strength can be determined (Poulos *et al*, 1985). An examination of the triaxial results for Sulphur Point indicate a significant range of "undrained strengths" determined from an examination of the stress paths (Figure 7). Undrained strengths have been evaluated as summarised above in Table 3.

These results indicate a characteristic undrained strength of 80 kPa would be appropriate (conservative) in the consideration of post seismic stability.

It is interesting to compare the strength of these Sulphur Point soils with the tentative relationship proposed by Seed (1987) which is presented as Figure 8. Sulphur Point SPT "N" values are typically in the range 16-20 (although higher and lower values are recorded) which indicates residual strengths (Figure 8) in the range 36 to +54 kPa. Based on this, it was considered prudent to check stability for a lower strength of 36 kPa.

8.3 Factor of Safety Against Collapse

Poulos *et al* (1985) consider that F_L = 1.1 is acceptable where the insitu void ratios and steady state conditions are well defined and appropriate corrections have been made. Noting that the steady state strength is sensitive to void ratio (ie small changes in void ratio can result in large changes in undrained strength) and that no corrections to the undrained strength have been made it was considered that F_L > 2.0 should be achieved for the Sulphur Point stability.

Based on the measured undrained strength values and the calculated mobilised shear stress values (surfaces shown on Figure 6) the following factors of safety are calculated:

Circle C3 $F_L = \frac{80}{23} = 3.5$ ($F_L = \frac{36}{23} = 1.50$)

Circle C5 $F_L = \frac{80}{19} = 4.1$ ($F_L = \frac{36}{19} = 1.9$)

Circle C6 $F_L = \frac{80}{31} = 2.6$ ($F_L = \frac{36}{31} = 1.2$)

This analysis indicates that the Sulphur Point Wharf has an acceptable factor of safety against collapse failure (without considering the strength contribution provided by the piles). It is noted that the stability results in parenthesis based on Figure 8 (Seed, 1987) indicate marginal stability (ie, it is less than F_L > 2.0).

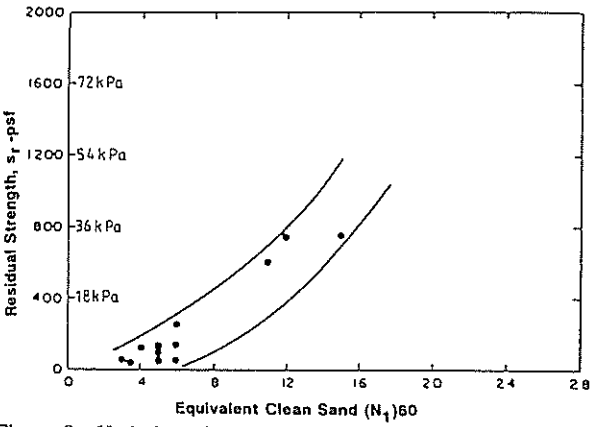

Figure 8 : Undrained Strength Data (after Seed)

9. STRUCTURE DISPLACEMENT

Structure horizontal displacement has been assessed on the basis of the measured soil properties and published data. Displacement estimate are summarised in Table 4.

Event	Axial Strain (Dynamic Triaxial)	Estimated Shear Strain	Displacement
Operating Earthquake	2%	1 - 3%	0.2 - 0.4m
Contingency Earthquake	20%	3 - 20%	2 - 4m

Table 4 : Summary of Wharf Displacement

A structural assessment based on these displacements indicates that the wharf structure will not collapse.

10. CONCLUSIONS

The assessment of seismic stability of structures constructed over recent sediments is complex. While engineering criteria exist for the assessment of liquefaction and the stability of structures on level ground there is less information regarding the determination of the stability of sloping sites.

Based on level ground methodology it is observed that the Sulphur Point site does have a significant liquefaction potential without any closer consideration of the soil properties. This suggests that the wharf will experience collapse.

The procedure developed by Poulos *et al* (1985) provides a rational basis for the assessment of seismic stability based on the consideration of the undrained strength of the soil. Using this procedure it is demonstrated that the Sulphur Point Wharf will remain stable against collapse even under the contingency earthquake.

Displacement behaviour of structures under seismic loading is difficult to assess. Estimates of displacement have been made based on measured and published data.

By consideration of the actual properties of the soils at Sulphur Point it has been possible to demonstrate that the wharf structure adopted for the development will satisfy the seismic design philosophy and criteria adopted.

11. ACKNOWLEDGEMENTS

The permission of the Chief Executive Officer of the Port of Tauranga Ltd and the General Manager of Works Consultancy Services Ltd to publish this paper is acknowledged. The many constructive discussions with colleagues during the course of this project are appreciated by the authors.

12. REFERENCES

Bracegirdle A (1980): "Seismic stability of reinforced earth retaining walls", Bulletin NZNSEE Vol 13, No.4, December 1980.

Casagrande A (1975): "Liquefaction and Cyclic Deformation of Sands - A Critical Review", Harvard Soil Mechanics Series No. 88, Harvard University, 1975 (Also Proc 5th Pan Am Conference on SM & FE, Buenos Aires, 1975).

Dobry R (1985) unpublished data - see NRC (1985).

Franklin A G (1986) : "Use of the piezocone for evaluating soil liquefaction potential", Proc 8th European Conference on Earthquake Engineering, Lisbon, 1986.

Houghton B F and Hegan B D (1980): "A preliminary assessment of geological factors influencing slope stability and land slipping in and around Tauranga City", DSIR NZ Geological Survey Engineering Geology Report No.EG348, October 1980.

Iwasaki T (1986): "Soil Liquefaction Studies in Japan: State-of -the-Art" Soil Dynamics and Earthquake Engineering, Volume 5, No.1, January 1986.

Martin G R (1991): "A practical assessment of site liquefaction effects and remedial measures", Proc 2nd Int Conf on Recent Advances in Geotechnical Earthquake Engineering and Soil Dynamics, St Louis, March 1991 (also NZ Geomechanics News No.42, July 1991.)

Matuschka *et al* (1985) : "New Zealand seismic hazard analysis", Bulletin of NZNSEE, Vol 18, No.4, December 1985.

NRC (1985): "Liquefaction of Soils During Earthquakes", Committee of Earthquake Engineering, National Research Council, Washington, 1985.

Poulos S J, Castro G, and France J W (1985): "Liquefaction Evaluation Procedure", Proc ASCE Journal Geot Eng Vol III, No.6, June 1985.

Seed H B (1987): "Design Problems in Soil Liquefaction", Proc ASCE Journal of Geot Eng, Vol 1B, No.GT8, August 1987.

The Liquefaction Potential in Christchurch

I.F. McCAHON
B.E.(Hons), M.I.P.E.N.Z.
Senior Engineer, Soils & Foundations Ltd, Christchurch
D.McG. ELDER
B.E.(Hons.), Ph.D., M.I.P.E.N.Z.
Soils & Foundations Ltd, seconded to Jacques Whitford Ltd, Halifax, Canada
M.D. YETTON
B.Sc., M.Sc.(Hons.) (Engineering Geology)
Manager, Soils & Foundations Ltd, Christchurch

SUMMARY As part of a recent study, information pertaining to the liquefaction hazard in Christchurch has been reviewed. At least one third of the Christchurch urban area is sited on a general soil profile dominated by sand with a high water table, which would be susceptible to liquefaction if the grading is uniform and the soil sufficiently loose. For a number of sites that have adequate test data, analysis shows that liquefaction is likely to occur during earthquake shaking with an average return period suggested by regional seismicity levels of about 30 years. Liquefaction has not been reported in Christchurch historically, but it appears that the city has not experienced earthquake shaking severe enough to cause liquefaction since European settlement. It is concluded that the liquefaction hazard in Christchurch is significant, but the scarcity of available data on in situ densities and soil gradings does not yet allow delineation of liquefiable zones.

1. INTRODUCTION

Liquefaction is a common consequence of moderate to large earthquakes. It can be defined as "*the transformation of a granular material from a solid state into a liquefied state as a consequence of increased pore pressures*" (Youd, 1973). If the liquefaction in any event is sufficiently severe and extensive, loss in ground strength may result in damage to any proximate structures. Bearing capacity failure will cause buildings or superficial structures to settle and tilt, and buoyant, buried structures may float upwards. Liquefaction of a confined, subsurface stratum can cause both vertical and lateral displacement of surficial blocks of soil, and if the area is on a gentle slope, or close to a free face such as an incised river channel or open drain, then lateral spread can occur.

Generally, the assessment of liquefaction potential involves two steps:

(a) Evaluation of liquefaction susceptibility: Identifying those areas or layers which have the characteristics of a liquefiable soil.

Liquefaction hazard is site dependent; certain soil profiles are more liquefiable than others. Liquefaction is most likely to occur in saturated, relatively uniform fine sands or coarse silts in a loose state, at depths less than 10 to 15 m below ground level, where the groundwater level is within about 5 m of the ground surface.

(b) Evaluation of liquefaction opportunity: Identifying the relative probability for earthquake shaking strong enough to generate liquefaction in susceptible materials, based on an appraisal of the regional earthquake potential.

The liquefaction susceptibility and opportunity are considered together to determine the liquefaction potential or the relative likelihood that liquefaction will occur.

A recent study (Elder et al, 1991) has reviewed the probabilities for earthquake shaking in Christchurch, and the liquefaction opportunity is derived directly from this work. The study also assembled the majority of site investigation data available for Christchurch which has been used to assess the liquefaction susceptibility of the city area.

2. LIQUEFACTION SUSCEPTIBILITY

The Christchurch soil profiles have been mapped by compiling all the available ground information records for the city, comprising some 20,000 soil records for about 15,000 sites. Most of these records are for shallow depths, and there are few records that contain any information other than soil description outside the central city area. The soil profile was mapped as representative soil types for five layers within the upper 30 m of soil.

Liquefaction occurs in relatively uniform cohesionless fine sands to silty sands, where the permeability is relatively low and drainage slow, and it is areas of these soil types that are of interest with respect to liquefaction potential. Much of the Christchurch area is underlain with sand and fine grained material, as shown on Figure 1. The map delineates soils in four categories:

(a) Predominantly sand (silty sand to sand), depth 2-10 m.
(b) Predominantly fine grained - clayey silts to sandy silts, depth 2-10 m.
(c) Predominantly sand - silty sand to sand, depth 2-5 m.
(d) Predominantly fine grained - clayey silts to sandy silts, depth 2-5 m.

Not all of the soils within these representative types will have particle size gradings that are susceptible to liquefaction, and there is only limited information available on soil gradings. The majority of samples tested for particle size distribution curves from Christchurch sites lie within the envelope for liquefiable soils. At this stage, there is no reason to believe that these gradings are not representative of the sand dominated soils in Christchurch, and therefore it is concluded at this stage that most of the area shown in Figure 1 has underlying soils that are susceptible to liquefaction if sufficiently loose.

To be susceptible the soil must also be below the groundwater level, and generally the groundwater level must be within a few metres of the ground surface. Christchurch has a high groundwater level, and virtually the whole city east of a line from Halswell - Ilam - Bishopdale has water table within 2 m of the ground level.

Liquefaction is observed only in relatively loose soils. While dense sands and silts may show initial liquefaction, this is rapidly inhibited due to the dilatancy characteristics of such

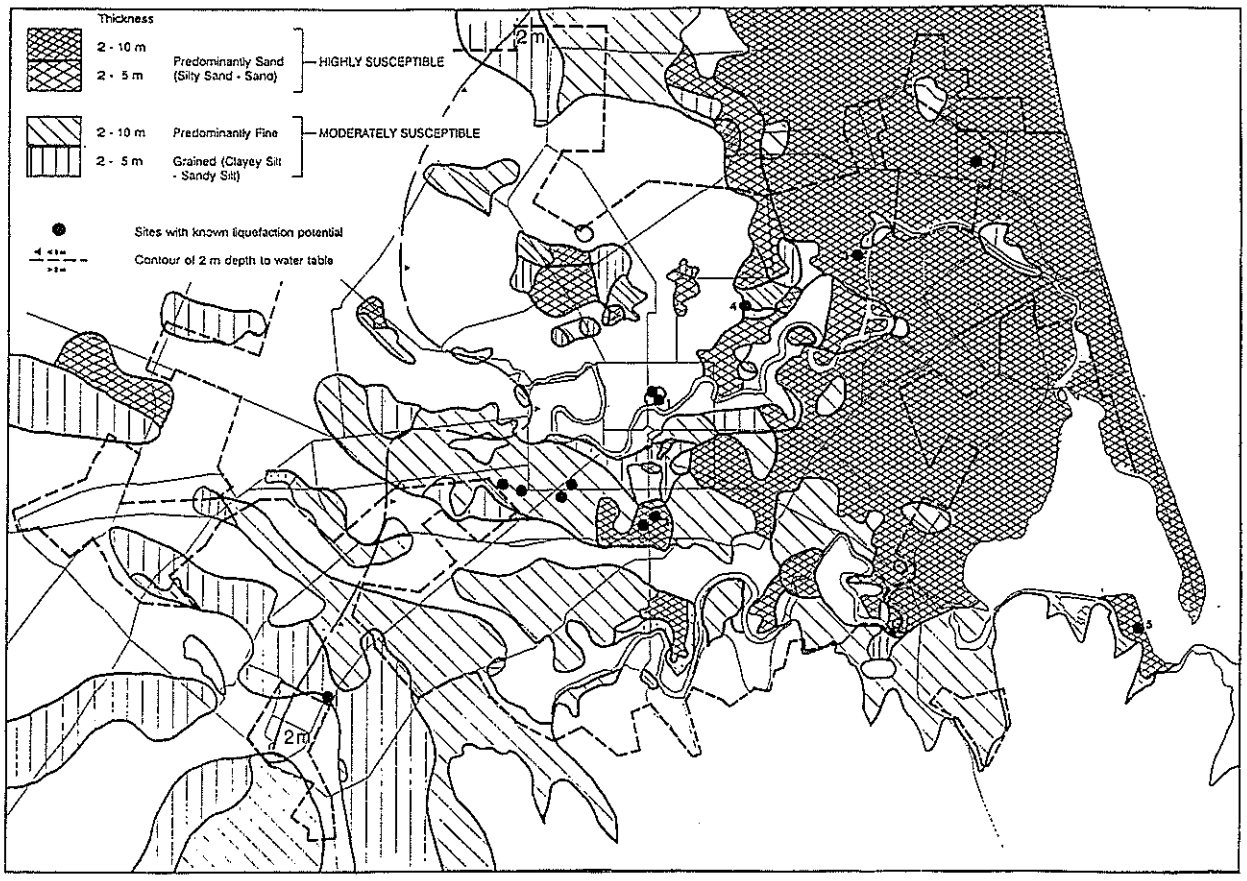

Figure 1 **Map of Soil Types susecptible to Liquefaction in Christchurch.**

materials.

The relative density of the soils will depend on the manner of deposition, and not all the area shown as complying with the general grain size requirement in Figure 1 will be liquefiable. Much of the Brighton area soil was probably deposited in a high wave energy beach environment, and former beach deposits of a similar nature now distant from the coast are unlikely to be liquefiable.

There is very limited information on relative densities of soils in Christchurch below the water table except in the central city area. It is therefore not possible to delineate areas of looser soils across the city. A number of sites where test information is available and liquefaction hazard has been identified are shown on Figure 1.

At this stage it is possible to draw only tentative conclusions on the liquefaction susceptibility of Christchurch soils: at least one-third of the urban area overlies a general soil profile dominated by saturated sand. The limited data on uniformity characteristics of the sands and in situ densities suggest that a significant proportion of this area is likely to be susceptible to liquefaction.

3. LIQUEFACTION ANALYSIS

There are four general methodologies for liquefaction prediction

- Case history methods, where earthquake magnitude required to produce liquefaction is related to distance from the epicentre.
- In situ soil data methods, using empirical relationships between test data (usually SPT 'N' values) and depth, for given degrees of shaking.
- Methods involving comparison between dynamic shear strength and earthquake induced stress, modified for earthquake magnitude, soil size grading and the thickness of surface confinement, and using ground accelerations.
- Methods using theories of excess pore water pressure generation, relating pore water pressure to dissipated energy, and hence earthquake magnitude and distance.

The first approach is typified by the method proposed by Kuribayashi & Toitsuoka (1975) where Japanese liquefaction observations are included on a plot of earthquake magnitude vs epicentral distance. The line defining the distance from the epicentre to the farthest site of liquefaction is given by

$$\log_{10} R_{max} = 0.77M - 3.6 \qquad (R_{max} \text{ in km}) \qquad (1)$$

New Zealand data has also been plotted (Fairless & Berrill, 1984) and found to approximate this relationship. This gives some confidence in applying this relationship to New Zealand, and the line defining maximum distance for liquefaction is shown in Figure 2, showing probable earthquake magnitudes for the seismic zones in the Christchurch region. This plot clearly indicates that maximum magnitude earthquakes in the Pegasus, Banks Peninsula, and Canterbury Plains Seismicity Zones, or the Porters Pass Tectonic Zone, and the central section of the Alpine Fault are all capable of inducing liquefaction in susceptible soils within Christchurch. A map defining these zones is shown in Figure 3.

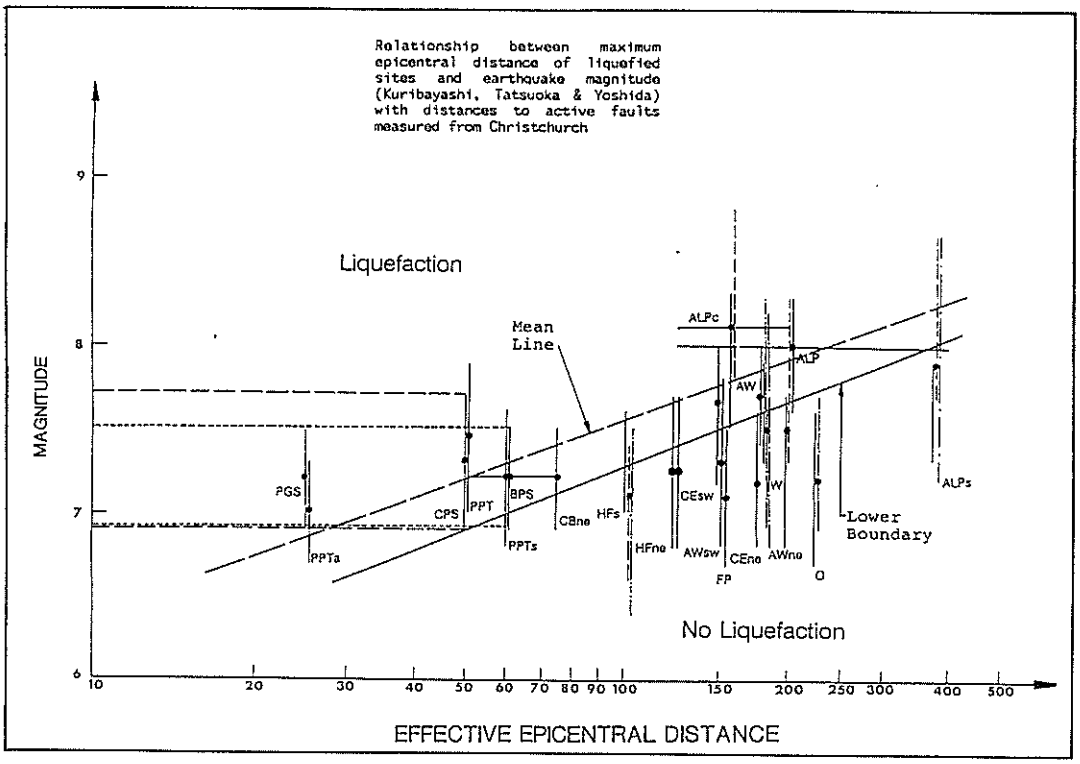

Figure 2 **Relationship between Maximum Epicentral distance of Liquefied sites and Earthquake Magnitude (after Kurilsayashi et al 1975)**

Key	
CPS	Cant. Plains Seismic
BPS	Banks Pen. Seismic
PGS	Pegasus Seismic
PPT	Porters Pass TZ
PPTa	- Ashley section
PPTs	- Southern section
CBne	Kaiwara
HF	Hope
HFs	- SW section
HFne	- NE section
CE	Clarence/Eliot
CEsw	- SW section
CEne	- NE section
AW	Awatere
AWsw	- SW section
AWne	- NE section
W	Wairau
FP	Fox's Peak
O	Ostler
ALP	Alpine Fault
ALPc	- Central section
ALPs	- South section

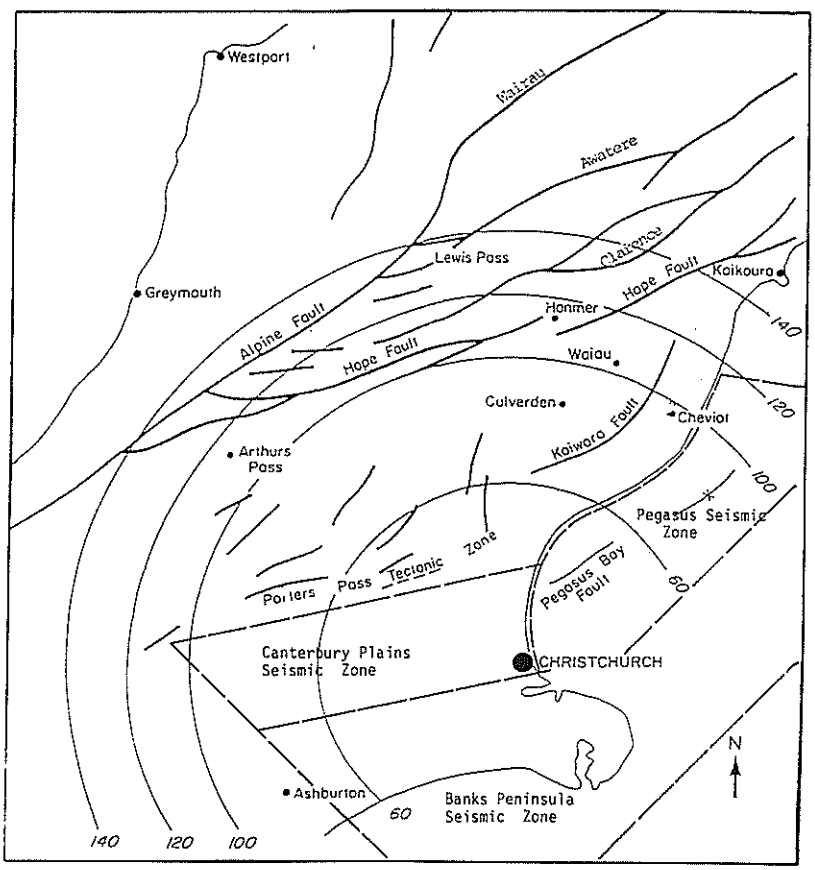

Figure 3 **Known Active Faults and Seismicity Zones in the Canterbury Region.**

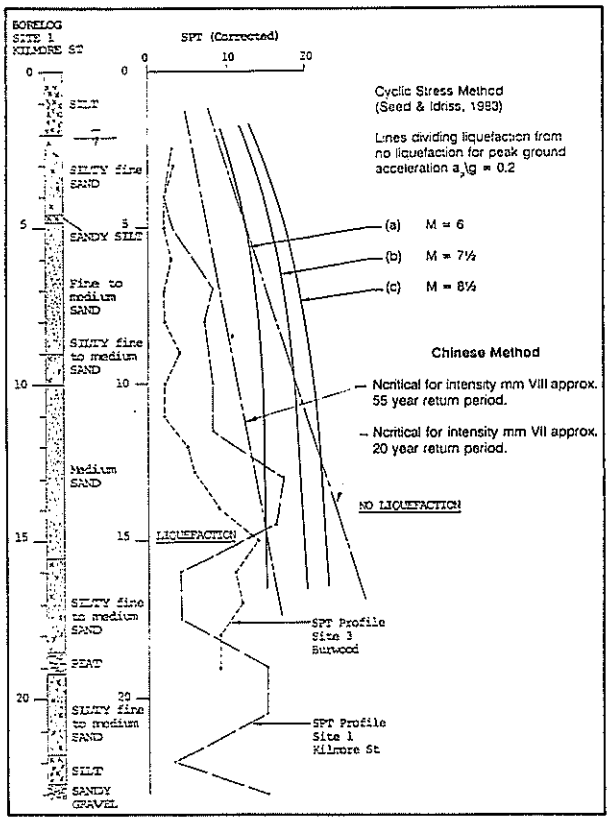

Figure 4 **Liquefaction Analysis for Two sites in Christchurch - Chinese and Cyclic Stress Methods.**

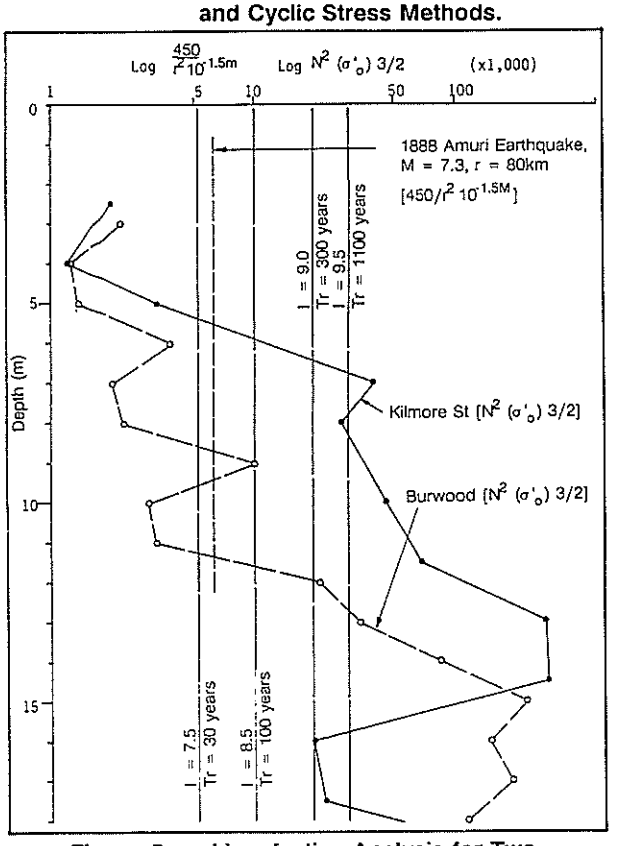

Figure 5 **Liquefaction Analysis for Two sites in Christchurch - Seismic Energy Method.**

The second approach is illustrated by the empirical relationship commonly referred to in New Zealand as the "Chinese" method. The method identifies a threshold value of SPT 'N', below which liquefaction can be expected to occur.

$$N_{crit} = N_o [1 + 0.125 (dx - 3) - 0.05 (dw - 2)] \qquad (2)$$

in which dx equals the depth to the layer being considered in metres, dw is the depth to the water table, and N_o is a function of shaking intensity.

A plot of N_{crit} versus depth for intensities MM VII and MM VIII is shown on Figure 4 which includes SPT N values (corrected) for two sites: one in Kilmore Street in the central city, and the second near Horseshoe Lake in the eastern city. Clearly the site N values are predominantly less than the N_{crit} values. This method predicts that liquefaction would occur at these two sites for earthquake shaking greater than MM VII (return period of about 20 years allowing for some increase in intensity from deep alluvium amplification).

The third approach compares dynamic shear strength of the soil and earthquake induced stress. The method, described by Seed et al (1983), uses the cyclic stress ratio, which is the ratio of the average cyclic shear stress τ_n developed as a result of the earthquake loading, to the initial vertical effective stress σ_o, and which can be computed from

$$\frac{\tau_n}{\sigma_o} = 0.65 \frac{a_p}{g} \cdot \frac{\sigma_o}{\sigma'_o} \cdot r_d \qquad (3)$$

where a_p = maximum acceleration at the ground surface, σ_o = total overburden pressure on the layer under consideration, σ'_o = initial effective overburden stress, and r_d = stress reduction factor varying from 1 at the ground surface to a value of 0.9 at a depth of 10 m.

Correlation with field and test data, using SPT N values as the measure of in situ density, gives a curve dividing cases where liquefaction is likely from those where liquefaction is unlikely. The position of this curve varies with the number of cycles of stress induced by earthquakes of different magnitudes, as shown in Figure 4, which shows data for the site in Kilmore Street, using a peak ground acceleration of $a_p/g = 0.2$, again indicating that liquefaction is likely to occur.

The cyclic stress method has also been adapted for use of in situ test data from the static cone penetration test (CPT) (Robertson & Campanella, 1985). CPT data for the same site in Kilmore Street confirms that liquefaction is expected for peak ground acceleration $a_p/g = 0.2$.

The fourth method assumes that the pore pressure increase during an earthquake is a function of the density of dissipated seismic energy, where the dissipation rate depends on the initial soil stress and density, characterised by the SPT-N value (Berrill et al, 1988). For level ground, liquefaction occurs when the increase in pore pressure equals the initial vertical effective stress. Extensive liquefaction case history records were used by Berrill et al to determine the values of constants in the proposed relationship for liquefaction prediction. The likelihood of liquefaction occurring is determined by plotting

$$r^2 \sigma'^{3/2}_o 10^{-1.5M} \text{ v } N \qquad (4)$$

where r is the distance from the earthquake source, σ'_o is the initial effective overburden stress and M is the earthquake magnitude. Liquefiable and non-liquefiable cases are separated by the line

$$450 N^{-2} = r^2 (\sigma'_o)^{3/2} 10^{-1.5M} \qquad (5)$$

This equation can be rewritten in the form

$$N^2(\sigma'_o)^{3/2} = \frac{450}{r^2\, 10^{-1.5M}} \quad (6)$$

Where the right hand side is determined by the seismic event and the left hand side is derived from the site specific data, which can be plotted as a function of depth at the site. From the seismicity model for Christchurch, values of r and M can be selected for a range of seismic intensities, each with return period.

The right hand side of the equation can therefore be plotted as vertical lines on the $N^2(\sigma'_o)^{3/2}$ v. depth profile, representing liquefaction thresholds for different shaking intensities.

Data from the Kilmore Street and Burwood sites are plotted on Figure 5 and again show that these sites have a considerable liquefaction potential, but not to the extent that the previous analysis methods predict, with little likelihood of liquefaction below 5-6 m at Kilmore Street, and 12 m at Burwood.

4. LIQUEFACTION OPPORTUNITY

The seismicity of the central and northern South Island has been reviewed in detail (Elder et al, 1991). The analysis indicates that potential exists for relatively rare but very large earthquakes (magnitude approximately 8) along the Alpine Fault, which essentially marks the western edge of the Southern Alps. More frequent moderate to large earthquakes (magnitude around 6-7.5) can be expected in the Canterbury Plains foothills and North Canterbury area, and less frequent moderate earthquakes under the Canterbury Plains and Christchurch itself.

It is clear that Christchurch will be subject to moderately severe seismic shaking at relatively short return periods, and average return periods of about 20 years for MM VII and 55 years for MM VIII have been calculated from regional seismicity levels. The historical record since 1930 indicates a considerably lower level of large earthquake activity than during the early years of Christchurch settlement.

5. PROBABILITY OF LIQUEFACTION

For the two sites used to illustrate this paper, the methods using the cyclic stress approach indicate liquefaction is likely to occur over virtually the whole soil profile with peak ground accelerations less than $a_p\backslash g = 0.2$, and this acceleration has a return of about 90 years. The method based on the density of dissipated seismic energy predicts a somewhat different hazard, with only the soils between 2 and 5-6 m liquefying at Kilmore Street, and between 2 and 11 m at Burwood, but with seismic events as low as 30 year return period. The empirical relationship of the "Chinese" method suggests liquefaction could occur with intensities of MM VII or greater, with a return period of about 20 years. The relationship between Magnitude and distance can be used to provide another estimate of the likelihood of liquefaction in Christchurch. Using only earthquakes of magnitude greater than the mean line in Figure 2 gives an annual frequency of occurrence of 0.0046 (215 year return period) with a probability of liquefaction occurring in any 50 year period of 20%.

There is therefore a wide range in estimated likelihood of liquefaction. Some of this range may be due to the effects of duration in liquefaction; a peak ground acceleration in excess of $a_p\backslash g = 0.2$ may not induce liquefaction unless the shaking is of sufficient duration. However, even for the lower probability of seismic shaking sufficient to cause liquefaction occurring, there is a significant risk to any potentially liquefiable site.

Similar analyses have been carried out for the other sites marked on Figure 1, and confirm that liquefaction is also predicted at these sites under similar earthquake conditions.

6. HISTORICAL EVIDENCE FOR LIQUEFACTION IN NORTH CANTERBURY

The most widespread occurrences of liquefaction in New Zealand since 1943 were caused by the 1848 Marlborough, 1855 Wairarapa, 1931 Napier, and 1987 Edgecumbe earthquakes. All these earthquakes occurred in coastal regions with plentiful fine-grained, recent alluvial deposits (Fairless & Berrill 1984). Generally liquefaction in New Zealand has been reported for earthquakes of magnitude 6.9 or greater (Edgecumbe, M = 6.3, was smaller, but unusually shallow).

There is little historical evidence of liquefaction occurring in Christchurch. The most destructive earthquake effects experienced in Christchurch since European settlement were during an earthquake (M = 5.5 - 6.0) on 4th June 1869, centred 10 km east of the city. It caused considerable damage to chimneys, masonry and household contents but there are no reports of liquefaction (Dibble et al, 1980). This may reflect the low population and sparse nature of development at the time, but the size of the earthquake was probably insufficient for widespread liquefaction.

Earthquakes have damaged chimneys in Christchurch and the Cathedral spire on at least three occasions: 5th December 1881 (M = 6.25, 80 km from Christchurch near Castle Hill), 1st September 1888 (M = 7.0 - 7.3, 80 km distant on the Hope Fault), and 16th November 1901 (M = 6.5, at a distance of over 100 km). Liquefaction effects were reported in the Hanmer area in 1888 and in the Cheviot, Hurunui and Kaiapoi areas in 1901.

The Motunau earthquake (M = 6.75) on 25th December 1922 caused liquefaction at Waikuku and Leithfield beaches. It appears from press reports that water ejection occurred behind the Waikuku sandhills, and loss of ground support caused a tree to topple, and motor cars to become bogged.

These historical earthquake events have been used to check the predicted liquefaction effect by the various methods, and some contradicting results emerge.

The general relationship between magnitude and the distance from the epicentre of an earthquake to the farthest site of liquefaction as proposed by Kuribayashi & Tatsuoka (1975) (refer to Figure 2), would not predict liquefaction in Christchurch for any of the historic earthquakes, and that the 1901 liquefaction at Kaiapoi, and the 1922 Waikuku liquefaction effects were close to the furthest distance from the epicentre that liquefaction could be expected for those events. Other large earthquakes (1929 Arthurs Pass, 1929 Murchison and 1968 Inangahua) were all too distant for liquefaction in Christchurch to be expected. This relationship is consistent with the lack of reported liquefaction in Christchurch.

However, for the sites where a site-specific liquefaction potential has been identified, a back analysis for these historical earthquakes indicates that liquefaction would have occurred. The seismic energy value for the 1888 Amuri earthquake is plotted on Figure 5 and indicates that for both the Kilmore Street and Burwood sites, liquefaction should theoretically have occurred in the top 5-10 m of metres of soil. This earthquake (M7.3, 80 km distance) is assessed as having produced up to MM VII shaking in Christchurch (Cowan, 1991), which would have a likely peak ground acceleration of 0.05 - 0.1 g. The cyclic stress method would predict liquefaction at both sites for 0.1 g acceleration, and liquefaction at Burwood for 0.05 g acceleration. Similarly three earthquakes (1868, 1881 and 1921) all produced MM VII

shaking in Christchurch, and the "Chinese" method plotted in Figure 4 indicates that liquefaction would have occurred.

It may be that liquefaction has in fact occurred in Christchurch since European settlement, but was not recognised or reported. It is also conceivable that the very deep alluvium under Christchurch which has a marked effect on predicted response spectra (Elder et al, 1991) in some fashion makes Christchurch soils less susceptible to liquefaction than in most reported sites used in determining the analysis methods.

7. CONCLUSIONS

A substantial area of Christchurch City is underlain by layers of sand or silts which would be susceptible to liquefaction if sufficiently loose. Although insufficient soil testing has been carried out to characterise densities in all areas, a number of sites where testing and analysis has been carried out demonstrate that some silts and sands in the city are loose and vulnerable to liquefaction. At this stage, there is no evidence to suggest that the conditions and soil gradings at those sites are not typical of Christchurch soils, and it is concluded that a large part of the eastern city is potentially subject to liquefaction.

There is some discrepancy between the lack of liquefaction effects reported from historical earthquakes, and the liquefaction potential predicted by liquefaction analyses.

ACKNOWLEDGEMENT

Most of the work described here was funded by the Earthquake and War Damage Commission.

REFERENCES

Berrill, J.B., Davis, R.O., Mullenger, G., and Fairless, G.J. (1988) Seismic Liquefaction Research by the University of Canterbury. Transactions, IPENZ, Vol. 15, No. 2/CE, July 1988.

Cowan, H.A. (1991) The North Canterbury earthquake of Sept 1, 1888. Journal of the Royal Society of New Zealand, Vol. 21, No. 1, March, pp 1-12.

Elder, D.McG, McCahon, I.F., and Yetton, M.D. (1991) The Earthquake Hazard in Christchurch - a Detailed Evaluation. Unpublished report by Soils & Foundations Ltd to EQC. ISBN 0-473-01243-X.

Fairless, G.J. and Berrill, J.B. (1984) Liquefaction during Historic Earthquakes in New Zealand. Bulletin of N.Z. National Society for Earthquake Engineering, Vol. 17, No. 4, December.

Kuribayashi, E. and Tatsuoka, F. (1975) Brief Review of Liquefaction During Earthquakes in Japan, Soils and Foundations, 15, pp 81-92.

Robertson, P.K. and Campanella, R.G. (1985) Liquefaction Potential of Sands Using the CPT, Journal of Geotechnical Engineering Division, ASCE, Vol. 111, No. 3.

Seed, H., Bolton, Idriss, I.M. and Arango Ignacio (1983) Evaluation of Liquefaction Potential Using Field Performance Data, Journal Geotechnical Engineering Division, ASCE, Vol. 109, No. 3.

Youd, T.L. (1973) "Liquefaction, Flow, and Associated Ground Failure", U.S. Geological Survey Circular 688.

Landslide and Uplift of River Bed in Tal Valley, Carhwal Himalaya

G.S. MEHROTRA
M.Sc., Ph.D.
Scientist, Central Building Research Institute, Roorkee, India
ARCHANA GUPTA
B.E., M.E.
Research fellow, Central Building Research Institute, Roorkee, India
S. SARKAR
Scientist, M.Sc., M.Tech.
Scientist, Central Building Research Institute, Roorkee, India

SUMMARY In January 1990, a landslide occurred in Tal Valley of Garhwal Himalaya which caused uplift of the river bed by 6-8 m (upto April, 1990). Initially the rate of rise was 2 cm per day which gradually decreased, however, the process is still continued. A detailed geological and geotechnical studies of the area revealed that the slope mass movement was a rotational sliding with slumping triggered by heavy rainfall. The gravitational forces exerting upon highly weathered and sheared material formed a slip surface in the upper part of the slope which is terminating below the river bed. The paper highlights the mechanism of the slide which has been found directly related to the rise of the river bed.

1. INTRODUCTION

Landslides are annual recurring feature experienced in all hill ranges of India and other countries world wide. These are generally the natural events associated with heavy or substantial rainfall, cloud bursts, seismic shocks, river erosion etc.

In January, 1990, a large scale landslide with apparently deceptive movement occurred in the Tal Valley, Garhwal Himalaya, located near Village Bhukundi 15 kms from Chila power house, Hardwar. The most peculiar feature associated with this slide was the uplift (about 8 m) of the river bed (about 250 m long and 30 m wide) in twenty four hours time, after thirty six hours of continuous heavy rainfall. This event had caused enormous fear among the villagers. The slope conditions changed completely with the development of the series of escarpments in the upper part, numerous cracks in the middle portion of the slope and mass destruction of the trees in general on the slope. The river too has changed its course due to the uplift of the bed. In order to ascertain the gravity of the situation, geological, geotechnical & slope stability studies of the slide area were carried out with a view to understand the mechanism of failure and the causative factors of such mysterious movement which got terminated near the river bed due to counter-resistance by the underlying rocks. The paper highlights the findings of the study.

2. DESCRIPTION OF THE SLIDE AREA

The slide area is situated at the left bank of river Tal, 15 kms from Chila Power house, Hardwar. The river is eroding the foot of the hill striking almost in NW-SE direction. The slope area confined between two seasonal drains comprises predominantly of highly weathered rock-mass associated with clayey soil covered mostly by thick vegetation.

At the crown, an escarpment of 20-30 m high and about 300 m long was formed due to the landslide. The escarpment or slip surface is covered with gaugy material and stands at an angle of 50° to 60°. The thin shale bed associated with sandstone in the slip surface has shown the presence of slickenside surfaces at various locations indicating the direction of movement. It was further substantiated by the occurrence of sheared tree roots at the top of the escarpment.

In the middle portion of the slope, the landslide activity has resulted into development of numerous cracks mostly longitudinal or transverse to the slope. The length of the cracks varied from 10 m to 150 m, whereas width varied from few cms to 1 m and depth from 2 to 4 m. Many minor cracks obliquely branching out from the major cracks were also present. During the course of survey, it was observed that the areas lying between the cracks commonly showed several slumped portion clearly indicating subsidence of the slope. Inspite of the fact that the slope was reasonably well vegetated, yet it was marred by tilted and uprooted trees.

3. GEOLOGY OF THE AREA

The main rocks exposed in the slide area are shales and sandstones of Eocene age. Outcrops were found exposed near the slip surface and in the surrounding areas. The shales were generally moderate to highly weathered and fractured in the slide area, associated with exposures of hard and massive sandstones. The rock beds were dipping inside the hill with E-W strike and $20\text{-}30^{\circ}$ dip towards south. The sheared rocks with pulverised material indicated the presence of shear zone, the extent of which could not be identified due to lack of continuous exposure of rocks and also due to the thick vegetation on the slope. However, on the basis of some abrupt variation in attitudes of beds the presence of local folding in the area can not be ruled out. Geologically, the area may be considered as weak zone due to the presence of highly fractured and weathered rock mass on the slope.

4. FIELD INVESTIGATIONS AND LANDSLIDE MONITORING

In order to have better understanding of the sliding phenomenon in this region, it was planned to carry out detailed scientific investigations of the area. It involved detailed geological, geomorphological and geotechnical surveying and mapping of the area, monitoring the rise of river bed and displacements in cracks. A contour map alongwith the location of slide boundary and major cracks was prepared (Fig.1).

For the monitoring of the uplift of the river bed, few wooden markers of 90 cm length were installed covering the full stretch of the uplift portion, each going 50 cm below the ground surface. The data of sloping distance, horizontal distance and elevation of these markers were taken using Elec-

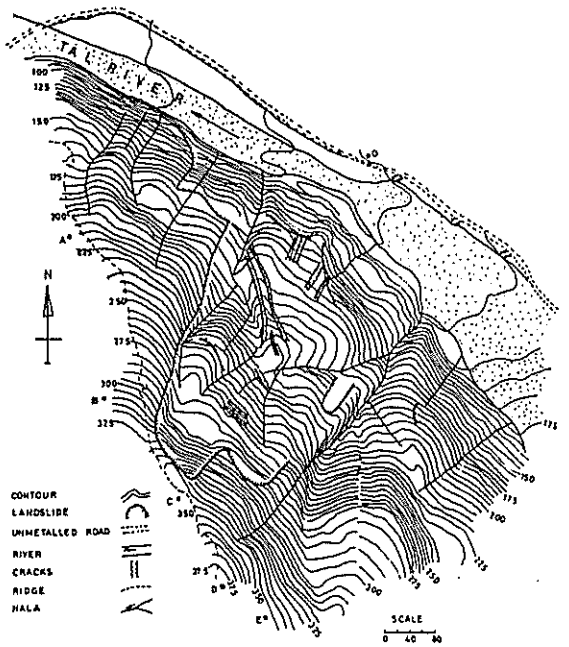

Figure 1 Map of slide area

tronic distance meter, from a fixed bench mark. The observations were taken at different time intervals for assessing the horizontal and vertical displacements. The analysis of the monitoring data clearly exhibits that there was no considerable movement in the horizontal direction, whereas there was significant change in vertical direction. Due to the rise of river bed, most of the markers fixed on the outer profile of the uplift portion got covered with debris and some tilted forward. The angle of tilt varied from 7 to 45 degrees. The rise of different portions of the river bed was found to vary from 0.75 to 2.5 meters in thirty days indicating an average rate of rise of 1.5 cm/day (Fig.2).

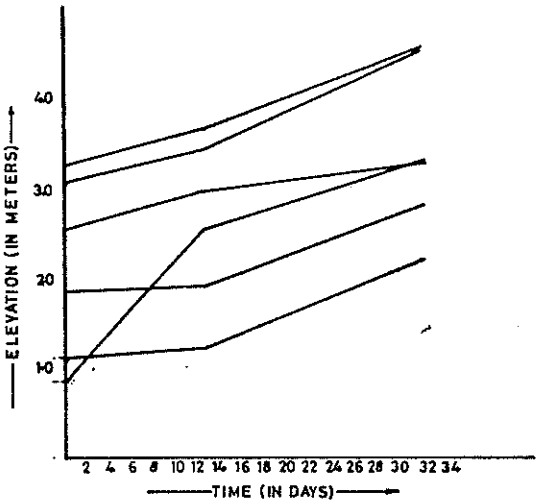

Figure 2 Rise of river bed with time

For the monitoring of movement in cracks, markers (iron bars) were fixed on both the walls of the cracks and the displacements in forward as well as vertical directions were measured from time to time. The analysis of the data obtained for the cracks at different intervals of time have clearly revealed widening of the cracks as well as subsidence of the ground along the cracks. Some of the cracks were found to have widened by 2 cms to 1 m while the subsidence was recorded to vary from 1 to 6 cms. It was observed that there was no relative displacement along the cracks. It is significant to note that during the period of investigations the soil mass close to the slip surface has moved by 20 to 40 cms (in ten days time) indicating the process of subsidence still active in the region.

5. MECHANISM OF THE LANDSLIDE

This is a successive rotational landslide in the weathered rock formation consisting of sandstones interbedded with Shales (Fig.3). Evidence of sliding at the interface of shale and sandstone are prominent & large displacements have been inferred due to presence of slickenside surfaces.

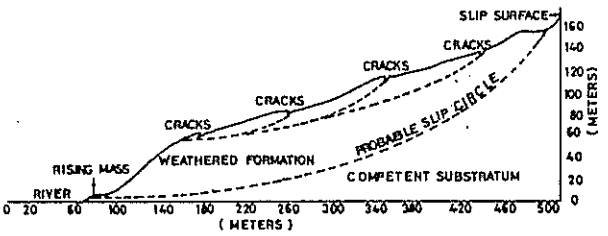

Figure 3 Section showing mechanism of slide

The laboratory testing of the weathered product of the rock formation has shown a low value of cohesion with an average angle of internal friction. The uniaxial compressive strength obtained through point load tests have shown fairly good compressive strength for sandstones, whereas the shales were found to be so soft that even undisturbed sampling was difficult.

It has also been observed that just at the interface of sandstone and shale the particle size of clay material is very fine which indicates that initially because of breakdown of bigger particles proportion of the clay size fraction at the boundary tends to decrease but later on clay fraction records marked increase, as could be expected corresponding to large movements (Mehrotra, 1988). The another important feature is wet conditions of clay surface which indicates high water retaining capacity and obstruction to the water flow causing high pore pressure for sliidng to take place.

6. SLOPE STABILITY ANALYSIS

The main objective of the stability analysis was to evaluate the factor of safety of the hill slope along various sections, compatible with the existing field conditions. The present study area shows the existence of highly weathered and fractured rockmass with soil cover indicating the slip surface to take a circular path. Hence to determine the existing factor of safety, rotational equilibrium analysis has been applied for stability analysis.

A software for circular failure analysis, was developed and run, both for static and dynamic conditions. The program was developed based on Bishop's Simplified Equation (Bishop 1955) with modifications to account for the effects of earthquake forces and pore water pressure. The program also takes into account the effect of tension cracks and water in the tension cracks on the Factory of Safety of the slope. The mathematical equation used is given below :

TABLE I

FACTOR OF SAFETY AT CHILA SLIDE AREA

Seismic Coefficient	0.0, 0.00				0.05, 0.25			
Profile	Pore pressure ratio				Pore pressure ratio			
	0.0	0.1	0.2	0.3	0.0	0.1	0.2	0.3
OA	1.209	0.988	0.899	0.776	1.111	0.936	0.823	0.705
OB	1.086	0.912	0.779	0.677	1.002	0.840	0.712	0.612
OC	1.012	0.843	0.715	0.599	1.974	0.775	0.662	0.538
OD	1.004	0.813	0.673	0.547	1.963	0.748	0.612	0.489
OE	1.066	0.863	0.752	0.619	1.992	0.796	0.687	0.558

$$F = \frac{\Sigma[c.b + W(1 - \bar{B})\tan(\emptyset)] \dfrac{\sec(\alpha)}{1 + \tan(\emptyset).\tan(\alpha)/F}}{W + \Sigma[W\sin(\alpha) + \alpha_h W' \cos(\alpha)]}$$

where,

F = Factor of safety of slope

c = Cohesion of soil

b = Width of the slice

W' = Weight of the slice

W = $(1 + \alpha_v)W'$

$\bar{B}$ = Pore water pressure/W'

$\emptyset$ = Angle of internal friction

α = Angle of the base of slice with horizontal

α_h = Coefficient of horizontal E.Q. acceleration

α_v = Coefficient of vertical E.Q. acceleration = $1/2\alpha_h$

VV = Driving moment due to water force/ radius of arc

The input data included the coordinates of the slope profile, depth of hard strata at the toe, cohesion, angle of internal friction, unit weight of soil, unit weight of water, pore pressure ratio and coefficients of horizontal and vertical components of earthquake acceleration.

The analysis was carried out in dry and wet condition with varying amount of pore pressure ratios along five selected sections of the slope. For selection of the sections, change in slope and presence of cracks were taken into cosideration. The depth of hard strata was considered to be 10 metres, as observed from the field investigations. Since the pore water pressure could not be measured in the field, assumed values of pore pressure ratios were considered to evaluate the variation in factor of safety with water saturation. For dynamic analysis of the slope, the values of horiontal and vertical coefficient of earthquake acceleration were taken according to the seismic zones of India (IS:1893-1948). Parameters of soil and seismicity coefficients used in the stability analysis are :

Cohesion of soil	-	250 kN/m^2
Friction angle of soil	-	30^o
Unit weight of the soil	-	17.0 kN/m^3
Unit weight of water	-	10.0 kN/m^3
Pore pressure ratio	-	0.00, 0.1, 0.2 & 0.3
Seismic coefficient :		
Horizontal	-	0.05
Vertical	-	0.025

The existing factor of safety values are tabulated in Table I. The analysis has shown that in dry condition the slope is just stable while with little increment in pore pressure and considering the seismicity, factor of safety for all the sections drop below 1, showing instability.

The existing factor of safety (Table I) along OA, OB & OE ranges from 1.066 to 1.209 without any pore pressure and seismic coefficient and decreased to 0.558 to 0.705 at 0.3 pore pressure & 0.05 seismic coefficient. Whereas along OC and OD, factor of safety ranges from 1.004 to 1.012 without any pore pressure and seismic co-efficient and decreased to 0.489 to 0.538 at 0.3 pore pressure & 0.05 seismic coefficient. Among all the sections, the central portion of the slide area i.e. along OC and OD, has shown the minimum factor of safety indicating unstable zone. This inference is further confirmed by the presence of numerous cracks and signs of subsidence in the central zone.

7. CONCLUSION

The study carried out has established that the uplift of the river bed as well as the development of series of cracks on the slope were caused by the landslide. The manifestation at the crown where slip surface has been developed clearly indicated a shear failure of weathered rockmass. It could be also inferred that the slope movement was initially triggered by gravitational force exerted upon sheared material which have subsequently caused slumping along a slip surface forming an escarpment at the top and terminatig at the toe of the slide.

The evidences produced by the formation of successive layers clearly point towards successive rotational failure of weathered rockmass overlying a hard substrata.

The monitoring data confirming the rise of river bed has led to the conclusion that the area is still rising, though it is not uniform throughout. The river bed material being very loose almost without any cohesion could not resist the stresses which are pushing up the material. The counter resistance of the rocks below the river bed must have been responsible for the uplift. Hence the uplift of the river bed is directly related of the nature of the slide.

The slope stability analysis has shown that the slope appears to be stable with no pore pressure and seismicity. But with marginal rise of water pressure, which is common in this area during monsoon, the slope tends to be highly unstable. The combined effect of seismicity and pore pressure makes the slope highly unstable when the factor of safety drops down to 0.489 from 1.209.

8. ACKNOWLEDGEMENT

For providing all the facilities to carry out the study, authors are thankful to the Director, Central Building Research Institute, Roorkee (U.P.), India. Thanks go to Mr. R. Dharmaraju, Mr. D.G. Rao and Mr. A. Paul who helped us in carrying out the field investigations. Thanks are also due to Ms. Heera Bhatt for nicely wordprocessing the paper. The paper has been published with the kind permission of Director Central Building Research Institute, Roorkee.

9. REFERENCES

1. Bishop, A.W. (1955), "The Use of Slip Circle in the Stability Analysis of Slopes", Geotechnique, Vol. 5, No. 1.

2. Viwkesm Hiseogm, E. (1986), "Engineering Properties of Soils and their Measurements", McGraw Hill Book Company, Singapore.

3. Choudhury, R.N. (1978), "Slope Analysis", Elsevier Scientific Publishing Company, Amsterdam.

4. Eco Development in the Garhwal Himalaya with Particular Reference to Field Study and Monitoring of Landslides and Development of Innovative Control Measures, Central Building Research Institute, Roorkee (1988), (Published Report).

5. Hoek, E. and Bray, J.W. (1981), "Rock Slope Engineering", The Institution of Mining and Metallurgy, London.

6. IS:1893-1984, (1984) "Criteria for Earthquake Resistant Design of Structures".

7. Mehrotra, G.S., Bhandari, R.K. (1988), "A Geological Appraisal of Slope Instability and Proposed Remedial Measures at Kaliasaur Slide on National Highway, Garhwal Himalaya", 2nd Int. Conf. on Case Histories in Geotech. Engg., St. Louis, U.S.A.

8. Rajaraman, V. (1984), "Computer Programming in Fortran IV", Prentice Hall of India Pvt. Ltd., New Delhi.

Stability Analysis in Stiff Fissured Clay at Raby Bay, Queensland

A.T. MOON
B.Sc., M.Sc.
Principal, Coffey Partners International Pty Ltd, Brisbane

SUMMARY. The Raby Bay Project in southeast Queensland consists of a coastal residential and recreational complex based around a system of canals. Construction failures and the presence of fissured clay had caused concern about canal slope stability and the adoption of remedial works. Most of the stiff clays is of volcanic origin but sedimentary clay occurs in parts of the site. Defects (fissures) occur in layers and trends were identified in the occurrence and character of defects across the site. Stability charts have been developed based on a generalised model which takes into account the depth and thickness of the layer containing defects (weak layer) and the dip and continuity of the defects. The concept of a Strength Reduction Factor has been developed to characterise the strength of the weak layer.

1. INTRODUCTION

1.1 Background And Approach

Raby Bay is situated about 25km east of Brisbane in southeast Queensland. The Raby Bay Project consists of a coastal residential and recreational complex based around a system of tidal canals. Construction of the canals started in 1983 and design slopes of 3 to 1 (horizontal to vertical) were adopted early in the project. The canals are excavated to a depth of RL -3.8m and fill is placed between the canals to construct road and residential areas to about RL +3m.

The presence of closely spaced slickensided and/or polished defects in the stiff soils ("fissured clay") was recognised in 1983 following a slope failure next to an overdeepened borrow area. During the period 1983 to 1988 the presence of fissured clay was observed in several areas and appeared to contribute to several construction slope failures. Back analyses appeared to indicate that the mass strength parameters at the time of failure were between residual and fully softened although there was uncertainty about the pore water pressure assumptions.

Remedial measures in the form of excavation and replacement of the slopes were adopted where fissured clay occurred. Flatter slopes were not considered. The soil profile was described as extremely variable and decisions on replacement were made on a lot by lot basis. During 1988 construction was underway in a part of the site where, in places, fissured clay occurred at depths greater than RL -7m. The scale (and therefore the cost) of earthworks replacement in this area was a major concern to the developer.

This paper presents some of the results of the work carried out by the writer on the project during 1989. The initial engagement was to carry out a review of the site geology. Subsequent engagements during that year were to carry out investigations and provide advice on slope design for various parts of the project. Some construction monitoring was also carried out and the results of previous studies were reviewed and used where relevant to the development and quantification of the geotechnical model.

Excavations or large test pits were the preferred method of field investigation as they provide the most complete picture of subsurface conditions. Where depth limitations occurred, or there were problems with pit stability or access, large diameter cored boreholes (100mm diameter core) were used. The work was carried out as a number of individual studies of different parts of the project area. However, emphasis was placed on obtaining an overall understanding of the site geology so that an overall approach to stability analysis and slope design could be developed for the entire project area.

2. GEOTECHNICAL MODEL

2.1 Geological Setting

According to published geological maps the Raby Bay Project area consists of estuarine deposits underlain by volcanics of the Tertiary age Lamington Group. The estuarine deposits are described as consisting of mud, silt, sand, clay, gravel, and minor peat and coral debris. While the Lamington Group consists mainly of basalt, some pyroclastic material (ash or tuff) and sediments also occur.

2.2 Site Geology

2.2.1 Soil and rock materials

Figure 1 is a diagrammatic cross section showing the site geology. A brief description of the materials is given in the legend. Seven materials were identified with subdivision of each material based on both geological origin and engineering properties. From the engineering point of view the information on materials may be summarised as follows:-

- Most of the material consists of soil. Very little rock was encountered.
- Most of Materials 3, 4 and 5 consist of stiff to very stiff clay. Parts of Material 2 were observed to be soft to firm.
- The upper parts of Materials 3 and 4 are lateritised. They are mottled red and include ironstone gravels.

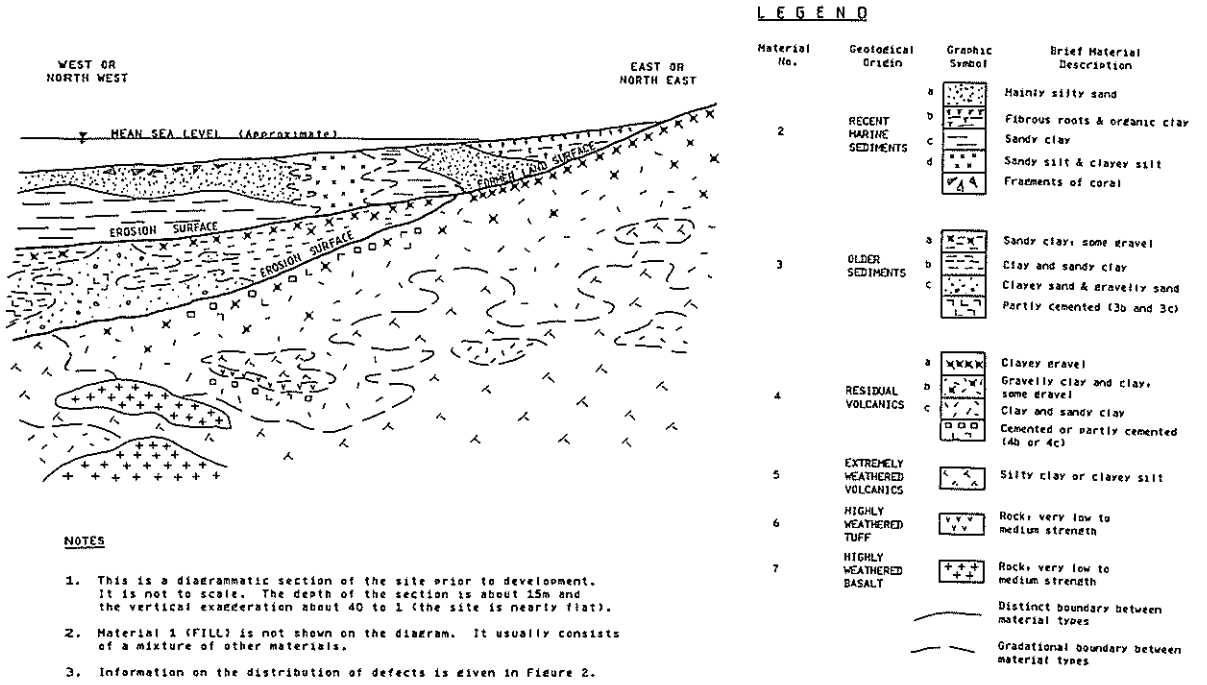

Figure 1 Diagrammatic cross section showing site geology

2.2.2 Defects

In geotechnical engineering, defects may be defined as discontinuities or breaks in the continuity of a material. All rock masses and many soil masses contain defects. Stiff cohesive soils such as occur at Raby Bay almost invariably contain defects. Defects in cohesive soils are sometimes referred to as fissures although there is no consistent definition of fissures in the literature. Sometimes the term is applied specifically to short closely spaced defects with dull surfaces, sometimes to all defects.

Several different types of defects as defined by Stapledon (1970) occur at Raby Bay, but emphasis has been placed on the systematic collection of information on defects with slickensided and/or polished surfaces. As is discussed in Section 3 these defects are the most significant to slope design. Unless stated otherwise, subsequent references to defects will refer to those defects with slickensided and/or polished surfaces.

Information was collected on the following aspects of defects:-

- Occurrence.
- Thickness of layers containing defects.
- Dip and preferred orientation.
- Shape.
- Spacing.
- Intersections.
- Length and effective continuity.

Defects do not occur in all materials and where they do occur they tend to be confined to layers which are typically 1 to 2m thick. Most defects dip between 30° and 50° and do not show a preferred orientation. Flatter defects occur at greater depths. Most dips are curved or undulose although some planar defects occur. Defect spacing varies but is typically 0.1 to 1m. In most areas few defect intersections were observed but in some local areas where defects were closely spaced there are many intersections. Defects are generally less than 1m in length.

The concept of the Effective Continuity Assessment (ECA) was developed after observations in test pits and construction excavations indicated that defects are not continuous and that flatter defects are often shorter than the steeper defects. The ECA is defined as an assessment of the continuity of defects at the lower angle in the dip range of a particular defect set. It is expressed as a percentage of the maximum length possible at this angle across the thickness of the layer in which the defect set occurs.

A schematic section showing the distribution of defects is given in Figure 2. The defects were not uniformly distributed across the site. Further from the original shore defects are less common, occur in deeper and thinner layers, and are more widely spaced.

2.2.3 Origin of defects

The pattern of defects observed at Raby Bay is very similar to that reported in South Africa by Williams and Jennings (1977). High horizontal stresses associated with wetting and drying in a semi arid climate was considered to be the most likely origin of the South African defects. Similar conditions would have applied to the Raby Bay area during periods of Pleistocene lower sea levels and probably during the Tertiary when the lateritisation is likely to have occurred. The pattern of defects at Raby Bay appears to differ from the pattern reported in some of the London Clay in Britain (Skempton, Schuster, and Petley, 1969).

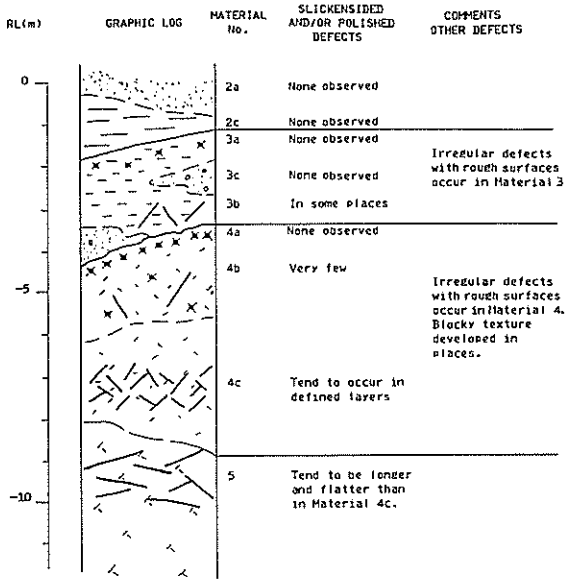

Figure 2 Schematic section showing the distribution of defects

2.3 Material Properties

2.3.1 Introduction

Skempton (1977), Moon (1984) and Burland (1990) discuss the effective strength parameters applicable to the mass strength of stiff fissured clay. They describe the different approaches to the assessment of the strength parameters applicable to the first time failure of largely intact material or material that does not contain extensive slickensided and/or polished defects. Terms which have been used to describe those strength parameters include fully softened, remoulded, post peak and post rupture. At low stress levels the different approaches appear to result in strengths similar to those derived from back analysis. The term fully softened has been used in this paper. If movement occurs on pre-existing shear failure surfaces it is the residual strength which is applicable.

The approach to the assessment of the design effective strength parameters was as follows:-

- To define materials according to their geological origin and engineering properties (Figure 1).
- To use index tests to categorise each material type, assess its variability, and make preliminary predictions of strength parameters based on published and unpublished work on similar soils.
- To carry out effective shear strength testing using methods discussed by Moon (1984) to assess the fully softened strength of the soils and the residual strength of all materials in which slickensided and/or polished defects occur. Test results from previous studies at Raby Bay were used wherever possible.

Back analysis of past slope failures is also a potential method of assessing strength parameters. The usefulness of back analysis at Raby Bay is limited by the fact that all the past failures are "construction failures" in the sense that they occurred after excavation. In most cases fill placement had also occurred. Pore pressure measurements were not available and there is uncertainty about the rate of pore pressure equilibration following unloading (excavation) and loading (fill placement). No major slope failures occurred in parts of the project investigated by the writer but previous back analyses appeared to indicate that mass strengths were less than the fully softened strength in some places.

2.3.2 Test results and strength parameters

The results of the Atterberg Limits tests given in Figure 3 illustrates how the geological origin and material classification may be related to the engineering properties. The test results for Material 5 fall below the A line (diagonal line) which is typical of weathered volcanics. Further weathering produces residual volcanic soil (Material 4c). Such weathering has produced a greater proportion of clay minerals which is reflected by the higher liquid limit and plasticity index. Lateritisation, on the other hand, involves oxidation and a reduction in plasticity (Materials 4a and 4b). Material 3 is a sedimentary cohesive soil and the test results occupy the typical position of just above the A line for such materials. The Recent Marine Sediments (Material 2) are lower plasticity materials because the fine fraction tends to consist of silt rather than clay.

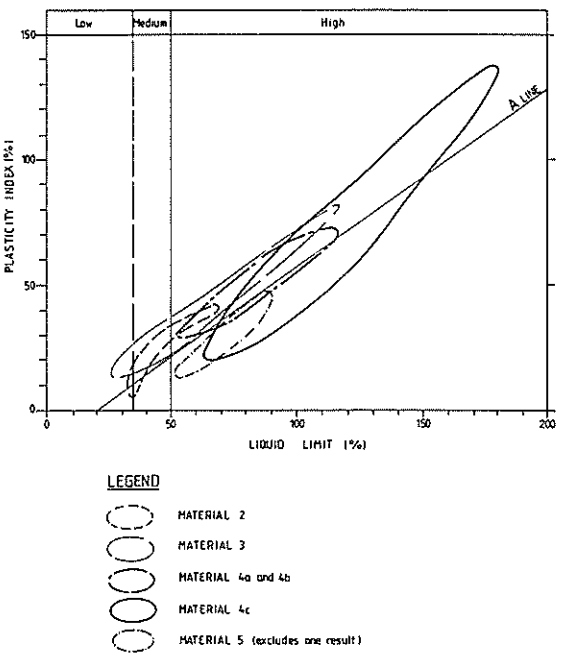

Figure 3 Summary of Atterberg Limits results

The design parameters adopted for stability analysis of the relevant material types are given in Table I.

TABLE I

STRENGTH PARAMETERS ADOPTED FOR STABILITY ANALYSIS

Material No. [1]	Density t/m³	Fully softened cohesion kPa	Fully softened friction angle	Residual cohesion kPa	Residual friction angle
1 (Fill)	1.9	5	27		
2a	1.8	0	36		
2b (Not assessed, organic material removed)					
2c	1.8	2	29		
2d	1.8	0	33		
3a	2	5	24	2	12
3b	2	5	24	2	12
3c	2	2	30		
4a	2	2	36		
4b	1.7	5	29	2	11
4c	1.7	5	27	2	11
5	1.7	10	26	2	11
6,7 (not assessed, rock)					
G[2]	1.9	5	27	2	11

NOTES:
[1] Brief descriptions of materials are given in Figure 1.
[2] Generalised strength parameters for the entire soil profile.

3. APPROACH TO THE STABILITY ANALYSIS

3.1 Present Practice In Fissured Clay

At Raby Bay the past topography appears to have been subdued and pre-existing slope failures prior to construction are not likely to have occurred. However, on a smaller scale, slickensided and/or polished defects are failure surfaces for which residual strength parameters will apply. Parts of potential large scale failure surfaces may occur along such defects. Present practice in assessing the effective strength parameters for slope design in stiff soils with non-continuous defects appears to include the following approaches:-

1. assume fully softened parameters on the basis of observations that defects are not continuous;

2. assume residual strength parameters in situations where extensive closely spaced defects occur;

3. assume intermediate values between fully softened and residual (or in some cases peak and residual).

The first approach developed for the London Clay (Skempton, 1977) appears to be widely used (Chandler, 1984). Descriptions of defects in London Clay in Skempton, Schuster, and Petley (1969) indicate most defects are short (less than 100mm) are not slickensided and polished, and are flat lying or steeply dipping. For soils where longer, slickensided and/or polished, inclined defects occur the use of fully softened strength may lead to an over-estimate of shear strength.

The second approach is appropriate if slope movement, or any form of shear movement on an extensive scale has taken place and continuous pre-existing failure surfaces exist. This approach is likely to result in an underestimate of shear strength if applied to slopes where continuous, unfavourably oriented, slickensided and/or polished defects do not occur.

The third approach has been used by Thorne (1984) and Macgregor, Olds, and Fell (1990). In both cases intermediate strength values were based on laboratory testing and observations in materials where closely spaced slickensided and polished defects occurred. Intermediate strength values had also been applied at Raby Bay prior to this study because mass strengths lower than fully softened had been indicated by back analysis. In all of these cases a single value had been adopted to apply to the "highly fissured" material.

In this study a generalised model has been developed which provides a method of quantifying a range of strengths intermediate between fully softened and residual which is based on observations of the defects occurring at particular test locations.

3.2 Development Of The Generalised Slope Model

The starting point of the model is the generalised density and fully softened strength given in Table I. These parameters were adopted as being representative of the soil profile where no defects occur. If there are defects, the layer in which the defects occur is referred to as the weak layer. A density of 1.7 t/m³ was adopted for the weak layer. The strength of the weak layer is assumed to vary between the fully softened value and the residual value according to the proportion of potential failure surfaces which may occur along pre-existing defects. In assessing this proportion the following variables were taken into account:-

- the thickness of the weak layer;
- the dip of the defects;
- the continuity of the defects.

The influence of the thickness and dip were taken into account in a single factor referred to as the Thickness Dip Factor or TDF. The TDF is a measure of the proportion of failure surface that can occur along pre-existing defects within the weak layer assuming the defects are continuous. Geometrical constraints mean that the feasible failure surfaces cannot entirely occur along pre-existing defects unless the defects are near horizontal or the layer containing defects is sufficiently thick. A mathematical expression of this geometrical constraint is given in Figure 4.

Stability analyses indicate that the length of critical failure surfaces in the weak layer is reasonably constant even when the depth and strength of the weak layer is varied. On the assumption that L is constant general TDF charts have been developed for the Raby Bay Project. Figure 5 is a TDF chart for weak layers below the canal floor with defects which do not show a preferred orientation.

The TDF assumes that defects are continuous and thus overestimates the proportion of potential failure surfaces on pre-existing defects. This lack of continuity may be taken into account by multiplying the TDF by the Effective Continuity Assessment (ECA). The product of the TDF and the ECA has been defined as the Strength Reduction Factor (SRF) of the weak layer. It has been assumed that the reduction in effective strength of the weak layer from fully softened to residual is linearly proportional to the SRF. Examples of the SRF are given in Table II.

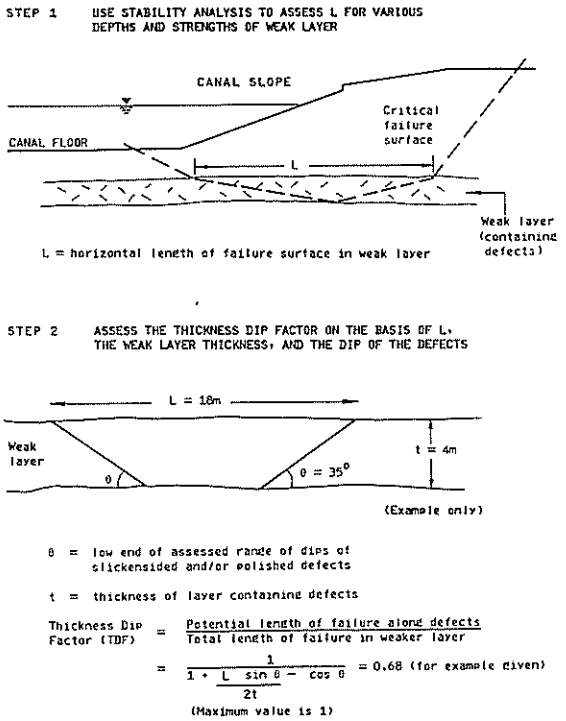

Figure 4 Development and definition of the Thickness Dip Factor

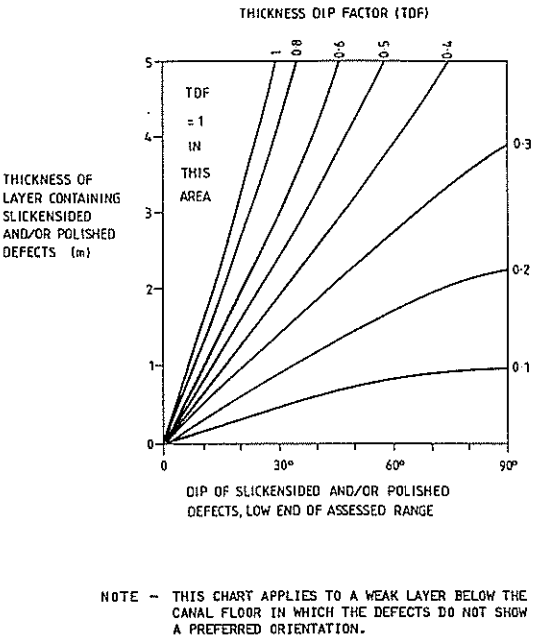

Figure 5 Example of a Thickness Dip Factor chart

TABLE II

EXAMPLES OF THE WEAK LAYER STRENGTH REDUCTION FACTOR

Strength Reduction Factor %	Adopted strength for weak layer cohesion kPa	friction angle[1]	Comment
0	5	27	Fully softened strength
25	4.3	23.3	
50	3.5	19.4	
75	2.8	15.3	
100	2	11	Residual strength

[1] based on a linear relationship between the Strength Reduction Factor and the tangent of the friction angle.

Figure 6 is a stability chart which shows the variation in factor of safety with SRF and depth of the top of the weak layer. Rapid assessment of factors of safety for any combination of weak layer depth and thickness and defect dip and continuity can be made by using the TDF and stability charts.

Although the thickness of the weak layer is taken into account in the TDF (and hence the SRF) the actual stability analyses used to develop the stability chart are based on an assumed defect layer thickness of 1.5m. Observations indicate that this is a typical thickness and sensitivity analyses indicated that factors of safety were not particularly sensitive to increased thicknesses of the weak layer. Increasing the weak layer thickness to 4m reduced the factor of safety by less than 5%.

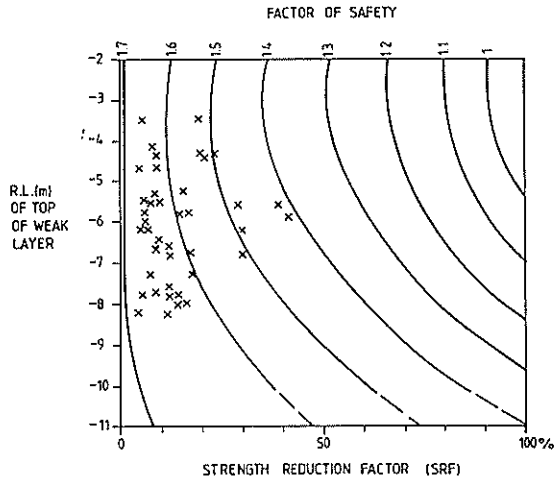

Figure 6 Stability chart showing results for part of the project area

3.3 Method Of Analysis And Design Factor Of Safety

Janbu's Simplified Method was used for the stability analyses. For particular analyses comparisons have been made with other non-circular methods of stability analysis such as Spencer's Method and Morgenstern and Price's Method. Where such comparisons have been made factors of safety have been within 5% of the values obtained by Janbu's Simplified Method.

The stability chart based on the generalised model allows rapid assessment of the approximate factor of safety to be made for particular slope models. The slope models are based on information on the depth and thickness of the layer containing defects and the dip and continuity of the defects from the area concerned. In order to make decisions based on these stability assessments it is necessary to adopt a design factor of safety below which further action is taken. Such further action might consist of one or more of the following activities:-

- carry out individual stability analyses of more complex slope models representative of the area concerned;
- carry out further site investigation in order to provide more information and confirm or revise the geotechnical model;
- assess remedial measures to improve the stability.

A design factor of safety of 1.5 was adopted for the Raby Bay Project based on sensitivity and probabilistic analyses.

4. RESULTS OF STABILITY ANALYSES

The results of the stability assessments based on the generalised model carried out for part of the project area are presented on Figure 6. In this area the comprehensive logging of the sides of the excavations and test pits in the base of the canal provided a more complete picture of the geotechnical model than in the other areas investigated. The crosses on the chart indicate the test pit locations.

The assessment using the generalised model stability chart indicated that most factors of safety were greater than the adopted design value of 1.5 but several marginal or lower values occurred. Individual stability analyses based on the detailed profile at the particular test pit location were carried out for all slopes where the preliminary assessment indicated a factor of safety of less than or close to 1.5. The individual analyses confirmed the marginal values and can be regarded as a check on the validity of the generalised model. The two sets of results compared very well with differences of less than 5% in all cases.

The marginal factors of safety occur at the inland end of the area investigated. The principal reason for this is that flatter defects occur higher in the profile in this area. Some overdeepening of the canal had also contributed to a lower factor of safety. Trial excavations were carried out in order to confirm or revise the geotechnical model and, in particular, reassess the continuity of defects in larger exposures of the weak layer. This resulted in a reduction in the Effective Continuity Assessment (ECA) and no remedial measures were required. If remedial measures had been required, restoring the canal depth to RL -3.8m and limited replacement of the weak layer in critical areas with granular material were the options considered.

5. DISCUSSION AND CONCLUSIONS

This paper presents a quantitative approach to the assessment of the effect of slickensided and/or polished defects on the effective shear strength of soil for the Raby Bay Project. Decision-making using this approach is based on careful observation of the distribution and character of defects (the structural geology) of the soil. Generalised descriptions such as "fissured" are of limited use in slope design for soil masses in the same way as the description of a rock mass as "jointed" is inadequate for rock slope design. In both cases the starting point for slope design should be an adequate understanding and description of the structural geology using clearly defined terms.

As far as geotechnical risk is concerned it is considered that the risk of overconservatism in the Raby Bay slope design has been reduced by the improved understanding of the site geology. The risk of unexpectedly adverse conditions is also likely to be lessened by an approach which is dependent on detailed observations and construction monitoring.

6. ACKNOWLEDGMENTS

Permission to publish by Civic Projects (Raby Bay) Pty.Ltd. and constructive criticism during the preparation of this paper by Maurice Philp and Philip Shaw is gratefully acknowledged.

7. REFERENCES

Burland, J.B. (1990). On the compressibility and shear strength of natural clays. Geotechnique Vol. 40 No.3 pp 329-378.

Chandler, R.J. (1984). Recent European experience of landslides in overconsolidated clays and soft rocks. Proc. Fourth International Symposium on Landslides Toronto. Vol. 1 pp. 61-81.

MacGregor, J.P., Olds R. and Fell R. (1990). Landsliding in extremely weathered basalt, Plantes Hill, Victoria. In Engineering Geology of Weak Rocks. Proc. Twenty Sixth Annual Conference of the Geological Society, edited by Cripps, J.C. and Moon, C.F., University of Leeds.

Moon, A.T. (1984). Effective shear strength parameters for stiff fissured clays. Proc. Fourth Australia New Zealand Conference on Geomechanics, Perth. Vol. I pp 107-111.

Skempton, A.W. (1977). Slope stability of cuttings in brown London Clay. Special Lecturers Volume, Ninth International Conference on Soil Mechanics and Foundation Engineering, Tokyo. pp 22-33.

Skempton, A.W., Schuster, R.L. and Petley, D.J. (1969). Joints and fissures in the London Clay at Wraysbury and Edgware. Geotechnique. Vol. 19 No.2 pp 205-217.

Stapledon, D.H. (1970). Changes and structural defects developed in some South Australian clays and their engineering consequences. Symposium on Soils and Earth Structures in Arid Climates, Adelaide. Institution of Engineers, Australia pp 39-48.

Thorne, C.P. (1984). Strength assessment and stability analysis for fissured clay. Geotechnique. Vol. 34 No.3 pp 305-322.

Williams, A.A.B. and Jennings, J.E. (1977). The in situ shear behaviour of fissured soils. Proc. Ninth International Conference on Soil Mechanics and Foundation Engineering, Tokyo. Vol. 2, pp 169-176.

The Effect of Auto-correlation on the Probability of Failure of Slopes

G.R. MOSTYN
B.E., M.Eng.Sc., B.A., M.I.E.Aust.
Senior Lecturer, University of New South Wales, Kensington, Australia
S. SOO
B.Sc., B.E.
University of New South Wales, Kensington, Australia

SUMMARY Probabilistic analyses of slopes are generally based on treating only the most significant variables as random variables. Usually simplifications are made regarding the correlation structure of these variables. This is especially so with respect to the correlation of each variable with itself in space (i.e. auto-correlation). Most analyses ignore this auto-correlation. The paper presents several cases from the literature for which probabilities of failure have been determined where auto-correlation has been ignored. These are re-analysed and the sensitivity of the computed probability of failure to various assumptions regarding the auto-correlation structure is determined. It is found that, in general, realistic assumptions regarding auto-correlation result in very significant reductions in the computed probabilities of failure for most civil engineering slopes. Thus most methods of probabilistic slope analysis can at best be regarded as producing only an index of slope stability.

1 INTRODUCTION

In the last twenty years many methods have been developed to determine the probability of failure of a slope, many of these are discussed in Mostyn and Small (1), but there is no single method that has attained the degree of acceptance as, say, Bishop's method has for deterministic analysis of slopes. For this reason it is difficult to assign acceptable limits to probabilities of failure to assist with decision making. This paper presents the results of an investigation into the effect of auto-correlation on the computed probabilities of failure for some slopes that have been analysed by various probabilistic methods.

2 PROBABILISTIC METHODS OF SLOPE ANALYSIS

The conventional method to assess the stability of a slope is to determine the factor of safety, FOS, by one of several generally accepted methods, such methods are described in almost every geotechnical engineering textbook and do not need to be further described here. The factor of safety has several drawbacks which are described by Li and Lumb (2).

An alternate method of analysis of a slope is to determine the probability of failure and use this to assess the stability or decide on further action. Acceptance of probabilistic methods has been slow, Chowdhury (3) suggests three reasons why this may be so. First, the results are not readily used by engineers; second, extra data is required to statistically describe the soil; and third, there is no agreement as to what probability of failure constitutes an unsafe slope.

Most of the methods in use to determine the probability of failure, P_f, of a slope treat the slope material as layers with given means, μ, and standard deviations, σ, for the strength parameters, generally the cohesion, c, and angle of friction, ϕ. While sometimes the correlation of c with ϕ is taken into account, it is very rare for the correlation of each of these parameters with itself in space to be taken into account, this property is called auto-correlation. Thus most methods of probabilistic slope analysis assume that a random variable, e.g. ϕ, is perfectly correlated with itself over infinite distances, so that each realisation consists of layers of soil of fixed strength.

Auto-correlation is reflected in the fact that the property of a soil within a particular layer will vary in space, but the value of this property at two points close together is likely to be similar, while the values for points remote from each other are likely to be independent of each other. Probabilistic analyses are often undertaken with the unstated assumption of perfect auto-correlation, this would only be acceptable if the resulting probabilities were similar to those obtained from analyses taking the actual auto-correlation structure into consideration.

The assumption of perfect auto-correlation allows the material property to be sometimes either very high or low throughout the layer, auto-correlation on a realistic scale acts to reduce the variance and thus these homogenous outriders are less likely.

There are several methods of describing auto-correlation, one method is to add a third parameter, the scale of fluctuation, δ, to the statistical description of the layer. This parameter is a measure of the distance within which the soil property shows relatively strong correlation with itself. In other words, the values of the parameter lying within a distance δ of each other are both likely to be either above or below the mean. Thus a small δ implies rapid fluctuations about the mean and a large reduction in variance over any failure plane; this results in a small "spread" of the performance function and for factors of safety greater than unity a smaller P_f. Conversely a large δ means much longer variations about the mean.

The concept can be extended to three dimensions, in which case δ_x, δ_y and δ_z are used. Li and White (4) have examined the literature and indicate that δ_x and δ_y are often about an order of magnitude larger than δ_z and are often of the order of 3 to 30m.

Various funtions have been used to model auto-correlation, these are generally of an exponential form and four have been described by Li and White (4).

3 PROGRAM PROBSN

Li has written a program, PROBSN, which uses a first order second moment, FOSM, method to determine the probability of failure of a slope using the generalised procedure of slices, GPS, method of analysis. Non circular and circular surfaces can be analysed and the method is rigorous in that it satisfies both force and moment equilibrium. The performance function adopted in the analysis is not the factor of safety but the safety margin, as this is more likely to be Normally distributed. The reliability of the critical surface is determined as the Hasofer-Lind reliability index, β_{HL}, described by Hasofer and Lind (5). PROBSN was ported to personal computers by Waddell (6) and Furrer & Steele (7). The resulting code contained several errors that were detected and corrected by Soo (8).

4 CASE STUDIES

In order to examine the influence of autocorrelation on the values determined for the probability of failure, several cases that had been analysed and then published in the literature were re-analysed taking into account auto-correlation. The first two cases also formed a check on the accuracy of PROBSN.

4.1 Case 1: Catalan & Cornell

Catalan and Cornell (9) used a level crossing method to determine the probability of failure of a slope, the analyses was based on a circular failure surface using the simplified Bishop method and did take account of auto-correlation.

The slope analysed was a uniform slope over a rigid base, 11 m high with a face angle of approximately 26 degrees. The slope was comprised of material with an undrained shear strength of 33.5 kPa and unit weight of 16.5 kN/m^3. The reported value of the FOS was 1.53 and equalled that obtained by PROBSN. The analyses were completed with coefficients of variation (V_s, i.e. standard deviation divided by the mean) on the undrained shear strength of 0.2 and 0.4.

The results of the analyses run by Catalan and Cornell and those obtained using PROBSN are given on Table I.

The differences between the values of P_f derived by PROBSN and those reported by Catalan and Cornell are probably due to the fact that the relationship between the scale of fluctuation, δ, in PROBSN and the correlation distances used in the refernce had to be estimated. Equally parts of the slope geometry were estimated. As expected these matters and assumptions regarding the distribution of the performance function can have a large effect on estimation of small failure probabilities. Notwithstanding these matters the broad agreement for the larger values of P_f is reasonable. In addition the rapid reduction in P_f with a decrease in δ is very apparent.

TABLE I
P_f FOR CASE 1

δ_x	δ_y	P_f PROBSN	P_f Reported
V_s = 0.2			
10000	100	3.9E-2	**
91.5	3.05	1.6E-3	7.0E-3
30.5	1.53	2.0E-4	1.0E-3
3.05	1.53	1.0E-6	1.0E-4
1.0	0.01	4.0E-8	**
V_s = 0.4			
10000	100	1.9E-1	**
100	1.0	3.2E-2	**
30.5	1.53	3.7E-2	6.0E-2
3.05	1.53	1.5E-2	9.0E-3
1.0	0.01	3.5E-3	**

** Results not reported

4.2 Case 2: Alonso

Alonso (10) analysed the Green Creek slide and included auto-correlation in his analysis. The slope analysed is shown on Figure 1, the critical circle was the conventional minimum FOS circle obtained using Bishop's method. The correlation distance was assumed to be the same in all directions. Slope material properties were (mean & standard deviation): cohesion of 30 & 9 kPa, co-efficient of friction of 0.34 & 0.052, density of 16 and 0.4 kN/m^3. Alonso obtained an FOS of 1.40 compared with 1.38 from PROBSN. The results of the analyses completed by Alonso and those obtained using PROBSN are given on Table II.

TABLE II
RESULTS FOR CASE 2

δ	c = 30 kPa		c = 15 kPa
	P_f PROBSN	P_f Reported	P_f PROBSN
10000	0.11	**	0.77
1000	0.084	**	0.78
100	0.067	**	0.82
10	0.0056	**	0.92
8	0.0043	0.008	0.93
4	0.0023	0.004	0.94
1	0.0009	0.001	0.95
0.1	0.0008	0.001	0.95
0.01	0.0008	0.001	0.95

** Not reported in reference

As can be seen from Table II there is reasonable agreement between the estimates of P_f for the two methods. In addition P_f reduces rapidly with reductions in δ, this behaviour is shown on Figure 2.

Cases 1 and 2 provide some support for the accuracy of PROBSN in that there is broad agreement with the few reported cases from the literature that have included auto-correlation in probabilistic slope analysis. The discrepancies at small P_f would be expected with almost any probabilistic analysis, but the broad agreement at higher P_f is encouraging.

All the cases analysed in the literature had estimated probabilities of failure less than 0.5 (i.e. FOS greater than

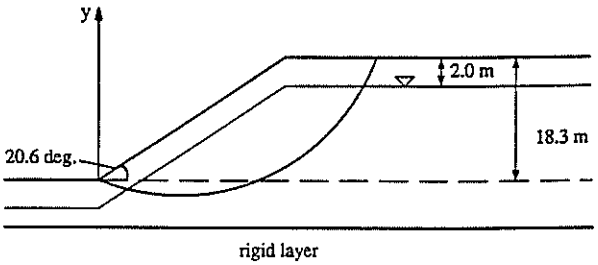

Figure 1 Slope adopted in Case 2

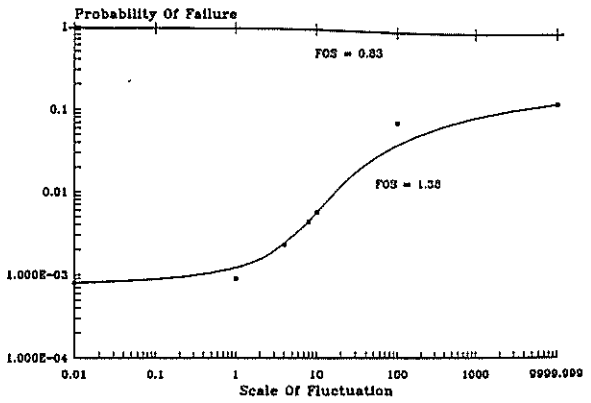

Figure 2 P_f versus δ for Case 2

one). In order to investigate the effect of autocorrelation on high values of P_f the cohesion in Case 2 was reduced to 15 kPa, this resulted in a reduction in the FOS to 0.83 and the P_f values are contained in the fourth column of Table II. It can be seen that P_f increases with a reduction in δ, as the resulting reduction in variance now acts to draw more of the realisations to failure conditions.

4.3 Case 3: Chowdhury (11)

Chowdhury (11) analysed a slope as shown in Figure 3 comprised of materials with (mean & coefficient of variation) a cohesion of 30 kPa and 30%, angle of friction of 20 degrees and 10% and unit weight of 18.8 kN/m^3 and zero. The analysis was based on circular failure surfaces and the simplified Bishop method with the critical circle being that with the minimum FOS. Auto-correlation was not considered by Chowdhury. The reported value of FOS was 1.36 with a P_f of 2.3E-2, this should be compared with the FOS obtained from PROBSN of 1.40 and the probabilities of failure given in Table III as a function of the scales of fluctuation.

TABLE III
P_f FOR CASE 3

δ_x (m)	δ_y (m)	P_f
10000	10000	1.9E-2
100	10	1.3E-3
10	10	6.6E-5
10	1	2.0E-5
1	1	8.4E-6
0.001	0.001	6.0E-6

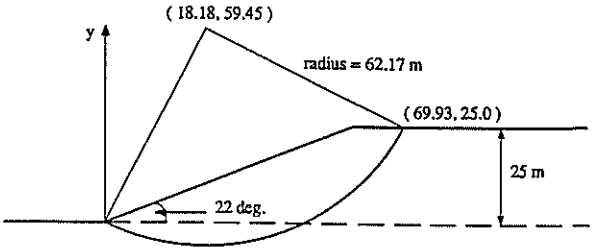

Figure 3 Slope adopted in Case 3

Here it can be seen that there is good agreement between the output of PROBSN for δ equal to 10000m and the results from the literature which were obtained ignoring auto-correlation but these P_f are one to three orders of magnitude too high if real scales of fluctuations of between 1 and 100 m in the horizontal plane are taken into account.

4.4 Case 4: Chowdhury (12)

Chowdhury (12) developed a probabilistic analysis of progressive failure, the slope analysed is shown in Figure 4 comprised of materials with a mean cohesion of 23.94 kPa and a co-efficient of variation of 50%, an angle of friction of 38 degrees and unit weight of 18.8 kN/m^3. Analyses were completed with the coefficient of variation of the angle of friction (V_ϕ) varying from 0.1 to 0.5. The analysis was based on circular failure surfaces and the simplified Bishop method. Auto-correlation was not considered. The FOS obtained from PROBSN was 2.41 for circle A. The probabilities of failure as functions of V_ϕ and δ are given in Table IV.

TABLE IV
P_f FOR CASE 4

δ_x	δ_y	P_f for $V_\phi = 0.10$	P_f for $V_\phi = 0.50$
Chowdhury			
∞	∞	8.4E-3	3.3E-2
PROBSN			
10000	10000	8.9E-3	2.7E-2
10000	100	7.8E-3	2.6E-2
100	10	1.9E-3	1.2E-2
100	1	8.2E-7	1.2E-4
10	1	2.4E-7	6.0E-5
0.001	0.001	≈ 0	6.0E-8

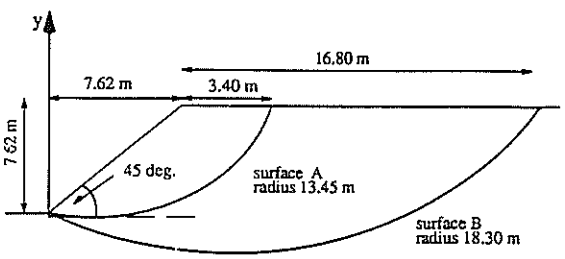

Figure 4 Slope adopted in Case 4

It can be seen that there is good agreement between Chowdhury and PROBSN when δ is large relative to the slope but as δ approaches realistic values then P_f reduces by several orders of magnitude.

4.5 Case 5: D'Andrea & Sangrey

D'Andrea and Sangrey (13) analysed the slope shown on Figure 5 using conventional critical slip circle, simplified Bishop analysis. Auto-correlation was not considered. The slope was comprised of material with a mean cohesion of 24.75 kPa and unit weight of 16.33 kn/m^3. The coefficient of variation of the cohesion (V_c) was varied between 0.05 and 0.35, a comparison of the results obtained by PROBSN with the referenced paper for "no auto-correlation" is given in Table V.

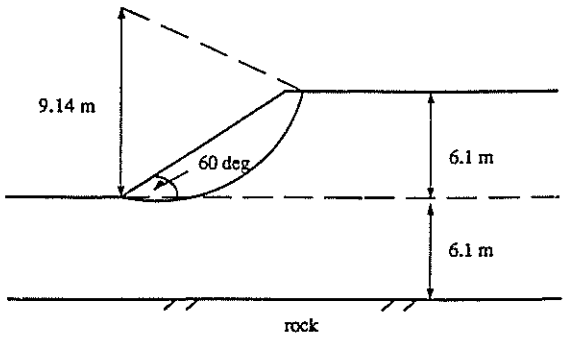

Figure 5 Slope adopted in Case 5

TABLE V
COMPARISON OF P_f FOR CASE 5

V_c	P_f PROBSN *	P_f Reported
0.05	0.021	0.054
0.15	0.112	0.136
0.25	0.210	0.221
0.35	0.277	0.281

* Determined with $\delta_x = \delta_y = 10000$

These results are in good agreement, especially for the larger P_f.

The effects of auto-correlation on the probabilities of failure as functions of V_c and δ are given in Table VI.

TABLE VI
P_f FOR CASE 5

δ_x	δ_y	P_f for $V_c = 0.05$	P_f for $V_c = 0.35$
10000	100	0.021	0.27
1000	10	0.018	0.24
100	10	0.016	0.24
10	1	0.007	0.12
1	0.01	0.004	0.055
0.001	0.001	0.004	0.052

As seen above there is good agreement between D'Andrea & Sangrey and PROBSN when δ is large relative to the slope but as δ approaches realistic values then P_f reduces five fold. This is a smaller drop than for some of the other cases as P_f is larger and the greatest effects are in the tails of the probability curves. It should also be noted that this slope has a FOS of 1.3, but using the common methods of probabilistic slope analysis (i.e. ignoring auto-correlation) has a P_f of between 2 and 27% depending on the variance of the cohesion. These are large P_f for an "apparently" stable slope.

If the strength is reduced so that the FOS falls below unity then the effect of δ on P_f is much reduced. For a cohesion of 18 kPa, the FOS is 0.93 and the P_f varies between 57 and 71 percent depending on auto-correlation and the coefficient of variation for the strength.

5 CONCLUSIONS

A summary of the comparisons contained in the previous sections is presented on Figure 6. The horizontal axis is the P_f obtained by PROBSN assuming perfect auto-correlation (i.e. δ=10000m) for the different slopes. The vertical axis gives the P_f for the same slope when δ_x is set at 10m, some of these had to be interpolated from other values of δ_x. PROBSN was used even for the perfect auto-correlation cases to eliminate any variation between different analyses.

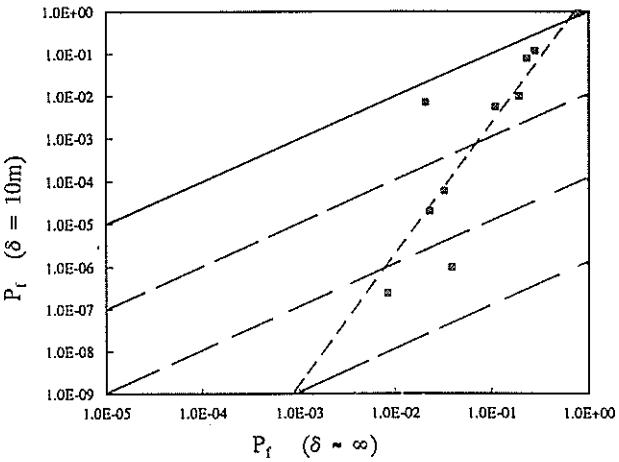

Figure 6 Effect of auto-correlation on P_f

A number of features evident on this figure are:

* The solid line represents equality between the two analyses, the broken lines below this are contours at ratios of two orders of magnitude between the answers obtained with and without auto-correlation.
* For a P_f of 50% there is no difference between the answers as a reduction in variance does not change P_f but only a change in the mean of the performance function would.
* Above a P_f of 50% ignoring auto-correlation is not conservative, this is not really significant as P_f values of this magnitude will always present a problem.
* As the P_f decreases the ratio between the two results increases rapidly, from unity at P_f equal to 50% to 10^5 for P_f ($\delta=\infty$) equal to 1%.
* A line of best fit to the logrithmic data is shown as a dashed line. It can be seen from this that for realistic values of P_f ($\delta=\infty$) for civil engineering structures, say 10 to 0.1%, there is between two and

six orders of magnitude difference between the results generally reported and the more realistic results obtained taking account of auto-correlation. These artificially high values of P_f are likely to explain some practising engineers reluctance to adopt probabilistic analyses.

* The results are monotonically increasing preserving rank of P_f on both axes, thus results of analysis based on perfect auto-correlation can be used as an index of stability (and may be better than FOS).
* Even though the results obtained ignoring auto-correlation are conservative, the fact that they are several orders of magnitude in error indicates that they should not be used in economic analysis but only as an index.

It should be noted that for P_f lower than about 1% other factors such as assumed distribution of the performance function, method of analysis, etc can also have large effects on the derived P_f.

6 ACKNOWLEDGEMENTS

The authors would like to acknowledge the work undertaken by Peter Waddell in undertaking most of the transfer of PROBSN from mainframe to PC. This work was extended by Matt Furrer and John Steele as a final year project. Finally the assistance provided by K.S. (Victor) Li and earlier Weeks White with PROBSN is gratefully acknowledged.

7 REFERENCES

1. Mostyn, G.R. and Small, J. "Methods of Stability Analysis", Soil Slope Instability and Stabilization (eds Walker, B.F. and Fell, R.), pp71-120, Balkema, 1987.

2. Li, K.S. and Lumb, P. "Probabilistic Design of Slopes", Canadian Geotechnical Journal, V24, pp520-531, 1987.

3. Chowdhury, R. "Analysis Methods for Assessing Landslide Risk - Recent Developments", Proc. 5th Int. Sym. on Landslides, Lausanne, V1, pp515-524, 1987.

4. Li, K.S. and White, W. "Probabilistic Characterisation of Soil Profiles", Research Report No. 19, Department of Civil Engineering, The University of New South Wales, Australian Defence Force Academy, Canberra, 54p, 1987.

5. Hasofer, A.M. and Lind, N.C. "Exact and Invariant Second Moment Code Format", J. Eng. Mech. Div, A.S.C.E., Vol 100, pp111-121, 1974.

6. Waddell, P. "Application of a Computer Program to the Study of the Effects of Autocorrelation on a Probabilistic Slope Stability Analysis", Master of Engineering Science Report, School of Civil Engineering, The University of New South Wales, Sydney, 1988.

7. Furrer, M. and Steele, J. "Use of PROBSN in Examining the Effects of Autocorrelation on the Probability of Failure of a Slope", Final Year Report, School of Civil Engineering, The University of New South Wales, Sydney, 1989.

8. Soo, S. "The Effects of Autocorrelation on the Probability of Failure of a Slope", Final Year Thesis, School of Civil Engineering, The University of New South Wales, Sydney, 1990.

9. Catalan, J.M. and Cornell, C.A. "Earth Slope Reliability by a Level Crossing Method", J. Geot. Eng. Div, A.S.C.E., V102, GT6, June, pp591-604, 1976.

10. Alonso, E.E. "Risk Analysis of Slopes and its Application to Slopes in Canadian Sensitive Clays", Geotechnique, V26, No 3, pp453-472, 1976.

11. Chowdhury, R. "Practical Aspects of Probabilistic Studies for Slopes", Soil Slope Instability and Stabilization (eds Walker, B.W. and Fell, R.), pp299-304, Balkema, 1987.

12. Chowdhury, R. "Reliability and Interdependence in Geomechanics", Proc. 4th Int. Conf. on the Application of Statistics and Probability to Soil and Structural Engineering, Florence, pp1629-1642, 1983.

13. D'Andrea, R.A. and Sangrey, D.A. "Safety Factors for Probabilistic Slope Design", J. Geot. Eng. Div., A.S.C.E., V108, GT9, Sept, pp1101-1118, 1982

Beanpole Corner Landslide Stabilisation

G.J. SAUL
B.E., M.Sc., M.I.P.E.N.Z.
Senior Engineer, Works Consultancy Services Ltd
C.K. ANDERSON*
B.E., M.Sc., M.I.P.E.N.Z.
Geotechnical Engineer, Barrett Fuller & Partners Ltd
C.J. GRAHAM
B.E., Ph.D., M.I.P.E.N.Z.
Director, Barrett Fuller & Partners Ltd
*Formerly with Works Consultancy Services Ltd, New Zealand

1. INTRODUCTION

The Pukerua to Paekakariki Bay section of the North Island, New Zealand main trunk railway line and State Highway One (Figure 1) are located at the foot of a steep 45° coastal rock slope with a 35° head slope. The rock slope was formed by wave action during the last interglacial period and comprises weathered and closely jointed greywacke and argillite which rises 250 to 300m above sea level. The 35° head slope comprises colluvium derived from greywacke. Extensive old scree deposits have accumulated at the toe of the slope and several localised areas of slope instability have caused problems in the past.

The Beanpole Corner slide is a shallow rockslide located on a broad spur above the railway line. The landslide has a long history of instability which started before 1940 as a small slide just above the railway line and progressed 65 m up the rock slope in a series of failures, one of which derailed a freight train in the 1960s. During 1979, a portion of the slide is believed to have moved up to 5 m during or following a period of heavy rainfall and continued creep movement was observed. This portion was located on the head slope immediately above the steeper rockface, 65 m above the railway. The positions of these features are shown in Figure 1.

Preliminary slope assessment concluded that without stabilisation there was an unacceptably high risk of complete and rapid failure closing the railway below. This paper describes the investigation, monitoring, stability assessment, design and construction of engineering works to stabilize the slide. Design and construction supervision of the remedial works was carried out by Works Consultancy Services Ltd for New Zealand Rail Ltd.

2. SCOPE OF INVESTIGATIONS AND INSTRUMENTATION

An engineering geological assessment of the slide was carried out in 1981 by New Zealand Geological Survey, (DSIR), based on surface mapping of the geology and a review of previous instability problems. Site investigation and monitoring was recommended to enable remedial works to be designed.

The following techniques were used to investigate and instrument the slide mass.

(a) A topographical survey.

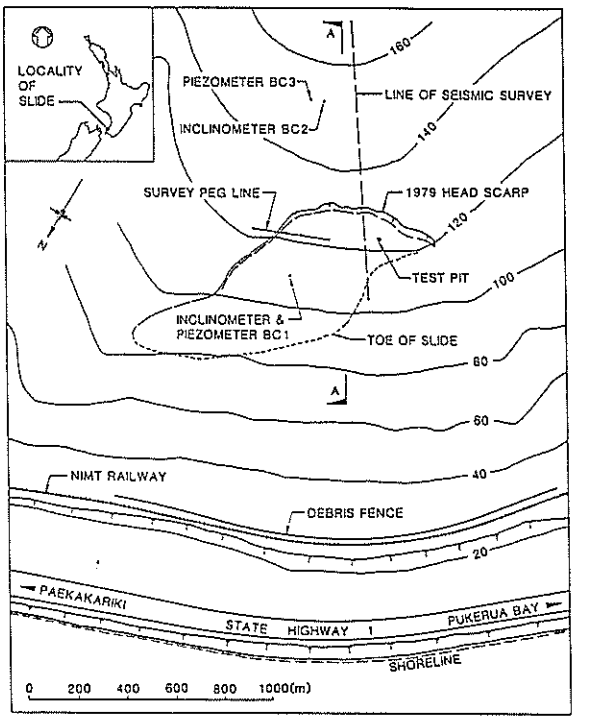

Figure 1 Plan of Landslide Area.

(b) A seismic profiling survey.

(c) One cored borehole to 16 metres depth (BC 1).

(d) A test pit to 9 m depth within the slide mass.

(e) A line of survey pegs across the head scarp area.

(f) Two inclinometers (BC 1 and BC 2).

(g) Two pneumatic piezometers (BC 1 and BC 3).

(h) Installation of a rain gauge.

The position of these investigations and instruments is shown on Figure 1.

3. SITE OBSERVATIONS

The geological mapping, test pit and cored bore hole indicated that the sliding mass was a greywacke derived colluvium comprising loose to moderately dense, angular gravel in a silty matrix with occasional clay lenses. A 4.5 m thick, silty clay layer with greywacke gravel sized inclusions was located at the base of the slide mass. Total slide thickness was

approximately 10 m. Bedrock below the slide comprised closely jointed, argillaceous greywacke with irregular beds 200-500 mm thick, dipping 45° to 65° into the slope.

The location and geometry of the active failure surface was determined from the results of both investigations and monitoring, with inclinometer results providing the most valuable data. The failure plane was believed to lie within the thick silty clay layer. Figure 2 illustrates the section geometry adopted for slide analysis and remedial works design. Total slide volume was estimated at 30,000 m^3.

Accurate determination of piezometric levels was not achieved from the pneumatic piezometers although water was observed seeping into the test pit at 5 m depth. Correlation of slide movement with rainfall indicated that increased movement occurred when the three month average rainfall exceeded 100 mm, which suggested a link between slide stability and piezometric pressure. Figure 3 illustrates the correlation developed.

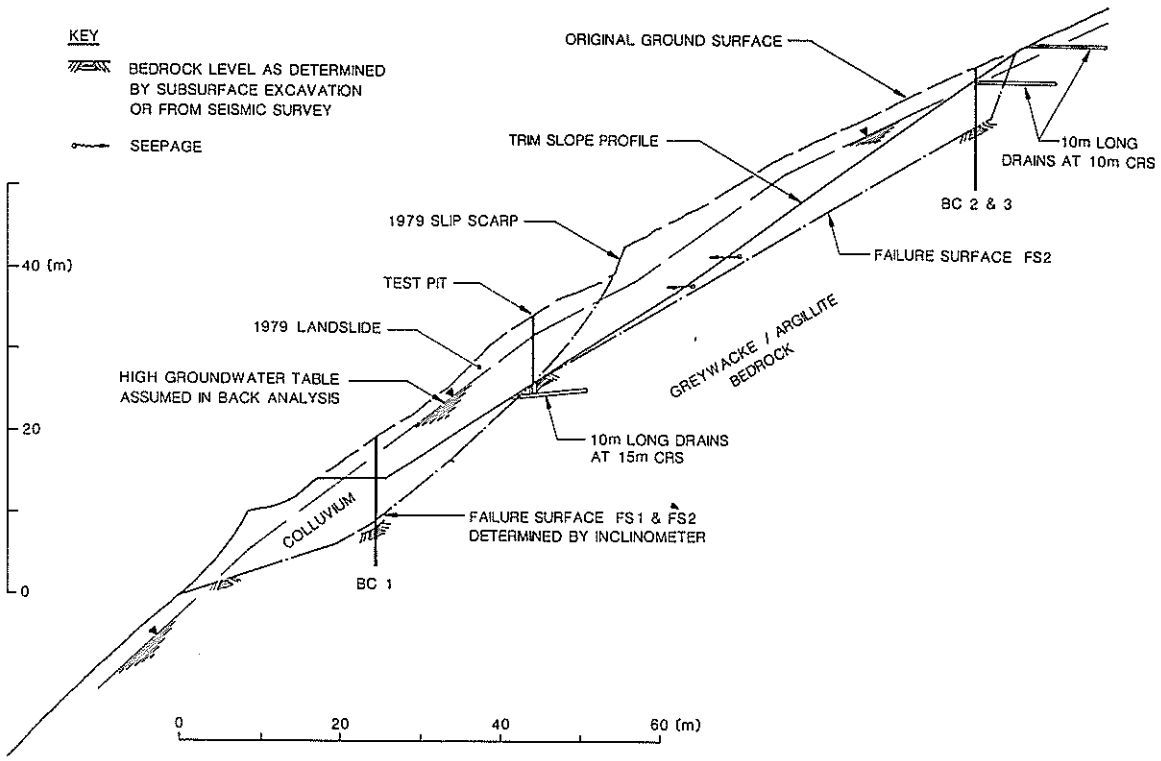

Figure 2 Cross Section A-A through Landslide.

The movement history prior to 1982 is uncertain although there is anecdotal evidence of a slide displacement of up to 5 m following heavy rain in 1979. Monitoring of slide movement using survey pegs began in mid 1982 and Figure 3 illustrates the history of movement up to 1985, and the relationship between rainfall and slide velocity. Movement continued at an average rate of 70 mm/year from 1985 to 1989. Inclinometer BC1 in the active slide was sheared off in December 1983 after 70 mm of deformation in 11 months. Inclinometer BC2 confirmed that the slope above the slip scarp was not moving. However, materials above the scarp were similar to the actively sliding materials and there was the potential for progressive slope failure.

4. HAZARD AND RISK ASSESSMENT

Continued creep movements of the slide, coupled with the observed acceleration of movement following wet weather, indicated that there was an unacceptably high risk of a rapid failure blocking the railway. This could have led to disruption of commuter and freight traffic and possible loss of life.

A 4 m high debris fence had been installed just above the track through the slide area in the 1960s and had proved effective in preventing boulders and small rock falls from reaching the track. After the 1979 failure, an alarm was installed on the fence to trigger signal lights should the fence be deformed by falling material.

5. STABILITY ASSESSMENTS

Observations of slide movement and the relationship between slide movement and rainfall were used to establish that the slide was at limiting equilibrium prior to stabilization works. No clear correlation was established between piezometric level and slide movement.

The history of slide movement and the consequences of failure were considered sufficient reason to establish the requirement for stabilization works. Remedial works

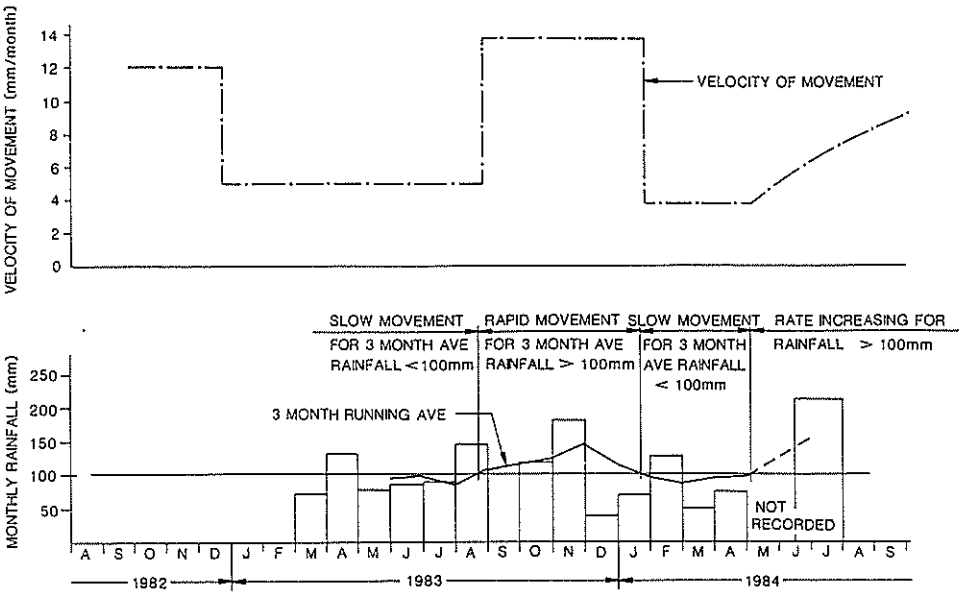

Figure 3 Graphs of Slide Velocity and Rainfall.

including slope trimming and drainage to control groundwater rise during prolonged wet periods were considered.

A geotechnical model of the slide was established which comprised ground topography based on available survey data, the failure surface geometry derived from subsurface geological observations and surface mapping together with material strengths derived from back analyses of the slide. The model is illustrated in Figure 2.

Back analysis assuming limiting equilibrium conditions and two different piezometric cases (dry and wet slopes) were used to determine material shear strength parameters for remedial work design because materials in the slide base were variable and it was not possible to establish shear strength with certainty. The piezometric line assumed for the wet slope case is shown in Figure 2. These analyses yielded the following effective shear strength parameters:

Dry Slope $c' = 0$ kPa $\quad \phi' = 31^{o}$

Wet Slope $c' = 27$ kPa $\quad \phi' = 35^{o}$

The "wet slope" parameters were considered more representative of the materials observed and high ground water conditions inferred during the movement event. Therefore the wet slope strength parameters were adopted for final design. Limit equilibrium analysis of the geotechnical model was carried out using the vertical slice Sarma method (1). The stability analysis results for the following three cases are presented in Table 1:

(a) The Original Situation; which models the original level as shown in Figure 2.

(b) Post Construction - Wet Slope; which models the design slope trim as shown in Figure 2 with a groundwater level coincident with the design trim profile.

(c) Post construction - Drained Slope; which models the slope trim with fully effective drainage (an ideal but impractical situation).

TABLE I

STABILITY ANALYSIS RESULTS

Failure Surface	Original Situation	Post Construction Wet Slope	Post Construction Drained Slope
Active Portion (SF1) .	1.0	1.3	2.5
Headslope (FS2)	1.0	1.6	2.2

Drainage is generally more cost effective than earthworks for improving slide stability. However, because of the uncertainties in the specific relationship between slide movement and groundwater pressure, uncertainty in level of control achievable with drainage, and the possibility of progressive upslope development of the slide, slope trimming was adopted as the primary means of stabilizing the slide. The extent of slope trimming was determined from analysis and is illustrated in Figure 2.

Analysis indicated slope trimming gave an acceptable stability increase for the two modelled surfaces (FS1 and FS2). However nominal drainage was considered desirable to stabilise the head slope (FS2) because of the difficulty in predicting future mechanisms for progressive development of the slide and because access to the site would be difficult after remedial work.

6. REMEDIAL WORK

Access to the site was constructed from farm land above the landslide and only tracked vehicles were able to negotiate the steep gradients along the access track.

Slope trimming involved a 60 m high cut at a grade of 1.4H to 1V and removal of 31,000 cubic metres of material. Earthworks were carried out between January and September 1990. Material was cut from the slope and pushed into and down a side gully to the railway line where it was loaded out by trucks to a dump site. Excavation was halted while trains passed beneath the site because of the steep slopes and potential for boulders loosened by construction to roll downslope and bounce over the debris fence onto the railway.

Three rows of 10 m long horizontal drains at 10 m centres were planned from benches formed in the head of the cut slope to control ground water in the slope above the active portion. The lower two rows of five drain holes were dry and the highest row was not installed. A seepage area was observed during excavation at about mid slope and a bench was formed just below the seepage to channel increased flow during wet weather into the side gully. The seepage continued beneath the bench and a row of 10 m long horizontal drains at 15 m centres was installed from a bench formed at RL 110 m. A slight flow (less than 1 li/m) was encountered from only one of these drains.

7. POST CONSTRUCTION PERFORMANCE

Geological conditions encountered during construction were similar to conditions predicted from investigation results. The previous monitoring instrumentation was removed during earthworks and surface survey marks have been installed since. Regular repeat surveys of these marks is planned with a re-survey after the first winter.

8. SUMMARY AND CONCLUSIONS

The Beanpole Corner slide presented a potential hazard to the operation of a busy section of the main trunk railway line. The slide was investigated and monitored, remedial works were designed and constructed. Principal conclusions from the work follow:

a) A possible relationship between slide movement and rainfall was identified but with the limited instrumentation it was not possible to establish a relationship between groundwater pressure and movement.

b) The design standard for the active part of the slide and the slope above was based on an assessment of geological and groundwater uncertainties, the hazard and the difficult site access after remedial work was completed.

c) Slope stabilisation measures were able to be designed accounting for uncertainties of material strengths and piezometric pressures.

d) Drainage was installed but no appreciable flows from these holes were observed. Drainage holes may act as a control on future groundwater rise during prolonged wet periods.

Post construction monitoring has been installed but at the time of paper preparation results of resurvey were not available.

9. ACKNOWLEDGEMENTS

The authors wish to thank New Zealand Rail Ltd and Works Consultancy Services Ltd for their permission to publish this paper. Acknowledgement is made to the many members of Works Consultancy Services Ltd (formerly the Ministry of Works and Development) and DSIR who worked on the investigation, design and construction of this project.

10. REFERENCES

1. Sarma, S.K., Analysis of Embankments and Slopes. Geotechnique, Vol.25, No.3 1973.

A Simple Method for Assessing Effects of Earthquakes on Slopes

T.J.E. SINCLAIR
M.A., M.Sc., D.I.C., C.Eng., M.I.C.E., M.I.P.E.N.Z.
Principal, Tonkin & Taylor Ltd, Auckland

SUMMARY A simple method is proposed for assessing the reduction in factor of safety of a slope due to an earthquake or of estimating the yield acceleration at which deformations might occur. The method is suitable for first approximations or for multi-point calculations such as required for risk or hazard mapping, where accuracy can be sacrificed in favour of highlighting regions of concern needing more detailed investigation or analysis. The simple "rule-of-thumb" is derived and the limitations discussed in relation to some validation calculations.

1. INTRODUCTION

For quantitative Risk Assessments, it is often convenient to have a quick and easy method of assessing the effects of an earthquake on soil slopes without the need for detailed analysis and computer methods.

Examples of such situations might be:

- Small budget tasks such as assessing stability of house sites
- Multi-site analyses such as assessing stability of road cuts or fills over long distances or mapping landslip hazard over large areas of irregular terrain

The purpose of this paper is to suggest a simple method of estimating the reduction in factor of safety of a slope due to an earthquake or, conversely, of estimating the "yield" acceleration at which an earthquake may cause deformation of a slope.

The recognised methods of taking account of earthquakes in slope stability evaluation have been extensively documented. For example, Martin (1988) gives a state-of-the-art account based primarily on the Makdisi and Seed (1978) method of assessing stability in terms of deformation. This, however, derives from the pseudo-static stability approach, using any of the various conventional analytical methods (See Bromhead, 1986). Sarma (1973, 1987) adopts a different approach, defining stability of a slope in terms of the critical acceleration which would just cause "failure". These methods may or may not require a computer. Simplified methods using charts or tables have been described by Prater (1979, 1985), Koppula (1984) and Hadj-Hamou & Kavazanjian (1985). All of the above examples, including the simplified methods, are more rigorous than that proposed in this paper but tend to require some consideration of the site specific complexities. The proposed simple "rule-of-thumb" depends only on the slope angle and the factor of safety of the slope immediately prior to the earthquake.

2. CONCEPT

The great majority of natural soils have sufficient fines to allow the sudden loading (or unloading) of an earthquake event to be considered undrained. In this situation, soil mechanics theory suggests that the shear strength on a potential slip surface during the first sudden shearing movements of an earthquake is the same as immediately before the earthquake. This implies that an earthquake only changes the "driving" forces and does not affect the "resisting" forces.

Of course, such a statement ignores the potential for strength loss due to cyclic loading, a factor which will be discussed in the next section.

Consider simple slopes as shown in Figure 1. The factor of safety (F) is defined by:

$$F = \frac{\text{Resisting forces/moments}}{\text{Driving forces/moments}} = \frac{R}{D} \quad \text{- (1)}$$

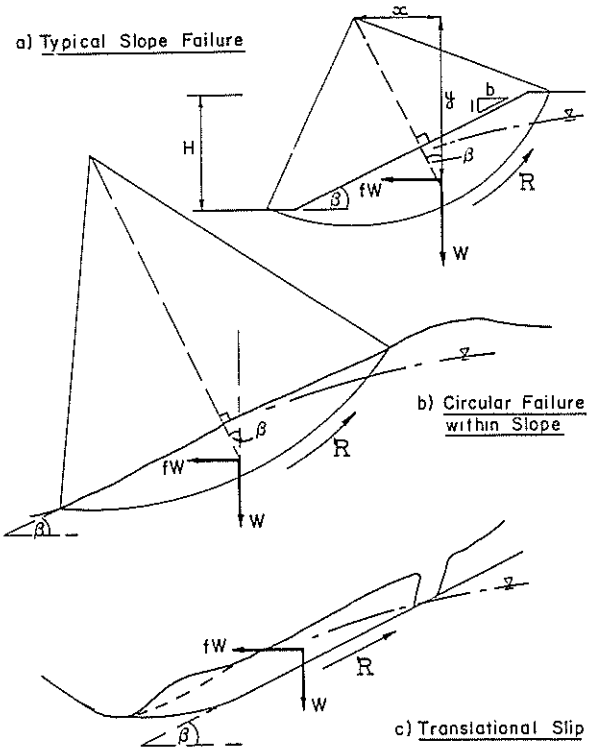

Figure 1: Failure modes

For static conditions, the factor of safety (F_o) is given by:

$$F_o = \frac{R}{Wx} \quad \text{for Figures 1(a) and (b)} \quad \text{- (2a)}$$

where x is the horizontal distance between the centre of the slip circle and the centre of (slip) mass

$$\text{or } F_o = \frac{R}{W\sin\beta} \quad \text{for Figure 1(c)} \quad \text{- (2b)}$$

Now, if an earthquake causes a horizontal acceleration (fg) to be applied to the slip mass, then the "factor of safety" under earthquake (F_e) becomes:

$$F_e = \frac{R}{fWy+Wx} \quad \text{for Figures 1(a) and 1(b)} \quad \text{-(3a)}$$

where y is the vertical distance between the centre of the slip circle and the centre of (slip) mass

$$\text{or } F_e = \frac{R}{fW\cos\beta+W\sin\beta} \quad \text{for Figure 1(c)} \quad \text{-(3b)}$$

From equations (2) and (3), the ratios of earthquake to static factors of safety are:

$$\frac{F_e}{F_o} = \frac{1}{1+f(y/x)} \quad \text{for Figures 1(a) and (b)} \quad \text{-(4a)}$$

$$\text{or } \frac{F_e}{F_o} = \frac{1}{1+f\cot\beta} \quad \text{for Figure 1(c)} \quad \text{-(4b)}$$

For any circular slip contained entirely within a homogeneous slope, as illustrated in Figure 1(b), the ratio (y/x) is equal to $\cot\beta$. By examination of Figure 1(a), it is clear that (y/x) is approximately equal to $\cot\beta$ for most typical slips which are not deep seated and for slopes flatter than about 34° ($\cot\beta = 1.5$). This can be checked using computer methods or stability charts (e.g. Janbu, 1968 or Cousins, 1978) and for either total stress or effective stress parameters. Further validation of this is discussed in the following section.

In summary, therefore, the reduction in factor of safety of any slope of face angle β, subjected to a horizontal acceleration (fg), is given approximately by:

$$F_e/F_o = 1/(1+f\cot\beta) = 1/(1+fb) \quad \text{-(5)}$$

where $b = \cot\beta$

Alternatively, the yield acceleration coefficient (f_y) is given by equation (5) when $F_o = 1$:

$$f_y = (F_o-1)/\cot\beta = (F_o-1)/b \quad \text{-(6)}$$

3. VALIDITY

There are several factors which lay the simple formulae of equations (5) and (6) open to question. For example:

(a) Strength loss:

Almost all soils exhibit some tendency to increase pore pressures on repeated cyclic loading. However, it is now generally recognised (e.g. Seed and Idriss, 1982) that substantial strength loss does not occur until the effective onset of "liquefaction". Soils susceptible to liquefaction, though dangerous, are relatively infrequent in slopes and would, of course, negate the purpose of this paper.

(b) Shear surface:

One of the simplifying assumptions is that the critical slip surfaces for the static and dynamic conditions are the same. This, of course, may not be true because the static factor of safety (F_o) could be calculated using effective stress methods whereas the factor of safety under earthquake conditions (F_e) would be calculated using total stress methods. This does not appear to make much difference (see paragraph d following).

(c) Vertical acceleration:

The simple method allows for only horizontal accelerations. This is the normal assumption in almost all other dynamic stability methods. Prater (1979) points out that the peaks of the horizontal and vertical components of acceleration are generally not in phase and suggests that a value of 0.3 for the ratio of vertical/horizontal acceleration would be realistic. Equation (5) can be modified to allow for a vertical acceleration to give:

$$\frac{F_e}{F_o} = \frac{1}{1+f_v+f_hb} \simeq \frac{1}{1+f_h(b+0.3)} \quad \text{-(7)}$$

where f_v and f_h are the vertical and horizontal acceleration coefficients and $f_v \simeq 0.3\, f_h$.

(d) Geometry:

As discussed previously, the geometric assumptions are only true for translational slides and circular slips contained entirely within a slope. Such failure modes, however, make up a large proportion of the types of slips which do occur in natural slopes as a result of an earthquake (e.g. Hopkins et al., 1991). Deep seated "base" failures tend to be rare in this context, particularly because accelerations tend to be greater towards the top of a slope.

To validate the approach for more generalised conditions and slopes typical of road cuts or water retention embankments (for example), conventional pseudo-static stability studies were carried out using the autosearch facility of the computer program UTEXAS2 (Wright, 1985). The cases tested are summarised in Figure 2 and the results are shown in Figure 3. It can be seen that, despite the varied geometry and groundwater conditions, the relationship holds reasonably well for $b > 1.5$, though it can't be accused of being conservative.

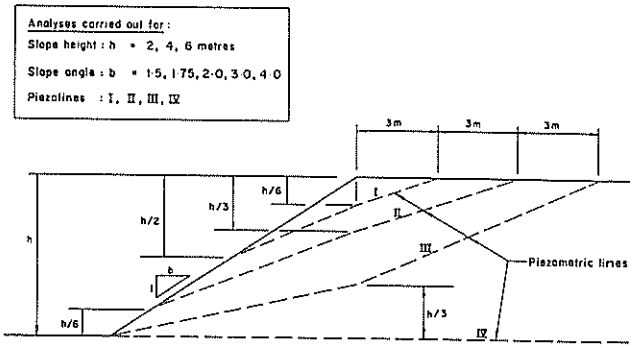

Figure 2: Validation test examples

4. CONCLUSION

A simple method has been suggested for assessing the effects of earthquakes on a slope. It is probably best to use the method for estimating the "yield" acceleration for subsequent estimates of slope deformation. Ignoring vertical accelerations, the relationship is given as:

$$f_y = (F_o-1)/b$$

where f_yg = the "yield" acceleration (g = gravity)

F_o = the static factor of safety immediately prior to the earthquake

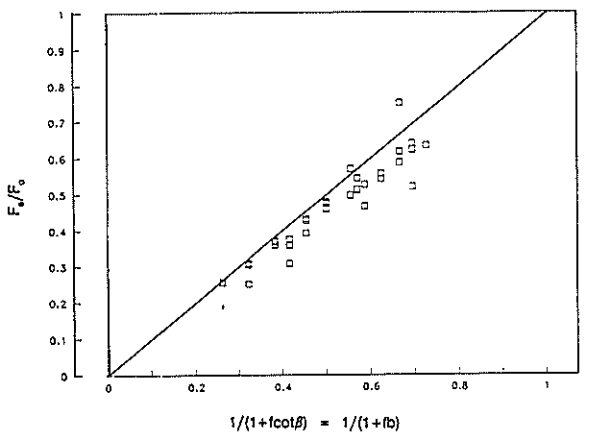

Figure 3: Results of validation tests (excluding results with numerical problems)

b = the slope "gradient" or the cotangent of the slope angle

To allow for the vertical component of ground acceleration, it is suggested that the value of 0.3 may be added to "b" in the above relationship.

There are many limitations of this very simple "rule-of-thumb" but if it is used for just approximate estimates (as would be the case for any deformation estimate) or for multi-site analyses such as would be required for risk analyses for road cuts, flood defences or landslip hazard mapping, then the approximations compare very favourably with other assumptions relating to variations in geometry, groundwater conditions and soil parameters.

5. REFERENCES

1. Bromhead, E.N. (1986). The stability of slopes. Surrey University Press, London or Chapman and Hall, New York.

2. Chang, C.J., Chen, W.F. and Yao, J.T.P. (1984). Seismic displacements in slopes by limit analysis. Journ. Geotech. Eng. Div., ASCE, Vol.110, No.7, pp 860-874.

3. Cousins, B.F. (1978). Stability charts for simple earth slopes. Journ.Geotech. Eng. Div., ASCE, Vol.104, GT2 pp 267-279.

4. Hadj-Hamou, T. and Kavazanjian, E. (1985). Seismic stability of gentle infinite slopes. Journ. Geotech. Eng. Div., ASCE, Vol.111, No.6., pp 681-697.

5. Hopkins, D.C., Clark, W.D., Matuschka, T. and Sinclair, J.C. (1991). The Philippines earthquake of July 16, 1990; Report on field visit by the NZNSEE reconnaissance team. Bulletin of the NZ Nat.Soc. for Earthquake Eng., Vol.24, No.1, pp 3-95.

6. Janbu, N. (1968). Slope stability computations. Soil Mechanics and Foundation Engineering Report, Technical University of Norway, Trondheim.

7. Koppula, S.D. (1984). Pseudo-static analysis of clay slopes subjected to earthquakes. Geotechnique 34, No.1, pp 71-79.

8. Makdisi, F.I. and Seed, H.B. (1978). A simplified procedure for estimating dam and embankment earthquake - induced deformations. Journ. Geotech.Eng.Div., ASCE, Vol.104, No. GT7, pp 849-877.

9. Martin, G.R. (1988). Geotechnical aspects of earthquake engineering, State-of-the-art Report No.2. 5th ANZ Geomechanics Conference, Sydney.

10. Prater, E.G. (1979). Yield acceleration for seismic stability of slopes. Journ. Geotech. Eng. Div., ASCE, Vol.105, No. GT5, pp 682-687.

11. Prater, E.G. (1985). Stability of cuttings considering variable cohesion and earthquake effects. Proc. 11th Int.Conf. Soil Mech. & Found.Eng., San Francisco, Balkema, Rotterdam.

12. Sarma, S.K. (1973). Stability analysis of embankments and slopes. Geotechnique, 23 No.3, pp 423-433.

13. Sarma, S.K. (1987). A note on the stability analysis of slopes, Geotechnique 37, No.1, pp 107-111.

14. Seed, H.B. and Idriss, I.M., (1982). Ground motions and soil liquefaction during earthquakes, Monograph Series, Earthquake Engineering Research Institute, Berkeley, Calif.

15. Wright, S.G. (1985). UTEXAS2: A computer program for slope stability calculations. Report to US Army Engineer District, Fort Worth, Corps of Engineers.

Assessment of Strong Motion During 1989 Newcastle Earthquake

D.J. WILLIAMS
B.E., Ph.D., M.I.E.Aust.
Senior Lecturer in Civil Engineering, The University of Queensland

SUMMARY The strong motion data collected during recent earthquakes, particularly those occurring in seismically active regions of the world, has highlighted the importance of site conditions in determining amplification and the greater hazard posed by continental earthquakes compared with plate margin earthquakes of the same magnitude. The paper outlines an approach for assessing the strong motion during the 1989 Newcastle, Australia continental earthquake, for which only intensity data were available. It is shown that a rational and useful assessment is possible. From this assessment, estimates are made of the likely level of amplification which occurred during the Newcastle event, giving rise to the widespread damage observed. The estimated amplifications are shown to be in line with available worldwide data.

1. INTRODUCTION

The state-of-the-art of earthquake engineering has made rapid advances over the last few years, due largely to the strong motion data which has been collected during recent earthquakes in seismically active regions of the world. Acceleration data collected during the 1985 Michoachan earthquake, which caused considerable devastation to parts of Mexico City, demonstrated the extent to which soft soil deposits and structures of certain critical aspect ratios can amplify rock motions, particularly those of low amplitude and low frequency. While the possibility of amplification was known before this event (1,2), the level of amplification measured at Mexico City was far higher than anticipated. The 1989 Loma Prieta earthquake and subsequent aftershocks triggered numerous accelerometers in the surrounding area, providing the most valuable strong motion database in existence.

There is increasing appreciation of the importance of frequency and of the greater damage potential of a continental earthquake compared with one of similar magnitude occurring at a plate margin. However, there is a difficulty in assessing ground motions during the relatively infrequent and widely scattered earthquakes which occur in regions of relatively low earthquake hazard, due to the absence of strong motion instruments. Reliance must be placed on far-field seismograph records and macroseismic data in the form of "felt reports", from which intensities are assigned. In this paper, an assessment is made of the ground motions experienced during the damaging 1989 Newcastle, Australia continental earthquake, drawing on the data available for this event and making use of worldwide data to provide some validation of the results obtained. From this assessment, estimates are made of the likely level of amplification which occurred during the Newcastle event, giving rise to the widespread damage observed. The estimated amplifications are shown to be in line with available worldwide data.

2. SITE SPECIFIC AMPLIFICATION

Okamoto (1) suggested that the considerable differences in the levels of earthquake damage sustained at sites roughly equi-distant from the epicentre of a given earthquake are due mainly to differences in ground conditions. The amplification of ground shaking and resulting greater damage which can occur at soft soil sites was explained in terms of the resonance of the soil column due to multiple reflections of the incident waves. Resonance is a function of the thickness, density, and shear wave velocity of the soil profile, the density and shear wave velocity of the bedrock, and the amplitude and frequency content of the earthquake ground motions. The soil profile is generally non-homogeneous and multi-layered, and the properties of the bedrock may also vary. Okamoto presented measured data indicating amplification up through a weathered rock profile in excess of 2-fold, and similar amplifications up through a soft soil profile. Reclaimed land overlying soft soils was identified as being particularly susceptible to amplification and earthquake damage.

The degree of amplification across a material boundary is a function of the impedance gradient across the boundary, impedance being the square root of the product of the material density and its shear wave velocity. Simplified analyses (1) involving a single homogeneous, elastic soil layer overlying homogeneous, elastic bedrock suggested amplifications of up to 10-fold. Up to a 2-fold amplification was predicted across the rock/soil interface, although the greater the impedance gradient from hard to soft material, the more difficult it is for the earthquake energy to be transmitted. The reflection of ground motion at the ground surface can lead to a further doubling of the incident ground motion. Resonance accounted for the remainder of the amplification. In the more general case of a non-homogeneous, multi-layered subsurface conditions, complex ground motions will result from the transmission and relection of ground motions at material boundaries. The most marked amplification will occur close to the ground surface, particularly if, as is likely, the softest layer exists at the surface. The effects of reflection, refraction and scattering of ground motions across a material interface can reduce the amplitude of the ground motions significantly (a 35 % reduction is suggested in 3). Non-elastic material behaviour may result in only about half the amplification predicted for elastic material behaviour.

Joyner and Boore (4) suggested that resonance of

the soil column does not usually dominate amplification since ground shaking covers a range of frequencies apart from the resonant one. They suggested that amplification is more usually dominated by the low shear wave velocity or, more precisely, low impedance of the layers towards the ground surface. For strong ground motion frequencies of greater than 3 Hz, attenuation in soils appears to dominate over amplification.

Finn (5) noted that at low levels of earthquake shaking the ground response will be essentially elastic. With increasing shaking level, the elastic shear modulus of the ground G, which controls the instantaneous response, will soften raising the site period and the damping, thus changing the response. While the response of Mexico City's lakebed deposits to the distant (hence low level input ground motions) 1985 Michoacan earthquake was largely elastic, the response of the San Francisco Bay region to the 1989 Loma Prieta earthquake was decidedly non-elastic. In the former case, the input ground motions were amplified 3 to 5-fold, producing peak ground surface accelerations approaching 0.2 g (where g is the gravitational constant equal to 9.81 $m.s^{-2}$). The response of the lakebed clays remained essentially elastic because the shear modulus of these high plasticity clays did not show substantial degradation until a shear strain level of about 0.1 %, and hysteretic damping was also low. This allowed greater amplification close to the ground surface than would have occurred if non-elastic effects had been substantial. At Treasure Island, in the San Francisco Bay region, the observed amplification during the Loma Prieta mainshock was 2 to 3-fold, limited by the non-elastic response of the soft bay mud and surface fill. Amplification at the same site during the smaller amplitude aftershocks was much greater, since the ground response to these was essentially elastic.

Based on limited data, Seed and Idriss (2) proposed approximate relationships between peak accelerations on rock and those on other ground conditions, indicating attenuation of rock accelerations greater than 0.1 g through soils, and amplification of rock accelerations less than 0.1 g. Based on acceleration data collected at soft soil sites during the Michoacan and Loma Prieta earthquakes, and on the results of analyses, Idriss (6) proposed for empirical correlation a median relationship between peak accelerations on rock and those on soft soil sites indicating amplification through overlying soft soils of rock motions up to 0.4 g.

3. CONTINENTAL VERSUS PLATE MARGIN EARTHQUAKES

Seed and Idriss (2) showed that attenuation relationships for continental eastern United States earthquakes indicated lower peak horizontal ground accelerations in the near-field, but a slower rate of decay and consequently higher accelerations in the far-field, compared with those for plate margin western United States earthquakes. Whitman and Algermissen (7) reported that peak ground accelerations measured during recent eastern Canadian (continental) earthquakes were much larger, for comparable magnitude and epicentral distance, than those recorded during Californian (plate margin) earthquakes, and had much higher predominant periods. The midwestern region of the United States shows relatively slow attenuation of intensity, which is thought to be due to the hard, intact nature of the bedrock, and the considerable depth of poorly consolidated materials overlying the rock, particularly in the Mississippi floodplain.

Jacob (8) noted that the rock shear wave velocity adopted as a reference in the United States Uniform Building Code (UBC) is 800 $m.s^{-1}$. While this may be appropriate for Californian bedrock, the eastern United States bedrock typically has a shear wave velocity about 4 times this value. Since amplification is proportional to the square root of the shear wave velocity contrast across a material boundary, for a given soil shear wave velocity, the higher rock shear wave velocity for the eastern United States compared with California should lead to about twice the amplification.

For the same size earthquake, continental earthquakes produce much larger damage and felt areas than plate margin earthquakes. Algermesson (9) observed that the 1811 Ms 8.3 New Madrid (continental) earthquake had a damage area of about 5000000 km^2, compared with about 180000 km^2 for the 1906 Ms 8.3 San Francisco (plate margin) earthquake. The 1989 Richter local magnitude M_L 5.6 Newcastle (continental) earthquake had a damage area of about 9000 km^2 and caused damage estimated at US$4 billion, compared with about 50 km^2 causing damage estimated at US$10 million for the 1989 M_L 5.5 Upland, Los Angeles (plate margin) earthquake (10). The corresponding felt areas were about 200000 km^2 and about 9000 km^2, respectively.

4. BRIEF DESCRIPTION OF 1989 NEWCASTLE EARTHQUAKE

4.1 Seismology

Rynn (11) presented a detailed assessment of the seismology of the 1989 Newcastle earthquake, which is briefly summarised herein. The earthquake occurred on 28 December 1989. It was of M_L 5.6, caused 13 fatalities, 160 injuries, and A$4 billion damage, including an insured loss of about A$1.2 billion, making it the most costly single natural disaster in Australian history. The damage area covered about 9000 km^2, and the felt area about 200000 km^2, with isolated felt reports up to 800 km from the epicentre. The epicentre was approximately located near Boolaroo, about 15 km west south west of the Newcastle Central Business District, based on far-field seismograph records. The epicentral location is only accurate to ± 15 km. The focus was approximately located at a depth of 11.5 km, based on data picked up at a seismograph station in Scotland. It could be more shallow. The focal mechanism was interpreted as a thrust mechanism with near horizontal principle stress direction, but no evidence of faulting or tectonic movement could be found at the ground surface. Significant recorded aftershocks were of M_L 2.7 on 29 December 1989, located 9 km west south west of the Newcastle Central Business District at a focal depth of 13.6 km, and M_L 2.5 on 27 February 1990 also near Boolaroo. No additional damage was reported after either event. Previous earthquakes of similar size to the mainshock occurred in the same area in 1868 and 1925.

Little strong motion data are available due to the lack of accelerometers in the region. The duration of shaking can only be guessed from personal observations, which put it in the range from 5 to 42 s. From instruments at coal mines in the region, 30 to 90 km from the epicentre, peak rock accelerations in the range 0.02g to 0.1g were obtained. A significant amount of long period energy was observed on distant seismograph records. The Brisbane seismograph station, located 630 km from the epicentre, recorded 8 s period energy lasting for longer than 2 min.

Macroseismic data includes over 30000 "felt reports". Modified Mercalli intensity (MMI) values assigned to these reports ranged from MMI VIII to IX in Newcastle, to MMI I representing several reports of buildings swaying at the Gold Coast (550 km distant) and in Melbourne (800 km distant). The area within which significant damage was sustained, corresponding to MMI VI to IX, extended from Newcastle south to Liverpool (Sydney, 135 km), north west to Scone (118 km) and Cassilis (200 km), and north to Gladstone (near Kempsey, 250 km). In the absence of strong motion data, the required engineering parameters must be obtained indirectly from assigned intensity values.

4.2 Ground Movement and Damage

Ground movements included a 50 mm settlement of the southern abutment to the Stockton bridge, and ground waves (11). Surveying of damaged buildings after the earthquake suggested building and ground settlements of up to 50 mm in Newcastle. No evidence of liquefaction was observed at the ground surface.

The majority of the building damage was associated with unreinforced masonry construction, particularly where lime mortar had been used and was in a poor state of repair. Much of the damage occurred at alluvial sites, particularly distant from the epicentre. More than 50000 buildings sustained damage as a result of the earthquake. These included commercial buildings of up to 8 storeys, low level apartment buildings, and dwellings. A number of buildings in the Central Business District of Newcastle suffered partial collapse. These included the Newcastle Workers' Club of reinforced concrete construction (where 9 fatalities occurred), and the Newcastle Returned Servicemans' League Club. Damage to a number of other buildings was sufficient for them to be condemned. These included the Junction Motel of reinforced concrete construction, apartment buildings incorporating a "soft-storey" at ground level for garages, and part of the Royal Newcastle Hospital.

Damage to masonry walls, including infill panels, cavity brick and brick veneer was widespread. Damage included in-plane shear, out-of plane peeling, and corner, racking and torsional failures. There was extensive evidence of masonry veneers not being adequately tied to the structure. Buildings affected included the Kent Hotel (where 2 fatalities occurred), schools, churches and shops. The collapse of parapets, verandas and free-standing chimneys was widespread. Cracked plaster walls, minor cracks in masonry, cracked and dislodged roof tiles, and cracks in concrete paths and masonry fences were observed throughout the damage area. While building services generally performed satisfactorily, damage to internal fittings was extensive. Damage to electricity supply switchyards caused by the earthquake resulted in the Newcastle area being without power for a number of hours following the earthquake.

4.3 Site Conditions

Brennan (12) reported that the Newcastle earthquake observations show a high degree of correlation between areas of significant damage and alluvial soil and/or fill, with about 80 % of the damage being located on saturated, unconsolidated sediments. With increasing epicentral distance, the damage on rock falls away and damage becomes almost entirely confined to alluvial areas. Based on damage levels in the near-field, peak ground accelerations as high as 0.25g were estimated.

The occurrence of amplification may be inferred from the observed level of damage, particularly in the far-field, given the relatively moderate size of the earthquake. For example, at Scone (MMI VI at 118 km distant), large cracks appeared in the masonry walls of buildings such as the swimming pool, the Parish Hall, and some houses, which were founded on the alluvial floodplain of Middlebrook. Elsewhere in the town, the earthquake was barely felt. The peak rock acceleration at Scone is estimated to have been less than 0.01g. At Cassilis (MMI VI at 200 km), a sandstone block chapel founded on recent alluvium suffered cracks through the walls and masonry blocks. The peak rock acceleration here was probably less than 0.005g. The unreinforced masonry Police Station at Gladstone east of Kempsey, and 320 km north east of the epicentre, suffered minor cracking. This building is located on the Macleay River floodplain and is the only masonry building in the town. The brick Children's Hospital at Liverpool (Sydney), 138 km south west of the epicentre, and built on the Georges River floodplain, suffered cracking sufficiently extensive to force its closure.

5. ASSESSMENT OF STRONG MOTIONS DURING 1989 NEWCASTLE EARTHQUAKE

5.1 Approach to Assessment

Chapman et al. (13) assessed the attenuation/ amplification effects during the 1886 Ms 7.65 Charleston earthquake based on assigned intensities. Aki and Irikura (14) found a remarkably positive correlation between site-dependent, weak motion amplification and intensity, suggesting that intensity may be a more versatile seismic hazard parameter than the conventional peak ground acceleration. This is not too surprising since intensity is a direct, if qualitative, measure of the effect of the earthquake shaking reaching the ground surface. Attempts have also been made to predict site amplification based on surface geology. The younger the geology, the greater the site amplification tends to be. Borcherdt et al. (15) reported that amplification is quite well correlated with geological unit, shear wave velocity V_s and MMI. The combination most susceptible to amplification is fill and recent very soft to soft alluvium of low V_s (of the order of 130 $m.s^{-1}$), which on average may cause amplification of 5.7, and an increase of 2.4 intensity units.

On the basis of these observations, an approach involving assigned intensities and surface geology was adopted in the assessment of the strong motion during the 1989 Newcastle earthquake. This approach was combined with the mean attenuation relationship for a M_L 5.6 earthquake in this region.

5.2 Methodology and Results

Jorss and Wishart (16) grouped a significant sample of the preliminary macroseismic data collected by the Centre for Earthquake Research at the University of Queensland from the 1989 Newcastle earthquake (594 data points), according to identified surface geology. In particular, attention was focused on sites underlain by Quaternary alluvium (201 data points), and sites underlain by the older Palaeozoic sedimentary bedrock (105 data points). Much of the collected near-field data was excluded because the large volume of data collected in this area remains to be analysed. The selected data was plotted against epicentral distance, as shown in Figure 1. The

right hand axis of Figure 1 is the peak ground acceleration normalised by g, to a logarithmic scale. Also included in Figure 1 are the upper and lower bounds for the alluvium and older bedrock sites, the estimated mean attenuation relationship for a ML 5.6 earthquake in eastern Australia after Rynn (17), and a liquefaction lower bound after Williams (18).

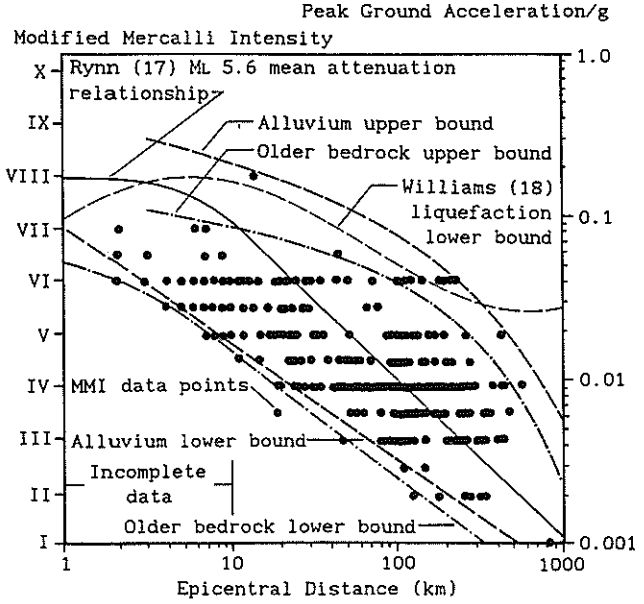

Figure 1 Selected Modified Mercalli intensity data from the 1989 Newcastle earthquake

It can be seen from Figure 1 that the alluvium upper bound is about one intensity unit above the older bedrock upper bound, while the alluvium lower bound is up to half an intensity unit above the older bedrock lower bound. It is also apparent from Figure 1 that the slopes of the bounds to the intensity data are considerably flatter than the slope of the attenuation relationship beyond an epicentral distance of 10 km. A few of the Newcastle intensity data points plot above the lower bound for the surface expression of liquefaction. In the near-field, intensities of up to MMI IX were assigned (not plotted in Figure 1). This corresponds to a peak ground acceleration approaching 0.4 g. About 10 km from the epicentre, limited intensity data suggest a peak ground acceleration approaching 0.2 g, dropping to 0.04 g with increasing epicentral distance. This acceleration level persists to about 230 km from the epicentre.

Taking the mean attenuation relationship to be representative of peak bedrock accelerations for the 1989 Newcastle earthquake, and the alluvium upper bound to represent the maximum degree of amplification through soft soils, maximum amplification factors may be estimated as a function of epicentral distance. The results are plotted as a curve in Figure 2, in which the estimated amplification factors are seen to rise rapidly with increasing epicentral distance, before tapering off at large distances. By way of comparison, a simplified calculation may be carried out to estimate the likely amplification in the far-field caused by the Newcastle earthquake. In the Newcastle region, the shear wave velocity of the bedrock is typically about 3500 $m.s^{-1}$, and that of the overlying alluvial soil is typically about 35 $m.s^{-1}$. The densities of the two materials may be taken as 22 $kN.m^{-3}$ and 18 $kN.m^{-3}$ for the rock and soil, respectively. Allowing for the impedance contrast between the bedrock and overlying soil, in the far-field a maximum amplification of the order of $[(3500x22)/(35x18)]^{0.5} \simeq 11$ is indicated. Allowing for some loss of energy, say 35 %, a more realistic estimate might be about 7. These values are in reasonable agreement with the maximum plotted value of about 9.

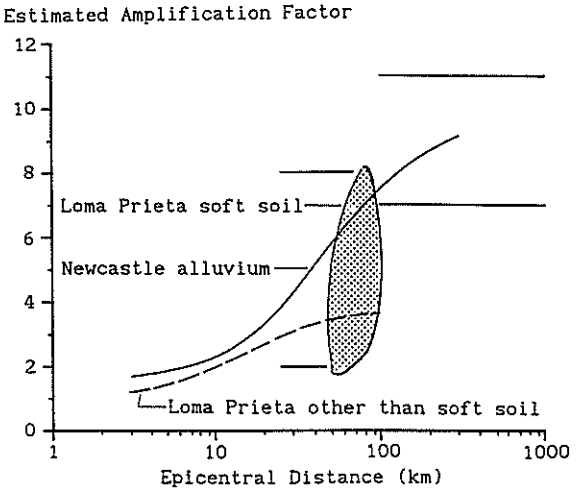

Figure 2 Estimated amplification factor versus epicentral distance

5.3 Comparison with Strong Motion Data Measured During 1989 Loma Prieta Earthquake

The acceleration data measured during the 1989 Loma Prieta earthquake provide an opportunity to check the validity of the approach adopted to assess the strong motion during the 1989 Newcastle earthquake. Seed et al. (19) reported that the Loma Prieta earthquake occurred when a segment of the San Andreas fault north east of Santa Cruz ruptured over a length of about 45 km, commencing at a depth of about 18 km near the centre of the rupture. It produced a magnitude of Ms 7.1 with a duration of 8 to 12 s, and damage over an area of about 7500 km^2, to a maximum of about 112 km from the epicentre. At least 62 fatalities occurred, with more than 2400 treated for injuries, and more than 12000 people displaced from their homes. Numerous aftershocks were recorded.

The mainshock caused numerous and widespread landslides, liquefaction and other soil failures surrounding San Francisco Bay and elsewhere, structural distress and failures in residential and commercial buildings, damage to non-structural elements and building contents, damage to critical road systems, and widespread disruption of utilities and other lifelines. More than 105000 homes, 500 apartment buildings, and 3500 businesses were damaged, with more than 1000 structures being condemned and demolished. Direct costs of up to US$10 billion, make it the most costly single natural disaster in United States history.

The affected region was unusually well instrumented with strong motion recorders (accelerometers), in the free-field, in buildings and on dams. The acceleration data collected confirmed the amplification of moderate and low amplitude bedrock motions by overlying weathered rock and, in particular, by overlying soft soils in the San Francisco Bay area (64 to 80 km from the epicentre). The latter preferentially amplified

long period motions, and resulted in a massive concentration of damage (well over half) and loss of life (more than 80 %) at soft soil (typically loose sandy fill over deep, clayey alluvium) sites comprising less than 1 % of the affected area.

The moderate amplitude mainshock peak horizontal bedrock accelerations reaching the San Francisco Bay area were in the range 0.06g to 0.12g, and were amplified through the soil cover to peak ground surface accelerations estimated to be in the range 0.16g to 0.33g (2 to 3-fold). Amplification of the low peak bedrock accelerations reaching the area from the aftershocks was 4 to 8-fold. For two to four storey buildings such as those in the Marina District, there is further amplification through the structure of up to 2-fold as a result of resonant interaction with the amplified long period ground surface motions.

Seed et al. (20) compared well established (Ms 7.1) mean attenuation relationships for the western United States with peak ground accelerations measured on different ground conditions during the Loma Prieta earthquake. The Idriss (21) relationship is a good mean to the "rock" site and "stiff soil" site acceleration data. The Joyner and Boore (4) relationship is a little low to represent the mean to the "rock" site, "stiff soil" site and "deep soil" site acceleration data, but their mean ± 2 standard deviation curves bound the data well. Idriss (6) tended to favour the Joyner and Boore mean relationship. Peak ground acceleration data recorded at the surface of "soft soil" sites during the Loma Prieta mainshock and aftershocks plot well above both attenuation relationships, straddling the Joyner and Boore mean + 2 standard deviation curve. The Idriss mean relationship, the Joyner and Boore mean relationship and mean ± 2 standard deviation curves, and the Loma Prieta soft soil data cloud are shown in Figure 3. Also reproduced for comparison in Figure 3 are the curves plotted in Figure 1.

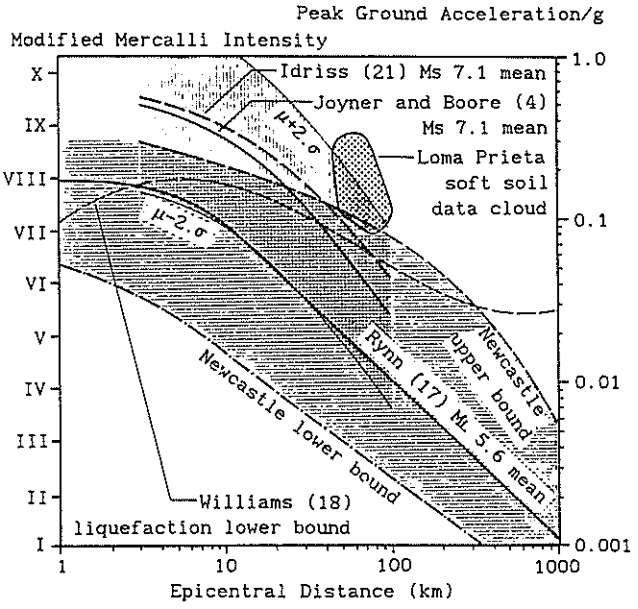

Figure 3 Comparison between Newcastle and Loma Prieta data

Conservatively (since the aftershocks to which some of the data apply were of much smaller magnitude than the mainshock) taking the Joyner and Boore mean attenuation relationship to be representative of peak bedrock accelerations for the Loma Prieta earthquake, the amplification factor through the soft soils may be estimated for each data point within the cloud. The results are shown as a data cloud in Figure 2. The cloud shows an amplification factor ranging from about 2 to about 8, in agreement with that reported by Seed et al. (19). The estimated Loma Prieta soft soil amplification factors are also of a similar order to those for the Newcastle region alluvium sites, estimated using a similar approach.

Again taking the Joyner and Boore mean attenuation relationship to be representative of peak bedrock accelerations for the Loma Prieta earthquake, the maximum degree of amplification through other than soft soil cover may be estimated from the upper bound to the measured acceleration data. The results are plotted as a curve in Figure 2, in which the estimated amplification factors are seen to rise with increasing epicentral distance, before tapering off at about 100 km. The trend of the curve is similar to that of the Newcastle alluvium curve, except that the stiffer ground to which the Loma Prieta data apply produce far less amplification than the soft Newcastle region alluvium, as would be expected.

The amplification factors estimated for the Newcastle region alluvium sites are plotted with the Idriss (6) median relationship between peak accelerations on rock and those on soft soil sites in Figure 4. The Newcastle estimates are in remarkably close agreement with the median relationship.

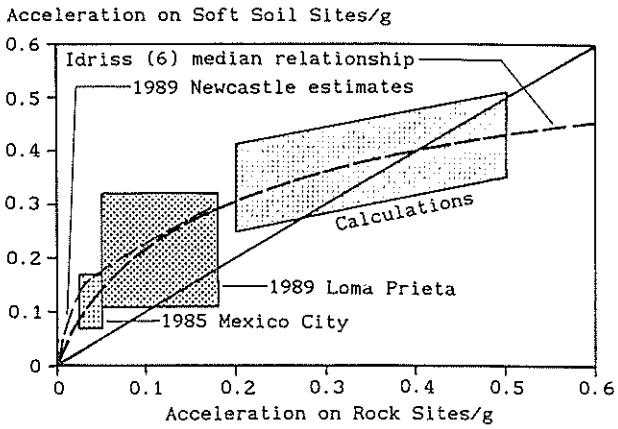

Figure 4 Comparison between Newcastle estimated amplifications and Idriss (6) median relationship

6. CONCLUSIONS

An assessment of the strong motion during the 1989 ML 5.6 Newcastle earthquake has been carried out using available macroseismic data from the earthquake, together with the mean attenuation relationship for the earthquake magnitude and region, and information on surface geology. The results obtained compare well with worldwide data analysed in a similar way, again emphasising the importance of site conditions and the very much greater hazard posed by continental earthquakes compared with plate margin earthquakes of the same magnitude. When the complete macroseismic database from the Newcastle event becomes available, more complete analyses will be carried out.

7. ACKNOWLEDGEMENTS

The author is indebted to the many colleagues whose freely given views and information were invaluable in formulating an understanding of the phenomenon of site amplification. These include Drs Rynn and Morris of The University of Queensland, Ted Brennan of Brisbane, Drs Byrne, Finn, Anderson and Campanella of The University of British Columbia, and Dr Jacobs of Columbia University. Special appreciation is extended to former students Nick Jorss and Vaughan Wishart at The University of Queensland for their dedication in collating and plotting the Newcastle intensity data.

8. REFERENCES

1. Okamoto, S. (1973). Introduction to earthquake engineering. Univ. of Tokyo Press.

2. Seed, H.B. and Idriss, I.M. (1982). Ground motions and soil liquefaction during earthquakes. Earthquake Eng. Research Inst. Monograph Series.

3. Stewart, W.P. and Campanella, R.G. (1991). Insitu measurement of damping in soils. Proc. Second Int. Conf. on Recent Advances in Geotechnical Earthquake Eng. and Soil Dynamics, St Louis, Missouri, Vol. I, pp. 83-92.

4. Joyner, W.B. and Boore, D.M. (1988). Measurement, characterization, and prediction of strong ground motion. Proc. A.S.C.E. Geotechnical Eng. Div. Spec. Conf. on Earthquake Eng. and Soil Dynamics II - Recent Advances in Ground-Motion Evaluation, Park City, Utah, Geotechnical Spec. Pub. No. 20, pp. 43-102.

5. Finn, W.D.L. (1991). Geotechnical engineering aspects of microzonation. Proc. Fourth Int. Conf. on Seismic Zonation, Stanford, California, Vol. I, pp. 199-259.

6. Idriss, I.M. (1990). Response of soft soil sites to earthquakes. Proc. H.Bolton Seed Memorial Symposium, Vol. 2, pp. 273-289. BiTech Publishers Ltd., Vancouver, Canada.

7. Whitman, R.V. and Algermissen, S.T. (1991). Seismic zonation in eastern United States. Proc. Fourth Int. Conf. on Seismic Zonation, Stanford, California, Vol. I, pp. 845-869.

8. Jacob, K.H. (1991). Seismic zonation and site response: are Building-code soil-factors adequate to account for variability of site conditions across the US? Proc. Fourth Int. Conf. on Seismic Zonation, Stanford, California, Vol. II, pp. 695-702.

9. Algermesson, S.T. (1983). An introduction to the seismicity of the United States. Earthquake Eng. Research Inst. Monograph Series.

10. Rynn, J.M.W. (1990). Introduction - Earthquakes and the Australian Community. Proc. Fourth Earthquake Eng. Workshop, The Univ. of Queensland, Australia, 9 pp.

11. Rynn, J.M.W. (1990). The 28 December 1989 Newcastle, Australia, earthquake. Proc. Fourth Earthquake Eng. Workshop, The Univ. of Queensland, Australia, 22 pp.

12. Brennan, E. (1990). Geological controls on damage patterns resulting from the 1989 Newcastle earthquake. Proc. Fourth Earthquake Eng. Workshop, The Univ. of Queensland, Australia, 9 pp.

13. Chapman, M.C., Bollinger, G.A., Sibol, M.S. and Stephenson, D.E. (1990). The influence of the coastal plain sedimentary wedge on strong ground motions from the 1886 Charleston, South Carolina, earthquake. Earthquake Spectra, Vol. 6, No. 4, pp. 617-640.

14. Aki, K. and Irikura, K. (1991). Characterisation and mapping of earthquake shaking for seismic zonation. Proc. Fourth Int. Conf. on Seismic Zonation, Stanford, California, Vol. I, pp. 61-110.

15. Borcherdt, R., Wentworth, C.M., Janssen, A., Fumai, T. and Gibbs, J. (1991). Methodology for predictive *GIS* mapping of special study zones for strong ground shaking in the San Francisco Bay region, CA. Proc. Fourth Int. Conf. on Seismic Zonation, Stanford, California, Vol. III, pp. 545-552.

16. Jorss, N.C. and Wishart, V. (1991). Application of Newcastle earthquake data to Queensland. Fourth year thesis, Dept. of Civil Eng., The Univ. of Queensland.

17. Rynn, J.M.W. (1988). The assessment of seismic risk in north eastern Australia. Civil Eng. Trans., I.E.Aust., Vol. CE30, No. 2, pp. 45-56.

18. Williams, D.J. (1988). Potential engineering risks in the earthquake hazard to the east coast of Queensland. Civil Eng. Trans., I.E.Aust., Vol. CE30, No. 5, pp. 307-316.

19. Seed, R.B., Dickenson, S.E., Riemer, M.F., Bray, J.D., Sitar, N., Mitchell, J.K., Idriss, I.M., Kayan, R.E., Kroop, A., Harder, L.F. and Power, M.S. (1990). Preliminary report on the principle geotechnical aspects of the October 17, 1989 Loma Prieta earthquake. Earthquake Eng. Research Center, College of Engineering, University of California at Berkeley, Report No. UCB/EERC-90/05.

20. Seed, R.B., Dickenson, S.E. and Idriss, I.M. (1991). Principal geotechnical aspects of the 1989 Loma Prieta earthquake. Soils and Foundations, Vol. 31, No. 1, pp. 1-26.

21. Idriss, I.M. (1985). Evaluating seismic risk in engineering practice. Proc. Eleventh Int. Conf. on Soil Mechanics and Foundation Eng., San Francisco, Vol. 1, pp. 255-320.

General Report Session 7
Professional & Legal Issues

D.C. STARR
B.Sc., M.Sc., C.Eng., M.I.C.E., M.H.K.I.E., F.G.S.
Principal, Hollingsworth Dames & Moore

SUMMARY The involvement of geotechnical engineers and engineering geologists in litigation and contractual disputes has an important bearing on the image of the profession. Three papers on professional and legal issues are briefly summarized and reviewed. Selected ideas emerging from treatment of the common theme of risk and uncertainty are presented as part of a cohesive approach to the subject. These ideas cover the relationship between acceptable levels of risk and previous experience, the evaluation of relevant experience by an independent agency, and the allocation of risk. The Reviewer emphasizes the importance of education in dissemination of information relating to risk minimisation. Reference is made by the Reviewer to existing guidelines on the presentation of information on sub-surface conditions, and to recent comments by others on the subject of uncertainty. Attention is drawn to the role of further education both within and outside the geotechnical engineering profession in achieving a common approach to risk management and professional liability.

1. INTRODUCTION

The experience of many professional geotechnical engineers and engineering geologists is that involvement in litigation cases causes divisions which harm the image of the geomechanics profession. The publicity given to the Coledale embankment failure, and the trial and subsequent acquittal of those indicted on charges of manslaughter and negligence has focused attention on the matter of potential liability (Christie 1991).

Risk management and professional liability are now matters which consulting firms, public bodies and individuals take seriously. For a conference theme of "Geotechnical Risk" it would seem reasonable to expect a degree of interest in professional and legal issues. However, only three papers have been submitted for general review under this heading.

An attempt has been made by the Reviewer to briefly summarize each paper, with some general observations, followed by a discussion of common themes.

2. REVIEW OF PAPERS SUBMITTED

2.1 Geohazard Risk Assessment (Grocott & Olsen)

The paper entitled "Geohazard risk assessment and reasons for alternative expert opinion" (Grocott G.G. & A.J. Olsen), deals with a dispute about the suitability of a subdivision site subject to potential instability.

An earth flow type landslide caused damage to a dwelling forming part of a rural-residential subdivision.

The landslide event led to litigation between the subdivision property owners on one hand, and the local authority and developers on the other hand.

The geotechnical advisors for the Plaintiffs considered that the site had an unacceptable risk of future instability, while the Defendant's advisors concluded the site was suitable.

The parties concerned agreed to mutual disclosure of evidence before an independent adjudicator in the form of a "mini trial". This course of action was chosen as a means of indicating the likely outcome of the full High Court hearing. On the basis of the evidence submitted, the "mini trial" found the site to be unsuitable for safe residential development.

The expert evidence submitted on behalf of the Plaintiffs and Defendants is compared. A slight difference in the extent of subsurface investigation is noted, although both parties appear to have favoured an observational approach, rather than sampling, testing and numerical stability analysis. The risk assessment was based on engineering judgement, supplemented in the Plaintiff's case by an analysis of the return period of slip-inducing

storms.

The major issue in dispute related to what constitutes an acceptable level of risk. The difference in opinion between the Plaintiff's experts and those of the Defendants is attributed by the authors, to the level of previous site specific experience and involvement with stability assessments in the immediate environs.

The circumstances described in the paper appear to categorise the geotechnical setting as one where engineering judgement is more important than numerical results of a stability analysis.

In such cases, engineering judgement requires to be based on adequate knowledge and experience of local conditions. In the Reviewer's opinion, precedents have been established elsewhere usually on the initiative of government agencies, in the development of a suitable body of local knowledge and experience. The guidelines established by the Geotechnical Control office in Hong Kong are a prime example of the formalisation of such practice (G.C.O., 1984). A further example is provided by the second paper submitted for the current theme, which is reviewed below.

2.2 Elements of an Effective Geologic Hazard Mitigation Program (Rold)

The paper by R.W. Rold deals with the mitigation of potential geological hazards by a three-element approach of evaluation, education and enforcement. It describes the experience of the Colorado Geological Survey, who were charged with delineating areas of natural geologic hazards that would affect the safety of citizens, and with providing advice to agencies of the state and local government. At the time concerned, the spread of urbanization into areas which had less favourable geological conditions caused major problems for government agencies.

An initial evaluation of the areas of interest comprised a review of available historical data and an assessment of experience drawn from areas with similar geological conditions. The second phase of the evaluations comprised detailed site investigations. This stage was generally conducted by consultants, whose work was reviewed by the Colorado Geological Survey. The survey then made recommendations for approval to the regulatory agency concerned. As an agency independent of the clients concerned, the Colorado Geological Survey were able to effect the necessary degree of quality control, and establish credibility with the regulatory agencies, developers and public.

The education phase was introduced to inform the decision makers and general public as to the character, severity and extent of potential geological hazards, and the consequences if such hazards were ignored. Local professional bodies (AIPG and AEG) were instrumental in enhancing the education process by hosting conferences. Travelling road shows and field trips helped to educate local government, elected officials and citizens. In addition, a policy was established to publicise guidelines and information about hazards ranging from construction on swelling and shrinking soils, to subsidence above disused coal mines.

The enforcement authority in Colorado resides with county commissions and town councils. The mechanism of enforcement began with the Colorado Geological Survey's enabling statute, which required the survey to advise and counsel governmental agencies and to delineate natural hazardous areas. A statewide subdivision law requires developers to conduct investigations to show that potential hazards have been identified, and that proposed uses are compatible with the soil or topographic conditions. As part of the approval process, counties are required to submit geological reports provided by the developer's consultants for evaluation by the Colorado Geological Survey.

A House Bill passed in 1973 defined geological practice, and has improved the standing of the profession.

The author concludes that although the Colorado system could stand improvement, it has worked well. The present Reviewer endorses the author's belief that a program of evaluation, education and enforcement could mitigate geological hazards at any location in the world. This concept is considered further in the discussion which follows in Section 3.

2.3 Dealing with Technical Uncertainty (Hollands)

The paper by D.E. Hollands deals with the matter of risk management. The author notes that in the engineering profession, there will always be uncertainties, and that additional effort and money spent on assessing risk will produce diminishing returns. Risk should be allocated according to who has control, who can foresee the risk, who can best bear the risk, and who benefits or suffers if the risk materialises. It is suggested that all risks should be borne by the principal, unless transferred in return for fair compensation. The party who has control should usually accept the risk.

Uncertainty is compounded by the unreliability of human judgement, and a distinction is made in law between "facts" and "opinion".

In discussing expertise, the author notes that the study of the physical behaviour of soil, rock and water is an ancient art, and that theory and numerical methods have mainly developed in recent decades. The usefulness of computers in checking the sensitivity of models to changes in parameters is acknowledged, as is the improvement in knowledge with the benefit of hindsight when engineering judgement and experience is combined in a panel of experts. Importance is also attributed to the way engineering judgement is presented, through good communication with technical and non-technical people.

Legal liability can be assumed due to incompetence, or from working outside ones range of experience. It is more common to find that risk or uncertainty has been overlooked. Liability can arise from duties which are more onerous than the obligation to exercise reasonable care and skill. The degree of skill to be expected from a specialist is higher than that expected from a general practitioner. Failure to obtain specialist advice may be considered negligent.

Advice is provided by the author on managing professional liability risks. These can be minimised by competence and thoroughness, and by seeking independent advice and review. Liability can be inadvertently increased by the manner in which work is described, and the wording of reports, records, contracts of engagement, and even invoices can misrepresent the degree of involvement.

With regard to giving evidence on professional standards, the author suggests that careful research is needed to describe the general practices of an average competent member of the profession.

Methods of settling technical disputes are discussed, with arbitration as the preferred judicial method. Mention is made of ADR and collaboration, the latter being defined as the constructive management of differences. An example is given of the successful application of collaboration to a case involving aspects of a proposed refuse landfill.

3. COMMON THEMES - RISK AND UNCERTAINTY

Each of the papers reviewed deals with a different aspect of risk and uncertainty. The following discussion draws together some thoughts which emerge from this common theme.

Grocott & Olsen (Geohazard risk assessment) deal with the matter of what constitutes an acceptable level of risk. According to the authors, this is influenced by the level of previous site specific experience and involvement with stability assessments in the immediate environs.

Rold suggests a three-element approach to the mitigation of geological hazards, with the first stage comprising evaluation of experience drawn from areas with similar geological conditions. This stage is followed by site-specific sub-surface investigations which are reviewed by an independent agency.

Hollands suggests that technical uncertainty be dealt with by allocation of risk according to who can foresee the risk, who can bear the risk, and who benefits or suffers if the risk materialises. The author suggests that the party who has control should usually accept the risk. Importance is attributed to the way engineering judgement is communicated, and it is suggested that risks can be minimised by competence and thoroughness, and by seeking independent advice and review.

The ideas expressed above could form part of a cohesive approach to the subject of risk and uncertainty, by application of the following guidelines:-

(a) Acceptable levels of risk are largely influenced by previous experience and familiarity with the particular setting. Hence relevant experience (and competence) are essential prerequisites of workers in this field.

(b) Evaluation of relevant experience by an independent agency can lead to mitigation of geological (and geotechnical) hazards, through education and enforcement.

(c) Uncertainty can be dealt with by appropriate allocation of risk. Due attention should be paid to the way engineering judgement is communicated, and judgement should be backed-up by independent advice and review.

The present reviewer wishes to emphasize the importance of education in dissemination of information relating to risk minimisation. The document "Guidelines for the Provision of Geotechnical Information in Construction Contracts" (I.E. Aust., 1987), provides some useful suggestions for dealing with uncertainty. The document also covers the matter of "facts", "interpretation" and "opinion".

In the context of geotechnical information, facts should be the same, regardless of the observer (e.g. sample locations, soil and rock descriptions, water levels). Interpretation involves judgement exercised in the knowledge of geological conditions or processes, and interpretations may differ from one

geotechnical specialist to another. The Guidelines stress the importance of appreciating that although often considered to be basically factual, borelogs are interpretations. Professional opinion is dependent on conclusions or recommendations derived from consideration of relevant facts and interpretations, together with analysis and/or the exercise of judgement.

The Institution of Engineers, Australia, Guidelines suggest that where areas of significant uncertainty or doubt exist, these should be brought to the attention of the users of geotechnical information. The present Reviewer considers that these guidelines form a good basis for educating members of the profession and non-specialists about the nature of geotechnical information.

Another aspect of the importance of communication and education is dealt with in a guest editorial in a recent edition of Australian Geomechanics (Miller, 1991). This touches on the matter of uncertainty, and in particular focuses on the validity of boundary conditions. Dr Miller refers to the Institution of Engineers' discussion paper "Are you at Risk", which argues that people do not properly understand uncertainty, and as a consequence expectations are distorted. The author of the guest editorial (who is a structural engineer) is struck by the difficulty geotechnical engineers face in assembling information about the distribution and properties of materials underlying a particular site. He points out that if we need to assume discrete boundary conditions for the purpose of modelling, we should constantly remind ourselves of the assumptions made, and convey them to those we serve.

In the same edition of Australian Geomechanics (October 1991), the Editorial Committee questions the abrogation of liability by the use of disclaimer clauses and "weasel words" in technical reports. The Queensland State Group of the Australian Geomechanics Society has set up a sub-committee on litigation, with terms of reference which include an examination of the feasibility of providing guidelines on reducing professional liability claims in terms of the manner in which technical reports and recommendations are presented. One of the recommendations given in an interim report from the sub-committee is that consideration be given to the preparation of guidelines on presentation of information in geotechnical reports. Such a document would enhance and compliment the "Guidelines for the Provision of Geotechnical Information in Construction Contracts" (I.E. Aust., 1987).

It is the Reviewer's opinion that although the geotechnical engineering profession is concerned about risk management and professional liability, there is a need for further education and acceptance of a common approach. The education process is required both within the profession and outside, and it would appear that engineers of other disciplines, architects and lawyers should be targeted in this respect.

4. CONCLUSIONS

Three papers have been reviewed under the heading of Professional and Legal Issues. Each deals with different aspects of risk hazard assessment, and uncertainty. Case histories are used by the authors as a means of illustrating points made. It is considered by the present Reviewer that the ideas expressed could form part of a cohesive approach to the subject of risk and uncertainty, by application of appropriate guidelines.

In considering the common theme of risk and uncertainty, the Reviewer emphasizes the need for education and dissemination of information. This is required in order to obtain consensus on a common approach within the profession to risk management and professional liability.

5. REFERENCES

Christie, H.D. (1991). Railway embankment failure at Coledale, NSW - 1988. Australian Geomechanics No. 20 Oct. pp. 40-48.

GCO (1984). Geotechnical Manual for Slopes (Second edition). Geotechnical Control Office, Hong Kong, 195p.

I.E. Aust., (1987) Guidelines for the Provision of Geotechnical Information in Construction Contracts. The Institution of Engineers, Australia, Canberra, 19p.

Miller, P. (1991). Uncertainty. Australian Geomechanics No 20 Oct. pp. 3-4.

Geohazard Risk Assessment and Reasons For Alternative Expert Opinion

G.G. GROCOTT
B.Sc.(Hons.), M.Sc.(Eng.Geol.),
Ian R. Brown Associates Ltd
A.J. OLSEN
B.E., M.Sc., D.I.C.
Worley Consultants Ltd

SUMMARY In 1983, a highly mobile earth flow type landslide was initiated as a result of heavy rainfall, causing damage to a single dwelling forming part of a rural-residential subdivision in the Bay of Plenty, New Zealand. The event led to litigation between the subdivision property owners on the one hand, who found through their geotechnical advisers that all of the site had an unacceptable risk of future instability, and the local territorial authority, the developers and their engineering consultants on the other hand, who concluded that the site was suitable. Possible reasons for this extreme difference between the expert witnesses included alternative opinions on what constitutes acceptable risk, unduly conservative attitudes, and differences in site specific geotechnical experience.

1. INTRODUCTION :

Some engineering disciplines particularly those using precise design codes based on known material properties or performance criteria are more amenable to risk assessment than others. Assessment of geohazard risk however relies heavily on judgement and experience, as the vagaries of the material properties and the unpredictability of their behaviour and performance under adverse conditions often preclude meaningful numerical analysis. Engineering failures commonly lead to community demands for decreasing levels of risk associated with development projects, such that "state of the art" standards are constantly changing. Given these degrees of uncertainty, questions relating to geohazard risk assessment such as is the site "safe" or "safe enough" are likely to result in highly subjective responses from the technical experts.

This paper illustrates by way of a New Zealand case history how divergent the assessment of geohazard risk can be. Reasons for this divergence of opinion are explored.

2. GEOTECHNICAL CHARACTERISTICS OF THE SITE

In 1983, a small area of a 10 hectare rural-residential subdivision located in the Bay of Plenty (Figure 1) was overrun by a rapidly moving earth flow[1] type landslide following a period of heavy rain. The failure involved a large volume (approx. 1200 m^3) of soil debris which moved rapidly down to the floor and partially up the flank of the adjacent valley side, a total distance of 250 m.

The landslide caused extensive damage to a dwelling located in its path, necessitating partial rebuilding of the structure.

The local geology comprises variably weathered rhyolite bedrock, overlain by a surficial mantle of successive showers of ignimbrite and volcanic ash. The surficial deposits are characterised by high natural water content, extreme sensitivity, and variable strength and permeability. These soil properties have given rise to failures of natural and engineered slopes elsewhere in the Bay of Plenty (Institute of Professional Engineers New Zealand, 1983; Tonkin & Taylor, 1980).

The subdivision is contained on the lower portions of a northeasterly - facing slope which rises 80 m in elevation from valley floor to slope crest. Slopes within the subdivision are inclined at 15° to 30°, steepening up to 45° at the slope crest above the site.

Landforms both within and surrounding the subdivision reflect an association with past slope instability. Above the subdivision, the topography comprises several well developed gullies and ridges, resulting in a "scolloped" outline in plan. A major landslide feature, identified on aerial photographs, occupies one of the gullies, and extends below onto slopes comprising a part of the subdivision. The site of the 1983 slide is located within a separate gully.

The subdivision is characterised by hummocky, undulating and irregularly contoured slopes. Exposures showed these slopes to be underlain by colluvium, indicating mass movement from higher areas. Similar land forms exist in areas adjacent to the site.

Investigations established that the 1983 landslide was probably triggered by excessive groundwater pressures at the interface between the surficial deposits and the underlying bedrock, resulting in a reduction of effective stresses. Other factors such as steepness of slope, devegetation, and stormwater runoff were considered by various parties to also be contributory.

Analysis of the 1983 landslide causing storm event showed that rainfall over a 72 hour period exceeded 260 mm, which was preceded by a 10 day period of lesser (94 mm) rain. The characteristics of this rainfall event were found to have a return period of about seven to eight years. A smaller earth flow which occurred on adjacent land to the subdivision in 1986, was found to have been initiated by a rainfall event similar to the 1983 storm.

(1) *Earth flow : Movement within displaced mass such that the form taken by moving material or the apparent distribution of velocities and displacements resemble those of viscous fluids (Varnes, in Schuster and Kriyek, 1978).*

3. BASIS OF LITIGATION

In 1983 prior to the landslide event the relevant local authority initiated an independent consultant's study of the slope stability risk of the general area surrounding and including the subdivision. This work, completed in 1984 after the landslide event, resulted in the production of a plan showing a three-tiered zonation of slope stability risk. Most of the subdivision formed part of a larger area which because of "the steepness of the slopes, the colluvial debris, and the evidence of mass movement", it was considered there was a moderate to severe risk of future instability. As a consequence of this finding, the local authority amended the district scheme in 1985, the affect of which was to severely restrict development in all of the deemed risk areas including the subdivision.

In 1984 the individual subdivision property owners (Plaintiffs) collectively engaged geotechnical consultants to investigate in detail the suitability of their land for residential development. This study concluded that the level of risk of further damaging landslides was sufficiently high as to render the entire site unsuitable. It was further concluded that no suitable remedial measures could be implemented to mitigate the landslide hazard.

This advice to the Plaintiffs which adversely impacted on development and resale prospects for their land resulted in their initiating litigation proceedings against the local authority, the developers, and the engineering consultants to the developers (collectively the Defendants) to seek compensation for loss of value of their asset. The Defendants initiated their own independent geotechnical study which concluded that the site was essentially stable but to meet the concerns of the Plaintiffs' experts, the stability could be enhanced by remedial drainage and other works.

In 1988, the parties concerned agreed to mutual disclosure of evidence before an independent adjudicator in the form of a "mini trial", in order to indicate the likely outcome in the event of litigation proceeding to a full High Court hearing. The "mini trial" found the site to be unsuitable for safe residential development on the basis of the evidence (ie in favour of the Plaintiffs). Subsequently, an out of court settlement was agreed to by the parties.

4. ASSESSMENT OF EXPERT EVIDENCE

Table 1 summarises the evidence of the expert witnesses acting for the parties concerned.

Examination of Table 1 shows there were a number of similarities but also some differences between the evidence of the opposing expert witnesses.

The experts for both parties were in philosophical agreement on the appropriate method of geotechnical investigation for this site, involving an observational approach of the site conditions, rather than a sampling, testing and numerical stability analysis method. This agreement arose out of both parties recognising the complexities of the ground conditions which rendered the latter approach inappropriate.

One difference between the parties was the level of site investigation, which differed slightly, but which both considered appropriate in the light of individual experience and knowledge of site conditions.

While both parties relied on their respective engineering judgements and experience at arriving at their conclusions, an important addition to the Plaintiffs case was to attempt to quantify the frequency of past instability as an aid to assessing risk. However, it was not possible to establish the recurrence interval of damaging events from the geological record, because of the destructive nature of previous landsliding. An alternative method of establishing frequency was used, based on analysis of the rainfall record to assess the return period of slip-inducing storms.

TABLE 1
ASSESSMENT OF EXPERT EVIDENCE

	Plaintiff Evidence	Defendant Evidence
Professional disciplines involved in dispute :	Engineering geology Geotechnical engineering Civil engineering Hydrological engineering Statistical analysis	Engineering geology Geotechnical engineering Civil engineering
Scope of geotechnical assessment of site :		
■ air photo interpretation	Yes	Yes
■ walk over field study	Yes	Yes
■ subsurface investigations	Yes	None before "mini trial"; limited investigations after "mini trial"
■ laboratory testing	No	No
■ numerical stability analysis	No	No
Basis for risk assessment :	Engineering judgement, statistical analysis of slip-inducing rainfall events	Engineering judgement
Relevant previous experience :		
■ within district	Yes	Yes
■ site specific	Yes	No

5. DIFFERENCES OF OPINIONS ON ASSESSED RISK

The assessment of geohazard risk poses special problems due to the high level of uncertainty compared with other engineering disciplines. Some of the factors contributing to the divergence of opinion in this case history are discussed.

5.1 Differences In Acceptable Risk Levels

At this site, recognition of the geohazard risk was not the issue in dispute, as both parties provided ample description of the slope instability history.

Clearly the major issue of dispute related to differences as to what constituted an acceptable level of risk. Without specific codes or standards on which to base their response, the experts were invited not to identify whether the site had been affected by past instability, but to define the term "safe". This was expressed by the Defendants: "There can be no general definition of the level of acceptable (slope stability) risk because this is based on subjective judgement and will therefore vary between one person and another".

The Plaintiffs approach to the problem of defining "safe" was to invoke the principle of precedence, which assumes that the past instability of the site is a guide to its future behaviour. An attempt was made to quantify the return period of damaging storm events, which formed the basis for an engineering judgment that the site was unsuitable for "safe" living.

Although major slumping on the site was recognised, the Defendants considered that there was sufficient difference between the character of the subdivision and that of the surrounding areas to conclude that evidence of active slipping elsewhere was unlikely to impinge on the site. The 1983 landslide was considered to be an isolated event in terms of recent activity on the site, with human factors such as devegetation and stormwater runoff being probable contributory factors. These observations formed the basis for their opinion that as the site exhibited no signs of present instability, then future failures were unlikely.

The subdivision residents had their own concepts of what constituted acceptable risk. Because of their exposure to involuntary risk, the residents requested and were provided with rainfall threshold criteria. This prompted the evacuation of some of their homes on a number of occasions.

5.2 Conservatism

Following the 1983 landslide, the Plaintiff's experts were involved in evaluating slope stability issues for other clients affected by the same storm event, for a considerable period following the failure. This level of detailed involvement with a particularly damaging event was suggested by the Defendants to be possibly responsible for a more conservative attitude than would normally be warranted.

5.3 Relevant Experience

The experts involved with this dispute were all experienced geotechnical practitioners, having carried out similar projects elsewhere in the area. However, the Plaintiff's experts had previous site specific experience and involvement with other stability assessments in the immediate environs to the subdivision. The Plaintiff's experts were of the opinion that had the other party had access to this level of detailed site specific experience, the differences in opinion between them might have been less divergent.

6. CONCLUSIONS

Many geohazard problems are beyond meaningful numerical analysis due to the complexities of the ground conditions. These situations pose special problems, as evaluation of the risk requires that the recurrence interval of the damaging event be quantified. Even if the recurrence interval of the hazard can be determined, and inevitably insufficient or unreliable data preclude an accurate assessment of this aspect, the absence of specific codes or standards relating to the assessment of risk for these types of hazards makes the definition of the term "safe" unverifiable. Risk assessment is then reduced to engineering judgement, often presented as "scientific fact".

REFERENCES

Institute of Professional Engineers New Zealand, 1983. Report of the President's Committee on the Ruahihi Canal Collapse.

Strachan, CM (Chairman) et al, 1983. Engineering risk. Report of the Presidents Task Committee on Professional Practice and Risk. Institution of Professional Engineers New Zealand, Wellington.

Tonkin & Taylor, 1980. Omokoroa Point. Land stability investigation. Consultants report for Tauranga County Council, reference 4487/2. Unpublished.

Varnes, DJ in Schuster and Krijek (Editors), 1978. Transportation Research Board Special Report 176. National Research Council, Washington, DC.

DISCLOSURE

The objective of this Paper has been to present the events of this case history in an as unbiased as possible manner without interpretation or investigation of the legal outcome. However, it is inevitable that in places a bias may penetrate, and for this reason we record our involvement with the Plaintiffs. The Defendants experts were invited to co-author the Paper, but declined.

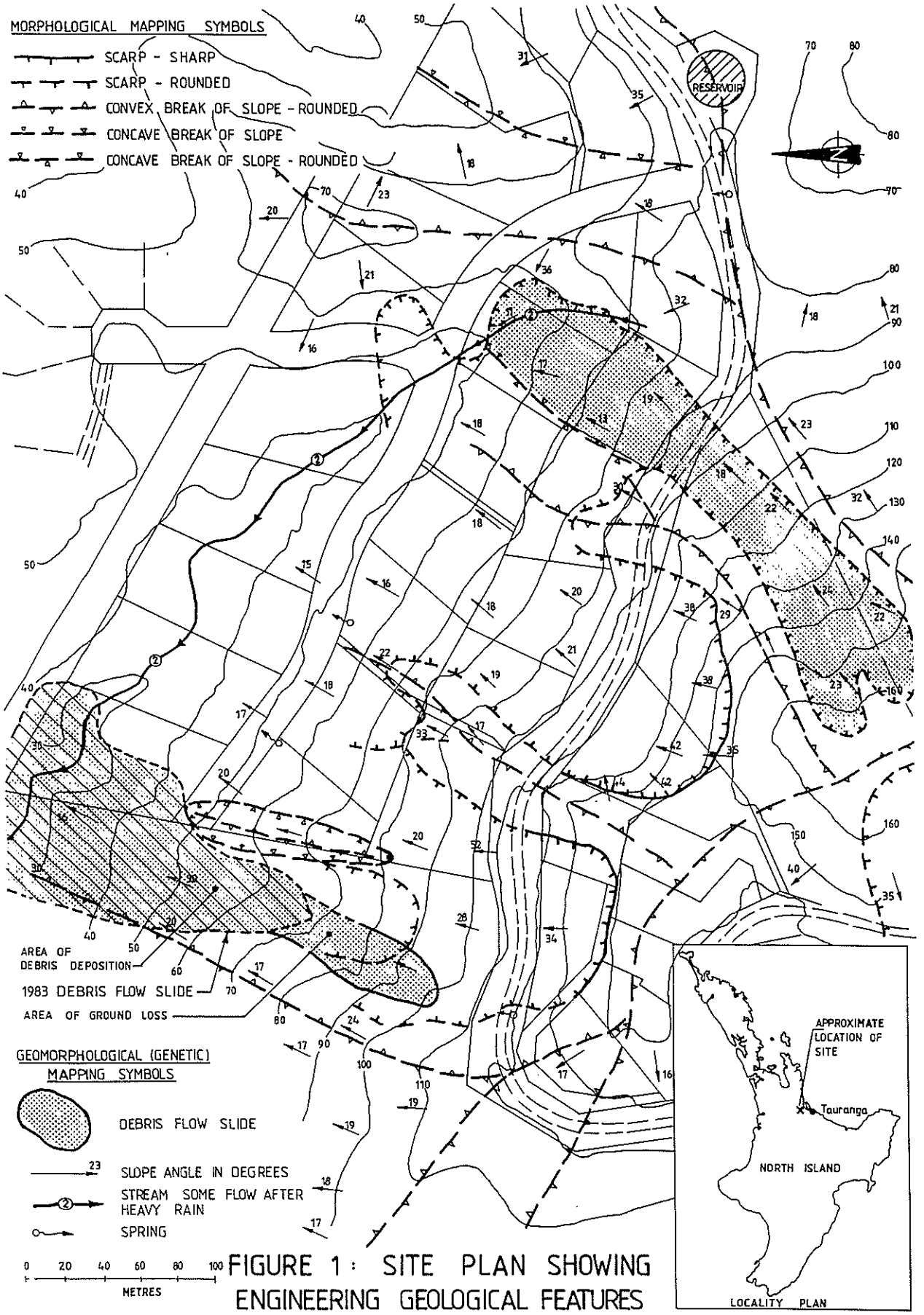

FIGURE 1 : SITE PLAN SHOWING ENGINEERING GEOLOGICAL FEATURES

Dealing with Technical Uncertainty

DAVID E. HOLLANDS
F.I.C.E., F.C.I.Arb., F.I.P.E.N.Z., F.I.E.Aust., F.I.Arb.A., F.Arb.I.N.Z., M.A.S.C.E., M.N.Z.I.S.
Consulting Engineer & Arbitrator, Auckland, N.Z.

SUMMARY Professional engineers are involved in managing risk through investigation and design. This involves anticipating what might go wrong. The risks must be balanced and allocated, through statutory, contractural and insurance means. Some of these risks are beyond engineering control and may be uninsurable. Others may not even be recognised, except with the benefit of hindsight.

It is inevitable there will be technical uncertainty. Strategies for dealing with this include expertise, good judgement, independent review and good communication. When a risk materialises, the cause and responsibility for any resulting loss and damage may be disputed. Consideration of the legal and technical factors involved is required to substantiate or refute claims.

In disputes which depend on the interpretation of scientific or technical data, there is a need to deal wisely with uncertainty. Traditional legal forums tend to encourage adversarial science and have difficulty in coping with complex technical matters. Collaborating is a process being used to deal with technical uncertainty, both in decision making and dispute resolution. A workshop on groundwater aspects of a proposed refuse landfill is a New Zealand example of applying this process to a technical issue.

1. RISK ASSESSMENT

Professional engineering is an art, not a science. There will always be uncertainties. The engineer's work involves anticipating what might go wrong and balancing risks to achieve practical and economic answers. There are also political, industrial and commercial risks, many of which may be beyond the control of the engineer or contractor and be uninsurable. However, the acceptance of risk may provide opportunities for increased profit.

Some of the geotechnical risks which may be present in construction projects arise from factors such as:

(i) physical conditions:
- unforeseen or differing site conditions
- instability of natural or constructed slopes
- soft ground, rock, old fill
- groundwater, subsurface erosion

(ii) artificial obstructions:
- underground services
- wells, pits, shafts, boreholes
- debris, refuse, contaminated ground

(iii) adverse weather and natural disasters
- affecting site conditions
- surface flooding, erosion, siltation
- earthquake, volcanic activity, tsunami, typhoon

(iv) defective materials or workmanship of contractor, sub-contractor or supplier
- lack of quality

(v) defective design

Risk assessment is important if decision-makers are to evaluate the potential gains and losses associated with any particular course of action. The odds may be unacceptable, in which case the course of action can either be rejected or a method found by which the odds are improved.

When new technology is involved, there may be no information on potential failures. Even when existing technology is to be applied, risk data may be inadequate or inconsistent. Moreover, useful information on past or potential failures may have been suppressed.

Limits on the extent of risk assessment have been described (IPENZ, 1983) as follows:

> "The law of diminishing returns applies where the purpose of a risk assessment is to provide information for decision-making. Because any assessment contains some uncertainties, a decision based on it must also be subject to uncertainties. Additional effort and money spent on an assessment to improve its quality will produce a less than proportionate improvement in the reliability of the decision. Ultimately a point will be reached where the costs of additional investigations and studies, plus the costs due to the delay in the decision, will exceed any benefits from a more reliable assessment."

2. RISK ALLOCATION

In construction projects, risk is allocated between the principal and contractor through the general and special conditions of

contract. Traditionally, the allocation of risk depends on:

(a) which party can best control the risk;
(b) which party can best foresee the risk;
(c) which party can best bear the risk; and
(d) which party most benefits or suffers if the risk materialises.

Basically, all risks should be those of the principal, unless transferred to or assumed by another party in return for fair compensation. However, the other party needs to have the competence to assess the risk, the opportunity and expertise necessary to control or minimise it, and the financial resources to pay for damages if the risk materialises. Indeed, control is the essence of risk allocation. The party who has control should usually accept the risk. Thus, during construction, the contractor has control of the site and usually takes primary responsibility.

The principal usually carries the risk of unforeseen physical conditions. Increased costs arising from conditions that could not reasonably have been foreseen by an experienced contractor are paid for as a variation. Thorough site investigation and evaluation, by a competent geotechnical engineer, will minimise this risk.

3. INSURANCE

Few construction contracts are undertaken without some form of insurance cover. Contract Works insurance is usually referred to as Contractors All Risks insurance, but it never covers all the risks! It insures the works against physical damage, and includes cover on material and plant on the site. Public Liability insurance covers property other than that owned by or in the charge of the contractor and other than the contract works.

The engineer will also need the protection of Professional Liability insurance. The policy should cover any claim arising from work done earlier in the insured's professional career, have automatic reinstatement (i.e. become fully operative again after a claim), cover employees as joint insured, cover legal costs (even if, in the final analysis, the claim does not involve any payment), etc.

There can be gaps between the various insurance policies. Also, claims may fail. For example, construction insurance is based on the assumption that events causing damage are not foreseeable and are therefore accidental. If damage can reasonably be foreseen or is expected to occur, it should be avoided by intentional design or action and not by wishful thinking. Where there is a lack of fortuity, the claim may be declined.

A common exception provides that construction insurance does not apply to "loss or damage caused by defective design". In this context, "defective design" may refer to the broad concept of the condition of a thing and not be limited to any non-compliance with proper standards by the engineer or by the contractor; i.e. it need not imply that there was any negligent designing. However, exclusions for defective design or faulty workmanship are now usually limited to the defective part, in which case damage to other property affected (i.e. to adjacent parts of the works) is covered.

It is absolutely essential that all relevant information (including all investigation results, reports, letters, etc), known to the principal or its consultants, be listed and made available both to tenderers and to insurers. The importance of this onerous task is often underestimated, with the result that the principal can be faced with unexpected costs due to avoidable claims for extras from the contractor or the declining of an insurance claim during or after construction.

4. UNCERTAINTY

The dictionary tells us that when something is "uncertain" it is not able to be accurately known or predicted, not precisely determined, liable to variation, or changeable. On the other hand, a "fact" is an event or truth known to have happened or existed, or a piece of information.

The law makes a distinction between "facts" (which rely on direct observation or other sensing of some thing or event) and "opinion" (which depends on the judgment of someone with special skill or experience in interpreting the facts). However, the reality is that many such "facts" are either generalised descriptions of variable things or faulty memories of complex events.

Human thinking is only a description of reality, not the real thing. Put another way, people respond to their map of reality, not to reality itself. We try to make meaning out of all the information which is constantly bombarding our senses. But where uncertainty is involved, human judgement can be unreliable. We may lock onto an answer too soon, focus on detail and overlook the context, or behave as if chance events are subject to control. Data that contradicts our opinion may harden rather than soften that opinion. Experts are particularly prone to getting stuck in grooves, while still insisting they are making subtle judgements.

Compounding all these potential judgement malfunctions, we tend to use language which makes fact out of opinion (e.g. using "it's" to preface our opinion, which makes it sound as if everyone agrees; turning verbs into abstract nouns, which sound more authoritative).

5. EXPERTISE

Geotechnical engineering attempts to apply logic to understanding the physical behaviour of the soil, rock and water which comprise the earth's surface. The art is ancient, but theory and numerical methods have mainly developed in recent decades.

Subsurface information is mostly obtained from borings or test pits. Only a small part of a site can be sampled, partly because of the cost but also because drilling and excavation are destructive test methods.

Groundwater, an important factor in all soil behaviour, can be used to illustrate the limitations of expertise. Theory may be based on the assumption that soil is relatively uniform, so there is a uniform increase in hydrostatic pressure with depth below a free water surface. In fact the soil is almost never uniform, and vagaries of rainfall and drainage through permeable strata result in a complex and changing pattern of groundwater pressure (Hollands, 1985).

Slope stability analysis is also fraught with difficulties. There are various methods of strength testing, options for interpreting stress-strain-pore pressure relationships, parameters to describe soil performance, assumptions regarding subsurface conditions, and methods of expressing results. Computer programmes convert all these uncertain factors into an apparently simple answer, which can lead to a false sense of confidence. Computers are of course helpful to check the sensitivity of models to variations in the assumptions.

Because we have developed scientific and mathematical models to encode our experience, engineers are perceived as dealing in facts. We tend to present our opinions as answers to problems. Indeed we are often so inordinately proud of them that we do not present their limitations to our clients or the community, leaving the impression that the models are precise and comprehensive. We hide our risk judgements in factors of safety, even convincing ourselves that nothing can go wrong. Nevertheless, failures do occur regularly and the public has become sceptical about expertise.

Sound judgement is important, especially in geotechnical engineering. Dr Ralph Peck said:

> "As long as the myth persists that only what can be calculated constitutes engineering, engineers will have little incentive or opportunity to apply the best judgement to the crucial problems that cannot be solved by calculation."

The report of the failure of the Teton dam shows the remarkable results that can be achieved when a great body of engineering judgement and experience is combined in a panel of experts. (Dunnicliff & Deere, 1984)

Equally important is the way engineering judgement is presented, through good communication that can be understood by both technical and non-technical people. Care is also needed to recognise the state of knowledge of others, and not take too much for granted.

6. LEGAL LIABILITY

Many engineering failures can be attributed, at least in part, to lapses in logical reasoning, misinterpretation of site conditions, inadequate construction control, or lack of maintenance. Some could be more bluntly described as resulting from incompetence, by engineers or contractors working outside the range of their training and experience. However, it is more common to find that some detail or risk or uncertainty has been overlooked. Professional liability claims also arise due to misunderstanding of the engineer's true role and legal responsibilities.

The courts have held that a professional person must exercise a reasonable degree of care and skill. Failure to do so is usually referred to as professional negligence. Liability in contract is governed by the terms of the contract. These can include duties which are more onerous than the basic obligation to exercise reasonable care and skill. An engineer can also be liable in tort to other parties, irrespective of any contract. A tort is a civil wrong, for which there are legal remedies which do not depend on any provisions of contract or criminal law.

The standard which the engineer must meet has been described as the reasonable skill, care and diligence of an ordinary and competent engineer. This usually means the degree of skill and care which the majority of the profession would have brought to the same task. However, the court is not bound to accept such practices as sufficient and retains its own freedom to conclude that the general practice falls below the standard required by the law. Employed engineers are bound by the same obligation to use reasonable care and skill.

The degree of skill to be expected from a specialist is higher than that to be expected of a general practitioner. Furthermore, with the increasing development of specialisation, the general practitioner is expected to know when a particular problem may require specialist advice. If it was reasonable to do so, a failure to obtain specialist advice, or at least to recommend it, may be considered negligent.

7. MANAGING PROFESSIONAL LIABILITY RISKS

The most effective way for an engineer to minimise professional liability risks is to be competent and thorough. Where appropriate, independent advice and review should be sought. Then, as far as possible, any remaining risks should be identified, be drawn to the client's attention and be clearly explained in terms that can be understood by non-technical people. Communication of risk is essential.

An engineer may feel that any review of work implies criticism or lack of confidence. On the contrary, the real professional encourages and welcomes independent review. It may identify some detail or risk that has been overlooked, thus helping to ensure that the project will be successful and enhancing the engineer's reputation. In the unlikely event of a future problem, the review itself will be good evidence that the care and skill of the profession has been exercised and that the problem could not have been reasonably anticipated by the ordinary competent engineer.

The engineer's liability can be inadvertently increased by the way work is described. The wording of reports, certificates, inspection records, contracts of engagement, and even

fee accounts, may imply a degree of involvement that exceeds the true function of a professional adviser. For example, words like "ensure" and "supervise" can lead to unintended warranties.

Experienced engineers are often asked to give an opinion on engineering matters, with a view to giving evidence in a court or arbitration hearing if a claim cannot be resolved. When giving evidence, the engineer must do so objectively and fairly. The expert witness is not there to advance a party's cause, but to assist the tribunal. If experience is lacking or preparation has been inadequate or there has been a lack of objectivity, the "expert" can be made to look a fool and this may be recorded in a decision for all to read.

When giving evidence on professional standards, the engineer is normally required to describe the general practices of an average competent member of the profession at the time, and not what the witness would have done in the circumstances. This requires careful research. Care must be taken to avoid any temptation to base such opinions on what is known now, with the benefit of hindsight, or on more recent practices.

8. TECHNICAL DISPUTES

The keys to resolving technical disputes are:

- identifying the main issues in dispute
- establishing the relevant "facts"
- interpreting the technical factors (technical opinions)
- interpreting the legal factors (legal opinions)
- recognising any possible different interpretations of technical and legal factors (grey areas/uncertainties)
- quantification (most losses are converted into money)

The person claiming must prove the claims, so good evidence is needed - e.g. minutes, instructions, correspondence, photographs, investigation results, expert opinion, etc.

An expert may give opinion evidence on the interpretation of facts. However, in adversarial proceedings both parties may produce experts. This often introduces two models, into each of which one can feed disputed "facts". Both models may give an impression of rationality and reality. Any fallibility may be concealed, consciously or unconsciously, but uncertainty still remains. Traditional judicial forums therefore have difficulty in coping with complex technical matters.

Arbitration is the preferred judicial method of deciding technical disputes. Construction contracts have a submission in their general conditions, providing for one or more arbitrators to decide any dispute. If necessary, a properly procured award will be enforced by the court as a judgement. Arbitration has potential advantages of privacy, informality, convenience, efficiency, finality, and the option to choose a technical tribunal. (Hollands, 1989)

Alternative dispute resolution (ADR) methods involve a neutral party as mediator or conciliator in voluntary processes to reach agreement. The parties retain the power to make their own decision. ADR seeks to minimise the costs inherent in adversarial processes; i.e. costs of money, time, self-respect, relationships with others, opportunities lost, etc. ADR can avoid a win-lose result by incorporating factors into the outcome which are beyond the scope of the contractual and legal remedies available from litigation or arbitration. It allows the parties to deal with the uncertainty inherent in differing legal and technical opinions. To realise its potential, ADR should be used at an early stage and emphasise getting the parties to work together as joint problem solvers. Dispute resolution can then be transformed into an opportunity to improve relationships and develop skills in avoiding and dealing with future problems. (Hollands, 1988)

9. COLLABORATING

Our traditional engineering methodology has not dealt well with technical uncertainty. For example, during initial project assessment, investigation, design and decision-making, a "we know best what is good for you" philosophy supported by "good public relations" (the "decide-announce-defend" syndrome) has too often resulted in opposition to technical proposals and to the professions involved. So-called public consultation has been unsatisfactory, due to such factors as: the use of complex technical reports, difficulties in validating information, inadequate involvement and power of the parties, etc.

Increased attention is being given to working together, in a consensual process called collaborating. (McCarthy, 1984; Gray, 1989; Susskind & Cruikshank, 1987; Hollands, 1991) Collaborating has been defined as the constructive management of differences. It provides a methodology for dealing with uncertainty, power imbalances, cultural differences, politics and problem solving. It is a form of ADR which is particularly applicable to multi-party decision making and environmental dispute resolution. Collaborating involves interweaving two processes: conflict resolution, and the advancement of common understandings and shared visions.

10. GROUNDWATER WORKSHOP

A workshop on groundwater issues is a New Zealand example of successfully applying collaborating to a specific technical issue. There were different technical opinions about leachate and groundwater aspects of a proposed Auckland Regional Council (ARC) refuse landfill at Mt Wellington, Auckland. For example, a concern that, if the landfill proceeded, there could be pollution of existing groundwater resources in the vicinity.

Twelve technical experts, who were advising the ARC and other parties including objectors, were involved. Several others attended periodically as observers and/or were on the mailing list and had the

opportunity to comment. The author, who had previously acted as auditor for the environmental impact assessment, convened and facilitated the workshop. The objective was to produce a "single-text" report (i.e. a report to which all participants could agree), to summarise the relevant information and deal with the groundwater concerns.

The process was funded by the ARC, as part of its public participation programme for the proposed refuse landfill. The author was not a consultant to the ARC, but an independent neutral facilitator endeavouring to assist all parties. The involvement of a geotechnical engineer advising a local community objector group was assisted by intervenor funding provided by the ARC.

Most participants had to rely on basic information provided by others. Also, some participants were only involved in particular facets of the topic. New and more detailed information could emerge in the future. It was therefore not intended that the report should represent the complete and final technical opinion of those involved. Nevertheless, it was intended to make the information clearer, more accurate, more complete, and more accessible to non-technical people.

Concern was expressed that design of the landfill's leachate and groundwater control systems continued to evolve during the workshop. This was because the workshop proceeded in parallel with on-going development of the conceptual design, and some changes were made in response to submissions by workshop participants other than the ARC and its consultants. However, it was finally agreed that this was quite normal, as engineering designs are not fixed but are developed and refined in response to further information, changes in technology, and new perceptions of the many factors involved. Indeed, it was considered important that further refinement should continue during the detailed design stage and in response to subsurface conditions actually exposed during construction, if the landfill proceeded.

The workshop met on six occasions over a period of six months. During that period, a sub-committee also met and developed wording and diagrams for the report. The concerns of each participant were incorporated. The author collated and edited the report, often rewording technical material in more neutral terms. The participants finally reached general agreement on the technical factors and complete agreement on wording of the report (Hollands, 1990).

11. CONCLUSIONS

It is inevitable that there will be technical uncertainty. We must acknowledge this uncertainty and identify the risks. Strategies for dealing with this involve both technical competence and risk management. Sharing the problem, through review or collaborative processes, is worthwhile. When disputes arise, an appropriate process is needed to resolve differences and improve future relationships.

12. REFERENCES

1. IPENZ (1983). Engineering Risk. Institution of Professional Engineers, New Zealand
2. Dunnicliff & Deere (1984). Judgement in Geotechnical Engineering - the professional legacy of Ralph B Peck. John Wiley & Sons.
3. McCarthy, Jane (1984). Negotiating Settlements - a guide to environmental mediation. American Arbitration Association.
4. Hollands, David E (1985). Geotechnical Engineering - a set of four 1-hour audio tapes. Continuing Education Programme, Institution of Professional Engineers, New Zealand.
5. Susskind, Lawrence & Cruikshank, Jeffrey (1987). Breaking the Impasse - consensual approaches to resolving public disputes. MIT-Harvard Public Disputes Programme, Basic Books.
6. Hollands, David E (1988). Conciliation or Mediation of Construction Contract Disputes. New Zealand Engineering, June 1988. Arbitration, the Journal of The Chartered Institute of Arbitrators, August 1989.
7. Gray, Barbara (1989). Collaborating - finding common ground for multiparty problems. Jossey-Bass Publishers.
8. Hollands, David E (1989). Initiating the Arbitration of a Construction Contract Dispute. New Zealand Engineering, October 1989.
9. Hollands, David E; Facilitator & Editor (1990). Groundwater Aspects of Proposed Refuse Landfill, Lunn Avenue Quarry, Mt Wellington - single text report of joint workshop. Auckland Regional Council.
10. Hollands, David E (1991). Trade Waste Controls for Auckland - a collaborative process. Water Supply & Disposal Association Conference, Wairakei.

Very large changes in sea level

P.M. JAMES
B.Sc., M.Sc.(Eng.), Ph.D., D.I.C., M.I.E.Aust
Geotechnical & Geological Engineer, Brisbane

SUMMARY Very large changes in sea level are postulated for the Tertiary and Quaternary Periods using submarine valley data, the findings of the Deep Sea Drilling Program, and certain geological sequences. A potential mechanism to account for the changes is sought in periods of instability in the earth's mode of spin. Conditions for similar occurrences in the future are possibly still extant.

1 INTRODUCTION

The phenomenon of sea level changes during historical times has been documented by Vita-Finzi (1). Concern, today, is focussed on a possible sea level rise through the greenhouse effect. While such changes pose an obvious risk to civil structures and developments, the majority of these changes are what might be termed minor. It is not necessary to look very far back into geological time, however, to come to the conclusion that very large relative changes in sea level, several orders of magnitude greater than predicted for the greenhouse effect, can occur. Further, it is but a small step to recognise that such variations could well be a normal part of earth history.

Environmental changes of this nature are beyond the capabilities of engineering solutions. It is therefore important to establish past sea level fluctuations and also to try to assess the probability of future occurrences. This paper is presented in the hope that its brief outline of evidence might stimulate further research in this area. Geotechnical engineers are often in a useful position to record data on the recent past.

Discussions, below, deal in turn with: the morphology of submarine valleys, the findings of the Deep Sea Drilling Program (DSDP), and certain geological sequences. A potential mechanism for sea level change is then proposed.

2 SUBMARINE VALLEYS

Submarine valleys occur in all the oceans and seas of the world and almost ninety percent of them can be seen as direct extensions of existing terrestrial systems. Many are disturbed on the continental shelf area, but can typically be traced down the continental slopes; most continue out onto the abyssal plains of the oceans. Along their various courses, submarine valleys exhibit nearly all of the features which characterise terrestrial drainage systems: tributaries, levees, huge fan deposits with incised channels, steep sided gorges in hard rock as spectacular as the Grand Canyon...

The origin of these features is puzzling. Marine scientists traditionally seek explanations based on turbidity current activity and the merits of this mechanism will be touched on, below, when relevant. According to Shepard and Dill (2), the most logical and comprehensive explanation of submarine valleys would be a drowned river origin, if only a mechanism were available to explain the huge changes in sea level required.

It is instructive to look initially at submarine valleys for which a drowned river origin is not in question: those in the Mediterranean. The submarine valleys of Corsica, for example, begin as small rocky gorges just above present day sea level and continue, with increasing relief, down to the Mediterranean Sea floor at some 3 km depth. Here, deposits of shallow water sediments and sea grass are found.

Now, the Mediterranean is known to have been dry on at least one occasion, notably around 5 million years ago, and hence these submarine valleys can be seen as happily eroding their precipitous channels during one or more of the dry periods. No turbidity current activity is required and, indeed, none could be realistically postulated on the rocky Corsican coastline.

The east coast of Sri Lanka contains several submarine valleys which are almost identical to the above examples. The largest of these, the Trincomalee Canyon, extends off the island's largest river, the Mahaweli, and runs a twisting and precipitous course in a V-shaped canyon which is deeply incised into hard Pre Cambrian quartzites and granites. The canyon runs a distance of 60 km from land and reaches a depth of 4 km below sea level.

The Mahaweli carries a reasonable sediment load and hence an origin related to turbidity currents can not therefore be ruled out entirely, provided one can also explain how turbidity currents are capable of developing such an impressive erosive power, under water. To the south of Trincomalee, however, there are several other submarine valleys which occur in locations where the associated terrestrial streams are minor and where, like the Corsican examples, the action of turbidity currents can not realistically be invoked. The submarine canyons have nonetheless developed to a degree which is only marginally less impressive than the one at Trincomalee. That is, deep gorges have been eroded into hard rock without any apparent assistance from turbidity currents.

Across the Bay of Bengal, the Ganges submarine valley system also begins as a set of canyons on the continental slope. Although the sediment load of the Ganges is far beyond anything available in Sri Lanka, the size of its submarine gorge does not reflect this potential for turbidity current activity. Again, it has to be inferred that the size of a submarine gorge is not influenced by either present

past sediment loads of their terrestrial counterparts.

In the case of the Ganges system, the huge sediment load is evident as a submarine alluvial fan which covers most of the floor of the Bay of Bengal, over 1000 km in length and up to 12 km thick, in water depths ranging from 3 to 5 km. Deposition of this fan appears to have taken place in four major pulses of sedimentation, the last being Pleistocene in age. Since that time, the surface of the fan has become eroded by a "braided stream" network. The gradients of the eroded channels in the fan are no more than 1 in 1000, over lengths of hundreds of kilometres.

The traditionally accepted hypothesis for this deposit is, again, turbidity current activity, but there are some difficulties. Veritable turmoil, involving the whole of the Bay of Bengal is implied, while it is necessary to postulate turbidity current transportation over 1000 km on almost horizontal surfaces. Following deposition, there still remains the problem of how discrete channels could have been eroded in the fan, under water. Currents, even in restricted channels on continental slope areas, are seldom sufficient to move fine sands.

Abyssal fans also occur off both the east and west coasts of the USA. Borehole evidence reveals that distinct bedding planes separating clays and sands occur in these. Age sequences can also be identified. In the Hudson Canyon, cobbles, gravel and shallow water shells have been recorded at depths of over 3 km.

These features, to name but a few, again militate aganist any explanation based on turbidity current activity. By their nature, turbidity currents mix sediments and then redeposit them, down slope, as a graded sediment. On the other hand, all of the above features fit well into a scenario of normal fluviatile processes - which, of course, would require huge changes in sea level.

3 DEEP SEA DRILLING

An enormous amount of new data has been made available on the sea floor by the Deep Sea Drilling Program (DSDP). One of the common features of many of the boreholes drilled hundreds of kilometres from land is the presence of terriginous material such as coarse sediment, wood, leaves, etc. Such findings can, of course, be explained by major turbidity currents, but there are certain other associated features which do not fit into the framework. Some examples are:-

Bh 156, in the Galapagos area, revealed the presence of oxidised basalt under 2.5 km of water.

Bh 240, drilled 500 km east of equatorial Africa, encountered sand and reef materials in the upper stratigraphic units under almost 5 km of water.

In Bh 661, off NW Africa, a deposit of Cretaceous anhydrite was encountered in the sediments of the ocean depths. Anhydrite requires shallow, enclosed, subtropical basins for its formation.

The above brief examples indicate that either the sea had withdrawn ephemerally from the relevant areas, or that the areas have been subject to massive and localised subsidence over the past few million years.

It is worth mentioning here that the Bay of Bengal was also dry in the Cretaceous. Here, subsidence is not considered an option, owing to problems arising out of trying to adjust the hydraulic gradients of the associated river systems.

In other words, if subsidence of the crust is found to be an option of little attraction, one is left again with the problem of massive sea level changes.

4 GEOLOGICAL INDICATORS

The discussions above have been concerned with low sea levels. If the sea level goes down in one part of the globe, it might well be expected to go up in another, in order to maintain volume. Unfortunately evidence for high sea levels on land is susceptible to eradication by normal geological processes and it could therefore be expected to be scanty. Some useful examples are nonetheless available.

Elevated marine benches, known as tablazos, have been recorded along stretches of the western coastline of South America. Heights of 300 m above sea level occur in Peru, gradually decreasing to around 100 m in the south. These tablazos are believed to be Upper Pleistocene in age and the result of sea level change rather than uplift of the continent.

The geological records for the north of Malaya cite Pleistocene (?) wave cut platforms in granite at elevations of almost 200 m. In Hawaii, evidence has recently been found of marine effects at more than 100 m elevation, which would appear beyond the limit of tsunamis as we know them, in the open ocean.

The island of Barbados provides directly observable evidence of enormous oscillations between land and sea. Tertiary coals, now exposed on the island, are overlain by globigerina ooze: a slow forming deposit of ocean depths in excess of 4 km. The stratigraphic association indicates that, over the past ten million years or so, Barbados has gone from tropical swamp conditions to the ocean's depths; has stayed there long enough for the ooze to be deposited; and then has been returned to the surface again.

A similar situation has been recorded in Indonesia, where deep sea radiolarian ooze is sandwiched between Tertiary shallow water sediments.

Both of the above sequences are located in areas of active crust, which makes it difficult to differentiate between sea level changes and/or subsidence-uplift of the crust. On the other hand, the almost perfect reversibility of the movement makes any mechanism of crustal dynamics somewhat suspect.

5 A MECHANISM FOR SEA LEVEL CHANGE ?

As things stand at present, the oceans form an evenly spread veneer over the earth's spinning surface. The pattern of centripetal forces which acts on this veneer is, however, far from uniform. Neglecting minor gravitational changes and tidal effects, the height to which a column of water should rise under the centripetal forces applicable at any location on the surface of the earth can be approximately determined by equating potential and kinetic energy.

$$m.g.h. = \tfrac{1}{2}\, m.v^2$$

where v = angular velocity, given by one complete rotation in 24 hrs, at a radius of spin appropriate to any latitude. At the equator, the radius is 6375 km; at the poles the radius of spin is zero.

The heights to which a column of water should therefore rise are equal to zero at the poles and around 11.9 km at the equator. Ideally, then, water should tend to accumulate at the equator, leaving the poles dry.

This distribution does not occur in practice and the

reason appears to be that the earth is not a spinning sphere but distorts in a quasi-hydrostatic fashion. That is, the earth shape, with its equatorial bulge and polar flattening, develops the same distorted shape which is preferred by the water veneer. In other words, the distorted earth shape forces the water out into the reasonably even distribution we see today.

Let us now assume that the earth's mode of spin is amenable to change: for example a transient period of chaos manifest as either polar wander or (major) precessional wobble.

In the former case, geographical polar migration would alter the existing pattern of centripetal forces and this could be expected to find an immediate response in the oceans. Water would attempt to ammass at the new equatorial location, while draining away from the new poles. Large changes in sea level would be experienced in some regions, although not necessarily at nodal points.

Whether the equatorial bulge would also adjust to the new regime, by some sort of creep process, is a subject for geophysical debate. However, if the bulge did migrate towards the new equator it would have the effect of adjusting sea levels gradually to the situation which obtained prior to the polar shift. Alternatively, one might argue that the inertia provided by the bulge would eventually restore the earth to its original position and, in consequence, return the sea levels to normal.

As an example of the effect of polar migration, we could consider the last Ice Age, around 15,000 years bp, when the centre of the northern ice cap was located in the vicinity of Baffin Island. At the time, ice sheets covered parts of north west Europe and North America, but Siberia was much warmer than today. The ice sheet at Baffin Island thus looks suspiciously like a polar position. If this assumption is made, then the associated equator of the time would have run through Rio de Janiero and, on the opposite side of the globe, Hong Kong. According to the model, oceanic waters would have gravitated to this new equatorial location and away from those regions which found themselves in a higher latitude.

The patterns of sea level from that time provide some remarkable coincidences with prediction.

* The high level tablazos on the west coast of South America and the elevated wave cut platforms in north Malaya both lie close to the predicted equatorial position.

* No changes in sea level are evident in the Gilbert & Ellis Islands, according to Vita-Finzi, but this location would be close to a nodal point, remaining equatorial.

* North America, north west Europe and antipodean Australasia are all regions which would have moved to a higher latitude by the above polar shift. In all these areas low sea levels have been recorded at the appropriate time.

If the change in the earth's mode of spin involved precessional wobble rather than polar migration, a somewhat similar outcome might be anticipated for the oceans. Under precessional wobble, some of the earth's rotational energy would be transferred to gyroscopic action, causing a slowing down in the rate of spin as well as other complex changes. Thus, one might expect the oceans to drain away from the equatorial regions, causing sea level rises in the higher latitudes.

Circumstantial evidence from the megalithic period, from early historical eclipse data, and from myths, have been collated by the writer. Two periods of major sea level change appear to have been associated with times of significant, transient, precession over the past four thousand years.

Such changes are very recent. The conditions which brought them into being, assuming the above interpretation has some validity, could therefore be considered as still potentially active. Geotechnical specialists are concerned with the detailed investigation of sites and are in a unique position to observe features which might throw light on the matter.

6 REFERENCES

1. Vita-Finzi, C.,"Recent Earth History", Macmillan London, 1973.

2. Shepard, F.P. and Dill, R.F., "Submarine Canyons and Other Sea Valleys", Rand McNally & Co, Chicago, 1966.

7 SELECTED BIBLIOGRAPHY

Deep Sea Drilling Program, (Selected Boreholes)

Gold, T., "Instability of the earth's axis of spin", Nature, Vol 175, p526 ff, 1955.

James, P.M., "Prehistorical evidence for precession", Spec. in Science & Tech., 7:5:303-315, 1984.

James, P.M., "Polar Wander & Crustal Deformation, an alternative geological model", (unpubl. ms)

Elements of an Effective Geologic Hazard Mitigation Program

J.W. ROLD
AB & MS University of Colorado, State Geologist and Director Colorado Geological Survey

SUMMARY Effective geologic hazard mitigation requires evaluation, education and enforcement. Evaluation requires geologic hazard mapping to determine the location, and seriousness of the hazards and a hazard investigation prior to land use changes or construction. In developed areas investigations should be undertaken at the first indication of a problem. These should be conducted by qualified private consultants or government staffs. If by consultants they should be subject to governmental review. Publication and availability of results furthers the education element. Education informs decision makers and the general public as to the character and extent of the geologic hazards and the consequences if ignored. Decision makers include regulatory government officials, landowners, industry and financiers. Educational efforts should include graphically illustrated talks, publications and the media. Reports must interest and inform the layman and be scientifically credible. Enforcement must ensure that information gained by evaluation guides land use decision-making and construction location and design. Enforcement can be hazard zoning, grading codes, subdivision regulation, and building codes, as well as economic decisions by enlightened developers or investors. Enforcement must utilize geological review of land use changes and construction sites by competent geologic staff of a governmental agency free from political and economic pressures.

1. INTRODUCTION

Throughout the world society has struggled to mitigate the serious economic, safety, health and social impacts of geologic hazards. Long-term consideration of this problem by the staff of the Colorado Geological Survey and our experience leads to the conclusion that an effective geologic hazard mitigation program must utilize three interrelated elements. They consist of evaluation, education and enforcement. Like the three-legged stool, the program will fail if any of the legs or elements are missing or deficient.

The Colorado Survey's involvement with geologic hazard mitigation began with its reestablishment in 1969. Two of its major statutory charges were: "to delineate areas of natural geologic hazards that would affect the safety of or cause economic loss to the citizens" and "to provide advice and counsel to all agencies of state and local government on geologic problems". At that time the burgeoning spread of Front Range metropolitan urbanization onto geologically less favorable sites and the exploding alpine recreational developments caused major problems for government agencies. The impact of geologic hazards on these developments certainly caused economic loss to and affected the safety of our citizens. Therefore the fledgling Survey began a long-range program to evaluate the seriousness of the problem, educate public and private decision makers to the character and magnitude of geologic hazards and to provide a mechanism for enforcement of the consideration of geologic hazards information in public and private construction or major changes of land use.

2. EVALUATION

The evaluation element consists of two phases. The first must be a determination of the overall magnitude, character and seriousness of the hazards to be mitigated. This step forms the critical basis of and provides the information for the educational element. Conduct of the evaluation must be credible to be accepted by government officials, private decision makers and the general public. In Colorado we utilized previous work of the U.S. Geological Survey, academicians, consultants and investigations by our own small staff. Particularly in the early stages we drew heavily on examples from areas such as California.

Even in areas where little or no geologic mapping has been done, a review of historical records and analogies drawn from areas of similar geologic environments will satisfy many of the requirements of this first phase of evaluation.

The second phase of the evaluation element consists of detailed site investigations prior to significant land use changes or construction. As such it provides the information to be used by decision makers or by regulators in the enforcement element. Colorado adopted the philosophy that site investigations for the second evaluation phase would be conducted by consultants and that the costs therefore, would be borne by the development applicant. The consultant's work then would be reviewed by the Colorado Geological Survey who made recommendations for approval, denial or modification to the regulatory agency in the enforcement element. This process provided considerable additional work for geological consultants, validated high quality work, screened out the shoddy work and provided state wide objective uniformity of evaluation. As an agency with total responsibility to the public rather than to any specific client, we were able with careful quality control to establish the necessary strong credibility with the regulatory agencies, development applicants and the public.

3. EDUCATION

The critical education element follows and utilizes information derived from the first phase of the evaluation element. The education process must provide the evidence and justification for the second evaluation phase and for the establishment of an enforcement element. It must inform decision makers and the general public as to the character, severity and extent of the geologic hazard and the consequences to be suffered if the hazard is ignored. In Colorado the education element was enhanced immeasurably by the dedicated work of many members of the local sections of the American Institute of Professional Geologists (AIPG) and the Association of Engineering Geologists (AEG). Their cooperative efforts in hosting five Governor's Conferences on environmental geology helped to educate geologists, planners, legislators and the public. Road shows with accompanying field trips over wide areas of the state helped to educate local government staffs, elected officials and influential citizens. The careful tutoring and education of several newspaper and television reporters aided them in providing accurate and extensive media coverage of current newsworthy hazard events. We found that colored-slide, illustrated talks presented to legislative hearings, service clubs, geological societies and any other interested audiences throughout the state were extremely effective. The Colorado Survey's early successful involvement in several high visibility, controversial projects increased the public's sensitivity to the problem.

Early on we established a policy that geologic hazard publications especially should be timely, accurate and understandable to the non-geologist. Publications such as Special Publication 12, Nature's Building Codes - Geology and Construction in Colorado; Special Publication 6 - Guidelines and Criteria for Identification and Land Use Controls of Geological Hazards and Mineral Resource Areas; Special Publication 11 - Home Construction on Shrinking and Swelling Soils; Special Publication 14 - Home Landscaping and Maintenance on Swelling Soils; and Special Publication 26 - Subsidence Above Inactive Coal Mines - Information For the Home Owner, have been widely accepted and widely distributed. They are effective educational tools for geologists, engineers, architects, lawyers, planners, builders and private citizens.

4. ENFORCEMENT

Even after massive and successful efforts at education and evaluation, the hard facts in many situations require strict enforcement with statutory backup. Though many development proponents and regulatory agencies can be persuaded by the merits of a geological review of a project, sometimes the bottom line must be a legal requirement that an evaluation must be conducted, and that the consideration of the results of that evaluation must be part of the decision making process.

A successful enforcement mechanism to ensure that the hazard knowledge gained by the evaluation element can only be set in place after a successful education effort. The enforcement element must ensure that the information gained by the evaluation phase guides land use decision making and construction site location and design. The enforcement mechanism may be by hazard zoning, grading codes, subdivision regulations, building codes, deed restrictions, easements or covenants. In Colorado the legislature has maintained that all land use controls shall be at the local government level. The enforcement authority therefore resides with county commissions and town councils. The function of statewide evaluation, review, recommendations and technical advice by the Colorado Survey to the regulatory bodies is mandated by the statues.

The enforcement mechanism in Colorado actually began with the Colorado Geological Survey's enabling statute (34-1-101 CRS 1973) which required the Survey to advise and counsel governmental agencies and to delineate natural hazardous areas. Importantly the laws gave the Colorado Survey no regulatory authority but required it to give advice, counsel and recommendations to those that had that authority.

One of the strongest portions of Colorado's enforcement strategy is its statewide subdivision law, Senate Bill (SB)-35 (30-28-101 and 113 et seq. CRS 1973). SB-35 requires the developer of a subdivision which is outside city limits to conduct an investigation of the "geological characteristics of the area significantly affecting the land use and the impacts of such characteristics on the proposed subdivision. Evidence to show that the areas of subdivision which involve soil or topographic conditions presenting hazards or requiring special precautions have been identified and that proposed uses of such areas are compatible with such conditions." (Subdivision was defined as breaking land into two or more parcels, one of which was less than 35 acres).

As part of the subdivision approval process, counties are required to submit a geologic report provided by the developer's consultants and the subdivision plan "to the Colorado Geological Survey for an evaluation of those factors which would have a significant impact on the proposed use of the land". The Colorado Survey must make its recommendation to the county commissioners within 35 days.

The geological portion of this subdivision law has been the most successful part of the evaluation and enforcement framework. Most subdividers now realize that the cost of an adequate subdivision geological investigation is an investment in their project's success, rather than an unnecessary expense. Most consulting geologists are now conducting adequate subdivision investigations. Most county commissioners and planning commissions and staff now realize that geologic factors can be a critical part of their land use decisions.

Success of the program is validated by the fact that since 1973 over 12,000 subdivisions have been reviewed. Except for swelling soil problems, we are not aware of any serious geologic problems which have occurred when the geologic recommendations of the consultant and our staff were followed.

In 1973 House Bill (HB)-1574 (34-1-201 and 202 CRS 1973) was passed. It defined geological practice and required that geologic work be done by a legally defined

professional geologist. That statute does not require licensing or registration and has no enforcement clause but it has improved the stature of the geological profession and has essentially kept non-geologists from making geological reports.

In 1974 HB-1034 (29-20-101 CRS 1973) specifically gave local governments the power to "plan for and regulate the use of land by regulating developments and activities in hazardous areas". This gave broad powers, but did not require cities, towns and counties to address and mitigate geologic hazards in a broad variety of land use cases.

Also in 1974 HB-1041 (24-65.1-101 CRS 1973) specifically defined geologic hazards and those geologic conditions which could constitute a geologic hazard. It gave local governments the power for, but did not require the identification, official designation, and administration of hazard areas. It also required the Colorado Survey to promulgate a model geologic hazard area control regulation (Rogers 1974). Most local governments with potential hazard problems used the Colorado Survey or consultants to map and identify potential geologic hazard areas within their jurisdiction. This evaluation work provided immense amounts of hazard information and increased local governments' awareness of their geologic hazard problems. Although most governments utilize this information in their planning, zoning, and land use decisions, none have carried out their full authority to formally designate and manage geologic hazard areas. Political and philosophical controversies over the non-geologic portions of this broad land use control act caused it to fall in disrepute and prevented its full implementation. However, the widespread hazard identification studies and legal definition of geologic hazards and hazard areas served to institutionalize the rational concern for the geologic impacts on future developments.

In 1984 concerns for extensive swelling soil damage to residential construction in several Denver suburbs spurred the passage of SB-13 (6-6.5-101 CRS 1973). With the title of Soil and Hazard Analysis of Residential Construction, that statute requires "that very builder shall provide the purchaser of a new home with a copy of a summary report of the analysis and the site recommendations. For sites in which significant potential for expansive soils is recognized, the builder shall supply each buyer with a copy of a publication detailing the problems associated with such soils, the building methods to address these problems during construction and suggestions for care and maintenance to address such problems". Not coincidentally the Colorado Survey's SP-14, Home Landscaping and Maintenance on Swelling Soils fit that description and is now widely and routinely distributed by builders to home buyers. The statute served to educate and raise the consciousness of all home builders, government agencies and home buyers to the serious swelling soil problems.

Also in 1984 HB-1045 (22-32-124 CRS 1973) required the Colorado Survey to "determine the geologic suitability" of new school construction or school site acquisitions. This requires a geologic review of school construction sites and forces the consideration of geologic problems that could be encountered.

5. CONCLUSIONS

Colorado has over the years devised a workable though imperfect set of procedures to: educate the public and decision makers; evaluate or review with Colorado Geological Survey's staff most development activities before they are approved or become certain and most importantly the enforcement through a statutory framework which requires geological hazard information to be acquired, reviewed and addressed for most development projects.

The education effort, though extensive and fairly successful, has been seriously hampered by the lack of funding. Many worthwhile projects to provide hazard information have had to be shelved.

The first phase of the evaluation element has essentially been terminated. Although we have learned to identify potential hazard areas, considerable research into the causal mechanisms and the temporal predictability of geologic hazards needs to be conducted. Fortunately the second phase of the evaluation element has been included in and interwoven with the enforcement strategy.

The enforcement or statutory framework for geologic hazard mitigation has been relatively successful. Statutes now require all subdivisions in the state's unincorporated areas to undergo geological investigations, state Survey review, and consideration of those results by planning commissions and county commissioners. Both cities and towns have broad powers to consider geologic hazard information and most require geologic investigations and review of suspected problem areas. The National Environmental Policy Act, the Environmental Impact Statement process, the old federal A-95 process and the state Joint Review Process ensure the geological investigation and review for major projects and those which require federal decisions or federal funding. School sites now require geological investigations. Homes built on suspected swelling soils require an evaluation, analysis and disclosure of mitigation methods to the home buyers. A strong network of local government staff, geologists and informed citizens throughout the state bring the Survey into the picture on many controversial or geologically suspect projects even though geological review may not be legally required.

One must realize that an enforcement program does not consist of simply passing a law. Regulators must have ready access to and utilize competent, objective, credible geologic advice. The source of that advice should be as free as possible from political and economic pressures. The objective evaluation of controversial or politically sensitive developments or projects is fraught with difficulty. Reviewers soon learn that a person's mettle is forged in the crucible of controversy.

Last year Governor Romer signed an executive order establishing a Colorado Natural Hazard Mitigation Council. The Council's charge is to manage the mitigation of natural hazards such as floods, wild fires, earth-

quakes, drought, avalanches, and landslides. It should assess the vulnerability of those situations, evaluate and prioritize mitigation options, seek funding for the most immediate needs and coordinate all levels of government and private sector in effective responses to such hazards. The council is made up of 25 official and 27 ex-officio positions representing the legislature, the governor's office, the affected departments of state government, local governments, the universities, and professional societies. The Hazard Mitigation Council should serve to institutionalize concerns for mitigating geological hazards. Hopefully it will carry forward the three key elements of a hazard mitigation program.

The Colorado system is far from perfect and could stand considerable improvement, but it has worked remarkably well in mitigating the impacts of geologic hazards. We firmly believe that a program of evaluating the seriousness of a geologic hazard, educating the decision makers to its seriousness and a statutory enforcement mechanism could mitigate geological hazards any place in the world.

6. REFERENCES

1. Colorado Land Use Act, House Bill 1041 of 1974, Title 24, Article 65.1, Section 101-502, Colorado Revised Statues 1973.

2. Enabling Act Reestablishing The Colorado Geological Survey, Title 34, Article 1, Section 101-305, Colorado Revised Statues 1973

3. Geological Practice Definition Act, House Bill 1574 of 1973, Title 34, Article 1, Section 201 and 202, Colorado Revised Statutes 1973.

4. Holtz, W.G. and Hart, S.S., "Home Construction on Shrinking and Swelling Soils," Special Publication 11, Colorado Geological Survey, 1978.

5. Jochim, C.L., "Home Landscaping and Maintenance on Swelling Soil," Special Publication 14, Colorado Geological Survey, 1981.

6. Land Use Control Enabling Act, House Bill 1034 of 1974, Title 29, Article 20, Section 101-106, Colorado Revised Statutes 1973.

7. Rogers, W.P., et al. "Guidelines and Criteria for Identification and Land Use Controls of Geologic Hazard and Mineral Resource Areas," Special Publication 6, Colorado Geological Survey, 1974.

8. School Building Codes-Zoning-Planning Act, House Bill 1045 of 1984, Title 22, Article 32, Section 124, Colorado Revised Statutes 1973

9. Shelton, D.C. and Prouty D., "Nature's Building Codes -Geology and Construction in Colorado," Special Publication 12, Colorado Geological Survey, 1979.

10. Soil and Hazard Analyses of Residential Construction, Senate Bill 13 of 1984, Title 6, Article 6.5, Section 101, Colorado Revised Statutes 1973.

11. The Subdivision Regulation Act, Senate Bill 35 of 1972, Title 30, Article 28, Section 101-113, Colorado Revised Statutes 1973.

12. Turney, J.E., "Subsidence Above Inactive Coal Mines: Information for the Homeowner," Special Publication 26, Colorado Geological Survey, 1985.

ABSTRACTS

Keynote Address

John Jaeger Memorial Address

Session One
Earth Structures, Dams, Soil Improvement and Geofabrics

Session Two
Foundations and Retaining Walls

Session Three
Mining, Tunnels and Excavations

Session Four
Soil Properties and Testing

Session Five
Analytical and Probabilistic Methods

Session Six
Slope Stability and Seismic Hazard

Session Seven
Professional and Legal Issues

MITIGATION OF GROUND FAILURE RISK — SOME LESSONS FROM THE LOMA PRIETA EARTHQUAKE

KEYWORDS: Earthquakes; Fills; *Geotechnical risk; Ground improvement methods;* Ground response; Lateral spreading; Liquefaction; *Risk evaluation; Risk mitigation; Seismic safety;* Settlements; Stability.

ABSTRACT: The identification, evaluation, and mitigation of risk increasingly defines the nature of modern geotechnical engineering practice. The aftermath of the October 17, 1989 Loma Prieta earthquake in California is used to illustrate how geotechnical risk has been identified and evaluated in the Marina District of San Francisco as a basis for recommendations for mitigative actions for both private citizens and the government to prevent loss of life and massive damage in a large earthquake which is predicted with a high degree of probability to occur within the next 30 years. Special studies were done in the Marina District which showed that the heavy damage in 1989 was the result of deep soft soil layers, uncompacted liquefiable fills, and structually deficient buildings. Actions to prevent loss of life and even more devastation in future earthquakes include ground improvement to prevent liquefaction and lateral spreading, seismic retrofitting of structures, upgrading of utility systems, and the development of emergency response plans. Geotechnical risks are ubiquitous, and as geotechnical engineers we have a special obligation to apply our special scientific and technical skills for their identification, evaluation, and mitigation. These include zonation studies, keeping the public and governments informed, early participation in site selection, helping in the development of consensus on assumption of responsibilities, participation in the development of emergency response plans, and insuring that the public and policy makers have correct perceptions and understanding of geotechnical issues that directly affect their safety and that of the environment around them.

REFERENCE: MITCHELL, James K. (1992) Mitigation of Ground Failure Risk — Some Lessons from the Loma Prieta Earthquake.

Proc. of 6th Australia New Zealand Conf. on Geomechanics, Christchurch, New Zealand, Feb 3-7.

MODELLING INTERACTIVE LOAD DEFORMATION AND FLOW PROCESSES IN SOILS

KEYWORDS: Load; Deformation; Failure; Simulation; Interactive.

ABSTRACT: This paper presents a general conceptual model for the practical simulation of a number of interactive physical properties in a wide range of soils. This model has been developed over more than 25 years as a finite element computer program incorporating the theoretical and practical experience gained by the author during this period. The processes simulated are load — deformation — failure and the simultaneous flow of water, solutes and heat. While a wide range of soils and soil conditions have been analysed successfully, the modelling procedures were originally developed to handle the particular problems of unsaturated and swelling soils, which are of great significance in Australia and which because of their nature need to be analysed as non-linear and hysteretic materials. The procedures presented are designed so that they can be related to currently available experimental measurements, rather than to idealized theories developed for materials other than soils. As such, this has been applied successfully to a wide range of practical problems, involving a variety of soil types. A brief description of the procedures used in the model, comparisons with previous theoretical and experimental data, and some practical applications are given in this paper.

REFERENCE: RICHARDS, B.G. (1992) Modelling Interactive Load Deformation and Flow Processes in Soils.

Proc. of 6th Australia New Zealand Conf. on Geomechanics, Christchurch, New Zealand, Feb 3-7.

EARTH STRUCTURES, DAMS, SOIL IMPROVEMENT AND GEOFABRICS — GENERAL REPORT

KEYWORDS: Earth structures; Dams; Geofabrics; Soil improvement.

ABSTRACT: This is the general report on a total of twelve papers presented at the session on Earth Structures, Dams, Soil Improvement and Geofabrics during the 1992 6th ANZ Conference on Geomechanics.

REFERENCE: FELL, R. (1992) Earth Structures, Dams, Soil Improvement and Geofabrics — General Report.

Proc. of 6th Australia New Zealand Conf. on Geomechanics, Christchurch, New Zealand, Feb 3-7.

THE APPLICATION OF REINFORCEMENT MATERIALS FOR EARTH STRUCTURES — RISK AND ACCEPTABILITY

KEYWORDS: Reinforced soil; Reinforcement materials; Risk; Application; Safety factors.

ABSTRACT: Reinforcement materials for the reinforcement or stabilisation of earth structures come in many forms. The key characteristics of earth reinforcement are strength, extensibility, soil interaction and durability. In applying reinforcement materials to earth structures an assessment needs to be made of risk. Risk is defined as function of hazard, vulnerability and uncertainty. Hazard relates to the potential for loss of life or function. Vulnerability relates to the criticality of the reinforcement to the performance and stability of the structure. Uncertainty relates primarily to the ability to predict behaviour over the service life required. Application categories for earth reinforcing materials are derived which are based on an overall risk assessment of both the materials and the application. Such categories can be used for the application of material types or for the definition of appropriate safety factors.

REFERENCE: BOYD, M.S. (1992) The Application of Reinforcement Materials for Earth Structures — Risk and Acceptability.

Proc. of 6th Australia New Zealand Conf. on Geomechanics, Christchurch, New Zealand, Feb 3-7.

GROUND IMPROVEMENT TO REDUCE GEOTECHNICAL RISK: WAINGAKE FINAL WATER TREATMENT PLANT

KEYWORDS: *Earthquakes; Foundations;* Ground improvement; Retaining wall; *Risk; Settlement;* Slope stability; Soils; *Stone columns.*

ABSTRACT: Site investigations for the Waingake Final Water Treatment Plant near Gisborne in New Zealand identified poor ground conditions under the proposed retaining walls which also carry the treatment plant buildings. Due to the poor ground conditions, there was a potential for damaging settlements and foundation failure. The risk was exacerbated by the potential for strong earthquakes in the region. Ground improvement using stone columns provided a cost effective solution to mitigate the risk of damaging settlements and foundation failure. This solution also allows the retaining wall to undergo small translational movements during large seismic events with minimal disruption to the treatment facility. The stone columns were constructed using a dry compaction technique. Settlement monitoring confirmed the effectiveness of the stone columns in reducing settlements.

REFERENCE: BRABHAHARAN, P. (1992) Ground Improvement to Reduce Geotechnical Risk: Waingake Final Water Treatment Plant.

Proc. of 6th Australia New Zealand Conf. on Geomechanics, Christchurch, New Zealand, Feb 3-7.

DESIGN PROCEDURE FOR THE SEISMIC ANALYSIS OF EARTH STRUCTURES

KEYWORDS: *Dam design; Earthquake analysis;* Embankment risk analysis; *Seismic risk.*

ABSTRACT: A simple procedure is described for the seismic analysis of earth structures such as dams, tailings dams and embankments. The procedure is based upon the state of the practice used in California, and although by no means a rigorous analysis, represents an improvement on the pseudostatic analyses commonly used. The seismic analysis results in an estimate of the measure of performance of an earth structure under a particular earthquake loading. In order to assess the acceptability of the estimated deformations for seismic design, a simple set of criteria is proposed which relate the estimated performance to the lifetime seismic probability of the structure. An assessment of the relative risk of failure, i.e. lifetime failure probability versus consequence/cost of failure, provides a reasonable basis for assessing the structure's performance under seismic loading.

REFERENCE: ELIAS, D.C., NOVELLO, E.A. and GLENISTER, D. (1992) Design Procedure for the Seismic Analysis of Earth Structures.

Proc. of 6th Australia New Zealand Conf. on Geomechanics, Christchurch, New Zealand, Feb 3-7.

GEOTECHNICAL INVESTIGATIONS FOR THE ASSESSMENT OF THE RISK OF WATER LEAKAGE FROM PRESSURE TUNNELS

KEYWORDS: *Water tunnels; Tunnel lining; Stress measurement; Pump tests;* Rock structure; topography.

ABSTRACT: The role of rock stress measurements and borehole pumping tests in the assessment of potential for hydraulic jacking of rock joints and fractures is discussed in relation to three pressure tunnel projects in Australia. Investigations for the siting of steel pressure linings, carried out in varied geological and topographical conditions, have shown that rock stresses and hydraulic jacking potential may vary strongly over short distances within rock masses, with structural effects appearing to have a particularly strong influence on variability. The results of these studies suggest that conventional methods of design for placement of steel linings should be supplemented by direct field measurements to assist in reducing the risk of water leakage from pressure tunnels, and in achieving the economical placement of full pressure linings.

REFERENCE: ENEVER, J.R., WOLD, M.B. and WALTON, R.J. (1992) Geotechnical Investigations for the Assessment of the Risk of Water Leakage from Pressure Tunnels.

Proc. of 6th Australia New Zealand Conf. on Geomechanics, Christchurch, New Zealand, Feb 3-7.

STRAIN COMPATIBILITY AND DESIGN CRITERIA FOR REINFORCED EARTH

KEYWORDS: *Reinforced earth; Design; Analysis;* Factors of Safety; Finite difference analysis.

ABSTRACT: As new types of reinforcing elements are tried in a variety of types of soils and rocks, there is considerable scope for further study of the most appropriate design assumptions and techniques for analysis and design of soil and rock reinforcement.

A modified "displacement method" of analysis is used to study the significance of various design assumptions and to provide some insight into choice of appropriate Factors of Safety. It is thought that displacement methods, while relatively simple and expedient, offer significant advantages because they can show the inter-relationship between the relative stiffness of the various components of the system and the safety with respect to failure of these individual components.

Results of analyses using the modified displacement method and analyses using an elasto-plastic finite difference program are studied to provide insights into the effect of the method of determining the normal stress distribution on the failure surface and the significance of choice of Factors of Safety.

REFERENCE: FIDLER, S.R. and WALLACE, K.B. (1992) Strain Compatibility and Design Criteria for Reinforced Earth

Proc. of 6th Australia New Zealand Conf. on Geomechanics, Christchurch, New Zealand, Feb 3-7..

FLEXURAL SLIP, AN OFTEN NEGLECTED HAZARD

KEYWORDS: *Bedding plane shear; Foliation shear; Origin of slickensides;* Stability; Dams; Slopes.

ABSTRACT: Flexural slip seams, resulting from tectonic folding, are typically manifest as bedding plane shears in sedimentary rocks and foliation shears in metamorphic rocks. Residual or near residual strengths apply along the seams, depending on rock type and intensity of folding. Although of great lateral extent and frequent occurrence, these seams are often missed in site investigations; when encountered, they are sometimes incorrectly diagnosed. Major re-design of dams and occasional failures have resulted from a non-recognition of the hazard, while landslides initiated by these features have been wrongly attributed to progressive failure. Illustrated examples are described from the literature and the writer's experience.

REFERENCE: JAMES, P.M. (1992) Flexural Slip, An Often Neglected Hazard

Proc. of 6th Australia New Zealand Conf. on Geomechanics, Christchurch, New Zealand, Feb 3-7..

GEOMEMBRANES, GEOTEXTILES AND SLOPE STABILITY

KEYWORDS: Heap Leach; Geotextiles; Geomembranes; Sliding; Friction.

ABSTRACT: This paper is about the potential for instability that can arise when a soil mass is to be placed over a geomembrane. This can occur in heap leach mining, solid waste dumping or aesthetic soil cover in lagoons. Typical geomembranes have relatively low friction coefficients to soils and these coefficients are lower still for geomembrane to geotextile interfaces — an important factor since the two are often used together.

A case study sliding failure of a heap leach is discussed in some detail and some potential remedies are discussed with particular reference to heap leach mining applications.

REFERENCE: HAUSMANN, M.R., SADLIER, M.A. and BECKINGSALE, C. (1992) Geomembranes, Geotextiles and Slope Stability.

Proc. of 6th Australia New Zealand Conf. on Geomechanics, Christchurch, New Zealand, Feb 3-7.

REDUCTION OF PAVEMENT DAMAGE FROM EXPANSIVE SOILS USING MOISTURE BARRIERS

KEYWORDS: *Barrier;* Deformation; *Expansive soil; Geomembrane;* Moisture migration; *Pavement* road construction; Seasonal movement; Trees.

ABSTRACT: Two field trials were carried out at an experimental site on the Sunraysia Highway, north-western Victoria, where the road had to be reconstructed because of the pavement damage caused by the effects of a Victorian semi-arid climate and trees on the expansive clay subgrade. Using a plastic geomembrane, a vertical moisture barrier was installed in each verge in order to stop the lateral migration of moisture to and from the subgrade. A barrier depth of 1.8m below verge surface level was not deep enough to prevent the significant seasonal pavement movements being caused by roadside trees. However, a deeper barrier that was at least 2.5m below verge level greatly reduced or virtually eliminated seasonal movements.

REFERENCE: HOLDEN, J.C. (1992) Reduction of Pavement Damage from Expansive Soils using Moisture Barriers

Proc. of 6th Australia New Zealand Conf. on Geomechanics, Christchurch, New Zealand, Feb 3-7..

THE DEVELOPMENT, TESTING AND APPLICATION OF A NON-STEEL TENDON FOR ARTIFICIAL GROUND SUPPORT

KEYWORDS: *Ground support;* Polyethylene bar; *Rib bolts;* Tendons; Corrosion; *Mining.*

ABSTRACT: BHP has developed an innovative high strength polyethylene (HOPE) bar for artificial ground support applications. The tendon is currently being trialled for use as a rib bolt in underground coal mining applications, as a corrosion proof bolt for use in open pit mines and as a soil nail for improving embankment stability. The properties of the bar, laboratory tests and field trials are discussed.

REFERENCE: HOWARTH, D.F. and RENWICK, M.T. (1992) The Development, Testing and Application of a Non-Steel Tendon for Artificial Ground Support.

Proc. of 6th Australia New Zealand Conf. on Geomechanics, Christchurch, New Zealand, Feb 3-7.

A METHOD OF RISK ASSESSMENT FOR ROADWAY EMBANKMENTS UTILISING EXPANSIVE MATERIALS

KEYWORDS: Risk; Expansive Clays; In-service conditions; Roadway Embankments; Moisture Content Monitoring; Soil Suction Profile; Tolerable Movement.

ABSTRACT: In roadway construction, risk is defined in terms of pavement distress. A risk criterion in terms of the tolerable movements in roadways is proposed for expansive clay road embankments. A design approach is outlined. Valuable information for future designs using expansive clays are found in already constructed road embankments. Their performance in terms of surface distress and associated maintenance requirements can be the yardstick for similar construction. Initial movements may be minimised by designing at the in-service conditions. The soil suction profile for an existing roadway embankment is used as a predictive model for movements accompanying moisture changes, and the risks involved with constructing at the in-service conditions are outlined.

REFERENCE: LOOK-HONG, B., WIJEYAKULASURIYA, V. and REEVES, I. (1992) A Method of Risk Assessment for Roadway Embankments Utilising Expansive Materials.

Proc. of 6th Australia New Zealand Conf. on Geomechanics, Christchurch, New Zealand, Feb 3-7.

SEEPAGE AND SALINITY CONTROL FOR THE WURDEE BOLUC RESERVOIR ENLARGEMENT PROJECT

KEYWORDS: Water supply; Reservoirs; Seepage; Salination; Drainage.

ABSTRACT: The Geelong and District Water Board operates the Wurdee Boluc Reservoir for purposes of domestic and industrial water supply. The Board is currently raising the reservoir by 4m to increase the capacity from 19,200 ML to 40,000 ML. Groundwater studies have shown that raised groundwater levels and associated salination could result from the enlargement. Computer models have been used to assess the problem and have identified a deep drainage trench supplemented by simple relief wells as the most effective method of seepage control. A sensitivity study indicated that large variations in the required length and depth of the drainage trench occurred depending on the foundation conditions assumed in design. Because the embankment is 8 km long it would have been very expensive to adopt a drainage system that provided an acceptable level of risk against downstream salination. However, as there would be a significant time between increase in reservoir level and spread of salination it was decided to adopt an observational approach to achieve an economic design for the system with minimal risk. An extensive groundwater monitoring system has been installed and field trials carried out. Seepage control measures based on a reasonable but not conservative assessment of ground conditions are now being installed. The changes in groundwater levels are being monitored as the reservoir level is raised and supplementary seepage control measures will be installed if required. This paper discusses the design, monitoring and implementation of the seepage control system.

REFERENCE: O'FLAHERTY, P.J., BARKLEY, D. and TRUSCOTT, E.G. (1992) Seepage and Salinity Control for the Wurdee Boluc Reservoir Enlargement Project.

Proc. of 6th Australia New Zealand Conf. on Geomechanics, Christchurch, New Zealand, Feb 3-7.

SEAVIEW MARINA, GEOTECHNICAL DESIGN OF BREAKWATERS

KEYWORDS: *Breakwaters;* Case Study; Geotechnical *Design; Marinas;* Soft *Soils.*

ABSTRACT: Seaview Marina is located in the northeast corner of Wellington Harbour. When completed it will provide sheltered moorings and berths for some 560 pleasure craft. The construction of the associated breakwater is virtually complete. The breakwaters are of rubble mound type, 630m in length and rise up to 8.5m above seabed. They are founded on 14m thickness of very soft and soft alluvial silts. The investigation, design and construction monitoring of the breakwaters is discussed. The design was based on traditional slip circle analyses and undrained soil strength parameters determined by in situ shear vane tests. Consolidation settlement of the breakwaters is closely following that predicted from one dimensional consolidation theory.

REFERENCE: PALMER, S.J. (1992) Seaview Marina, Geotechnical Design of Breakwaters

Proc. of 6th Australia New Zealand Conf. on Geomechanics, Christchurch, New Zealand, Feb 3-7..

TRIAL LOADING OF FAILED SECTION OF RIVER BANK, FISHERMAN ISLAND

KEYWORDS: Analysis; Failure; Field tests; Instrumentation; Pore pressures; Slope stability; Soil mechanics.

ABSTRACT: In November 1985 180m of the partially completed bank of the new Fisherman Islands No. 3 berth collapsed into the Brisbane River. In the course of the failure, shearing had occurred in the river deposits, with displacements of up to about 4m. At the toe the dredging had resulted in overconsolidated conditions and laboratory reversing shearbox tests had shown low residual friction angles. The costs of remedial measures were very dependent on whether residual strength behaviour would apply, on the extent of pore pressures remaining from the failure and on pore pressures which would be developed during reconstruction.

To provide information on these matters it was decided to carry out a trial to near failure by loading the failed section. Major findings were that in the failed and disturbed areas the operational strength was essentially the critical state value, and that substantial pore pressures were developed near the toe because even at relatively high factors of safety against overall failure, the area near the toe became highly stressed and experienced pore pressure increases approximating the maximum total principal stress increase, i.e. Skempton's "A"=1. Near the rear of the slope, the pore pressure increase approximated the increase in total bulk stress, i.e. Skempton's "A"=0.33.

REFERENCE: THORNE, C.P. (1992) Trial Loading of Failed Section of River Bank, Fisherman Island.

Proc. of 6th Australia New Zealand Conf. on Geomechanics, Christchurch, New Zealand, Feb 3-7.

TECHNICAL SESSION 2: FOUNDATIONS AND RETAINING WALLS — GENERAL REPORT

KEYWORDS: Foundations; Retaining walls; Risk.

ABSTRACT: This is the general report on a total of 13 papers presented at the session on Foundations and Retaining Walls during the 1992 6th ANZ Conference on Geomechanics.

REFERENCE: SINCLAIR, T.J.E. (1992) General Report: Technical Session 2 — Foundations and Retaining Walls.

Proc. of 6th Australia New Zealand Conf. on Geomechanics, Christchurch, New Zealand, Feb 3-7.

DESIGN OF GROUTED OFFSHORE PILES IN CALCAREOUS SOILS

KEYWORDS: Piles; *Calcareous;* Design; Cone penetration testing.

ABSTRACT: It is well known that conventional driven steel pipe piles in calcareous soils may show very low unit skin friction values and as a result drilled and grouted insert piles have generally been used for support of offshore platforms in such soils. This paper reviews the current state of practice in design of grouted piles in calcareous soils, and proposes a new alternative to the existing methods using cone penetration test cone resistance values to determine peak skin friction for design. The method proposed also uses load transfer analysis and brittle load transfer curves to calculate axial pile capacity. The effect of cyclic loading on axial capacity is also incorporated in the proposed procedure.

REFERENCE: ABBS, A.F. (1992) Design of Grouted Offshore Piles in Calcareous Soils.

Proc. of 6th Australia New Zealand Conf. on Geomechanics, Christchurch, New Zealand, Feb 3-7.

SENSITIVITY ANALYSIS OF LATERALLY LOADED PILES

KEYWORDS: Design; *Finite element method; Pile foundation; Sensitivity analysis;* Variational principles.

ABSTRACT: A simple on-dimensional idealization in conjunction with the beam-on-elastic-foundation approach is used for sensitivity analysis of laterally loaded piles. The first order variations of an arbitrary displacement and an internal force at a specific cross-section due to some variations of the design variables are derived using the adjoint method. The pile cross-section dimensions, the pile material constants and the soil constants are considered to be the design variables. The consideration is valid both for linear and non-linear range of behaviour of the pile material and the soil. An accuracy of the approximation of the changes of the displacements due to the design variable increments by virtue of their first order variations is also discussed. Some numerical examples dealing with the linear structure are given.

REFERENCE: BUDKOWSKA, B.B. and SZYMCZAK, C. (1992) Sensitivity Analysis of Laterally Loaded Piles.

Proc. of 6th Australia New Zealand Conf. on Geomechanics, Christchurch, New Zealand, Feb 3-7.

IDENTIFICATION OF FAILURE MECHANISMS IN SOFT ROCK USING STEREO-PHOTOGRAMMETRY

KEYWORDS: *Base failure; Bored pile;* Foundations; Instrumentation; *Model test; Photogrammetry; Rock.*

ABSTRACT: In order to determine the failure mechanisms which occur when a soft rock is deformed by a loaded foundation, a series of laboratory tests were conducted on a model footing. The footing and foundation rock were modelled by a semi-cylindrical section which was held against the smooth rigid surface of a transparent window. By taking successive photographs from a fixed camera position as the footing was loaded, it was possible to produce a series of stereo-photographic pairs. When these were viewed under a stereoscope, the three dimensional images could be used to produce qualitative and quantitative data on the evolution of the displacement field in the plane of the section examined.

REFERENCE: CHOI, S.K. and JOHNSTON, I.W. (1992) Identification of Failure Mechanisms in Soft Rock by Stereo-Photogrammetry.

Proc. of 6th Australia New Zealand Conf. on Geomechanics, Christchurch, New Zealand, Feb 3-7.

DETERMINING OF RETAINING WALL STABILITY USING THE FINITE ELEMENT METHOD

KEYWORDS: Finite elements; *Nodal Displacement Method; Retaining walls; Safety factors.*

ABSTRACT: Conventional methods of stability analysis for retaining walls are compared with two approaches based on finite element analyses, namely the modified conventional analysis and the recently developed Nodal Displacement Method (NDM). The NDM has considerable potential as it is able to model construction sequences and gives due attention to soil and wall displacements as well as stresses. The physical meaning of safety factor is discussed and the NDM shown to be capable of giving a range of values, depending upon which problem variables are considered to be significant.

REFERENCE: DONALD, I.B. and GOH, A.T.C. (1992) Determination of Retaining Wall Stability using the Finite Element Method.

Proc. of 6th Australia New Zealand Conf. on Geomechanics, Christchurch, New Zealand, Feb 3-7.

LATERAL SOIL MOVEMENT LOADING ON BRIDGE FOUNDATION PILES

KEYWORDS: Construction fills; *Lateral soil movements; Soft clay; Piles;* Analysis; Case study; Bridge foundations.

ABSTRACT: A case in which large amounts of construction filling led to overstressing of piles supporting a bridge foundation is presented. Despite efforts to minimise the lateral soil movements, e.g. employing light fill and strong geotextiles, lateral sub-soil movement of the very soft estuarine clays were caused by the temporary construction fill and severe over-loading of two groups of pier piles ensued. The situation may have been influenced by a previous failure of the soil near the two pile groups, when fill without geotextile reinforcing had been employed during site investigation. A numerical analysis confirmed the likelihood of pile failure and assisted with the assessment of the integrity of other piles at the site.

REFERENCE: HULL, T.S. and McDONALD, P. (1992) Lateral Soil Movement Loading on Bridge Foundation Piles

Proc. of 6th Australia New Zealand Conf. on Geomechanics, Christchurch, New Zealand, Feb 3-7..

BEHAVIOUR OF FIXED AND FREE HEAD PILES IN A LATERALLY SLIDING SOIL

KEYWORDS: Lateral load; *Sliding soil;. Fixed head pile; Free head pile;* Pile design; Slope stability improvement; Axial pile stresses; Numerical analysis.

ABSTRACT: The effect of soil sliding laterally past a pile is investigated for both the fixed and free head boundary conditions. A numerical method is employed and the limitations imposed by small deformation assumptions are highlighted. Axial response of the pile is incorporated in an approximate manner and leads to limits on the pile response in terms of axial pile stresses. The results can be of aid in the design of piles to withstand lateral soil movements while supporting structures and the design of piles to increase slope stability. The influence of head fixity is found to be restricted to a limited range of sliding soil depths.

REFERENCE: HULL, T.S., LEE, C.Y., and POULOS, H.G. (1992) Behaviour of Fixed and Free Head Piles in a Laterally Sliding Soil.

Proc. of 6th Australia New Zealand Conf. on Geomechanics, Christchurch, New Zealand, Feb 3-7.

ANALYTICAL PREDICTIONS FOR SIDE RESISTANCE OF PILES IN ROCK

KEYWORDS: *Analytical model; Bored piles;* Design curves; *Rock; Side resistance.*

ABSTRACT: The side resistance of a bored pile in rock is largely controlled by the roughness of the interface between the concrete of the pile and the surrounding rock mass. On the basis of a large number of laboratory tests, an analytical model has been developed to describe the behaviour of this interface. By making a number of reasonable assumptions, the model has been used to produce some simplified design charts for the estimation of adhesion factors for miles in Melbourne mudstone.

REFERENCE: KODIKARA, J.K., JOHNSTON, I.W. and HABERFIELD, C.M. (1992) Analytical Predictions for Side Resistance of Piles in Rock.

Proc. of 6th Australia New Zealand Conf. on Geomechanics, Christchurch, New Zealand, Feb 3-7.

STABILITY OF RETAINING WALLS WITH COMPACTED BACKFILLS

KEYWORDS: *Compaction;* Finite elements; *Nodal Displacement Method; Retaining walls; Stability.*

ABSTRACT: A new technique referred to as the "Nodal Displacement Method" — based on the Finite Element Method — was developed at Monash University for the evaluation of the stability of geotechnical structures and slopes. A compaction simulation algorithm was also developed and incorporated with an elastoplastic finite element model to simulate the compaction of the fill behind retaining walls. This paper describes the application of the model displacement method to evaluate the stability of retaining walls where the backfill has been compacted.

REFERENCE: KULATHILAKA, S.A.S. and DONALD, I.B. (1992) Stability of Retaining Walls with Compacted Backfills.

Proc. of 6th Australia New Zealand Conf. on Geomechanics, Christchurch, New Zealand, Feb 3-7.

RISK ASSOCIATED WITH CONSTRUCTION OF LARGE DIAMETER BORED PILES IN CAVERNOUS MARBLE

KEYWORDS: Foundation; Cavernous marble; Bored piles; Soil cavity; Sinkholes; Soil piping.

ABSTRACT: The method used for the construction of large diameter bored piles for the Light Rail Transit Development Project in Hong Kong are discussed. The piles were founded on cavernous marble bedrock with large cavity systems, one of which is believed to be connected as far as 30m horizontally and 20m vertically. The paper discusses the risks involved in bored piling in cavernous marble. The major risks include the formation of sinkholes and collapse of soil cavities. The techniques used for minimising these risks are described.

REFERENCE: LI, K.S. (1992) Risk Associated with Construction of Large Diameter Bored Piles in Cavernous Marble.

Proc. of 6th Australia New Zealand Conf. on Geomechanics, Christchurch, New Zealand, Feb 3-7.

PREDICTION AND MEASUREMENT OF A HEAVILY LOADED RAFT

KEYWORDS: Settlement; Pressuremeter; Raft footing.

ABSTRACT: Settlement of a heavily loaded raft was predicted on the basis of pressuremeter test results and other data using a layered elastic model, and the computer program FOCALS. Settlement measurements taken during construction allow assessment of these predictions, and the effectiveness of the approach used.

REFERENCE: OLDS, R.J. (1992) Prediction and Measurement of a Heavily Loaded Raft.

Proc. of 6th Australia New Zealand Conf. on Geomechanics, Christchurch, New Zealand, Feb 3-7.

THE CELLULAR RAFT AND HORIZONTAL GROUND STRAINS

KEYWORDS: Mining subsidence; Heaving clay; Swelling rock; Earthquakes; *Ground strain; Foundations;* Base isolation.

ABSTRACT: The development of a cellular raft foundation (called the BOUCELL raft) is described and compared with the conventional slab-on-ground or stiffened raft foundation in a number of applications. The potential of the cellular raft to reduce the risk of distress to buildings caused by horizontal soil stain is discussed. Areas of application where this mechanism of horizontal soil strain should be considered, include:

- Buildings on ground to be undermined, particularly with longwall mining techniques for total extraction of coal.
- Buildings in seismically active zones where large ground motions may be involved.
- Buildings on swelling soft rock which has been weathered to considerable depth.

REFERENCE: PELLISSIER, J.P. and WILLIAMS, A.A.B. (1992) The Cellular Raft and Horizontal Ground Strains.

Proc. of 6th Australia New Zealand Conf. on Geomechanics, Christchurch, New Zealand, Feb 3-7.

CLASS A PREDICTIONS OF PILE BEHAVIOUR

KEYWORDS: Analysis; Bearing capacity; Field tests; Pile foundations; Residual loads; Settlement; Soil mechanics.

ABSTRACT: Class A (before the event) predictions were made of the load-settlement behaviour of four different test piles at a site in Evanston, Illinois:

1. a driven steel tube pile;
2. a driven steel H pile;
3. a drilled pier constructed under slurry;
4. a drilled cased pier.

The paper describes the prediction procedures adopted and the correlations employed to assess the required geotechnical parameters. Predictions are presented for the load-settlement behaviour, the distribution of load with depth and the distribution of residual load after installation of the driven piles. These are then compared with the measured behaviour of the test piles.

REFERENCE: POULOS, H.G. (1992) Class A Predictions of Pile Behaviour.

Proc. of 6th Australia New Zealand Conf. on Geomechanics, Christchurch, New Zealand, Feb 3-7.

STUDY OF A CASE OF UNSUITABLE STRUCTURAL SYSTEM ON HETEROGENEOUS SOIL

KEYWORDS: *Soil mechanics; Foundations; Buildings; Damage; Differential movement;* Rigidity; Cracking; Water effect; Soil replacement; Repair works.

ABSTRACT: This paper presents a case of group of residential low-cost buildings constructed in new desert area in Egypt. The geotechnical properties of the soil and its behaviour were not well studied before construction. The adopted foundation type and structural system were unsuitable and could not afford sufficient rigidity for the buildings to withstand the occurred differential movements due to water penetration through the bearing stratum. Severe cracks and damages had taken place in most bearing walls. The paper presents also all the carried out investigations, inspections and studies to identify the case. The proposed remedy includes soil replacement, foundation support, different repair works and the necessary precautions to stop deterioration and make the houses ready for use without any future troubles.

REFERENCE: REYAD, M.M. (1992) Study of a Case of Unsuitable Structural System on Heterogeneous Soil.

Proc. of 6th Australia New Zealand Conf. on Geomechanics, Christchurch, New Zealand, Feb 3-7.

THE ANALYSIS OF AXIALLY LOCATED PILES IN LAYERED OR NON-HOMOGENEOUS SOILS

KEYWORDS: *Elastic theory;* Finite layer method; Non-homogeneous soil; *Pile foundations; Settlement (structural); Soil mechanics.*

ABSTRACT: A finite layer method of analysis is presented which may be used to compute the settlement of end bearing piles in soils which are horizontally layered or for which the modulus increases linearly with depth. Comparisons are made with the solutions of other authors and with the results of finite element analyses for piles subjected to axial loading. It is found that for all the cases examined, the finite layer approach can produce highly accurate results.

REFERENCE: SMALL, J.C. and LEE, C.Y. (1992) The Analysis of Axially Loaded Piles in Layered or Non-Homogeneous Soils.

Proc. of 6th Australia New Zealand Conf. on Geomechanics, Christchurch, New Zealand, Feb 3-7.

PILED BRIDGE ABUTMENTS ON SOFT CLAY — EXPERIMENTAL DATA AND SIMPLE DESIGN METHODS

KEYWORDS: Bridge abutments; Centrifuge modelling; *Embankments;* Lateral loads; *Piles; Soft clay.*

ABSTRACT: Construction of bridge approach embankments on soft clay can result in the development of significant lateral soil movements, which impose lateral loads on the abutment piles. Estimation of these loads is highly uncertain at present. Centrifuge model tests of piled bridge abutments have been conducted with a view to obtaining data from which a new design method may be developed. Results from two of these tests are presented and compared with predictions from several current simple design methods. Some of the factors influencing the loads induced in piles adjacent to embankments are discussed.

REFERENCE: STEWART, D.P., JEWELL, R.J. and RANDOLPH, M.F. (1992) Piled Bridge Abutments on Soft Clay — Experimental Data and Simple Design Methods.

Proc. of 6th Australia New Zealand Conf. on Geomechanics, Christchurch, New Zealand, Feb 3-7.

THE ANALYSIS OF RECTANGULAR RAFTS OF FINITE FLEXIBILITY SUBJECTED TO CONCENTRATED LOADS

KEYWORDS: Bending moments; *Elastic analysis;* Finite element method; Finite layer analysis; *Foundations;* Rafts; Soil mechanics; *Numerical analysis;* Soil-structure interaction.

ABSTRACT: A method is presented which may be used to analyse the behaviour of rafts resting on elastic soil layers. The soil layer may be of finite depth and the soil properties may vary vertically and in one lateral direction. Finite elements are used for the analysis of the raft and finite layer theory is used for the analysis of the soil. Examples are presented, with values of differential displacements and moments in the raft being evaluated for the case where point loads are applied to the raft.

REFERENCE: ZHANG, B.Q. and SMALL, J.C. (1992) The Analysis of Rectangular Rafts of Finite Flexibility Subjected to Concentrated Loads.

Proc. of 6th Australia New Zealand Conf. on Geomechanics, Christchurch, New Zealand, Feb 3-7.

MINING, TUNNELLING AND EXCAVATIONS — GENERAL REPORT

KEYWORDS: Mining; Tunnelling; Excavations.

ABSTRACT: This is the general report on a total of twelve papers presented at the session on mining, tunnelling and excavations during the 1992 6th ANZ Conference on Geomechanics.

REFERENCE: BENNET, A.G. (1992) General Report — Mining, Tunnelling and Excavations.

Proc. of 6th Australia New Zealand Conf. on Geomechanics, Christchurch, New Zealand, Feb 3-7.

SUBSIDENCE DUE TO ABANDONED MINES: RISK, EVALUATION AND MITIGATION

KEYWORDS: Pillar failure; Sags; Void migration; Site investigation; Hazard zoning; Rafts; Bulk grouting.

ABSTRACT: Abandoned mine workings, especially those at shallow depth, because of their potential to cause ground subsidence, often represent significant problems in urban areas where development or redevelopment is to take place. In the United Kingdom information needed to locate potential hazards due to mineworkings is available but occurs in numerous scattered locations and considerable time and effort may be involved in its collection. In recent years thematic geological maps have been produced for certain coalfield areas where workings have long since closed. These can be used as an initial aid to hazard avoidance when such areas undergo redevelopment.

Nonetheless old workings should be located prior to the development of a site, and their layout and condition determined, wherever possible. This can be accomplished by a combination of indirect and direct methods of exploration. The site then can be zoned according to the degree of risk that the workings present. This may result in buildings not being permitted to those areas of maximum risk unless the ground is stabilized beforehand. Stabilization measures may involve occupying the workings with hydraulic fill or cheap bulk grouts. In areas of less risk special foundation structures may be used.

REFERENCE: BELL, F.G. and MORTIMER, B. (1992) Subsidence due to Abandoned Mines: Risk, Evaluation and Mitigation.

Proc. of 6th Australia New Zealand Conf. on Geomechanics, Christchurch, New Zealand, Feb 3-7.

STUDY OF PERIPHERAL FRACTURED ZONES AT THE SIDES OF ROADWAYS IN UNDERGROUND COAL MINES IN NEW SOUTH WALES BY SEISMIC METHODS

KEYWORDS: *Fractured zones; Pillar; Continuous ribside; Seismic refraction; Uphole method;* P-wave velocity.

ABSTRACT: A study of the depth and degree of fracturing at the sides of pillars and continuous ribs in roadways was conducted at two underground coal mines in New South Wales, using the seismic refraction and a modified form of the uphole method. The depths of the fractured zones determined by the refraction method were lower than the corresponding ones by the uphole method, the latter being closer to the findings of other investigators.

REFERENCE: BHATTACHARYYA, A.K. and BELLEZA, G.B. (1992) Study of the Peripheral Fractured Zones at the Sides of Roadways in Underground Coal Mines in New South Wales by Seismic Methods

Proc. of 6th Australia New Zealand Conf. on Geomechanics, Christchurch, New Zealand, Feb 3-7..

A RELIABILITY-BASED APPROACH FOR THE ASSESSMENT OF STABILITY AND SUPPORT REQUIREMENTS IN JOINTED ROCK EXCAVATIONS

KEYWORDS: Joint Statistics; Reliability; Stability; Support Requirements.

ABSTRACT: A reliability-based approach has been adopted for the assessment of stability and support requirements for three case study jointed rock excavations. The assessment of excavation stability has been based on the distributions of individual volumes of potentially unstable blocks surrounding each excavation. The assessment of support requirements has been based on the distributions of block depths and their occurrence per excavation advance. The dimensions and occurrence of potentially unstable blocks has been quantified by examining the interaction of excavation geometry with the rock mass structural patterns on 2D joint trace maps for selected section views through each rock mass. Joint trace maps have been generated using joint statistics and a simple rock mass structural model. By repetitively superimposing the respective excavation geometrics on the corresponding joint trace map it was possible to identify potentially unstable blocks according to simple geometric criteria and quantify their dimensions to construct distributions of block geometry. The probabilities of encountering individual block volumes per excavation advance have been represented on cumulative frequency distributions to provide reliability-based predictions of excavation instability. Confidence levels have been represented on cumulative frequency distributions for block depths to provide reliability-based predictions of support requirements in terms of required lengths of rock bolts to support potentially unstable blocks. Predicted rock bolt spacings have been calculated based on the number of potentially unstable blocks identified per excavation advance. A reasonably good correlation has been found to exist between the reliability-based predictions and actual and/or recommended support requirements for the three case study rock excavations that have been investigated.

REFERENCE: BROX, D.R. (1992) A Reliability-Based Approach for the Assessment of Stability and Support Requirements in Jointed Rock Excavations.

Proc. of 6th Australia New Zealand Conf. on Geomechanics, Christchurch, New Zealand, Feb 3-7.

IN SITU STRESS MEASUREMENTS USING HYDRAULIC FRACTURING IN JOINTED ROCK IN HONG KONG

KEYWORDS: In situ stress; Hydraulic fracturing; Tunnels; Hong Kong.

ABSTRACT: In situ stress measurements using the hydraulic fracturing technique have been conducted in Hong Kong during the preliminary design site investigation for the Cheung Ching Tunnel as part of the Route 3 Project. Measurements were conducted in shallow boreholes completed along the eastern low rock cover section of the proposed tunnel alignment on Tsing Yi Island. The magnitude and orientation of the minimum principal horizontal stress was of concern along this critical section of tunnel where rock cover varies between 16 and 30 metres above crown level. Information concerning the in situ state of stress was significant for the evaluation of the stability of the 1.5 km long, twin arrangement of unprecedented 17 metre span tunnels. Rock mass conditions along this section of the proposed tunnel alignment are characterised with closely spaced jointing and slightly to moderately weathered granitic rock. Near consistent minimum principal horizontal stresses were measured slightly in excess of overburden stress. Results from numerical modelling of the variable topography indicate a generally good agreement with the measured stresses.

REFERENCE: BROX, D.R., KONIETZKY, H., RUMMEL, F. (1992) In Situ Stress Measurements using Hydraulic Fracturing Techniques.

Proc. of 6th Australia New Zealand Conf. on Geomechanics, Christchurch, New Zealand, Feb 3-7.

RISK OF MINE RELATED SUBSIDENCE AT OCEAN VIEW

KEYWORDS: Earthquake; Hazard; *Mining; Risk Analysis;* Subsidence.

ABSTRACT: In July 1989 a subsidence pit appeared in a residential area at Ocean View above the one hundred year old abandoned Walker No. 1 Coal Mine. Subsidence hazard for the residential area was examined. The extent of the mine was assessed together with overlying ground conditions and condition of the mine. Strata overlying the mine were found to be extremely weak. Mine workings were found to be deteriorating and in an open and flooded condition. The subsidence pit was attributed to localised catastrophic collapse of the mine roof and consequent subsidence of water charged sandy gravel into the mine opening, causing the sudden collapse at the ground surface. Other similar pits were observed above nearby abandoned mines. The risk of further subsidence pits forming was assessed to be very probable. Fourteen private properties were determined to be at risk, and the degree of risk to residents and property was assessed as 'risky to some risk". Courses of action for the Local Authority were prepared and in August 1990 the Crown accepted some liability for the situation.

REFERENCE: FARQUHAR, G.B. and DOUGLAS, B.J. (1992) Risk of Mine Related Subsidence at Ocean View.

Proc. of 6th Australia New Zealand Conf. on Geomechanics, Christchurch, New Zealand, Feb 3-7.

APPLICATION OF ADVANCED ELECTRONIC GEOTECHNICAL MONITORING TECHNIQUES IN AUSTRALIAN UNDERGROUND COAL MINING

KEYWORDS: *Geotechnical monitoring; Coal mining;* Automated monitoring; *Intrinsic safety.*

ABSTRACT: Excavation instability is a major problem in underground coal mining in terms of the potential risk to both personnel and production, lowering safety levels and reducing efficiency. In this environment there is a clear need for effective geotechnical monitoring to be undertaken. To be of maximal value and most cost effective, this type of routine data retrieval is best undertaken by automated computer controlled systems.

The potential role and value of automated geotechnical sensors and monitoring systems is clear. The advantages of the utilisation of such technology in the modern underground coal mine would manifest themselves as improved excavation design reducing instability, higher efficiency and profitability of operations by avoiding costly delays and by promoting a safer working environment in underground coal mines.

REFERENCE: FOLLINGTON, I.L. and MEDHURST, T.P. (1992) Application of Advanced Electronic Geotechnical Monitoring Techniques in Australian Underground Coal Mining.

Proc. of 6th Australia New Zealand Conf. on Geomechanics, Christchurch, New Zealand, Feb 3-7.

BACK ANALYSIS OF A DUG EXCAVATION IN SOFT CLAY

KEYWORDS: Underground excavation; Tunnels; Soft clay; Back analysis; Singapore.

ABSTRACT: One of the more complex projects in the construction of the mass rapid transit system in Singapore was the construction of the Marina Bay station and tunnels. The complexity of the site conditions made conventional excavation methods uneconomical. The construction involved the construction of a series of cofferdams and submerged excavation of the soil. Back analyses were carried out using the finite element method in which the soil is modelled by a non-linear, hyperbolic stress-strain relationship.

REFERENCE: GOH, A.T.C., WONG, K.S. and PREBAHARAN, N. (1992) Back Analysis of a Dug Excavation in Soft Clay.

Proc. of 6th Australia New Zealand Conf. on Geomechanics, Christchurch, New Zealand, Feb 3-7.

RESIDUAL ROCK BURSTING IN THE HOMER TUNNEL, FIORDLAND, N.Z.

KEYWORDS: Explosive spalling; Residual stress; Denudation.

ABSTRACT: The Homer Tunnel pilot heading and the full tunnel encountered zones of explosive rock spalling the causes of which had to be quantified and controlled before public use was allowed. Because of a turbulent recent geological history there were several possible causes.

The spalling occurred in strong massive rock, but was not continuous, and it attenuated with time, so it was postulated that the cause was residual stresses locked in from past geological time and released by the tunnel excavation.

Four years of monitoring confirmed this diagnosis. Denudation of 18 kms of this piece of Gondwana basement in the last 6 M years was the most likely mechanism, leaving a high horizontal stress component locked in, with a relatively small vertical component from present overburden.

REFERENCE: GORDON, F.R. (1992) Residual Rock Bursting in the Homer Tunnel, Fiordland N.Z.

Proc. of 6th Australia New Zealand Conf. on Geomechanics, Christchurch, New Zealand, Feb 3-7.

SLOPE STABILITY DURING BLASTING: A CASE HISTORY

KEYWORDS: *Blasting;* Blast monitoring; Blast modelling; *Slope stability.*

ABSTRACT: The paper discusses the effects of open pit production blasting on the stability of the main footwall slope in pit 1A of the Telfer Gold Mine in Western Australia. The paper presents results of blast monitoring and blast modelling. These data are used in the back analysis of failed sections of slope to assess blast-induced accelerations pertaining during slope failure, and the results of this analysis are used to assess failure risk in the slope during future blasting operations. A good correlation is obtained between blast acceleration and distance from the blast divided by the square root of the TOTAL charge weight in the blast (when plotted on a log-log scale), which makes the risk assessment credible.

REFERENCE: LILY, P.A. and THOMPSON, P.W. (1992) Slope Stability During Blasting: A Case History.

Proc. of 6th Australia New Zealand Conf. on Geomechanics, Christchurch, New Zealand, Feb 3-7.

THE USE OF DIAPHRAGM WALLS TO REDUCE RISK IN DEEP EXCAVATION

KEYWORDS: *Bentonite;* Construction; Deep excavation; *Diaphragm; Walls foundations;* Ground-water; Grout; Risk management; Slurry walls.

ABSTRACT: Diaphragm walls are permanent foundations structures constructed in place before excavation is carried out. Knowing and understanding their inherent features not only provides designers with a cost effective alternative to other temporary and permanent construction forms, but can also offer managers of construction a safer option during the building phase when risk to workers and adjoining structures is high.

REFERENCE: RESSI DI CERVIA, A.L. (1992) The Use of Diaphragm Walls to Reduce Risk in Deep Excavation.

Proc. of 6th Australia New Zealand Conf. on Geomechanics, Christchurch, New Zealand, Feb 3-7.

MODELLING SURFACE AND SUBSURFACE SUBSIDENCE OVER COAL MINES

KEYWORDS: *Subsidence; Centrifuge modelling;* Total extraction.

ABSTRACT: A series of geotechnical centrifuge model tests are reported in which coal extraction at relatively shallow depth (60 metres) has been simulated and surface and subsurface movements of the overlying strata recorded. A trap-door system was designed and developed to replicate the total extraction of panels of coal by either Wongawilli or Longwall extraction. The centrifuge model tests were performed on the Acutronic 661 centrifuge at the University Of Western Australia. From post-test examination of the deformed models using a scanning Laser displacement transducer, settlement data for both the surface and subsurface strata was determined. The effectiveness of the centrifuge modelling technique for modelling subsidence problems, and its capabilities for calibrating numerical models is well demonstrated.

REFERENCE: STONE, K.J.L. and MISICH, I. (1992) Modelling Surface and Subsurface Subsidence over Coal Mines.

Proc. of 6th Australia New Zealand Conf. on Geomechanics, Christchurch, New Zealand, Feb 3-7.

A REVIEW AND ANALYSIS OF ROCK DISCONTINUITY MAPPING METHODS

KEYWORDS: *Geological Mapping; Rock Mass Discontinuities; Sampling Biases.*

ABSTRACT: Conventional rock discontinuity mapping methods use a line or an areal intersection criterion in order to determine a statistically representative sample of the rock mass structural properties. In the present case, line transect, semi-trace length and cell mapping techniques are described and compared. Finally, the line sampling method is recommended based on practicality and the mathematical analysis of the observed discontinuity trace length distributions.

REFERENCE: VILLAESCUSA, E. (1992) A Review and Analysis of Rock Discontinuity Mapping Methods.

Proc. of 6th Australia New Zealand Conf. on Geomechanics, Christchurch, New Zealand, Feb 3-7.

ASSESSMENT OF APPLICABILITY OF FOUR EMPIRICAL STRENGTH CRITERIA FOR INTACT COAL

KEYWORDS: Strength criterion; Coal; Triaxial testing; Axial compressive strength.

ABSTRACT: The applicability of four empirical strength criteria, namely, Bieniawski, Hock and Brown, Johnston and Ramamurthy has been assessed for intact coal by using the published triaxial test data. For non-linear regression analysis, the PC package FFIT has been selected. The best fit has been found by minimising the sum of the squares of the relative errors between the function and the data points. Although unique values of the constants in all criteria have been determined with good coefficients of determination ranging from 0.83 to 0.86 for overall data, a wide variation has been noticed in the values of the constants when individual data sets have been analysed. A strong negative correlation has been observed between B in Bieniawksi's criterion and uniaxial compressive strength, σ (coefficient of determination, r^2=0.86), m in Hoek and Brown's criterion and σ (r^2=0.71) and B in Ramamurthy's criterion and σ (r^2=0.88). An empirical strength equation which best describes the triaxial strength test data analysed for intact coal is presented. An estimate of the axial compressive stress at failure at any confining pressure can be made if only the uniaxial compressive strength of the intact coal is known.

REFERENCE: VUTUKURI, V.S., HOSSAINI, M.E. (1992) Assessment of Applicability of Four Empirical Strength Criteria for Intact Coal.

Proc. of 6th Australia New Zealand Conf. on Geomechanics, Christchurch, New Zealand, Feb 3-7.

SESSION 4: SOIL PROPERTIES AND TESTING — GENERAL REPORT

KEYWORDS: Soil properties; Testing; Risk.

ABSTRACT: This is the general report on a total of 21 papers presented at the session on soil properties and testing during the 1992 6th ANZ Conference on Geomechanics.

REFERENCE: ELDER, D. McG. and TRAYLEN, N.J. (1992) General Report, Session 4: Soil Properties and Testing.

Proc. of 6th Australia New Zealand Conf. on Geomechanics, Christchurch, New Zealand, Feb 3-7.

POLLUTANT MIGRATION THROUGH CLAY

KEYWORDS: Hydraulic conductivity; Permeability; Clay; Pollution Migration; Kerosene.

ABSTRACT: Tests have been performed on a remoulded clay to establish the variation of its hydraulic conductivity with stress history and void ratio. The hydraulic conductivity has been determined by both a direct flow method and indirectly from the consolidation response, and a comparison of these methods is presented. A pollutant, kerosene, has been forced through the samples and the hydraulic conductivity determined. No flow of the kerosene was detected until a breakthrough pressure, dependent on the void ratio, was exceeded. Thereafter, the hydraulic conductivity was almost linearly related to the flow rate. The high relative permeabilities suggest that significant chemical effects occur as kerosene displaces the water.

REFERENCE: AIREY, D.W. (1992) Pollutant Migration Through Clay.

Proc. of 6th Australia New Zealand Conf. on Geomechanics, Christchurch, New Zealand, Feb 3-7.

STRESS PATH TESTS TO INVESTIGATE YIELDING OF K_0 CONSOLIDATED SOIL

KEYWORDS: *Yielding; Triaxial testing; Clay.*

ABSTRACT: An important feature of soil behaviour is the existence of a state boundary, or yield, surface which marks a clear change in behaviour from relatively high stiffness to relatively low stiffness. Parts of the surface can be identified in oedometer and one-dimensional compression tests in which the yield stress is identified by the preconsolidation pressure. However, in different parts of foundations and other structures soils experience many different stress paths and it is necessary to examine the complete state boundary surface. Conventional methods, using undrained triaxial compression and extension tests are unsatisfactory for this purpose as there is no guarantee that undrained stress paths reach and follow that state boundary surface. An alternative method is to use special drained stress paths in which the stress path is constrained to follow the state boundary surface causing continuous yielding.

The paper describes a short series of special tests on a K_o consolidated, reconstituted silty clay. The test results demonstrate that the state boundary surface observed in the tests on K_o consolidated samples is approximately symmetrical for compression and extension and it is close to the surface for isotropically consolidated samples given by Cam-clay.

REFERENCE: ALLMAN, M.A., ATKINSON, J.H. and JORDAN, D.O. (1992) Stress Path Tests to Investigate Yielding of K_o Consolidated Soil.

Proc. of 6th Australia New Zealand Conf. on Geomechanics, Christchurch, New Zealand, Feb 3-7.

SCREW PLATE INSERTION DISTURBANCE IN SAND

KEYWORDS: *Sand; Laboratory testing; Modulus of elasticity;* Screw plate.

ABSTRACT: This paper gives the results of a series of laboratory tests carried out in clean dry sand, in which load-displacement tests were used for evaluation of Young's modulus of the sand. Tests were carried out using a miniature screw plate embedded in the sand during the process of sand raining, and a screw plate inserted by rotation into the sand from the sand surface. The inserted screw plate was under the control of a threaded rod having the same pitch as the screw plate.

The purpose of the tests was to determine the effect of insertion disturbance on values of Young's modulus obtained from a test with an inserted screw plate. Tests were carried out at relative densities of about 0.15, 0.65 and 0.85 with surcharge pressures of 35 kPa and 100 kPa. Comparison of the results from embedded and inserted screw plates indicates that the effect of the disturbance caused by insertion is small when the sand is loose, but may be considerable when the sand is more dense.

REFERENCE: BROWN, P.T. and ABDEL-LATIF, M.F. (1992) Screw Plate Insertion Disturbance in Sand.

Proc. of 6th Australia New Zealand Conf. on Geomechanics, Christchurch, New Zealand, Feb 3-7.

SCREW PLATE INSERTION DISTURBANCE IN SAND

KEYWORDS: *Clay;* Consolidation; *Laboratory testing; Modulus of elasticity;* Screw plate.

ABSTRACT: This paper gives the results of a series of laboratory tests carried out in kaolin consolidated from slurry, in which load-displacement tests were used for evaluation of Young's modulus of the clay. Tests were carried out using a flat circular disc and a miniature screw plate both being embedded in the clay prior to consolidation, and a screw plate inserted by rotation into the clay from the clay surface after consolidation.

The purpose of the tests was to determine the effect of screw plate shape and insertion disturbance on values of undrained and drained modulus and coefficient of consolidation obtained from a test with an inserted screw plate. Tests were carried out with OCR = 5 and 10. Comparison of the results from embedded and inserted screw plates, despite scatter, indicates that the effect of the disturbance caused by insertion is small when OCR = 5, but is considerable when OCR = 10.

REFERENCE: BROWN, P.T. and ABDEL-LATIF, M.F. (1992) Screw Plate Insertion Disturbance in Clay.

Proc. of 6th Australia New Zealand Conf. on Geomechanics, Christchurch, New Zealand, Feb 3-7.

STRAIN SOFTENING OF A GRANULAR SOIL IN TRIAXIAL AND MULTI-AXIAL TESTING

KEYWORDS: Granular soil; Multi-axial testing; Strain softening; Strain path; Stress path; Triaxial testing.

ABSTRACT: An intensive research program was carried out to investigate the strain softening behaviour of a dense granular soil. Strain path testing technique was developed and adopted for the study. Both strain softening observed from triaxial and multi-axial tests were reported. The factors affecting the occurrence of strain softening were discussed.

REFERENCE: CHU, J., LO, S-C. R. and LEE, I.K. (1992) Strain Softening of a Granular Soil in Triaxial and Multi-Axial Testing.

Proc. of 6th Australia New Zealand Conf. on Geomechanics, Christchurch, New Zealand, Feb 3-7.

SOME ENGINEERING IMPLICATIONS OF CHEMICAL WEATHERING OF SOIL FORMATIONS AT NILE VALLEY BOUNDARIES

KEYWORDS: Silica/sesquioxide ratio; Nile clay; Desert clay; Genesis; Lateritic soil; Geomorphology; Chemical weathering.

ABSTRACT: Analysis of result, of silica/sesquioxide ratio of clayey deposit in Egypt showed that there are significant variations in the values of this ratio depending upon whether the soil is inside or outside the Nile Valley. It is observed that the clayey deposits outside the Nile Valley (desert region) are poorly developed even though they are quite old compared to inside the Nile Valley. These changes could be attributed to genesis of soil deposits. The alluvial formations of the Nile Valley have been enriched by lateritic soil carried down by the Nile River from tropical zone of Abyssinia. Furthermore it was found that the morphological conditions affected the silica/sesquioxide ratio indicating differential weathering that chemical weathering modified geotechnical properties significantly.

REFERENCE: EL-SOHBY, M.A., MAZEN, S.O. and ABOUSHOOK, M.I. (1992) Some Engineering Implications of Chemical Weathering of Soil Formations at Nile Valley Boundaries.

Proc. of 6th Australia New Zealand Conf. on Geomechanics, Christchurch, New Zealand, Feb 3-7.

EVALUATION OF TERTIARY AGE GRAVEL DEPOSITS USING PLATE LOAD TESTS

KEYWORDS: *Gravel; Compressibility; Insitu testing;* Design; Settlement.

ABSTRACT: Refurbishment of an eight storey building resulted in footing loads increasing by up to 25% above the original design value. Site investigations showed the footings were founded on gravels, not siltstone as expected. Plate load testing was carried out to evaluate the settlement characteristics of the gravel. Stress of up to 1500 kPa were applied, using the existing building for reaction. Settlements were able to be confidently predicted.

REFERENCE: ERVIN, M.C. and KURZEME, M. (1992) Evaluation of Tertiary Age Gravel Deposits Using Plate Load Tests.

Proc. of 6th Australia New Zealand Conf. on Geomechanics, Christchurch, New Zealand, Feb 3-7.

EVALUATION OF SWELLING OF AN EXPANSIVE CLAY SHALE FROM MAE MOH, THAILAND

KEYWORDS: Clay shale; Expansive clay; Free swell; Oedometer; Swell pressure.

ABSTRACT: Slope instability problems and some failures of linings in the Mae Moh diversion channel in Northern Thailand have been caused by the presence of expansive clay shales. The paper describes the results of some laboratory tests conducted on block samples of this clay shale composed of fine grained and fissured material. The tests were conducted using the oedometer, the triaxial apparatus, the hydraulically pressurized consolidometer and the pressure membrane apparatus. Undisturbed, remoulded and pressurized samples were used. Experimental results indicated that the clay shale was highly cemented. The moderate expansive behaviour of the clay shale can be attributed to the presence of some active and expansive materials. The swelling pressure was about 400 kPa for the majority of tests conducted. The Huder-Amberg test was found to be the most reliable for measuring the swelling pressure. A rather high expansion was recorded when the sample was tested in its unconfined state and differential swelling was observed in the sub-parallel directions. Therefore, the swelling of the clay shale was possibly due to the mineral orientation as well as the horizontally bedded fissures.

REFERENCE: INDRARATNA, B. and HUSIN, M.R.B. (1992) Evaluation of Swelling of an Expansive Clay Shale from Mae Moh, Thailand.

Proc. of 6th Australia New Zealand Conf. on Geomechanics, Christchurch, New Zealand, Feb 3-7.

NORMALISED SHEAR STRENGTH AND COMPRESSIBILITY CHARACTERISTICS OF ADELAIDE EXPANSIVE CLAY

KEYWORDS: *Shear strength; Compressibility; Expansive clay; Total suction; Earth pressure;* Undrained; In-situ.

ABSTRACT: Extensive data on the engineering properties of expansive clay soils, which underlie the City of Adelaide, have been determined as part of the many construction projects in the central business district. The expansive clays have large in-situ total soil suctions, of the order of pF=4. Also, high values of undrained shear strength and undrained Young's modulus have been measured, which are typical of an overconsolidated clay. This paper examines the available data on the shear strength and compressibility characteristics of these clay soils. It is shown that by taking into account the large total suctions acting within the soil samples, the undrained shear strength and Young's modulus, when normalised with respect to the effective stresses, are comparable to data determined for other over-consolidated clays. The range of values is indicated in a normalised format although a statistical treatment of the trends is not presented in this paper.

REFERENCE: KAGGWA, W.S. and JAKSA, M.A. (1992) Normalised Shear Strength and Compressibility Characteristics of Adelaide Expansive Clay.

Proc. of 6th Australia New Zealand Conf. on Geomechanics, Christchurch, New Zealand, Feb 3-7.

DEGREE OF SATURATION OF THE KESWICK CLAY WITHIN THE ADELAIDE CITY AREA ABOVE THE GENERAL GROUNDWATER TABLE.

KEYWORDS: *Specific gravity; Keswick Clay; Hindmarsh Clay; Degree of saturation.*

ABSTRACT: The available data on in-situ bulk density and moisture content, and the specific gravity of solids of the Keswick Clay within the Adelaide city area are examined. It is found that for clay samples located at depths above the general water table the degree of saturation is typically greater than 95%, whereas these soils have been previously treated as unsaturated, and as a consequence, the in-situ effective stresses equated to the total stresses.

The paper also presents an evaluation of the sensitivity of the degree of saturation to the average value of specific gravity of the clay particles, using estimates from laboratory measurements and those based on crystal structure and mineral composition.

REFERENCE: JAKSA, M.B. and KAGGWA, W.S. (1992) Degree of Saturation of the Keswick Clay Within the Adelaide City Area Above the General Groundwater Table.

Proc. of 6th Australia New Zealand Conf. on Geomechanics, Christchurch, New Zealand, Feb 3-7.

THE DYNAMIC RESPONSE OF VOLCANIC SOILS

KEYWORDS: Dynamic properties; Shear modulus; Earthquake response; Earthquake hazard; Laboratory Torsion Test; Volcanic Soil Properties.

ABSTRACT: This paper presents the results of a series of laboratory experiments to measure the shear modulus and equivalent viscous damping factor of two volcanic soils. This data is compared with the international data base of the dynamic properties of clays and sands and important differences noted. An example seismic site response analysis is presented to show the sensitivity of the results to the dynamic soil properties. The estimate of the seismic hazard at a site is significantly effected by the choice of material properties.

REFERENCE: LARKIN, T.J. and CHAN, S.Y. (1992) The Dynamic Response of Volcanic Soils.

Proc. of 6th Australia New Zealand Conf. on Geomechanics, Christchurch, New Zealand, Feb 3-7.

MOUNTINGS FOR MEASUREMENT OF GROUND VIBRATIONS

KEYWORDS: *Vibrations; Instrumentation;* Machine foundations; Earthquakes; Blasts.

ABSTRACT: Studies have shown that mountings which support vibration transducers for free field vibration measurement may interact with the ground in such a way as to reduce the accuracy of vibration measurement particularly for high frequency vibrations. These theoretical studies form the basis for assessment of the accuracy of the vibration measurements in the field using different mountings. Geophysical surveys have been carried out at a field site to establish the ground geometry and the stiffness characteristics of the ground. Comparisons were made between the observed vibration amplitudes measured on different mountings placed on or just below the surface of the ground. The mountings used were either plates (surface mounted) or rods (varying depth of embedment), an accelerometer being attached to the upper surface of the mounting in each case. The source of vibration used was an electromagnetic vibrator which generated sinusoidal steady state vibrations. Study of the experimental data shows an approximate measure of agreement with theoretical predictions for some series of measurements, but for other measurements there was relatively little agreement for reasons that are not understood at this stage.

REFERENCE: MOORE, P.J., STYLES, J.R. and CHANG, A. (1992) Mountings for Measurement of Ground Vibrations.

Proc. of 6th Australia New Zealand Conf. on Geomechanics, Christchurch, New Zealand, Feb 3-7.

SMALL SCALE VARIABILITY OF REACTIVE SOILS IN WESTERN SYDNEY

KEYWORDS: Reactive soils; Expansive soils; Shrink-swell; Soil suction; Variability; Site investigations; Sydney.

ABSTRACT: The Australian Standards AS2870 deal with the design of slabs and footings for residential construction, several methods of site classification are countenanced by these standards. One such method is the estimation of the maximum ground surface movement (y_s) and this is often based on shrink-swell index (I_{ss}) test results. The standard provides no guidance on the number of tests that should be completed. The paper describes a detailed site investigation on one site in western Sydney aimed at determining the small scale variability of the shrink-swell index. The site was selected with a view to minimising this variability. A comprehensive programme of laboratory testing was completed on samples obtained during the site investigation. The results of this programme were then analysed to determine the variability across the site. The results indicate that the variability is such that a single shrink-swell test result can be a very poor indicator of site reactivity even for this "low variability" site. In general at least two to three tests are required to classify a site with even low confidence. A detailed geotechnical log increases the value of test results almost three fold. For the site with relatively low variability two or three tests and a detailed log result in a site classification which is also relatively low in variability.

REFERENCE: MOSTYN, G.R. and WATERS, M. (1992) Small Scale Variability of Reactive Soils in Western Sydney.

Proc. of 6th Australia New Zealand Conf. on Geomechanics, Christchurch, New Zealand, Feb 3-7.

MODEL PILE TESTING IN CALCAREOUS SAND AND SILT IN A LABORATORY CALIBRATION CHAMBER

KEYWORDS: Calcareous sediments; Calibration chamber; Cone penetrometer; Large-scale testing; Offshore; Pile testing; Sand; Silt.

ABSTRACT: The Monash sand calibration chamber has been modified to allow large (1.2m diameter by 1.8m) triaxial samples of calcareous sand and silt to be prepared, and, after saturation, to be used for a program of model pile testing for application to platforms in Bass Strait, Australia. Three model piles, of 100 and 150mm diameter, could be driven through the chamber lid into each sample and cyclically loaded both before and after grouting. Raining techniques of sample formation were found to be barely possible because of silty fines, and new procedures for compaction in place were required for the finer materials. A pile clearance of 2D was shown to be adequate for independent action in such materials and pile skin frictions were shown to decrease rapidly up the pile shaft.

REFERENCE: PARKIN, A.K., TAN, C.P. and YEE, Y.W. (1992) Model Pile Testing in Calcareous Sand and Silt in a Laboratory Calibration Chamber.

Proc. of 6th Australia New Zealand Conf. on Geomechanics, Christchurch, New Zealand, Feb 3-7.

CYCLIC UNDRAINED STIFFNESS OF STIFF CLAY AND VOLCANIC ASH

KEYWORDS: Soil testing; Cyclic undrained triaxial test; *Dynamic properties; Apparent shear modulus; Equivalent viscous damping ratio; Volcanic ash;* Site response.

ABSTRACT: The paper presents results of strain and stress controlled cyclic undrained triaxial tests on specimens of Auckland clays and on volcanic ash specimens from Tauranga. The change in shear modulus and damping with strain amplitude over a range of $\pm 0.1\%$ to $\pm 2\%$ is presented. Most of the tests were done at frequencies of 0.2 Hertz. In addition monitoring of the pore pressure changes, which were measured at mid-height of the specimen, is discussed. The Auckland clay is found to be insensitive to the number of cycles. The damping values and rate of change in apparent shear Modulus with strain amplitude follow established relationships. The volcanic ash generates excess pore water pressure. It is suggested that the liquidity index may be a useful parameter in categorising the cyclic pore pressure response.

REFERENCE: PENDER, M.J., DUSKE, G.C. and PEPLOE, R.J. (1992) Cyclic Undrained Stiffness of Stiff Clay and Volcanic Ash.

Proc. of 6th Australia New Zealand Conf. on Geomechanics, Christchurch, New Zealand, Feb 3-7.

SIMPLE SHEAR COMPACTION OF BASECOURSE AGGREGATES

KEYWORDS: *Basecourse* aggregate; *Compaction; Shear stiffness;* Fatigue; Pavement design.

ABSTRACT: The paper reports on a research project in which the densification and stiffening of basecourse aggregate were measured during cyclic loading in a simple shear compactor. The intention of the simple shear compaction device is to provide a rapid means of categorising various basecourse aggregates. The apparatus, which uses a servo controlled hydraulic loading system under the control of a small computer, is described briefly. Good quality greywacke and basalt aggregates and a lesser quality argillite aggregate from the Auckland region were tested. The differences between the good quality basecourse materials and the lesser quality argillite is readily apparent from the test results. The dependence of the shear modulus and change in density of the basecourse on normal stress, strain amplitude and numbers of cycles (up to 500,000) is described.

REFERENCE: PENDER, M.J., PEPLOE, R.J. and DUSKE, G.C. (1992) Simple Shear Compaction of Basecourse Aggregates.

Proc. of 6th Australia New Zealand Conf. on Geomechanics, Christchurch, New Zealand, Feb 3-7.

INFLUENCE OF SOIL DENSITY ON PILE SKIN FRICTION IN CALCAREOUS SEDIMENTS

KEYWORDS: Bearing capacity; Calcareous sediments; Foundations; Model tests; Piles; Settlements; Soil mechanics.

ABSTRACT: Model tests on jacked piles in calcareous sand have been performed to study the influence of density on the shaft friction under static and cyclic loading. Two types of test vessel have been used, in which dense and medium dense samples of New North Rankin calcareous sand have been consolidated under various overburden pressures. Model instrumented piles have been jacked into the sand samples and a study made of the influence of the sand density on the following aspects:
a. the jacking force required to install the pile
b. the skin friction and soil modulus for static loading
c. the degradation of skin friction under cyclic loading
d. the skin friction of the soil following the cyclic loading.
It has been found that the initial density of the sand has a significant effect on all these aspects.

REFERENCE: POULOS, H.G. and AL-DOURI, R.H. (1992) Influence of Soil Density on Pile Skin Friction in Calcareous Sediments.

Proc. of 6th Australia New Zealand Conf. on Geomechanics, Christchurch, New Zealand, Feb 3-7.

SOME RESIDUAL STRENGTH MEASUREMENTS ON NEW ZEALAND SOILS

KEYWORDS: Residual strength; Ring shear; New Zealand; Allophane; Plasticity index; Clay fraction.

ABSTRACT: Results of residual strength of measurements on a number of New Zealand soils are presented. Samples were taken from the upper half of the North Island and included soils derived from weathered Waitemata formations, Pleistocene deposits in the Auckland area, Onerahi Chaos and volcanic ash. The tests were carried out in a Bromhead ring shear apparatus. Results showed a wide scatter, but apart from the volcanic ash samples, generally conformed to published data for overseas soils. The lowest measured $\varnothing_r$ value was 7.4°, this was from a highly plastic clay obtained from an existing shear zone in weathered Waitemata materials. The $\varnothing_r$ values obtained from the weathered volcanic ash soils were high with a range from 18° to 37°. For these soils there did not appear to be any correlation between $\varnothing_r$ values and plasticity index or clay fraction.

REFERENCE: WESLEY, L.D. (1992) Some Residual Strength Measurements on New Zealand Soils.

Proc. of 6th Australia New Zealand Conf. on Geomechanics, Christchurch, New Zealand, Feb 3-7.

RISKS IN USING MATERIALS DATA OBTAINED FROM REPEATED LOAD TRIAXIAL TESTS IN PAVEMENT DESIGN AND ANALYSIS

KEYWORDS: Pavements; Triaxial testing; Basecourse.

ABSTRACT: To design and to analyse granular pavements requires resilient moduli and Poisson's ratios for the granular base and sub-grade materials concerned. They can be obtained from repeated load triaxial tests. A typical basecourse crushed rock was tested using a range of cyclic and static confining pressures and the resilient moduli were derived and fitted to available models for resilient modulus. One of the models was found to produce comparable constants for both test types and, therefore, could provide a basis for correcting the moduli obtained from different methods of applying confining pressure. All the models were used in the program NONCIRL to predict the lives of some typical granular pavements selected from the NAASRA Pavement Design Guide. The predicted lives range from 0.3 to 3 times the NAASRA design lives and this indicates that the risks associated with the use of different characterisation models in pavement design and analysis are significant.

REFERENCE: VUONG, B. (1992) Risks in Using Materials Obtained from Repeated Load Triaxial Tests in Pavement Design and Analysis.

Proc. of 6th Australia New Zealand Conf. on Geomechanics, Christchurch, New Zealand, Feb 3-7.

SUGGESTED REVISION OF THE PINHOLE TEST EROSION CLASSES

KEYWORDS: Lab Testing; Pinhole Test; Erosion; Dispersion; Loess.

ABSTRACT: The Pinhole Test was developed by Sherard et al (1976) as a test of dispersion in fine grained soils. Although the test is a good indication of erodibility in Banks Peninsula loessial soils it is not a reliable measure of dispersion. Dispersion is just one of a number of processes which can contribute to erodibility in soils. In view of this we suggest the test classes to which samples are assigned following testing be revised to remove the dispersive/non-dispersive implication inherent in the original classification.

REFERENCE: YETTON, M.D. and BELL, D.H. (1992) Suggested Revision of the Pinhole Erosion Test Classes.

Proc. of 6th Australia New Zealand Conf. on Geomechanics, Christchurch, New Zealand, Feb 3-7.

SETTLEMENT DETERMINATION ON SAND

KEYWORDS: Settlement prediction; Sand; Plate load tests; Standard penetration tests.

ABSTRACT: Settlements of alluvial sands on a site in Sydney were predicted using an elastic method. Moduli were determined from standard penetration test blow counts. Rather than use published correlations, a limited number of in situ screw plate tests were undertaken at depth in a borehole to relate elastic modulus to blow count. Settlements were monitored as construction proceeded and were found to be in good agreement with predictions.

REFERENCE: YOUNG, G.S., PHILLIPS, A.B. and BROWN, P.T. (1992) Settlement Determination on Sand.

Proc. of 6th Australia New Zealand Conf. on Geomechanics, Christchurch, New Zealand, Feb 3-7.

FATIGUE FAILURE OF A CEMENTED SAND

KEYWORDS: Fatigue; Cemented Sand; Triaxial Tests; Frequency.

ABSTRACT: A series of monotonic and cyclic undrained triaxial tests have been performed on an artificially cemented carbonate sand. The effects of the stress level and frequency on the number of cycles to failure have been investigated. It has been found that the number of cycles to failure increases with frequency for a given stress level, and that the time for which the load is applied is more important than the number of cycles of loading. The test results have been used to produce fatigue S — N curves with fatigue failures occurring at stress levels as low as 60% of the static peak strength.

REFERENCE: ZHAO, M.M., HUANG, J.T. and AIREY, D.W. Fatigue Failure of Cemented Sand.

Proc. of 6th Australia New Zealand Conf. on Geomechanics, Christchurch, New Zealand, Feb 3-7.

GENERAL REPORT: ANALYTICAL AND PROBABILISTIC METHODS

KEYWORDS: *Deterministic analysis; Probability theory;* Finite elements; *Slopes;* Grey system theory; Fuzzy mathematics; Seismic analysis.

ABSTRACT: This General Report reviews the papers allocated to the session on Analytical and Probabilistic Methods. It also gives a brief overview of the other important developments in these areas that have taken place recently. The methods of analysis covered include finite element, boundary element and distinct element techniques, stochastic methods, limit states approach, and risk assessment in rock engineering.

REFERENCE: CARTER, J.P. (1992) General Report: Analytical and Probabilistic Methods.

Proc. of 6th Australia New Zealand Conf. on Geomechanics, Christchurch, New Zealand, Feb 3-7.

STABILITY OF SLOPES IN COHESIVE-FRICTION SOIL

KEYWORDS: Analysis; Finite elements; Plasticity; Stability; Slope.

ABSTRACT: The upper and lower bound theorems of classical plasticity are used to examine the drained stability of slopes under conditions of plane strain loading. Rigorous bounds on the loads needed to support the slope against active failure are derived using two numerical techniques that are based on a finite element type of discretisation. The soil is idealised as a perfectly plastic solid which obeys the Mohr-Coulomb yield criterion and has a uniform effective cohesion, friction angle and self-weight. Both of these techniques lead to large linear programming problems. The solution to the lower bound linear programming problem defines a statistically admissible stress field whereas the solution to the upper bound linear programming problem defines a kinematically admissible velocity field. For the range of slope geometrics considered, the results bracket the exact collapse load quite closely.

REFERENCE: ASSADI, A. and SLOAN, S.W. (1992) Stability of Slopes in Cohesive-Friction Soil.

Proc. of 6th Australia New Zealand Conf. on Geomechanics, Christchurch, New Zealand, Feb 3-7.

NUMERICAL SIMULATION OF THE TIME-DEPENDANT STRATIFIED VISCOELASTIC SOIL MEDIUM WITH CRACKS

KEYWORDS: Numerical analysis; Time dependant behaviour; Recurrent integration; Finite element technique; Viscoelasticity.

ABSTRACT: The paper contains the numerical analysis of viscoelastic stratified half space with cracks filled out by air. The cracks are of different type, size and location. The employed constitutive model assumes the proportionality relationship between the spherical components of stress and strain tensor and viscoelasticity law between deviators. With respect to time variables the recurrent integral method is applied, while with respect to spatial variables — the finite element is employed.

In order to analyze the effect of cracks on the displacement and stress field, the computer program was prepared and some numerical examples are investigated. The conclusions connected with risk induced by the variably located cracks are drawn on the basis of numerical results.

REFERENCE: BUDKOWSKA, B.B., GRZESIAK, W. (1992) Numerical Simulation of the Time Dependant Stratified Viscoelastic Soil Medium with Cracks.

Proc. of 6th Australia New Zealand Conf. on Geomechanics, Christchurch, New Zealand, Feb 3-7.

EXPERIENCE WITH THE SEARCH OF MINIMUM FACTOR OF SAFETY OF SLOPES

KEYWORDS: Slope stability; Factor of safety; Limit equilibrium analysis; Non-linear failure criterion; Method of optimization.

ABSTRACT: The author's experience with the searching technique for the minimum factors of safety in slope stability analysis is summarized as follows: (1) For soil slopes where geological heterogeneity and discontinuities are not dominating, using circular slip surfaces and the Bishop's simplified method generally produce results as good as any more rigorous approach does in the light of both the value of minimum factor of safety and the location of the critical slip surface; (2) When performing the calculation for non-circular slip surfaces, the smoothly curved part of the slip surface should be simulated by splines rather than a broken line since it requires more nodal points and hence, more degrees of freedom, than a curve to produce equally good simulation; (3) For slopes composed of uniform compacted granular materials, a non-linear strength envelope generally gives physically more reasonable critical slip surfaces than a linear cohensionless strength envelope does; (4) The random search technique has been proposed to aid in finding the global minimum factor of safety; (5) The computation results of the two test examples that possess closed form solutions indicated that the searching technique described in this paper provides not only practically feasible but also theoretically reliable solutions to stability problems.

REFERENCE: CHEN, Z. (1992) Experience with the Search of Minimum Factor of Safety of Slopes.

Proc. of 6th Australia New Zealand Conf. on Geomechanics, Christchurch, New Zealand, Feb 3-7.

GEOTECHNICAL RISK AND THE USE OF GREY EXTRAPOLATION TECHNIQUE

KEYWORDS: Grey system theory; Grey extrapolation technique; Geotechnical risk; Pore water pressure.

ABSTRACT: This paper is concerned with an aspect of the assessment of geotechnical risk with particular reference to observational data and interpretation. The use of a grey prediction model (grey extrapolation technique) is discussed. This is part of what is known as the grey system theory which is concerned with systems subject to uncertainty. An illustrative example concerned with data on pore pressure equilibrium in an excavated slope of overconsolidated clay has been presented.

REFERENCE: CHOWDHURY, R.N., ZHANG, S. and LI, J. (1992) Geotechnical Risk and the Use of Grey Extrapolation Technique.

Proc. of 6th Australia New Zealand Conf. on Geomechanics, Christchurch, New Zealand, Feb 3-7.

EXPLORE — AN EXPERT SYSTEM FOR SUBSURFACE EXPLORATION

KEYWORDS: Expert systems; Subsurface exploration

ABSTRACT: Expert systems are computer programs that are capable of incorporating empirical and qualitative knowledge. Because many geomechanics solutions require judgement and rules of thumb, there is potential that expert systems can be utilised to assist the geotechnical engineer in the decision making process. In this paper, an overview of expert systems is presented. The methodology involved in building a geotechnical expert system for subsurface exploration is then described.

REFERENCE: GOH, A.T.C. (1992) Explore — An Expert System for Subsurface Exploration.

Proc. of 6th Australia New Zealand Conf. on Geomechanics, Christchurch, New Zealand, Feb 3-7.

ROCK ENGINEERING RISK ASSESSMENT THROUGH CRITICAL MECHANISM AND PARAMETER EVALUATION

KEYWORDS: Systems approach; Interaction matrix; Fei-Tsui Dam (Taiwan); *Remit/Response;* Discontinuities; Slope Stability; Parameter significance.

ABSTRACT: A new methodology for complete rock engineering problems has recently been developed (with the acronym *Remit/Response*) that allows a comprehensive listing of all geotechnical parameters, focusing in on the ones most relevant for a particular project. Moreover, this methodology has been extended to the ability to identify and present all rock engineering mechanisms associated with a particular project. A matrix configuration is used for this technique — the rock mechanics interaction matrix.

By considering the rows (representing essentially the influence of the parameter on the system) and the columns (representing essentially the effect of the system on the parameter), the significance of each mechanism and parameter can be identified for any engineering scheme. Hence, through the systematic consideration of the mechanisms and their interactions, it is possible, not only to identify the critical parameters, but also to obtain a clear idea of their priority in terms of potential failure.

The basic rock engineering method is presented and explained, and its use illustrated via a case study of the construction and performance of the Fei-Tsui Dam in Taiwan. The case study shows directly the applicability of the generic model by highlighting the crucial effect of the discontinuities and the method by which they were strengthened.

REFERENCE: HUDSON, J.A., SHENG, J. and ARNOLD, P.N. (1992) Rock Engineering Risk Assessment Through Critical Mechanism and Parameter Evaluation.

Proc. of 6th Australia New Zealand Conf. on Geomechanics, Christchurch, New Zealand, Feb 3-7.

A POINT ESTIMATE METHOD FOR CALCULATING THE RELIABILITY INDEX OF SLOPES

KEYWORDS: Reliability analysis; *Reliability index; Point estimate method;* Random field model.

ABSTRACT: The point estimate method developed by Rosenblueth has been used for calculating the reliability index of slopes. If there are n random variables, Rosenblueth's method will require 2^n evaluations of the factor-of-safety function at 2^n different combinations of input parameters. This method becomes impracticable when the number of random variables is large. In this paper, a more efficient point estimate method is proposed. This new method has the same order of accuracy as Rosenblueth's method, but requires only $(n^2+3n+2)/2$ evaluations of the factor-of-safety function. The results of an illustrative example also indicate that the reliability indices given by Rosenblueth's method and the proposed method are practically identical.

REFERENCE: LI, K.S. (1992) A Point Estimate Method for Calculating the Reliability Index of Slopes.

Proc. of 6th Australia New Zealand Conf. on Geomechanics, Christchurch, New Zealand, Feb 3-7.

LIMIT STATE DESIGN OF PILE FOUNDATIONS: A PROBABILISTIC APPRAISAL

KEYWORDS: *Limit state design; Pile foundations;* Partial safety factor; Calibration; Reliability index.

ABSTRACT: The current Australian piling code AS2159-1978 is under review. In the draft revised piling code, a limit state method is used for the design of pile foundations. This paper describes the probabilistic basis for the limit state method, with special reference to the draft piling code. The theory for the limit state method is reviewed and the procedure for determining the partial safety factors in the limit state format is also described. It is observed that the use of a variable strength reduction factor is required to give effective control on the reliability level of pile designs. The value of the strength reduction factor can also be directly related to the level of confidence which can be quantified in terms of the variability of the pile capacity.

REFERENCE: LO, S-C. R., LI, K.S. and LEE, I.K. (1992) Limit State Design of Pile Foundations: A Probabilistic Appraisal.

Proc. of 6th Australia New Zealand Conf. on Geomechanics, Christchurch, New Zealand, Feb 3-7.

RELIABILITY ANALYSIS OF FAILED SLOPES, A BACK ANALYSIS VIEW OF THE SENSITIVITY TO INPUT PARAMETERS

KEYWORDS: Slope stability; *Probability of failure; Reliability analysis;* Slope back-analysis.

ABSTRACT: Many probabilistic slope analysis techniques have been presented in the literature over the last two decades, however these methods are not used routinely and appear to be restricted to special cases where a reliability approach is desirable. This paper investigates slopes, mostly taken from surface coal mines, that have failed and uses a back analysis reliability approach. A method based on the first-order second moment method was formulated capable of dealing with spatial variability of the random strength variables, circular and non-circular slip surfaces. This model was extended to account for end resistance and variance reduction along the failure width in a quasi 3-D formulation. The case studies were analysed in probabilistic terms in both 2-D and 3-D. The 3-D aspects of failure were investigated in detail and a lateral release factor was introduced to assess the importance of end resistance on the failure probability. The sensitivity to the various probabilistic and deterministic inputs is discussed.

REFERENCE: ST GEORGE, J.D. (1992) Reliability Analysis of Failed Slopes, a Back Analysis View of the Sensitivity to Input Parameters.

Proc. of 6th Australia New Zealand Conf. on Geomechanics, Christchurch, New Zealand, Feb 3-7.

RESONANCE AVOIDANCE IN SEISMIC DESIGN

KEYWORDS: *Natural frequency; Seismic design;* Vibrations; Resonance.

ABSTRACT: In seismic design the minimization of structural damage from an earthquake is assisted if positive steps for resonance avoidance for buildings and building elements are taken. Resonance avoidance refers to lack of coincidence between the dominant ground frequencies and the natural frequencies of buildings and building elements. For many sites the dominant ground frequencies lie between one and five hertz. With raft and footing foundations resonance effects may be encountered, particularly for deep deposits of soft soil. The foundation natural frequency rises as the ground becomes stiffer or the depth to a solid stratum decreases. Natural frequency of the foundation may also be varied by altering foundation dimensions and loads. It is unlikely that the natural frequencies of individual beams and columns in a building would coincide with dominant frequencies experienced in an earthquake. However, for some buildings, coincidence between the natural frequencies for the building as a whole and the ground motion will occur. Factors which affect the natural frequency of a building include: aspect ratio; column/beam in-fill material; rigidity of connections; rigidity of base and rotational stiffness of foundation; disposition of lift and stair cores.

REFERENCE: STYLES, J.R., MOORE, P.J. and GUPTA, R.K. (1992) Resonance Avoidance in Seismic Design.

Proc. of 6th Australia New Zealand Conf. on Geomechanics, Christchurch, New Zealand, Feb 3-7.

LOCATION OF CRITICAL SLIP SURFACES IN COAL MINE SPOIL PILES

KEYWORDS: Coal mine; *Critical slip surface; Dynamic programming;* Spoil pile stability; *Stochastic finite element method; Wedge analysis.*

ABSTRACT: In Australia, the spoil removed to expose coal during surface mining is conventionally loose dumped in piles within the already mined pit, where it is free to ravel at about its angle of repose. This, together with the frequent occurrence of water softened material at the base of the piles, results in a considerable risk of spoil pile instability. The failure of coal mine spoil piles is characterised by a deep-seated, essentially two-wedge mechanism. In the paper, the location of the critical slip surface within a spoil pile of particular geometry, comprising spoil having various strength parameters, is determined by two independent techniques. The first makes use of the stochastic finite element method to determine the stresses within the spoil pile and indicate the probable location of the critical slip surface, which are then used in an improved dynamic programming method to search for the critical slip surface and determine the corresponding minimum factor of safety. The second uses a pattern search within a generalised limit equilibrium wedge analysis to locate the critical slip surface and determine the corresponding minimum factor of safety. The two results are compared.

REFERENCE: WILLIAMS, D.J. and ZOU, J.-Z. (1992) Location of Critical Slip Surfaces in Coal Mine Spoil Piles.

Proc. of 6th Australia New Zealand Conf. on Geomechanics, Christchurch, New Zealand, Feb 3-7.

SOME APPLICATIONS OF FUZZY MATHEMATICS TO ROCK ENGINEERING AND SLOPE STABILITY

KEYWORDS: *Rock engineering; Fuzzy mathematics;* Fuzzy arithmetical operations; Fuzzy stability factor.

ABSTRACT: In this paper, the basic components of fuzzy mathematics are described and applied to several important problems in rock engineering. A method is presented for determining the fuzzy values of typical rock mass parameters. The limit equilibrium method is used as the basis for calculation of the stability factor for a rock slope and fuzzy arithmetical operations are required to evaluate this factor because the parameters used in the calculation are considered to be indistinct. The techniques presented in the paper are illustrated by typical example calculations.

REFERENCE: XIAO, B., CARTER, J.P. and YU, X. (1992) Some Applications of Fuzzy Mathematics to Rock Engineering and Slope Stability.

Proc. of 6th Australia New Zealand Conf. on Geomechanics, Christchurch, New Zealand, Feb 3-7.

FINITE ELEMENT ANALYSIS OF PRESSUREMETER TESTS IN SOIL

KEYWORDS: Finite Element; Soil; Pressuremeter; Strength Parameter; Analysis.

ABSTRACT: It is well accepted that the strength parameters from the self-boring pressuremeter tests are often much higher than those obtained from good laboratory tests or other in-situ tests. It is the authors belief that these disagreements may be largely due to the influence of the finite length of the pressuremeter. Although the Gibson and Anderson analysis has been widely used to interpret self-boring pressuremeter tests in clay, significant uncertainty remains due to the fact that the pressuremeter is assumed to be infinitely long in the analysis. To quantify possible effects of the finite length of the pressuremeter on soil parameters derived from the tests, a two-dimensional axisymmetric finite element analysis of the self-boring presuremeter tests is carried out in this paper. It has been concluded that serious over-estimation of the strength parameters of soil may be deduced by applying the Gibson and Anderson method to field pressuremeter tests. A new interpretation procedure is proposed to eliminate the effects of the simple assumptions used in the conventional interpretation method.

REFERENCE: YU, H.S. (1992) Finite Element Analysis of Pressuremeter Tests in Soil.

Proc. of 6th Australia New Zealand Conf. on Geomechanics, Christchurch, New Zealand, Feb 3-7.

GENERAL REPORT — SLOPE STABILITY AND SEISMIC HAZARD

KEYWORDS: Slope stability; Hazard assessment; Stabilisation; Seismic hazard; Liquefaction.

ABSTRACT: This paper gives an overview of eleven papers allocated to the session entitled "Slope Stability and Seismic Hazard" at the Sixth Australia-New Zealand Conference on Geomechanics held at Christchurch, New Zealand in February 1992.

REFERENCE: RIDDOLLS, B.W. and BROWN, I.R. (1992) General Report — Slope Stability and Seismic Hazard.

Proc. of 6th Australia New Zealand Conf. on Geomechanics, Christchurch, New Zealand, Feb 3-7.

DEVELOPMENT OF ECONOMICAL SOLUTIONS TO MITIGATE GEOTECHNICAL RISKS: WAIPAOA WATER TREATMENT AUGMENTATION PLANT

KEYWORDS: Earthquakes; *Economic analysis;* Foundations; Ground improvement; *Liquefaction;* Preloading; *Risk; Settlement;* Soils; Tanks.

ABSTRACT: A case study of the Waipaoa Treatment Plant illustrates the use of engineering evaluation to assess the geotechnical and seismic risks, and develop economical solutions to civil engineering projects. At the Waipaoa site, geotechnical assessment identified a high risk of damage to the main plant due to settlements, and a moderate risk of damage due to liquefaction during large earthquake events. An economic evaluation provided the likely financial benefits from ground improvement measures to mitigate these risks, and enabled a comparison of the capital expenditure and the likely costs during the life of the facility. This enabled the client to decide on the level of risk mitigation appropriate for the facility and provided a basis for the design of the treatment plant and ground improvement measures.

REFERENCE: BRABHAHARAN, P. and VESSEY, J.V. (1992) Development of Economical Solutions to Mitigate Geotechnical Risks: Waipaoa Water Treatment Augmentation Plant.

Proc. of 6th Australia New Zealand Conf. on Geomechanics, Christchurch, New Zealand, Feb 3-7.

ASSESSING GEOTECHNICAL RISK OF INSTABILITY BETWEEN ADJACENT MINING OPERATIONS — A CASE STUDY

KEYWORDS: Coal mining; Pit stability; Mylonite; Probabilistic analysis.

ABSTRACT: Instability of a 60m highwall excavated to a common boundary between two adjoining but separately owned coal mining operations represented significant potential loss for both parties. A probabilistic approach to stability analysis was adopted to quantify the risk and value the cost of insuring against losses incurred by inadvertent failure.

REFERENCE: DUNBAVAN, M. and BOYD, G. (1992) Assessing Geotechnical Risk of Instability Between Adjacent Mining Operations — A Case Study.

Proc. of 6th Australia New Zealand Conf. on Geomechanics, Christchurch, New Zealand, Feb 3-7.

THE EFFECT OF REGIONAL GEOLOGY ON THE SEISMIC HAZARD IN CHRISTCHURCH, NEW ZEALAND

KEYWORDS: Seismic hazard; Active faults; Site response; Amplification; Alluvial soils.

ABSTRACT: A detailed seismic hazard assessment has been carried out from Christchurch, New Zealand. Active faults were evaluated and recent seismicity analysed to produce a seismicity model for the central South Island. By combining over 15,000 borelogs for the city representative soil profiles were developed for nodal points on a 500m grid over the city. Amplification effects were modelled by computer methods to predict likely variations in amplification across the city. The overall seismic hazard is considerably greater than has previously been thought.

REFERENCE: ELDER, D.McG., McCAHON, I.F. and YETTON, M.D. (1992) Effect of Regional Geology on the Seismic Hazard in Christchurch, New Zealand.

Proc. of 6th Australia New Zealand Conf. on Geomechanics, Christchurch, New Zealand, Feb 3-7.

SOME LANDSLIDE RISK ZONING SCHEMES IN USE IN EASTERN AUSTRALIA AND THEIR APPLICATION

KEYWORDS: Landslides; Hazard; Risk; Insurance.

ABSTRACT: Landslide risk zoning schemes in use in Eastern Australia have developed with mixed terminology to describe the probability and the consequences of landsliding. The terms "hazard" and "risk" have been interchanged. The zoning schemes have also been influenced by the lack of insurance to cover damage due to landsliding, and have generally made inadequate allowance for the situation where loss of life is possible. It is suggested that some standardisation of terms and approach is needed, and steps taken to introduce landslide insurance.

REFERENCE: FELL, R. (1992) Some Landslide Risk Zoning Schemes in Use in Eastern Australia and their Application.

Proc. of 6th Australia New Zealand Conf. on Geomechanics, Christchurch, New Zealand, Feb 3-7.

ROCK SLOPE INSTABILITY ZONING WITH KINEMATIC AND MORPHOLOGICAL FACTORS

KEYWORDS: *Instability Zoning; Block Type Slope Movements;* Block Toppling; Kinematics; Morphology.

ABSTRACT: Within this paper, the analyses of morphological factors and the slope kinematics were used as crucial criteria to detect and subdivide instability zones. A case study at a disintegrating rock slope in the Austrian Alps was conducted. An inclined limestone slab, some 30m thick, is distintegrating into large blocks which are resting upon a layered and weak sequence of clastic and calcareous sedimentary rocks.

The kinematic behaviour of the rock slope has been monitored for several years using state-of-the-art monitoring systems. The zoning of the whole slope by its kinematics is based on the results of high resolution, quasi-continuous readings taken from extensometers, clinometers, optical-mechanical devices and from geodetical measurements. Furthermore, failure mechanisms could be detected and were monitored utilizing particular combinations of survey systems. The slope is being characterized into zones with similar quantity and character of deformation, indicated by the amount of displacement and the kinematic response of the rock mass to the influence of external factors.

The analyses of the morphological systems such as open joints, graben-shaped and rifting structures were used for the morphological zoning. It is considered that, after all possible kinematic methods of disintegration have occurred, a particular distribution of stress could cause failure mechanisms, which are independent of the pre-existing rock mass structures. This stress distribution is explained. Finally, the important parameters for an 'engineering approach' to block type slope movements were analyzed: these are presented in terms of the consequential risk of instability.

REFERENCE: GLAWE, U. and HUDSON, J.A. (1992) Rock Slope Instability Zoning with Kinematic and Morphological Factors.

Proc. of 6th Australia New Zealand Conf. on Geomechanics, Christchurch, New Zealand, Feb 3-7.

SEISMIC STABILITY OF THE SULPHUR POINT WHARF

KEYWORDS: Ports; Liquefaction; Slope Stability; Seismic Design.

ABSTRACT: The Sulphur Point Wharf development is a major expansion of the Port of Tauranga Ltd's port facilities in Tauranga Harbour involving an area of some 60 hectares. Initial development of the reclaimed site involves the construction of some 600 metres of wharf with a design dredge depth of 14.5 metres.

The Tauranga Harbour consists of deep deposits of predominantly sands interspersed with layers of silts and fine gravels. The wharf structure consists of a reinforced concrete deck supported on driven precast prestressed concrete piles. The sands at the site which form the marginal slope under the open piled wharf structure are protected with rock buttressing.

This paper describes the seismic design philosophy developed for the wharf structures and the design criteria adopted. "Operating" and "contingency" design earthquakes are defined together with performance expectations relative to the design life of the facility. The features and considerations associated with the assessment of seismic stability in the geotechnical engineering design process are presented.

Initial investigations at Sulphur Point indicated that the recent sands did have a liquefaction potential. Site investigations and the evaluation of soil properties with respect to seismic shaking is described. Extensive piezo cone penetrometer testing together with static and dynamic triaxial testing of undisturbed piston samples has enabled the behaviour of the soils to be assessed. In-situ geophysical testing including shearwave velocity measurement is described.

The wharf structure/soil interaction associated with the marginal slope and soil behaviour have been addressed in the design process. Wharf stability and estimated deformation behaviour under the operating and contingency design earthquakes is presented.

REFERENCE: JENNINGS, D.N. and THOMPSON, G.S. (1992) Seismic Stability of the Sulphur Point Wharf.

Proc. of 6th Australia New Zealand Conf. on Geomechanics, Christchurch, New Zealand, Feb 3-7.

THE LIQUEFACTION POTENTIAL IN CHRISTCHURCH

KEYWORDS: Liquefaction; Seismic hazard; Liquefaction analysis.

ABSTRACT: This paper reviews information pertaining to the liquefaction hazard in Christchurch. At least one third of the Christchurch urban area is sited on a general soil profile dominated by sand with a high water table, which would be susceptible to liquefaction if the grading is uniform and the soil sufficiently loose. Analysis for a number of sites that have adequate test data indicates liquefaction is likely to occur during seismic shaking with an average return period of about 30 years. The lack of historical liquefaction reports suggests some discrepancy between the analysis predictions and the actual response, but it is concluded that the liquefaction hazard in Christchurch is significant. Scarcity of data on in-situ densities and soil gradings does not yet allow delineation of liquefiable zones.

REFERENCE: McCAHON, I.F., ELDER, D. McG. and YETTON, M.D. (1992) The Liquefaction Potential in Christchurch.

Proc. of 6th Australia New Zealand Conf. on Geomechanics, Christchurch, New Zealand, Feb 3-7.

LANDSLIDE AND UPLIFT OF RIVER BED IN TAL VALLEY, GARHWAL HIMALAYA

KEYWORDS: Instability seismicity; Pore pressure; Landslide; Shear zone; Cohesion; Internal angle of friction.

ABSTRACT: The present paper deals with a case history of a landslide which occurred in Tal Valley of Garhwal Himalaya, India in January 1990, causing upliftment of the river-bed by 6-8m. A detailed geological and geotechnical study of the area revealed that the slope mass movement was a rotational sliding with slumping triggered by heavy rainfall. The gravitational forces exerting upon highly weathered and sheared material formed a slip surface in the upper part of the slope which is terminating below the river-bed. This paper highlights the mechanism of the slide which has been found directly related to the rise of the river-bed. The study carried out has established that the uplift of the river-bed as well as the development of cracks on the slope were caused by the landslide. The monitoring data confirming the rise of river-bed has led to the conclusion that the area is still rising, though it is not uniform throughout. The slope stability analysis has shown that the slope appears to be stable with no pore pressure and seismicity. But with marginal rise of water pressure, which is very common in this area during monsoon, the slope tends to be highly unstable. Considering the effect of seismicity in dynamic condition, the factor of safety drastically drops below 0.5.

REFERENCE: MEHROTRA, G.S., GUPTA, A. and SARKAR, S. (1992) Landslide and Uplift of River Bed in Tal Valley, Garhwal Himalaya.

Proc. of 6th Australia New Zealand Conf. on Geomechanics, Christchurch, New Zealand, Feb 3-7.

STABILITY ANALYSIS IN STIFF FISSURED CLAY AT RABY BAY, QUEENSLAND

KEYWORDS: Fissures; Fully softened strength; Residual strength; Slope stability analysis; Soil defects; Stability charts; Stiff clays; Structural geology.

ABSTRACT: The Raby Bay Project in southeast Queensland consists of a coastal residential and recreational complex based around a system of canals. Construction failures and the presence of fissured clay had caused concern about canal slope stability and the adoption of remedial works. Most of the stiff clay is of volcanic origin but sedimentary clay occurs in parts of the site. Defects (fissures) occur in layers and trends were identified in the occurrence and character of defects across the site. Stability charts have been developed based on a generalised model which takes into account the depth and thickness of the layer containing defects (weak layer) and the dip and continuity of the defects. The concept of a Strength Reduction Factor has been developed to characterise the strength of the weak layer.

REFERENCE: MOON, A.T. (1992) Stability Analysis in Stiff Fissured Clay at Raby Bay, Queensland.

Proc. of 6th Australia New Zealand Conf. on Geomechanics, Christchurch, New Zealand, Feb 3-7.

THE EFFECT OF AUTO-CORRELATION ON THE PROBABILITY OF FAILURE OF SLOPES

KEYWORDS: Slope stability; Probability; Probabilistic methods; Auto-correlation; Reliability.

ABSTRACT: Probabilistic analyses of slopes are generally based on treating only the most significant variables as random variables. Usually simplifications are made regarding the correlation structure of these variables. This is especially so with respect to the correlation of each variable with itself in space (i.e. auto-correlation). Most analyses ignore this auto-correlation. The paper presents several cases from the literature for which probabilities of failure have been determined where auto-correlation has been ignored. These are re-analysed and the sensitivity of the computed probability of failure to various assumptions regarding the auto-correlation structure is determined. It is found that, in general, realistic assumptions regarding auto-correlation result in very significant reductions in the computed probabilities of failure for most civil engineering slopes. Thus most methods of probabilistic slope analysis can at best be regarded as producing only an index of slope stability.

REFERENCE: MOSTYN, G.R. and SOO, S. (1992) The Effect of Auto-Correlation on the Probability of Failure of Slopes.

Proc. of 6th Australia New Zealand Conf. on Geomechanics, Christchurch, New Zealand, Feb 3-7.

BEANPOLE CORNER LANDSLIDE STABILISATION

KEYWORDS: *Landslide;* Investigations; Monitoring; Stability; Analysis; Remedial.

ABSTRACT: In 1979 a 30,000m^3 rockslide in greywacke colluvium at Beanpole Corner above the North Island, New Zealand, main trunk railway line, moved 5m presenting a potential hazard to the railway. The slide was the most recent in a series of progressive movements which have occurred since 1940. Investigation and monitoring was carried out and movement was found to occur at an average rate of 70mm/year. Back analysis was used to design a slope trim unloading the 1979 slide mass and regarding the slope above. Nominal drainage of the regraded slope was considered desirable to ensure long term stability of the slope. The remedial works were carried out in 1990 and survey monitoring of the new slope is planned.

REFERENCE: SAUL, G.J., ANDERSON, C.K. and GRAHAM, C.J. (1992) Beanpole Corner Landslide Stabilisation.

Proc. of 6th Australia New Zealand Conf. on Geomechanics, Christchurch, New Zealand, Feb 3-7.

A SIMPLE METHOD FOR ASSESSING EFFECTS OF EARTHQUAKES ON SLOPES

KEYWORDS: *Slope stability; Earthquake; Yield acceleration.*

ABSTRACT: A simple method is proposed for assessing the reduction in factor of safety of a slope due to an earthquake or of estimating the yield acceleration at which deformations might occur. The method is suitable for first approximations or for multi-point calculations such as required for risk or hazard mapping, where accuracy can be sacrificed in favour of highlighting regions of concern needing more detailed investigation or analysis. The simple "rule-of-thumb" is derived and the limitations discussed in relation to some validation calculations.

REFERENCE: SINCLAIR, T.J.E. (1992) A Simple Method for Assessing Effects of Earthquakes on Slopes.

Proc. of 6th Australia New Zealand Conf. on Geomechanics, Christchurch, New Zealand, Feb 3-7.

ASSESSMENT OF STRONG MOTION DURING 1989 NEWCASTLE EARTHQUAKE

KEYWORDS: *Amplification; Continental earthquakes; Earthquake-induced liquefaction;* Earthquake damage; Earthquake hazard assessment; *Peak ground acceleration;* Soft soil sites; *Strong motion.*

ABSTRACT: Australia is located in the middle of a large stable tectonic plate and is perceived to have a relatively low earthquake hazard. However, as evidenced by the devastating 1989 ML 5.6 Newcastle event, damaging earthquakes can occur in such regions. Because continental earthquakes are relatively infrequent and widely scattered, strong motion instruments are not installed and the assessment of the strong motion must be based on fair-field seismograph records and assigned intensities. A rational and useful assessment of the strong motion during the 1989 Newcastle earthquake using the available intensity data, the mean attenuation relationship for the magnitude and region, and information on surface geology was carried out. From this assessment, estimates were made of the likely level of amplification which occurred during the Newcastle event, giving rise to the widespread damage observed. The estimated amplifications are shown to be in line with available worldwide data.

REFERENCE: WILLIAMS, D.J. (1992) Assessment of Strong Motion During 1989 Newcastle Earthquake.

Proc. of 6th Australia New Zealand Conf. on Geomechanics, Christchurch, New Zealand, Feb 3-7.

PROFESSIONAL AND LEGAL ISSUES

KEYWORDS: *Risk; Uncertainty; Liability; Education; Guidelines.*

ABSTRACT: The involvement of geotechnical engineers and engineering geologists in litigation and contractual disputes has an important bearing on the image of the profession. Selected ideas emerging from a review of three papers on professional and legal issues are presented, and cover the relationship between acceptable levels of risk and previous experience, evaluation of relevant experience by an independent agency, and the allocation of risk. Reference is made to guidelines on the presentation of information on sub-surface conditions, and to comments by others on uncertainty. Attention is drawn to the role of education in achieving a common approach to risk management and professional liability.

REFERENCE: STARR, D.C. (1991) Professional and Legal Issues.

Proc. of 6th Australia New Zealand Conf. on Geomechanics, Christchurch, New Zealand, Feb 3-7.

GEOHAZARD RISK ASSESSMENT AND REASONS FOR ALTERNATIVE EXPERT OPINION

KEYWORDS: Slope stability; Earthflows; Risk assessment; Expert evidence.

ABSTRACT: Some engineering disciplines particularly those using precise design codes based on known material properties or performance criteria are more amenable to risk assessment than others. Assessment of geohazard risk however relies heavily on judgement and experience, as the vagaries of the material properties and the unpredictability of their behaviour and performance under adverse stress conditions often preclude meaningful numerical analysis. This New Zealand case history examines the affect of a highly mobile earthflow landslide which caused damage to a rural residential subdivision. Compensation which was sought by the affected property owners resulted in a divergence of opinion between various experts engaged to evaluate the risk. Reasons for this divergence of expert opinion are given in the paper.

REFERENCE: GROCOTT, G.G. and OLSEN, A.J. (1992) Geohazard Risk Assessment and Reasons for Alternative Expert Opinion.

Proc. of 6th Australia New Zealand Conf. on Geomechanics, Christchurch, New Zealand, Feb 3-7.

DEALING WITH TECHNICAL UNCERTAINTY

KEYWORDS: Collaborating; *Disputes;* Expertise; Groundwater; Insurance; *Liability; Risk; Uncertainty.*

ABSTRACT: Professional engineers are involved in managing risk through investigation and design. This involves anticipating what might go wrong. The risks must be balanced and allocated, through statutory, contractural and insurance means. Some of these risks are beyond engineering control and may be uninsurable. Others may not even be recognised, except with uncertainty. Strategies for dealing with this include expertise, good judgement, independent review and good communication. When a risk materialises, the cause and responsibility for any resulting loss and damage may be disputed. Consideration of the legal and technical factors involved is required to substantiate or refute claims. In disputes which depend on the interpretation of scientific or technical data, there is a need to deal wisely with uncertainty. Traditional legal forums tend to encourage adversarial science and have difficulty in coping with complex technical matters. Collaborating is a process being used to deal with technical uncertainty, both in decision making and dispute resolution. A workshop on groundwater aspects of a proposed refuse landfill is a New Zealand example of applying this process to a technical issue.

REFERENCE: HOLLANDS, D.E. (1992) Dealing With Technical Uncertainty.

Proc. of 6th Australia New Zealand Conf. on Geomechanics, Christchurch, New Zealand, Feb 3-7.

VERY LARGE CHANGES IN SEA LEVEL

KEYWORDS: Sea level changes; *Submarine valleys; Ocean drilling;* Earth instability.

ABSTRACT: Very large changes in sea level are postulated for the Tertiary and Quaternary Periods, using data from submarine valleys, the Deep Sea Drilling Program, and certain geological sequences. A potential mechanism to account for the changes is sought in periods of instability in the earth's mode of spin. Conditions for similar occurrences in the future are possibly still extant.

REFERENCE: JAMES, P.M. (1992) Very Large Changes in Sea Level.

Proc. of 6th Australia New Zealand Conf. on Geomechanics, Christchurch, New Zealand, Feb 3-7.

ELEMENTS OF AN EFFECTIVE GEOLOGIC HAZARD MITIGATION PROGRAM

KEYWORDS: *Geologic Hazards; Mitigation; Education; Evaluation; Enforcement; Review.*

ABSTRACT: Effective geologic hazard mitigation requires evaluation, education and enforcement. Evaluation requires geologic hazard mapping to determine the location, and seriousness of the hazards and a hazard investigation prior to land use changes or construction. In developed areas investigations should be undertaken at the first indication of a problem. These should be conducted by qualified private consultants or government staffs. If by consultants they should be subject to governmental review. Publication and availability of results furthers the education element. Education informs decision makers and the general public as to the character and extent of the geologic hazards and the consequences if ignored. Decision makers include regulatory government officials, landowners, industry and financiers. Educational efforts should include graphically illustrated talks, publications and the media. Reports must interest and inform the layman and be scientifically credible. Enforcement must ensure that information gained by evaluation guides land use decision-making and construction location and design. Enforcement can be hazard zoning, grading codes, subdivision regulation, and building codes, as well as economic decisions by enlightened developers or investors. Enforcement must utilize geological review of land use changes and construction sites by competent geologic staff of a governmental agency free from political and economic pressures. Colorado's efforts and its experience with utilizing the three elements will be discussed.

REFERENCE: ROLD, J.W. (1992) Elements of an Effective Geologic Hazard Mitigation Program.

Proc. of 6th Australia New Zealand Conf. on Geomechanics, Christchurch, New Zealand, Feb 3-7.

AUTHOR'S INDEX

NOTES

NOTES

NOTES

NOTES

NOTES

NOTES

NOTES

NOTES